The development of small molecule inhibitors of the essential *Leishmania* bromodomain *Ld*BDF5

Jennifer Louise Carter

Hertford College, University of Oxford

Thesis submitted for the degree of:

Doctor of Philosophy in Organic Chemistry

Michaelmas Term 2023

Under the supervision of:

Prof. Stuart J. Conway (University of Oxford)

Dr Jacob T. Bush (GlaxoSmithKline)

Table of Contents

Abstract i

Acknowledgements iii

Abbreviations v

Chapter 1 **Introduction** 1

1.1 Epigenetics 1

1.1.1 The biological importance of bromodomains 2

1.1.2 Structure of bromodomains 2

1.1.3 Ligands for human bromodomains 4

1.2 Bromodomains as therapeutic targets for infectious diseases 8

1.3 Leishmaniasis and antileishmanials 9

1.3.1 Lifecycle of the *Leishmania* parasite 12

1.3.2 Importance of epigenetic regulation in *Leishmania* for global transcription control 12

1.3.3 Chemical validation of epigenetic targets in *Leishmania* 14

1.3.4 Bromodomains in *Leishmania* 15

1.3.5 Homology of *Ld*BDF5 16

1.3.6 Structural information on *Leishmania* bromodomains 16

1.4 Project aims 21

1.5 Biophysical Assays – a brief introduction 22

1.5.1 WaterLOGSY 22

1.5.2 Thermal Shift Assay 23

1.5.3 Microscale thermophoresis 24

1.5.4 Isothermal calorimetry 26

Chapter 2 **Fragment-based screening** 27

2.1 Introduction and aims 27

2.2 Library design and synthesis 28

2.2.1 Triazolo-fused heterocycles 32
2.2.2 Pyridazinones 35
2.2.3 3,5-Dimethylisoxazoles 36
2.2.4 Benzo-fused Isoxazoles 42
2.2.5 Benzimidazoles 43
2.2.6 Dihydroquinaxolinones, dihydroquinazolinones, and dihydroquinolinones 45
2.2.7 Summary of the fragment library synthesis 48
2.3 Recombinant protein expression and purification 50
2.4 Fragment-based screening assays 54
2.4.1 WaterLOGSY 55
2.4.2 Thermal Shift Assay 59
2.5 Docking studies with **18** in *Ld*BDF5.1 63
2.6 Conclusions and further work 65
Chapter 3 **Exploring the SAR of modifications to the *N*-1 and *C*-2 positions of fragment 18** 67
3.1 Introduction and aims 67
3.2 Library design 69
3.3 Library synthesis 70
3.3.1 Optimisation of the benzimidazole cyclisation 75
3.3.2 HATU-promoted benzimidazole formation 77
3.3.3 Synthesis of compound **107** 79
3.3.4 Summary of the synthetic library of analogues of compound **18** 81
3.4 Determination of compound binding affinities for *Ld*BDF5.1 using microscale thermophoresis 81
3.4.1 MST binding affinity data for R^1-functionalised compounds 82
3.4.2 MST binding affinity data for R^2-functionalised compounds 85
3.5 Docking studies of *C*-2 nitrophenyl containing compounds 88

3.5.1 Evaluation of nitriles as nitro bioisosteres 89
3.6 Development of *C*-2 cyanophenyl containing compounds 91
3.6.1 Synthesis of compounds **156** and **157** 92
3.6.2 MST data for compounds **156** and **157** 93
3.6.3 Design and synthesis of compound **168** 94
3.6.4 MST data for compound **168** 95
3.7 Exploring the additivity of modifications at the *N*-1 and *C*-2 position 95
3.8 Validation of affinity data using ITC 97
3.9 Conclusions and further work 98
Chapter 4 **The development of chemical probes for *Ld*BDF5.1** 101
4.1 Introduction and aims 101
4.2 Evaluation of high affinity compounds in parasites 102
4.2.1 Results from the initial phenotypic assays 103
4.3 The design and synthesis of compounds to investigate the physicochemical properties required for potency in *Leishmania* promastigotes 107
4.3.1 The synthesis of analogues of **156** 109
4.4 Determining the affinity and potency of analogues of compound **156** 110
4.4.1 Determination of the binding affinity of analogues of compound **156** for *Ld*BDF5.1 111
4.4.2 Validation of binding affinities using ITC 112
4.4.3 Evaluation of the effect of physicochemical variation on the activity of compounds in the promastigote assays 113
4.5 Investigation of binding modes using X-ray crystallography studies 117
4.6 Evaluation of selectivity for *Ld*BDF5.1 over human bromodomains 121
4.6.1 Binding affinity of compound **174** in human BRD4(1) and CREBBP 121
4.6.2 Differences in the binding sites of *Ld*BDF5.1, BRD4(1) and CREBBP 122
4.7 Evaluation of the selectivity of **174** for BDF5.1 over BDF5.2 126

4.8 The selectivity of ligands optimised for *Ld*BDF5.1 over the bromodomains in *Ld*BDF1-4 129
4.9 Determination of ADMET properties of ligands for *Ld*BDF5.1 129
4.10 Conclusions and further work 132
Chapter 5 **Conclusions and future work** 135
5.1 Conclusions 135
5.2 Future work 139
Chapter 6 **Experimental** 142
6.1 General Chemistry Methods 142
6.2 Procedures and Compound Data 146
6.2.1 Fragment Library 146
6.2.2 Ligands for *Ld*BDF5.1 183
6.3 General Biology Methods 303
6.3.1 Protein Expression 303
6.3.2 Protein Purification 308
6.4 Biophysical Assays 310
6.4.1 WaterLOGSY 310
6.4.2 Thermal Shift Assay (Differential Scanning Fluorimetry) 311
6.4.3 Microscale Thermophoresis 311
6.4.4 Isothermal Titration Calorimetry 312
6.5 Leishmania Promastigote Cell Viability Assay 313
6.6 Docking of ligands in GOLD 313
6.7 Affinity Selection Mass Spectrometry (ASMS) 314
6.8 Protein X-ray crystallography 314
References 317
Appendices 345
A1 WaterLOGSY Spectra 345

A2 Thermal Shift Data 352
A3 Microscale Thermophoresis (MST) Data 360
A4 MST and Chromlog$D_{7.4}$ Data Tables 412
A5 NMR Spectra of Novel Compounds 416
A6 Isothermal Titration Calorimetry (ITC) Data 514
A7 Image Permissions 523

Abstract - The development of small molecule inhibitors of the essential *Leishmania* bromodomain *Ld*BDF5

The leishmaniases are a collection of neglected tropical diseases caused by *Leishmania* parasites that are epidemic across Africa, Asia, and Latin America. *Leishmania* have complex lifecycles, adopting a range of phenotypes to survive in multiple hosts. Epigenetic processes link genotype to phenotypic diversity in a population and play a crucial role in regulation of the *Leishmania* lifecycle. Targeting the epigenetic mechanisms may therefore be a promising strategy for the treatment of leishmaniasis. Bromodomain-containing proteins (BCPs) are epigenetic proteins that recognise acetylated lysine (KAc) residues in histones and regulate transcription. *Ld*BDF5 is a BCP that contains two bromodomains (*Ld*BDF5.1 and *Ld*BDF5.2) and interprets histone acetylation marks in *Leishmania* to maintain normal levels of gene expression. Inducible gene deletion has shown that BDF5 in *Leishmania* is essential for parasite survival in its two main lifecycle stages: the promastigote and the amastigote, demonstrating it as a suitable target for the disruption of epigenetic processes. The work in this dissertation describes the development of high affinity, potent, and selective ligands that have enabled chemical validation of *Ld*BDF5 as a target for antileishmanial drug discovery.

A fragment-based screening approach was adopted to identify ligands for *Ld*BDF5. A range of KAc-mimicking fragments were synthesised and evaluated using biophysical assays. Compound **18** was identified as a hit with a K_d value of 1410 ± 84 nM (microscale thermophoresis) for *Ld*BDF5.1. Analogues of **18** were synthesised with modifications at two positions (*N*-1 and *C*-2 of the benzimidazole) to probe the structure-activity relationship (SAR) of *Ld*BDF5.1 (Figure 0.1). The highest affinity compounds resulted from modifications at the *C*-2 position with an ethyl linker functionalised with 3-cyano-4-methylbenzene. The binding mode of these compounds was confirmed using X-ray crystallography with compound **181** complexed to *Lmx*BDF5.1. The 3-cyano-4-methylbenzene on the *C*-2 ethylene forms effective π-stacking interactions with Y96, enabling the nitrile to form a key hydrogen bonding interaction with the T99 hydroxyl in the binding site of *Ld*BDF5.1. Compounds designed to target *Ld*BDF5.1 were tested in cell viability assays and exhibited growth inhibition of the *Leishmania* promastigotes, supporting the genetic studies that demonstrated the essentiality of BDF5 for promastigote viability. Five compounds showed increased

activity (EC_{50} values of 0.41–1.72 µM) relative to the clinically approved anti-leishmanial miltefosine (EC_{50} = 1.79 µM). It was also demonstrated that the compounds have >100-fold selectivity for *Ld*BDF5.1 over the human BRD4(1) and CREBBP bromodomains. This work provides a foundation for the future exploration of BDF5 inhibitors in antileishmanial drug discovery.

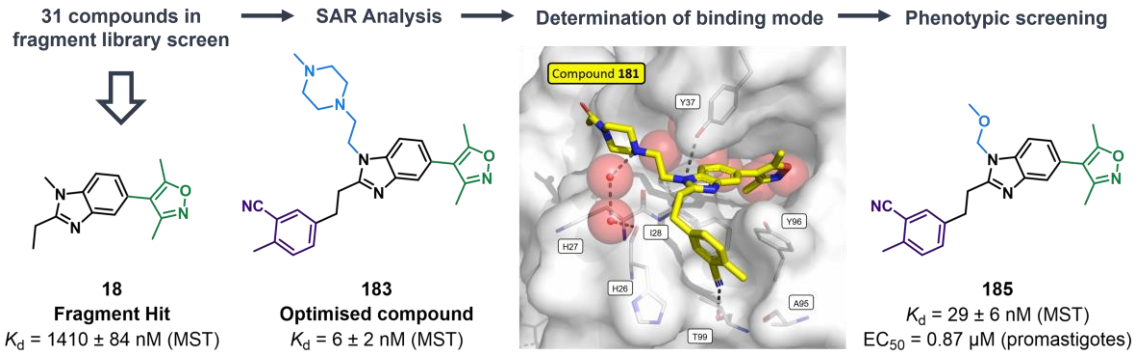

Figure 0.1. The development of high affinity (**183**) and potent compounds (**185**) for *Ld*BDF5.1 from **18**.

Acknowledgements

Firstly, thank you Stuart for your support with this project and for your mentorship over the past four years. Thank you for all the scientific discussion, life/career advice, running chat, pep talks, and encouragement when I needed it. I have learnt so much from you and thoroughly enjoyed my time in your group. A big thank you goes to my collaborators at the University of York: Nathaniel, Catherine, Jeremey and Tony, for the productive meetings that helped to shape the project, and for conducting the biological work with my compounds. Thank you to Marius and Martin at the University of Freiburg for your help with obtaining a crystal structure, and to Andreas at the Helmholtz Centre for conducting the ADMET assays. Thank you to Jacob and collaborators at GSK, and to my Part II and summer students, Ali and Alex, who also worked on this project.

I would like to acknowledge all the NMR, MS, admin, and facilities staff who have supported my research. Thank you to David for welcoming me into the Biochemistry department and teaching me the biophysical assays, and Adam, for your help with troubleshooting the ÄKTAs. Thank you to the Schofield group for accommodating me in LG2 and for lending me hand with the biology. A special mention goes to Raph, Klem, Giorgia, Patrick, Freddy and Karina.

To all the members of the Conway Group – past and present – it has been a great pleasure! There has never been a dull day in the labs with you guys and I am very lucky to have worked alongside such an amazing group of scientists and friends. Thank you to the postdocs: Glen, Marta, Antoine, Pascal, Maria, and Debs, for always being so approachable and imparting your postdoc skills and wisdom. Jess and Holly, thank you for initially welcoming me into the group and helping me find my feet. Thank you Adam for bringing the “Good Energy” and Sophie for maintaining the “Good Energy” in the lab when Adam left. Thanks Pascal for initiating the SJCCC and providing excellent company (and tows) on long café rides. Glen, thank you for propelling The Beatles to my top artist for Spotify Wrapped this year. Thank you Katrina for always being up for a coffee and for being there whenever I needed a good chat. Bernie, you are a star baker - thank you for boosting group morale with your incredible cakes! Thank you Darius for keeping me company late at night in the CRL when protein purification was taking its sweet time. Thank you to my reliable lunch pals for providing good company and good

laughs: Ceri, Harriet, Michael and Patrick. Alistair, thank you for being a great friend, listening to my woes, and boosting my mood with chocolate! Oli, I have enjoyed being your desk buddy. Thank you for humouring my nonsense conversations and offering me great advice. Ada and Keefe, thanks for teaching me how to macarena!

I have made so many fantastic friends during my time in Oxford. It would be impossible to mention you all, but thank you for entertaining me outside of the lab and keeping me (relatively) sane while I've been working on my DPhil. Thank you to my family for being there for me every step of the way and for being so loving and supportive of all that I do. And finally, thank you Tim, for all the adventures, tasty dinners, runs and rides, silliness and fun. I am forever grateful for meeting you in Oxford. You have been my biggest cheerleader and supported me throughout – I could not have got through this without you!

Abbreviations

Ac	Acetyl
ADDP	1,1-(Azodicarbonyl)dipiperidine
ADMET	Absorption, Distribution, Metabolism, Excretion, and Toxicity
ASMS	Affinity Selection Mass Spectrometry
ATAD2	ATPase Family AAA Domain-Containing Protein 2
Base J	β-D-Glucopyranosyloxymethyluracil
BAZ2A/B	Bromodomain Adjacent to Zinc Finger Domain 2A/B
BCP	Bromodomain Containing Protein
BDF	Bromodomain Factor
BET	Bromodomain and Extra-Terminal domain
BNIP	Bisnaphthalimidopropyl
Boc	*tert*-Butyloxycarbonyl
br	Broad
BRD	Bromodomain
BRET	Bioluminescence Resonance Energy Transfer
BRPF1	Bromodomain and PHD Finger-containing protein 1
CDI	1,1'-Carbonyldiimidazole
CECR2	Cat Eye syndrome Chromosome Region, candidate 2
CETSA	Cellular Thermal Shift Assays
CHI	Chromatographic Hydrophobicity Index
CL	Cutaneous Leishmaniasis
COSY	Correlated spectroscopy
CREB	cAMP-Response Element Binding protein

CREBBP	CREB-Binding Protein
CRISPR	Clustered Regularly Interspaced Short Palindromic Repeats
CYP	Cytochrome P450
Da	Dalton
DABCO	1,4-Diazabicyclo[2.2.2]octane
dba	Dibenzylideneacetone
DEAD	Diethyl azodicarboxylate
DIAD	Diisopropyl azodicarboxylate
DiCre	Dimerisable Cre-recombinase
DIPEA	*N*,*N*-Diisopropylethylamine
DMAP	4-Dimethylaminopyridine
DME	Dimethoxyethane
DMF	*N*,*N*-Dimethylformamide
DNA	Deoxyribonucleic Acid
Dppf	1,1'-bis(diphenylphosphino)ferrocene
DSF	Differential Scanning Fluorimetry
E. coli	*Escherichia coli*
EC_{50}	Half maximal effective concentration
EDTA	Ethylenediaminetetraacetic Acid
eq.	Equivalents
ESI	Electrospray Ionisation
Et	Ethyl
E-value	Expectation value
FA	Formic Acid
FBDD	Fragment-Based Drug Discovery

FPLC	Fast Protein Liquid Chromatography
GCN5	General Control Non-depressible 5
GOLD	Genetic Optimisation for Ligand Docking
GSK	GlaxoSmithKline
h	Hour(s)
HAT	Histone Acetyltransferase
HATU	Hexafluorophosphate Azabenzotriazole Tetramethyl Uronium
HBA	Hydrogen Bond Acceptor
HBTU	Hexafluorophosphate Benzotriazole Tetramethyl Uronium
HDAC	Histone Deacetylase
HEPES	4-(2-Hydroxyethyl)-1-piperazineethanesulfonic acid
HOAt	1-Hydroxy-7-azabenzotriazole
HPLC	High-Performance Liquid Chromatography
HRMS	High Resolution Mass Spectrometry
HSQC	Heteronuclear Single Quantum Coherence
HTS	High-Throughput Screening
IBD	Iodobenzene Diacetate
IMAC	Immobilised-Metal Affinity Chromatography
IPTG	Isopropyl β-D-1-thiogalactopyranoside
IR	Infrared
ITC	Isothermal Titration Calorimetry
KAc	Acetylated lysine
K_d	Equilibrium dissociation constant
LC	Liquid Chromatography
LCMS	Liquid Chromatography–Mass Spectrometry

LRMS	Low Resolution Mass Spectrometry
m	Medium
MCL	Mucocutaneous Leishmaniasis
Me	Methyl
MetID	Metabolite identification studies
MLM	Mouse Liver Microsomes
MRG	MORF-mortality factor on chromosome 4-Related Gene
MS	Molecular Sieves
MST	Microscale Thermophoresis
MUSCLE	Multiple Sequence Comparison by Log-Expectation
MW	Molecular Weight
MWCO	Molecular Weight Cut Off
NAD^+	Nicotinamide Adenine Dinucleotide
NMP	*N*-methyl-2-pyrrolidone
NMR	Nuclear Magnetic Resonance
NOE	Nuclear Overhauser Effect
PBS	Phosphate-Buffered Saline
PBS-T	1X Phosphate-Buffered Saline, 0.1% Tween® 20 Detergent
PCAF	P300/CBP-Associated Factor
PDB	Protein Data Bank
PKDL	Post-Kala-azar Dermal Leishmaniasis
ppm	Parts per million
PROTAC	Proteolysis-Targeting Chimera
PSA	Polar Surface Area
PTM	Post Translational Modifications

PTU	Polycistronic Transcriptional Unit
RBA%	Relative Binding Affinity percentage
RBP	RNA Binding Protein
RNA	Ribonucleic Acid
ROS	Reactive Oxygen Species
rt	Room temperature
s	Second(s)
SAR	Structure-Activity Relationship
SDS-PAGE	Sodium Dodecyl Sulfate-Polyacrylamide Gel Electrophoresis
SEC	Size-Exclusion Chromatography
SEM	Standard Error of the Mean
SET	Single Electron Transfer
SFI	Solubility Forecast Index
SGC	Structural Genomics Consortium
SIR2rp1	Silent Information Regulator 2 related protein 1
SMARCA2/4	SWI/SNF-related, matrix-associated, actin-dependent regulator of chromatin subfamily A member 2/4
S_NAr	Nucleophilic aromatic substitution
SPR	Surface Plasmon Resonance
T3P	Propylphosphonic anhydride
TAF1	TATA-box binding protein Associated Factor 1
TAF1L	TATA-Box Binding Protein Associated Factor 1 Like
TFA	Trifluoroacetic acid
THF	Tetrahydrofuran
TLC	Thin Layer Chromatography

TMS	Tetramethylsilane
TPSA	Topological Polar Surface Area
Triflic anhydride	Trifluoromethanesulfonic anhydride
TRIM	Tripartite Motif
TSA	Thermal Shift Assay
TSS	Transcription Start Site
TTS	Transcription Termination Site
UV	Ultraviolet
VL	Visceral Leishmaniasis
w	Weak
WaterLOGSY	Water-Ligand Observed *via* Gradient Spectroscopy
YEATS domains	(Yaf9, ENL, AF9, Taf14, and Sas5) domains

Chapter 1 - Introduction

1.1 Epigenetics

The term "epigenetics" refers to heritable changes in gene expression or phenotype that occur without variation in the underlying deoxyribonucleic acid (DNA) sequence.[1, 2] In eukaryotic cells, DNA is wrapped around core histone proteins and packaged into nucleosomes, the building blocks of chromatin. Epigenetic changes in gene expression are, in part, a result of chemical modifications to DNA bases, and post translational modifications (PTMs) to the histone proteins, which alter the structure of chromatin and affect the transcription of genes (Figure 1.1).[3, 4] While certain DNA modifications, such as the methylation of cytosine, are stable and heritable epigenetic regulators, histone PTMs, including acetylation, methylation, ubiquitination and phosphorylation, play a role in dynamic epigenetic regulation.[5, 6]

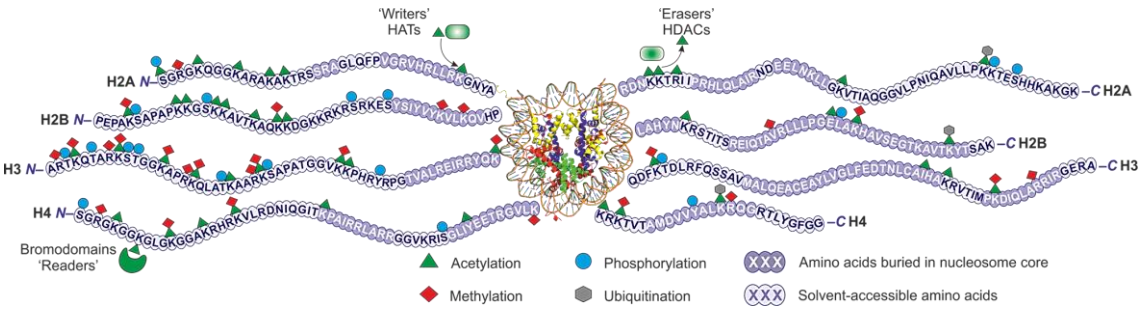

Figure 1.1. A cartoon depicting DNA wrapped around histone proteins and PTMs on the histone tails (displayed as single letter amino acid sequences). Different modifications, such as acetylation, phosphorylation, methylation, and ubiquitination are shown. Acetyl groups are appended by histone acetyltransferases (HATs) and removed by histone deacetylases (HDACs). Bromodomains are the "reader" proteins and interpret acetylation of histone proteins. Image reproduced with permission from Jennings *et al.* Copyright 2014, Future Science Group.[7]

ε-*N*-Acetylation of lysine residues (KAc) is one of the most frequently occurring PTMs, which controls chromatin configuration and its interaction with other proteins.[8] Large-scale proteomics studies have demonstrated that KAc occurs in over 1750 proteins with a diverse array of cellular functions such as cell cycle regulation, transcription and replication, nuclear transport and chromatin remodelling.[8] On histones, the acetyl functionality is appended to lysine residues by histone acetyltransferase (HAT) enzymes

and is removed by histone deacetylases (HDACs). Acetylation of histone tail lysine residues neutralises the positively charged amine side chain, and reduces the electrostatic interactions between DNA and histones. This leads to a more relaxed and open chromatin structure, euchromatin, that is associated with transcriptionally active genes.[9] In addition to modulating chromatin structure, KAc residues affect gene transcription through interaction with bromodomain-containing proteins (BCPs). The bromodomain recognises and interprets the lysine acetylation state.[10]

1.1.1 The biological importance of bromodomains

BCPs play an essential role in the regulation of gene expression, as part of larger protein complexes, through chromatin remodelling, histone modification, histone recognition, and transcriptional machinery regulation.[11] Dysregulation of bromodomains in humans is associated with a variety of diseases, including cancers, inflammation, cardiovascular diseases, and viral infections.[12-15] As a result, the development of bromodomain inhibitors as therapeutic agents is now an intense area of research.[3, 13] In the past decade, over thirty bromodomain inhibitors have entered clinical trials for different human disorders, many of which target the bromodomain and extra-terminal domain (BET) family of BCPs.[11, 16-22]

1.1.2 Structure of bromodomains

First reported in 1992, and named after the *Drosophila* gene *brahma*, bromodomains are protein interaction modules of ~110 amino acids.[23] The human genome codes for 61 distinct bromodomains that are distributed across 46 separate BCPs. The 61 bromodomains cluster into eight families based on their sequence homology and structural similarity (Figure 1.2).[24]

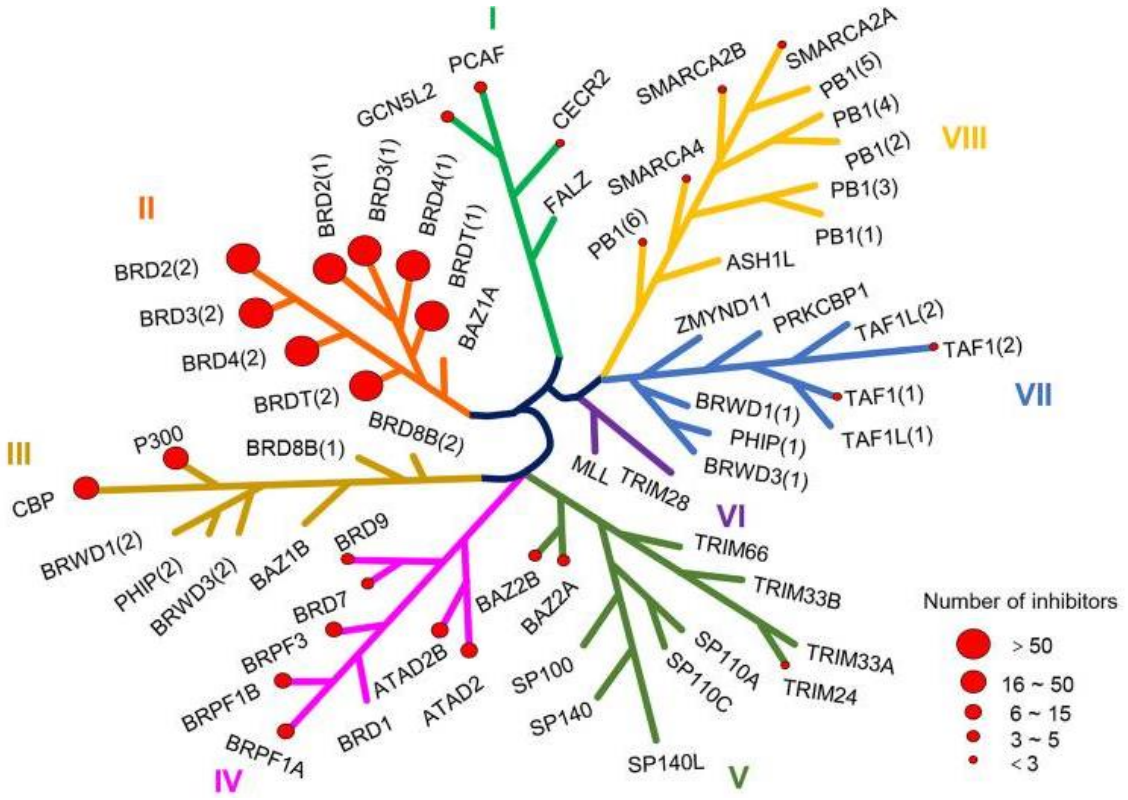

Figure 1.2. Phylogenetic tree of the human bromodomain family. The eight families are shown in different colours and indicated by Roman numerals. The number of inhibitors reported is indicated by the different sizes of red dots (current as of May 2023). Image from: Pan *et al.*, Copyright 2023.[12]

The tertiary structure of the bromodomains is a bundle of four α-helices (αZ, αA, αB, and αC), linked by loop regions of variable length (ZA and BC loops).[25] Crystal structures of bromodomains with bound cognate peptides have shown that KAc is recognised within a binding pocket that is largely hydrophobic in nature, although a network of four or five well-ordered water molecules typically form the base of the binding site.[26] The binding of KAc occurs *via* two main interactions: i) a hydrogen bond between the KAc carbonyl and the amide of a highly conserved asparagine residue, and ii) a water-mediated hydrogen bond between the KAc carbonyl and the hydroxyl of a conserved tyrosine residue (Figure 1.3). It is typical for these key interactions to be competitively mimicked when developing synthetic ligands for bromodomains. The variable ZA and BC loops that shape the KAc binding pocket contribute to binding specificity and allow for the development of selective bromodomain ligands.[24, 27]

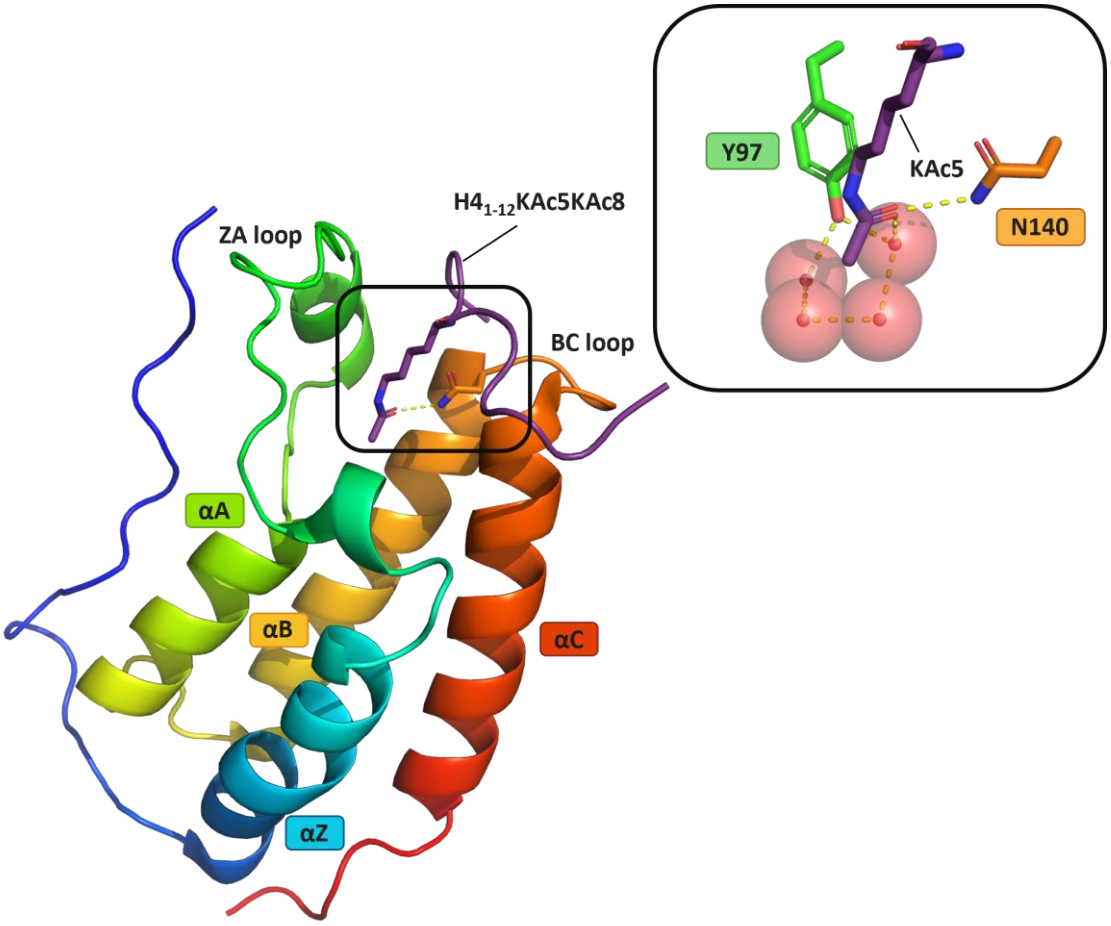

Figure 1.3. A view of an X-ray crystal structure of the first domain of BRD4 in complex with the diacetylated histone H4-mimicking peptide H4$_{1-12}$KAc5KAc8 (PDB code 3UVW, carbon = purple).[28] There is a hydrogen bond between the KAc5 carbonyl and the amide of the highly conserved asparagine residue, N140, and a water-mediated hydrogen bond between the KAc5 carbonyl and the hydroxyl of the conserved tyrosine residue, Y97.

1.1.3 Ligands for human bromodomains

The first potent and selective bromodomain ligands were two diazepine-based inhibitors of the BET bromodomains, **(+)-JQ1** and **I-BET762**, published simultaneously by Filippakopoulos *et al.* and Nicodeme *et al.* (Figure 1.4).[20, 21, 29] The structures of these inhibitors were inspired by and modified from compounds disclosed in a patent by Mitsubishi Tanabe Pharma.[29] **(+)-JQ1** and **I-BET762** helped define the role of the BET proteins in oncology and inflammation and ignited significant interest in bromodomains as therapeutic targets.[30]

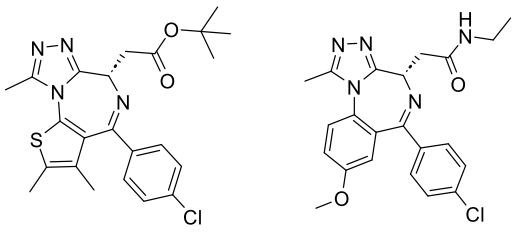

Figure 1.4. The structure of **(+)-JQ1** and **I-BET726** bromodomain ligands.[20, 21]

Since the discovery of **(+)-JQ1** and **I-BET762** in 2010, BET bromodomains have been the focus of extensive research and it is only more recently that bromodomains outside of the BET family have received more attention. There are, however, a growing number of bromodomains for which there are multiple chemical probes from a diverse range of chemotypes (Figure 1.5).[31, 32] Examples include CECR2, PCAF/GCN5, CREBBP/p300, ATAD2, BRD9, BRPF-1B, TAF1, SMARCA2/4, and BAZ2A/B, highlighting the tractability of numerous bromodomains to small molecule binding.[33-43]

Small molecule inhibitors of bromodomains are typically designed to mimic a KAc residue, giving them the ability to disrupt the interaction between an acetylated histone and the KAc binding site within a bromodomain.[44] Canonical bromodomains feature conserved asparagine and tyrosine residues that are involved in the recognition process. As described in section 1.1.2, the asparagine nitrogen forms a direct hydrogen bond with the carbonyl oxygen atom of the KAc of acetylated histones, whereas the tyrosine forms a hydrogen bond to the oxygen of the carbonyl through a bridged water molecule. High affinity ligands usually mimic these interactions and most bromodomain inhibitors comprise a rigid scaffold bearing hydrogen bond acceptors and donors such as triazole-fused heterocycles, 3,5-dimethylisoxazoles, pyridazinones, benzimidazoles, quinazolinones and quinolinones (Figure 1.6).[45] The two key interactions that are formed by KAc mimics in canonical bromodomains are either made by two different atoms (Figure 1.6, A&B), or by the same atom (Figure 1.6, C&D). Some bromodomain ligands, e.g. **PFI-1**, feature a third hydrogen bond to the carbonyl oxygen atom of the asparagine (Figure 1.6, C).

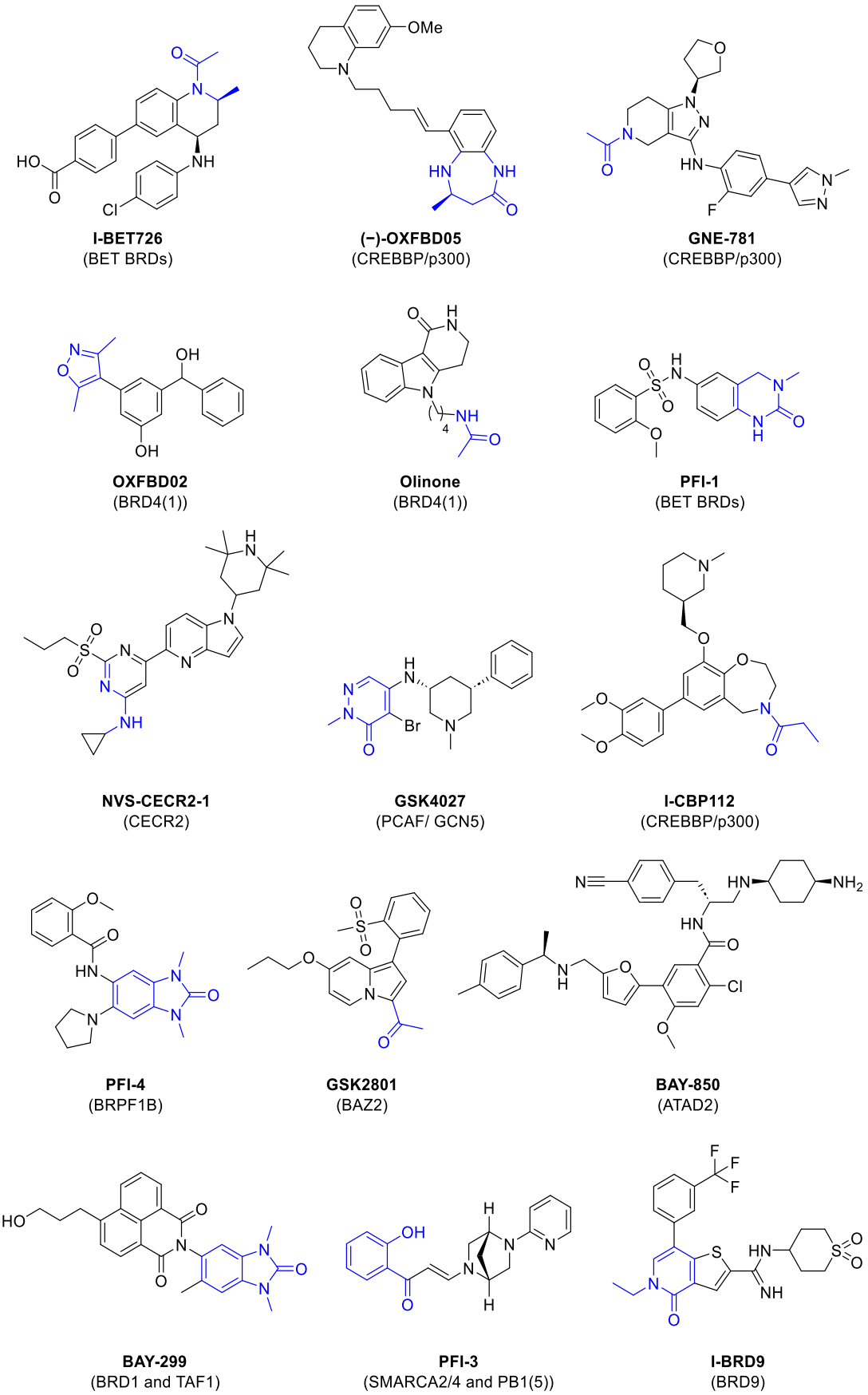

Figure 1.5. The structures of a diverse range of chemotypes found in bromodomain ligands. The KAc mimic, where known, is highlighted in blue.[35-43, 46-51]

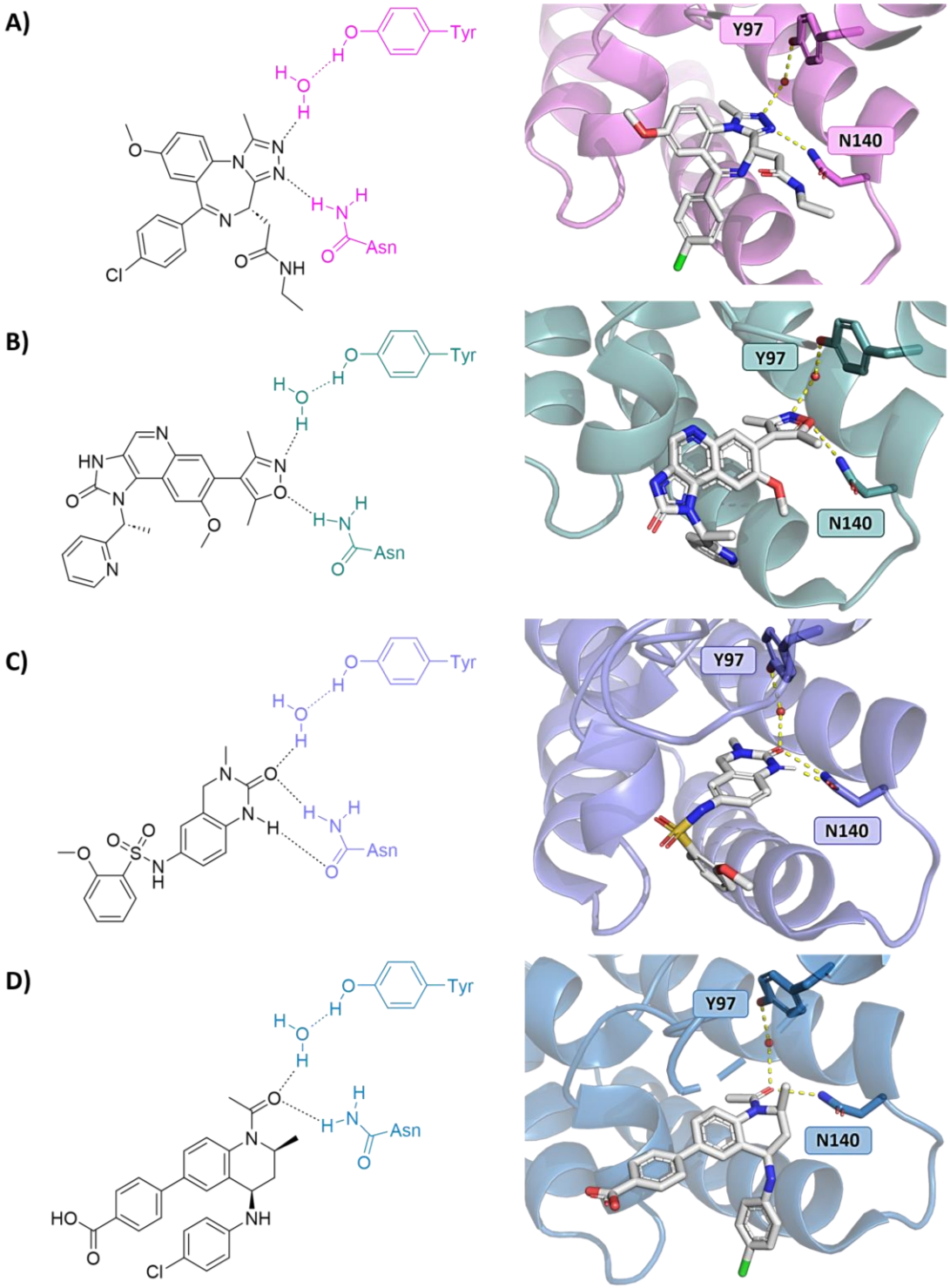

Figure 1.6. Examples of KAc mimics that feature in human bromodomain inhibitors and their hydrogen bonding interactions with the conserved asparagine and tyrosine residues in canonical bromodomains. **A)** Hydrogen bonding interactions of triazole-based KAc mimics and the X-ray crystal structure of **I-BET762** (carbon = white) in complex with BRD4(1) (cartoon and carbon = pink, PDB code 3P5O).[52] **B)** Hydrogen bonding interactions of 3,5-dimethylisoxazole-based KAc mimics and the X-ray crystal structure of **I-BET151** (carbon = white) in complex with BRD4(1) (cartoon and carbon = teal, PDB code 3ZYU).[53] **C)** Hydrogen bonding interactions of the 1,3- dimethyl-3,4-dihydroquinazolin-2(1*H*)-one KAc mimic and the X-ray crystal structure of **PFI-1** (carbon = white) in complex with BRD4(1) (cartoon and carbon = purple, PDB code 4E96).[54] **D)** Hydrogen bonding interactions of N^1-acetyl-based KAc mimics and the X-ray crystal structure of **I-BET726** (carbon = white) in complex with BRD4(1) (cartoon and carbon = blue, PDB code 4BJX).[55]

1.2 Bromodomains as therapeutic targets for infectious diseases

Outside of human physiology and disease, emerging evidence suggests that BCPs are important mediators of gene expression relating to the invasion, metamorphosis, and viability of parasites including *Plasmodium* spp. (causative agents of malaria), *Toxoplasma gondii* (toxoplasmosis), *Trypanosoma brucei* (African trypanosomiasis/sleeping sickness), *Trypanosoma cruzi* (American trypanosomiasis/Chagas disease) and *Leishmania* (leishmaniasis).[56, 57] In these parasites, the proteins containing bromodomains are referred to as bromodomain factors (BDFs). A number of BDFs have been identified as essential for parasite viability and might serve as novel epigenetic targets for the treatment of neglected diseases.[57]

A limited number of studies have aimed to understand and target the epigenetic mechanisms in kinetoplastid parasites, including the role of BDFs. Gene editing approaches have confirmed the essentiality of bromodomain genes for parasite viability. For example, in *T. brucei*, *Tb*BDF3-7 were genetically validated using ribonucleic acid (RNA) interference (RNAi) target sequencing and were observed to be essential for the survival and growth of the bloodstream form.[58, 59] CRISPR/Cas9 genome editing was employed to demonstrate the essentiality of *Tc*BDF2 in *T. cruzi* for host cell invasion, amastigote replication, and differentiation of the parasite.[60] Jones *et al.* used Cas9-driven gene deletions to show that BDF1-5 are essential for *L. mexicana* promastigote survival, while DiCre (dimerisable Cre-recombinase) inducible gene deletion of BDF5 identified the protein to be essential for *Leishmania* promastigotes and amastigotes.[61]

In parallel, the BDFs in *T. brucei* and *T. cruzi* have been investigated through chemical inhibition with human bromodomain ligands. Yang *et al.* demonstrated that **GSK2801** competitively inhibits hyperacetylated H2AZ binding to the *T. brucei* BDF2.[62] Additionally, **I-BET15** was shown to bind to *T. brucei* BDF2 (Figure 1.7), and reports on these compounds suggest that inhibition of *T. brucei* BDF2 results in disrupted parasite growth and abnormal lifecycle progression from the procyclic form to the bloodstream form.[59, 62] *T. brucei* BDF2 may therefore serve as a potential chemotherapeutic target for the treatment of trypanosomiasis. The inhibitory effect of **SGC-CBP30** (Figure 1.7) to *T. brucei* BDF5 has been disclosed in a patent.[63] *T. cruzi* BDF2, which recognises H4K10Ac and H4K14Ac, and *T. cruzi* BDF3, which plays a key role in parasite morphogenesis and

differentiation, have also been investigated as therapeutic targets.[60, 64-67] *T. cruzi* BDF3 interacts with the human bromodomain inhibitors **(+)-JQ1** and **I-BET151** (IC_{50} = 7.14 μM, and 6.35 μM, respectively), and a fragment-based approach was applied to identify novel ligands for this bromodomain.[64, 68] These studies demonstrate that targeting the bromodomains of parasites can be a promising therapeutic strategy, and that existing inhibitors of human bromodomains can serve as effective starting points for the development of parasite-specific bromodomain inhibitors.

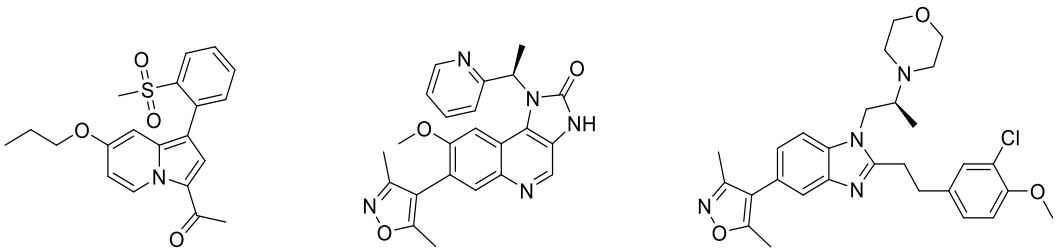

Figure 1.7. The structure of **GSK2801**, **I-BET151**, and **SGC-CBP30** bromodomain ligands.[43, 53, 69]

1.3 Leishmaniasis and antileishmanials

Leishmaniases are a collection of neglected tropical diseases caused by parasitic protozoa of the genus *Leishmania.* The disease is endemic in approximately 100 countries with an annual occurrence of 700,000 to 1 million new cases.[70] Leishmaniasis manifests in three main forms: cutaneous (CL, the most common); mucocutaneous leishmaniasis (MCL); and visceral (VL, also known as kala-azar, the most serious form of the disease).[71] CL is characterised by skin lesions, mainly ulcers, that can be severely disfiguring and stigmatising.[72] MCL can lead to the destruction of the mucosal membranes. VL causes fever, weight loss, spleen and liver enlargement, and is fatal if left untreated in 95% of cases.[73] VL is predominantly caused by *L. donovani* and *L. infantum* species. Even following a cure of primary VL, a sequela can develop in the form of PKDL (post-kalar-azar dermal leishmaniasis).[74]

The threats posed by leishmaniasis epidemics are particularly severe in some of the poorest communities in Africa, Asia, and Latin America.[75] Although treatments exist — current drugs include antimonials, amphotericin B, paromomycin sulfate, pentamidine, and miltefosine (Figure 1.8) — the duration of treatments are often long, the drugs are costly, and they exhibit severe adverse side effects. Moreover, emerging resistance in

Leishmania to existing therapies is an increasingly pressing issue (Table 1.1).[76] The majority of the current treatments require parenteral administration, which provides challenges for healthcare in rural areas. The only oral drug available for leishmaniasis treatment is miltefosine, which is teratogenic and cannot be issued to women of childbearing age.[77]

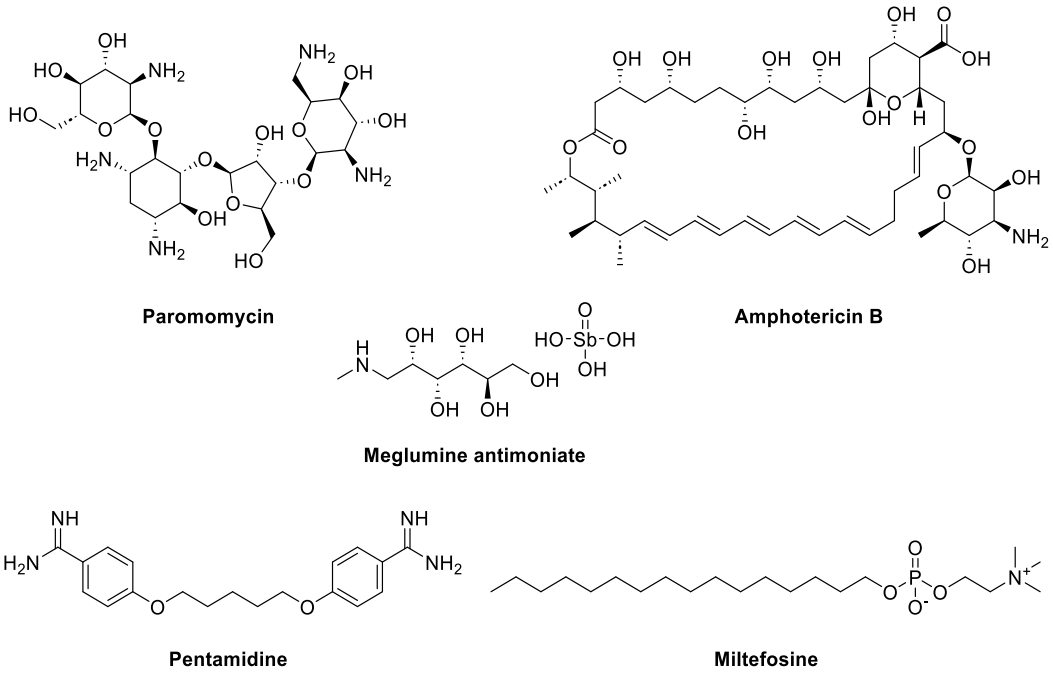

Figure 1.8. The chemical structures of FDA-approved drugs for the treatment of leishmaniasis.

Table 1.1. The FDA-approved drugs (structures shown in Figure 1.8) for leishmaniasis, summarising the mode of action, efficacy, resistance, and side effects of the treatment. The intended use of the drug, in terms of the form of leishmaniasis it is design to treat, is given in parentheses. Adapted from Singh *et al.*[76]

Drug	Mode of Action	Efficacy	Resistance	Toxicity
Paromomycin [78, 79] (CL/PKDL)	Inhibits protein synthesis by inhibiting 30S ribosomal subunit. Premature termination of mRNA.	95% Cure rate in a Phase III trial (15 mg kg^{-1}, 11 mg base) for 21 days. Effective against PKDL.	No effective resistance.	Pain at the injection site, kidney toxicity, liver toxicity, and hearing toxicity.
Amphotericin B [80-82] (VL)	Binds to cell wall sterols, preferentially to ergosterols. Lowers glucose and amino acid intake, results in apoptosis.	>90%	No effective resistance.	Infusion-related reactions, anemia, nephrotoxicity myocarditis, and even death of the patient.
Meglumine Antimoniate [83] (VL/CL)	DNA degradation leading to apoptosis. Inhibits glycolysis and β-oxidation.	Varies between 35% and 95% based on area.	High resistance in some regions of India.	Cardiotoxicity arthralgia, anorexia, fever, urticaria and significant toxicity to the liver, kidneys, and spleen. Hospitalisation and constant monitoring of patients during treatment.

Drug	Mode of Action	Efficacy	Resistance	Toxicity
Pentamidine [84, 85] (VL)	Inhibits the synthesis of DNA and RNA, and causes mitochondrial damage.	Cure rates range from 35% with *L. braziliensis*in Peru to 90% with *L. guyanensis*in Suriname, efficacy is very variable.	Prevalent.	Heart damage, joint pain, loss of appetite, fever, urticaria, and serious liver, kidneys, and spleen damage. Hospitalisation and monitoring of patients during treatment required.
Miltefosine [86, 87] (CL/VL)	Induces apoptosis. Modulates membrane permeability.	93–95% in India, 65–85% in Africa.	No effective resistance described.	Can cause birth defects, stomach problems, kidney damage, and liver damage. Cannot be given to pregnant women.

Thus far, the majority of new lead compounds (or pre-clinical candidates) for *Leishmania* have been identified by phenotypic-based drug discovery and target deconvolution.[88] This approach has been successful: the GSK "Leish-Box" of inhibitors came from screening large libraries of compounds against *Leishmania*, and some natural product inhibitors were identified from the Davis natural product-based library.[89, 90] Ongoing drug discovery programmes have identified new chemical entity antileishmanials that have progressed into clinical development in recent years (Figure 1.9).[91, 92] Unlike phenotypic-based drug discovery studies, there has been limited success in developing antileishmanial compounds using target-based approaches. The poor outcomes from these structure-based studies are often due to inhibition of the target in a cell-free context not translating to the desired activity in phenotypic assays.[93] There also remains a lack of robustly validated molecular targets that can be exploited for antileishmanial drug discovery, highlighting the need for thorough genetic and chemical validation of potential targets.[94]

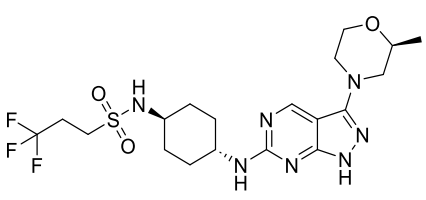

DDD853651/ GSK3186899
inhibitor of CRK12
Intra-macrophage: EC_{50} = 1.4 μM

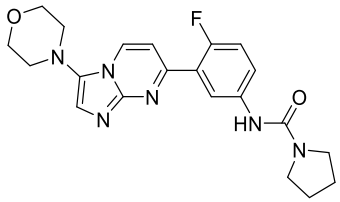

DDD01305143/ GSK3494245
proteasome inhibitor
Intra-macrophage: EC_{50} = 1.6 μM

Figure 1.9. Structures of two compounds in clinical development for the treatment of leishmaniasis.[91, 92]

1.3.1 Lifecycle of the *Leishmania* parasite

Leishmania spp. exhibit complex lifecycles with different developmental stages in more than one host (Figure 1.10).[95] *Leishmania* metacyclic promastigotes are transmitted to humans through the bites of infected female phlebotomine sandflies. In the bloodstream, the parasites invade mammalian macrophages and other phagocytic cells. In the tissue stage, promastigotes transform into amastigotes, which multiply in the cells and proceed to infect other phagocytes. At this stage, the infection may become symptomatic in the host. When a sandfly next takes a meal of parasite-containing blood from an infected human, ingested amastigotes transform in the fly gut into several forms of promastigote, including the metacyclic form that is infective to humans.[96] To rapidly transition between these morphological states and sustain chronic infection in the mammalian host, the parasite must employ transcriptional and post-transcriptional regulation of gene expression, translational repression, and PTMs of histones and transcription factors.[97-99]

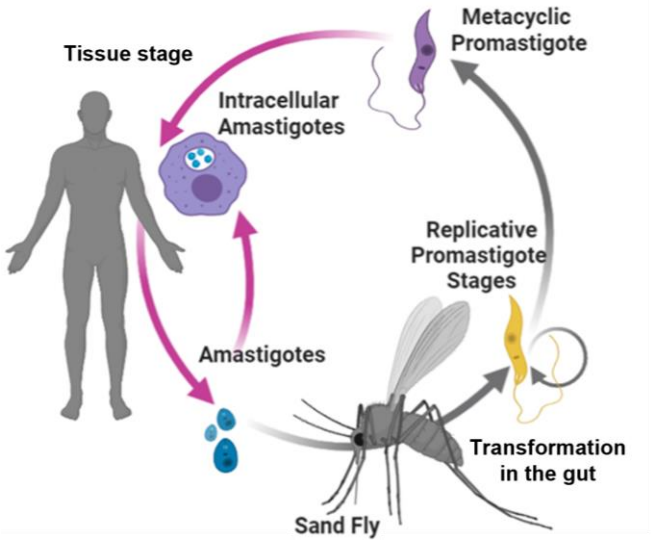

Figure 1.10. A simplified cartoon of the lifecycle of *Leishmania* depicting the promastigote and amastigote forms of the parasite, found in the sandfly and human, respectively. Image was created with Biorender.com.

1.3.2 Importance of epigenetic regulation in *Leishmania* for global transcription control

Leishmania heavily depend on post-transcriptional mechanisms for gene regulation.[100, 101] Unlike other eukaryotes, *Leishmania* have an unusual arrangement of their genes in large polycistronic transcriptional units (PTUs) containing tens to hundreds of protein-

coding genes on the same strand of DNA (Figure 1.11).[102-105] All the genes within a PTU are transcribed at the same rate to generate a single polycistronic pre-mRNA strand, then individual genes within the primary transcript are *trans*-spliced and polyadenylated to form mature individual mRNAs.[106, 107] Consequently, the *Leishmania* genome contains far fewer transcription start sites (TSSs) and transcription termination sites (TTSs) than other eukaryotes. *Leishmania* rely almost exclusively on post-transcriptional mechanisms to regulate differential gene expression, which are not yet completely understood.[108, 109] In parallel, transcription appears to be controlled by both histone and non-histone proteins, which form part of protein complexes that regulate chromatin accessibility.[61]

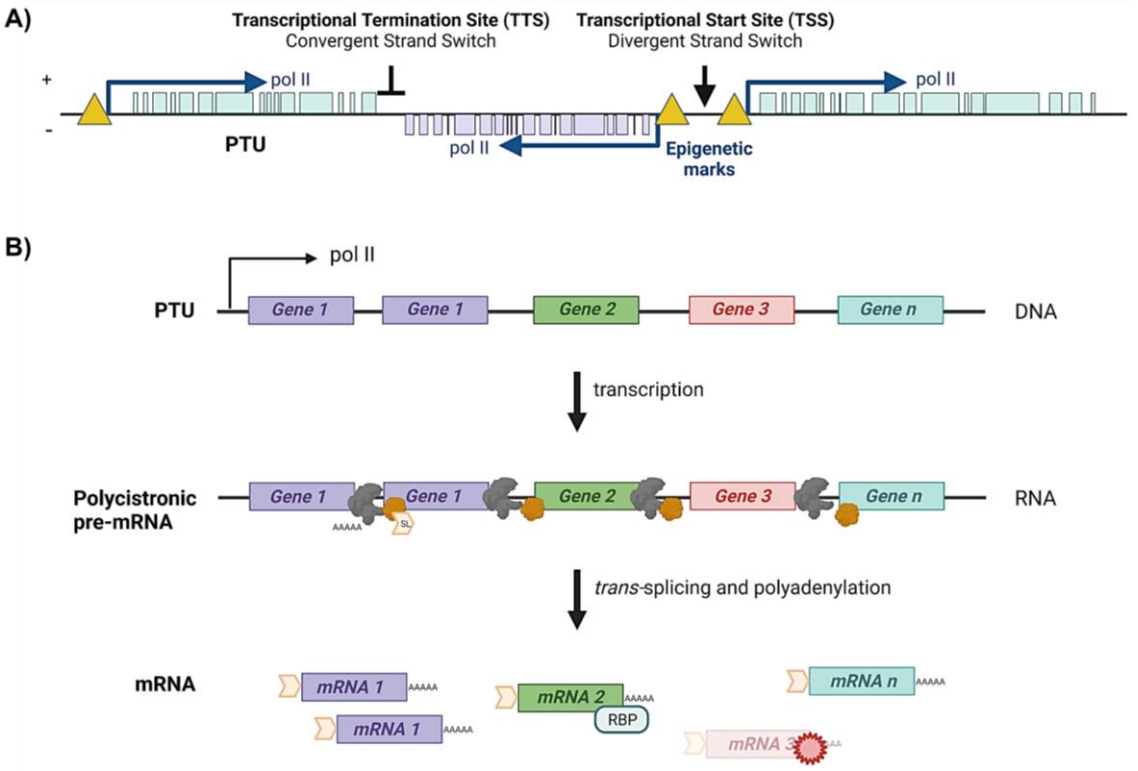

Figure 1.11. A) The arrangement of genes in PTUs separated by divergent or convergent strand-switch regions in the *Leishmania* parasite. Transcription start sites are indicated by arrows. Epigenetic marks on DNA have been identified at TSS and TTSs. **B)** Transcription occurs *via* transcription of a polycistronic pre-mRNA that is trans-spliced into mRNA fragments. The initial transcripts are individualised in monocistronic mRNAs after the addition of a capped splice leader (SL) RNA through a trans-splicing reaction coupled to polyadenylation. pol II = RNA polymerase II; RBP = RNA binding protein. Image was created with Biorender.com.

There are numerous examples that epigenetic regulation plays an important role in *Leishmania* for gene expression. Following the sequencing of the *L. major* genome, bioinformatics analyses predicted the existence of genes encoding HATs, HDACs,

bromodomains, and YEATS domains.[103] A number of epigenetic marks have been identified at TSSs and TTSs in *Leishmania*, including histone variants, histone modifications, and the DNA modification base J (β-D-glucosyl-hydroxymethyluracil).[103, 110-115] Evidence indicates that TSSs in *Leishmania* are actively regulated through histone acetylation, and chromatin accessibility might mediate the initiation of transcription of protein-coding genes.[110] H3 acetylation has been identified at TSSs in *L. major* and H4 acetylation marks have been identified at TSSs in *L. donovani*.[108, 110, 112-115] However, the proteins and processes which interpret these epigenetic marks in *Leishmania* are not yet defined.

1.3.3 Chemical validation of epigenetic targets in *Leishmania*

The development of chemical tools targeting epigenetic regulation will enable a better understanding of the mechanisms underlying the success of *Leishmania* and may open exciting new avenues for antileishmanial therapies. The essentiality of histone acetylation determined by genetic experiments is underlined by a limited amount of chemical validation on HDACs in *Leishmania*. Following the discovery that the human HDAC inhibitor vorinostat demonstrates some anti-parasitic activity in *Leishmania,* several efforts have been made to improve the structure-activity relationships of hydroxamate-based HDAC inhibitors with anti-leishmanial activity.[116-121] The most recent development was an *O*-alkyl hydroxamate derivative **1** (Figure 1.12) that displays potent *in vitro* activity against the amastigote stage of *L. infantum* (IC_{50} = 3.21 ± 1.2 μM) and no observed activity against promastigotes – supporting evidence for lifecycle stage-dependent HDAC isoforms.[104, 118, 122, 123] A human sirtuin (NAD^+-dependent HDAC) inhibitor, **KH-TFMDI** (Figure 1.12), was found to be potent against *L. amazonesis* promastigotes (IC_{50} = 1.98 μM) and amastigotes (IC_{50} = 1.15 μM).[124] Treatment of the promastigotes with **KH-TFMDI** induced morphological changes, increased levels of acetyl-tubulin, altered mitochondrial function, and resulted in cell death.[124] Bisnaphthalimidopropyl (BNIP) compounds are a known series of antileishmanials that are also proposed to act through inhibition of the *L. infantum* sirtuin, SIR2rp1, at the low micromolar level (Figure 1.12).[125, 126] Whilst parasite HDAC inhibitors demonstrate therapeutic potential against *Leishmania*, key factors to address in

the development of these compounds are species selectivity and potency.[127] Demonstration of cellular target engagement is also required to confirm the mechanism of action of the inhibitors.

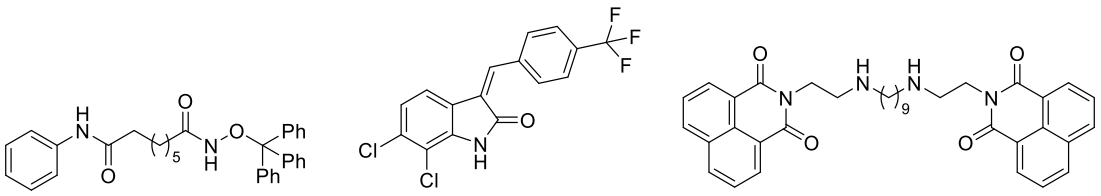

1
Amastigotes: IC_{50} = 3.21 μM
Promastigotes: no activity

KH-TFMDI
Amastigotes: IC_{50} = 1.15 μM
Promastigotes: IC_{50} = 1.98 μM

BNIPDanon
Amastigotes: IC_{50} = 6.03 μM
Promastigotes: *no data*

Figure 1.12. Structures of HDAC inhibitors that have shown potency against *Leishmania*.[122, 124, 125]

Unlike for the HDACs, at the start of this project, there were no known bromodomain inhibitors for *Leishmania* and this field of research remained largely unexplored. Five X-ray crystal structures featuring human bromodomains inhibitors bound to *L. donovani* BDFs were available on the PDB, however there was no information regarding the binding affinity or phenotypic effect of the ligands on the parasite.[128-132]

1.3.4 Bromodomains in *Leishmania*

There are five canonical BDFs in the *Leishmania* genome (BDF1–BDF5) and three additional non-canonical bromodomains (BDF6–BDF8) that do not feature the conserved asparagine and tyrosine residues.[56, 61, 103] BDF1–3 are small proteins (<500 residues) and contain only a single bromodomain, whereas BDF4 is a larger protein that also bears a CW-type zinc finger domain. BDF5 has *N*-terminal tandem bromodomains and a *C*-terminal MRG domain-like region (MORF-mortality factor on chromosome 4-related gene).[61] MRG domains are typically associated with chromatin remodeling and transcription regulation proteins.[133] BDF5 is expressed in both *Leishmania* lifecycle stages and plays an essential role in RNA polymerase II-mediated transcription. As a component of a larger assembly of proteins that includes other bromodomain factors and HAT2, BDF5 associates with TSSs to influence transcription.[61] Jones *et al.* demonstrated that inducible deletion of BDF5 leads to a disruption of transcriptional activity and global

defects in gene expression.[61] BDF5 was shown to be essential for the cellular viability of both *Leishmania* promastigotes and amastigotes. The genetic target validation of BDF5 provides a strong rationale for the investigation of the protein as a therapeutic target.

1.3.5 Homology of *Ld*BDF5

*Ld*BDF5 lacks structural homology to known human protein domains. A PHMMER search was used to identify human bromodomain homologues of *Ld*BDF5.[134] No hits were detected in the search with the entire protein sequence in the query against the UniProt database. However, *Ld*BDF5.1 shares limited identity (28.8%, E-value = 0.027) with human BRD3 and BRD9 (30.5%, E-value = 0.23). The low levels of sequence homology between the organisms provides a potential advantage in terms of developing selective compounds without negatively affecting human biology.

1.3.6 Structural information on *Leishmania* bromodomains

Valuable structural data have been obtained for *Leishmania* BDFs, particularly for *Ld*BDF5 (Table 1.2). Two human bromodomains inhibitors have been co-crystallised with the first domain of BDF5 in *L. donovani* (*Ld*BDF5.1): **BI-2536** and **SGC-CBP30** (PDB codes 5TCM and 6BYA).[130, 131] The structure of the second bromodomain of *Ld*BDF5 (*Ld*BDF5.2) was solved with **bromosporine** (PDB code 5TCK), a pan-selective human bromodomain inhibitor.[132, 135] **Bromosporine** was also co-crystallised with *Ld*BDF2 (PDB code 5C4Q) and *Ld*BDF3 (PDB code 5FEA).[128, 129] More recently, Wilkinson *et al.* solved the apo structure of *Ld*BDF5.2 (PDB code 8BPT).[136, 137] While no information regarding the binding affinity or effect of the human bromodomain ligands co-crystallised with the aforementioned structures was available at the start of this project, the existing structural information could be utilised for the development of highly specific small molecule inhibitors to validate bromodomains as targets in leishmaniasis.

Table 1.2. PDB codes for the available structures of *L. donovani* bromodomains.[128-132, 137]

Bromodomain	*L. donovani* gene	PDB code	Ligand
BDF2	LdBPK_363130.1	5C4Q	Bromosporine
BDF3	LdBPK_363520.1	5FEA	Bromosporine
BDF5.1	LdBPK_091320.1	5TCM/6BYA	BI-2536/SGC-CBP30
BDF5.2	LdBPK_091320.1	5TCK/8BPT	Bromosporine/*none*

1.1.3.1 X-Ray crystal structures of the *Ld*BDF5 bromodomains

The crystal structures of the *Ld*BDF5 bromodomains (PDB codes: 6BYA and 5TCK) show a similar overall fold to human bromodomains (Figure 1.13).[131, 132] Both bromodomains are canonical and feature conserved asparagine and tyrosine residues (Y44 & N90 in *Ld*BDF5.1, and N257 & Y201 in *Ld*BDF5.2) that bind to cognate KAc substrates. The base of the binding site of *Ld*BDF5.1 has a network of five well-ordered water molecules, which do not feature in *Ld*BDF5.2.

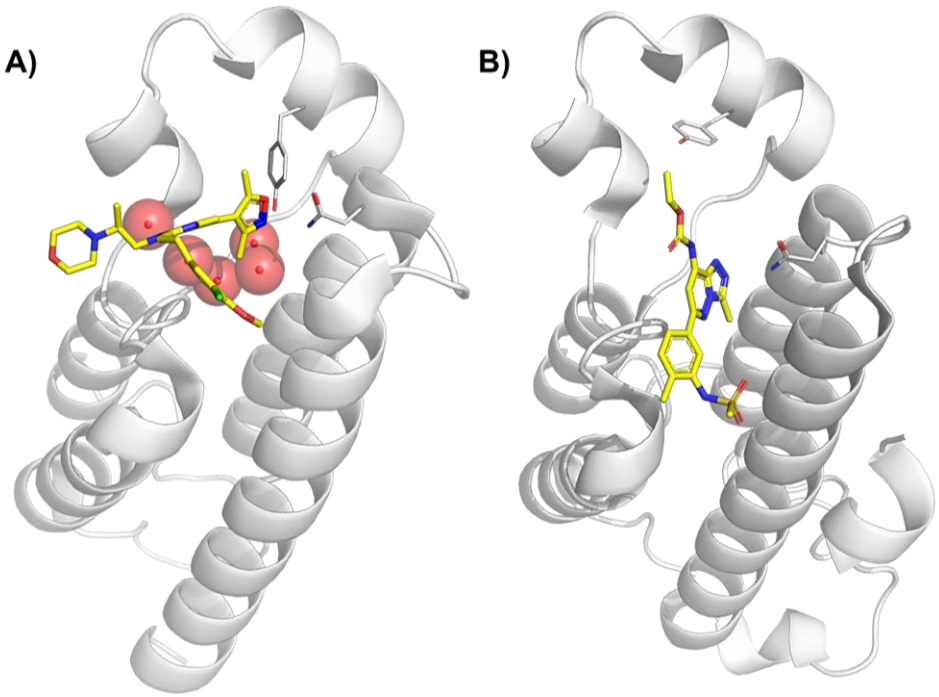

Figure 1.13. A) A view of the X-ray crystal structure of **SGC-CBP30** (carbon = yellow) in complex with *Ld*BDF5.1 (cartoon and carbon = white, PDB code 6BYA).[131] **B)** A view of the X-ray crystal structure of **bromosporine** (carbon = yellow) in complex with *Ld*BDF5.2 (cartoon and carbon = white, PDB code 5TCK).[132]

The crystal structure of **SGC-CBP30** in complex with *Ld*BDF5.1 was overlaid with an X-ray crystal structure of CREBBP, the target protein of **SGC-CBP30** in humans (PDB code: 4NR7, Figure 1.14).[138, 139] There is close alignment between the tyrosine (Y1125) and asparagine (N1168) residues in CREBBP and the corresponding residues (Y44 and N90) in *Ld*BDF5.1. The 3,5-dimethylisoxazole motif of **SGC-CBP30** acts as a KAc mimetic in the binding site of *Ld*BDF5.1 by hydrogen bonding to N90 with its oxygen atom, and forming a water-mediated hydrogen bond to Y44 with its nitrogen atom (Figure 1.14, A).[140] However, there are differences close to the inhibitor within the KAc pocket of *Ld*BDF5 and CREBBP, which suggest that it may be possible to generate selective ligands for the parasite bromodomain. One region in CREBBP that is particularly valuable in enhancing inhibitor potency and selectivity is the LPF shelf, which comprises of residues L1109, P1110, and F1111.[50, 69, 141] In *Ld*BDF5.1, the LPF residues, are replaced by a HIF motif (H27, I28 and, F29; Figure 1.14, B). Another residue that is key for attaining selectivity toward CREBBP is R1173, located at the entrance of the binding site of this bromodomain.[69, 142, 143] The aromatic ring of the **SGC-CBP30** ligand forms cation-π interactions with the R1173 side chain in CREBBP. However, the R1173 residue corresponds to A95 in *Ld*BDF5.1 (Figure 1.14, C), therefore the cation-π interaction would not form in the parasite protein. The **SGC-CBP30** ligand adopts different binding conformations in the *Ld*BDF5.1 and CREBBP binding sites due to the structural differences resulting from the replacement of the R1173 and V1174 residues in CREBBP with A95 and Y96 in *Ld*BDF5.1 (Figure 1.14, D). These structural differences may be exploited to generate parasite-specific inhibitors of the bromodomain.

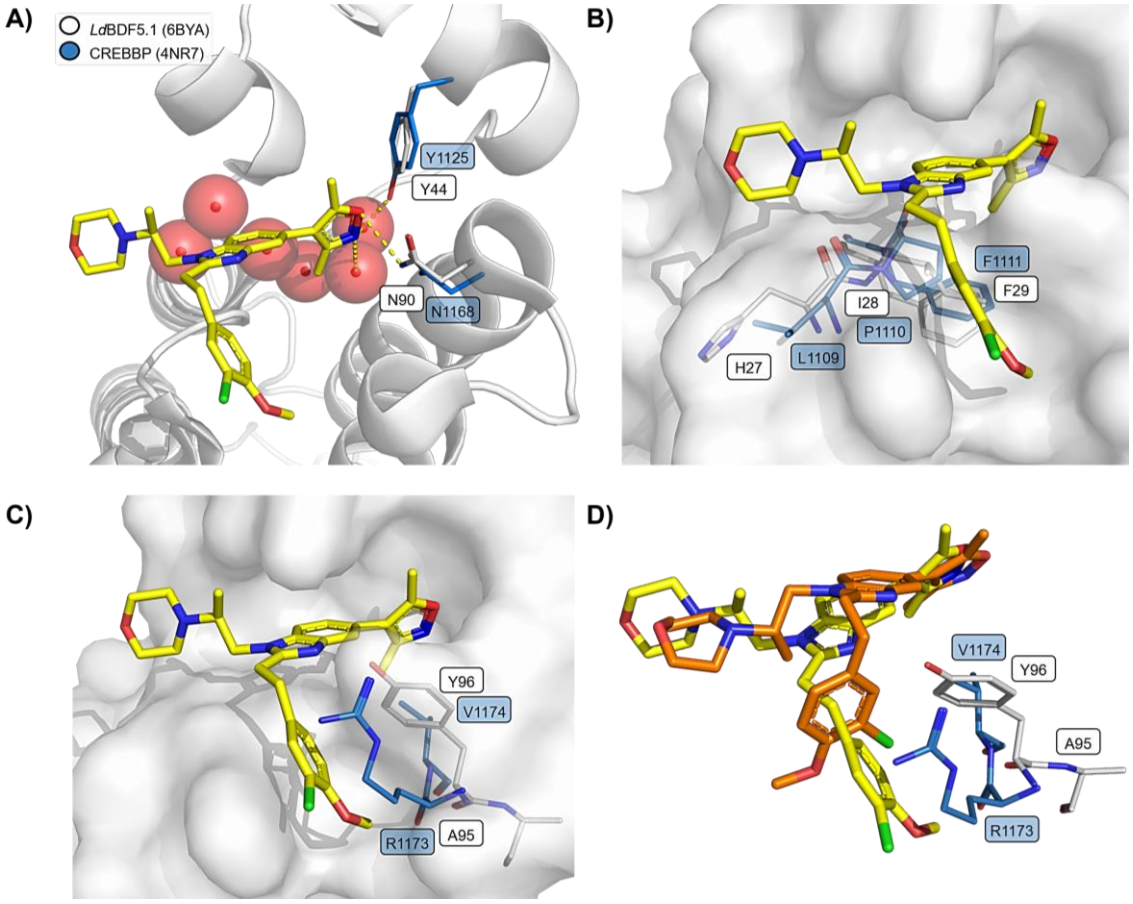

Figure 1.14. The X-ray crystal structure of **SGC-CBP30** (carbon = yellow) in complex with *Ld*BDF5.1 (PDB code 6BYA).[131] **A)** A view of the X-ray crystal structure of **SGC-CBP30** (carbon = yellow) in complex with *Ld*BDF5.1 (cartoon and carbon = white, PDB code 6BYA) overlaid with the X-ray crystal structure of human CREBBP (carbon = blue, PDB code 4NR7).[131, 138] The N and Y residues important for binding KAc/KAc mimics is conserved between the two proteins. **B)** A view of the LPF shelf region of CREBBP (carbon = blue, PDB code 4NR7) and the HIF motif in *Ld*BDF5.1 (carbon = white, PDB code 6BYA). **C)** A view of the structural differences between *Ld*BDF5.1 and CREBBP. The R1173 and V1174 residues in CREBBP (carbon = blue, PDB code 4NR7) correspond to A95 and Y96 in *Ld*BDF5.1 (carbon = white, PDB code 6BYA). **D)** The different binding conformations of the **SGC-CBP30** ligand in *Ld*BDF5.1 (ligand carbon = yellow; protein carbon = white, PDB code 6BYA) and the **SGC-CBP30** ligand in CREBBP (ligand carbon = orange; protein carbon = blue, PDB code 4NR7).

The binding mode of **bromosporine** in *Ld*BDF5.2 is very different to its binding mode in human BRD4(1) (Figure 1.15, A). In the crystal structure of **bromosporine** bound to human BRD4(1), the triazole ring acts as a KAc mimic and hydrogen bonds to the conserved asparagine and tyrosine residues (N140 and Y97). The methyl substituent of the core bicyclic ring in **bromosporine** is oriented such that it points into the KAc binding pocket and the sulfonamide-containing side chain projects along the ZA channel. In the co-crystal structure of *Ld*BDF5.2 with **bromosporine** the plane of the triazolopyridazine moiety is almost perpendicular to its orientation in BRD4(1), with the sulfonamide and ethyl carbamate moieties projecting in different directions. The triazole KAc mimicking

motif in **bromosporine** does not form the expected interactions with the N257 and Y201 residues in *Ld*BDF5.2 (equivalent to N140 and Y97 in BRD4(1)). The **bromosporine** ligand appears to form π-stacking interactions with W263 (Figure 1.15, B). Moreover, the *Ld*BDF5.2 crystal structure shows an A and B chain of the bromodomain and two **bromosporine** ligands, which are situated at the interface of two molecules and form interactions with both chains. Therefore, the **bromosporine** ligand may be an artifact of crystal packing.

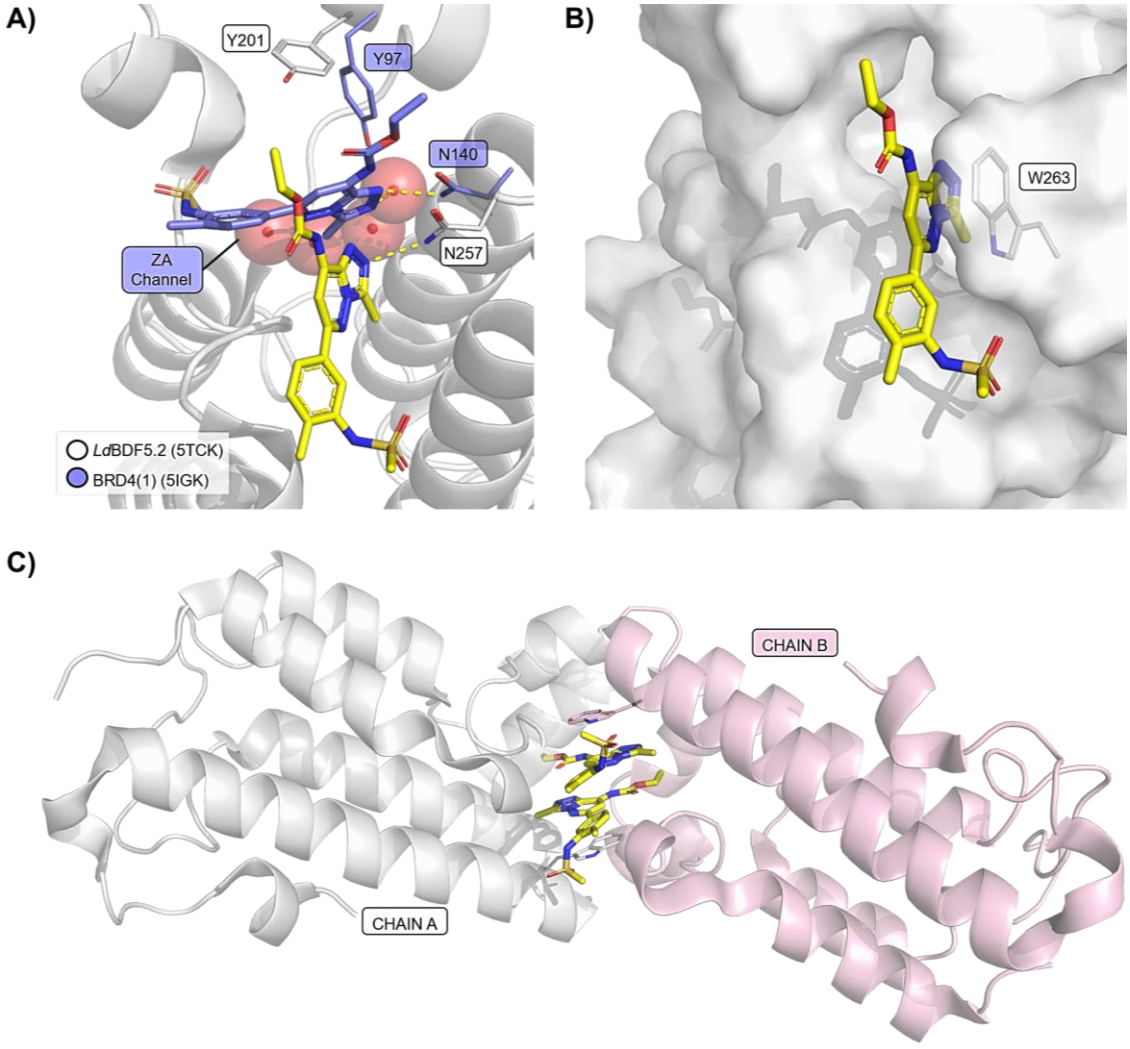

Figure 1.15. The X-ray crystal structure of **bromosporine** (carbon = yellow) in complex with *Ld*BDF5.2 (PDB code 5TCK).[132] **A)** The different binding modes of **bromosporine** in *Ld*BDF5.2 (ligand carbon = yellow; protein carbon = white, PDB code 5TCK) and **bromosporine** in human BRD4(1) (ligand carbon = purple; protein carbon = purple, PDB code 5IGK).[132, 144] The N257 and Y201 residues in *Ld*BDF5.2 are not well aligned to N140 and Y97 in BRD4(1). The triazole KAc mimic in **bromosporine** does not bind as expected in *Ld*BDF5.2. **B)** A view of **bromosporine** (carbon = yellow) in complex with *Ld*BDF5.2 (carbon = white, PDB code 5TCK). The ligand appears to form π-stacking interactions with W263. **C)** A view of the X-ray crystal structure of *Ld*BDF5.2 showing the A and B chains of the bromodomain with two **bromosporine** ligands (carbon = yellow) bound at the interface (PDB code 5TCK).

1.4 Project aims

There remains an unmet medical need to develop new therapeutic agents with novel modes of action for the treatment of leishmaniasis, and drug discovery efforts have been hampered by the lack of well-validated molecular drug targets. *Leishmania* parasites have complex lifecycles, adopting a range of phenotypes to survive in multiple hosts. Epigenetic processes link genotype to phenotypic diversity in a population and therefore must play a crucial role in regulating the *Leishmania* lifecycle. Inducible gene deletion has shown that BDF5 in *Leishmania* is essential for parasite survival in its two main lifecycle stages: the promastigote and the amastigote, demonstrating it as a suitable target for the disruption of epigenetic processes.[61] The traction that bromodomain inhibitors have gained in cancer research, the discoveries of small molecule bromodomain ligands for other parasitic protozoa, in conjunction with the recent genetic target validation of *Leishmania* BDF5, provide strong rationale for the investigation of BDF5 as a drug target.

The overarching aim of this thesis was to chemically validate *Ld*BDF5 as a therapeutic target against *Leishmania*. Chemical validation of *Ld*BDF5 required the development of high affinity, potent, and selective ligands for the target. The strategy to achieve this goal was as follows:

- Conduct fragment-based screening to identify hit compounds for the bromodomains (BDF5.1 and BDF5.2) in *Ld*BDF5 (Chapter 2).
- Optimise hits into high affinity compounds through analysis of the structure activity relationship (SAR) (Chapter 3).
- Evaluate high affinity compounds in the *Leishmania* parasite to provide insight into the phenotypic effect of BDF5 inhibition (Chapter 4).
- Demonstrate target engagement in the parasite.

The validation of BDF5 as a viable therapeutic target in *Leishmania* will provide valuable information for future drug discovery efforts for combating leishmaniasis.

1.5 Biophysical Assays – a brief introduction

A crucial component of any successful target-based ligand discovery programme is the establishment of robust biophysical assays to evaluate the binding interactions between ligands and the target of interest. High-throughput screening of ligands against a target protein is widely used in the early stages of drug discovery to identify initial hits.[145] Qualitative assays can be employed to rapidly identify weakly binding compounds with the potential to be optimised into higher affinity ligands. More accurate quantitative assays are typically used in the later stages of drug discovery projects to obtain precise binding affinity data on a smaller number of ligands, due to the lower throughput and/or high sample consumption of these assays.[146] The methods discussed here include techniques suitable for fragment screening (waterLOGSY and thermal shift), and quantitative techniques suitable for the characterisation of higher affinity ligands (microscale thermophoresis and isothermal calorimetry). Although assays involving these techniques are widely applicable to multiple targets, optimisation is required to ensure that the assay is as sensitive as is required for the target of interest.

1.5.1 WaterLOGSY

Water-ligand observed *via* gradient spectroscopy (waterLOGSY) is a nuclear magnetic resonance (NMR)-based assay that relies on intermolecular nuclear Overhauser effect (NOE) and spin diffusion to transfer magnetisation from excited bulk water molecules to the ligand.[147] This occurs either directly from water protons to ligands, or indirectly through the initial transfer of magnetisation to protons at a protein surface, which is then relayed onto a protein-bound ligand (Figure 1.16).[148, 149] The interaction of a bound ligand with water is either through water–ligand–protein or protein–ligand complexes, both of which have a slow tumbling regime and result in a negative NOE. Unbound ligands interact directly with bulk water molecules and experience much faster tumbling in solution, resulting in a positive NOE. A comparison of the ligand signals in the absence and presence of a protein receptor indicates whether ligand binding has occurred, with a difference in signal intensity being suggestive of binding.

WaterLOGSY is a sensitive technique and offers a key advantage in its ability to check compound solubility, which serves as a useful filter to exclude compounds that aggregate in solution. Aggregation of small molecules causes a false positive response in the waterLOGSY experiment because the aggregate adopts the tumbling behaviour of a macromolecular species and thus gives waterLOGSY responses as if the ligand were bound. The first step in any waterLOGSY experiment determines whether the ligand aggregates in solution by running an NMR experiment of the ligand in the absence of any protein.[148] One disadvantage of waterLOGSY is that the assay can be relatively low-throughput due to the long acquisition times and slow sample switching of NMR experiments.

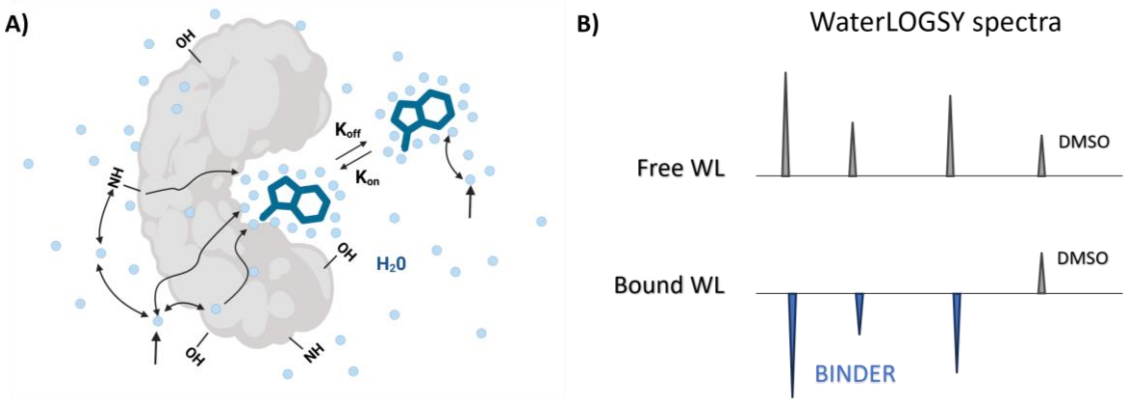

Figure 1.16. A) A diagram illustrating the different mechanisms through which magnetisation is transferred from bulk excited water molecules to bound and unbound ligands. Image adapted from Dalvit *et al.*[148] and created in BioRender.com. **B)** Theoretical WaterLOGSY (WL) spectra, in the absence and in the presence of the protein receptor. The bound WL spectra indicates ligand binding because the compound peaks are inverted relative to DMSO.

1.5.2 Thermal Shift Assay

The thermal shift assay (TSA), also known as differential scanning fluorimetry (DSF), studies the thermal stabilisation of a protein upon ligand binding.[150] The temperature at which a protein unfolds is monitored by a hydrophobic dye in solution, such as SYPRO Orange®. The dye is highly fluorescent in hydrophobic environments but quenched in polar solvents such as aqueous buffer. In the assay, the protein in solution is gradually heated, and it unfolds to expose hydrophobic sites that interact with the dye, leading to an increase in fluorescence. The melting point (T_M) of the protein is determined from the midpoint of the melting curve generated in the experiment (Figure 1.17). Ligand binding

can alter protein stability, resulting in a shift in the melting temperature (ΔT_M). The relationship between binding affinity and the magnitude of the observed temperature shift in TSA is not a simple correlation (i.e. a larger ΔT_M does not necessarily mean tighter binding) and can be complicated by interactions between the ligand and the denatured state of the protein.[151] ΔT_M is also dependent on whether ligand binding is entropically or enthalpically driven.[152] Consequently, TSA provides a source of qualitative information on ligand binding rather than a fully quantitative measurement of binding affinity. The advantage of this assay is that it is high-throughput, allowing a large number of compounds to be screened in parallel.

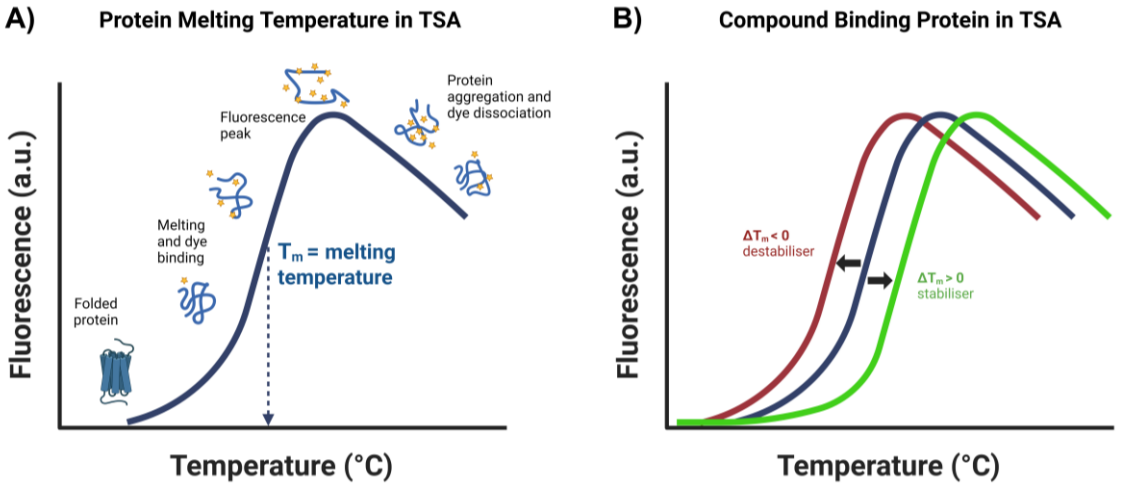

Figure 1.17. **A)** Schematic representation of fluorescence intensity versus temperature for the unfolding of protein in the presence of SYPRO Orange® dye for the TSA. The fluorescence of the dye is quenched in buffer but increases as the protein unfolds and hydrophobic surfaces are exposed. Fluorescence intensity decreases again as the protein aggregates and hydrophobic patches become inaccessible for the dye to bind. The midpoint of the melting curve, which is also the inflection point of the sigmoidal curve, defines the melting temperature (T_M) of the denaturation process. **B)** A representation of compounds binding and changing the T_M of the protein. Images were created with Biorender.com.

1.5.3 Microscale thermophoresis

Microscale thermophoresis (MST) is a powerful technique for determining the binding affinity of a ligand for a target protein.[153] The technique is based on thermophoresis: the directed movement of molecules in a microscopic temperature gradient. MST is highly sensitive and enables the measurement of compound affinities in the pM to mM range.[154]

Thermophoresis is monitored by the fluorescence of proteins that are either covalently labelled with a fluorophore or intrinsically fluorescent.[154] In the MST assay, the fluorescent protein is mixed with a concentration range of the ligand, and the solution is

loaded into capillaries (Figure 1.18). A temperature gradient is applied to samples in the capillaries using an infrared (IR) laser, and the movement of the fluorescent molecules in the temperature gradient is detected and recorded. The interaction of a ligand with the fluorescent protein will alter the molecular properties of the protein, such as charge, size, and hydration shell, leading to a change in movement behaviour. The effect of different concentrations of the ligand on the movement of the fluorescent protein in MST are quantified to determine binding affinity.[155] The MST assay is generally high-throughput and requires low sample consumption of the protein and ligand, however the cost of consumables for this assay can be prohibitive for screening large libraries of compounds.

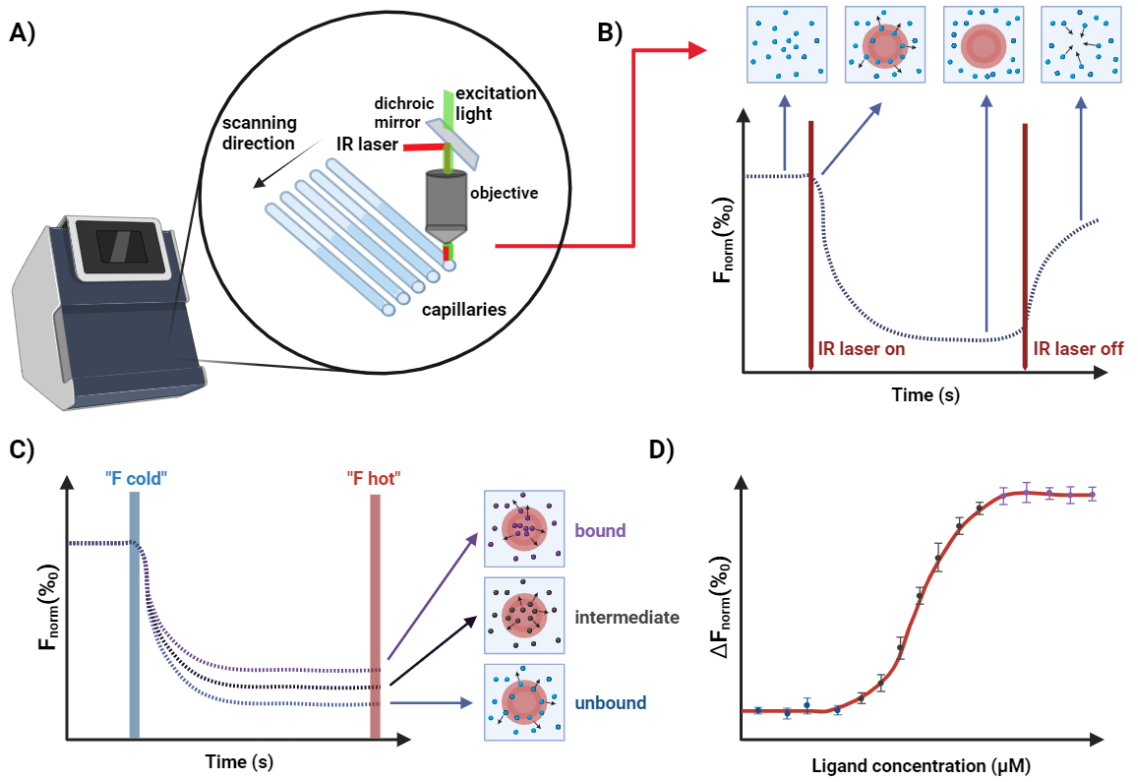

Figure 1.18. A) Overview of an MST apparatus. A tray in the Monolith NT.115 machine is loaded with capillaries and MST is measured in the capillaries. The fluorescence within the capillary is excited and detected through the same objective. A focused IR-laser is used to locally heat a defined sample volume. Thermophoresis of fluorescent molecules through the temperature gradient is detected. **B)** The typical signal from an MST experiment. Initially, the molecules are homogeneously distributed, and a constant "initial fluorescence" is detected. Within the first second after activation of the IR laser, the "T-Jump" is observed, which corresponds to a rapid change in fluorophore properties due to the fast temperature change. Subsequently, thermophoretic movement of the fluorescently labelled molecules out of the heated sample volume can be detected. Typically, the fluorescence change is measured for 30 s. After deactivation of the IR-Laser, an inverse T-Jump occurs, followed by the "back-diffusion" of molecules, which is solely driven by mass diffusion. **C)** A typical binding experiment readout. The thermophoretic movement of a fluorescent protein (blue trace; "unbound") changes upon binding to a non-fluorescent ligand (purple trace; "bound"), resulting in different traces. **D)** For analysis, the change in thermophoresis is expressed as the change in the normalised fluorescence (ΔF_{norm}), which is defined as F_{hot}/F_{cold} (F-values correspond to average fluorescence values between defined areas marked by the red and blue areas in plot C, respectively). Titration of the ligand results in a gradual change in thermophoresis, which is plotted as ΔF_{norm}, to yield a binding curve, which can be fitted to derive the binding affinity. Image adapted from Jerabek-Willemsen *et al.*[154] Created in Biorender.com.

1.5.4 Isothermal calorimetry

Isothermal titration calorimetry (ITC) is a quantitative technique used to establish the thermodynamic properties of small molecule interactions with a protein.[156, 157] ITC can determine the binding equilibrium constant K_d, the enthalpy ΔH, the Gibbs energy ΔG, and the molarity of binding. It is a direct thermodynamic measurement of the interaction between a ligand and protein that works by detecting the heat changes upon ligand binding by measuring the power required to keep a sample cell at the same temperature as a reference cell (Figure 1.19).[158] ITC is suitable for detecting medium to high affinity interactions (K_d values from around 1 nM to 100 µM), hence the technique is typically used to determine the K_d of an interaction previously identified in a high-throughput screening assay. One of the drawbacks of this assay is that high protein concentrations and volumes are required for weaker interactions (in the micromolar range), making it less suited to early stage fragment screening where binding affinities are typically lower.

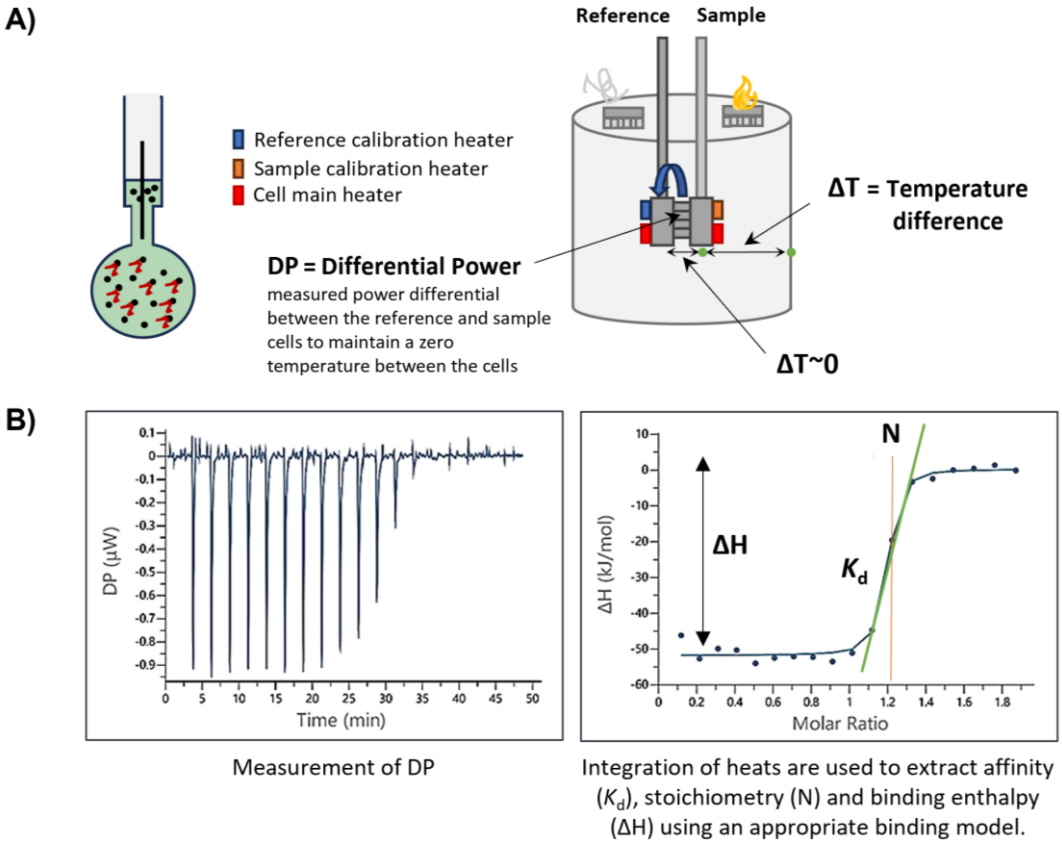

Figure 1.19. A) Instrumentation of the typical isothermal titration calorimetry and representative model showing how ITC works. **B)** The resulting change of the thermal power released by the calorimeter, needed to keep the difference of temperature between the sample cell and the reference cell constant, is represented as a deviation of the baseline in the produced raw data. The peak integration of the power input can be plotted against the titration molar ratio to enable the determination of the thermodynamic parameters including the stoichiometry of the interaction (N), affinity constant (K_d), and change in enthalpy (ΔH).

Chapter 2- Fragment-based screening

2.1 Introduction and aims

Chemically validating *Ld*BDF5 as a target for antileishmanial drug discovery requires the development of high affinity ligands for its bromodomains. The initial aim of this project was to synthesise a small library of compounds containing a diverse range of KAc mimics, which have previously been employed in human bromodomain ligands, and screen them against the two bromodomains in *Ld*BDF5. The identification of KAc mimics that bind to *Ld*BDF5 bromodomains may provide a starting point for the further development of the fragments into high-affinity ligands.

Therefore, the aims of the work described in this chapter were as follows:

- Synthesise a fragment library of compounds encompassing motifs that are known to act as KAc mimics in human bromodomain ligands.
- Express and purify recombinant *Ld*BDF5.1 and *Ld*BDF5.2 proteins on an appropriate scale for fragment screening.
- Assess the binding of KAc mimics to the *Ld*BDF5 proteins using biophysical assays to determine the bromodomain ligandability.

2.2 Library design and synthesis

To identify new ligands for the *Ld*BDF5 bromodomains, a fragment-based screening approach was adopted (Figure 2.1).[159] Fragment-based screening enables efficient exploration of a broad chemical space through assessing a structurally diverse library of small fragments for binding affinity. The compounds in a fragment screen typically have a molecular mass of <300 Da and consequently low binding affinity to their target proteins. The fragments that bind will likely form a small number of high-quality binding interactions with the target. Initial hits from fragment-based screens provide starting points for subsequent chemical optimisation and structure-activity relationship (SAR) studies. In the process of fragment-based drug discovery (FBDD), the fragments are elaborated to generate larger molecules with improved affinity or potency.

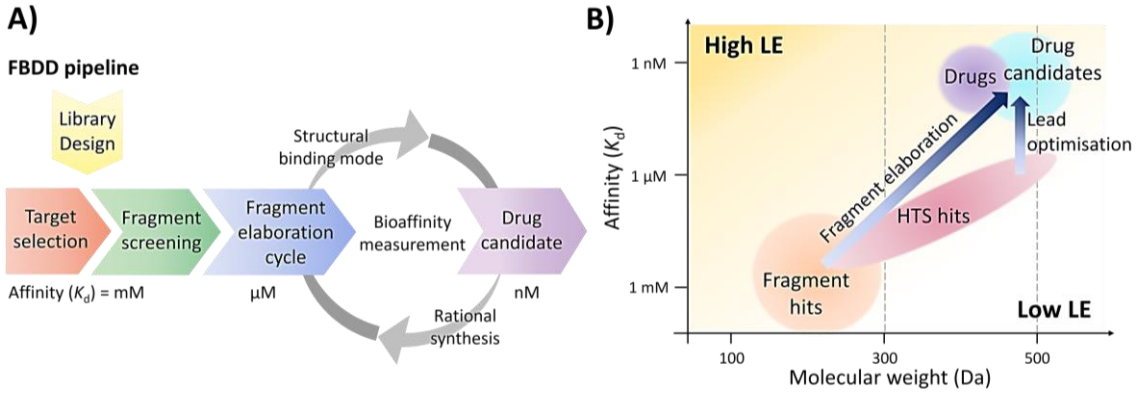

Figure 2.1. A) The general workflow of FBDD. Validated fragments are taken through to a lead series. Iterative cycle of design, binding mode determination, and affinity measurement incrementally improve affinity and physicochemical properties to deliver drug candidates; **B)** A comparison of molecular mass *vs* the affinity of leads developed from conventional high-throughput screening (HTS) and FBDD approaches. Images adapted with permission from Scott *et al.*, *Biochemistry*, **2012**, *51* (25), 4990–5003. Copyright 2012, American Chemical Society.[159]

Extensive structural studies on the human BCPs have identified the residues that are important for its interactions with KAc residues in target proteins, in particular an asparagine and tyrosine. In human BRD4(1), these residues are Y97 and N140; N140 forms a hydrogen bond directly with KAc, while Y97 interacts with KAc through a water-mediated hydrogen bond.[10, 26] The primary sequences of *Ld*BDF5.1 and *Ld*BDF5.2 indicate that both of these bromodomains possess equivalent residues to Y97 and N140, [Y44 & N90 in *Ld*BDF5.1 and Y257 & N201 in *Ld*BDF5.2, (Figure 2.2)], indicating that they are canonical bromodomains and that they can bind to KAc.

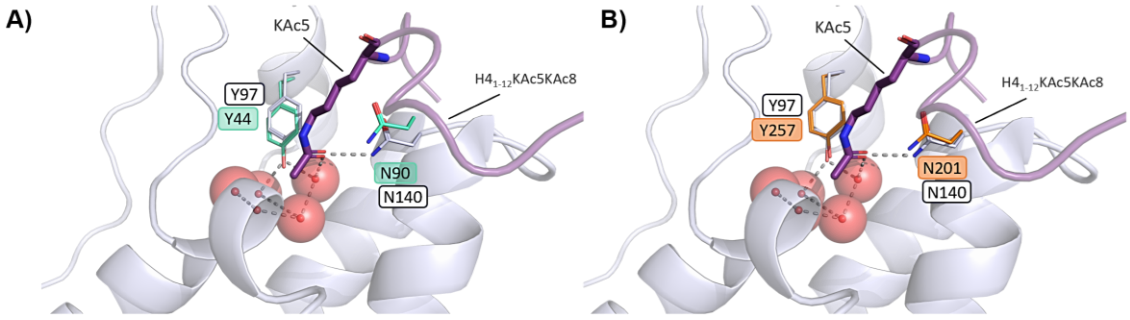

C)

```
                LdBDF5.1        6BYA_1|Chains   MHHHHHHSSGRENLYFQ----------------------GYNEADVAALVRSL-------
                LdBDF5.2        8BPT_1|Chains   AAA-----------------------------------PPSTREMVQLVDSL-------
I)              CERC2           3NXB_1|Chains   SMREEKKTKDLFEL------------------------DDDFTAMYKVLDVV-------
II)             BRD4(1)         3ZYU_1|Chains   SMNPPPPETSNPNKPKRQT-------------------NQLQYLLRVVLKTL-------
III)            CBP             4NYX_1|Chain    SMRKKIFKP-----------------------------EELRQALMPTLEAL-------
IV)             BRD9            4UIU_1|Chain    GAENES--------------------------------TPIQQLLEHFLRQL-------
V)              BAZ2A           4QBM_1|Chains   SMH-----------------------------------SDLTFCEIILMEM--------
VI)             MLL1            3LQH_1|Chain    SGNFCPLCDKCYDDDDYESKMMQCGKCDRWVHSKCENLSDEMYEILSNLPESVAYTCVNC
VII)            TAF1(2)         6DF7_1|Chains   MHHHHHHASDYKDDDDKGSLVPRGSPLLD----------DDDQVAFSFILDNI-------
VIII)           PB1(5)          5FH8_1|Chains   SMSGISPKKSKYMTPMQQKL------------------NEVYEAVKNYTDKR-------
VIII)           PB1(5)          5FH8_1|Chains   RDLEGD---------------------------

                LdBDF5.1        6BYA_1|Chains   -DRAE-----DHHIFAVD---------VLETYPYLAESYTKVCP----RRCDLATAAQKA
                LdBDF5.2        8BPT_1|Chains   -NRRE-----DGGAFSVD---------VAEAYPDLRDSYRKICP----RPMNLILMRQRA
I)              CERC2           3NXB_1|Chains   -KAHK-----DSWPFLEP---------VDESY--APN-YYQIIK----APMDISSMEKKL
II)             BRD4(1)         3ZYU_1|Chains   -WKHQ-----FAWPFQQP---------VDAVKLNLPD-YYKIIK----TPMDMGTIKKRL
III)            CBP             4NYX_1|Chain    -YRQD----PESLPFRQP---------VDPQLLGIPD-YFDIVK----NPMDLSTIKRKL
IV)             BRD9            4UIU_1|Chain    -QRKD----PHGF-FAFP---------VTDAI--APG-YSMIIK----HPMDFGTMKDKI
V)              BAZ2A           4QBM_1|Chains   -ESHD-----AAWPFLEP---------VNPRL--VSG-YRRIIK----NPMDFSTMRERL
VI)             MLL1            3LQH_1|Chain    TERHP-----AEWRLALEKELQISLKQVLTALLNSRT-TSHLLRYRQQQPLDLEGVKRKM
VII)            TAF1(2)         6DF7_1|Chains   -VTQKMMAVPDSWPFHHP---------VNKKF--VPD-YYKVIV----NPMDLETIRKNI
VIII)           PB1(5)          5FH8_1|Chains   -GRRL-----SAIFLRLP---------SRSEL---PD-YYLTIK----KPMDMEKIRSHM
                                                                :                        ::      .

                LdBDF5.1        6BYA_1|Chains   LEGAYSYD----------LRLEGLKADIALMASNCVAYNGPTSAYAETAAKFERYALEQI
                LdBDF5.2        8BPT_1|Chains   KEGYYTSGSATVYGDTVAASLTRLREDIELLVRNCITFNVKVESWVTLARSFQAFAHRRV
I)              CERC2           3NXB_1|Chains   NGGLY-------------CTKEEFVNDMKTMFRNCRKYNGESSEYTKMSDNLERCFHRAM
II)             BRD4(1)         3ZYU_1|Chains   ENNYY-------------WNAQECIQDFNTMFTNCYIYNKPGDDIVLMAEALEKLFLQKI
III)            CBP             4NYX_1|Chain    DTGQY-------------QEPWQYVDDVWLMFNNAWLYNRKTSRVYKFCSKLAEVFEQEI
IV)             BRD9            4UIU_1|Chain    VANEY-------------KSVTEFKADFKLMCDNAMTYNRPDTVYYKLAKKILHAGFKMM
V)              BAZ2A           4QBM_1|Chains   LRGGY-------------TSSEEFAADALLVFDNCQTFNEDDSEVGKAGHIMRRFFESRW
VI)             MLL1            3LQH_1|Chain    DQGNY-------------TSVLEFSDDIVKIIQAAINSDGGQPEIKKANSMVKSFFIRQM
VII)            TAF1(2)         6DF7_1|Chains   SKHKY-------------QSRESFLDDVNLILANSVKYNGPESQYTKTAQEIVNVCYQTL
VIII)           PB1(5)          5FH8_1|Chains   MANKY-------------QDIDSMVEDFVMMFNNACTYNEPESLIYKDALVLHKVLLETR
                                                      *                    *   :   .   :           .

                LdBDF5.1        6BYA_1|Chains   DAFVLEHNG-------GC----------------
                LdBDF5.2        8BPT_1|Chains   DDFVLRHAAFLRGTTMGAEVYE-------------
I)              CERC2           3NXB_1|Chains   MKH-----------------------------
II)             BRD4(1)         3ZYU_1|Chains   NELPTEE--------------------------
III)            CBP             4NYX_1|Chain    DPVMQSLG-----------------------
IV)             BRD9            4UIU_1|Chain    S------------------------------
V)              BAZ2A           4QBM_1|Chains   EEFYQ----------------------------
VI)             MLL1            3LQH_1|Chain    ERVFPWFSVKKSRFWEPNKVSS-----------
VII)            TAF1(2)         6DF7_1|Chains   TEYDEHLTQLEKDICTAKEAALEEAELESLDPMT
```

COLOUR	RESIDUE	PROPERTY
RED	AVFPMILW	Small (small + hydrophobic (incl. aromatic -Y))
BLUE	DE	Acidic
PINK	RK	Basic - H
GREEN	STYHCNGQ	Hydroxyl + sulfhydryl + amine + G

Figure 2.2. A) Overlaid X-ray crystal structures of *Ld*BDF5.1 (PDB code 6BYA, carbon = teal) with the diacetylated histone H4-mimicking peptide H4$_{1-12}$KAc5KAc8 (PDB code 3UVW, carbon = purple) bound to BRD4(1) (carbon = white), showing the conserved Y and N residues that are important for interactions with KAc. **B)** Overlaid X-ray crystal structures of *Ld*BDF5.2 (PDB code 8BPT, carbon = orange) with the diacetylated histone H4-mimicking peptide H4$_{1-12}$KAc5KAc8 (PDB code 3UVW, carbon = purple) bound to BRD4(1) (carbon = white), showing the conserved Y and N residues that are important for interactions with KAc. **C)** Multiple sequence alignment of *Ld*BDF5.1, *Ld*BDF5.2 and individual representatives of all 8 bromodomain families (labelled I-VIII). Multiple sequence alignment was carried out using MUSCLE[160] and the amino acid sequences of *Ld*BDF5.1 (Uniprot ID: A0A3Q8I8I6), *Ld*BDF5.2 (Uniprot: A0A3Q8I8I6), CERC2 (Uniprot: Q9BXF3), BRD4(1) (Uniprot: O60885), CBP (Uniprot: Q92793), BRD9 (Uniprot: Q9H8M2), BAZ2A (Uniprot: Q9UIF9), MLL1 (Uniprot: Q03164), TAF1(2) (Uniprot: U3KMH2), PB1(5) (Uniprot: Q86U86). Highlighted in yellow are the conserved tyrosine and asparagine residues in canonical bromodomains. An * (asterisk) indicates positions which have a single, fully

conserved residue. A : (colon) indicates conservation between groups of strongly similar properties. A . (period) indicates conservation between groups of weakly similar properties.

Chemical probes have been developed for multiple subfamilies of human bromodomains and they have been used to understand the role of these proteins as well as validate them as drug targets.[17, 26, 31, 32, 34, 161-163] Additionally, these chemical probes have been applied to investigate the functions of non-human bromodomains, including those in parasites such as *Trypanosoma* spp., *Plasmodium falciparum*, and *Schistosoma mansoni*.[56, 57, 64, 164] Despite these tool compounds not being optimised for parasite bromodomains, their binding and activity indicate that they are promising starting points for subsequent chemical optimisation into potent and selective compounds for parasite bromodomains. Given the bromodomains in *Ld*BDF5 are canonical, it was proposed that KAc mimics that have been employed in the development of human bromodomain ligands could be used as starting points in the development of ligands for the *Leishmania* bromodomains. A fragment-growing approach would be used to optimise the interactions of any KAc mimicking fragments that bind *Ld*BDF5 to develop higher affinity ligands. Building out from the conserved KAc binding residues could also help achieve selectivity of our ligands for the parasite bromodomain, over its human counterparts.

To investigate this idea, a small library of thirty-one compounds, encompassing motifs that are known to act as KAc mimics in human bromodomain ligands, was designed and synthesised (Figure 2.3). The fragment library consisted of the following molecules: triazole-fused heterocycles (compounds **2**, **3**, **4**, **5**, and **6**), which are KAc mimics based on the pan-bromodomain inhibitors **(+)-JQ1** and **bromosporine**; a selection of 5-amino-4-chloro-2-methylpyridazin-3(2*H*)-one derivatives (compounds **7**, **8**, **9**, **10**, and **11**), which have been used as the basis to develop P300/CBP-associated factor (PCAF) and General control non-depressible 5 (GCN5) bromodomain ligands; and compounds featuring the 3,5-dimethylisoxazole KAc bioisostere that is found in several potent bromodomain and extra-terminal domain (BET) bromodomain ligands, such as **I-BET151** and **OXFBD02** (compounds **12**, **13**, **14**, **15**, **16**, **17**, **18**, **19**, **20**, and **21**).[20, 36, 135, 139, 140, 165, 166] Benzo-fused isoxazoles were included (compounds **22** and **23**), alongside dihydroquinoxalinone fragments and related chemotypes found in CREB-binding protein (CREBBP) ligands, such as **(-)-OXFBD05** (compounds **24**, **25**, **26**, and **27**).[50, 142, 167-169] Benzimidazole motifs, which feature in a series of inhibitors selective for the bromodomain and PHD finger containing (BRPF1) bromodomain, and ligands which

bind to the tripartite motif (TRIM) bromodomains, were screened (compounds **28**, **29**, and **30**). A couple of other compounds that are structurally similar to fragments that are known to occupy KAc binding sites were also added to the library (compounds **31** and **32**).

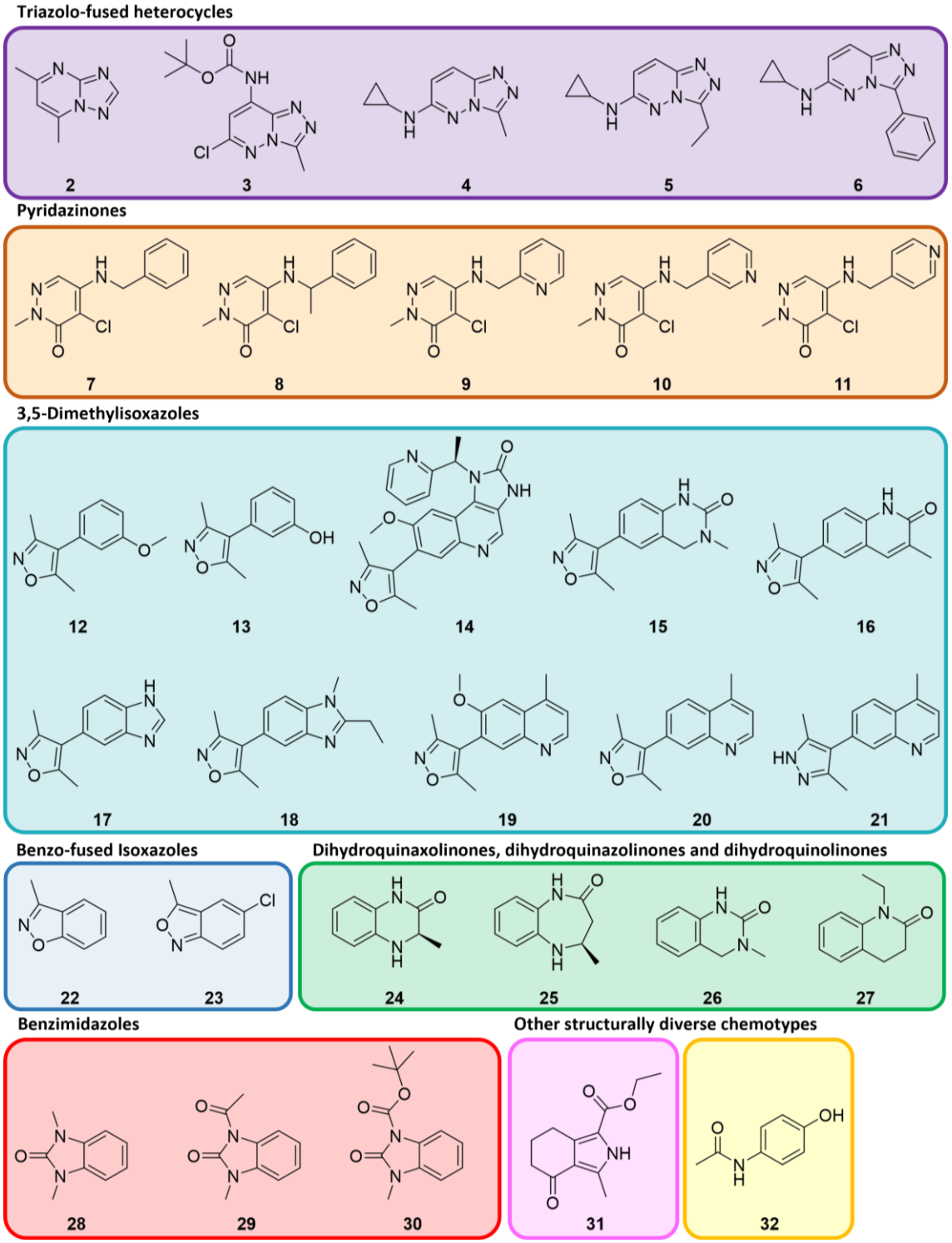

Figure 2.3. Fragment library of the thirty-one compounds (MW: 133-284 Da) encompassing motifs that are known to act as KAc mimics in human bromodomain ligands. Compound **14** (MW of 415 Da) is a human bromodomain ligand that was included in the library screening.[20, 36, 46, 50, 69, 139, 140, 142, 167, 168, 170-174]

2.2.1 Triazolo-fused heterocycles

Triazole-fused heterocycles are motifs commonly found in ligands for human bromodomains (Figure 2.4).[170] The potent and selective BET family inhibitor **(+)-JQ1** features a triazole ring.[20] Within the BET bromodomain KAc binding sites, this triazole ring forms key hydrogen bonding interactions with the highly conserved asparagine in the KAc binding pocket [N140 in BRD4(1) and N429 in BRD2(2); Figure 2.5]. Like most BET bromodomain inhibitors, **(+)-JQ1** has a methyl group adjacent to the hydrogen bond acceptor *N*-1, which mimics the acetyl group of acetyl lysine (Figure 2.5, D). There are two regions that have been found to be particularly valuable in enhancing inhibitor potency and selectivity for the BET proteins: the WPF shelf (a conserved tryptophan-proline-phenylalanine motif) and the ZA channel.[175] The selectivity of **(+)-JQ1** for the BETs has been attributed to the 4-chlorophenyl moiety, which forms hydrophobic interactions with residues on the edge of the acetyl-lysine binding pocket, including W81 of the WPF shelf (Figure 2.5, B).[20] **Bromosporine** is a structurally related but more promiscuous bromodomain inhibitor than **(+)-JQ1** that interacts with both BET and non-BET bromodomains, including CERC2, BRD9, and TAF1L(2).[135] The triazole forms interactions with conserved asparagine residues (N100 in BRD9, N140 in BRD4(1) and N1602 in TAF1L(2)), while the sulfonamide interacts with the ZA channel.

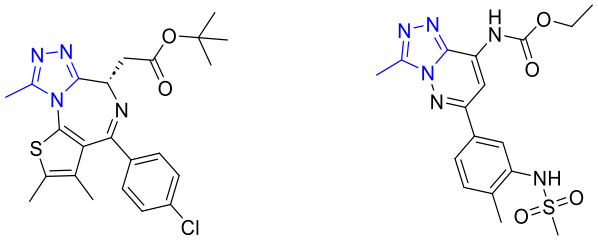

Figure 2.4. Structures of human bromodomain ligands: **(+)-JQ1** and **Bromosporine**.[20, 135] Highlighted in blue are the KAc mimicking motifs.

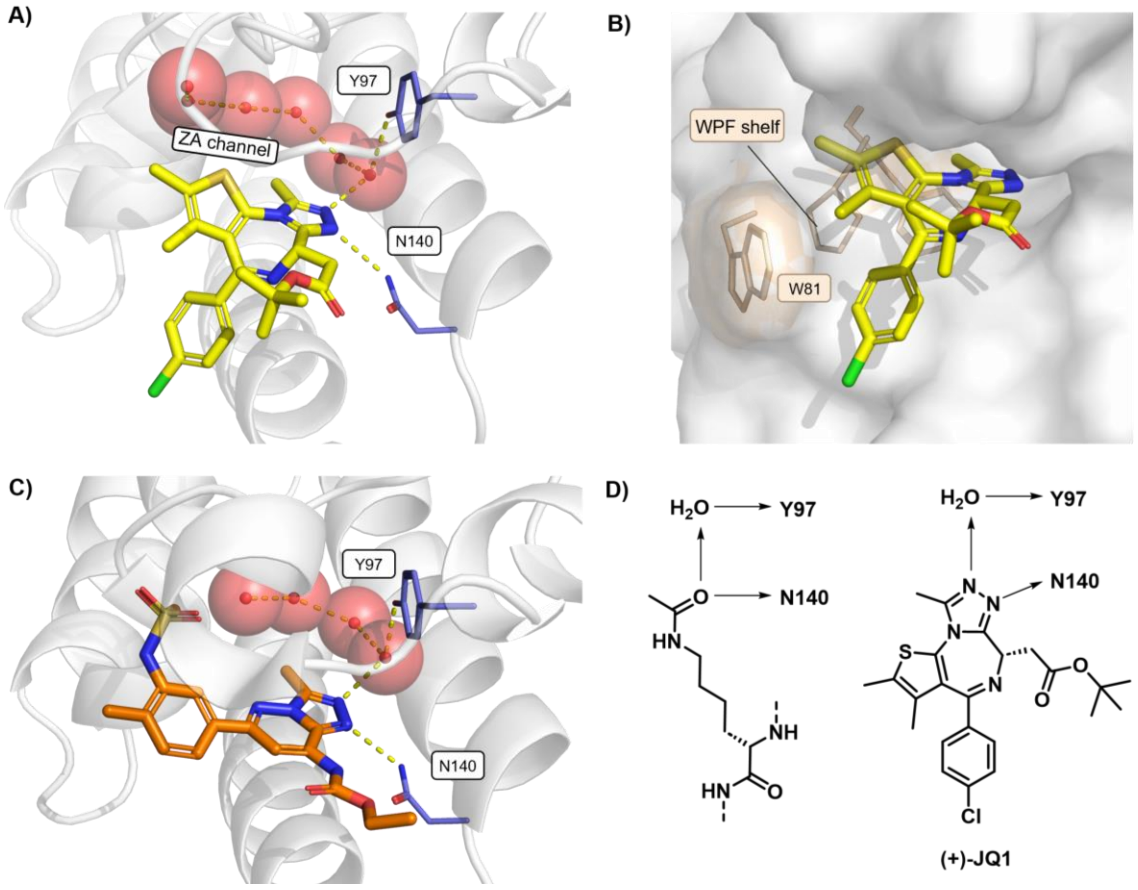

Figure 2.5. A) A view of **(+)-JQ1** (carbon = yellow) bound to BRD4(1) (carbon = purple, PDB code: 3MXF).[176] The triazole of **(+)-JQ1** forms a hydrogen bond with residues N140 and Y97 (through a bridged water molecule); **B)** The 4-chlorophenyl moiety of **(+)-JQ1** forms hydrophobic interactions with W81 of the WPF shelf in BRD4(1); **C)** A view of **bromosporine** (carbon = orange) bound to BRD4(1) (carbon = purple, PDB code: 6V0U).[177] The triazole of **bromosporine** is hydrogen bonding N140 and Y97 (through a bridged water molecule); **D)** The triazole of **(+)-JQ1** is a KAc mimic and forms equivalent hydrogen bonding interactions to those made by KAc in the binding site of BRD4(1).

Thus, fragments containing triazolo-fused heterocycles were included in the library of KAc mimics. The triazolopyrimidine **2** was prepared in high yield (96%) *via* condensation of 1*H*-1,2,4-triazol-5-amine **33** with acetylacetone (Scheme 2.1).

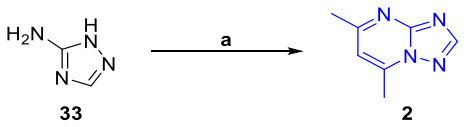

Scheme 2.1. Synthesis of **2**. *Reagents and conditions:* **a)** Pentane-2,4-dione, acetic acid, reflux, 3 h, 96%.

The triazolopyridazine fragment **3** was synthesised in three steps from the commercially available 3,6-dichloropyridazin-4-amine **34**. First, 3,6-dichloropyridazin-4-amine **34** was heated under reflux with hydrazine monohydrate to afford **35** in a 39% yield. The

triazolopyridazine group was then formed in an acetic acid-mediated ring closure, followed by Boc protection of the amine **36** to give **3** (Scheme 2.2).

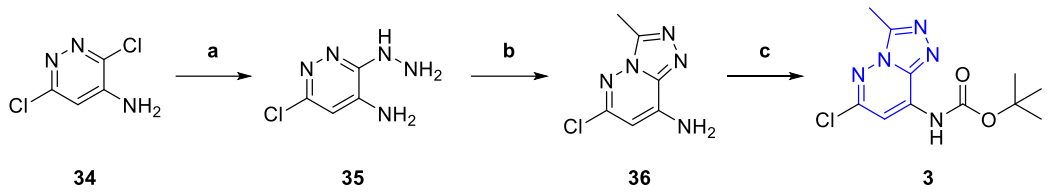

Scheme 2.2. Synthesis of **3**. *Reagents and conditions:* **a)** Hydrazine monohydrate, reflux, 4 h, 39%; **b)** Acetic acid, reflux, 7 h, 71%; **c)** di-*tert*-Butyl dicarbonate anhydride, 4-DMAP, pyridine, THF, rt, 24 h, 30%.

Compounds **4**, **5**, and **6** were synthesised from 3-chloro-6-hydrazineylpyridazine **37** (Scheme 2.3). Compound **37** was reacted with an equimolar amount of the appropriate aldehyde and heated under reflux in ethanol to afford the intermediates **38** and **39**. Intramolecular oxidative cyclisation of **38** or **39** with iodobenzene diacetate (IBD) in dichloromethane at room temperature provided compounds **40** and **41**. These compounds were subsequently reacted in neat cyclopropylamine to give the desired compounds **4** and **5**, respectively. To synthesise **6**, the intermediate **42** was formed *via* oxidative cyclisation using manganese dioxide, then compound **42** was heated under reflux in cyclopropylamine to afford **6**.

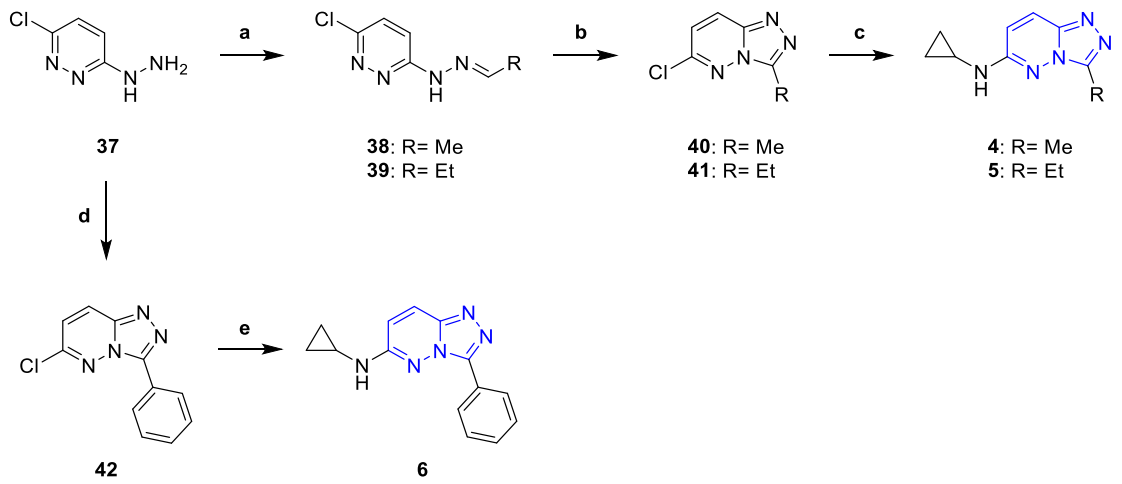

Scheme 2.3. Synthesis of **4** and **5**. *Reagents and conditions*: **a)** EtOH, acetaldehyde/propionaldehyde, reflux, 1-2 h, **38:** 36%, **39:** 48%; **b)** [Bis(acetoxy)iodo]benzene, CH_2Cl_2, rt, 2-3 h, **40:** 80%, **41:** 76%; **c)** Cyclopropylamine, 70 °C, 3.5 h, **4:** 38%, **5:** 100%. Synthesis of **6**. *Reagents and conditions*: **d)** 4-Toluenesulfonic acid, benzaldehyde, MnO_2, toluene, 80 °C, 2 h, 10%; **e)** Cyclopropylamine, 70 °C, 4 h, 58%.

2.2.2 Pyridazinones

Humphreys *et al.* published a pyridazinone-based chemical probe (**GSK4027**) for the PCAF/GCN5 bromodomain with pIC_{50} 7.4 ($IC_{50} = 40$ nM) measured in the PCAF NanoBRET assay (Figure 2.6).[36] The probe was optimised from a non-selective, weakly active pyridazinone hit **43** (pIC_{50} 4.8; $IC_{50} = 12.5$ µM). Hydrogen bonding to the conserved asparagine in the bromodomain (N803 in PCAF/N808 in GCN5) occurs through the carbonyl of **GSK4027**. An additional hydrogen bond forms to a conserved water molecule bound to Y760 in PCAF (Y765 in GCN5).

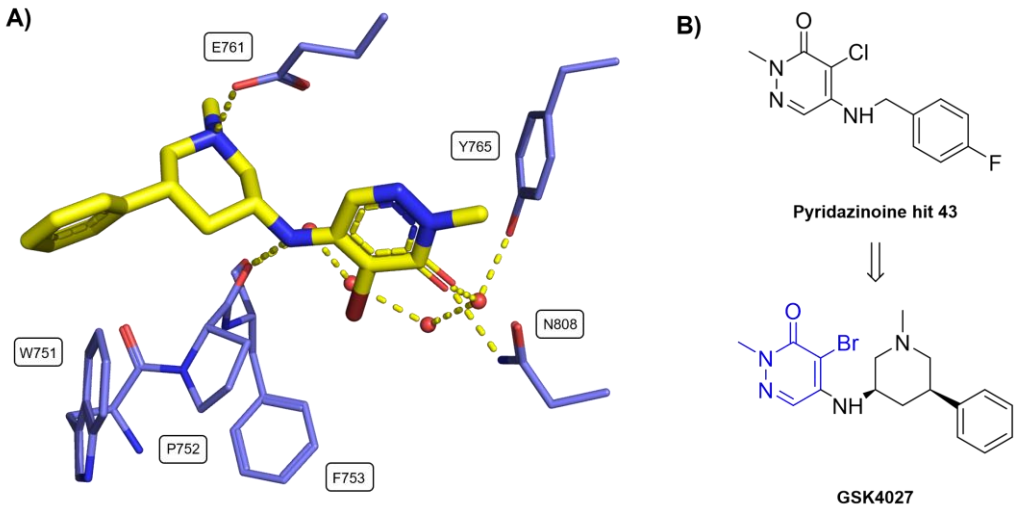

Figure 2.6. A) GSK4027 (carbon = yellow) in complex with GCN5 (carbon = purple, PDB code: 5MLJ).[178] The pyridazinone is acting as a KAc mimic, hydrogen bonding to the conserved N808 and Y765 residues; **B)** Struture of pyridazinone hit compound **43** and the optimised chemical probe **GSK4027** for the PCAF/GCN5 bromodomain.[36]

Five compounds were designed for the fragment library encompassing the pyridazinone KAc mimetic, with variable aromatic groups at the 5-position. Compounds **7-11** were synthetically accessible in one step *via* an S_NAr reaction with the commercially available 4,5-dichloropyridazinone **44** (Scheme 2.4). The methodology was reported to yield a mixture of 4- and 5-positional isomers.[36] However, for all compounds (**7-11**) the S_NAr reaction was regioselective and amines preferentially reacted at the 5-position, likely due to the steric bulk of the amine substituents. Considering the mechanism of the reaction, reaction at the 5-position also delocalises the intermediate anion to the oxygen of the carbonyl, which is a better electron sink than the pyridazinone nitrogen.

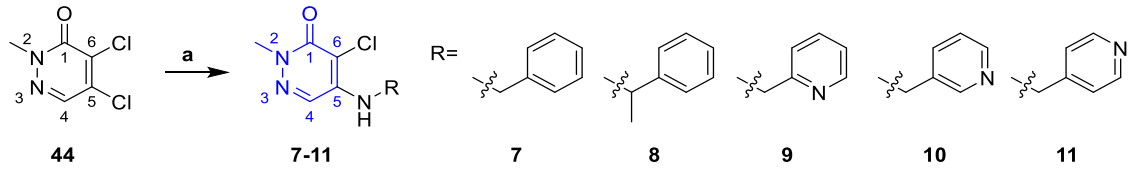

Scheme 2.4. Synthesis of pyridazinones **7-11**. *Reagents and conditions:* **a)** R-NH_2, NMP, 100 °C, 7 h, **7:** 70%, **8:** 50%, **9:** 69%, **10:** 12%, **11:** 24%.

2.2.3 3,5-Dimethylisoxazoles

4-Substituted 3,5-dimethylisoxazoles can act as KAc mimetics and are found in several potent BET bromodomain ligands, such as **OXFBD02** and **I-BET151**, which bind to BRD4(1) and other BET-bromodomains (Figure 2.7).[46, 139] The 3,5-dimethylisoxazole accepts a hydrogen bond from the conserved asparagine residue within the bromodomain binding pocket [N140 in BRD4(1)], which mimics the key interaction made with the carbonyl oxygen of KAc.

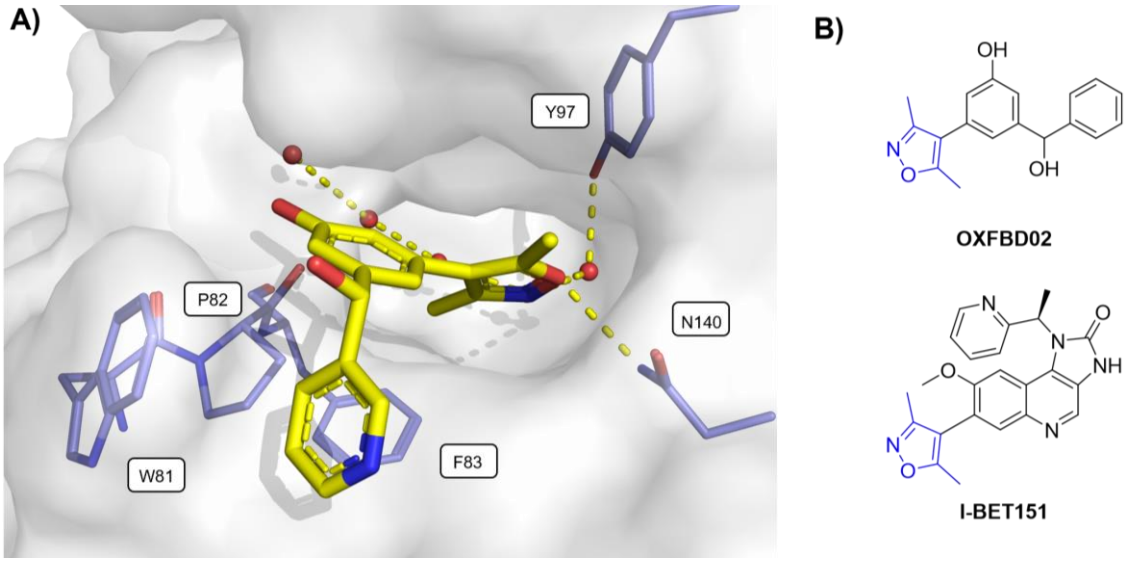

Figure 2.7. A) A view of **OXFBD02** (carbon = yellow) in complex with BRD4(1) (carbon = purple, PDB code: 6FSY).[179] The 3,5-dimethylisoxazole is acting as a KAc lysine mimic, hydrogen bonding to conserved N140 and Y97; **B)** Structures of human bromodomain ligands **OXFBD02** and **I-BET151**. The KAc mimic is highlighted in blue.

Collaborators at GlaxoSmithKline (GSK) performed an Affinity Selection Mass Spectrometry (ASMS) screen with *Ld*BDF5.1 and *Ld*BDF5.2 (a brief description of the assay is provided in the Experimental Section 6.7). Results from the ASMS screen indicate that compounds featuring a 3,5-dimethylisoxazole substituent on a quinoline

core, as found in compounds **45**, **46**, and **47** (Table 2.1), bind *Ld*BDF5.1.[180] The compounds that bound *Ld*BDF5.2 possess different chemotypes: for example, **48** features the benzimidazole core typically found in BRPF1 and TRIM bromodomain inhibitors, while **49** contains a 3-methylpyridinone that features in BET bromodomain inhibitors.[168, 171, 174] To probe the SAR of the two *Ld*BDF5 bromodomains, fragments **12** and **13**, three quinoline-based fragments with either an isoxazole or pyrazole motif at the 7-position (**19-21**), and structures **16** and **50**, which are related to **49** and **51** (Figure 2.8) were synthesised.

Table 2.1. Selected hits from ASMS screen with *L. donovani* bromodomains. Details of the assay are provided in the Experimental Section 6.7. A relative binding affinity percentage (% RBA) is reported for the ligands that are hits. A higher affinity is indicated by a greater % RBA.

Compound	Structure	% RBA	Target
45	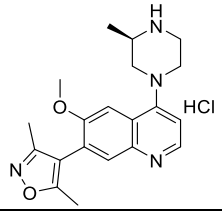	36	*Ld*BDF5.1
46	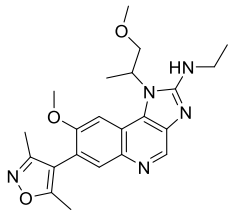	9	*Ld*BDF5.1
47	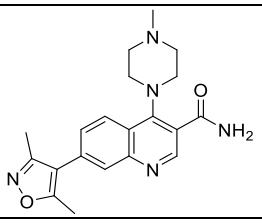	23	*Ld*BDF5.1
51	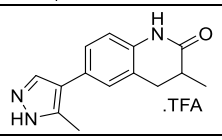	29	*Ld*BDF5.1
48	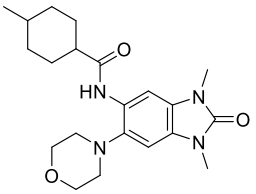	6	*Ld*BDF5.2
49	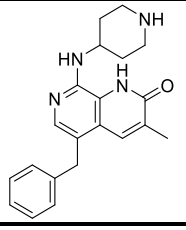	37	*Ld*BDF5.2

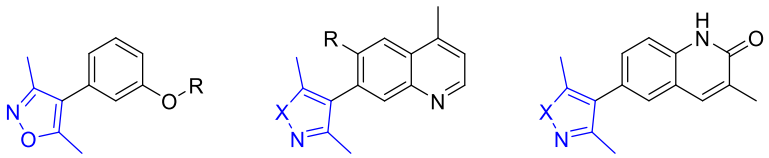

12: R= Me
13: R= H

19: X= O, R= OMe
20: X= O, R= H
21: X= NH, R= H

16: X= O
50: X= NH

Figure 2.8. Structures of compounds **12**, **13**, **19-21**, **16**, and **50** synthesised for the fragment library. The KAc mimic is highlighted in blue.

Suzuki-Miyaura cross-coupling of 3-bromoanisole **52** with trifluoroborate **53** afforded the methoxy substituted compound **12**.[181] It has been reported that direct coupling of aryl bromides with boronic acids can be very low yielding due to rapid hydrodeborylation of the heterocyclic boronic acids.[182] Therefore, the trifluoroborate derivative **53** was employed to ensure efficient coupling with 3-bromoanisole **52**, through slow release of the boronic acid into the reaction.[183] The related phenol derivative **13** was obtained in a subsequent demethylation step using BBr_3 in dichloromethane, based on the method of McOmie, Watts, and West (Scheme 2.5).[184]

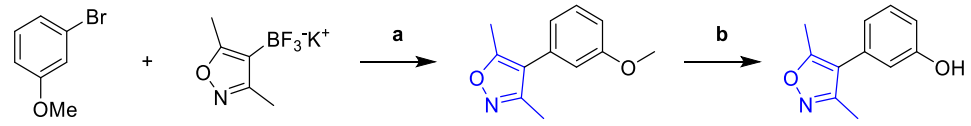

52 **53** **12** **13**

Scheme 2.5. Synthesis of dimethyl isoxazole containing fragments **12** and **13**. *Reagents and conditions:* **a)** Na_2CO_3, RuPhos, $Pd(OAc)_2$, EtOH, 80 °C, 17 h, 85%; **b)** BBr_3, CH_2Cl_2, 0 °C to rt, 30 min, 68%.

Trifluoroborate salts were also employed in Suzuki-Miyaura coupling reactions with 7-bromo-4-methylquinoline **54** to generate compounds **20** and **21** (Scheme 2.6).

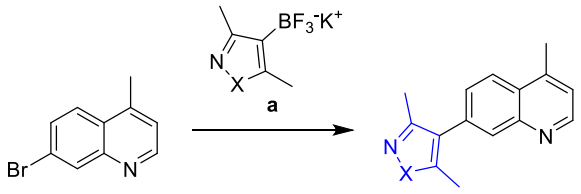

54

20: X= O
21: X= NH

Scheme 2.6. Synthesis of **20** and **21**. *Reagents and conditions:* **a)** K_2CO_3, 1,4-dioxane/H_2O, $Pd(dppf)Cl_2 \cdot CH_2Cl_2$, 100 °C, 16-20 h, **20:** 50%, **21:** 42%.

7-Bromo-6-methoxy-4-methylquinoline **55** was not commercially available, and attempts to synthesise this compound *via* bromination of **56** resulted in 5-bromo-6-methoxy-4-

methylquinoline **57** as the major product. A range of bromination conditions were screened (Table 2.2), but none yielded the desired 7-bromo-6-methoxy-4-methylquinoline **55**. The triflate **58** of 6-methoxy-4-methylquinoline **56** was instead employed as a pseudohalide coupling partner with **53** to generate compound **19** (Scheme 2.7). The triflate **58** was synthesised in 32% yield over four steps from 4-chloro-6-methoxyquinolin-7-ol **59**. To aid with purification, compound **59** was benzyl protected to give **60**, which was methylated to give compound **61**. Deprotection of **61** gave **62**, which was converted to the triflate **58** using triflic anhydride.

Table 2.2. Conditions screened for the bromination of **56** and strutures of the major product(s) isolated in each reaction.

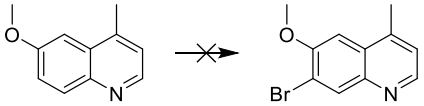

56 **55**

Products isolated in bromination reactions 1-5:

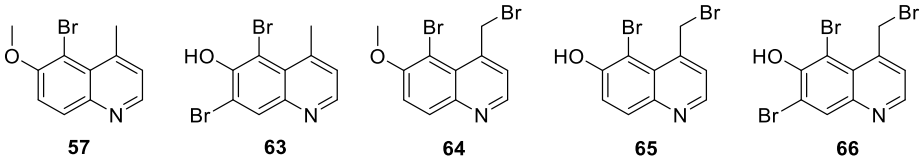

57 **63** **64** **65** **66**

	Brominating agent	Temperature	Solvent	Major product(s)
1	**NBS**	rt to reflux	MeCN	**57**
2	**NBS**	100 °C, µW	DCE	**63, 64, 65**
3	**Br_2**	0 °C to rt	CH_3Cl	**57**
4	**Br_2**	50 °C	CH_3Cl	**57, 66**
5	**Br_2, HOAc**	50 °C	CH_3Cl	**57, 63, 64**

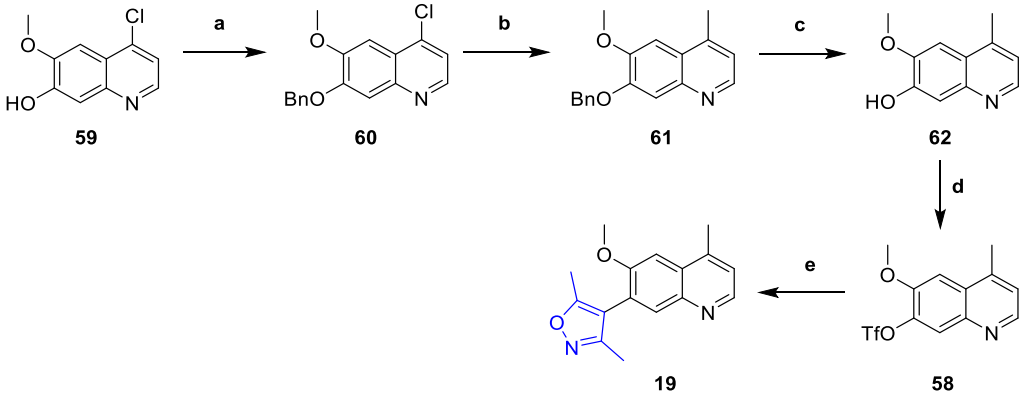

Scheme 2.7. Synthesis of **19**. *Reagents and conditions:* **a)** K_2CO_3, benzyl bromide, DMF, 45 °C, 2 h, **100%**; **b)** Methyl boronic acid, K_2CO_3, $Pd(dppf)Cl_2 \cdot CH_2Cl_2$, 1,4-dioxane/$H_2O$, 110 °C, 5 h, **48%**; **c)** 10% Pd/C, acetic acid, $H_{2\,(g)}$, rt, 15 h, **100%**; **d)** Triflic anhydride, pyridine, CH_2Cl_2, 0 °C, 1 h, **67%**; **e)** 3,5-Dimethylisoxazol-4-yl-4-boronic acid, K_2CO_3, $Pd(dppf)Cl_2 \cdot CH_2Cl_2$, 1,4-dioxane/$H_2O$, 110 °C, 4 h, **31%**.

The initial step in the synthesis of **16** involved a Baylis-Hillman reaction of 5-bromo-2-nitrobenzaldehyde **67** with methyl acrylate (Scheme 2.8).[185] Reduction of the phenyl propenoate **68** to phenyl propanoate **69** was achieved using Wilkinson's catalyst under an atmosphere of hydrogen gas. The hydrogenation was conducted with the rhodium-based catalyst rather than Pd/C to selectively reduce the alkene and avoid the potential reduction of the aryl bromide.[186-188] A Béchamp reduction of the nitro group and *in situ* cyclisation primarily afforded **70**. However, compound **71** was also observed in the ^{1}H NMR of the isolated product.[189] A longer reaction time might have enabled full conversion of **70** to **71**. The isolated intermediate **70** was heated under reflux in toluene using Dean and Stark apparatus with a sub-stoichiometric amount of tosic acid to give compound **71**. Compound **71** was then coupled to potassium (3,5-dimethylisoxazol-4-yl)trifluoroborate **53** to yield **16** in 54% yield.

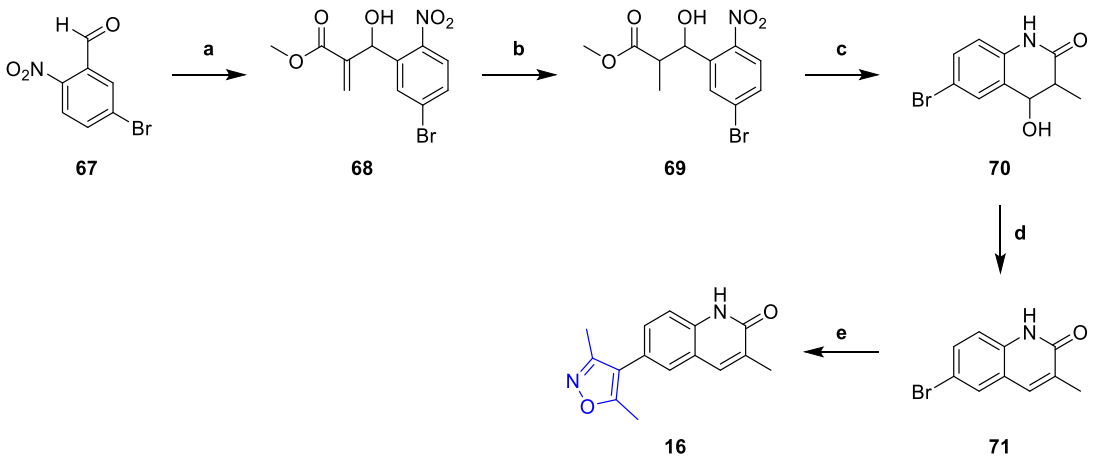

Scheme 2.8. Synthesis of **16**. *Reagents and conditions*: **a)** Methyl acrylate, DABCO, DMF, rt, 4 h, 93%; **b)** Wilkinson's catalyst, THF, $H_{2\,(g)}$, 50 °C, 24 h, 100%; **c)** Fe powder, acetic acid, 50 °C, 1 h, 88%; **d)** 4-Toluenesolfonic acid, toluene, reflux with Dean Stark apparatus, 19 h, 88%; **e)** Potassium (3,5-dimethylisoxazol-4-yl)trifluoroborate, K_2CO_3, $Pd(dppf)Cl_2 \cdot CH_2Cl_2$, 1,4-dioxane/$H_2O$, 110 °C, 5.5 h, 54%.

5- And 6-isoxazolyl-benzimidazoles feature in high affinity inhibitors of both BET and CREBBP bromodomains.[69, 190] Hay *et al.* developed a high affinity, selective ligand for the CREBBP bromodomain from a series of 5-isoxazole-benzimidazoles based on the fragment hit **17**.[69] Selectivity for CREBBP over BRD4(1) was achieved by varying substituents at *N*-1 and *C*-2 on the benzimidazole. The optimised compound became the Structural Genomics Consortium (SGC)-nominated probe **SGC-CBP30**. **SGC-CBP30** has been co-crystallised with *Ld*BDF5.1, allowing for the determination of its binding mode (PDB code: 6BYA).[131] As expected, the 3,5-dimethylisoxazole group acts as a KAc

mimic, forming hydrogen bonding interactions to the conserved N90 and Y44 in the KAc binding site (Figure 2.9). As the effect of this human bromodomain inhibitor on *Leishmania* had not yet been reported, compounds **17** and **18** were added to the synthetic library to be evaluated in biophysical assays with *Ld*BDF5.1.

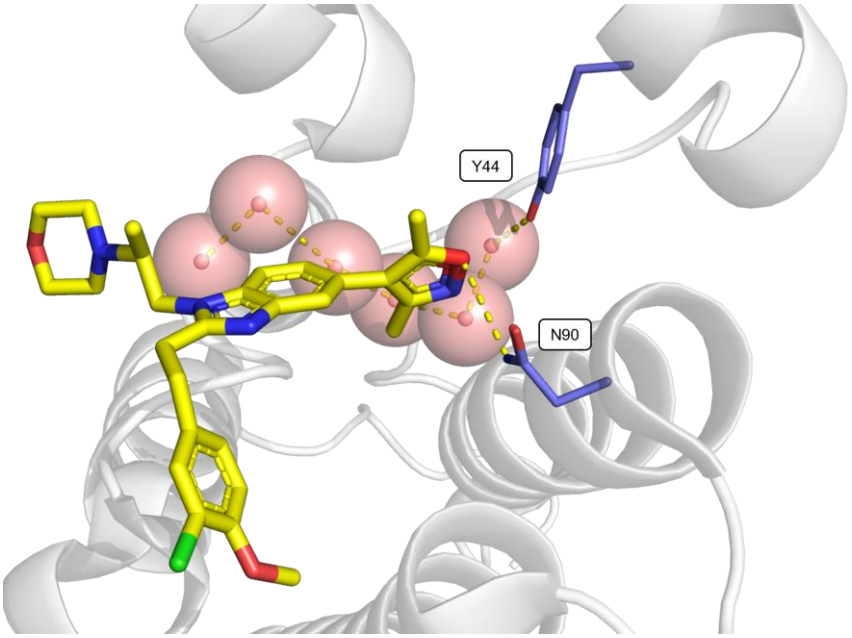

Figure 2.9. A view of the X-ray crystal structure of **SGC-CBP30** (carbon = yellow) co-crystallised with *Ld*BDF5.1 (carbon = purple, PDB code: 6BYA).[131]

Fragment **17** was synthesised in one step from commercially available **72** (Scheme 2.9). Compound **18** was synthesised in four steps (Scheme 2.10). The reaction of 4-bromo-1-fluoro-2-nitrobenzene **73** in a Suzuki-Miyaura coupling with the 3,5-dimethylisoxazole potassium trifluoroborate salt **53** gave **74** in 76% yield.[69] An S_NAr reaction with methylamine hydrochloride provided **75**, which was subsequently reduced in a Pd/C-catalysed hydrogenation to give the aniline **76**. Condensation of **76** with proprionic acid afforded benzoimidazole **18** in a yield of 62%.

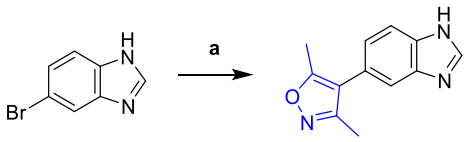

72 **17**

Scheme 2.9. Synthesis of **17**. *Reagents and conditions*: **a)** Potassium (3,5-dimethylisoxazol-4-yl)trifluoroborate, Na_2CO_3, $Pd(dppf)Cl_2 \cdot CH_2Cl_2$, DMF/$H_2O$, 130 °C, µW, 30 min, 40%.

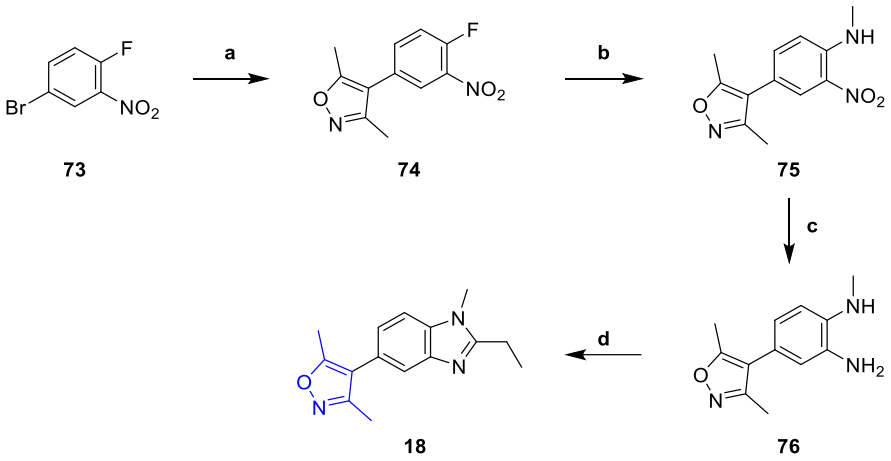

73 74 75 76 18

Scheme 2.10. Synthesis of **18**. *Reagents and conditions:* **a) 53**, $NaHCO_3$, $Pd(dppf)Cl_2 \cdot CH_2Cl_2$, DME/$H_2O$, 110 °C, 17 h, 76%; **b)** Methylamine hydrochloride, DIPEA, NMP, 80 °C, 2 h, 99%; **c)** 10 wt. % Pd/C, H_2, EtOH, 18 h, 38%; **d)** T3P (≥50 wt. % in ethyl acetate), propionic acid, DIPEA, ethyl acetate, 80 °C, 6 h, 62%.

2.2.4 Benzo-fused Isoxazoles

Planar systems incorporating the isoxazole KAc-mimicking chemotype were also synthesised. These compounds have the isoxazole moiety fused to a benzene ring. The 1,2-benzisoxazole **22** was obtained following the procedure from Chen *et al.*[191] The imine **77** of 2-hydroxyacetophenone **78** was formed by treating with methanolic ammonia, followed by NCS-mediated cyclisation, which was facilitated by generating the N-Cl imine intermediate **79** *in situ* (Scheme 2.11, steps **a** and **b**). The cyclisation gave a mixture of products which made the purification challenging. An alternative preparation from 2-hydroxyacetophenone proceeding *via* the oxime **80** (Scheme 2.11, steps **c** and **d**)[192] resulted in a cleaner and quicker reaction that gave the desired 1,2-benzisoxazole **22** in a greater yield (49% compared to 69% yield over two steps).

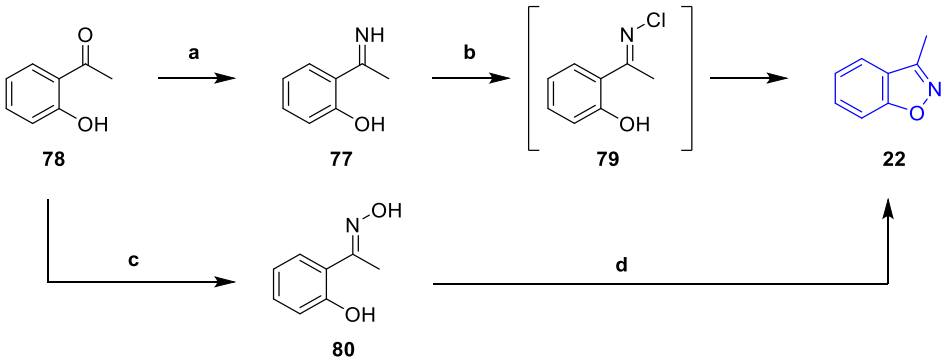

78 77 79 22 80

Scheme 2.11. Synthesis of 1,2-benzisoxazole **22**. *Reagents and conditions:* **a)** 7 M Methanolic ammonia solution, rt, 41 h, 73%; **b)** NCS, K_2CO_3, THF, rt, 21 h, 67%; **c)** Hydroxylamine hydrochloride, NaOAc, EtOH, reflux, 2 h, 100%; **d)** DMF-DMA, 1,4-dioxane, reflux, 1 h, 69%.

The 2,1-benzisoxazole **81** was obtained in a reductive cyclisation of 2-nitroacetophenone **82** following the procedure of Kim *et al*. (Scheme 2.12).[193] The authors proposed that the role of 2-bromo-2-nitropropane in this reduction is likely to be an electron acceptor with a low lying antibonding non-bonding orbital. The desired product **81** was obtained in 34% yield, with 2-aminobenzaldehyde observed as a by-product. Unfortunately, 2,1-benzisoxazole **81** was found to be volatile and therefore not suitable for evaluation in biophysical assays with the *Leishmania* bromodomains. Therefore, the chloro- substituted 2,1-benzisoxazole **23** was prepared under the same reaction conditions from **83**. The halogen substituent both increases the molecular weight of the fragment to provide a compound with a higher boiling point and gives a derivative which may be useful for further functionalisation, for example in cross coupling reactions.

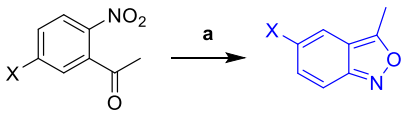

82: X= H
83: X= Cl

81: X= H
23: X= Cl

Scheme 2.12. Synthesis of 2,1-benzisoxazoles **81** and **23**. *Reagents and conditions*: **a)** Zinc dust, 2-bromo-2-nitropropane, MeOH, 50 °C, 28-31 h, **81**: 34%, **23:** 54%.

2.2.5 Benzimidazoles

The first high affinity and selective inhibitors discovered for the BRPF1 bromodomain encompass the benzimidazole motif, which is also present in the core of ligands that bind to the bromodomains of TRIM24 and TRIM33.[167, 168] **GSK6853** contains a benzimidazole and is a chemical probe for BRPF1 with a reported pK_d of 9.5 (K_d = 0.31 nM).[169] Similarly, compound **84** contains a benzimidazole moiety and is a selective BRPF1B/TRIM24 dual inhibitor with reported pK_d values of 6.9 and 6.7 (K_d = 137 nM and 222 nM), respectively (Figure 2.10).[168] Additionally, the benzimidazole **48** was shown to bind *Ld*BDF5.2 in the GSK ASMS screening assay. Given the apparent affinity of the benzimidazole moiety for bromodomains, fragments containing benzimidazole motifs were included in the fragment library to probe the SAR of the *Leishmania* bromodomain.

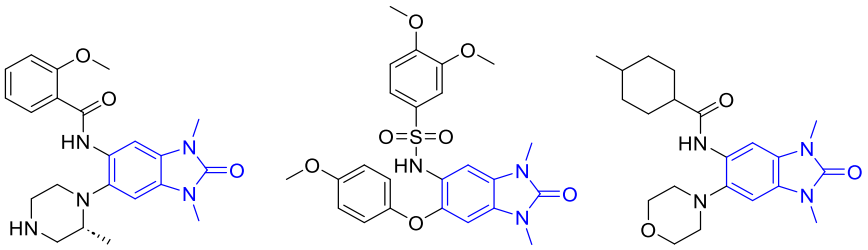

GSK6853 84 48

Figure 2.10. Benzimidazoles in human bromodomain ligands with KAc mimetic highlighted in blue.

Compound **28** was synthesised in two steps starting from 1,2-phenylenediamine **85** (Scheme 2.13). An imide condensation reaction between compound **85** and *N,N'*-carbonyldiimidazole (CDI) yielded compound **86**, which was methylated to afford fragment **28**.

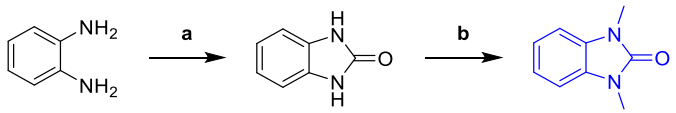

85 **86** **28**

Scheme 2.13. Synthesis of benzimidazole **28**. *Reagents and conditions*: **a)** CDI, DMF, rt, 24 h, 23%; **b)** Iodomethane, K_2CO_3, DMF, rt, 23 h, 98%.

An alternative route to synthesise more diverse benzimidazolone structures was also employed (Scheme 2.14). 1-Fluoro-2-nitrobenzene **87** was reacted with methylamine hydrochloride to afford **88** in a quantitative yield. Compound **88** was subsequently reduced to the aniline in a Pd/C-catalysed hydrogenation and the crude product **89** reacted with CDI to afford **90**. Acetic anhydride and di-*tert*-butyl dicarbonate each reacted cleanly with **90** to give fragments **29** and **30**, respectively.

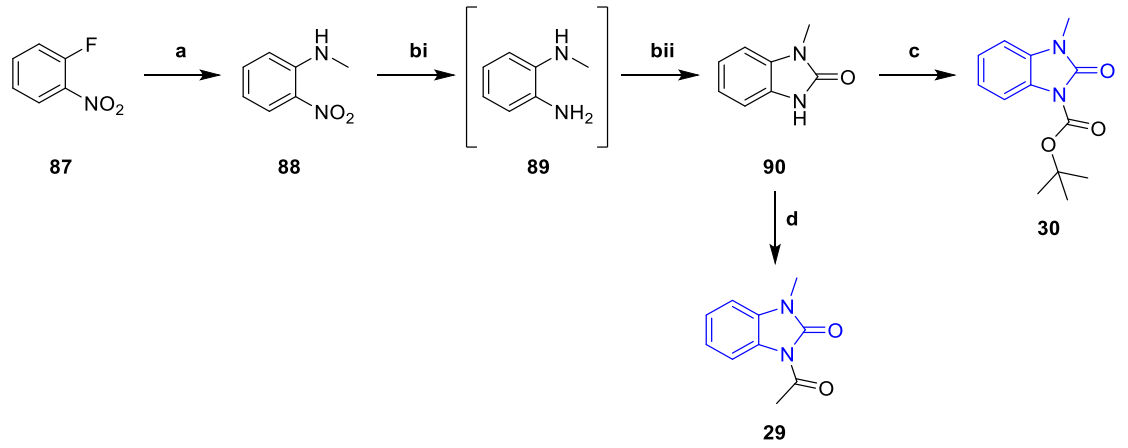

87 88 89 90 30 29

Scheme 2.14. Synthesis of **29** and **30**. *Reagents and conditions*: **a)** Methylamine hydrochloride, DIPEA, NMP, 85 °C, 5 h, 99%; **b) i)** 10% Pd/C, H_2, EtOH, 48 h, **ii)** CDI, THF, reflux, 24 h, 23%; **c) 29:** 4-DMAP, Et_3N, acetic anhydride, THF, rt, 3 h, 87%; **30:** 4-DMAP, di-*tert*-butyl dicarbonate, Et_3N, THF, 0 °C to rt, 3 h, 81%.

2.2.6 Dihydroquinaxolinones, dihydroquinazolinones, and dihydroquinolinones

The dihydroquinaxolinone ligand **91** was discovered by Rooney *et al.* to be a high affinity binder of the CREBBP bromodomain (Figure 2.11).[142] The dihydroquinaxolinone amide forms two key hydrogen bond interactions with the highly conserved asparagine residue (N1168) in the KAc binding pocket.

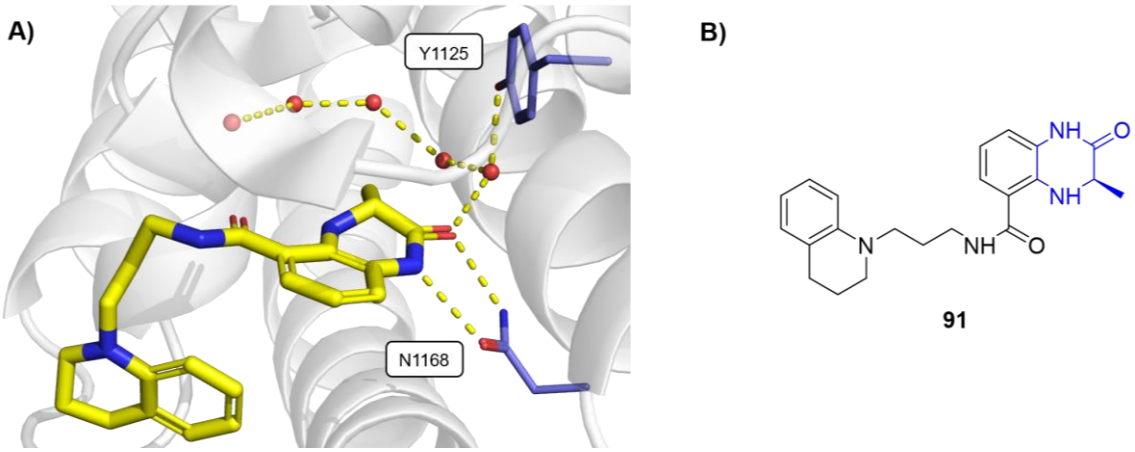

91

Figure 2.11. A) Compound **91** in complex with the CREBBP bromodomain (PDB code: 4NYW).[194] The dihydroquinaxolinone amide forms two hydrogen bonds to N1168 and one water-mediated hydrogen bond with Y1125; **B)** Dihydroquinaxolinone ligand **91** for the CREBBP bromodomain with KAc mimetic highlighted in blue.

The dihydroquinoxalinone **24** was synthesised from commercially available 1-fluoro-2-nitrobenzene **87** in two steps. The nucleophilic aromatic substitution of **87** with D-alanine

methyl ester was initially performed in toluene at 85 °C with caesium carbonate as the base, as these conditions were previously employed in-house for a similar substrate, benzyl 2-fluoro-3-nitrobenzoate. However, the reaction was found to be slow, with only 2% conversion of the starting material observed by LCMS after 24 h. The poor conversion was likely due to the lower reactivity of compound **87** compared to benzyl 2-fluoro-3-nitrobenzoate, which has a more electron deficient aromatic ring. Other factors that might explain low conversion are the poor solubility of caesium carbonate in toluene, or too little base in the reaction mixture. Alternative conditions for the S_NAr were investigated; reacting 1-fluoro-2-nitrobenzene with D-alanine methyl ester in DMF at 85 °C with 4.0 eq. of DIPEA as a base gave the desired product **92** in 75% yield. The reduction of the nitro group of **92** with Zn and ammonium chloride, followed by *in situ* cyclisation, afforded the dihydroquinoxalinone **24** in 89% yield (Scheme 2.15).

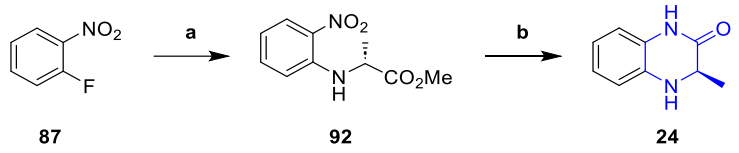

87 92 24

Scheme 2.15. Synthesis of dihydroquinoxalinone **24**. *Reagents and conditions*: **a)** D-Alanine methyl ester hydrochloride, DIPEA, DMF, 85 °C, 22 h, 75%; **b)** Zinc powder, NH_4Cl, DMF, rt, 25 h, 89%.

Since the dihydroquinoxalinone moiety is moderately stable to oxidation and has the propensity to form the corresponding quinoxalinone, the more stable 7-membered dihydroquinoxalinone ring **25** was also prepared (Scheme 2.16).[50] 1-Fluoro-2-nitrobenzene **87** was subjected to an S_NAr reaction with *tert*-butyl (*R*)-3-aminobutanoate to provide **93**. The Boc group of compound **93** was de-protected using TFA, then, the reduction of the nitro group with Fe powder in acetic acid allowed for an intramolecular ring closure, which yielded the KAc-mimicking fragment **25**.

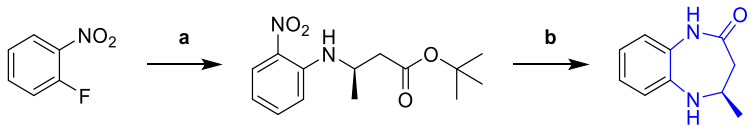

87 93 25

Scheme 2.16. Synthesis of 7-membered dihydroquinoxalinone **25**. *Reagents and conditions*: **a)** *tert*-Butyl (*R*)-3-aminobutanoate, DIPEA, DMF, 75 °C, 22 h, **40%**; **b)i)** TFA, CH_2Cl_2, rt, 45 min, **ii)** Fe powder, acetic acid, reflux, 3 h, **22%.**

A similar chemotype, the dihydroquinazolinone **26**, was synthesised in three steps starting from isatoic anhydride **94** (Scheme 2.17). Reaction of **94** with methylamine hydrochloride gave **95**, then the amide was reduced using RedAl® to afford **96**. The final step involved a ring closure reaction, facilitated by CDI, to produce **26**. Given the structural similarity of both the dihydroquinazlinone and the 3,5-dimethylisoxazole moiety to KAc, it was proposed that the dihydroquinazoline-containing 3,5-dimethylisoxazloe derivative **15** might bind *Ld*BDF5 bromodomains in two different ways, with either the dihydroquinazlinone or 3,5-dimethylisoxazole moiety acting as the KAc bioisostere.[140] Fragment **15** was synthesised *via* bromination of **26** with *N*-bromosuccinimide. The intermediate **97** was then coupled to potassium (3,5-dimethylisoxazol-4-yl)trifluoroborate **53** to yield **15**.

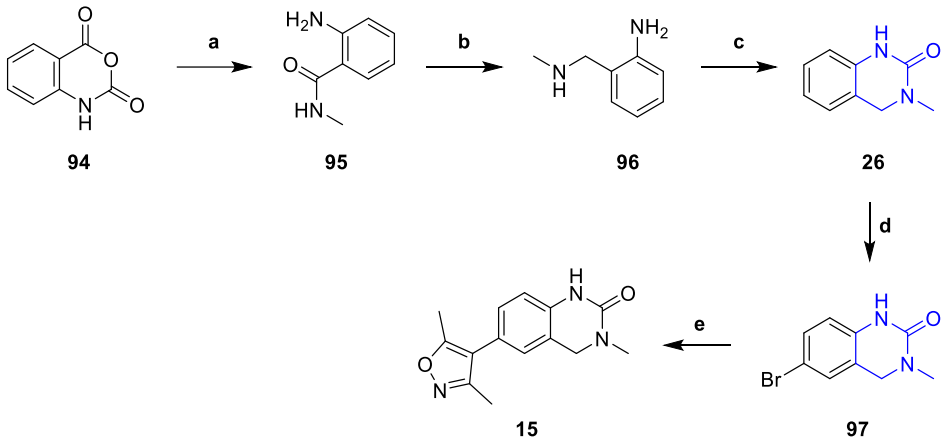

Scheme 2.17. Synthesis of fragments **26** and **15**. *Reagents and conditions*: **a)** Methylamine hydrochloride, Et_3N, DMF, 70 °C, 5 h, 92%; **b)** Red-Al® (60 wt % in toluene), toluene, reflux, 2 h 15 min, 42%; **c)** *N,N'*-Carbonyldiimidazole, THF, reflux, 24 h, 64%; **d)** *N*-Bromosuccinimide, CH_2Cl_2, rt, 2.5 h, 65%; **e)** Potassium (3,5-dimethylisoxazol-4-yl)trifluoroborate, Na_2CO_3, $Pd(OAc)_2$, RuPhos, EtOH, 110 °C, µW, 3 h, 25%.

Dihydroquinolinone **27** was synthesised from aniline **98** (Scheme 2.18) *via* the acylation of **98** with 2-chloropropionyl chloride to give **99**. An intramolecular Friedel-Crafts alkylation of **99** using neat $AlCl_3$ provided **100**, which was subsequently alkylated with ethyl iodide to form **27**.[195]

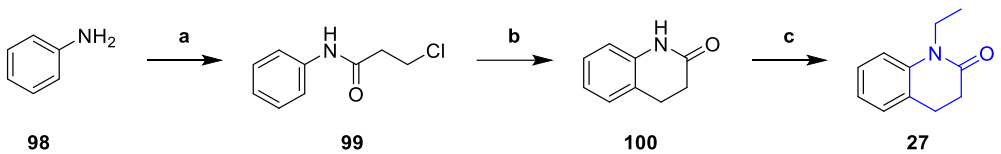

Scheme 2.18. Synthesis of **27**. *Reagents and conditions*: **a)** 3-Chloropropionyl chloride, Et_3N, CH_2Cl_2, 0 °C, 1 h, 88%; **b)** $AlCl_3$, 150 °C, 1 h, 64%; **c)** Ethyl iodide, sodium hydride, DMF, 0 °C, 2 h, 88%.

Other structurally diverse compounds that were synthesised for the fragment library include compound **31** and **32**. Compound **31** was co-crystalised with BRD4(2) and the X-ray crystallographic structure can be found in the PDB (PDB code: 5UEP).[172] Compound **31** was synthesised from 2-acetylcyclohexane-1,3-dione **101** in a Knorr-type reductive condensation (Scheme 2.19).[196]

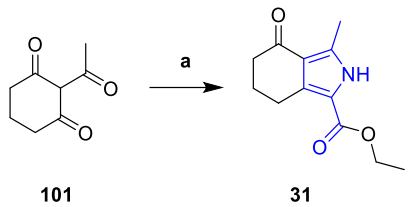

Scheme 2.19. Synthesis of **31**. *Reagents and conditions*: **a)** Diethyl-2-aminomalonate hydrochloride, sodium acetate, acetic acid, 100 °C, 17 h, **58%**.

One of the most commonly used drugs, acetaminophen (paracetamol **32**) is structurally similar to fragments that are known to occupy KAc binding sites.[173] Acetaminophen **32** was synthesised to include in the fragment library in one-pot from 4-hydroxyacetophenone **102** (Scheme 2.20).[197] In this reaction, hydroxylamine hydrochloride acts to form an oxime and the *in situ* production of hydrochloric acid enables a Beckmann rearrangement of the oxime to form the corresponding amide **32**.

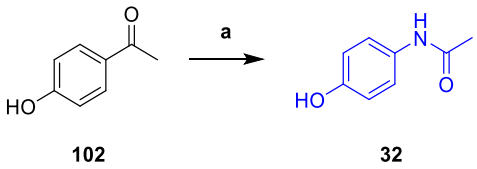

Scheme 2.20. Synthesis of **32**. *Reagents and conditions*: **a)** Hydroxylamine hydrochloride, acetonitrile, 95 °C, 2 h, 50%.

2.2.7 Summary of the fragment library synthesis

In summary, a variety of fragments inspired by a broad range of known KAc mimics used in the inhibition of human bromodomains were synthesised for a fragment-based screen to identify potential binders of the *Ld*BDF5 bromodomains. Following the preparation of the fragment library, the thirty-one compounds were then screened against the *Ld*BDF5.1 and *Ld*BDF5.2 proteins to provide information on whether the KAc-mimicking motifs present in the panel of compounds are capable of binding to the bromodomains.

2.3 Recombinant protein expression and purification

The production of *Ld*BDF5.1 and *Ld*BDF5.2 proteins provided the biological targets necessary for the biophysical assays employed in the fragment screen. The target proteins, *Ld*BDF5.1 and *Ld*BFD5.2, were recombinantly expressed in *Escherichia coli* following protocols produced by collaborators in the Mottram Group at the University of York (see the Experimental Section 6.3.1 for full details). Plasmids containing the *Leishmania* bromodomain coding sequences were provided by Dr Nathanial Jones (Mottram Group). Briefly, the plasmid DNA for *Ld*BDF5.1 and *Ld*BFD5.2 were amplified and their sequences were confirmed by Sanger sequencing. *Ld*BDF5.1 was expressed in *E. coli* Rosetta™ competent cells, then purified using immobilised-metal affinity (IMAC) and size-exclusion (SEC) chromatography techniques, following the conditions used by Dr Catherine Russell (Mottram group). 81 mg of the His-tagged *Ld*BDF5.1 was obtained from 10 L of culture. The protein purity was confirmed using sodium dodecyl sulfate-polyacrylamide gel electrophoresis (SDS-PAGE) and protein mass spectrometry (Figure 2.12 and Figure 2.13).

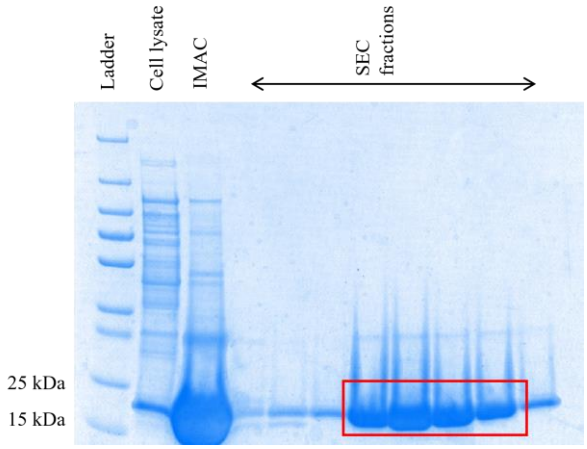

Figure 2.12. SDS-PAGE gel of purified *Ld*BDF5.1 fractions stained with InstantBlue® Coomassie protein stain. Highlighted in red are the fractions eluted from the SEC column that were combined. These fractions contain *Ld*BDF5.1 (MW= 15.2 kDa).

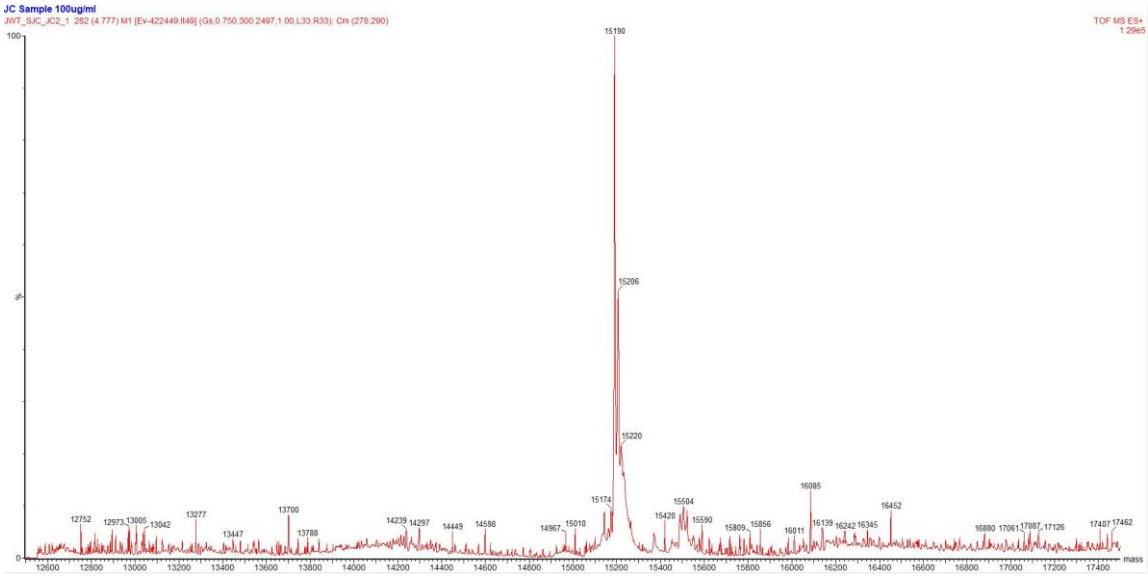

Figure 2.13. Confirmation of purification of *Ld*BDF5.1 by protein mass spectrometry (method detailed in the Experimental section 6.3.2) *Ld*BDF5.1 with 6 His-tags has MW: 15.19 kDa.

Initial attempts to express and purify *Ld*BDF5.2 in Rosetta™ 2 cells following the established protocol were unsuccessful. Therefore, small scale expression trials were conducted to judge the effects of varied growth conditions on expression levels and solubility of the recombinant protein. The results from these expression trials are summarised in Table 2.3. Rosetta™ 2 cells were transformed with the *Ld*BDF5.2 plasmid on selection plates (containing ampicillin and chloramphenicol) and 100 mL starter cultures were made from surviving colonies. Expression tests were performed using 100 mL cultures (with glucose, ampicillin, and chloramphenicol). The following parameters were varied: temperature, time, OD_{600} at point of inoculation, and IPTG concentration (Table 2.3). Following incubation, the cells were pelleted and lysed, then micro-scale purification (using 1.5 mL of cell lysate) was performed using Ni-NTA Agarose.

The Ni resin is an affinity chromatography matrix for purifying recombinant proteins carrying a His-tag, such as *Ld*BDF5.2. Histidine residues in the His-tag bind to the vacant positions in the coordination sphere of the immobilised nickel ions with high specificity and affinity. Cell lysates were loaded onto the matrices and the His-tagged proteins bound, whilst other proteins passed through the matrix. After washing, any His-tagged proteins were eluted in imidazole-containing buffer. The purified samples were then evaluated for expression levels of the target protein by SDS-PAGE gel chromatography (Figure 2.14).

Table 2.3. Experimental conditions for *Ld*BDF5.2 expression trials. The media was LB with 100 µg/mL ampicillin, 25 µg/mL chloramphenicol and 0.2% glucose.

Experiment	OD_{600} before lowering temperature	OD_{600} at inoculation point	Growth temperature (°C)	IPTG concentration (mM)	Induction temperature (°C)	Expression time (h)
1	0.6	0.8	37	0.1	30	4
2	0.6	0.8	37	0.5	30	4
3	0.6	0.8	37	1	30	4
4	0.8	0.8	37	0.1	37	4
5	0.8	0.8	37	0.5	37	4
6	0.8	0.8	37	1	37	4
7	0.6	0.6	37	0.1	16	15
8	0.6	0.6	37	0.5	16	15
9	0.6	0.6	37	1	16	15
10	0.8	0.8	37	0.1	16	15
11	0.8	0.8	37	0.5	16	15
12	0.8	0.8	37	1	16	15

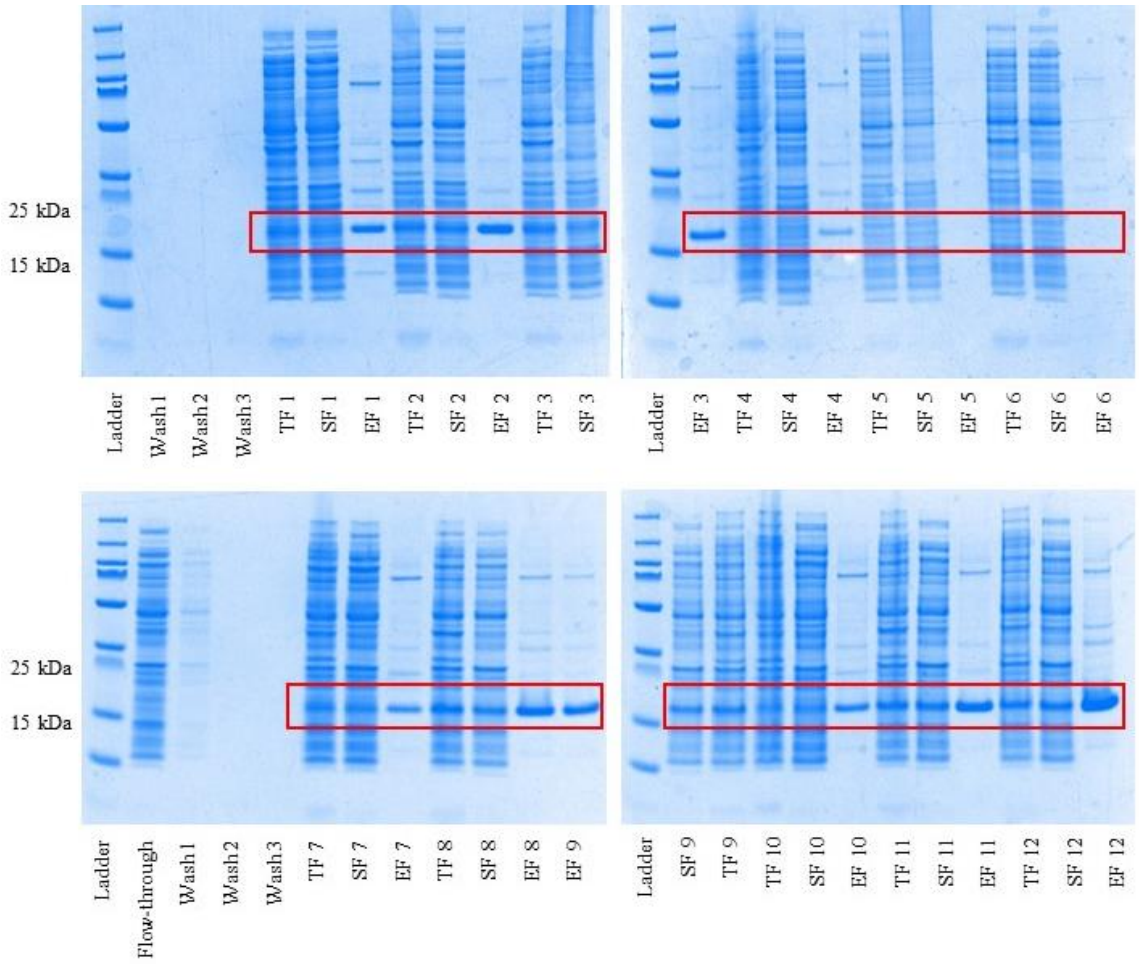

Figure 2.14. SDS-PAGE gels with InstantBlue® Coomassie protein stain. Highlighted in red is the band containing *Ld*BDF5.2 (MW= 17.9 kDa). Experiment numbers are listed along the x axis. TF = Total fraction (re-suspended cell lysate); SF = Soluble fraction (supernatant after spinning down cell debris); EF = Eluted fraction (sample eluted from nickel resin in high imidazole buffer). Experiment 12 provided the optimal conditions for expression of *Ld*BDF5.2.

The gels in Figure 2.14 show that expression of *Ld*BDF5.2 was favoured when the incubation temperature post inoculation with IPTG was lowered from 37 °C to 30 °C, or 16 °C (as in Experiments 1-3 and 7-12). From these results, it appeared that higher levels of protein expression were achieved when the bacteria were grown at a slower rate and for longer. This may be because a slower rate of protein production allows more time for newly translated recombinant proteins to fold properly and reduce the chances of protein aggregation.[198] The concentration of IPTG added can influence the formation of undesirable inclusion bodies and limit protein expression.[199] Generally, a higher concentration of IPTG (0.5 mM or 1 mM) gave increased expression. Following the expression trial summarised in Table 2.3, the optimised expression conditions for *Ld*BDF5.2 were determined to be those found in Experiment 12: incubation at 37 °C until the OD_{600} reached 0.8, then inoculation with 1 mM IPTG followed by an incubation at 16 °C overnight. The expression of *Ld*BDF5.2 was then performed on large scale (6 L culture) using the conditions described above to obtain a 30 g cell pellet. 17 g of this cell pellet was purified using fast protein liquid chromatography (FPLC) techniques to yield 22 mg of *Ld*BDF5.2 (see the Experimental Section 6.3.2 for full details on the protocol). The protein purity was confirmed using SDS-PAGE (Figure 2.15) and protein mass spectrometry (Figure 2.16). The deconvoluted mass spectra confirmed that we had expressed *Ld*BDF5.2. Additionally, a second peak with a mass 178 Da higher than the expected mass of *Ld*BDF5.1 was detected. This additional peak may be the result of gluconoylation of the *N*-terminal His-tag which is a known occurrence during expression of proteins in *E.coli*.[200]

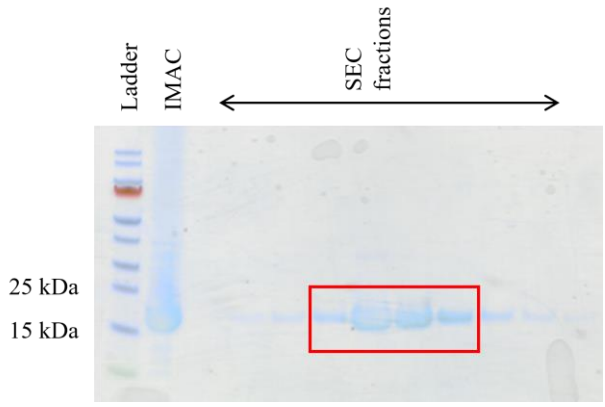

Figure 2.15. SDS-PAGE gel with InstantBlue® Coomassie protein stain. Highlighted in red are the fractions eluted from the SEC column that were combined. These fractions contain *Ld*BDF5.2 (MW= 17.9 kDa).

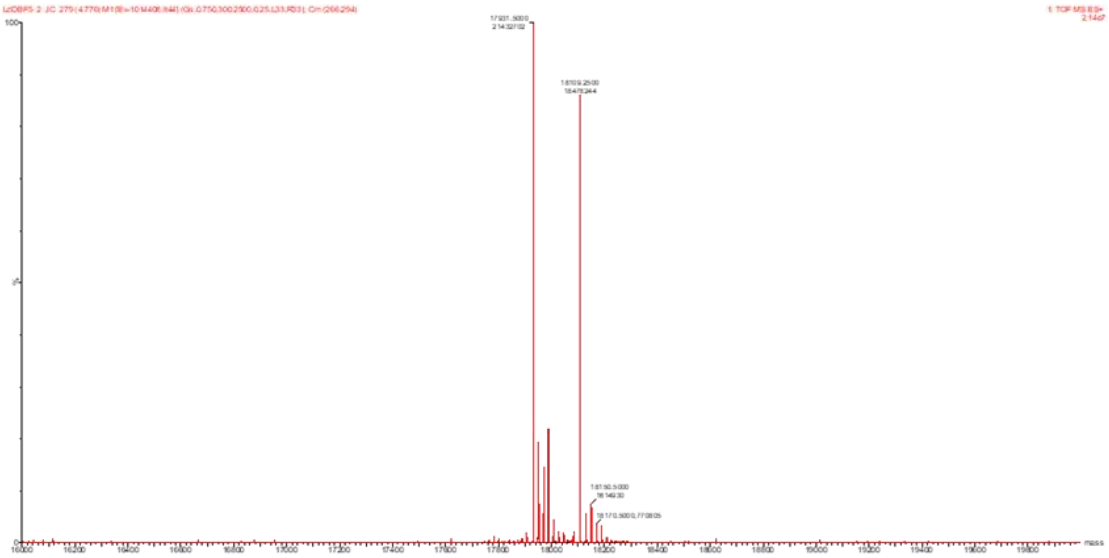

Figure 2.16. Confirmation of purification of *Ld*BDF5.2 by protein mass spectrometry (method detailed in the Experimental section 6.3.2). *Ld*BDF5.2 with 6 His-tags has MW: 17.93 kDa. A mass of 17.93 kDa was detected. A second peak with mass of 18.10 kDa was also found, corresponding to α-*N*-gluconoylation of a His-tag on the recombinant protein.

2.4 Fragment-based screening assays

The binding of the synthetic library of thirty-one compounds (Figure 2.3) to the bromodomains *Ld*BDF5.1 and *Ld*BDF5.2 was evaluated using a range of biophysical assays. Biophysical assays are well-suited to fragment-based screening as they are sufficiently sensitive to detect weak interactions and reliable enough to avoid false positive hits.[201] Techniques including NMR, Surface Plasmon Resonance (SPR), and X-ray crystallography are typically applied to fragment screening, but more recently MST and TSA have also been used.[202]

At the time of the fragment-based screening, two of these techniques were readily accessible: waterLOGSY and TSA. TSA offers clear advantages over other biophysical techniques: the method is easy to develop; rapidly generates data; and requires small amounts of sample.[203] The reagents are low cost and the method does not require specialised instrumentation. TSA can be performed in 96-well format in standard thermocyclers, making it useful for high-throughput screening of large compound libraries. However, both the binding affinity and the thermodynamics of protein unfolding determine the melting temperature of a protein in the presence of a ligand. Thus, not all proteins are amenable to the approach, and both false positives and false negatives are

common.[201] WaterLOGSY was chosen as an initial assay to assess fragments binding to the *Ld*BDF5 bromodomains because the technique is highly sensitive and offers a key advantage in its ability to check compound solubility, which serves as a useful filter to exclude compounds that aggregate in solution and may cause false positive hits in fragment screening experiments.[148] WaterLOGSY relies on fast exchange of the binding event, hence tight binding (compounds with nanomolar affinity) with a slow off-rate might appear as false negative. This effect is more commonly observed for large ligands but would be surprising for fragments (MW < 300) with low affinity.

2.4.1 WaterLOGSY

The KAc mimicking fragments designed and synthesised in section 2.2 were screened in the waterLOGSY assay (Table 2.4; spectra stacks are in section A1 of the Appendices). First, a water-supressed ^{1}H NMR spectrum from a compound-only sample (without protein) was run. Then, a waterLOGSY ^{1}H sequence was acquired. Negative ligand resonances in the compound-only waterLOGSY spectrum (positive NOEs) indicated suitable solubility. Positive peaks in the compound-only waterLOGSY spectrum are indicative that the studied small molecule displays large-molecule like NOE, which is indicative of aggregate formation in solution despite appearing as clear solutions in the NMR tubes.[204] When positive peaks in the compound-only waterLOGSY spectrum were observed, the concentration of the ligand was reduced until a suitable concentration was found. Following the determination of the optimal concentration for each compound, the compounds were then screened in the presence of the protein. Positive peaks in the presence of the protein indicate binding, as shown for compound **18** (Figure 2.17). No changes in the peak sign upon the addition of protein indicate that no binding was detected under the screening conditions, as shown for compound **2** (Figure 2.18).

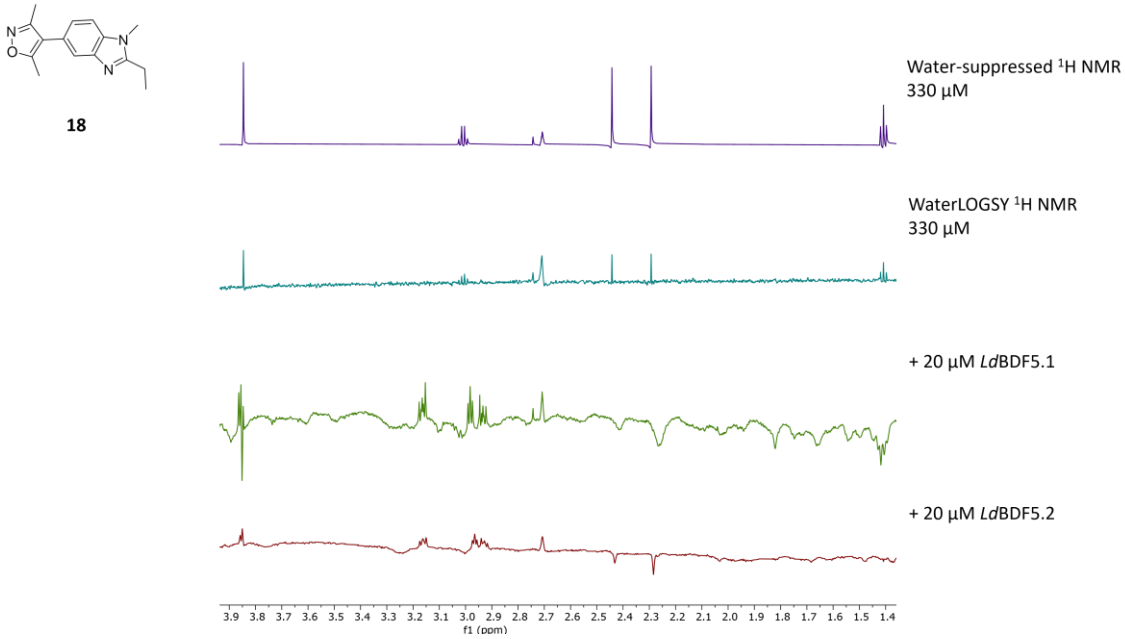

Figure 2.17. Partial waterLOGSY spectra of **18**. The water suppressed ^{1}H spectrum is shown in purple. The waterLOGSY NMR of the compound only (blue) shows no inversion of the compound peaks indicating suitable solubilisation at 330 µM. Inversion of the ligand peaks on addition of 20 µM *Ld*BDF5.1 (green), suggests weak binding to *Ld*BDF5.1. The waterLOGSY spectrum in the presence of 20 µM *Ld*BDF5.2 (red) also shows inversion of the ligand peaks which indicates potential weak binding.

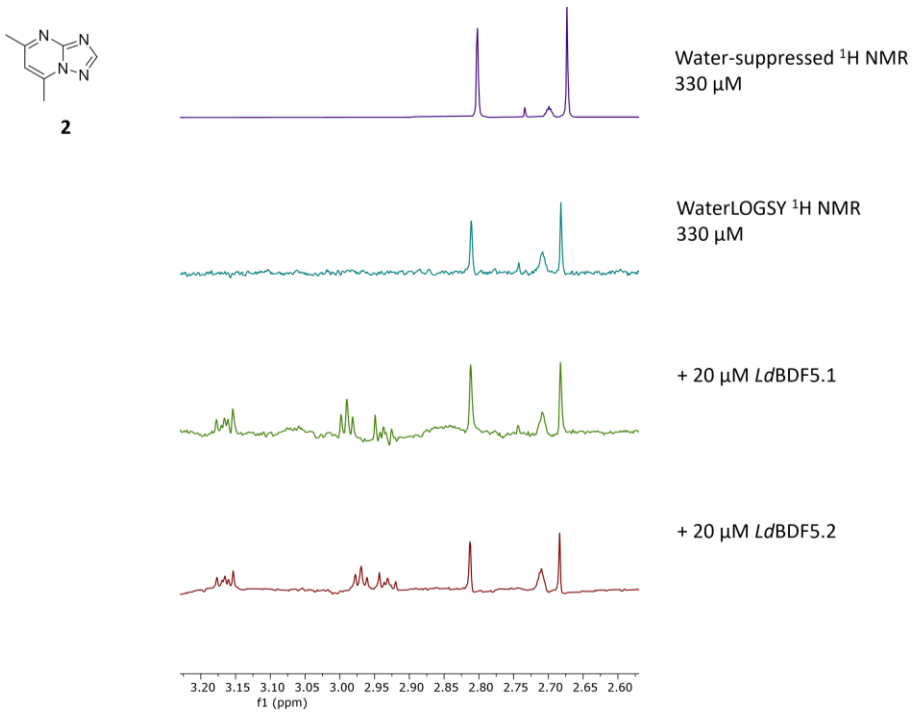

Figure 2.18. Partial waterLOGSY spectra of **2**. The water suppressed ^{1}H spectrum is shown in purple. The waterLOGSY NMR of the compound only (blue) shows no inversion of the compound peaks indicating suitable solubilisation at 330 µM. No inversion of the ligand peaks on addition of 20 µM *Ld*BDF5.1 (green), suggests no binding to *Ld*BDF5.1. The waterLOGSY spectrum in the presence of 20 µM *Ld*BDF5.2 (red) also shows no inversion of the ligand peaks which suggests no binding.

The results from the waterLOGSY assays are summarised in Table 2.4. Unfortunately, compounds **12**, **20**, **21** and **103** all formed soluble aggregates in solution down to a concentration of 63 µM, which was the lowest detectable concentration of ligand, and protein binding could not be distinguished from aggregation behaviours using this technique. At low concentrations, the assay became lower throughput because more scans were required in the NMR experiment to achieve high resolution spectra. Due to the solubility and throughput constraints of waterLOGSY, TSA was selected as an alternative qualitative binding assay.

Table 2.4. Results of the waterLOGSY assay for KAc mimicking fragments and the *Ld*BDF5.1, or *Ld*BDF5.2 protein. LogD values were calculated using MarvinSketch 23.12 software plugins, ChemAxon: http://www.chemaxon.com). MW is the molecular weight of the compound; SFI is the solubility forecast index (SFI = *c* log $D_{pH7.4}$ + number of aromatic rings).[205]

Compound	Structure	MW	cLogD	SFI	Solubility	*Ld*BDF5.1	*Ld*BDF5.2
7	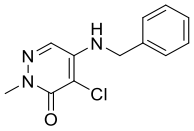	249.70	1.6	3.6	Soluble at 500 µM	Binds	Binds
9	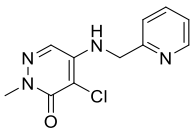	250.70	0.5	2.5	Soluble at 500 µM	No binding	No binding
8	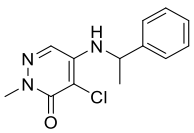	263.73	2.0	4.0	Soluble at 500 µM	Binds	Binds
29	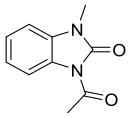	190.20	0.6	2.6	Soluble at 63 µM	No binding	No binding
28	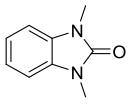	162.19	1.2	3.2	Soluble at 330 µM	No binding	Inconclusive
13	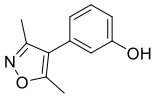	189.21	2.0	4.0	Soluble at 63 µM	Binds	Binds

Compound	Structure	MW	cLogD	SFI	Solubility	*Ld*BDF5.1	*Ld*BDF5.2
3	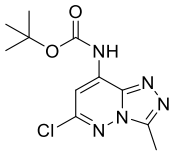	283.72	1.6	3.6	Soluble at 63 µM	Binds	Binds
2	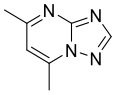	148.17	0.5	2.5	Soluble at 500 µM	No binding	No binding
24	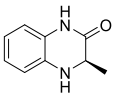	162.19	1.0	2.0	Soluble at 250 µM	No binding	No binding
26	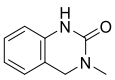	162.19	1.1	2.0	Soluble at 125 µM	Inconclusive	Inconclusive
25	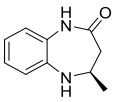	17.22	1.0	2.0	Soluble at 500 µM	No binding	No binding
18	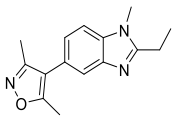	255.32	2.6	5.6	Soluble at 330 µM	Binds	Inconclusive
20	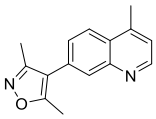	238.29	3.0	6.0	Not soluble at 63 µM	---	---
21	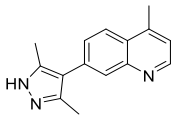	237.31	2.9	5.9	Not soluble at 63 µM	---	---
103	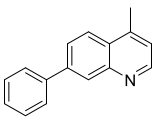	219.29	4.3	7.3	Not soluble at 63 µM	---	---

Compound	Structure	MW	cLogD	SFI	Solubility	*Ld*BDF5.1	*Ld*BDF5.2
12	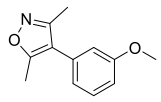	203.24	2.2	4.2	Not soluble at 63 µM	---	---
30	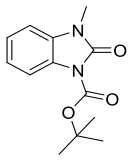	248.28	2.5	4.5	Soluble at 63 µM	Inconclusive	Poor resolution

2.4.2 Thermal Shift Assay

TSA was employed to screen the thirty-one fragments against the *Ld*BDF5 bromodomains (Table 2.5 and Table 2.6). A threshold of $\Delta T_M \geq 2$ °C was deemed to be a thermal shift that was indicative of a binding event (Figure 2.19). The fragment library compounds were screened using TSA at a range of concentrations (125 µM, 250 µM, and 500 µM) against *Ld*BDF5.2. However, no thermal shifts greater than the 2 °C threshold were observed. Compounds **3**, **7**, **8**, and **13** that were identified as binding *Ld*BDF5.2 in waterLOGSY and all produced a $\Delta T_M < 0.5$ °C at 250 µM in TSA (Table 2.5). The discrepancy between the TSA and waterLOGSY results for these compounds may be because waterLOGSY was able to detect weaker binders than TSA and is a more sensitive technique.[147, 206] The library of fragments was then screened against *Ld*BDF5.1 using TSA. The results of this screen are summarised in Table 2.6.

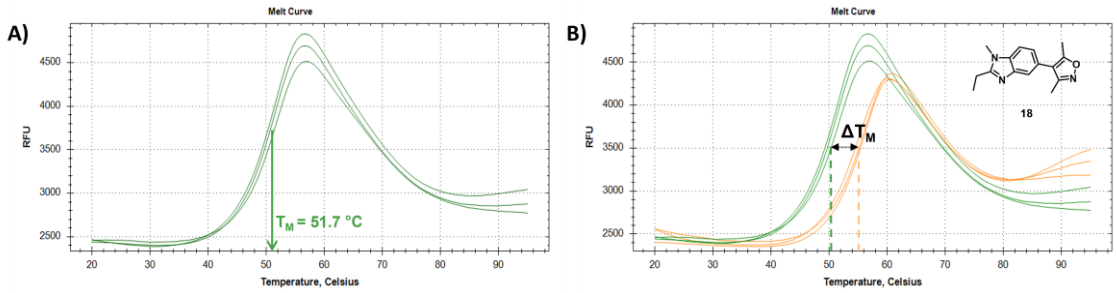

Figure 2.19. A) Thermal shift assay melting curve for *Ld*BDF5.1. The inflection point of the sigmoidal curve defines the melting temperature of the denaturation process (T_M = 51.7 °C). **B)** Thermal shift assay melting curve for *Ld*BDF5.1 + compound **18** at 250 µM. The curve shows three replicate samples of protein with the compound (orange) alongside DMSO control samples (green). Compound **18** binds to *Ld*BDF5.1 and results in a shift in the melting temperature of the protein (ΔT_M).

Table 2.5. Fragments screened in the DSF assay and the thermal shift (ΔT_M) of the melting curve of *Ld*BD5.2 for each compound (250 µM); T_M (*Ld*BD5.2) = 48.4 °C. The error quoted is the standard error of the mean (SEM) of n = 3 repeats.

	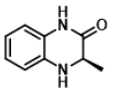	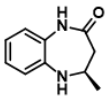	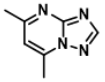	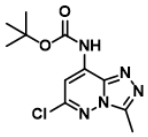	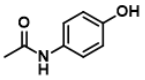
ID	**24**	**25**	**2**	**3**	**32**
ΔT_M (°C)	**0.17 ± 0.11**	**0.10 ± 0.15**	**0.20 ± 0.10**	**0.20 ± 0.07**	**0.00 ± 0.05**
	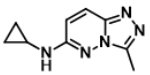	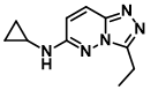	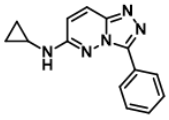	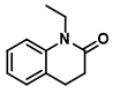	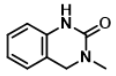
ID	**4**	**5**	**6**	**27**	**26**
ΔT_M (°C)	**0.10 ± 0.04**	**0.03 ± 0.03**	**0.07 ± 0.04**	**0.16 ± 0.04**	**0.20 ± 0.07**
	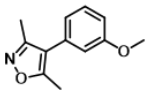	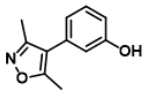	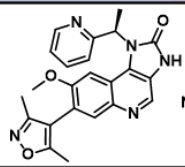	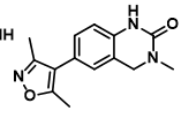	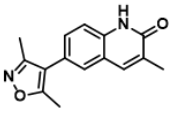
ID	**12**	**13**	**14**	**15**	**16**
ΔT_M (°C)	**0.47 ± 0.07**	**0.33 ± 0.00**	**0.07 ± 0.07**	**-0.03 ± 0.03**	**0.13 ± 0.04**
	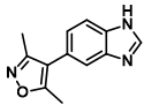	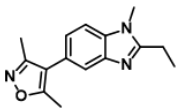	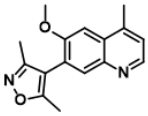	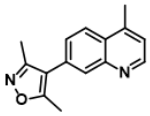	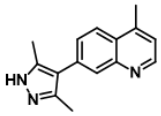
ID	**17**	**18**	**19**	**20**	**21**
ΔT_M (°C)	**n.d.**	**0.20 ± 0.12**	**0.00 ± 0.00**	**0.33 ± 0.00**	**0.17 ± 0.06**
	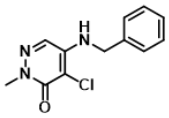	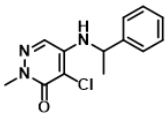	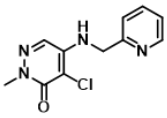	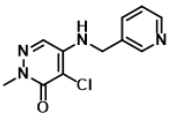	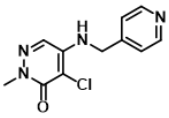
ID	**7**	**8**	**9**	**10**	**11**
ΔT_M (°C)	**0.17 ± 0.11**	**-0.06 ± 0.24**	**0.10 ± 0.08**	**0.07 ± 0.04**	**0.57 ± 0.03**
	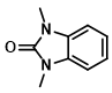	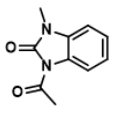	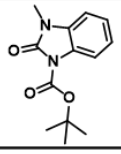		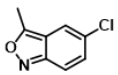
ID	**28**	**29**	**30**	**22**	**23**
ΔT_M (°C)	**0.27 ± 0.00**	**0.40 ± 0.07**	**0.33 ± 0.00**	**0.33 ± 0.00**	**0.03 ± 0.03**
	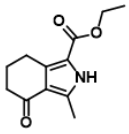				
ID	**31**				
ΔT_M (°C)	**0.77 ± 0.10**				

$\Delta T_M = 0$ **Largest ΔT_M**

Table 2.6. Fragments screened in the DSF assay and the thermal shift (ΔT_M) of the melting curve of *Ld*BD5.1 for each compound (250 µM); T_M (*Ld*BD5.1) = 51.7 °C. The error quoted is the standard error of the mean (SEM) of n = 3 repeats.

	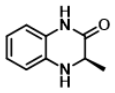	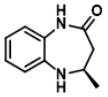	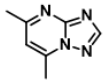	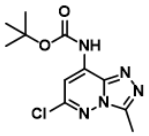	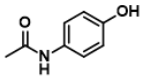
ID	24	25	2	3	32
ΔT_M (°C)	0.12 ± 0.07	0.35 ± 0.20	0.23 ± 0.13	-0.20 ± 0.47	0.52 ± 0.25
	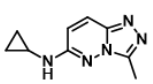	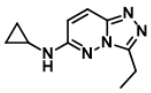	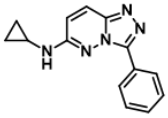	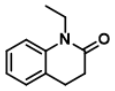	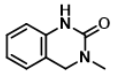
ID	4	5	6	27	26
ΔT_M (°C)	0.37 ± 0.19	0.12 ± 0.10	0.52 ± 0.17	0.72 ± 0.22	-0.19 ± 0.40
	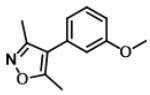	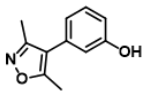	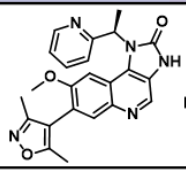	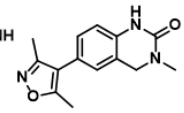	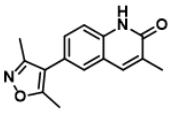
ID	12	13	14	15	16
ΔT_M (°C)	0.79 ± 0.21	-0.31 ± 0.62	0.94 ± 0.16	0.87 ± 0.14	1.42 ± 0.25
	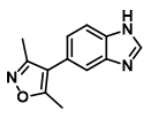	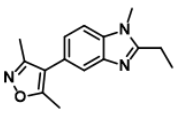	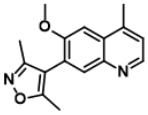	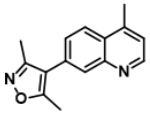	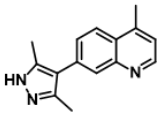
ID	17	18	19	20	21
ΔT_M (°C)	2.12 ± 0.12	4.67 ± 0.37	2.42 ± 0.43	1.31 ± 0.49	0.31 ± 0.20
	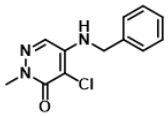	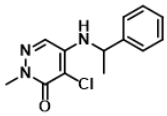	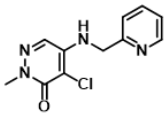	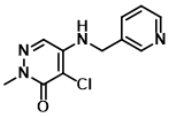	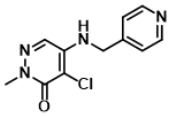
ID	7	8	9	10	11
ΔT_M (°C)	0.12 ± 0.07	0.23 ± 0.13	0.31 ± 0.18	0.22 ± 0.25	0.47 ± 0.12
	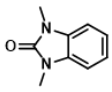	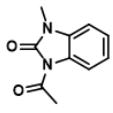	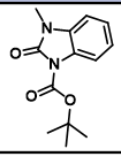		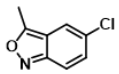
ID	28	29	30	22	23
ΔT_M (°C)	0.31 ± 0.18	-1.06 ± 0.41	-0.97 ± 0.44	0.23 ± 0.13	0.04 ± 0.09
	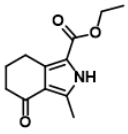				
ID	31				
ΔT_M (°C)	0.92 ± 0.13				



$\Delta T_M = 0$ Largest ΔT_M

Three compounds from the panel (**17**, **18**, and **19**) demonstrated $\Delta T_M \geq 2$ °C of the melting curve of *Ld*BD5.1 (Table 2.6). All three hit fragments for *Ld*BD5.1 are bicyclic and incorporate a 3,5-dimethylisoxaozle, the KAc bioisostere that binds human BET family and CREBBP bromodomains (Figure 2.20).[69, 139, 140, 190, 207] Compound **17** produced a positive thermal shift for *Ld*BD5.1 with $\Delta T_M = 2.12 \pm 0.12$ °C. The largest thermal shift of the melting curve of *Ld*BD5.1 was observed with **18** ($\Delta T_M = 4.67 \pm 0.37$ °C), which is *N*-1 methyl and *C*-2 ethyl-substituted analogue of **17**. Compounds **17** and **18** are fragments based on the CREBBP/EP300-selective chemical probe, **SGC-CBP30**.[207] Work in parallel with Russell *et al.* identified **SGC-CBP30** as an inhibitor of *Ld*BD5.1 with $K_d = 280 \pm 12$ nM measured using ITC.[136] The interaction of **18** with *Ld*BD5.1 was validated and quantified using ITC. Compound **18** binds *Ld*BD5.1 with $K_d = 2.7 \pm 0.4$ µM (n=3).

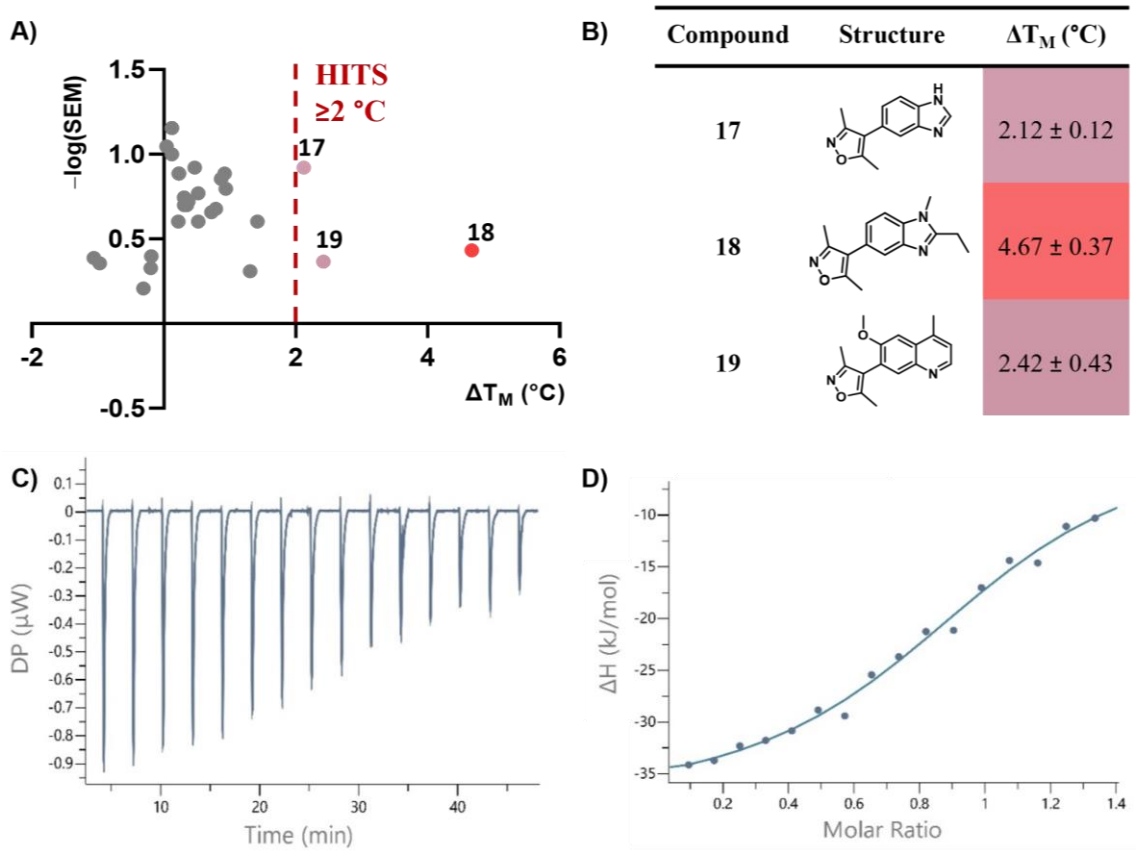

Figure 2.20. A) A scatter plot of ΔT_M (°C) plotted against –log(SEM) of thirty-one compounds screened against *Ld*BD5.1. Red coloured dots represent the compounds with a ΔT_M (°C) greater than 2 °C. SEM = standard error of the mean. **B)** Structures of hit fragments, **17**, **18** and **19**, and their respective thermal shift values, ΔT_M (°C). **C)** Representative trace from ITC with **18** (20 µM) and *Ld*BDF5.1 (160 µM). **D)** Integrated ITC binding curve from ITC with **18** (20 µM) and *Ld*BDF5.1 (160 µM). The thermodynamic parameters of the binding interation are detailed in the Appendix section A6.

The presence of the dimethylisoxazole fused to a bicyclic heterocyclic ring in all three of the hits identified from the TSA, and the absence of such a motif in non-binders, provides confidence in the hit compounds. Subsequent quantification of the binding affinity for **18** using ITC demonstrated that compound **18** was a suitable fragment for further development (Figure 2.20).

2.5 Docking studies with 18 in *Ld*BDF5.1

Following the identification of compound **18** as having low-micromolar affinity to *Ld*BDF5.1, this compound was chosen for further SAR development. To predict how compound **18** might be interacting with the protein, a series of *in silico* docking studies were performed by Bernadette Lee. An X-ray crystal structure of the *Ld*BD5.1 bromodomain bound to ligand **SGC-CBP30** has been solved in the literature (PDB code: 6BYA).[131] The crystal structure of the protein was used to dock **18** in *Ld*BD5.1 and to define the ligand binding site. Examination of compound **18** docked in the binding site of *Ld*BDF5.1 predicts that the dimethylisoxazole moiety forms similar interactions typically made by native KAc residues to human bromodomains (Figure 2.21). Notably, the oxygen of the dimethylisoxazole **18** is predicted to form a hydrogen bonding interaction with the conserved asparagine residue, N90, of *Ld*BDF5.1. The nitrogen from the dimethylisoxazole is predicted to form a water-mediated hydrogen bond with Y44 (Figure 2.21, A). The benzimidazole occupies the KAc binding pocket, with the *N*-1 hydrogen bonding to Y37, and the *N*-methyl group orientated to extend out of the ZA channel (Figure 2.21, B). A common motif found in human BET bromodomains is the WPF shelf, which comprises of the W81, P82 and F83 residues in BRD4(1).[46] Structural differences in the WPF shelf between different human bromodomains have been exploited in the development of higher affinity selective bromodomain inhibitors.[175] Similar motifs have been found in parasite bromodomains, such as the HFF shelf in BRD3(2) of *S. mansoni.*[164] In *Ld*BDF5.1, the WPF shelf is replaced with the residues H27, I28 and F29 (highlighted in blue, Figure 2.21, B). The *C*-2 ethyl of **18** sits over I28 of the HIF shelf and may be forming hydrophobic interactions in this area.

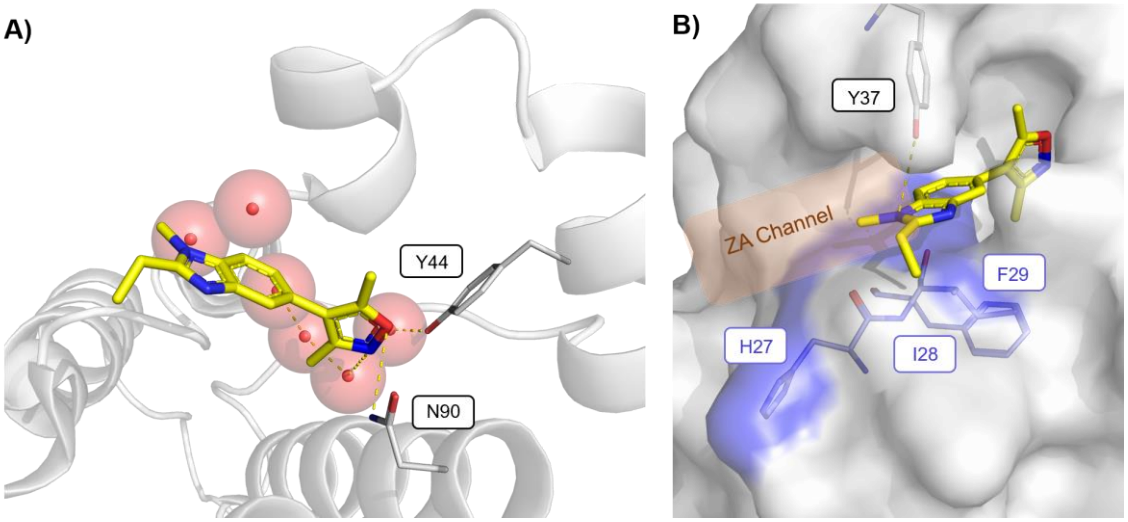

Figure 2.21. Compound **18** (carbon = yellow) docked in the binding site of X-ray *Ld*BD5.1 (carbon = white, PDB code 6BYA) using GOLD docking software.[131, 208] **A)** The oxygen of the 3,5-dimethylisoxazole hydrogen bonds to N90, and the nitrogen forms a water-mediated hydrogen bond with Y44; **B)** The benzimidazole *N*-1 hydrogen bonds to Y37, and the *N*-methyl group is orientated to extend out of the ZA channel (highlighted in orange). The residues analogous to those in the WPF shelf, H27, I28 and F29, are highlighted in blue.

Two regions were identified in the *Ld*BDF5.1 structure where additional functionality could be added to improve the binding affinity of **18** (Figure 2.22). The *C*-2 ethyl of **18** appears to project into a pocket defined by the residues H26, T99, A95 and Y96 (Figure 2.22, region highlighted in purple). It was proposed that analogues of **18** with an aromatic ring on the *C*-2 ethyl could occupy this region and may form π-stacking interactions with Y96 or H26. Substituents on the aromatic ring could be used to fine-tune the electronics and sterics of the π-system and optimise any interactions with the protein. Substituents on *N*-1 of **18** may project out of the ZA channel and into the more solvent exposed region (Figure 2.22, region highlighted in blue). The additional functionality at *N*-1 may have the potential to H-bond or displace one of the ZA channel water molecules, which could lead to an increase in affinity of the compound. Overall, the *in silico* studies revealed two promising areas for further compound development and SAR studies, which are described in the next chapter.

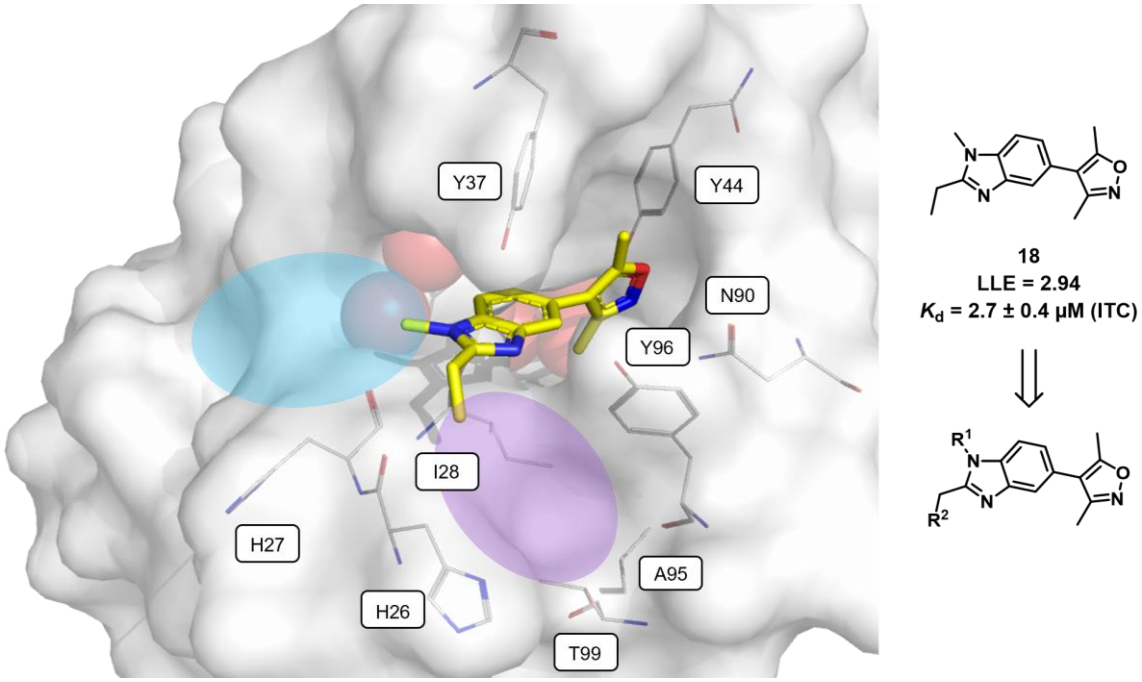

Figure 2.22. Compound **18** (carbon = yellow) docked in the binding site of *Ld*BD5.1 (carbon = white, PDB code: 6BYA) using GOLD docking software.[131, 208] Highlighted in purple is the region where analogues of **18** with aromatic substituents (R^2 group) on the *C*-2 ethyl may be able to π-stack with Y96 and H26. Highlighted in blue is the region where substituents on *N*-1 (R^1 group) would extend. The general structure of analogues of **18** is shown on the right.

2.6 Conclusions and further work

The aims of the work described in this chapter were to synthesise a fragment library of compounds containing known human bromodomain ligand KAc mimics to screen against the bromodomains in *Ld*BDF5 and to determine whether any of the motifs bind. It was not feasible to screen all the fragments with *Ld*BDF5.1 and *Ld*BDF5.2 in the waterLOGSY assay due to the solubility and throughput constraints, therefore TSA was employed as an alternative qualitative binding assay. Of the thirty-one KAc mimicking fragments that were synthesised and screened against the *Ld*BDF5.1 and *Ld*BDF5.2 proteins, three compounds (**17**, **18**, and **19**) indicated a binding interaction with the first domain in *Ld*BDF5 in TSA. The TSA with *Ld*BDF5.2 did not indicate any fragments binding to the domain, despite four compounds (**3**, **7**, **8**, and **13**) having been identified as binders in the waterLOGSY assay. To investigate this further, an orthogonal technique, such as ITC, should be used to validate the results of the screening assays with both of the *Ld*BDF5 domains.

All three hit compounds for *Ld*BDF5.1 that were identified in TSA featured a dimethylisoxazole fused to a bicyclic heterocyclic ring. Docking studies with compound **18** indicate that the 3,5-dimethylisoxazole motif acts as an effective KAc bioisostere in the binding site of *Ld*BDF5.1. ITC was used to validate and quantify the binding interaction of compound **18** (K_d = 2.7 ± 0.4 μM).

The fragment screens described in this chapter resulted in the identification of a lead compound that provides a starting point for future SAR studies in *Ld*BDF5.1. Docking of **18** in *Ld*BDF5.1 informed the design of ligands that could be synthesised to investigate the SAR of *Ld*BDF5.1 by identifying two regions within the binding site that are unique to *Ld*BDF5.1 and appear to be able to accommodate additional functionalisation. Thus, a thorough exploration of the SAR between *Ld*BDF5.1 and **18** was undertaken in Chapter 3 to identify higher affinity ligands for the parasite bromodomain, which may help chemically validate the biological importance of *Ld*BDF5.1.

Chapter 3 - Exploring the SAR of modifications to the *N*-1 and *C*-2 positions of fragment 18

3.1 Introduction and aims

Following the fragment-based screening described in Chapter 2, compound **18** was identified as the most promising fragment for further development into ligands for *Ld*BDF5.1. The work described in this chapter focussed on diversifying the scaffold of **18** with the goal of developing compounds with high affinity ($K_d \leq 0.1$ μM) for *Ld*BDF5.1. Docking studies of compound **18** with *Ld*BDF5.1 were undertaken to identify regions where fragment modification may be beneficial. From these docking studies, two regions of the fragment were identified for functionalisation (Figure 3.1). In particular, the *C*-2 ethyl group projects into a cleft where π-stacking interactions with Y96 and H26 could be optimised with aromatic substituents. The docking studies showed that the *N*-1 methyl group projected along the ZA channel region of the KAc binding pocket and into a solvent exposed region. The addition of functional groups at the *N*-1 position may form non-covalent binding interactions with the protein or conserved water molecules in the binding pocket. The 3,5-dimethylisoxazole appeared to act as an effective KAc mimic in *Ld*BDF5.1 and therefore was not modified. The affinities of the compounds synthesised for *Ld*BDF5.1 were evaluated using MST. A thorough exploration of the SAR between *Ld*BDF5.1 and compound **18** was undertaken to identify higher affinity ligands for the parasite bromodomain, which may help chemically validate the biological importance of *Ld*BDF5.1. Thus, the aims of the work described in this chapter were as follows:

- Synthesise analogues of **18** with modifications at the *N*-1 and *C*-2 positions of the fragment benzimidazole core.
- Explore the SAR of the modifications at the *N*-1 and *C*-2 positions of **18** by determining the binding affinities of compounds for *Ld*BDF5.1 using MST.

- Apply the results from the SAR studies to design and synthesise compounds with optimised substituents at the *N*-1 and *C*-2 positions to achieve $K_d \leq 0.1$ μM for *Ld*BDF5.1.

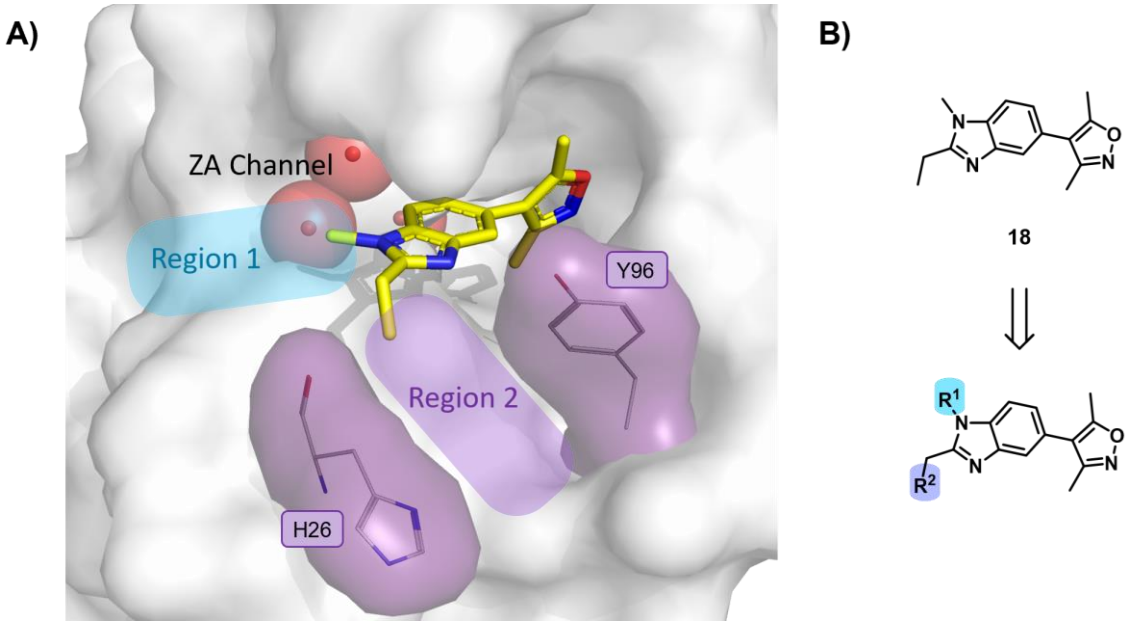

Figure 3.1. A) A view of compound **18** (carbon = yellow**)** docked in the binding site of the X-ray crystal structure of *Ld*BDF5.1 (carbon = white) (PDB code: 6BYA) using GOLD docking software.[131, 208] Highlighted in blue is Region 1, where substituents on *N*-1 (R^1 group) could extend. Highlighted in purple is Region 2, where analogues of **18** with aromatic substituents (R^2 group) on the *C*-2 ethyl may be able to π-stack with Y96 and H26. Docking was performed by Bernadette Lee. **B)** The general structure of analogues of compound **18**.

3.2 Library design

Based on the docking studies discussed in Chapter 2, section 2.5, it was proposed that the functionalisation of the *N*-1 position of **18** with extended side chains containing amino moieties could occupy the ZA channel and the more solvent exposed region in *Ld*BDF5.1, forming additional hydrogen bonding interactions in this area (Figure 3.2, A). Thus, compounds featuring dimethylamine (**104**), *N*-methyl piperazine (**105**), morpholine (**106** and **107**) and pyridine rings (**108** and **109**) at the *N*-1 position were synthesised (Figure 3.2, B). A compound functionalised with a cyclopropane ring (**110**) was also prepared to probe any unexpected hydrophobic interactions that might occur. The ethyl group at the *C*-2 position of this set of compounds was kept consistent to enable matched pair analysis.

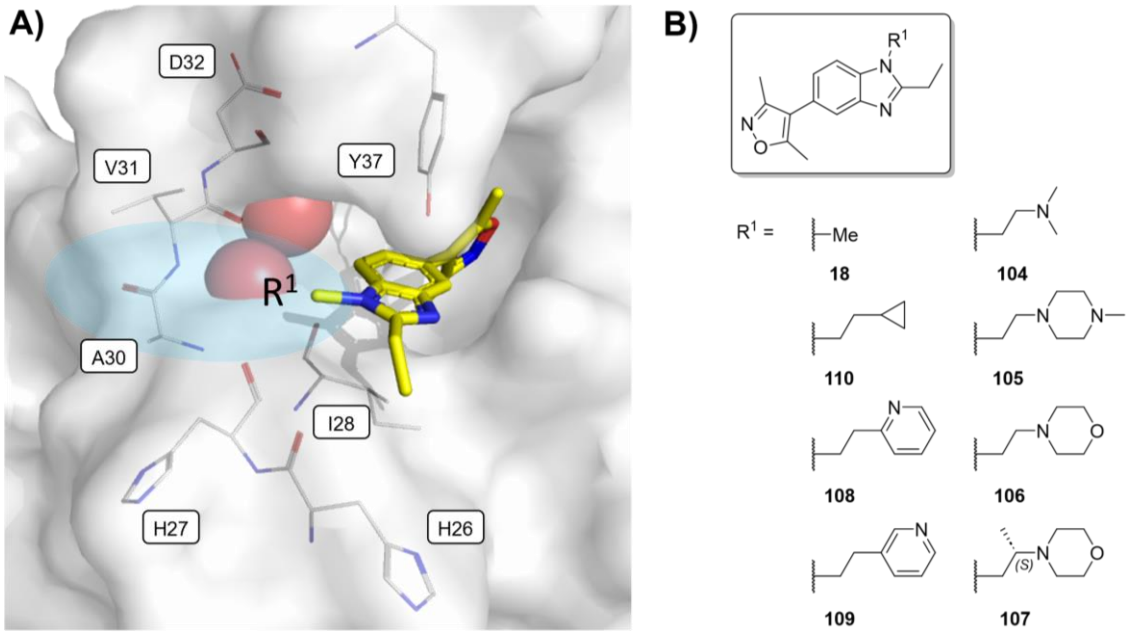

Figure 3.2. A) A view of **18** (carbon = yellow**)** docked in the binding site of the X-ray crystal structure of *Ld*BDF5.1 (carbon = white) (PDB code 6BYA) using GOLD docking software.[131, 208] Highlighted in blue is a region where substituents on *N*-1 (R^1 group) might interact with the protein. Docking was performed by Bernadette Lee. **B)** The general structure of analogues of compound **18**.

Another set of analogues of compound **18** bearing aromatic functional groups at the *C*-2 position were designed and synthesised. It was envisaged that the aryl-functionalised derivatives on the *C*-2 ethyl of **18** might form π-stacking interactions with Y96 and H26 (Figure 3.3). To probe the electronic and steric interactions in the region, aryl rings with

a variety of electron withdrawing and donating groups, as well as substituents of different sizes at either the *meta*- or *para*- positions were synthesised. Two compounds with a methylene linker (**111** and **112**) were included in this library to explore the effects of shortening the ethyl linker. As with the compounds functionalised at *N*-1, the *C*-2 functionalised compounds all contained a methyl group at *N*-1, as featured in compound **18**, such that the effect of the *C*-2 functionalisation could be directly evaluated.

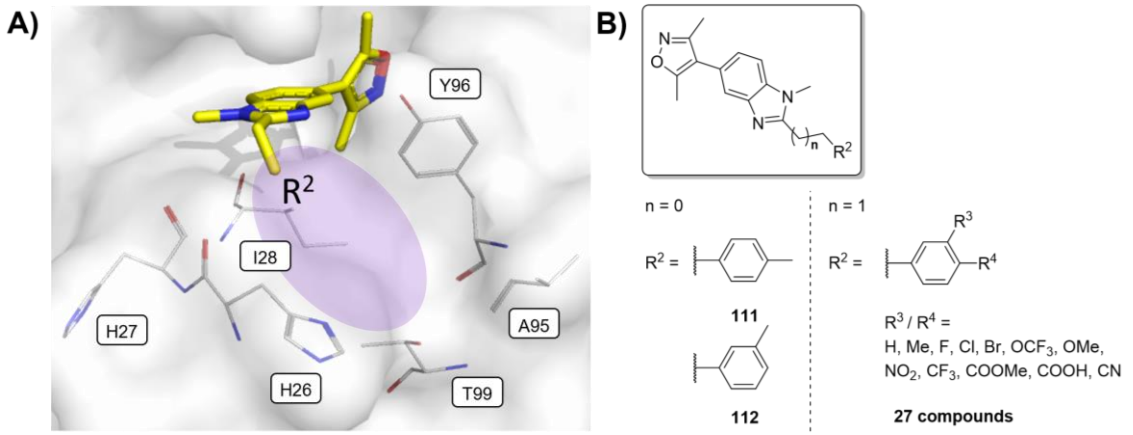

Figure 3.3. A view of **18** (carbon = yellow) docked in the binding site of an X-ray crystal structure of *Ld*BDF5.1 (carbon = white) (PDB code 6BYA) using GOLD docking software.[131, 208] Highlighted in purple is a region where analogues of compound **18** with aromatic substituents (R^2 group) on the *C*-2 ethyl may be able to π-stack with Y96 and H26. Docking was performed by Bernadette Lee.

3.3 Library synthesis

A general synthetic strategy was designed to generate analogues of **18** (Scheme 3.1). The synthetic strategy began with the installation of the dimethylisoxazole moiety — the key KAc mimicking headgroup. A Suzuki coupling was employed for the attachment of the dimethylisoxazole moiety to provide compound **74**. The presence of the nitro group *ortho*- to the fluorine of compound **74** allowed for a high diversity of functional groups to be installed *para*- to the dimethylisoxazole *via* S_NAr substitutions. It was envisioned that a coupled reduction/cyclisation step following procedures reported by Hay *et al.* would afford the desired benzimidazole targets (general structure of compound **113**) with further diversification at *C*-2 (step **d** and step **e** in Scheme 3.1).[69]

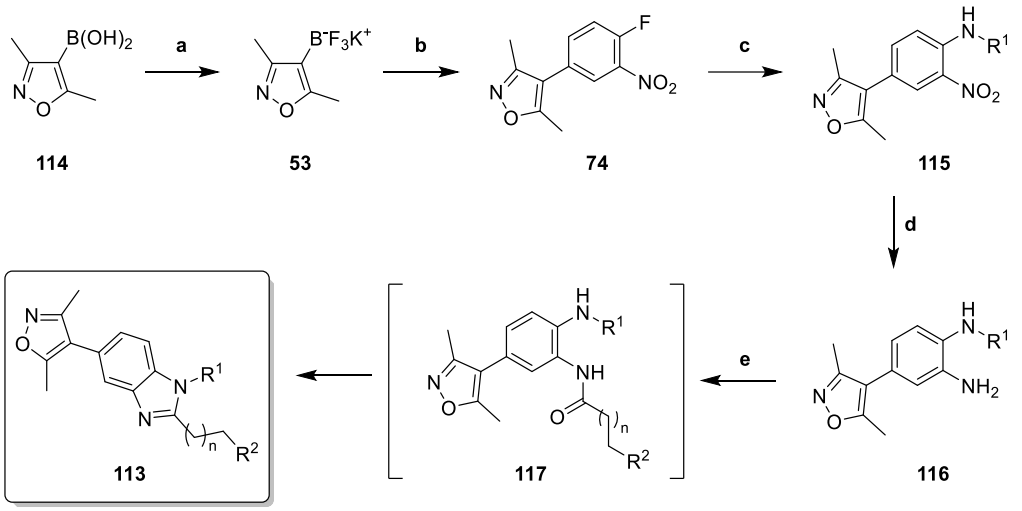

Scheme 3.1. General synthetic route to synthesise analogues of **18** with diversification at R^1 and R^2. *Reagents and conditions:* **a)** Potassium fluoride, L-(+)-tartaric acid, THF, acetonitrile, rt, 30 min, 73%; **b)** 4-Bromo-1-fluoro-2-nitrobenzene, $NaHCO_3$, $Pd(dppf)Cl_2 \cdot CH_2Cl_2$, DME/$H_2O$, 110 °C, 3 h, 76%; **c)** R^1-NH_2, DIPEA, DMF, 80 °C, 51–99%; **d)** 1 M $Na_2S_2O_{4\,(aq)}$, EtOH, 80 °C, crude; **e)** see Table 3.1. Yields are reported in Table 3.2 and Table 3.3.

Table 3.1. Methods and the reagents and conditions for step **e** in Scheme 3.1. The methods are colour coded for future reference.

Method	Reagents and conditions
A	Propylphosphonic anhydride (≥50 wt. % in ethyl acetate), propionic acid, DIPEA, ethyl acetate, 80 °C, 6-17 h
B	**i)** Propionic acid, HATU, DIPEA, DMF, rt, 16 h; **ii)** propionic acid, reflux, 17 h
C	**i)** (R^2)-Propionic acid, HATU, DIPEA, DMF, rt, 16 h; **ii)** (R^2)-propionic acid, toluene, reflux with 3 Å MS, 17-72 h
D	**i)** R^2-propionic acid, HATU, DIPEA, DMF, rt, 3-16 h; **ii)** toluene, reflux with 3 Å MS, 24-48 h
E	**i)** R^2-propionic acid, HATU, DIPEA, DMF, rt, 3-16 h; **ii)** acetic acid, reflux, 17-32 h
F	Propylphosphonic anhydride (≥50 wt. % in ethyl acetate), 3-(3-chloro-4-methoxyphenyl)propionic acid, DIPEA, ethyl acetate, 80 °C, 1 h

As discussed in Chapter 2, section 2.2.3, due to the tendency of the boronic acid **114** to undergo proto-deborylation, the trifluoroborate **53** was instead used as a coupling partner.[182] Potassium 3,5-dimethylisoxazole-4-trifluoroborate **53** was synthesised from 3,5-dimethylisoxazole-4-boronic acid **114**, then the Suzuki coupling of the trifluoroborate with commercially available 4-bromo-1-fluoro-2-nitrobenzene yielded compound **74** in 76% yield (Scheme 3.1). The key intermediate **74** was synthesised on a 10 g scale. Analogues of **18** with different functional groups installed at the *N*-1 position were prepared from 4-(4-fluoro-3-nitrophenyl)-3,5-dimethylisoxazole **74** by aromatic nucleophilic substitution with different amines. These reactions proceeded in yields ranging from 51–99% (Table 3.2). Then, sodium dithionite provided a fast (5–15 min) and efficient reduction of the aromatic nitro group in compounds of the general structure

115. The reducing reagent acts as a single electron transfer donor to facilitate reduction *via* hydroxylamines by a six electron mechanism (Figure 3.4).[209]

Table 3.2. Yields for the reactions in step **c** for analogues of **18** varied at the R^1 position ranged from 51-99%.

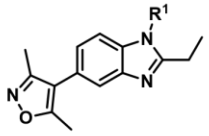

Compound	R^1	Yield in step c
18		93%*
110	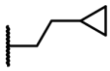	71%
108	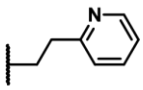	62%
109	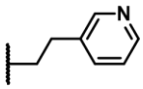	85%
104		51%
105	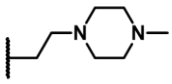	83%
106	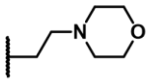	99%

*yield for 15 g scale reaction

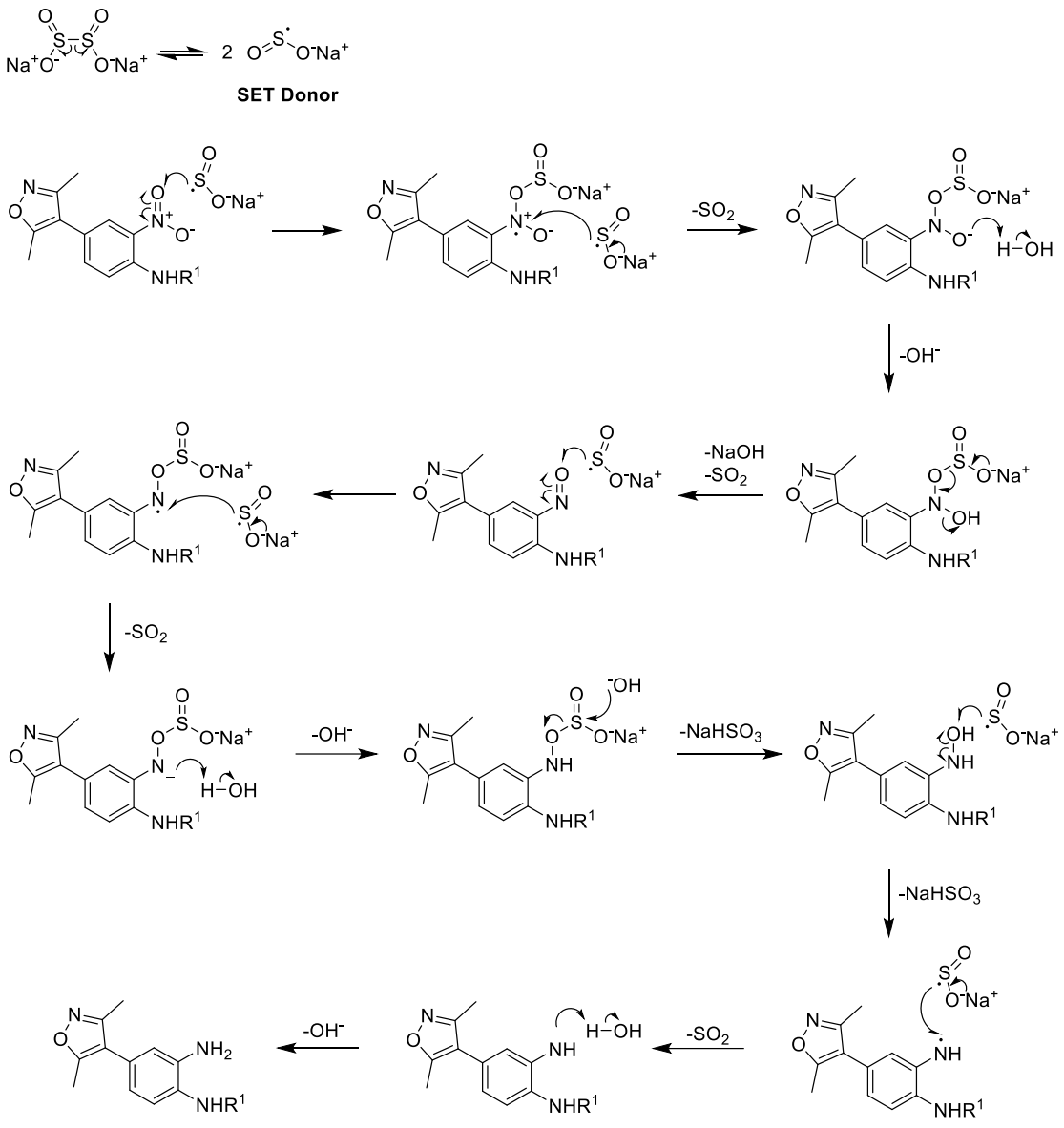

Figure 3.4. Proposed mechanism for sodium dithionite-mediated reduction of the aromatic nitro group in compounds of the general structure **115**.[209]

Anilines of the general structure **116** were carried forward without purification after the reduction in step **d**, Scheme 3.1. A range of different methods were employed to form the benzimidazole rings in compounds of the general structure **113** (Scheme 3.1). The methods A–F for step **e**, (Table 3.1) involve either a one-pot, T3P-promoted cyclodehydration with propionic acid, or a two-step procedure in which a HATU-mediated amide coupling is followed by an intramolecular cyclisation (promoted by heating under reflux in toluene, or under acidic conditions).

Table 3.3. Yield and method used for the reactions in step **e** to generate analogues of **18** varied at either the R^1 or R^2 position.

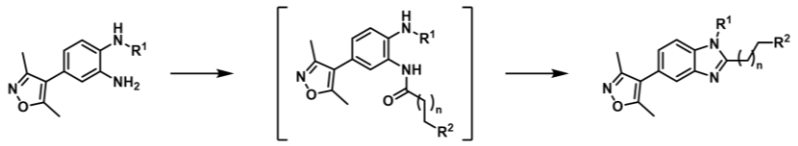

Compound	n	R^1	R^2	Method for step e	Yield in step e
18	0	Me	H	A	62%
110	0		H	A	25%
108	0	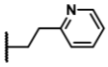	H	A	24%
137	1	Me		C	38%
121	1	Me		E	21%
122	1	Me		E	19%
149	1	Me		C	21%
150	1	Me		C	39%
120	1	Me	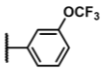	E	21%
139	1	Me	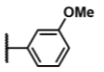	C	11%
151	1	Me		C	99%
153	1	Me		D	55%
145	1	Me	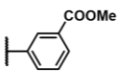	D	71%
147	1	Me	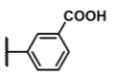	D*	89%
112	0	Me		C	96%
141	1	Me	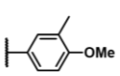	C	43%

Compound	n	R^1	R^2	Method for step e	Yield in step e
104	0		H	B	30%
109	0	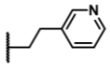	H	B	26%
105	0	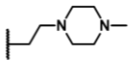	H	C	56%
106	0	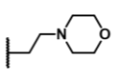	H	C	58%
138	1	Me		C	89%
123	1	Me		E	45%
176	1	Me	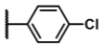	D	84%
125	1	Me	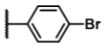	D	95%
144	1	Me	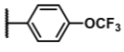	D	87%
142	1	Me	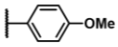	C	46%
152	1	Me	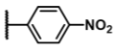	C	50%
177	1	Me	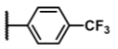	C	77%
146	1	Me	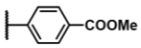	D	79%
148	1	Me	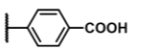	D*	90%
111	0	Me		C	72%
143	1	Me	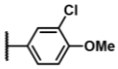	F	32%

*Compound **147** was synthesised from **145**. Compound **148** was synthesised from **146**. *Reagents and conditions*: 2 M NaOH in EtOH, 50 °C, 1.5 h.

3.3.1 Optimisation of the benzimidazole cyclisation

A number of different methods (A–F, Table 3.1) were employed to promote the intramolecular cyclisation and the benzimidazole ring formation to produce final compounds. The methodology was optimised to improve the synthetic efficiency and yields throughout the project. Initial conditions for the cyclisation step involved heating the anilines **116** with propionic acid under dehydrating conditions with propylphosphonic anhydride (T3P) to yield the final compounds **18**, **110** and **108**. T3P functioned as both a coupling agent and water scavenger in the cyclisation reaction (Figure 3.5).[210] However, the rate of T3P-promoted cyclodehydration appeared to be slow for compounds **18**, **110** and **108**, and the reaction did not go to completion after stirring for 17 h at rt. The amide (general structure of **117**), hemiaminal intermediate, and desired product (general structure of **113**), all exhibited very similar R_f values by TLC, which made both the monitoring of the reaction by TLC and purification using flash column chromatography challenging. Consequently, the yields for this reaction with **110** and **108** were low (Table 3.3). The T3P reaction may have been improved by increasing the temperature of the reaction, or heating in a microwave reactor.[211] However, it was decided that isolating the amide intermediate prior to cyclisation would give two cleaner synthetic steps, hopefully improving the overall yield of the cyclodehydration. For compounds **109**, **104**, **105** and **106**, the amide intermediates (general structure of **117**) were synthesised using a HATU-mediated amide coupling approach with propionic acid. The amides were then heated under reflux in propionic acid to provide the desired benzimidazoles **109** and **104** in 26–30% yield. Higher yields (56–58%) were achieved for compounds **105** and **106** by heating under reflux in toluene with a sub-stoichiometric amount of propionic acid (Table 3.2). 3 Å molecular sieves were also used in the reaction vial to keep the reaction mixture anhydrous and facilitate the elimination of water in the final step of benzimidazole formation.

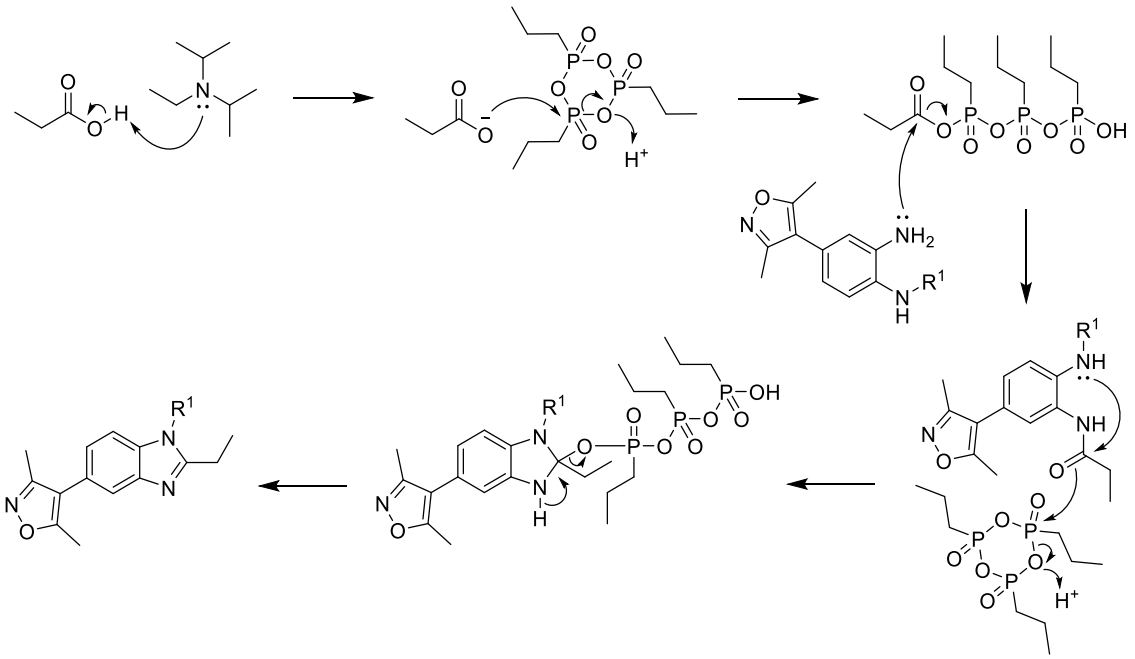

Figure 3.5. Proposed mechanism for T3P promoted cyclodehydration.

For compounds bearing aromatic functional groups at the *C*-2 position, the synthetic approach required the initial installation of a methyl group at *N*-1. Compound **75** was synthesised on a 15 g scale from 4-(4-fluoro-3-nitrophenyl)-3,5-dimethylisoxazole **74** by nucleophilic aromatic substitution with methylamine (Scheme 3.2). The compounds featuring a methyl group at *N*-1 were prepared from the same common intermediate **75** *via* the reduction, amidation, and cyclisation steps described in Scheme 3.1. When intermediates were heated under reflux in acetic acid during the benzimidazole ring formation (step **d** in Scheme 3.2, method E in Table 3.3), the formation of side product **118** was commonly observed and the yields of the product were low (19–45%). To decrease the formation of **118**, the cyclisation was optimised by heating the amide intermediates (general structure of **119**) under reflux in toluene with 3 Å molecular sieves. A sub-stoichiometric amount of acid was found to be unnecessary in this step. Compounds **125**, **144-146, 153**, and **176** synthesised using this method (method D, Table 3.3) had the highest yields (55–95%).

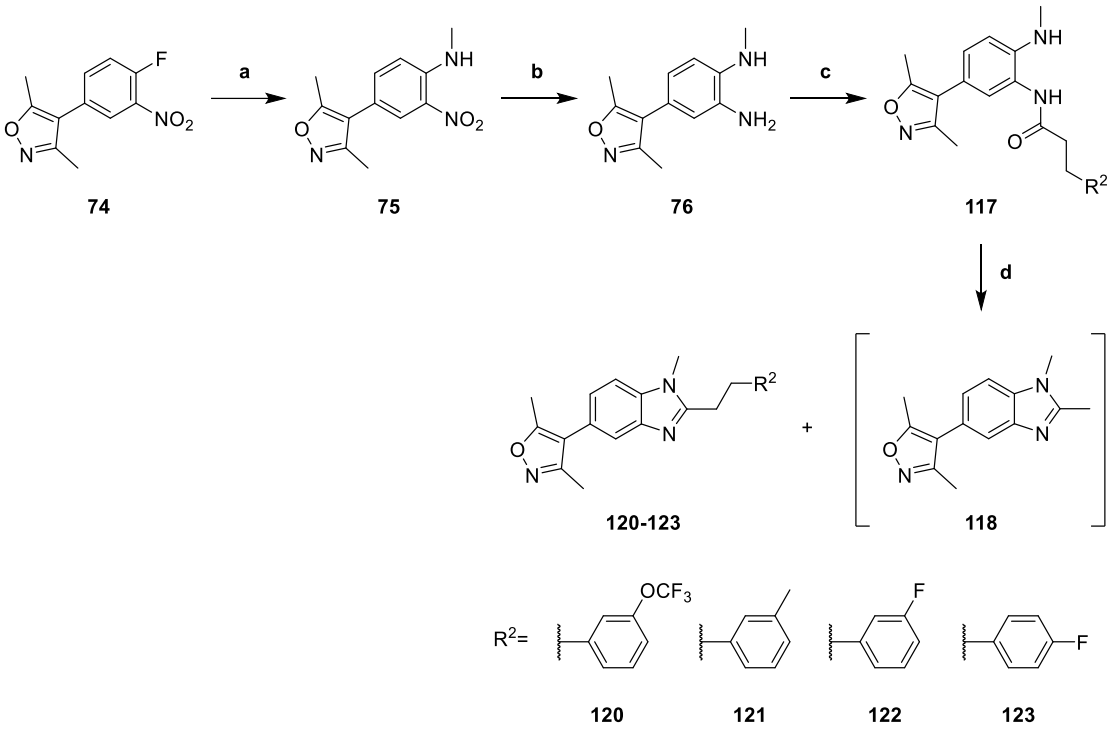

Scheme 3.2. Synthesis of compounds **120**, **121**, **122** and **123**. *Reagents and conditions:* **a)** $MeNH_2$, DIPEA, DMF, 80 °C, 1 h, 93%; **b)** 1 M $Na_2S_2O_{4\ (aq)}$, EtOH, 80 °C, 10 min, crude; **c)** HATU, DIPEA, DMF, rt, 3-16 h, crude; **d)** Acetic acid, reflux, 17–32 h, **120:** 21%, **121:** 21%, **122:** 19%, **123:** 45%.

3.3.2 HATU-promoted benzimidazole formation

It was thought that using HATU as a coupling reagent would solely yield the amide intermediate (general structure of **117**) in step **e** (Scheme 3.1). Although the HATU coupling approach did effectively provide the amide intermediates **117**, the products isolated after column chromatography were not always pure when assessed using ^{1}H NMR. Some of the ring-closed benzimidazole was also observed in the ^{1}H NMR of the amide intermediates (for an example, see Figure 3.6).

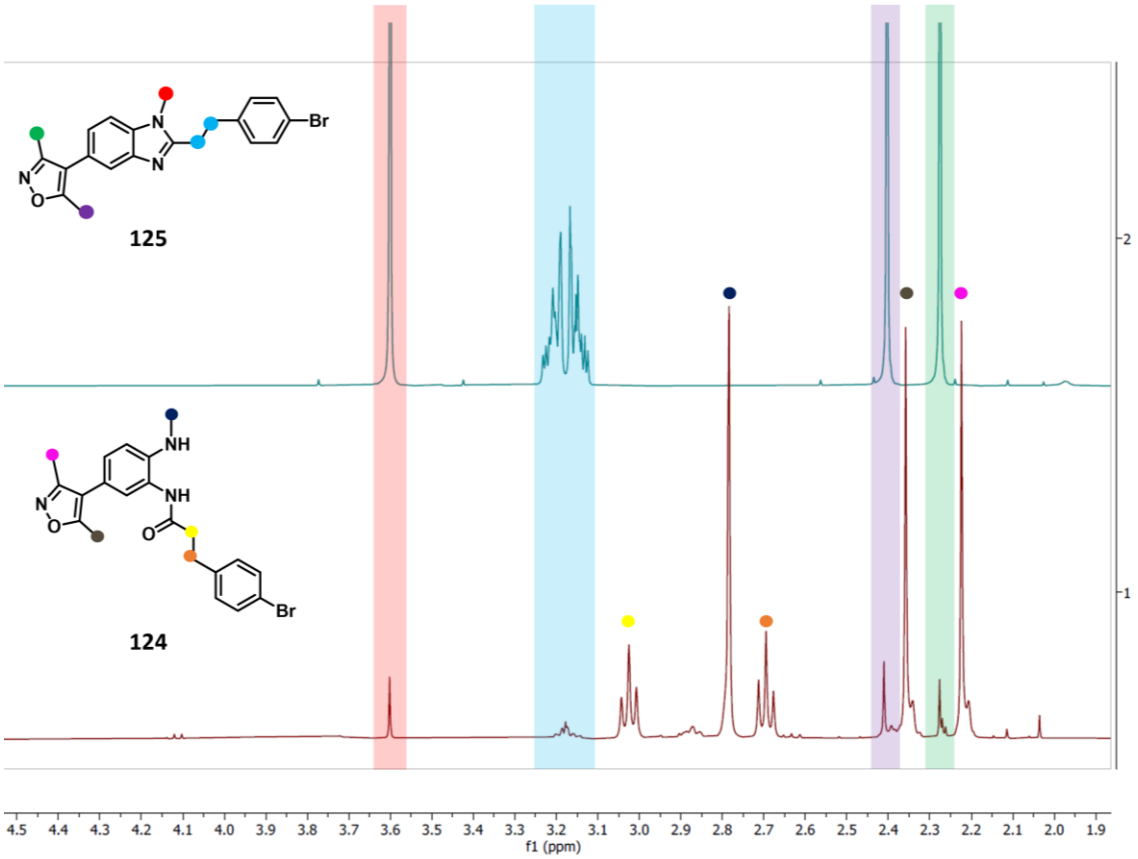

Figure 3.6. Partial ^{1}H NMR spectra of the amide intermediate **124** (bottom spectrum) and benzimidazole **125** (top spectrum). Highlighted in red, blue, purple and green are signals present in compound **125** that were also present in the NMR spectrum of the amide intermediate **124**.

Barasa and Yoganathan have shown that the hexafluorophosphate benzotriazole tetramethyl uronium (HBTU) coupling reagent can act as an effective promoter of benzimidazole synthesis.[212] The authors suggest that HBTU behaves as an activating agent and promotes benzimidazole formation by activation of the aryl amide intermediate.[212] HATU is structurally similar to HBTU, but exhibits increased reactivity, and was likely playing a similarly important mechanistic role in the formation of benzimidazoles (Scheme 3.3).[213] It was proposed that the intermediate amide **117** was activated by HATU, where the amide oxygen reacted with the uronium and a molecule of 1-hydroxy-7-azabenzotriazole (HOAt, **126**) was eliminated. Then, the aryl amine **127** reacted to eliminate a molecule of tetramethylurea **128** and formed the desired benzimidazole **113**.

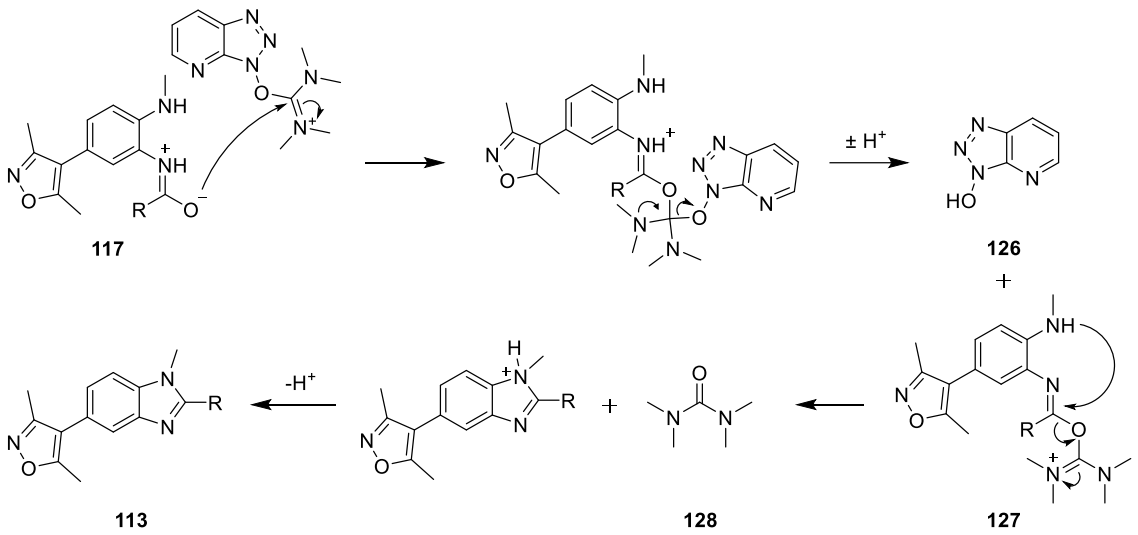

Scheme 3.3. A proposed mechanism of the HATU promoted cyclisation.

As the conditions used for the amide coupling to produce the intermediate (general structure of **117**) also produced some amount of the desired benzimidazole (general structure of **113**), the mixture of the intermediate **117** and final product **113** were carried forward in the synthesis without further purification.

3.3.3 Synthesis of compound 107

Compound **107** was synthesised with a methyl group on the morpholino-ethylene moiety *N*-1 position of the core benzimidazole, as features in the **SGC-CBP30** human bromodomain inhibitor. The synthesis of compound **107** required a modified synthetic route to the one outlined in Scheme 3.1 because (*S*)-2-morpholinopropan-1-amine was not commercially available for the S_NAr reaction in step **c**. A retrosynthetic analysis of the desired S_NAr product (compound **129**) revealed compound **130** to be a key building block (Scheme 3.4). It was important to have diamine **130** mono-protected to achieve regioselectivity in the S_NAr reaction.

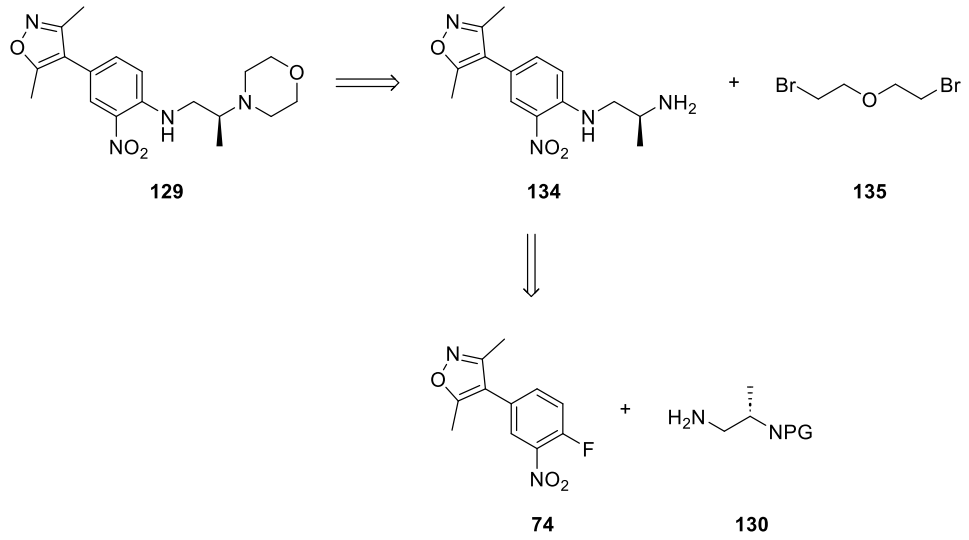

Scheme 3.4. Retrosynthetic analysis of compound **129**. NPG = nitrogen protecting group.

Compound **130** was synthesised from commercially available (*S*)-2-aminopropan-1-ol **131** (Scheme 3.5). The alcohol **131** was activated by PPh_3 and DIAD followed by reaction with phthalimide to produce **132**. The mono-protected diamine **130** was generated by reaction of **132** with hydrazine. Reaction of **130** with 4-bromo-1-fluoro-2-nitrobenzene **74** gave **133**. Compound **133** was then deprotected using TFA to give primary amine **134**. Reaction of **134** with 1-bromo-2-(2-bromoethoxy)ethane **135** afforded compound **129**. The desired compound **107** was obtained by reduction of the nitro group in compound **129**, coupling the aniline intermediate to propionic acid to give **136**, and subsequent cyclisation to form the benzimidazole ring (Scheme 3.5).

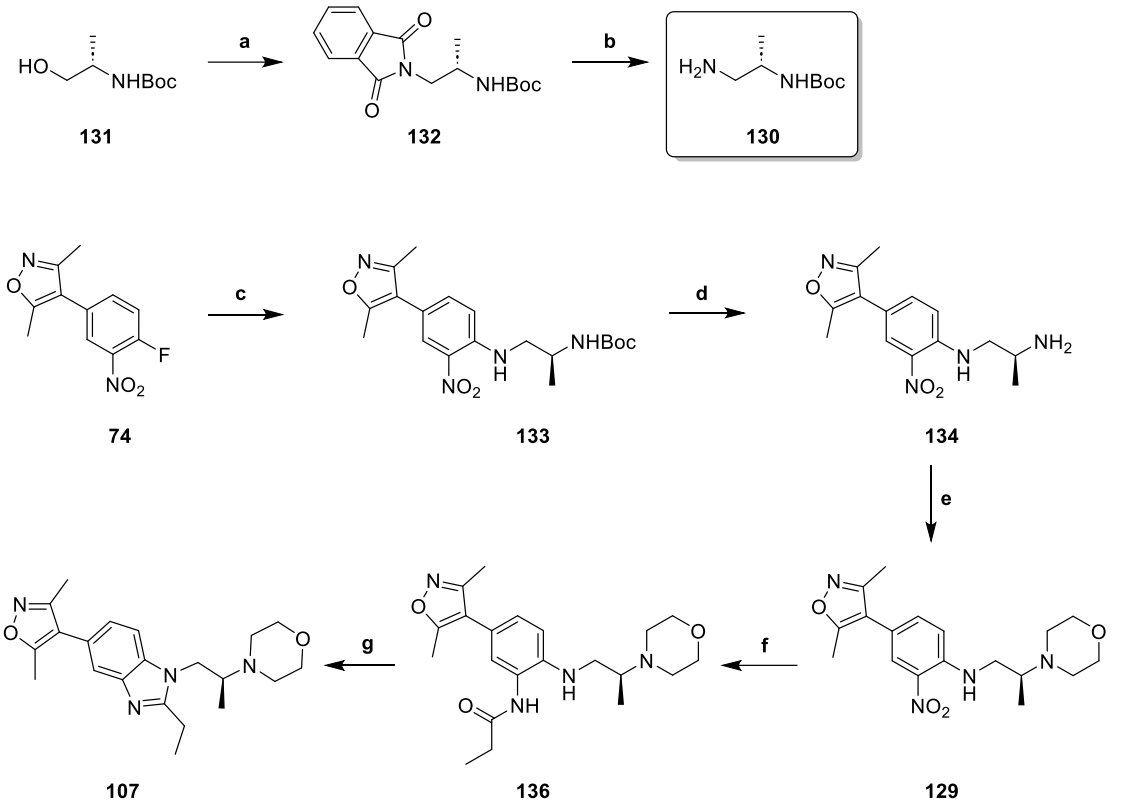

Scheme 3.5. Synthesis of **107**. *Reagents and conditions:* **a)** Phthalimide, DIAD, PPh_3, THF, 0 °C to rt, 3 h, 40%; **b)** Hydrazine monohydrate, ethanol, reflux, 2 h, 88%; **c) 130**, DIPEA, DMF, 80 °C, 17 h, 62%; **d)** TFA, CH_2Cl_2, rt, 2 h, 54%; **e)** 1-Bromo-2-(2-bromoethoxy)ethane, K_2CO_3, DMF, 80 °C, 3 h, 22%; **f) i)** 1 M $Na_2S_2O_{4\,(aq)}$, EtOH, 80 °C, 10 min; **f) ii)** Propylphosphonic anhydride (≥50 wt.% in ethyl acetate), propionic acid, DIPEA, ethyl acetate, 80 °C, 17 h; **g)** Toluene, reflux, 17 h, 23% (3 steps).

3.3.4 Summary of the synthetic library of analogues of compound 18

A total of thirty-two analogues of compound **18** were synthesised with modifications at either the *C*-2, or *N*-1 position on the core benzimidazole to investigate the SAR in two different regions of the binding site in *Ld*BDF5.1. The binding affinities of these compounds with *Ld*BDF5.1 were then evaluated using MST.

3.4 Determination of compound binding affinities for *Ld*BDF5.1 using microscale thermophoresis

MST was used to determine compound affinity for *Ld*BDF5.1. The MST assay was chosen to screen the library of analogues of **18** because it is a high-throughput technique and enables quantification of the compound binding affinities for *Ld*BDF5.1 with low

consumption of the protein and ligand. In this assay, the His tags on the *Ld*BDF5.1 recombinant protein were labelled with a RED-tris-NTA dye.

3.4.1 MST binding affinity data for R[1]-functionalised compounds

The compounds synthesised in section 3.3 with functionalisation at the *N*-1 position were analysed for binding affinity to *Ld*BDF5.1 using MST as described above. The results of these experiments are summarised in Table 3.4. The chromlog$D_{7.4}$ value and the solubility forecast index (SFI) value for each compound are also reported. These are useful parameters for predicting compound solubility, which can impact the generation of quality binding data in biophysical assays. Lipophilicity reflects the affinity of a molecule for an aqueous or lipophilic environment and is often quantified using logD, which is the distribution coefficient in octanol-water at a given pH.[214] A chromatographic logD assay (as detailed in the Experimental section 6.1) was conducted to calculate the chromlog$D_{7.4}$ value for each compound.[215] The solubility Forecast Index (SFI = clog$D_{7.4}$ + #Ar) accounts for the number of aromatic rings in a compound, since increased aromaticity in a compound is generally associated with reduced solubility.[205] If the SFI value is < 5 then there is a reasonable chance of having good solubility.

Table 3.4. Analogues of **18** substituted at *N*-1 and the binding affinity (K_d) for each compound measured in the MST assay. The error quoted is the standard error of the mean (SEM) of n = 3 technical repeats. SFI is the solubility forecast index (SFI = Chromlog$D_{pH7.4}$ + number of aromatic rings).[205]

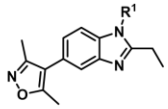

Low affinity — High affinity

Compound	R[1]	K_d (nM)	Chrom log$D_{7.4}$	SFI	Compound	R[1]	K_d (nM)	Chrom log$D_{7.4}$	SFI
18		1410 ± 84.0	3.6	6.6	**104**		1120 ± 120	3.2	6.2
110		1640 ± 296	5.5	8.5	**105**	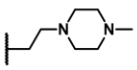	1540 ± 323	2.0	5.0
108	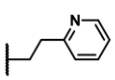	5130 ± 833	3.9	7.9	**106**	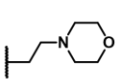	594 ± 84.0	3.4	6.4
109	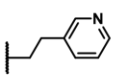	1720 ± 195	3.3	7.3	**107**	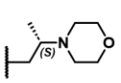	580 ± 195	3.9	6.9

These data show that the presence of a cyclopropane group at the R^1 position did not improve the binding affinity for *Ld*BDF5.1. The cyclopropane analogue **110** measured a similar binding affinity to the initial hit compound **18** (*cf.* K_d = 1640 ± 296 nM and 1410 ± 84.0 nM, respectively). The similar binding affinity of **110** to **18** could be due to the absence of additional binding interactions between the cyclopropyl group and the suspected region of binding for R^1-functionalised compounds in ZA channel.

The addition of a 2-pyridyl group to the *N*-1 ethyl on the core scaffold of **18** resulted in a decrease in binding affinity for *Ld*BDF5.1. For compound **109**, the binding affinity was comparable to that of **18** (*cf.* K_d = 1720 ± 195 nM and 1410 ± 84.0 nM), whereas for compound **108**, there was a two to three-fold decrease in affinity (K_d = 5130 ± 833 nM). The small structural change between **108** and **109**— the presence of the pyridyl nitrogen atom at the 2-position instead of the 3-position — appeared to have an effect on binding affinity. It is possible that the two compounds adopt different binding poses in the *Ld*BDF5.1 binding site, or that the presence of the pyridyl nitrogen at the 2-position allows for an intramolecular non-covalent interaction that prevents binding to the target. The 3-pyridyl nitrogen in compound **109** could also be H-bonding to a water molecule in the ZA channel.

The compounds **104**, **106** and **107**, which feature more hydrophilic sidechains, showed increased binding affinity for *Ld*BDF5.1 compared to **18** (*cf.* K_d = 1120 ± 120 nM, 598 ± 84 nM and 580 ± 121 nM, with 1410 ± 84.0 nM, respectively). Notably, the morpholine-containing analogues **106** and **107** showed over a two-fold increase in affinity. Compound **107** was synthesised with a methyl group on the morpholino-ethylene moiety to constrain the conformation of the linker. However, compound **107** did not show any change in binding affinity compared to **106** (*cf.* K_d = 580 ± 121 nM and 598 ± 84.0 nM). The larger increase in affinity for analogues **106** and **107** may be because the compounds are forming an additional interaction in the binding site. From an inspection of compound **106** docked in the *Ld*BDF5.1 protein, it appeared that the nitrogen atom of the morpholine ring could form a hydrogen bonding interaction to a conserved water molecule in *Ld*BDF5.1 (Figure 3.7).

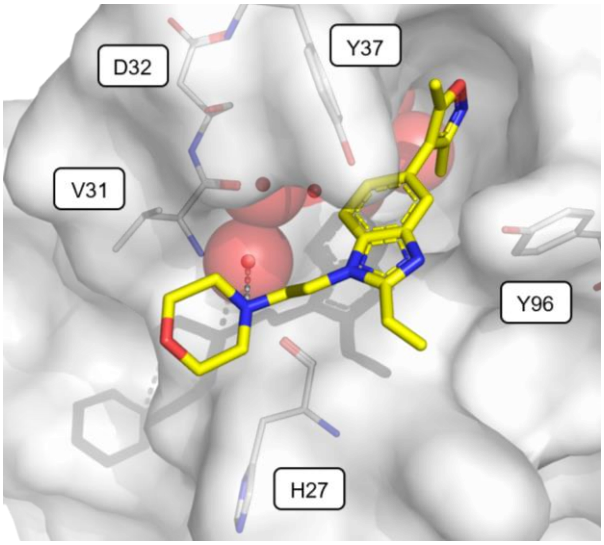

Figure 3.7. A view of compound **106** (carbon = yellow) docked in binding site of an X-ray crystal structure of *Ld*BDF5.1 (carbon = white) (PDB code 6BYA) using GOLD docking software.[131, 208] The nitrogen atom of the morpholine ring appears to form a hydrogen bonding interaction to a conserved water molecule in the ZA channel. Docking was performed by Bernadette Lee.

While compound **104** features a nitrogen at the same position as in compounds **106** and **107**, the dimethylamine group of compound **104** is more likely to be protonated at pH 7.4 due to the higher pKa of the dimethylamine compared to that of the nitrogen in the morpholine ring. Protonation of the dimethylamine nitrogen would prevent the nitrogen lone pair from forming hydrogen bonding interactions with the water molecule highlighted in Figure 3.7. The absence of this interaction with compound **104** could explain why the binding affinity was lower than that of the morpholine-containing compounds **107** and **106**. The *N*-methyl piperazine-containing compound **105** gave similar binding affinity to that of **18** (*cf.* K_d = 1540 ± 323 nM and 1410 ± 84.0 nM, respectively). The pKa of the piperazine nitrogen at the 4-position in compound **105** is largely influenced by the *N*-methyl group. In the MST assay conditions at pH 7.4, some species of **105** may be protonated at the piperazine nitrogen, decreasing the ability of this compound to form the same proposed hydrogen bonding interaction to the water molecule in *Ld*BDF5.1. To further probe the influence of the pKa of the nitrogen atom on the binding affinity of analogues of **18**, it would be interesting to synthesise the unmethylated piperazine analogue, or a piperidine at the same position.

The MST binding affinity data for R^1-functionalised compounds indicated that compounds **107** and **106**, which feature a morpholino-ethyl group, displayed the greatest binding affinities for *Ld*BDF5.1. Thus, the morpholino-ethylene was deemed the best

substitution at R^1. Given that compound **106** could be synthesised in fewer steps than **107** and exhibited similar binding affinity, **106** was selected as the lead compound from this set of *N*-1-functionalised analogues.

3.4.2 MST binding affinity data for R^2-functionalised compounds

Table 3.5 shows the MST results for compounds whose structures vary at the *C*-2 position of the benzimidazole. The *C*-2 ethyl of **18** was initially functionalised with a benzene ring to generate compound **137**, which had a K_d of 2470 ± 702 nM. Although the error (SEM) in affinity measurements for compound **137** was large, the data suggest that binding to *Ld*BDF5.1 did not improve with an unsubstituted aromatic ring at the *C*-2 ethyl of **18**. However, when the aromatic ring was functionalised at the *meta*- or *para*- position, it was possible to increase the binding affinity of **137** for *Ld*BDF5.1 (Table 3.5).

Table 3.5. Analogues of **18** substituted at *C*-2 and the binding affinity (K_d) for each compound measured in the MST assay. The error quoted is the standard error of the mean (SEM) of n = 3 technical repeats.

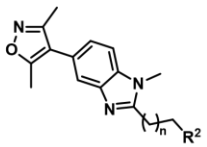

Low affinity — High affinity

Compound	n	R²	K_d (nM)	Chrom $logD_{7.4}$	Compound	n	R²	K_d (nM)	Chrom $logD_{7.4}$
18	1	H	1410 ± 84.0	3.6	**137**	1		2470 ± 702	5.4
121	1		599 ± 29.4	6.0	**138**	1	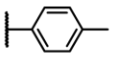	526 ± 131	6.0
122	1		1290 ± 145	5.5	**123**	1	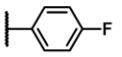	962 ± 13.8	5.4
149	1		3140 ± 449	5.9	**176**	1	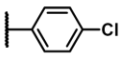	1450 ± 146	5.9
150	1		309 ± 33.0	6.0	**125**	1	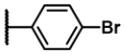	600 ± 38.9	6.0
120	1	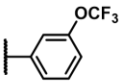	840 ± 46.4	6.2	**144**	1	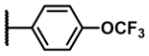	656 ± 61.5	6.3
139	1	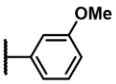	770 ± 143	5.3	**142**	1	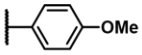	845 ± 120	5.3
151	1	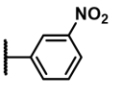	96.4 ± 10.2	5.2	**152**	1	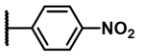	308 ± 20.4	5.2
153	1	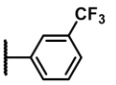	3610 ± 770	6.2	**177**	1	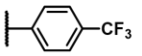	1830 ± 148	6.2
145	1	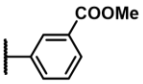	814 ± 131	5.1	**146**	1	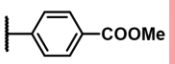	383 ± 48.0	5.0
147	1	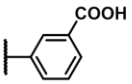	2550 ± 296	2.2	**148**	1	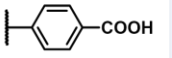	1150 ± 261	2.1
112	0		1080 ± 121	5.5	**111**	0	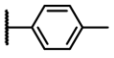	2420 ± 218	5.5
141	1	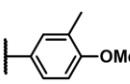	218 ± 104	5.9	**143**	1	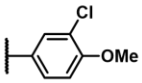	353 ± 89.2	5.5

An electron-donating methyl group on the aryl ring was tolerated with **121** and **138** showing more than two-fold increase in binding affinity for *Ld*BDF5.1 compared to **18** (*cf.* K_d = 599 ± 29.4 nM, 526 ± 131 nM, and 1410 ± 84.0 nM respectively). When the ethyl linker in compound **121** was shortened to a methylene in compound **112**, the binding affinity decreased from K_d = 599 ± 29.4 nM to K_d = 1080 ± 121 nM. Similarly, shortening the linker in compound **138** to generate compound **111** resulted in a small decrease in binding affinity from K_d = 526 ± 131 nM to K_d = 2420 ± 218 nM. These results indicate that the *C*-2 ethyl linker length and flexibility may be important for maintaining key binding interactions of the methyl-substituted aryl ring with *Ld*BDF5.1.

Compounds containing methoxy groups on the phenyl ring at R^2, showed comparable affinity for *Ld*BDF5.1 to the analogous methyl-functionalised compounds. *Meta*-methoxy substituted compound **139** had K_d = 770 ± 143 nM, compared to the *meta*-methyl substituted compound **121** with K_d = 599 ± 29.4 nM. Similarly, the *para*-methoxy substituted compound **140** had K_d = 845 ± 120 nM, compared to the *para*-methyl substituted compound **138** with K_d = 526 ± 131 nM. However, the combination of a *meta*-methyl and *para*-methoxy group in **141** resulted in a higher affinity compound than the mono-substituted analogues **121** and **142** (*cf.* K_d = 218 ± 104 nM, K_d = 599 ± 29.4 nM and K_d = 845 ± 120 nM, respectively). The combination of a *meta*-chloro and *para*-methoxy group in **143** also resulted in a high affinity compound (K_d = 353 ± 89.2 nM). It is possible that the addition of a substituent at the *meta*-position of **142** induces a favourable conformational change of the compound in the binding site of *Ld*BDF5.1 or improves the π-stacking interaction with Y96.

The trifluoromethoxy is a strong electron-withdrawing group, whereas the methoxy group is electron-donating. Although the trifluoromethoxy group and the methoxy group alter the electronics of the aromatic ring in different ways, the binding affinities for compounds **120**, **139**, **142**, and **144** were similar (*cf.* K_d = 840 ± 46.4 nM, K_d = 770 ± 143 nM, K_d = 845 ± 120 nM, and K_d = 656 ± 61.5 nM, respectively). The binding affinities for the methyl ester analogues **145** and **146** were K_d = 814 ± 131 μM and K_d = 383 ± 48.0 μM, respectively. The binding affinity of compounds **145** and **146** for *Ld*BDF.1 were three to four-fold higher than they were for the related carboxylic acid analogues, **147** (K_d = 2550 ± 296 nM) and **148** (K_d = 1150 ± 261 nM). However, the differences in affinities between these two sets of molecules can likely be attributed to the poor solubility of the carboxylic acid-containing compounds in the assay conditions.

The addition of a fluorine to the *meta*- or *para*-position of the phenyl ring did not result in a significant increase in affinity. Compounds **122** and **123** had a K_d of 1290 ± 145 nM and K_d = 962 ± 13.8 nM, respectively. The binding affinity decreased by two-fold when a chlorine was substituted at the *meta*-position of the phenyl ring — **149** had a binding affinity of K_d = 3140 ± 449 nM. Conversely, when the *meta*-position of the phenyl ring was substituted with a bromine, the binding affinity increased by more than four-fold (**150** had K_d = 309 ± 33.0 nM whereas **18** had a K_d of 1410 ± 84.0 nM). The high affinity for the bromo-containing compound **150** might be explained by the greater potential for bromine to form halogen bonds with the protein compared to chlorine. Halogen bonds can form between a halogenated ligand and accessible Lewis bases in a protein binding site.[216] The backbone carbonyl oxygen is the most prominent Lewis base involved in halogen bonding in protein binding sites, however, halogen bonds can also be formed with side chain groups such as hydroxyl, sulfurs, and π-surfaces.[216] Halogen bonding would be stronger for the bromine substituent compared to the chlorine or fluorine because polarisability significantly increases with atomic size, playing a key role in stabilising halogen bonding interactions.

The most promising compound tested was **151** which featured a *meta*-nitrophenyl group at R^2. Compound **151** had a K_d of 96.4 ± 10.2 nM — a ten-fold increase in binding affinity for *Ld*BDF5.1 compared to **18** (K_d = 1410 ± 84.0 nM). Compound **152**, functionalised with a *para*-nitrophenyl group, demonstrated four-fold lower binding affinity than compound **152** (*cf.* K_d = 308 ± 20.4 nM and K_d = 96.4 ± 10.2 nM, respectively). Given that other compounds with electron-withdrawing functionalities in the *meta*-position, such as the trifluoromethyl in compound **153**, the carboxylic acid in compound **147** and the ester in compound **145**, were weaker binders for *Ld*BDF5.1 (*cf.* K_d = 3610 ± 770 nM, K_d = 2550 ± 296 nM and K_d = 814 ± 131 nM), it was hypothesised that there must be a distinctive interaction between the nitro group at the *meta*-position and the binding site of *Ld*BDF5.1 that was driving the increase in affinity for compound **151**.

3.5 Docking studies of *C*-2 nitrophenyl containing compounds

To explore whether the nitro groups present in **151** and **152** were forming additional non-covalent interactions with the target, docking studies were performed in the binding

site of *Ld*BDF5.1 by Bernadette Lee. The results from these docking studies indicated that the nitrophenyl group may be forming a hydrogen bond to the hydroxyl group of T99 (Figure 3.8, A). The flexible *C*-2 ethyl linker enables the phenyl ring to sandwich between Y96 and H26 and π-stack. This conformation directs the *meta*-nitro towards T99, enabling a key H-bonding interaction. The docking studies indicate that the *meta*-nitro group in **151** and *para*-nitro group in **152** appear to accommodate the same position in *Ld*BDF5.1 and form hydrogen bonds to the threonine residue T99 (Figure 3.8, B). The *meta*-nitro group does not appear to be any closer to the T99 residue than the *para*-nitro, therefore, it is unlikely that it is the relative proximity of the nitro group to the T99 residue that is responsible for the increased binding affinity of **151** compared to **152**. However, the differences in the conformation of the *C*-2 ethyl linker can be seen for the two compounds. It could be that compound **151** adopts a more energetically favourable conformation due to stronger π-stacking interactions with either Y96 or H26 compared to **152**, which results in a higher binding affinity.

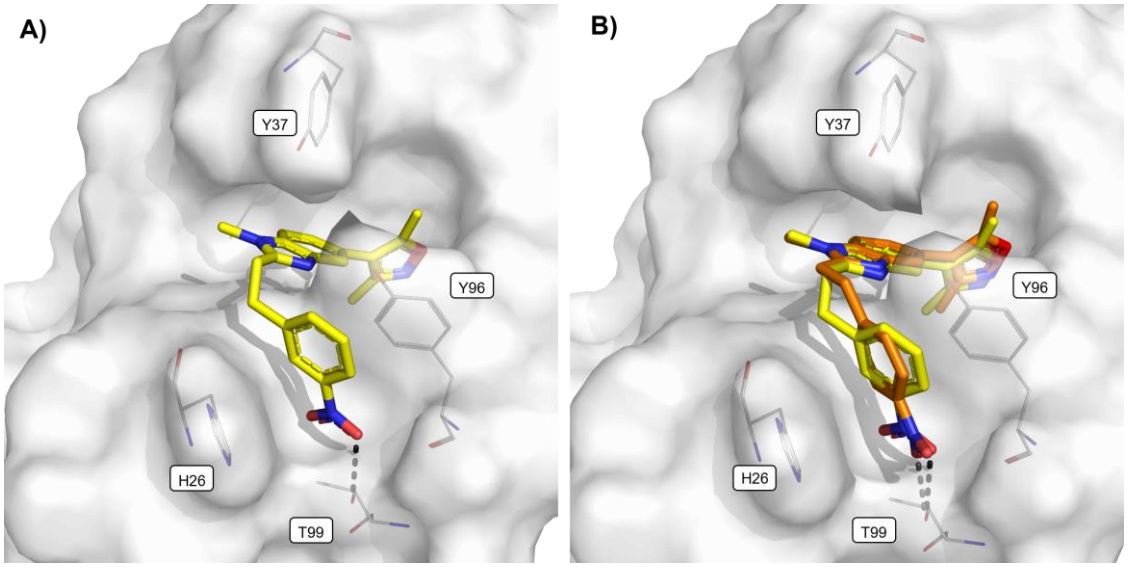

Figure 3.8. A) A view of compound **151** (carbon = yellow) docked in the binding site of *Ld*BDF5.1 (carbon = white) (PDB code 6BYA) using GOLD docking software.[131, 208] The key hydrogen bond interaction between the nitro group and T99 is highlighted. **B)** A view of docked compounds **151** (carbon = yellow) and **152** (carbon = orange) overlaid in the binding site of *Ld*BDF5.1 (carbon = white). The conformation of the *C*-2 ethyl linker is different for the two compounds. Docking was performed by Bernadette Lee.

3.5.1 Evaluation of nitriles as nitro bioisosteres

Nitroaromatic compounds have been investigated, but not widely used, in the treatment of leishmaniasis. However, they have shown therapeutic potential in the treatment of

human African trypanosomiasis.[217-220] Nitro groups undergo enzymatic bioreduction and their oxidation back to the nitro-group gives reactive oxygen species (ROS) *in vivo*.[221, 222] In many anti-parasitic drugs, these reactive species are responsible for the biological effect of the drug. However, the presence of a nitro group in drug compounds administered to humans can also result in several toxicity issues.[217, 223] Consequently, nitro groups are often avoided in drug discovery programmes where there are suitable alternatives. It was anticipated that future development of a tool compound containing a nitro group and testing in *in vivo* experiments could be problematic. The potential generation of ROS may obfuscate the source of antiparasitic activity as it would be difficult to differentiate between activity due to inhibition of the target bromodomain and the ROS. Therefore, a suitable nitro bioisostere was sought that would maintain the proposed H-bond to the threonine residue in the binding site of *Ld*BDF5.1. Nitriles share the ability of the nitro group to act as a good hydrogen bond acceptor.[224] Unlike the nitro group, nitriles are not readily metabolised.[224] Pleasingly, when the nitro group was substituted for the nitrile in **154** and **155**, the compounds showed comparable binding affinities to their nitro-functionalised analogues **151** and **152** (Table 3.6): **154** and **155** have binding affinities of K_d =120 ± 16 nM and 330 ± 120 nM, respectively, compared to 96 ± 10 nM and 310 ± 20 nM for **151** and **152**.

Table 3.6. The binding affinity (K_d) for compounds measured in the MST assay. The error quoted is the standard error of the mean (SEM) of n = 3 technical repeats.

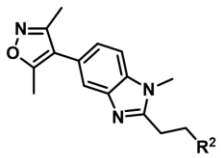

Compound	R²	K_d (nM)	Chrom $logD_{7.4}$	Compound	R²	K_d (nM)	Chrom $logD_{7.4}$
151	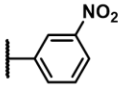	96 ± 10	5.2	**152**	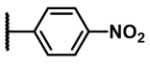	310 ± 20	5.2
154	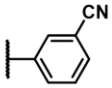	120 ± 16	4.9	**155**	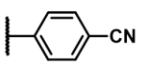	330 ± 120	4.8

3.6 Development of *C*-2 cyanophenyl containing compounds

The introduction of a methyl group on compounds can lead to small improvements in binding affinity due to favourable desolvation energetics, tailored hydrophobic interactions, and induced conformational effects.[225-229] In aqueous solution, formation of a hydrogen bond requires the desolvation of both the hydrogen bond donor and acceptor. It was hypothesised that installation of a methyl group adjacent to the nitrile on the aromatic ring of compound **154** might reduce the enthalpic penalty associated with the desolvation of the nitrile and further increase the binding affinity. Docking studies (performed by Bernadette Lee) also revealed that a *para*-methyl group may form additional hydrophobic interactions with A95 (Figure 3.9). Thus, compound **156** was synthesised with 3-cyano-4-methylphenyl at the *C*-2 ethyl position, and **157** was synthesised as an analogue of **155** with a 4-cyano-3-methylphenyl at the *C*-2 ethyl position.

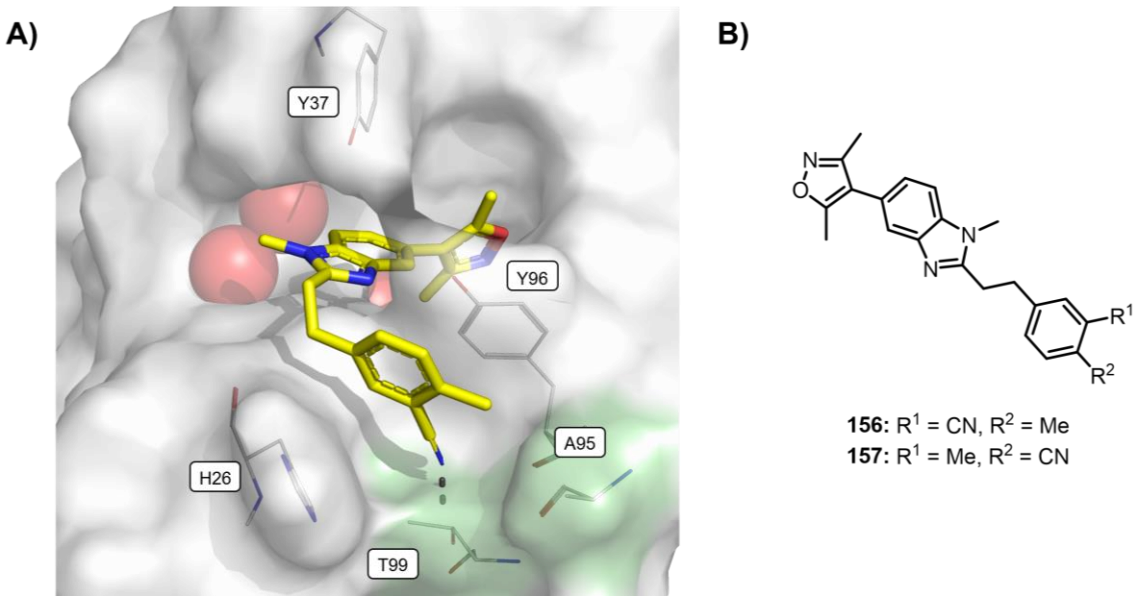

Figure 3.9. A) A view of compound **156** (carbon = yellow) docked in the binding site of *Ld*BDF5.1 (carbon = white) (PDB code 6BYA) using GOLD docking software.[131, 208] The *meta*-cyano group is shown to hydrogen bond with T99. The *para*-methyl group is near A95 and may form additional hydrophobic interactions with this residue. The surface areas of the T99 and A95 residues are highlighted in green. Docking was performed by Bernadette Lee. **B)** The general structure of compounds **156** and **157**.

3.6.1 Synthesis of compounds 156 and 157

Acids **158** and **159** were not commercially available for the synthesis of compounds **156** and **157**. However, a large-scale (5 g) synthesis of **159** was reported in a patent procedure.[230] Compound **159** was generated in two steps (Scheme 3.6).

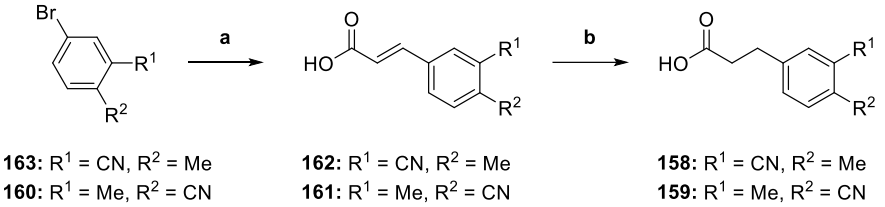

163: R^1 = CN, R^2 = Me
160: R^1 = Me, R^2 = CN

162: R^1 = CN, R^2 = Me
161: R^1 = Me, R^2 = CN

158: R^1 = CN, R^2 = Me
159: R^1 = Me, R^2 = CN

Scheme 3.6. Synthesis of compounds **158** and **159**. *Reagents and conditions*: **a)** Tris(2-methylphenyl)phosphane, acrylic acid, Et_3N, palladium(II) acetate, acetonitrile, 200 °C, MW, 45 min, **162:** 49%, **161:** 22%; **b)** 10% Pd/C, $H_{2\,(g)}$, 2:1 THF : MeOH, rt, 17 h, **158:** 87%, **159:** 0%.

A Heck reaction between 4-bromo-2-methylbenzonitrile **160** and acrylic acid provided the cinnamic acid intermediate **161**, which was subjected to hydrogenation with 10% Pd/C to yield **159**.[231] The patent procedure was adapted for a smaller scale (500 mg) synthesis of **158** and **159**: the Heck reaction conditions were changed from a 2 h reaction at 200 °C under microwave irradiation, to a 45 minute reaction. The work-up procedure was performed as described in the patent: the catalyst was removed by filtration and the reaction mixture was acidified by the addition of HCl to precipitate the cinnamic acid intermediate, **161** or **162**. The Heck reaction with **163** and acrylic acid provided **162** in 49% yield (Scheme 3.6). A mixture of THF and water solubilised intermediate **162** for the Pd/C catalysed hydrogenation to generate **158** in 87% yield. Unfortunately, the Heck reaction with 4-bromo-2-methylbenzonitrile **160** and acrylic acid to give **161** was low yielding (22%), and the product isolated was impure by ^{1}H NMR. The hydrogenation of **161** to provide **159** was then hindered by the poor solubility of the cinnamic acid **161** in organic solvent.

The synthesis of compounds **158** and **159** was later optimised (Scheme 3.7). Benzyl acrylate was employed in the Heck reaction instead of acrylic acid, and the reaction was performed at a lower temperature (80 °C) for a longer duration (5 h). The intermediates **164** and **165** were synthesised in 80% and 74% yields respectively, using the optimised

Heck reaction conditions. The benzyl protecting group and the double bond in intermediates **164** and **165** were hydrogenated in a single step with a 10% Pd/C catalyst to provide compounds **158** and **159**. It was then possible to use compounds **158** and **159** in the HATU-assisted amide coupling with compound **76** (step **c**, Scheme 3.7) to generate compounds **166** and **167**. Compounds **166** and **167** were then heated under reflux in toluene to form the benzimidazole ring, completing the synthesis of compounds **156** and **157**.

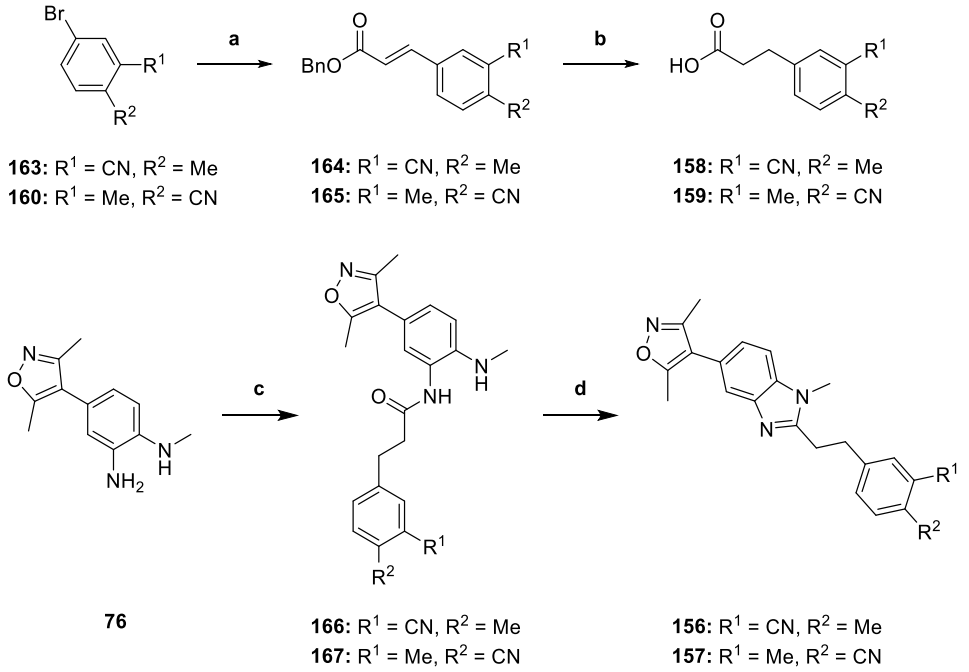

Scheme 3.7. Optimised synthetic route to compounds **156** and **157**. *Reagents and conditions*: **a)** Tris(2-methylphenyl)phosphane, benzyl acrylate, Et_3N, palladium(II) acetate, acetonitrile, 80 °C, 5 h, **164:** 80%, **165:** 74%; **b)** 10% Pd/C, $H_{2\,(g)}$, MeOH, rt, 5 h, **158:** 78%, **159:** 84%; **c) 158** or **159**, HATU, DIPEA, DMF, rt, 3 h, **166:** 57%, **167:** 36%; **d)** Toluene, reflux with 3 Å MS, 17 h, **156:** 81%, **157:** 62%.

3.6.2 MST data for compounds 156 and 157

Pleasingly, the addition of the methyl group to compounds **156** and **157** resulted in greater binding affinities for *Ld*BDF5.1 compared to the analogous compounds **154** and **155** without the methyl group on the aromatic ring (*cf.* K_d = 33 ± 4.0 nM, 110 ± 22 nM and K_d = 120 ± 16 nM, 330 ± 120 nM, respectively). Notably, compound **156** showed a four-fold increase in binding affinity over compound **154**.

Table 3.7. The binding affinity (K_d) for compounds **154-157** measured in the MST assay. The error quoted is the standard error of the mean (SEM) of n = 3 technical repeats.

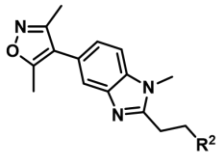

Compound	R^2	K_d (nM)	Chrom $logD_{7.4}$	Compound	R^2	K_d (nM)	Chrom $logD_{7.4}$
156	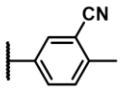	33 ± 4.0	5.1	**157**	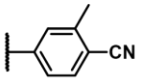	110 ± 22	5.1
154	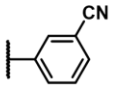	120 ± 16	4.9	**155**	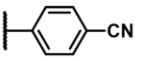	330 ± 120	4.8

3.6.3 Design and synthesis of compound 168

To investigate how increasing the electron density of the phenyl ring would modulate the binding of 3-cyano-4-methylphenyl containing compound **156**, compound **168**, which featured an oxygen atom adjacent to the phenyl ring, was synthesised according to the procedure shown in Scheme 3.8. It was postulated that this π-electron donating group would increase the electron density of the aromatic ring and thereby increase the ability of the nitrile to hydrogen bond T99. Compound **168** was synthesised in two steps from the diamine **76** (Scheme 3.8). The reaction of **76** with glycolic acid and 6 M HCl provided **169** in 74% yield. Compound **168** was obtained from a Mitsunobu reaction of **169** with 5-hydroxy-2-methylbenzonitrile, where tributylphosphine and 1,1-(azodicarbonyl)dipiperidine (ADDP) were employed to enhance the reactivity of the phenol with the primary alcohol in **169**.[232]

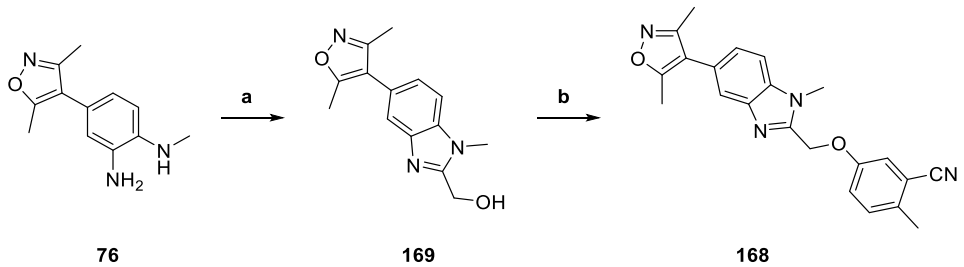

Scheme 3.8. Synthesis of compound **168**. *Reagents and conditions:* **a)** Glycolic acid, 6 M $HCl_{(aq)}$, 80 °C, 17 h, 74%; **b)** Tributylphosphine, 5-hydroxy-2-methylbenzonitrile, 1,1-(azodicarbonyl)dipiperidine, dichloromethane, rt, 17 h, 86%.

3.6.4 MST data for compound 168

Unexpectedly, compound **168** was measured to have a lower affinity for *Ld*BDF5.1 in the MST assay compared to **156** (*cf.* K_d = 190 ± 19 nM and K_d = 33 ± 4.0 nM, respectively, Table 3.8). The lower binding affinity for compound **168** could be due to the change in electronics of the π-system, and/or a conformational change of the molecule that reduced its ability to π-stack with residues Y96 and H26 optimally. It is also possible that the ability of the nitrile to form the proposed hydrogen bonding interaction with T99 was reduced because the nitrile lone pair was situated further from the threonine. To more definitively identify the binding interactions and conformations adopted by compound **168** and others, crystal structures of these compounds in complex with *Ld*BDF5.1 should be obtained, which would allow for future compounds to be designed with key binding interactions and steric requirements in mind.

Table 3.8. The binding affinity (K_d) for compounds **156** and **168** measured in the MST assay. The error quoted is the standard error of the mean (SEM) of n = 3 technical repeats.

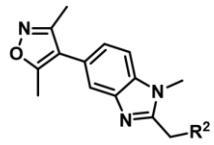

Compound	R^2	K_d (nM)	Chrom $logD_{7.4}$
156	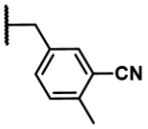	33 ± 4.0	5.1
168	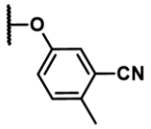	190 ± 19	5.2

3.7 Exploring the additivity of modifications at the *N*-1 and *C*-2 position

To probe whether the observed SAR of the modifications at the *N*-1 and *C*-2 positions of **18** were additive, a selection of compounds were synthesised with permutations of the

highest affinity moieties at each position. Compounds featuring a morpholino-ethylene at *N*-1 and a *C*-2 linked aryl ring substituted with either a nitro, nitrile, methyl or combination of the nitrile and methyl were synthesised, as displayed in Table 3.9. The morpholino-ethyl was an attractive group to incorporate because of its ability to improve the solubility of compounds — an important property for obtaining reliable *in vitro* and *in vivo* assay results.[233]

Table 3.9. The binding affinities (K_d) of compounds incorporating a morpholine substutient at R^1 compared to analogues with a methyl substituent at R^1, measured in the MST assay. Units are nM, error is the standard error of the mean (SEM) of n = 3.

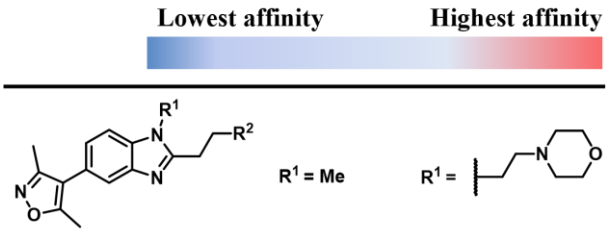

	Lowest affinity → Highest affinity	
R^2 = H	**18** 1400 ± 84	**106** 600 ± 84
R^2 = 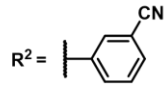	**154** 120 ± 16	**170** 66 ± 1.0
R^2 = 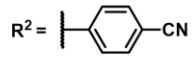	**155** 330 ± 120	**178** 160 ± 14
R^2 = 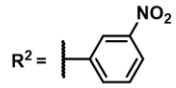	**151** 96 ± 10	**172** 93 ± 5.0
R^2 = 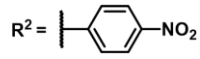	**152** 310 ± 20	**173** 400 ± 18
R^2 = 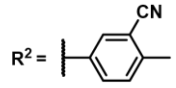	**156** 33 ± 4.0	**174** 52 ± 3.0
R^2 = 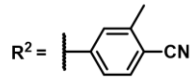	**157** 110 ± 22	**175** 93 ± 6.0
R^2 = 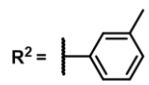	**121** 600 ± 29	**171** 220 ± 63
R^2 = 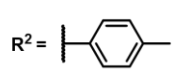	**138** 530 ± 130	**179** 240 ± 60

When the *C*-2 phenyl ring was mono-substituted with a nitrile and the *N*-1 methyl was replaced with a morpholino-ethylene substituent, the binding affinity improved by roughly two-fold. For example, **170** had a K_d of 66 ± 1.0 nM whereas its *N*-1 methyl-functionalised analogue **154** had a K_d of 120 ± 16 nM. The same trend was apparent for compounds where the *C*-2 phenyl ring was mono-substituted with a methyl group. For example, **171** had K_d = 220 ± 63 nM compared to its *N*-1 methyl analogue **121** which had K_d = 600 ± 29 nM. The improvement in binding affinity indicates that there was an additive effect when the morpholino-ethylene was incorporated into these compounds.

Unfortunately, there were instances where modifications to both the *N*-1 and *C*-2 positions was not additive. For nitro-containing compounds **172** and **173**, an additive effect was not observed with the morpholino-ethyl group at R^1. **172** binds with comparable affinity (K_d = 93 ± 5.0 nM) to **151** (K_d = 96 ± 10 nM). The affinity of **173** for *Ld*BDF5.1 was lower than that of **152** (*cf.* K_d = 400 ± 18 nM and K_d = 310 ± 20 nM, respectively). Compound **174** which features a morpholino-ethylene at *N*-1, had lower affinity compared to compound **156** which had a simple methyl substitution (*cf.* K_d = 52 ± 3.0 nM and K_d = 33 ± 4.0 nM, respectively). It is difficult to elucidate the reason for the non-additive SAR of these specific modifications at the *N*-1 and *C*-2 position without more definitive structural information from a crystal structure. However, the most common causes of non-additivity are interactions between substituents, different binding modes, rearrangements in the water network, and changes in protein conformation.[234, 235]

3.8 Validation of affinity data using ITC

To validate the results from the MST assay, ITC data were collected for compounds **170**, **174** and **175**. The ITC measurements corroborated the results from the MST assay (Figure 3.10).

A)

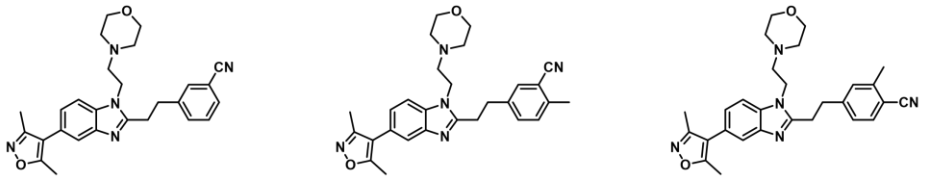

Compound	170	174	175
K_d (ITC)	92 ± 1.0 nM	37 ± 12 nM	120 ± 13 nM
K_d (MST)	66 ± 1.0 nM	52 ± 3.0 nM	93 ± 6.0 nM

B)

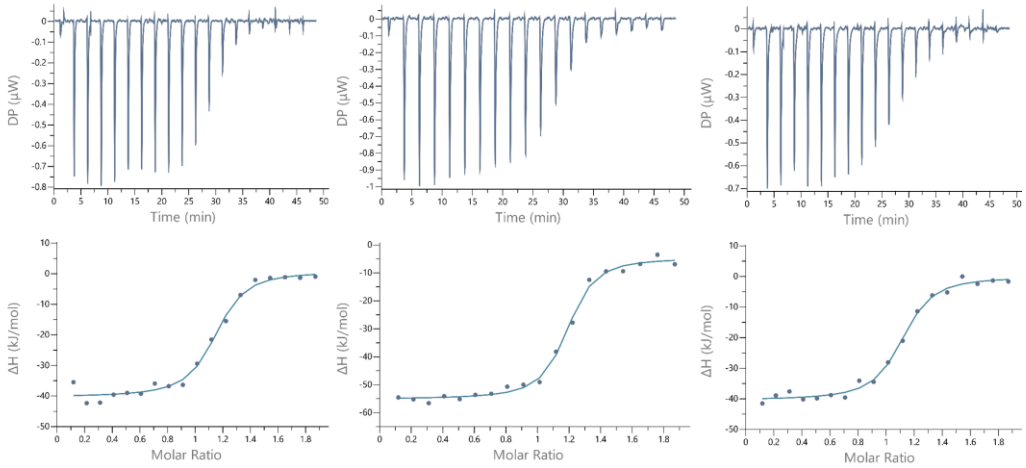

Figure 3.10. A) A comparison of the binding affinity data for compounds **170**, **174** and **175** measured in the MST and ITC assays. The error is the standard error of the mean (SEM) of n = 3 repeats; **B)** Representative ITC traces for **170**, **174** and **175** demonstrating binding to *Ld*BDF5.1. The compound concentration was 10 µM and the protein concentraion was 100 µM. The thermodynamic parameters of the binding interactions are detailed in the Appendix section A6.

Using ITC, compounds **170**, **174** and **175** were shown to bind with K_d = 92 ± 1.0 nM, K_d = 37 ± 12 nM, and K_d = 120 ± 13 nM, respectively. The corroboration of the affinity data for the compounds listed above using an orthogonal technique confirmed that MST was an effective tool for establishing the binding affinities of compounds in high-throughput experiments.

3.9 Conclusions and further work

The work described in this chapter details the SAR investigation of a synthetic library of analogues of **18**. Analogues of compound **18** were synthesised with modifications at two positions (R^1 and R^2 at *N*-1 and *C*-2 of the benzimidazole, respectively) to probe the SAR of two regions in the binding site of *Ld*BDF5.1 that may be able to accommodate additional functionality. An MST assay was used for the initial assessment of compound

binding in a high-throughput manner, which was orthogonally validated using ITC. These studies resulted in the generation of high affinity ligands for *Ld*BDF5.1, including six compounds with $K_d \leq 0.1$ μM for the parasite bromodomain.

When the substitutions at R^1 and R^2 were assessed independently, the morpholino-ethyl group was the optimal substituent at R^1. It was postulated that the nitrogen atom of the morpholine group could form an additional hydrogen bonding interaction with a conserved water molecule in the ZA channel of *Ld*BDF5.1, which increased the affinity of compounds **106** and **107** (K_d of 598 ± 84.0 nM and, 580 ± 121 nM respectively). Functionalisation at R^2 focused on targeting potential π-stacking interactions with aromatic residues (Y96 and H26) through the inclusion of phenyl substituents at the *C*-2 position. Substantial improvements in binding affinity of **18** were seen when the *C*-2 ethyl group was functionalised with a 3-nitrophenyl (**151**) or 3-cyanophenyl (**154**) group. Compounds **151** and **154** demonstrated a greater than ten-fold increase in affinity compared to **18** (*cf.* K_d = 96 ± 10 nM, 120 ± 16 nM, and 1400 ± 84 nM, respectively, measured using MST). The high affinity of nitrophenyl and cyanophenyl-containing compounds was attributed to effective π-stacking interactions with Y96 and a key hydrogen bonding interaction with the T99 hydroxyl in the binding site of *Ld*BDF5.1. Further affinity was gained through the addition of a methyl group to the *C*-2 aromatic ring, which was hypothesised to reduce the enthalpic penalty associated with the desolvation of the nitrile and enhance the interaction with T99. Indeed, the highest affinity compound (**156**, K_d = 33 ± 4.0 nM) featured a 4-methyl-3-cyanobenzene substituent at R^2. Thus, targeting the ZA channel and the region adjacent to Y96 in *Ld*BDF5.1 with appropriate functionality on analogues of **18** was an effective SAR strategy for increasing *Ld*BDF5.1 affinity.

Matched pair analysis of the MST data for compounds with either a methyl or mopholino-ethyl group at *N*-1 revealed that the SAR for modifications at the *C*-2 ethyl and the *N*-1 position were not always additive. To further explore the non-additivity, compounds with different permutations at the *N*-1 and *C*-2 positions could be evaluated. Additionally, it was clear that an X-ray crystal structure of one of these compounds in complex with *Ld*BDF5.1 would be highly valuable to validate docking studies and confirm the binding mode of compounds. Thus, efforts to solve such a crystal structure are discussed in the next chapter (Chapter 4).

The SAR studies described in this chapter identified several compounds with sufficient binding affinity for *Ld*BDF5.1 to begin phenotypic assays against the *Leishmania* parasite. The evaluation of the potency of these lead compounds would provide insight into the physicochemical requirements for activity in cells and will inform the design of subsequent chemical probes for *Ld*BDF5.1.

Chapter 4 - The development of chemical probes for *Ld*BDF5.1

4.1 Introduction and aims

The work described in Chapter 3 explored the SAR of modifications at the *N*-1 and *C*-2 position of the benzimidazole ring in **18** and led to the development of high affinity ligands for *Ld*BDF5.1. The work described in this chapter focused on optimising the high affinity ligands into chemical probes.

A chemical probe is a potent and selective ligand for its target protein that modulates the biochemical activity of the target in cells.[236] To be useful in the study of a complex biological system, the chemical probe must be active in cells at a reasonable concentration, typically low micromolar or nanomolar range, and it cannot be generally toxic to the host organism.[237] A chemical probe should also have the ability to permeate living cells and be sufficiently selective for its target to build confidence that the observed effects are due to modulation of the intended molecular target.[238] Potency, selectivity, and permeability are therefore key fundamental properties of chemical probes.[239]

To determine the biological role of BDF5 in *Leishmania* and validate the protein as a molecular target for therapeutic exploration, the high affinity ligands identified in Chapter 3 needed to demonstrate activity against the parasite in a cellular based assay. The phenotypic assays required an investigation into the physicochemical properties that were necessary for compound permeability in the parasites. It was also crucial that compounds chosen for development into chemical probes for *Ld*BDF5.1 had a high degree of selectivity to ensure that the biological insights could confidently be ascribed to the function of the bromodomain of interest. Therefore, the binding affinities of *Ld*BDF5.1 ligands to other bromodomains, particularly human bromodomains, needed to be evaluated. Additionally, determining the mode of binding of compounds using X-ray crystallography could provide valuable structural information to explain on-target selectivity and support future efforts to derivatise these compounds into versatile chemical tools.

Therefore, the aims of the work described in this Chapter were to:

- Assess the activity of *Ld*BDF5.1 ligands in the *Leishmania* parasite.
- Evaluate and optimise the physicochemical properties of the *Ld*BDF5.1 ligands.
- Investigate the selectivity of compounds for *Ld*BDF5.1 over human bromodomains.
- Use X-ray crystallography to validate the binding modes and provide a structural basis for any observed selectivity.

4.2 Evaluation of high affinity compounds in parasites

The first step to assess the potency of *Ld*BDF5.1 ligands against their target in the *Leishmania* parasites was to conduct a promastigote viability assay. The assay employs free-living parasites and has the main advantage of allowing fast and easy screening of a large number of compounds. However, the drawback of the assay is that promastigotes represent the insect life-stage of the *Leishmania* parasite so there is risk of identifying compounds that do not affect the relevant disease-causing life-stage. The promastigote cell viability assay was carried out by Dr Nathaniel Jones at The University of York. In brief, *L. donovani* promastigotes were treated with 0–30 μM of the compound then incubated for 5 days at 25 °C. Resazurin, a fluorometric growth indicator, was added to the cells after the 5 days to quantitatively measure the viability of promastigotes using fluorescence and determine the EC_{50} values of compounds.

The compounds chosen for the initial screen were high affinity ligands for *Ld*BDF5.1 or had diverse physicochemical properties to probe the factors that influence cell permeability (Table 4.1). In particular, the highest affinity compound from Chapter 3, **156** (K_d = 33 ± 4.0 nM), which features a 3-cyano-4-methylbenzene at R^2 and a methyl group at R^1, and the analogue of this compound, **174** (K_d = 52 ± 3.0 nM), which has a morpholino-ethyl group in the place of the methyl group at R^1, were included. Matched pairs of compounds with the methyl and morpholino-ethyl group at R^1 were chosen to be evaluated in the cellular assay to explore the effect of the morpholine on potency. Morpholino-containing compounds are known to demonstrate increased solubility,[233] therefore it was postulated that the morpholino-containing compounds **170**, **174**, and **175**

may have increased potency compared to their matched pairs with the methyl group at R^1 (**154**, **156**, and **157**, respectively).

Compounds **151** and **152**, which have a nitrophenyl group at R^2, were screened alongside compounds **154** and **155**, which have a bioisosteric cyanophenyl group at R^2, to investigate the potential differences in activity because of ROS generation.

To investigate the effect of lipophilicity and charge state on parasite viability, compound **145**, which features a methyl ester at the *meta*-position, and **147** which features a carboxylate group at the same position, were included in the assay. It was proposed that the increased lipophilicity and absence of a negative charge on **145** would render the compound more membrane permeable then **147**, thereby increase the potency of **145**. Finally, compound **168** was included in the panel of compounds to evaluate the effect of variations to the *C*-2 linker.

4.2.1 Results from the initial phenotypic assays

The results from the promastigote assay are summarised in Table 4.1. The compounds tested demonstrated promising activity in the promastigotes, with four compounds (**152**, **155**, **157**, and **151**) outperforming the positive control miltefosine (EC_{50} = 1.79 ± 0.22 μM), the current oral drug approved for the treatment of visceral leishmaniasis.[240]

Table 4.1. Compounds assessed in the 5-day *L. donovani* promastigote viability assay. The EC_{50} values are reported, alongside the compound K_d from the MST assay. The error is the SEM of n =3 repeats. MW = molecular weight, ND = no data.

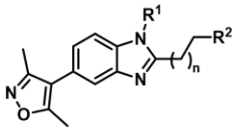

Lowest affinity/ potency — Highest affinity/ potency

Compound	n	R^1	R^2	EC_{50} (μM)	K_d (nM)	Chrom $logD_{7.4}$	MW (Da)
152	1	Me	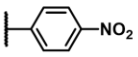	0.41 ± 0.09	310 ± 20	5.2	376.42
155	1	Me	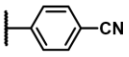	0.70 ± 0.16	330 ± 120	4.8	356.43
157	1	Me	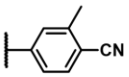	0.84 ± 0.31	110 ± 22	5.1	370.46
151	1	Me	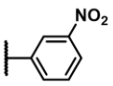	1.72 ± 0.45	96 ± 10	5.2	376.42
156	1	Me	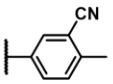	1.83 ± 0.20	33 ± 4.0	5.1	370.46
145	1	Me	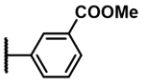	2.24 ± 1.0	810 ± 130	5.1	389.45
154	1	Me	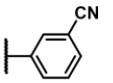	2.94 ± 0.60	120 ± 16	4.9	356.43
168	0	Me	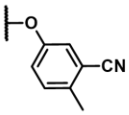	4.38 ± 0.34	190 ± 19	5.2	372.43
174	1	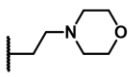	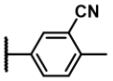	6.36 ± 0.91	52 ± 3.0	5.1	469.59
170	1	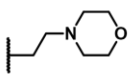	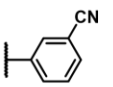	7.43 ± 0.43	66 ± 1.0	4.7	455.56
175	1	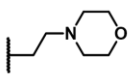	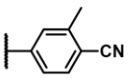	>30	93 ± 6.0	4.8	469.59
147	1	Me	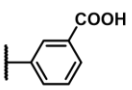	>30	2500 ± 300	2.2	375.43
Miltefosine		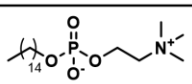		1.79 ± 0.22	ND	ND	407.57

The most potent compound was **152** with EC_{50} = 0.41 ± 0.09 μM. Compound **152** contains a nitro-group, which can generate ROS intracellularly.[241] It is known that *Leishmania* are susceptible to oxidative stress, so the potential formation of intracellular ROS could result in cell death independent of the inhibition of bromodomains.[242] However, **155**, which has a nitrile in the place of the nitro group, showed similar binding affinity to *Ld*BDF5.1 and retained high potency in the parasites (EC_{50} = 0.70 ± 0.16 μM). The compounds **151** and **154**, which have a nitro and nitrile at the *meta*- position, respectively, followed the same trend: the nitrile compound possessed similar binding affinity to the nitro (*cf.* K_d = 96 ± 10 nM and 120 ± 16 nM), and their efficacy in the parasites were comparable (*cf.* EC_{50} = 1.72 ± 0.45 μM and 2.94 ± 0.60 μM). As nitriles are not known to generate ROS, and the binding affinities between the nitro compounds and their respective nitrile-functionalised analogues are similar, it is more likely that the efficacy of the nitro-containing compounds is derived from inhibition of bromodomains (or an alternative mechanism) rather than ROS generation.

Interestingly, the compounds with *para*- substituted aryl rings, **152** and **155**, were more effective in the parasites than the *meta*- substituted analogues, **151** and **154** (*cf.* EC_{50} = 0.41 ± 0.09 μM, and 1.72 ± 0.45 μM, with EC_{50} = 0.70 ± 0.09 μM, and 2.94 ± 0.60 μM, respectively), despite having three-fold lower binding affinities (*cf.* K_d = 310 ± 20 nM and 330 ± 120 nM, with K_d = 96 ± 10 nM and 120 ± 16 nM, respectively). The reasons for the higher activity of the compounds containing *para*-substituted aryl rings over the *meta*- substituted analogues cannot be determined from this assay. However, an assay that quantifies the intracellular concentrations of these compounds may provide insight into whether the difference in potency is due to differences in cell permeability.

Compound **147** did not demonstrate any activity at the highest concentration used in this assay (30 μM). The low potency correlates with the low affinity of this compound for *Ld*BDF5.1 (K_d = 2500 ± 300 nM). The methyl ester analogue **145** had substantially higher efficacy than the acid **147** (*cf.* EC_{50} = 2.24 ± 1.0 μM and > 30 μM), despite its low affinity for *Ld*BDF5.1 (K_d = 810 ± 130 nM). It was postulated that the increased lipophilicity and absence of a negative charge on **145** resulted in greater permeability through cell membranes and, consequently, higher potency.

Compound **168** is an analogue of **156** that differs by an oxygen atom in the *C*-2 linker. **168** demonstrated a six-fold lower binding affinity for *Ld*BDF5.1 compared to **156** (*cf*. K_d = 190 ± 19 nM and K_d = 33 ± 4.0 nM, respectively), but only a two-fold decrease in potency (*cf*. EC_{50} = 4.38 ± 0.45 μM and EC_{50} = 1.83 ± 0.20 μM, respectively), suggesting that the lower binding affinity of **168** may be compensated for by the increase in intracellular concentration of the compound. The knowledge that compounds are potent with additional heteroatoms in the *C*-2 linker might prove useful in tuning the physicochemical properties of these compounds.

Unexpectedly, the compounds featuring the morpholino-ethyl group at R^1 (**170**, **174**, and **175**) demonstrated low potency (EC_{50} = 7.43 ± 0.43 μM, 6.36 ± 0.91 μM, and > 30 μM, respectively). When the morpholino-ethyl group at R^1 was replaced with a methyl group, the potency substantially improved (*cf*. **154**, **156**, and **157** with EC_{50} = 2.94 ± 0.60 μM, 1.83 ± 0.20 μM, and 0.84 ± 0.31 μM, respectively). Given the high binding affinity of compounds **170**, **174**, and **175** (K_d = 66 ± 1.0 nM, 52 ± 3.0 nM, and K_d = 93 ± 6.0 nM, respectively), the lack of efficacy is likely due to the differences in the physicochemical properties of these compounds that influence cell permeability. From the set of compounds assessed in the parasites, **170**, **174**, and **175** had the largest molecular weights. The size of the additional morpholino-ethyl group at R^1 could have reduced the ability of these compounds to permeate the parasite cells, thereby reducing their potency. The charge state of the nitrogen in the morpholine ring could also influence the permeability.

Overall, the potency data and the MST binding affinity data are not strongly correlated. For example, **174** had high affinity for *Ld*BDF5.1 (K_d = 52 ± 3.0 nM) but low potency in the promastigotes (EC_{50} = 6.36 ± 0.91 μM). Conversely, compound **155** was a weaker binder (K_d = 330 ± 120 nM) that demonstrated high potency (EC_{50} = 0.70 ± 0.16 μM). Other compounds, such as **156**, were high affinity binders (K_d = 33 ± 4.0 nM) and relatively potent (EC_{50} = 1.83 ± 0.20 μM). The weak correlation between MST and cellar assay data could be related to compound permeability or solubility, compound metabolism, or off-target effects. Lipophilicity, H-bonding capacity, and molecular size and shape descriptors are all known to influence molecular transport through membranes.[243, 244] The parasite cell viability data demonstrates the importance of having phenotypic assays included in the compound development pipeline. Before attempting to improve the *Ld*BDF5.1 binding affinity of compounds any further, it was important to investigate the physicochemical properties of compounds that influence their potency.

4.3 The design and synthesis of compounds to investigate the physicochemical properties required for potency in *Leishmania* promastigotes

It was hypothesised that the low biological activity for some of the compounds evaluated in the promastigotes could be attributed to the compounds not having the necessary physicochemical properties to permeate the cell membranes. To investigate the factors that influence compound permeability and result in increased potency, a set of compounds was designed that varied in molecular weight (MW), and size, lipophilicity, ionisation state, and hydrogen-bonding capacity (Table 4.2).[243] The compounds all featured a 3-cyano-4-methylbenzene attached to the *C*-2 ethyl linker but differed at the R^1 position. Modifications at the R^1 group were used to modulate the physicochemical properties of compounds. The R^2 group was kept consistent because the functionality at R^2 was determined to be important for the high binding affinity of compounds.

Table 4.2. Molecular descriptors of compounds designed to investigate the physicochemical properties required for potency in *Leishmania* promastigotes. MW = molecular weight (Da); TPSA = topological polar surface area (Å^2); HBA = number of hydrogen bond acceptors (pH 7.4). Calculator Plugins were used for structure property prediction and calculations, Marvin 23.12, 2023, ChemAxon (http://www.chemaxon.com). OSIRIS DataWarrior 5.5.0 software was used to calculate TPSA.[245]

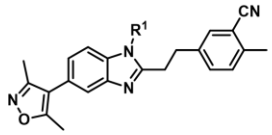

R^1	Me	O	O	N O	N	N F F	N NMe	N NAc
Compound	**156**	**185**	**186**	**174**	**180**	**182**	**183**	**181**
MW	370.46	414.51	468.60	469.59	467.62	503.60	482.63	510.64
Chrom $logD_{7.4}$	5.1	5.4	5.7	5.1	6.6	6.0	4.7	4.1
TPSA	67.6	76.9	76.9	80.1	70.9	70.9	74.1	91.2
HBA	3	4	4	5	3	3	4	5
pK_a	N/A	N/A	N/A	7.0	9.1	8.2	3.1/ 8.3	7.7

Most drug-like compounds diffuse across cell membranes *via* passive transport and the rate at which this occurs is highly dependent on MW and size of the molecule.[246] Generally, larger molecules will diffuse more slowly across membranes and demonstrate

decreased passive permeability. The set of compounds designed to be evaluated in the parasites included compounds with a MW ranging from 370.46–510.64 Da.

Lipophilicity reflects the affinity of a molecule for an aqueous or lipophilic environment and can be used to predict the ability of molecules to cross cell membranes and bind to proteins, which are mostly hydrophobic in nature.[247] In the context of drug candidates, logP values beyond Lipinksi's rule-of-five criteria (>5) are often associated with undesirable features, such as rapid metabolic turnover, poor aqueous solubility, high plasma protein binding, and tissue accumulation.[247, 248] However, a drug will generally display poor absorption, distribution, metabolism, excretion, and toxicity (ADMET) properties if the lipophilicity is too low.[247, 249] Lipophilicity is often quantified using logD, which is the distribution coefficient in octanol-water at a given pH.[214] Of particular interest is the logD at pH = 7.4 (the physiological pH of blood serum). A chromatographic logD assay was conducted to calculate the chromlog$D_{7.4}$ value for each compound in Table 4.2.[215] The most lipophilic compound was **180** with a chromlog$D_{7.4}$ value of 6.6. The high value is likely due to the high proportion of methylene and methyl units in this compound and the low number of heteroatoms capable of hydrogen bonding. Compound **181** was the least lipophilic compound with a chromlog$D_{7.4}$ value of 4.1.

The surface area that is solvent accessible on a compound is another potential influence on its membrane permeability.[250] Polar surface area (PSA) is the sum of the contributions to the molecular surface area of polar atoms such as oxygen, nitrogen and their attached hydrogens. Ertl *et al.* developed a fast additive fragment method of calculating PSA termed topological PSA (TPSA).[251] The TPSA molecular descriptor correlates well with passive molecular transport through membranes; molecules with high TPSA may exhibit poor permeability.[252] Compounds in Table 4.2 were designed with a range of TPSA values ranging from 67.6 $Å^2$ (**156**) to 91.2 $Å^2$ (**181**).

Hydrogen bonds can play key roles in molecular recognition. However, too many hydrogen bond donors/acceptors can have a deleterious effect on the membrane permeability of a molecule.[253] Polar groups can decrease the affinity for the hydrophobic membrane and also increase the water desolvation penalty when the compound binds to its target.[253] The compounds designed in Table 4.2 varied in the number and nature of the heteroatoms that they contained. Additionally, the pK_a values of the heteroatoms in the molecules influenced the number of hydrogen bonding interactions that could be made.

The degree of ionisation of a compound is a function of both its pK_a value and pH at the membrane surface. Membranes are generally more permeable to non-ionised forms of compounds because of their greater lipid solubility.[254] It was possible to modulate the pK_a values of the nitrogen atom(s) in the R^1 group with heteroatoms and additional substituents. For example, the pK_a of the nitrogen atom of the piperidine ring in compound **180** was decreased from 9.1 to 8.2 by the incorporation of electron withdrawing fluorine atoms at the 4-position of the cyclic ring (as in **182**). The pK_a of the piperidine was further decreased to 7.0 in compound **174** with a morpholine substitution.

4.3.1 The synthesis of analogues of 156

The seven analogues of **156** were synthesised following the general synthetic route outlined in Scheme 4.1. It was possible to make the modifications to the R^1 group on the benzimidazole ring by employing different amines in the S_NAr reaction (Scheme 4.1, step **c**). The yields for these reactions are summarised in Table 4.3.

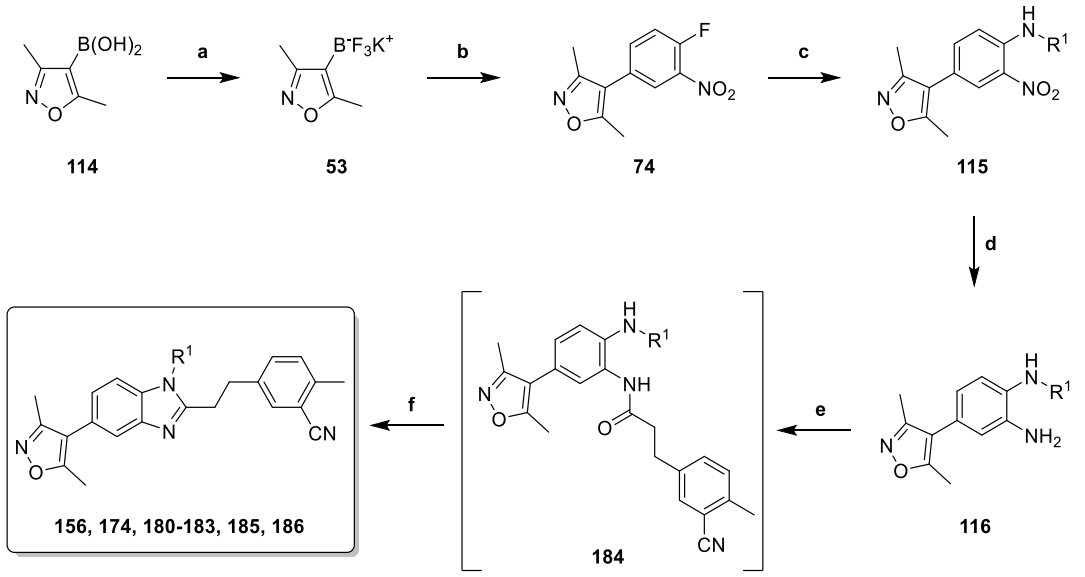

Scheme 4.1. General synthetic route to synthesise analogues of **156** with diversification at R^1. *Reagents and conditions:* **a)** Potassium fluoride, L-(+)-tartaric acid, THF, acetonitrile, rt, 30 min, 73%; **b)** 4-Bromo-1-fluoro-2-nitrobenzene, $NaHCO_3$, $Pd(dppf)Cl_2 \cdot CH_2Cl_2$, DME/$H_2O$, 110 °C, 3 h, 76%; **c)** R^1-NH_2, DIPEA, DMF, 80 °C, 50 min-2 h 30 min; 51-99%; **d)** 1 M $Na_2S_2O_{4\,(aq)}$, EtOH, 80 °C, 5 min, crude; **e)** 3-(3-Cyano-4-methylphenyl)propanoic acid, HATU, DIPEA, DMF, rt, 3 h, 57-97%; **f)** Toluene, reflux, 3 Å MS, 24-48 h; 39-86%.

Table 4.3. Yields for steps **c**, **e** and **f** in Scheme 4.1.

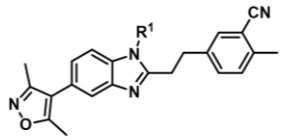

Compound	R^1	step c (%)	step e (%)	step f (%)
156		99	57	81
185		97	97	84
186	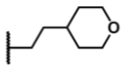	88	65	48
174	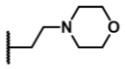	99	85	84
180	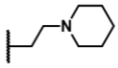	92	93	46
182	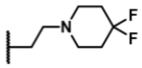	85	88	86
183	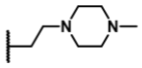	83	61	81
181	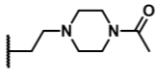	51	59	39

4.4 Determining the affinity and potency of analogues of compound 156

The binding affinities of analogues of compound **156** with modifications at the R^1 position were determined prior to evaluating their potency in the parasites using the biophysical assays discussed in Chapter 3 to confirm that their affinities were comparable to **156** and that variations in potency were due to changes in physicochemical properties rather than binding affinity.

4.4.1 Determination of the binding affinity of analogues of compound 156 for *Ld*BDF5.1

Analogues of **156** were evaluated in the MST assay to determine their binding affinities for *Ld*BDF5.1 (Table 4.4).

Table 4.4. Binding affinity (K_d) data for each compound measured in the MST assay. The error quoted is the SEM of n = 3 technical repeats.

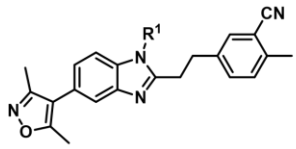

Lowest affinity — Highest affinity

Compound	R^1	K_d (nM)
183	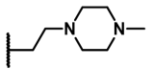	6.0 ± 2.0
181	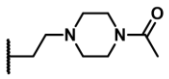	11 ± 6.0
180	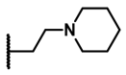	28 ± 15
185		29 ± 6.0
156		33 ± 4.0
186	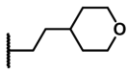	36 ± 2.0
174	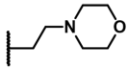	52 ± 3.0
182	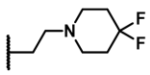	ND

The results show that the compounds featuring a piperidine, methoxymethyl, and THP at the R^1 group all had binding affinities comparable to **156**, which has a methyl group at R^1 (*cf.* K_d = 28 ± 5.0 nM, 29 ± 6.0 nM, 36 ± 2.0 nM and K_d = 33 ± 4.0 nM, respectively).

Compound **174**, which has a morpholine at R^1, was only a slightly weaker binder than **156** (*cf*. K_d = 33 ± 4.0 nM and K_d = 52 ± 3.0 nM, respectively). These data indicated that the piperidine, methoxymethyl, THP and morpholine substituents the R^1 position were not detrimental to the binding affinity of compound **156** and therefore could be used to evaluate the physicochemical properties required increase the potency of compounds in parasites. Two compounds, **183** and **181**, demonstrated binding affinities that were substantially higher than the binding affinity of **156** (*cf*. K_d = 6.0 ± 2.0 nM, 11 ± 6.0 nM and K_d = 33 ± 4.0 nM, respectively). Both compounds feature a piperazine ring at R^1 that is substituted at the 4-position with either a methyl (**183**) or acetyl group (**181**). A binding affinity could not be determined for **182** because the compound formed aggregates in the buffer solution across the range of concentrations used in the assay.

4.4.2 Validation of binding affinities using ITC

ITC was used to validate the binding affinity of compounds **181** and **183**, which measured the highest affinity in the MST assay (Figure 4.1). The ITC data for these compounds were in good agreement with the MST data. Compound **183** had K_d = 7.0 ± 2.0 nM in the ITC assay, which correlates strongly with the binding affinity measured in MST (K_d = 6.0 ± 2.0 nM). Similarly, the binding affinity of **181** using ITC was K_d = 26 ± 5.0 nM, and in MST it measured K_d = 11 ± 6.0 nM. ITC confirmed the identification of high affinity binders for *Ld*BDF5.1.

A)

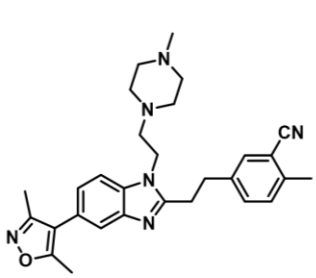

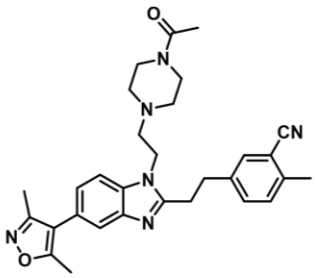

Compound	183	181
K_d (ITC)	7.0 ± 2.0 nM	26 ± 5.0 nM
K_d (MST)	6.0 ± 2.0 nM	11 ± 6.0 nM

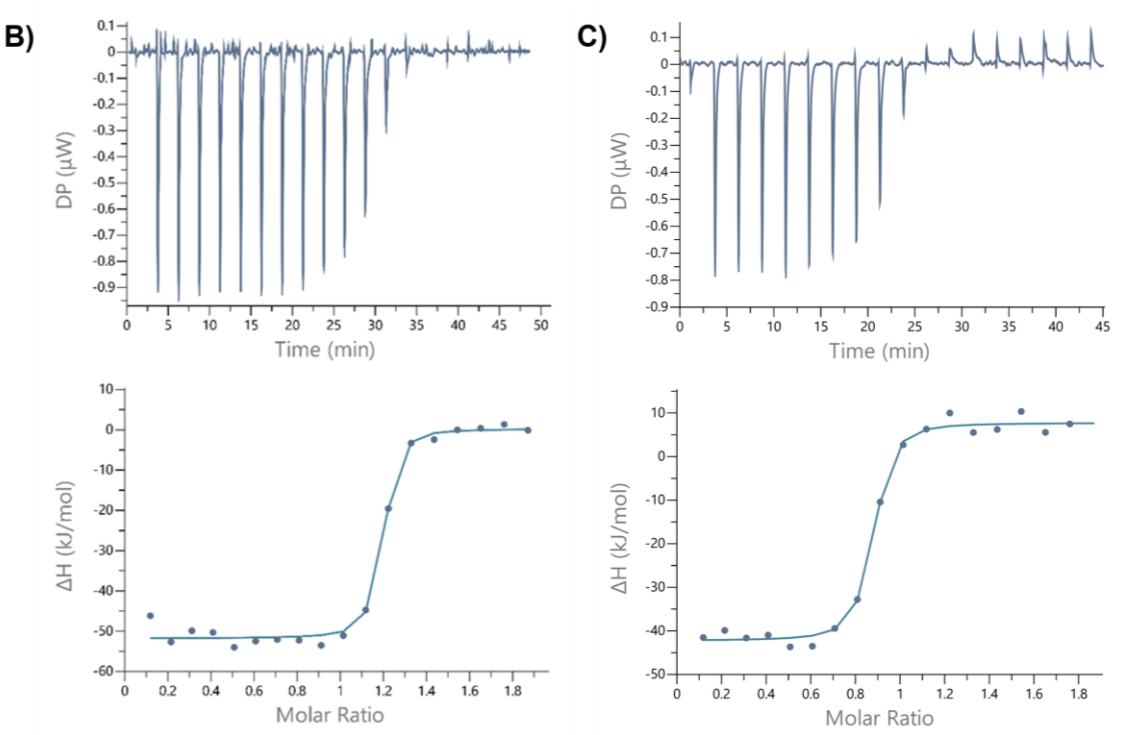

Figure 4.1. A) Comparison of the binding affinity (K_d) data for compounds **183** and **181** measured using ITC and MST. The error quoted is the SEM from n = 3 repeats. **B)** Representative trace from ITC with **183** (10 µM) and *Ld*BDF5.1 (100 µM). **C)** Representative trace from ITC with **181** (10 µM) and *Ld*BDF5.1 (100 µM). The thermodynamic parameters of the binding interations are detailed in the Appendix section A6.

4.4.3 Evaluation of the effect of physicochemical variation on the activity of compounds in the promastigote assays

The analogues of **156** with varied physicochemical properties were assessed in the 5-day promastigote viability assay (conducted by Dr Nathaniel Jones at the University of York), as described in section 4.2, to determine their potency. The results of the assay and the

physiochemical properties of the compounds were compared to explain the differences in activity observed in the parasites (Table 4.5 and Figure 4.2).

Table 4.5. Compounds assessed in the 5-day *L. donovani* promastigote viability assay. The EC_{50} values are reported alongside the compound K_d from the MST assay. The error is the SEM from n =3 repeats. MW = molecular weight (Da); TPSA = topological polar surface area (Å^2); HBA = number of hydrogen bond acceptors calculated in ChemAxon from the protonation state of the compound at pH 7.4. Calculator Plugins were used for structure property prediction and calculation, Marvin 23.12, 2023, ChemAxon (http://www.chemaxon.com). OSIRIS DataWarrior 5.5.0 software was used to calculate TPSA.[245]

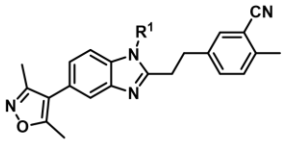

Lowest affinity/ potency — **Highest affinity/ potency**

Compound	R^1	EC_{50} (μM)	K_d (nM)	Chrom $logD_{7.4}$	MW	TPSA	HBA	pK_a
185		0.87 ± 0.03	29 ± 6.0	5.4	414.51	76.9	4	N/A
156		1.83 ± 0.20	33 ± 4.0	5.1	370.46	67.6	3	N/A
180	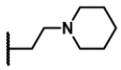	5.33 ± 0.37	28 ± 15	6.6	467.62	70.9	3	9.1
186	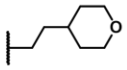	6.00 ± 0.39	36 ± 2.0	5.7	468.60	76.9	4	N/A
174	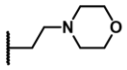	6.36 ± 0.91	52 ± 3.0	5.1	469.59	80.1	5	7.0
183	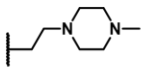	9.81 ± 2.72	6.0 ± 2.0	4.7	482.63	74.1	4	3.1/8.3
181	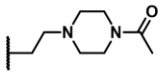	>30	11 ± 6.0	4.1	510.64	91.2	5	7.7
182	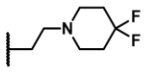	ND	ND	6.0	503.60	70.9	3	8.2

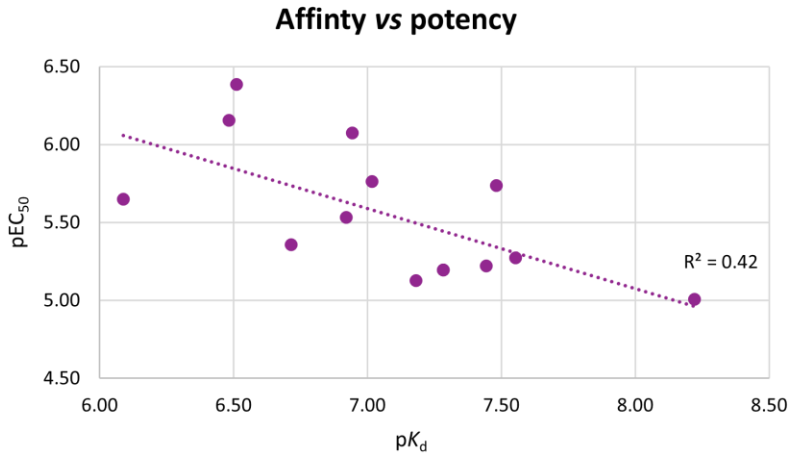

Figure 4.2. Scatter plot of affinity *vs* potency for all compounds evaluated in the promastigote viability assay showing a weak negative correlation ($R^2 = 0.42$).

Compounds **156**, **174**, **180**, **185**, and **186** all exhibited similar binding affinities for *Ld*BDF5.1. However, the compounds were not equally potent in the parasites (Table 4.5 and Figure 4.2). Compounds **185** and **156** were the most potent in the cell viability assay with EC_{50} values of 0.87 ± 0.03 µM and 1.83 ± 0.20 µM, respectively. Compounds **174**, **180**, and **186** exhibited lower potency (EC_{50} = 6.36 ± 0.91 µM, 5.33 ± 0.37 µM, and 6.00 ± 0.39 µM, respectively). These results could be rationalised by comparing the relative size of the group at R^1. Compounds **174**, **180**, and **186** all feature a heterocycle attached to an ethyl linker at R^1, whereas compounds **156** and **185** feature smaller methyl and methoxymethyl groups at this position. The smaller groups at the R^1 position, and lower MW compounds, appear to result in compounds with higher potency (Figure 4.3, A). The larger molecules may have demonstrated decreased permeability because they were slower to diffuse across membranes in the parasites.

The TPSA varied for compounds **174**, **180**, and **186** (*cf.* 80.1 Å^2, 70.9 Å^2, and 76.9 Å^2, respectively). However, all three compounds exhibited similar potencies (between 5.33 and 6.36 µM). The TPSA of one of the least potent compounds, **186** (EC_{50} = 6.00 ± 0.39 µM), was the same as the most potent compound, **185** (76.9 Å^2), indicating that TPSA was not an important factor in influencing the potency of compounds. The decreased potency of **186** was more likely due to the bulkier THP group at R^1 (Figure 4.3, B). Additionally, there did not appear to be any correlation between chromlog$D_{7.4}$ and efficacy (Figure 4.3, C).

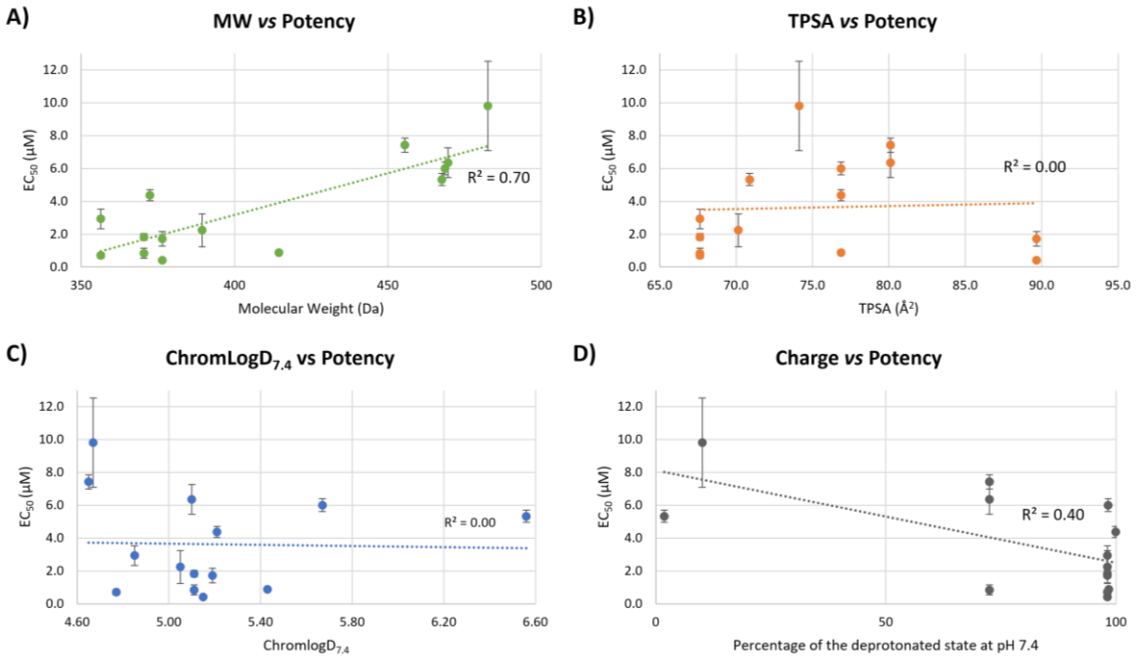

Figure 4.3. A) Scatter plot of MW *vs* potency for all compounds evaluated in the promastigote viability assay showing a positive correlation (R^2 = 0.70). **B)** Scatter plot of TPSA *vs* potency for all compounds evaluated in the promastigote viability assay showing no correlation (R^2 = 0.00). **C)** Scatter plot of chromlog$D_{7.4}$ *vs* potency for all compounds evaluated in the promastigote viability assay showing no correlation (R^2 = 0.00). **D)** Scatter plot of charge *vs* potency for all compounds evaluated in the promastigote viability assay showing a weak negative correlation (R^2 = 0.40).

Interestingly, the highest affinity compounds, **183** and **181** (K_d = 6.0 ± 2.0 nM and 11 ± 6.0 nM, respectively) measured the lowest potencies in the parasites (EC_{50} = 9.81 ± 2.72 µM and >30 µM). The pKa of piperazine nitrogen atoms in compounds **181** and **183** renders these compounds more likely to be protonated at pH 7.4. The charged state of compounds **181** and **183** in the assay might have reduced their ability to permeate the lipid membrane and reduced their activity in the parasites. The high MWs and large piperazine ring on the ethyl linker at R^1 in compounds **181** and **183** may have also contributed to their decreased permeability.

Overall, the results from the promastigote viability assay indicated that both size and charge were important determinants of potency in the parasites than the binding affinity of a compound. Compound **182** was not soluble in the cell viability assay, and the lack of binding affinity and potency data for this compound hindered its use as a chemical probe for *Ld*BDF5.1.

Work is ongoing to evaluate the activity of ligands that were most potent in the promastigote viability assays in intracellular amastigotes, the medically relevant stage of

the *Leishmania* parasite. The amastigotes reside inside macrophages which provide an additional barrier of macrophage cell membrane permeability for the compounds. Therefore, it is likely that the physicochemical properties required for compounds to be potent against the amastigotes will differ from those necessary for potency in the promastigotes.

4.5 Investigation of binding modes using X-ray crystallography studies

An X-ray crystal structure was sought to validate the binding mode of high affinity compounds in *Ld*BDF5.1. A collaborator at the University of Freiburg, Marius Amann, had established a co-crystallisation workflow for the highly analogous *Lmx*BDF5.1. Compound **181** was co-crystallised with *Lmx*BDF5.1 and the X-ray crystal structure was solved by Dr Martin Hügle (the methods and structural refinement are detailed in the Experimental, Section 6.8). There are only two differentiated residues in the sequences of the BDF5.1 protein in *L. mexicana* and *L. donovani,* and neither of these mutations are located within the binding pocket (Figure 4.4). Therefore, this X-ray crystal structure also provided a highly valuable insight into the binding mode of compound **181** in *Ld*BDF5.1.

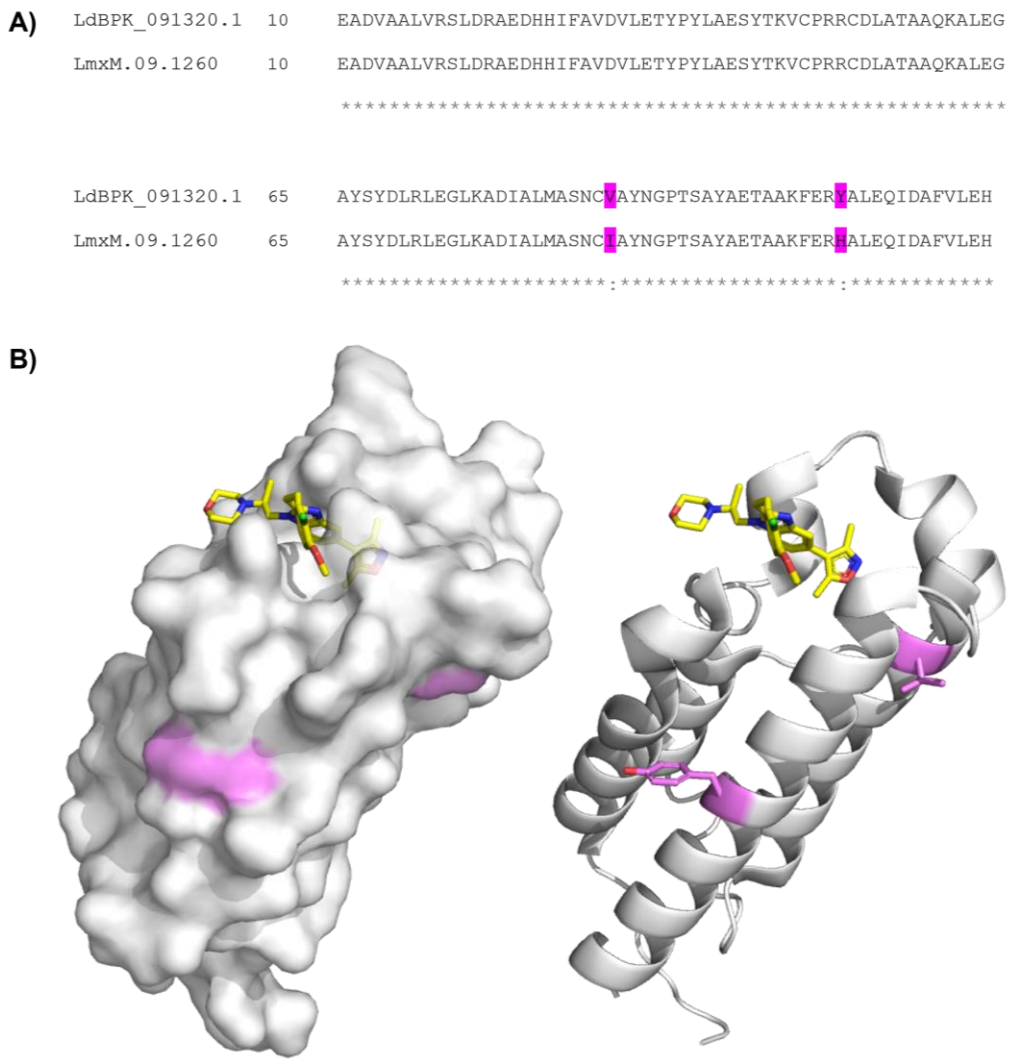

Figure 4.4. A) A sequence alignment with *Ld*BDF5.1 (LdBPK_091320.1, top) and *Lmx*BDF5.1 (LmxM.09.1260, bottom). Highlighted in pink are the two residues that differ in the BDF5.1 proteins. The sequence alignment was carried out using MUSCLE.[160] **B)** Views of X-ray crystal structures of **SGC-CBP30** (carbon = yellow) in *Ld*BDF5.1 (cartoon and surface = white; PDB code: 6BYA). Highlighted in pink are the residues that are different in *L. mexicana* and *L. donovani.*

The crystal structure demonstrates that the 3,5-dimethylisoxazole acts as a KAc mimic in the binding site of BDF5.1 and forms a hydrogen bond with N90 and a water-mediated hydrogen bond with Y44 (Figure 4.5).

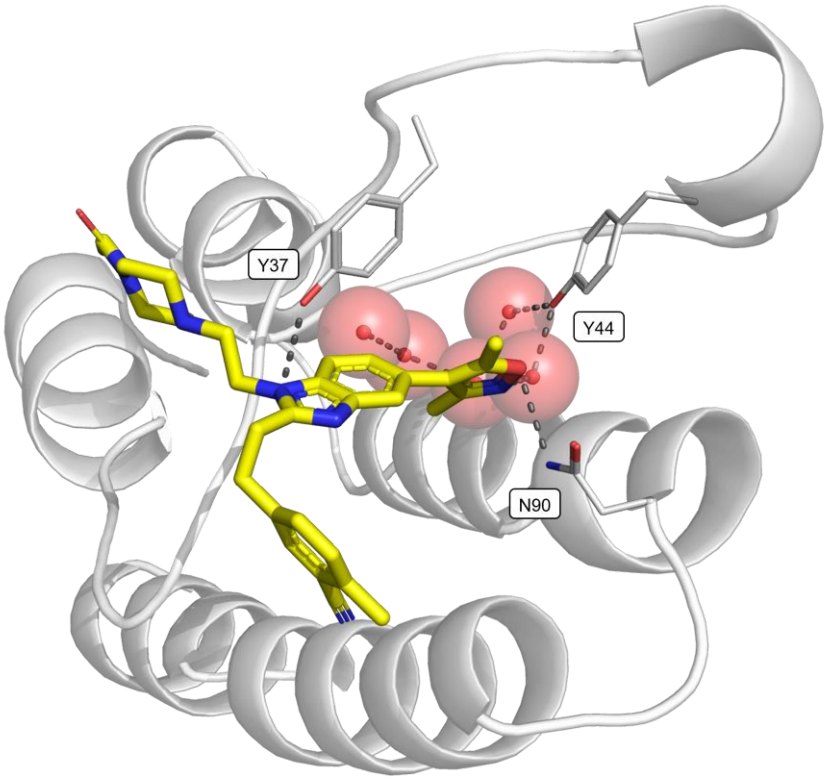

Figure 4.5. View of the X-ray crystal structure of **181** (carbon = yellow) in the binding site of *Lmx*BDF5.1 (cartoon and carbon = white). The 3,5-dimethylisoxazole acts as a KAc mimic and forms a hydrogen bond with N90 and a water-mediated hydrogen bond with Y44. The benzimidazole core hydrogen bonds with Y37.

Hydrogen bonding interactions appear to be formed between the nitrogen atoms in the benzimidazole core and the hydroxyl of Y37. The *C*-2 ethyl linker sits over I28 (part of the "HIF shelf" — analogous to the "WPF shelf" in human BRD4(1))[21] and forms hydrophobic interactions in this area (Figure 4.6, A). The X-ray crystal structure validates the binding modes proposed from the docking studies in Chapter 3, section 3.5. Notably, the 3-cyano-4-methylbenzene ring is π-stacking with Y96 to direct the nitrile group at the T99 residue, enabling the nitrile to hydrogen bond with the T99 hydroxyl group.

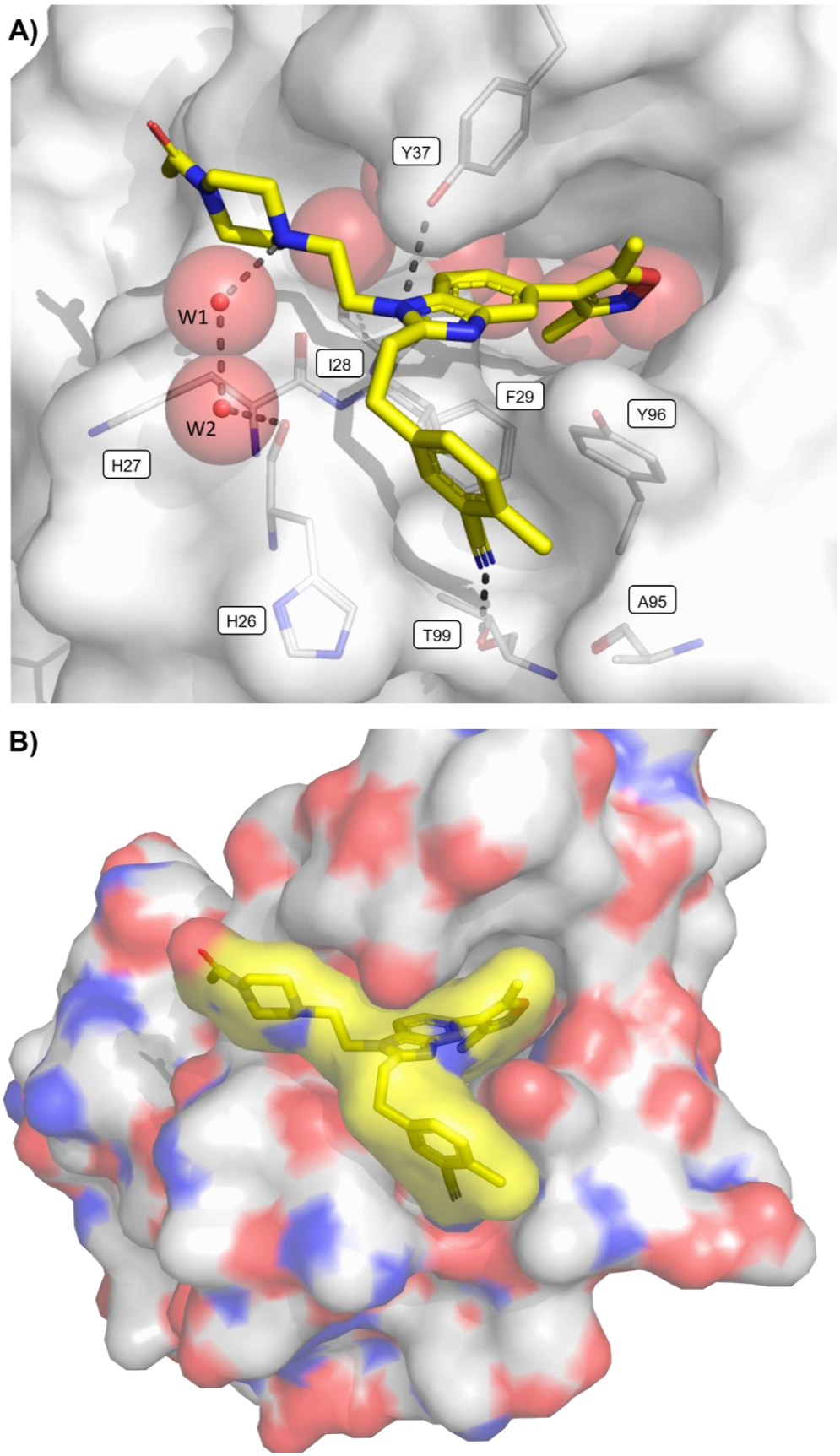

Figure 4.6. A) View of an X-ray crystal structure of **181** (carbon = yellow) in the binding site of *Lmx*BDF5.1 (carbon = white). **B)** The space fill of compound **181** (carbon = yellow) in the binding site of *Lmx*BDF5.1 (carbon = white).

As hypothesised, the *N*-1 ethylene linker extends out of the ZA channel such that the *N*-acetyl piperazine ring is in a solvent exposed region of the protein (Figure 4.6, A). In the X-ray crystal structure, the nitrogen of the *N*-acetyl piperazine can form hydrogen bonds with water molecules, W1 and W2, in this area. W1 and W2 appear to be bulk water molecules, rather than the conserved water molecules in the *Ld*BDF5.1 binding site. As the *N*-acetyl group projects into the bulk solvent, it may be a suitable location for further derivatisation without affecting the binding affinity.

4.6 Evaluation of selectivity for *Ld*BDF5.1 over human bromodomains

Chemical probes must be highly selective to ensure that their biological activity is due to an on-target effect, and to reduce off-target activity.[255] The high structural conservation of bromodomain proteins posed a significant challenge toward developing selective chemical probes for *Ld*BDF5.1.[255] However, the low levels of sequence homology between the parasitic bromodomains and human bromodomains provided a potential advantage in terms of achieving selective compounds without negatively affecting human biology.[56]

4.6.1 Binding affinity of compound 174 in human BRD4(1) and CREBBP

To investigate the selectivity of the ligands optimised for *Ld*BDF5.1, the binding of compound **174** to the human CREBBP and BRD4(1) proteins (provided by other members of the Conway Group) was assessed using ITC (Table 4.6). BRD4(1) was chosen as a representative human bromodomain because it is the most extensively characterised BET protein and has implications in multiple disease states.[256, 257] The binding affinity of **174** to CREBBP was evaluated since the compounds that were optimised for *Ld*BDF5.1 were very similar in structure to the **SGC-CBP30** ligand that is selective for CREBBP.[69]

Table 4.6. Binding affinity (K_d) data for compounds **174** and **SGC-CBP30** for the *Ld*BDF5.1, human CREBBP and human BRD4(1) proteins measured using ITC. The error quoted is the SEM from n = 3 biological repeats.

Compound	Structure	*Ld*BD5.1 K_d (nM)	CREBBP K_d (nM)	BRD4(1) K_d (nM)
174	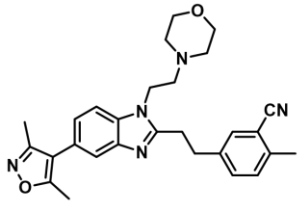	37 ± 12	5620 ± 334	9540 ± 1700
SGC-CBP30	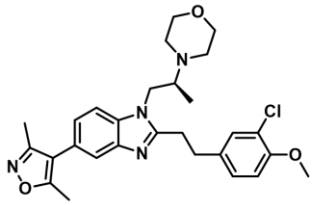	280 ± 12	21 ± 2*	850 ± 96*

*binding affinity data for **SGC-CBP30** from *Hay et al.*[69]

Compound **174** displayed greater than 100-fold selectivity for *Ld*BDF5.1 over human CREBBP and human BRD4(1) determined using ITC (*cf.* K_d = 37 ± 12 nM with K_d = 5620 ± 334 nM and K_d = 9540 ± 1700 nM, respectively). The **SGC-CBP30** ligand had a binding affinity of 280 ± 12 nM for *Ld*BDF5.1, yet the small structural differences between this ligand and **174** resulted in the **SGC-CBP30** compound being 10-fold more selective for human CREBBP than the parasite bromodomain (K_d = 21 ± 2 nM).[69] Selectivity can therefore be achieved for both parasitic and human targets.

4.6.2 Differences in the binding sites of *Ld*BDF5.1, BRD4(1) and CREBBP

Bromodomains share a conserved fold comprising a bundle of four α-helices (named αZ, αA, αB and αC) linked by more diverse loop regions.[10] Bromodomain substrate specificity has been achieved with human bromodomain inhibitors by targeting the loop regions (ZA and BC) that surround the KAc binding site and show large sequence variations.[56] In particular, selective and high affinity inhibitors for human BET bromodomains have been developed by designing compounds to fill the region of space adjacent to a conserved stretch of three amino acids adjacent to the KAc binding site known as the 'WPF shelf'.[26] For example, the potent and selective BRD4(1) inhibitor

(*R*)-OXFBD04 (K_d = 247 ± 80 nM) features a pyridine ring that occupies the space next to the WPF shelf (Figure 4.7).[26, 46] The WPF motif is inherent to BET bromodomains but absent in most non-BET bromodomains.

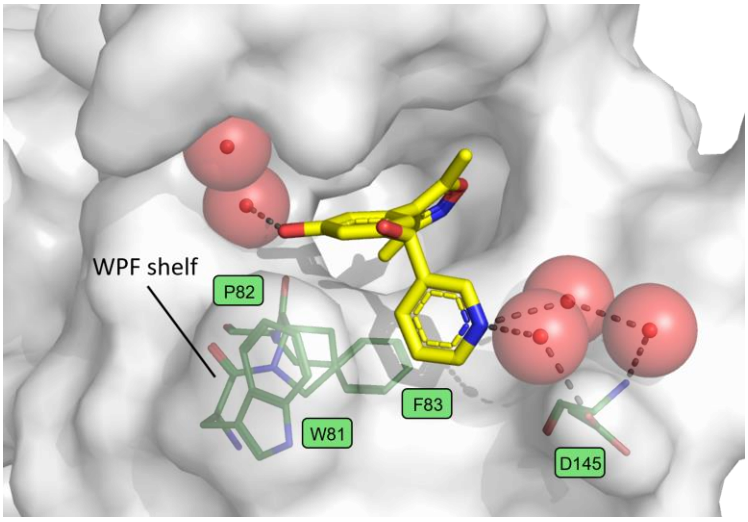

Figure 4.7. A view of **(*R*)-OXFBD04** (carbon = yellow) in BRD4(1) (carbon = green; PDB code: 6FSY) that highlights the pyridine ring occupies the space next to the WPF shelf.[46, 179]

A few residues differ between the CREBBP and the BET bromodomains binding sites (Figure 4.8).[139] First, W81 from the top of the WPF shelf of BET bromodomains corresponds to a leucine in the CREBBP bromodomain, making this part of the binding site of CREBBP more suitable to accommodate bulkier ligands. Another residue that is key for attaining selectivity toward CREBBP is R1173, located at the entrance of the binding site of this bromodomain. This residue corresponds to D145 in BRD4(1). Some selectivity for the CREBBP bromodomain has resulted in part from exploiting specific cation–π interactions from ligands to the R1173 side chain (Figure 4.8, B).[69, 142, 143]

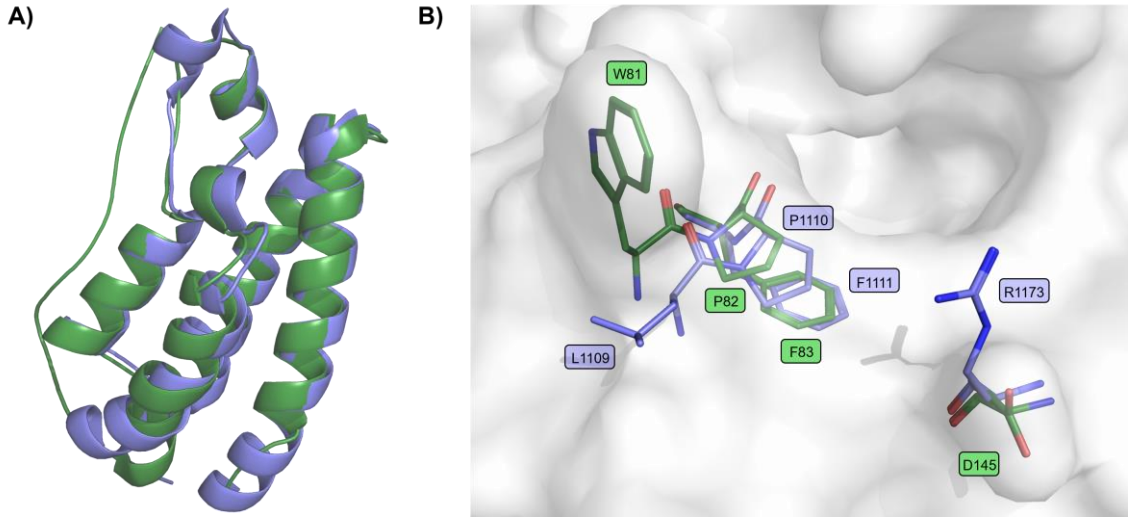

Figure 4.8. A) The overall fold of BRD4(1) (green cartoon; PDB code: 4NR8) is similar to that of CREBBP (purple cartoon; PDB code: 4NR7).[138, 258] **B)** A view of the X-ray crystal structure of CREBBP (purple cartoon; PDB code: 4NR7) overlaid with the X-ray crystal structure of BRD4(1) (surface = white, carbon = green; PDB code: 4NR8). This overlay shows that the WPF shelf region of BRD4(1) is altered to an LPF motif in CREBBP. The D145 residue in BRD4(1) is equivalent to R1173 in CREBBP.

The structural differences in the binding sites of *Ld*BDF5.1 and the human bromodomains help to rationalise the selectivity of **174** for the parasite bromodomain. In *Ld*BDF5.1, the WPF residues, are replaced by a HIF motif (H27, I28, F29; Figure 4.9). Compound **174** fills the region of space adjacent to the HIF motif with the *N*-1 ethyl substitution on the benzimidazole core extending out of the ZA channel. This part of the binding site of BRD4(1) will not accommodate **174** because the ligand would sterically clash with W81. Compound **174** is also not optimised to interact with the hydrophobic region of BRD4(1) – the morpholino-ethyl was designed to reside in a solvent exposed region of *Ld*BDF5.1.

The key interaction that results in the high affinity of compound **174** for *Ld*BDF5.1 was attributed to the hydrogen bonding interaction of the nitrile of the 3-cyano-4-methylphenyl ring with T99. The directionality of this interaction is facilitated by the π-stacking of the phenyl ring with Y96 in *Ld*BDF5.1. In human BRD4(1) the Y96 residue of *Ld*BDF5.1 is replaced by I146, and the T99 residue is replaced by M149 (Figure 4.9). The structural differences in this key binding region of *Ld*BDF5.1 result in significantly lower binding affinity for **174** in BRD4(1).

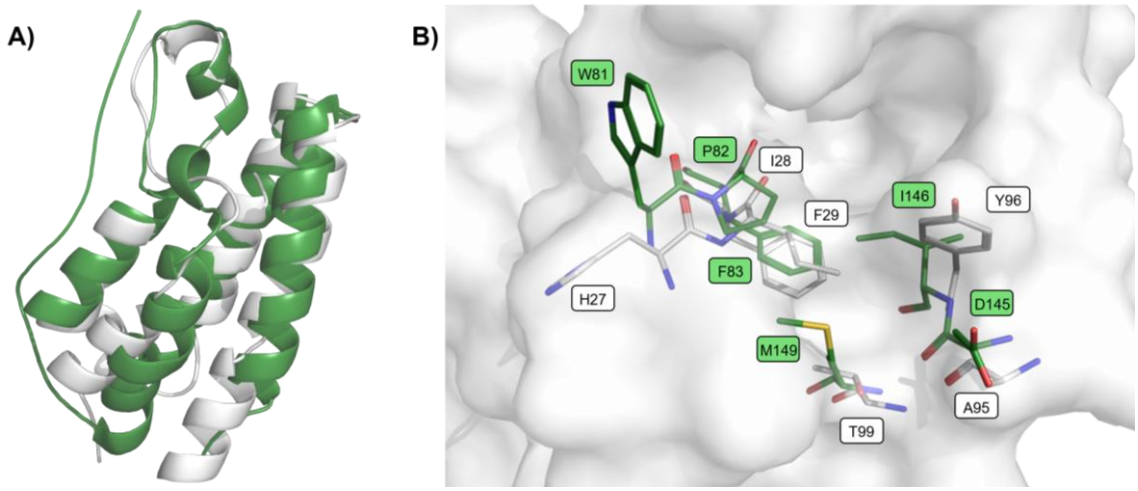

Figure 4.9. A) The overall fold of BRD4(1) (green cartoon; PDB code: 4NR8) is similar to that of *Ld*BDF5.1 (white cartoon; PDB code: 6BYA).[131, 258] **B)** A view of the X-ray crystal structure of BRD4(1) (carbon = green; PDB code: 4NR8) overlaid with the X-ray crystal structure of *Ld*BDF5.1 (surface = white, carbon = white; PDB code: 6BYA). This overlay shows that the WPF shelf region of BRD4(1) is altered to a HIF motif in *Ld*BDF5.1. The M149, D145 and I146 residues in BRD4(1) are equivalent to T99, A95 and Y96 in *Ld*BDF5.1.

A comparison of the binding modes of the **SGC-CBP30** compound to *Ld*BDF5.1 and CREBBP helps to explain the low affinity of **174** for CREBBP (Figure 4.10, A & B). The **SGC-CBP30** ligand adopts different binding conformations in the *Ld*BDF5.1 and CREBBP binding sites due to the flexible *C*-2 ethyl linker. The residue R1173 is key for attaining the selectivity and high affinity for the **SGC-CBP30** ligand towards CREBBP.[69] The **SGC-CPB30** compound has an electron rich ring which forms cation–π interactions with the positively charged R1173 side chain. Compound **174** features a relatively electron poor ring, owing to the nitrile substituent at the *meta*-position, which may reduce its ability to form these interactions. Additionally, the nitrile is at the same position as the chlorine atom in the **SGC-CBP30** ligand, which sits in a hydrophobic section of the induced pocket between V1174 and F1177.[69] The longer nitrile in compound **174** could sterically clash with the protein at this position.

The **SGC-CBP30** ligand was optimised for binding to CREBBP and did not exhibit as high affinity for *Ld*BDF5.1 (*cf.* $K_d = 21 \pm 2$ nM and 280 ± 12 nM, respectively). The lower affinity for *Ld*BDF5.1 may be due to the absence of a hydrogen bond acceptor at the *meta*-position of the phenyl ring, which prevents the formation of the key hydrogen bonding interaction with T99 in *Ld*BDF5.1.

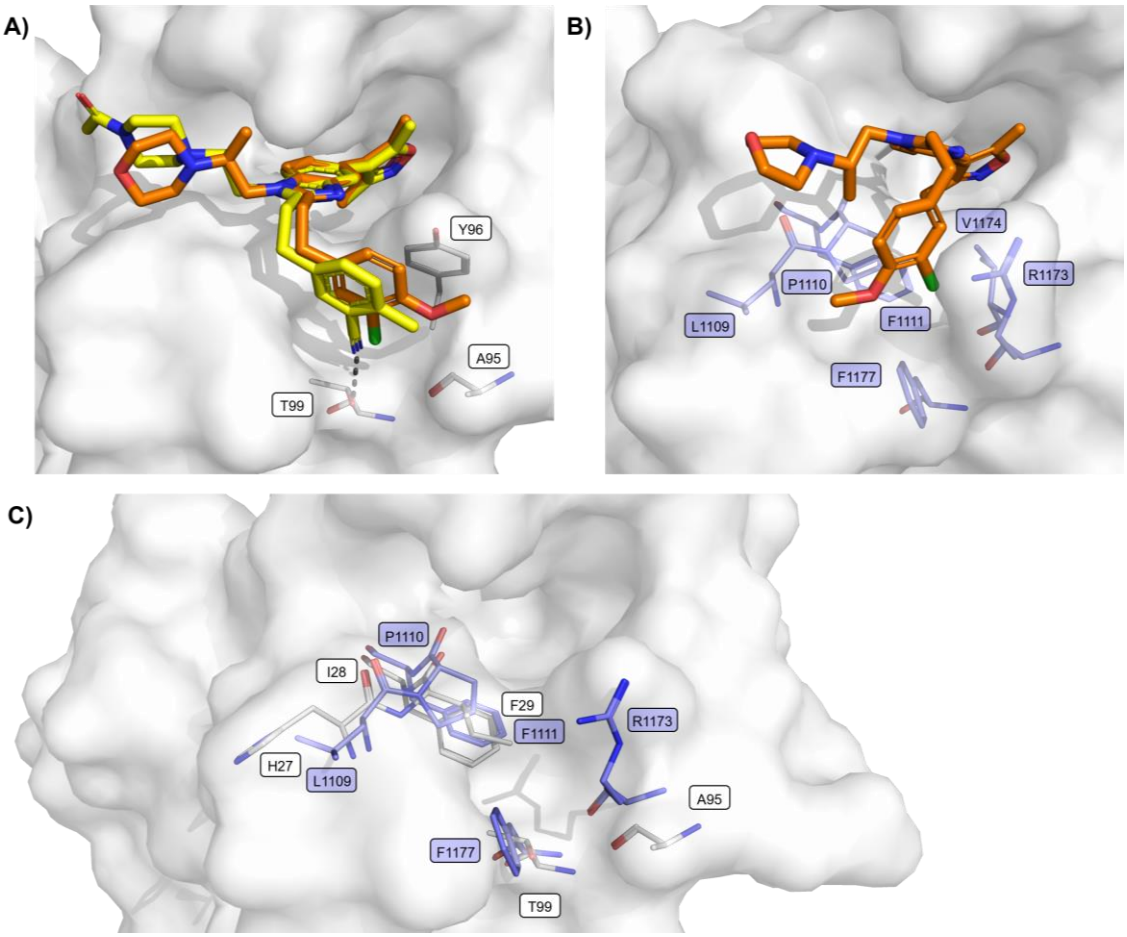

Figure 4.10. A) A view of the X-ray crystal structure of compound **181** (carbon = yellow) bound to *Lmx*BDF5.1 (carbon = white) overlaid with the X-ray crystal structure of **SGC-CBP30** (carbon = orange) in the binding site of *Ld*BDF5.1 (PDB code: 6BYA).[131] **B)** A view of the X-ray crystal structure of **SGC-CBP30** (carbon = orange) in the binding site of CREBBP (carbon = purple; PDB code: 4NR7).[138] **SGC-CBP30** is shown to form cation–π interactions with R1173. **C)** A view of the X-ray crystal structure of CREBBP (carbon = purple; PDB code: 4NR7) overlaid with the X-ray crystal structure of *Ld*BDF5.1 (surface = white, carbon = white; PDB code: 6BYA).[131, 138] This overlay highlights that the A95 and T99 residues in *Ld*BDF5.1 are replaced by R1173 and F1177 in CREBBP.

4.7 Evaluation of the selectivity of 174 for BDF5.1 over BDF5.2

Chemical probes for *Ld*BDF5.1 need to be selective over BDF5.2 to enable the effects of bromodomain inhibition to be attributed to the specific protein domain. Selective probes would also enable experiments to investigate whether inhibition of the single bromodomain in BDF5 is sufficient to perturb the entire function of the protein.

The selectivity of compound **174** for BDF5.1 over BDF5.2 was evaluated using ITC. Due to limited protein availability, *Lmx*BDF5.2 was used in the ITC assay rather than *Ld*BDF5.2. However, given the 7 mutated residues in the sequences of BDF5.2 in

L. mexicana and *L. donovani* are not located within the KAc binding pocket, it was reasonable to assume that the binding affinity of **174** in *Lmx*BDF5.2 and *Ld*BDF5.2 would be similar enough to evaluate the selectivity of **174** for BDF5.1 (Figure 4.11).

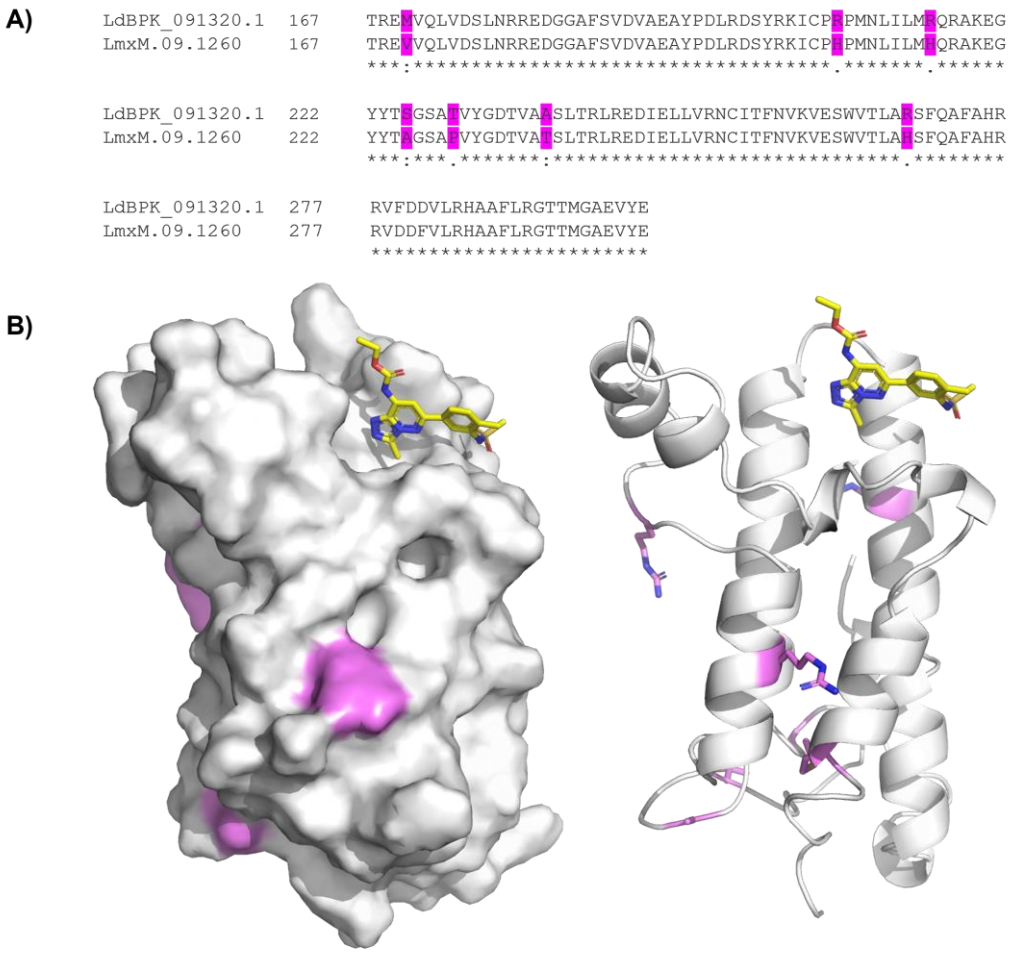

Figure 4.11. A) A sequence alignment with *Ld*BDF5.2 (LdBPK_091320.1, top) and *Lmx*BDF5.2 (LmxM.09.1260, bottom). Highlighted in pink are the seven residues that differ in the BDF5.2 proteins. The sequence alignment was carried out using MUSCLE.[160] **B)** Views of the X-ray crystal structure of **bromosporine** (carbon = yellow) bound to *Ld*BDF5.2 (cartoon and surface = white; PDB code: 5TCK).[132] Highlighted in pink are the residues that are different in *L. mexicana* and *L. donovani.*

The binding affinity for compound **174** in *Lmx*BDF5.2 was 36 ± 5.9 µM (Table 4.7). Compound **174** exhibits 974-fold selectivity for *Ld*BDF5.1 over *Lmx*BDF5.2. The ITC results highlight that it should be possible to develop domain specific ligands for BDF5 in *Leishmania*.

Table 4.7. Binding affinity (K_d) data for compound **174** to *Ld*BDF5.1 and *Lmx*BDF5.2 measured using ITC (assay performed by Marius Amann at University of Freiburg). The error quoted is the SEM from n = 2 biological repeats.

Compound	Structure	*Ld*BD5.1 K_d (nM)	*Lmx*BD5.2 K_d (nM)	Fold selectivity
174	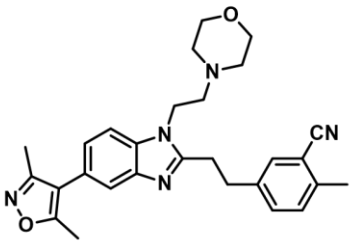	37 ± 12	36050 ± 5850	974

BDF5.2 has a canonical bromodomain structure, featuring conserved N257 and Y201 residues that bind KAc and KAc mimetics (Figure 4.12, A). Structural differences between BDF5.1 and BDF5.2 surround the KAc binding site (Figure 4.12, B). For example, the HIF motif of BDF5.1 is replaced by G184, A185 and F186 in BDF5.2. The Y96 that features in *Ld*BDF5.1 is replaced by W263 in BDF5.2. One reason for the low binding affinity of **174** in BDF5.2 may be that the bulkier W263 residue sterically clashes with the substituted phenyl ring of **174**. Moreover, the hydrogen bonding interaction between the nitrile of **174** and BDF5.2 would be absent due to the replacement of T99 with L266.

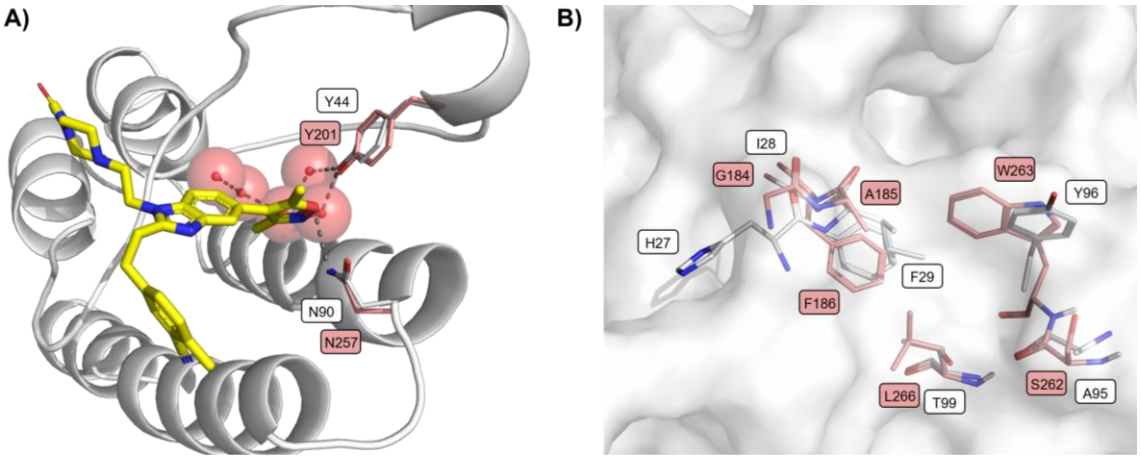

Figure 4.12. A) A view of the X-ray crystal structure of compound **181** (carbon = yellow) bound to *Lmx*BDF5.1 (carbon and cartoon = white) overlaid with the X-ray crystal structure of *Ld*BDF5.2 (carbon = pink; PDB code: 8BPT).[137] This comparison shows that the NY motif, which is important for KAc and KAc-mimic binding, is conserved between the proteins. **B)** A view of the X-ray crystal structure of *Ld*BDF5.2 (surface = white, carbon = pink; PDB code: 8BPT) overlaid with the X-ray crystal structure of *Ld*BDF5.1 (carbon = white; PDB code: 6BYA).[131, 137] This overlay highlights that the HIF motif in BDF5.1 is replaced by a GAF motif in BDF5.2. A95, Y96 and T99 residues in BDF5.1 are replaced by S262, W263 and L266 in BDF5.2.

4.8 The selectivity of ligands optimised for *Ld*BDF5.1 over the bromodomains in *Ld*BDF1-4

Selectivity for *Ld*BDF5.1 over the other *L. donovani* bromodomains is important for chemical validation of *Ld*BDF5.1 in a phenotypic context. A sequence alignment of the canonical bromodomains in *Ld*BDF1-5 (Figure 4.13) revealed large sequence variation in the loop regions that surround the KAc binding site in *Ld*BDF5.1. Moreover, the bromodomains in *Ld*BDF1-4 all lack the key residues (Y97 and T99) that were targeted to develop high affinity ligands for *Ld*BDF5.1. Thus, it was hypothesised that the ligands that were optimised for binding to *Ld*BDF5.1 would demonstrate low affinity for *Ld*BDF1-4. To confirm this hypothesis, biophysical assays with recombinant *Ld*BDF1-4 bromodomains should be conducted.

```
LdBDF5.1          YNGPTSAYAETAAKFERYALEQIDAFVLEHNG-------GC----

LdBDF1            YNGIQAPASKLARTMEVLMEDRFV----------------------
LdBDF2            FNEKGSQWHDLAKQLKKRYLTLAQESGLSFDA-----DQAFIPTK
LdBDF3            FNGANSLLATEAGKCRSALDRIRRAYQDDQRI-------TVEEAE
LdBDF4            YNGGGSELSRQASALLSAGVKALRDSQAEED--------------
LdBDF5.2          FNVKVESWVTLARSFQAFAHRRVDDFVLRHAAFLRGTTMGAEVYE
                  :*          *
```

Figure 4.13. A section of the sequence alignment (starting at residue Y89 in LdBDF5.1) with the canonical bromodomains in *L. donovani* (*Ld*BDF1-5). Highlighted in green are the residues that are in the same position as Y96 and T99 in *Ld*BDF5.1. The bromodomains in *Ld*BDF1-4 and *Ld*BDF5.2 do not have a tyrosine or threonine at these positions. The sequence alignment was carried out using MUSCLE.[160]

4.9 Determination of ADMET properties of ligands for *Ld*BDF5.1

A selection of compounds designed to target *Ld*BDF5.1 were profiled for their ADMET properties (the assays were conducted by Dr Andreas Kany at the Helmholtz Institute for Pharmaceutical Research Saarland). The compounds were assessed for murine microsomal clearance and plasma stability (Table 4.8 and Table 4.9). The compounds proved to be prone to liver metabolism and exhibited a low half-life in most cases e.g. compound **145** had a half-life of 1.3 ± 0 min. The low half-lives may, in part, be due to cytochrome P450 mediated oxidation of the aromatic rings.[259] There were two exceptions: compounds **147** and **148** were not metabolised after 2 hours. These compounds both feature a carboxylic acid, which might render them polar enough for renal excretion and

could be a reason why no liver metabolism was observed.[260] The plasma stability of the compounds tested was generally high, with no degradation over a 4 hour period for all compounds except **145** and **146**. Compound **145** had a half-life of 32.1 ± 1.5 min in the mouse plasma, and **146** had a half-life of 77.2 ± 10.3 min. These compounds both feature ester groups and therefore may have been prone to plasma esterases leading to formation of the corresponding carboxylic acid.[261]

In the future development of these compounds as chemical probes for *Ld*BDF5.1, efforts should be made to improve the stability of compounds *in vivo.* Achieving low clearance will prolong the half-life of the compound *in vivo* and help increase its exposure to the target protein. Cl_{int} is hydrophobicity-dependent — compounds with higher lipophilicity are more likely to bind to non-polar active sites of metabolic cytochrome P450 (CYP) enzymes, which reduces metabolic stability and increases unbound clearance.[262] Decreasing the lipophilicity of the compounds might help to improve compound metabolic stability. However, the $logD_{7.4}$ must be optimised to enhance metabolic stability, while maintaining the cell permeability required for potency.

Table 4.8. Murine microsomal clearance and plasma stability data. MLM = mouse liver microsomes; Cl_{int} = intrinsic clearance.

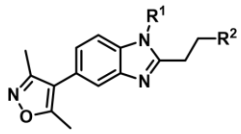

Compound	R^1	R^2	$t_{1/2}$ [min] MLM	Cl_{int} [µl/min/mg]	$t_{1/2}$ [min] Mouse Plasma/% at 4 h
154		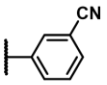	1.5 ± 0.71	1047 ± 480	>240
151		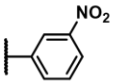	2.9 ± 0.78	508 ± 136	>240
145		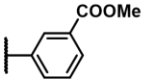	1.3 ± 0	1061 ± 43	32.1 ± 1.5
147		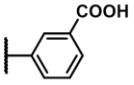	>120	<11.6	>240
121			1.4 (n = 1)	1003 (n = 1)	>240
171	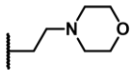		1.4 ± 0.28	1016 ± 179	>240
155		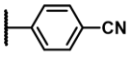	3.4 ± 0.35	422 ± 46	>240
152		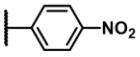	1.9 ± 0.42	745 ± 157	>240
146		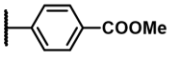	2.5 ± 0.28	566 ± 70	77.2 ± 10.3
148		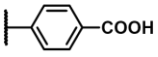	>120	<11.6	>240
138		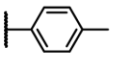	1.4 ± 0.07	1016 ± 33	>240
179	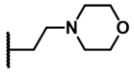	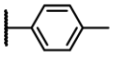	1.4 ± 0.28	998 ± 211	>240

Table 4.9. Murine microsomal clearance and plasma stability data. MLM = mouse liver microsomes; Cl_{int} = intrinsic clearance.

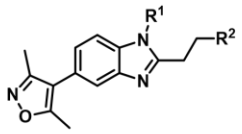

Compound	R^1	R^2	$t_{1/2}$ [min] MLM	Cl_{int} [µl/min/mg]	$t_{1/2}$ [min] Mouse Plasma/% at 4 h
156		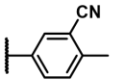	1.5 ± 0.14	710 ± 216	>240
157		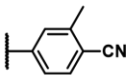	1.4 ± 0.0	977 ± 0.7	>240
168		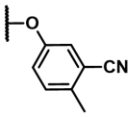	16.6 ± 10.1	103 ± 63	>240
185		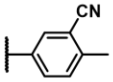	1.8 ± 0.49	836 ± 229	>240
180	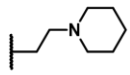	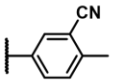	2.5 ± 0.63	579 ± 144	>240
186	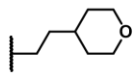	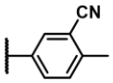	2.0 ± 0.78	763 ± 294	>240
174	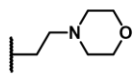	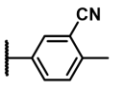	1.7 ± 0.07	853 ± 29	>240
183	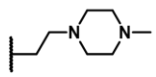	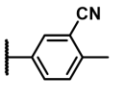	3.8 ± 0.42	369 ± 43	>240
181	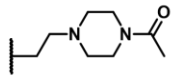	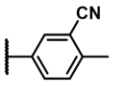	3.2 ± 0.63	103 ± 63	>240
182	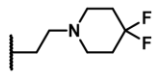	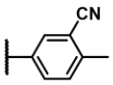	2.3 ± 0.57	617 ± 139	>240

4.10 Conclusions and further work

The work described in this chapter aimed to further develop the hit compounds identified in Chapter 3 into chemical probes for *Ld*BDF5.1. The Structural Genomics Consortium (SGC) has proposed the following criteria for a compound to be nominated as a chemical

probe: IC_{50} or K_d <100 nM, significant cellular activity below 1 μM, and selectivity >30-fold over proteins in the same family.[236] These criteria are similar to the guidelines proposed by Workman *et al.* for high-quality selective chemical probes.[236, 239]

In the development of ligands for *Ld*BDF5.1, 11 compounds were identified with K_d <100 nM. Notably, compounds **183** and **181** demonstrated the highest binding affinities of 6.0 ± 2.0 nM, and 11 ± 6.0 nM, respectively. These binding affinities measured using MST were validated in an orthogonal binding assay using ITC.

Compounds designed to target *Ld*BDF5.1 demonstrated promising activity in the promastigote cell viability assay, with five compounds: **151** **152**, **155**, **157** and **185** showing increased activity relative to miltefosine (EC_{50} < 1.79 μM). The cellular assays revealed that the size and charge state of the R^1 group of compounds had the greatest influence on potency, resulting in smaller and more lipophilic molecules demonstrating higher potency. The binding affinity of compounds did not strongly correlate with their potency, possibly because larger R^1 groups provided additional binding interactions with the protein to improve the affinity, but the increased size of the compound tended to reduce the cell permeability and decrease potency. Work is ongoing to evaluate the potency of compounds against intracellular amastigotes, the medically relevant stage of the *Leishmania* parasite. It is possible that the physicochemical properties of the compounds required to demonstrate activity in the intracellular amastigotes may differ from those necessary for activity against the promastigotes.

The X-ray crystal structure obtained for **181** bound to *Lmx*BDF5.1, provided a highly valuable insight into the binding mode of the compound and confirmed the key hydrogen bonding interaction of the nitrile on the phenyl ring with T99 that resulted in increased binding affinity of compounds.

Compound **174** demonstrated high selectivity (>100 fold) for *Ld*BDF5.1 over human BRD4(1) and CREBBP, and almost 1000-fold selectivity over *Lmx*BDF5.2 (*cf.* K_d = 37 ± 12 nM with K_d = 5620 ± 334 nM, 9540 ± 1700 nM and 36 ± 5.9 μM, respectively, using ITC). The structural differences in the binding sites of *Ld*BDF5.1 and the human bromodomains rationalised the high selectivity of **174** for the parasite bromodomain. In particular, the R^1 group on **174** would sterically clash with the WPF shelf present in BRD4(1) (replaced by a HIF motif in the parasite bromodomain). For CREBBP, the low binding affinity of compound **174** was likely to result from sub-optimal

cation-π interactions of the electron deficient π ring (3-cyano-4-methylbenzene) with R1173. It was postulated that ligands such as **174** may also exhibit selectivity over other *Leishmania* bromodomains in *Ld*BDF1-4 because these proteins lack the threonine residue (T99) and tyrosine residue (Y97) that were targeted by high affinity and selective ligands for *Ld*BDF5.1.

In summary, the work described in this chapter led to the development of several compounds that have the potential to fulfil the criteria to be a chemical probe for *Ld*BDF5.1. The entire panel of compounds were not screened for their selectivity due to time constraints, however, given the structural similarities with high affinity compounds featuring the 3-cyano-4-methylbenzene group at R^2, it was hypothesised that analogues of **174** would also be selective for *Ld*BDF5.1. The ADMET properties of the compounds discussed in this chapter are an area for future improvement and enhancing the metabolic stability of compounds whilst maintaining the cell permeability required for potency will require the correct balance of physicochemical properties.

Chapter 5 - Conclusions and future work

5.1 Conclusions

Epigenetic processes play a key role in the lifecycle of *Leishmania*, enabling the parasite to transition between the different lifecycle stages to survive in multiple hosts. It was hypothesised that interfering with the epigenetic mechanisms in *Leishmania* would be detrimental to the survival of the parasite, and may be an effective strategy for the treatment of leishmaniasis. The main aims of the work described in this dissertation were to design, synthesise, and optimise small molecule ligands for *Ld*BDF5 to chemically validate the protein as a therapeutic target.

Initially, a fragment-based screening approach was adopted to identify KAc mimics that bound to *Ld*BDF5.1 or *Ld*BDF5.2 (Chapter 2). Although no fragments were identified that demonstrated binding to *Ld*BDF5.2 using TSA, three compounds (**17**, **19** and **18**) featuring a 3,5-dimethylisoxazole KAc mimicking motif were identified as binding to *Ld*BDF5.1. The compound displaying the greatest thermal shift, **18**, was subsequently validated as a hit using ITC and its K_d for *Ld*BDF5.1 was measured to be 2.7 ± 0.4 μM. The identification of a lead compound with low micromolar affinity for *Ld*BDF5.1 provided a starting point for the development of higher affinity ligands for *Ld*BDF5.1.

Docking of **18** in *Ld*BDF5.1 informed the design of ligands that were synthesised to investigate the SAR of *Ld*BDF5.1 by identifying two regions within the binding site, which are unique to *Ld*BDF5.1 and appeared to accommodate additional functionalisation. 44 analogues of **18** were synthesised with a diverse range of functionality at the *N*-1 and *C*-2 positions of the benzimidazole core (Chapter 3). The 3,5-dimethylisoxazole is a known KAc mimic and therefore was not modified. The greatest improvement in binding affinity of **18** was seen when the *C*-2 ethyl was functionalised with a 3-nitrophenyl or 3-cyanophenyl group. Compounds **151** and **154** demonstrated a greater than ten-fold increase in affinity compared to **18** (*cf.* K_d = 96 ± 10 nM, 120 ± 16 nM, and 1400 ± 84 nM, respectively, measured using

MST). The high affinity of nitrophenyl and cyanophenyl-containing compounds was attributed to effective π-stacking interactions with Y96 and a key hydrogen bonding interaction with the T99 hydroxyl in the binding site of *Ld*BDF5.1. Targeting these residues in *Ld*BDF5.1 was an effective SAR strategy for increasing *Ld*BDF5.1 affinity and resulted in the development of 11 compounds with K_d <100 nM. Notably, compounds **183** and **181** demonstrated the highest binding affinities of 6.0 ± 2.0 nM, and 11 ± 6 .0 nM, respectively, measured using MST (Table 5.1).

Table 5.1. The binding affinities of analogues of **18** measured using MST. The ligand efficiency (LE) for each compound is given in (kcalmol^{-1})/heavy atom.[263]

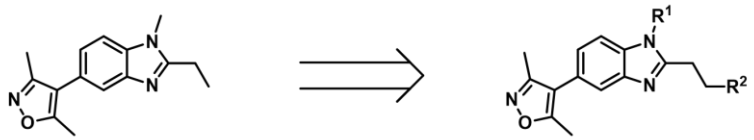

18
K_d = 1400 ± 84 nM (MST)

44 analogues

Compound	R^1	R^2	K_d (MST)	LE
151		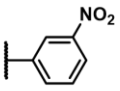	96 ± 10 nM	0.35
154		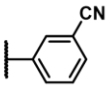	120 ± 16 nM	0.36
183	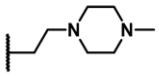	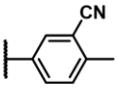	6.0 ± 2.0 nM	0.32
181	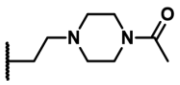	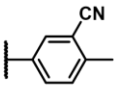	11 ± 6.0 nM	0.29

Compounds designed to target *Ld*BDF5.1 were tested in cell viability assays and exhibited growth inhibition of *Leishmania* promastigotes, supporting previous genetic studies that demonstrated the essentiality of *Ld*BDF5 function for parasite survival (Chapter 4).[61] Five compounds (**151**, **152**, **155**, **157**, and **185**) showed increased activity (EC_{50} = 0.41–1.72 μM) relative to miltefosine (EC_{50} = 1.79 μM). However, the binding affinity of the *Ld*BDF5.1 ligands did not strongly correlate with their potency in promastigotes (Table 5.2). A combination of the size and charge state of the group at *N*-1 of compounds influenced the potency in cellular assays, with smaller and more lipophilic molecules demonstrating higher potency. The importance of cell penetration for efficacy

means that these physicochemical properties will be key considerations for the design of future *Ld*BDF5.1 chemical probes and therapeutics.

Table 5.2. The potency of *Ld*BDF5.1 ligands and their binding affinities measured using MST.

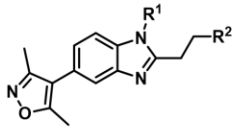

Lowest affinity/ potency — Highest affinity/ potency

Compound	R^1	R^2	EC_{50} (μM)	K_d (nM)	MW (Da)
152	Me	NO_2	0.41 ± 0.09	310 ± 20	376.42
155	Me	CN	0.70 ± 0.16	330 ± 120	356.43
157	Me	CN	0.84 ± 0.31	110 ± 22	370.46
185	O—	CN	0.87 ± 0.03	29 ± 6.0	414.51
151	Me	NO_2	1.72 ± 0.45	96 ± 10	376.42
Miltefosine			1.79 ± 0.22	ND	407.57

The X-ray crystal structure obtained for **181** bound to *Lmx*BDF5.1, confirmed the binding mode of compounds predicted by docking (Figure 5.1). As expected, the 3,5-dimethylisoxazole acts as a KAc mimic in the binding site of *Ld*BDF5.1 and forms a hydrogen bond with N90 and a water-mediated hydrogen bond with Y44. The *N*-1 ethylene linker extends out of the ZA channel into a solvent exposed region of the protein, while the phenyl ring at the *C*-2 ethyl π-stacks with Y96. In high affinity compounds, the nitrile group is directed towards the T99 residue, enabling the hydrogen bond formation with the T99 hydroxyl group.

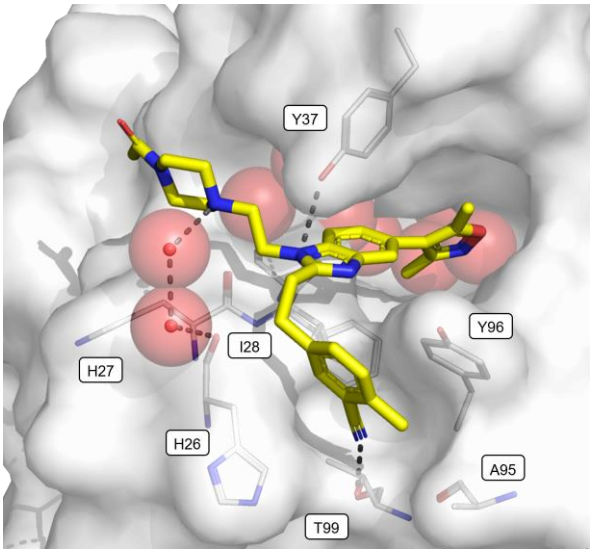

Figure 5.1. View of an X-ray crystal structure of **181** (carbon = yellow) in the binding site of *Lmx*BDF5.1 (carbon = white).

It was possible to achieve selectivity for *Ld*BDF5.1 over human BRD4(1) and CREBBP (Table 5.3). The structural differences in the binding sites of *Ld*BDF5.1 and human BRD4(1) or CREBBP rationalised the high (>100 fold) selectivity of **174** for the parasite bromodomain. This level of selectivity is ideal for chemical validation of a specific protein. It was also shown that compound **174** was 974-fold more selective for *Ld*BDF5.1 over *Lmx*BDF5.2 (*cf.* K_d = 37 ± 12 nM with K_d = 36 ± 5.9 μM, respectively, using ITC). Given the BDF5 protein is highly conserved in *L. donovani* and *L. mexicana*, it was reasonable to assume that compound **174** would demonstrate high selectivity for *Ld*BDF5.1 over *Ld*BDF5.2.

Table 5.3. Binding affinity (K_d) data for compound **174** to *Ld*BDF5.1, *Lmx*BDF5.2, human CREBBP and human BRD4(1) proteins measured using ITC. The error quoted is the SEM from n = 3 biological repeats.

Compound	Structure	*Ld*BD5.1 K_d (nM)	*Lmx*BD5.2 K_d (nM)	CREBBP K_d (nM)	BRD4(1) K_d (nM)
174	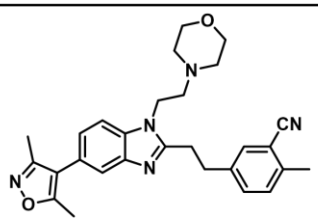	37 ± 12	36050 ± 5850	5620 ± 334	9540 ± 1700
		Fold selectivity:	974	152	258

The work in this dissertation describes the development of high affinity, selective, and potent compounds that have the potential to fulfil the criteria to become chemical probes for *Ld*BDF5.1. Further work is required to confirm that the potency of compounds is due to inhibition of *Ld*BDF5.1, which will provide a strong rationale for the future exploration of BDF5 inhibitors in antileishmanial drug discovery.

5.2 Future work

The compounds discussed in this dissertation are currently being tested in cell viability assays with intracellular amastigotes – the medically relevant stage of the *Leishmania* parasite. Given that the amastigotes reside in a more acidic macrophage environment, it is likely that the physicochemical properties of the compounds required to demonstrate activity in the amastigotes will differ from those necessary for activity against the promastigotes. Therefore, future efforts should focus on optimising the physicochemical properties of compounds to the environment where the amastigote form is found. It was demonstrated that variation at the *N*-1 position of the benzimidazole ring is tolerated without substantial loss in binding affinity, so there is chemical space to make these modifications.

It was postulated that high affinity compounds that exhibited lower activity against the promastigotes were less cell membrane permeant, and so exhibited an inhibitory effect in the parasites. To test this hypothesis, an LCMS assay could be established to provide insight into cell permeability. Treatment of the parasites with the compounds, followed by a washing step and LCMS analysis of the parasite lysate, may give an indication of whether compounds are permeating the cell membrane.

The metabolic studies in Chapter 4 suggested that compounds were readily metabolised by mouse liver microsomes. Metabolite identification (MetID) studies are underway to identify the metabolites of compounds and elucidate their clearance mechanisms. It is hoped that these studies will inform the design of future compounds with enhanced stability *in vivo*, which will help increase compound exposure to the target protein.

There is precedent that a phenotypic effect can be observed for multi-bromodomain proteins even when only one of the bromodomains is targeted by a high affinity ligand.[61,

[264] However, to enhance on-target selectivity and efficacy, potent compounds described in this thesis could also be used as a starting point for a PROTAC (Proteolysis-Targeting Chimera) strategy to degrade BDF5; however, this is caveated by the current lack of validated ubiquitin ligase binding compounds that can recruit parasite E3 ligases to target proteins.[265]

To confirm that the inhibitory effect of compounds is due to inhibition of *Ld*BDF5.1, future work should focus on assessment of target engagement inside cells. Techniques such as chemical proteomics, cellular thermal shift assays (CETSA), and methods using bioluminescence resonance energy transfer (BRET), such as NanoBRET, could be employed.[266-268] Furthermore, a CRISPR-Cas9 genetic screening approach could be adopted to derive and identify drug resistance mutations in *Ld*BDF5 and provide evidence for target engagement.[269-271]

Human BRD4(1) and CREBBP were chosen as representative human bromodomains to assess the selectivity of compound **174** for *Ld*BDF5.1. However, there are at least 61 bromodomains in the human genome that could interact with the inhibitors designed for *Ld*BDF5.1. The selectivity of future chemical probes for *Ld*BDF5.1 should be evaluated using a standardised commercial assay such as BROMO*scan*®, which will measure the binding affinity of test compounds to a wider panel of human bromodomains.[272] The sequence alignment of the bromodomains in *Ld*BDF1-5 (Chapter 4, section 4.8) indicated that there was large sequence variation in the loop regions that surround the KAc binding site in *Ld*BDF5.1. Specifically, the bromodomains in *Ld*BDF1-4 and *Ld*BDF5.2 lack the threonine residue (T99) and tyrosine residue (Y97) that were proposed to be key in achieving high affinity and selective ligands for *Ld*BDF5.1. However, it is necessary to show that the ligands are selective for *Ld*BDF5.1 over *Ld*BDF1-4 to chemically validate BDF5.1 in a phenotypic context. Biophysical assays should be conducted with recombinant *Ld*BDF1-4 to evaluate the binding affinity of highly potent compounds against these proteins.

Finally, given the highly conserved nature of BDF5 across different species of *Leishmania*, the development of potent bromodomain inhibitors may demonstrate broad antileishmanial activity. Compounds should also be screened against different species of *Leishmania* responsible for different forms leishmaniasis. In all, the work described in this dissertation has built a strong foundation for the future development of selective

bromodomain inhibitors that may meet the unmet need for novel antileishmanials and have the potential to alleviate the heavy burden of the parasitic disease.

Chapter 6 - Experimental

6.1 General Chemistry Methods

Reagents and solvents were of commercially available reagent grade quality from Sigma-Aldrich, Fluorochem or Alfa Aesar, and used without purification unless otherwise stated. All non-aqueous reactions requiring anhydrous conditions were carried out under an inert atmosphere of argon or nitrogen, unless otherwise stated. Anhydrous solvents were obtained from an MBRAUN MB5 Solvent Purification System and stored over 3 Å molecular sieves under an inert argon atmosphere. Concentration *in vacuo* refers to removal of solvent on a Buchi^{TM} rotary evaporator under reduced pressure in a water bath at 40 °C. Celite® refers to Celite® 545 filter aid, treated with sodium carbonate, flux-calcined (Sigma Aldrich). Brine refers to a saturated aqueous solution of sodium chloride. Petroleum Ether refers to the fraction in the boiling point range 40–60 °C.

^{1}H NMR spectra were measured on a Bruker AVIII HD 400 (400 MHz), AVII 500 (500 MHz), AVIIIHD 600 (600 MHz) or NEO 600 (600 mHz) spectrometer in the stated solvents as a reference for the internal deuterium lock. The chemical shift data for each signal are given as δ in units of parts per million (ppm) relative to tetramethylsilane (TMS) where δ(TMS) = 0.00. The spectra are calibrated using the solvent peak with the data provided by Fulmer *et al*.[273] The multiplicity of each signal is indicated by: s (singlet); br s (broad singlet); d (doublet); t (triplet); br t (broad triplet); q (quartet); m (multiplet); sp (septet) or combinations thereof. The number of protons (n) for a given resonance signal is indicated by nH. Where appropriate, coupling constants (*J*) are quoted in Hz, recorded to the nearest 0.1 Hz. Spectra were assigned using COSY, HSQC and HMBC experiments as necessary. H_aH_b-X refers to diastereotopic protons at position X, where the specific proton is unassigned. Relative stereochemistry was assigned *via* NOESY experiments.

^{13}C NMR spectra were measured on a Bruker AVII 500 (126 MHz), AVIIIHD 600 (151 MHz) or NEO 600 (151 MHz) spectrometer in the stated solvents as a reference for the internal deuterium lock. The chemical shift data for each signal are given as δ in units of ppm relative to TMS where δ(TMS) = 0.00. The spectra are calibrated using the solvent

peak with the data provided by Fulmer *et al.*[273] The chemical shift is quoted to 1 decimal place, unless two different shifts are indistinguishable, where the shifts are then quoted to 2 decimal places. Spectra were assigned using HSQC and HMBC as necessary.

^{11}B NMR spectra were measured on a Bruker AVIII HD 400 (128 MHz) spectrometer in the stated solvents as a reference for the internal deuterium lock. The chemical shift data for each signal are given as δ in units of ppm relative to TMS where δ(TMS) = 0.00. The spectra are uncalibrated. Coupling constants (*J*) are quoted in Hz, recorded to the nearest 0.1 Hz.

^{19}F NMR spectra were measured on a Bruker AVIII HD 400 (376 MHz) spectrometer in the stated solvents as a reference for the internal deuterium lock. The chemical shift data for each signal are given as δ in units of ppm relative to TMS where δ(TMS) = 0.00. The multiplicity of each signal is indicated by: s (singlet); d (doublet); t (triplet); q (quartet); m (multiplet); sp (septet) or combinations thereof. The number of fluorines (n) for a given resonance signal is indicated by nF. The spectra are uncalibrated. Coupling constants (*J*) are quoted in Hz, recorded to the nearest 0.1 Hz.

^{31}P NMR spectra were measured on a Bruker AVIII HD 400 (162 MHz) or NEO 600 (243 MHz) spectrometer in the stated solvents as a reference for the internal deuterium lock. The chemical shift data for each signal are given as δ in units of ppm relative to TMS where δ(TMS) = 0.00. The spectra are uncalibrated. Coupling constants (*J*) are quoted in Hz, recorded to the nearest 0.1 Hz.

Mass spectra were acquired on either an Agilent 6120 (low resolution), Waters LCT Premier XE bench-top, Waters LCT Premier bench-top orthogonal acceleration time-of-flight LC-MS system (low resolution) or Bruker microToF spectrometer (high resolution) using electrospray ionisation (ESI) from solutions of methanol or acetonitrile. *m/z* values are reported in Daltons and followed by their percentage abundance in parentheses.

Melting points were determined using a Griffin capillary tube melting point apparatus (Registered Design No. 889339) or Leica Galen III hot stage microscope and are uncorrected. The solvent(s) from which the sample was crystallised is given in parentheses. *Dec.* is used to indicate that the sample decomposed at the stated temperature.

Infrared (IR) spectra were obtained from neat samples or thin liquid films. The spectra were recorded using a Bruker Tensor 27 spectrometer with a diamond ATR module. Absorption maxima are given in wavenumbers (cm^{-1}) and reported as s (strong), m (medium), w (weak), or broad (*br*).

Specific optical rotations were measured using a Schmidt Haensch Unipol polarimeter, using a sodium lamp at 589 nm and a path length of 1.0 dm. The concentration (c) is expressed in g/100 mL (equivalent to g/0.1 dm^3). Specific rotations are denoted $[\alpha]_D^T$ and are given in implied units of 10^{-1} deg cm^2g^{-1} (where T = ambient temperature in °C).

Analytical thin layer chromatography (TLC) was carried out on Merck silica gel 60 F_{254} aluminium-supported thin layer chromatography sheets. Visualisation was by absorption of UV light (λ_{max} 254 nm), or thermal development after staining in either an: aqueous basic solution of potassium permanganate, or ethanolic solution of ninhydrin.

Flash column chromatography was carried out using Merck silica gel (40–63 μm), eluting using solvents as supplied under a positive pressure of N_2 gas.

Analytical high performance liquid chromatography (HPLC): *Method 1* was carried out on a PerkinElmer Flexar system with a Binary LC Pump and UV/vis LC Detector using a Dionex Acclaim reverse phase 120 column (C_{18}, 5 μm, 120 Å, 4.6 × 150 mm); [95:5 H_2O: MeCN → 5:95 H_2O : MeCN: H_2O with 0.1% TFA modifier, 10 min; 5 min hold; 1.5 mL min^{-1}]. *Method 2* was carried out on a PerkinElmer Flexar system with a Binary LC Pump and UV/vis LC Detector using a Dionex Acclaim reverse phase 120 column (C_{18}, 5 μm, 120 Å, 4.6 × 150 mm); [95:5 H_2O : MeCN → 5:95 H_2O : MeCN, 10 min; 5 min hold; 1.5 mL min^{-1}]. *Method 3* was carried out on an Agilent 1260 Infinity II® system with a Poroshell 120 EC-C_{18} column [4 μm, 4.6 × 100 mm]; [95:5 H_2O: MeCN → 5:95 H_2O: MeCN with 0.1% FA modifier, 10 min; 5 min hold; 1 mL min^{-1}]. *Method 4* was carried out on an Agilent 1260 Infinity II® system with an XBridge reverse phase column [C_{18}, 5 μm, 120 Å, 4.6 × 150 mm]; [95:5 H_2O : MeCN → 5:95 H_2O : MeCN with 0.1% TFA modifier, 10 min; 2 min hold; 1 mL min^{-1}]. Sample purity was measured using the UV absorbance at 254 nm and another wavelength (either 220 nm or 280 nm). The reported purity is the UV absorbance at 254 nm.

Semi-preparative high performance liquid chromatography (HPLC) was carried out on an Agilent 1260 Infinity II® with an Agilent 5 Prep C_{18} column [5 μm, 21.2 × 50 mm];

[95:5 H_2O : MeCN with 0.1% FA modifier (1 min), 95:5 H_2O : MeCN → 5:95 H_2O : MeCN with 0.1% FA modifier (10 min), 5 min hold; 20 mL min^{-1}].

ChromlogD assay was carried out on an Agilent 1260 Infinity II® system with a Poroshell 120 EC-C_{18} column [4 µm, 4.6 × 100 mm]; [95:5 H_2O (50 mM NH_4.OAc) : MeCN → 5:95 H_2O (50 mM NH_4.OAc) : MeCN, with starting mobile phase at pH 7.4, 10 min; 5 min hold; 1 mL min^{-1}]. The Chromatographic Hydrophobicity Index (CHI)[215, 249] values were derived directly from the gradient retention times using calibration parameters for standard compounds. The CHI value approximates to the volume % organic concentration when the compound elutes. CHI was linearly transformed into a ChromlogD value by least-square fitting of experimental CHI values using the following formula: ChromlogD = 0.0857*CHI - 2.[262]

6.2 Procedures and Compound Data

6.2.1 Fragment Library

5,7-Dimethyl[1,2,4]triazolo[1,5-*a*]pyrimidine 2

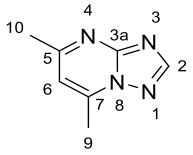

3-Amino-1,2,4-triazole (84.1 mg, 1.00 mmol, 1.0 eq.) was placed in a microwave vial and dissolved in acetic acid (0.5 mL). Acetylacetone (102 µL, 1.00 mmol, 1.0 eq.) was added then the vial was sealed. The reaction mixture refluxed in an oil bath at 135 °C for 3 h. The resulting mixture was then cooled before being concentrated *in vacuo* to give 5,7-dimethyl[1,2,4]triazolo[1,5-*a*]pyrimidine **2** (143 mg, 96%) as a colourless solid: R_f 0.10 (ethyl acetate); m.p. 127-129 °C ($CDCl_3$) [lit.[274] 130–132 °C (ethyl acetate)]; ^{1}H NMR (400 MHz, $CDCl_3$) δ 8.45 (1H, s, C^2-H), 6.84 (1H, d, *J* 1.0, C^6-H), 2.83 (3H, d, *J* 1.0, C^7-CH_3), 2.70 (3H, s, C^5-CH_3); LRMS *m/z* (ESI^+) 149 ($[M+H]^+$, 100%); Analytical HPLC (RP, *Method 4*) rt 5.3 min, purity 100%. The spectroscopic data are in good agreement with the literature.[275, 276]

(3*Z*)-6-Chloro-3-hydrazinylidene-2,3-dihydropyridazin-4-amine 35

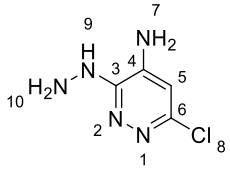

4-Amino-3,6-dichloropyridazine (5.00 g, 30.5 mmol, 1.0 eq.) and hydrazine monohydrate (141 mL, 2.91 mol, 96 eq.) were refluxed for 4 h. The reaction mixture was cooled to rt then water (100 mL) was added to aid precipitation. The resulting solid was collected by filtration, washed with water, then dried under high vacuum to give (3*Z*)-6-chloro-3-hydrazinylidene-2,3-dihydropyridazin-4-amine **35** (1.91 g, 39%) as an off-white solid: R_f 0.35 (reverse phase, water : methanol, 1:1); m.p. 189-190 °C (EtOH) [lit.[277] 185-190 °C]; ^{1}H NMR (400 MHz, DMSO-d_6) δ 7.29 (1H, br s, N*H*NH_2), 6.38 (1H, s, C^5-H), 6.27 (2H, br s, C^4-NH_2), 4.25 (2H, br s, NHNH_2); LRMS *m/z* (ESI^+) 160 ($[M+H]^+$, 100%). The spectroscopic data are in good agreement with the literature.[278, 279]

6-Chloro-3-methyl[1,2,4]triazolo[4,3-*b*]pyridazin-8-amine 36

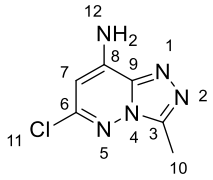

(3*Z*)-6-Chloro-3-hydrazinylidene-2,3-dihydropyridazin-4-amine **35** (1.85 g, 12.0 mmol, 1.0 eq.) was dissolved in acetic acid (27 mL) then refluxed for 7 h. The reaction mixture was cooled to rt then quenched with ice-cold water (40 mL). The resulting light brown precipitate was collected by filtration. Acetic acid was removed by azeotroping with cyclohexane then the solid was purified by recrystallisation from methanol. The resulting solid was suspended in a solution of sat. $Na_2CO_{3\ (aq)}$ then stirred for 30 min. The solid was filtered off then dried under high vacuum to give 6-chloro-3-methyl[1,2,4]triazolo[4,3-*b*]pyridazin-8-amine **36** (1.52 g, 71%) as an off-white solid: R_f 0.46 (CH_2Cl_2 : MeOH, 1:1); m.p. 222-223 °C (MeOH) [lit.[280] 234-235 °C]; ^{1}H NMR (400 MHz, DMSO-d_6) δ 7.87 (2H, br s, C^8-NH_2), 6.11 (1H, s, C^7-H), 2.58 (3H, s, C^3-CH_3); LRMS *m/z* (ESI^+) 184 ($[M+H]^+$, 100%). The spectroscopic data are in good agreement with the literature.[278, 279]

***Tert*-butyl (6-chloro-3-methyl[1,2,4]triazolo[4,3-*b*]pyridazin-8-yl)carbamate 3**

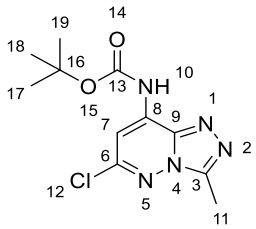

6-Chloro-3-methyl[1,2,4]triazolo[4,3-*b*]pyridazin-8-amine **36** (1.45 g, 8.00 mmol, 1.0 eq.), di-*tert*-butyl dicarbonate anhydride (2.58 g, 12.0 mmol, 1.5 eq.), 4-DMAP (96.5 mg, 0.790 mmol, 0.1 eq.) and pyridine (636 µL, 8.00 mmol, 1.0 eq.) were combined in anhydrous THF (25 mL) then the reaction mixture was stirred at rt for 24 h. The solvent was removed *in vacuo* then the residue re-dissolved in ethyl acetate (300 mL), then washed with sat. aq. NH_4Cl (2 × 150 mL), water (2 × 150 mL) and brine (150 mL). The organic layer was dried over $MgSO_{4\ (s)}$, filtered, then the filtrate was concentrated *in vacuo* to give a light brown oil. Both the desired Boc-protected product and doubly Boc-protected product were visible in the ^{1}H NMR (in a ratio of 1:0.15). The light brown oil was suspended in a solution of MeOH (72 mL) and 2 M NaOH (18 mL) then stirred

at rt for 1.5 h. The reaction mixture was neutralised with sat. aq. NH_4Cl then extracted with ethyl acetate (3 × 150 mL). The combined organic layers were washed with water (2 × 100 mL), brine (100 mL) then dried over $Na_2SO_{4\,(s)}$, filtered, then the filtrate was concentrated *in vacuo*. The residue was purified by flash column chromatography eluting with petroleum ether : ethyl acetate (85:15 to 0:1) to yield *tert*-butyl (6-chloro-3-methyl[1,2,4]triazolo[4,3-*b*]pyridazin-8-yl)carbamate **3** (681 mg, 30%) as a colourless solid: R_f 0.25 (petroleum ether : ethyl acetate, 2:3); m.p. 118-120 °C ($CDCl_3$) [lit.[279]129-131 °C (ethyl acetate)]; ^{1}H NMR (400 MHz, $CDCl_3$) δ 8.07 (1H, s, N^{10}-H), 7.63 (1H, s, C^7-H), 2.71 (3H, s, C^{11}-H_3), 1.49 (9 H, s, C^{16}-$(CH_3)_3$); LRMS *m/z* (ESI^-) 282 ($[M-H]^-$, 100%); Analytical HPLC (RP, *Method 4*) rt 10.2 min, purity 100%. The spectroscopic data are in good agreement with the literature.[279, 281]

(6*E*)-3-Chloro-6-[(2*E*)-ethylidenehydrazinylidene]-1,6-dihydropyridazine 38

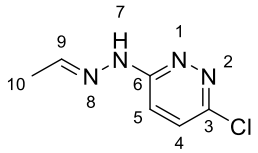

3-Chloro-6-hydrazineylpyridazine (200 mg, 1.38 mmol, 1.0 eq.) was dissolved in ethanol (10 mL) and acetaldehyde (85.9 µL, 1.52 mmol, 1.1 eq.) was added. The reaction mixture was refluxed for 1 h. The solvent was evaporated *in vacuo.* Recrystallisation from ethanol gave (6*E*)-3-chloro-6-[(2*E*)-ethylidenehydrazinylidene]-1,6-dihydropyridazine **38** (84 mg, 36%) as a brown solid: R_f 0.40 (petroleum ether : ethyl acetate, 1:1); m.p. 163-165 °C (ethyl acetate) [lit.[282] 205-206 °C]; ^{1}H NMR (400 MHz, $CDCl_3$) δ 10.04 (1H, s, N-H), 7.51 (1H, d, *J* 9.4, C^4-H), 7.46 (1H, q, *J* 5.4, C^9-H), 7.30 (1H, d, *J* 9.4, C^5-H), 2.02 (3H, d, *J* 5.4, C^{10}-H_3); LRMS *m/z* (ESI^+) 171 ($[M+H]^+$, 100%). The spectroscopic data are in good agreement with the literature.[283]

6-Chloro-3-methyl[1,2,4]triazolo[4,3-*b*]pyridazine 40

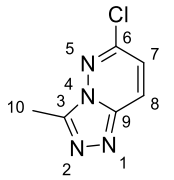

(6*E*)-3-Chloro-6-[(2*E*)-ethylidenehydrazinylidene]-1,6-dihydropyridazine **38** (70.0 mg, 0.410 mmol, 1.0 eq.) was dissolved in CH_2Cl_2 (5 mL) and [bis(acetoxy)iodo]benzene (145 mg, 0.451 mmol, 1.1 eq.) was added portion-wise. The reaction mixture was stirred at rt for 2.5 h. The solvent was then evaporated *in vacuo.* The residue was purified by flash column chromatography eluting CH_2Cl_2 : methanol (1:0 to 9:1). Pure fractions were combined and concentrated *in vacuo* to yield 6-chloro-3-methyl[1,2,4]triazolo[4,3-*b*]pyridazine **40** (55 mg, 80%) as a cream solid: R_f 0.38 (CH_2Cl_2 : methanol, 9:1); m.p. 88-90 °C (MeOH) [lit.[283] 75.5 °C (H_2O/EtOH), lit.[282] 104-105 °C]; ^{1}H NMR (400 MHz, $CDCl_3$) δ 8.06 (1H, d, *J* 9.6, C^8-H), 7.09 (1H, d, *J* 9.6, C^7-H), 2.80 (3H, s, C^{10}-H_3); LRMS *m/z* (ESI^+) 169 ($[M+H]^+$, 100%). The spectroscopic data are in good agreement with the literature.[282, 283]

***N*-Cyclopropyl-3-methyl[1,2,4]triazolo[4,3-*b*]pyridazin-6-amine 4**

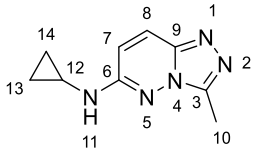

6-Chloro-3-methyl[1,2,4]triazolo[4,3-*b*]pyridazine **40** (45 mg, 0.27 mmol, 1.0 eq.) was dissolved in cyclopropylamine (0.50 mL) then the reaction mixture was heated to 70 °C for 3.5 h. The reaction mixture was cooled to rt and partitioned between water and CH_2Cl_2. The organic layer was separated then the aqueous layer was extracted with CH_2Cl_2 (3 × 5 mL). The combined organic layers were dried over $MgSO_{4\,(s)}$, filtered, then the filtrate was concentrated *in vacuo.* The residue was purified by flash column chromatography eluting with CH_2Cl_2 : methanol (1:0 to 85:15) to yield *N*-cyclopropyl-3-methyl[1,2,4]triazolo[4,3-*b*]pyridazin-6-amine **4** (19 mg, 38%) as a yellow solid: R_f 0.11 (CH_2Cl_2 : methanol, 9:1); m.p. 183-185 °C ($CDCl_3$); ν_{max} (thin film)/ cm^{-1} 1684 (C=N, m), 1602 (C=C, m), 1511 (N-H, m), 1424 (C-H, w), 1362 (C-H, w), 1250 (C-N, m), 912 (C=C, m), 820 (C=C, m); ^{1}H NMR (400 MHz, $CDCl_3$) δ 7.77 (1H, d, *J* 9.8, C^8-H), 6.72

(1H, d, *J* 9.8, C^7-H), 5.19 (1H, s, N-H), 2.75-2.68 (1H, m, C^{12}-H), 2.68 (3H, s, C^{10}-H_3), 0.94-0.81 (2H, m, C^{13}-H_a, C^{14}-H_a), 0.69-0.56 (2H, m, C^{13}-H_b, C^{14}-H_b); ^{13}C NMR (101 MHz, $CDCl_3$) δ 155.0 (C^6), 146.6 (C^3), 143.2 (C^9), 124.7 (C^8), 114.4 (C^7), 24.3 (C^{12}), 9.8 (C^{10}), 7.7 (C^{13}, C^{14}); LRMS *m/z* (ESI^+) 190 ($[M+H]^+$, 100%); HRMS Analytical HPLC (RP, *Method 4*) rt 5.8 min, purity 100%.

(6*E*)-3-Chloro-6-[(2*E*)-propylidenehydrazinylidene]-1,6-dihydropyridazine 39

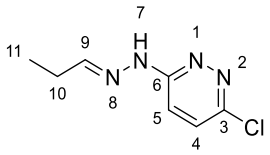

3-Chloro-6-hydrazineylpyridazine (200 mg, 1.38 mmol, 1.0 eq.) was dissolved in ethanol (10 mL) then propionaldehyde (110 µL, 1.52 mmol, 1.1 eq.) was added. The reaction mixture was refluxed for 2 h. The reaction mixture was cooled to rt then the solvent was evaporated *in vacuo.* Recrystallisation from ethanol gave (6*E*)-3-chloro-6-[(2*E*)-propylidenehydrazinylidene]-1,6-dihydropyridazine **39** (123 mg, 48%) as a beige solid: R_f 0.39 (petroleum ether : ethyl acetate, 1:1); m.p. 147-149 °C (ethyl acetate) [lit.[283] 144.5 °C (EtOH), lit.[284] 156-158 °C]; ^{1}H NMR (400 MHz, $CDCl_3$) δ 10.2 (1H, s, N-H), 7.55-7.48 (2H, m, C^4-H, C^9-H), 7.30 (1H, d, *J* 9.3, C^5-H), 2.36 (2H, qd, *J* 7.5, 5.0, C^{10}-H_2), 1.15 (3H, t, *J* 7.5, C^{11}-H_3); LRMS *m/z* (ESI^+) 185 ($[M+H]^+$, 100%). The spectroscopic data are in good agreement with the literature.[283]

6-Chloro-3-ethyl[1,2,4]triazolo[4,3-*b*]pyridazine 41

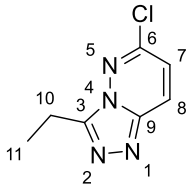

(6*E*)-3-Chloro-6-[(2*E*)-propylidenehydrazinylidene]-1,6-dihydropyridazine **39** (80.0 mg, 0.433 mmol, 1.0 eq.) was dissolved in CH_2Cl_2 (5 mL) and [bis(acetoxy)iodo]benzene (153 mg, 0.477 mmol, 1.1 eq.) was added portion-wise. The reaction mixture was stirred at rt for 3 h. The solvent was evaporated *in vacuo* then the residue was purified by flash column chromatography eluting with CH_2Cl_2 : methanol (1:0 to 9:1). Pure fractions were

combined and concentrated *in vacuo* to yield 6-chloro-3-ethyl[1,2,4]triazolo[4,3-*b*]pyridazine **41** (60 mg, 76%) as a cream solid: R_f 0.50 (CH_2Cl_2 : methanol, 9:1); m.p. 78-80 °C (CH_2Cl_2) [lit.[283] 93 °C (H_2O/EtOH)]; ^{1}H NMR (400 MHz, $CDCl_3$) δ 8.05 (1H, d, *J* 9.6, C^8-H), 7.08 (1H, d, *J* 9.6, C^7-H), 3.20 (2H, q, *J* 7.6, C^{10}-H_2), 1.49 (3H, t, *J* 7.6, C^{11}-H_3); LRMS *m/z* (ESI^+) 183 ($[M+H]^+$, 100%). The spectroscopic data are in good agreement with the literature.[283]

_N_-Cyclopropyl-3-ethyl[1,2,4]triazolo[4,3-*b*]pyridazin-6-amine 5

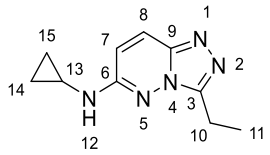

6-Chloro-3-ethyl[1,2,4]triazolo[4,3-*b*]pyridazine **41** (50 mg, 0.27 mmol, 1.0 eq.) was dissolved in cyclopropylamine (0.50 mL) then the reaction mixture was heated to 70 °C for 3.5 h. The reaction mixture was cooled to rt then partitioned between water and CH_2Cl_2. The organic layer was separated then the aqueous layer was extracted with CH_2Cl_2 (3 × 5 mL). The combined organic layers were dried over $MgSO_{4\,(s)}$, filtered, then the filtrate was concentrated *in vacuo*. The residue was purified by flash column chromatography eluting with CH_2Cl_2 : methanol (1:0 to 85:15) to yield *N*-cyclopropyl-3-ethyl[1,2,4]triazolo[4,3-*b*]pyridazin-6-amine **5** (55 mg, 100%) as a colourless solid: R_f 0.32 (CH_2Cl_2 : methanol, 9:1); m.p. 172-174 °C (CH_2Cl_2); ν_{max} (thin film)/ cm^{-1} 1634 (C=C, w), 1586 (C=C, w), 1506 (N-H, m), 1347 (C-N, m), 1309 (C-H, w), 818 (C=C, m); ^{1}H NMR (400 MHz, $CDCl_3$) δ 7.85 (1H, d, *J* 9.8, C^8-H), 7.61 (1H, d, *J* 3.1, N-H), 6.72 (1H, d, *J* 9.8, C^7-H), 2.96 (2H, q, *J* 7.5, C^{10}-H_2), 2.65 (1H, ttd, *J* 7.0, 3.7, 1.7, C^{13}-H), 1.34 (3H, t, *J* 7.5, C^{11}-H_3), 0.81-0.68 (2H, m, C^{14}-H_a, C^{15}-H_a), 0.56-0.44 (2H, m, C^{14}-H_b, C^{15}-H_b); ^{13}C NMR (101 MHz, $CDCl_3$) δ 154.8 (C^6), 150.9 (C^3), 143.3 (C^9), 124.5 (C^8), 114.7 (C^7), 24.3 (C^{13}), 18.1 (C^{10}), 10.9 (C^{11}), 7.7 (C^{14}, C^{15}); LRMS *m/z* (ESI^+) 204 ($[M+H]^+$, 100%); HRMS *m/z* (ESI^+) [Found: 226.1070, $C_{10}H_{13}N_5$ requires $[M+Na]^+$ 226.1063)]; Analytical HPLC (RP, *Method 3*) rt 6.5 min, purity 100%.

6-Chloro-3-phenyl[1,2,4]triazolo[4,3-*b*]pyridazine 42

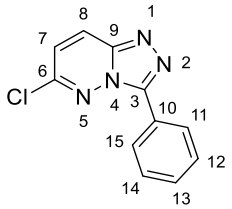

p-Toluenesulfonic acid (11.9 mg, 69.0 µmol, 0.05 eq.) and MnO_2 (481 mg, 5.53 mmol, 4.0 eq.) were added to a stirred solution of 3-chloro-6-hydrazineylpyridazine (200 mg, 1.38 mmol, 1.0 eq.) and benzaldehyde (169 µL, 1.66 mmol, 1.2 eq.) in toluene (12 mL), in a round bottom flask covered with tinfoil. The reaction mixture was heated to 80 °C for 2 h. The reaction mixture was cooled to rt, filtered through a sinter funnel then the filtrate was evaporated *in vacuo.* The residue was purified by flash column chromatography eluting with petroleum ether : ethyl acetate (1:0 to 0:1) to yield 6-chloro-3-phenyl[1,2,4]triazolo[4,3-*b*]pyridazine **42** (33 mg, 10%) as a brown solid: R_f 0.12 (petroleum ether : ethyl acetate, 1:1); m.p. 184-186 °C ($CDCl_3$) [lit.[285] 197-199 °C, lit.[286] 199-201 °C,]; ^{1}H NMR (400 MHz, $CDCl_3$) δ 8.46 (2H, m, C^{11}-H, C^{15}-H), 8.15 (1H, d, *J* 9.6, C^8-H), 7.64-7.48 (3H, m, C^{12}-H, C^{13}-H, C^{14}-H), 7.15 (1H, d, *J* 9.6, C^7-H); LRMS *m/z* (ESI^+) 231 ($[M+H]^+$, 100%). The spectroscopic data are in good agreement with the literature.[287, 288]

***N*-Cyclopropyl-3-phenyl[1,2,4]triazolo[4,3-*b*]pyridazin-6-amine 6**

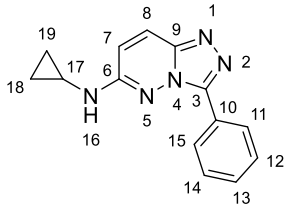

6-Chloro-3-phenyl[1,2,4]triazolo[4,3-*b*]pyridazine **42** (20 mg, 0.087 mmol, 1.0 eq.) was dissolved in cyclopropylamine (0.2 mL) then the reaction mixture was heated to 70 °C for 4 h. The reaction mixture was cooled to rt and partitioned between water and CH_2Cl_2. The organic layer was separated then the aqueous layer was extracted with CH_2Cl_2 (3 × 5 mL). The combined organic layers were dried over $Na_2SO_{4\,(s)}$, filtered, then the filtrate was concentrated *in vacuo.* The residue was purified by flash column chromatography eluting with CH_2Cl_2 : methanol (1:0 to 93:7) to yield *N*-cyclopropyl-3-phenyl[1,2,4]triazolo[4,3-*b*]pyridazin-6-amine **6** (13 mg, 58%) as a light brown solid:

R_f 0.54 (CH_2Cl_2 : methanol, 9:1); m.p. 212-214 °C ($CDCl_3$) [lit.[7] 183-185 °C (EtOH)]; ν_{max} (thin film)/ cm^{-1} 3233 (N-H, m), 2924 (N-H, m), 1633 (C=C, m), 1584 (N-H, m), 1499 (C-H, m), 1263 (C-N, m), 1023 (C-N, m); ^{1}H NMR (600 MHz, $CDCl_3$) δ 8.61-8.56 (2H, m, C^{11}-H, C^{15}-H), 7.88 (1H, d, *J* 9.8, C^8-H), 7.54-7.49 (2H, m, C^{12}-H, C^{14}-H), 7.49-7.44 (1H, m, C^{13}-H), 6.73 (1H, d, *J* 9.8, C^7-H), 5.21 (1H, s, N-H), 2.76 (1H, ttd, *J* 6.9, 3.7, 1.7, C^{17}-H), 0.97-0.85 (2H, m, C^{18}-H_a, C^{19}-H_a), 0.73-0.60 (2H, m, C^{18}-H_b, C^{19}-H_b); ^{13}C NMR (151 MHz, $CDCl_3$) δ 154.9 (C^6), 147.4 (C^3), 144.2 (C^9), 129.7 (C^{13}), 128.6 (C^{12}, C^{14}), 127.6 (C^{11}, C^{15}), 127.2 (C^{10}), 125.0 (C^8), 114.5 (C^7), 24.4 (C^{17}), 7.7 (C^{18}, C^{19}); LRMS *m/z* (ESI^+) 252 ($[M+H]^+$, 100%); HRMS *m/z* (ESI^+) [Found: 274.1076, $C_{14}H_{13}N_5$ requires $[M+Na]^+$ 274.1063)]; Analytical HPLC (RP, *Method 2*) rt 8.1 min, purity 100%.

5-(Benzylamino)-4-chloro-2-methylpyridazin-3(2*H*)-one 7

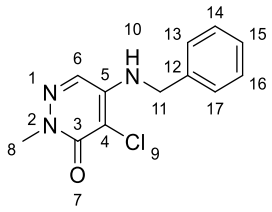

4,5-Dichloro-2-methylpyridazin-3(2*H*)-one (89.5 mg, 0.50 mmol, 1.0 eq.) was dissolved in NMP (1 mL). Phenylmethanamine (109 µL, 1.00 mmol, 2.0 eq.) was added then the reaction was stirred in an oil bath at 80 °C for 3 h. The temperature of the oil bath was increased to 100 °C for 1 h. The reaction mixture was left to stir at rt for 72 h. The reaction mixture was diluted with water (25 mL) then extracted with ethyl acetate (3 × 60 mL). The combined organic layers were washed with 10% w/v LiCl aq. (4 × 60 mL), dried over anhydrous $MgSO_{4\,(s)}$, then the filtrate was concentrated *in vacuo*. The crude product was purified using flash column chromatography eluting with petroleum ether : ethyl acetate (1:1 to 1:9) to yield 5-(benzylamino)-4-chloro-2-methylpyridazin-3(2*H*)-one **7** (87 mg, 70%) as an off-white solid: R_f 0.16 (petroleum ether : ethyl acetate, 1:1); m.p. 168-169 °C ($CDCl_3$) [lit.[289] 183-185 °C (EtOH)]; ^{1}H NMR (400 MHz; $CDCl_3$); δ 7.43 (1H, s, C^6-H), 7.35 – 7.20 (3H, m, C^{13}-H, C^{14}-H, C^{15}-H), 5.04 (1H, s, NH), 4.48 (2H, d, *J* 6.0, C^{11}-H_2), 3.67 (4H, s, N^2-CH_3). LRMS *m/z* (ESI^+) 250 ($[M+H]^+$, 100%). Analytical HPLC (RP, *Method 2*) rt 6.8 min, purity 97%. The spectroscopic data are in good agreement with the literature values.[36, 289-291]

4-Chloro-2-methyl-5-[(1-phenylethyl)amino]pyridazin-3(2*H*)-one 8

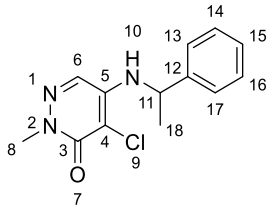

A solution of 4,5-dichloro-2-methylpyridazin-3(2*H*)-one (89.5 mg, 0.500 mmol, 1.0 eq.) and phenylethylamine (127 µL, 1.00 mmol, 2.0 eq.) in NMP (1 mL) was stirred at 100 °C for 7 h. The reaction mixture was then stirred at rt for 16 h. The reaction mixture was diluted with water (25 mL) then extracted with ethyl acetate (3 × 30 mL). The combined organic components were washed with 10% w/v LiCl aq. (3 × 50 mL), then dried over anhydrous $Na_2SO_{4\ (s)}$, filtered, then the filtrate was concentrated *in vacuo*. The crude product was purified using flash column chromatography eluting with petroleum ether : ethyl acetate (1:0 to 0:1) to yield 4-chloro-2-methyl-5-((1-phenylethyl)amino)pyridazin-3(2*H*)-one **8** (66 mg, 50%) as a colourless solid: R_f 0.10 (petroleum ether : ethyl acetate, 1:1); m.p. 139-141 °C (ethyl acetate) [lit.[290] 106-108 °C (ethyl acetate)]; ^{1}H NMR (400 MHz, $CDCl_3$) δ 7.40–7.34 (2H, m, C^{13}-H, C^{17}-H), 7.30 (1H, s, C^6-H), 7.31–7.26 (3H, m, C^{14}-H, C^{15}-H and C^{16}-H), 4.95 (1H, d, *J* 6.2, N-H), 4.70 (1H, dq, *J* 6.2, 6.7, C^{11}-H), 3.69 (3H, s, N^2-CH_3), 1.6 (3H, d, *J* 6.7, C^{18}-H_3); LRMS *m/z* (ESI^+) 286 ($[M+Na]^+$, 70%); Analytical HPLC (RP, *Method 4*) rt 9.1 min, purity 99%. The spectroscopic data are in good agreement with the literature values.[290]

4-Chloro-2-methyl-5-{[(pyridin-2-yl)methyl]amino}pyridazin-3(2*H*)-one 9

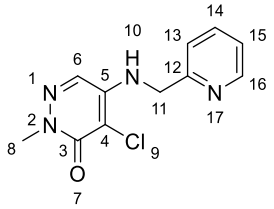

A solution of 4,5-dichloro-2-methylpyridazin-3(2*H*)-one (89.5 mg, 0.500 mmol, 1.0 eq.) and 2-(aminomethyl)pyridine (103 µL, 1.00 mmol, 2.0 eq.) in NMP (1 mL) was stirred at 100 °C for 7 h. The reaction mixture was then stirred at rt for 16 h. The reaction mixture was diluted with water (25 mL), then extracted with ethyl acetate (3 × 30 mL). The combined organic components were washed with 10% w/v LiCl aq. (3 × 50 mL), dried over anhydrous $Na_2SO_{4\ (s)}$, filtered, then the filtrate was concentrated *in vacuo*. The crude

product was purified using flash column chromatography eluting with petroleum ether : ethyl acetate (1:1 to 1:3) to yield 4-chloro-2-methyl-5-((pyridin-2-ylmethyl)amino)pyridazin-3(2*H*)-one **9** (86 mg, 69%) as a colourless solid: R_f 0.17 (petroleum ether : ethyl acetate, 1:1); m.p. 88-89 °C ($CDCl_3$); ^{1}H NMR (400 MHz, $CDCl_3$) δ 8.60 (1H, d, *J* 4.9, C^{16}-H), 7.67 (1H, ddd, *J* 7.7, 7.7, 1.8, C^{14}-H), 7.50 (1H, s, C^6-H), 7. 28–7.18 (2H, m, C^{13}-H, C^{15}-H), 7.02 (1H, br s, NH), 5.09 (2H, d, *J* 5.7, C^{11}-H_2), 3.75 (3H, s, C^8-H_3); LRMS *m/z* (ESI^+) 251 ($[M+H]^+$, 100 %); Analytical HPLC (RP, *Method 4*) rt 5.5 min, purity 100%. The spectroscopic data are in good agreement with the literature values.[290]

4-Chloro-2-methyl-5-{[(pyridin-3-yl)methyl]amino}pyridazin-3(2*H*)-one 10

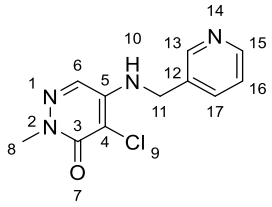

4,5-Dichloro-2-methylpyridazin-3(2*H*)-one (180 mg, 1.00 mmol, 1.0 eq.) was dissolved in NMP (1.5 mL). 3-(Aminomethyl)pyridine (509 µL, 5.00 mmol, 5.0 eq.) was added then the reaction was stirred in an oil bath at 80 °C for 21 h. The reaction mixture was diluted with water (15 mL) then extracted with ethyl acetate (3 × 30 mL). The combined organic layers were washed with 10% w/v LiCl aq. (4 × 20 mL), dried over anhydrous $MgSO_{4\ (s)}$, filtered, then the filtrate was concentrated *in vacuo*. The crude product was purified by flash column chromatography eluting with petroleum ether : ethyl acetate (1:0 to 0:1) to yield 4-chloro-2-methyl-5-{[(pyridin-3-yl)methyl]amino}pyridazin-3(2*H*)-one **10** (31 mg, 12%) as a light beige solid: R_f 0.15 (ethyl acetate); m.p. 93-95 °C ($CDCl_3$); ^{1}H NMR (400 MHz; $CDCl_3$) δ 8.57 (2H, m, C^{13}-H, C^{15}-H), 7.67-7.59 (1H, m, C^{16}-H), 7.49 (1H, s, C^6-H), 7.29 (1H, ddd, *J* 8.0, 4.8, 0.9, C^{17}-H), 6.16 (1H, br s, NH), 4.96 (2H, d, *J* 6.8, C^{11}-H_2), 3.74 (3H, s, C^8-H_3); LRMS *m/z* (ESI^+) 251 ($[M+H]^+$, 100%); Analytical HPLC (RP, *Method 2*) rt 5.0 min, purity 100%. The spectroscopic data are in good agreement with the literature values.[290]

4-Chloro-2-methyl-5-{[(pyridin-4-yl)methyl]amino}pyridazin-3(2*H*)-one 11

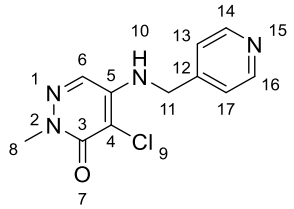

4,5-Dichloro-2-methylpyridazin-3(2*H*)-one (180 mg, 1.00 mmol, 1.0 eq.) was dissolved in NMP (1.5 mL). 4-(Aminomethyl)pyridine (508 μL, 5.00 mmol, 5.0 eq.) was added then the reaction was stirred in an oil bath at 80 °C for 22 h. The reaction mixture was diluted with water (15 mL) then extracted with ethyl acetate (3 × 30 mL). The combined organic layers were washed with 10% w/v LiCl aq. (4 × 20 mL), dried over anhydrous $MgSO_{4\ (s)}$ then the filtrate was concentrated *in vacuo*. The crude product was purified by flash column chromatography eluting with petroleum ether : ethyl acetate (1:0 to 0:1) to yield 4-chloro-2-methyl-5-{[(pyridin-4-yl)methyl]amino}pyridazin-3(2*H*)-one **11** (60 mg, 24%) as a brown oil: R_f 0.20 (ethyl acetate); ^{1}H NMR (400 MHz; $CDCl_3$) δ 8.64-8.53 (2H, m, C^{14}-H, C^{16}-H), 7.48 (1H, s, C^6-H), 7. 19 (2H, m, C^{13}-H, C^{17}-H), 6.28 (1H, br s, NH), 4.94 (2H, d, *J* 7.3, C^{11}-H_2), 3.75 (3H, s, C^8-H_3); LRMS *m/z* (ESI^+) 251 ($[M+H]^+$, 100%); Analytical HPLC (RP, *Method 2*) rt 4.9 min, purity 100%. The spectroscopic data are in good agreement with the literature values.[290]

Potassium (3,5-dimethylisoxazol-4-yl)trifluoroborate 53

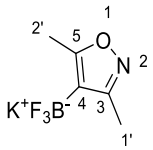

(3,5-Dimethylisoxazol-4-yl)boronic acid (2.00 g, 14.2 mmol, 1.0 eq.) was suspended in MeCN (50 mL). An aqueous solution of potassium fluoride (10 M, 5.68 mL, 56.8 mmol, 4.0 eq.) was added then the suspension was stirred vigorously until the boronic acid dissolved. L-(+)-tartaric acid (4.37 g, 29.2 mmol, 2.1 eq.) was suspended in THF (30 mL) and added dropwise to the reaction mixture over a period of 10 min, whilst stirring vigorously. The reaction mixture was stirred for a further 20 min at rt. The reaction mixture was filtered then the filter cake was washed with MeCN (100 mL). The filtrate was concentrated *in vacuo* to yield potassium (3,5-dimethylisoxazol-4-yl)trifluoroborate **53** (2.09 g, 73%) as a colourless solid: R_f 0.10 (petroleum ether : diethyl ether, 1:1); m.p. >300 °C (MeCN) [lit.[46] >300 °C (acetone)]; ^{1}H NMR (400 MHz, DMSO-d_6) δ 2.19 (3H,

s, H-2'), 2.04 (3H, s, H-1'); ^{11}B NMR (160 MHz, DMSO-d_6) δ 2.39 (q, J 49.6); ^{19}F NMR (377 MHz, DMSO-d_6) δ -134.53 (d, J 44.5); LRMS m/z (ESI)$^-$ 164 ([M-K]$^-$, 100%). The spectroscopic data are in good agreement with the literature.[46]

4-(3-Methoxyphenyl)-3,5-dimethylisoxazole 12

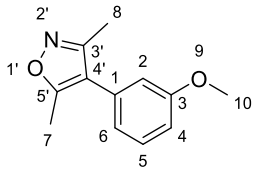

Potassium (3,5-dimethylisoxazol-4-yl)trifluoroborate **53** (50.0 mg, 246 µmol, 1.2 eq.), Na_2CO_3 (65.3 mg, 61.6 µmol, 3.0 eq.), RuPhos (19.2 mg, 41.0 µmol, 0.2 eq.), and $Pd(OAc)_2$ (4.71 mg, 21.0 µmol, 0.1 eq.) were placed in a microwave vial. The vial was evacuated under vacuum for 5 min then refilled with argon. 3-Bromoanisole (26.0 µL, 205 µmol, 1.0 eq.) and EtOH (1 mL) were added. The vial was sealed then the reaction was stirred at 80 °C for 17 h. The reaction mixture was filtered through a plug of silica then the plug was washed with ethyl acetate (4 × 10 mL). The combined washings were concentrated *in vacuo*. The residue was purified using flash column chromatography eluting with petroleum ether : ethyl acetate (1:0 to 3:1) to yield 4-(3-methoxyphenyl)-3,5-dimethylisoxazole **12** (35.5 mg, 85%) as a light yellow oil: R_f 0.33 (petroleum ether : ethyl acetate, 5:1); ^{1}H NMR (400 MHz, $CDCl_3$) δ 7.28 (1H, dd, J 8.0, 8.0, C^5-H), 6.83 (1H, ddd, J 8.0, 2.6, 1.0, C^6-H), 6.77 (1H, ddd, J 8.0, 1.6, 1.0, C^4-H), 6.71 (1H, dd, J 2.6, 1.6, C^2-H), 3.77 (3H, s, O-CH_3), 2.34 (3H, C$^{5'}$-CH_3), 2.21 (3H, s, C$^{3'}$-CH_3); LRMS m/z (ESI$^+$) 204 ([M+H]$^+$, 100%); Analytical HPLC (RP, *Method 2*) rt 9.3 min, purity 99%. The spectroscopic data are in good agreement with the literature.[290, 292]

3-(3,5-Dimethylisoxazol-4-yl)phenol 13

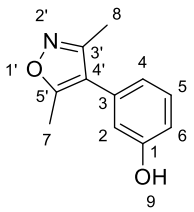

To a vigorously stirred solution of 4-(3-methoxyphenyl)-3,5-dimethylisoxazole **12** (13.5 mg, 0.066 mmol, 1.0 eq.) in anhydrous CH_2Cl_2 (0.5 mL) at 0 °C was added BBr_3

(399 µL, 4.21 mmol, 64.0 eq.) dropwise over 15 min. The reaction mixture was warmed to rt then stirred for an additional 30 min. The reaction mixture was poured into a cooled sat. aq. $NaHCO_3$ solution (100 mL) at 0 °C then extracted with ethyl acetate (3 × 100 mL). The combined organic components were washed with sat. aq. $NaHCO_3$ (50 mL), dried over anhydrous $MgSO_{4\,(s)}$, filtered, then the filtrate was concentrated *in vacuo*. The residue was dissolved in MeOH then concentrated *in vacuo* three successive times. The residue was purified using flash column chromatography eluting with petroleum ether : ethyl acetate (1:0 to 0:1) to yield 3-(3,5-dimethylisoxazol-4-yl)phenol **13** (8.5 mg, 68%) as an off-white solid: R_f 0.42 (petroleum ether : ethyl acetate, 1:1); m.p. 103-104°C ($CDCl_3$) [lit.[290] 102–106 °C (ethyl acetate)]; ^{1}H NMR (400 MHz, $CDCl_3$) δ 7.22 (1H, dd, *J* 8.0, 7.8, C^5-H), 6.80 (1H, ddd, *J* 8.0, 2.5, 1.3, C^6-H), 6.73 (1H, ddd, *J* 7.8, 1.4, 1.3 C^4-H), 6.69 (1H, dd, *J* 2.5, 1.4 C^2-H), 6.09 (1H, s, O-H), 2.34 (3H, s, $C^{5'}$-H_3), 2.21 (3H, s, $C^{3'}$-H_3); LRMS *m/z* (ESI^+) 190 ($[M+H]^+$, 100%); Analytical HPLC (RP, *Method 2*) rt 6.6 min, purity 100%. The spectroscopic data are in good agreement with the literature.[290]

Methyl 2-[(5-bromo-2-nitrophenyl)(hydroxy)methyl]prop-2-enoate 68

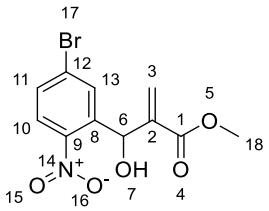

5-Bromo-2-nitrobenzaldehyde (750 mg, 3.26 mmol, 1.0 eq.) and DABCO (36.6 mg, 0.326 mmol, 0.1 eq.) were combined in DMF (2 mL). Methyl acrylate (443 µL, 4.89 mmol, 1.5 eq.) was added then the reaction mixture was stirred at rt for 4 h. Methyl acrylate (295 µL, 3.26 mmol, 1.0 eq.) and DABCO (36.6 mg, 0.326 mmol, 0.1 eq.) were added then the reaction mixture was stirred for a further 2 h at rt, until the starting material had all been consumed. The solvent was evaporated *in vacuo.* The residue was purified by flash column chromatography eluting with petroleum ether : ethyl acetate (4:1 to 0:1) to yield methyl 2-[(5-bromo-2-nitrophenyl)(hydroxy)methyl]prop-2-enoate **68** (930 mg, 93%) as an orange oil: R_f 0.30 (petroleum ether : ethyl acetate, 9:1); ν_{max} (thin film)/ cm^{-1} 3201 (O-H, m), 2953 (C-H, m), 1726 (C=O, s), 1525 (N-O, s), 1355 (C-H, m); ^{1}H NMR (400 MHz, $CDCl_3$) δ 7.96 (1H, dd, *J* 2.2, 0.5, C^{13}-H), 7.87 (1H, d, *J* 8.7, C^{10}-H), 7.62 (1H,

dd, *J* 8.7, 2.2, C^{11}-H), 6.39 (1H, s, C^{3}-H), 6.24 (1H, s, C^{6}-H), 5.71 (1H, dd, *J* 1.3, 0.6, C^{3}-H'), 3.79 (3H, s, C^{18}-H_3), 3.42 (1H, s, C^{6}-OH); ^{13}C NMR (101 MHz, $CDCl_3$) δ 166.3 (C^{1}), 140.4 (C^{9}), 138.2 (C^{2}), 132.1 (C^{13}), 131.9 (C^{11}), 128.7 (C^{8}), 126.7 (C^{3}), 126.2 (C^{10}), 67.5 (C^{6}), 60.4 (C^{12}), 52.3 (C^{18}); LRMS *m/z* (ESI^+) 339 ([M(^{79}Br) +Na]$^+$); HRMS *m/z* (ESI^+) [Found: 315.9816, $C_{11}H_{10}BrNO_5$ requires M+H^+ 315.9815)]; Analytical HPLC (RP, *Method 1*) rt 9.6 min, purity 95%.

Methyl 3-(5-bromo-2-nitrophenyl)-3-hydroxy-2-methylpropanoate 69

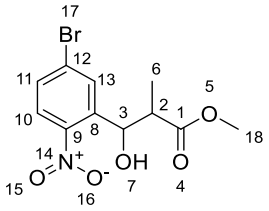

To a solution of methyl 2-((5-bromo-2-nitrophenyl)(hydroxy)methyl)acrylate **68** (400 mg, 1.27 mmol, 1.0 eq.) in degassed THF (10 mL) and saturated by hydrogen was added Wilkinson's catalyst (117 mg, 0.127 mmol, 0.1 eq.). The reaction mixture was stirred under $H_{2\,(g)}$ at 50 °C for 24 h. The solvent was evaporated *in vacuo* then the residue was purified using flash column chromatography eluting with petroleum ether : ethyl acetate (1:0 to 7:3) to yield methyl 3-(5-bromo-2-nitrophenyl)-3-hydroxy-2-methylpropanoate **69** (402 mg, 100%) as a yellow oil: R_f 0.40 (petroleum ether : ethyl acetate, 4:1); ν_{max} (thin film)/ cm^{-1} 2998 (O-H, m), 2884 (O-H, m), 2360, 1740 (C=O, s), 1566 (N-O, s), 1460 (C-H, m), 1352 (N-O, s), 1175 (C-O, s); ^{1}H NMR (400 MHz, $CDCl_3$) δ 7.90 (1H, d, *J* 2.1, C^{13}-H), 7.87 (1H, d, *J* 8.7, C^{10}-H), 7.60 (1H, dd, *J* 8.7, 2.1, C^{11}-H), 5.47 (1H, d, *J* 5.4, C^{3}-H), 3.89 (1H, d, *J* 18.6, C^{3}-OH), 3.68 (3H, s, C^{18}-H_3), 2.97 (1H, qd, *J* 7.3, 5.4, C^{2}-H), 1.31 (3H, d, *J* 7.3, C^{6}-H_3); ^{13}C NMR (101 MHz, $CDCl_3$) δ 175.6 (C^{1}), 146.8 (C^{12}), 139.7 (C^{15}), 131.8 (C^{11}, C^{13}), 128.6 (C^{9}), 126.2 (C^{10}), 70.8 (C^{3}), 52.1 (C^{18}), 45.7 (C^{2}), 15.1 (C^{6}); LRMS *m/z* (ESI^+) 304 ([M(^{79}Br)-CH_3+H]$^+$, 100%); HRMS *m/z* (ESI^+) [Found: 317.9972, $C_{11}H_{12}BrNO_5$ requires [M+H]$^+$ 317.9978)]; Analytical HPLC (RP, *Method 1*) rt 9.8 min, purity 92%.

6-Bromo-4-hydroxy-3-methyl-3,4-dihydroquinolin-2(1*H*)-one 70

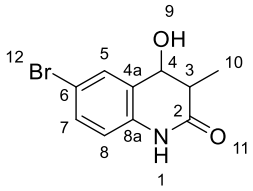

Methyl 3-(5-bromo-2-nitrophenyl)-3-hydroxy-2-methylpropanoate **69** (250 mg, 0.790 mmol, 1.0 eq.) was dissolved in acetic acid (6 mL) and iron (439 mg, 3.93 mmol, 5.0 eq.) was added. The reaction mixture was stirred at 50 °C for 1 h. The reaction mixture was neutralised with $NaHCO_{3\ (aq)}$, filtered then extracted with ethyl acetate. The organic layer was washed with water then brine, then dried over $Na_2SO_{4\ (s)}$, filtered, then the filtrate was concentrated *in vacuo.* The residue was purified by flash column chromatography eluting with petroleum ether : ethyl acetate (1:0 to 0:1) to yield 6-bromo-4-hydroxy-3-methyl-3,4-dihydroquinolin-2(1*H*)-one **70** (176 mg, 88%) as a light yellow solid: R_f 0.15 (petroleum ether : ethyl acetate, 1:1); m.p. 142-144 °C ($CDCl_3$); ν_{max} (thin film)/ cm^{-1} 3113 (N-H, m), 2942 (O-H, m), 2007 (C-H, w), 1667 (C=O, s), 1453 (C-H, m), 1383 (C-H, m); ^1H NMR (400 MHz, $CDCl_3$) δ 7.74 (1H, br s, N-H), 7.50 (1H, d, *J* 2.0, C^5-H), 7.42 (1H, dt, *J* 8.3, 2.0, C^7-H), 6.71 (1H, dd, *J* 8.3, 2.0, C^8-H), 5.32 (1H, s, C^4-H), 4.77 (1H, br s, C^4-OH), 2.88-2.65 (1H, m, C^3-H), 1.40 (3H, d, *J* 7.1, C^{10}-H_3); ^{13}C NMR (126 MHz, $CDCl_3$) δ 171.8 (C^2), 135.7 (C^{8a}), 132.6 (C^7), 131.0 (C^5), 127.6 (C^{4a}), 117.3 (C^8), 115.7 (C^6), 70.4 (C^4), 41.5 (C^3), 10.4 (C^{10}); LRMS *m/z* (ESI^-) 255 ([M(^{79}Br) -H]$^-$, 100%); HRMS *m/z* (ESI^+) [Found: 255.9957, $C_{10}H_{10}BrNO_2$ requires $[M+H]^+$ 255.9968)]; Analytical HPLC (RP, *Method 2*) rt 7.1 min, purity 100%.

6-Bromo-3-methylquinolin-2(1*H*)-one 71

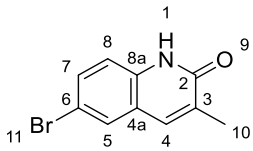

6-Bromo-4-hydroxy-3-methyl-3,4-dihydroquinolin-2(1*H*)-one **70** (115 mg, 0.449 mmol, 1.0 eq.) and *p*-toluenesolfonic acid (42.7 mg, 0.225 mmol, 0.5 eq.) were refluxed in toluene (10 mL) for 19 h using a Dean Stark apparatus. The solvent was evaporated *in vacuo* then the residue re-dissolved in ethyl acetate and washed with $NaHCO_{3\ (aq)}$ then brine. The organic layer was concentrated *in vacuo.* The residue was purified by flash

column chromatography eluting with petroleum ether : ethyl acetate (1:0 to 0:1) to yield 6-bromo-3-methylquinolin-2(1*H*)-one **71** (93 mg, 88%) as an off-white powder: R_f 0.27 (petroleum ether : ethyl acetate, 1:1); m.p. 230-231 °C ($CDCl_3$) [lit.[293] 248-251 °C ($CHCl_3$/ hexane)]; ^{1}H NMR (600 MHz, DMSO-*d*$_6$) δ 11.86 (1H, s, N-H), 7.82 (1H, d, *J* 2.2, C^5-H), 7.74 (1H, s, C^4-H), 7.57 (1H, dd, *J* 8.7, 2.2, C^7-H), 7.24 (1H, d, *J* 8.7, C^8-H), 2.10 (3H, d, *J* 1.3, C^{10}-H_3); ^{13}C NMR (151 MHz, DMSO-*d*$_6$) δ 162.6 (C^2) 137.4 (C^{8a}), 135.6 (C^4), 132.1 (C^7), 131.8 (C^3), 129.4 (C^5), 121.7 (C^{4a}), 117.3 (C^8), 113.7 (C^6), 17.0 (C^{10}); LRMS *m/z* (ESI$^+$) 239 ([M(^{79}Br)+H]$^+$, 100%). The spectroscopic data are in good agreement with the literature.[293]

6-(3,5-Dimethyl-1,2-oxazol-4-yl)-3-methylquinolin-2(1*H*)-one 16

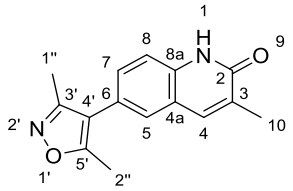

6-Bromo-3-methylquinolin-2(1*H*)-one **71** (30.0 mg, 126 µmol, 1.0 eq.), potassium (3,5-dimethylisoxazol-4-yl)trifluoroborate **53** (30.7 mg, 151 µmol, 1.2 eq.) and K_2CO_3 (31.1 mg, 227 µmol, 1.5 eq.) were combined in 1,4-dioxane : H_2O (10:1, 1.5 mL) then the reaction mixture was degassed with $N_{2\,(g)}$ for 15 min. Pd(dppf)Cl_2·CH_2Cl_2 (10.0 mg, 13.0 µmol, 0.1 eq.) was added then the reaction mixture was stirred at 110 °C for 5.5 h. Pd(dppf)Cl_2·CH_2Cl_2 (10.0 mg, 13.0 µmol, 0.1 eq.) was added then the reaction mixture was stirred for a further 16 h at 110 °C . The reaction mixture was cooled to rt and filtered through Celite®. The filtrate was partitioned between ethyl acetate and water. The organic layer was separated, then the aqueous layer was extracted with ethyl acetate (3 × 5 mL). The combined organic layers were dried over $MgSO_{4\,(s)}$, filtered, then the filtrate was concentrated *in vacuo.* The residue was purified by flash column chromatography eluting with petroleum ether : ethyl acetate (88:12 to 0:1). Pure fractions were combined and concentrated *in vacuo* to yield 6-(3,5-dimethyl-1,2-oxazol-4-yl)-3-methylquinolin-2(1*H*)-one **16** (20 mg, 54%) as a colourless solid: R_f 0.18 (petroleum ether : ethyl acetate, 1:1); m.p. 245-248 °C (ethyl acetate); ν_{max} (thin film)/ cm^{-1} 3142 (N-H, m), 2986 (C-H, m), 1643 (C=O, s), 1423 (C-H, m); ^{1}H NMR (400 MHz, $CDCl_3$) δ 11.66 (1H, s, N-H), 7.68 (1H, s, C^4-H), 7.46 (1H, d, *J* 8.3, C^8-H), 7.37 (1H, d, *J* 1.8, C^5-H), 7.34 (1H, dd, *J* 8.3, 1.8, C^7-H), 2.42 (3H, s, $C^{2''}$-H_3), 2.33 (3H, d, *J* 1.2, C^{10}-H_3), 2.28 (3H, s, $C^{1''}$-H_3);

^{13}C NMR (101 MHz, $CDCl_3$) δ 165.3 (C^2), 164.4 ($C^{5'}$), 158.7 ($C^{3'}$), 137.0 (C^4), 136.8 (C^{8a}), 131.1 (C^3), 130.2 (C^7), 127.3 (C^5), 124.7 (C^{4a}), 120.6 (C^6), 116.0 (C^8, $C^{4'}$), 16.9 (C^{10}), 11.6 ($C^{2''}$), 10.8 ($C^{1''}$); HRMS *m/z* (ESI^+) [Found: 255.1134, $C_{15}H_{14}N_2O_2$ requires $[M+H]^+$ 255.1128)]; LRMS *m/z* (ESI^+) 255 ($[M+H]^+$, 100%); Analytical HPLC (RP, *Method 2*) rt 7.7 min, purity 100%.

4-(1*H*-Benzo[*d*]imidazol-5-yl)-3,5-dimethylisoxazole 17

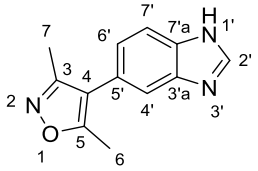

DMF : water (4:1) (5 ml) was degassed with Ar $_{(g)}$ for 20 min. 5-Bromo-1*H*-benzo[*d*]imidazole (500 mg, 2.52 mmol, 1.0 eq.), potassium (3,5-dimethylisoxazol-4-yl)trifluoroborate (618 mg, 3.05 mmol, 1.2 eq.), Na_2CO_3 (1.08 g, 10.2 mmol, 4.0 eq.) and $Pd(dppf)Cl_2 \cdot CH_2Cl_2$ (207 mg, 0.250 mmol, 0.1 eq.) were added. The reaction was stirred at 130˚C in a microwave reactor for 30 min. The reaction mixture was cooled to rt then filtered through Celite®, washing with CH_2Cl_2. The reaction mixture was partitioned between CH_2Cl_2 (15 mL) and sat. $NaHCO_{3\ (aq)}$ (10 mL) then the layers were separated. The organic layer was washed with H_2O (10 mL) and brine (10 mL), then dried over anhydrous $MgSO_{4\ (s)}$, filtered, then the filtrate was concentrated *in vacuo*. The residue was purified by flash column chromatography eluting with CH_2Cl_2 : methanol (1:0 to 9:1) to yield 4-(1*H*-benzo[*d*]imidazol-5-yl)-3,5-dimethylisoxazole **17** (216 mg, 40%) as a yellow solid: m.p. 245 °C (*dec.*); ν_{max} (thin film)/ cm^{-1} 2926 (N-H, s *br*), 1666 (N-H, m), 1637 (C=C, m), 1483 (C-H, w), 1425 (C-H, w), 911 (C=C, m); R_f 0.26 (CH_2Cl_2 : methanol, 9:1); ^{1}H NMR (400 MHz, DMSO-d_6) δ 12.5 (1H, s, $N^{1'}$-H), 8.25(1H, s, $C^{2'}$-H), 7.55 (2H, m, $C^{4'}$-H, $C^{7'}$-H), 7.15 (1H, d, *J* 8.2, $C^{6'}$-H), 2.38 (3H, s, C^6-H_3), 2.21 (3H, s, C^7-H_3); LRMS *m/z* (ESI^-) 212 ($[M-H]^-$, 100%); HRMS *m/z* (ESI^+) [Found: 236.0797, $C_{12}H_{11}N_3O$ requires $[M+Na]^+$ 236.0794)]; Analytical HPLC (RP, *Method 2*) rt 5.3 min, purity 100%. The spectroscopic data are in good agreement with the literature.[190, 295]

4-(2-Ethyl-1-methyl-1*H*-benzo[*d*]imidazol-5-yl)-3,5-dimethylisoxazole 18

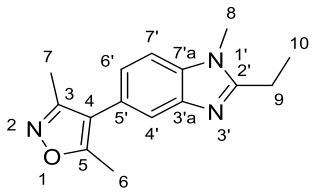

4-(3,5-Dimethylisoxazol-4-yl)-N^1-methylbenzene-1,2-diamine **76** (50.0 mg, 0.230 mmol, 1.0 eq.) was dissolved in ethyl acetate (1.5 mL) then propionic acid (17.2 µL, 0.230 mmol, 1.0 eq.) was added. 50 wt.% T3P in ethyl acetate (356 µL, 1.19 mmol, 5.2 eq.) and DIPEA (88.1 µL 0.506 mmol, 2.2 eq.) were added then the reaction mixture was stirred at 80 °C for 6 h. The reaction mixture was quenched with 1 M $NaOH_{(aq)}$ then the organic layer was separated. The aqueous layer was extracted with ethyl acetate (3 × 15 mL). The combined organic layers were dried over $MgSO_{4\ (s)}$, filtered, then the filtrate was concentrated *in vacuo*. The residue was purified by flash column chromatography eluting with petroleum ether : ethyl acetate (1:0 to 0:1) to yield 4-(2-ethyl-1-methyl-1*H*-benzo[*d*]imidazol-5-yl)-3,5-dimethylisoxazole **18** (37 mg, 62%) as an off-white solid: m.p. 109-110 °C ($CDCl_3$); R_f 0.14 (petroleum ether : ethyl acetate, 1:9); ν_{max}(thin film)/ cm^{-1} 1519 (C-H, w), 1409 (C-H, m), 1310 (C-O, s); ^{1}H NMR (400 MHz, $CDCl_3$) δ 7.59 (1H, d, *J* 1.1, $C^{4'}$-H), 7.34 (1H, d, *J* 8.3, $C^{7'}$-H), 7.11 (1H, dd, *J* 8.3, 1.1, $C^{6'}$-H), 3.75 (3H, s, C^8-H_3), 2.93 (2H, q, *J* 7.5, C^9-H_2), 2.39 (3H, s, C^6-H_3), 2.26 (3H, s, C^7-H_3), 1.47 (3H, t, *J* 7.5, C^{10}-H_3); ^{13}C NMR (101 MHz, $CDCl_3$) δ 164.9 (C^5), 159.0 (C^3), 157.2 ($C^{2'}$), 142.8 ($C^{3'a}$), 135.3 ($C^{7'a}$), 124.0 ($C^{5'}$), 123.3 ($C^{6'}$), 119.8 ($C^{4'}$), 117.2 (C^4), 109.1 ($C^{7'}$), 29.7 (C^8), 20.9 (C^9), 11.6 (C^{10}), 11.5 (C^6), 10.8 (C^7); LRMS *m/z* (ESI^+) 256 ($[M+H]^+$, 100%); HRMS *m/z* (ESI^+) [Found: 256.1444, $C_{15}H_{17}N_3O$ requires $[M+H]^+$ 256.1444)]; Analytical HPLC (RP, *Method 1*) rt 6.2 min, purity 100%.

7-(Benzyloxy)-4-chloro-6-methoxyquinoline 60

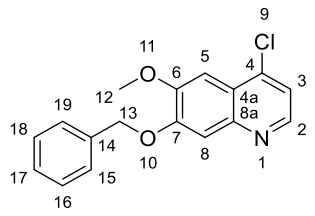

4-Chloro-6-methoxy-7-hydroxyquinoline (700 mg, 3.34 mmol, 1.0 eq.) and potassium carbonate (2.31 g, 16.7 mmol, 5.0 eq.) were combined in anhydrous DMF (15 mL).

Benzyl bromide (436 µL, 3.67 mmol, 1.1 eq.) was added then the reaction mixture was stirred at 45 °C for 2 h. The reaction mixture was cooled to rt then the solvent was evaporated *in vacuo.* The residue was suspended in water and sonicated. The suspension was filtered then the filter cake washed with water, then hexane and dried under vacuum to give 7-(benzyloxy)-4-chloro-6-methoxyquinoline **60** (1.00 g, 100%) as a brown solid: R_f 0.68 (petroleum ether : ethyl acetate, 1:1); m.p. 125-126°C ($CDCl_3$) [lit.[296] 132-133 °C]; ^{1}H NMR (400 MHz, $CDCl_3$) δ 8.58 (1H, d, *J* 4.9, C^2-H), 7.56-7.30 (9H, m, C^3-H, C^5-H, C^8-H, C^{15}-H, C^{16}-H, C^{17}-H, C^{18}-H, C^{19}-H,), 5.34 (2H, s, C^{13}-H), 4.09 (3H, s, C^{12}-H_3); LRMS *m/z* (ESI^+) 300 ($[M+H]^+$, 100%). The spectroscopic data are in good agreement with the literature.[296]

7-(Benzyloxy)-6-methoxy-4-methylquinoline 61

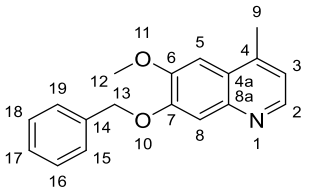

7-(Benzyloxy)-4-chloro-6-methoxyquinoline **60** (600 mg, 2.00 mmol, 1.0 eq.), methyl boronic acid (180 mg, 3.00 mmol, 1.5 eq.) and K_2CO_3 (830 mg, 6.01 mmol, 3.0 eq.) were combined in 1,4-dioxane : H_2O (10:1, 20 mL) then the reaction mixture was degassed with $N_{2\,(g)}$ for 15 min. $Pd(dppf)Cl_2 \cdot CH_2Cl_2$ (164 mg, 0.200 mmol, 0.1 eq.) was added then the reaction mixture was stirred at 110 °C for 5 h. The reaction mixture was cooled to rt and filtered through Celite®. The filtrate was partitioned between ethyl acetate and water. The organic layer was separated, then the aqueous layer was extracted with ethyl acetate (3 × 20 mL). The combined organic layers were washed with brine, dried over $MgSO_{4\,(s)}$, filtered, then the filtrate was concentrated *in vacuo.* The residue was purified by flash column chromatography eluting with petroleum ether : ethyl acetate (1:0 to 0:1). Pure fractions were combined and concentrated *in vacuo* to yield 7-(benzyloxy)-6-methoxy-4-methylquinoline **61** (266 mg, 48%) as an orange solid: R_f 0.17 (petroleum ether : ethyl acetate, 1:1); m.p. 107-109 °C ($CHCl_3$); ν_{max} (thin film)/ cm^{-1} 1620 (C=C, w), 1592 (C=C, w), 1505 (N=C, m), 1487 (N-C, m), 1262 (C-O, s), 1246 (C-O, s), 1167 (C-N, m), 855 (C=C, m); ^{1}H NMR (600 MHz, $CDCl_3$) δ 8.56 (1H, d, *J* 4.5, C^2-H), 7.53-7.48 (2H, m, C^{19}-H, C^{15}-H), 7.46 (1H, s, C^5-H), 7.40-7.36 (2H, m, C^{16}-H, C^{18}-H), 7.34-7.28 (1H, m, C^{17}-H), 7.16 (1H, s, C^8-H), 7.09 (1H, dd, *J* 4.5, 1.0, C^3-H), 5.31 (2H, s, C^{13}-H_2),

4.03 (1H, s, C^{12}-H_3), 2.63 (3H, d, *J* 0.9, C^9-H_3); ^{13}C NMR (151 MHz, $CDCl_3$) δ 151.2 (C^7), 150.0 (C^6), 148.1 (C^2), 145.1 (C^4), 142.4 (C^{8a}), 136.5 (C^{14}), 128.8 (C^{16}, C^{18}), 128.2 (C^{17}), 127.6 (C^{15}, C^{19}), 123.8 (C^{4a}), 120.6 (C^3), 110.4 (C^5), 102.0 (C^8), 70.8 (C^{13}), 56.2 (C^{12}), 19.0 (C^9); LRMS *m/z* (ESI^+) 280 ($[M+H]^+$, 100%); HRMS *m/z* (ESI^+) [Found: 302.1139, $C_{18}H_{17}NO_2$ requires $[M+Na]^+$ 302.1152)]. Analytical HPLC (RP, *Method 2*) rt 7.4 min, purity 95%.

6-Methoxy-4-methylquinolin-7-ol 62

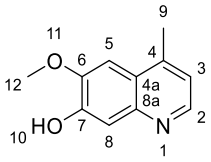

10% Palladium on carbon (15 mg, 10 wt. % of substrate) was added to a degassed solution of 7-(benzyloxy)-6-methoxy-4-methylquinoline **61** (150 mg, 0.537 mmol, 1.0 eq.) in acetic acid (10 mL). The reaction mixture was stirred under $H_{2\ (g)}$ at rt for 15 h. The reaction mixture was filtered through Celite® then eluted with ethyl acetate. The filtrate was evaporated *in vacuo* then the residue was purified by flash column chromatography eluting with ethyl acetate : methanol (1:0 to 7:3). Pure fractions were combined and concentrated *in vacuo* to yield 6-methoxy-4-methylquinolin-7-ol **62** (101 mg, 100%) as a light yellow solid: R_f 0.63 (ethyl acetate : methanol, 10:1); m.p. 229-230 °C (MeOH) [lit.[297] 187 °C (benzene)]; ν_{max} (thin film)/ cm^{-1} 2962 (O-H, m), 2852 (C-H, m), 1471 (C-H, m), 1423 (O-H, m), 1249 (C-N, m), 1205 (C-O, s); ^{1}H NMR (400 MHz, DMSO-*d*$_6$) δ 10.03 (1H, s, C^7-OH), 8.45 (1H, d, *J* 4.4, C^2-H), 7.24 (1H, s, C^5-H), 7.24 (1H, s, C^8-H), 7.10 (1H, d, *J* 4.4, C^3-H), 3.94 (3H, s, C^{12}-H_3), 2.60 (3H, s, C^9-H_3); ^{13}C NMR (101 MHz, $CDCl_3$) δ 149.8 (C^{8a}), 148.9 (C^7), 147.4 (C^2), 144.7 (C^6), 141.9 (C^{4a}), 122.4 (C^4), 119.5 (C^3), 111.2 (C^5), 102.3 (C^8), 55.6 (C^{12}), 18.3 (C^9); HRMS *m/z* (ESI^+) [Found: 190.0855, $C_{11}H_{11}NO_2$ requires $[M+H]^+$ 190.0863)]; LRMS *m/z* (ESI^+) 190 ($[M+H]^+$); Analytical HPLC (RP, *Method 1*) rt 5.5 min, purity 96%.

6-Methoxy-4-methylquinolin-7-yl trifluoromethanesulfonate 58

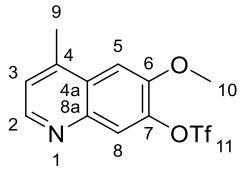

6-Methoxy-4-methylquinolin-7-ol **62** (34 mg, 0.18 mmol, 1.0 eq.) was dissolved in anhydrous CH_2Cl_2 (3.0 mL) and cooled to 0 °C. Anhydrous pyridine (29 µL, 0.36 mmol, 2.0 eq.) then trifluoromethanesulfonic anhydride (36 µL, 0.22 mmol, 1.2 eq.) were added then the reaction mixture was stirred in an ice bath for 1 h. The reaction mixture was quenched with water (5 mL) then extracted with CH_2Cl_2 (2 × 5 mL). The combined organic layers were dried over $Na_2SO_{4\,(s)}$, filtered, then the filtrate was concentrated *in vacuo.* The residue was purified by flash column chromatography eluting with petroleum ether : ethyl acetate (1:0 to 0:1) to yield 6-methoxy-4-methylquinolin-7-yl trifluoromethanesulfonate **58** (39 mg, 67%) as a colourless solid: R_f 0.52 (petroleum ether : ethyl acetate, 1:1); m.p. 52-54 °C (ethyl acetate); ν_{max} (thin film)/ cm^{-1} 1427 (S=O, s), 1308 (C-N, s), 1250 (C-O, s), 1211 (C-F, s), 1141 (C-O, s), 1074 (C=O, s), 891 (C=C, s), 858 (C=C, m); ^{1}H NMR (400 MHz, $CDCl_3$) δ 8.69 (1H, d, *J* 4.4, C^2-H), 7.96 (1H, s, C^8-H), 7.31 (1H, s, C^5-H), 7.26 (1H, dd, *J* 4.5, 1.1, C^3-H), 4.06 (3H, s, C^{10}-H_3), 2.67 (3H, s, C^9-H_3); ^{13}C NMR (101 MHz, $CDCl_3$) δ 150.0 (C^6), 149.5 (C^2), 143.0 (C^4), 143.2 (C^{8a}), 141.3 (C^7), 128.7 (C^{4a}), 123.2 (C^3), 123.1 (C^8), 118.9 (q, *J* 321, C^{11}), 104.0 (C^5), 56.5 (C^{10}), 19.1 (C^9); ^{19}F NMR (376 MHz, $CDCl_3$) δ -73.64 (3F, s, C-F_3); HRMS *m/z* (ESI^+) [Found: 322.0350, $C_{12}H_{10}F_3NO_4S$ requires $[M+H]^+$ 322.0355)]; LRMS *m/z* (ESI^+) 322 ($[M+H]^+$, 100%); Analytical HPLC (RP, *Method 3*) rt 9.7 min, purity 100%.

7-(3,5-Dimethyl-1,2-oxazol-4-yl)-6-methoxy-4-methylquinoline 19

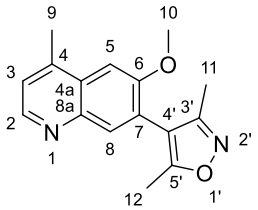

6-methoxy-4-methylquinolin-7-yl trifluoromethanesulfonate **58** (35 mg, 0.11 mmol, 1.0 eq.), 3,5-dimethylisoxazol-4-yl-4-boronic acid (19 mg, 0.13 mmol, 1.2 eq.) and K_2CO_3 (43 mg, 0.33 mmol, 3.0 eq.) were combined in 1,4-dioxane (2.0 mL) then the

reaction mixture was degassed with $N_{2\ (g)}$ for 15 min. $Pd(dppf)Cl_2 \cdot CH_2Cl_2$ (8.0 mg, 0.011 mmol, 0.1 eq.) was added then the reaction mixture was stirred at 110 °C for 4 h. The reaction mixture was cooled to rt and filtered through Celite®. The filtrate was concentrated *in vacuo.* The residue was purified by flash column chromatography eluting with petroleum ether : ethyl acetate (1:0 to 0:1). Pure fractions were combined and concentrated *in vacuo* to yield 7-(3,5-dimethyl-1,2-oxazol-4-yl)-6-methoxy-4-methylquinoline **19** (9 mg, 31%) as a colourless solid: R_f 0.21 (petroleum ether : ethyl acetate, 1:1); m.p. 133-135 °C (ethyl acetate); ν_{max} (thin film)/ cm^{-1} 1596 (C=C, m), 1472 (C-H, m), 1426 (C-H, m), 1242 (C-O, s), 1214 (C-O, s), 1034 (C-N, m), 906 (C=C, m); ^1H NMR (400 MHz, $CDCl_3$) δ 8.69 (1H, d, *J* 4.4, C^2-H), 7.88 (1H, s, C^8-H), 7.27 (1H, d, *J* 4.4, C^5-H), 7.26 (1H, dd, *J* 4.4, 0.9, C^3-H), 3.97 (1H, s, O-CH_3), 2.72 (1H, d, *J* 0.9, C^9-H_3), 2.37 (3H, s, C^{12}-H_3), 2.22 (3H, s, C^{11}-H_3); ^{13}C NMR (101 MHz, $CDCl_3$) δ 166.5 ($C^{5'}$), 159.9 (C^6), 155.8 ($C^{3'}$), 148.5 (C^2), 143.7 (C^{8a}), 142.7 (C^4), 133.0 (C^8), 129.2 (C^{4a}), 124.3 (C^7), 112.9 ($C^{4'}$), 101.6 (C^5), 55.7 (C^{10}), 19.0 (C^9), 11.8 (C^{12}), 10.9 (C^{11}); HRMS *m/z* (ESI^+) [Found: 291.1111, $C_{16}H_{16}N_2O_2$ requires $[M+Na]^+$ 291.1104)]; LRMS *m/z* (ESI^+) 269 ($[M+H]^+$, 100%); Analytical HPLC (RP, *Method 3*) rt 6.4 min, purity 95%.

3,5-Dimethyl-4-(4-methylquinolin-7-yl)isoxazole 20

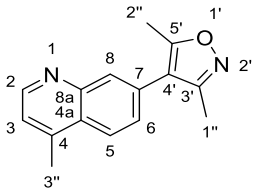

7-Bromo-4-methylquinoline (100 mg, 0.45 mmol, 1.0 eq.), potassium (3,5-dimethylisoxazol-4-yl)trifluoroborate **53** (110 mg, 0.54 mmol, 1.2 eq.) and K_2CO_3 (93 mg, 0.68 mmol, 1.5 eq.) were combined in 1,4-dioxane : H_2O (10:1, 1 mL) then the reaction mixture was degassed with $N_{2\ (g)}$ for 15 min. $Pd(dppf)Cl_2 \cdot CH_2Cl_2$ (37 mg, 0.045 mmol, 0.1 eq.) was added then the reaction mixture was stirred at 100 °C for 16 h. The reaction mixture was filtered through Celite® then the filtrate was partitioned between ethyl acetate and water. The organic layer was separated, then the aqueous layer was extracted with ethyl acetate (3 × 5 mL). The combined organic layers were dried over $MgSO_{4\ (s)}$, filtered, then the filtrate was concentrated *in vacuo.* The residue was purified by flash column chromatography eluting with petroleum ether : ethyl acetate (1:0

to 1:4) to yield 3,5-dimethyl-4-(4-methylquinolin-7-yl)isoxazole **20** (54 mg, 50%) as a beige solid: R_f 0.10 (petroleum ether : ethyl acetate, 7:3); m.p. 91-93 °C ($CHCl_3$); ν_{max} (thin film)/ cm^{-1} 3042 (C-H, m), 2930 (C-H, m), 1313 (C-N, s), 1185 (N-O, m); ^1H NMR (400 MHz, $CDCl_3$) δ 8.83 (1H, d, *J* 4.3, C^2-H), 8.10 (1H, d, *J* 8.6, C^5-H), 8.03 (1H, d, *J* 1.8, C^8-H), 7.50 (1H, dd, *J* 8.6, 1.8, C^6-H), 7.30 (1H, dd, *J* 4.3, 1.0, C^3-H), 2.77 (3H, d, *J* 1.0, $C^{3"}$-H_3), 2.51 (3H, s, $C^{1"}$-H_3), 2.38 (3H, s, $C^{2"}$-H_3); ^{13}C NMR (101 MHz, $CDCl_3$) δ 165.8 ($C^{5'}$), 158.7 ($C^{3'}$), 150.8 (C^2), 148.0 (C^{8a}), 144.4 (C^4), 131.5 (C^7), 129.9 (C^8), 127.4 (C^{4a}), 127.2 (C^6), 124.5 (C^5), 122.2 (C^3), 116.1 ($C^{4'}$), 18.6 ($C^{3"}$), 11.8 ($C^{1"}$), 11.0 ($C^{2"}$); LRMS *m/z* (ESI^+) 239 ($[M+H]^+$, 100%); HRMS *m/z* (ESI+) [Found: 239.1180, $C_{15}H_{14}N_2O$ requires $[M+H]^+$ 239.1179)]; Analytical HPLC (RP, *Method 1*) rt 6.1 min, purity 100%.

7-(3,5-Dimethyl-1*H*-pyrazol-4-yl)-4-methylquinoline 21

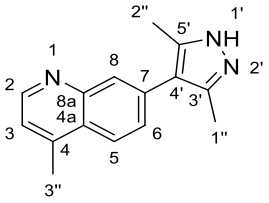

7-Bromo-4-methylquinoline (100 mg, 0.45 mmol, 1.0 eq.) was dissolved in 1,4-dioxane : water (10:1) (5 ml). 3,5-Dimethylpyrazole-4-boronic acid pinacol ester (66 mg, 0.54 mmol, 1.2 eq.) and potassium carbonate (94 mg, 0.68 mmol, 1.5 eq.) were added then the reaction was degassed for 30 min. $Pd(dppf)Cl_2 \cdot CH_2Cl_2$ (30 mg, 0.42 mmol, 0.1 eq.) was added then the reaction was stirred at 110˚C for 20 h. The reaction mixture was cooled to rt, filtered through Celite®, eluted using ethyl acetate (10 mL) then the eluate was washed with water (2 × 10 mL) then brine (5 mL). The organic components were combined, dried over $MgSO_{4\ (s)}$, filtered, then the filtrate was concentrated *in vacuo.* The residue was purified by flash column chromatography eluting with ethyl acetate (100%) to yield 7-(3,5-dimethyl-1*H*-pyrazol-4-yl)-4-methylquinoline **21** (44 mg, 42%) as a dark orange solid: R_f 0.10 (ethyl acetate); m.p. 111–113 °C (ethyl acetate); ν_{max} (thin film)/ cm^{-1} 3157 (N-H), 2901 (C-H, w); ^1H NMR (400 MHz, $CDCl_3$) δ 8.78 (1H, d, J 4.4, C^2-H), 8.03 (1H, d, J 8.6, C^5-H), 8.00 (1H, d, J 1.7, C^8-H), 7.54 (1H, dd, J 8.6, 1.7, C^6-H), 7.22 (1H, dd, J 4.4, 1.0, C^3-H), 2.73 (3H, d, J 1.0, $C^{3"}$-H), 2.39 (6H, s, $C^{1"}$-H_3, $C^{2"}$-H_3); ^{13}C NMR (101 MHz, $CDCl_3$) δ 171.2 ($C^{3'}$, $C^{5'}$), 150.5 (C^2),

148.2 (C^{8a}), 144.2 (C^{4}), 135.0 (C^{7}), 131.3 (C^{4a}), 129.4 (C^{8}), 128.1 (C^{6}), 126.7 ($C^{4'}$), 123.9 (C^{5}), 121.6 (C^{3}), 18.6 ($C^{3''}$), 11.8 ($C^{1''}$, $C^{2''}$); LRMS *m/z* (ESI^{+}) 238 ($[M+H]^{+}$, 100%); HRMS *m/z* (ESI^{+}) [Found: 238.1340, $C_{15}H_{16}N_3$ requires $[M+H]^{+}$ 238.1339]; Analytical HPLC (RP, *Method 1*) rt 7.5 min, purity 99%.

2-[(1*E*)-*N*-Hydroxyethanimidoyl]phenol 80

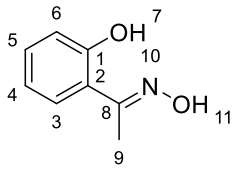

2'-Hydroxyacetophenone (1.00 mL, 8.31 mmol, 1.0 eq.), hydroxylamine hydrochloride (924 mg, 13.3 mmol, 1.6 eq.) and NaOAc (1.09 g, 13.3 mmol, 1.6 eq.) were refluxed at 80 °C in EtOH : H_2O, 3:1 (20 mL) for 2 h. The reaction mixture was cooled to rt and EtOH was evaporated *in vacuo* to give a colourless solid. Water was added to dissolve the ionic impurities. The solid was filtered and the filter cake dried under high vacuum to give 2-[(1*E*)-*N*-hydroxyethanimidoyl]phenol **80** (1.31 g, 100%); R_f 0.41 (petroleum ether : ethyl acetate, 3:1); m.p. 107-110 °C ($CDCl_3$) [lit.[298] 104-107 °C, lit.[299] 118-120 °C, lit.[300] 206-208 °C]; ^{1}H NMR (400 MHz, $CDCl_3$) δ 11.41 (1H, s, C^{1}-OH), 7.69 (1H, s, N^{10}-OH), 7.45 (1H, dd, *J* 7.9, 1.6, C^{3}-H), 7.27 (1H, ddd, *J* 8.5, 7.3, 1.6, C^{5}-H), 6.98 (1H, dd, *J* 8.5, 1.3, C^{6}-H), 6.92 (1H, ddd, *J* 7.9, 7.3, 1.3, C^{4}-H), 2.37 (3H, s, C^{9}-H_3); LRMS *m/z* (ESI^{+}) 152 ($[M+H]^{+}$, 100%). The spectroscopic data are in good agreement with the literature.[299]

3-Methyl-1,2-benzoxazole 22

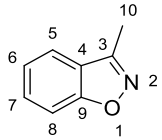

2-[(1*E*)-*N*-Hydroxyethanimidoyl]phenol **80**(1.00 g, 6.36 mmol, 1.0 eq.) was dissolved in 1,4-dioxane (5.30 mL) and DMF-DMA (4.90 mL, 36.9 mmol, 5.8 eq.) was added. The reaction mixture was refluxed at 100 °C for 1 h. The reaction mixture was cooled to rt then partitioned between ethyl acetate (20 mL) and water (20 mL). The aqueous layer was

extracted with ethyl acetate (3 × 20 mL). Combined organic layers were washed with brine (20 mL), dried over anhydrous $Na_2SO_{4\,(s)}$, filtered and concentrated *in vacuo*. The residue was purified using silica column chromatography eluting with diethyl ether in petroleum ether (3:7) to yield 3-methyl-1,2-benzoxazole **22** (581 mg, 69%) as a yellow oil: R_f 0.51 (petroleum ether : diethyl ether, 20:1); ^{1}H NMR (400 MHz, $CDCl_3$) δ 7.61 (1H, ddd, *J* 7.9, 0.9, 0.8, C^5-H), 7.55-7.47 (1H, m, C^7-H, C^8-H), 7.28 (1H, ddd, *J* 7.9, 4.4, 3.4, C^6-H), 2.57 (3H, s, C^{10}-H_3); ^{13}C NMR (126 MHz, $CDCl_3$) δ 162.8 (C^9), 155.0 (C^3), 129.7 (C^8), 123.2 (C^6), 122.2 (C^4), 121.2 (C^5), 109.8 (C^7), 10.1 (C^{10}); LRMS *m/z* (ESI^+) 134 ($[M+H]^+$, 100%); Analytical HPLC (RP, *Method 4*) rt 9.3 min, purity 100%. The spectroscopic data are in good agreement with the literature.[301]

5-Chloro-3-methyl-2,1-benzoxazole 23

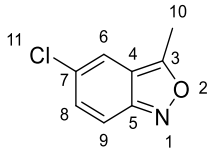

1-(5-Chloro-2-nitrophenyl)ethan-1-one (200 mg, 1.00 mmol, 1.0 eq.), zinc dust (327 mg, 5.00 mmol, 5.0 eq.) and 2-bromo-2-nitropropane (128 µL, 1.20 mmol, 1.2 eq.) were combined in a microwave vial then placed under argon. Degassed MeOH (3 mL) was added then the reaction mixture was stirred at 50 °C for 31 h. The reaction mixture was filtered through Celite®, eluting with CH_2Cl_2. The filtrate was evaporated *in vacuo* then the residue was partitioned between CH_2Cl_2 (15 mL) and sat. aq. NH_4Cl (10 mL). The aqueous layer was extracted with CH_2Cl_2 (2 × 15 mL). The combined organic layers were washed with water (15 mL), dried over anhydrous $MgSO_{4\,(s)}$, filtered, then the filtrate was concentrated *in vacuo.* The residue was purified by flash column chromatography eluting with petroleum ether : ethyl acetate (1:0 to 76:24) to yield 5-chloro-3-methyl-2,1-benzoxazole **23** (90 mg, 54%) as an off-white solid: R_f 0.27 (petroleum ether : ethyl acetate, 15:1); m.p. 87-89 °C ($CHCl_3$) [lit.[302] 97-98 °C ($CHCl_3$)]; ^{1}H NMR (400 MHz, $CDCl_3$) δ 7.49 (1H, dd, *J* 9.4, 0.9, C^9-H), 7.44 (1H, dd, *J* 1.8, 0.9, C^6-H), 7.19 (1H, dd, *J* 9.4, 1.8, C^8-H), 2.77 (3H, s, C^{10}-H_3); HRMS *m/z* (ESI+) [Found: 168.0211, C_8H_6ClNO requires $[M+H]^+$ 168.0211)]; LRMS *m/z* (ESI^+) 168 ($[M+H]^+$); Analytical HPLC (RP, *Method 2*) rt 8.7 min, purity 100%. The spectroscopic data are in good agreement with the literature.[302]

Methyl-*N*-(2-nitrophenyl)alaninate 92

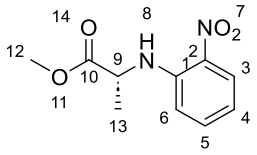

To a stirred solution of 1-fluoro-2-nitrobenzene (747 µL, 7.09 mmol, 1.0 eq.) and D-alanine methyl ester hydrochloride (1.09 g, 7.80 mmol, 1.1 eq.) in DMF (14.2 mL) was added DIPEA (4.94 mL, 28.3 mmol, 4.0 eq.). The reaction mixture was heated to 85 °C then stirred for 22 h. The reaction mixture was cooled to rt, quenched with a solution of sat. $NaHCO_{3\,(aq)}$ then extracted with ethyl acetate (3 × 100 mL). The combined organic layers were washed with 10% w/v LiCl aq. (100 mL), dried over $Na_2SO_{4\,(s)}$, filtered, then the filtrate was concentrated *in vacuo*. The residue was purified using flash column chromatography eluting with petroleum ether : ethyl acetate (12:88 to 0:1) to yield methyl *N*-(2-nitrophenyl)alaninate **92** (1.20 g, 75%) as a yellow oil: R_f 0.20 (petroleum ether : ethyl acetate, 10:1); $[\alpha]_D^{25}$= -135.1 (*c* 1.0, $CHCl_3$); ^{1}H NMR (400 MHz, $CDCl_3$) δ 8.29 (1H, d, *J* 7.0, N-H), 8.20 (1H, dd, *J* 8.7, 1.6, C^3-H), 7.43 (1H, dddd, *J* 8.7, 7.0, 1.6, 0.6, C^5-H), 6.77-6.66 (2H, m, C^4-H, C^6-H), 4.31 (1H, p, *J* 7.0, C^9-H), 3.78 (3H, s, C^{12}-H_3), 1.61 (3H, d, *J* 7.0, C^{13}-H_3); LRMS *m/z* (ESI^-) 209 ([M-CH_3-H]$^-$, 100%). The spectroscopic data are in good agreement with the literature.[303]

(3*R*)-3-Methyl-3,4-dihydroquinoxalin-2(1*H*)-one 24

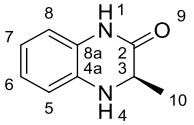

Methyl *N*-(2-nitrophenyl)alaninate **92** (1.10 g, 4.90 mmol, 1.0 eq.), zinc powder (8.02 g, 123 mmol, 25 eq.) and NH_4Cl (6.56 g, 123 mmol, 25.0 eq.) were combined in DMF (55 mL) then the reaction mixture was stirred at rt for 25 h. The suspension was diluted with ethyl acetate (100 mL) then filtered through Celite®. The filtrate was washed with brine (2 × 100 mL) and 10% w/v LiCl aq. (100 mL). The organic layer was dried over $MgSO_{4\,(s)}$, filtered, then the filtrate was concentrated *in vacuo*. The residue was purified using flash column chromatography eluting with petroleum ether : ethyl acetate (3:1 to 1:1) to yield (3*R*)-3-methyl-3,4-dihydroquinoxalin-2(1*H*)-one **24** (703 mg, 89%) as a brown solid: R_f 0.41 (petroleum ether : ethyl acetate, 1:1); $[\alpha]_D^{25}$= -61.2 (*c* 1.0, $CHCl_3$);

m.p. 112-114 °C ($CHCl_3$) [lit.[304] 117-119 °C]; ^{1}H NMR (400 MHz, $CDCl_3$) δ 9.57 (1H, s, N^1-H), 6.88 (1H, ddd, *J* 7.6, 7.5, 1.6, C^8-H), 6.81 (1H, dd, *J* 7.8, 1.6, C^6-H), 6.75 (1H, ddd, *J* 7.6, 7.5, 1.3, C^7-H), 6.67 (1H, dd, *J* 7.8, 1.3, C^5-H), 4.03 (1H, q, *J* 6.6, C^3-H), 3.93 (1H, s, N^4-H), 1.46 (3H, d, 6.6, C^{10}-H_3); LRMS *m/z* (ESI^+) 163.0 ($[M+H]^+$, 100%); Analytical HPLC (RP, *Method 4*) rt 6.6 min, purity 100%. The spectroscopic data are in good agreement with the literature.[305]

***Tert*-butyl (*R*)-3-((2-nitrophenyl)amino)butanoate 93**

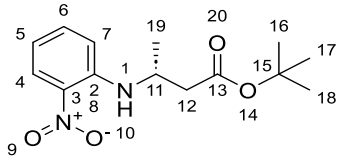

Tert-butyl (*R*)-3-aminobutanoate (380 mg, 2.39 mmol, 2.0 eq.), 1-fluoro-2-nitrobenzene (126 µL, 1.19 mmol, 1.0 eq.), DIPEA (831 µL, 4.77 mmol, 4.0 eq.) and DMF (3 mL) were combined in a dry microwave vial. The vial was sealed then the reaction mixture was stirred under argon at 75 °C for 22 h. The reaction mixture was cooled to rt, quenched with sat. $NaHCO_{3\ (aq)}$ then extracted with ethyl acetate (3 × 50 mL). The combined organic layers were washed with 10% w/v LiCl aq. (50 mL), then dried over $Na_2SO_{4\ (s)}$, filtered, then the filtrate was concentrated *in vacuo*. The residue was purified by flash column chromatography eluting with petroleum ether : ethyl acetate (1:0 to 86:14) to yield *tert*-butyl (*R*)-3-((2-nitrophenyl)amino)butanoate **93** (132 mg, 40%) as a dark yellow oil: R_f 0.14 (petroleum ether : ethyl acetate, 20:1); $[\alpha]_D^{25}$= -165.7 (*c* 1.0, $CHCl_3$); ν_{max} (thin film)/ cm^{-1} 3361 (N-H, m), 1723 (C=O, s), 1615 (N-H, m), 1504 (N-O, s), 1301 (N-O, s), 1163 (C-O, s); ^{1}H NMR (400 MHz, $CDCl_3$) δ 8.16 (1H, dd, *J* 8.6, 1.6, C^4-H), 8.12 (1H, d, *J* 8.1, N^1-H), 7.43 (1H, dddd, *J* 8.7, 7.0, 1.7, 0.7, C^6-H), 6.91 (1H, dt, *J* 8.5, 0.9, C^7-H), 6.63 (1H, ddd, *J* 8.4, 6.9, 1.2, C^5-H), 4.19-4.06 (1H, m, C^{11}-H), 2.61 (1H, dd, *J* 14.9, 5.8, C^{12}-H), 2.45 (1H, dd, *J* 14.9, 7.0, C^{12}-H'), 1.44 (9H, s, C^{16}-H, C^{17}-H, C^{18}-H), 1.37 (3H, d, *J* 6.5, C^{19}-H_3); ^{13}C NMR (101 MHz, $CDCl_3$) δ 170.4 (C^{13}), 144.4 (C^2), 136.39 (C^6), 132.2 (C^3), 127.2 (C^4), 115.5 (C^5), 114.1 (C^7), 81.5 (C^{15}), 45.7 (C^{11}), 42.7 (C^{12}), 28.2 (C^{16}, C^{17}, C^{18}), 20.7 (C^{19}); HRMS *m/z* (ESI^+) [Found: 281.1487, $C_{14}H_{20}N_2O_4$ requires $[M+H]^+$ 281.1496)]; LRMS *m/z* (ESI^+) 303 ($[M+Na]^+$); Analytical HPLC (RP, *Method 2*) rt 11.2 min, purity 100%.

(4*R*)-4-Methyl-1,3,4,5-tetrahydro-2*H*-1,5-benzodiazepin-2-one 25

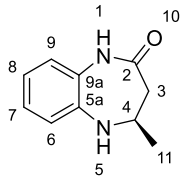

To a solution of *tert*-butyl (3S)-3-(2-nitroanilino)butanoate **93** (125 mg, 0.446 mmol, 1.0 eq.) in CH_2Cl_2 (1 mL) was added TFA (1 mL). The reaction mixture was stirred at rt for 45 min. The reaction mixture was concentrated *in vacuo* then the residue re-dissolved in acetic acid (2 mL). Iron powder (125 mg, 2.23 mmol, 5.0 eq.) was added then the reaction mixture heated under reflux for 3 h. Potassium carbonate (1 M aq. sol, 15 mL) was added then the resulting mixture was extracted with ethyl acetate (3 × 15 mL). The combined organic layers were washed with brine (15 mL), dried over $MgSO_{4\ (s)}$, filtered, then the filtrate was concentrated *in vacuo.* The residue was purified by flash column chromatography eluting with petroleum ether : ethyl acetate (78:22 to 0:1) to yield (4*R*)-4-methyl-1,3,4,5-tetrahydro-2*H*-1,5-benzodiazepin-2-one **25** (18 mg, 22%) as a beige solid: R_f 0.21 (petroleum ether : ethyl acetate, 1:9); $[\alpha]_D^{25}$= +1.44 (*c* 1.0, $CHCl_3$); m.p. 176-177 °C ($CHCl_3$); ^{1}H NMR (400 MHz, $CDCl_3$) δ 7.82 (1H, s, N-H^1), 7.04-6.95 (1H, m, C^8-H), 6.92-6.84 (2H, m, C^6-H, C^7-H), 6.78 (1H, d, *J* 7.3, C^9-H), 4.03 (1H, dqd, *J* 7.8, 6.4, 4.1, C^4-H), 3.50 (1H, br s, N-H^5), 2.64 (1H, dd, *J* 13.6, 4.1, C^3-H'), 2.44 (1H, dd, *J* 13.6, 7.8, C^3-H''), 1.33 (3H, d, *J* 6.4, C^{11}-H$_3$); LRMS *m/z* (ESI$^+$) 177 ([M+H]$^+$); Analytical HPLC (RP, *Method 2*) rt 5.6 min, purity 100%. The spectroscopic data are in good agreement with the literature.[302]

2-Amino-*N*-methylbenzamide 95

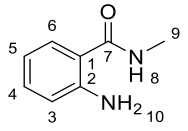

Isatonic anhydride (600 mg, 3.68 mmol, 1.0 eq.), methylamine hydrochloride (1.24 g, 18.4 mmol, 5.0 eq.) and Et_3N (2.56 mL, 6.13 mmol, 5.0 eq.) were combined in anhydrous DMF (10 mL) then stirred in an oil bath at 70 °C for 5 h. The reaction mixture was left to stir, cooling to rt, overnight. The reaction mixture was poured into water (30 mL) then extracted with ethyl acetate (3 × 30 mL). The aqueous layer was adjusted to pH 10 with the addition of 2 M NaOH $_{(aq)}$. The organic layers were washed with 10% w/v LiCl $_{(aq)}$

(3 × 30 mL), dried over $Na_2SO_{4\,(s)}$, filtered, then the filtrate was concentrated *in vacuo*. The residue was purified by flash column chromatography eluting with petroleum ether : ethyl acetate (1:1) to yield 2-amino-*N*-methylbenzamide **95** (363 mg, 66%) as an orange solid: R_f 0.20 (petroleum ether : ethyl acetate, 1:1); m.p. 71-73°C ($CDCl_3$) [lit.[306] 66-67 °C, lit.[307] 75-76 °C (ethyl acetate), lit.[308] 79-80 °C (Et_2O)]; ^{1}H NMR (400 MHz, $CDCl_3$) δ 7.29 (1H, dd, *J* 8.0, 1.5, C^6-H), 7.19 (1H, ddd, *J* 8.2, 7.2, 1.5, C^4-H), 6.67 (1H, dd, *J* 8.2, 1.2, C^3-H), 6.63 (1H, ddd, *J* 8.0, 7.2, 1.2, C^5-H), 6.08 (1H, *br* s, N-H), 5.50 (2H, *br* s, N-H_2), 2.96 (3H, d, *J* 4.9, C^9-H_3); LRMS *m/z* (ESI$^+$) 173 ([M+Na]$^+$, 100%). The spectroscopic data are in good agreement with the literature.[306]

2-[(Methylamino)methyl]aniline 96

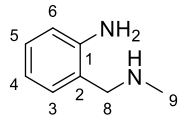

2-Amino-*N*-methylbenzamide **95** (350 mg, 2.33 mmol, 1.0 eq.) was dissolved in toluene (5 mL). Red-Al® (60 wt % in toluene, 5 mL, 15.4 mmol, 6.6 eq.) was added dropwise over a period of 5 min then the reaction mixture refluxed for 1.3 h. The reaction mixture was cooled to rt then added dropwise to 60 mL of a stirred solution of 1 M NaOH at 0 °C. The organic layer was separated, then the aqueous layer extracted with toluene (2 × 30 mL). The combined organic layers were dried over $MgSO_{4\,(s)}$, filtered, then concentrated *in vacuo*. The residue was purified by flash column chromatography eluting in acetone : toluene (1:1) with 1% Et_3N to yield 2-[(methylamino)methyl]aniline **96** (297 mg, 94%) as a light yellow oil: R_f 0.16 (1% Et_3N in acetone : toluene, 1:1); ^{1}H NMR (400 MHz, $CDCl_3$) δ 7.02 (1H, td, *J* 7.9, 7.4, 1.0, C^5-H), 6.94 (1H, dd, *J* 7.5, 1.0, C^3-H), 6.68 (1H, td, *J* 7.5, 7.4, 1.1, C^4-H), 6.52 (1H, dd, *J* 7.9, 1.1, C^6-H), 3.89 (2H, s, C^8-H_2), 3.83 (1H, *br* s, N-H), 2.35 (3H, s, C^9-H_3); LRMS *m/z* (ESI$^+$) 137 ([M+H]$^+$). The spectroscopic data are in good agreement with the literature.[309-311]

3-Methyl-3,4-dihydroquinazolin-2(1*H*)-one 26

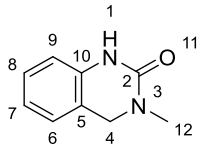

2-[(Methylamino)methyl]aniline **96** (280 mg, 2.06 mmol, 1.0 eq.) and *N,N'*-carbonyldiimidazole (433 mg, 2.67 mmol, 1.3 eq.) were dissolved in anhydrous THF (10 mL) and refluxed for 2 h. The reaction mixture was poured into water (10 mL) then extracted with ethyl acetate (3 × 20 mL). Organic layers were dried over $MgSO_{4\,(s)}$, filtered, then the filtrate was concentrated *in vacuo*. The crude product was purified by flash column chromatography eluting with petroleum ether : ethyl acetate (1:0 to 0:1) to yield 3-methyl-3,4-dihydroquinazolin-2(1*H*)-one **26** (181 mg, 54%) as an off-white solid: R_f 0.20 (petroleum ether : ethyl acetate, 2:3); m.p. 190-193°C ($CDCl_3$) [lit.[312] 198-202 °C]; ^{1}H NMR (400 MHz, $CDCl_3$) δ 7.24 (1H, *br* s, N^1-H), 7.20-7.12 (1H, m, C^8-H), 7.03 (1H, ddt, *J* 7.5, 1.6, 0.8, 0.8, C^6-H), 6.93 (1H, td, *J* 7.5, 7.5, 1.0, C^7-H), 6.68 (1H, dd, *J* 7.9, 0.8, C^9-H), 4.45 (2H, s, C^4-H_2), 3.04 (3H, s, C^{12}-H_3); LRMS *m/z* (ESI^+) 163 ($[M+H]^+$, 100%); Analytical HPLC (RP, *Method 2*) rt 6.7 min, purity 100%. The spectroscopic data are in good agreement with the literature.[311, 313]

6-Bromo-3-methyl-3,4-dihydroquinazolin-2(1*H*)-one 97

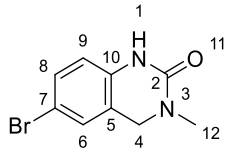

To a degassed solution of **26** (170 mg, 1.05 mmol, 1.0 eq.) in anhydrous CH_2Cl_2 (3 mL), was added *N*-bromosuccinimide (224 mg, 1.26 mmol, 1.2 eq.). The reaction mixture was stirred at rt for 2.5 h. The yellow solid was removed by filtration. The filtrate was washed with water (2 × 5 mL) then dried over $Na_2SO_{4\,(s)}$, filtered, then concentrated *in vacuo* to yield 6-bromo-3-methyl-3,4-dihydroquinazolin-2(1*H*)-one **97** (165 mg, 65%) as an off-white solid: R_f 0.20 (petroleum ether : ethyl acetate, 1:4); m.p. 197-199 °C ($CDCl_3$) [lit.[140] 195-197 °C (EtOH)]; ^{1}H NMR (400 MHz, $CDCl_3$) δ 7.53 (1H, *br* s, N^1-H), 7.30-7.23 (1H, m, C^8-H), 7.16 (1H, dt, *J* 2.1, 0.9, 0.9, C^6-H), 6.59 (1H, d, *J* 8.4, C^9-H), 4.41 (2H, s, C^4-H_2), 3.03 (3H, s, C^{12}-H_3); LRMS *m/z* (ESI^+) 241 [M(^{79}Br) +H]$^+$, 100%). The spectroscopic data are in good agreement with the literature.[140, 314]

6-(3,5-Dimethyl-1,2-oxazol-4-yl)-3-methyl-3,4-dihydroquinazolin-2(1*H*)-one 15

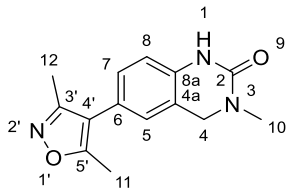

To a dry 2-5 mL microwave vial were added 6-bromo-3-methyl-3,4-dihydroquinazolin-2(1*H*)-one **97** (50.0 mg, 0.207 mmol, 1.0 eq.), potassium (3,5-dimethylisoxazol-4-yl)trifluoroborate **53** (50.5 mg, 0.249 mmol, 1.2 eq.), palladium diacetate (4.70 mg, 0.021 mmol, 0.1 eq.), RuPhos (29.0 mg, 0.062 mmol, 0.3 eq.) and anhydrous Na_2CO_3 (44.0 mg, 0.414 mmol, 2.0 eq.). The vial was sealed and purged with argon. De-gassed ethanol (1.5 mL) was added then the reaction mixture was heated in a microwave at 110 °C for 3 h. The reaction mixture was filtered through Celite® eluting with CH_2Cl_2 then the eluate concentrated *in vacuo*. The residue was purified by flash column chromatography eluting with petroleum ether : ethyl acetate (1:0 to 0:1) to yield 6-(3,5-dimethyl-1,2-oxazol-4-yl)-3-methyl-3,4-dihydroquinazolin-2(1*H*)-one **15** (13 mg, 25%) as a light yellow solid: R_f 0.15 (petroleum ether : ethyl acetate, 1:1); m.p. 220-222 °C ($CDCl_3$) [lit. [140] 224-226 °C (MeOH)]; ^{1}H NMR (400 MHz, $CDCl_3$) δ 7.85 (1H, *br* s, N-H), 6.98 (1H, dd, *J* 8.1, 1.8, C^8-H), 6.84 (1H, d, *J* 1.8, C^5-H), 6.73 (1H, d, *J* 8.1, C^7-H), 4.43 (2H, s, C^4-H_2), 3.00 (3H, s, C^{10}-H_3), 2.31 (3H, s, C^{11}-H_3), 2.17 (3H, s, C^{12}-H_3); LRMS *m/z* (ESI^+) 258 ($[M+H]^+$, 100%); Analytical HPLC (RP, *Method 4*) rt 7.3 min, purity 100%. The spectroscopic data are in good agreement with the literature.[140]

3-Chloro-*N*-phenylpropanamide 99

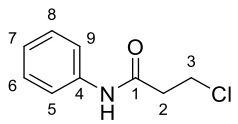

Aniline (500 mg, 5.36 mmol, 1.0 eq.) was slowly added to a solution of trimethylamine (681 µL, 4.88 mmol, 0.9 eq.) in anhydrous CH_2Cl_2 (3 mL) at 0 °C. A solution of 3-chloropropionyl chloride (804 mg, 6.32 mmol, 1.2 eq.) in anhydrous CH_2Cl_2 (4 mL) was cooled to 0 °C then slowly added to the aniline solution. The reaction mixture was stirred at 0 °C for 1 h. The reaction mixture was quenched with 2M $HCl_{(aq)}$ then extracted with CH_2Cl_2. The organic layer was dried over $MgSO_{4\,(s)}$, filtered, then the filtrate was

concentrated *in vacuo* to yield 3-chloro-*N*-phenylpropanamide **99** (866 mg, 88 %) as a light pink solid: R_f 0.57 (petroleum ether : ethyl acetate, 1:1); m.p. 112-115 °C ($CDCl_3$) [lit.[315] 115-117 °C, lit.[316] 119-121°C, lit.[294] 118-120°C]; ^{1}H NMR (400 MHz, $CDCl_3$) δ 7.64 (1H, *br* s, N-H), 7.52 (2H, dd, *J* 8.0, 1.2, C^5-H, C^9-H), 7.37-7.28 (2H, m, C^6-H, C^8-H), 7.41 (1H, dt, *J* 8.0, 1.3, 1.2, C^7-H), 3.87 (2H, t, *J* 6.4, C^3-H_2), 2.80 (2H, t, *J* 6.4, C^2-H_2); LRMS *m/z* (ESI^+) 184 ($[M+H]^+$, 100%). The spectroscopic data are in good agreement with the literature.[316, 317]

3,4-Dihydroquinolin-2(1*H*)-one 100

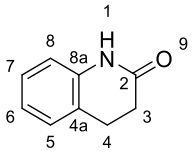

3-Chloro-*N*-phenylpropanamide **99** (600 mg, 3.27 mmol, 1.0 eq.) and $AlCl_3$ (1.31 g, 9.80 mmol, 3.0 eq.) were combined in an anhydrous 2-5 mL microwave reaction vial. The vial was sealed then the reaction mixture was heated to 150 °C for 1 h. Crushed ice was added to the reaction mixture then the formed solid was filtered, then the filter cake washed with water. The solid was dried *in vacuo* then purified by flash column chromatography eluting with petroleum ether : ethyl acetate (1:0 to 0:1) to yield 3,4-dihydroquinolin-2(1*H*)-one **100** (307 mg, 64%) as an off-white solid: R_f 0.15 (petroleum ether : ethyl acetate, 7:3); m.p. 155-156 °C ($CDCl_3$) [lit.[318] 154-155 °C, lit.[319] 162-164 °C, lit.[320] 159-161 °C]; ^{1}H NMR (400 MHz, $CDCl_3$) δ 9.12 (1H, *br* s, N-H), 7.22-7.12 (2H, m, C^7-H, C^5-H), 6.98 (1H, td, *J* 7.5, 7.5, 1.0, C^6-H), 6.84 (1H, dd, *J* 7.5, 1.0, C^8-H), 2.97 (2H, dd, *J* 8.6, 6.6, C^4-H_a, C^4-H_a), 2.65 (2H, m, C^3-H_a, C^3-H_b); LRMS *m/z* (ESI^+) 148 ($[M+H]^+$, 100%). The spectroscopic data are in good agreement with the literature.[321-323]

1-Ethyl-3,4-dihydroquinolin-2(1*H*)-one 27

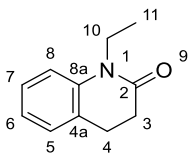

3,4-Dihydroquinolin-2(1*H*)-one **100** (200 mg, 1.36 mmol, 1.0 eq.) and ethyl iodide (530 µL, 6.52 mmol, 4.8 eq.) were combined in anhydrous DMF (2 mL). The reaction

mixture was cooled to 0 °C then sodium hydride (50% in mineral oil, 71.7 mg, 1.49 mmol, 1.1 eq.) was added portion-wise. The reaction mixture was stirred at 0 °C for 2 h. The reaction was quenched with the addition of glacial acetic acid then partitioned between ethyl acetate and water. The reaction mixture was extracted with ethyl acetate (3 × 10 mL). The combined organic layers were washed with 10% w/v $LiCl_{(aq)}$ (3 × 30 mL), dried over $Na_2SO_{4\,(s)}$, filtered, then concentrated *in vacuo.* The residue was purified by flash column chromatography eluting with petroleum ether : ethyl acetate (1:0 to 0:1) to yield 1-ethyl-3,4-dihydroquinolin-2(1*H*)-one **27** (209 mg, 88%) as a colourless oil: R_f 0.46 (petroleum ether : ethyl acetate, 1:1); ^{1}H NMR (400 MHz, $CDCl_3$) δ 7.24 (1H, m, C^6-H), 7.16 (1H, dd, *J* 7.3, 1.3, C^5-H), 7.05-6.96 (2H, m, C^7-H, C^8-H), 3.99 (2H, q, *J* 7.1, C^{10}-H_2), 2.88 (2H, dd, *J* 8.7, 6.1, C^4-H_a, C^4-H_a), 2.71-2.57 (2H, m, C^3-H_a, C^3-H_b), 1.26 (3H, t, *J* 7.1, C^{11}-H_3); LRMS *m/z* (ESI$^+$) 176 ([M+Na]$^+$, 100%). Analytical HPLC (RP, *Method 3*) rt 8.4 min, purity 100%. The spectroscopic data are in good agreement with the literature.[318, 324]

1,3-Dihydro-2*H*-benzimidazol-2-one 86

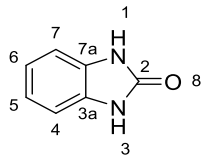

1,2-Diaminobenzene (108 mg, 1.00 mmol, 1.0 eq.) was dissolved in anhydrous DMF (2 mL) then *N,N'*-carbonyldiimidazole (178 mg, 1.10 mmol, 1.1 eq.) in anhydrous DMF (0.5 mL) was added dropwise over a period of 5 min. The reaction mixture was stirred for rt for 24 h. The solvent was removed *in vacuo* then the resulting colourless solid was washed with water (4 × 5 mL). The crude product was triturated with ethyl acetate, then the filtered solid was dried under high vacuum to yield 1,3-dihydro-2*H*-benzimidazol-2-one **86** (31 mg, 23%) as a colourless solid: R_f 0.26 (ethyl acetate); m.p. >300 °C (ethyl acetate) [lit.[325] 305-308 °C, lit.[326] 318-320 °C (EtOH), lit.[327] 320-322 °C]; ^{1}H NMR (400 MHz, DMSO-d_6) δ 10.56 (2H, s, N-H^1, N-H^3), 6.91 (4H, s, C^4-H, C^5-H, C^6-H, C^7-H); LRMS *m/z* (ESI$^+$) 135 ([M+H]$^+$, 100%). The spectroscopic data are in good agreement with the literature.[328]

1,3-Dimethyl-1,3-dihydro-2*H*-benzimidazol-2-one 28

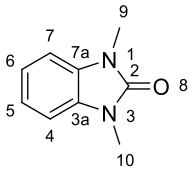

1,3-Dihydro-2*H*-benzimidazol-2-one **86** (25.0 mg, 0.186 mmol, 1.0 eq.), iodomethane (69.6 μL, 1.12 mmol, 6.0 eq.) and K_2CO_3 (155 mg, 1.12 mmol, 6.0 eq.) were combined in anhydrous DMF (0.5 mL) then the reaction mixture was stirred at rt for 23 h. The reaction mixture was partitioned between water (10 mL) and ethyl acetate (10 mL) then the aqueous layer was extracted with ethyl acetate (3 × 10 mL). The combined organic layers were washed with 10% w/v LiCl aq. (2 × 10 mL), dried over anhydrous $MgSO_{4\,(s)}$, filtered, then the filtrate was concentrated *in vacuo* to give 1,3-dimethyl-1,3-dihydro-2*H*-benzimidazol-2-one **28** (30 mg, 98%) as a yellow solid: R_f 0.36 (ethyl acetate); m.p. 98-100 °C ($CDCl_3$) [lit.[329] 104-106 °C, lit.[330] 107-108 °C, lit.[331] 112-113 °C]; ^{1}H NMR (400 MHz, $CDCl_3$) δ 7.04 (2H, dd, *J* 5.7, 3.2, C^6-H, C^5-H), 6.91 (2H, dd, *J* 5.7, 3.2, C^7-H, C^4-H), 3.36 (6H, s, *J* 8.0, 1.7, C^9-H_3, C^{10}-H_3); LRMS *m/z* (ESI^+) 163 ($[M+H]^+$, 100%); Analytical HPLC (RP, *Method 4*) rt 7.5 min, purity 98%. The spectroscopic data are in good agreement with the literature.[331]

***N*-Methyl-2-nitroaniline 88**

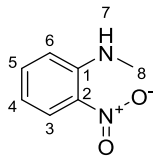

2-Fluoronitrobenzene (1.49 mL, 14.0 mmol, 1.0 eq.) and methylamine hydrochloride (1.91 g, 28.0 mmol, 2.0 eq.) were dissolved in NMP (20 mL). DIPEA (12.3 mL, 71.0 mmol, 5.0 eq.) was added then the reaction mixture was stirred at 85 °C for 5 h. Water (70 mL) was added then the mixture was extracted with ethyl acetate (2 × 200 mL). The combined organic layers were washed with 10% w/v LiCl aq. (2 × 10 mL), dried over anhydrous $MgSO_{4\,(s)}$, filtered, then the filtrate was concentrated *in vacuo.* The residue was purified using flash column chromatography eluting with petroleum ether : ethyl acetate (1:0 to 9:1) to yield *N*-methyl-2-nitroaniline **88** (2.1 g, 99%) as an orange solid: R_f 0.24 (petroleum ether : CH_2Cl_2, 4:1); m.p. 37-39 °C (ethyl acetate) [lit.[332] 34-35 °C (MeCN)]; ^{1}H NMR (400 MHz, $CDCl_3$) δ 8.17 (1H, dd, *J* 8.5, 1.6, C^3-H),

8.04 (1H, s, N-H), 7.46 (1H, dddd, *J* 8.5, 6.9, 1.6, 0.7, C^5-H), 6.84 (1H, dd, *J* 8.5, 1.2, C^6-H), 6.65 (1H, ddd, *J* 8.5, 6.9, 1.2, C^4-H), 3.03 (3H, d, *J* 5.1, C^8-H_3); LRMS *m/z* (ESI^+) 153 ($[M+H]^+$, 100%). The spectroscopic data are in good agreement with the literature.[290]

1-Methyl-1,3-dihydro-2*H*-benzimidazol-2-one 90

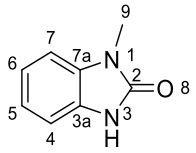

To a solution of *N*-Methyl-2-nitroaniline **88** (1.90 g, 12.3 mmol, 1.0 eq.) in ethanol (25 mL) was added 10 wt. % palladium on carbon (66.4 mg, 0.624 mmol, 0.05 eq.) then the reaction mixture was stirred at rt under $H_{2\ (g)}$ for 48 h. The reaction mixture was filtered through Celite® eluting with ethyl acetate then the filtrate was evaporated *in vacuo* to give *N*-methylbenzene-1,2-diamine (1.90 g) as a brown oil. The intermediate was dissolved in anhydrous THF (40 mL) then CDI (2.02 g, 12.3 mmol, 1.0 eq.) was added. The reaction mixture refluxed for 24 h. The reaction mixture was cooled to rt, then poured into water (60 mL) then extracted with ethyl acetate (3 × 100 mL). The combined organic layers were dried over anhydrous $Na_2SO_{4\ (s)}$, filtered, then the filtrate was concentrated *in vacuo.* The residue was purified using flash column chromatography eluting with petroleum ether : ethyl acetate (88:12 to 0:1) to yield 1-methyl-1,3-dihydro-2*H*-benzimidazol-2-one **90** (1.36 g, 74%) as a brown foam: R_f 0.30 (petroleum ether : ethyl acetate, 1:2); m.p. 182-183 °C (ethyl acetate) [lit.[333] 187-190 °C (EtOH)]; ^{1}H NMR (400 MHz, $CDCl_3$) δ 10.45 (1H, s, N^3-H), 7.16-7.04 (1H, m, C^4-H, C^5-H, C^7-H), 7.00-6.95 (1H, m, C^6-H), 3.43 (1H, s, C^9-H_3); LRMS *m/z* (ESI^+) 149 ($[M+H]^+$, 100%). The spectroscopic data are in good agreement with the literature.[334]

1-Acetyl-3-methyl-1,3-dihydro-2*H*-benzimidazol-2-one 29

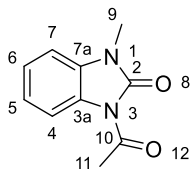

1-Methyl-1,3-dihydro-2*H*-benzimidazol-2-one **90** (50.0 mg, 0.337 mmol, 1.0 eq.) and 4-DMAP (8.25 mg, 0.068 mmol, 0.2 eq.) were dissolved in anhydrous THF (1 mL). Et_3N

(56.0 μL, 0.402 mmol, 1.2 eq.) and acetic anhydride (35.0 μL, 0.371 mmol, 1.1 eq.) were added then the reaction mixture was stirred at rt for 1 h. The reaction mixture was concentrated *in vacuo* then the residue re-dissolved in CH_2Cl_2 (5 mL), washed with water (5 mL), then 1 M aq. HCl (5 mL), then water (5 mL), then sat. aq. $NHCO_3$ (5 mL). The organic layer was dried over anhydrous $MgSO_{4\,(s)}$, filtered, then the filtrate was concentrated *in vacuo* to yield 1-acetyl-3-methyl-1,3-dihydro-2*H*-benzimidazol-2-one **29** (56 mg, 87%) as a colourless solid: R_f 0.70 (CH_2Cl_2 : MeOH, 10:1); m.p. 105-106 °C (MeOH) [lit.[335] 121-122 °C (EtOH, H_2O)]; ^{1}H NMR (400 MHz, $CDCl_3$) δ 8.21 (1H, ddd, *J* 8.0, 1.2, 0.6, C^4-H), 7.25 (1H, dd, *J* 7.7, 1.2, C^6-H), 7.18 (1H, ddd, *J* 8.0, 1.3, C^5-H), 6.99 (1H, ddd, *J* 7.7, 1.3, 0.6, C^7-H), 3.42 (3H, s, C^9-H_3), 2.78 (3H, s, C^{11}-H_3); HRMS *m/z* (ESI+) [Found: 213.0258, $C_{10}H_{10}N_2O_2$ requires $[M+Na]^+$ 213.0635)]; LRMS *m/z* (ESI^+) 213 ($[M+Na]^+$, 100%). Analytical HPLC (RP, *Method 2*) rt 8.2 min, purity 100%. The spectroscopic data are in good agreement with the literature.[336]

***Tert*-butyl 3-methyl-2-oxo-2,3-dihydro-1*H*-benzimidazole-1-carboxylate 30**

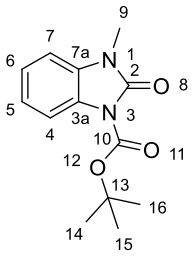

1-Methyl-1,3-dihydro-2*H*-benzimidazol-2-one **90** (50.0 mg, 0.34 mmol, 1.0 eq.) and 4-DMAP (2.0 mg, 16.0 μmol, 0.05 eq.) were dissolved in THF (1 mL). Et_3N (50 μL, 0.36 mmol, 1.1 eq.) was added then the reaction mixture was cooled to 0 °C. Di-*tert*-butyl dicarbonate (90 μL, 0.36 mmol, 1.1 eq.) was added then the reaction mixture was stirred at rt for 1 h. The reaction mixture was concentrated *in vacuo* then the residue re-dissolved in CH_2Cl_2 (5 mL). Water (2 mL) was added then the mixture was extracted with CH_2Cl_2 (2 × 5 mL). The combined organic layers were washed with 1 M aq. HCl (5 mL) then water (5 mL), dried over anhydrous $MgSO_{4\,(s)}$, filtered, then the filtrate was concentrated *in vacuo.* The residue was purified using flash column chromatography eluting with petroleum ether : ethyl acetate (1:0 to 0:1) to yield *tert*-butyl 3-methyl-2-oxo-2,3-dihydro-1*H*-benzimidazole-1-carboxylate **30** (78 mg, 94%) as a light yellow oil: R_f 0.63 (MeOH: CH_2Cl_2, 1:10); ^{1}H NMR (400 MHz, $CDCl_3$) δ 7.85-7.79 (1H, m, C^4-H), 7.20 (1H, ddd,

J 7.7, 1.2, C^6-H), 7.12 (1H, ddd, *J* 7.7, 1.3, C^5-H), 6.98-6.92 (1H, m, C^7-H), 3.38 (3H, s, C^9-H_3), 1.67 (9H, s, C^{14}-H_3, C^{15}-H_3, C^{16}-H_3); LRMS *m/z* (ESI^+) 271 ($[M+Na]^+$, 100%); HRMS *m/z* (ESI^+) [Found: 249.1487, $C_{13}H_{16}N_2O_3$ requires $[M+H]^+$ 249.1234)]; Analytical HPLC (RP, *Method 1*) rt 10.0 min, purity 98%. The spectroscopic data are in good agreement with the literature.[290]

Ethyl 3-methyl-4-oxo-4,5,6,7-tetrahydro-2*H*-isoindole-1-carboxylate 31

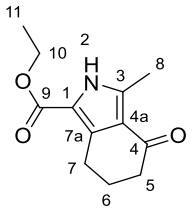

To a solution of 2-acetylcyclohexane-1,3-dione (500 mg, 3.24 mmol, 1.0 eq.) in glacial acetic acid (2.5 mL) under $N_{2\,(g)}$ was added anhydrous sodium acetate (1.06 g, 13.0 mmol, 4.0 eq.). A solution of diethyl-2-aminomalonate hydrochloride (1.37 g, 6.49 mmol, 2.0 eq.) in glacial acetic acid (2.5 mL) was slowly added. The reaction mixture was heated to 100 °C then stirred for 17 h. The reaction mixture was cooled to rt then poured into ice water (20 mL). The reaction mixture was extracted with ethyl acetate (3 × 30 mL). The combined organic layers were washed with 1 M NaOH $_{(aq)}$, then brine, dried over $Na_2SO_{4\,(s)}$, filtered, then the filtrate was concentrated *in vacuo.* The residue was purified by flash column chromatography eluting with petroleum ether : ethyl acetate (1:0 to 0:1) to yield ethyl 3-methyl-4-oxo-4,5,6,7-tetrahydro-2*H*-isoindole-1-carboxylate **31** (460 mg, 58%) as a cream solid: R_f 0.54 (petroleum ether : ethyl acetate, 1:1); m.p. 143-145 °C ($CDCl_3$) [lit.[196] 160-162 °C]; ^{1}H NMR (400 MHz, $CDCl_3$) δ 9.75 (1H, *br* s, N-H), 4.33 (2H, q, *J* 7.1, C^{10}-H_2), 2.95 (2H, t, *J* 6.2, C^5-H_2), 2.58 (3H, s, C^8-H_3), 2.50-2.42 (2H, m, C^7-H_2), 2.11-2.01 (2H, m, C^6-H_2), 1.73 (3H, t, *J* 7.1, C^{11}-H_3); LRMS *m/z* (ES^+) 222 ($[M+H]^+$, 100%); Analytical HPLC (RP, *Method 2*) rt 1.7 min, purity 100%. The spectroscopic data are in good agreement with the literature.[337]

_N_-(4-Hydroxyphenyl)acetamide 32

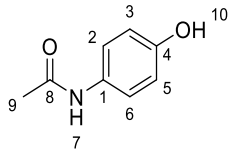

4'-Hydroxyacetophenone (500 mg, 3.67 mmol, 1.0 eq.) and hydroxylamine hydrochloride (766 mg, 11.0 mmol, 3.0 eq.) were combined in acetonitrile (36 mL). The reaction mixture was refluxed at 70 °C for 1 h. The temperature was increased to 95 °C then the reaction was stirred for a further 2 h. The reaction mixture was cooled to rt then the solvent was evaporated *in vacuo.* The residue was purified by flash column chromatography eluting with petroleum ether : ethyl acetate (22:3 to 0:1) to yield *N*- (4-hydroxyphenyl)acetamide **32** (275 mg, 50%) as a brown solid: R_f 0.12 (petroleum ether : ethyl acetate, 1:1); m.p. 167-168 °C ($CDCl_3$) [lit.[338] 169-170 °C, lit.[339] 168-170 °C]; ^{1}H NMR (400 MHz, DMSO-d_6) δ 9.63 (1H, s, N-H), 9.15 (1H, *br* s, C^4-OH), 7.41-7.26 (2H, m, C^2-H, C^6-H), 6.70-6.59 (2H, m, C^3-H, C^5-H), 1.97 (3H, s, C^9-H_3); HRMS *m/z* (ESI^+) [Found: 174.0527, $C_8H_9NO_2$ requires $[M+Na]^+$ 174.0526)]; LRMS *m/z* (ESI^+) 152 ($[M+H]^+$, 100%); Analytical HPLC (RP, *Method 2*) rt 4.5 min, purity 98%. The spectroscopic data are in good agreement with the literature.[340, 341]

6.2.2 Ligands for *Ld*BDF5.1

4-(4-Fluoro-3-nitrophenyl)-3,5-dimethylisoxazole 74

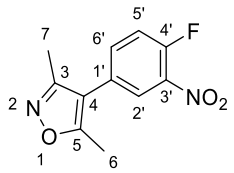

4-Bromo-1-fluoro-2-nitrobenzene (2.00 mL, 16.2 mmol, 1.0 eq.) and potassium (3,5-dimethylisoxazol-4-yl)(trifluoro)borate **53** (3.96 g, 19.4 mmol, 1.2 eq.) were combined in DME (30.0 mL). Sat. aq. $NaHCO_3$ (30.0 mL) was added then the reaction mixture was degassed with $N_{2\,(g)}$ for 20 min. $Pd(dppf)Cl_2.CH_2Cl_2$ (1.33 g, 1.62 mmol, 0.1 eq.) was added then the reaction mixture was stirred at 110 °C for 17 h. The reaction mixture was filtered through Celite® (eluting with ethyl acetate) then the filtrate was partitioned between water and ethyl acetate. The aqueous layer was extracted with ethyl acetate (3 × 120 mL). The combined organic layers were dried over $MgSO_{4\,(s)}$, filtered,

then the filtrate was concentrated *in vacuo*. The residue was purified by flash column chromatography eluting with petroleum ether : ethyl acetate (1:0 to 0:1) to yield 4- (4-fluoro-3-nitrophenyl)-3,5-dimethylisoxazole **74** (2.87 g, 76%) as a light brown solid: R_f 0.50 (petroleum ether : ethyl acetate, 7:3); m.p. 112-113 °C ($CDCl_3$) [lit.[69] 128-131 °C]; ^{1}H NMR (400 MHz, $CDCl_3$) δ 7.95 (1H, dd, *J* 6.9, 2.3, $C^{2'}$-H), 7.53 (1H, ddd, *J* 8.6, 4.2, 2.3, $C^{6'}$-H), 7.40 (1H, dd, *J* 10.4, 8.6, $C^{5'}$-H), 2.43 (3H, s, C^6-H_3), 2.28 (3H, s, C^7-H_3); ^{19}F NMR (376 MHz, $CDCl_3$) δ -118.6 (s, 1 F); LRMS *m/z* (ESI^+) 237 ($[M+H]^+$, 100%). The spectroscopic data are in good agreement with the literature.[69]

_N_-(2-Cyclopropylethyl)-4-(3,5-dimethylisoxazol-4-yl)-2-nitroaniline 187

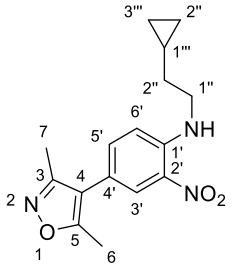

4-(4-fluoro-3-nitrophenyl)-3,5-dimethylisoxazole **74** (200 mg, 0.847 mmol, 1.0 eq.) was dissolved in anhydrous DMF (1.2 mL). 2-Cyclopropylethanamine hydrochloride (206 mg, 1.69 mmol, 2.0 eq.) and DIPEA (737 µL, 4.23 mmol, 5.0 eq.) were added. The reaction mixture was stirred at 60 °C for 3 h. The reaction mixture was cooled to rt and partitioned between ethyl acetate and water. The aqueous layer was extracted with ethyl acetate (3 × 10 mL). The combined organic layers were dried over $MgSO_{4\ (s)}$, filtered, then the filtrate was concentrated *in vacuo*. The residue was purified by flash column chromatography eluting with petroleum ether : ethyl acetate (1:0 to 4:1) to yield *N*- (2-cyclopropylethyl)-4-(3,5-dimethylisoxazol-4-yl)-2-nitroaniline **187** (181 mg, 71%) as an orange oil: R_f 0.52 (petroleum ether : ethyl acetate, 3:2); ν_{max} (thin film)/ cm^{-1} 3380 (N-H, m), 1626 (N-H, m), 1527 (N-O, s), 1357 (C-N, s), 1260 (C-N, s); ^{1}H NMR (400 MHz, $CDCl_3$) δ 8.26 (1H, br s, N-H), 8.08 (1H, d, *J* 2.1, $C^{3'}$-H), 7.33 (1H, ddd, *J* 8.9, 2.1, 0.7, $C^{6'}$-H), 6.96 (1H, d, *J* 8.9, $C^{5'}$-H), 3.45 (2H, dt, *J* 6.9, 5.1, $C^{1''}$-H_2), 2.40 (3H, s, C^6-H_3), 2.26 (3H, s, C^7-H_3), 1.67 (2H, q, *J* 6.9, $C^{2''}$-H_2), 0.89-0.72 (1H, m, $C^{1'''}$-H), 0.63-0.49 (2H, m, $C^{2'''}$-H_a, $C^{3'''}$-H_a), 0.27-0.12 (2H, m, $C^{2'''}$-H_b, $C^{3'''}$-H_b); ^{13}C NMR (101 MHz, $CDCl_3$) δ 165.5 (C^5), 158.3 (C^3), 145.0 ($C^{1'}$), 136.9 ($C^{5'}$), 127.2 ($C^{3'}$), 117.4 ($C^{2'}$), 115.4 ($C^{4'}$), 114.6 ($C^{6'}$), 100.4 (C^4), 43.5 ($C^{1'''}$), 34.0 ($C^{2'''}$), 11.7 (C^6),

10.9 (C^{7}), 8.9 ($C^{1'''}$), 4.5 ($C^{2'''}$, $C^{3'''}$); LRMS *m/z* (ESI^{+}) 302 ([M+H^{+}], 100%); HRMS *m/z* (ESI^{+}) [Found: 302.1500, $C_{16}H_{19}O_3N_3$ requires $[M+H]^{+}$ 302.1499)]; Analytical HPLC (RP, *Method 1*) rt 12.1 min, purity 96%.

4-(1-(2-Cyclopropylethyl)-2-ethyl-*1H*-benzo[*d*]imidazol-5-yl)-3,5-dimethylisoxazole 110

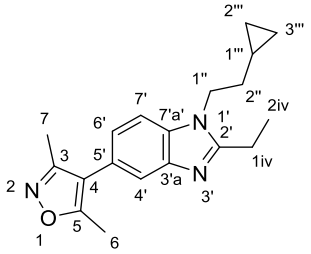

N-(2-Cyclopropylethyl)-4-(3,5-dimethylisoxazol-4-yl)-2-nitroaniline **187** (150 mg, 0.498 mmol, 1.0 eq.) was suspended in EtOH (2.6 mL) and 1 M $Na_2S_2O_4$ (2.6 mL, 2.59 mmol, 5.2 eq.) was added. The reaction mixture was stirred at 80 °C for 30 min. The reaction mixture was cooled to rt and partitioned between ethyl acetate (10 mL) and 10% aq. ammonia solution (5 mL). The phases were separated then the organic phase was evaporated *in vacuo*. The crude material was dissolved in ethyl acetate (7.5 mL). DIPEA (191 µL, 1.10 mmol, 2.2 eq.), propionic acid (37.2 µL, 0.498 mmol, 1.0 eq.) and 50 wt% T3P in ethyl acetate (1.5 mL, 2.59 mmol, 5.2 eq.) were added. The reaction mixture was stirred at 80 °C for 17 h. The reaction mixture was cooled to rt then partitioned between ethyl acetate and 1 M $NaOH_{(aq)}$. The organic layer was separated then the aqueous layer was extracted with ethyl acetate (3 × 10 mL). The combined organic layers were dried over $MgSO_{4\,(s)}$, filtered, then the filtrate was concentrated *in vacuo*. The residue was purified by flash column chromatography eluting with petroleum ether : ethyl acetate (1:0 to 3:7) to yield 4-(1-(2-cyclopropylethyl)-2-ethyl-*1H*-benzo[*d*]imidazol-5-yl)-3,5-dimethylisoxazole **110** (38 mg, 25%) as a yellow solid: R_f 0.21 (petroleum ether : ethyl acetate, 1:1); m.p. 60-61 °C ($CDCl_3$); ν_{max} (thin film)/ cm^{-1} 1620 (C=C, m), 1512 (N-O, m), 1426 (C-H, m), 1308 (C-N, m), 1244 (C-O, m); ^{1}H NMR (400 MHz, $CDCl_3$) δ 7.59 (1H, dd, *J* 1.6, 0.7, $C^{4'}$-H), 7.36 (1H, dd, *J* 8.2, 0.7, $C^{7'}$-H), 7.08 (1H, dd, *J* 8.2, 1.6, $C^{6'}$-H), 4.22 (2H, t, *J* 7.0, $C^{1''}$-H_2), 2.94 (2H, q, *J* 7.5, C^{1iv}-H_2), 2.40 (3H, s, C^{6}-H_3), 2.27 (3H, s, C^{7}-H_3), 1.72 (2H, q, *J* 7.0, $C^{2''}$-H_2), 1.49 (3H, t, *J* 7.5, C^{2iv}-H_3), 0.73-0.56 (1H, m, $C^{1'''}$-H), 0.55-0.39 (2H, m, $C^{2'''}$-H_a, $C^{3'''}$-H_a), 0.06 (2H, dt, *J* 5.8, 4.5, $C^{2'''}$-H_b, $C^{3'''}$-H_b); ^{13}C NMR

(101 MHz, $CDCl_3$) δ 165.1 ($C^{2'}$), 159.2 (C^5), 157.1 (C^3), 143.1 ($C^{3'a}$), 134.7 ($C^{7'a}$), 123.9 ($C^{5'}$), 123.3 ($C^{6'}$), 120.0 ($C^{4'}$), 117.3 (C^4), 109.6 ($C^{7'}$), 43.9 ($C^{1'''}$), 34.9 ($C^{2'''}$), 21.0 (C^{1iv}), 11.9 (C^{2iv}), 11.7 (C^6), 11.0 (C^7), 8.7 ($C^{1'''}$), 4.6 ($C^{2'''}$, $C^{3'''}$); LRMS *m/z* (ESI^+) 310 ($[M+H]^+$, 100%); HRMS *m/z* (ESI^+) [Found: 310.1911, $C_{19}H_{23}ON_3$ requires $[M+H]^+$ 310.1914)]; Analytical HPLC (RP, *Method 1*) rt 7.7 min, purity 98%.

4-(3,5-Dimethylisoxazol-4-yl)-2-nitro-*N*-(2-(pyridin-2-yl)ethyl)aniline 188

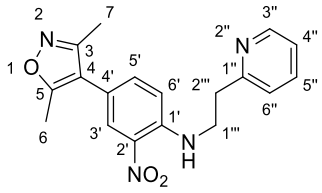

4-(4-Fluoro-3-nitrophenyl)-3,5-dimethylisoxazole **74** (200 mg, 0.847 mmol, 1.0 eq.) was dissolved in anhydrous DMF (1.2 mL). 2-(Pyridin-2-yl)ethan-1-amine (203 µL, 1.69 mmol, 2.0 eq.) and DIPEA (737 µL, 4.23 mmol, 5.0 eq.) were added. The reaction mixture was stirred at 60 °C for 3 h. The reaction mixture was cooled to rt and partitioned between ethyl acetate and water. The aqueous layer was extracted with ethyl acetate (3 × 10 mL). The combined organic layers were dried over $MgSO_{4\ (s)}$, filtered, then the filtrate was concentrated *in vacuo*. The residue was purified by flash column chromatography eluting with CH_2Cl_2 : methanol (1:0 to 90:10) to yield 4-(3,5-dimethylisoxazol-4-yl)-2-nitro-*N*-(2-(pyridin-2-yl)ethyl)aniline **188** (178 mg, 62%) as an orange solid: R_f 0.63 (ethyl acetate : petroleum ether, 7:3); m.p. 75-77 °C ($CDCl_3$); ν_{max} (thin film)/ cm^{-1} 3388 (N-H, m), 1617 (N-H, m), 1528 (N-O, s), 1395 (C-H, m), 1226 (C-N, s), 1149 (C=C, s); ^1H NMR (400 MHz, $CDCl_3$) δ 8.60 (1H, ddd, *J* 4.9, 1.9, 1.0, $C^{3"}$-H), 8.40 (1H, t, *J* 5.4, N-H), 8.04 (1H, d, *J* 2.2, $C^{3'}$-H), 7.63 (1H, td, *J* 7.7, 1.8, $C^{5"}$-H), 7.32 (1H, ddd, *J* 8.9, 2.2, 0.6, $C^{5'}$-H), 7.22 (1H, dt, *J* 7.7, 1.1, $C^{6"}$-H), 7.17 (1H, ddd, *J* 7.7, 4.9, 1.2, $C^{4"}$-H), 7.01 (1H, d, *J* 8.9, $C^{6'}$-H), 3.78 (2H, td, *J* 6.8, 5.3, $C^{1'''}$-H_2), 3.20 (2H, t, *J* 6.8, $C^{2'''}$-H_2), 2.38 (3H, s, C^6-H_3), 2.24 (3H, s, C^7-H_3); ^{13}C NMR (101 MHz, $CDCl_3$) δ 165.3 (C^5), 158.6 ($C^{1"}$), 158.3 (C^3), 149.7 ($C^{3"}$), 144.5 ($C^{1'}$), 136.8 ($C^{5'}$), 136.7 ($C^{5"}$), 131.9 ($C^{2'}$), 127.0 ($C^{3'}$), 123.4 ($C^{6"}$), 121.9 ($C^{4"}$), 117.4 ($C^{4'}$), 114.9 (C^4), 114.5 ($C^{6'}$), 42.7 ($C^{1'''}$), 37.1 ($C^{2'''}$), 11.6 (C^6), 10.7 (C^7); LRMS *m/z* (ESI^+) 339 ($[M+H^+]$, 100%); HRMS *m/z* (ESI^+) [Found: 339.1451, $C_{18}H_{18}N_4O_3$ requires $[M+H]^+$ 339.1452)]; Analytical HPLC (RP, *Method 1*) rt 6.9 min, purity 100%.

4-(2-Ethyl-1-(2-(pyridin-2-yl)ethyl)-*1H*-benzo[*d*]imidazol-5-yl)-3,5-dimethylisoxazole 108

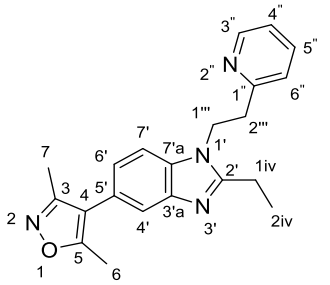

4-(3,5-Dimethylisoxazol-4-yl)-2-nitro-*N*-(2-(pyridin-2-yl)ethyl)aniline **188** (80.0 mg, 0.236 mmol, 1.0 eq.) was suspended in EtOH (1.23 mL) and 1 M $Na_2S_2O_4$ (1.23 mL, 1.23 mmol, 5.2 eq.) was added. The reaction mixture was stirred at 80 °C for 1 h. The reaction mixture was cooled to rt and partitioned between ethyl acetate (10 mL) and 10 % aq. ammonia solution (5 mL). The phases were separated then the organic phase was washed with water (5 mL) and brine (5 mL), dried over $MgSO_{4\,(s)}$, filtered, then the filtrate was concentrated *in vacuo*. The crude material was dissolved in ethyl acetate (4.0 mL). DIPEA (90.6 µL, 0.520 mmol, 2.2 eq.), propionic acid (17.7 µL, 0.236 mmol, 1.0 eq.) and 50 wt% T3P in ethyl acetate (1.37 mL, 0.615 mmol, 2.6 eq.) were added. The reaction mixture was stirred at 80 °C for 17 h. The reaction mixture was cooled to rt and partitioned between ethyl acetate and water. The organic layer was separated then the aqueous layer was extracted with ethyl acetate (3 × 10 mL). The combined organic layers were washed with brine, dried over $MgSO_{4(s)}$, filtered, then the filtrate was concentrated *in vacuo*. The residue was purified by preparative HPLC eluting with water : acetonitrile (95:5 to 5:95) to yield 4-(2-ethyl-1-(2-(pyridin-2-yl)ethyl)-1*H*-benzo[*d*]imidazol-5-yl)-3,5-dimethylisoxazole **108** (20 mg, 24%) as a colourless oil: R_f 0.16 (0.1% Et_3N in CH_2Cl_2 : methanol, 9:1); ν_{max} (thin film)/ cm^{-1} 1591 (C=C, m), 1468 (C-H, m), 1311 (C-N, s); ^{1}H NMR (400 MHz, $CDCl_3$) δ 8.62 (1H, ddd, *J* 4.9, 1.8, 0.9, $C^{3"}$-H), 7.60 (1H, dd, *J* 1.6, 0.7, $C^{4'}$-H), 7.52 (1H, td, *J* 7.6, 1.8, $C^{5"}$-H), 7.36 (1H, dd, *J* 8.3, 0.7, $C^{7'}$-H), 7.18 (1H, ddd, *J* 7.6, 4.9, 1.1, $C^{4"}$-H), 7.09 (1H, dd, *J* 8.2, 1.6, $C^{6'}$-H), 6.86 (1H, dt, *J* 7.7, 1.1, $C^{6"}$-H), 4.58 (2H, t, *J* 7.1, $C^{1'''}$-H_2), 3.27 (2H, t, *J* 7.1, $C^{2'''}$-H_2), 2.68 (2H, q, *J* 7.5, C^{1iv}-H_2), 2.40 (3H, s, C^6-H_3), 2.28 (3H, s, C^7-H_3), 1.37 (3H, t, *J* 7.5, C^{2iv}-H_3); ^{13}C NMR (101 MHz, $CDCl_3$) δ 165.1 (C^5), 159.2 (C^3), 157.5 ($C^{2'}$), 157.2 ($C^{1"}$), 149.9 ($C^{3"}$), 142.9 ($C^{3'a}$), 136.9 ($C^{5"}$), 134.3 ($C^{7'a}$), 124.2 ($C^{5'}$), 123.8 ($C^{6"}$), 123.5 ($C^{6'}$), 122.3 ($C^{4"}$), 119.9 ($C^{4'}$), 117.3 (C^4), 109.6 ($C^{7'}$), 43.5 ($C^{1'''}$), 38.1 ($C^{2'''}$), 20.6 (C^{1iv}), 11.8 (C^6), 11.7 (C^{2iv}), 11.0 (C^7); LRMS *m/z* (ESI^+) 347 ([M+H^+], 100%); HRMS *m/z* (ESI^+) [Found: 347.1867,

$C_{21}H_{22}N_4O$ requires $[M+H]^+$ 347.1866)]; Analytical HPLC (RP, *Method 1*) rt 5.7 min, purity 99%.

4-(3,5-Dimethylisoxazol-4-yl)-2-nitro-*N*-(2-(pyridin-3-yl)ethyl)aniline 189

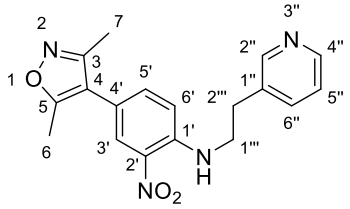

4-(4-Fluoro-3-nitrophenyl)-3,5-dimethylisoxazole **74** (200 mg, 0.847 mmol, 1.0 eq.) was dissolved in anhydrous DMF (1.2 mL). 2-(Pyridin-3-yl)ethan-1-amine (199 µL, 1.69 mmol, 2.0 eq.) and DIPEA (737 µL, 4.23 mmol, 5.0 eq.) were added. The reaction mixture was stirred at 60 °C for 3 h. The reaction mixture was cooled to rt and partitioned between ethyl acetate and water. The aqueous layer was extracted with ethyl acetate (3 × 10 mL). The combined organic layers were dried over $MgSO_{4\ (s)}$, filtered, then the filtrate was concentrated *in vacuo*. The residue was purified by flash column chromatography eluting with petroleum ether : ethyl acetate (1:0 to 0:1) to yield 4-(3,5-dimethylisoxazol-4-yl)-2-nitro-*N*-(2-(pyridin-3-yl)ethyl)aniline **189** (242 mg, 85%) as an orange oil: R_f 0.48 (petroleum ether : ethyl acetate, 7:3); ν_{max} (thin film)/ cm^{-1} 1624 (N-H, m), 1528 (N-O, s), 1231 (C-N, s), 1026 (C-N, m); ^{1}H NMR (400 MHz, $CDCl_3$) δ 8.56 (1H, s, $C^{2"}$-H), 8.55-8.49 (1H, d, *J* 4.3, $C^{4"}$-H), 8.14 (1H, t, *J* 5.1, N-H), 8.07 (1H, d, *J* 2.1, $C^{3'}$-H), 7.60 (1H, dt, *J* 7.8, 2.0, $C^{6"}$-H), 7.34 (1H, ddd, *J* 8.8, 2.1, 0.6, $C^{5'}$-H), 7.30-7.27 (1H, m, $C^{5"}$-H), 6.94 (1H, d, *J* 8.8, $C^{6'}$-H), 3.64 (2H, td, *J* 7.1, 5.4, $C^{1'''}$-H_2), 3.07 (2H, t, *J* 7.1, $C^{2'''}$-H_2), 2.39 (3H, s, C^6-H_3), 2.25 (3H, s, C^7-H); ^{13}C NMR (101 MHz, $CDCl_3$) δ 165.4 (C^5), 158.5 (C^3), 150.1 ($C^{2"}$), 148.5 ($C^{4"}$), 144.2 ($C^{1'}$), 136.9 ($C^{5'}$), 136.2 ($C^{6"}$), 133.6 ($C^{1"}$), 132.1 ($C^{2'}$), 127.1 ($C^{3'}$), 123.6 ($C^{5"}$), 118.0 (C^4), 114.8 ($C^{4'}$), 114.2 ($C^{6'}$), 44.1 ($C^{1'''}$), 32.6 ($C^{2'''}$), 11.6 (C^6), 10.8 (C^7); LRMS *m/z* (ESI^-) 337 ($[M-H]^-$, 100%); HRMS *m/z* (ESI^+) [Found: 339.1451, $C_{18}H_{18}N_4O_3$ requires $[M+H]^+$ 339.1452)]; Analytical HPLC (RP, *Method 1*) rt 7.1 min, purity 100%.

***N*-(5-(3,5-Dimethylisoxazol-4-yl)-2-((2-(pyridin-3-yl)ethyl)amino)phenyl)propionamide 190**

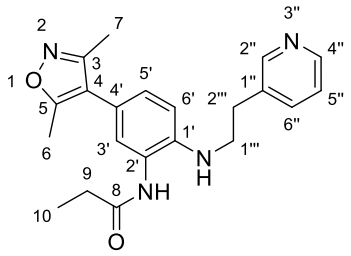

4-(3,5-Dimethylisoxazol-4-yl)-2-nitro-*N*-(2-(pyridin-3-yl)ethyl)aniline **189** (200 mg, 0.591 mmol, 1.0 eq.) was suspended in EtOH (3.1 mL) and 1 M $Na_2S_2O_4$ (3.1 mL, 3.07 mmol, 5.2 eq.) was added. The reaction mixture was stirred at 80 °C for 10 min. The reaction mixture was cooled to rt and partitioned between ethyl acetate (10 mL) and 10% aq. ammonia solution (5 mL). The phases were separated then the organic phase was washed with water (5 mL) and brine (5 mL), dried over $MgSO_{4\,(s)}$, filtered, then the filtrate was concentrated *in vacuo*. The crude material was dissolved in DMF (1.5 mL). DIPEA (108 µL, 0.621 mmol, 1.05 eq.), propionic acid (46.3 µL, 0.621 mmol, 1.05 eq.) and HATU (236 mg, 0.621 mmol, 1.05 eq.) were added. The reaction mixture was stirred at rt for 3 h. The reaction mixture was partitioned between ethyl acetate and water. The organic layer was separated then the aqueous layer was extracted with ethyl acetate (3 × 10 mL). The combined organic layers were washed with brine, dried over $MgSO_{4\,(s)}$, filtered, then the filtrate was concentrated *in vacuo*. The residue was purified by flash column chromatography eluting with CH_2Cl_2 : methanol (1:0 to 9:1) to yield *N*-(5-(3,5-dimethylisoxazol-4-yl)-2-((2-(pyridin-3-yl)ethyl)amino)phenyl)propionamide **190** (203 mg, 94%) as an off-white semi-solid: R_f 0.26 (0.1% Et_3N in CH_2Cl_2 : methanol, 9:1); ^{1}H NMR (400 MHz, $CDCl_3$) δ 8.52 (1H, d, *J* 2.0, $C^{2"}$-H), 8.48 (1H, dd, *J* 4.9, 2.0, $C^{4"}$-H), 8.01 (1H, s, $C^{1'}$-NH), 7.65 (1H, ddd, *J* 8.0, 2.0, 2.0, $C^{6"}$-H), 7.38-7.28 (2H, m, $C^{5"}$-H, N-H), 7.15 (1H, d, *J* 2.0, $C^{6'}$-H), 7.02 (1H, dd, *J* 8.3, 2.0, $C^{4'}$-H), 6.82 (1H, d, *J* 8.3, $C^{3'}$-H), 3.44 (2H, t, *J* 6.9, $C^{1'''}$-H_2), 2.99 (2H, t, *J* 6.9, $C^{2'''}$-H_2), 2.42 (2H, q, *J* 7.5, C^9-H_2), 2.37 (3H, s, C^6-H_3), 2.24 (3H, s, C^7-H_3), 1.22 (3H, t, *J* 7.5, C^{10}-H_3); ^{13}C NMR (101 MHz, $CDCl_3$) δ 173.5 (C^8), 165.0 (C^5), 159.0(C^3), 149.5 ($C^{2"}$), 147.1 ($C^{4"}$), 141.6 ($C^{2'}$), 137.5 ($C^{6"}$), 135.6 ($C^{1"}$), 128.2 ($C^{4'}$), 126.7 ($C^{6'}$), 126.3 ($C^{2'}$), 124.5 ($C^{5'}$), 124.0 ($C^{5"}$), 116.2 (C^4), 113.3 ($C^{3'}$), 44.9 ($C^{1'''}$), 32.86 ($C^{2'''}$), 30.1 (C^9), 11.7 (C^6), 11.0 (C^7), 10.0 (C^{10}); LRMS *m/z* (ESI^+) 365 ($[M+H]^+$, 100%).

4-(2-Ethyl-1-(2-(pyridin-3-yl)ethyl)-*1H*-benzo[*d*]imidazol-5-yl)-3,5-dimethylisoxazole 109

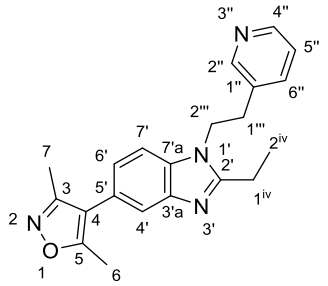

N-(5-(3,5-Dimethylisoxazol-4-yl)-2-((2-(pyridin-3-yl)ethyl)amino)phenyl)propionamide **190** (202 mg, 0.555 mmol, 1.0 eq.) was refluxed in propionic acid (0.5 mL) for 17 h. The reaction mixture was cooled to rt then the solvent was evaporated *in vacuo.* The residue was purified by RP flash column chromatography eluting with water : acetonitrile (95:5 to 5:95) to yield 4-(2-ethyl-1-(2-(pyridin-3-yl)ethyl)-*1H*-benzo[*d*]imidazol-5-yl)-3,5-dimethylisoxazole **109** (50 mg, 26%) as a brown oil: R_f 0.13 (water : acetonitrile, 1:9); ν_{max} (thin film)/ cm^{-1} 1423 (C-H, m), 1309 (C-N, s), 1209 (C-N, m), 1106 (C-N, m); ^{1}H NMR (400 MHz, DMSO-d_6) δ 8.42 (1H, dd, *J* 4.8, 1.7, $C^{4"}$-H), 8.36 (1H, d, *J* 1.7, $C^{4'}$-H), 7.66-7.57 (2H, m, $C^{7'}$-H, C^{6}-H), 7.54 (1H, d, *J* 1.4, $C^{2"}$-H), 7.28 (1H, ddd, *J* 7.8, 4.8, 0.9, $C^{5'}$-H), 7.14 (1H, dd, *J* 8.3, 1.7, $C^{6'}$-H), 4.45 (2H, t, *J* 7.2, $C^{2'''}$-H_2), 3.07 (2H, t, *J* 7.2, $C^{1'''}$-H_2), 2.66 (2H, q, *J* 7.4, C^{1iv}-H_2), 2.40 (3H, s, C^{6}-H_3), 2.23 (3H, s, C^{7}-H_3), 1.24 (3H, t, *J* 7.4, C^{2iv}-H_3); ^{13}C NMR (101 MHz, DMSO-d_6) δ 164.5 ($C^{2'}$), 158.3 (C^{5}), 156.7 (C^{3}), 150.0 ($C^{4'}$), 147.8 ($C^{4"}$), 142.6 ($C^{3'a}$), 136.5 ($C^{6"}$), 134.3 ($C^{7'a}$), 133.7 ($C^{1"}$), 123.4 ($C^{5"}$), 122.7 ($C^{5'}$), 122.6 ($C^{6'}$), 118.9 ($C^{2'}$), 116.7 (C^{4}), 110.3 ($C^{7'}$), 43.9 ($C^{2'''}$), 32.3 ($C^{1'''}$), 19.7 (C^{1iv}), 11.3 (C^{2iv}), 11.3 (C^{6}), 10.5 (C^{7}); LRMS *m/z* (ESI^+) 347 ([$M+H^+$], 100%); HRMS *m/z* (ESI^+) [Found: 347.1864, $C_{21}H_{22}N_4O$ requires $[M+H]^+$ 347.1866)]; Analytical HPLC (RP, *Method 1*) rt 4.5 min, purity 100%.

N^1-(4-(3,5-Dimethylisoxazol-4-yl)-2-nitrophenyl)-N^2,N^2-dimethylethane-1,2-diamine 191

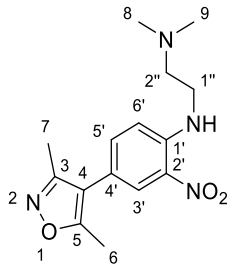

4-(4-Fluoro-3-nitrophenyl)-3,5-dimethylisoxazole **74** (200 mg, 0.847 mmol, 1.0 eq.) was dissolved in anhydrous DMF (1.2 mL). N^1,N^1-dimethylethane-1,2-diamine (185 µL, 1.69 mmol, 2.0 eq.) and DIPEA (737 µL, 4.23 mmol, 5.0 eq.) were added. The reaction mixture was stirred at 60 °C for 3 h. The reaction mixture was cooled to rt and partitioned between ethyl acetate and water. The aqueous layer was extracted with ethyl acetate (3 × 10 mL). The combined organic layers were dried over $MgSO_{4\ (s)}$, filtered, then the filtrate was concentrated *in vacuo*. The residue was purified by flash column chromatography eluting with CH_2Cl_2 : methanol (1:0 to 90:10) to yield N^1-(4-(3,5-dimethylisoxazol-4-yl)-2-nitrophenyl)-N^2,N^2-dimethylethane-1,2-diamine **191** (132 mg, 51%) as an orange solid: R_f 0.30 (CH_2Cl_2 : methanol, 9:1); m.p. 108-110 °C ($CDCl_3$) [lit.[69] 118-119 °C]; ^{1}H NMR (400 MHz, $CDCl_3$) δ 8.39 (1H, br s, N-H), 8.07 (1H, d, *J* 2.2, $C^{3'}$-H), 7.33 (1H, ddd, *J* 8.8, 2.2, 0.6, $C^{5'}$-H), 6.92 (1H, d, *J* 8.8, $C^{6'}$-H), 3.38 (2H, td, *J* 6.2, 4.6, $C^{1"}$-H_2), 2.65 (2H, t, *J* 6.2, $C^{2'}$-H_2), 2.39 (3H, s, C^6-H_3), 2.32 (6H, s, $N(CH_3)_2$), 2.25 (3H, s, C^7-H_3); ^{13}C NMR (151 MHz, $CDCl_3$) δ 165.5 (C^5), 158.8 (C^3), 144.7 ($C^{1'}$), 136.8 ($C^{5'}$), 132.0 (C^4), 127.2 ($C^{3'}$), 117.3 ($C^{2'}$), 115.1 ($C^{4'}$), 114.7 ($C^{6'}$), 57.5 ($C^{2"}$), 45.4 (C^8, C^9), 40.9 ($C^{1"}$), 11.7 (C^6), 10.9 (C^7); LRMS *m/z* (ESI^+) 305 ($[M+H]^+$, 100%); HRMS *m/z* (ESI^+) [Found: 305.1598, $C_{15}H_{20}O_4N_3$ requires $[M+H]^+$ 305.1608)]; Analytical HPLC (RP, *Method 1*) rt 6.8 min, purity 100%. The spectroscopic data are in good agreement with the literature.[69]

***N*-(2-((2-(Dimethylamino)ethyl)amino)-5-(3,5-dimethylisoxazol-4-yl)phenyl)propionamide 192**

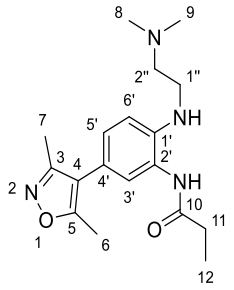

N^1-(4-(3,5-dimethylisoxazol-4-yl)-2-nitrophenyl)-N^2,N^2-dimethylethane-1,2-diamine **191** (195 mg, 0.641 mmol, 1.0 eq.) was suspended in EtOH (3.0 mL) and 1 M $Na_2S_2O_4$ (3.3 mL, 3.33 mmol, 5.2 eq.) was added. The reaction mixture was stirred at 80 °C for 15 min. The reaction mixture was cooled to rt and partitioned between ethyl acetate (15 mL) and 10% aq. ammonia solution (7 mL). The phases were separated, then the organic phase was washed with water (5 mL) and brine (5 mL), dried over $MgSO_{4\ (s)}$, filtered, then the filtrate was concentrated *in vacuo*. The crude material was dissolved in DMF (2.0 mL). DIPEA (117 µL, 0.673 mmol, 1.05 eq.), propanoic acid (50.0 µL, 0.673 mmol, 1.05 eq.), HATU (256 mg, 0.673 mmol, 1.05 eq.) and HOBT (90.9 mg, 0.673 mmol, 1.05 eq.) were added. The reaction mixture was stirred at rt for 16 h. The reaction mixture was partitioned between ethyl acetate and water. The organic layer was separated then the aqueous layer was extracted with ethyl acetate (3 × 10 mL). The combined organic layers were washed with brine, dried over $MgSO_{4\ (s)}$, filtered, then the filtrate was concentrated *in vacuo*. The residue was purified by flash column chromatography eluting with CH_2Cl_2 : methanol (1:0 to 85:15) to yield *N*-(2-((2-(dimethylamino)ethyl)amino)-5-(3,5-dimethylisoxazol-4-yl)phenyl)propionamide **192** (64 mg, 30%) as a brown oil: R_f 0.41 (CH_2Cl_2 : methanol, 9:1); ^{1}H NMR (400 MHz, $CDCl_3$) δ 10.83 (1H, s, $OC^{10}N$-H), 8.07 (1H, d, *J* 2.0, $C^{3'}$-H), 7.17 (1H, d, *J* 8.1, $C^{5'}$-H), 7.05 (1H, dd, *J* 8.0, 2.0, $C^{6'}$-H), 4.89 (1H, *br* s, $C^{1'}N$-H), 2.80 (6H, s, C^8-H_3, C^9-H_3), 2.49 (3H, s, C^6-H_3), 2.34 (3H, s, C^7-H_3), 2.32 (2H, q, *J* 8.0, C^{11}-H_2), 1.93 (3H, m, $C^{1''}$-H_3), 1.21 (3H, t, *J* 8.0, C^{12}-H_3), 0.99 (2H, t, *J* 7.4, $C^{2''}$-H_2); ^{13}C NMR (101 MHz, $CDCl_3$) δ 172.9 (C^{10}), 165.8 (C^5), 158.5 (C^3), 140.9 ($C^{1'}$), 131.3 ($C^{2'}$), 128.2 ($C^{5'}$), 125.4 ($C^{6'}$), 124.7 ($C^{3'}$), 124.1 ($C^{4'}$), 115.7 (C^4), 38.6 (C^8, C^9), 30.4 (C^{11}), 27.1 ($C^{1''}$), 11.8 (C^6), 11.0 (C^7), 9.9 (C^{12}), 9.2 ($C^{2''}$); LRMS *m/z* (ESI^+) 369 ($[M+K]^+$, 100%).

2-(5-(3,5-Dimethylisoxazol-4-yl)-2-ethyl-1*H*-benzo[*d*]imidazol-1-yl)-*N*,*N*-dimethylethan-1-amine 104

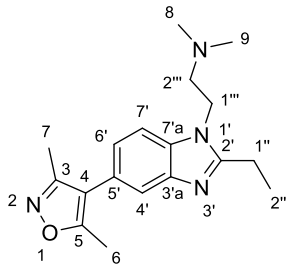

N^1-(4-(3,5-dimethylisoxazol-4-yl)-2-nitrophenyl)-N^2,N^2-dimethylethane-1,2-diamine **191** (80.0 mg, 0.263 mmol, 1.0 eq.) was suspended in EtOH (1.37 mL) and 1 M $Na_2S_2O_4$ (1.37 mL, 1.37 mmol, 5.2 eq.) was added. The reaction mixture was stirred at 80 °C for 1 h. The reaction mixture was cooled to rt and partitioned between ethyl acetate (10 mL) and 10% aq. ammonia solution (5 mL). The organic layer was separated then the aqueous layer was extracted with ethyl acetate (10 mL). The combined organic layers were washed with brine, dried over $MgSO_{4\ (s)}$, filtered, then the filtrate was concentrated *in vacuo*. The crude material was dissolved in ethyl acetate (4 mL). DIPEA (101 µL, 0.580 mmol, 2.2 eq.), propionic acid (19.7 µL, 0.263 mmol, 1.0 eq.) and 50 wt% T3P in ethyl acetate (407 µL, 1.37 mmol, 2.6 eq.) were added. The reaction mixture was stirred at 80 °C for 17 h. The reaction mixture was cooled to rt and partitioned between ethyl acetate and 1 M $NaOH_{(aq.)}$. The organic layer was separated then the aqueous layer was extracted with ethyl acetate (3 × 10 mL). The combined organic layers were dried over $MgSO_{4\ (s)}$, filtered, then the filtrate was concentrated *in vacuo*. The residue was purified by flash column chromatography eluting with CH_2Cl_2 : methanol (1:0 to 90:10) to yield 2-(5-(3,5-dimethylisoxazol-4-yl)-2-ethyl-1*H*-benzo[*d*]imidazol-1-yl)-*N*,*N*-dimethylethan-1-amine **104** (24 mg, 30%) as a colourless oil: R_f 0.13 (0.1% Et_3N in CH_2Cl_2 : methanol, 9:1); m.p. 97-98 °C ($CDCl_3$); ν_{max} (thin film)/ cm^{-1} 2361 (C-H, m), 1483 (C-H, m), 1311 (C-N, s), 1250 (C-N, m); ^{1}H NMR (400 MHz, $CDCl_3$) δ 7.61 (1H, dd, *J* 1.6, 0.7, $C^{4'}$-H), 7.38 (1H, dd, *J* 8.3, 0.7, $C^{7'}$-H), 7.12 (1H, dd, *J* 8.3, 1.6, $C^{6'}$-H), 4.28-4.16 (2H, t, *J* 7.4, $C^{1'''}$-H_2), 2.93 (2H, q, *J* 7.5, $C^{1''}$-H_2), 2.73 (2H, t, *J* 7.4, $C^{2'''}$-H_2), 2.40 (3H, s, C^6-H_3), 2.39 (6H, s, $N(CH_3)_2$), 2.27 (3H, s, C^7-H_3); ^{13}C NMR (101 MHz, $CDCl_3$) δ 165.0 (C^5), 159.1 ($C^{2'}$), 157.1 (C^3), 143.1 ($C^{3'a}$), 134.5 ($C^{7'a}$), 124.0 ($C^{5'}$), 123.3 ($C^{6'}$), 120.0 (C^4), 117.2 (C^4), 109.3 ($C^{7'}$), 58.5 ($C^{2'''}$), 45.9 (C^8, C^9), 42.2 ($C^{1'''}$), 20.8 ($C^{1''}$), 11.7 ($C^{2''}$), 11.5 (C^6), 10.9 (C^7); LRMS *m/z* (ESI^+) 335 ($[M+Na]^+$, 100%); HRMS *m/z* (ESI^+) [Found: 313.2018,

$C_{18}H_{24}N_4O$ requires $[M+H]^+$ 313.2023)]; Analytical HPLC (RP, *Method 1*) rt 5.5 min, purity 98%.

4-(3,5-Dimethylisoxazol-4-yl)-*N*-(2-(4-methylpiperazin-1-yl)ethyl)-2-nitroaniline 193

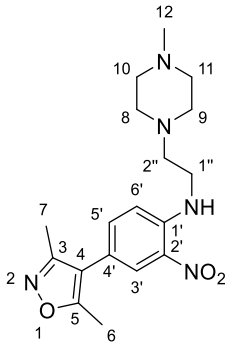

4-(4-Fluoro-3-nitrophenyl)-3,5-dimethylisoxazole **74** (200 mg, 0.847 mmol, 1.0 eq.) was dissolved in anhydrous DMF (1.2 mL). 2-(4-Methylpiperazin-1-yl)ethan-1-amine (254 µL, 1.69 mmol, 2.0 eq.) and DIPEA (737 µL, 4.23 mmol, 5.0 eq.) were added. The reaction mixture was stirred at rt for 17 h. The solvent was evaporated *in vacuo* then the residue was partitioned between ethyl acetate and water. The aqueous layer was extracted with ethyl acetate (3 × 15 mL). The combined organic layers were washed with 10% w/v $LiCl_{(aq)}$ (3 × 10 mL), then dried over $MgSO_{4\,(s)}$, filtered, then the filtrate was concentrated *in vacuo*. The residue was purified by flash column chromatography eluting with CH_2Cl_2 : methanol (1:0 to 9:1) to yield 4-(3,5-dimethylisoxazol-4-yl)-*N*-(2-(4-methylpiperazin-1-yl)ethyl)-2-nitroaniline **193** (251 mg, 83%) as an orange oil: R_f 0.28 (CH_2Cl_2 : methanol, 9:1); ν_{max} (thin film)/ cm^{-1} 3345 (N-H, m), 1620 (N-H, m), 1558 (N-O, s), 1452 (C-H, m), 1353 (C-N, m), 1224 (C-N, m), 1154 (C-N, m); ^1H NMR (400 MHz, $CDCl_3$) δ 8.56 (1H, t, *J* 4.5, N-H), 8.07 (1H, d, *J* 2.2, $C^{3'}$-H), 7.33 (1H, dd, *J* 8.8, 2.2, $C^{5'}$-H), 6.90 (1H, d, *J* 8.8, $C^{6'}$-H), 3.39 (2H, td, *J* 6.2, 4.6, $C^{1"}$-H_2), 2.75 (2H, t, *J* 6.2, $C^{2"}$-H_2), 2.70-2.45 (8H, m, C^8-H_2, C^9-H_2, C^{10}-H_2, C^{11}-H_2), 2.39 (3H, s, C^6-H_3), 2.34 (3H, s, C^{12}-H_3), 2.25 (3H, s, C^7-H_3); ^{13}C NMR (101 MHz, $CDCl_3$) δ 165.4 (C^5), 158.7 (C^3), 144.6 ($C^{1'}$), 136.9 ($C^{5'}$), 132.0 ($C^{2'}$), 127.1 ($C^{3'}$), 117.3 (C^4), 115.1 ($C^{4'}$), 114.9 ($C^{6'}$), 55.5 ($C^{2"}$), 55.1 (C^8, C^9), 52.5 (C^{10}, C^{11}), 45.9 (C^{10}), 39.8 (C^{12}), 11.7 (C^6), 10.9 (C^7); LRMS *m/z* (ESI^+) 360 ($[M+H]^+$, 100%); HRMS *m/z* (ESI^+) [Found: 360.2029, $C_{18}H_{25}N_5O_3$ requires $[M+H]^+$ 360.2030)]; Analytical HPLC (RP, *Method 2*) rt 6.7 min, purity 100%.

***N*-(5-(3,5-Dimethylisoxazol-4-yl)-2-((2-(4-methylpiperazin-1-yl)ethyl)amino)phenyl)propionamide 194**

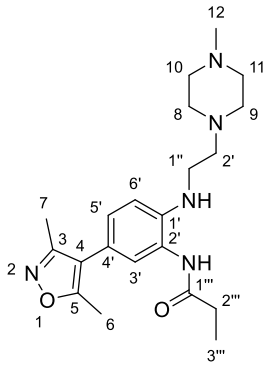

1 M $Na_2S_2O_{4\,(aq)}$ (2.58 mL, 2.58 mmol, 5.2 eq.) was added to 4-(3,5-dimethylisoxazol-4-yl)-*N*-(2-(4-methylpiperazin-1-yl)ethyl)-2-nitroaniline **193** (178 mg, 0.495 mmol, 1.0 eq.) in EtOH (2.58 mL). The reaction mixture was stirred at 80 °C for 10 min. The reaction mixture was cooled to rt then the solvent was evaporated *in vacuo.* The residue was partitioned between 10% aq. ammonia solution and ethyl acetate. The aqueous layer was separated then extracted with ethyl acetate (3 × 15 mL). 2 M $NaOH_{(aq)}$ was added to the aqueous layer and this was further extracted with ethyl acetate (3 × 15 mL). The combined organic layers were dried over $MgSO_{4\,(s)}$, filtered, then the filtrate was concentrated *in vacuo*. The residue was dissolved in anhydrous DMF (1.0 mL). Propanoic acid (37.0 µL, 0.97 mmol, 1.05 eq.), HATU (198 mg, 0.522 mmol, 1.05 eq.) and DIPEA (91.0 µL, 0.522 mmol, 1.05 eq.) were added. The reaction mixture was stirred at rt for 17 h. The solvent was evaporated *in vacuo.* The residue was re-dissolved in ethyl acetate (10 mL) and water (5 mL) was added. The organic layer was separated then the aqueous layer was extracted with ethyl acetate (3 × 10 mL). The combined organic layers were washed with 10% w/v $LiCl_{(aq)}$ (3 × 10 mL), dried over $MgSO_{4\,(s)}$, filtered, then the filtrate was concentrated *in vacuo*. The residue was purified by flash column chromatography eluting with CH_2Cl_2 : methanol (1:0 to 9:1) to yield *N*-(5-(3,5-dimethylisoxazol-4-yl)-2-((2-(4-methylpiperazin-1-yl)ethyl)amino)phenyl)propionamide **194** (89 mg, 98%) as a cream solid: R_f 0.10 (CH_2Cl_2 : methanol, 9:1); ^{1}H NMR (400 MHz, $CDCl_3$) δ 7.40-7.29 (1H, *br* s, $OC^{1'''}N$-H), 7.32 (1H, d, *J* 2.1, $C^{6'}$-H), 6.99 (1H, dd, *J* 8.3, 2.1, $C^{5'}$-H), 6.75 (1H, d, *J* 8.3, $C^{6'}$-H), 4.59 (1H, s, $C^{1'}$-NH), 3.21 (2H, t, *J* 5.8, $C^{1''}$-H_2), 2.75 (2H, t, *J* 5.8, $C^{2''}$-H_2), 2.69-2.47 (8H, m, C^8-H_2, C^9-H_2, C^{10}-H_2, C^{11}-H_2), 2.50 (2H, q, *J* 7.6, $C^{2'''}$-H_2), 2.38 (3H, s, C^6-H_3), 2.34 (3H, s, C^{12}-H_3), 2.25 (3H, s, C^7-H_3); 1.30 (3H, t, *J* 7.6, $C^{3'''}$-H_3); ^{13}C NMR (101 MHz, $CDCl_3$)

δ 172.9 ($C^{1'''}$), 164.9 (C^{5}), 159.0 (C^{3}), 141.4 ($C^{1'}$), 127.7 ($C^{5'}$), 126.3 ($C^{3'}$), 124.4 ($C^{2'}$), 119.9 ($C^{4'}$), 116.3 (C^{4}), 112.9 ($C^{6'}$), 56.3 ($C^{2'}$), 54.8 (C^{8}, C^{9}), 52.5 (C^{10}, C^{11}), 45.9 (C^{12}), 40.2 ($C^{1''}$), 30.4 ($C^{2'''}$), 11.7 (C^{6}), 11.0 (C^{7}), 10.2 ($C^{3'''}$); LRMS *m/z* (ESI^+) 386 ($[M+H]^+$, 100%).

4-(2-Ethyl-1-(2-(4-methylpiperazin-1-yl)ethyl)-1*H*-benzo[*d*]imidazol-5-yl)-3,5-dimethylisoxazole 105

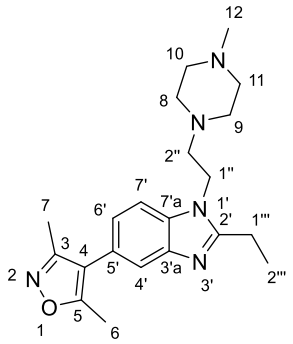

N-(5-(3,5-Dimethylisoxazol-4-yl)-2-((2-(4-methylpiperazin-1-yl)ethyl)amino)phenyl)propionamide **194** (75 mg, 195 µmol, 1.0 eq.) and propanoic acid (1.5 µL, 19.0 µmol, 0.1 eq.) were combined in toluene (1 mL) in a microwave vial containing 3 Å molecular sieves. The reaction mixture was stirred at 130 °C for 72 h. The reaction mixture was cooled to rt, filtered then the solvent was evaporated *in vacuo.* The residue was purified by RP flash column chromatography eluting with water : acetonitrile (95:5 to 5:95) to yield 4-(2-ethyl-1-(2-(4-methylpiperazin-1-yl)ethyl)-*1H*-benzo[*d*]imidazol-5-yl)-3,5-dimethylisoxazole **105** (40 mg, 56%) as a yellow solid: R_f 0.16 (CH_2Cl_2 : methanol, 9:1); m.p. 84-86 °C ($CDCl_3$); ν_{max} (thin film)/ cm^- 1618 (C=C, w), 1453 (C-H, m), 1409 (C-H, m), 1310 (C-N, m), 1166 (C-N, m), 1011 (C-H, m); ^1H NMR (600 MHz, $CDCl_3$) δ 7.60 (1H, d, *J* 1.6, $C^{4'}$-H), 7.35 (1H, d, *J* 8.2, $C^{7'}$-H), 7.10 (1H, dd, *J* 8.2, 1.6, $C^{6'}$-H), 4.23 (2H, t, *J* 7.0, $C^{1''}$-H_2), 2.94 (2H, q, *J* 7.5, $C^{1'''}$-H_2), 2.74 (2H, t, *J* 7.0, $C^{2''}$-H_2), 2.66-2.56 (4H, m, C^{8}-H_2, C^{9}-H_2), 2.50 (4H, m, C^{10}-H_2, C^{11}-H_2), 2.40 (3H, s, C^{6}-H_3), 2.33 (3H, s, C^{12}-H_3), 2.28 (3H, s, C^{7}-H_3), 1.50 (3H, t, *J* 7.5, $C^{2'''}$-H_3); ^{13}C NMR (151 MHz, $CDCl_3$) δ 165.1 (C^{5}), 159.2(C^{3}), 157.3 (C^{1}), 143.2 ($C^{2'}$), 134.6 ($C^{7'a}$), 124.2 ($C^{5'}$), 123.4 ($C^{6'}$), 120.1 ($C^{4'}$), 117.3 (C^{4}), 109.4 ($C^{7'}$), 57.3 ($C^{2''}$), 55.1 (C^{10}, C^{11}), 53.5 (C^{8}, C^{9}), 45.9 (C^{12}), 41.9 ($C^{1''}$), 21.0 ($C^{1'''}$), 11.9 ($C^{2'''}$), 11.7 (C^{6}), 11.0 (C^{7}); LRMS *m/z* (ESI^+) 368 ($[M+H]^+$, 100%); HRMS *m/z* (ESI^+) [Found: 368.2462,

$C_{21}H_{29}N_5O$ requires $[M+H]^+$ 368.2445)]; Analytical HPLC (RP, *Method 3*) rt 4.9 min, purity 100%.

4-(3,5-Dimethylisoxazol-4-yl)-*N*-(2-morpholinoethyl)-2-nitroaniline 195

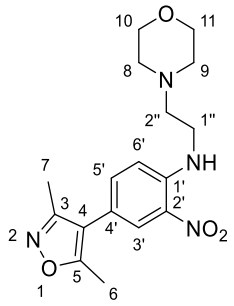

4-(4-Fluoro-3-nitrophenyl)-3,5-dimethylisoxazole **74** (200 mg, 0.847 mmol, 1.0 eq.) was dissolved in anhydrous DMF (1.2 mL). 2-Morpholinoethan-1-amine (221 mg, 1.69 mmol, 2.0 eq.) and DIPEA (737 µL, 4.24 mmol, 5.0 eq.) were added. The reaction mixture was stirred at 60 °C for 19 h. The reaction mixture was cooled to rt and partitioned between ethyl acetate and water. The aqueous layer was extracted with ethyl acetate (3 × 15 mL). The combined organic layers were dried over $MgSO_{4\,(s)}$, filtered, then the filtrate was concentrated *in vacuo*. The residue was purified by flash column chromatography eluting with CH_2Cl_2 : methanol (1:0 to 85:15) to yield 4-(3,5-dimethylisoxazol-4-yl)-*N*-(2-morpholinoethyl)-2-nitroaniline **195** (291 mg, 99%) as an orange oil: R_f 0.64 (CH_2Cl_2 : methanol, 9:1); ν_{max} (thin film)/ cm^{-1} 2981 (N-H, m), 1623 (N-H, m), 1555 (N-O, s), 1461 (C-H, m), 1383 (C-N, m), 1226 (C-O, s), 1157 (C-O, s); ^{1}H NMR (400 MHz, $CDCl_3$) δ 8.56 (1H, t, *J* 4.5, N-H), 8.05 (1H, d, *J* 2.2, $C^{3'}$-H), 7.32 (1H, ddd, *J* 8.8, 2.2, 0.7, $C^{5'}$-H), 6.90 (1H, d, *J* 8.8, $C^{6'}$-H), 3.77-3.67 (4H, dd, *J* 4.8, 4.8, C^{10}-H_2, C^{11}-H_2), 3.44-3.33 (2H, m, $C^{1''}$-H_2), 2.73 (2H, dd, *J* 6.6, 5.6, $C^{2''}$-H_2), 2.60-2.47 (4H, m, C^8-H_2, C^9-H_2), 2.37 (3H, s, C^6-H_3), 2.22 (3H, s, C^7-H_3); ^{13}C NMR (101 MHz, $CDCl_3$) δ 165.4 (C^5), 158.7 (C^3), 144.5 ($C^{1'}$), 136.9 ($C^{5'}$), 132.0 ($C^{2'}$), 127.1 ($C^{3'}$), 117.4 (C^4), 115.0 ($C^{4'}$), 114.8 ($C^{6'}$), 67.1 (C^{10}, C^{11}), 56.1 ($C^{2''}$), 53.3 (C^8, C^9), 39.5 ($C^{1''}$), 11.7 (C^6), 10.9 (C^7); LRMS *m/z* (ESI^+) 347 ($[M+H]^+$, 100%); HRMS *m/z* (ESI^+) [Found: 347.1703, $C_{17}H_{22}N_4O_4$ requires $[M+H]^+$.1714)]; Analytical HPLC (RP, *Method 1*) rt 6.9 min, purity 100%. The spectroscopic data are in good agreement with the literature.[342]

***N*-(5-(3,5-Dimethylisoxazol-4-yl)-2-((2-morpholinoethyl)amino)phenyl)propionamide 196**

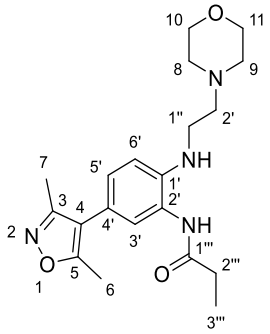

1 M $Na_2S_2O_{4\,(aq)}$ (1.50 mL, 1.50 mmol, 5.2 eq.) was added to 4-(3,5-dimethylisoxazol-4-yl)-*N*-(2-morpholinoethyl)-2-nitroaniline **195** (100 mg, 0.289 mmol, 1.0 eq.) in EtOH (1.50 mL). The reaction mixture was stirred at 80 °C for 10 min. The reaction mixture was cooled to rt then the solvent was evaporated *in vacuo.* The residue was partitioned between 10% aq. ammonia solution and ethyl acetate. The aqueous layer was separated then extracted with ethyl acetate (3 × 15 mL). 2 M $NaOH_{\,(aq)}$ was added to the aqueous layer and this was further extracted with ethyl acetate (3 × 15 mL). The combined organic layers were dried over $MgSO_{4\,(s)}$, filtered, then the filtrate was concentrated *in vacuo*. The residue was dissolved in anhydrous DMF (1.0 mL). Propanoic acid (16.0 µL, 0.215 mmol, 1.0 eq.), HATU (85.8 mg, 0.226 mmol, 1.05 eq.) and DIPEA (39.4 µL, 0.226 mmol, 1.05 eq.) were added. The reaction mixture was stirred at rt for 17 h. The solvent was evaporated *in vacuo.* The residue was re-dissolved in ethyl acetate (10 mL) and 1 M NaOH (5 mL) was added. The organic layer was separated then the aqueous layer was extracted with ethyl acetate (3 × 10 mL). The combined organic layers were washed with 10% w/v $LiCl_{\,(aq)}$ (3 × 10 mL), dried over $MgSO_{4\,(s)}$, filtered, then the filtrate was concentrated *in vacuo*. The residue was purified by flash column chromatography eluting with CH_2Cl_2 : methanol (1:0 to 9:1), followed by EtOH with 1% Et_3N to yield *N*-(5-(3,5-dimethylisoxazol-4-yl)-2-((2-morpholinoethyl)amino)phenyl)propionamide **196** (46 mg, 58%) as a colourless oil: R_f 0.38 (CH_2Cl_2 : methanol, 9:1); ^{1}H NMR (400 MHz, $CDCl_3$) δ 7.22 (1H, d, *J* 2.0, $C^{3'}$-H), 7.01 (1H, dd, *J* 8.3, 2.0, $C^{5'}$-H), 6.79 (1H, d, *J* 8.3, $C^{6'}$-H), 3.86-3.62 (4H, m, C^{10}-H_2, C^{11}-H_2), 3.29-3.17 (2H, m, $C^{1"}$-H_2), 2.77-2.64 (2H, m, $C^{2"}$-H_2), 2.50 (2H, q, *J* 7.5, $C^{2'''}$-H_2), 2.38 (3H, s, C^6-H_3), 2.25 (3H, s, C^7-H_3), 1.51-1.41 (4H, m, C^8-H_2, C^9-H_2), 1.31 (3H, t, *J* 7.5, $C^{3'''}$-H_3); LRMS *m/z* (ESI^+) 373 ($[M+H]^+$, 100%).

4-(2-(5-(3,5-Dimethylisoxazol-4-yl)-2-ethyl-1*H*-benzo*[d]*imidazol-1-yl)ethyl)morpholine 106

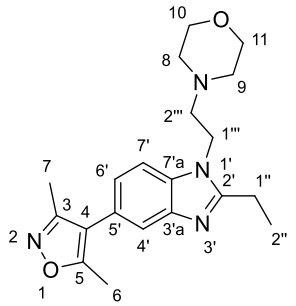

N-(5-(3,5-dimethylisoxazol-4-yl)-2-((2-morpholinoethyl)amino)phenyl)propionamide **196** (40.0 mg, 0.107 mmol, 1.0 eq.) and propanoic acid (1.60 µL, 0.021 mmol, 0.2 eq.) were combined in toluene (1 mL) in a microwave vial containing 3 Å molecular sieves. The reaction mixture was stirred at 130 °C for 48 h. The reaction mixture was cooled to rt, filtered then the solvent was evaporated *in vacuo.* The residue was purified by RP flash column chromatography eluting with water : acetonitrile (95:5 to 5:95) to yield 4-(2-(5-(3,5-dimethylisoxazol-4-yl)-2-ethyl-1*H*-benzo*[d]*imidazol-1-yl)ethyl)morpholine **106** (22 mg, 58%) as a yellow oil: R_f 0.52 (CH_2Cl_2 : methanol, 9:1); ν_{max} (thin film)/ cm^{-1} 1619 (C-H, w), 1512 (N-O, m), 1483 (C-H, m), 1452 (C-H, m), 1410 (C-H, m), 1309 (C-H, m), 1246 (C-N, m), 1116 (C-O, s), 1009 (C-H, w); ^{1}H NMR (600 MHz, $CDCl_3$) δ 7.60 (1H, d, *J* 1.6, $C^{4'}$-H), 7.35 (1H, d, *J* 8.2, $C^{7'}$-H), 7.10 (1H, dd, *J* 8.2, 1.6, $C^{6'}$-H), 4.24 (2H, t, *J* 6.9, $C^{1'''}$-H_2), 3.77-3.60 (4H, m, C^{10}-H_2, C^{11}-H_2), 2.94 (2H, q, *J* 7.5, $C^{1''}$-H_2), 2.72 (2H, t, *J* 6.9, $C^{2'''}$-H_3), 2.51 (4H, t, *J* 4.6, C^8-H_2, C^9-H_2), 2.40 (3H, s, C^6-H_3), 2.27 (3H, s, C^7-H_3), 1.50 (3H, t, *J* 7.5, $C^{2''}$-H_3); ^{13}C NMR (151 MHz, $CDCl_3$) δ 165.0 (C^5), 159.0 (C^3), 157.1 ($C^{2'}$), 143.2 ($C^{3'a}$), 134.5 ($C^{7'a}$), 124.1 ($C^{5'}$), 123.3 ($C^{6'}$), 120.0 ($C^{4'}$), 117.2 (C^4), 109.3 ($C^{7'}$), 66.9 (C^{10}, C^{11}), 57.7 ($C^{2'''}$), 54.1 (C^8, C^9), 41.6 ($C^{1'''}$), 20.9 ($C^{1''}$), 11.7 ($C^{2''}$), 11.5 (C^6), 10.9 (C^7); LRMS *m/z* (ESI^+) 355 ($[M+H]^+$, 100%); HRMS *m/z* (ESI^+) [Found: 355.2130, $C_{20}H_{26}N_4O_2$ requires $[M+H]^+$ 355.2129)]; Analytical HPLC (RP, *Method* 1) rt 5.5 min, purity 100%.

***Tert*-butyl (*S*)-(1-(1,3-dioxoisoindolin-2-yl)propan-2-yl)carbamate 132**

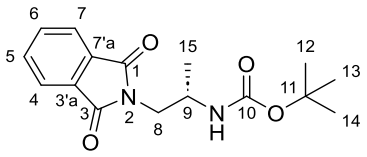

Tert-butyl (*S*)-(1-hydroxypropan-2-yl)carbamate (800 mg, 4.57 mmol, 1.0 eq.) was dissolved in anhydrous THF (10.0 mL). Phthalimide (734 mg, 5.02 mmol, 1.1 eq.) and triphenylphosphine (1.36 g, 5.02 mmol, 1.1 eq.) were added. DIAD (988 µL, 5.02 mmol, 1.1 eq.) was dropwise added. The reaction mixture was stirred at rt for 3 h. The solvent was evaporated *in vacuo* then the crude reaction mixture loaded onto Celite®. The crude material was purified by flash column chromatography eluting with petroleum ether : ethyl acetate (1:0 to 0:1) to yield *tert*-butyl (*S*)-(1-(1,3-dioxoisoindolin-2-yl)propan-2-yl)carbamate **132** (561 mg, 40%) as an off-white solid: R_f 0.64 (petroleum ether : ethyl acetate, 1:1); $[\alpha]_D^{25}$ = +13.1 (*c* 1.0, $CHCl_3$); m.p. 112-113 °C ($CDCl_3$); ^{1}H NMR (400 MHz, $CDCl_3$) δ 7.86-7.77 (2H, m, C^4-H, C^7-H), 7.72-7.64 (2H, m, C^5-H, C^6-H), 5.02-4.86 (1H, m, C^9-H), 4.74 (1H, *br* d, *J* 8.8, N-H), 4.15-3.96 (1H, m, C^8-H_a), 3.73-3.59 (1H, m, C^8-H_b), 1.23 (3H, s, C^{15}-H_3), 1.22 (9H, s, C^{11}-$(CH_3)_3$); ^{13}C NMR (101 MHz, $CDCl_3$) δ 168.7 (C^{10}), 155.5 (C^1, C^3), 134.0 (C^5, C^6), 132.1 ($C^{7'a}$, $C^{3'a}$), 123.5 (C^7, C^4), 79.2 (C^{11}), 70.0 (C^9), 43.5 (C^8), 28.2 (C^{12}, C^{13}, C^{14}), 22.0 (C^{15}); LRMS *m/z* (ESI^+) 327 ($[M+Na]^+$, 100%); Analytical HPLC (RP, *Method 2*) rt 9.2 min, purity 100%. The spectroscopic data are in good agreement with the literature.[343, 344]

***Tert*-butyl (*S*)-(1-aminopropan-2-yl)carbamate 130**

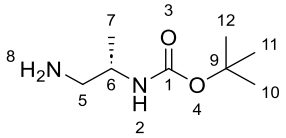

Hydrazine monohydrate (2.53 mL, 52.2 mmol, 5.3 eq.) was added to a mixture of *tert*-butyl (*S*)-(1-(1,3-dioxoisoindolin-2-yl)propan-2-yl)carbamate **132** (3.00 g, 9.86 mmol, 1.0 eq.) in ethanol (18.0 mL). The reaction mixture was refluxed for 2 h, then cooled to rt and filtered. The filtrate was concentrated *in vacuo* to yield *tert*-butyl (*S*)-(1-aminopropan-2-yl)carbamate **130** (1.50 g, 88%) as a colourless solid: m.p. 83-84 °C ($CDCl_3$); R_f 0.16 (CH_2Cl_2 : methanol, 9:1); $[\alpha]_D^{25}$ = +3.68 (*c* 1.0, MeOH); ^{1}H NMR (400 MHz, DMSO-d_6) δ 6.53 (1H, d, *J* 8.1, N-H), 4.73 (2H, p, *J* 6.2, N-H_2), 3.33-3.22

(1H, m, C^6-H), 2.46-2.31 (2H, m, C^5-H_a, C^5-H_b), 1.34 (9H, s, C^9-$(CH_3)_3$), 1.14 (3H, d, *J* 6.2, C^7-H_3); ^{13}C NMR (101 MHz, DMSO-*d*$_6$) δ 155.6 (C^1), 67.2 (C^9), 48.0 (C^6), 46.3 (C^5), 27.7 (C^{10}, $C^{11,}$ C^{12}), 21.3 (C^7); LRMS *m/z* (ESI$^+$) 175 ([M+H]$^+$, 100%). The spectroscopic data are in good agreement with the literature.[344, 345]

Tert-butyl (_S_)-(1-((4-(3,5-dimethylisoxazol-4-yl)-2-nitrophenyl)amino)propan-2-yl)carbamate 133

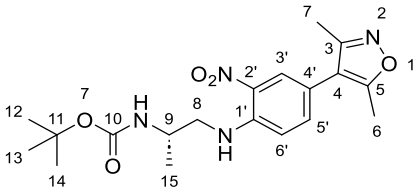

4-(4-Fluoro-3-nitrophenyl)-3,5-dimethylisoxazole **74** (100 mg, 0.423 mmol, 1.0 eq.) was dissolved in anhydrous DMF (2.0 mL). *Tert*-butyl (*S*)-(1-aminopropan-2-yl)carbamate **130** (89.0 mg, 0.508 mmol, 1.2 eq.) and DIPEA (147 µL, 0.847 mmol, 2.0 eq.) were added. The reaction mixture was stirred at 80 °C for 17 h. The reaction mixture was cooled to rt and partitioned between ethyl acetate and water. The aqueous layer was extracted with ethyl acetate (3 × 10 mL). The combined organic layers were dried over $MgSO_{4\ (s)}$, filtered, then the filtrate was concentrated *in vacuo*. The residue was purified by flash column chromatography eluting with petroleum ether : ethyl acetate (1:0 to 1:1) to yield *tert*-butyl (*S*)-(1-((4-(3,5-dimethylisoxazol-4-yl)-2-nitrophenyl)amino)propan-2-yl)carbamate **133** (123 mg, 62%) as an orange oil: R_f 0.58 (ethyl acetate : petroleum ether, 1:1); $[\alpha]_D^{25}$= +7.98 (*c* 1.0, $CHCl_3$); ν_{max} (thin film)/ cm^{-1} 3368 (N-H, m), 1702 (C=O, s), 1622 (N-H, m), 1530 (N-O, s) 1227 (C-N, m), 1165 (C-O, m); ^{1}H NMR (400 MHz, $CDCl_3$) δ 8.35 (1H, t, *J* 4.6, $C^{1'}$N-H), 8.07 (1H, d, *J* 2.2, $C^{3'}$-H), 7.35 (1H, dd, *J* 9.0, 2.2, $C^{5'}$-H), 7.14 (1H, d, *J* 9.0, $C^{6'}$-H), 4.54 (1H, d, *J* 4.9, OC^{10}N-H), 4.00 (1H, m, C^9-H), 3.55-3.42 (1H, m, C^8-H_a), 3.39-3.32 (1H, m, C^8-H_b), 2.40 (3H, s, C^6-H_3), 2.26 (3H, s, C^7-H_3), 1.45 (9H, s, C^{11}-$(CH_3)_3$), 1.26 (3H, d, *J* 6.2, C^{15}-H_3); ^{13}C NMR (101 MHz, $CDCl_3$) δ 165.4 (C^5), 158.6 (C^3), 156.1 (C^{10}), 144.7 ($C^{1'}$), 136.9 ($C^{5'}$), 132.0 ($C^{2'}$), 127.0 ($C^{3'}$), 117.7 ($C^{4'}$), 114.9 (C^4), 114.7 ($C^{6'}$), 48.5 (C^8), 45.5 (C^9), 28.4 (C^{12}, C^{13}, C^{14}), 22.0 (C^{15}), 11.6 (C^6), 10.8 (C^7); LRMS *m/z* (ESI$^-$) 389 ([M-H]$^-$, 100%); HRMS *m/z* (ESI$^+$) [Found: 391.1984, $C_{19}H_{27}N_4O_5$ requires [M+H]$^+$ 391.1976)]; Analytical HPLC (RP, *Method 2*) rt 10.4 min, purity 100%.

(2*S*)-*N*^{1}-[4-(3,5-Dimethyl-1,2-oxazol-4-yl)-2-nitrophenyl]propane-1,2-diamine 134

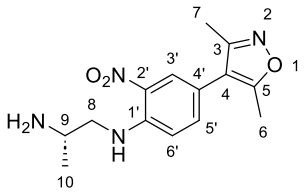

Tert-butyl (*S*)-(1-((4-(3,5-dimethylisoxazol-4-yl)-2-nitrophenyl)amino)propan-2-yl)carbamate **133** (300 mg, 0.768 mmol, 1.0 eq.) was dissolved in CH_2Cl_2 (1.5 mL). Trifluoroacetic acid (1.5 mL) was slowly added. The reaction mixture was stirred at rt for 2 h then slowly poured into a saturated solution of $NaHCO_3$. The organic phase was separated then the aqueous layer was extracted with CH_2Cl_2 (3 × 20 mL). The combined organic layers were washed with brine, dried over $MgSO_{4\,(s)}$, filtered, then the filtrate was concentrated *in vacuo*. The residue was purified by flash column chromatography eluting with CH_2Cl_2 : methanol (1:0 to 9:1) to yield (2*S*)-*N*^{1}-[4-(3,5-dimethyl-1,2-oxazol-4-yl)-2-nitrophenyl]propane-1,2-diamine **134** (240 mg, 54%) as an orange oil: R_f 0.21 (CH_2Cl_2 : methanol: Et_3N, 98:2:0.1); $[\alpha]_D^{25}$= +8.83 (*c* 1.0, $CHCl_3$); ^{1}H NMR (400 MHz, MeOD) δ 8.12 (1H, d, *J* 2.2, C$^{3'}$-H), 7.53 (1H, dd, *J* 8.8, 2.2, C$^{5'}$-H), 7.21 (1H, d, *J* 8.8, C$^{6'}$-H), 3.65-3.49 (3H, m, C^{8}-H$_2$, C^{9}-H), 2.41 (3H, s, C^{6}-H$_3$), 2.25 (3H, s, C^{7}-H$_3$); LRMS *m/z* (ESI$^+$) 291 ([M+H]$^+$, 100%). The spectroscopic data are in good agreement with the literature.[69]

(*S*)-4-(3,5-Dimethylisoxazol-4-yl)-*N*-(2-morpholinopropyl)-2-nitroaniline 129

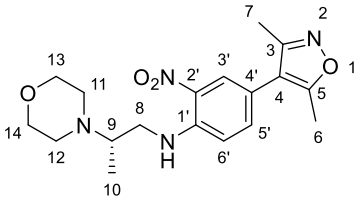

(2*S*)-*N*^{1}-[4-(3,5-Dimethyl-1,2-oxazol-4-yl)-2-nitrophenyl]propane-1,2-diamine **134** (150 mg, 0.52 mmol, 1.0 eq.) was dissolved in DMF (3.0 mL). K_2CO_3 (214 mg, 1.55 mmol, 3.0 eq.) and 2-bromoethyl ether (71.4 μL, 0.57 mmol, 1.0 eq.) were added. The reaction mixture was stirred at 80 °C for 3 h. The reaction was cooled to rt then partitioned between ethyl acetate and water. The organic phase was separated then the aqueous layer was extracted with ethyl acetate (3 × 20 mL). The combined organic layers were washed with brine, dried over $MgSO_{4\,(s)}$, filtered, then the filtrate was concentrated

in vacuo. The residue was purified by flash column chromatography eluting with *c*-hexane : acetone (1:0 to 2:3) to yield (*S*)-4-(3,5-dimethylisoxazol-4-yl)-*N*-(2-morpholinopropyl)-2-nitroaniline **129** (40 mg, 22%) as an orange solid: R_f 0.55 (*c*-hexane : acetone, 1:0 to 2:3); $[\alpha]_D^{25}$= +43.5 (*c* 1.0, $CHCl_3$); m.p. 164-165 °C ($CDCl_3$) [lit.[69]126-129 °C]; ^{1}H NMR (400 MHz, $CDCl_3$) δ 8.86 (1H, d, *J* 5.9, N-H), 8.09 (1H, d, *J* 2.2, C$^{3'}$-H), 7.32 (1H, dd, *J* 8.8, 2.2, C$^{5'}$-H), 6.88 (1H, d, *J* 8.8, C$^{6'}$-H), 3.89-3.69 (4H, m, C^{13}-H_2, C^{14}-H_2), 3.32 (1H, ddd, *J* 11.5, 5.6, 5.6, C^8-H_a), 3.13 (1H, ddd, *J* 12.2, 9.9, 2.3, C^8-H_b), 3.07-2.96 (1H, m, C^9-H), 2.73-2.60 (2H, m, C^{11}-H_a, C^{12}-H_a), 2.55-2.46 (2H, m, C^{11}-H_b, C^{12}-H_b), (3H, s, C^6-H_3), 2.26 (3H, s, C^7-H_3); LRMS *m/z* (ESI$^+$) 361 ([M+H]$^+$, 100%). The spectroscopic data are in good agreement with the literature.[69]

(*S*)-4-(1-(5-(3,5-Dimethylisoxazol-4-yl)-2-ethyl-1*H*-benzo[*d*]imidazol-1-yl)propan-2-yl)morpholine 107

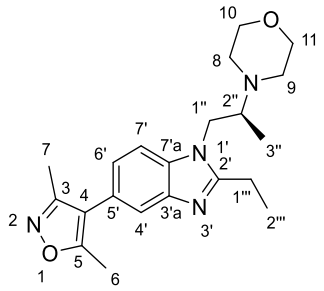

1M $Na_2S_2O_{4\,(aq)}$ (361 µL, 0.361 mmol, 5.2 eq.) was added to (*S*)-4-(3,5-dimethylisoxazol-4-yl)-*N*-(2-morpholinopropyl)-2-nitroaniline **129** (25.0 mg, 0.069 mmol, 1.0 eq.) in EtOH (400 µL). The reaction mixture was stirred at 80 °C for 10 min. The reaction mixture was cooled to rt then the solvent was evaporated *in vacuo.* The residue was partitioned between 10% aq. ammonia solution and ethyl acetate. The aqueous layer was separated then extracted with ethyl acetate (3 × 10 mL). The combined organic layers were dried over $MgSO_{4\,(s)}$, filtered, then the filtrate was concentrated *in vacuo*. The residue was dissolved in ethyl acetate (1 mL). Propanoic acid (4.5 µL, 0.061 mmol, 1.0 eq.), 50 wt. % T3P in ethyl acetate (185 µL, 0.317 mmol, 5.2 eq.) and DIPEA (23.2 µL, 0.133 mmol, 2.2 eq.) were added. The reaction mixture was stirred at 80 °C for 17 h. The reaction was cooled to rt and sat. aq. $NaHCO_3$ was added. The organic layer was separated then the aqueous layer was extracted with ethyl acetate (3 × 10 mL). The combined organic layers were dried over $MgSO_{4\,(s)}$, filtered, then the filtrate was concentrated *in vacuo*. The residue was dissolved in toluene (1 mL) and refluxed at

110 °C for 17 h in a microwave vial containing 3 Å molecular sieves. The reaction mixture was cooled to rt, filtered then the solvent was evaporated *in vacuo.* The residue was purified by column chromatography eluting with petroleum ether : ethyl acetate (1:0 to 0:1) then ethanol (100%) to yield (*S*)-4-(1-(5-(3,5-dimethylisoxazol-4-yl)-2-ethyl-1*H*-benzo[*d*]imidazol-1-yl)propan-2-yl)morpholine **107** (5 mg, 23%) as a yellow oil: R_f 0.30 (CH_2Cl_2 : methanol, 9:1); $[\alpha]_D^{25}$= +15.5 (*c* 1.0, $CHCl_3$); ν_{max} (thin film)/ cm^{-1} 1614 (C=C, w), 1483 (C-H, w); ^{1}H NMR (400 MHz, $CDCl_3$) δ 7.62 (1H, dd, *J* 1.6, 0.6, $C^{4'}$-H), 7.33 (1H, dd, *J* 8.3, 0.6, $C^{7'}$-H), 7.10 (1H, dd, *J* 8.3, 1.6, $C^{6'}$-H), 4.26 (1H, dd, *J* 14.5, 6.4, $C^{1''}$-H_a), 3.96 (1H, dd, *J* 14.5, 7.4, $C^{1''}$-H_b), 3.76-3.63 (4H, m, C^{10}-H_2, C^{11}-H_2), 3.11-3.01 (1H, dtd, *J* 14.1, 7.4, 7.0, $C^{2''}$-H), 3.01-2.85 (2H, m, $C^{1'''}$-H_a, $C^{1'''}$-H_b), 2.75-2.65 (2H, m, C^8-H_a, C^9-H_a), 2.59-2.48 (2H, m, C^8-H_b, C^9-H_b), 2.41 (3H, s, C^6-H_3), 2.28 (3H, s, C^7-H_3), 1.51 (3H, t *J* 7.5, $C^{2'''}$-H_3), 1.05 (3H, d, *J* 6.8, $C^{3''}$-H_3); ^{13}C NMR (101 MHz, $CDCl_3$) δ 165.1 (C^5), 159.2 (C^3), 157.5 ($C^{2'}$), 143.1 ($C^{3'a}$), 134.9 ($C^{7'a}$), 124.2 ($C^{5'}$), 123.4 ($C^{6'}$), 120.1 ($C^{4'}$), 117.3 (C^4), 109.7 ($C^{7'}$), 67.3 (C^{10}, C^{11}), 59.6 ($C^{2''}$), 49.6 (C^8, C^9), 47.0 ($C^{1''}$), 21.1 ($C^{1'''}$), 12.5 ($C^{3''}$), 11.8 ($C^{2'''}$), 11.7 (C^6), 10.9 (C^7); LRMS *m/z* (ESI^+) 369 ($[M+H]^+$, 100%); HRMS *m/z* (ESI^+) [Found: 369.2276, $C_{21}H_{28}N_4O_2$ requires $[M+H]^+$ 369.2285)]; Analytical HPLC (RP, *Method 3*) rt 5.5 min, purity 100%

4-(3,5-Dimethyl-1,2-oxazol-4-yl)-*N*-methyl-2-nitroaniline 75

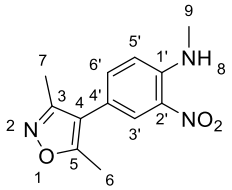

4-(4-Fluoro-3-nitrophenyl)-3,5-dimethylisoxazole **74** (3.00 g, 12.7 mmol, 1.0 eq.) and methylamine hydrochloride (1.72 g, 25.4 mmol, 2.0 eq.) were combined in NMP (18.0 mL). DIPEA (11.1 mL, 65.5 mmol, 5.0 eq.) was added then the reaction mixture was stirred at 80 °C for 2 h. The reaction mixture was cooled to rt then partitioned between ethyl acetate and water. The aqueous layer was extracted with ethyl acetate (3 × 50 mL). The combined organic layers were washed with 10% w/v LiCl aq. (3 × 30 mL) dried over $MgSO_{4\,(s)}$, filtered, then the filtrate was concentrated *in vacuo*. The residue was purified by silica column chromatography eluting with petroleum ether : ethyl acetate (1:0 to 1:4) to yield 4-(3,5-dimethyl-1,2-oxazol-4-yl)-*N*-methyl-2-nitroaniline **75** (3.10 g, 99%) as an orange solid: R_f 0.48 (petroleum ether : ethyl acetate,

1:1); m.p. 136-137 °C ($CDCl_3$); ν_{max} (thin film)/ cm^{-1} 3398 (N-H, m), 1625 (N-H, m), 1531 (N-O, s), 1356 (C-N, s), 1264 (C-N, s), 1228 (C-N, m), 1181 (C-N, s); ^1H NMR (400 MHz, $CDCl_3$) δ 8.11 (2H, br s, $C^{3'}$-H, N-H), 7.40 (1H, dd, *J* 8.8, 2.2, $C^{6'}$-H), 6.96 (1H, d, *J* 8.8, $C^{5'}$-H), 3.10 (3H, d, *J* 3.8, C^9-H_3), 2.43 (3H, s, C^6-H_3), 2.29 (3H, s, C^7-H_3); ^{13}C NMR (101 MHz, $CDCl_3$) δ 165.4 (C^5), 158.6 (C^3), 148.6 ($C^{2'}$), 145.5 ($C^{1'}$), 136.9 ($C^{6'}$), 126.9 ($C^{3'}$), 117.4 ($C^{4'}$), 114.1 (C^4), 29.8 (C^9), 11.6 (C^6), 10.8 (C^7); LRMS *m/z* (ESI^+) 248 ([M+H^+], 100%); HRMS *m/z* (ESI^+) [Found: 248.1019, $C_{12}H_{12}O_3N_3$ requires $[M+H]^+$ 248.1030)]; Analytical HPLC (RP, *Method 2*) rt 9.4 min, purity 100%.

4-(3,5-Dimethylisoxazol-4-yl)-*N*^{1}-methylbenzene-1,2-diamine 76

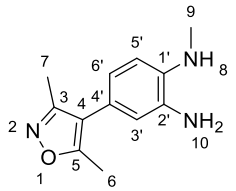

4-(3,5-Dimethyl-1,2-oxazol-4-yl)-*N*-methyl-2-nitroaniline **75** (3.21 g, 0.016 mmol, 1.0 eq.) was dissolved in EtOH (120 mL) then the solvent was degassed for 30 min. 10 wt. % Palladium on carbon (321 mg, 10 wt. % of substrate) was added then the reaction mixture was stirred at rt under $H_{2\,(g)}$ for 18 h. The reaction mixture was filtered through Celite® eluting with ethyl acetate. The filtrate was washed with water then the organic layer was dried over $MgSO_{4\,(s)}$, filtered, then the filtrate was concentrated *in vacuo*. The residue was purified by silica column chromatography eluting with petroleum ether : ethyl acetate (1:0 to 0:1) to yield 4-(3,5-dimethylisoxazol-4-yl)-*N*^{1}-methylbenzene-1,2-diamine **76** (1.33 g, 38%) as a yellow solid: R_f 0.27 (petroleum ether : ethyl acetate, 1:1); m.p. 154-156 °C ($CDCl_3$); ν_{max} (thin film)/ cm^{-1} 3321 (N-H, m), 1528 (N-H, m), 1309 (C-N, s), (C-N, m), 1214 (C-N, m); ^1H NMR (400 MHz, $CDCl_3$) δ 6.73 (1H, dd, *J* 8.0, 1.9, $C^{6'}$-H), 6.70 (1H, d, *J* 8.0, $C^{5'}$-H), $C^{3'}$-H), 3.39 (3H, br s, N-H, N-H_2), 2.90 (3H, s, C^9-H_3), 2.38 (3H, s, C^6-H_3), 2.25 (3H, s, C^7-H_3); ^{13}C NMR (101 MHz, $CDCl_3$) δ 164.6 (C^5), 159.2 (C^3), 138.6 ($C^{2'}$), 134.3 ($C^{1'}$), 121.9 ($C^{6'}$), 120.3 ($C^{4'}$), 117.0 ($C^{5'}$), 116.9 (C^4), 111.0 ($C^{3'}$), 31.0 (C^9), 11.7 (C^6), 11.0 (C^7); LRMS *m/z* (ESI^+) 218 ([M+H^+], 100%); HRMS *m/z* (ESI^+) [Found: 218.1278, $C_{12}H_{14}N_3O$ requires $[M+H]^+$ 218.1288)]; Analytical HPLC (RP, *Method 2*) rt 6.1 min, purity 100%.

***N*-(5-(3,5-Dimethylisoxazol-4-yl)-2-(methylamino)phenyl)-3-phenylpropanamide 197**

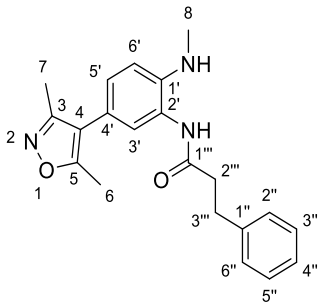

4-(3,5-Dimethylisoxazol-4-yl)-N^1-methylbenzene-1,2-diamine **76** (100 mg, 0.462 mmol, 1.0 eq.) was dissolved in DMF (1.0 mL). 3-Phenylpropanoic acid (72.1 mg, 0.485 mmol, 1.05 eq.) and HATU (185 mg, 0.485 mmol, 1.05 eq.) were added. The reaction mixture was stirred at rt for 17 h. The solvent was evaporated *in vacuo.* The residue was re-dissolved in ethyl acetate (10 mL) and sat. aq. $NaHCO_3$ (5 mL) was added. The organic layer was separated then the aqueous layer was extracted with ethyl acetate (3 × 10 mL). The combined organic layers were washed with brine, dried over $MgSO_{4\ (s)}$, filtered, then the filtrate was concentrated *in vacuo*. The residue was purified by flash column chromatography eluting with CH_2Cl_2 : methanol (1:0 to 9:1) to yield *N*-(5-(3,5-dimethylisoxazol-4-yl)-2-(methylamino)phenyl)-3-phenylpropanamide **197** (66 mg, 41%) as a brown oil: R_f 0.60 (CH_2Cl_2 : methanol, 9:1); ^{1}H NMR (400 MHz, $CDCl_3$) δ 7.65 (1H, dd, *J* 1.5, 0.7, $C^{3'}$-H), 7.37-7.21 (6H, m, $C^{6'}$-H, $C^{2''}$-H, $C^{3''}$-H, $C^{4''}$-H, $C^{5''}$-H, $C^{6''}$-H), 7.15 (1H, dd, *J* 8.2, 1.5, $C^{5'}$-H), 3.58 (3H, s, C^8-H_3), 3.28-3.18 (4H, m, $C^{2'''}$-H_2, $C^{3'''}$-H_2), 2.44 (3H, s, C^6-H_3), 2.31 (3H, s, C^7-H_3); LRMS *m/z* (ESI^+) 332 ($[M+2H-CH_3]^+$, 100%).

3,5-Dimethyl-4-(1-methyl-2-phenethyl-1*H*-benzo[*d*]imidazol-5-yl)isoxazole 137

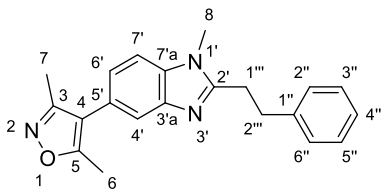

N-(5-(3,5-Dimethylisoxazol-4-yl)-2-(methylamino)phenyl)-3-phenylpropanamide **197** (60 mg, 0.17 mmol, 1.0 eq.) and 3-phenylpropanoic acid (26 mg, 0.17 mmol, 1.0 eq.) were combined in toluene (700 μL) in a microwave vial containing 3 Å molecular sieves. The reaction mixture was stirred at 120 °C for 18 h. The reaction mixture was cooled to

rt, filtered and then the solvent evaporated *in vacuo*. The residue was purified by RP flash column chromatography eluting with water : acetonitrile (95:5 to 5:95) to yield 3,5-dimethyl-4-(1-methyl-2-phenethyl-1*H*-benzo[*d*]imidazol-5-yl)isoxazole **137** (22 mg, 38%) as a colourless solid: R_f 0.21 (petroleum ether : ethyl acetate, 3:7); m.p. 140-142 °C ($CDCl_3$); ν_{max} (thin film)/ cm^{-1} 1507 (N-O, w), 1420 (C-H, m), 1317 (C-N, s) 1032 (C-N, m); ^1H NMR (400 MHz, $CDCl_3$) δ 7.65 (1H, d, *J* 1.6, $C^{4'}$-H), 7.39-7.22 (6H, m, $C^{7'}$-H, $C^{2''}$-H, $C^{3''}$-H, $C^{4''}$-H, $C^{5''}$-H, $C^{6''}$-H), 7.15 (1H, dd, *J* 8.2, 1.6, $C^{6'}$-H), 3.60 (3H, s, C^8-H_3), 3.36-3.14 (4H, m, $C^{1'''}$-H_2, $C^{2'''}$-H_2), 2.44 (3H, s, C^6-H_3), 2.31 (3H, s, C^7-H_3); ^{13}C NMR (101 MHz, $CDCl_3$) δ 165.0 (C^5), 159.0 (C^3), 155.4 ($C^{2'}$), 142.9 ($C^{3'a}$), 140.7 ($C^{1''}$), 135.1 ($C^{7'a}$), 128.7 ($C^{2'''}$, $C^{6''}$), 128.4 ($C^{3''}$, $C^{5''}$), 126.5 ($C^{4''}$), 124.2 ($C^{5'}$), 123.4 ($C^{6'}$), 119.8 ($C^{4'}$), 117.2 (C^4), 109.3 ($C^{7'}$), 34.0 ($C^{2'''}$), 29.7 ($C^{1'''}$), 29.7 (C^8), 11.6 (C^6), 10.9 (C^7); LRMS *m/z* (ESI^+) 332 ($[M+H]^+$, 100%); HRMS *m/z* (ESI^+) [Found: 332.1759, $C_{21}H_{21}N_3O$ requires $[M+H]^+$ 332.1757)]; Analytical HPLC (RP, *Method 1*) rt 7.7 min, purity 100%.

_N_-(5-(3,5-Dimethylisoxazol-4-yl)-2-(methylamino)phenyl)-3-(*m*-tolyl)propanamide 198

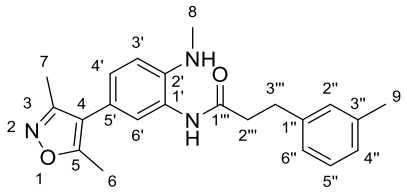

3-(3-(Methylphenyl)propanoic acid (34.3 mg, 0.209 mmol, 1.0 eq.), HATU (79.5 mg, 0.209 mmol, 1.0 eq.) and DIPEA (72.9 µL, 0.418 mmol, 2.0 eq.) were combined in anhydrous DMF (1.0 mL). 4-(3,5-Dimethylisoxazol-4-yl)-N^1-methylbenzene-1,2-diamine **76** (50.0 mg, 0.230 mmol, 1.1 eq.) in anhydrous DMF (500 µL) was added. The reaction mixture was stirred at rt for 17 h. The solvent was evaporated *in vacuo.* The residue was re-dissolved in ethyl acetate (10 mL) and water (5 mL) was added. The organic layer was separated, then the aqueous layer was extracted with ethyl acetate (3 × 10 mL). The combined organic layers were washed with 10% w/v $LiCl_{(aq)}$ (3 × 10 mL), dried over $MgSO_{4\,(s)}$, filtered, then the filtrate was concentrated *in vacuo*. The residue was purified by flash column chromatography eluting with CH_2Cl_2 : methanol (1:0 to 9:1) to yield *N*-(5-(3,5-dimethylisoxazol-4-yl)-2-(methylamino)phenyl)-3-(*m*-tolyl)propanamide **198** (73 mg, 87%) as an off-white solid: R_f 0.44 (CH_2Cl_2 :

methanol, 9:1); ^{1}H NMR (400 MHz, $CDCl_3$) δ 7.20 (1H, dd, *J* 7.5, 7.5, $C^{5''}$-H), 7.13 (1H, *br* s, $C^{2'}$N-H), 7.10-6.98 (4H, m, $C^{6'}$-H, $C^{2''}$-H, $C^{4''}$-H, $C^{6''}$-H), 6.99 (1H, dd, *J* 8.3, 2.1, $C^{4'}$-H), 6.70 (1H, d, *J* 8.3, $C^{3'}$-H), 3.02 (2H, t, *J* 7.2, $C^{3'''}$-H_2), 2.76-2.67 (2H, m, $C^{2'''}$-H_2), 2.73 (3H, s, C^{9}-H_3), 2.34 (3H, s, C^{6}-H_3), 2.31 (3H, s, C^{8}-H_3), 2.21 (3H, s, C^{7}-H_3); LRMS *m/z* (ESI^+) 364 ($[M+H]^+$, 100%).

3,5-Dimethyl-4-(1-methyl-2-(3-methylphenethyl)-1*H*-benzo[*d*]imidazol-5-yl)isoxazole 121

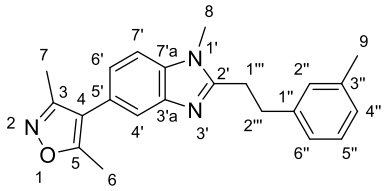

N-(5-(3,5-Dimethylisoxazol-4-yl)-2-(methylamino)phenyl)-3-(*m*-tolyl)propanamide **198** (70.0 mg, 0.193 mmol, 1.0 eq.) was refluxed in toluene (1.0 mL) in a microwave vial containing 3 Å molecular sieves for 24 h. The reaction mixture was cooled to rt, filtered, then the solvent was evaporated *in vacuo.* The residue was purified by flash column chromatography eluting with CH_2Cl_2 : methanol (1:0 to 9:1) to yield 3,5-dimethyl-4-(1-methyl-2-(3-methylphenethyl)-1*H*-benzo[*d*]imidazol-5-yl)isoxazole **121** (45 mg, 68%) as a colourless solid: R_f 0.50 (CH_2Cl_2 : methanol, 9:1); m.p. 120-121 °C ($CDCl_3$); ν_{max} (thin film)/ cm^{-1} 1512 (N-O, m), 1485 (C-H, m), 1444 (C-H, m), 1422 (C-H, m), 1322 (C-N, s), 1245 (C-N, m); ^{1}H NMR (600 MHz, $CDCl_3$) δ 7.62 (1H, dd, *J* 1.6, 0.7, $C^{4'}$-H), 7.33 (1H, dd, *J* 8.3, 0.7, $C^{7'}$-H), 7.19 (1H, td, *J* 7.3, 0.8, $C^{5''}$-H), 7.13 (1H, dd, *J* 8.2, 1.6, $C^{6'}$-H), 7.08-7.00 (3H, m, $C^{2''}$-H, $C^{4''}$-H, $C^{6''}$-H), 3.61 (3H, s, C^{8}-H_3), 3.25-3.13 (4H, m, $C^{1'''}$-H_2, $C^{2'''}$-H_2), 2.41 (3H, s, C^{6}-H_3), 2.32 (3H, s, C^{9}-H_3), 2.29 (3H, s, C^{7}-H_3); ^{13}C NMR (151 MHz, $CDCl_3$) δ 165.1 (C^{5}), 159.1 (C^{3}), 155.6 ($C^{2'}$), 143.1 ($C^{3'a}$), 140.8 ($C^{1''}$), 138.4 ($C^{3''}$), 135.3 ($C^{7'a}$), 129.3 ($C^{4''}$), 128.7 ($C^{5''}$), 127.3 ($C^{2''}$), 125.5 ($C^{6''}$), 124.2 (C^{4}), 123.5 ($C^{6'}$), 119.9 ($C^{4'}$), 117.3 (C^{4}), 109.3 ($C^{7'}$), 34.0 ($C^{1'''}$), 29.9 ($C^{1'''}$), 29.8 (C^{8}), 21.5 (C^{9}), 11.6 (C^{6}), 11.0 (C^{7}); LRMS *m/z* (ESI^+) 346 ($[M+H]^+$, 100%); HRMS *m/z* (ESI^+) [Found: 368.1745, $C_{22}H_{23}ON_3$ requires $[M+Na]^+$ 368.1733)]; Analytical HPLC (RP, *Method 3*) rt 7.6 min, purity 100%.

4-(2-(3-Fluorophenethyl)-1-methyl-1*H*-benzo[*d*]imidazol-5-yl)-3,5-dimethylisoxazole 122

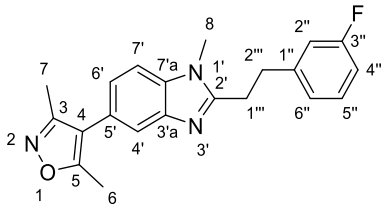

4-(3,5-Dimethylisoxazol-4-yl)-N^1-methylbenzene-1,2-diamine **76** (100 mg, 0.460 mmol, 1.0 eq.) was dissolved in DMF (2.0 mL). DIPEA (240 µL, 1.37 mmol, 3.0 eq.), 3-(3-fluorophenyl)-propionic acid (98.0 mg, 0.552 mmol, 1.2 eq.) and HATU (350 mg, 0.920 mmol, 2.0 eq.) were added. The reaction mixture was stirred at rt for 16 h. The reaction mixture was diluted with diethyl ether and partitioned with the addition of water. The layers were separated then the aqueous layer was extracted with diethyl ether. The organic layer was dried with $MgSO_{4\,(s)}$, then filtered, then the filtrate was concentrated *in vacuo*. The residue was dissolved in acetic acid (0.5 mL) and 3-(3-fluorophenyl)-propionic acid (82.0 mg, 0.488 mmol, 1.05 eq.) was added. The reaction mixture was stirred at 90 °C for 32 h. The reaction mixture was cooled to rt then the solvent was evaporated *in vacuo*. The crude product was purified by flash column chromatography eluting with ethyl acetate : petroleum ether (1:0 to 1:0) to yield 4-(2-(3-fluorophenethyl)-1-methyl-1*H*-benzo[*d*]imidazol-5-yl)-3,5-dimethylisoxazole **122** (31 mg, 19%) as a colourless oil: R_f 0.61 (ethyl acetate); ν_{max} (thin film)/ cm^{-1} 1513 (C-H, w), 1424 (C-H, m), 1312 (C-F, s), 1243 (C-O, s); ^{1}H NMR (600 MHz, $CDCl_3$) δ 7.62 (1H, dd, *J* 1.6, 0.7, $C^{4'}$-H), 7.34 (1H, dd, *J* 8.3, 0.7, $C^{7'}$-H), 7.29-7.23 (1H, m, $C^{5''}$-H), 7.14 (1H, dd, *J* 8.3, 1.6, $C^{6'}$-H), 7.02 (1H, ddd, *J* 7.6, 1.6, 0.9, $C^{6''}$-H), 6.98-6.90 (2H, m, $C^{2''}$-H, $C^{4''}$-H), 3.64 (3H, s, C^8-H_3), 3.30-3.24 (2H, m, $C^{2'''}$-H_2), 3.22-3.16 (2H, m, $C^{1'''}$-H_2), 2.42 (3H, s, C^6-H_3), 2.29 (3H, s, C^7-H_3); ^{13}C NMR (151 MHz, $CDCl_3$) δ 165.0 (C^5), 163.0 (d, *J* 246.2, $C^{3''}$), 159.0 (C^3), 155.0 ($C^{2'}$), 143.2 (d, *J* 7.1, $C^{1''}$), 142.9 ($C^{3'a}$), 135.2 ($C^{7'a}$), 130.1 (d, *J* 8.4, $C^{5''}$), 124.2 ($C^{5'}$), 124.1 (d, *J* 2.8, $C^{6''}$), 123.5 ($C^{6'}$), 119.9 ($C^{4'}$), 117.2 (C^4), 115.3 (d, *J* 21.2, $C^{2''}$), 113.3 (d, *J* 21.1, $C^{4''}$), 109.3 ($C^{7'}$), 33.5 (d, *J* 1.7, $C^{2'''}$), 29.7 (C^8), 29.3 ($C^{2'''}$), 11.6 (C^6), 10.9 (C^7); ^{19}F NMR (565 MHz, $CDCl_3$) δ -113.12 (td, *J* 9.0, 6.0, $C^{3''}$-F); LRMS *m/z* (ESI^+) 351 ($[M+2H]^+$, 100%); HRMS *m/z* (ESI^+) [Found: 350.1662, $C_{21}H_{20}FN_3O$ requires $[M+H]^+$ 350.1663)]; Analytical HPLC (RP, *Method 1*) rt 8.3 min, purity 100%.

3-(3-Chlorophenyl)propanoyl chloride 199

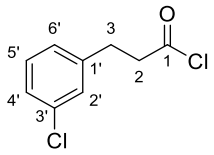

To a stirred solution of 3-(3-chlorophenyl)propanoic acid (200 mg, 1.08 mmol, 1.0 eq.) in CH_2Cl_2 (5.0 mL) was added DMF (20 µL). The reaction mixture was cooled to 0 °C and oxalyl chloride (186 µL, 2.17 mmol, 2.0 eq.) was dropwise added. The reaction mixture was warmed to rt then stirred for 2.5 h. The volatile components were evaporated *in vacuo* then the compound carried forward as crude.

3-(3-Chlorophenyl)-*N*-(5-(3,5-dimethylisoxazol-4-yl)-2-(methylamino)phenyl)propenamide 200

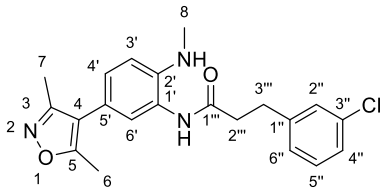

3-(3-Chlorophenyl)propanoyl chloride **199** (185 mg, 1.00 mmol, 1.05 eq.) was dissolved in CH_2Cl_2 (5.0 mL) and Et_3N (265 µL, 1.90 mmol, 2.0 eq.) was added. The reaction mixture was cooled to 0 °C and 4-(3,5-dimethylisoxazol-4-yl)-N^1-methylbenzene-1,2-diamine **76** (207 mg, 0.952 mmol, 1.0 eq.) was added dropwise. The reaction mixture was stirred at rt for 2.5 h. The reaction mixture was concentrated *in vacuo* then the residue was purified by flash column chromatography eluting with petroleum ether : ethyl acetate (1:0 to 3:7) to yield 3-(3-chlorophenyl)-*N*-(5-(3,5-dimethylisoxazol-4-yl)-2-(methylamino)phenyl)propenamide **200** (92 mg, 25%) as a yellow oil: R_f 0.16 (petroleum ether : ethyl acetate, 1:1); ^{1}H NMR (400 MHz, $CDCl_3$) δ 7.25-7.05 (5H, m, $C^{6'}$-H, $C^{2"}$-H, $C^{4"}$-H, $C^{5"}$-H, $C^{6"}$-H), 7.00 (1H, dd, *J* 8.1, 2.0, $C^{4'}$-H), 6.90 (1H, d, *J* 8.1, $C^{3'}$-H), 2.94 (3H, d, *J* 4.7, C^8-H_3), 2.85 (2H, t, *J* 7.2, $C^{3'''}$-H_2), 2.62 (2H, t, *J* 7.2, $C^{2'''}$-H_2), 2.49 (3H, s, C^6-H_3), 2.35 (3H, s, C^7-H_3); LRMS *m/z* (ESI^+) 386 ($[M+2+H]^+$, 100%).

4-(2-(3-Chlorophenethyl)-1-methyl-1*H*-benzo[*d*]imidazol-5-yl)-3,5-dimethylisoxazole 149

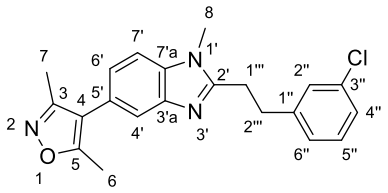

3-(3-Chlorophenyl)-*N*-(5-(3,5-dimethylisoxazol-4-yl)-2-(methylamino)phenyl)propenamide **200** (75 mg, 0.20 mmol, 1.0 e.q.) and 3-(3-chlorophenyl)propanoic acid (36 mg, 0.20 mmol, 1.0 eq.) were combined in toluene (300 µL) in a microwave vial containing 3 Å molecular sieves. The reaction mixture was stirred at 130 °C for 72 h. The reaction mixture was cooled to rt, filtered through a PTFE filter then the solvent was evaporated *in vacuo.* The residue was purified by flash column chromatography eluting with petroleum ether : ethyl acetate (1:0 to 0:1) to yield 4-(2-(3-chlorophenethyl)-1-methyl-1*H*-benzo[*d*]imidazol-5-yl)-3,5-dimethylisoxazole **149** (15 mg, 21%) as a yellow solid: R_f 0.10 (petroleum ether : ethyl acetate, 1:1); m.p. 119-122 °C (EtOAc); ν_{max} (thin film)/ cm^{-1} 1598 (N-H, m), 1424 (C-H, m), 1312 (C-N, s), 783 (C-Cl, s); ^{1}H NMR (400 MHz, $CDCl_3$) δ 7.62 (1H, d, *J* 0.9, $C^{4'}$-H), 7.34 (1H, d, *J* 8.2, $C^{7'}$-H), 7.28-7.18 (3H, m, $C^{2''}$-H, $C^{4''}$-H, $C^{5''}$-H), 7.14 (1H, dd, *J* 8.2, 1.6, $C^{6'}$-H), 7.14-7.09 (1H, m, $C^{6''}$-H), 3.65 (3H, s, C^8-H_3), 3.32-3.10 (4H, m, $C^{1'''}$-H_2, $C^{2'''}$-H_2), 2.42 (3H, s, C^6-H_3), 2.29 (3H, s, C^7-H_3); ^{13}C NMR (101 MHz, $CDCl_3$) δ 165.0 (C^5), 159.0 (C^3), 154.9 ($C^{2'}$), 142.9 ($C^{1''}$), 142.7 ($C^{3'a}$), 135.2 ($C^{3''}$), 134.4 ($C^{7'a}$), 130.0 ($C^{5''}$), 128.5 ($C^{4''}$), 126.7 ($C^{6''}$), 126.7 ($C^{2''}$), 124.2 ($C^{5'}$), 123.6 ($C^{6'}$), 119.9 ($C^{4'}$), 117.2 (C^4), 109.3 ($C^{7'}$), 33.4 ($C^{1'''}$), 29.8 (C^8), 29.3 ($C^{2'''}$), 11.6 (C^6), 10.9 (C^7); LRMS *m/z* (ESI^+) 366 ($[M+H]^+$, 100%); HRMS *m/z* (ESI^+) [Found: 366.1362, $C_{21}H_{21}ClN_3O$ requires $[M+H]^+$ 366.1368)]; Analytical HPLC (RP, *Method 3*) rt 7.8 min, purity 100%.

3-(3-Bromophenyl)-*N*-(5-(3,5-dimethylisoxazol-4-yl)-2-(methylamino)phenyl)propenamide 201

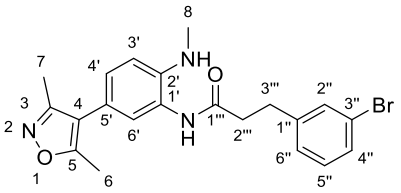

4-(3,5-Dimethylisoxazol-4-yl)-N^1-methylbenzene-1,2-diamine **76** (100 mg, 0.462 mmol, 1.0 eq.) was dissolved in DMF (1.0 mL). 3-(3-Bromophenyl)propanoic acid (111 mg, 0.485 mmol, 1.05 eq.) and HATU (185 mg, 0.485 mmol, 1.05 eq.) were added. The reaction mixture was stirred at rt for 17 h. The solvent was evaporated *in vacuo.* The residue was re-dissolved in ethyl acetate (10 mL) then water (5 mL) was added. The organic layer was separated then the aqueous layer was extracted with ethyl acetate (3 × 10 mL). The combined organic layers were washed with brine, dried over $MgSO_{4\ (s)}$, filtered, then the filtrate was concentrated *in vacuo*. The residue was purified by flash column chromatography eluting with CH_2Cl_2 : methanol (1:0 to 9:1) to yield 3-(3-bromophenyl)-*N*-(5-(3,5-dimethylisoxazol-4-yl)-2-(methylamino)phenyl)propenamide **201** (100 mg, 51%) as a brown oil: R_f 0.60 (CH_2Cl_2 : methanol, 9:1); ^{1}H NMR (400 MHz, $CDCl_3$) δ 8.01 (1H, s, $OC^{1'''}N$-H), 7.63 (1H, dd, *J* 1.6, 0.7, $C^{6'}$-H), 7.42-7.29 (3H, m, $C^{3'}$-H, $C^{2'''}$-H, $C^{4'''}$-H), 7.19-7.10 (3H, m, $C^{4'}$-H, $C^{5'''}$-H, $C^{6'''}$-H), 3.62 (3H, s, C^8-H_3), 2.99-2.90 (3H, m, $C^{3'''}$-H_2), 2.67 (2H, t, *J* 7.7, $C^{2'''}$-H_2), 2.41 (3H, s, C^6-H_3), 2.28 (3H, s, C^7-H_3); LRMS *m/z* (ESI^-) 426 ([M(^{79}Br) -H]$^-$, 100%).

4-(2-(3-Bromophenethyl)-1-methyl-1*H*-benzo[*d*]imidazol-5-yl)-3,5-dimethylisoxazole 150

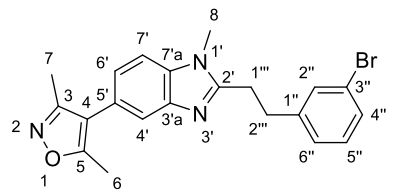

3-(3-Bromophenyl)-*N*-(5-(3,5-dimethylisoxazol-4-yl)-2-(methylamino)phenyl)propenamide **201** (90 mg, 0.21 mmol, 1.0 eq.) and 3-(3-bromophenyl)propanoic acid (48 mg, 0.21 mmol, 1.0 eq.) were combined in toluene (400 µL) in a microwave vial containing 3 Å molecular sieves. The reaction mixture was

stirred at 120 °C for 18 h. The reaction mixture was cooled to rt, filtered then the solvent was evaporated *in vacuo.* The residue was purified by RP flash column chromatography eluting with water : acetonitrile (95:5 to 5:95) to yield 4-(2-(3-bromophenethyl)-1-methyl-1*H*-benzo[*d*]imidazol-5-yl)-3,5-dimethylisoxazole **150** (33 mg, 39%) as a colourless solid: R_f 0.38 (petroleum ether : ethyl acetate, 3:7); m.p. 122-123 °C ($CDCl_3$); ν_{max} (thin film)/ cm^{-1} 1420 (C-H, m), 1312 (C-N, s), 697 (C-Br); ^1H NMR (400 MHz, $CDCl_3$) δ 7.62 (1H, dd, *J* 1.6, 0.7, $C^{4'}$-H), 7.41 (1H, m, $C^{2''}$-H), 7.37 (1H, ddd, *J* 5.7, 3.4, 2.0, $C^{4''}$-H), 7.34 (1H, dd, *J* 8.2, 0.7, $C^{7'}$-H), 7.17 (2H, m, $C^{5''}$-H, $C^{6''}$-H), 7.14 (1H, dd, *J* 8.2, 1.6, $C^{6'}$-H), 3.65 (3H, s, C^8-H_3), 3.33-3.08 (4H, m, $C^{1'''}$-H_2, $C^{2'''}$-H_2), 2.42 (3H, s, C^6-H_3), 2.29 (3H, s, C^7-H_3); ^{13}C NMR (101 MHz, $CDCl_3$) δ 165.0 (C^5), 159.0 ($C^{2'}$), 154.9 (C^3), 143.0 ($C^{1''}$), 142.9 ($C^{3'a}$), 135.1 ($C^{7'a}$), 131.5 ($C^{2''}$), 130.2 ($C^{5''}$), 129.7 ($C^{4''}$), 127.1 ($C^{6''}$), 124.2 ($C^{5'}$), 123.6 ($C^{6'}$), 122.7 ($C^{3''}$), 119.9 ($C^{4'}$), 117.1 (C^4), 109.3 ($C^{7'}$), 33.4 ($C^{1'''}$), 29.8 (C^8), 29.3 ($C^{2'''}$), 11.6 (C^6), 10.9 (C^7); LRMS *m/z* (ESI^+) 412 ($[M(^{79}Br)+H]^+$, 100%). HRMS *m/z* (ESI^+) [Found: 412.0844, $C_{21}H_{21}ON_3Br$ requires M+2 412.0842)]; Analytical HPLC (RP, *Method 3*) rt 7.9 min, purity 100%.

3,5-Dimethyl-4-(1-methyl-2-(3-methylphenethyl)-1*H*-benzo[*d*]imidazol-5-yl)isoxazole 120

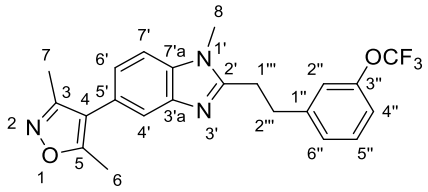

DIPEA (67.6 µL, 0.388 mmol, 1.05 eq.) was added to a mixture of 4-(3,5-dimethylisoxazol-4-yl)-N^1-methylbenzene-1,2-diamine **76** (80.0 mg, 0.370 mmol, 1.0 eq.), 3-(3-(trifluoromethoxy)phenyl)propanoic acid (90.9 mg, 0.388 mmol, 1.05 eq.) and HATU (148 mg, 0.388 mmol, 1.05 eq.) in DMF (0.8 mL). The reaction mixture was stirred at rt for 22 h. The reaction mixture was partitioned between CH_2Cl_2 and sat. aq. $NaHCO_3$. The organic layer was separated then the aqueous layer was extracted with CH_2Cl_2 (3 × 5 mL). The combined organic layers were washed with brine, dried over $MgSO_{4\,(s)}$, filtered, then the filtrate was concentrated *in vacuo*. The residue was purified by flash column chromatography eluting with CH_2Cl_2 : methanol (1:0 to 93:7) to yield *N*-(5-(3,5-dimethylisoxazol-4-yl)-2-(methylamino)phenyl)-3-(*m*-tolyl)propanamide (115 mg) as a yellow oil: R_f 0.50 (CH_2Cl_2 : methanol, 9:1). The amide was refluxed in

acetic acid (1.0 mL) for 72 h. The reaction mixture was cooled to rt then the solvent was evaporated *in vacuo.* The residue was dissolved in ethyl acetate and washed with sat. aq. $NaHCO_3$. The aqueous layer was extracted with ethyl acetate (3 × 5 mL). The combined organic layers were washed with water, dried over $MgSO_{4\,(s)}$, filtered, then the filtrate was concentrated *in vacuo*. The residue was purified by flash column chromatography eluting with CH_2Cl_2 : methanol (1:0 to 9:1) to yield 3,5-dimethyl-4-(1-methyl-2-(3-methylphenethyl)-1*H*-benzo[*d*]imidazol-5-yl)isoxazole **120** (16 mg, 21%) as a colourless solid: R_f 0.60 (CH_2Cl_2 : methanol, 9:1); m.p. 120-122 °C ($CDCl_3$); ν_{max} (thin film)/ cm^{-1} 1424 (C-H, m), 1313 (C-N, s), 1258 (C-O, s), 1214 (C-F, s); ^{1}H NMR (600 MHz, $CDCl_3$) δ 7.62 (1H, d, *J* 1.5, $C^{4'}$-H), 7.36-7.29 (2H, m, $C^{7'}$-H, $C^{5''}$-H), 7.17 (1H, d, *J* 7.6, $C^{6''}$-H), 7.14 (1H, dd, *J* 8.2, 1.5, $C^{6'}$-H), 7.12-7.07 (2H, m, $C^{2''}$-H, $C^{4''}$-H), 3.62 (3H, s, C^8-H_3), 3.29 (2H, dd, *J* 9.2, 6.5, $C^{2'''}$-H_2), 3.19 (2H, dd, *J* 9.2, 6.5, $C^{1'''}$-H_2), 2.42 (3H, s, C^6-H_3), 2.29 (3H, s, C^7-H_3); ^{13}C NMR (151 MHz, $CDCl_3$) δ 165.4 (C^5), 159.4 (C^3), 155.1 ($C^{2'}$), 149.8 (q, *J* 1.6, $C^{3''}$), 143.3 ($C^{1''}$), 143.2 ($C^{3'a}$), 135.5 ($C^{7'a}$), 130.3 ($C^{5''}$), 127.3 ($C^{6''}$), 124.6 ($C^{5'}$), 123.9 ($C^{6'}$), 121.3 ($C^{2''}$), 120.8 (q, *J* 257, C-F_3), 119.4 ($C^{4''}$), 117.5 ($C^{4'}$), 109.7 ($C^{7'}$), 33.9 ($C^{2'''}$), 30.0 (C^8), 29.6 ($C^{1'''}$), 11.9 (C^6), 11.2 (C^7); ^{19}F NMR (565 MHz, $CDCl_3$) δ -57.75 (s, OCF_3); LRMS *m/z* (ESI^+) 434 ($[M+K]^+$, 100%). HRMS *m/z* (ESI^+) [Found: 416.1578, $C_{22}H_{20}F_3N_3O_2$ requires $[M+H]^+$ 416.1580)]; Analytical HPLC (RP, *Method 4*) rt 9.1 min, purity 100%.

_N_-(5-(3,5-Dimethylisoxazol-4-yl)-2-(methylamino)phenyl)-3-(3-methoxyphenyl)propenamide 202

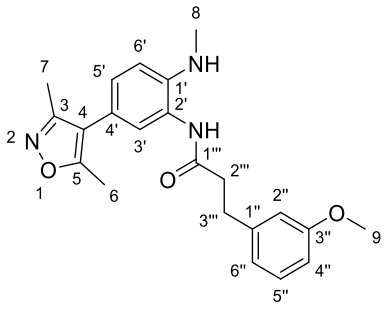

1 M $Na_2S_2O_{4\,(aq)}$ (3.15 mL, 3.15 mmol, 5.2 eq.) was added to 4-(3,5-dimethylisoxazol-4-yl)-*N*-methyl-2-nitroaniline **75** (150 mg, 0.606 mmol, 1.0 eq.) in EtOH (3.15 mL). The reaction mixture was stirred at 80 °C for 10 min. The reaction mixture was cooled to rt and the solvent was evaporated *in vacuo.* The residue was partitioned between 10% aq.

ammonia solution and ethyl acetate. The aqueous layer was separated then extracted with ethyl acetate (3 × 15 mL). The combined organic layers were dried over $MgSO_{4\,(s)}$, filtered, then the filtrate was concentrated *in vacuo*. The residue was dissolved in anhydrous DMF (500 µL) and added to a mixture of 3-(3-methoxyphenyl)propanoic acid (91.4 mg, 0.439 mmol, 1.0 eq.), HATU (167 mg, 0.439 mmol, 1.0 eq.) and DIPEA (153 µL, 0.879 mmol, 2.0 eq.) in anhydrous DMF (1.0 mL). The reaction mixture was stirred at rt for 18 h. The reaction mixture was partitioned between ethyl acetate and water. The organic layer was separated then the aqueous layer was extracted with ethyl acetate (3 × 10 mL). The combined organic layers were washed with brine, dried over $MgSO_{4\,(s)}$, filtered, then the filtrate was concentrated *in vacuo*. The residue was purified by flash column chromatography eluting with CH_2Cl_2 : methanol (1:0 to 9:1) to yield *N*-(5-(3,5-dimethylisoxazol-4-yl)-2-(methylamino)phenyl)-3-(3-methoxyphenyl)propenamide **202** (132 mg, 57%) as a yellow solid: R_f 0.18 (CH_2Cl_2 : methanol, 9:1); m.p. 48-50 °C ($CDCl_3$); ^{1}H NMR (400 MHz, $CDCl_3$) δ 7.25 (1H, dd, *J* 8.0, 8.0, $C^{5"}$-H), 7.04-6.96 (2H, m, $C^{3'}$-H, $C^{5'}$-H), 6.89-6.76 (3H, m, $C^{2"}$-H, $C^{4"}$-H, $C^{6"}$-H), 6.72 (1H, m, $C^{6'}$-H), 3.77 (3H, s, C^9-H_3), 3.05 (2H, t, *J* 7.2, $C^{3'''}$-H_2), 2.76 (3H, s, C^8-H_3), 2.72 (2H, t, *J* 7.2, $C^{2'''}$-H_2), 2.36 (3H, s, C^6-H_3), 2.22 (3H, s, C^7-H_3); ^{13}C NMR (101 MHz, $CDCl_3$) δ 171.3 ($C^{1'''}$), 164.9 (C^5), 160.0 ($C^{3"}$), 159.0 (C^3), 143.0 ($C^{1"}$), 142.2 ($C^{1'}$), 129.9 ($C^{5"}$), 128.3 ($C^{5'}$), 126.5 ($C^{3'}$), 123.5 ($C^{2'}$), 120.9 ($C^{6"}$), 119.3 ($C^{4'}$), 116.3 (C^4), 114.5 ($C^{2"}$), 112.1 ($C^{6'}$), 111.9 ($C^{4"}$), 55.3 (C^9), 39.0 ($C^{2'''}$), 32.1 ($C^{3'''}$), 30.7 (C^8), 11.7 (C^6), 10.9 (C^7); LRMS *m/z* (ESI^+) 378 ($[M+H]^+$, 100%).

4-(2-(3-Methoxyphenethyl)-1-methyl-1*H*-benzo[*d*]imidazol-5-yl)-3,5-dimethylisoxazole 139

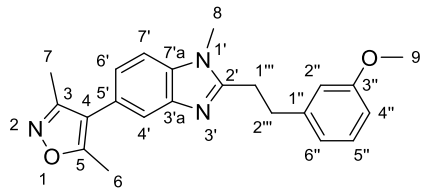

N-(5-(3,5-Dimethylisoxazol-4-yl)-2-(methylamino)phenyl)-3-(3-methoxyphenyl)propenamide **202** (600 mg, 1.58 mmol, 1.0 eq.) and 3-(3-methoxyphenyl)propanoic acid (51.0 mg, 0.316 mmol, 0.2 eq.) were combined in toluene (1.0 mL) in a microwave vial containing 3 Å molecular sieves. The reaction mixture was stirred at 130 °C for 18 h. The reaction mixture was cooled to rt, filtered then the solvent

was evaporated *in vacuo.* The residue was purified by RP flash column chromatography eluting with H_2O : acetonitrile (95:5 to 5:95) to yield 4-(2-(3-methoxyphenethyl)-1-methyl-1*H*-benzo[*d*]imidazol-5-yl)-3,5-dimethylisoxazole **139** (65 mg, 11%) as a yellow solid: R_f 0.62 (CH_2Cl_2 : methanol, 9:1); m.p. 113-115 °C ($CDCl_3$); ν_{max} (thin film)/ cm^{-1} 1594 (N-H, m), 1424 (C-H, m), 1261 (C-O, s), 1040 (C-O, m); ^1H NMR (400 MHz, $CDCl_3$) δ 7.62 (1H, dd, *J* 1.7, 0.7, $C^{4'}$-H), 7.33 (1H, dd, *J* 8.2, 0.7, $C^{6'}$-H), 7.22 (1H, t, *J* 7.8, $C^{5''}$-H), 7.13 (1H, dd, *J* 8.2, 1.7, $C^{7'}$-H), 6.83 (1H, dt, *J* 8.0, 1.2, $C^{4''}$-H), 6.78 (2H, ddd, *J* 8.0, 2.6, 0.9, $C^{6''}$-H), 6.75 (1H, m, $C^{2''}$-H), 3.73 (3H, s, C^8-H_3), 3.59 (3H, s, C^9-H_3), 3.27-3.14 (4H, m, $C^{1'''}$-H_2, $C^{2'''}$-H_2), 2.41 (3H, s, C^6-H_3), 2.29 (3H, s, C^7-H_3); ^{13}C NMR (101 MHz, $CDCl_3$) δ 165.1 (C^5), 159.9 ($C^{3''}$), 159.1 (C^3), 155.5 ($C^{2'}$), 143.1 ($C^{3'a}$), 142.4 ($C^{1''}$), 135.3 ($C^{7'a}$), 129.8 ($C^{5''}$), 124.2 ($C^{5'}$), 123.5 ($C^{7'}$), 120.9 ($C^{2''}$), 120.0 ($C^{4'}$), 117.3 (C^4), 114.2 ($C^{2''}$), 112.0 ($C^{6''}$), 109.4 ($C^{6'}$), 55.2 (C^8), 34.2 ($C^{1'''}$), 29.8 (C^9), 29.7 ($C^{2'''}$), 11.7 (C^6), 11.0 (C^7); LRMS *m/z* (ESI^+) 362 ($[M+H]^+$, 100%); HRMS *m/z* (ESI^+) [Found: 362.1863, $C_{22}H_{23}N_3O_2$ requires $[M+H]^+$ 362.1857)]; Analytical HPLC (RP, *Method 3*) rt 7.3 min, purity 100%.

_N_-(5-(3,5-Dimethylisoxazol-4-yl)-2-(methylamino)phenyl)-3-(3-nitrophenyl)propenamide 203

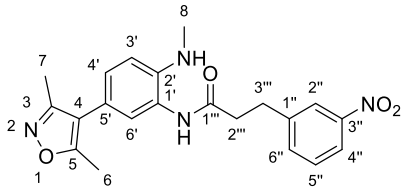

4-(3,5-Dimethyl-1,2-oxazol-4-yl)-*N*-methyl-2-nitroaniline **75** (150 mg, 0.607 mmol, 1.0 eq.) was suspended in EtOH (3.2 mL) and 1 M $Na_2S_2O_4$ (3.2 mL, 3.16 mmol, 5.2 eq.) was added. The reaction mixture was stirred at 80 °C for 15 min. The reaction mixture was cooled to rt and partitioned between ethyl acetate (15 mL) and 10% aq. ammonia solution (7 mL). The phases were separated then the organic phase was washed with water (5 mL) and brine (5 mL), dried over $MgSO_{4\,(s)}$, filtered, then the filtrate was concentrated *in vacuo*. The crude material (100 mg) was dissolved in DMF (1.0 mL). DIPEA (70.2 µL, 0.403 mmol, 1.05 eq.), 3-(3-nitrophenyl)propanoic acid (74.9 mg, 0.384 mmol, 1.05 eq.), HATU (153 mg, 0.403 mmol, 1.05 eq.) and HOBT (54.5 mg, 0.403 mmol, 1.05 eq.) were added. The reaction mixture was stirred at rt for 20 h. The reaction mixture was partitioned between ethyl acetate and water. The organic layer was separated then the

aqueous layer was extracted with ethyl acetate (3 × 10 mL). The combined organic layers were washed with brine, dried over $MgSO_{4\ (s)}$, filtered, then the filtrate was concentrated *in vacuo*. The residue was purified by flash column chromatography eluting with petroleum ether : ethyl acetate (1:0 to 0:1) to yield *N*-(5-(3,5-dimethylisoxazol-4-yl)-2-(methylamino)phenyl)-3-(3-nitrophenyl)propenamide **203** (138 mg, 76%) as a yellow foam: R_f 0.45 (CH_2Cl_2 : methanol, 9:1); ^{1}H NMR (400 MHz, $CDCl_3$) δ 8.13(1H, s, $C^{2"}$-H), 8.08 (1H, dd, *J* 8.3, 2.0, $C^{4"}$-H), 7.61 (1H, d, *J* 7.6, $C^{6"}$-H), 7.47 (1H, dd, *J* 7.9, 7.9, $C^{5"}$-H), 7.29 (1H, s, $C^{1'''}$N-H), 7.07 (1H, d, *J* 2.0, $C^{6'}$-H), 7.03 (1H, dd, *J* 8.3, 2.0, $C^{3'}$-H), 6.78 (1H, d, *J* 8.3, $C^{4'}$-H), 3.19 (2H, t, *J* 7.4, $C^{3'''}$-H_2), 2.82 (2H, t, *J* 7.4, $C^{2'''}$-H_2), 2.81 (3H, s, C^8-H_3), 2.35 (3H, s, C^6-H_3), 2.21 (3H, s, C^7-H_3); ^{13}C NMR (101 MHz, $CDCl_3$) δ 170.6 ($C^{1'''}$), 165.0 (C^5), 159.0 (C^3), 148.6 ($C^{3"}$), 142.8 ($C^{2'}$), 142.8 ($C^{1"}$), 135.2 ($C^{6"}$), 129.7 ($C^{5"}$), 128.5 ($C^{4'}$), 126.2 ($C^{6'}$), 123.7 ($C^{1'}$), 123.3 ($C^{2"}$), 121.7 ($C^{4"}$), 119.8 ($C^{5'}$), 116.2 (C^4), 112.8 ($C^{3'}$), 37.9 (C^8), 31.0 ($C^{2'''}$), 30.9 ($C^{3'''}$), 11.7 (C^6), 10.9 (C^7); LRMS *m/z* (ESI^+) 395 ($[M+H]^+$, 100%).

3,5-Dimethyl-4-(1-methyl-2-(3-nitrophenethyl)-1*H*-benzo[*d*]imidazol-5-yl)isoxazole 151

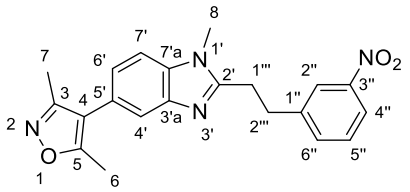

N-(5-(3,5-dimethylisoxazol-4-yl)-2-(methylamino)phenyl)-3-(3-nitrophenyl)propanamide **203** (100 mg, 254 μmol, 1.0 eq.) and 3-(3-nitrophenyl)propanoic acid (10.0 mg, 51.0 μmol, 0.2 eq.) were combined in toluene (2.0 mL) in a microwave vial containing 3 Å molecular sieves. The reaction mixture was refluxed for 24 h. The reaction mixture was cooled to rt, filtered then the solvent was evaporated *in vacuo.* The residue was purified by RP flash column chromatography eluting with H_2O : acetonitrile (95:5 to 5:95) to yield 3,5-dimethyl-4-(1-methyl-2-(3-nitrophenethyl)-1*H*-benzo[*d*]imidazol-5-yl)isoxazole **151** (95 mg, 99%) as an off-white solid: R_f 0.48 (CH_2Cl_2 : methanol, 9:1); m.p. 165-166 °C ($CDCl_3$); ν_{max} (thin film)/ cm^{-1} 1528 (N-O, s), 1442 (C-H, m), 1424 (C-H, m), 1350 (C-N, s), 1314 (C-N, s), 1244 (C-N, m); ^{1}H NMR (600 MHz, $CDCl_3$) δ 8.16 (1H, t, *J* 2.0, $C^{2"}$-H), 8.10 (1H, ddd, *J* 8.2, 2.0, 1.1, $C^{4"}$-H), 7.64-7.62 (1H, m, $C^{4'}$-H), 7.61-7.57 (1H, m, $C^{6"}$-H), 7.48 (1H, dd, *J* 8.0,

$C^{5''}$-H), 7.36 (1H, dd, *J* 8.2, 0.7, $C^{7'}$-H), 7.15 (1H, dd, *J* 8.2, 1.6, $C^{6'}$-H), 3.71 (3H, s, C^{8}-H_3), 3.42 (2H, m, $C^{2'''}$-H_2), 3.24 (2H, dd, *J* 8.9, 6.9, $C^{1'''}$-H_2), 2.42 (3H, s, C^{6}-H_3), 2.29 (3H, s, C^{7}-H_3); ^{13}C NMR (151 MHz, $CDCl_3$) δ 165.2 (C^5), 159.1 (C^3), 154.4 ($C^{2'}$), 148.6 ($C^{3''}$), 143.0 ($C^{3'a}$), 142.8 ($C^{1''}$), 135.3 ($C^{7'a}$), 135.0 ($C^{6''}$), 129.7 ($C^{5''}$), 124.5 ($C^{5'}$), 123.8 ($C^{6'}$), 123.3 ($C^{2''}$), 121.8 ($C^{4''}$), 120.1 ($C^{4'}$), 117.2 (C^4), 109.5 ($C^{7'}$), 33.1 ($C^{2'''}$), 30.0 (C^8), 29.0 ($C^{1'''}$), 11.7 (C^6), 11.0 (C^7); LRMS *m/z* (ESI^+) 377 ($[M+H]^+$, 100%); HRMS *m/z* (ESI^+) [Found: 377.1606, $C_{21}H_{20}O_3N_4$ requires $[M+H]^+$ 377.1608)]; Analytical HPLC (RP, *Method 3*) rt 7.4 min, purity 100%.

3-(3-Cyanophenyl)-*N*-(5-(3,5-dimethylisoxazol-4-yl)-2-(methylamino)phenyl)propanamide 204

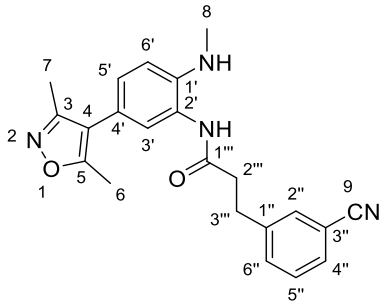

1 M $Na_2S_2O_{4\,(aq)}$ (3.15 mL, 3.15 mmol, 5.2 eq.) was added to 4-(3,5-dimethylisoxazol-4-yl)-*N*-methyl-2-nitroaniline **75** (150 mg, 0.606 mmol, 1.0 eq.) in EtOH (3.15 mL). The reaction mixture was stirred at 80 °C for 30 min. The reaction mixture was cooled to rt then the solvent was evaporated *in vacuo.* The residue was partitioned between 10% aq. ammonia solution and ethyl acetate. The aqueous layer was separated then extracted with ethyl acetate (3 × 15 mL). The combined organic layers were dried over $MgSO_{4\,(s)}$, filtered, then the filtrate was concentrated *in vacuo*. The residue was dissolved in anhydrous DMF (1.0 mL). 3-(3-Cyanophenyl)propanoic acid (96.5 mg, 0.551 mmol, 1.0 eq.), HATU (210 mg, 0.578 mmol, 1.05 eq.) and DIPEA (101 µL, 0.578 mmol, 1.05 eq.) were added. The reaction mixture was stirred at rt for 17 h. The solvent was evaporated *in vacuo.* The residue was re-dissolved in ethyl acetate (10 mL) and water (5 mL) was added. The organic layer was separated then the aqueous layer was extracted with ethyl acetate (3 × 10 mL). The combined organic layers were washed with 10% w/v $LiCl_{(aq)}$ (3 × 10 mL), dried over $MgSO_{4\,(s)}$, filtered, then the filtrate was concentrated *in vacuo*. The residue was purified by flash column chromatography eluting with

petroleum ether : ethyl acetate (1:0 to 0:1) to yield 3-(3-cyanophenyl)-*N*-(5-(3,5-dimethylisoxazol-4-yl)-2-(methylamino)phenyl)propanamide **204** (163 mg, 79%) as a brown oil: R_f 0.60 (petroleum ether : ethyl acetate, 1:4); ^{1}H NMR (400 MHz, $CDCl_3$) δ 7.56 (1H, d, *J* 1.8, $C^{2"}$-H), 7.55-7.49 (2H, m, $C^{4"}$-H, $C^{6"}$-H), 7.41 (1H, dd, *J* 7.6, 7.6, $C^{5"}$-H), 7.22 (1H, s, $C^{1'}$N-H), 7.05 (1H, s, $C^{2"}$-H), 7.04 (1H, dd, *J* 8.2, 2.1, $C^{5'}$-H), 6.78 (1H, d, *J* 8.2, $C^{6'}$-H), 3.11 (2H, t, *J* 7.4, $C^{3'''}$-H_2), 2.82 (3H, s, C^8-H_3), 2.75 (2H, t, *J* 7.4, $C^{3'''}$-H_2), 2.36 (3H, s, C^6-H_3), 2.22 (3H, s, C^7-H_3); ^{13}C NMR (101 MHz, $CDCl_3$) δ 170.5 ($C^{1'''}$), 164.9 (C^5), 159.0 (C^3), 143.0 ($C^{1"}$), 142.3 ($C^{1'}$), 133.5 ($C^{6"}$), 132.1 ($C^{2"}$), 130.3 ($C^{4"}$), 129.5 ($C^{5"}$), 128.4 ($C^{5'}$), 126.2 ($C^{3'}$), 123.6 ($C^{2'}$), 119.5 ($C^{4'}$), 118.9 (C^9), 116.2 (C^4), 112.7 ($C^{3"}$), 112.6 ($C^{6'}$), 38.0 ($C^{2'''}$), 31.1 ($C^{3'''}$), 30.8 (C^8), 11.7 (C^6), 11.0 (C^7) ; LRMS *m/z* (ESI^+) 373 ($[M+H]^+$, 100%).

3-(2-(5-(3,5-Dimethylisoxazol-4-yl)-1-methyl-1*H*-benzo[*d*]imidazol-2-yl)ethyl)benzonitrile 154

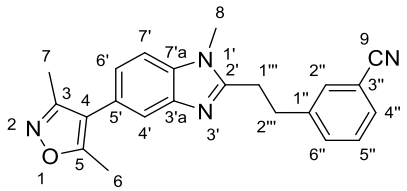

3-(3-Cyanophenyl)-*N*-(5-(3,5-dimethylisoxazol-4-yl)-2-(methylamino)phenyl)propanamide **204** (140 mg, 374 µmol, 1.0 eq.) and 3-(3-cyanophenyl)propanoic acid (6.6 mg, 37.0 µmol, 0.1 eq.) were combined in toluene (1.0 mL) in a microwave vial containing 3 Å molecular sieves. The reaction mixture was stirred at 130 °C for 72 h. The reaction mixture was cooled to rt, filtered then the solvent was evaporated *in vacuo*. The residue was purified by RP flash column chromatography eluting with water : acetonitrile (95:5 to 5:95) to yield 3-(2-(5-(3,5-dimethylisoxazol-4-yl)-1-methyl-1*H*-benzo[*d*]imidazol-2-yl)ethyl)benzonitrile **154** (98 mg, 74%) as a yellow solid: R_f 0.27 (petroleum ether : ethyl acetate, 7:3); m.p. 130-132 °C ($CDCl_3$); ν_{max} (thin film)/ cm^{-1} 2361 (C-H, m), 2229 (C≡N, m), 1619 (C=C, w), 1510 (C-H, m), 1484 (C-H, m), 1424 (C-H, m), 1322 (C-N, m), 1242 (C-N, m); ^{1}H NMR (600 MHz, $CDCl_3$) δ 7.62 (1H, d, *J* 1.0, $C^{4'}$-H), 7.56 (1H, br t, *J* 1.75, $C^{2"}$-H), 7.53 (1H, dt, *J* 7.7, 1.4, $C^{4"}$-H), 7.50 (1H, dt, *J* 8.0, 1.5, $C^{6"}$-H), 7.41 (1H, t, *J* 7.7, $C^{5"}$-H), 7.35 (1H, d, *J* 8.2, $C^{7'}$-H), 7.15 (1H, dd, *J* 8.2, 1.0, $C^{6'}$-H), 3.68 (3H, s, C^8-H_3), 3.33 (2H, dd, *J* 9.1, 6.6, $C^{2'''}$-H_2), 3.19 (2H, dd, *J* 9.1, 6.6, $C^{1'''}$-H_2), 2.42 (3H, s, C^6-H_3), 2.28 (3H, s, C^7-H_3); ^{13}C NMR (151 MHz, $CDCl_3$)

δ 165.2 (C^5), 159.1 (C^3), 154.4 ($C^{2'}$), 142.9 ($C^{3'a}$), 142.3 ($C^{1''}$), 135.3 ($C^{7'a}$), 133.2 ($C^{6''}$), 132.0 ($C^{2''}$), 130.5 ($C^{4''}$), 129.6 ($C^{5''}$), 124.5 ($C^{5'}$), 123.8 ($C^{6'}$), 120.0 ($C^{4'}$), 118.9 (C^9), 117.2 (C^4), 112.9 ($C^{3''}$), 109.5 ($C^{7'}$), 33.1 ($C^{2'''}$), 29.9 (C^8), 29.1 ($C^{1'''}$), 11.7 (C^6), 11.0 (C^7); LRMS *m/z* (ESI^+) 357 ($[M+H]^+$, 100%); HRMS *m/z* (ESI^+) [Found: 357.1719, $C_{22}H_{20}N_4O$ requires $[M+H]^+$ 357.1710)]; Analytical HPLC (RP, *Method 3*) rt 6.3 min, purity 96%.

_N_-(5-(3,5-Dimethylisoxazol-4-yl)-2-(methylamino)phenyl)-3-(3-(trifluoromethyl)phenyl)propanamide 205

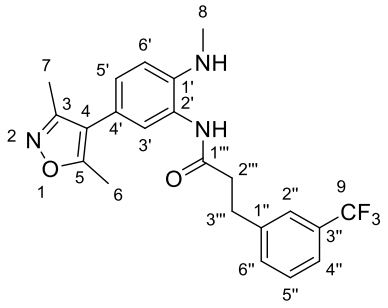

1 M $Na_2S_2O_{4\,(aq)}$ (3.15 mL, 3.15 mmol, 5.2 eq.) was added to 4-(3,5-dimethylisoxazol-4-yl)-*N*-methyl-2-nitroaniline **75** (150 mg, 0.606 mmol, 1.0 eq.) in EtOH (3.15 mL). The reaction mixture was stirred at 80 °C for 15 min. The reaction mixture was cooled to rt then the solvent was evaporated *in vacuo.* The residue was partitioned between 10% aq. ammonia solution and ethyl acetate. The aqueous layer was separated then extracted with ethyl acetate (3 × 15 mL). The combined organic layers were dried over $MgSO_{4\,(s)}$, filtered, then the filtrate was concentrated *in vacuo*. The residue was dissolved in anhydrous DMF (1.0 mL). 3-(3-(Trifluoromethyl)phenyl)propanoic acid (120 mg, 0.551 mmol, 1.0 eq.), HATU (220 mg, 0.578 mmol, 1.05 eq.) and DIPEA (101 µL, 0.578 mmol, 1.05 eq.) were added. The reaction mixture was stirred at rt for 3 h. The solvent was evaporated *in vacuo.* The residue was re-dissolved in ethyl acetate (10 mL) and 1 M NaOH (5 mL) was added. The organic layer was separated then the aqueous layer was extracted with ethyl acetate (3 × 10 mL). The combined organic layers were washed with 10% w/v $LiCl_{(aq)}$ (3 × 10 mL), dried over $MgSO_{4\,(s)}$, filtered, then the filtrate was concentrated *in vacuo*. The residue was purified by flash column chromatography eluting with petroleum ether : ethyl acetate (1:0 to 0:1) to yield *N*-(5-(3,5-dimethylisoxazol-4-yl)-2-(methylamino)phenyl)-3-(3-(trifluoromethyl)phenyl)propanamide **205** (181 mg, 79%) as a yellow foam: R_f 0.22

(petroleum ether : ethyl acetate, 1:1); ^{1}H NMR (400 MHz, $CDCl_3$) δ 7.55-7.28 (4H, m, $C^{3'}$-H, $C^{2''}$-H, $C^{4''}$-H, $C^{5''}$-H), 7.07-6.97 (2H, m, $C^{5'}$-H, $C^{6''}$-H), 6.75 (1H, d, *J* 8.1, $C^{6'}$-H), 3.12 (2H, t, *J* 7.4, $C^{3'''}$-H_2), 2.78 (3H, s, C^{8}-H_3), 2.75 (2H, t, *J* 7.4, $C^{2'''}$-H_2), 2.33 (3H, s, C^{6}-H_3), 2.20 (3H, s, C^{7}-H_3); ^{13}C NMR (101 MHz, $CDCl_3$) δ 170.8 ($C^{1'''}$), 164.8 (C^{5}), 158.9 (C^{3}), 142.9 ($C^{1''}$), 141.6 ($C^{1'}$), 132.1 ($C^{5''}$), 130.8 (q, *J* 34.1, $C^{3''}$), 129.1 ($C^{3'}$), 128.2 ($C^{6''}$), 126.2 ($C^{5'}$), 125.1 (q, *J* 4.0, $C^{2''}$), 124.3 (q, *J* 272.3, C^{9}), 123.5 ($C^{2'}$), 123.3 (q, *J* 4.0, $C^{4''}$), 119.2 ($C^{4'}$), 116.2 (C^{4}), 112.2 ($C^{6'}$), 38.2 ($C^{2'''}$), 31.3 ($C^{3'''}$), 30.6 (C^{8}), 11.5 (C^{6}), 10.8 (C^{7}); ^{19}F NMR (565 MHz, $CDCl_3$) δ -62.26 (s, CF_3); LRMS *m/z* (ESI^+) 418 ($[M+H]^+$, 100%).

3,5-Dimethyl-4-(1-methyl-2-(3-(trifluoromethyl)phenethyl)-1*H*-benzo[*d*]imidazol-5-yl)isoxazole 153

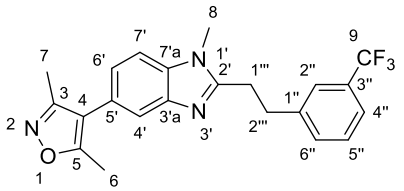

N-(5-(3,5-Dimethylisoxazol-4-yl)-2-(methylamino)phenyl)-3-(3-(trifluoromethyl)phenyl)propanamide **205** (80.0 mg, 0.192 mmol, 1.0 eq.) and 3-(3-(trifluoromethyl)phenyl)propanoic acid (4.2 mg, 0.019 mmol, 0.1 eq.) were combined in toluene (1.0 mL) in a microwave vial containing 3 Å molecular sieves. The reaction mixture was stirred at 130 °C for 72 h. The reaction mixture was cooled to rt, filtered then the solvent was evaporated *in vacuo.* The residue was purified by RP flash column chromatography eluting with water : acetonitrile (95:5 to 5:95) to yield 3,5-dimethyl-4-(1-methyl-2-(3-(trifluoromethyl)phenethyl)-1*H*-benzo[*d*]imidazol-5-yl)isoxazole **153** (43 mg, 55%) as a colourless solid: R_f 0.61 (CH_2Cl_2 : methanol, 9:1); m.p. 129-131 °C ($CDCl_3$); ν_{max} (thin film)/ cm^{-1} 1619 (C=C, w), 1511 (C-H, w), 1486 (C-H, w), 1330 (C-F, s), 1248 (C-N, w), 1164 (C-H, m), 1123 (C-F, s), 1074 (C-H, m); ^{1}H NMR (600 MHz, $CDCl_3$) δ 7.65 (1H, d, *J* 1.3, $C^{4'}$-H), 7.52-7.47 (2H, m, $C^{2''}$-H, $C^{4''}$-H), 7.47-7.39 (2H, m, $C^{5''}$-H, $C^{5''}$-H), 7.36 (1H, d, *J* 8.2, $C^{7'}$-H), 7.16 (1H, dd, *J* 8.2, 1.3, $C^{6'}$-H), 3.64 (3H, s, C^{8}-H_3), 3.35 (2H, dd, *J* 9.3, 6.5, $C^{2'''}$-H_2), 3.24 (2H, dd, *J* 9.3, 6.5, $C^{1'''}$-H_2), 2.41 (3H, s, C^{6}-H_3), 2.28 (3H, s, C^{7}-H_3); ^{13}C NMR (151 MHz, $CDCl_3$) δ 165.2 (C^{5}), 159.1 (C^{3}), 154.7 ($C^{2'}$), 142.0 ($C^{3'a}$), 141.5 ($C^{1''}$), 134.9 ($C^{7'a}$), 132.1 ($C^{6''}$), 131.1 (q, *J* 32.1, $C^{3''}$), 129.3 ($C^{5''}$), 125.2 (q, *J* 3.8, $C^{2''}$), 124.9 ($C^{5'}$), 124.1 ($C^{6'}$), 124.1 (q, *J* 274.1, C^{9}), 123.3 (q,

J 3.8, $C^{4''}$), 119.7 ($C^{4'}$), 117.1 (C^{4}), 109.6 ($C^{7'}$), 33.6 ($C^{2'''}$), 29.9 (C^{8}), 29.2 ($C^{1'''}$), 11.7 (C^{6}), 11.0 (C^{7}); ^{19}F NMR (565 MHz, $CDCl_3$) δ -62.26 (s, CF_3); LRMS *m/z* (ESI^+) 400 ($[M+H]^+$, 100%); HRMS *m/z* (ESI^+) [Found: 400.1606, $C_{22}H_{20}F_3N_3O$ requires $[M+H]^+$ 400.1631)]; Analytical HPLC (RP, *Method 3*) rt 7.4 min, purity 95%.

Methyl 3-(3-((5-(3,5-dimethylisoxazol-4-yl)-2-(methylamino)phenyl)amino)-3-oxopropyl)benzoate 206

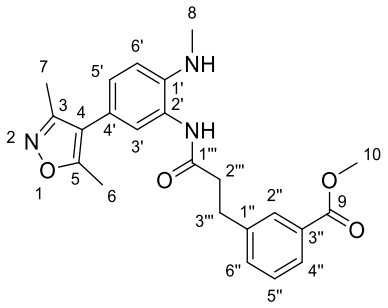

1 M $Na_2S_2O_{4\,(aq)}$ (3.15 mL, 3.15 mmol, 5.2 eq.) was added to 4-(3,5-dimethylisoxazol-4-yl)-*N*-methyl-2-nitroaniline **75** (150 mg, 0.606 mmol, 1.0 eq.) in EtOH (3.15 mL). The reaction mixture was stirred at 80 °C for 10 min. The reaction mixture was cooled to rt and partitioned between 10% aq. ammonia solution and ethyl acetate. The aqueous layer was separated then extracted with ethyl acetate (3 × 15 mL). The combined organic layers were dried over $MgSO_{4\,(s)}$, filtered, then the filtrate was concentrated *in vacuo*. The residue was dissolved in anhydrous DMF (1.0 mL). 3-(3-(Methoxycarbonyl)phenyl)propanoic acid (95.8 mg, 0.460 mmol, 1.0 eq.), HATU (175 mg, 0.460 mmol, 1.0 eq.) and DIPEA (160 µL, 0.921 mmol, 2.0 eq.) were added. The reaction mixture was stirred at rt for 4 h. The solvent was evaporated *in vacuo.* The residue was re-dissolved in ethyl acetate (10 mL) and 1 M NaOH (5 mL) was added. The organic layer was separated then the aqueous layer was extracted with ethyl acetate (3 × 10 mL). The combined organic layers were washed with 10% w/v $LiCl_{(aq)}$ (3 × 10 mL), dried over $MgSO_{4\,(s)}$, filtered, then the filtrate was concentrated *in vacuo*. The residue was purified by flash column chromatography eluting with petroleum ether : ethyl acetate (1:0 to 3:7) to yield methyl 3-(3-((5-(3,5-dimethylisoxazol-4-yl)-2-(methylamino)phenyl)amino)-3-oxopropyl)benzoate **206** (141 mg, 75%) as a brown foam: R_f 0.12 (ethyl acetate : petroleum ether, 1:1); ^1H NMR (400 MHz, $CDCl_3$) δ 7.96 (1H, s, $C^{2'}$N-H), 7.91 (1H, dt, *J* 7.7, 1.5, $C^{4''}$-H), 7.47 (1H, dt, *J* 7.7, 1.5, $C^{6''}$-H), 7.38

(1H, dd, *J* 7.7, $C^{5''}$-H), 7.03 (1H, s, $C^{3'}$-H), 7.04-7.02 (1H, m, $C^{5'}$-H), 6.98 (1H, s, $C^{2''}$-H), 6.74 (1H, d, *J* 8.4, $C^{6'}$-H), 3.90 (3H, s, C^{10}-H_3), 3.13 (2H, t, *J* 7.3, $C^{2'''}$-H_2), 2.83-2.71 (5H, m, $C^{3'''}$-H_2, C^{8}-H_3), 2.35 (3H, s, C^{6}-H_3), 2.22 (3H, s, C^{7}-H_3); LRMS *m/z* (ESI^+) 408 ($[M+H]^+$, 100%).

Methyl 3-(2-(5-(3,5-dimethylisoxazol-4-yl)-1-methyl-1*H*-benzo[*d*]imidazol-2-yl)ethyl)benzoate 145

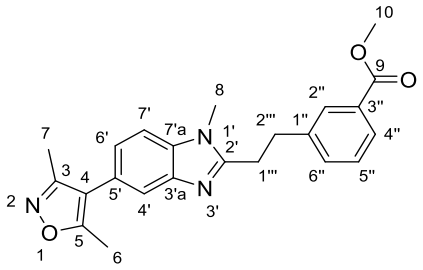

Methyl 3-(3-((5-(3,5-dimethylisoxazol-4-yl)-2-(methylamino)phenyl)amino)-3-oxopropyl)benzoate **206** (86.0 mg, 0.211 mmol, 1.0 eq.) was refluxed in toluene (2.0 mL) in a microwave vial containing 3 Å molecular sieves for 48 h. The reaction mixture was cooled to rt, filtered then the solvent was evaporated *in vacuo.* The residue was purified by flash column chromatography eluting with CH_2Cl_2 : methanol (1:0 to 93:7) to yield methyl 3-(2-(5-(3,5-dimethylisoxazol-4-yl)-1-methyl-1*H*-benzo[*d*]imidazol-2-yl)ethyl)benzoate **145** (58 mg, 71%) as a yellow solid: R_f 0.13 (ethyl acetate : petroleum ether, 1:1); m.p. 174-175 °C ($CDCl_3$); ν_{max} (thin film)/ cm^{-1} 1723 (C=O, s), 1308 (C-O, s); ^{1}H NMR (600 MHz, $CDCl_3$) δ 7.96 (1H, d, *J* 1.6, $C^{2''}$-H), 7.91 (1H, dt, *J* 7.7, 1.6, $C^{4''}$-H), 7.64-7.60 (1H, m, $C^{4'}$-H), 7.42 (1H, dt, *J* 7.7, 1.6, $C^{6''}$-H), 7.37 (1H, dd, *J* 7.7, 7.7, $C^{5''}$-H), 7.33 (1H, d, *J* 8.2, $C^{7'}$-H), 7.14 (1H, dd, *J* 8.2, 1.6, $C^{6'}$-H), 3.91 (3H, s, C^{10}-H_3), 3.64 (3H, s, C^{8}-H_3), 3.31 (2H, dd, *J* 9.4, 6.5, $C^{2'''}$-H_2), 3.21 (2H, dd, *J* 9.4, 6.5, $C^{1'''}$-H_2), 2.42 (3H, s, C^{6}-H_3), 2.29 (3H, s, C^{7}-H_3); ^{13}C NMR (151 MHz, $CDCl_3$) δ 167.1 (C^9), 165.0 (C^5), 159.0 (C^3), 155.0 ($C^{2'}$), 142.9 ($C^{3'a}$), 141.0 ($C^{1''}$), 135.2 ($C^{7'a}$), 133.2 ($C^{6''}$), 130.5 ($C^{3''}$), 129.4 ($C^{5''}$), 128.8 ($C^{2''}$), 127.8 ($C^{4''}$), 124.2 ($C^{5'}$), 123.5 ($C^{6'}$), 119.9 ($C^{4'}$), 117.2 (C^4), 109.3 ($C^{7'}$), 52.2 (C^{10}), 33.5 ($C^{2'''}$), 29.8 (C^8), 29.4 ($C^{1'''}$), 11.6 (C^6), 10.9 (C^7); LRMS *m/z* (ESI^+) 390 ($[M+H]^+$, 100%); HRMS *m/z* (ESI^+) [Found: 390.1831, $C_{23}H_{23}N_3O_3$ requires $[M+H]^+$ 390.1812)]; Analytical HPLC (RP, *Method 3*) rt 7.3 min, purity 100%.

3-(2-(5-(3,5-Dimethylisoxazol-4-yl)-1-methyl-1*H*-benzo[*d*]imidazol-2-yl)ethyl)benzoic acid 147

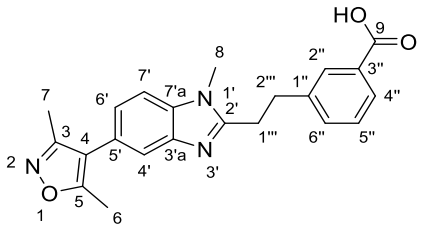

Methyl 3-(2-(5-(3,5-dimethylisoxazol-4-yl)-1-methyl-1*H*-benzo[*d*]imidazol-2-yl)ethyl)benzoate **145** (15.0 mg, 0.039 mmol, 1.0 eq.) was dissolved in ethanol (0.3 mL). 2 M NaOH $_{(aq)}$ (193 µL, 0.385 mmol, 10.0 eq.) was dropwise added. The reaction mixture was stirred at 50 °C for 1.5 h. The reaction was then cooled to rt and the pH adjusted to pH 2 with 2 M HCl $_{(aq)}$. The aqueous layer was extracted with ethyl acetate. The organic layer was dried over $MgSO_{4\ (s)}$, filtered, then the filtrate was concentrated *in vacuo.* The residue was lyophilised to yield 3-(2-(5-(3,5-dimethylisoxazol-4-yl)-1-methyl-1*H*-benzo[*d*]imidazol-2-yl)ethyl)benzoic acid **147** (13 mg, 89%) as a pale yellow solid: R_f 0.10 (CH_2Cl_2 : methanol, 9:1); m.p. 250 °C *dec.* ($CDCl_3$); ν_{max} (thin film)/ cm^{-1} 3415 (O-H, s *br*), 1697 (C=O, s), 1293 (O-H, m), 1246 (C-O, s); ^{1}H NMR (600 MHz, DMSO-d_6) δ 7.97 (1H, d, *J* 8.5, $C^{7'}$-H), 7.92 (1H, d, *J* 1.8, $C^{2"}$-H), 7.82 (1H, dt, *J* 7.7, 1.4, $C^{4"}$-H), 7.76 (1H, d, *J* 1.6, $C^{4'}$-H), 7.62 (1H, dt, *J* 7.7, 1.5, $C^{6"}$-H), 7.53 (1H, dd, *J* 8.5, 1.6, $C^{6'}$-H), 7.46 (1H, dd, *J* 7.7, 7.7, $C^{5"}$-H), 3.94 (3H, s, C^8-H_3), 3.52 (2H, dd, *J* 9.3, 6.9, $C^{1"'}$-H_2), 3.29 (2H, dd, *J* 9.3, 6.9, $C^{2"'}$-H_2), 2.42 (3H, s, C^6-H_3), 2.23 (3H, s, C^7-H_3); ^{13}C NMR (151 MHz, DMSO-d_6) δ 167.2 (C^9), 165.5 (C^5), 158.2 (C^3), 154.1 ($C^{2'}$), 140.0 ($C^{1"}$), 133.0 ($C^{6"}$), 132.2 ($C^{7'a}$), 131.1 ($C^{3"}$), 129.3 ($C^{2"}$), 128.8 ($C^{5"}$), 127.6 ($C^{4"}$), 127.1 ($C^{5'}$), 126.1 ($C^{6'}$), 115.6 (C^4), 114.7 ($C^{4'}$), 112.9 ($C^{7'}$), 31.7 ($C^{2"'}$), 31.0 (C^8), 26.8 ($C^{1"'}$), 11.3 (C^6), 10.4 (C^7). $C^{3'a}$ was not distinguishable in the ^{13}C NMR; LRMS *m/z* (ESI^+) 376 ($[M+H]^+$, 100%); HRMS *m/z* (ESI^-) [Found: 374.1517, $C_{22}H_{21}N_3O_3$ requires $[M-H]^-$ 374.1510)]; Analytical HPLC (RP, *Method 3*) rt 6.6 min, purity 100%.

***N*-(5-(3,5-Dimethylisoxazol-4-yl)-2-(methylamino)phenyl)-3-(*p*-tolyl)propenamide 207**

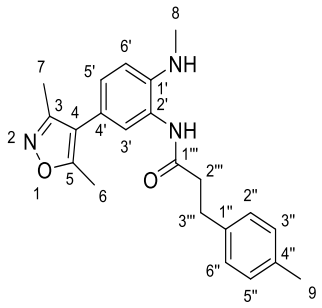

4-(3,5-Dimethyl-1,2-oxazol-4-yl)-*N*-methyl-2-nitroaniline **75** (150 mg, 0.61 mmol, 1.0 eq.) was dissolved in EtOH (3.2 mL) and 1 M $Na_2S_2O_4$ (3.2 mL, 3.2 mmol, 5.2 eq.) was added. The reaction mixture was stirred at 80 °C for 15 min. The reaction mixture was cooled to rt and partitioned between ethyl acetate (20 mL) and 10% aq. ammonia solution (10 mL). The phases were separated then the organic phase was washed with water (10 mL) and brine (10 mL), dried over $MgSO_{4\,(s)}$, filtered, then the filtrate was concentrated *in vacuo*. The crude material was dissolved in DMF (2.0 mL). DIPEA (70.2 µL, 0.0403 mmol, 1.05 eq.), 3-(*p*-tolyl)propanoic acid (63.1 mg, 0.384 mmol, 1.0 eq.), HATU (153 mg, 0.403 mmol, 1.05 eq.) and HOBT (54.5 mg, 0.403 mmol, 1.05 eq.) were added. The reaction mixture was stirred at rt for 20 h. The reaction mixture was partitioned between ethyl acetate and water. The organic layer was separated then the aqueous layer was extracted with ethyl acetate (3 × 15 mL). The combined organic layers were washed with 10% w/v $LiCl_{(aq)}$ (3 × 10 mL), dried over $MgSO_{4\,(s)}$, filtered, then the filtrate was concentrated *in vacuo*. The residue was purified by flash column chromatography eluting with petroleum ether : ethyl acetate (1:0 to 0:1) to yield *N*-(5-(3,5-dimethylisoxazol-4-yl)-2-(methylamino)phenyl)-3-(*p*-tolyl)propenamide **207** (141 mg, 84%) as a cream solid: R_f 0.27 (ethyl acetate : petroleum ether, 1:1); ^{1}H NMR (400 MHz, $CDCl_3$) δ 7.20-7.11 (4H, m, $C^{2''}$-H, $C^{3''}$-H, $C^{5''}$-H, $C^{6''}$-H), 7.03 (1H, d, *J* 2.1, $C^{3'}$-H), 7.01 (1H, dd, *J* 8.2, 2.1, $C^{5'}$-H), 6.71 (1H, d, *J* 8.2, $C^{6'}$-H), 3.04 (2H, t, *J* 7.1, $C^{2'''}$-H_2), 2.73 (3H, s, C^8-H_3), 2.70 (2H, t, *J* 7.1, $C^{3'''}$-H_2), 2.36 (3H, s, C^6-H_3), 2.34 (3H, s, C^9-H_3), 2.25 (3H, s, C^{7}-H_3); ^{13}C NMR (101 MHz, $CDCl_3$) δ 171.4 ($C^{1'''}$), 164.8 (C^5), 159.0 (C^3), 142.9 ($C^{1'}$), 137.5 ($C^{1''}$), 136.2 ($C^{4''}$), 129.6 ($C^{3''}$, $C^{5''}$), 128.6 ($C^{2''}$, $C^{6''}$), 128.2 ($C^{5'}$), 126.4 ($C^{3'}$), 123.6 ($C^{2'}$), 119.5 ($C^{4'}$), 116.3 (C^4), 112.0 ($C^{6'}$), 39.2 ($C^{2'''}$), 31.6 ($C^{3'''}$), 30.7 (C^8), 21.2 (C^9), 11.7 (C^6), 10.9 (C^7); LRMS *m/z* (ESI^-) 362 ($[M-H]^-$, 100%).

3,5-Dimethyl-4-(1-methyl-2-(4-methylphenethyl)-1*H*-benzo[*d*]imidazol-5-yl)isoxazole 138

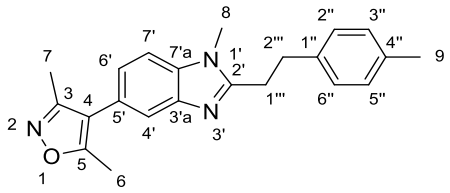

N-(5-(3,5-Dimethylisoxazol-4-yl)-2-(methylamino)phenyl)-3-(*p*-tolyl)propenamide **207** (100 mg, 275 µmol, 1.0 eq.) and 3-(*p*-tolyl)propanoic acid (9.0 mg, 55.0 µmol, 0.2 eq.) were refluxed in toluene (2.0 mL) in a microwave vial containing 3 Å molecular sieves for 24 h. The reaction mixture was cooled to rt, filtered then the solvent was evaporated *in vacuo.* The residue was purified by RP flash column chromatography eluting with H_2O : acetonitrile (95:5 to 5:95) to yield 3,5-dimethyl-4-(1-methyl-2-(4-methylphenethyl)-1*H*-benzo[*d*]imidazol-5-yl)isoxazole **138** (85 mg, 89%) as a light brown solid: R_f 0.50 (CH_2Cl_2 : methanol, 9:1); m.p. 149-151 °C ($CDCl_3$); ν_{max} (thin film)/ cm^{-1} 1613 (C=C, w), 1513 (C-H, w), 1484 (C-H, m), 1246 (C-O, s); ^{1}H NMR (600 MHz, $CDCl_3$) δ 7.62 (1H, d, *J* 1.5, $C^{4'}$-H), 7.33 (1H, d, *J* 8.2, $C^{7'}$-H), 7.12 (1H, dd, *J* 8.2, 1.6, $C^{6'}$-H), 7.11-7.13 (4H, m, $C^{2"}$-H, $C^{3"}$-H, $C^{5"}$-H, $C^{6"}$-H), 3.59 (3H, s, C^8-H_3), 3.23-3.13 (4H, m, $C^{1'''}$-H_2, $C^{2'''}$-H_2), 2.42 (3H, s, C^6-H_3), 2.33 (3H, s, C^9-H_3), 2.29 (3H, s, C^7-H_3); ^{13}C NMR (151 MHz, $CDCl_3$) δ 165.0 (C^5), 159.0 (C^3), 155.6 ($C^{2'}$), 143.0 ($C^{3'a}$), 137.6 ($C^{1"}$), 136.1 ($C^{4"}$), 135.1 ($C^{7'a}$), 129.3 ($C^{3"}$, $C^{5"}$), 128.3 ($C^{2"}$, $C^{6"}$), 124.1 ($C^{5'}$), 123.4 ($C^{6'}$), 119.8 ($C^{4'}$), 117.2 (C^4), 109.3 ($C^{7'}$), 33.6 ($C^{2'''}$), 29.9 ($C^{1'''}$), 29.7 (C^8), 21.0 (C^9), 11.6 (C^6), 10.9 (C^7); LRMS *m/z* (ESI^+) 346 ($[M+H]^+$, 100%); HRMS *m/z* (ESI^+) [Found: 346.1899, $C_{22}H_{23}N_3O$ requires $[M+H]^+$ 346.1914)]; Analytical HPLC (RP, *Method 3*) rt 7.6 min, purity 100%.

***N*-(5-(3,5-Dimethylisoxazol-4-yl)-2-(methylamino)phenyl)-3-(4-fluorophenyl)propenamide 208**

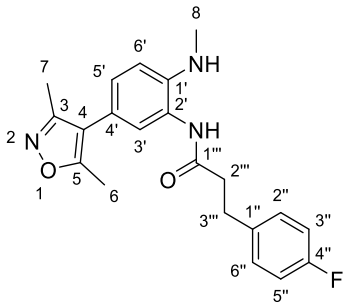

4-(3,5-Dimethyl-1,2-oxazol-4-yl)-*N*-methyl-2-nitroaniline **75** (200 mg, 0.81 mmol, 1.0 eq.) was suspended in EtOH (4.2 mL) and 1 M $Na_2S_2O_4$ (4.2 mL, 4.2 mmol, 5.2 eq.) was added. The reaction mixture was stirred at 80 °C for 15 min. The reaction mixture was cooled to rt and partitioned between ethyl acetate (15 mL) and 10% aq. ammonia solution (7 mL). The phases were separated then the organic phase was washed with water (5 mL) and brine (5 mL), dried over $MgSO_{4\,(s)}$, filtered, then the filtrate was concentrated *in vacuo*. The crude material was dissolved in DMF (2.0 mL). DIPEA (148 µL, 0.85 mmol, 1.05 eq.), 3-(4-fluorophenyl)propanoic acid (143 mg, 0.85 mmol, 1.05 eq.), HATU (323 mg, 0.85 mmol, 1.05 eq.) and HOBT (115 mg, 0.85 mmol, 1.05 eq.) were added. The reaction mixture was stirred at rt for 3 h. The reaction mixture was partitioned between ethyl acetate and water. The organic layer was separated then the aqueous layer was extracted with ethyl acetate (3 × 10 mL). The combined organic layers were washed with brine, dried over $MgSO_{4\,(s)}$, filtered, then the filtrate was concentrated *in vacuo*. The residue was purified by flash column chromatography eluting with petroleum ether : ethyl acetate (1:0 to 0:1) to yield *N*-(5-(3,5-dimethylisoxazol-4-yl)-2-(methylamino)phenyl)-3-(4-fluorophenyl)propenamide **208** (186 mg, 63%) as yellow oil: R_f 0.38 (petroleum ether : ethyl acetate, 1:4); ^{1}H NMR (400 MHz, $CDCl_3$) δ 8.00 (1H, s, $C^{1'''}$N-H), 7.23 (2H, m, $C^{2''}$-H, $C^{6''}$-H), 7.17-6.84 (4H, m, $C^{4'}$-H, $C^{6'}$-H, $C^{3''}$-H, $C^{5''}$-H), 6.74 (1H, d, *J* 8.2, $C^{3'}$-H), 3.04 (2H, t, *J* 7.2, $C^{3'''}$-H_2), 2.79 (3H, s, C^8-H_3), 2.70 (2H, t, *J* 7.2, $C^{2'''}$-H_2), 2.36 (3H, s, C^6-H_3), 2.22 (3H, s, C^7-H_3); ^{13}C NMR (101 MHz, $CDCl_3$) δ 171.0 ($C^{1'''}$), 164.9 (C^5), 161.6 (d, *J* 244.6, $C^{4''}$), 159.0 (C^3), 143.0 ($C^{2'}$), 136.3 ($C^{1''}$), 130.2 (d, *J* 7.6, $C^{2''}$, $C^{6''}$), 128.3 ($C^{4'}$), 136.4 ($C^{6'}$), 123.6 ($C^{1'}$), 119.4 ($C^{5'}$), 116.2 (C^4), 115.6 (d, *J* 7.6, $C^{3''}$, $C^{5''}$), 112.3 ($C^{3'}$), 39.1 ($C^{2'''}$), 31.1 ($C^{3'''}$), 30.7 (C^8), 11.7 (C^6), 10.9 (C^7); LRMS *m/z* (ESI^+) 368 ($[M+H]^+$, 100%).

4-(2-(4-Fluorophenethyl)-1-methyl-1*H*-benzo[*d*]imidazol-5-yl)-3,5-dimethylisoxazole 123

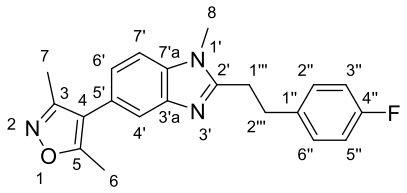

DIPEA (42.3 µL, 0.243 mmol, 1.05 eq.) was added to a mixture of 4-(3,5-dimethylisoxazol-4-yl)-N^1-methylbenzene-1,2-diamine **76** (50.0 mg, 0.231 mmol, 1.0 eq.), 3-(4-(fluorophenyl)propanoic acid (40.8 mg, 0.243 mmol, 1.05 eq.) and HATU (92.3 mg, 0.243 mmol, 1.05 eq.) in DMF (0.5 mL). The reaction mixture was stirred at rt for 20 h. The reaction mixture was partitioned between CH_2Cl_2 and sat. aq. $NaHCO_3$. The organic layer was separated then the aqueous layer was extracted with CH_2Cl_2 (3 × 5 mL). The combined organic layers were washed with brine, dried over $MgSO_{4\,(s)}$, filtered, then the filtrate was concentrated *in vacuo*. The residue was purified by flash column chromatography eluting with CH_2Cl_2 : methanol (1:0 to 93:7) to yield *N*-(5-(3,5-dimethylisoxazol-4-yl)-2-(methylamino)phenyl)-3-(4-fluorophenyl)propanamide (17 mg) as a colourless semi-solid: R_f 0.48 (CH_2Cl_2 : methanol, 9:1). The amide was refluxed in acetic acid (1.0 mL) for 72 h. The reaction mixture was cooled to rt then the solvent was evaporated *in vacuo.* The residue was dissolved in ethyl acetate and washed with sat. aq. $NaHCO_3$. The aqueous layer was extracted with ethyl acetate (3 × 5 mL). The combined organic layers were washed with water, dried over $MgSO_{4\,(s)}$, filtered, then the filtrate was concentrated *in vacuo*. The residue was purified by flash column chromatography eluting with CH_2Cl_2 : methanol (1:0 to 9:1) to yield 4-(2-(4-fluorophenethyl)-1-methyl-1*H*-benzo[*d*]imidazol-5-yl)-3,5-dimethylisoxazole **123** (37 mg, 45%) as a light yellow solid: R_f 0.37 (petroleum ether : ethyl acetate, 1:4); m.p. 129-130 °C (EtOAc); ν_{max} (thin film)/ cm^{-1} 1509 (C=C, s), 1315 (C-N, s), 1243 (C-F, s); ^{1}H NMR (400 MHz, $CDCl_3$) δ 7.62 (1H, d, *J* 1.6, $C^{4'}$-H), 7.33 (1H, dd, *J* 8.3, $C^{7'}$-H), 7.22-7.16 (2H, m, $C^{3''}$-H, $C^{5''}$-H), 7.13 (1H, dd, *J* 8.3, 1.6, $C^{6'}$-H), 7.03-6.93 (2H, m, $C^{2''}$-H, $C^{6''}$-H), 3.60 (3H, s, C^8-H_3), 3.29-3.09 (4H, m, $C^{1'''}$-H_2, $C^{2'''}$-H_2), 2.42 (3H, s, C^6-H_3), 2.29 (3H, s, C^7-H_3); ^{13}C NMR (101 MHz, $CDCl_3$) δ 165.1 (C^5), 161.8 (d, *J* 244.4, $C^{4''}$), 159.1 (C^3), 155.2 ($C^{2'}$), 143.0 ($C^{3'a}$), 136.5 (d, *J* 3.7, $C^{1''}$), 135.2 ($C^{7'a}$), 130.0 (d, *J* 8.4, $C^{2''}$, $C^{6''}$), 124.4 ($C^{5'}$), 123.6 ($C^{6'}$), 120.0 ($C^{4'}$), 117.3 (C^4), 115.7 (d, *J* 20.9, $C^{3''}$, $C^{5''}$), 109.4 ($C^{7'}$), 33.3 ($C^{1'''}$), 29.8 ($C^{2'''}$), 29.8 (C^8), 11.7 (C^6), 11.0 (C^7); ^{19}F NMR

(400 MHz, $CDCl_3$) δ -116.4 (s, 1 F); LRMS *m/z* (ESI^+) 350 ($[M+H]^+$, 100%). HRMS *m/z* (ESI^+) [Found: 350.1661, $C_{21}H_{20}FN_3O$ requires $[M+H]^+$ 350.1663)]; Analytical HPLC (RP, *Method 1*) rt 8.2 min, purity 100%.

3-(4-Chlorophenyl)-*N*-(5-(3,5-dimethylisoxazol-4-yl)-2-(methylamino)phenyl)propanamide 209

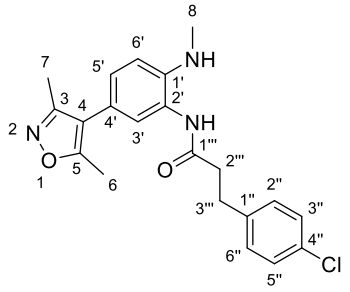

3-(4-Chlorophenyl)propanoic acid (38.5 mg, 0.209 mmol, 1.0 eq.), HATU (79.5 mg, 0.209 mmol, 1.0 eq.) and DIPEA (72.9 µL, 0.418 mmol, 2.0 eq.) were combined in anhydrous DMF (1.0 mL). 4-(3,5-Dimethylisoxazol-4-yl)-N^1-methylbenzene-1,2-diamine **76** (50.0 mg, 0.230 mmol, 1.1 eq.) in anhydrous DMF (500 µL) was added. The reaction mixture was stirred at rt for 17 h. The solvent was evaporated *in vacuo.* The residue was re-dissolved in ethyl acetate (10 mL) and water (5 mL) was added. The organic layer was separated then the aqueous layer was extracted with ethyl acetate (3 × 10 mL). The combined organic layers were washed with 10% w/v $LiCl_{(aq)}$ (3 × 10 mL), dried over $MgSO_{4\ (s)}$, filtered, then the filtrate was concentrated *in vacuo*. The residue was purified by flash column chromatography eluting with CH_2Cl_2 : methanol (1:0 to 9:1) to yield 3-(4-chlorophenyl)-*N*-(5-(3,5-dimethylisoxazol-4-yl)-2-(methylamino)phenyl)propanamide **209** (69 mg, 78%) as a yellow oil: R_f 0.52 (CH_2Cl_2 : methanol, 9:1); ^1H NMR (400 MHz, $CDCl_3$) δ 7.30-7.26 (2H, d, *J* 8.4, $C^{3''}$-H, $C^{5''}$-H), 7.19 (2H, d, *J* 8.4, $C^{2''}$-H, $C^{6''}$-H), 7.07 (1H, *br* s, $C^{1'}$N-H), 7.04-6.98 (2H, m, $C^{3'}$-H, $C^{5'}$-H), 6.74 (1H, d, *J* 8.0, $C^{6'}$-H), 3.03 (2H, t, *J* 7.2, $C^{3'''}$-H_2), 2.78 (3H, d, *J* 1.8, C^8-H_3), 2.70 (2H, t, *J* 7.2, $C^{2'''}$-H_2), 2.35 (3H, s, C^6-H_3), 2.21 (3H, s, C^7-H_3); LRMS *m/z* (ESI^+) 384 ($[M+H]^+$, 100%).

4-(2-(4-Chlorophenethyl)-1-methyl-1*H*-benzo[*d*]imidazol-5-yl)-3,5-dimethylisoxazole 176

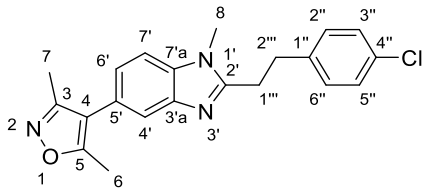

3-(4-Chlorophenyl)-*N*-(5-(3,5-dimethylisoxazol-4-yl)-2-(methylamino)phenyl)propana mide **209** (60 mg, 0.16 mmol, 1.0 eq.) was refluxed in toluene (2.0 mL) in a microwave vial containing 3 Å molecular sieves for 20 h. The reaction mixture was cooled to rt, filtered then the solvent evaporated *in vacuo.* The residue was purified by flash column chromatography eluting with CH_2Cl_2 : methanol (1:0 to 9:1) to yield 4-(2-(4-chlorophenethyl)-1-methyl-1*H*-benzo[*d*]imidazol-5-yl)-3,5-dimethylisoxazole **176** (48 mg, 84%) as a colourless solid: R_f 0.39 (CH_2Cl_2 : methanol, 9:1); m.p. 128-130 °C ($CDCl_3$); ν_{max} (thin film)/ cm^{-1} 1510 (N-O, m), 1492 (C-H, m), 1320 (C-N, s), 1152 (C-O, m), 910 (C=C, s), 732 (C-Cl, s); ^{1}H NMR (600 MHz, $CDCl_3$) δ 7.61 (1H, dd, *J* 1.5, 0.7, $C^{4'}$-H), 7.33 (1H, dd, *J* 8.3, 0.7, $C^{7'}$-H), 7.27-7.24 (2H, m, $C^{3''}$-H, $C^{5''}$-H), 7.18-7.14 (2H, m, $C^{2''}$-H, $C^{6''}$-H), 7.13 (1H, dd, *J* 8.3, 1.5, $C^{6'}$-H), 3.61 (3H, s, C^8-H_3), 3.26-3.20 (2H, m, $C^{2'''}$-H_2), 3.18-3.12 (2H, m, $C^{1'''}$-H_2), 2.41 (3H, s, C^6-H_3), 2.28 (3H, s, C^7-H_3); ^{13}C NMR (151 MHz, $CDCl_3$) δ 165.1 (C^5), 159.1 (C^3), 155.1 ($C^{2'}$), 143.0 ($C^{3'a}$), 139.2 ($C^{1''}$), 135.2 ($C^{7'a}$), 132.4 ($C^{4''}$), 129.9 ($C^{2''}$, $C^{6''}$), 128.9 ($C^{3''}$, $C^{5''}$), 124.3 ($C^{6'}$), 120.0 ($C^{4'}$), 117.3 (C^4), 109.4 ($C^{7'}$), 33.3 ($C^{2'''}$), 29.8 (C^8), 29.6 ($C^{1'''}$), 11.7 (C^6), 11.0 (C^7); LRMS *m/z* (ESI^+) 366 ([M+H]$^+$, 100%); HRMS *m/z* (ESI^+) [Found: 388.1205, $C_{21}H_{20}ClN_3O$ requires [M+Na]$^+$ 388.1187)]; Analytical HPLC (RP, *Method 3*) rt 7.7 min, purity 100%.

3-(4-Bromophenyl)-*N*-(5-(3,5-dimethylisoxazol-4-yl)-2-(methylamino)phenyl)propanamide 124

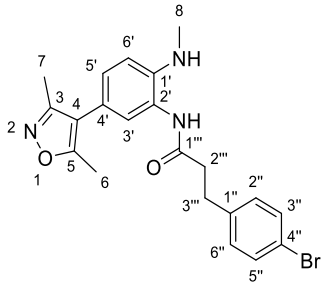

3-(4-Bromophenyl)propanoic acid (47.9 mg, 0.209 mmol, 1.0 eq.), HATU (79.5 mg, 0.209 mmol, 1.0 eq.) and DIPEA (72.9 µL, 0.418 mmol, 2.0 eq.) were combined in

anhydrous DMF (1.0 mL). 4-(3,5-Dimethylisoxazol-4-yl)-N^1-methylbenzene-1,2-diamine **76** (50.0 mg, 0.230 mmol, 1.1 eq.) in anhydrous DMF (500 µL) was added. The reaction mixture was stirred at rt for 17 h. The solvent was evaporated *in vacuo.* The residue was re-dissolved in ethyl acetate (10 mL) and water (5 mL) was added. The organic layer was separated then the aqueous layer was extracted with ethyl acetate (3 × 10 mL). The combined organic layers were washed with 10% w/v $LiCl_{(aq)}$ (3 × 10 mL), dried over $MgSO_{4\ (s)}$, filtered, then the filtrate was concentrated *in vacuo*. The residue was purified by flash column chromatography eluting with CH_2Cl_2 : methanol (1:0 to 9:1) to yield 3-(4-bromophenyl)-*N*-(5-(3,5-dimethylisoxazol-4-yl)-2-(methylamino)phenyl)propanamide **124** (78 mg, 87%) as a yellow solid: R_f 0.45 (CH_2Cl_2 : methanol, 9:1); ^{1}H NMR (400 MHz, $CDCl_3$) δ 7.44 (2H, d, *J* 8.4, $C^{3"}$-H, $C^{5"}$-H), 7.15 (2H, d, *J* 8.4, $C^{2"}$-H, $C^{6"}$-H), 7.08-7.00 (2H, m, $C^{3'}$-H, $C^{5'}$-H), 6.89 (1H, *br* s, $C^{1'}$N-H), 6.75 (1H, d, *J* 8.1, $C^{6'}$-H), 3.03 (2H, t, *J* 7.2, $C^{3'''}$-H_2), 2.79 (3H, d, *J* 1.0, C^8-H_3), 2.70 (2H, t, *J* 7.2, $C^{2'''}$-H_2), 2.36 (3H, s, C^6-H_3), 2.23 (3H, s, C^7-H_3); LRMS *m/z* (ESI^+) 430 ([M(^{79}Br)+H]$^+$, 100%).

4-(2-(4-Bromophenethyl)-1-methyl-1*H*-benzo[*d*]imidazol-5-yl)-3,5-dimethylisoxazole 125

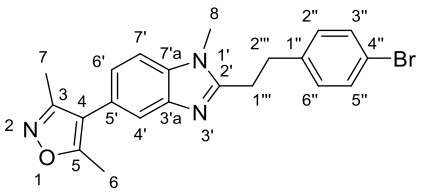

3-(4-Bromophenyl)-*N*-(5-(3,5-dimethylisoxazol-4-yl)-2-(methylamino)phenyl)propanamide **124** (70 mg, 0.16 mmol, 1.0 eq.) was refluxed in toluene (2.0 mL) in a microwave vial containing 3 Å molecular sieves for 24 h. The reaction mixture was cooled to rt, filtered then the solvent was evaporated *in vacuo.* The residue was purified by flash column chromatography eluting with CH_2Cl_2 : methanol (1:0 to 9:1) to yield 4-(2-(4-bromophenethyl)-1-methyl-1*H*-benzo[*d*]imidazol-5-yl)-3,5-dimethylisoxazole **125** (64 mg, 95%) as a colourless solid: R_f 0.56 (CH_2Cl_2 : methanol, 9:1); m.p. 135-137 °C (MeOH); ν_{max} (thin film)/ cm^{-1} 1510 (N-O, m), 1451 (C-H, m), 1321 (C-N, s), 1244 (C-O, m), 910 (C=C, m), 809 (C=C, m), 731 (C-Br, s); ^{1}H NMR (600 MHz, $CDCl_3$) δ 7.61 (1H, dd, *J* 1.5, 0.8, $C^{4'}$-H), 7.43-7.38 (2H, m, $C^{3"}$-H, $C^{5"}$-H), 7.33 (1H, d, *J* 8.2, $C^{7'}$-H), 7.13 (1H, dd, *J* 8.2, 1.5, $C^{6'}$-H), 7.10 (2H, d, *J* 8.1, $C^{2"}$-H, $C^{6"}$-H), 3.24-3.18

(2H, m, $C^{2'''}$-H_2), 3.18-3.12 (2H, m, $C^{1'''}$-H_2), 2.41 (3H, s, C^6-H_3), 2.28 (3H, s, C^7-H_3); ^{13}C NMR (151 MHz, $CDCl_3$) δ 165.1 (C^5), 159.1 (C^3), 155.0 ($C^{2'}$), 143.0 ($C^{3'a}$), 139.7 ($C^{1''}$), 135.2 ($C^{7'a}$), 131.8 ($C^{3''}$, $C^{5''}$), 130.3 ($C^{2''}$, $C^{6''}$), 124.3 ($C^{5'}$), 123.6 ($C^{6'}$), 120.4 ($C^{4''}$), 119.9 ($C^{4'}$), 117.2 (C^4), 109.4 ($C^{7'}$), 33.3 ($C^{2'''}$), 29.8 (C^8), 29.4 ($C^{1'''}$), 11.7 (C^6), 11.0 (C^7); LRMS *m/z* (ESI^+) 410 ([M(^{79}Br)+H]$^+$, 100%); HRMS *m/z* (ESI^+) [Found: 410.0875, $C_{21}H_{20}BrN_3O$ requires $[M+H]^+$ 410.0863)]; Analytical HPLC (RP, *Method 3*) rt 7.9 min, purity 100%.

_N_-(5-(3,5-Dimethylisoxazol-4-yl)-2-(methylamino)phenyl)-3-(4-(trifluoromethoxy)phenyl)propanamide 210

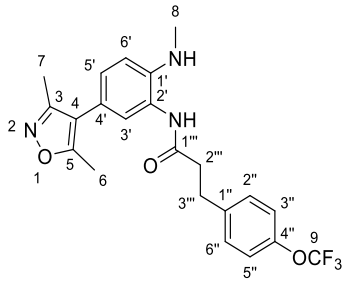

3-(4-(Trifluoromethoxy)phenyl)propanoic acid (48.9 mg, 0.209 mmol, 1.0 eq.), HATU (79.5 mg, 0.209 mmol, 1.0 eq.) and DIPEA (72.9 µL, 0.418 mmol, 2.0 eq.) were combined in anhydrous DMF (1.0 mL). 4-(3,5-Dimethylisoxazol-4-yl)-N^1-methylbenzene-1,2-diamine **76** (50.0 mg, 0.230 mmol, 1.1 eq.) in anhydrous DMF (500 µL) was added. The reaction mixture was stirred at rt for 17 h. The solvent was evaporated *in vacuo.* The residue was re-dissolved in ethyl acetate (10 mL) and water (5 mL) was added. The organic layer was separated then the aqueous layer was extracted with ethyl acetate (3 × 10 mL). The combined organic layers were washed with 10% w/v $LiCl_{(aq)}$ (3 × 10 mL), dried over $MgSO_{4\,(s)}$, filtered, then the filtrate was concentrated *in vacuo*. The residue was purified by flash column chromatography eluting with CH_2Cl_2 : methanol (1:0 to 9:1) to yield *N*-(5-(3,5-dimethylisoxazol-4-yl)-2-(methylamino)phenyl)-3-(4-(trifluoromethoxy)phenyl)propanamide **210** (63 mg, 63%) as an off-white solid: R_f 0.43 (CH_2Cl_2 : methanol, 9:1); ^{1}H NMR (400 MHz, $CDCl_3$) δ 7.30 (2H, d, *J* 8.5, $C^{3''}$-H, $C^{5''}$-H), 7.17 (2H, d, *J* 8.5, $C^{2''}$-H, $C^{6''}$-H), 7.07-7.01 (2H, m, $C^{3'}$-H, $C^{5'}$-H), 6.89 (1H, *br* s, $C^{1'}$N-H), 6.77 (1H, d, *J* 8.2, $C^{6'}$-H), 3.09 (2H, t, *J* 7.3, $C^{3'''}$-H_2), 2.79 (3H, s, C^8-H_3), 2.73 (2H, t, *J* 7.3, $C^{2'''}$-H_2), 2.36 (3H, s, C^6-H_3), 2.23 (3H, s, C^7-H_3);

^{19}F NMR (376 MHz, $CDCl_3$) δ -57.93 (3F, s, OCF_3); LRMS *m/z* (ESI^+) 434 ($[M+H]^+$, 100%).

3,5-Dimethyl-4-(1-methyl-2-(4-(trifluoromethoxy)phenethyl)-1*H*-benzo[*d*]imidazol-5-yl)isoxazole 144

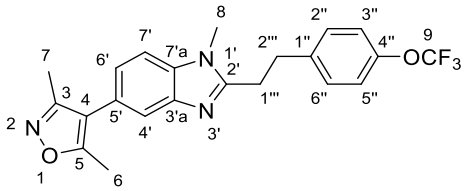

N-(5-(3,5-Dimethylisoxazol-4-yl)-2-(methylamino)phenyl)-3-(4-(trifluoromethoxy)phenyl)propanamide **210** (55 mg, 0.13mmol, 1.0 eq.) was refluxed in toluene (2.0 mL) in a microwave vial containing 3 Å molecular sieves for 24 h. The reaction mixture was cooled to rt, filtered and then the solvent evaporated *in vacuo*. The residue was purified by flash column chromatography eluting with CH_2Cl_2 : methanol (1:0 to 9:1) to yield 3,5-dimethyl-4-(1-methyl-2-(4-(trifluoromethoxy)phenethyl)-1*H*-benzo[*d*]imidazol-5-yl)isoxazole **144** (46 mg, 87%) as a colourless oil: R_f 0.44 (CH_2Cl_2 : methanol, 9:1); ν_{max} (thin film)/ cm^{-1} 1510 (N-O, m), 1485 (C-H, m), 1320 (C-N, s), 1264 (C-O, s), 1223 (C-F, s), 1163 (C-O, s); ^{1}H NMR (600 MHz, $CDCl_3$) δ 7.62 (1H, d, *J* 1.5, $C^{4'}$-H), 7.33 (1H, d, *J* 8.2, $C^{7'}$-H), 7.25 (2H, d, *J* 8.7, $C^{3"}$-H, $C^{5"}$-H), 7.18-7.11 (3H, m, $C^{6'}$-H, $C^{2"}$-H, $C^{6"}$-H), 3.61 (3H, s, C^8-H_3), 3.30-3.24 (2H, m, $C^{2'''}$-H_2), 3.20-3.15 (2H, m, $C^{1'''}$-H_2), 2.41 (3H, s, C^6-H_3), 2.28 (3H, s, C^7-H_3); ^{13}C NMR (151 MHz, $CDCl_3$) δ 165.1 (C^5), 159.1 (C^3), 155.0 ($C^{2'}$), 148.0 (q, *J* 2.2, $C^{4"}$), 143.0 ($C^{3'a}$), 139.6 ($C^{1"}$), 135.2 ($C^{7'a}$), 129.8 ($C^{3"}$, $C^{5"}$), 124.3 ($C^{5'}$), 123.7 ($C^{2"}$, $C^{6"}$), 121.3 ($C^{6'}$), 120.7 (q, *J* 257.1, C^9), 120.0 ($C^{4'}$), 117.2 (C^4), 109.4 ($C^{7'}$), 33.2 ($C^{2'''}$), 29.8 (C^8), 29.6 ($C^{1'''}$), 11.7 (C^6), 11.0 (C^7); ^{19}F NMR (565 MHz, $CDCl_3$) δ -57.93 (3F, s, OCF_3); LRMS *m/z* (ESI^+) 416 ($[M+H]^+$, 100%); HRMS *m/z* (ESI^+) [Found: 416.1578, $C_{22}H_{20}F_3N_3O_2$ requires $[M+H]^+$ 416.1580)]; Analytical HPLC (RP, *Method 3*) rt 8.2 min, purity 100%.

***N*-(5-(3,5-dimethylisoxazol-4-yl)-2-(methylamino)phenyl)-3-(4-methoxyphenyl)propanamide 211**

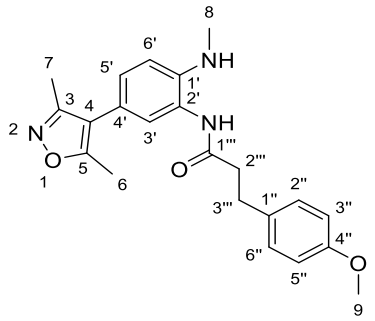

4-(3,5-Dimethylisoxazol-4-yl)-N^1-methylbenzene-1,2-diamine **76** (100 mg, 0.462 mmol, 1.0 eq.) was dissolved in DMF (1.0 mL). 3-(4-Methoxyphenyl)propanoic acid (87.5 mg, 0.485 mmol, 1.05 eq.) and HATU (185 mg, 0.485 mmol, 1.05 eq.) were added. The reaction mixture was stirred at rt for 17 h. The reaction mixture was partitioned between ethyl acetate (10 mL) and sat. aq. $NaHCO_3$ (5 mL). The organic layer was separated then the aqueous layer was extracted with ethyl acetate (3 × 10 mL). The combined organic layers were washed with brine, dried over $MgSO_{4\,(s)}$, filtered, then the filtrate was concentrated *in vacuo*. The residue was purified by flash column chromatography eluting with CH_2Cl_2 : methanol (1:0 to 9:1) to yield *N*-(5-(3,5-dimethylisoxazol-4-yl)-2-(methylamino)phenyl)-3-(4-methoxyphenyl)propanamide **211** (45 mg, 26%) as a brown oil: R_f 0.60 (CH_2Cl_2 : methanol, 9:1); ^{1}H NMR (400 MHz, $CDCl_3$) δ 7.64 (1H, d, *J* 1.6, $C^{3'}$-H), 7.32 (1H, d, *J* 8.3, $C^{6'}$-H), 7.18-7.08 (3H, m, $C^{5'}$-H, $C^{2''}$-H, $C^{6''}$-H), 6.87-6.78 (2H, m, $C^{3''}$-H, $C^{5''}$-H), 3.79 (3H, s, C^9-H_3), 3.21-3.12 (4H, m, $C^{2'''}$-H_2, $C^{3'''}$-H_2), 2.80 (3H, s, C^8-H_3), 2.42 (3H, s, C^6-H_3), 2.29 (3H, s, C^7-H_3); ^{13}C NMR (101 MHz, $CDCl_3$) δ 176.7 ($C^{1'''}$), 165.2 (C^5), 159.1 (C^3), 158.4 ($C^{4''}$), 142.4 ($C^{1'}$), 134.9 ($C^{2'}$), 132.7 ($C^{1''}$), 129.5 ($C^{2''}$, $C^{6''}$), 124.5 ($C^{4'}$), 123.7 ($C^{5'}$), 119.7 ($C^{3'}$), 117.2 (C^4), 114.2($C^{3''}$, $C^{4''}$), 109.5 ($C^{6'}$), 55.4 (C^9), 33.4 ($C^{3'''}$), 30.2 ($C^{2'''}$), 29.9 (C^8), 11.7 (C^6), 11.0 (C^7); LRMS *m/z* (ESI^+) 362 ($[M+2H-CH_3]^+$, 100%).

4-(2-(4-Methoxyphenethyl)-1-methyl-1*H*-benzo[*d*]imidazol-5-yl)-3,5-dimethylisoxazole 142

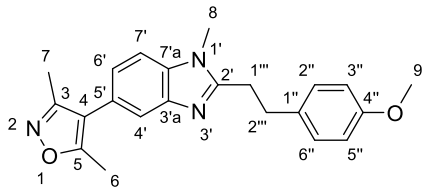

N-(5-(3,5-dimethylisoxazol-4-yl)-2-(methylamino)phenyl)-3-(4-methoxyphenyl)propanamide **211** (39.0 mg, 0.103 mmol, 1.0 eq.) and 3-(4-methoxyphenyl)propanoic acid (19.0 mg, 0.103 mmol, 1.0 eq.) were combined in toluene (400 µL) in a microwave vial containing 3 Å molecular sieves. The reaction mixture was stirred at 120 °C for 18 h. The reaction mixture was cooled to rt, filtered then the solvent was evaporated *in vacuo.* The residue was purified by RP flash column chromatography eluting with water : acetonitrile (95:5 to 5:95) to yield 4-(2-(4-methoxyphenethyl)-1-methyl-1*H*-benzo[*d*]imidazol-5-yl)-3,5-dimethylisoxazole **142** (17 mg, 46%) as an off-white solid: R_f 0.33 (petroleum ether : ethyl acetate, 3:7); m.p. 128-130 °C ($CDCl_3$); ν_{max} (thin film)/ cm^{-1} 1511 (N-O, s), 1242 (C-O, s), 1037 (C-N, m); ^1H NMR (400 MHz, $CDCl_3$) δ 7.32 (1H, dd, *J* 8.3, 0.7, $C^{7'}$-H), 7.18-7.09 (3H, m, $C^{6'}$-H, $C^{2''}$-H, $C^{6''}$-H), 6.88-6.80 (2H, m, $C^{3''}$-H, $C^{5''}$-H), 3.79 (3H, s, C^9-H_3), 3.58 (3H, s, C^8-H_3), 3.17 (4H, m, $C^{1'''}$-H_2, $C^{2'''}$-H_2), 2.42 (3H, s, C^6-H_3), 2.29 (3H, s, C^7-H_3); ^{13}C NMR (101 MHz, $CDCl_3$) δ 165.0 (C^5), 159.0 ($C^{4''}$), 158.3 (C^3), 155.5 ($C^{2'}$), 142.9 ($C^{3'a}$), 135.1 ($C^{7'a}$), 132.8 ($C^{1''}$), 129.4 ($C^{6''}$, $C^{2''}$), 124.1 ($C^{5'}$), 123.4 ($C^{6'}$), 119.8 ($C^{4'}$), 117.2 (C^4), 114.1 ($C^{3''}$, $C^{5''}$), 109.3 ($C^{7'}$), 55.3 (C^9), 33.2 ($C^{2'''}$), 30.0 ($C^{1'''}$), 29.7 (C^8), 11.6 (C^6), 10.9 (C^7); LRMS *m/z* (ESI^+) 362 ($[M+H]^+$, 100%). HRMS *m/z* (ESI^+) [Found: 362.1859, $C_{22}H_{23}O_2N_3$ requires $[M+H]^+$ 362.1863)]; Analytical HPLC (RP, *Method 1*) rt 7.9 min, purity 100%.

***N*-(5-(3,5-dimethylisoxazol-4-yl)-2-(methylamino)phenyl)-3-(4-nitrophenyl)propenamide 212**

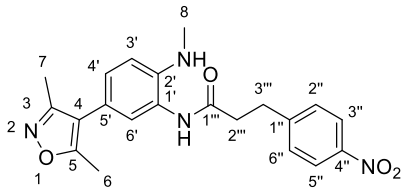

4-(3,5-Dimethyl-1,2-oxazol-4-yl)-*N*-methyl-2-nitroaniline **75** (200 mg, 0.81 mmol, 1.0 eq.) was suspended in EtOH (4.2 mL) and 1 M $Na_2S_2O_4$ (4.2 mL, 4.2 mmol, 5.2 eq.) was added. The reaction mixture was stirred at 80 °C for 15 min. The reaction mixture was cooled to rt and partitioned between ethyl acetate (15 mL) and 10% aq. ammonia solution (7 mL). The phases were separated then the organic phase was washed with water (5 mL) and brine (5 mL), dried over $MgSO_{4\,(s)}$, filtered, then the filtrate was concentrated *in vacuo*. The crude material was dissolved in DMF (2.0 mL). DIPEA (168 µL, 0.97 mmol, 1.05 eq.), 3-(4-nitrophenyl)propanoic acid (189 mg, 0.97 mmol, 1.05 eq.), HATU (368 mg, 0.97 mmol, 1.05 eq.) and HOBT (131 mg, 0.97 mmol, 1.05 eq.) were added. The reaction mixture was stirred at rt for 2 h. The reaction mixture was partitioned between ethyl acetate and water. The organic layer was separated then the aqueous layer was extracted with ethyl acetate (3 × 10 mL). The combined organic layers were washed with brine, dried over $MgSO_{4\,(s)}$, filtered, then the filtrate was concentrated *in vacuo*. The residue was purified by flash column chromatography eluting with petroleum ether : ethyl acetate (3:2 to 0:1) to yield *N*-(5-(3,5-dimethylisoxazol-4-yl)-2-(methylamino)phenyl)-3-(4-nitrophenyl)propenamide **212** (44 mg, 13%) as a yellow oil: R_f 0.38 (petroleum ether : ethyl acetate, 1:9); ^{1}H NMR (400 MHz, $CDCl_3$) δ 8.20-8.14 (2H, m, $C^{3'''}$-H, $C^{5'''}$-H), 7.48-7.40 (2H, m, $C^{2''}$-H, $C^{6''}$-H), 7.09 (1H, d, *J* 2.0, $C^{6'}$-H), 7.07-7.01 (1H, m, $C^{4'}$-H), 6.80 (1H, d, *J* 8.3, $C^{3'}$-H), 3.19 (2H, t, *J* 7.4, $C^{2'''}$-H_2), 2.80 (3H, s, C^8-H_3), 2.77 (2H, t, *J* 7.4, $C^{3'''}$-H_2), 2.36 (3H, s, C^6-H_3), 2.23 (3H, s, C^7-H_3); ^{13}C NMR (101 MHz, $CDCl_3$) δ 170.2 ($C^{1'''}$), 164.9 (C^5), 159.0 (C^3), 148.5 ($C^{4''}$), 146.9 ($C^{1''}$), 142.8 ($C^{2'}$), 129.6 ($C^{2''}$, $C^{6''}$), 128.5 ($C^{4'}$), 126.1 ($C^{6'}$), 124.0 ($C^{3''}$, $C^{5''}$), 123.7 ($C^{1'}$), 119.9 ($C^{5'}$), 116.1 (C^4), 112.8 ($C^{3'}$), 38.0 ($C^{3'''}$), 31.3 ($C^{2'''}$), 30.9 (C^8), 11.7 (C^6), 10.9 (C^7); LRMS *m/z* (ESI^-) 393 ($[M+Na]^-$, 100%).

3,5-Dimethyl-4-(1-methyl-2-(4-nitrophenethyl)-1*H*-benzo[*d*]imidazol-5-yl)isoxazole 152

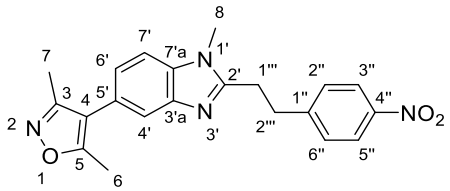

N-(5-(3,5-Dimethylisoxazol-4-yl)-2-(methylamino)phenyl)-3-(4-nitrophenyl)propenamide **212** (30 mg, 80.0 µmol, 1.0 eq.) and 3-(4-nitrophenyl)propanoic acid (3.1 mg, 16.0 µmol, 0.2 eq.) were combined in toluene (0.7 mL) in a microwave vial containing 3 Å molecular sieves. The reaction mixture was refluxed for 48 h. The reaction mixture was cooled to rt, filtered then the solvent was evaporated *in vacuo.* The residue was purified by RP flash column chromatography eluting with H_2O : acetonitrile (95:5 to 5:95) to yield 3,5-dimethyl-4-(1-methyl-2-(4-nitrophenethyl)-1*H*-benzo[*d*]imidazol-5-yl)isoxazole **152** (15 mg, 50%) as a yellow solid: R_f 0.39 (CH_2Cl_2 : methanol, 9:1); m.p. 194-195 °C ($CDCl_3$); ν_{max} (thin film)/ cm^{-1} 1519 (N-O, s), 1449 (C-H, m), 1346 (C-N, s); ^{1}H NMR (400 MHz, $CDCl_3$) δ 8.21-8.12 (2H, m, $C^{3''}$-H, $C^{5''}$-H), 7.26 (1H, d, *J* 1.5, $C^{4'}$-H), 7.46-7.40 (2H, m, $C^{2''}$-H, $C^{6''}$-H), 7.35 (1H, d, *J* 8.3, $C^{7'}$-H), 7.15 (1H, dd, *J* 8.3, 1.5, $C^{6'}$-H), 3.67 (3H, s, C^8-H_3), 3.41 (2H, dd, *J* 8.9, 6.7, $C^{1'''}$-H_2), 3.23 (2H, dd, *J* 8.9, 6.7, $C^{2'''}$-H_2), 2.42 (3H, s, C^6-H_3), 2.29 (3H, s, C^7-H_3); ^{13}C NMR (101 MHz, $CDCl_3$) δ 165.2 (C^5), 159.1 (C^3), 154.3 ($C^{2'}$), 148.5 ($C^{1''}$), 146.9 ($C^{4''}$), 142.9 ($C^{3'a}$), 135.2 ($C^{7'a}$), 129.5 ($C^{2''}$, $C^{6''}$), 124.6 ($C^{5'}$), 124.1 ($C^{3''}$, $C^{5''}$), 123.9 ($C^{6'}$), 120.0 ($C^{4'}$), 117.2 (C^4), 109.5 ($C^{7'}$), 33.4 ($C^{1'''}$), 29.9 (C^8), 28.9 ($C^{2'''}$), 11.7 (C^6), 11.0 (C^7); LRMS *m/z* (ESI^+) 377 ($[M+H]^+$, 100%); HRMS *m/z* (ESI^+) [Found: 332.1764, $C_{21}H_{20}ON_3$ requires $[M+H]^+$ 332.1757)]; Analytical HPLC (RP, *Method 3*) rt 7.4 min, purity 100%.

***N*-(5-(3,5-Dimethylisoxazol-4-yl)-2-(methylamino)phenyl)-3-(*p*-tolyl)propanamide 213**

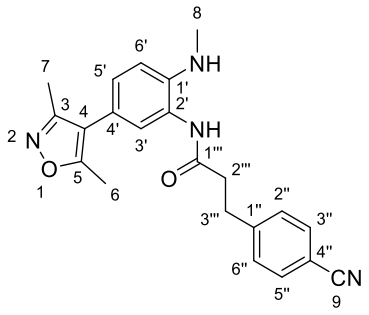

1 M $Na_2S_2O_{4\,(aq)}$ (3.15 mL, 3.2 mmol, 5.2 eq.) was added to 4-(3,5-dimethylisoxazol-4-yl)-*N*-methyl-2-nitroaniline **75** (150 mg, 0.61 mmol, 1.0 eq.) in EtOH (3.15 mL). The reaction mixture was stirred at 80 °C for 15 min. The reaction mixture was cooled to rt then the solvent was evaporated *in vacuo.* The residue was partitioned between 10% aq. ammonia solution and ethyl acetate. The aqueous layer was separated then extracted with ethyl acetate (3 × 15 mL). The combined organic layers were dried over $MgSO_{4\,(s)}$, filtered, then the filtrate was concentrated *in vacuo*. The residue was dissolved in anhydrous DMF (1.0 mL). 3-(4-Cyanophenyl)propanoic acid (80.6 mg, 0.46 mmol, 1.0 eq.), HATU (184 mg, 0.48 mmol, 1.05 eq.) and DIPEA (84.2 µL, 0.48 mmol, 1.05 eq.) were added. The reaction mixture was stirred at rt for 17 h. The solvent was evaporated *in vacuo.* The residue was re-dissolved in ethyl acetate (10 mL) and water (5 mL) was added. The organic layer was separated then the aqueous layer was extracted with ethyl acetate (3 × 10 mL). The combined organic layers were washed with 10% w/v $LiCl_{(aq)}$ (3 × 10 mL), dried over $MgSO_{4\,(s)}$, filtered, then the filtrate was concentrated *in vacuo*. The residue was purified by flash column chromatography eluting with petroleum ether : ethyl acetate (1:0 to 0:1) to yield *N*-(5-(3,5-dimethylisoxazol-4-yl)-2-(methylamino)phenyl)-3-(*p*-tolyl)propanamide **213** (168 mg, 89%) as a brown solid: R_f 0.46 (CH_2Cl_2 : methanol, 9:1); ^{1}H NMR (400 MHz, $CDCl_3$) δ 7.59 (2H, d, *J* 8.3, $C^{3"}$-H, $C^{5"}$-H), 7.37 (2H, d, *J* 8.3, $C^{2"}$-H, $C^{6"}$-H), 7.29 (1H, s, $OC^{1'''}N$-H), 7.08 (1H, d, *J* 2.0, $C^{3'}$-H), 7.03 (1H, dd, *J* 8.3, 2.0, $C^{5'}$-H), 6.77 (1H, d, *J* 8.3, $C^{6'}$-H), 3.13 (2H, t, *J* 7.4, $C^{3'''}$-H_2), 2.79 (3H, d, *J* 12.7, C^8-H_3), 2.75 (2H, t, *J* 7.4, $C^{2'''}$-H_2), 2.35 (3H, s, C^6-H_3), 2.21 (3H, s, C^7-H_3); ^{13}C NMR (101 MHz, $CDCl_3$) δ 170.4 ($C^{1'''}$), 164.9 (C^5), 159.0 (C^3), 146.5 ($C^{1'}$), 142.9 ($C^{1"}$), 132.5 ($C^{3"}$, $C^{5"}$), 129.5 ($C^{2"}$, $C^{6"}$), 128.4 ($C^{5'}$), 126.1 ($C^{3'}$), 123.7 ($C^{2'}$), 119.5 ($C^{4'}$), 119.0 (C^9), 116.2 (C^4), 112.5 ($C^{6'}$), 110.4 ($C^{4"}$), 38.7 ($C^{2'''}$), 31.6 ($C^{3'''}$), 30.8 (C^8), 11.7 (C^6), 10.9 (C^7); LRMS *m/z* (ESI^+) 375 ($[M+H]^+$, 100%).

4-(2-(5-(3,5-Dimethylisoxazol-4-yl)-1-methyl-1*H*-benzo[*d*]imidazol-2-yl)ethyl)benzonitrile 155

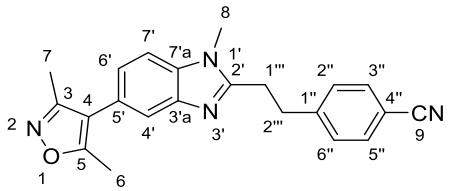

N-(5-(3,5-Dimethylisoxazol-4-yl)-2-(methylamino)phenyl)-3-(*p*-tolyl)propanamide **213** (100 mg, 0.27 mmol, 1.0 eq.) and 3-(4-cyanophenyl)propanoic acid (4.7 mg, 0.027 mmol, 0.1 eq.) were combined in toluene (1.0 mL) in a microwave vial containing 3 Å molecular sieves. The reaction mixture was stirred at 130 °C for 72 h. The reaction mixture was cooled to rt, filtered then the solvent was evaporated *in vacuo.* The residue was purified by column chromatography eluting with petroleum ether : ethyl acetate (1:0 to 0:1) to yield 4-(2-(5-(3,5-dimethylisoxazol-4-yl)-1-methyl-1*H*-benzo[*d*]imidazol-2-yl)ethyl)benzonitrile **155** (49 mg, 52%) as a light yellow solid: R_f 0.61 (CH_2Cl_2 : methanol, 9:1); m.p. 169-171 °C ($CDCl_3$); ν_{max} (thin film)/ cm^{-1} 2229 (C≡N, w), 1423 (C-H, m), 1321 (C-H, m); ^{1}H NMR (600 MHz, $CDCl_3$) δ 7.62 (1H, d, *J* 1.6, $C^{4'}$-H), 7.59 (2H, d, *J* 7.9, $C^{3''}$-H, $C^{5''}$-H), 7.37 (1H, d, *J* 8.0, $C^{7'}$-H), 7.35 (2H, d, *J* 7.9, $C^{2''}$-H, $C^{6''}$-H), 7.16 (1H, dd, *J* 8.0, 1.6, $C^{6'}$-H), 3.65 (3H, s, C^8-H_3), 3.36 (2H, dd, *J* 9.0, 6.8, $C^{2'''}$-H_2), 3.21 (2H, dd, *J* 9.0, 6.8, $C^{1'''}$-H_2), 2.42 (3H, s, C^6-H_3), 2.28 (3H, s, C^7-H_3); ^{13}C NMR (151 MHz, $CDCl_3$) δ 165.2 (C^5), 159.1 (C^3), 154.4 ($C^{2'}$), 146.3 ($C^{3'a}$), 142.5 ($C^{1''}$), 135.1 ($C^{7'a}$), 132.6 ($C^{3''}$, $C^{5''}$), 129.4 ($C^{2''}$, $C^{6''}$), 124.7 ($C^{5'}$), 124.0 ($C^{6'}$), 119.9 ($C^{4'}$), 118.9 (C^9), 117.2 (C^4), 110.7 ($C^{4''}$), 109.6 ($C^{7'}$), 33.7 ($C^{2'''}$), 29.9 (C^8), 28.9 ($C^{1'''}$), 11.7 (C^6), 11.0 (C^7); LRMS *m/z* (ESI^+) 357 ($[M+H]^+$, 100%); HRMS *m/z* (ESI^+) [Found: 357.1713, $C_{22}H_{20}N_4O$ requires $[M+H]^+$ 357.1710)]; Analytical HPLC (RP, *Method 3*) rt 6.5 min, purity 100%.

***N*-(5-(3,5-Dimethylisoxazol-4-yl)-2-(methylamino)phenyl)-3-(4-(trifluoromethyl)phenyl)propanamide 214**

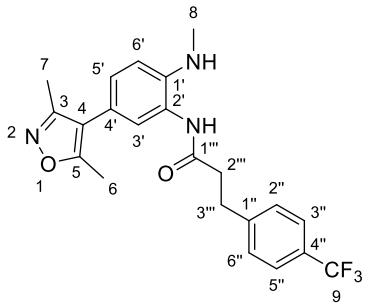

1 M $Na_2S_2O_{4\,(aq)}$ (3.15 mL, 3.15 mmol, 5.2 eq.) was added to 4-(3,5-dimethylisoxazol-4-yl)-*N*-methyl-2-nitroanilinae **75** (150 mg, 0.606 mmol, 1.0 eq.) in EtOH (3.15 mL). The reaction mixture was stirred at 80 °C for 30 min. The reaction mixture was cooled to rt and partitioned between 10% aq. ammonia solution and ethyl acetate. The aqueous layer was separated then extracted with ethyl acetate (3 × 15 mL). The combined organic layers were dried over $MgSO_{4\,(s)}$, filtered, then the filtrate was concentrated *in vacuo*. The residue was dissolved in anhydrous DMF (1.0 mL). 3-(4-(Trifluoromethyl)phenyl)propanoic acid (120 mg, 0.551 mmol, 1.0 eq.), HATU (220 mg, 0.578 mmol, 1.05 eq.) and DIPEA (101 µL, 0.578 mmol, 1.05 eq.) were added. The reaction mixture was stirred at rt for 5 h. The solvent was evaporated *in vacuo.* The residue was re-dissolved in ethyl acetate (10 mL) and 1 M NaOH (5 mL) was added. The organic layer was separated then the aqueous layer was extracted with ethyl acetate (3 × 10 mL). The combined organic layers were washed with 10% w/v $LiCl_{(aq)}$ (3 × 10 mL), dried over $MgSO_{4\,(s)}$, filtered, then the filtrate was concentrated *in vacuo*. The residue was purified by flash column chromatography eluting with petroleum ether : ethyl acetate (1:0 to 0:1) to yield *N*-(5-(3,5-dimethylisoxazol-4-yl)-2-(methylamino)phenyl)-3-(4-(trifluoromethyl)phenyl)propanamide **214** (156 mg, 68%) as a light brown solid: R_f 0.46 (petroleum ether : ethyl acetate, 1:4); ^{1}H NMR (400 MHz, $CDCl_3$) δ 7.57 (4H, d, *J* 8.0, $C^{3''}$-H_2, $C^{5''}$-H_2), 7.39 (4H, d, *J* 8.0, $C^{2''}$-H_2, $C^{6''}$-H_2), 7.09-7.00 (2H, m, $C^{3'}$-H, $C^{5'}$-H), 6.76 (1H, d, *J* 8.2, $C^{6'}$-H), 3.12 (2H, t, *J* 7.3, $C^{3''''}$-H_2), 2.77 (3H, s, C^8-H_3), 2.76 (2H, t, *J* 7.3, $C^{2''''}$-H_2), 2.35 (3H, s, C^6-H_3), 2.22 (3H, s, C^7-H_3); ^{13}C NMR (101 MHz, $CDCl_3$) δ 170.7 ($C^{1''''}$), 164.9 (C^5), 159.0 (C^3), 144.8 ($C^{1''}$), 142.9 ($C^{1'}$), 130.6 (m, $C^{4''}$), 129.1 ($C^{2''}$, $C^{6''}$), 128.4 ($C^{3'}$), 127.1 (q, *J* 273.1, C^9), 126.3 ($C^{5'}$), 125.7 (q, *J* 4.0, $C^{3''}$, $C^{5''}$), 123.5 ($C^{2'}$), 119.5 ($C^{4'}$), 116.2 (C^4), 112.5 ($C^{6'}$),

38.4 ($C^{2'''}$), 31.5 ($C^{3'''}$), 30.7(C^{8}), 11.6 (C^{6}), 10.9 (C^{7}); ^{19}F NMR (565 MHz, $CDCl_3$) δ -62.26 (s, CF_3); LRMS *m/z* (ESI^+) 418 ($[M+H]^+$, 100%).

3,5-Dimethyl-4-(1-methyl-2-(4-(trifluoromethyl)phenethyl)-1*H*-benzo[*d*]imidazol-5-yl)isoxazole 177

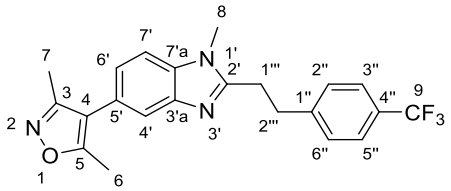

N-(5-(3,5-Dimethylisoxazol-4-yl)-2-(methylamino)phenyl)-3-(4-(trifluoromethyl)phenyl)propanamide **214** (130 mg, 310 µmol, 1.0 eq.) and 3-(4-(trifluoromethyl)phenyl)propanoic acid (6.8 mg, 19.0 µmol, 0.1 eq.) were combined in toluene (1.0 mL) in a microwave vial containing 3 Å molecular sieves. The reaction mixture was stirred at 130 °C for 72 h. The reaction mixture was cooled to rt, filtered then the solvent was evaporated *in vacuo.* The residue was purified by RP flash column chromatography eluting with water : acetonitrile (95:5 to 5:95) to yield 3,5-dimethyl-4-(1-methyl-2-(4-(trifluoromethyl)phenethyl)-1*H*-benzo[*d*]imidazol-5-yl)isoxazole **177** (96 mg, 77%) as a colourless solid: R_f 0.38 (CH_2Cl_2 : methanol, 9:1); m.p. 124-126 °C ($CDCl_3$); ν_{max} (thin film)/ cm^{-1} 1619 (C=C, w), 1420 (C-H, w), 1325 (C-F, s), 1164 (C-H, w), 1122 (C-F, m), 1067 (C-H, m); ^1H NMR (600 MHz, $CDCl_3$) δ 7.63 (1H, s, $C^{4'}$-H), 7.56 (2H, d, *J* 7.8, $C^{2''}$-H, $C^{6''}$-H), 7.36 (1H, d, *J* 8.3, $C^{7'}$-H), 7.35 (2H, d, *J* 9.3, $C^{3''}$-H, $C^{5''}$-H), 7.15 (1H, d, *J* 8.3, $C^{6'}$-H), 3.64 (3H, s, C^{8}-H_3), 3.34 (2H, t, *J* 8.0, C^{2iv}-H_2), 3.21 (2H, t, *J* 8.0, C^{1iv}-H_2), 2.41 (3H, s, C^{6}-H_3), 2.28 (3H, s, C^{7}-H_3); ^{13}C NMR (151 MHz, $CDCl_3$) δ 165.2 (C^{5}), 159.1 (C^{3}), 154.8 ($C^{2'}$), 144.9 ($C^{1''}$), 142.7 ($C^{3'a}$), 135.2 ($C^{7'a}$), 129.0 (q, *J* 35.3, $C^{1''}$), 128.9 ($C^{2''}$, $C^{6''}$), 125.7 (q, *J* 3.8, $C^{3''}$, $C^{5''}$), 124.5 ($C^{5'}$), 124.3 (q, *J* 273.0, C^{9}), 123.8 ($C^{6'}$), 119.9 ($C^{4'}$), 117.2 (C^{4}), 109.5 ($C^{7'}$), 33.6 ($C^{2'''}$), 29.9 (C^{8}), 29.2 ($C^{1'''}$), 11.7 (C^{6}), 11.0 (C^{7}); ^{19}F NMR (565 MHz, $CDCl_3$) δ -62.43 (s, CF_3); LRMS *m/z* (ESI^+) 400 ($[M+H]^+$, 100%); HRMS *m/z* (ESI^+) [Found: 400.1646, $C_{22}H_{20}F_3N_3O$ requires $[M+H]^+$ 400.1631)]; Analytical HPLC (RP, *Method 3*) rt 7.4 min, purity 95%.

Methyl 4-(3-((5-(3,5-dimethylisoxazol-4-yl)-2-(methylamino)phenyl)amino)-3-oxopropyl)benzoate 215

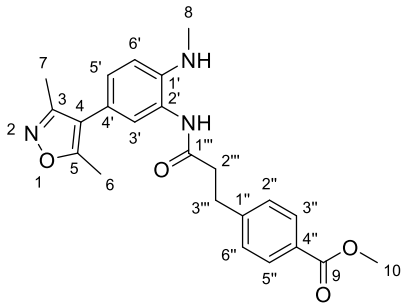

1 M $Na_2S_2O_{4\,(aq)}$ (3.15 mL, 3.15 mmol, 5.2 eq.) was added to 4-(3,5-dimethylisoxazol-4-yl)-*N*-methyl-2-nitroaniline **75** (150 mg, 0.606 mmol, 1.0 eq.) in EtOH (3.15 mL). The reaction mixture was stirred at 80 °C for 10 min. The reaction mixture was cooled to rt and partitioned between 10% aq. ammonia solution and ethyl acetate. The aqueous layer was separated then extracted with ethyl acetate (3 × 15 mL). The combined organic layers were dried over $MgSO_{4\,(s)}$, filtered, then the filtrate was concentrated *in vacuo*. The residue was dissolved in anhydrous DMF (1.0 mL). 3-(4-(Methoxycarbonyl)phenyl)propanoic acid (95.8 mg, 0.460 mmol, 1.0 eq.), HATU (175 mg, 0.460 mmol, 1.0 eq.) and DIPEA (160 µL, 0.921 mmol, 2.0 eq.) were added. The reaction mixture was stirred at rt for 3 h. The solvent was evaporated *in vacuo.* The residue was re-dissolved in ethyl acetate (10 mL) and 1 M aq NaOH (5 mL) was added. The organic layer was separated then the aqueous layer was extracted with ethyl acetate (3 × 10 mL). The combined organic layers were washed with 10% w/v $LiCl_{(aq)}$ (3 × 10 mL), dried over $MgSO_{4\,(s)}$, filtered, then the filtrate was concentrated *in vacuo*. The residue was purified by flash column chromatography eluting with CH_2Cl_2 : methanol (1:0 to 9:1) to yield methyl 4-(3-((5-(3,5-dimethylisoxazol-4-yl)-2-(methylamino)phenyl)amino)-3-oxopropyl)benzoate **215** (118 mg, 63%) as an off-white solid: R_f 0.31 (CH_2Cl_2 : methanol, 1:0 to 9:1); m.p. 150-152 °C ($CDCl_3$); ^{1}H NMR (400 MHz, $CDCl_3$) δ 8.03-7.95 (2H, d, *J* 8.3, $C^{3"}$-H, $C^{5"}$-H), 7.37-7.31 (2H, d, *J* 8.3, $C^{2"}$-H, $C^{6"}$-H), 7.05-6.98 (2H, m, $C^{3'}$-H, $C^{5'}$-H), 6.89 (1H, *br* s, $C^{1'}$N-H), 6.74 (1H, dd, *J* 8.7, 1.3, $C^{6'}$-H), 3.91 (3H, s, C^{10}-H_3), 3.13 (2H, t, *J* 7.3, $C^{3'''}$-H_2), 2.76 (3H, s, C^{8}-H_3), 2.74 (2H, t, *J* 7.3, $C^{2'''}$-H_2), 2.36 (3H, s, C^{6}-H_3), 2.22 (3H, s, C^{7}-H_3); ^{13}C NMR (101 MHz, $CDCl_3$) δ 170.8 ($C^{1'''}$), 167.0 (C^{9}), 164.9 (C^{5}), 159.0 (C^{3}), 146.1 ($C^{1"}$), 143.0 ($C^{1'}$), 130.1 ($C^{3"}$, $C^{5"}$), 128.8 ($C^{2"}$, $C^{6"}$), 128.7 ($C^{4"}$), 128.4 ($C^{5'}$), 126.4 ($C^{3'}$), 123.5 ($C^{2'}$), 119.5 ($C^{4'}$), 116.2 (C^{4}), 112.4 ($C^{6'}$), 52.3 (C^{10}), 38.6 ($C^{2'''}$), 31.8 ($C^{3'''}$), 30.7 (C^{8}),

11.7 (C^6), 10.9 (C^7); LRMS *m/z* (ESI^-) 406 ($[M-H]^-$, 100%); HRMS *m/z* (ESI^+) [Found: 430.1756, $C_{23}H_{25}N_3O_4$ requires $[M+Na]^+$ 430.1737)].

Methyl 4-(2-(5-(3,5-dimethylisoxazol-4-yl)-1-methyl-1*H*-benzo[*d*]imidazol-2-yl)ethyl)benzoate 146

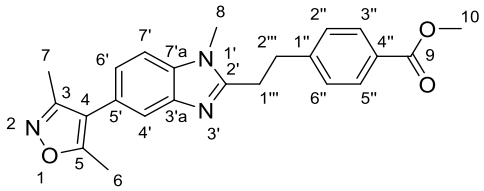

Methyl 4-(3-((5-(3,5-dimethylisoxazol-4-yl)-2-(methylamino)phenyl)amino)-3-oxopropyl)benzoate **215** (100 mg, 0.25 mmol, 1.0 eq.) was refluxed in toluene (1.0 mL) in a microwave vial containing 3 Å molecular sieves for 72 h. The reaction mixture was cooled to rt, filtered then the solvent was evaporated *in vacuo.* The residue was purified by column chromatography eluting with CH_2Cl_2 : methanol (1:0 to 93:7) to yield methyl 4-(2-(5-(3,5-dimethylisoxazol-4-yl)-1-methyl-1*H*-benzo[*d*]imidazol-2-yl)ethyl)benzoate **146** (75 mg, 79%) as a light yellow solid: R_f 0.43 (CH_2Cl_2 : methanol, 9:1); m.p. 175-176 °C ($CDCl_3$); ν_{max} (thin film)/ cm^{-1} 1718 (C=O, s), 1612 (C=C, w), 1511 (C-H, w), 1436 (C-H, m), 1282 (C-O, s); ^1H NMR (600 MHz, $CDCl_3$) δ 7.97 (2H, d, *J* 8.0, $C^{3"}$-H, $C^{5"}$-H), 7.62 (1H, d, *J* 1.6, $C^{4'}$-H), 7.33 (1H, d, *J* 8.2, $C^{7'}$-H), 7.30 (2H, d, *J* 8.0, $C^{2"}$-H, $C^{6"}$-H), 7.16 (1H, dd, *J* 8.2, 1.6, $C^{6'}$-H), 3.90 (3H, s, C^{10}-H_3), 3.60 (3H, s, C^8-H_3), 3.32 (2H, dd, *J* 9.1, 6.6, $C^{2'''}$-H_2), 3.21 (2H, dd, *J* 9.1, 6.6, $C^{1'''}$-H_2), 2.42 (3H, s, C^6-H_3), 2.29 (3H, s, C^7-H_3); ^{13}C NMR (151 MHz, $CDCl_3$) δ 167.1 (C^9), 165.2 (C^5), 159.1 (C^3), 155.0 ($C^{2'}$), 146.1 ($C^{1"}$), 142.8 ($C^{3'a}$), 135.2 ($C^{7'a}$), 130.1 ($C^{3"}$, $C^{5"}$), 128.7 ($C^{4"}$), 128.6 ($C^{2"}$, $C^{6"}$), 124.5 ($C^{5'}$), 123.8 ($C^{6'}$), 119.9 ($C^{4'}$), 117.2 (C^4), 109.5 ($C^{7'}$), 52.2 (C^{10}), 34.0 ($C^{2'''}$), 29.9 (C^8), 29.2 ($C^{1'''}$), 11.7 (C^6), 11.0 (C^7); LRMS *m/z* (ESI^+) 390 ($[M+H]^+$, 100%); HRMS *m/z* (ESI^+) [Found: 390.1831, $C_{23}H_{23}N_3O_3$ requires $[M+H]^+$ 390.1812)]; Analytical HPLC (RP, *Method 3*) rt 7.2 min, purity 100%.

4-(2-(5-(3,5-Dimethylisoxazol-4-yl)-1-methyl-1*H*-benzo[*d*]imidazol-2-yl)ethyl)benzoic acid 148

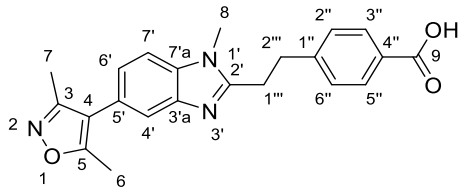

Methyl 4-(2-(5-(3,5-dimethylisoxazol-4-yl)-1-methyl-1*H*-benzo[*d*]imidazol-2-yl)ethyl)benzoate **146** (30.0 mg, 77.0 µmol, 1.0 eq.) was dissolved in ethanol (0.5 mL). 2 M NaOH $_{(aq)}$ (385 µL, 770 µmol, 10.0 eq.) was dropwise added. The reaction mixture was stirred at 50 °C for 1.5 h. The reaction was then cooled to rt then the pH adjusted to pH 2 with 2 M HCl $_{(aq)}$. The aqueous layer was extracted with ethyl acetate. The organic layer was dried over $MgSO_{4\ (s)}$, filtered, then the filtrate was concentrated *in vacuo.* The residue was lyophilised to yield 4-(2-(5-(3,5-dimethylisoxazol-4-yl)-1-methyl-1*H*-benzo[*d*]imidazol-2-yl)ethyl)benzoic acid **148** (26 mg, 90%) as a light yellow solid: R_f 0.17 (petroleum ether : ethyl acetate, 1:4); m.p. 257 °C *dec.* ($CDCl_3$); ν_{max} (thin film)/ cm^{-1} 2981 (O-H, s *br*), 1703 (C=O, s), 1382 (O-H, m), 1246 (C-O, s); ^{1}H NMR (600 MHz, DMSO-d_6) δ 7.87 (2H, d, *J* 8.1, $C^{3"}$-H, $C^{5"}$-H), 7.57 (1H, d, *J* 8.3, $C^{7'}$-H), 7.55 (1H, d, *J* 1.6, $C^{4'}$-H), 7.45 (2H, d, *J* 8.1, $C^{2"}$-H, $C^{6"}$-H), 7.18 (1H, dd, *J* 8.3, 1.6, $C^{6'}$-H), 3.73 (3H, s, C^8-H_3), 3.23 (4H, s, $C^{1'''}$-H_2, $C^{2'''}$-H_2), 2.39 (3H, s, C^6-H_3), 2.22 (3H, s, C^7-H_3); ^{13}C NMR (151 MHz, DMSO-d_6) δ 167.2 (C^9), 164.5 (C^5), 158.3 (C^3), 155.2 ($C^{2'}$), 146.3 ($C^{1"}$), 142.5 ($C^{3'a}$), 135.2 ($C^{7'a}$), 129.4 ($C^{3"}$, $C^{5"}$), 128.6 ($C^{4"}$), 128.6 ($C^{2"}$, $C^{6"}$), 122.7 ($C^{5'}$), 122.7 ($C^{6'}$), 118.8 ($C^{4'}$), 116.7 (C^4), 110.1 ($C^{7'}$), 32.5 ($C^{2'''}$), 29.5 (C^8), 27.8 ($C^{1'''}$), 11.3 (C^6), 10.5 (C^7); LRMS *m/z* (ESI^+) 376 ($[M+H]^+$, 100%); HRMS *m/z* (ESI^+) [Found: 376.1665, $C_{22}H_{21}N_3O_3$ requires $[M+H]^+$ 376.1656)]; Analytical HPLC (RP, *Method 3*) rt 6.5 min, purity 100%.

***N*-(5-(3,5-Dimethylisoxazol-4-yl)-2-(methylamino)phenyl)-2-(*m*-tolyl)acetamide 216**

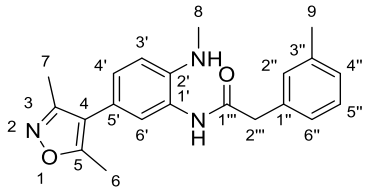

4-(3,5-Dimethyl-1,2-oxazol-4-yl)-*N*-methyl-2-nitroaniline **75** (200 mg, 0.809 mmol, 1.0 eq.) was suspended in EtOH (4.2 mL) and 1 M $Na_2S_2O_4$ (4.2 mL, 4.21 mmol, 5.2 eq.)

was added. The reaction mixture was stirred at 80 °C for 15 min. The reaction mixture was cooled to rt and partitioned between ethyl acetate (15 mL) and 10% aq. ammonia solution (7 mL). The phases were separated then the organic phase was washed with water (5 mL) and brine (5 mL), dried over $MgSO_{4\,(s)}$, filtered, then the filtrate was concentrated *in vacuo*. The crude material was dissolved in DMF (2.0 mL). DIPEA (168 µL, 0.967 mmol, 1.05 eq.), 2-(*m*-tolyl)acetic acid (159 mg, 0.967 mmol, 1.05 eq.), HATU (368 mg, 0.967 mmol, 1.05 eq.) and HOBT (131 mg, 0.967 mmol, 1.05 eq.) were added. The reaction mixture was stirred at rt for 2.5 h. The reaction mixture was partitioned between ethyl acetate and water. The organic layer was separated then the aqueous layer was extracted with ethyl acetate (3 × 10 mL). The combined organic layers were washed with brine, dried over $MgSO_{4\,(s)}$, filtered, then the filtrate was concentrated *in vacuo*. The residue was purified by silica column chromatography eluting with petroleum ether : ethyl acetate (1:0 to 3:7) to yield *N*-(5-(3,5-dimethylisoxazol-4-yl)-2-(methylamino)phenyl)-2-(*m*-tolyl)acetamide **216** (165 mg, 51%) as a yellow solid: R_f 0.33 (petroleum ether : ethyl acetate, 1:1); ^{1}H NMR (400 MHz, $CDCl_3$) δ 7.30 (1H, dd, *J* 7.5, 7.5, $C^{5"}$-H), 7.22-7.13 (3H, m, $C^{2"}$-H, $C^{4"}$-H, $C^{6"}$-H), 7.10 (1H, d, *J* 2.1, $C^{6'}$-H), 7.01 (1H, dd, *J* 8.3, 2.1, $C^{4'}$-H), 6.97 (1H, s, $C^{2'}$N-H), 6.75 (1H, d, *J* 8.3, $C^{3'}$-H), 3.75 (2H, s, $C^{2'''}$-H_2), 2.38 (3H, s, C^8-H_3), 2.35 (3H, s, C^6-H_3), 2.22 (3H, s, C^7-H_3); ^{13}C NMR (101 MHz, $CDCl_3$) δ 170.4 ($C^{1'''}$), 164.9 (C^5), 159.0 (C^3), 142.8 ($C^{2'}$), 139.3 ($C^{3"}$), 134.7 ($C^{1"}$), 130.2 ($C^{2"}$), 129.4 ($C^{5"}$), 128.7 ($C^{4"}$), 128.3 ($C^{4'}$), 126.5 ($C^{6"}$), 126.0 ($C^{6'}$), 123.9 ($C^{1'}$), 119.7 ($C^{5'}$), 116.2 (C^4), 112.5 ($C^{3'}$), 44.4 ($C^{2'''}$), 30.9 (C^8), 21.5 (C^9), 11.6 (C^6), 10.9 (C^7); LRMS *m/z* (ESI^+) 348 ($[M-H]^+$, 100%).

3,5-Dimethyl-4-(1-methyl-2-(3-methylbenzyl)-1*H*-benzo[*d*]imidazol-5-yl)isoxazole 112

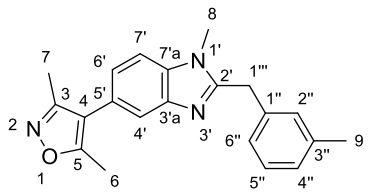

N-(5-(3,5-Dimethylisoxazol-4-yl)-2-(methylamino)phenyl)-2-(*m*-tolyl)acetamide **216** (120 mg, 0.343 mmol, 1.0 eq.) and 2-(*m*-tolyl)acetic acid (11.0 mg, 0.069 mmol, 0.2 eq.) were combined in toluene (1.5 mL) in a microwave vial containing 3 Å molecular sieves. The reaction mixture was refluxed for 24 h. The reaction mixture was cooled to rt, filtered

then the solvent was evaporated *in vacuo*. The residue was purified by flash column chromatography eluting with CH_2Cl_2 : methanol (1:0 to 9:1) to yield 3,5-dimethyl-4-(1-methyl-2-(3-methylbenzyl)-1*H*-benzo[*d*]imidazol-5-yl)isoxazole **112** (109 mg, 96%) as a cream solid: R_f 0.39 (CH_2Cl_2 : methanol, 9:1); m.p. 163-164 °C ($CDCl_3$); ν_{max} (thin film)/ cm^{-1} 1484 (C-H, m), 1460 (C-H, m), 1247 (C-N, m); ^{1}H NMR (400 MHz, $CDCl_3$) δ 7.64 (1H, dd, *J* 1.6, 0.7, $C^{4'}$-H), 7.34 (1H, dd, *J* 8.3, 0.7, $C^{7'}$-H), 7.20 (1H, t, *J* 7.5, $C^{5''}$-H), 7.14 (1H, dd, *J* 8.3, 1.6, $C^{6'}$-H), 7.10-7.02 (3H, m, $C^{2''}$-H, $C^{4''}$-H, $C^{6''}$-H), 4.31 (2H, s, $C^{1'''}$-H_2), 3.64 (3H, s, C^8-H_3), 2.42 (3H, s, C^6-H_3), 2.30 (3H, s, C^9-H_3), 2.29 (3H, s, C^7-H_3); ^{13}C NMR (101 MHz, $CDCl_3$) δ 165.2 (C^5), 159.1 (C^3), 154.5 ($C^{2'}$), 142.9 ($C^{3'a}$), 138.8 ($C^{3''}$), 135.9 ($C^{1''}$), 135.6 ($C^{7'a}$), 129.3 ($C^{2''}$), 128.9 ($C^{5''}$), 128.0 ($C^{4''}$), 125.6 ($C^{6''}$), 124.3 ($C^{5'}$), 123.7 ($C^{6'}$), 120.2 ($C^{4'}$), 117.2 (C^4), 109.5 ($C^{7'}$), 34.6 ($C^{1'''}$), 30.4 (C^8), 21.5 (C^9), 11.7 (C^6), 11.0 (C^7); LRMS *m/z* (ESI^+) 332 ($[M+H]^+$, 100%); HRMS *m/z* (ESI^+) [Found: 332.1742, $C_{21}H_{21}N_3O$ requires $[M+H]^+$ 332.1757)]; Analytical HPLC (RP, *Method 3*) rt 7.5 min, purity 100%.

_N_-(5-(3,5-dimethylisoxazol-4-yl)-2-(methylamino)phenyl)-2-(_p_-tolyl)acetamide 217

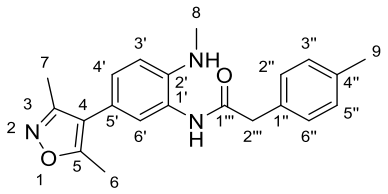

4-(3,5-Dimethyl-1,2-oxazol-4-yl)-*N*-methyl-2-nitroaniline **75** (200 mg, 0.809 mmol, 1.0 eq.) was suspended in EtOH (4.2 mL) and 1 M $Na_2S_2O_4$ (4.2 mL, 4.21 mmol, 5.2 eq.) was added. The reaction mixture was stirred at 80 °C for 15 min. The reaction mixture was cooled to rt and partitioned between ethyl acetate (15 mL) and 10% aq. ammonia solution (7 mL). The phases were separated then the organic phase was washed with water (5 mL) and brine (5 mL), dried over $MgSO_{4\,(s)}$, filtered, then the filtrate was concentrated *in vacuo*. The crude material was dissolved in DMF (2.0 mL). DIPEA (168 µL, 0.967 mmol, 1.05 eq.), 2-(*p*-tolyl)acetic acid (145 mg, 0.967 mmol, 1.05 eq.), HATU (368 mg, 0.967 mmol, 1.05 eq.) and HOBT (131 mg, 0.967 mmol, 1.05 eq.) were added. The reaction mixture was stirred at rt for 2 h. The reaction mixture was partitioned between ethyl acetate and water. The organic layer was separated then the aqueous layer was extracted with ethyl acetate (3 × 10 mL). The combined organic layers were washed with brine, dried over $MgSO_{4\,(s)}$, filtered, then the filtrate was concentrated *in vacuo*. The

residue was purified by flash column chromatography eluting with petroleum ether : ethyl acetate (9:1 to 3:7) to yield *N*-(5-(3,5-dimethylisoxazol-4-yl)-2-(methylamino)phenyl)-2-(*p*-tolyl)acetamide **217** (26 mg, 9%) as a colourless solid: R_f 0.36 (petroleum ether : ethyl acetate, 1:9); ^{1}H NMR (400 MHz, $CDCl_3$) δ 7.26 (2H, d, *J* 7.7, $C^{3"}$-H, $C^{5"}$-H), 7.22 (1H, d, *J* 7.7, $C^{6"}$-H, $C^{2"}$-H), 7.08 (1H, d, *J* 2.1, $C^{6'}$-H), 7.02 (1H, dd, *J* 8.3, 2.1, $C^{4'}$-H,), 6.90 (1H, *br* s, $C^{2'}$N-H), 6.77 (1H, d, *J* 8.3, $C^{3'}$-H), 3.76 (2H, s, $C^{2'''}$-H_2), 2.80 (3H, s, C^8-H_3), 2.37 (3H, s, C^9-H_3), 2.35 (3H, s, C^6-H_3), 2.22 (3H, s, C^7-H_3); LRMS *m/z* (ESI^+) 350 ($[M+H]^+$, 100%).

3,5-Dimethyl-4-(1-methyl-2-(4-methylbenzyl)-1*H*-benzo[*d*]imidazol-5-yl)isoxazole 111

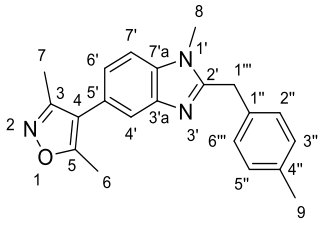

N-(5-(3,5-Dimethylisoxazol-4-yl)-2-(methylamino)phenyl)-2-(*p*-tolyl)acetamide **217** (15 mg, 45.0 μmol, 1.0 eq.) and 2-(*p*-tolyl)acetic acid (1.4 mg, 9.00 μmol, 0.2 eq.) were combined in toluene (0.5 mL) in a microwave vial containing 3 Å molecular sieves. The reaction mixture was refluxed for 24 h. The reaction mixture was cooled to rt, filtered then the solvent was evaporated *in vacuo.* The residue was purified by RP flash column chromatography eluting with H_2O : acetonitrile (95:5 to 5:95) to yield 3,5-dimethyl-4-(1-methyl-2-(4-methylbenzyl)-1*H*-benzo[*d*]imidazol-5-yl)isoxazole **111** (11 mg, 72%) as a yellow film: R_f 0.39 (CH_2Cl_2 : methanol, 9:1); ν_{max} (thin film)/ cm^{-1} 1672 (C=N, w), 1421 (C-H, m), 1189 (C-N, m); ^{1}H NMR (400 MHz, $CDCl_3$) δ 7.85 (1H, s, $C^{4'}$-H), 7.47 (1H, d, *J* 8.4, $C^{7'}$-H), 7.30 (1H, dd, *J* 8.4, 1.4, $C^{6'}$-H), 7.21-7.11 (4H, m, $C^{2"}$-H, $C^{3"}$-H, $C^{5"}$-H, $C^{6"}$-H), 4.55 (2H, s, $C^{1'''}$-H_2), 3.77 (3H, s, C^8-H_3), 2.41 (3H, s, C^6-H_3), 2.32 (3H, s, C^9-H_3), 2.27 (3H, s, C^7-H_3); ^{13}C NMR (151 MHz, $CDCl_3$) δ 165.8 (C^5), 158.7 (C^3), 153.4 ($C^{2'}$), 138.0 ($C^{4"}$), 133.2 ($C^{7'a}$), 131.5 ($C^{3'a}$), 130.2 ($C^{3"}$,$C^{5"}$), 129.3 ($C^{5'}$), 128.6 ($C^{2"}$,$C^{6"}$), 128.0 ($C^{1"}$), 126.3 ($C^{6'}$), 117.9 ($C^{4'}$), 116.2 (C^4), 110.7 ($C^{7'}$), 32.3 ($C^{1'''}$), 31.0 (C^8), 21.2 (C^9), 11.7 (C^6), 10.9(C^7); LRMS *m/z* (ESI^+) 332 ($[M+H]^+$, 100%); HRMS *m/z* (ESI^+) [Found: 332.1750, $C_{21}H_{21}N_3O$ requires $[M+H]^+$ 332.1757)]; Analytical HPLC (RP, *Method 3*) rt 7.6 min, purity 96%.

5-Bromo-*N*-methyl-3-nitropyridin-2-amine 218

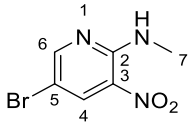

5-Bromo-2-chloro-3-nitropyridine (5.0 g, 2.11 mmol, 1.0 eq.) was dissolved in anhydrous THF (40 mL) and methylamine solution (33% wt. in EtOH, 8.65 mL, 6.95 mmol, 3.3 eq.) was slowly added at 0 °C. The reaction mixture was stirred at 0 °C for 1.5 h. The reaction mixture was diluted with ethyl acetate and quenched with sat. aq. $NaHCO_3$. The reaction mixture was separated then extracted with ethyl acetate (3 × 50 mL). The combined organic layers were dried over $MgSO_{4\ (s)}$, filtered, then the filtrate was concentrated *in vacuo* to yield 5-bromo-*N*-methyl-3-nitropyridin-2-amine **218** (4.7 g, 96%) as an orange solid: m.p. 136-139 °C (EtOAc); R_f 0.33 (petroleum ether : ethyl acetate, 9:1); ^{1}H NMR (400 MHz, $CDCl_3$) δ 8.53 (1H, d, *J* 2.3, C^4-H), 8.46 (1H, d, *J* 2.3, C^6-H), 8.17 (1H, s, N-H), 3.16 (3H, d, *J* 5.0, C^7-H_3); HRMS *m/z* (ESI^+) [Found: 231.9713, $C_6H_6BrN_3O_2$ requires $[M+H]^+$ 231.9716)]. The spectroscopic data are in good agreement with the literature.[346, 347]

5-Bromo-N^2-methylpyridine-2,3-diamine 219

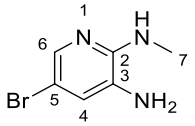

5-Bromo-*N*-methyl-3-nitropyridin-2-amine **218** (4.67 g, 20.0 μmol, 1.0 eq.) was dissolved in acetic acid (117 mL). Water (29 mL) and iron powder (4.67 g, 84.0 mmol, 4.2 eq.) were added then the reaction mixture was stirred at rt for 24 h. The reaction mixture was slowly poured into 6 M NaOH (500 mL) at 0 °C. The reaction mixture was then filtered through celite, washing with water, ethyl acetate, then 10% MeOH in CH_2Cl_2. The biphasic reaction mixture was separated then the aqueous layer was extracted with 10% MeOH in CH_2Cl_2. The combined organic layers were dried over $MgSO_{4\ (s)}$, filtered, and concentrated *in vacuo*. The residue was purified by flash column chromatography eluting with petroleum ether : ethyl acetate (1:0 to 0:1) to yield 5-bromo-N^2-methylpyridine-2,3-diamine **219** (3.34 g, 82%) as a purple solid: m.p. 90-93 °C ($CDCl_3$); R_f 0.29 (petroleum ether : ethyl acetate, 1:1); ^{1}H NMR (400 MHz, $CDCl_3$) δ 7.80 (1H, d, *J* 2.1, C^6-H), 6.95 (1H, d, *J* 2.1, C^4-H), 4.12 (1H, d, *J* 7.1, N-H), 3.22 (2H,

s, N-H_2), 2.98 (3H, d, *J* 4.8, C^7-H_3); LRMS *m/z* (ESI^+) 203 ($[M+2]^+$, 100%). The spectroscopic data are in good agreement with the literature.[347]

6-Bromo-2-ethyl-3-methyl-3*H*-imidazo[4,5-*b*]pyridine 220

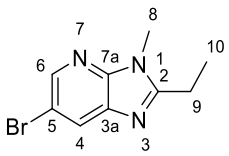

5-Bromo-N^2-methylpyridine-2,3-diamine **219** (1.0 g, 0.495 mol, 1.0 eq.) was dissolved in ethyl acetate (40 mL) and propionic acid (6.4 mL, 0.495 mol, 1.0 eq.) was added. 50 wt. % T3P in ethyl acetate (1.5 mL, 2.57 mol, 5.2 eq.) and DIPEA (1.9 mL 1.09 mol, 2.2 eq.) were added then the reaction mixture was stirred at 80 °C for 16 h. The reaction mixture was quenched with 1 M $NaOH_{(aq)}$ then the organic layer was separated. The aqueous layer was extracted with ethyl acetate (3 × 50 mL). The combined organic layers were dried over $MgSO_{4\ (s)}$, filtered, then the filtrate was concentrated *in vacuo*. The residue was purified by flash column chromatography eluting with petroleum ether : ethyl acetate (1:0 to 0:1) to yield *N*-(5-bromo-2-(methylamino)pyridin-3-yl)propionamide. This intermediate was refluxed in propionic acid (2.0 mL) for 24 h. The reaction mixture was cooled to rt then the solvent was evaporated *in vacuo.* The residue was purified by flash column chromatography eluting with petroleum ether : ethyl acetate (1:0 to 0:1) to yield 6-bromo-2-ethyl-3-methyl-3*H*-imidazo[4,5-*b*]pyridine **220** (420 mg, 36%) as a pale yellow solid: m.p. 94-97 °C ($CDCl_3$); R_f 0.23 (ethyl acetate); ^1H NMR (400 MHz, $CDCl_3$) δ 8.35 (1H, d, *J* 2.0, C^6-H), 8.08 (1H, d, *J* 2.0, C^4-H), 3.79 (3H, s, C^8-H_3), 2.93 (2H, q, *J* 7.5, C^9-H_2), 1.46 (1H, T, *J* 7.5, C^{10}-H_3); ^{13}C NMR (101 MHz, $CDCl_3$) δ 159.2 (C^2), 147.5 (C^{7a}), 143.8 (C^6), 136.0 (C^{3a}), 129.0 (C^4), 113.6 (C^5), 28.5 (C^8), 21.6 (C^9), 11.2 (C^{10}); LRMS *m/z* (ESI^+) 240 ($[M+H]^+$ 100%); HRMS *m/z* (ESI^+) [Found: 240.0127, $C_9H_{10}BrN_3$ requires $[M+H]^+$ 240.0131)].

4-(2-Ethyl-3-methyl-3*H*-imidazo[4,5-*b*]pyridin-6-yl)-3,5-dimethylisoxazole 221

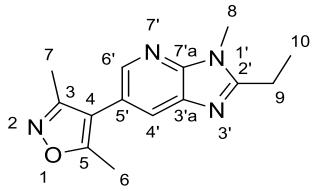

6-Bromo-2-ethyl-3-methyl-3*H*-imidazo[4,5-*b*]pyridine **220** (426 mg, 1.77 mmol, 1.0 eq.) and potassium (3,5-dimethylisoxazol-4-yl)trifluoroborate **53** (432 mg, 2.13 mmol, 1.2 eq.) were combined in DME (3.3 mL). Sat. aq. $NaHCO_3$ (3.3 mL) was added then the reaction mixture was degassed with $N_{2\,(g)}$ for 15 min. $Pd(dppf)Cl_2$, CH_2Cl_2 (145 mg, 17.7 mmol, 0.1 eq.) was added then the reaction mixture was stirred at 80 °C for 6.5 h. The reaction mixture was filtered through Celite® (eluting with ethyl acetate) then the filtrate partitioned between water and ethyl acetate. The aqueous layer was extracted with ethyl acetate (3 × 20 mL). The combined organic layers were dried over $MgSO_{4\,(s)}$, filtered, then the filtrate was concentrated *in vacuo*. The residue was purified by flash column chromatography eluting with petroleum ether : ethyl acetate (1:0 to 0:1) to yield 4-(2-ethyl-3-methyl-3*H*-imidazo[4,5-*b*]pyridin-6-yl)-3,5-dimethylisoxazole **221** (103 mg, 23%) as a brown solid: R_f 0.15 (ethyl acetate); m.p. 120-123 °C ($CDCl_3$); ν_{max} (thin film)/ cm^{-1} 1608 (C=C, w), 1518 (C-H, w), 1245 (C-O, s); ^1H NMR (600 MHz, $CDCl_3$) δ 8.21 (1H, d, *J* 1.9, $C^{6'}$-H), 7.85 (1H, d, *J* 1.9, $C^{4'}$-H), 3.85 (3H, s, C^8-H_3), 2.97 (2H, q, *J* 7.5, C^9-H_2), 2.41 (3H, s, C^6-H_3), 2.27 (3H, s, C^7-H_3), 1.50 (3H, t, *J* 7.5, C^{10}-H_3); ^{13}C NMR (151 MHz, $CDCl_3$) δ 165.8 (C^5), 159.0 (C^3), 158.8 ($C^{2'}$), 148.2 ($C^{7'a}$), 143.4 ($C^{6'}$), 134.8 ($C^{3'a}$), 126.8 ($C^{4'}$), 120.8 ($C^{5'}$), 114.3 (C^4), 28.3 (C^8), 21.4 (C^9), 11.5 (C^6), 11.0 (C^{10}), 10.7 (C^7); LRMS *m/z* (ESI^+) 258 ($[M+2H]^+$, 100%); HRMS *m/z* (ESI^+) [Found: 257.1409, $C_{14}H_{16}N_4O$ requires $[M+H]^+$ 257.1397)]; Analytical HPLC (RP, *Method 3*) rt 6.1 min, purity 100%.

***N*-(5-(3,5-Dimethylisoxazol-4-yl)-2-(methylamino)phenyl)-3-(4-methoxy-3-methylphenyl)propanamide 222**

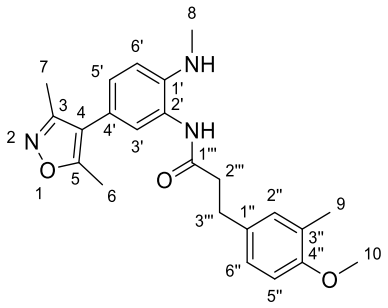

1 M $Na_2S_2O_{4\,(aq)}$ (3.15 mL, 3.15 mmol, 5.2 eq.) was added to 4-(3,5-dimethylisoxazol-4-yl)-*N*-methyl-2-nitroaniline **75** (150 mg, 0.606 mmol, 1.0 eq.) in EtOH (3.15 mL). The reaction mixture was stirred at 80 °C for 30 min. The reaction mixture was cooled to rt and partitioned between 10% aq. ammonia solution and ethyl acetate. The aqueous layer was separated then extracted with ethyl acetate (3 × 15 mL). The combined organic layers were dried over $MgSO_{4\,(s)}$, filtered, then the filtrate was concentrated *in vacuo*. The residue was dissolved in anhydrous DMF (1.0 mL). 3-(4-Methoxy-3-methylphenyl)propanoic acid (107 mg, 0.551 mmol, 1.0 eq.), HATU (220 mg, 0.578 mmol, 1.05 eq.) and DIPEA (101 µL, 0.578 mmol, 1.05 eq.) were added. The reaction mixture was stirred at rt for 3 h. The solvent was evaporated *in vacuo.* The residue was re-dissolved in ethyl acetate (10 mL) and 1 M $NaOH_{(aq)}$ (5 mL) was added. The organic layer was separated then the aqueous layer was extracted with ethyl acetate (3 × 10 mL). The combined organic layers were washed with 10% w/v $LiCl_{(aq)}$ (3 × 10 mL), dried over $MgSO_{4\,(s)}$, filtered, then the filtrate was concentrated *in vacuo*. The residue was purified by flash column chromatography eluting with petroleum ether : ethyl acetate (1:0 to 0:1) to yield *N*-(5-(3,5-dimethylisoxazol-4-yl)-2-(methylamino)phenyl)-3-(4-methoxy-3-methylphenyl)propanamide **222** (152 mg, 74%) as a yellow foam: R_f 0.40 (petroleum ether : ethyl acetate, 1:1); ^{1}H NMR (400 MHz, $CDCl_3$) δ 7.09-6.95 (3H, m, $C^{6''}$-H, $C^{3'}$-H, $C^{5'}$-H), 6.84 (1H, br s, $C^{2''}$-H), 6.77 (1H, d, *J* 8.9, $C^{6'}$-H), 6.70 (1H, d, *J* 8.1, $C^{5''}$-H), 3.80 (3H, s, C^{10}-H_3), 2.98 (2H, t, *J* 7.2, $C^{3'''}$-H_2), 2.72 (3H, s, C^{8}-H_3), 2.69 (2H, t, *J* 7.2, $C^{2'''}$-H_2), 2.35 (3H, s, C^{6}-H_3), 2.22 (3H, s, C^{7}-H_3), 2.20 (3H, s, C^{9}-H_3); ^{13}C NMR (101 MHz, $CDCl_3$) δ 171.5 ($C^{1''}$), 164.8 (C^{5}), 159.0 (C^{3}), 156.5 ($C^{4''}$), 142.8 ($C^{1'}$), 132.0 ($C^{1''}$), 130.9 ($C^{2''}$, $C^{6''}$), 128.1 ($C^{3'}$), 126.8 ($C^{5'}$), 126.4 ($C^{3''}$), 123.5 ($C^{2'}$), 119.2 ($C^{4'}$), 116.3 (C^{4}), 112.0 ($C^{5''}$), 110.1 ($C^{6'}$), 55.4 (C^{10}),

39.3 ($C^{2'''}$), 31.2 ($C^{3'''}$), 30.6 (C^{8}), 16.3 (C^{9}), 11.6 (C^{6}), 10.9 (C^{7}); LRMS *m/z* (ESI^+) 394 ($[M+H]^+$, 100%).

4-(2-(4-Methoxy-3-methylphenethyl)-1-methyl-1*H*-benzo[*d*]imidazol-5-yl)-3,5-dimethylisoxazole 141

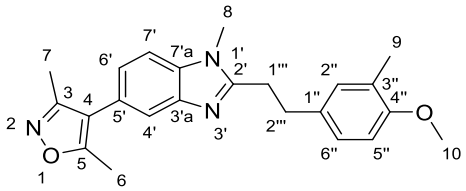

N-(5-(3,5-Dimethylisoxazol-4-yl)-2-(methylamino)phenyl)-3-(4-methoxy-3-methylphenyl)propanamide **222** (44 mg, 0.12 mmol, 1.0 eq.) and 3-(4-methoxy-3-methylphenyl)propanoic acid (2.3 mg, 0.012 mmol, 0.1 eq.) were combined in toluene (1.0 mL) in a microwave vial containing 3 Å molecular sieves. The reaction mixture was stirred at 130 °C for 72 h. The reaction mixture was cooled to rt, filtered then the solvent was evaporated *in vacuo.* The residue was purified by RP flash column chromatography eluting with water : acetonitrile (95:5 to 5:95) to yield 4-(2-(4-methoxy-3-methylphenethyl)-1-methyl-1*H*-benzo[*d*]imidazol-5-yl)-3,5-dimethylisoxazole **141** (19 mg, 43%) as a colourless solid: R_f 0.61 (CH_2Cl_2 : methanol, 9:1); m.p. 152-155 °C ($CDCl_3$); ν_{max} (thin film)/ cm^{-1} 1614 (C=C, w), 1506 (C-H, s), 1443 (C-H, m), 1320 (C-N, w), 1255 (C-O, s), 1226 (C-N, m), 1134 (C-H, m), 1103 (C-H, m), 1034 (C-O, s); ^{1}H NMR (600 MHz, $CDCl_3$) δ 7.69 (1H, s, $C^{4'}$-H), 7.37 (1H, d, *J* 8.3, $C^{7'}$-H), 7.19 (1H, dd, *J* 8.3, 1.6, $C^{6'}$-H), 6.98 (2H, m, $C^{2''}$-H, $C^{6''}$-H), 6.74 (2H, m, $C^{5''}$-H), 3.80 (3H, s, C^{10}-H_3), 3.58 (3H, s, C^{8}-H_3), 3.26 (2H, t, *J* 7.6, $C^{2'''}$-H_2), 3.18 (2H, t, *J* 7.6, $C^{1'''}$-H_2), 2.42 (3H, s, C^{6}-H_3), 2.28 (3H, s, C^{7}-H_3), 2.17 (3H, s, C^{9}-H_3); ^{13}C NMR (151 MHz, $CDCl_3$) δ 165.4 (C^{5}), 159.0 (C^{3}), 156.7 ($C^{4''}$), 155.3 ($C^{2'}$), 140.2 ($C^{3'a'}$), 134.3 ($C^{7'a}$), 131.8 ($C^{1''}$), 130.9 ($C^{2''}$), 127.1 ($C^{3''}$), 126.7 ($C^{6''}$), 125.6 ($C^{5'}$), 124.5 ($C^{6'}$), 119.0 ($C^{4'}$), 116.9 (C^{4}), 110.3 ($C^{5''}$), 109.9 ($C^{7'}$), 55.5 (C^{10}), 33.4 ($C^{1'''}$), 30.1 (C^{8}), 29.7 ($C^{2'''}$), 16.3 (C^{9}), 11.7 (C^{6}), 11.0 (C^{7}); LRMS *m/z* (ESI^+) 376 ($[M+H]^+$, 100%); HRMS *m/z* (ESI^+) [Found: 398.1835, $C_{23}H_{25}N_3O_2$ requires $[M+Na]^+$ 398.1839)]; Analytical HPLC (RP, *Method 3*) rt 7.1 min, purity 100%.

4-(2-(3-Chloro-4-methoxyphenethyl)-1-methyl-1*H*-benzo[*d*]imidazol-5-yl)-3,5-dimethylisoxazole 143

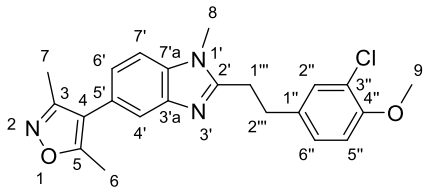

4-(3,5-Dimethylisoxazol-4-yl)-*N*^{1}-methylbenzene-1,2-diamine **76** (75.0 mg, 0.345 mmol, 1.0 eq.), 3-(3-chloro-4-methoxyphenyl)propionic acid (74.0 mg, 0.345 mmol, 1.0 eq.), 50 wt. % T3P in ethyl acetate (1.07 mL, 1.80 mmol, 5.2 eq.) and DIPEA (132 µL, 0.759 mmol, 2.2 eq.) were combined in ethyl acetate (1.0 mL). The reaction mixture was stirred at rt for 1 h. The reaction mixture was quenched with 1 M $NaOH_{(aq)}$ then extracted with ethyl acetate (3 × 15 mL). The combined organic layers were dried over $MgSO_{4\ (s)}$, filtered, then the filtrate was concentrated *in vacuo*. The residue was purified by flash column chromatography eluting with petroleum ether : ethyl acetate (1:0 to 0:1) to yield 4-(2-(3-chloro-4-methoxyphenethyl)-1-methyl-1*H*-benzo[*d*]imidazol-5-yl)-3,5-dimethylisoxazole **143** (44 mg, 32%) as an off-white solid: m.p. 103-105 °C ($CDCl_3$); R_f 0.23 (petroleum ether : ethyl acetate, 7:3); ν_{max} (thin film)/ cm^{-1} 1440 (C-H, m), 1311 (C-N, s), 1205 (C-O, s), 808 (C-Cl, s); ^{1}H NMR (700 MHz, $CDCl_3$) δ 7.62 (1H, d, *J* 1.5, $C^{4'}$-H), 7.34 (1H, d, *J* 8.2, $C^{7'}$-H), 7.26 (1H, d, *J* 2.0, $C^{2''}$-H), 7.14 (1H, dd, *J* 8.2, 1.5, $C^{6'}$-H), 7.08 (1H, dd, *J* 8.4, 2.0, $C^{6''}$-H), 6.85 (1H, d, *J* 8.4, $C^{5''}$-H), 3.88 (3H, s, C^{9}-H_3), 3.64 (3H, s, C^{8}-H_3), 3.17 (4H, m, $C^{1'''}$-H_2, $C^{2'''}$-H_2), 2.41 (3H, s, C^{6}-H_3), 2.28 (3H, s, C^{7}-H_3); ^{13}C NMR (176 MHz, $CDCl_3$) δ 165.2 (C^5), 159.1 (C^3), 155.1 ($C^{2'}$), 153.8 ($C^{4''}$), 142.6 ($C^{3'a}$), 135.1 ($C^{7'a}$), 133.9 ($C^{1''}$), 130.2 ($C^{2''}$), 127.8 ($C^{6''}$), 124.5 ($C^{5'}$), 123.8 ($C^{6'}$), 122.6 ($C^{3''}$), 119.9 ($C^{4'}$), 117.2 (C^4), 112.4 ($C^{5''}$), 109.5 ($C^{7'}$), 56.4 (C^9), 32.8 ($C^{2'''}$), 30.0 (C^8), 29.7 ($C^{1'''}$), 11.7 (C^6), 11.0 (C^7); LRMS *m/z* (ESI^+) 418 ($[M+Na]^+$, 100%); HRMS *m/z* (ESI^+) [Found: 396.1480, $C_{22}H_{22}ClN_3O_2$ requires $[M+H]^+$ 396.1473)]; Analytical HPLC (RP, *Method 3*) rt 7.7 min, purity 95%.

***N*-(5-(3,5-Dimethylisoxazol-4-yl)-2-((2-(4-methylpiperazin-1-yl)ethyl)amino)phenyl)-3-(3-nitrophenyl)propanamide 223**

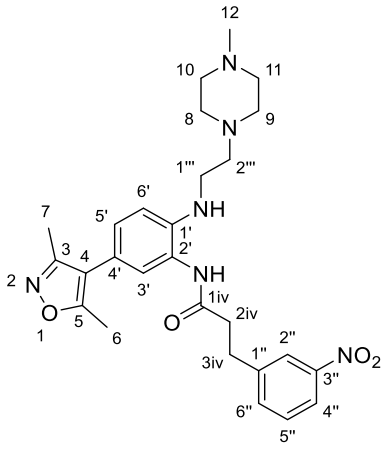

1 M $Na_2S_2O_{4\,(aq)}$ (1.73 mL, 1.73 mmol, 5.2 eq.) was added to 4-(3,5-dimethylisoxazol-4-yl)-*N*-(2-(4-methylpiperazin-1-yl)ethyl)-2-nitroaniline **193** (120 mg, 0.344 mmol, 1.0 eq.) in EtOH (1.73 mL). The reaction mixture was stirred at 80 °C for 20 min. The reaction mixture was cooled to rt then the solvent was evaporated *in vacuo.* The residue was partitioned between 10% aq. ammonia solution and ethyl acetate. The aqueous layer was separated then extracted with ethyl acetate (3 × 15 mL). The combined organic layers were dried over $MgSO_{4\,(s)}$, filtered, then the filtrate was concentrated *in vacuo*. The residue was dissolved in anhydrous DMF (2.0 mL). 3-(3-Nitrophenyl)propanoic acid (59.0 mg, 0.304 mmol, 1.05 eq.), HATU (121 mg, 0.319 mmol, 1.05 eq.) and DIPEA (55.5 µL, 0.319 mmol, 1.05 eq.) were added. The reaction mixture was stirred at rt for 17 h. The solvent was evaporated *in vacuo.* The residue was re-dissolved in ethyl acetate (10 mL) and 1 M NaOH (5 mL) was added. The organic layer was separated then the aqueous layer was extracted with ethyl acetate (3 × 10 mL). The combined organic layers were washed with 10% w/v $LiCl_{\,(aq)}$ (3 × 10 mL), dried over $MgSO_{4\,(s)}$, filtered, then the filtrate was concentrated *in vacuo*. The residue was purified by flash column chromatography eluting with CH_2Cl_2 : methanol (1:0 to 93:7) to yield *N*-(5-(3,5-dimethylisoxazol-4-yl)-2-((2-(4-methylpiperazin-1-yl)ethyl)amino)phenyl)-3-(3-nitrophenyl)propanamide **223** (59 mg, 38%) as a yellow oil: R_f 0.27 (CH_2Cl_2 : methanol, 9:1); ^{1}H NMR (400 MHz, $CDCl_3$) δ 8.15 (1H, t, *J* 2.9, $C^{2"}$-H), 8.12-8.05 (1H, m, $C^{4"}$-H), 7.64 (1H, dt, *J* 7.8, 1.4, $C^{6"}$-H), 7.48 (1H, dd, *J* 7.8, 7.8, $C^{5"}$-H), 7.37 (1H, s, OCN-H), 7.23 (1H, d, *J* 2.0, $C^{3'}$-H), 7.01 (1H, dd, *J* 8.3, 2.0, $C^{5'}$-H), 6.77 (1H, d, *J* 8.3, $C^{6'}$-H), 3.26-3.17 (4H, m, $C^{1'''}$-H_2, C^{3iv}-H_2), 2.83 (2H, t, *J* 7.6, C^{2iv}-H_2), 2.71 (2H, t, *J* 5.9, $C^{2'''}$-H_2), 2.66-2.56 (4H, m, C^{8}-H_2, C^{9}-H_2), 2.55-2.46 (4H, m, C^{10}-H_2, C^{11}-H_2), 2.38 (3H,

s, C^{6}-H_3), 2.30 (3H, s, C^{12}-H_3), 2.25 (3H, s, C^{7}-H_3); LRMS *m/z* (ESI^+) 507 ($[M+H]^+$, 100%).

3,5-Dimethyl-4-(1-(2-(4-methylpiperazin-1-yl)ethyl)-2-(3-nitrophenethyl)-1*H*-benzo[*d*]imidazol-5-yl)isoxazole 224

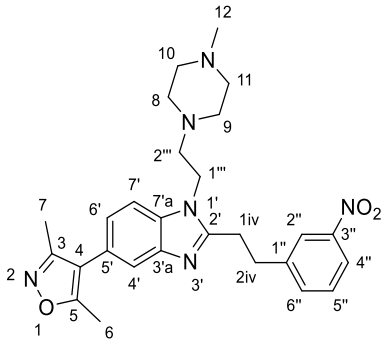

N-(5-(3,5-Dimethylisoxazol-4-yl)-2-((2-(4-methylpiperazin-1-yl)ethyl)amino)phenyl)-3-(3-nitrophenyl)propanamide **223** (20 mg, 40.0 µmol, 1.0 eq.) and 3-(3-nitrophenyl)propanoic acid (1.0 mg, 4.00 µmol, 0.1 eq.) were combined in toluene (1.0 mL) in a microwave vial containing 3 Å molecular sieves. The reaction mixture was stirred at 130 °C for 72 h. The reaction mixture was cooled to rt, filtered then the solvent was evaporated *in vacuo*. The residue was purified by flash column chromatography eluting with CH_2Cl_2 : methanol (1:0 to 85:15) to yield 3,5-dimethyl-4-(1-(2-(4-methylpiperazin-1-yl)ethyl)-2-(3-nitrophenethyl)-1*H*-benzo[*d*]imidazol-5-yl)isoxazole **224** (8 mg, 42%) as a yellow oil: R_f 0.30 (CH_2Cl_2 : methanol, 9:1); ν_{max} (thin film)/ cm^{-1} 1617 (C=C, w), 1528 (N-O, s), 1453 (C-H, m), 1410 (C-H, m), 1351 (N-O, s), 1322 (C-N, m), 1250 (N-H, w), 1167 (C-O, w); ^{1}H NMR (600 MHz, $CDCl_3$) δ 8.16 (1H, t, *J* 2.0, $C^{2"}$-H), 8.10 (1H, ddd, *J* 8.0, 2.4, 1.1, $C^{4"}$-H), 7.67-7.60 (2H, m, $C^{6"}$-H, $C^{4'}$-H), 7.49 (1H, dd, *J* 8.0, 8.0, $C^{5"}$-H), 7.35 (1H, d, *J* 8.2, $C^{7'}$-H), 7.14 (1H, dd, *J* 8.2, 1.0, $C^{6'}$-H), 4.19 (2H, t, *J* 6.6, $C^{1'''}$-H_2), 3.46 (2H, t, *J* 7.5, C^{2iv}-H_2), 3.26 (2H, t, *J* 7.5, C^{1iv}-H_2), 2.73 (2H, t, *J* 6.6, $C^{2'''}$-H_2), 2.68-2.62 (8H, m, C^{8}-H_2, C^{9}-H_2, C^{10}-H_2, C^{11}-H_2), 2.47 (3H, s, C^{12}-H_3), 2.42 (3H, s, C^{6}-H_3), 2.29 (3H, s, C^{7}-H_3); ^{13}C NMR (151 MHz, $CDCl_3$) δ 165.2 (C^5), 159.1 (C^3), 154.3 ($C^{2'}$), 148.6 ($C^{3"}$), 143.1 ($C^{3'a}$), 143.0 ($C^{1"}$), 135.1 ($C^{6"}$), 134.4 ($C^{7'a}$), 129.8 ($C^{5"}$), 124.7 ($C^{5'}$), 123.9 ($C^{6'}$), 123.2 ($C^{2"}$), 121.9 ($C^{4"}$), 120.2 ($C^{4'}$), 117.1 (C^4), 109.6 ($C^{7'}$), 57.0 ($C^{2'''}$), 54.6 (C^{10}, C^{11}), 52.4 (C^8, C^9), 45.1 (C^{12}), 41.9 ($C^{1'''}$), 32.9 (C^{2iv}), 29.0 (C^{1iv}), 11.7 (C^6), 11.0 (C^7); LRMS *m/z* (ESI^+) 489 ($[M+H]^+$, 100%); HRMS *m/z*

(ESI$^+$) [Found: 489.2631, $C_{27}H_{32}N_6O_3$ requires $[M+H]^+$ 489.2609)]; Analytical HPLC (RP, *Method 3*) rt 6.2 min, purity 96%.

_N_-(5-(3,5-Dimethylisoxazol-4-yl)-2-((2-(4-methylpiperazin-1-yl)ethyl)amino)phenyl)-3-(4-nitrophenyl)propanamide 225

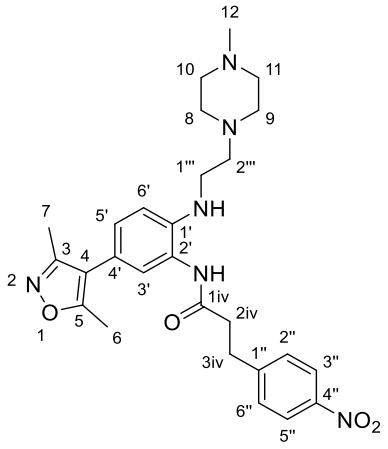

1 M $Na_2S_2O_{4\,(aq)}$ (1.45 mL, 1.45 mmol, 5.2 eq.) was added to 4-(3,5-dimethylisoxazol-4-yl)-*N*-(2-(4-methylpiperazin-1-yl)ethyl)-2-nitroaniline **193** (100 mg, 0.278 mmol, 1.0 eq.) in EtOH (1.45 mL). The reaction mixture was stirred at 80 °C for 5 min. The reaction mixture was cooled to rt then the solvent was evaporated *in vacuo.* The residue was partitioned between 10% aq. ammonia solution and ethyl acetate. The aqueous layer was separated then extracted with ethyl acetate (3 × 15 mL). The combined organic layers were dried over $MgSO_{4\,(s)}$, filtered, then the filtrate was concentrated *in vacuo*. The residue was dissolved in anhydrous DMF (1.0 mL). 3-(4-Nitrophenyl)propanoic acid (32.0 mg, 0.163 mmol, 1.05 eq.), HATU (65.0 mg, 0.171 mmol, 1.05 eq.) and DIPEA (29.8 µL, 0.171 mmol, 1.05 eq.) were added. The reaction mixture was stirred at rt for 2 h. The solvent was evaporated *in vacuo.* The residue was re-dissolved in ethyl acetate (10 mL) and 1 M NaOH (5 mL) was added. The organic layer was separated then the aqueous layer was extracted with ethyl acetate (3 × 10 mL). The combined organic layers were washed with 10% w/v $LiCl_{(aq)}$ (3 × 10 mL), dried over $MgSO_{4\,(s)}$, filtered, then the filtrate was concentrated *in vacuo*. The residue was purified by flash column chromatography eluting with CH_2Cl_2 : methanol (1:0 to 85:15) to yield *N*-(5-(3,5-dimethylisoxazol-4-yl)-2-((2-(4-methylpiperazin-1-yl)ethyl)amino)phenyl)-3-(4-nitrophenyl)propanamide **225** (58 mg, 64%) as an off-white solid: R_f 0.19 (CH_2Cl_2 : methanol, 9:1); ^{1}H NMR (400 MHz, $CDCl_3$) δ 8.17 (2H, d, *J* 8.7, $C^{3"}$-H,

$C^{5''}$-H), 7.45 (2H, d, *J* 8.7, $C^{2''}$-H, $C^{6''}$-H), 7.26 (1H, s, $C^{3'}$-H), 7.01 (1H, dd, *J* 8.3, 2.1, $C^{5'}$-H), 6.78 (1H, d, *J* 8.3, $C^{6'}$-H), 3.28-3.14 (4H, m, $C^{1'''}$-H_2, C^{3iv}-H_2), 2.80 (2H, t, *J* 7.6, C^{2iv}-H_2), 2.70 (2H, t, *J* 5.9, $C^{2'''}$-H_2), 2.64-2.54 (4H, m, C^{8}-H_2, C^{9}-H_2), 2.53-2.43 (4H, m, C^{10}-H_2, C^{11}-H_2), 2.38 (3H, s, C^{6}-H_3), 2.29 (3H, s, C^{12}-H_3), 2.25 (3H, s, C^{7}-H_3); LRMS *m/z* (ESI^+) 507 ($[M+H]^+$, 100%).

3,5-Dimethyl-4-(1-(2-(4-methylpiperazin-1-yl)ethyl)-2-(4-nitrophenethyl)-1*H*-benzo[*d*]imidazol-5-yl)isoxazole 226

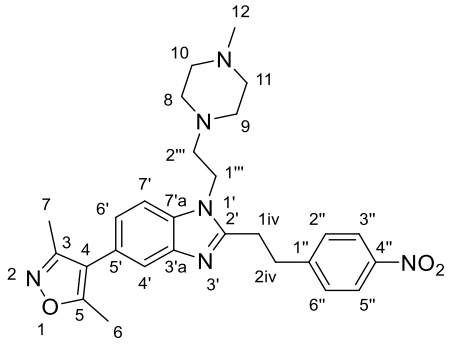

N-(5-(3,5-Dimethylisoxazol-4-yl)-2-((2-(4-methylpiperazin-1-yl)ethyl)amino)phenyl)-3-(4-nitrophenyl)propanamide **225** (33.0 mg, 65.0 µmol, 1.0 eq.) and 3-(4-nitrophenyl)propanoic acid (1.3 mg, 7.00 µmol, 0.1 eq.) were combined in toluene (1.0 mL) in a microwave vial containing 3 Å molecular sieves. The reaction mixture was stirred at 130 °C for 72 h. The reaction mixture was cooled to rt, filtered then the solvent was evaporated *in vacuo.* The residue was purified by flash column chromatography to yield 3,5-dimethyl-4-(1-(2-(4-methylpiperazin-1-yl)ethyl)-2-(4-nitrophenethyl)-1*H*-benzo[*d*]imidazol-5-yl)isoxazole **226** (17 mg, 53%) as a yellow oil: R_f 0.40 (1% Et_3N in CH_2Cl_2 : methanol, 9:1); ν_{max} (thin film)/ cm^{-1} 1601 (C=C, w), 1519 (N-O, s), 1458 (C-H, w), 1382 (C-H, m), 1347 (N-O, s), 1251 (N-H, w), 1150 (C-H, m); ^{1}H NMR (600 MHz, $CDCl_3$) δ 8.17 (1H, d, *J* 8.5, $C^{3''}$-H, $C^{5''}$-H), 7.63 (1H, d, *J* 1.6, $C^{4'}$-H), 7.44 (1H, d, *J* 8.5, $C^{2''}$-H, $C^{6''}$-H), 7.35 (1H, d, *J* 8.2, $C^{7'}$-H), 7.15 (1H, dd, *J* 8.2, 1.6, $C^{6'}$-H), 4.16 (2H, t, *J* 6.8, $C^{1'''}$-H_2), 3.45 (2H, t, *J* 7.8, C^{2iv}-H_2), 3.26 (2H, t, *J* 7.8, C^{1iv}-H_2), 2.70 (2H, t, *J* 6.8, $C^{2'''}$-H_2), 2.68-2.54 (8H, m, C^{8}-H_2, C^{9}-H_2, C^{10}-H_2, C^{11}-H_2), 2.43 (3H, s, C^{6}-H_3), 2.42 (3H, s, C^{12}-H_3), 2.30 (3H, s, C^{7}-H_3); ^{13}C NMR (151 MHz, $CDCl_3$) δ 165.2 (C^5), 159.1 (C^3), 154.3 ($C^{2'}$), 148.7 ($C^{4''}$), 147.0 ($C^{3'a}$), 143.0 ($C^{1''}$), 134.4 ($C^{7'a}$), 129.5 ($C^{2''}$, $C^{6''}$), 124.7 ($C^{5'}$), 124.1 ($C^{3''}$, $C^{5''}$), 123.9 ($C^{6'}$), 120.2 ($C^{4'}$), 117.1 (C^4), 109.6 ($C^{7'}$), 57.0 ($C^{2'''}$), 54.7 (C^8, C^9), 52.6 (C^{10}, C^{11}), 45.3 (C^{12}), 41.9 ($C^{1'''}$), 33.3 (C^{1iv}), 28.9 (C^{2iv}), 11.7 (C^6),

11.0 (C^7); LRMS *m/z* (ESI^+) 489 ($[M+H]^+$, 100%); HRMS *m/z* (ESI^+) [Found: 489.2600, $C_{27}H_{32}N_6O_3$ requires $[M+H]^+$ 489.2609)]; Analytical HPLC (RP, *Method 3*) rt 6.3 min, purity 95%.

_N_-(5-(3,5-Dimethylisoxazol-4-yl)-2-((2-morpholinoethyl)amino)phenyl)-3-(3-nitrophenyl)propanamide 227

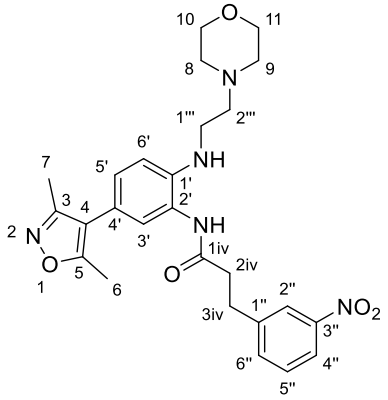

1 M $Na_2S_2O_{4\,(aq)}$ (2.3 mL, 2.25 mmol, 5.2 eq.) was added to 4-(3,5-dimethylisoxazol-4-yl)-*N*-(2-morpholinoethyl)-2-nitroaniline **195** (150 mg, 0.433 mmol, 1.0 eq.) in EtOH (2.0 mL). The reaction mixture was stirred at 80 °C for 30 min. The reaction mixture was cooled to rt then the solvent was evaporated *in vacuo.* The residue was partitioned between 10% aq. ammonia solution and ethyl acetate. The aqueous layer was separated then extracted with ethyl acetate (3 × 15 mL). 2 M $NaOH_{(aq)}$ was added to the aqueous layer and this was further extracted with ethyl acetate (3 × 15 mL). The combined organic layers were dried over $MgSO_{4\,(s)}$, filtered, then the filtrate was concentrated *in vacuo*. The residue was dissolved in anhydrous DMF (1.0 mL). 3-(3-Nitrophenyl)propanoic acid (59.0 mg, 0.303 mmol, 1.0 eq.), HATU (121 mg, 0.319 mmol, 1.05 eq.) and DIPEA (56.0 µL, 0.319 mmol, 1.05 eq.) were added. The reaction mixture was stirred at rt for 17 h. The solvent was evaporated *in vacuo.* The residue was re-dissolved in ethyl acetate (10 mL) and water (5 mL) was added. The organic layer was separated then the aqueous layer was extracted with ethyl acetate (3 × 10 mL). The combined organic layers were washed with 10% w/v $LiCl_{(aq)}$ (3 × 10 mL), dried over $MgSO_{4\,(s)}$, filtered, then the filtrate was concentrated *in vacuo*. The residue was purified by flash column chromatography eluting with CH_2Cl_2 : methanol (1:0 to 4:1) to yield *N*-(5-(3,5-dimethylisoxazol-4-yl)-2-((2-morpholinoethyl)amino)phenyl)-3-(3-nitrophenyl)propanamide **227** (55 mg, 36%) as a yellow solid: R_f 0.48 (CH_2Cl_2 :

methanol, 9:1); ^{1}H NMR (400 MHz, $CDCl_3$) δ 8.17-8.12 (1H, m, $C^{2"}$-H), 8.11-8.04 (1H, m, $C^{4"}$-H), 7.63 (1H, dt, *J* 7.9, 1.3, 1.3, $C^{6"}$-H), 7.47 (1H, dd, *J* 7.9, 7.9, $C^{5"}$-H), 7.17 (1H, d, *J* 2.0, $C^{3'}$-H), 7.02 (1H, dd, *J* 8.3, 2.0, $C^{5'}$-H), 6.76 (1H, d, *J* 8.3, $C^{6'}$-H), 3.83-3.73 (4H, m, C^{10}-H_2, C^{11}-H_2), 3.37-3.25 (2H, m, $C^{1'''}$-H_2), 3.20 (2H, t, *J* 7.5, C^{3iv}-H_2), 2.85 (2H, t, *J* 7.5, C^{2iv}-H_2), 2.88-2.82 (2H, m, $C^{2'''}$-H_2), 2.74-2.57 (4H, m, C^{8}-H_2, C^{9}-H_2), 2.37 (3H, s, C^{6}-H_3), 2.24 (3H, s, C^{7}-H_3); LRMS *m/z* (ESI^+) 492 ($[M+H]^+$, 100%).

4-(2-(5-(3,5-Dimethylisoxazol-4-yl)-2-(3-nitrophenethyl)-1*H*-benzo[*d*]imidazol-1-yl)ethyl)morpholine 172

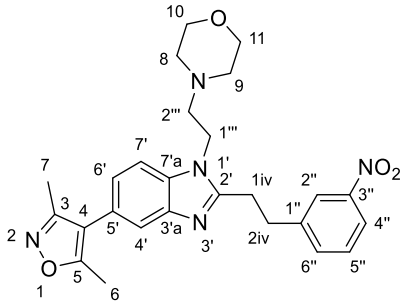

N-(5-(3,5-Dimethylisoxazol-4-yl)-2-((2-morpholinoethyl)amino)phenyl)-3-(3-nitrophenyl)propanamide **227** (40.0 mg, 81.0 µmol, 1.0 eq.) and 3-(3-nitrophenyl)propanoic acid (2.0 mg, 8.10 µmol, 0.1 eq.) were combined in toluene (1.0 mL) in a microwave vial containing 3 Å molecular sieves. The reaction mixture was stirred at 130 °C for 48 h. The reaction mixture was cooled to rt, filtered then the solvent was evaporated *in vacuo.* The residue was purified by RP flash column chromatography eluting with water : acetonitrile (95:5 to 5:95) to yield 4-(2-(5-(3,5-dimethylisoxazol-4-yl)-2-(3-nitrophenethyl)-1*H*-benzo[*d*]imidazol-1-yl)ethyl)morpholine **172** (16 mg, 42%) as a yellow oil: R_f 0.59 (CH_2Cl_2 : methanol, 9:1); ν_{max} (thin film)/ cm^{-1} 2361 (C-H, m), 2341 (C-H, m), 1528 (N-O, s), 1482 (C-H, m), 1450 (C-H, m), 1409 (C-H, m), 1351 (N-O, s), 1321 (C-N, m), 1246 (C-N, m), 1117 (C-O, s); ^{1}H NMR (600 MHz, $CDCl_3$) δ 8.16 (1H, t, *J* 2.0, $C^{2"}$-H), 8.09 (1H, ddd, *J* 8.0, 2.3, 1.1, $C^{5"}$-H), 7.63 (1H, m, $C^{6"}$-H), 7.62 (1H, d, *J* 1.6, $C^{4'}$-H), 7.48 (1H, dd, *J* 8.0, 8.0, $C^{5"}$-H), 7.37 (1H, d, *J* 8.2, $C^{7'}$-H), 7.14 (1H, dd, *J* 8.2, 1.6, $C^{6'}$-H), 4.21 (2H, t, *J* 6.7, $C^{1'''}$-H_2), 3.66 (4H, t, *J* 4.5, C^{10}-H_2, C^{11}-H_2), 3.46 (2H, t, *J* 8.5, C^{2iv}-H_2), 3.28 (2H, t, *J* 8.5, C^{1iv}-H_2), 2.68 (2H, t, *J* 6.7, $C^{2'''}$-H_2), 2.49 (4H, t, *J* 4.5, C^{8}-H_2, C^{9}-H_2), 2.42 (3H, s, C^{6}-H_3), 2.29 (3H, s, C^{7}-H_3); ^{13}C NMR (151 MHz, $CDCl_3$) δ 165.2 (C^{5}), 159.1 (C^{3}), 154.3 ($C^{2'}$), 148.6 ($C^{3"}$), 143.0 ($C^{3'a}$), 142.9 ($C^{1"}$),

135.0 ($C^{6''}$), 134.4 ($C^{7'a}$), 129.7 ($C^{5''}$), 124.6 ($C^{5'}$), 124.0 ($C^{6'}$), 123.2 ($C^{2''}$), 121.8 ($C^{4''}$), 120.1 ($C^{4'}$), 117.1 (C^{4}), 109.6 ($C^{7'}$), 66.9 (C^{10}, C^{11}), 57.8 ($C^{2'''}$), 54.2 (C^{8}, C^{9}), 41.7 ($C^{1'''}$), 32.9 (C^{2iv}), 28.9 (C^{1iv}), 11.7 (C^{6}), 11.0 (C^{7}); LRMS *m/z* (ESI^+) 476 ($[M+H]^+$, 100%); HRMS *m/z* (ESI^+) [Found: 476.2290, $C_{26}H_{29}N_5O_4$ requires $[M+H]^+$ 476.2292)]; Analytical HPLC (RP, *Method 3*) rt 6.4 min, purity 95%.

_N_-(5-(3,5-Dimethylisoxazol-4-yl)-2-((2-morpholinoethyl)amino)phenyl)-3-(4-nitrophenyl)propenamide 228

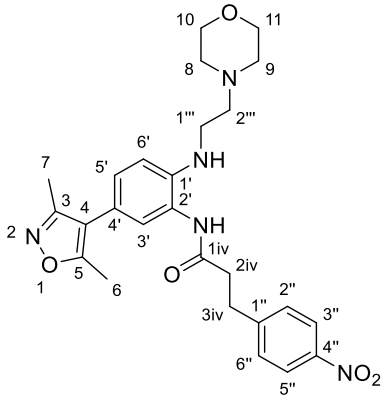

1 M $Na_2S_2O_{4\,(aq)}$ (2.3 mL, 2.25 mmol, 5.2 eq.) was added to 4-(3,5-dimethylisoxazol-4-yl)-*N*-(2-morpholinoethyl)-2-nitroaniline **195** (150 mg, 0.433 mmol, 1.0 eq.) in EtOH (2.0 mL). The reaction mixture was stirred at 80 °C for 30 min. The reaction mixture was cooled to rt then the solvent was evaporated *in vacuo.* The residue was partitioned between 10% aq. ammonia solution and ethyl acetate. The aqueous layer was separated then extracted with ethyl acetate (3 × 15 mL). 2 M $NaOH_{(aq)}$ was added to the aqueous layer and this was further extracted with ethyl acetate (3 × 15 mL). The combined organic layers were dried over $MgSO_{4\,(s)}$, filtered, then the filtrate was concentrated *in vacuo*. The residue was dissolved in anhydrous DMF (1.0 mL). 3-(4-Nitrophenyl)propanoic acid (85.0 mg, 0.433 mmol, 1.0 eq.), HATU (173 mg, 0.455 mmol, 1.05 eq.) and DIPEA (72.3 µL, 0.455 mmol, 1.05 eq.) were added. The reaction mixture was stirred at rt for 17 h. The solvent was evaporated *in vacuo.* The residue was re-dissolved in ethyl acetate (10 mL) and water (5 mL) was added. The organic layer was separated then the aqueous layer was extracted with ethyl acetate (3 × 10 mL). The combined organic layers were washed with 10% w/v $LiCl_{(aq)}$ (3 × 10 mL), dried over $MgSO_{4\,(s)}$, filtered, then the filtrate was concentrated *in vacuo*. The residue was purified by flash column chromatography eluting with CH_2Cl_2 : methanol (1:0 to 93:7) to yield *N*-(5-(3,5-

dimethylisoxazol-4-yl)-2-((2-morpholinoethyl)amino)phenyl)-3-(4-nitrophenyl)propenamide **228** (84 mg, 39%) as a yellow solid: R_f 0.25 (CH_2Cl_2 : methanol, 95:5); ^{1}H NMR (400 MHz, $CDCl_3$) δ 8.16 (2H, d, *J* 8.7, $C^{3"}$-H, $C^{5"}$-H), 7.44 (2H, d, *J* 8.7, $C^{2"}$-H, $C^{6"}$-H), 7.19 (1H, d, *J* 2.0, $C^{3'}$-H), 7.01 (1H, dd, *J* 8.3, 2.0, $C^{5'}$-H), 6.77 (1H, d, *J* 8.3, $C^{6'}$-H), 3.76-3.62 (4H, m, C^{10}-H_2, C^{11}-H_2), 3.27-3.12 (4H, m, $C^{1'''}$-H_2, C^{3iv}-H_2), 2.79 (2H, t, *J* 7.7, C^{2iv}-H_2), 2.67 (2H, t, *J* 5.9, $C^{2'''}$-H_2), 2.55-2.41 (4H, m, C^8-H_2, C^9-H_2), 2.37 (3H, s, C^6-H_3), 2.23 (3H, s, C^7-H_3); ^{13}C NMR (101 MHz, $CDCl_3$) δ 170.2 ($C^{1"}$), 164.9 (C^5), 159.0 (C^3), 148.6 ($C^{4"}$), 146.8 ($C^{1"}$), 141.5 ($C^{1'}$), 129.5 ($C^{2"}$, $C^{6"}$), 128.2 ($C^{5'}$), 126.2 ($C^{3'}$), 124.1 ($C^{2'}$), 124.0 ($C^{3"}$, $C^{5"}$), 120.0 ($C^{4'}$), 116.2 (C^4), 113.3 ($C^{6'}$), 67.0 (C^{10}, C^{11}), 57.0 ($C^{2'''}$), 53.4 (C^8, C^9), 40.1 ($C^{1'''}$), 37.9 (C^{2iv}), 31.4 (C^{3iv}), 11.7 (C^6), 11.0 (C^7); LRMS *m/z* (ESI^+) 494 ($[M+H]^+$, 100%).

4-(2-(5-(3,5-Dimethylisoxazol-4-yl)-2-(4-nitrophenethyl)-1*H*-benzo[*d*]imidazol-1-yl)ethyl)morpholine 173

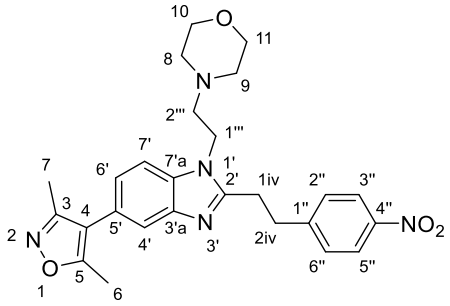

N-(5-(3,5-dimethylisoxazol-4-yl)-2-((2-morpholinoethyl)amino)phenyl)-3-(4-nitrophenyl)propenamide **228** (60 mg, 0.12 mmol, 1.0 eq.) and 3-(4-nitrophenyl)propanoic acid (2.4 mg, 0.012 mmol, 0.1 eq.) were combined in toluene (1.0 mL) in a microwave vial containing 3 Å molecular sieves. The reaction mixture was stirred at 130 °C for 72 h. The reaction mixture was cooled to rt, filtered then the solvent was evaporated *in vacuo.* The residue was purified by RP flash column chromatography eluting with water : acetonitrile (95:5 to 5:95) to yield 4-(2-(5-(3,5-dimethylisoxazol-4-yl)-2-(4-nitrophenethyl)-1*H*-benzo[*d*]imidazol-1-yl)ethyl)morpholine **173** (13 mg, 22%) as a yellow solid: R_f 0.20 (CH_2Cl_2 : methanol, 9:1); m.p. 89-91 °C ($CDCl_3$); ν_{max} (thin film)/ cm^{-1} 1518 (N-O, s), 1346 (N-O, s), 1116 (C-O, s); ^{1}H NMR (600 MHz, $CDCl_3$) δ 8.16 (2H, d, *J* 8.4, $C^{2"}$-H, $C^{6"}$-H), 7.63 (1H, d, *J* 1.6, $C^{4'}$-H), 7.44 (2H, d, *J* 8.4, $C^{3"}$-H, $C^{5"}$-H), 7.37 (1H, d, *J* 8.3, $C^{7'}$-H), 7.14 (1H, dd, *J* 8.3, 1.6, $C^{6'}$-H), 4.18 (2H, t, *J* 6.7,

$C^{1'''}$-H_2), 3.66 (4H, t, *J* 4.5, C^{10}-H_2, C^{11}-H_2), 3.46 (2H, t, *J* 7.9, C^{2iv}-H_2), 3.26 (2H, t, *J* 7.9, C^{1iv}-H_2), 2.66 (2H, t, *J* 6.7, $C^{2'''}$-H_2), 2.47 (4H, t, *J* 4.5, C^{8}-H_2, C^{9}-H_2), 2.42 (3H, s, C^{6}-H_3), 2.29 (3H, s, C^{7}-H_3); ^{13}C NMR (151 MHz, $CDCl_3$) δ 165.2 (C^5), 159.1 (C^3), 154.3 ($C^{2'}$), 148.7 ($C^{1''}$), 146.9 ($C^{4''}$), 143.0 ($C^{3'a}$), 134.4 ($C^{7'a}$), 129.4 ($C^{2''}$, $C^{6''}$), 124.7 ($C^{5'}$), 124.1 ($C^{3''}$, $C^{5''}$), 123.9 ($C^{6'}$), 120.1 ($C^{4'}$), 117.1 (C^4), 109.6 ($C^{7'}$), 66.9 (C^{10}, C^{11}), 54.2 (C^8, C^9), 41.7 ($C^{1'''}$), 33.3 (C^{2iv}), 28.8 (C^{1iv}), 11.7 (C^6), 11.0 (C^7); LRMS *m/z* (ESI^+) 476 ([M+H]$^+$, 100%); HRMS *m/z* (ESI^+) [Found: 476.2293, $C_{26}H_{29}N_5O_4$ requires [M+H]$^+$ 476.2292)]; Analytical HPLC (RP, *Method 3*) rt 6.4 min, purity 100%.

3-(3-Cyanophenyl)-*N*-(5-(3,5-dimethylisoxazol-4-yl)-2-((2-morpholinoethyl)amino)phenyl)propanamide 229

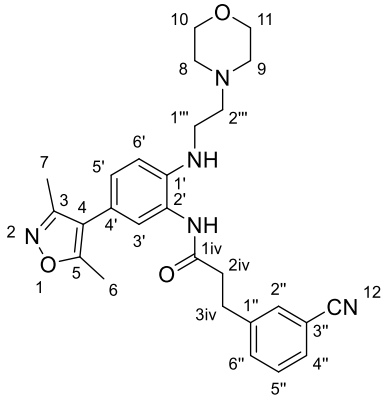

1 M $Na_2S_2O_{4\,(aq)}$ (2.25 mL, 2.25 mmol, 5.2 eq.) was added to 4-(3,5-dimethylisoxazol-4-yl)-*N*-(2-morpholinoethyl)-2-nitroaniline **195** (150 mg, 0.433 mmol, 1.0 eq.) in EtOH (2.30 mL). The reaction mixture was stirred at 80 °C for 15 min. The reaction mixture was cooled to rt then the solvent was evaporated *in vacuo.* The residue was partitioned between 10% aq. ammonia solution and ethyl acetate. The aqueous layer was separated then extracted with ethyl acetate (3 × 15 mL). The combined organic layers were dried over $MgSO_{4\,(s)}$, filtered, then the filtrate was concentrated *in vacuo*. The residue was dissolved in anhydrous DMF (1.0 mL). 3-(3-Cyanophenyl)propanoic acid (43.0 mg, 0.244 mmol, 1.0 eq.), HATU (93.0 mg, 0.244 mmol, 1.0 eq.) and DIPEA (85.0 µL, 0.488 mmol, 2.0 eq.) were added. The reaction mixture was stirred at rt for 17 h. The solvent was evaporated *in vacuo.* The residue was re-dissolved in ethyl acetate (10 mL) and water (5 mL) was added. The organic layer was separated then the aqueous layer was extracted with ethyl acetate (3 × 10 mL). The combined organic layers were washed with 10% w/v $LiCl_{(aq)}$ (3 × 10 mL), dried over $MgSO_{4\,(s)}$, filtered, then the

filtrate was concentrated *in vacuo*. The residue was purified by flash column chromatography eluting with eluting with CH_2Cl_2 : methanol (1:0 to 91:9) to yield 3-(3-cyanophenyl)-*N*-(5-(3,5-dimethylisoxazol-4-yl)-2-((2-morpholinoethyl)amino)phenyl)propanamide **229** (83 mg, 71%) as an off-white solid: R_f 0.39 (CH_2Cl_2 : methanol, 9:1); ^{1}H NMR (400 MHz, $CDCl_3$) δ 7.59-7.55 (1H, m, $C^{2"}$-H), 7.56-7.49 (2H, m, $C^{4"}$-H, $C^{6"}$-H), 7.41 (1H, dd, *J* 7.7, 7.7, $C^{5"}$-H), 7.33 (1H, *br* s, $C^{1'}$N-H), 7.16 (1H, d, *J* 2.0, $C^{3'}$-H), 7.01 (1H, dd, *J* 8.2, 2.0, $C^{5'}$-H), 6.77 (1H, d, *J* 8.2, $C^{6'}$-H), 3.73 (4H, m, C^{10}-H_2, C^{11}-H_2), 3.23 (2H, t, *J* 6.0, $C^{1'''}$-H_2), 3.13 (2H, t, *J* 7.5, C^{3iv}-H_2), 2.77 (2H, t, *J* 7.5, C^{2iv}-H_2), 2.71 (2H, t, *J* 6.0, $C^{2'''}$-H_2), 2.60-2.50 (4H, m, C^8-H_2, C^9-H_2), 2.37 (3H, s, C^6-H_3), 2.23 (3H, s, C^7-H_3); LRMS *m/z* (ESI^+) 474 ($[M+H]^+$, 100%).

3-(2-(5-(3,5-Dimethylisoxazol-4-yl)-1-(2-morpholinoethyl)-1*H*-benzo[*d*]imidazol-2-yl)ethyl)benzonitrile 170

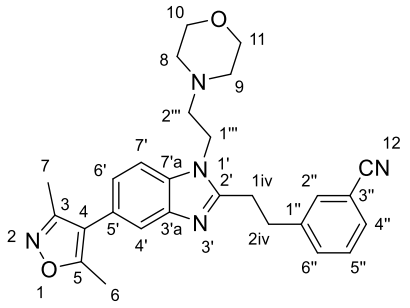

3-(3-Cyanophenyl)-*N*-(5-(3,5-dimethylisoxazol-4-yl)-2-((2-morpholinoethyl)amino)phenyl)propanamide **229** (70.0 mg, 0.148 mmol, 1.0 eq.) was refluxed in toluene (1.0 mL) in a microwave vial containing 3 Å molecular sieves for 48 h. The reaction mixture was cooled to rt, filtered then the solvent was evaporated *in vacuo*. The residue was purified by flash column chromatography eluting with eluting with CH_2Cl_2 : methanol (1:0 to 85:15) to yield 3-(2-(5-(3,5-dimethylisoxazol-4-yl)-1-(2-morpholinoethyl)-1*H*-benzo[*d*]imidazol-2-yl)ethyl)benzonitrile **170** (11 mg, 16%) as a red oil: R_f 0.35 (CH_2Cl_2 : methanol, 9:1); ν_{max} (thin film)/ cm^{-1} 2229 (C≡N, w), 1618 (C=C, w), 1583 (C-H, w), 1450 (C-H, m), 1322 (C-N, s), 1246 (C-O, s); ^{1}H NMR (700 MHz, $CDCl_3$) δ 7.62 (1H, d, *J* 1.5, $C^{4'}$-H), 7.57 (1H, d, *J* 1.7, $C^{2"}$-H), 7.55-7.51 (2H, m, $C^{4"}$-H, $C^{6"}$-H), 7.42 (1H, dd, *J* 7.7, 7.7, $C^{5"}$-H), 7.36 (1H, d, *J* 8.2, $C^{7'}$-H), 7.14 (1H, dd, *J* 8.2, 1.6, $C^{6'}$-H), 4.17 (2H, t, *J* 6.8, $C^{1'''}$-H_2), 3.69-3.63 (4H, m, C^{10}-H_2, C^{11}-H_2), 3.41-3.36 (2H, dd, *J* 8.9, 6.9, C^{2iv}-H_2), 3.22 (2H, dd, *J* 8.9, 6.9, C^{1iv}-H_2), 2.65 (2H, t, *J* 6.8,

$C^{2'''}$-H_2), 2.51-2.45 (4H, m, C^8-H_2, C^9-H_2), 2.42 (3H, s, C^6-H_3), 2.29 (3H, s, C^7-H_3); ^{13}C NMR (176 MHz, $CDCl_3$) δ 165.2 (C^5), 159.1 (C^3), 154.4 ($C^{2'}$), 143.0 ($C^{3'a}$), 142.5 ($C^{1''}$), 134.5 ($C^{7'a}$), 133.3 ($C^{6''}$), 132.0 ($C^{2''}$), 130.4 ($C^{4''}$), 129.6 ($C^{5''}$), 124.6 ($C^{5'}$), 123.8 ($C^{6'}$), 120.2 ($C^{4'}$), 118.9 (C^{12}), 117.2 (C^4), 112.9 ($C^{3''}$), 109.6 ($C^{7'}$), 67.0 (C^{10}, C^{11}), 57.8 ($C^{2'''}$), 54.2 (C^8, C^9), 41.8 ($C^{1'''}$), 32.9 (C^{2iv}), 29.0 (C^{1iv}), 11.7 (C^6), 11.0 (C^7); LRMS *m/z* (ESI^+) 456 ($[M+H]^+$, 100%); HRMS *m/z* (ESI^+) [Found: 478.2230, $C_{27}H_{29}N_5O_2$ requires $[M+Na]^+$ 478.2214)]; Analytical HPLC (RP, *Method 3*) rt 6.7 min, purity 100%.

3-(4-Cyanophenyl)-*N*-(5-(3,5-dimethylisoxazol-4-yl)-2-((2-morpholinoethyl)amino)phenyl)propanamide 230

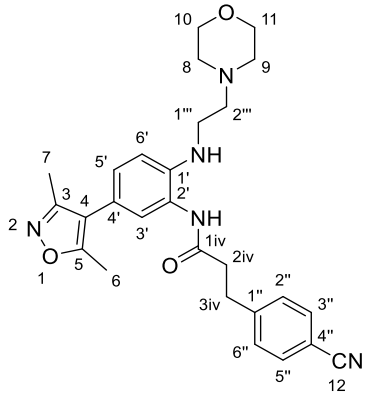

1 M $Na_2S_2O_{4\,(aq)}$ (2.25 mL, 2.25 mmol, 5.2 eq.) was added to 4-(3,5-dimethylisoxazol-4-yl)-*N*-(2-morpholinoethyl)-2-nitroaniline **195** (150 mg, 0.433 mmol, 1.0 eq.) in EtOH (2.30 mL). The reaction mixture was stirred at 80 °C for 15 min. The reaction mixture was cooled to rt then the solvent was evaporated *in vacuo.* The residue was partitioned between 10% aq. ammonia solution and ethyl acetate. The aqueous layer was separated then extracted with ethyl acetate (3 × 15 mL). The combined organic layers were dried over $MgSO_{4\,(s)}$, filtered, then the filtrate was concentrated *in vacuo*. The residue was dissolved in anhydrous DMF (1.0 mL). 3-(4-Cyanophenyl)propanoic acid (43.0 mg, 0.244 mmol, 1.0 eq.), HATU (93.0 mg, 0.244 mmol, 1.0 eq.) and DIPEA (85.0 µL, 0.488 mmol, 2.0 eq.) were added. The reaction mixture was stirred at rt for 17 h. The solvent was evaporated *in vacuo.* The residue was re-dissolved in ethyl acetate (10 mL) and water (5 mL) was added. The organic layer was separated then the aqueous layer was extracted with ethyl acetate (3 × 10 mL). The combined organic layers were washed with 10% w/v $LiCl_{(aq)}$ (3 × 10 mL), dried over $MgSO_{4\,(s)}$, filtered, then the filtrate was concentrated *in vacuo*. The residue was purified by flash column chromatography eluting

with eluting with CH_2Cl_2 : methanol (1:0 to 91:9) to yield 3-(4-cyanophenyl)-*N*-(5-(3,5-dimethylisoxazol-4-yl)-2-((2-morpholinoethyl)amino)phenyl)propanamide **230** (110 mg, 96%) as a yellow oil: R_f 0.39 (CH_2Cl_2 : methanol, 9:1); ^{1}H NMR (400 MHz, $CDCl_3$) δ 7.58 (2H, d, *J* 8.3, $C^{3"}$-H, $C^{5"}$-H), 7.51 (1H, *br* s, $C^{1'}$N-H), 7.39 (2H, d, *J* 8.3, $C^{4"}$-H, $C^{6"}$-H), 7.14 (1H, d, *J* 2.1, $C^{3'}$-H), 7.01 (1H, dd, *J* 2.1, 8.3, $C^{5'}$-H), 6.76 (1H, d, *J* 8.3, $C^{6'}$-H), 3.81-3.72 (4H, m, C^{10}-H_2, C^{11}-H_2), 3.35-3.22 (2H, m, $C^{1'''}$-H_2), 3.10 (2H, t, *J* 6.8, C^{3iv}-H_2), 2.83-2.72 (2H, m, $C^{2'''}$-H_2), 2.79 (2H, t, *J* 6.8, C^{2iv}-H_2), 2.69-2.53 (4H, m, C^8-H_2, C^9-H_2), 2.37 (3H, s, C^6-H_3), 2.23 (3H, s, C^7-H_3); LRMS *m/z* (ESI^+) 474 ($[M+H]^+$, 100%).

4-(2-(5-(3,5-Dimethylisoxazol-4-yl)-1-(2-morpholinoethyl)-1*H*-benzo[*d*]imidazol-2-yl)ethyl)benzonitrile 178

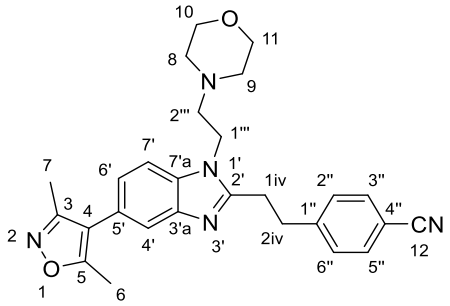

3-(4-Cyanophenyl)-*N*-(5-(3,5-dimethylisoxazol-4-yl)-2-((2-morpholinoethyl)amino)phenyl)propanamide **230** (100 mg, 0.211 mmol, 1.0 eq.) was refluxed in toluene (1.0 mL) in a microwave vial containing 3 Å molecular sieves for 48 h. The reaction mixture was cooled to rt, filtered then the solvent was evaporated *in vacuo*. The residue was purified by flash column chromatography eluting with eluting with CH_2Cl_2 : methanol (1:0 to 9:1) to yield 4-(2-(5-(3,5-dimethylisoxazol-4-yl)-1-(2-morpholinoethyl)-1*H*-benzo[*d*]imidazol-2-yl)ethyl)benzonitrile **178** (57 mg, 59%) as a yellow solid: R_f 0.33 (CH_2Cl_2 : methanol, 9:1); m.p. 135-137 °C (MeOH); ν_{max} (thin film)/ cm^{-1} 2227 (C≡N, w), 1246 (C-N, m), 1144 (C-O, s); ^{1}H NMR (700 MHz, $CDCl_3$) δ 7.62 (1H, d, *J* 1.5, $C^{4'}$-H), 7.61-7.59 (2H, m, $C^{3"}$-H, $C^{5"}$-H), 7.40-7.37 (2H, m, $C^{2"}$-H, $C^{6"}$-H), 7.36 (1H, d, *J* 8.2, $C^{7'}$-H), 7.14 (1H, dd, *J* 8.2, 1.5, $C^{6'}$-H), 4.15 (2H, t, *J* 6.8, $C^{1'''}$-H_2), 3.70-3.63 (4H, m, C^{10}-H_2, C^{11}-H_2), 3.44-3.35 (2H, m, C^{2iv}-H_2), 3.22 (2H, dd, *J* 8.9, 7.0, C^{1iv}-H_2), 2.64 (2H, t, *J* 6.8, $C^{2'''}$-H_2), 2.50-2.44 (4H, m, C^8-H_2, C^9-H_2), 2.42 (3H, s, C^6-H_3), 2.29 (3H, s, C^7-H_3); ^{13}C NMR (176 MHz, $CDCl_3$) δ 165.2 (C^5), 159.1 (C^3), 154.5 ($C^{2'}$), 146.6 ($C^{1"}$), 143.1 ($C^{3'a}$), 134.4 ($C^{7'a}$), 132.6 ($C^{3"}$, $C^{5"}$), 129.4 ($C^{2"}$, $C^{6"}$), 124.6 ($C^{5'}$),

123.8 ($C^{6'}$), 120.1 ($C^{4'}$), 118.9 (C^{12}), 117.1 (C^{4}), 110.6 ($C^{4''}$), 109.6 ($C^{7'}$), 66.9 (C^{10}, C^{11}), 57.8 ($C^{2'''}$), 54.2 (C^{8}, C^{9}), 41.8 ($C^{1'''}$), 33.6 (C^{2iv}), 28.9 (C^{1iv}), 11.7 (C^{6}), 11.0 (C^{7}); LRMS *m/z* (ESI^+) 456 ($[M+H]^+$, 100%); HRMS *m/z* (ESI^+) [Found: 456.2405, $C_{27}H_{29}N_5O_2$ requires $[M+H]^+$ 456.2394)]; Analytical HPLC (RP, *Method 3*) rt 6.6 min, purity 99%.

_N_-(5-(3,5-Dimethylisoxazol-4-yl)-2-((2-morpholinoethyl)amino)phenyl)-3-(*m*-tolyl)propenamide 231

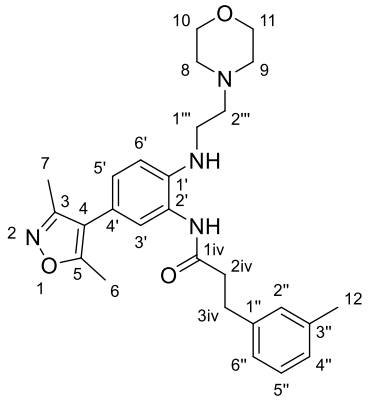

1 M $Na_2S_2O_{4\,(aq)}$ (3.29 mL, 3.29 mmol, 5.2 eq.) was added to 4-(3,5-dimethylisoxazol-4-yl)-*N*-(2-morpholinoethyl)-2-nitroaniline **195** (219 mg, 0.632 mmol, 1.0 eq.) in EtOH (3.29 mL). The reaction mixture was stirred at 80 °C for 10 min. The reaction mixture was cooled to rt then the solvent was evaporated *in vacuo.* The residue was partitioned between 10% aq. ammonia solution and ethyl acetate. The aqueous layer was separated then extracted with ethyl acetate (3 × 15 mL). The combined organic layers were dried over $MgSO_{4\,(s)}$, filtered, then the filtrate was concentrated *in vacuo*. The residue was dissolved in anhydrous DMF (2.0 mL). 3-(3-Methylphenyl)propanoic acid (109 mg, 0.663 mmol, 1.05 eq.), DIPEA (115 µL, 0.663 mmol, 1.05 eq.), HATU (252 mg, 0.663 mmol, 1.05 eq.) and HOBT (89.6 mg, 0.663 mmol, 1.05 eq.) were added. The reaction mixture was stirred at rt for 3 h. The solvent was evaporated *in vacuo.* The residue was re-dissolved in ethyl acetate (10 mL) and water (5 mL) was added. The organic layer was separated then the aqueous layer was extracted with ethyl acetate (3 × 10 mL). The combined organic layers were washed with brine, dried over $MgSO_{4\,(s)}$, filtered, then the filtrate was concentrated *in vacuo*. The residue was purified by flash column chromatography eluting with petroleum ether : ethyl acetate (1:0 to 0:1) to yield *N*-(5-(3,5-dimethylisoxazol-4-yl)-2-((2-morpholinoethyl)amino)phenyl)-3-(*m*-tolyl)propenamide **231** (294 mg, 99%) as a yellow oil: R_f 0.50 (CH_2Cl_2 : methanol, 9:1);

^{1}H NMR (400 MHz, $CDCl_3$) δ 7.68 (1H, *br* s, C^{1iv}N-H), 7.16 (1H, dd, *J* 7.5, $C^{5"}$-H), 7.08-6.96 (4H, m, $C^{5'}$-H, $C^{2"}$-H, $C^{4"}$-H, $C^{6"}$-H), 6.73 (1H, d, *J* 8.4, $C^{6'}$-H), 6.68 (1H, d, *J* 2.0, $C^{3'}$-H), 4.04-3.89 (4H, m, C^{10}-H_2, C^{11}-H_2), 3.76-3.65 (2H, m, $C^{1'''}$-H_2), 3.29-3.19 (2H, m, $C^{2'''}$-H_2), 3.04-2.93 (2H, m, C^{3iv}-H_2), 2.91-2.83 (2H, m, C^{2iv}-H_2), 2.83-2.75 (4H, m, C^{8}-H_2, C^{9}-H_2), 2.34 (3H, s, C^{6}-H_3), 2.27 (3H, s, C^{12}-H_3), 2.20 (3H, s, C^{7}-H_3); ^{13}C NMR (101 MHz, $CDCl_3$) δ 173.9 (C^{1iv}), 165.1 (C^{5}), 158.8 (C^{3}), 140.3 ($C^{1"}$), 139.6 ($C^{2'}$), 138.5 ($C^{3"}$), 129.4 ($C^{2"}$), 129.2 ($C^{5'}$), 128.7 ($C^{5"}$), 127.6 ($C^{3'}$), 127.4 ($C^{4"}$), 125.5 ($C^{6"}$), 123.9 ($C^{2'}$), 60.5 (C^{10}, C^{11}), 55.8 ($C^{2'''}$), 52.9 (C^{8}, C^{9}), 38.0 (C^{2iv}), 35.7 ($C^{1'''}$), 31.5 (C^{3iv}), 21.5 (C^{12}), 11.7 (C^{6}), 10.9 (C^{7}); LRMS *m/z* (ESI^+) 463 ($[M+H]^+$, 100%).

4-(2-(5-(3,5-Dimethylisoxazol-4-yl)-2-(3-methylphenethyl)-1*H*-benzo[*d*]imidazol-1-yl)ethyl)morpholine 171

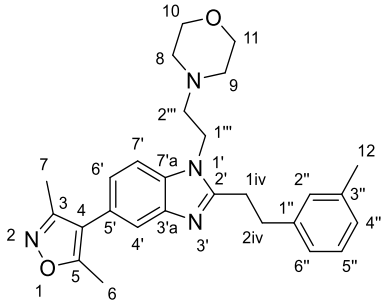

N-(5-(3,5-Dimethylisoxazol-4-yl)-2-((2-morpholinoethyl)amino)phenyl)-3-(*m*-tolyl)propenamide **231** (260 mg, 0.822 mmol, 1.0 eq.) and 3-(3-methylphenyl)propanoic acid (67.0 mg, 0.411 mmol, 1.0 eq.) were combined in toluene (1.0 mL) in a microwave vial containing 3 Å molecular sieves. The reaction mixture was stirred at 130 °C for 72 h. The reaction mixture was cooled to rt, filtered then the solvent was evaporated *in vacuo.* The residue was purified by flash column chromatography eluting with CH_2Cl_2 : methanol (1:0 to 9:1) followed by RP flash column chromatography eluting with water : acetonitrile (95:5 to 5:95) to yield 4-(2-(5-(3,5-dimethylisoxazol-4-yl)-2-(3-methylphenethyl)-1*H*-benzo[*d*]imidazol-1-yl)ethyl)morpholine **171** (28 mg, 8%) as a yellow oil: R_f 0.43 (CH_2Cl_2 : methanol, 9:1); ν_{max} (thin film)/ cm^{-1} 1451 (C-H, m), 1322 (C-N, m), 1247 (C-N, m), 1117 (C-O, s); ^{1}H NMR (400 MHz, $CDCl_3$) δ 7.63 (1H, d, *J* 1.6, $C^{4'}$-H), 7.35 (1H, dd, *J* 8.1, 0.5, $C^{7'}$-H), 7.20 (1H, dd, *J* 7.5, $C^{5"}$-H), 7.12 (1H, dd, *J* 8.1, 1.6, $C^{6'}$-H), 7.09-7.00 (3H, m, $C^{2"}$-H, $C^{4"}$-H, $C^{6"}$-H), 4.13 (2H, t, *J* 6.9, $C^{1'''}$-H_2), 3.74-3.61 (4H, m, C^{10}-H_2, C^{11}-H_2), 3.31-3.13 (4H, m, C^{1iv}-H_2, C^{2iv}-H_2), 2.61 (2H, t, *J* 6.9,

$C^{2'''}$-H_2), 2.50-2.44 (4H, m, C^8-H_2, C^9-H_2), 2.42 (3H, s, C^6-H_3), 2.33 (3H, s, C^{12}-H_3), 2.29 (3H, s, C^7-H_3); ^{13}C NMR (101 MHz, $CDCl_3$) δ 165.1 (C^5), 159.1 (C^3), 155.6 ($C^{2'}$), 143.2 ($C^{3'a}$), 141.0 ($C^{1''}$), 138.4 ($C^{3''}$), 134.4 ($C^{7'a}$), 129.3 ($C^{2''}$), 128.7 ($C^{5''}$), 127.4 ($C^{4''}$), 125.5 ($C^{6''}$), 124.3 ($C^{5'}$), 123.5 ($C^{6'}$), 120.1 ($C^{4'}$), 117.2 (C^4), 109.5 ($C^{7'}$), 66.9 (C^{10}, C^{11}), 57.7 ($C^{2'''}$), 54.2 (C^8, C^9), 41.6 ($C^{1'''}$), 33.9 (C^{2iv}), 29.9 (C^{1iv}), 21.5 (C^{12}), 11.7 (C^6), 11.0 (C^7); LRMS *m/z* (ESI^+) 445 ([M+H]$^+$, 100%); HRMS *m/z* (ESI^+) [Found: 445.2608, $C_{27}H_{32}N_4O_2$ requires [M+H]$^+$ 445.2598)]; Analytical HPLC (RP, *Method 3*) rt 7.1 min, purity 100%.

_N_-(5-(3,5-dimethylisoxazol-4-yl)-2-((2-morpholinoethyl)amino)phenyl)-3-(_p_-tolyl)propanamide 232

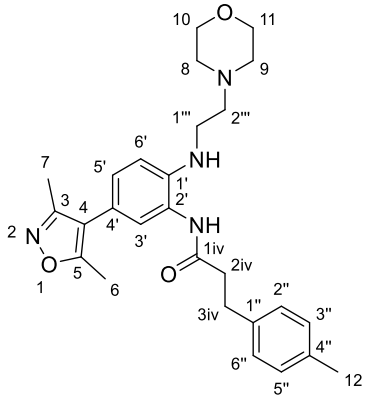

$Na_2S_2O_4$ (209 mg, 1.20 mmol, 5.2 eq.) was added to 4-(3,5-dimethylisoxazol-4-yl)-*N*-(2-morpholinoethyl)-2-nitroaniline **195** (80.0 mg, 0.231 mmol, 1.0 eq.) in EtOH (1.20 mL). H_2O (1.20 mL) was added then the reaction mixture was stirred at 80 °C for 10 min. The reaction mixture was cooled to rt then the solvent was evaporated *in vacuo.* The residue was partitioned between water and ethyl acetate. The aqueous layer was separated then extracted with ethyl acetate (3 × 10 mL). The combined organic layers were washed with brine, dried over $MgSO_{4\,(s)}$, filtered, then the filtrate was concentrated *in vacuo*. 3-(4-Methylphenyl)propanoic acid (29.9 mg, 0.182 mmol, 1.0 eq.), HATU (69.1 mg, 0.182 mmol, 1.0 eq.) and DIPEA (63.3 µL, 0.364 mmol, 2.0 eq.) were combined in anhydrous DMF (1.0 mL). 4-(3,5-Dimethylisoxazol-4-yl)-N^1-(2-morpholinoethyl)benzene-1,2-diamine (63.3 mg, 0.200 mmol, 1.1 eq.) in anhydrous DMF (500 µL) was added. The reaction mixture was stirred at rt for 17 h. The solvent was evaporated *in vacuo.* The residue was re-dissolved in ethyl acetate (10 mL) and water (5 mL) was added. The organic layer was separated then the aqueous layer was extracted

with ethyl acetate (3 × 10 mL). The combined organic layers were washed with 10% w/v LiCl $_{(aq)}$ (3 × 10 mL), dried over $MgSO_{4\ (s)}$, filtered and concentrated *in vacuo*. The residue was purified by flash column chromatography eluting with CH_2Cl_2 : methanol (1:0 to 9:1) to yield *N*-(5-(3,5-dimethylisoxazol-4-yl)-2-((2-morpholinoethyl)amino)phenyl)-3-(*p*-tolyl)propenamide **232** (73 mg, 79%) as an off-white solid: R_f 0.41 (CH_2Cl_2 : methanol, 9:1); ^{1}H NMR (400 MHz, $CDCl_3$) δ 7.17 (2H, d, *J* 8.0, $C^{2"}$-H, $C^{6"}$-H), 7.12 (2H, d, *J* 8.0, $C^{3"}$-H, $C^{5"}$-H), 7.08 (1H, d, *J* 2.0, $C^{3'}$-H), 7.00 (1H, dd, *J* 8.3, 2.0, $C^{5'}$-H), 6.92 (1H, *br* s, $C^{1'}$N-H), 6.76 (1H, d, *J* 8.3, $C^{6'}$-H), 3.75-3.68 (4H, m, C^{10}-H_2, C^{11}-H_2), 3.18 (2H, t, *J* 6.3, $C^{2'''}$-H_2), 3.06 (2H, t, *J* 7.5, C^{3iv}-H_2), 2.72 (2H, t, *J* 7.5, C^{2iv}-H_2), 2.68-2.60 (2H, m, $C^{1'''}$-H_2), 2.54-2.42 (4H, m, C^8-H_2, C^9-H_2), 2.38 (3H, s, C^6-H_3), 2.32 (3H, s, C^{12}-H_3), 2.24 (3H, s, C^7-H_3); LRMS *m/z* (ESI^+) 463 ($[M+H]^+$, 100%).

4-(2-(5-(3,5-Dimethylisoxazol-4-yl)-2-(4-methylphenethyl)-1*H*-benzo[*d*]imidazol-1-yl)ethyl)morpholine 179

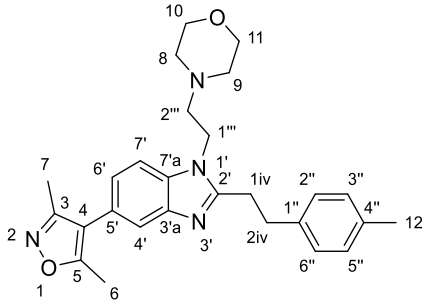

N-(5-(3,5-dimethylisoxazol-4-yl)-2-((2-morpholinoethyl)amino)phenyl)-3-(*p*-tolyl)propenamide **232** (50 mg, 0.108 mmol, 1.0 eq.) was refluxed in toluene (2.0 mL) in a microwave vial containing 3 Å molecular sieves for 24 h. The reaction mixture was cooled to rt, filtered then the solvent was evaporated *in vacuo.* The residue was purified by flash column chromatography eluting with CH_2Cl_2 : methanol (1:0 to 9:1) to yield 4-(2-(5-(3,5-dimethylisoxazol-4-yl)-2-(4-methylphenethyl)-1*H*-benzo[*d*]imidazol-1-yl)ethyl)morpholine **179** (44 mg, 91%) as a yellow oil: R_f 0.44 (CH_2Cl_2 : methanol, 9:1); ν_{max} (thin film)/ cm^{-1} 1451 (C-H, m), 1359 (C-N, m), 1247 (C-N, m), 1117 (C-O, s); ^{1}H NMR (600 MHz, $CDCl_3$) δ 7.63 (1H, dd, *J* 1.6, 0.7, $C^{4'}$-H), 7.34 (1H, d, *J* 8.3, 0.7, $C^{7'}$-H), 7.17-7.08 (5H, m, $C^{6'}$-H, $C^{2"}$-H, $C^{3"}$-H, $C^{5"}$-H $C^{6"}$-H), 4.12 (2H, t, *J* 6.9, $C^{1'''}$-H_2), 3.69-3.64 (4H, m, C^{10}-H_2, C^{11}-H_2), 3.29-3.21 (2H, m, C^{2iv}-H_2), 3.21-3.14 (2H, m,

C^{1iv}-H_2), 2.59 (2H, t, *J* 6.9, $C^{2'''}$-H_2), 2.48-2.43 (4H, m, C^8-H_2, C^9-H_2), 2.42 (3H, s, C^6-H_3), 2.32 (3H, s, C^{12}-H_3), 2.29 (3H, s, C^7-H_3); ^{13}C NMR (151 MHz, $CDCl_3$) δ 165.1 (C^5), 159.1 (C^3), 155.6 ($C^{2'}$), 143.2 ($C^{3'a}$), 137.9 ($C^{1''}$), 136.1 ($C^{4''}$), 134.4 ($C^{7'a}$), 129.5 ($C^{3''}$, $C^{5''}$), 128.4 ($C^{2''}$, $C^{6''}$), 124.3 ($C^{5'}$), 123.5 ($C^{6'}$), 120.1 ($C^{4'}$), 117.2 (C^4), 109.5 ($C^{7'}$), 66.9 (C^{10}, C^{11}), 57.7 ($C^{2'''}$), 54.2 (C^8, C^9), 41.6 ($C^{1'''}$), 33.9 (C^{2iv}), 29.9 (C^{1iv}), 21.1 (C^{12}), 11.7 (C^6), 11.0 (C^7); LRMS *m/z* (ESI^+) 445 ($[M+H]^+$, 100%); HRMS *m/z* (ESI^+) [Found: 445.2614, $C_{27}H_{32}N_4O_2$ requires $[M+H]^+$ 445.2598)]; Analytical HPLC (RP, *Method 3*) rt 7.0 min, purity 97%.

(*E*)-3-(3-Cyano-4-methylphenyl)acrylic acid 162

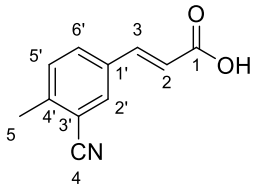

5-Bromo-2-methylbenzonitrile (500 mg, 2.55 mmol, 1.0 eq.), tris(2-methylphenyl)phosphane (155 mg, 0.510 mmol, 0.2 eq.), acrylic acid (175 µL, 2.55 mmol, 1.0 eq.) and Et_3N (1.42 mL, 10.2 mmol, 4.0 eq.) were dissolved in acetonitrile (4.0 mL). The reaction mixture was degassed for 20 min. Palladium(II) acetate (115 mg, 0.510 mmol, 0.2 eq.) was added. The reaction mixture was stirred under microwave irradiation for 45 min at 200 °C. The reaction mixture was cooled to rt and filtered through celite. The filtrate was concentrated *in vacuo.* The residue was partitioned between ethyl acetate (20 mL) and 3 M $NaOH_{(aq)}$ (15 mL). The aqueous layer was separated and washed with ethyl acetate. 2 M $HCl_{(aq)}$ (20 mL) was added to the aqueous solution and (*E*)-3-(3-cyano-4-methylphenyl)acrylic acid **162** precipitated as a colourless solid. The precipitate was filtered off and dried *in vacuo* to yield (*E*)-3-(3-cyano-4-methylphenyl)acrylic acid **162** (236 mg, 49%) as a colourless solid: R_f 0.22 (CH_2Cl_2 : methanol, 9:1); m.p. 214-216 °C ($CDCl_3$); ν_{max} (thin film)/ cm^{-1} 2361 (O-H, *br* s), 1706 (C=O, s), 1628 (C=C, m), 1427 (O-H, m); ^{1}H NMR (600 MHz, $CDCl_3$) δ 8.15 (1H, d, *J* 1.9, $C^{2'}$-H), 7.93 (1H, dd, *J* 8.1, 1.9, $C^{5'}$-H), 7.58 (1H, d, *J* 16.0, C^3-H), 7.50 (1H, d, *J* 8.1, $C^{6'}$-H), 6.64 (1H, d, *J* 16.0, C^2-H), 2.50 (3H, s, C^{12}-H_3); ^{13}C NMR (151 MHz, $CDCl_3$) δ 167.3 (C^1), 143.2 ($C^{4'}$), 141.6 (C^3), 132.9 ($C^{1'}$), 132.3 ($C^{5'}$), 132.2 ($C^{2'}$), 130.9 ($C^{6'}$), 120.8 (C^2), 117.5 (C^4), 112.5 ($C^{3'}$), 19.9 (C^5); LRMS *m/z* (ESI^+)

397 ([2M+Na]$^+$, 100%); HRMS *m/z* (ESI$^-$) [Found: 187.0636, $C_{11}H_9NO_2$ requires [M-H]$^-$ 187.0639)]; Analytical HPLC (RP, *Method 3*) rt 8.0 min, purity 100%.

3-(3-Cyano-4-methylphenyl)propanoic acid 158

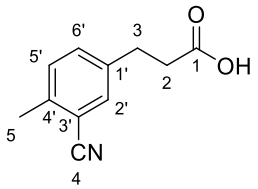

(*E*)-3-(3-Cyano-4-methylphenyl)acrylic acid **162** (50.0 mg, 0.267 mmol, 1.0 eq.) was dissolved in 2:1 THF : MeOH (6.0 mL) and the solvent was degassed for 15 min. 10 wt.% Palladium on carbon (5.0 mg, 10 wt. % of substrate) was added and the reaction mixture was stirred at rt under $H_{2\,(g)}$ for 17 h. The reaction mixture was filtered through Celite® eluting with ethyl acetate. The filtrate was concentrated *in vacuo* to yield 3-(3-cyano-4-methylphenyl)propanoic acid **158** (44 mg, 87%) as a colourless solid: R_f 0.36 (CH_2Cl_2 : methanol, 9:1); m.p. 74-76 °C ($CDCl_3$); ν_{max} (thin film)/ cm^{-1} 2929 (O-H, s, *br*), 2359 (C≡N, w), 1712 (C=O, s); ^{1}H NMR (600 MHz, $CDCl_3$) δ 7.42 (1H, d, *J* 1.9, C$^{2'}$-H), 7.31 (1H, dd, *J* 8.0, 1.9, C$^{5'}$-H), 7.22 (1H, d, *J* 8.0, C$^{6'}$-H), 2.92 (2H, t, *J* 7.6, C^3-H$_2$), 2.64 (2H, t, *J* 7.6, C^2-H$_2$), 2.49 (3H, s, C^5-H$_3$); ^{13}C NMR (151 MHz, $CDCl_3$) δ 178.2 (C^1), 140.1 (C$^{4'}$), 138.8 (C$^{1'}$), 133.0 (C$^{5'}$), 132.3 (C$^{2'}$), 130.6 (C$^{6'}$), 118.3 (C^4), 113.0 (C$^{3'}$), 35.5 (C^2), 29.9 (C^3), 20.1 (C^5); LRMS *m/z* (ESI$^+$) 401 ([2M+Na$^+$], 100%); HRMS *m/z* (ESI$^-$) [Found: 188.0722, $C_{11}H_{11}NO_2$ requires [M-H]$^-$ 188.0717)]; Analytical HPLC (RP, *Method 3*) rt 7.9 min, purity 99%.

Benzyl (*E*)-3-(3-cyano-4-methylphenyl)acrylate 164

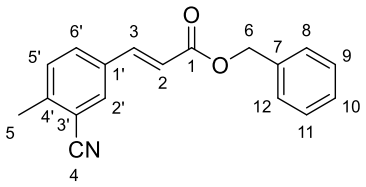

5-Bromo-2-methylbenzonitrile (1.25 g, 6.38 mmol, 1.0 eq.), tris(2-methylphenyl)phosphane (388 mg, 1.28 mmol, 0.2 eq.), benzyl acrylate (976 µL, 6.38 mmol, 1.0 eq.) and Et_3N (3.55 mL, 25.2 mmol, 4.0 eq.) were dissolved in acetonitrile (10 mL). The reaction mixture was degassed for 30 min. Palladium(II) acetate

(288 mg, 1.28 mmol, 0.2 eq.) was added. The reaction mixture was stirred at 80 °C for 5 h. The reaction mixture was cooled to rt and filtered through celite. The filtrate was partitioned between ethyl acetate (20 mL) and 2 M $HCl_{(aq)}$ (15 mL). The aqueous layer was separated then extracted with ethyl acetate (3 × 20 mL). The combined organic layers were dried over $MgSO_{4\ (s)}$, filtered, then the filtrate was concentrated *in vacuo*. The residue was purified by flash column chromatography eluting with petroleum ether : ethyl acetate (9:1) to yield benzyl (*E*)-3-(3-cyano-4-methylphenyl)acrylate **164** (1.41 g, 80%) as a yellow solid: R_f 0.30 (petroleum ether : ethyl acetate, 9:1); m.p. 64-66 °C ($CDCl_3$); ν_{max} (thin film)/ cm^{-1} 2229 (C≡N, w), 1715 (C=O, s), 1641 (C=C, m), 1160 (C-O, s), 983 (C=C, m); ^{1}H NMR (400 MHz, $CDCl_3$) δ 7.72 (1H, d, *J* 1.9, $C^{2'}$-H), 7.65 (1H, d, *J* 16.0, C^3-H), 7.61 (1H, dd, *J* 7.7, 1.9, $C^{6'}$-H), 7.45-7.31 (6H, m, $C^{5'}$-H, C^8-H, C^9-H, C^{10}-H, C^{11}-H, C^{12}-H), 6.48 (1H, d, *J* 16.0, C^2-H), 5.26 (2H, s, C^6-H_2), 2.57 (3H, s, C^5-H_3); ^{13}C NMR (101 MHz, $CDCl_3$) δ 166.3 (C^1), 144.0 ($C^{4'}$), 142.5 (C^3), 135.9 (C^7), 133.0 ($C^{1'}$), 132.0 ($C^{2'}$), 131.8 ($C^{6'}$), 131.0 ($C^{5'}$), 128.8 (C^9, C^{11}), 128.5 (C^{10}), 128.5 (C^8, C^{12}), 119.7 (C^2), 117.5 (C^4), 113.9 ($C^{3'}$), 66.8 (C^6), 20.6 (C^5); LRMS *m/z* (ESI^+) 278 ($[M+H]^+$, 100%); HRMS *m/z* (ESI^+) [Found: 278.1177, $C_{18}H_{15}NO_2$ requires $[M+H]^+$ 278.1176)]; Analytical HPLC (RP, *Method 3*) rt 11.0 min, purity 90%.

3-(3-Cyano-4-methylphenyl)propanoic acid 158

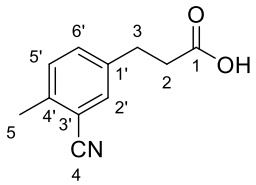

Benzyl (*E*)-3-(3-cyano-4-methylphenyl)acrylate **164** (1.30 g, 4.69 mmol, 1.0 eq.) was dissolved in MeOH (100 mL) and the solvent was degassed for 30 min. 10 wt.% Palladium on carbon (499 mg, 10 wt. % of substrate) was added and the reaction mixture was stirred at rt under $H_{2\ (g)}$ for 20 h. The reaction mixture was filtered through Celite® eluting with ethyl acetate. The filtrate was concentrated *in vacuo.* The residue was purified by flash column chromatography eluting with CH_2Cl_2 : methanol (1:0 to 9:1) to yield 3-(3-cyano-4-methylphenyl)propanoic acid **158** (693 mg, 78%) as a colourless solid: R_f 0.36 (CH_2Cl_2 : methanol, 9:1); m.p. 74-76 °C ($CDCl_3$); ν_{max} (thin film)/ cm^{-1} 2929 (O-H, s, *br*), 2359 (C≡N, w), 1712 (C=O, s); ^{1}H NMR (400 MHz, $CDCl_3$) δ 7.44 (1H, d, *J* 1.9, $C^{2'}$-H), 7.33 (1H, dd, *J* 7.9, 1.9, $C^{5'}$-H), 7.24 (1H, d, *J* 7.9, $C^{6'}$-H), 2.94 (2H, t, *J* 7.5,

C^3-H_2), 2.67 (2H, t, *J* 7.5, C^2-H_2), 2.50 (3H, s, C^5-H_3); ^{13}C NMR (101 MHz, $CDCl_3$) δ 178.5 (C^1), 140.2 ($C^{4'}$), 138.6 ($C^{1'}$), 133.0 ($C^{2'}$), 132.2 ($C^{6'}$), 130.6 ($C^{5'}$), 118.2 (C^4), 113.0 ($C^{3'}$), 35.2 (C^2), 29.7 (C^3), 20.2 (C^5); LRMS *m/z* (ESI^+) 401 ([2M+Na^+], 100%); HRMS *m/z* (ESI^-) [Found: 188.0722, $C_{11}H_{11}NO_2$ requires [M-H]$^-$ 188.0717)]; Analytical HPLC (RP, *Method 3*) rt 7.9 min, purity 99%.

3-(3-Cyano-4-methylphenyl)-*N*-(5-(3,5-dimethylisoxazol-4-yl)-2-(methylamino)phenyl)propanamide 166

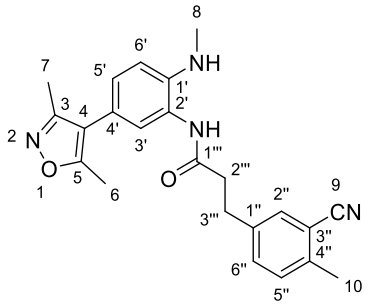

$Na_2S_2O_4$ (293 mg, 1.68 mmol, 5.2 eq.) was added to 4-(3,5-dimethylisoxazol-4-yl)-*N*-methyl-2-nitroaniline **75** (80.0 mg, 0.324 mmol, 1.0 eq.) in EtOH (1.70 mL). H_2O (1.70 mL) was added and the reaction mixture was stirred at 80 °C for 5 min. The reaction mixture was cooled to rt and the solvent was evaporated *in vacuo.* The residue was partitioned between sat. $NaHCO_{3\,(aq)}$ and ethyl acetate. The aqueous layer was separated then extracted with ethyl acetate (3 × 5 mL). The combined organic layers were dried over $MgSO_{4\,(s)}$, filtered, then the filtrate was concentrated *in vacuo*. 3-(3-Cyano-4-methylphenyl)propanoic acid **158** (44.3 mg, 0.234 mmol, 1.0 eq.), HATU (89.1 mg, 0.234 mmol, 1.0 eq.) and DIPEA (81.5 µL, 0.468 mmol, 2.0 eq.) were combined in anhydrous DMF (1.0 mL). 4-(3,5-Dimethylisoxazol-4-yl)-N^1-methylbenzene-1,2-diamine (56.0 mg, 0.258 mmol, 1.1 eq.) in anhydrous DMF (1.0 mL) was added. The reaction mixture was stirred at rt for 3 h. The solvent was evaporated *in vacuo.* The residue was re-dissolved in ethyl acetate (10 mL) and water (5 mL) was added. The organic layer was separated then the aqueous layer was extracted with ethyl acetate (3 × 10 mL). The combined organic layers were washed with 10% w/v $LiCl_{(aq)}$ (3 × 10 mL), dried over $MgSO_{4\,(s)}$, filtered and concentrated *in vacuo*. The residue was purified by flash column chromatography eluting with petroleum ether : ethyl acetate (1:0 to 1:4) to yield 3-(3-cyano-4-methylphenyl)-*N*-(5-(3,5-dimethylisoxazol-4-yl)-2-

(methylamino)phenyl)propanamide **166** (52 mg, 57%) as a colourless solid: R_f 0.32 (petroleum ether : ethyl acetate, 1:4); ^{1}H NMR (400 MHz, $CDCl_3$) δ 7.49 (1H, d, *J* 1.9, $C^{2''}$-H), 7.39 (1H, dd, *J* 8.0, 1.9, $C^{6''}$-H), 7.25 (1H, d, *J* 8.0, $C^{5''}$-H), 7.19 (1H, *br* s, $C^{1'}$N-H), 7.09-7.01 (2H, m, $C^{3'}$-H, $C^{5'}$-H), 6.78 (1H, d, *J* 8.2, $C^{6'}$-H), 3.06 (2H, t, *J* 7.4, $C^{2'''}$-H_2), 2.82 (3H, s, C^8-H_3), 2.72 (2H, t, *J* 7.4, $C^{3'''}$-H_2), 2.50 (3H, s, C^{10}-H_3), 2.36 (3H, s, C^6-H_3), 2.22 (3H, s, C^7-H_3); LRMS *m/z* (ESI^+) 389 ($[M+H]^+$, 100%).

5-(2-(5-(3,5-Dimethylisoxazol-4-yl)-1-methyl-1*H*-benzo[*d*]imidazol-2-yl)ethyl)-2-methylbenzonitrile 156

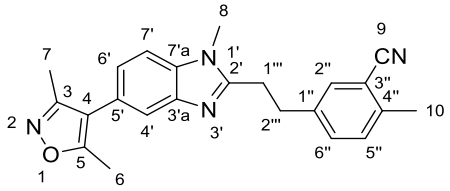

3-(3-Cyano-4-methylphenyl)-*N*-(5-(3,5-dimethylisoxazol-4-yl)-2-(methylamino)phenyl)propanamide **166** (31 mg, 0.080 mmol, 1.0 eq.) was refluxed in toluene (2.0 mL) in a microwave vial containing 3 Å molecular sieves for 24 h. The reaction mixture was cooled to rt, filtered then the solvent was evaporated *in vacuo*. The residue was purified by column chromatography eluting with petroleum ether : ethyl acetate (1:0 to 1:4) to yield 5-(2-(5-(3,5-dimethylisoxazol-4-yl)-1-methyl-1*H*-benzo[*d*]imidazol-2-yl)ethyl)-2-methylbenzonitrile **156** (24 mg, 81%) as a light yellow solid: R_f 0.25 (ethyl acetate : petroleum ether, 4:1); m.p. 133-135 °C ($CDCl_3$); ν_{max} (thin film)/ cm^{-1} 2228 (C≡N, w), 1510 (C-H, w), 1450 (C-H, m), 1322 (C-N, w); ^{1}H NMR (600 MHz, $CDCl_3$) δ 7.61 (1H, d, *J* 1.5, $C^{4'}$-H), 7.49 (1H, d, *J* 1.9, $C^{2''}$-H), 7.39-7.32 (2H, m, $C^{6'}$-H, $C^{6''}$-H), 7.24 (1H, d, *J* 7.9, $C^{5''}$-H), 7.17-7.12 (1H, m, $C^{7'}$-H), 3.67 (3H, s, C^8-H_3), 3.27 (2H, dd, *J* 9.2, 6.5, $C^{2'''}$-H_2), 3.16 (2H, dd, *J* 9.2, 6.5, $C^{2'''}$-H_2), 2.51 (3H, s, C^{10}-H_3), 2.41 (3H, s, C^6-H_3), 2.28 (3H, s, C^7-H_3); ^{13}C NMR (151 MHz, $CDCl_3$) δ 165.0 (C^5), 159.0 (C^3), 154.5 ($C^{2'}$), 142.8 ($C^{7'a'}$), 140.1 ($C^{1''}$), 139.0 ($C^{4''}$), 135.1 ($C^{3'a}$), 133.0 ($C^{6''}$), 132.1 ($C^{2''}$), 130.6 ($C^{5''}$), 124.3 ($C^{5'}$), 123.6 ($C^{7'}$), 119.9 ($C^{4'}$), 118.1 (C^9), 117.1 (C^4), 113.0 ($C^{3''}$), 109.3 ($C^{6'}$), 32.5 ($C^{2'''}$), 29.8 (C^8), 29.1 ($C^{1'''}$), 20.1 (C^{10}), 11.6 (C^6), 10.9 (C^7); LRMS *m/z* (ESI^+) 371 ($[M+H]^+$, 100%); HRMS *m/z* (ESI^+) [Found: 393.1700, $C_{23}H_{22}N_4O$ requires $[M+Na]^+$ 393.1686)]; Analytical HPLC (RP, *Method 3*) rt 7.4 min, purity 100%.

Benzyl (*E*)-3-(4-cyano-3-methylphenyl)acrylate 165

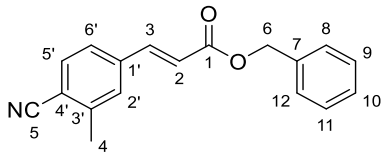

4-Bromo-2-methylbenzonitrile (962 mg, 4.91 mmol, 1.0 eq.), tris(2-methylphenyl)phosphane (299 mg, 0.981 mmol, 0.2 eq.), benzyl acrylate (751 µL, 4.91 mmol, 1.0 eq.) and Et_3N (2.72 mL, 19.6 mmol, 4.0 eq.) were dissolved in acetonitrile (10 mL). The reaction mixture was degassed for 30 min. Palladium(II) acetate (220 mg, 0.981 mmol, 0.2 eq.) was added. The reaction mixture was stirred at 80 °C for 6 h. The reaction mixture was cooled to rt and filtered through celite. The filtrate was partitioned between ethyl acetate (20 mL) and 2 M $HCl_{(aq)}$ (15 mL). The aqueous layer was separated then extracted with ethyl acetate (3 × 20 mL). The combined organic layers were dried over $MgSO_{4\,(s)}$, filtered, then the filtrate was concentrated *in vacuo*. The residue was purified by flash column chromatography eluting with petroleum ether : ethyl acetate (9:1) to yield benzyl (*E*)-3-(4-cyano-3-methylphenyl)acrylate **165** (1.0 g, 74%) as a yellow solid: R_f 0.29 (petroleum ether : ethyl acetate, 9:1); m.p. 63-65 °C ($CDCl_3$); ν_{max} (thin film)/ cm^{-1} 2225 (C≡N, w), 1717 (C=O, s), 1641 (C=C, m), 1166 (C-O, s), 982 (C=C, m); ^1H NMR (400 MHz, $CDCl_3$) δ 7.66 (1H, d, *J* 16.1, C^3-H), 7.60 (1H, d, *J* 8.0, $C^{5'}$-H), 7.46-7.32 (7H, m, $C^{2'}$-H, $C^{6'}$-H, C^8-H, C^9-H, C^{10}-H, C^{11}-H, C^{12}-H), 6.55 (1H, d, *J* 16.1, C^2-H), 5.26 (2H, s, C^6-H_2), 2.56 (3H, s, C^4-H_3); ^{13}C NMR (101 MHz, $CDCl_3$) δ 166.1 (C^1), 143.1 (C^3), 142.7 ($C^{3'}$), 138.5 ($C^{1'}$), 135.8 (C^7), 133.1 ($C^{5'}$), 129.7 ($C^{2'}$), 128.8 (C^9, C^{11}), 128.5 (C^{10}), 128.5 (C^8, C^{12}), 125.6 ($C^{6'}$), 121.3 (C^2), 117.8 (C^5), 114.1 ($C^{4'}$), 66.8 (C^6), 20.6 (C^4); LRMS *m/z* (ESI^+) 278 ($[M+H]^+$, 100%); HRMS *m/z* (ESI^+) [Found: 278.1183, $C_{18}H_{16}NO_2$ requires $[M+H]^+$ 278.1176)]; Analytical HPLC (RP, *Method 3*) rt 11.1 min, purity 100%.

3-(4-Cyano-3-methylphenyl)propanoic acid 159

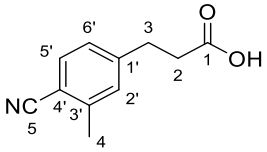

Benzyl (*E*)-3-(4-cyano-3-methylphenyl)acrylate **165** (900 mg, 3.25 mmol, 1.0 eq.) was dissolved in MeOH (90 mL) and the solvent was degassed for 30 min. 10 wt.% Palladium

on carbon (90 mg, 10 wt. % of substrate) was added and the reaction mixture was stirred at rt under $H_{2\,(g)}$ for 5 h. The reaction mixture was filtered through Celite® eluting with ethyl acetate. The filtrate was concentrated *in vacuo.* The residue was purified by flash column chromatography eluting with CH_2Cl_2 : methanol (95:5 to 9:1) to yield 3-(4-cyano-3-methylphenyl)propanoic acid **159** (516 mg, 84%) as a colourless solid: R_f 0.29 (CH_2Cl_2 : MeOH, 9:1); m.p. 122-123 °C ($CDCl_3$); ν_{max} (thin film)/ cm^{-1} 2225 (C≡N, w), 1717 (C=O, s), 1641 (C=C, m), 1166 (C-O, s), 982 (C=C, m); ^{1}H NMR (600 MHz, $CDCl_3$) δ 7.52 (1H, d, *J* 7.9, $C^{5'}$-H), 7.16 (1H, d, *J* 1.1, $C^{2'}$-H), 7.11 (1H, dd, *J* 7.9, 1.1, $C^{6'}$-H), 2.96 (2H, t, *J* 7.6, C^3-H_2), 2.69 (2H, t, *J* 7.6, C^2-H_2), 2.52 (3H, s, C^4-H_3); ^{13}C NMR (151 MHz, $CDCl_3$) δ 178.2 (C^1), 145.5 ($C^{3'}$), 142.2 ($C^{1'}$), 132.8 ($C^{5'}$), 130.3 ($C^{2'}$), 126.3 ($C^{6'}$), 118.1 (C^5), 110.8 ($C^{4'}$), 34.8 (C^2), 30.5 (C^3), 20.5 (C^4); LRMS *m/z* (ESI^+) 190 ($[M+H]^+$, 100%); HRMS *m/z* (ESI^-) [Found: 188.0726, $C_{11}H_{10}NO_2$ requires $[M-H]^-$ 188.0717)]; Analytical HPLC (RP, *Method 3*) rt 7.8 min, purity 96%.

3-(4-Cyano-3-methylphenyl)-*N*-(5-(3,5-dimethylisoxazol-4-yl)-2-(methylamino)phenyl)propanamide 167

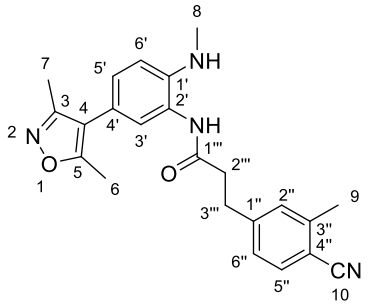

$Na_2S_2O_4$ (293 mg, 1.68 mmol, 5.2 eq.) was added to 4-(3,5-dimethylisoxazol-4-yl)-*N*-methyl-2-nitroaniline **75** (80.0 mg, 0.324 mmol, 1.0 eq.) in EtOH (1.70 mL). H_2O (1.70 mL) was added and the reaction mixture was stirred at 80 °C for 10 min. The reaction mixture was cooled to rt and the solvent was evaporated *in vacuo.* The residue was partitioned between water and ethyl acetate. The aqueous layer was separated then extracted with ethyl acetate (3 × 5 mL). The combined organic layers were dried over $MgSO_{4\,(s)}$, filtered, then the filtrate was concentrated *in vacuo*. 3-(4-Cyano-3-methylphenyl)propanoic acid **159** (43.5 mg, 0.230 mmol, 1.0 eq.), HATU (87.5 mg, 0.230 mmol, 1.0 eq.) and DIPEA (80.1 µL, 0.460 mmol, 2.0 eq.) were combined in anhydrous DMF (1.0 mL). 4-(3,5-Dimethylisoxazol-4-yl)-N^1-methylbenzene-1,2-

diamine (55.0 mg, 0.253 mmol, 1.1 eq.) in anhydrous DMF (1.0 mL) was added. The reaction mixture was stirred at rt for 3 h. The solvent was evaporated *in vacuo*. The residue was re-dissolved in ethyl acetate (10 mL) and water (5 mL) was added. The organic layer was separated then the aqueous layer was extracted with ethyl acetate (3 × 10 mL). The combined organic layers were dried over $MgSO_{4\,(s)}$, filtered, then the filtrate was concentrated *in vacuo*. The residue was purified by flash column chromatography eluting with petroleum ether : ethyl acetate (1:1 to 0:1) to yield 3-(4-cyano-3-methylphenyl)-*N*-(5-(3,5-dimethylisoxazol-4-yl)-2-(methylamino)phenyl)propanamide **167** (33 mg, 36%) as a pale red oil: R_f 0.26 (petroleum ether : ethyl acetate, 1:4); ^{1}H NMR (400 MHz, $CDCl_3$) δ 7.55 (1H, d, *J* 7.9, $C^{5''}$-H), 7.23 (1H, d, *J* 1.6, $C^{2''}$-H), 7.18 (1H, dd, *J* 7.9, 1.6, $C^{6''}$-H), 7.10 (1H, d, *J* 2.0, $C^{3'}$-H), 7.05 (1H, dd, *J* 8.3, 2.0, $C^{5'}$-H), 6.88 (1H, *br* s, $C^{1'}$N-H), 6.79 (1H, d, *J* 8.3, $C^{6'}$-H), 3.10 (2H, t, *J* 7.4, $C^{3'''}$-H_2), 2.74 (2H, t, *J* 7.4, $C^{2'''}$-H_2), 2.52 (3H, s, C^{8}-H_3), 2.37 (3H, s, C^{6}-H_3), 2.24 (3H, s, C^{7}-H_3); LRMS *m/z* (ESI^+) 389 ($[M+H]^+$, 100%).

4-(2-(5-(3,5-Dimethylisoxazol-4-yl)-1-methyl-1*H*-benzo[*d*]imidazol-2-yl)ethyl)-2-methylbenzonitrile 157

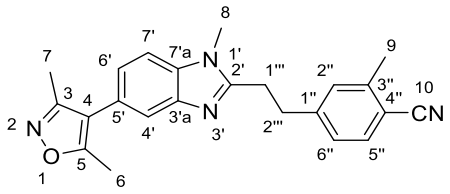

3-(4-Cyano-3-methylphenyl)-*N*-(5-(3,5-dimethylisoxazol-4-yl)-2-(methylamino)phenyl)propanamide **167** (72 mg, 0.19 mmol, 1.0 eq.) was refluxed in toluene (2.0 mL) in a microwave vial containing 3 Å molecular sieves for 24 h. The reaction mixture was cooled to rt, filtered then the solvent was evaporated *in vacuo*. The residue was purified by column chromatography eluting with CH_2Cl_2 : methanol (1:0 to 97:3) to yield 4-(2-(5-(3,5-dimethylisoxazol-4-yl)-1-methyl-1*H*-benzo[*d*]imidazol-2-yl)ethyl)-2-methylbenzonitrile **157** (43 mg, 62%) as a colourless solid: R_f 0.30 (CH_2Cl_2 : methanol, 9:1); m.p. 152-153 °C (MeOH); ν_{max} (thin film)/ cm^{-1} 2222 (C≡N, w), 1611 (C=C, w), 1511 (C-H, w), 1485 (C-H, m), 1423 (C-H, m), 1322 (C-N, m), 914 (C=C, m); ^{1}H NMR (600 MHz, $CDCl_3$) δ 7.62 (1H, dd, *J* 1.6, 0.7, $C^{4'}$-H), 7.53 (1H, d, *J* 8.0, $C^{5''}$-H), 7.35 (1H, dd, *J* 8.3, 0.7, $C^{7'}$-H), 7.22 (1H, m, $C^{2''}$-H), 7.19-7.13 (2H, m, $C^{6'}$-H, $C^{6''}$-H), 3.67 (3H, s, $C^{1'''}$-H_3), 3.33-3.27 (2H, m, C^{2iv}-H_2), 3.21-3.15 (2H, m, C^{1iv}-H_2), 2.52 (3H, s,

C^8-H_3), 2.42 (3H, s, C^6-H_3), 2.29 (3H, s, C^7-H_3); ^{13}C NMR (151 MHz, $CDCl_3$) δ 165.2 (C^5), 159.1 (C^3), 154.6 ($C^{2'}$), 146.2 ($C^{1''}$), 142.9 ($C^{3'a}$), 142.5 ($C^{3''}$), 135.3 ($C^{7'a}$), 133.0 ($C^{5''}$), 130.6 ($C^{2''}$), 126.5 ($C^{6''}$), 124.5 ($C^{5'}$), 123.8 ($C^{6'}$), 120.0 ($C^{4'}$), 118.3 (C^9), 117.2 (C^4), 111.1 ($C^{4''}$), 109.5 ($C^{7'}$), 33.7 (C^{2iv}), 29.9 ($C^{1'''}$), 29.0 (C^{1iv}), 20.6 (C^8), 11.7 (C^6), 11.0 (C^7); LRMS *m/z* (ESI^+) 371 ($[M+H]^+$, 100%); HRMS *m/z* (ESI^+) [Found: 393.1692, $C_{23}H_{22}N_4O$ requires $[M+Na]^+$ 393.1686)]; Analytical HPLC (RP, *Method 3*) rt 7.4 min, purity 100%.

3-(3-Cyano-4-methylphenyl)-*N*-(5-(3,5-dimethylisoxazol-4-yl)-2-((2-morpholinoethyl)amino)phenyl)propenamide 233

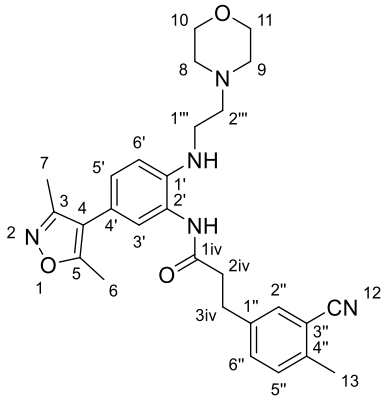

1 M $Na_2S_2O_{4\,(aq)}$ (660 µL, 0.660 mmol, 5.2 eq.) was added to 4-(3,5-dimethylisoxazol-4-yl)-*N*-(2-morpholinoethyl)-2-nitroaniline **195** (44.0 mg, 0.127 mmol, 1.0 eq.) in EtOH (660 µL). The reaction mixture was stirred at 80 °C for 10 min. The reaction mixture was cooled to rt then the solvent was evaporated *in vacuo.* The residue was partitioned between 10% aq. ammonia solution and ethyl acetate. The aqueous layer was separated then extracted with ethyl acetate (3 × 10 mL). The combined organic layers were dried over $MgSO_{4\,(s)}$, filtered, then the filtrate was concentrated *in vacuo*. 3-(3-Cyano-4-methylphenyl)propanoic acid **158** (15.0 mg, 0.080 mmol, 1.0 eq.), HATU (30.0 mg, 0.080 mmol, 1.0 eq.) and DIPEA (28.0 µL, 0.159 mmol, 2.0 eq.) were combined in anhydrous DMF (750 µL). 4-(3,5-Dimethylisoxazol-4-yl)-N^1-(2-morpholinoethyl)benzene-1,2-diamine (28.0 mg, 0.089 mmol, 1.1 eq.) in anhydrous DMF (750 µL) was added. The reaction mixture was stirred at rt for 2 h 45 min. The solvent was evaporated *in vacuo.* The residue was re-dissolved in ethyl acetate (10 mL) and 1 M $NaOH_{\,(aq)}$ (5 mL) was added. The organic layer was separated then the aqueous layer was extracted with ethyl acetate (3 × 10 mL). The combined organic layers were

washed with 10% w/v LiCl $_{(aq)}$ (3 × 10 mL), dried over $MgSO_{4\ (s)}$, filtered, then the filtrate was concentrated *in vacuo*. The residue was purified by flash column chromatography eluting with CH_2Cl_2 : methanol (1:0 to 85:15) to yield 3-(3-cyano-4-methylphenyl)-*N*-(5-(3,5-dimethylisoxazol-4-yl)-2-((2-morpholinoethyl)amino)phenyl)propenamide **233** (33 mg, 85%) as an off-white solid: R_f 0.29 (CH_2Cl_2 : methanol, 9:1); ^{1}H NMR (400 MHz, $CDCl_3$) δ 7.50 (1H, d, *J* 8.0, $C^{5''}$-H), 7.23 (1H, s, $C^{2''}$-H), 7.17 (1H, d, *J* 8.0, $C^{6''}$-H), 7.13 (1H, d, *J* 2.0, $C^{3'}$-H), 7.02 (1H, dd, *J* 8.3, 2.0, $C^{5'}$-H), 6.76 (1H, d, *J* 8.3, $C^{6'}$-H), 3.83-3.76 (4H, m, C^{10}-H_2, C^{11}-H_2), 3.40-3.29 (2H, m, $C^{1'''}$-H_2), 3.08 (2H, t, *J* 7.7, C^{3iv}-H_2), 2.90-2.80 (2H, m, $C^{2'''}$-H_2), 2.77 (2H, t, *J* 7.7, C^{2iv}-H_2), 2.76-2.64 (4H, m, C^{8}-H_2, C^{9}-H_2), 2.49 (3H, s, C^{13}-H_3), 2.37 (3H, s, C^{6}-H_3), 2.23 (3H, s, C^{7}-H_3); LRMS *m/z* (ESI^+) 486 ($[M+H]^+$, 100%).

5-(2-(5-(3,5-Dimethylisoxazol-4-yl)-1-(2-morpholinoethyl)-1*H*-benzo[*d*]imidazol-2-yl)ethyl)-2-methylbenzonitrile 174

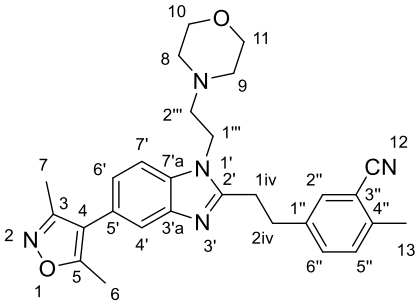

N-(5-(3,5-Dimethylisoxazol-4-yl)-2-((2-morpholinoethyl)amino)phenyl)propenamide **233** (30.0 mg, 0.062 mmol, 1.0 eq.) was refluxed in toluene (1.0 mL) in a microwave vial containing 3 Å molecular sieves for 48 h. The reaction mixture was cooled to rt, filtered, then the solvent was evaporated *in vacuo.* The residue was purified by flash column chromatography eluting with eluting with CH_2Cl_2 : methanol (1:0 to 9:1) to yield 5-(2-(5-(3,5-dimethylisoxazol-4-yl)-1-(2-morpholinoethyl)-1*H*-benzo[*d*]imidazol-2-yl)ethyl)-2-methylbenzonitrile **174** (24 mg, 84%) as yellow oil: R_f 0.37 (CH_2Cl_2 : methanol, 9:1); ν_{max} (thin film)/ cm^{-1} 2227 (C≡N, w), 1636 (C=C, w), 1509 (C-H, w), 1450 (C-H, m); ^{1}H NMR (600 MHz, $CDCl_3$) δ 7.62 (1H, dd, *J* 1.6, 0.6, $C^{4'}$-H), 7.50 (1H, d, *J* 2.0, $C^{2''}$-H), 7.38 (1H, dd, *J* 8.0, 2.0, $C^{6''}$-H), 7.36 (1H, dd, *J* 8.2, 0.6, $C^{7'}$-H), 7.25 (1H, d, *J* 8.0, $C^{5''}$-H), 7.13 (1H, dd, *J* 8.2, 1.6, $C^{6'}$-H), 4.17 (2H, t, *J* 6.8, $C^{1'''}$-H_2), 3.68-3.64 (4H, m, C^{10}-H_2, C^{11}-H_2), 3.36-3.29 (2H, m, C^{2iv}-H_2), 3.23-3.16 (2H, m, C^{1iv}-H_2), 2.65 (2H, t, *J* 6.8,

$C^{2'''}$-H_2), 2.51 (3H, s, C^{13}-H_3), 2.49-2.47 (4H, m, C^8-H_2, C^9-H_2), 2.42 (3H, s, C^6-H_3), 2.29 (3H, s, C^7-H_3); ^{13}C NMR (151 MHz, $CDCl_3$) δ 165.2 (C^5), 159.1 (C^3), 154.6 ($C^{2'}$), 143.1 ($C^{3'a}$), 140.2 ($C^{1''}$), 139.3 ($C^{4''}$), 134.5 ($C^{7'a}$), 133.1 ($C^{6''}$), 132.2 ($C^{2''}$), 130.7 ($C^{5''}$), 124.5 ($C^{5'}$), 123.8 ($C^{6'}$), 120.2 ($C^{4'}$), 118.2 (C^{12}), 117.2 (C^4), 113.1 ($C^{3''}$), 109.6 ($C^{7'}$), 67.0 (C^{10}, C^{11}), 57.8 ($C^{2'''}$), 54.2 (C^8, C^9), 41.8 ($C^{1'''}$), 32.5 (C^{2iv}), 29.1 (C^{1iv}), 20.2 (C^{13}), 11.7 (C^6), 11.0 (C^7); LRMS *m/z* (ESI^+) 470 ($[M+H]^+$, 100%); HRMS *m/z* (ESI^+) [Found: 470.2555, $C_{28}H_{31}N_5O_2$ requires $[M+H]^+$ 470.2551)]; Analytical HPLC (RP, *Method 3*) rt 7.1 min, purity 100%.

3-(4-Cyano-3-methylphenyl)-*N*-(5-(3,5-dimethylisoxazol-4-yl)-2-((2-morpholinoethyl)amino)phenyl)propenamide 234

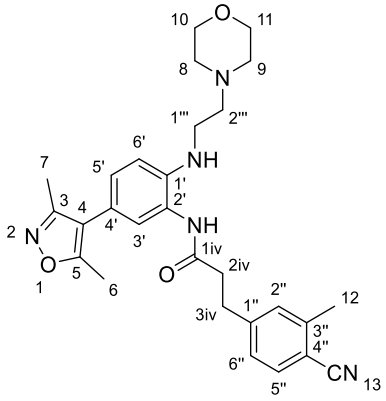

1 M $Na_2S_2O_{4\,(aq)}$ (660 µL, 0.660 mmol, 5.2 eq.) was added to 4-(3,5-dimethylisoxazol-4-yl)-*N*-(2-morpholinoethyl)-2-nitroaniline **195** (44.0 mg, 0.127 mmol, 1.0 eq.) in EtOH (660 µL). The reaction mixture was stirred at 80 °C for 10 min. The reaction mixture was cooled to rt then the solvent was evaporated *in vacuo.* The residue was partitioned between 10% aq. ammonia solution and ethyl acetate. The aqueous layer was separated then extracted with ethyl acetate (3 × 10 mL). The combined organic layers were dried over $MgSO_{4\,(s)}$, filtered, then the filtrate was concentrated *in vacuo*. 3-(4-Cyano-3-methylphenyl)propanoic acid **159** (16.0 mg, 0.085 mmol, 1.0 eq.), HATU (32.0 mg, 0.085 mmol, 1.0 eq.) and DIPEA (30.0 µL, 0.171 mmol, 2.0 eq.) were combined in anhydrous DMF (750 µL). 4-(3,5-Dimethylisoxazol-4-yl)-N^1-(2-morpholinoethyl)benzene-1,2-diamine (30.0 mg, 0.094 mmol, 1.1 eq.) in anhydrous DMF (750 µL) was added. The reaction mixture was stirred at rt for 3 h. The solvent was evaporated *in vacuo.* The residue was re-dissolved in ethyl acetate (10 mL) and 1 M $NaOH_{\,(aq)}$ (5 mL) was added. The organic layer was separated then the aqueous layer

was extracted with ethyl acetate (3 × 10 mL). The combined organic layers were washed with 10% w/v LiCl $_{(aq)}$ (3 × 5 mL), dried over $MgSO_{4\ (s)}$, filtered, then the filtrate was concentrated *in vacuo*. The residue was purified by flash column chromatography eluting with CH_2Cl_2 : methanol (1:0 to 9:1) to yield 3-(4-cyano-3-methylphenyl)-*N*-(5-(3,5-dimethylisoxazol-4-yl)-2-((2-morpholinoethyl)amino)phenyl)propenamide **234** (13 mg, 31%) as a red oil: R_f 0.54 (CH_2Cl_2 : methanol, 9:1); ^{1}H NMR (400 MHz, $CDCl_3$) δ 7.53 (1H, d, *J* 8.0, $C^{5''}$-H), 7.24-7.14 (3H, m, $C^{3'}$-H, $C^{2''}$-H, $C^{6''}$-H), 7.01 (1H, dd, *J* 8.3, 2.1, $C^{5'}$-H), 6.78 (1H, d, *J* 8.3, $C^{6'}$-H), 3.78-3.65 (4H, m, C^{10}-H_2, C^{11}-H_2), 3.19 (2H, t, *J* 5.8, $C^{1'''}$-H_2), 3.11 (2H, t, *J* 7.5, C^{3iv}-H_2), 2.75 (2H, t, *J* 7.5, C^{2iv}-H_2), 2.71-2.63 (2H, m, $C^{2'''}$-H_2), 2.51 (3H, s, C^{12}-H_3), 2.37 (3H, s, C^{6}-H_3), 2.24 (3H, s, C^{7}-H_3); LRMS *m/z* (ESI^+) 486 ($[M+H]^+$, 100%).

4-(2-(5-(3,5-Dimethylisoxazol-4-yl)-1-(2-morpholinoethyl)-1*H*-benzo[*d*]imidazol-2-yl)ethyl)-2-methylbenzonitrile 175

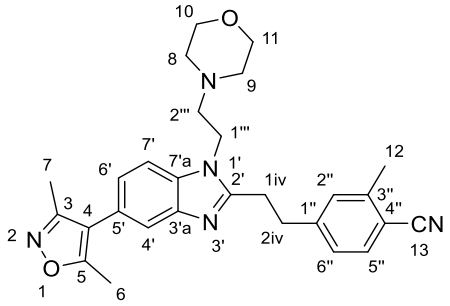

3-(3-Cyano-4-methylphenyl)-*N*-(5-(3,5-dimethylisoxazol-4-yl)-2-((2-morpholinoethyl)amino)phenyl)propenamide **234** (33 mg, 0.068 mmol, 1.0 eq.) was refluxed in toluene (1.0 mL) in a microwave vial containing 3 Å molecular sieves for 48 h. The reaction mixture was cooled to rt, filtered, then the solvent was evaporated *in vacuo.* The residue was purified by flash column chromatography eluting with eluting with CH_2Cl_2 : methanol (1:0 to 85:15) to yield 4-(2-(5-(3,5-dimethylisoxazol-4-yl)-1-(2-morpholinoethyl)-1*H*-benzo[*d*]imidazol-2-yl)ethyl)-2-methylbenzonitrile **175** (26 mg, 81%) as a yellow oil: R_f 0.48 (CH_2Cl_2 : methanol, 9:1); ν_{max} (thin film)/ cm^{-1} 2251 (C≡N, w), 1612 (C=C, w), 1509 (C-H, w), 1451 (C-H, m); ^{1}H NMR (600 MHz, $CDCl_3$) δ 7.62 (1H, dd, *J* 1.6, 0.7, $C^{4'}$-H), 7.54 (1H, d, *J* 8.0, $C^{5''}$-H), 7.36 (1H, dd, *J* 8.2, 0.7, $C^{7'}$-H), 7.23 (1H, m, $C^{2''}$-H), 7.17 (1H, dd, *J* 8.0, 1.7, $C^{6''}$-H), 7.14 (1H, dd, *J* 8.2, 1.6, $C^{6'}$-H), 4.16 (2H, t, *J* 6.8, $C^{1'''}$-H_2), 3.68-3.64 (4H, m, C^{10}-H_2, C^{11}-H_2), 3.37-3.32 (2H, m, C^{2iv}-H_2),

3.23-3.17 (2H, m, C^{1iv}-H_2), 2.65 (2H, t, *J* 6.8, $C^{2'''}$-H_2), 2.52 (3H, s, C^{12}-H_3), 2.49-2.45 (4H, m, C^{8}-H_2, C^{9}-H_2), 2.42 (3H, s, C^{6}-H_3), 2.29 (3H, s, C^{7}-H_3); ^{13}C NMR (151 MHz, $CDCl_3$) δ 165.2 (C^5), 159.1 (C^3), 154.6 ($C^{2'}$), 146.4 ($C^{3''}$), 143.1 ($C^{3'a}$), 142.4 ($C^{1''}$), 134.4 ($C^{7'a}$), 133.0 ($C^{5''}$), 130.5 ($C^{2''}$), 126.5 ($C^{6''}$), 124.6 ($C^{5'}$), 123.8 ($C^{6'}$), 120.1 ($C^{4'}$), 118.2 (C^{13}), 117.2 (C^4), 111.0 ($C^{4''}$), 109.6 ($C^{7'}$), 67.0 (C^{10}, C^{11}), 57.8 ($C^{2'''}$), 54.2 (C^8, C^9), 41.8 ($C^{1'''}$), 33.5 (C^{2iv}), 29.0 (C^{1iv}), 20.6 (C^{12}), 11.7 (C^6), 11.0 (C^7); LRMS *m/z* (ESI^+) 470 ($[M+H]^+$, 100%); HRMS *m/z* (ESI^+) [Found: 470.2558, $C_{28}H_{31}N_5O_2$ requires $[M+H]^+$ 470.2551)]; Analytical HPLC (RP, *Method 3*) rt 7.0 min, purity 100%.

3-(3-Cyano-4-methylphenyl)-*N*-(5-(3,5-dimethylisoxazol-4-yl)-2-((2-(4-methylpiperazin-1-yl)ethyl)amino)phenyl)propenamide 235

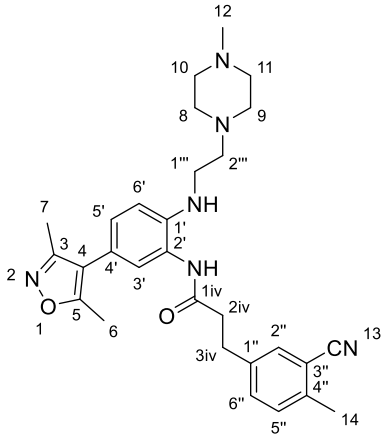

1 M $Na_2S_2O_4$ (202 mg, 1.15 mmol, 5.2 eq.) was added to 4-(3,5-dimethylisoxazol-4-yl)-*N*-(2-(4-methylpiperazin-1-yl)ethyl)-2-nitroaniline **193** (80.0 mg, 0.223 mmol, 1.0 eq.) in EtOH (1.15 mL). H_2O (1.15 mL) was added then the reaction mixture was stirred at 80 °C for 10 min. The reaction mixture was cooled to rt then the solvent was evaporated *in vacuo.* The residue was partitioned between 10% aq. ammonia solution and ethyl acetate. The aqueous layer was separated then extracted with ethyl acetate (3 × 10 mL). The combined organic layers were dried over $MgSO_{4\,(s)}$, filtered, then the filtrate was concentrated *in vacuo*. 3-(3-Cyano-4-methylphenyl)propanoic acid **158** (18.3 mg, 0.097 mmol, 1.0 eq.), HATU (36.7 mg, 0.097 mmol, 1.0 eq.) and DIPEA (33.6 µL, 0.193 mmol, 2.0 eq.) were combined in anhydrous DMF (1.0 mL). 4-(3,5-Dimethylisoxazol-4-yl)-N^1-(2-(4-methylpiperazin-1-yl)ethyl)benzene-1,2-diamine (35.0 mg, 0.106 mmol, 1.1 eq.) in anhydrous DMF (1.0 mL) was added. The reaction mixture was stirred at rt for 3 h. The solvent was evaporated *in vacuo.* The residue was

re-dissolved in ethyl acetate (10 mL) and water (5 mL) was added. The organic layer was separated then the aqueous layer was extracted with ethyl acetate (3 × 10 mL). The combined organic layers were washed with 10% w/v LiCl $_{(aq)}$ (3 × 10 mL), dried over $MgSO_{4\ (s)}$, filtered, then the filtrate was concentrated *in vacuo*. The residue was purified by flash column chromatography eluting with CH_2Cl_2 : methanol (1:0 to 9:1) to yield 3-(3-Cyano-4-methylphenyl)-*N*-(5-(3,5-dimethylisoxazol-4-yl)-2-((2-(4-methylpiperazin-1-yl)ethyl)amino)phenyl)propenamide **235** (29 mg, 61%) as a yellow oil: R_f 0.18 (Et_3N : CH_2Cl_2 : methanol, 1:99:0 to 1:89:10); ^{1}H NMR (400 MHz, $CDCl_3$) δ 7.53 (1H, d, *J* 1.9, C$^{2"}$-H), 7.40 (1H, dd, *J* 8.0, 1.9, C$^{5"}$-H), 7.30-7.19 (2H, m, C$^{6"}$-H, C$^{3'}$-H), 6.99 (1H, dd, *J* 8.3, 2.1, C$^{5'}$-H), 6.76 (1H, d, *J* 8.3, C$^{6'}$-H), 3.22 (2H, t, *J* 6.0, C$^{1'''}$-H_2), 3.09 (2H, t, *J* 7.6, C^{3iv}-H_2), 2.80-2.71 (4H, m, C$^{2'''}$-H_2, C^{2iv}-H_2), 2.68-2.44 (8H, m, C^8-H_2, C^9-H_2, C^{10}-H_2, C^{11}-H_2), 2.50 (3H, s, C^{12}-H_3), 2.38 (3H, s, C^6-H_3), 2.30 (3H, s, C^{14}-H_3), 2.25 (3H, s, C^7-H_3); LRMS *m/z* (ESI$^+$) 501 ([M+H]$^+$, 100%).

5-(2-(5-(3,5-Dimethylisoxazol-4-yl)-1-(2-(4-methylpiperazin-1-yl)ethyl)-1*H*-benzo[*d*]imidazol-2-yl)ethyl)-2-methylbenzonitrile 183

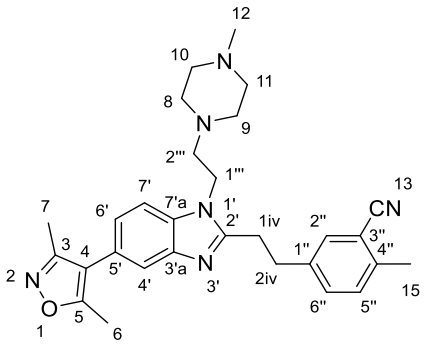

3-(3-Cyano-4-methylphenyl)-*N*-(5-(3,5-dimethylisoxazol-4-yl)-2-((2-(4-methylpiperazin-1-yl)ethyl)amino)phenyl)propenamide **235** (29.0 mg, 0.050 mmol, 1.0 eq.) was refluxed in toluene (2.0 mL) in a microwave vial containing 3 Å molecular sieves for 24 h. The reaction mixture was cooled to rt, filtered, then the solvent was evaporated *in vacuo.* The residue was purified by flash column chromatography eluting with eluting with CH_2Cl_2 : methanol (1:0 to 85:15) to yield 5-(2-(5-(3,5-dimethylisoxazol-4-yl)-1-(2-(4-methylpiperazin-1-yl)ethyl)-1*H*-benzo[*d*]imidazol-2-yl)ethyl)-2-methylbenzonitrile **183** (10 mg, 81%) as a colourless oil: R_f 0.31 (CH_2Cl_2 : methanol, 9:1); ν_{max} (thin film)/ cm^{-1} 2226 (C≡N, w), 1618 (C=C, w), 1509 (C-H, w), 1452 (C-H, m), 1358 (N-O, m), 1322 (C-N, m); ^{1}H NMR (600 MHz, $CDCl_3$) δ 7.61 (1H, d, *J* 1.6,

$C^{4'}$-H), 7.50 (1H, d, *J* 1.9, $C^{2''}$-H), 7.39 (1H, dd, *J* 7.9, 1.9, $C^{6''}$-H), 7.35 (1H, d, *J* 8.2, $C^{6'}$-H), 7.25 (1H, d, *J* 7.9, $C^{5''}$-H), 7.13 (1H, dd, *J* 8.3, 1.6, $C^{7'}$-H), 4.16 (2H, t, *J* 6.8, $C^{1'''}$-H_2), 3.34-3.29 (2H, m, C^{2iv}-H_2), 3.22-3.16 (2H, m, C^{1iv}-H_2), 2.66 (2H, t, *J* 6.8, $C^{2'''}$-H_2), 2.58-2.48 (4H, m, C^{8}-H_2, C^{9}-H_2), 2.51 (3H, s, C^{15}-H_3), 2.48-2.35 (4H, m, C^{10}-H_2, C^{11}-H_2), 2.42 (3H, s, C^{6}-H_3), 2.29 (3H, s, C^{12}-H_3), 2.29 (3H, s, C^{7}-H_3); ^{13}C NMR (151 MHz, $CDCl_3$) δ 165.2 (C^5), 159.1 (C^3), 154.7 ($C^{2'}$), 143.1 ($C^{3'a}$), 140.2 ($C^{4''}$), 139.4 ($C^{1''}$), 134.5 ($C^{7'a}$), 133.2 ($C^{6''}$), 132.2 ($C^{2''}$), 130.7 ($C^{5''}$), 124.5 ($C^{5'}$), 123.8 ($C^{7'}$), 120.1 ($C^{4'}$), 118.2 (C^{13}), 117.2 (C^4), 113.1 ($C^{3''}$), 109.6 ($C^{6'}$), 57.4 ($C^{2'''}$), 55.0 (C^{10}, C^{11}), 53.6 (C^8, C^9), 46.0 (C^{12}), 42.0 ($C^{1'''}$), 32.5 (C^{2iv}), 29.1 (C^{1iv}), 20.2 (C^{15}), 11.7 (C^6), 11.0 (C^7); LRMS *m/z* (ESI^+) 483 ($[M+H]^+$, 100%); HRMS *m/z* (ESI^+) [Found: 483.2875, $C_{29}H_{34}N_6O$ requires $[M+H]^+$ 483.2867)]; Analytical HPLC (RP, *Method 3*) rt 6.4 min, purity 100%.

1-(4-(2-((4-(3,5-Dimethylisoxazol-4-yl)-2-nitrophenyl)amino)ethyl)piperazin-1-yl)ethan-1-one 236

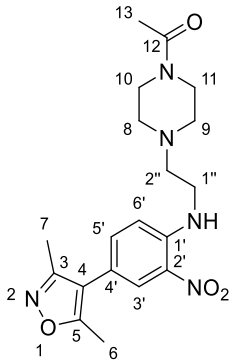

4-(4-Fluoro-3-nitrophenyl)-3,5-dimethylisoxazole **74** (200 mg, 0.847 mmol, 1.0 eq.) was dissolved in anhydrous DMF (2.5 mL). 1-(4-(2-Aminoethyl)piperazin-1-yl)ethan-1-one (250 mg, 1.46 mmol, 1.7 eq.) and DIPEA (369 µL, 2.17 mmol, 2.5 eq.) were added. The reaction mixture was stirred at 60 °C for 50 min. The reaction mixture was cooled to rt then the solvent was evaporated *in vacuo.* The residue was partitioned between CH_2Cl_2 and sat. $NaHCO_{3(aq)}$. The aqueous layer was extracted with CH_2Cl_2 (3 × 15 mL). The combined organic layers were dried over $MgSO_{4\ (s)}$, filtered, then the filtrate was concentrated *in vacuo*. The residue was purified by flash column chromatography eluting with CH_2Cl_2 : methanol (1:0 to 0:1) to yield 1-(4-(2-((4-(3,5-dimethylisoxazol-4-yl)-2-nitrophenyl)amino)ethyl)piperazin-1-yl)ethan-1-one **236** (167 mg, 51%) as an orange

solid: R_f 0.35 (CH_2Cl_2 : methanol, 9:1); m.p. 100-102 °C (MeOH); ν_{max} (thin film)/ cm^{-1} 3620 (N-H, m), 2926 (N-H, s *br*), 1615 (N-O, s), 1224 (C-N, m), 1005 (C-N, m); ^{1}H NMR (600 MHz, $CDCl_3$, at 25 °C there are two rotamers visible in 1:1 ratio; rot A and rot B) δ 8.57 (1H, t, *J* 4.4, N-H), 8.07 (1H, d, *J* 2.1, $C^{3'}$-H), 7.33 (1H, dd, *J* 8.8, 2.1, $C^{5'}$-H), 6.90 (1H, d, *J* 8.8, $C^{6'}$-H), 3.66 (rot A: 2H, m, C^{10}-H_2, C^{11}-H_2), 3.53 (rot B: 2H, m, C^{10}-H_2, C^{11}-H_2), 3.41 (2H, m, $C^{1''}$-H_2), 2.77 (2H, t, *J* 6.0, $C^{2''}$-H_2), 2.54 (rot A: 2H, m, C^8-H_2, C^9-H_2), 2.49 (rot B: 2H, m, C^8-H_2, C^9-H_2), 2.38 (3H, s, C^6-H_3), 2.24 (3H, s, C^7-H_3), 2.08 (3H, s, C^{13}-H_3); ^{13}C NMR (151 MHz, $CDCl_3$, at 25 °C there are two rotamers visible in 1:1 ratio; rot A and rot B) δ 168.9 (C^{12}), 165.3 (C^5), 158.6 (C^3), 144.4 ($C^{1'}$), 136.8 ($C^{5'}$), 132.0 ($C^{2'}$), 127.0 ($C^{3'}$), 117.4 (C^4), 114.9 ($C^{4'}$), 114.7 ($C^{6'}$), 55.4 ($C^{2''}$), 53.0 (rot A: C^8, C^9), 52.1 (rot B: C^8, C^9), 46.4 (rot B: C^{10}, C^{11}), 41.4 (rot A: C^{10}, C^{11}), 39.5 ($C^{1''}$), 21.4 (C^{13}), 11.6 (C^6), 10.8 (C^7); LRMS *m/z* (ESI^+) 388 ($[M+H]^+$, 100%); HRMS *m/z* (ESI^+) [Found: 388.1980, $C_{19}H_{25}N_5O_4$ requires $[M+H]^+$ 388.1979)]; Analytical HPLC (RP, *Method 3*) rt 6.4 min, purity 100%.

_N_-(2-((2-(4-Acetylpiperazin-1-yl)ethyl)amino)-5-(3,5-dimethylisoxazol-4-yl)phenyl)-3-(3-cyano-4-methylphenyl)propenamide 237

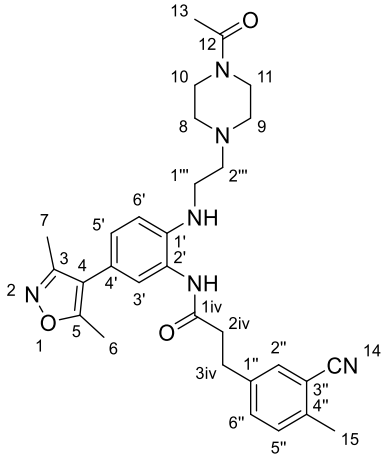

1 M $Na_2S_2O_4$ (257 mg, 0.336 mmol, 5.2 eq.) was added to 1-(4-(2-((4-(3,5-dimethylisoxazol-4-yl)-2-nitrophenyl)amino)ethyl)piperazin-1-yl)ethan-1-one **236** (130 mg, 0.336 mmol, 1.0 eq.) in EtOH (1.74 mL). H_2O (1.74 mL) was added then the reaction mixture was stirred at 80 °C for 10 min. The reaction mixture was cooled to rt then the solvent was evaporated *in vacuo.* The residue was partitioned between 10% aq. ammonia solution and ethyl acetate. The aqueous layer was separated then extracted with ethyl acetate (3 × 10 mL). The combined organic layers were dried over $MgSO_{4\,(s)}$,

filtered, then the filtrate was concentrated *in vacuo*. 3-(3-Cyano-4-methylphenyl)propanoic acid **158** (53.0 mg, 0.280 mmol, 1.0 eq.), HATU (106 mg, 0.280 mmol, 1.0 eq.) and DIPEA (98.0 µL, 0.560 mmol, 2.0 eq.) were combined in anhydrous DMF (750 µL). 1-(4-(2-((2-Amino-4-(3,5-dimethylisoxazol-4-yl)phenyl)amino)ethyl)piperazin-1-yl)ethan-1-one (100 mg, 0.280 mmol, 1.0 eq.) in anhydrous DMF (750 µL) was added. The reaction mixture was stirred at rt for 3 h. The solvent was evaporated *in vacuo.* The residue was re-dissolved in ethyl acetate (10 mL) and water (5 mL) was added. The organic layer was separated then the aqueous layer was extracted with ethyl acetate (3 × 10 mL). The combined organic layers were washed with 10% w/v LiCl $_{(aq)}$ (3 × 10 mL), dried over $MgSO_{4\,(s)}$, filtered, then the filtrate was concentrated *in vacuo*. The residue was purified by flash column chromatography eluting with CH_2Cl_2 : methanol (1:0 to 9:1) to yield *N*-(2-((2-(4-acetylpiperazin-1-yl)ethyl)amino)-5-(3,5-dimethylisoxazol-4-yl)phenyl)-3-(3-cyano-4-methylphenyl)propenamide **237** (87 mg, 59%) as a brown oil: R_f 0.38 (CH_2Cl_2 : methanol, 1:0 to 9:1); ^{1}H NMR (400 MHz, MeOD) δ 7.57 (1H, d, *J* 1.9, $C^{2''}$-H), 7.49 (1H, dd, *J* 8.0, 1.9, $C^{5''}$-H), 7.35 (1H, d, *J* 8.0, $C^{6''}$-H), 7.13 (1H, dd, *J* 8.4, 2.1, $C^{5'}$-H), 6.90 (1H, d, *J* 8.4, $C^{6'}$-H), 6.83 (1H, d, *J* 2.1, $C^{3'}$-H), 3.75-3.66 (4H, m, C^{10}-H_2, C^{11}-H_2), 3.48 (2H, t, *J* 6.0, $C^{1'''}$-H_2), 3.05 (2H, t, *J* 7.4, C^{3iv}-H_2), 3.00 (2H, t, *J* 6.0, $C^{2'''}$-H_2), 2.94-2.88 (2H, m, C^8-H_a, C^9-H_a), 2.88-2.81 (2H, m, C^8-H_b, C^9-H_b), 2.78 (2H, t, *J* 7.4, C^{2iv}-H_2), 2.48 (3H, s, C^{15}-H_3), 2.38 (3H, s, C^6-H_3), 2.23 (3H, s, C^7-H_3), 2.14 (3H, s, C^{13}-H_3); LRMS *m/z* (ESI^+) 529 ($[M+H]^+$, 100%).

5-(2-(1-(2-(4-Acetylpiperazin-1-yl)ethyl)-5-(3,5-dimethylisoxazol-4-yl)-1*H*-benzo[*d*]imidazol-2-yl)ethyl)-2-methylbenzonitrile 181

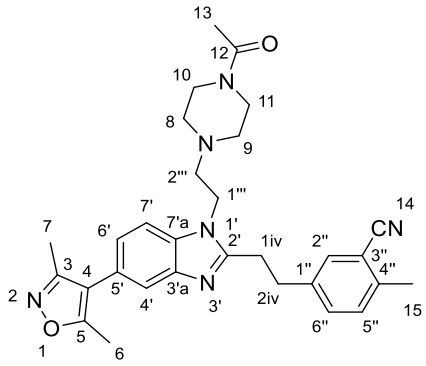

N-(2-((2-(4-Acetylpiperazin-1-yl)ethyl)amino)-5-(3,5-dimethylisoxazol-4-yl)phenyl)-3-(3-cyano-4-methylphenyl)propenamide **237** (70.0 mg, 0.132 mmol, 1.0 eq.) was refluxed in toluene (2.0 mL) in a microwave vial containing 3 Å molecular sieves for 48 h. The reaction mixture was cooled to rt, filtered, then the solvent was evaporated *in vacuo.* The residue was purified by flash column chromatography eluting with eluting with CH_2Cl_2 : methanol (1:0 to 85:15) to yield 5-(2-(1-(2-(4-acetylpiperazin-1-yl)ethyl)-5-(3,5-dimethylisoxazol-4-yl)-1*H*-benzo[*d*]imidazol-2-yl)ethyl)-2-methylbenzonitrile **181** (24 mg, 39%) as a beige solid: R_f 0.46 (CH_2Cl_2 : methanol, 9:1); m.p. 55-57 °C ($CDCl_3$); ν_{max} (thin film)/ cm^{-1} 2226 (C≡N, w), 1638 (C=O, s), 1440 (C-H, s), 1321 (C-N, m), 1148 (C-O, m), 1250 (C-N, s); ^{1}H NMR (600 MHz, $CDCl_3$, at 25 °C there are two rotamers visible in 1:1 ratio; rot A and rot B) δ 7.63 (1H, d, *J* 1.6, $C^{4'}$-H), 7.50 (1H, d, *J* 2.0, $C^{2''}$-H), 7.41-7.38 (1H, m, $C^{6''}$-H), 7.36 (1H, d, *J* 8.2, $C^{7'}$-H), 7.25 (1H, d, *J* 7.8, $C^{5''}$-H), 7.14 (1H, dd, *J* 8.2, 1.6, $C^{6'}$-H), 4.19 (2H, t, *J* 6.8, $C^{1'''}$-H_2), 3.59-3.55 (rot A: 2H, m, C^{10}-H_2, C^{11}-H_2), 3.44-3.39 (rot B: 2H, m, C^{10}-H_2, C^{11}-H_2), 3.36-3.30 (2H, m, C^{2iv}-H_2), 3.22-3.16 (2H, m, C^{1iv}-H_2), 2.68 (2H, t, *J* 6.8, $C^{2'''}$-H_2), 2.52 (3H, s, C^{15}-H_3), 2.48-2.43 (rot A and B: 4H, m, C^{8}-H_2, C^{9}-H_2), 2.43 (3H, s, C^{6}-H_3), 2.29 (3H, s, C^{7}-H_3), 2.07 (3H, s, C^{13}-H_3); ^{13}C NMR (151 MHz, $CDCl_3$, at 25 °C there are two rotamers visible in 1:1 ratio; rot A and rot B) δ 168.93 (C^{12}), 165.1 (C^{5}), 158.9 (C^{3}), 154.3 ($C^{2'}$), 142.8 ($C^{3'a}$), 140.2 ($C^{1''}$), 139.1 ($C^{4''}$), 134.2 ($C^{7'a}$), 133.0 ($C^{6''}$), 132.1 ($C^{2''}$), 130.6 ($C^{5''}$), 124.6 ($C^{5'}$), 123.8 ($C^{6'}$), 120.0 ($C^{4'}$), 118.1 (C^{12}), 117.0 (C^{4}), 113.0 ($C^{3''}$), 109.5 ($C^{7'}$), 57.1 ($C^{2'''}$), 53.9 (rot A: C^{10}, C^{11}), 53.2 (rot B: C^{10}, C^{11}), 46.1 (rot B: C^{8}, C^{9}), 41.8 ($C^{1'''}$), 41.2 (rot A: C^{8}, C^{9}), 32.4 (C^{2iv}), 29.0 (C^{1iv}), 21.3 (C^{13}), 20.1 (C^{15}), 11.6 (C^{6}), 10.9 (C^{7}); LRMS *m/z* (ESI^+) 511 ($[M+H]^+$, 100%); HRMS *m/z* (ESI^+) [Found: 511.2808, $C_{30}H_{34}N_6O_2$ requires $[M+H]^+$ 511.2816)]; Analytical HPLC (RP, *Method 3*) rt 7.0 min, purity 100%.

4-(3,5-Dimethylisoxazol-4-yl)-2-nitro-*N*-(2-(piperidin-1-yl)ethyl)aniline 238

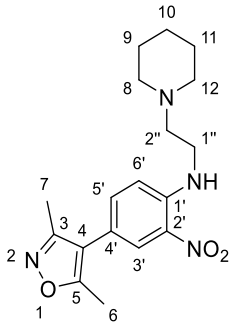

4-(4-Fluoro-3-nitrophenyl)-3,5-dimethylisoxazole **74** (100 mg, 0.423 mmol, 1.0 eq.) was dissolved in anhydrous DMF (2.0 mL). 2-(Piperidin-1-yl)ethan-1-amine (109 mg, 0.847 mmol, 2.0 eq.) and DIPEA (184 μL, 1.058 mmol, 2.5 eq.) were added. The reaction mixture was stirred at 80 °C for 2 h. The solvent was evaporated *in vacuo* then the residue was partitioned between ethyl acetate and water. The aqueous layer was extracted with ethyl acetate (3 × 15 mL). The combined organic layers were washed with 10% w/v $LiCl_{(aq)}$ (2 × 10 mL), then dried over $MgSO_{4\ (s)}$, filtered, then the filtrate was concentrated *in vacuo*. The residue was purified by flash column chromatography eluting with CH_2Cl_2 : methanol (1:0 to 9:1) to yield 4-(3,5-dimethylisoxazol-4-yl)-2-nitro-*N*-(2-(piperidin-1-yl)ethyl)aniline **238** (134 mg, 92%) as an orange oil: R_f 0.24 (CH_2Cl_2 : methanol, 9:1); ν_{max} (thin film)/ cm^{-1} 3340 (N-H, m, *br*), 1622 (N-H, s), 1558 (N-O, s), 1530 (N-O, s), 1298 (N-O, s), 1223 (C-N, m), 1160 (C-N, m); ^{1}H NMR (600 MHz, $CDCl_3$) δ 8.58 (1H, t, *J* 4.6, N-H), 8.07 (1H, d, *J* 2.1, $C^{3'}$-H), 7.32 (1H, dd, *J* 8.8, 2.1, $C^{5'}$-H), 6.91 (1H, d, *J* 8.8, $C^{6'}$-H), 3.38 (2H, td, *J* 6.2, 4.6, $C^{1''}$-H_2), 2.68 (2H, t, *J* 6.2, $C^{2''}$-H_2), 2.53-2.42 (4H, m, C^8-H_2, C^{12}-H_2), 2.39 (3H, s, C^6-H_3), 2.26 (3H, s, C^7-H_3), 1.63 (4H, p, *J* 5.6, C^9-H_2, C^{11}-H_2), 1.46 (2H, p, *J* 5.9, C^{10}-H_2); ^{13}C NMR (151 MHz, $CDCl_3$) δ 165.4 (C^5), 158.8 (C^3), 144.7 ($C^{1'}$), 136.8 ($C^{5'}$), 132.0 ($C^{2'}$), 127.1 ($C^{3'}$), 117.1 (C^4), 115.1 ($C^{4'}$), 114.9 ($C^{6'}$), 56.4 ($C^{2''}$), 54.4 (C^8, C^{12}), 40.1 ($C^{1''}$), 26.2 (C^9, C^{11}), 24.6 (C^{10}), 11.7 (C^6), 10.9 (C^7); LRMS *m/z* (ESI^+) 345 ($[M+H]^+$, 100%); HRMS *m/z* (ESI^+) [Found: 345.1929, $C_{18}H_{24}N_4O_3$ requires $[M+H]^+$ 345.1921)]; Analytical HPLC (RP, *Method 2*) rt 7.1 min, purity 100%.

3-(3-Cyano-4-methylphenyl)-*N*-(5-(3,5-dimethylisoxazol-4-yl)-2-((2-(piperidin-1-yl)ethyl)amino)phenyl)propanamide 239

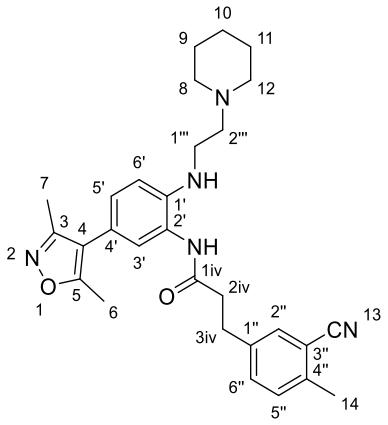

$Na_2S_2O_4$ (210 mg, 1.21 mmol, 5.2 eq.) was added to 4-(3,5-dimethylisoxazol-4-yl)-2-nitro-*N*-(2-(piperidin-1-yl)ethyl)aniline **238** (80.0 mg, 0.232 mmol, 1.0 eq.) in EtOH (1.20 mL). H_2O (1.20 mL) was added then the reaction mixture was stirred at 80 °C for 10 min. The reaction mixture was cooled to rt then the solvent was evaporated *in vacuo.* The residue was partitioned between water and ethyl acetate. The aqueous layer was separated then extracted with ethyl acetate (3 × 5 mL). The combined organic layers were dried over $MgSO_{4\ (s)}$, filtered, then the filtrate was concentrated *in vacuo*. 3-(3-Cyano-4-methylphenyl)propanoic acid **158** (28.4 mg, 0.150 mmol, 1.0 eq.), HATU (57.2 mg, 0.150 mmol, 1.0 eq.) and DIPEA (52.4 µL, 0.301 mmol, 2.0 eq.) were combined in anhydrous DMF (1.0 mL). 4-(3,5-Dimethylisoxazol-4-yl)-N^1-(2-(piperidin-1-yl)ethyl)benzene-1,2-diamine (52.0 mg, 0.165 mmol, 1.1 eq.) in anhydrous DMF (1.0 mL) was added. The reaction mixture was stirred at rt for 3 h. The solvent was evaporated *in vacuo.* The residue was re-dissolved in ethyl acetate (10 mL) and water (5 mL) was added. The organic layer was separated then the aqueous layer was extracted with ethyl acetate (3 × 10 mL). The combined organic layers were washed with 10% w/v $LiCl_{(aq)}$ (3 × 10 mL), dried over $MgSO_{4\ (s)}$, filtered, then the filtrate was concentrated *in vacuo*. The residue was purified by flash column chromatography eluting with CH_2Cl_2 : methanol (1:0 to 98:2) to yield 3-(3-cyano-4-methylphenyl)-*N*-(5-(3,5-dimethylisoxazol-4-yl)-2-((2-(piperidin-1-yl)ethyl)amino)phenyl)propanamide **239** (68 mg, 93%) as a brown oil: R_f 0.25 (CH_2Cl_2 : methanol, 9:1); ^{1}H NMR (400 MHz, $CDCl_3$) δ 8.12 (1H, *br* s, $C^{1'}$N-H), 7.48 (1H, d, *J* 2.0, $C^{2''}$-H), 7.37 (1H, dd, *J* 8.0, 2.0, $C^{6''}$-H), 7.19 (1H, d, *J* 8.0, $C^{5''}$-H), 7.16 (1H, d, *J* 2.0, $C^{3'}$-H), 6.98 (1H, dd, *J* 8.3, 2.0, $C^{5'}$-H), 6.72 (1H, d, *J* 8.3, $C^{6'}$-H), 3.42 (2H, t, *J* 5.8, $C^{1'''}$-H_2), 3.01 (2H, t, *J* 7.6, C^{3iv}-H_2),

2.97-2.88 (2H, m, C^{2iv}-H_2), 2.86-2.72 (4H, m, C^{8}-H_2, C^{12}-H_2), 2.45 (3H, s, C^{14}-H_3), 2.35 (3H, s, C^{6}-H_3), 2.21 (3H, s, C^{7}-H_3), 1.82-1.65 (4H, m, C^{9}-H_2, C^{11}-H_2), 1.64-1.46 (2H, m, C^{10}-H_2); LRMS *m/z* (ESI^+) 486 ($[M+H]^+$, 100%).

5-(2-(5-(3,5-Dimethylisoxazol-4-yl)-1-(2-(piperidin-1-yl)ethyl)-1*H*-benzo[*d*]imidazol-2-yl)ethyl)-2-methylbenzonitrile 180

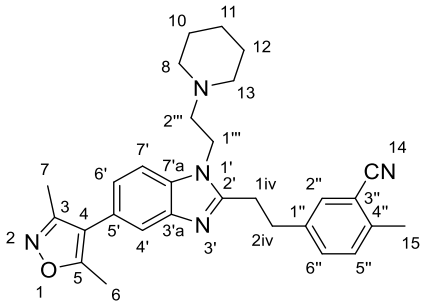

3-(3-Cyano-4-methylphenyl)-*N*-(5-(3,5-dimethylisoxazol-4-yl)-2-((2-(piperidin-1-yl)ethyl)amino)phenyl)propanamide **239** (55.0 mg, 0.174 mmol, 1.0 eq.) was refluxed in toluene (1.0 mL) in a microwave vial containing 3 Å molecular sieves for 48 h. The reaction mixture was cooled to rt, filtered, and then the solvent evaporated *in vacuo*. The residue was purified by flash column chromatography eluting with eluting with ethyl acetate : methanol (1:0 to 9:1) to yield 5-(2-(5-(3,5-dimethylisoxazol-4-yl)-1-(2-(piperidin-1-yl)ethyl)-1*H*-benzo[*d*]imidazol-2-yl)ethyl)-2-methylbenzonitrile **180** (37 mg, 46%) as a yellow oil: R_f 0.26 (CH_2Cl_2 : MeOH, 9:1); ν_{max} (thin film)/ cm^{-1} 2227 (C≡N, w), 1635 (C=C, w), 1510 (C-H, w), 1445 (C-H, m), 1321 (C-N, m), 1250 (C-N, m); ^{1}H NMR (600 MHz, $CDCl_3$) δ 7.61 (1H, dd, *J* 1.6, 0.7, $C^{4'}$-H), 7.50 (1H, d, *J* 1.9, $C^{2"}$-H), 7.38 (1H, dd, *J* 7.9, 1.9, $C^{6"}$-H), 7.36 (1H, d, *J* 8.2, $C^{7'}$-H), 7.24 (1H, d, *J* 7.9, $C^{5"}$-H), 7.12 (1H, dd, *J* 8.2, 1.6, $C^{6'}$-H), 4.17 (2H, t, *J* 6.8, $C^{1'''}$-H_2), 3.34-3.28 (2H, m, C^{2iv}-H_2), 3.22-3.16 (2H, m, C^{1iv}-H_2), 2.58 (2H, t, *J* 6.8, $C^{2'''}$-H_2), 2.51 (3H, s, C^{15}-H_3), 2.43-2.40 (4H, m, C^{8}-H_2, C^{13}-H_2), 2.42 (3H, s, C^{6}-H_3), 2.29 (3H, s, C^{7}-H_3), 1.55 (4H, p, *J* 5.6, C^{10}-H_2, C^{12}-H_2), 1.44 (2H, q, *J* 5.6, C^{11}-H_2); ^{13}C NMR (151 MHz, $CDCl_3$) δ 165.0 (C^5), 159.0 (C^3), 154.6 ($C^{2'}$), 143.0 ($C^{3'a}$), 140.0 ($C^{4"}$), 139.3 ($C^{1"}$), 134.4 ($C^{7'a}$), 133.0 ($C^{6"}$), 132.1 ($C^{2"}$), 130.6 ($C^{5"}$), 124.2 ($C^{5'}$), 123.6 ($C^{6'}$), 119.9 ($C^{4'}$), 118.1 (C^{14}), 117.1 (C^4), 112.9 ($C^{3"}$), 109.5 ($C^{7'}$), 58.1 ($C^{2'''}$), 55.2 (C^8, C^{13}), 41.9 ($C^{1'''}$), 32.5 (C^{2iv}), 28.9 (C^{1iv}), 25.9 (C^{10}, C^{12}), 24.1 (C^{11}), 20.1 (C^{15}), 11.6 (C^6), 10.9 (C^7); LRMS *m/z* (ESI^+)

468 ([M+H]$^+$, 100%); HRMS *m/z* (ESI$^+$) [Found: 468.2735, $C_{29}H_{33}N_5O$ requires [M+H]$^+$ 468.2758)]; Analytical HPLC (RP, *Method 3*) rt 6.8 min, purity 100%.

_N_-(2-(4,4-Difluoropiperidin-1-yl)ethyl)-4-(3,5-dimethylisoxazol-4-yl)-2-nitroaniline 240

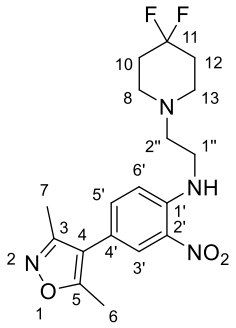

4-(4-Fluoro-3-nitrophenyl)-3,5-dimethylisoxazole **74** (100 mg, 0.423 mmol, 1.0 eq.) was dissolved in anhydrous DMF (2.0 mL). 2-(4,4-Difluoropiperidin-1-yl)ethan-1-amine (139 mg, 0.847 mmol, 2.0 eq.) and DIPEA (184 µL, 1.058 mmol, 2.5 eq.) were added. The reaction mixture was stirred at 80 °C for 2 h. The solvent was evaporated *in vacuo* then the residue was partitioned between ethyl acetate and water. The aqueous layer was extracted with ethyl acetate (3 × 15 mL). The combined organic layers were washed with 10% w/v LiCl $_{(aq)}$ (2 × 10 mL), then dried over $MgSO_{4\ (s)}$, filtered, then the filtrate was concentrated *in vacuo*. The residue was purified by flash column chromatography eluting with petroleum ether : ethyl acetate (1:0 to 0:1) to yield *N*-(2-(4,4-difluoropiperidin-1-yl)ethyl)-4-(3,5-dimethylisoxazol-4-yl)-2-nitroaniline **240** (138 mg, 85%) as an orange oil: R_f 0.42 (ethyl acetate : petroleum ether, 1:1); ν_{max} (thin film)/ cm^{-1} 3369 (N-H, m, *br*), 1622 (N-H, s), 1560 (N-O, s), 1530 (N-O, s), 1354 (N-O, s), 1224 (C-N, m), 1100 (C-F, s); ^{1}H NMR (600 MHz, $CDCl_3$) δ 8.57 (1H, t, *J* 4.5, N-H), 8.08 (1H, d, *J* 2.1, C$^{3'}$-H), 7.32 (1H, dd, *J* 8.8, 2.2, C$^{5'}$-H), 6.91 (1H, d, *J* 8.8, C$^{6'}$-H), 3.40 (2H, td, *J* 6.1, 4.6, C$^{1"}$-H_2), 2.81 (2H, t, *J* 6.1, C$^{2"}$-H_2), 2.70-2.60 (4H, m, C^8-H_2, C^{13}-H_2), 2.40 (3H, s, C^6-H_3), 2.26 (3H, s, C^7-H_3), 2.06 (4H, ddd, *J* 19.3, 11.8, 5.7, C^{10}-H_2, C^{12}-H_2); ^{13}C NMR (151 MHz, $CDCl_3$) δ 165.3 (C^5), 158.6 (C^3), 144.4 (C$^{1'}$), 136.8 (C$^{5'}$), 132.0 (C$^{2'}$), 127.1 (C$^{3'}$), 121.9 (t, ^1J 241.7, C^{11}), 117.4 (C^4), 114.9 (C$^{4'}$), 114.7 (C$^{6'}$), 54.7 (C$^{2"}$), 49.7 (t, ^3J 5.4, C^8, C^{13}), 40.0 (C$^{1"}$), 34.1 (t, ^2J 23.2, C^{10}, C^{12}), 11.6 (C^6), 10.8 (C^7); ^{19}F NMR (565 MHz, $CDCl_3$) δ -98.1 (2F, *br* s, C^{11}-F_2); LRMS *m/z* (ESI$^+$) 381 ([M+H]$^+$, 100%); HRMS *m/z* (ESI$^+$)

[Found: 381.1749, $C_{18}H_{22}F_2N_4O_3$ requires $[M+H]^+$ 381.1733)]; Analytical HPLC (RP, *Method 2*) rt 7.5 min, purity 100%.

3-(3-Cyano-4-methylphenyl)-*N*-(2-((2-(4,4-difluoropiperidin-1-yl)ethyl)amino)-5-(3,5-dimethylisoxazol-4-yl)phenyl)propanamide 241

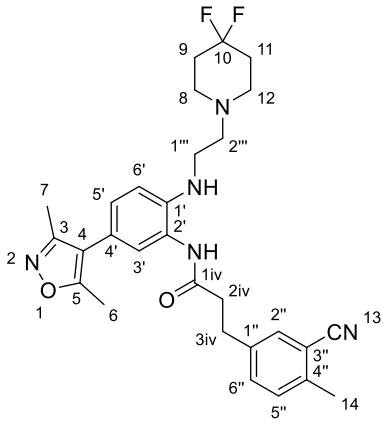

$Na_2S_2O_4$ (190 mg, 1.09 mmol, 5.2 eq.) was added to *N*-(2-(4,4-difluoropiperidin-1-yl)ethyl)-4-(3,5-dimethylisoxazol-4-yl)-2-nitroaniline **240** (80.0 mg, 0.210 mmol, 1.0 eq.) in EtOH (1.10 mL). H_2O (1.10 mL) was added then the reaction mixture was stirred at 80 °C for 10 min. The reaction mixture was cooled to rt then the solvent was evaporated *in vacuo.* The residue was partitioned between water and ethyl acetate. The aqueous layer was separated then extracted with ethyl acetate (3 × 5 mL). The combined organic layers were dried over $MgSO_{4\,(s)}$, filtered, then the filtrate was concentrated *in vacuo*. 3-(3-Cyano-4-methylphenyl)propanoic acid **158** (28.4 mg, 0.150 mmol, 1.0 eq.), HATU (57.2 mg, 0.150 mmol, 1.0 eq.) and DIPEA (52.4 µL, 0.301 mmol, 2.0 eq.) were combined in anhydrous DMF (1.0 mL). N^1-(2-(4,4-Difluoropiperidin-1-yl)ethyl)-4-(3,5-dimethylisoxazol-4-yl)benzene-1,2-diamine (58.0 mg, 0.166 mmol, 1.1 eq.) in anhydrous DMF (1.0 mL) was added. The reaction mixture was stirred at rt for 3 h. The solvent was evaporated *in vacuo.* The residue was re-dissolved in ethyl acetate (10 mL) and water (5 mL) was added. The organic layer was separated then the aqueous layer was extracted with ethyl acetate (3 × 10 mL). The combined organic layers were washed with 10% w/v $LiCl_{(aq)}$ (3 × 10 mL), dried over $MgSO_{4\,(s)}$, filtered, then the filtrate was concentrated *in vacuo*. The residue was purified by flash column chromatography eluting with CH_2Cl_2 : methanol (1:0 to 98:2) to yield 3-(3-cyano-4-methylphenyl)-*N*-(2-((2-(4,4-difluoropiperidin-1-yl)ethyl)amino)-5-(3,5-dimethylisoxazol-4-yl)phenyl)propenamide

241 (69 mg, 88%) as an off-white solid: R_f 0.23 (CH_2Cl_2 : methanol, 9:1); ^{1}H NMR (400 MHz, $CDCl_3$) δ 7.50 (1H, d, *J* 1.9, $C^{2"}$-H), 7.39 (1H, dd, *J* 8.0, 1.9, $C^{6"}$-H), 7.24 (1H, *br* s, $C^{1'}$N-H), 7.10 (1H, d, *J* 2.0, $C^{3'}$-H), 7.06-7.00 (2H, m, $C^{5'}$-H, $C^{5"}$-H), 6.79 (1H, d, *J* 8.4, $C^{6'}$-H), 3.19 (2H, m, $C^{1'''}$-H_2), 3.07 (2H, t, *J* 7.5, C^{3iv}-H_2), 2.75-2.67 (4H, m, $C^{2'''}$-H_2, C^{2iv}-H_2), 2.62-2.56 (4H, m, C^8-H_2, C^{12}-H_2), 2.50 (3H, s, C^{14}-H_3), 2.37 (3H, s, C^6-H_3), 2.24 (3H, s, C^7-H_3), 2.08-1.96 (4H, m, C^9-H_2, C^{11}-H_2); ^{19}F NMR (376 MHz, $CDCl_3$) δ -98.1 (2F, *br* s, C^{10}-F_2); LRMS *m/z* (ESI^+) 522 ($[M+H]^+$, 100%).

5-(2-(1-(2-(4,4-Difluoropiperidin-1-yl)ethyl)-5-(3,5-dimethylisoxazol-4-yl)-1*H*-benzo[*d*]imidazol-2-yl)ethyl)-2-methylbenzonitrile 182

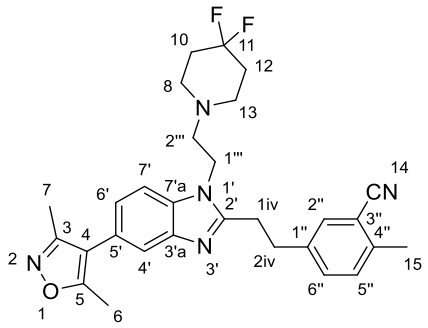

3-(3-Cyano-4-methylphenyl)-*N*-(2-((2-(4,4-difluoropiperidin-1-yl)ethyl)amino)-5-(3,5-dimethylisoxazol-4-yl)phenyl)propenamide **241** (60.0 mg, 0.115 mmol, 1.0 eq.) was refluxed in toluene (1.0 mL) in a microwave vial containing 3 Å molecular sieves for 24 h. The reaction mixture was cooled to rt, filtered, and then the solvent evaporated *in vacuo*. The residue was purified by flash column chromatography eluting with eluting with CH_2Cl_2 : methanol (1:0 to 9:1) to yield 5-(2-(1-(2-(4,4-difluoropiperidin-1-yl)ethyl)-5-(3,5-dimethylisoxazol-4-yl)-1*H*-benzo[*d*]imidazol-2-yl)ethyl)-2-methylbenzonitrile **182** (50 mg, 86%) as an off-white solid: R_f 0.24 (CH_2Cl_2 : methanol, 9:1); m.p. 218-220 °C (MeOH); ν_{max} (thin film)/ cm^{-1} 2227 (C≡N, w), 1654 (C=C, w), 1536 (C-H, w), 1445 (C-H, m), 1263 (C-N, s), 1098 (C-F, s); ^{1}H NMR (600 MHz, DMSO-d_6) δ 9.34 (1H, s, N-H), 7.65 (1H, d, *J* 1.9, $C^{2"}$-H), 7.50 (1H, dd, *J* 7.9, 1.9, $C^{6"}$-H), 7.39 (1H, d, *J* 7.9, $C^{5"}$-H), 7.05 (1H, dd, *J* 8.3, 2.1, $C^{6'}$-H), 6.94 (1H, d, *J* 2.1, $C^{4'}$-H), 6.74 (1H, d, *J* 8.3, $C^{7'}$-H), 5.00 (1H, t *J* 5.3, N-H), 3.16 (2H, q, *J* 6.1, $C^{1'''}$-H_2), 2.94 (2H, t, *J* 7.5, C^{2iv}-H_2), 2.66 (2H, t, *J* 7.5, C^{1iv}-H_2), 2.61 (2H, t, *J* 6.4, $C^{2'''}$-H_2), 2.56-2.51 (4H, m, C^8-H_2, C^{13}-H_2), 2.43 (3H, s, C^{15}-H_3), 2.35 (3H, s, C^6-H_3), 2.17 (3H, s, C^7-H_3), 2.02-1.92 (4H, m, C^{10}-H_2, C^{12}-H_2),; ^{13}C NMR (151 MHz, DMSO-d_6) δ 170.4 ($C^{2'}$), 164.0 (C^5), 158.1 (C^3),

142.4 ($C^{7'a}$), 139.7 ($C^{1''}$), 139.1 ($C^{4''}$), 133.4 ($C^{6''}$), 132.0 ($C^{2''}$), 130.4 ($C^{5''}$), 127.2 ($C^{6'}$), 126.5 ($C^{4'}$), 122.8 (t, *J* 248.1, C^{11}), 123.6 ($C^{3'a}$), 118.1 (C^{14}), 116.9 ($C^{5'}$), 115.7 (C^{4}), 111.6 ($C^{7'}$), 111.5 ($C^{3''}$), 55.0 ($C^{2'''}$), 49.3 (t, *J* 5.2, C^{8}, C^{13}), 39.9 ($C^{1'''}$), 36.7 (C^{1iv}), 33.5 (t, *J* 22.5, C^{10}, C^{12}), 30.0 (C^{2iv}), 19.4 (C^{15}), 11.2 (C^{6}), 10.5 (C^{7}); ^{19}F NMR (376 MHz, DMSO-*d*$_6$) δ -97.9 (2F, *br* s, C^{11}-F_2); LRMS *m/z* (ESI^+) 522 ($[M+NH_4+H]^{2+}$, 100%); HRMS *m/z* (ESI^+) [Found: 504.2583, $C_{29}H_{32}F_2N_5O$ requires $[M+H]^+$ 504.2569)]; Analytical HPLC (RP, *Method 3*) rt 7.7 min, purity 100%.

4-(3,5-Dimethylisoxazol-4-yl)-2-nitro-*N*-(2-(tetrahydro-2*H*-pyran-4-yl)ethyl)aniline 242

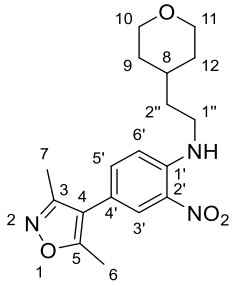

4-(4-Fluoro-3-nitrophenyl)-3,5-dimethylisoxazole **74** (100 mg, 0.423 mmol, 1.0 eq.) was dissolved in anhydrous DMF (2.0 mL). 2-(Tetrahydro-2*H*-pyran-4-yl)ethanamine hydrochloride (140 mg, 0.847 mmol, 2.0 eq.) and DIPEA (184 µL, 1.06 mmol, 2.5 eq.) were added. The reaction mixture was stirred at 80 °C for 2 h. The reaction mixture was cooled to rt. The solvent was evaporated *in vacuo.* The residue was dissolved in ethyl acetate and the solution was partitioned with the addition of water. The aqueous layer was separated then extracted with ethyl acetate (3 × 10 mL). The combined organic layers were dried over $MgSO_{4\,(s)}$, filtered, then the filtrate was concentrated *in vacuo*. The residue was purified by flash column chromatography eluting with petroleum ether : ethyl acetate (7:3 to 1:1) to yield 4-(3,5-dimethylisoxazol-4-yl)-2-nitro-*N*-(2-(tetrahydro-2*H*-pyran-4-yl)ethyl)aniline **242** (129 mg, 88%) as an orange solid: R_f 0.33 (petroleum ether : ethyl acetate, 1:1); ν_{max} (thin film)/ cm^{-1} 2980 (N-H, m), 1622 (N-H, m), 1565 (C=C, m), 1530 (N-O, s), 1450 (C-H, m), 1261 (N-O, s), 1240 (C-O, s), 1163 (C-O, s); ^{1}H NMR (600 MHz, $CDCl_3$) δ 8.11-8.03 (2H, m, N-H, $C^{3'}$-H), 7.34 (1H, ddd, *J* 8.8, 2.2, 0.6, $C^{5'}$-H), 6.93 (1H, d, *J* 8.8, $C^{6'}$-H), 4.02-3.94 (2H, m, C^{10}-H_a, C^{11}-H_a), 3.46-3.35 (4H, m, $C^{1''}$-H_2, C^{10}-H_b, C^{11}-H_b), 2.40 (3H, s, C^{6}-H_3), 2.26 (3H, s, C^{7}-H_3), 1.78-1.64 (5H, m, $C^{2''}$-H_2, C^{8}-H, C^{9}-H_a, C^{12}-H_a), 1.45-1.35 (2H, m, C^{9}-H_b, C^{12}-H_b); ^{13}C NMR (151 MHz, $CDCl_3$)

δ 165.4 (C^5), 158.6 (C^3), 144.6 ($C^{1'}$), 136.9 ($C^{5'}$), 131.8 ($C^{2'}$), 127.1 ($C^{3'}$), 117.5 ($C^{4'}$), 114.9 (C^4), 114.3 ($C^{6'}$), 67.8 (C^{10}, C^{11}), 40.3 ($C^{1''}$), 35.9 ($C^{2''}$), 32.9 (C^8, C^9), 32.8 (C^8), 11.6 (C^6), 10.8 (C^7); LRMS *m/z* (ESI^+) 346 ($[M+H]^+$, 100%); HRMS *m/z* (ESI^+) [Found: 346.1766, $C_{18}H_{23}N_3O_4$ requires $[M+H]^+$ 346.1761)]; Analytical HPLC (RP, *Method 3*) rt 10.3 min, purity 100%.

3-(3-Cyano-4-methylphenyl)-*N*-(5-(3,5-dimethylisoxazol-4-yl)-2-((2-(tetrahydro-2*H*-pyran-4-yl)ethyl)amino)phenyl)propenamide 243

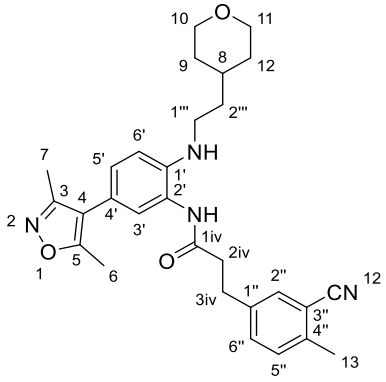

$Na_2S_2O_4$ (210 mg, 1.20 mmol, 5.2 eq.) was added to 4-(3,5-dimethylisoxazol-4-yl)-2-nitro-*N*-(2-(tetrahydro-2*H*-pyran-4-yl)ethyl)aniline **242** (80.0 mg, 0.232 mmol, 1.0 eq.) in EtOH (1.20 mL). H_2O (1.20 mL) was added and the reaction mixture was stirred at 80 °C for 10 min. The reaction mixture was cooled to rt and the solvent was evaporated *in vacuo.* The residue was partitioned between water and ethyl acetate. The aqueous layer was separated then extracted with ethyl acetate (3 × 5 mL). The combined organic layers were dried over $MgSO_{4\,(s)}$, filtered, then the filtrate was concentrated *in vacuo*. 3-(3-Cyano-4-methylphenyl)propanoic acid **158** (45.8 mg, 0.242 mmol, 1.0 eq.), HATU (92.1 mg, 0.242 mmol, 1.0 eq.) and DIPEA (84.3 µL, 0.484 mmol, 2.0 eq.) were combined in anhydrous DMF (1.0 mL). 4-(3,5-Dimethylisoxazol-4-yl)-N^1-(2-(tetrahydro-2*H*-pyran-4-yl)ethyl)benzene-1,2-diamine (84.0 mg, 0.266 mmol, 1.1 eq.) in anhydrous DMF (1.0 mL) was added. The reaction mixture was stirred at rt for 3 h. The solvent was evaporated *in vacuo.* The residue was re-dissolved in ethyl acetate (10 mL) and water (5 mL) was added. The organic layer was separated then the aqueous layer was extracted with ethyl acetate (3 × 10 mL). The combined organic layers were washed with 10% w/v $LiCl_{(aq)}$ (3 × 10 mL), dried over $MgSO_{4\,(s)}$, filtered, then the filtrate was concentrated *in vacuo*. The residue was purified by flash column chromatography eluting

with petroleum ether : ethyl acetate (1:1 to 0:1) to yield 3-(3-cyano-4-methylphenyl)-*N*-(5-(3,5-dimethylisoxazol-4-yl)-2-((2-(tetrahydro-2*H*-pyran-4-yl)ethyl)amino)phenyl)propenamide **243** (77 mg, 65%) as a light yellow oil: R_f 0.48 (petroleum ether : ethyl acetate, 1:4); ^{1}H NMR (400 MHz, $CDCl_3$) δ 7.49 (1H, d, *J* 2.0, $C^{2"}$-H), 7.42-7.36 (1H, dd, *J* 8.0, 2.0, $C^{6"}$-H), 7.25 (1H, d, *J* 8.0, $C^{5"}$-H), 7.07-6.98 (3H, m, $C^{1'}$N-H, $C^{3'}$-H, $C^{5'}$-H), 6.79 (1H, d, *J* 8.3, $C^{6'}$-H), 4.02-3.91 (2H, m, C^{10}-H_a, C^{11}-H_a), 3.47-3.33 (2H, m, C^{10}-H_b, C^{11}-H_b), 3.19-3.11 (2H, m, $C^{1'''}$-H_2), 3.07 (2H, t, *J* 7.4, C^{3iv}-H_2), 2.73 (2H, t, *J* 7.4, C^{2iv}-H_2), 2.50 (3H, s, C^{13}-H_3), 2.36 (3H, s, C^{6}-H_3), 2.23 (3H, s, C^{7}-H_3), 1.70-1.50 (5H, m, C^{8}-H, C^{9}-H_2, C^{12}-H_2), 1.44-1.29 (2H, m, $C^{2'''}$-H_2); LRMS *m/z* (ESI^+) 487 ($[M+H]^+$, 100%).

5-(2-(5-(3,5-Dimethylisoxazol-4-yl)-1-(2-(tetrahydro-2*H*-pyran-4-yl)ethyl)-1*H*-benzo[*d*]imidazol-2-yl)ethyl)-2-methylbenzonitrile 186

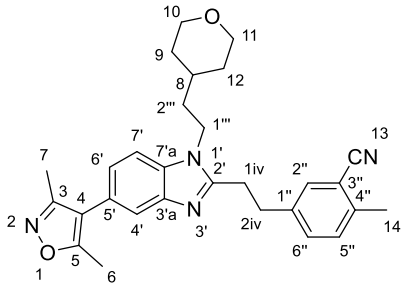

3-(3-Cyano-4-methylphenyl)-*N*-(5-(3,5-dimethylisoxazol-4-yl)-2-((2-(tetrahydro-2*H*-pyran-4-yl)ethyl)amino)phenyl)propenamide **243** (50.0 mg, 0.103 mmol, 1.0 eq.) was refluxed in toluene (1.0 mL) in a microwave vial containing 3 Å molecular sieves for 24 h. The reaction mixture was cooled to rt, filtered, and then the solvent evaporated *in vacuo*. The residue was purified by flash column chromatography eluting with eluting with petroleum ether : ethyl acetate (1:1 to 0:1) to yield 5-(2-(5-(3,5-dimethylisoxazol-4-yl)-1-(2-(tetrahydro-2*H*-pyran-4-yl)ethyl)-1*H*-benzo[*d*]imidazol-2-yl)ethyl)-2-methylbenzonitrile **186** (35 mg, 48%) as a yellow oil: R_f 0.56 (EtOAc); m.p. 120-122 °C (MeOH); ν_{max} (thin film)/ cm^{-1} 2228 (C≡N, w), 1619 (C=C, w), 1508 (C-H, w), 1446 (C-H, m), 1322 (C-N, m), 1239 (C-O, s), 1094 (C-O, s), 911 (C=C, m); ^{1}H NMR (600 MHz, $CDCl_3$) δ 7.63 (1H, dd, *J* 1.5, 0.6, $C^{4'}$-H), 7.49 (1H, d, *J* 1.9, $C^{2"}$-H), 7.38 (1H, dd, *J* 7.9, 1.9, $C^{6"}$-H), 7.33 (1H, dd, *J* 8.3, 0.6, $C^{7'}$-H), 7.25 (1H, d, *J* 7.9, $C^{5"}$-H), 7.14 (1H, dd, *J* 8.3, 1.5, $C^{6'}$-H), 4.11-4.05 (2H, m, $C^{1'''}$-H_2), 4.02-3.95 (2H, m, C^{10}-H_a, C^{11}-H_a), 3.39 (2H, td, *J* 11.8, 1.9, C^{10}-H_b, C^{11}-H_b), 3.34-3.29 (2H, m, C^{2iv}-H_2), 3.16-3.10 (2H, m,

C^{1iv}-H_2), 2.52 (3H, s, C^{14}-H_3), 2.42 (3H, s, C^6-H_3), 2.29 (3H, s, C^7-H_3), 1.71-1.58 (4H, m, $C^{2'''}$-H_2, C^8-H, C^9-H_a, C^{12}-H_a), 1.44-1.34 (2H, m, C^9-H_b, C^{12}-H_b); ^{13}C NMR (151 MHz, $CDCl_3$) δ 165.2 (C^5), 159.1 (C^3), 154.0 ($C^{2'}$), 142.9 ($C^{3'a}$), 140.3 ($C^{4''}$), 139.2 ($C^{1''}$), 134.3 ($C^{7'a}$), 133.1 ($C^{6''}$), 132.2 ($C^{2''}$), 130.8 ($C^{5''}$), 124.6 ($C^{5'}$), 123.9 ($C^{6'}$), 120.1 ($C^{4'}$), 118.2 (C^{13}), 117.2 (C^4), 113.1 ($C^{3''}$), 109.5 ($C^{7'}$), 67.8 (C^{10}, C^{11}), 41.4 ($C^{1'''}$), 37.0 ($C^{2'''}$), 33.1 (C^8), 33.0 (C^9, C^{12}), 32.7 (C^{2iv}), 29.1 (C^{1iv}), 20.9 (C^{14}), 11.7 (C^6), 11.0 (C^7); LRMS *m/z* (ESI^+) 469 ($[M+H]^+$, 100%); HRMS *m/z* (ESI^+) [Found: 469.2598, $C_{29}H_{33}N_4O_2$ requires $[M+H]^+$ 469.2606)]; Analytical HPLC (RP, *Method 3*) rt 8.0 min, purity 96%.

4-(3,5-Dimethylisoxazol-4-yl)-*N*-(2-methoxyethyl)-2-nitroaniline 244

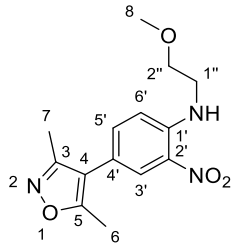

4-(4-Fluoro-3-nitrophenyl)-3,5-dimethylisoxazole **74** (100 mg, 0.423 mmol, 1.0 eq.) was dissolved in anhydrous DMF (2.0 mL). 2-Methoxyethan-1-amine (73.6 µL, 0.847 mmol, 2.0 eq.) and DIPEA (184 µL, 1.06 mmol, 2.5 eq.) were added. The reaction mixture was stirred at 60 °C for 2.5 h. The reaction was cooled to rt and the solvent was evaporated *in vacuo.* The residue was partitioned between ethyl acetate and water. The aqueous layer was extracted with ethyl acetate (3 × 15 mL). The combined organic layers were washed with 10% w/v LiCl $_{(aq)}$ (3 × 10 mL), then dried over $MgSO_{4\ (s)}$, filtered, then the filtrate was concentrated *in vacuo*. The residue was purified by flash column chromatography eluting with petroleum ether : ethyl acetate (1:0 to 7:3) to yield 4-(3,5-dimethylisoxazol-4-yl)-*N*-(2-methoxyethyl)-2-nitroaniline **244** (120 mg, 97%) as an orange solid: R_f 0.46 (ethyl acetate : petroleum ether, 1:1); m.p. 75-76 °C; ν_{max} (thin film)/ cm^{-1} 3379 (N-H, m), 2933 (C-H, m), 1624 (C=C, m), 1565 (N-H, m), 1531 (N-O, s), 1355 (N-O, s), 1260 (C-O, s), 1241 (C-O, s), 1196 (C-N, m); ^{1}H NMR (600 MHz, $CDCl_3$) δ 8.26 (1H, t, *J* 5.3, N-H), 8.08 (1H, d, *J* 2.2, $C^{3'}$-H), 7.34 (1H, dd, *J* 8.8, 2.1, $C^{5'}$-H), 6.96 (1H, d, *J* 8.8, $C^{6'}$-H), 3.70 (2H, t, *J* 5.4, $C^{2''}$-H_2), 3.54 (2H, dd, *J* 5.4, 5.3, $C^{1''}$-H_2), 3.45 (3H, s, C^8-H_3), 2.40 (3H, s, C^6-H_3), 2.26 (3H, s, C^7-H_3); ^{13}C NMR (151 MHz, $CDCl_3$) δ 165.5 (C^5), 158.7 (C^3), 144.8 ($C^{1'}$), 136.9 ($C^{5'}$), 132.2 ($C^{2'}$), 127.2 ($C^{3'}$), 117.7 ($C^{4'}$), 115.0 (C^4), 114.6 ($C^{6'}$), 70.6 ($C^{2''}$), 59.3 (C^8), 43.0 ($C^{1''}$), 11.7 (C^6), 10.9 (C^7); LRMS *m/z* (ESI^+) 292 ($[M+H]^+$,

100%); HRMS *m/z* (ESI^+) [Found: 292.1305, $C_{14}H_{16}N_3O_4$ requires $[M+H]^+$ 292.1292)]; Analytical HPLC (RP, *Method 3*) rt 9.6 min, purity 100%.

3-(3-Cyano-4-methylphenyl)-*N*-(5-(3,5-dimethylisoxazol-4-yl)-2-((2-methoxyethyl)amino)phenyl)propanamide 245

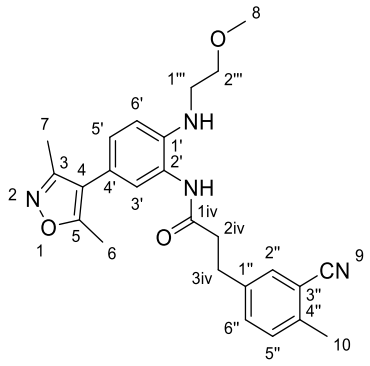

$Na_2S_2O_4$ (249 mg, 1.43 mmol, 5.2 eq.) was added to 4-(3,5-dimethylisoxazol-4-yl)-*N*-(2-methoxyethyl)-2-nitroaniline **244** (80.0 mg, 0.275 mmol, 1.0 eq.) in EtOH (1.40 mL). H_2O (1.40 mL) was added then the reaction mixture was stirred at 80 °C for 10 min. The reaction mixture was cooled to rt then the solvent was evaporated *in vacuo.* The residue was partitioned between water and ethyl acetate. The aqueous layer was separated then extracted with ethyl acetate (3 × 5 mL). The combined organic layers were dried over $MgSO_{4\,(s)}$, filtered, then the filtrate was concentrated *in vacuo*. 3-(3-Cyano-4-methylphenyl)propanoic acid **158** (29.6 mg, 0.157 mmol, 1.0 eq.), HATU (59.5 mg, 0.157 mmol, 1.0 eq.) and DIPEA (54.5 µL, 0.313 mmol, 2.0 eq.) were combined in anhydrous DMF (1.0 mL). 4-(3,5-Dimethylisoxazol-4-yl)-N^1-(2-methoxyethyl)benzene-1,2-diamine (45.0 mg, 0.172 mmol, 1.1 eq.) in anhydrous DMF (1.0 mL) was added. The reaction mixture was stirred at rt for 3 h. The solvent was evaporated *in vacuo.* The residue was re-dissolved in ethyl acetate (10 mL) and water (5 mL) was added. The organic layer was separated then the aqueous layer was extracted with ethyl acetate (3 × 10 mL). The combined organic layers were washed with 10% w/v $LiCl_{(aq)}$ (3 × 10 mL), dried over $MgSO_{4\,(s)}$, filtered, then the filtrate was concentrated *in vacuo*. The residue was purified by flash column chromatography eluting with CH_2Cl_2 : methanol (1:0 to 98:2) to yield 3-(3-cyano-4-methylphenyl)-*N*-(5-(3,5-dimethylisoxazol-4-yl)-2-((2-methoxyethyl)amino)phenyl)propanamide **245** (66 mg, 97%) as an off-white solid: R_f 0.48 (CH_2Cl_2 : methanol, 9:1); ^1H NMR (400 MHz, $CDCl_3$) δ 7.49 (1H, d, *J* 2.0,

$C^{2''}$-H), 7.39 (1H, dd, *J* 8.1, 2.0, $C^{6''}$-H), 7.37 (1H, d, *J* 2.1, $C^{3'}$-H), 7.24 (1H, d, *J* 8.1, $C^{5''}$-H), 6.99 (1H, dd, *J* 8.3, 2.1, $C^{5'}$-H), 6.84 (1H, d, *J* 8.3, $C^{6'}$-H), 3.59 (2H, t, *J* 5.1, $C^{2'''}$-H_2), 3.40 (3H, s, C^{8}-H_3), 3.26 (2H, t, *J* 5.1, $C^{1'''}$-H_2), 3.07 (2H, t, *J* 7.5, C^{2iv}-H_2), 2.72 (2H, t, *J* 7.5, C^{3iv}-H_2), 2.51 (3H, s, C^{10}-H_3), 2.39 (3H, s, C^{6}-H_3), 2.25 (3H, s, C^{7}-H_3); LRMS *m/z* (ESI^+) 433 ($[M+H]^+$, 100%).

5-(2-(5-(3,5-Dimethylisoxazol-4-yl)-1-(2-methoxyethyl)-1*H*-benzo[*d*]imidazol-2-yl)ethyl)-2-methylbenzonitrile 185

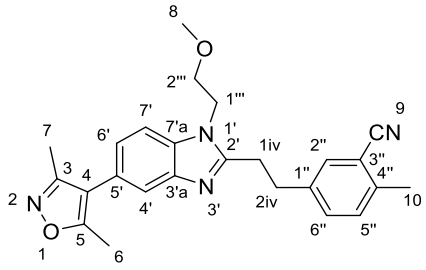

3-(3-Cyano-4-methylphenyl)-*N*-(5-(3,5-dimethylisoxazol-4-yl)-2-((2-methoxyethyl)amino)phenyl)propanamide **245** (49.0 mg, 0.113 mmol, 1.0 eq.) was refluxed in toluene (2.0 mL) in a microwave vial containing 3 Å molecular sieves for 24 h. The reaction mixture was cooled to rt, filtered, and then the solvent evaporated *in vacuo.* The residue was purified by flash column chromatography eluting with eluting with petroleum ether : ethyl acetate (1:1 to 0:1) to yield 5-(2-(5-(3,5-dimethylisoxazol-4-yl)-1-(2-methoxyethyl)-1*H*-benzo[*d*]imidazol-2-yl)ethyl)-2-methylbenzonitrile **185** (39 mg, 84%) as a light yellow solid: R_f 0.61 (ethyl acetate); m.p. 102-104 °C (EtOAc); ν_{max} (thin film)/ cm^{-1} 2227 (C≡N, w), 1635 (C=C, w), 1510 (C-H, w), 1451 (C-H, m), 1321 (C-N, m), 1117 (C-O, s), 912 (C=C, m); ^{1}H NMR (600 MHz, $CDCl_3$) δ 7.63 (1H, dd, *J* 1.6, 0.6, $C^{4'}$-H), 7.51 (1H, d, *J* 1.9, $C^{2''}$-H), 7.40 (1H, dd, *J* 7.9, 1.9, $C^{6''}$-H), 7.36 (1H, dd, *J* 8.3, 0.6, $C^{7'}$-H), 7.25 (1H, d, *J* 7.9, $C^{5''}$-H), 7.13 (1H, dd, *J* 8.3, 1.6, $C^{6'}$-H), 4.27 (2H, dd, *J* 5.2, 5.2, C^{2iv}-H_2), 3.67 (2H, dd, *J* 5.2, 5.2, C^{1iv}-H_2), 3.32-3.27 (5H, m, $C^{2'''}$-H_2, C^{8}-H_3), 3.23-3.18 (2H, m, $C^{1'''}$-H_2), 2.51 (3H, s, C^{10}-H_3), 2.42 (3H, s, C^{6}-H_3), 2.29 (3H, s, C^{7}-H_3); ^{13}C NMR (151 MHz, $CDCl_3$) δ 165.2 (C^5), 159.1 (C^3), 155.3 ($C^{2'}$), 142.8 ($C^{3'a}$), 140.1 ($C^{4''}$), 139.5 ($C^{1''}$), 134.4 ($C^{7'a}$), 133.2 ($C^{6''}$), 132.2 ($C^{2''}$), 130.6 ($C^{5''}$), 124.6 ($C^{5'}$), 123.8 ($C^{6'}$), 120.0 ($C^{4'}$), 118.3 (C^9), 117.2 (C^4), 113.0 ($C^{3''}$), 109.7 ($C^{7'}$), 70.8 (C^{1iv}), 59.3 (C^8), 44.1 (C^{2iv}), 32.6 ($C^{2'''}$), 29.0 ($C^{1'''}$), 20.1 (C^{10}), 11.7 (C^6), 11.0 (C^7); LRMS *m/z* (ESI^+) 415 ($[M+H]^+$, 100%); HRMS *m/z* (ESI^+) [Found: 415.2145,

$C_{25}H_{26}N_4O_2$ requires $[M+H]^+$ 415.2129)]; Analytical HPLC (RP, *Method 3*) rt 7.9 min, purity 100%.

(5-(3,5-Dimethylisoxazol-4-yl)-1-methyl-1*H*-benzo[*d*]imidazol-2-yl)methanol 169

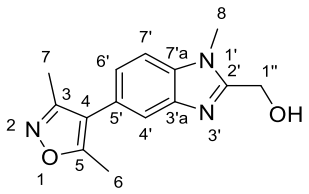

$Na_2S_2O_4$ (549 mg, 3.15 mmol, 5.2 eq.) was added to 4-(3,5-dimethylisoxazol-4-yl)-*N*-methyl-2-nitroaniline **76** (150 mg, 0.607 mmol, 1.0 eq.) in EtOH (3.15 mL). H_2O (3.15 mL) was added and the reaction mixture was stirred at 80 °C for 5 min. The reaction mixture was cooled to rt and the solvent was evaporated *in vacuo.* The residue was partitioned between water and ethyl acetate. The aqueous layer was separated then extracted with ethyl acetate (3 × 5 mL). The combined organic layers were dried over $MgSO_{4\,(s)}$, filtered, then the filtrate was concentrated *in vacuo*. Glycolic acid (69.3 mg, 0.911 mmol, 1.5 eq.) and 6 M $HCl_{(aq.)}$ (2.0 mL) were added. The reaction mixture was stirred at 80 °C for 17 h. The reaction mixture was cooled to rt and basified with 2 M $NaOH_{(aq.)}$. The reaction mixture was extracted with ethyl acetate (15 mL). The organics were washed with water (5 mL), dried over $MgSO_{4\,(s)}$, filtered, then the filtrate was concentrated *in vacuo*. The residue was purified by flash column chromatography eluting with eluting with CH_2Cl_2 : methanol (1:0 to 9:1) to yield (5-(3,5-dimethylisoxazol-4-yl)-1-methyl-1*H*-benzo[*d*]imidazol-2-yl)methanol **169** (116 mg, 74%) as an off-white solid: R_f 0.22 (CH_2Cl_2 : methanol, 9:1); m.p. 211-212 °C (MeOH); ν_{max} (thin film)/ cm^{-1} 3035 (O-H, w *br*), 1487 (C-H, m), 1425 (C-H, m), 1325 (O-H, m), 1029 (C-N, m); ^{1}H NMR (400 MHz, DMSO-d_6) δ 7.62 (1H, dd, *J* 8.4, 0.7, $C^{7'}$-H), 7.57 (1H, dd, *J* 1.6, 0.7, $C^{4'}$-H), 7.23 (1H, dd, *J* 8.4, 1.6, $C^{6'}$-H), 5.60 (1H, t, *J* 5.8, $C^{1"}$-OH), 4.73 (2H, d, *J* 5.8, $C^{1"}$-H_2), 3.86 (3H, s, C^8-H_3), 2.39 (3H, s, C^6-H_3), 2.22 (3H, s, C^7-H_3); ^{13}C NMR (101 MHz, DMSO-d_6) δ 164.6 (C^5), 158.3 (C^3), 154.8 ($C^{2'}$), 142.1 ($C^{7'a}$), 135.5 ($C^{3'a}$), 123.3 ($C^{6'}$), 122.9 ($C^{5'}$), 119.4 ($C^{7'}$), 116.7 (C^4), 110.3 ($C^{4'}$), 56.4 ($C^{1"}$), 30.0 (C^8), 11.3 (C^6), 10.5 (C^7); LRMS *m/z* (ESI^+) 258 ($[M+H]^+$, 100%); HRMS *m/z* (ESI^+) [Found: 258.1244, $C_{14}H_{15}N_3O_2$ requires $[M+H]^+$ 258.1237)]; Analytical HPLC (RP, *Method 3*) rt 5.5 min, purity 100%.

5-((5-(3,5-Dimethylisoxazol-4-yl)-1-methyl-1*H*-benzo[*d*]imidazol-2-yl)methoxy)-2-methylbenzonitrile 168

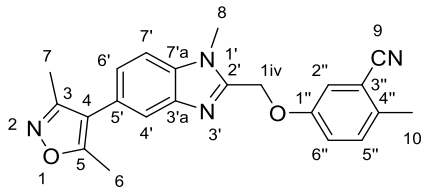

Tributylphosphine (77.7 μL, 0.311 mmol, 2.0 eq.) was added to a mixture of (5-(3,5-dimethylisoxazol-4-yl)-1-methyl-1*H*-benzo[*d*]imidazol-2-yl)methanol **169** (40.0 mg, 0.155 mmol, 1.0 eq.), 5-hydroxy-2-methylbenzonitrile (31.3 mg, 0.233 mmol, 1.5 eq.) and 1,1-(azodicarbonyl)dipiperidine (78.5 mg, 0.311 mmol, 2.0 eq.) in CH_2Cl_2 (1.0 mL). The reaction mixture was stirred at rt for 17 h. The reaction mixture was partitioned between CH_2Cl_2 and water. The organic layer was separated, dried over $MgSO_{4\,(s)}$, filtered, then the filtrate was concentrated *in vacuo*. The residue was purified by flash column chromatography eluting with eluting with petroleum ether : ethyl acetate (1:0 to 1:4) to yield 5-((5-(3,5-dimethylisoxazol-4-yl)-1-methyl-1*H*-benzo[*d*]imidazol-2-yl)methoxy)-2-methylbenzonitrile **168** (50 mg, 86%) as a colourless solid: R_f 0.48 (ethyl acetate : petroleum ether, 4:1); m.p. 180-181 °C (EtOAc); ν_{max} (thin film)/ cm^{-1} 2227 (C≡N, w), 1610 (C=C, w), 1502 (C-H, w), 1381 (C-N, m), 1252 (C-O, s), 1162 (C-O, s), 954 (C=C, s); ^{1}H NMR (600 MHz, $CDCl_3$) δ 7.67 (1H, dd, *J* 1.6, 0.7, $C^{4'}$-H), 7.45 (1H, dd, *J* 8.3, 0.7, $C^{7'}$-H), 7.30 (1H, d, *J* 2.6, $C^{2''}$-H), 7.29-7.20 (3H, m, $C^{6'}$-H, $C^{5''}$-H, $C^{6''}$-H), 5.41 (2H, s, C^{1iv}-H_2), 3.94 (3H, s, C^8-H_3), 2.47 (3H, s, C^{10}-H_3), 2.42 (3H, s, C^6-H_3), 2.29 (3H, s, C^7-H_3); ^{13}C NMR (151 MHz, $CDCl_3$) δ 165.2 (C^5), 159.0 (C^3), 155.8 ($C^{2'}$), 149.6 ($C^{1''}$), 142.6 ($C^{3'a}$), 135.7 ($C^{7'a}$), 135.3 ($C^{4''}$), 131.7 ($C^{5''}$), 124.9 ($C^{5'}$), 124.9 ($C^{6'}$), 120.9 ($C^{2''}$), 119.9 ($C^{4'}$), 118.4 ($C^{6''}$), 117.8 (C^9), 117.0 (C^4), 113.6 ($C^{3''}$), 110.0 ($C^{7'}$), 63.7 (C^{1iv}), 30.6 (C^8), 19.6 (C^{10}), 11.6 (C^6), 10.9 (C^7); LRMS *m/z* (ESI^+) 373 ($[M+H]^+$, 100%); HRMS *m/z* (ESI^+) [Found: 373.1671, $C_{22}H_{20}N_4O_2$ requires $[M+H]^+$ 373.1659)]; Analytical HPLC (RP, *Method 3*) rt 8.9 min, purity 100%.

***Tert*-butyl 4-(2-((4-(3,5-dimethylisoxazol-4-yl)-2-nitrophenyl)amino)ethyl)piperazine-1-carboxylate 246**

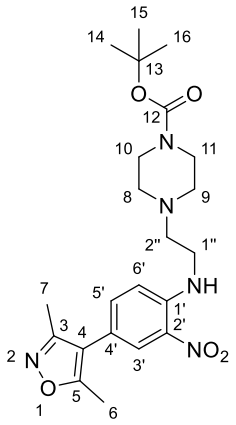

4-(4-Fluoro-3-nitrophenyl)-3,5-dimethylisoxazole **74** (500 mg, 2.12 mmol, 1.0 eq.) was dissolved in anhydrous DMF (3.0 mL). *Tert*-butyl 4-(2-aminoethyl)piperazine-1-carboxylate (971 mg, 4.23 mmol, 2.0 eq.) and DIPEA (1.84 mL, 10.6 mmol, 5.0 eq.) were added. The reaction mixture was stirred at rt for 45 min. The solvent was evaporated *in vacuo* then the residue was partitioned between ethyl acetate and water. The aqueous layer was extracted with ethyl acetate (3 × 15 mL). The combined organic layers were washed with 10% w/v LiCl $_{(aq)}$ (3 × 10 mL), then dried over $MgSO_{4\ (s)}$, filtered, then the filtrate was concentrated *in vacuo*. The residue was purified by flash column chromatography eluting with petroleum ether : ethyl acetate (1:0 to 0:1) to yield *tert*-butyl 4-(2-((4-(3,5-dimethylisoxazol-4-yl)-2-nitrophenyl)amino)ethyl)piperazine-1-carboxylate **246** (745 mg, 79%) as an orange solid: R_f 0.31 (petroleum ether : ethyl acetate, 1:1); m.p. 58-60 °C (ethyl acetate); ν_{max} (thin film)/ cm^{-1} 1695 (C=O, m), 1451 (N-O, s), 1246 (C-O, s); ^{1}H NMR (600 MHz, $CDCl_3$) δ 8.57 (1H, t, *J* 4.4, N-H), 8.07 (1H, d, *J* 2.1, $C^{3'}$-H), 7.33 (1H, dd, *J* 8.8, 2.1, $C^{5'}$-H), 6.90 (1H, d, *J* 8.8, $C^{6'}$-H), 3.52-3.46 (4H, m, C^{10}-H_2, C^{11}-H_2), 3.40 (2H, dd, *J* 6.1, 5.6, $C^{1''}$-H_2), 2.75 (2H, t, *J* 6.1, $C^{2''}$-H_2), 2.53-2.44 (4H, m, C^8-H_2, C^9-H_2), 2.39 (3H, s, C^6-H_3), 2.25 (3H, s, C^7-H_3), 1.46 (9H, s, $C^{13}(C\text{-}H_3)_3$); ^{13}C NMR (151 MHz, $CDCl_3$) δ 165.3 (C^5), 158.6 (C^3), 154.8 (C^{12}), 144.4 ($C^{1'}$), 136.8 ($C^{5'}$), 132.0 ($C^{2'}$), 127.0 ($C^{3'}$), 117.3 (C^4), 114.9 ($C^{4'}$), 114.7 ($C^{6'}$), 79.7 (C^{13}), 55.6 ($C^{2''}$), 52.5 (broadening from two rotamers, C^8, C^9), 44.2 (rot A: C^{10}, C^{11}), 43.2 (rot B: C^{10}, C^{11}), 39.6 ($C^{1''}$), 28.4 (C^{14}, C^{15}, C^{16}), 11.6 (C^6), 10.8 (C^7); LRMS *m/z* (ESI^+) 390 ($[M+H\ -Boc]^+$, 100%); HRMS *m/z* (ESI^+) [Found: 446.2408, $C_{22}H_{31}N_5O_5$ requires $[M+H]^+$ 446.2398)]; Analytical HPLC (RP, *Method 3*) rt 7.7 min, purity 100%.

6.3 General Biology Methods

Standard sterile techniques were followed thoroughly. Media and equipment were sterilised by autoclaving at 121 °C for 20 min. Solutions of IPTG, antibiotics and other labile compounds were sterilised by filtration through 0.22 µm filters (Millex®GP, Merck Millipore). Final concentrations of antibiotics, unless otherwise stated, were: Ampicillin 100 µg/mL, Chloramphenicol 25 µg/mL.

The pH of solutions was determined using a Jenway pH Meter 3305, with an Aldrich glass/calomel combination electrode. Calibration was carried out between pH 4.0-7.0 or 7.0-10.0 immediately before use, with buffer solutions of phthalate (pH 4.0), phosphate (pH 7.0) and borate (pH 10.0) from Fisher Scientific. Electrodes were stored in a 4 M aqueous potassium chloride solution.

Cell growth media and cell lysates were centrifuged in a Beckman Avanti J-25 (8500 rpm: JA-10 rotor; 15,000 rpm: JA-16.250 rotor and 24,000 rpm: JA-25.50 rotor, respectively). Proteins were concentrated using a Beckman Allegra X-30R centrifuge (4000 rpm, SX4400 swing bucket) at 4 °C.

Cells were incubated in a New Brunswick G-25 Shaker Incubator at 37 °C and 220 rpm. Optical density at 600 nm was measured with a Novaspec III visible spectrophotometer.

Purified (Milli-Q) water was obtained from a Millipore Elix® Reverse Osmosis system which was further purified by a Millipore Milli-Q® Synthesis system with a 0.22 µm filter on the outlet. Reagent quantities given as weight per volume (w/v) correspond to g/mL unless otherwise stated.

6.3.1 Protein Expression

6.1.3.1 Plasmid DNA

The Leishmania bromodomain coding sequences were cloned in the pET15-MHL vector from the Structural Genomics Consortium.

6.1.3.2 Details of the pET15-MHL Vector (GenBank accession EF456738)

Antibiotic resistance	Ampicillin 100 ug/ml
Promoter	T7 - lacO
Initiation Codon	ATG site in vector at bp 5317, NcoI site was destroyed
N – terminal fusion sequence	MHHHHHHSSGRENLYFQG
Termination codons	TGATGA included in 3’ PCR primer and vector cloning site. No amino acid residues added at cloning junction
5’ sequencing primer T7- Fwd	5’ TTG TAT TTC CAG GGC --- 3’
3’ sequencing primer T7- Rev	5’ ATG CTA GTT ATT GCT CAG CGG 3’

6.1.3.3 Protein information

LdBDF5.1	**MW with 6×His tag Da**	**kDa**
	15190.9219	15.1909219
Bromodomain sequence	CCGAAGCTCTATAATGAGGCAGATGTAGCTGCGCTGGTGCGGAGCC TGGATCGTGCGGAGGATCATCATATCTTTGCCGTCGATGTTCTGGAA ACCTATCCGTACTTAGCGGAAAGCTACACCAAAGTATGCCCGCGTCG CTGCGATTTGGCGACCGCAGCCCAAAAGGCACTGGAGGGAGCTTAT AGCTACGACCTGCGGTTGGAAGGCCTCAAAGCCGACATCGCTCTTAT GGCGTCTAACTGCGTCGCCTATAATGGGCCGACGAGCGCGTATGCCG AAACTGCCGCCAAATTTGAACGGTATGCCCTGGAACAGATTGATGCT TTCGTGTTGGAACATAACGGGGGTTGC	

LdBDF5.2	**MW with 6×His tag Da**	**kDa**
	17931.1934	17.9311934
Bromodomain sequence	GCGGCGCCTCCAAGTACACGTGAGATGGTTCAGCTGGTTGATAGCCT TAATCGTCGCGAAGATGGTGGCGCCTTTTCCGTTGATGTAGCAGAAG CATACCCCGATTTGCGCGACAGTTATCGCAAAATTTGTCCACGCCCTA TGAACCTGATTCTGATGCGCCAACGCGCTAAAGAGGGTTACTACACCT CGGGGTCTGCCACGGTTTACGGTGACACGGTAGCAGCATCCCTGACGC GCTTGCGTGAGGACATTGAGCTGTTAGTGCGCAACTGTATCACATTCA ATGTCAAAGTAGAGTCTTGGGTCACTTTGGCACGCAGCTTCCAAGCGT TCGCGCACCGTCGCGTGGACGACTTCGTGCTTCGCCACGCAGCATTCCT GCGTGGGACGACCATGGGCGCGGAAGTTTACGAG	

Eurofins Genomics' TubeSeq Service was used for plasmid sequencing.

Escherichia coli (E. coli) bacterial strains of the following genotypes were used:

NEB® 5-alpha: for plasmid amplification purposes.

Rosetta™ (DE3): for protein expression of LdBDF5.1. Host strains are BL21 derivatives designed to enhance the expression of eukaryotic proteins that contain codons rarely used in *E. coli*. These strains supply tRNAs for AGG, AGA, AUA, CUA, CCC, GGA codons on a compatible chloramphenicol-resistant plasmid. DE3 denotes a chromosomal copy of the T7 RNA polymerase gene, transcribing genes under T7 promoter.

Rosetta™ 2(DE3): for protein expression of *Ld*BDF5.2. Host strains are BL21 derivatives designed to enhance the expression of eukaryotic proteins that contain codons rarely used in *E. coli*. These strains supply tRNAs for 7 rare codones (AGA, AGG, AUA, CUA, GGA, CCC, and CGG) on a compatible chloramphenicol-resistant plasmid. The tRNA genes are driven by their native promoters.

6.1.3.4 Media and Growth Conditions

E. coli strains were cultured in LB medium (10 g/L Oxoid™ Tryptone, 5 g/L Oxoid™ Yeast Extract, 5 g/L NaCl) at 37 °C and 220 rpm. When solid medium was required, Bacto agar was added to a final concentration of 1.5% (w/v). Standard sterile practices were followed using an open flame, on sterilised surfaced using aq. EtOH (70% v/v). Media and equipment were sterilised by autoclaving at 121 °C for 15 min. Solutions of IPTG, antibiotics and other labile compounds were sterilised by filtering through 0.22 µm filters (Minisart®, Sartorius Stedim). Final concentrations of ampicillin unless indicated otherwise was 100 µg/mL. Final concentrations of chloramphenicol unless indicated otherwise was 25 µg/mL.

6.1.3.5 Transformation of *E. Coli*

Competent cells were thawed on ice for 15 min before 5.0 µL of plasmid DNA was added to 50 µL of the competent cells. The tubes of cells were flicked 4-5 times to mix the cells and DNA, then placed on ice for 10 min. The tubes were heat shocked in a water bath at 42 °C for 30 s. The tubes were returned to ice for 3 min. 200 µL of room temperature SOC medium was added to each tube, then 50 µL of the mixture was spread onto a selection plate containing the appropriate antibiotic and incubated overnight at 37 °C.

Plasmid DNA was transformed into E. coli Rosetta™ (DE3) or Rosetta™ 2(DE3) cells for protein purification, and NEB5®α cells for plasmid amplification purposes.

Amplified plasmid DNA was purified using a GeneJET Plasmid Miniprep Kit (Thermo Scientific) according to manufacturer's instructions.

DNA concentration was estimated by measuring absorbance at 280 nm using a Nanodrop® ND-1000 spectrophotometer (Nanodrop® Technologies Inc.).

6.1.3.6 Small-scale expression trials for *Ld*BDF5.2

Small-scale recombinant protein expression was performed using 100 mL flasks containing 100 mL of LB medium containing glucose (0.2%), chloramphenicol (25 µg/mL) and ampicillin (100 µg/mL). Flasks were inoculated with 1 % of the bacterial starter culture and grown at 37 °C until they reached the desired OD_{600}. Cultures were induced with IPTG, then incubated at the specified temperature for the specified length of time. Cells were then harvested by centrifuging at 5000 rpm at 4 °C for 30 min. The resulting bacterial pellet was frozen in a sealable plastic bag at −80 °C.

Cell pellets were thawed on ice, resuspended in Lysis buffer (10 mL) and vortexed. Cells were sonicated on ice for 3.5 min, using 5 sec bursts interrupted by 5 sec pauses at 60% intensity. A sample of the cell lysate was taken at this stage for SDS PAGE gel analysis (Total fraction, TF sample). 1.5 mL of the cell lysate was clarified by centrifugation at 14800 rpm at 4 °C for 15 min. A second sample was removed from the supernatant at this stage (Soluble fraction, SF sample). The supernatant was added to 100 µL of Ni resin beads (equilibrated in Binding buffer) and the sample rotated at 25 rpm for 75 min at 4 °C using a Stuart Tube Rotator with Free Microcentrifuge Tube Holder, 120 VAC. The sample was spun down at 500 rpm for 6 min at 4 °C and the supernatant removed. A sample of the supernatant was kept as a control sample for the SDS PAGE gel (Flow through sample). The Ni resin was washed with 1 mL Binding buffer three times. The Ni beads were spun down at 500 rpm for 5 min at 4 °C and the supernatant discarded between each wash. Samples were taken from each consecutive wash for analysing on the SDS PAGE gel. The His-tagged proteins were eluted from the Ni resin by the addition of 200 µL Elution buffer. Samples were rotated at 25 rpm for 15 min at 4 °C using a Stuart Tube Rotator with Free Microcentrifuge Tube Holder. The eluent was removed, and a sample taken for the SDS PAGE gel (Eluted fraction, EF sample). Protein concentration

was estimated by measuring the absorbance at 280 nm using a Nanodrop® ND-1000 spectrophotometer (Nanodrop® Technologies Inc.).

Table 6.1. Composition of buffers for small-scale purification.

Buffers (pH 7.5)

Reagent	Lysis*	Binding	Elution
HEPES	20 mM	20 mM	20 mM
NaCl	500 mM	500 mM	500 mM
Imidazole	30 mM	30 mM	300 mM
DTT	1 mM	1 mM	1 mM
$MgCl_2$	5 mM	-	-
DNAse I	5 µg/ mL	-	-

* 1 Roche cOmplete mini EDTA free protease tablet per 100 mL buffer

Table 6.2. Masses of cell pellets obtained and concentration of eluted protein from small-scale expression and purification trials.

Experiment	**Mass of cell pellet (mg)**	**Protein concentration (mg/ mL)**
1	654	0.581
2	415	0.235
3	380	0.208
4	781	0.084
5	533	0.034
6	491	0.020
7	662	0.318
8	364	0.353
9	401	0.296
10	449	0.435
11	302	0.454
12	296	0.694

6.1.3.7 Large-scale growth for *Ld*BDF5.1

Large-scale recombinant protein expression was performed using 2 L flasks containing 1 L of LB medium containing the appropriate antibiotic. Flasks were inoculated with 1 % of the bacterial starter culture and grown at 37 °C until they reached an OD_{600} of 0.6. Cultures were induced with IPTG (0.10 mM), then incubated at 37 °C for a further 2-3 h. After this time, cells were harvested by centrifuging at 5000 rpm at 4 °C for 30 min. The resulting bacterial pellet was frozen in a sealable plastic bag at −80 °C.

6.1.3.8 Large-scale growth for *Ld*BDF5.2

Large-scale recombinant protein expression was performed using 2 L flasks containing 1 L of LB medium containing the appropriate antibiotic. Flasks were inoculated with 1 % of the bacterial starter culture and grown at 37 °C until they reached an OD_{600} of 0.8. Cultures were induced with IPTG (1 mM), then incubated at 16 °C for a 15 h. After this time, cells were harvested by centrifuging at 5000 rpm at 4 °C for 30 min. The resulting bacterial pellet was frozen in a sealable plastic bag at −80 °C.

6.3.2 Protein Purification

Cell pellets were resuspended in Binding buffer (100 mL per 20 g cell mass) with the addition of 5 mM $MgCl_2$, one cOmplete™ Mini EDTA-free tablet and DNase I (5 µg/ mL). The cells were lysed by sonication on ice for 15 min, using 30 sec bursts interrupted by 30 sec pauses. Polyethyleneimine (PEI, 0.15% *v/v*) was added, and the cells were incubated on ice for 15 mins. The lysate was clarified by centrifugation at 15 000 rpm at 4 °C for 40 min. The supernatant was decanted, filtered through a 0.45 µm filter, and applied to a purification column.

Immobilised metal affinity chromatography (IMAC) was performed with a HisTrap™ (6 mL) column (GE Healthcare) charged with 20 mL of 100 mM $NiSO_4$ and washed with 50 mL of binding buffer prior to loading the cell lysate at 1 mL/min. The protein was eluted using a gradient of 100% binding buffer to 100% elution buffer over 20 column volumes (CVs). Eluted protein was collected and fractionated; fractions containing the highest levels of pure protein (as determined by SDS-PAGE gels and UV trace) were

concentrated using Coming® SpinX® UF concentrators (30 K MWCO) in a Beckmann Allegra™ 21R centrifuge.

Size exclusion chromatography (SEC) was used for further purification. Concentrated fractions (<1.5 mL) were loaded on a HiLoad Superdex S75 16/600 column using a loop, then eluted using 1 CV of Gel filtration buffer. Eluted protein was collected and fractionated; fractions containing the highest levels of pure protein (as determined by SDS-PAGE gels) were concentrated (to 50-500 μM) using Coming® SpinX® UF concentrators (30 K MWCO) in a Beckmann Allegra™ 21R centrifuge.

Table 6.3. Composition of buffers for IMAC and SEC purification steps.

IMAC and SEC buffers (pH 7.5)

Reagent	Binding	Elution	Strip	Gel filtration
HEPES	20 mM	20 mM	20 mM	20 mM
NaCl	500 mM	500 mM	500 mM	500 mM
Imidazole	30 mM	300 mM	–	–
EDTA	–	–	100 mM	–
DTT*	1 mM	1 mM	–	1 mM

*Addition only prior to loading column

Protein concentration was estimated by measuring the absorbance at 280 nm using a Nanodrop® ND-1000 spectrophotometer (Nanodrop® Technologies Inc.) with the 'Protein A280' programme module according to the manufacturer's instructions.

Protein molecular weight and **molar extinction coefficient** were calculated using ProtParam on the ExPASy Bioinformatics Resource Portal.

Intact Protein Mass Spectrometry for *Ld*BDF5.1 was carried out on a Waters LCT Premier XE mass spectrometer coupled with a Water Aqcuity sample and column manager. A ProSwift™ RP-2H monolithic 4.6 mm × 50 mm column (Thermo Scientific™) was used with a constant flow rate of 0.2 mL/min and a gradient of 5 min from H_2O:MeCN (95:5) to H_2O:MeCN (5:95). All samples were run with 0.1% formic acid in the elution solvents. Mass spectra were deconvoluted using Waters MassLynx™ software (MaxEnt1 algorithm, 12.5–17.5 kDa range, 1.0 Da resolution).

Intact Protein Mass Spectrometry for *Ld*BDF5.2 was carried out on a Waters Xevo G2-XS QTOF mass spectrometer, equipped with a Waters Acquity UPLC. A ProSwift™ RP-2H monolithic 4.6 mm × 50 mm column (Thermo Scientific™) was used with a constant flow rate of 0.4 mL/min and a gradient method of 10 min from H_2O:MeCN (95:5) to H_2O:MeCN (5:95) with a 5 min hold. All samples were run with 0.1% formic acid in the elution solvents. Mass spectra were deconvoluted using Waters MassLynx™ software (MaxEnt1 algorithm, 16–20 kDa range, 1.0 Da resolution).

Sodium Dodecyl-Sulfate Polyacrylamide Gel Electrophoresis (SDS-PAGE) was used to determine protein purity. NuPAGE™ Bis-Tris Mini Gels (ThermoFisher) were used to perform denaturing protein gel electrophoresis. For denaturing PAGE analysis, samples were prepared by mixing with Laemmli 2X sample loading buffer (1:1) and incubated at 100 °C for 2 min. All gels were loaded with a molecular weight ladder: PageRuler Plus Prestained Protein Ladder. 50 mL of 20X NuPAGE™ MES was added to 950 mL of deionised water to prepare 1X SDS Running Buffer. The gel was run at 180 V for 30 mins. Following Electrophoresis, gels were stained for 15 mins with InstantBlue™ Coomasie® stain. De-ionised water was used to de-stain the gels.

6.4 Biophysical Assays

6.4.1 WaterLOGSY

Proteins were buffer exchanged from HEPES storage buffer into PBS (NaH_2PO_4/Na_2HPO_4 50 mM, NaCl 150 mM, pH 7.4 in filtered milli Q) using GE Healthcare PD SpinTrap G-25 columns. Protein concentrations in the phosphate buffer were calculated by measuring the absorbance at 280 nm using a NanoDrop Lite spectrophotometer (Nanodrop® Technologies Inc.) by using the predicted protein absorbance (*Ld*BDF5.1: ε280: 12800 M^{-1} cm^{-1}, *Ld*BDF5.2: ε280: 14650 M^{-1} cm^{-1}). For each compound, a water-suppressed ^1H NMR spectrum was recorded as a reference, followed by a waterLOGSY spectrum of the compound in the absence of protein as a negative control, and then another waterLOGSY spectrum in the presence of the specified protein. Samples were prepared to a total volume of 160 µL in PBS buffer

(NaH_2PO_4/Na_2HPO_4 50 mM, NaCl 150 mM, pH 7.4 in filtered milli Q), with 500 μM compound from 50 mM *d*-DMSO stock solutions, 10% D_2O for signal locking, and 20 μM protein for samples with protein. Where compounds formed soluble aggregates the compound and protein concentration were decreased. After loading into 3 mm Hilgenberg NMR tubes for Bruker Match^{TM} system, samples were briefly centrifuged in a manual benchtop rotor. Spectra were recorded on a Bruker AVIII 700 MHz spectrometer with inverse TCI cryoprobe using a standard waterLOGSY pulse sequence.[148]

6.4.2 Thermal Shift Assay (Differential Scanning Fluorimetry)

Protein thermal shift assay was carried out using CFX Connect Real-time PCR system, and 5 μM *Ld*BDF5.1 (or *Ld*BDF5.2) protein and 20 μM test compounds were used for this assay. The assay buffer comprised 20 mM Hepes and 500 mM NaCl at pH 7.5. The compounds were prepared as 2 mM stock solutions in DMSO, then diluted with buffer to 200 μM. 2.5 μL Compound was added to each well of a 96-well PCR plate (Axygen). 22.5 μL Buffer containing SYPRO® orange (Sigma) and protein was added to the individual wells of the plate to give a final concentration of 5× SYPRO® orange (Sigma) and 5 μM protein in each well. The 96-well PCR plates were sealed and centrifuged (1000 rpm, 1 min, 25 °C) before measurement. Fluorescence signal was monitored and collected from 20 to 95 °C. Each compound was tested in triplicate. The T_M values of *Ld*BDF5.1 and *Ld*BDF5.2 with test compounds were determined by Bio-Rad CFX Maestro 1.1 Software. The thermal shift (ΔT_M) was calculated as the difference in melting temperatures of the protein in the absence/presence of ligand.

6.4.3 Microscale Thermophoresis

The *Ld*BD5.1 protein was labelled with the Monolith His-Tag Labeling Kit (RED-tris-NTA 2nd Generation kit, NanoTemper Technologies, Catalog# MO-L018) according to the manufacturer's protocol. The test compound was serially diluted in 16-steps in PBS-T buffer (137 mM NaCl, 2.7 mM KCl, 10 mM Na_2HPO_4, 1.8 mM KH_2PO_4, 0.1% Tween-20, pH 7.4) with 0.5% DMSO. Equivalent volume of labelled

protein and compound were mixed. The labelled protein was at a final concentration of 25 nM. The samples were loaded into Monolith premium capillaries (Catalog# MO-K025), and thermophoresis was measured on a Monolith NT.115 equipment (NanoTemper Technologies) with an IR laser power of 40% and an LED intensity of 60%. Each compound was tested in triplicate. The binding curve was calculated from the gradual difference of thermophoresis between the fluorescent molecules of both unbound and bound states, which is plotted as F_{norm} (defined as F_{hot}/ F_{cold}) against ligand concentration. The binding constants (K_d) were determined from the binding curve by fitting to log(agonist) vs. response in GraphPad Prism version 9.5.1. for Windows, GraphPad Software, San Diego, California USA, www.graphpad.com.

6.4.4 Isothermal Titration Calorimetry

All calorimetric experiments were performed on a MicroCal iTC200 or MicroCal PEAQ-ITC Automated (Malvern) and analysed with the MicroCal PEAQ-ITC Analysis software (Malvern 1.1.0.1262) using a single binding site model. The first data point was excluded from the analysis. The *Ld*BDF5.1, *Ld*BDF5.2, *Hm*CREBBP and *Hm*BRD4(1) bromodomains were dialysed at 4 °C overnight in a Slide-A-Lyzer® MINI Dialysis Device (2000 MWCO; Thermo Scientific Life Technologies) into PBS buffer (137 mM NaCl, 2.7 mM KCl, 10 mM Na_2HPO_4, 1.8 mM KH_2PO_4, pH 7.4) containing 0.5% DMSO. Proteins were centrifuged to remove aggregates (2 min, 3,000 rpm, 4 °C). Protein concentration was determined by measuring the absorbance at 280 nm using a NanoDrop Lite spectrophotometer (Nanodrop® Technologies Inc.) by using the predicted protein absorbance (*Ld*BDF5.1: ε280: 12800 M^{-1} cm^{-1}, *Ld*BDF5.2: ε280: 14650 M^{-1} cm^{-1}, CREBBP: ε280: 26930 M^{-1} cm^{-1} and BRD4(1): ε280: 28545 M^{-1} cm^{-1}). Small molecules ligands were dissolved as 20 mM DMSO stock solution and diluted to the required concentration using dialysis buffer. The cell was stirred at 750 rpm, reference power set to 5 µcal/sec and temperature held at 25 ˚C. After an initial delay of 60 sec, 20 × 2 µL injections (first injection 0.4 µL) were performed with a spacing of 150 sec. Heated dilutions were measured under the same conditions and subtracted for analysis. Small molecule solutions in the calorimetric cell (250 µL, 10 to 40 µM) were titrated with the protein solutions in the syringe (60 µL, 100 to 220 µM).

6.5 Leishmania Promastigote Cell Viability Assay

L. donovani LV9 (MHOM/ET/67/HU3) promastigotes were grown at 25 °C in hemoflagellate-modified minimum essential medium (HOMEM) (Gibco) supplemented with 10% (v/v) heat-inactivated fetal calf serum (hi-FCS) (Gibco) and 1% (v/v) penicillin/streptomycin solution (Sigma-Aldrich). Cell cultures were passaged weekly into fresh medium using dilutions of 1/40 or 1/100 culture in fresh medium. Cell density was determined by fixing cells using a 1/10 dilution in 2% (v/v) formaldehyde and manually counted using a Neubauer hemocytometer.

For cell viability dose–response assays, cultures were grown to mid log (exponential) phase and dilutions were prepared to 5×10^3 cells/ml in medium (HOMEM with 10% hi-FCS and 1% penicillin/streptomycin solution). 60 μM compound solutions were also prepared in medium. 100 μL cells were seeded into triplicate wells of 96-well plates at 500 cells per well, alongside 100 μL compounds were serially diluted in medium to obtain final concentrations of 0–30 μM. A miltefosine positive control was included, along with DMSO, parasites-only, and media-only controls. Empty wells were filled with 200 μL of PBS, then plates were incubated for 5 days at 25 °C, after which time, 40 μL of resazurin (Sigma-Aldrich) was added to each well (final concentration, 80 μM) and the plates were incubated for a further 8 h at 25 °C. Fluorescence readings were taken using a BMG LABTECH CLARIOstar microplate reader and data was processed using BMG LABTECH Mars software with subsequent analysis and graph plotted in GraphPad Prism. Mean, blank-corrected fluorescence measurements (over compound concentrations 0.23–30 μM) were normalised to give values as % cell viability. Three biological replicates were performed, with fluorescence measurements averaged, and data fitted to an [Inhibitor] vs normalised response, variable slope dose–response curve to calculate EC_{50}. The standard error of the mean was calculated for the averaged mean values.

6.6 Docking of ligands in GOLD

Docking of ligands into *Ld*BDF5.1 (PDB: 6BYA, chain A) was performed in GOLD (v2021.2.0) by Bernadette Lee.[208] The .mol2 files for the ligands were generated from SMILES strings using OpenBabel (v3.1.0).[348] The ligands were protonated during this process, with all ligands modelled in the neutral state. The protein structure was protonated in GOLD, and the bound 2LO ligand extracted from the binding site. Seven waters were retained in the bromodomain pocket, and the remaining solvent molecules were removed. The 2LO ligand's coordinates were used to define the binding site for ligands, with protein atoms within 6.0 Å of the ligand included in the binding site definition. Docking was then carried out in GOLD using the ChemPLP scoring function, with 20 solutions requested. Poses generated by GOLD were visually inspected to identify possible binding modes for ligands.

6.7 Affinity Selection Mass Spectrometry (ASMS)

ASMS is a high-throughput technology that directly assesses ligand/target interactions.[349] This technique was performed by collaborators at GSK to generate hits for the *Ld*BDF5.1 and *Ld*BDF5.2 proteins from a classified library of in-house compounds. In this process, hundreds of small molecules are incubated with the protein and specific protein−ligand complexes are allowed to form. Size exclusion chromatography is then used to remove the molecules with weak or no affinity from solution. The ligands with affinity for the protein are carried though in the eluate and reversed-phase accurate-mass liquid chromatography−mass spectrometry (LC−MS) analysis detects the mass of the ligands. A relative binding affinity percentage (% RBA) is reported for the ligands that are hits. This is calculated from the amount of ligand bound (selection), normalised to the signal detected from the small molecule in the absence of the protein target (control). A stronger affinity is, in most cases, indicated by a greater %RBA.

6.8 Protein X-ray crystallography

Crystallisation of *Lmx*BDF5.1 with **181** was conducted by Marius Amann at the University of Freiburg. The X-ray crystal structure was solved by Dr Martin Hügle.

Table 6.4. Crystallisation of *Lmx*BDF5.1 with **181**, crystallographic data collection and refinement statistics. [a]Values in parentheses correspond to the outer resolution shell.

Structure	
*Lmx*BDF5.1 with **181**	
Crystallisation	
Crystallisation method	Vapour diffusion
Condition	0.1M Potassium thiocyanate, 30% w/v Polyethylene glycol monomethyl ether 2000
Temperature	277 K
Data collection	
X-ray wavelength (Å)	0.96770
Resolution range (Å)[a]	42.82 - 1.45 (1.502 - 1.45)
Space group	$P2_12_12_1$
Unit cell dimensions (*a* Å, *b* Å, *c* Å, α°, β°, γ°)	44.794 49.646 85.634 90 90 90
Total reflections [a]	359055 (36555)
Unique reflections [a]	34549 (3400)
Multiplicity [a]	10.4 (10.8)
Completeness (%)[a]	99.84 (99.85)
$I/\sigma(I)$ [a]	14.18 (2.42)
R_{merge} [a]	0.1042 (1.181)
R_{meas} [a]	0.1098 (1.24)
R_{pim} [a]	0.03391 (0.374)
CC(1/2)	0.997 (0.842)
CC*	0.999 (0.956)
Refinement	
Reflections used in refinement	34537 (3395)
Reflections used for R_{free}	1709 (179)
R_{work} **(%)**	0.1331 (0.1721)
R_{free} **(%)**	0.1725 (0.2335)

RMS (bonds)	0.009
RMS (angles)	1.00
Average *B* factor (Å)	20.70
Wilson B factor (Å)	15.29
Ramachandran favored (%)	100.00
Ramachandran allowed (%)	0.00
Ramachandran outliers (%)	0.00
Rotamer outliers (%)	0.00
Clashscore	2.60
Number of non-hydrogen atoms	2312
Macromolecules	1892
Ligands	121
Solvent	299
Protein residues	228

References

(1) Berger, S. L.; Kouzarides, T.; Shiekhattar, R.; Shilatifard, A. An operational definition of epigenetics. In *Genes & Development*, 2009; Vol. 23; pp 781-783.

(2) Felsenfeld, G. A Brief History of Epigenetics. *Cold Spring Harbor Perspectives in Biology* **2014**, *6* (1), a018200-a018200.

(3) Conway, S. J. Bromodomains: Are Readers Right for Epigenetic Therapy? *ACS Medicinal Chemistry Letters* **2012**, *3* (9), 691-694.

(4) Mcginty, R. K.; Tan, S. Nucleosome Structure and Function. *Chemical Reviews* **2015**, *115* (6), 2255-2273.

(5) Brasier, A. R. Orchestrating epigenetic readers: Progress in understanding the functions of bromodomain-containing protein 4 complexes. *Molecular Therapy - Nucleic Acids* **2023**, *32*, 340-342.

(6) Moore, L. D.; Le, T.; Fan, G. DNA Methylation and Its Basic Function. *Neuropsychopharmacology* **2013**, *38* (1), 23-38.

(7) Jennings, L. E.; Measures, A. M.; Wilson, B. G.; Conway, S. J. Phenotypic screening and fragment-based approaches to the discovery of small-molecule bromodomain ligands. *Future Medicinal Chemistry* **2014**, *6* (2), 179-204.

(8) Choudhary, C.; Kumar, C.; Gnad, F.; Nielsen, M. L.; Rehman, M.; Walther, T. C.; Olsen, J. V.; Mann, M. Lysine Acetylation Targets Protein Complexes and Co-Regulates Major Cellular Functions. *Science* **2009**, *325* (5942), 834-840.

(9) Bannister, A. J.; Kouzarides, T. Regulation of chromatin by histone modifications. *Cell Research* **2011**, *21*, 381-395.

(10) Filippakopoulos, P.; Knapp, S. The bromodomain interaction module. *FEBS Letters* **2012**, *586*, 2692-2704.

(11) Zaware, N.; Zhou, M.-M. Bromodomain biology and drug discovery. *Nature Structural & Molecular Biology* **2019**, *26* (10), 870-879.

(12) Pan, Z.; Zhao, Y.; Wang, X.; Xie, X.; Liu, M.; Zhang, K.; Wang, L.; Bai, D.; Foster, L. J.; Shu, R.*; et al.* Targeting bromodomain-containing proteins: research advances of drug discovery. *Molecular Biomedicine* **2023**, *4* (13), 1-38.

(13) Cochran, A. G.; Conery, A. R.; Sims, R. J. Bromodomains: a new target class for drug development. *Nature Reviews Drug Discovery* **2019**, *18* (8), 609-628.

(14) Brand, M.; Measures, A. M.; Wilson, B. G.; Cortopassi, W. A.; Alexander, R.; Höss, M.; Hewings, D. S.; Rooney, T. P. C.; Paton, R. S.; Conway, S. J. Small Molecule Inhibitors of Bromodomain–Acetyl-lysine Interactions. *ACS Chemical Biology* **2015**, *10* (1), 22-39.

(15) Muller, S.; Filippakopoulos, P.; Knapp, S. Bromodomains as therapeutic targets. *Expert Reviews in Molecular Medicine* **2011**, *13* (e29).

(16) Wu, Q.; Heidenreich, D.; Zhou, S.; Ackloo, S.; Krämer, A.; Nakka, K.; Lima-Fernandes, E.; Deblois, G.; Duan, S.; Vellanki, R. N.*; et al.* A chemical toolbox for the study of bromodomains and epigenetic signaling. *Nature Communications* **2019**, *10* (1).

(17) Theodoulou, N. H.; Tomkinson, N. C.; Prinjha, R. K.; Humphreys, P. G. Clinical progress and pharmacology of small molecule bromodomain inhibitors. *Current Opinion in Chemical Biology* **2016**, *33*, 58-66.

(18) Shorstova, T.; Foulkes, W. D.; Witcher, M. Achieving clinical success with BET inhibitors as anti-cancer agents. *British Journal of Cancer* **2021**, *124* (9), 1478-1490.

(19) Quintela, M.; James, D. W.; Pociute, A.; Powell, L.; Edwards, K.; Coombes, Z.; Garcia, J.; Garton, N.; Das, N.; Lutchman-Singh, K.*; et al.* Bromodomain inhibitor i-BET858 triggers a unique transcriptional response coupled to enhanced DNA damage, cell cycle arrest and apoptosis in high-grade ovarian carcinoma cells. *Clinical Epigenetics* **2023**, *15* (1).

(20) Filippakopoulos, P.; Qi, J.; Picaud, S.; Shen, Y.; Smith, W. B.; Fedorov, O.; Morse, E. M.; Keates, T.; Hickman, T. T.; Felletar, I.*; et al.* Selective inhibition of BET bromodomains. *Nature* **2010**, *468* (7327), 1067-1073.

(21) Nicodeme, E.; Jeffrey, K. L.; Schaefer, U.; Beinke, S.; Dewell, S.; Chung, C.-W.; Chandwani, R.; Marazzi, I.; Wilson, P.; Coste, H.*; et al.* Suppression of inflammation by a synthetic histone mimic. *Nature* **2010**, *468* (7327), 1119-1123.

(22) To, K. K. W.; Xing, E.; Larue, R. C.; Li, P.-K. BET Bromodomain Inhibitors: Novel Design Strategies and Therapeutic Applications. *Molecules* **2023**, *28* (7), 3043.

(23) Haynes, S. R.; Dollard, C.; Winston, F.; Beck, S.; Trowsdale, J.; Dawid, I. B. The bromodomain: a conserved sequence found in human, *Drosophila* and yeast proteins. *Nucleic Acids Research* **1992**, *20* (10), 2603-2603.

(24) Filippakopoulos, P.; Picaud, S.; Mangos, M.; Keates, T.; Lambert, J.-P.; Barsyte-Lovejoy, D.; Felletar, I.; Volkmer, R.; Müller, S.; Pawson, T.*; et al.* Histone Recognition and Large-Scale Structural Analysis of the Human Bromodomain Family. *Cell* **2012**, *149* (1), 214-231.

(25) Filippakopoulos, P.; Knapp, S. Targeting bromodomains: epigenetic readers of lysine acetylation. *Nature Reviews Drug Discovery* **2014**, *13* (5), 337-356.

(26) Hewings, D. S.; Rooney, T. P. C.; Jennings, L. E.; Hay, D. A.; Schofield, C. J.; Brennan, P. E.; Knapp, S.; Conway, S. J. Progress in the Development and Application of Small Molecule Inhibitors of Bromodomain–Acetyl-lysine Interactions. *Journal of Medicinal Chemistry* **2012**, *55* (22), 9393-9413.

(27) Dhalluin, C.; Carlson, J. E.; Zeng, L.; He, C.; Aggarwal, A. K.; Zhou, M.-M.; Zhou, M.-M. Structure and ligand of a histone acetyltransferase bromodomain. *Nature* **1999**, *399* (6735), 491-496.

(28) Crystal Structure of the first bromodomain of human BRD4 in complex with a diacetylated histone 4 peptide (H4K5acK8ac). https://doi.org/10.2210/pdb3UVW/pdb (accessed Dec 7, 2023).

(29) Miyoshi, S.; Ooike, S.; Iwata, K.; Hikawa, H.; Sugahara, K. Antitumor agent. WO/2009/084693, 2007.

(30) Wang, Z.-Q.; Zhang, Z.-C.; Wu, Y.-Y.; Pi, Y.-N.; Lou, S.-H.; Liu, T.-B.; Lou, G.; Yang, C. Bromodomain and extraterminal (BET) proteins: biological functions, diseases, and targeted therapy. *Signal Transduction and Targeted Therapy* **2023**, *8* (1).

(31) Clegg, M. A.; Tomkinson, N. C. O.; Prinjha, R. K.; Humphreys, P. G. Advancements in the Development of non-BET Bromodomain Chemical Probes. *ChemMedChem* **2019**, *14* (4), 362-385.

(32) Theodoulou, N. H.; Tomkinson, N. C. O.; Prinjha, R. K.; Humphreys, P. G. Progress in the Development of non-BET Bromodomain Chemical Probes. *ChemMedChem* **2016**, *11* (5), 477-487.

(33) Smith, S. G.; Zhou, M.-M. The Bromodomain: A New Target in Emerging Epigenetic Medicine. *ACS Chemical Biology* **2016**, *11* (3), 598-608.

(34) Romero, F. A.; Taylor, A. M.; Crawford, T. D.; Tsui, V.; Côté, A.; Magnuson, S. Disrupting Acetyl-Lysine Recognition: Progress in the Development of Bromodomain Inhibitors. *Journal of Medicinal Chemistry* **2016**, *59* (4), 1271-1298.

(35) NVS-CECR2-1 A chemical probe for CECR2. https://www.thesgc.org/chemical-probes/NVS-CECR2-1 (accessed.

(36) Humphreys, P. G.; Bamborough, P.; Chung, C.-W.; Craggs, P. D.; Gordon, L.; Grandi, P.; Hayhow, T. G.; Hussain, J.; Jones, K. L.; Lindon, M.*; et al.* Discovery of a Potent, Cell Penetrant, and Selective p300/CBP-Associated Factor (PCAF)/General Control Nonderepressible 5 (GCN5) Bromodomain Chemical Probe. *Journal of Medicinal Chemistry* **2017**, *60* (2), 695-709.

(37) Picaud, S.; Fedorov, O.; Thanasopoulou, A.; Leonards, K.; Jones, K.; Meier, J.; Olzscha, H.; Monteiro, O.; Martin, S.; Philpott, M.*; et al.* Generation of a Selective Small Molecule Inhibitor of the CBP/p300 Bromodomain for Leukemia Therapy. *Cancer Research* **2015**, *75* (23), 5106-5119.

(38) PFI-4 A chemical probe for BRPF1B. https://www.thesgc.org/chemical-probes/PFI-4 (accessed.

(39) Fernández-Montalván, A. E.; Berger, M.; Kuropka, B.; Koo, S. J.; Badock, V.; Weiske, J.; Puetter, V.; Holton, S. J.; Stöckigt, D.; Ter Laak, A.*; et al.* Isoform-Selective ATAD2 Chemical Probe with Novel Chemical Structure and Unusual Mode of Action. *ACS Chemical Biology* **2017**, *12* (11), 2730-2736.

(40) Theodoulou, N. H.; Bamborough, P.; Bannister, A. J.; Becher, I.; Bit, R. A.; Che, K. H.; Chung, C.-W.; Dittmann, A.; Drewes, G.; Drewry, D. H.*; et al.* Discovery of I-BRD9, a Selective Cell Active Chemical Probe for Bromodomain Containing Protein 9 Inhibition. *Journal of Medicinal Chemistry* **2016**, *59* (4), 1425-1439.

(41) Bouché, L.; Christ, C. D.; Siegel, S.; Fernández-Montalván, A. E.; Holton, S. J.; Fedorov, O.; Ter Laak, A.; Sugawara, T.; Stöckigt, D.; Tallant, C.*; et al.* Benzoisoquinolinediones as Potent and Selective Inhibitors of BRPF2 and TAF1/TAF1L Bromodomains. *Journal of Medicinal Chemistry* **2017**, *60* (9), 4002-4022.

(42) Fedorov, O.; Castex, J.; Tallant, C.; Owen, D. R.; Martin, S.; Aldeghi, M.; Monteiro, O.; Filippakopoulos, P.; Picaud, S.; Trzupek, J. D.*; et al.* Selective targeting of the BRG/PB1 bromodomains impairs embryonic and trophoblast stem cell maintenance. *Science Advances* **2015**, *1* (10), e1500723.

(43) Chen, P.; Chaikuad, A.; Bamborough, P.; Bantscheff, M.; Bountra, C.; Chung, C.-W.; Fedorov, O.; Grandi, P.; Jung, D.; Lesniak, R.*; et al.* Discovery and Characterization of GSK2801, a Selective Chemical Probe for the Bromodomains BAZ2A and BAZ2B. *Journal of Medicinal Chemistry* **2016**, *59* (4), 1410-1424.

(44) Meslamani, J.; Smith, S. G.; Sanchez, R.; Zhou, M.-M. Structural features and inhibitors of bromodomains. *Drug Discovery Today: Technologies* **2016**, *19*, 3-15.

(45) Ferri, E.; Petosa, C.; McKenna, C. E. Bromodomains: Structure, function and pharmacology of inhibition. *Biochemical Pharmacology* **2016**, *106*, 1-18.

(46) Jennings, L.; Schiedel, M.; Hewings, D. S.; Picaud, S.; Laurin, C. M. C.; Bruno 3, P. A.; Bluck, J. P.; Scorah, A. R.; See, L.; Reynolds, J. K.*; et al.* BET bromodomain ligands: Probing the WPF shelf to improve BRD4 bromodomain affinity and metabolic stability. *Bioorganic & Medicinal Chemistry* **2018**, *26* (11), 2937-2957.

(47) Gacias, M.; Gerona-Navarro, G.; Plotnikov, N., Alexander; Zhang, G.; Zeng, L.; Kaur, J.; Moy, G.; Rusinova, E.; Rodriguez, Y.; Matikainen, B.*; et al.* Selective Chemical Modulation of Gene Transcription Favors Oligodendrocyte Lineage Progression. *Chemistry & Biology* **2014**, *21* (7), 841-854.

(48) Picaud, S.; Da Costa, D.; Thanasopoulou, A.; Filippakopoulos, P.; Fish, P. V.; Philpott, M.; Fedorov, O.; Brennan, P.; Bunnage, M. E.; Owen, D. R.*; et al.* PFI-1, a Highly Selective Protein Interaction Inhibitor, Targeting BET Bromodomains. *Cancer Research* **2013**, *73* (11), 3336-3346.

(49) Gosmini, R.; Nguyen, V. L.; Toum, J.; Simon, C.; Brusq, J.-M. G.; Krysa, G.; Mirguet, O.; Riou-Eymard, A. M.; Boursier, E. V.; Trottet, L.*; et al.* The Discovery of I-BET726 (GSK1324726A), a Potent Tetrahydroquinoline ApoA1 Up-Regulator and Selective BET Bromodomain Inhibitor. *Journal of Medicinal Chemistry* **2014**, *57* (19), 8111-8131.

(50) Brand, M.; Clayton, J.; Moroglu, M.; Schiedel, M.; Picaud, S.; Bluck, J. P.; Skwarska, A.; Bolland, H.; Chan, A. K. N.; Laurin, C. M. C.*; et al.* Controlling Intramolecular Interactions in the Design of Selective, High-Affinity Ligands for the CREBBP Bromodomain. *Journal of Medicinal Chemistry* **2021**, *64* (14), 10102-10123.

(51) Romero, F. A.; Murray, J.; Wah Lai, K.; Tsui, V.; Albrecht, B. K.; An, L.; Beresini, M. H.; de Leon Boenig, G.; Bronner, S. M.; Chan, E. W.*; et al.* GNE-781, A Highly Advanced Potent and Selective Bromodomain Inhibitor of Cyclic Adenosine

Monophosphate Response Element Binding Protein, Binding Protein (CBP). *Journal of Medicinal Chemistry* **2017**, *60* (22), 9162-9183.

(52) Crystal Structure of the First Bromodomain of Human BRD4 in complex with IBET inhibitor. https://doi.org/10.2210/pdb3P5O/pdb (accessed Dec 10, 2023).

(53) Crystal Structure of the first bromodomain of human BRD4 in complex with I-BET151(GSK1210151A). https://doi.org/10.2210/pdb3ZYU/pdb (accessed Dec 6, 2023).

(54) Crystal Structure of the first bromodomain of human BRD4 in complex with the inhibitor PFi-1. https://doi.org/10.2210/pdb4E96/pdb (accessed Dec 3, 2023).

(55) *N*-Terminal bromodomain of human BRD4 with GSK1324726A (I-BET726). https://doi.org/10.2210/pdb4BJX/pdb (accessed Dec 12, 2023).

(56) Tallant, C.; Bamborough, P.; Chung, C.-W.; Gamo, F. J.; Kirkpatrick, R.; Larminie, C.; Martín, J.; Prinjha, R.; Rioja, I.; Simola, D. F.*; et al.* Expanding Bromodomain Targeting into Neglected Parasitic Diseases. *ACS Infectious Diseases* **2021**, *7* (11), 2953-2958.

(57) Jeffers, V.; Yang, C.; Huang, S.; Sullivan, W. J. Bromodomains in Protozoan Parasites: Evolution, Function, and Opportunities for Drug Development. *Microbiology and Molecular Biology Reviews* **2017**, *81* (1), e00047-00016.

(58) Alsford, S.; Turner, D. J.; Obado, S. O.; Sanchez-Flores, A.; Glover, L.; Berriman, M.; Hertz-Fowler, C.; Horn, D. High-throughput phenotyping using parallel sequencing of RNA interference targets in the African trypanosome. *Genome Research* **2011**, *21* (6), 915-924.

(59) Schulz, D.; Mugnier, M. R.; Paulsen, E.-M.; Kim, H.-S.; Chung, C.-W. W.; Tough, D. F.; Rioja, I.; Prinjha, R. K.; Papavasiliou, F. N.; Debler, E. W. Bromodomain Proteins Contribute to Maintenance of Bloodstream Form Stage Identity in the African Trypanosome. *PLOS Biology* **2015**, *13* (12), e1002316.

(60) Pezza, A.; Tavernelli, L. E.; Alonso, V. L.; Perdomo, V.; Gabarro, R.; Prinjha, R.; Rodríguez Araya, E.; Rioja, I.; Docampo, R.; Calderón, F.*; et al.* Essential Bromodomain *Tc*BDF2 as a Drug Target against Chagas Disease. *ACS Infectious Diseases* **2022**, *8* (5), 1062-1074.

(61) Jones, N. G.; Geoghegan, V.; Moore, G.; Carnielli, J. B. T.; Newling, K.; Calderón, F.; Gabarró, R.; Martín, J.; Prinjha, R. K.; Rioja, I.*; et al.* Bromodomain factor 5 is an essential regulator of transcription in *Leishmania*. *Nature Communications* **2022**, *13* (1).

(62) Yang, X.; Wu, X.; Zhang, J.; Zhang, X.; Xu, C.; Liao, S.; Tu, X. Recognition of hyperacetylated *N*-terminus of H2AZ by *Tb*BDF2 from *Trypanosoma brucei*. *Biochemical Journal* **2017**, *474* (22), 3817-3830.

(63) Xiao, Y.; Shanhui, L.; Xiaoming, T. Compound capable of killing *trypanosoma brucei* and application of compound in treating trypanosomosis. CN107308167A, 2017.

(64) Laurin, C. M. C.; Bluck, J. P.; Chan, A. K. N.; Keller, M.; Boczek, A.; Scorah, A. R.; See, K. F. L.; Jennings, L. E.; Hewings, D. S.; Woodhouse, F.*; et al.* Fragment-Based Identification of Ligands for Bromodomain-Containing Factor 3 of *Trypanosoma cruzi*. *ACS Infectious Diseases* **2021**, *7* (8), 2238-2249.

(65) Villanova, G. V.; Nardelli, S. C.; Cribb, P.; Magdaleno, A.; Silber, A. M.; Motta, M. C. M.; Schenkman, S.; Serra, E. *Trypanosoma cruzi* bromodomain factor 2 (BDF2) binds to acetylated histones and is accumulated after UV irradiation. *International Journal for Parasitology* **2009**, *39* (6), 665-673.

(66) Alonso, V. L.; Tavernelli, L. E.; Pezza, A.; Cribb, P.; Ritagliati, C.; Serra, E. Aim for the readers! Bromodomains as new targets against Chagas' disease. *Current Medicinal Chemistry* **2019**, *26* (36), 6544-6563.

(67) Alonso, V. L.; Villanova, G. V.; Ritagliati, C.; Machado Motta, M. C.; Cribb, P.; Serra, E. C. *Trypanosoma cruzi* Bromodomain Factor 3 Binds Acetylated α-Tubulin and Concentrates in the Flagellum during Metacyclogenesis. *Eukaryotic Cell* **2014**, *13* (6), 822-831.

(68) Alonso, V. L.; Ritagliati, C.; Cribb, P.; Cricco, J. A.; Serra, E. C. Overexpression of bromodomain factor 3 in *Trypanosoma cruzi* (*Tc*BDF3) affects differentiation of the parasite and protects it against bromodomain inhibitors. *The FEBS Journal* **2016**, *283* (11), 2051-2066.

(69) Hay, D. A.; Fedorov, O.; Martin, S.; Singleton, D. C.; Tallant, C.; Wells, C.; Picaud, S.; Philpott, M.; Monteiro, O. P.; Rogers, C. M.*; et al.* Discovery and Optimization of Small-Molecule Ligands for the CBP/p300 Bromodomains. *Journal of the American Chemical Society* **2014**, *136* (26), 9308-9319.

(70) Burza, S.; Croft, S. L.; Boelaert, M. Leishmaniasis. *Lancet* **2018**, *329*, 951-970.

(71) Torres-Guerrero, E.; Quintanilla-Cedillo, M. R.; Ruiz-Esmenjaud, J.; Arenas, R. Leishmaniasis: a review. *F1000Research* **2017**, *6*, 750.

(72) Reithinger, R.; Dujardin, J.-C.; Louzir, H.; Pirmez, C.; Alexander, B.; Brooker, S. Cutaneous leishmaniasis. *The Lancet Infectious Diseases* **2007**, *7* (9), 581-596.

(73) Leishmaniasis. https://www.who.int/news-room/fact-sheets/detail/leishmaniasis#:~:text=Visceral%20leishmaniasis%20(VL)%2C%20also,Brazil%2C%20east%20Africa%20and%20India. (accessed Nov 22, 2023).

(74) Scarpini, S.; Dondi, A.; Totaro, C.; Biagi, C.; Melchionda, F.; Zama, D.; Pierantoni, L.; Gennari, M.; Campagna, C.; Prete, A.*; et al.* Visceral Leishmaniasis: Epidemiology, Diagnosis, and Treatment Regimens in Different Geographical Areas with a Focus on Pediatrics. *Microorganisms* **2022**, *10* (10), 1887.

(75) Georgiadou, S. P.; Makaritsis, K. P.; Dalekos, G. N. Leishmaniasis revisited: Current aspects on epidemiology, diagnosis and treatment. *Journal of Translational Internal Medicine* **2015**, *3* (2), 43-50.

(76) Singh, R.; Kashif, M.; Srivastava, P.; Manna, P. P. Recent Advances in Chemotherapeutics for Leishmaniasis: Importance of the Cellular Biochemistry of the Parasite and Its Molecular Interaction with the Host. *Pathogens* **2023**, *12* (5), 706.

(77) Dorlo, T. P. C.; Balasegaram, M.; Beijnen, J. H.; De Vries, P. J. Miltefosine: a review of its pharmacology and therapeutic efficacy in the treatment of leishmaniasis. *Journal of Antimicrobial Chemotherapy* **2012**, *67* (11), 2576-2597.

(78) Sundar, S.; Singh, A.; Tiwari, A.; Shukla, S.; Chakravarty, J.; Rai, M. Efficacy and Safety of Paromomycin in Treatment of Post-Kala-Azar Dermal Leishmaniasis. *ISRN Parasitology* **2014**, *2014*, 1-4.

(79) Sundar, S.; Jha, T. K.; Thakur, C. P.; Sinha, P. K.; Bhattacharya, S. K. Injectable Paromomycin for Visceral Leishmaniasis in India. *New England Journal of Medicine* **2007**, *356* (25), 2571-2581.

(80) Sundar, S.; Chakravarty, J.; Rai, V. K.; Agrawal, N.; Singh, S. P.; Chauhan, V.; Murray, H. W. Amphotericin B Treatment for Indian Visceral Leishmaniasis: Response to 15 Daily versus Alternate-Day Infusions. *Clinical Infectious Diseases* **2007**, *45* (5), 556-561.

(81) Sundar, S.; Chakravarty, J.; Agarwal, D.; Rai, M.; Murray, H. W. Single-Dose Liposomal Amphotericin B for Visceral Leishmaniasis in India. *New England Journal of Medicine* **2010**, *362* (6), 504-512.

(82) De Menezes, J. P. B.; Guedes, C. E. S.; Petersen, A. L. D. O. A.; Fraga, D. B. M.; Veras, P. S. T. Advances in Development of New Treatment for Leishmaniasis. *BioMed Research International* **2015**, *2015*, 1-11.

(83) Lyrio de Oliveira, A. L.; Brustoloni, Y. M.; Fernandes, T. D.; Cavalheiros Dorval, M. E.; da Cunha, R. V.; Bóia, M. N. Severe adverse reactions to meglumine antimoniate in the treatment of visceral leishmaniasis: a report of 13 cases in the southwestern region of Brazil. *Sage Journals* **2009**, *39* (3), 180-182.

(84) Andersen, E. M.; Cruz-Saldarriaga, M.; Llanos-Cuentas, A.; Luz-Cjuno, M.; Echevarria, J.; Miranda-Verastegui, C.; Colina, O.; Berman, J. D. Comparison of meglumine antimoniate and pentamidine for peruvian cutaneous leishmaniasis. *The American Journal of Tropical Medicine and Hygiene* **2005**, *72* (2), 133-137.

(85) J, B.; M, B. M.; Chanda, K. An Overview on the Therapeutics of Neglected Infectious Diseases—Leishmaniasis and Chagas Diseases. *Frontiers in Chemistry* **2021**, *9*.

(86) Antinori, S.; Schifanella, L.; Corbellino, M. Leishmaniasis: new insights from an old and neglected disease. *European Journal of Clinical Microbiology & Infectious Diseases* **2012**, *31* (2), 109-118.

(87) Bhattacharya, K., Sujit; Sinha, K., Prabhat; Sundar, S.; Thakur, P., Chandreshar; Jha, K., Tara; Pandey, K.; Das, R., Vidyanand; Kumar, N.; Lal, C.; Verma, N.*; et al.* Phase 4 Trial of Miltefosine for the Treatment of Indian Visceral Leishmaniasis. *The Journal of Infectious Diseases* **2007**, *196* (4), 591-598.

(88) Gilbert, I. H. Drug Discovery for Neglected Diseases: Molecular Target-Based and Phenotypic Approaches. *Journal of Medicinal Chemistry* **2013**, *56* (20), 7719-7726.

(89) Peña, I.; Pilar Manzano, M.; Cantizani, J.; Kessler, A.; Alonso-Padilla, J.; Bardera, A. I.; Alvarez, E.; Colmenarejo, G.; Cotillo, I.; Roquero, I.*; et al.* New Compound Sets Identified from High Throughput Phenotypic Screening Against Three Kinetoplastid Parasites: An Open Resource. *Scientific Reports* **2015**, *5* (1), 8771.

(90) Zulfiqar, B.; Jones, A.; Sykes, M.; Shelper, T.; Davis, R.; Avery, V. Screening a Natural Product-Based Library against Kinetoplastid Parasites. *Molecules* **2017**, *22* (10), 1715.

(91) Wyllie, S.; Thomas, M.; Patterson, S.; Crouch, S.; De Rycker, M.; Lowe, R.; Gresham, S.; Urbaniak, M. D.; Otto, T. D.; Stojanovski, L.*; et al.* Cyclin-dependent kinase 12 is a drug target for visceral leishmaniasis. *Nature* **2018**, *560* (7717), 192-197.

(92) Wyllie, S.; Brand, S.; Thomas, M.; De Rycker, M.; Chung, C.-W.; Pena, I.; Bingham, R. P.; Bueren-Calabuig, J. A.; Cantizani, J.; Cebrian, D.*; et al.* Preclinical candidate for the treatment of visceral leishmaniasis that acts through proteasome inhibition. *Proceedings of the National Academy of Sciences* **2019**, *116* (19), 9318-9323.

(93) Field, M. C.; Horn, D.; Fairlamb, A. H.; Ferguson, M. A. J.; Gray, D. W.; Read, K. D.; De Rycker, M.; Torrie, L. S.; Wyatt, P. G.; Wyllie, S.*; et al.* Anti-trypanosomatid drug discovery: an ongoing challenge and a continuing need. *Nature Reviews Microbiology* **2017**, *15* (4), 217-231.

(94) Jones, N. G.; Catta-Preta, C. M. C.; Lima, A. P. C. A.; Mottram, J. C. Genetically Validated Drug Targets in *Leishmania*: Current Knowledge and Future Prospects. *ACS Infectious Diseases* **2018**, *4* (4), 467-477.

(95) Sunter, J.; Gull, K. Shape, form, function and *Leishmania* pathogenicity: from textbook descriptions to biological understanding. *Open Biology* **2017**, *7* (9), 170165.

(96) Lidani, K. C. F.; Andrade, F. A.; Tizzot, M. R. P. A.; Costa-Ribeiro, M. C. V.; Beltrame, M. H.; Messias-Reason, I. J. Visceral Leishmaniasis and Natural Infection Rates of *Leishmania* in Lutzomyia longipalpis in Latin America. In *The Epidemiology and Ecology of Leishmaniasis*, 2017.

(97) R., M.-R.; Fuetes, M. Relevance and proteomics challenge of functional posttranslational modifications in Kinetoplastid parasites. *Journal of Proteomics* **2020**, *220*, 103762.

(98) Fernández-Moya, S. M.; Estévez, A. M. Posttranscriptional control and the role of RNA-binding proteins in gene regulation in trypanosomatid protozoan parasites. *WIREs RNA* **2010**, *1* (1), 34-46.

(99) Rochette, A.; Raymond, F.; Ubeda, J.-M.; Smith, M.; Messier, N.; Boisvert, S.; Rigault, P.; Corbeil, J.; Ouellette, M.; Papadopoulou, B. Genome-wide gene expression profiling analysis of *Leishmania major* and *Leishmania infantum* developmental stages reveals substantial differences between the two species. *BMC Genomics* **2008**, *9* (1), 255.

(100) De Pablos, L. M.; Ferreira, T. R.; Dowle, A. A.; Forrester, S.; Parry, E.; Newling, K.; Walrad, P. B. The mRNA-bound Proteome of *Leishmania mexicana*: Novel Genetic Insight into an Ancient Parasite. *Molecular & Cellular Proteomics* **2019**, *18* (7), 1271-1284.

(101) Grünebast, J.; Clos, J. *Leishmania*: Responding to environmental signals and challenges without regulated transcription. *Computational and Structural Biotechnology Journal* **2020**, *18*, 4016-4023.

(102) MartíNez-Calvillo, S.; Yan, S.; Nguyen, D.; Fox, M.; Stuart, K.; Myler, P. J. Transcription of *Leishmania major* Friedlin Chromosome 1 Initiates in Both Directions within a Single Region. *Molecular Cell* **2003**, *11* (5), 1291-1299.

(103) Ivens, A. C.; Peacock, C. S.; Worthey, E. A.; Murphy, L.; Aggarwal, G.; Berriman, M.; Sisk, E.; Rajandream, M.-A.; Adlem, E.; Aert, R.*; et al.* The Genome of the Kinetoplastid Parasite, *Leishmania major*. *Science* **2005**, *309* (5733), 436-442.

(104) Saxena, A.; Lahav, T.; Holland, N.; Aggarwal, G.; Anupama, A.; Huang, Y.; Volpin, H.; Myler, P. J.; Zilberstein, D. Analysis of the *Leishmania donovani* transcriptome reveals an ordered progression of transient and permanent changes in gene expression during differentiation. *Molecular and Biochemical Parasitology* **2007**, *152* (1), 53-65.

(105) MartíNez-Calvillo, S.; Nguyen, D.; Stuart, K.; Myler, P. J. Transcription Initiation and Termination on *Leishmania major* Chromosome 3. *Eukaryotic Cell* **2004**, *3* (2), 506-517.

(106) Jensen, B. C.; Phan, I. Q.; McDonald, J. R.; Sur, A.; Gillespie, M. A.; Ranish, J. A.; Parsons, M.; Myler, P. J. Chromatin-Associated Protein Complexes Link DNA Base J and Transcription Termination in *Leishmania*. *mSphere* **2021**, *6* (1).

(107) Clayton, C. Regulation of gene expression in trypanosomatids: living with polycistronic transcription. *Open Biology* **2019**, *9* (6), 190072.

(108) Mcdonald, J. R.; Jensen, B. C.; Sur, A.; Wong, I. L. K.; Beverley, S. M.; Myler, P. J. Localization of Epigenetic Markers in *Leishmania* Chromatin. *Pathogens* **2022**, *11* (8), 930.

(109) Clayton, C. E. Gene expression in Kinetoplastids. *Current Opinion in Microbiology* **2016**, *32*, 46-51.

(110) Thomas, S.; Green, A.; Sturm, N. R.; Campbell, D. A.; Myler, P. J. Histone acetylations mark origins of polycistronic transcription in *Leishmania major*. *BMC Genomics* **2009**, *10* (1), 152.

(111) Reynolds, D.; Cliffe, L.; Förstner, K. U.; Hon, C.-C.; Siegel, T. N.; Sabatini, R. Regulation of transcription termination by glucosylated hydroxymethyluracil, base J, in *Leishmania major* and *Trypanosoma brucei*. *Nucleic Acids Research* **2014**, *42* (15), 9717-9729.

(112) Kumar, D.; Rajanala, K.; Minocha, N.; Saha, S. Histone H4 lysine 14 acetylation in *Leishmania donovani* is mediated by the MYST-family protein HAT4. *Microbiology* **2012**, *158* (2), 328-337.

(113) Yadav, A.; Chandra, U.; Saha, S. Histone acetyltransferase HAT4 modulates navigation across G2/M and re-entry into G1 in *Leishmania donovani*. *Scientific Reports* **2016**, *6* (1), 27510.

(114) Kumar, D.; Saha, S. HAT3-mediated acetylation of PCNA precedes PCNA monoubiquitination following exposure to UV radiation in *Leishmania donovani*. *Nucleic Acids Research* **2015**, *43* (11), 5423-5441.

(115) Chandra, U.; Yadav, A.; Kumar, D.; Saha, S. Cell cycle stage-specific transcriptional activation of cyclins mediated by HAT2-dependent H4K10 acetylation of promoters in *Leishmania donovani*. *PLOS Pathogens* **2017**, *13*, e1006615

(116) Mai, A.; Cerbara, I.; Valente, S.; Massa, S.; Walker, L. A.; Tekwani, B. L. Antimalarial and Antileishmanial Activities of Aroyl-Pyrrolyl-Hydroxyamides, a New Class of Histone Deacetylase Inhibitors. *Antimicrobial Agents and Chemotherapy* **2004**, *48* (4), 1435-1436.

(117) de Souza, L. Â.; Silva e Bastos, M.; de Melo Agripino, J.; Onofre, T. S.; Calla, L. F. A.; Heimburg, T.; Ghazy, E.; Bayer, T.; da Silva, V. H. F.; Ribeiro, P. D.*; et al.* Histone deacetylases inhibitors as new potential drugs against *Leishmania braziliensis*, the main causative agent of new world tegumentary leishmaniasis. *Biochemical Pharmacology* **2020**, *180* (114191), 1-16.

(118) Corpas-López, V.; Díaz-Gavilán, M.; Franco-Montalbán, F.; Merino-Espinosa, G.; López-Viota, M.; López-Viota, J.; Belmonte-Reche, E.; Pérez-del Palacio, J.; de Pedro, N.; Gómez-Vidal, J. A.*; et al.* A nanodelivered Vorinostat derivative is a promising oral compound for the treatment of visceral leishmaniasis. *Pharmacological Research* **2019**, *139*, 375-383.

(119) Di Bello, E.; Noce, B.; Fioravanti, R.; Zwergel, C.; Valente, S.; Rotili, D.; Fianco, G.; Trisciuoglio, D.; Mourão, M. M.; Sales, P.*; et al.* Effects of Structurally Different HDAC Inhibitors against *Trypanosoma cruzi*, *Leishmania*, and *Schistosoma mansoni*. *ACS Infectious Diseases* **2022**, *8* (7), 1356-1366.

(120) Patil, V.; Guerrant, W.; Chen, P. C.; Gryder, B.; Benicewicz, D. B.; Khan, S. I.; Tekwani, B. L.; Oyelere, A. K. Antimalarial and antileishmanial activities of histone deacetylase inhibitors with triazole-linked cap group. *Bioorganic & Medicinal Chemistry* **2010**, *18* (1), 415-425.

(121) Guerrant, W.; Mwakwari, S. C.; Chen, P. C.; Khan, S. I.; Tekwani, B. L.; Oyelere, A. K. A Structure–Activity Relationship Study of the Antimalarial and Antileishmanial Activities of Nonpeptide Macrocyclic Histone Deacetylase Inhibitors. *ChemMedChem* **2010**, *5* (8), 1232-1235.

(122) Corpas-López, V.; Tabraue-Chávez, M.; Sixto-López, Y.; Panadero-Fajardo, S.; de Lima Franco, F. A.; Domínguez-Seglar, J. F.; Morillas-Márquez, F.; Franco-Montalbán, F.; Díaz-Gavilán, M.; Correa-Basurto, J.*; et al. O*-Alkyl Hydroxamates Display Potent and Selective AntileishmanialActivity. *Journal of Medicinal Chemistry* **2020**, *63* (11), 5625-6248.

(123) Alcolea, P. J.; Alonso, A.; Gómez, M. J.; Moreno, I.; Domínguez, M.; Parro, V.; Larraga, V. Transcriptomics throughout the life cycle of *Leishmania infantum*: High down-regulation rate in the amastigote stage. *International Journal for Parasitology* **2010**, *40* (13), 1497-1516.

(124) Verçoza, B. R. F.; Godinho, J. L. P.; De Macedo-Silva, S. T.; Huber, K.; Bracher, F.; De Souza, W.; Rodrigues, J. C. F. KH-TFMDI, a novel sirtuin inhibitor, alters the cytoskeleton and mitochondrial metabolism promoting cell death in *Leishmania amazonensis*. *Apoptosis* **2017**, *22* (9), 1169-1188.

(125) Tavares, J.; Ouaissi, A.; Kong Thoo Lin, P.; Loureiro, I.; Kaur, S.; Roy, N.; Cordeiro-Da-Silva, A. Bisnaphthalimidopropyl Derivatives as Inhibitors of *Leishmania* SIR2 Related Protein 1. *ChemMedChem* **2010**, *5* (1), 140-147.

(126) Tavares, J.; Ouaissi, A.; Silva, A. M.; Thoo Lin, P. K.; Roy, N.; Cordeiro-da-Silva, A. Anti-leishmanial activity of the bisnaphthalimidopropyl derivatives. *Parasitology International* **2012**, *61* (2), 360-363.

(127) Fioravanti, R.; Mautone, N.; Rovere, A.; Rotili, D.; Mai, A. Targeting histone acetylation/deacetylation in parasites: an update (2017–2020). *Current Opinion in Chemical Biology* **2020**, *57*, 65-74.

(128) Crystal Structure Analysis of bromodomain from *Leishmania donovani* complexed with bromosporine. https://doi.org/10.2210/pdb5C4Q/pdb (accessed Dec 3, 2023).

(129) Domain Swapped Bromodomain from *Leishmania donovani*. https://doi.org/10.2210/pdb5FEA/pdb (accessed Dec 4, 2023).

(130) First Bromodomain from *Leishmania donovani* LdBPK.091320 complexed with BI-2536. https://doi.org/10.2210/pdb5TCM/pdb (accessed Nov 23, 2023).

(131) Crystal structure of LdBPK_091320 with inhibitor bound. https://doi.org/10.2210/pdb6BYA/pdb (accessed Dec 12, 2023).

(132) Second Bromodomain from *Leishmania donovani* LdBPK.091320 complexed with Bromosporine. https://doi.org/10.2210/pdb5TCK/pdb (accessed Nov 23, 2023).

(133) Bowman, B. R.; Moure, C. M.; Kirtane, B. M.; Welschhans, R. L.; Tominaga, K.; Pereira-Smith, O. M.; Quiocho, F. A. Multipurpose MRG Domain Involved in Cell Senescence and Proliferation Exhibits Structural Homology to a DNA-Interacting Domain. *Structure* **2006**, *14* (1), 151-158.

(134) Potter, S. C.; Luciani, A.; Eddy, S. R.; Park, Y.; Lopez, R.; Finn, R. D. HMMER web server: 2018 update. *Nucleic Acids Research* **2018**, *46* (W1), W200-W204.

(135) Picaud, S.; Leonards, K.; Lambert, J.-P.; Dovey, O.; Wells, C.; Fedorov, O.; Monteiro, O.; Fujisawa, T.; Wang, C.-Y.; Lingard, H.*; et al.* Promiscuous targeting of bromodomains by bromosporine identifies BET proteins as master regulators of primary transcription response in leukemia. *Science Advances* **2016**, *2* (10).

(136) Russell, C. N.; Carter, J. L.; Borgia, J. M.; Bush, J.; Calderon, F.; Gabarro, R.; Conway, S. J.; Mottram, J. C.; Wilkinson, A. J.; Jones, N. G. Bromodomain Factor 5 as a

Target for Antileishmanial Drug Discovery. *ACS Infectious Diseases* **2023**, *9* (11), 2340-2357.

(137) Crystal structure of the second bromodomain of BRD5 from *Leishmania donovani*. https://doi.org/10.2210/pdb8BPT/pdb (accessed Dec 7, 2023).

(138) Crystal structure of the bromodomain of human CREBBP in complex with an isoxazolyl-benzimidazole ligand. https://doi.org/10.2210/pdb4NR7/pdb (accessed Dec 15, 2023).

(139) Hewings, D. S.; Fedorov, O.; Filippakopoulos, P.; Martin, S.; Picaud, S.; Tumber, A.; Wells, C.; Olcina, M. M.; Freeman, K.; Gill, A.*; et al.* Optimization of 3,5-Dimethylisoxazole Derivatives as Potent Bromodomain Ligands. *Journal of Medicinal Chemistry* **2013**, *56* (8), 3217-3227.

(140) Hewings, D. S.; Wang, M.; Philpott, M.; Fedorov, O.; Uttarkar, S.; Filippakopoulos, P.; Picaud, S.; Vuppusetty, C.; Marsden, B.; Knapp, S.*; et al.* 3,5-Dimethylisoxazoles Act As Acetyl-lysine-mimetic Bromodomain Ligands. *Journal of Medicinal Chemistry* **2011**, *54* (19), 6761-6770.

(141) Bronner, S. M.; Murray, J.; Romero, F. A.; Wah Lai, K.; Tsui, V.; Cyr, P.; Beresini, M. H.; de leon Boenig, G.; Chen, Z.; Choo, E. F.*; et al.* A Unique Approach to Design Potent and Selective Cyclic Adenosine Monophosphate Response Element Binding Protein, Binding Protein (CBP) Inhibitors. *Journal of Medicinal Chemistry* **2017**, *60* (24), 10151-10171.

(142) Rooney, T. P. C.; Filippakopoulos, P.; Fedorov, O.; Picaud, S.; Cortopassi, W. A.; Hay, D. A.; Martin, S.; Tumber, A.; Rogers, C. M.; Philpott, M.*; et al.* A Series of Potent CREBBP Bromodomain Ligands Reveals an Induced-Fit Pocket Stabilized by a Cation-π Interaction. *Angewandte Chemie International Edition* **2014**, *53* (24), 6126-6130.

(143) Sachchidanand; Resnick-Silverman, L.; Yan, S.; Mutjaba, S.; Liu, W.-j.; Zeng, L.; Manfredi, J. J.; Zhou, M.-M. Target Structure-Based Discovery of Small Molecules that Block Human p53 and CREB Binding Protein Association. *Chemistry & Biology* **2006**, *13*, 81-90.

(144) Crystal structure of the first bromodomain of human BRD4 in complex with bromosporine (BSP). https://doi.org/10.2210/pdb5IGK/pdb (accessed Dec 15, 2023).

(145) Hughes, J.; Rees, S.; Kalindjian, S.; Philpott, K. Principles of early drug discovery. *British Journal of Pharmacology* **2011**, *162* (6), 1239-1249.

(146) Renaud, J.-P.; Chung, C.-W.; Danielson, U. H.; Egner, U.; Hennig, M.; Hubbard, R. E.; Nar, H. Biophysics in drug discovery: impact, challenges and opportunities. *Nature Reviews Drug Discovery* **2016**, *15* (10), 679-698.

(147) Dalvit, C.; Pevarello, P.; Tatò, M.; Veronesi, M.; Vulpetti, A.; Sundström, M. Identification of compounds with binding affinity to proteins via magnetization transfer from bulk water. *Journal of Biomolecular NMR* **2000**, *18* (1), 65-68.

(148) Dalvit, C.; Fogliatto, G.; Stewart, A.; Veronesi, M.; Stockman, B. WaterLOGSY as a method for primary NMR screening: Practical aspects and range of applicability. *Journal of Biomolecular NMR* **2001**, *21* (4), 349-359.

(149) Raingeval, C.; Cala, O.; Brion, B.; Le Borgne, M.; Hubbard, R. E.; Krimm, I. 1D NMR WaterLOGSY as an efficient method for fragment-based lead discovery. *Journal of Enzyme Inhibition and Medicinal Chemistry* **2019**, *34* (1), 1218-1225.

(150) Niesen, F. H.; Berglund, H.; Vedadi, M. The use of differential scanning fluorimetry to detect ligand interactions that promote protein stability. *Nature Protocols* **2007**, *2* (9), 2212-2221.

(151) Waldron, T. T.; Murphy, K. P. Stabilization of Proteins by Ligand Binding: Application to Drug Screening and Determination of Unfolding Energetics. *Biochemistry* **2003**, *42* (17), 5058-5064.

(152) Hubbard, R. E.; Murray, J. B. Experiences in Fragment-Based Lead Discovery. **2011**, *493*, 509509-505315.

(153) Wienken, C. J.; Baaske, P.; Rothbauer, U.; Braun, D.; Duhr, S. Protein-binding assays in biological liquids using microscale thermophoresis. *Nature Communications* **2010**, *1* (1), 100.

(154) Jerabek-Willemsen, M.; André, T.; Wanner, R.; Roth, H. M.; Duhr, S.; Baaske, P.; Breitsprecher, D. MicroScale Thermophoresis: Interaction analysis and beyond. *Journal of Molecular Structure* **2014**, *1077*, 101-113.

(155) Rainard, J. M.; Pandarakalam, G. C.; McElroy, S. P. Using Microscale Thermophoresis to Characterize Hits from High-Throughput Screening: A European Lead Factory Perspective. *SLAS Discovery* **2018**, *23* (3), 225-241.

(156) Pierce, M. M.; Raman, C. S.; Nall, B. T. Isothermal Titration Calorimetry of Protein–Protein Interactions. *Methods* **1999**, *19* (2), 213-221.

(157) Freyer, M. W.; Lewis, E. A. Isothermal titration calorimetry: experimental design, data analysis, and probing macromolecule/ligand binding and kinetic interactions. *Methods in Cell Biology* **2008**, *84*, 79-113.

(158) Velázquez-Campoy, A.; Ohtaka, H.; Nezami, A.; Muzammil, S.; Freire, E. Isothermal Titration Calorimetry. *Current Protocols in Cell Biology* **2004**, *23* (1).

(159) Scott, D. E.; Coyne, A. G.; Hudson, S. A.; Abell, C. Fragment-Based Approaches in Drug Discovery and Chemical Biology. *Biochemistry* **2012**, *51* (25), 4990-5003.

(160) Edgar, R. C. MUSCLE: multiple sequence alignment with high accuracy and high throughput *Nucleic Acids Research* **2004**, *32* (5), 1792-1797.

(161) Schiedel, M.; Moroglu, M.; Ascough, D. M. H.; Chamberlain, A. E. R.; Kamps, J. J. A. G.; Sekirnik, A. R.; Conway, S. J. Chemical Epigenetics: The Impact of Chemical and Chemical Biology Techniques on Bromodomain Target Validation. *Angewandte Chemie International Edition* **2019**, *58* (50), 17930-17952.

(162) Pfister, S. X.; Ashworth, A. Marked for death: targeting epigenetic changes in cancer. *Nature Reviews Drug Discovery* **2017**, *16* (4), 241-263.

(163) Fujisawa, T.; Filippakopoulos, P. Functions of bromodomain-containing proteins and their roles in homeostasis and cancer. *Nature Reviews Molecular Cell Biology* **2017**, *18* (4), 246-262.

(164) Schiedel, M.; Mcardle, D.; Padalino, G.; Chan, A.; Forde-Thomas, J.; Mcdonough, M.; Whiteland, H.; Beckmann, M.; Cookson, R.; Hoffmann, K.*; et al.* Small Molecule Ligands of the BET-like Bromodomain, *Sm*BRD3, Affect *Schistosoma mansoni* Survival, Oviposition, and Development. *Journal of Medicinal Chemistry* **2023**, *66* (23), 15565-16454.

(165) Dawson, M. A.; Prinjha, R. K.; Dittmann, A.; Giotopoulos, G.; Bantscheff, M.; Chan, W.-I.; Robson, S. C.; Chung, C.-W.; Hopf, C.; Savitski, M. M.*; et al.* Inhibition of BET recruitment to chromatin as an effective treatment for MLL-fusion leukaemia. *Nature* **2011**, *478* (7370), 529-533.

(166) Martin, L. J.; Koegl, M.; Bader, G.; Cockcroft, X.-L.; Fedorov, O.; Fiegen, D.; Gerstberger, T.; Hofmann, M. H.; Hohmann, A. F.; Kessler, D.*; et al.* Structure-Based Design of an in Vivo Active Selective BRD9 Inhibitor. *Journal of Medicinal Chemistry* **2016**, *59* (10), 4462-4475.

(167) Demont, E. H.; Bamborough, P.; Chung, C.-W.; Craggs, P. D.; Fallon, D.; Gordon, L. J.; Grandi, P.; Hobbs, C. I.; Hussain, J.; Jones, E. J.*; et al.* 1,3-Dimethyl Benzimidazolones Are Potent, Selective Inhibitors of the BRPF1 Bromodomain. *ACS Medicinal Chemistry Letters* **2014**, *5* (11), 1190-1195.

(168) Bennett, J.; Fedorov, O.; Tallant, C.; Monteiro, O.; Meier, J.; Gamble, V.; Savitsky, P.; Nunez-Alonso, G. A.; Haendler, B.; Rogers, C.*; et al.* Discovery of a Chemical Tool Inhibitor Targeting the Bromodomains of TRIM24 and BRPF. *Journal of Medicinal Chemistry* **2016**, *59* (4), 1642-1647.

(169) Bamborough, P.; Barnett, H. A.; Becher, I.; Bird, M. J.; Chung, C.-W.; Craggs, P. D.; Demont, E. H.; Diallo, H.; Fallon, D. J.; Gordon, L. J.*; et al.* GSK6853, a Chemical Probe for Inhibition of the BRPF1 Bromodomain. *ACS Medicinal Chemistry Letters* **2016**, *7* (6), 552-557.

(170) Fedorov, O.; Lingard, H.; Wells, C.; Monteiro, O. P.; Picaud, S.; Keates, T.; Yapp, C.; Philpott, M.; Martin, S. J.; Felletar, I.*; et al.* [1,2,4]Triazolo[4,3-*a*]phthalazines: Inhibitors of Diverse Bromodomains. *Journal of Medicinal Chemistry* **2014**, *57* (2), 462-476.

(171) Divakaran, A.; Harki, D. A.; Pomerantz, W. C. K. Recent progress and structural analyses of domain-selective BET inhibitors. *Medicinal Research Reviews* **2023**, *43* (4), 972-1018.

(172) 5UEP. https://doi.org/10.2210/pdb5UEP/pdb (accessed Nov 23, 2023).

(173) Chung, C.-W.; Dean, A. W.; Woolven, J. M.; Bamborough, P. Fragment-Based Discovery of Bromodomain Inhibitors Part 1: Inhibitor Binding Modes and Implications for Lead Discovery. *Journal of Medicinal Chemistry* **2012**, *55* (2), 576-586.

(174) Watson, R. J.; Bamborough, P.; Barnett, H.; Chung, C.-w.; Davis, R.; Gordon, L.; Grandi, P.; Petretich, M.; Phillipou, A.; Prinjha, R. K.*; et al.* GSK789: A Selective Inhibitor of the First Bromodomains (BD1) of the Bromo and Extra Terminal Domain (BET) Proteins. *Journal of Medicinal Chemistry* **2020**, *63* (17), 9045–9069.

(175) Bamborough, P.; Chung, C.-W. Fragments in bromodomain drug discovery. *MedChemComm* **2015**, *6* (9), 1587-1604.

(176) 3MXF Crystal Structure of the first bromodomain of human BRD4 in complex with the inhibitor JQ1. https://doi.org/10.2210/pdb3MXF/pdb (accessed Nov 23, 2023).

(177) Crystal structure of the first bromodomain (BD1) of human BRD4 bound to bromosporine. https://doi.org/10.2210/pdb6V0U/pdb (accessed Dec 12, 2023).

(178) 5MLJ Bromodomain of Human GCN5 with 4-bromo-2-methyl-5-(((3*R*,5*R*)-1-methyl-5-phenylpiperidin-3-yl)amino)pyridazin-3(2*H*)-one.
https://doi.org/10.2210/pdb5MLJ/pdb (accessed Dec 12, 2023).

(179) 6FSY Crystal Structure of the first bromodomain of human BRD4 in complex with a 3,5-dimethylisoxazol ligand. https://doi.org/10.1016/j.bmc.2018.05.003 (accessed Nov 23, 2023).

(180) Prudent, R.; Annis, D. A.; Dandliker, P. J.; Ortholand, J.-Y.; Roche, D. Exploring new targets and chemical space with affinity selection-mass spectrometry. *Nature Reviews Chemistry* **2020**, *5* (1), 62-71.

(181) Miyaura, N.; Yanagi, T.; Suzuki, A. The Palladium-Catalyzed Cross-Coupling Reaction of Phenylboronic Acid with Haloarenes in the Presence of Bases. *Synthetic Communications* **1981**, *11* (7), 513-519.

(182) Hayes, H. L. D.; Wei, R.; Assante, M.; Geogheghan, K. J.; Jin, N.; Tomasi, S.; Noonan, G.; Leach, A. G.; Lloyd-Jones, G. C. Protodeboronation of (Hetero)Arylboronic Esters: Direct versus Prehydrolytic Pathways and Self-/Auto-Catalysis. *Journal of the American Chemical Society* **2021**, *143* (36), 14814-14826.

(183) Lennox, A. J. J.; Lloyd-Jones, G. C. The Slow-Release Strategy in Suzuki–Miyaura Coupling. *Israel Journal of Chemistry* **2010**, *50* (5-6), 664-674.

(184) McOmie, J. F. W.; Watts, M. L.; West, D. E. Demethylation of aryl methyl ethers by boron tribromide. *Tetrahedron* **1968**, *24* (5), 2289-2292.

(185) Familoni, O. B.; Klaas, P. J.; Lobb, K. A.; Pakade, V. E.; Kaye, P. T. The Baylis–Hillman approach to quinoline derivatives. *Org. Biomol. Chem.* **2006**, *4* (21), 3960-3965.

(186) Takahashi, M.; Konishi, H.; Iida, S.; Nakamura, K.; Yamamura, S.; Nishiyama, S. Phenolic oxidation of *o*,*o*′-dihalogenated phenols. *Tetrahedron* **1999**, *55* (17), 5295-5302.

(187) Jimenez, L.; Ramanathan, A. Reductive Dehalogenation of Aryl Bromides and Chlorides and Their Use as Aryl Blocking Groups. *Synthesis* **2010**, *2010* (02), 217-220.

(188) Shankar, R. B.; Pews, R. G. Synthesis of 1,2,4-triazolo[1,5-*a*]pyrimidine-2-sulfonamides. *Journal of Heterocyclic Chemistry* **1993**, *30* (1), 169-172.

(189) Béchamp, A. De l'action des protosels de fer sur la nitronaphtaline et la nitrobenzine. nouvelle méthode de formation des bases organiques artificielles de Zinin. *Annales de chimie et de physique* **1854**, *42*, 186–196.

(190) Hay, D.; Fedorov, O.; Filippakopoulos, P.; Martin, S.; Philpott, M.; Picaud, S.; Hewings, D. S.; Uttakar, S.; Heightman, T. D.; Conway, S. J.*; et al.* The design and synthesis of 5- and 6-isoxazolylbenzimidazoles as selective inhibitors of the BET bromodomains. *MedChemComm* **2013**, *4* (1), 140-144.

(191) Chen, C.-Y.; Andreani, T.; Li, H. A Divergent and Selective Synthesis of Isomeric Benzoxazoles from a Single N–Cl Imine. *Organic Letters* **2011**, *13* (23), 6300-6303.

(192) Zhang, M.; Zhang, Y.; Song, M.; Xue, X.; Wang, J.; Wang, C.; Zhang, C.; Li, C.; Xiang, Q.; Zou, L.*; et al.* Structure-Based Discovery and Optimization of Benzo[*d*]isoxazole Derivatives as Potent and Selective BET Inhibitors for Potential Treatment of Castration-Resistant Prostate Cancer (CRPC). *Journal of Medicinal Chemistry* **2018**, *61* (7), 3037-3058.

(193) Kim, B. H.; Moo Jun, Y.; Kim, T. K.; Lee, Y. S.; Baik, W.; Min Lee, B. 2-Bromo-2-nitropropane/Zn Promoted Reductive Cyclizations of Ortho-substituted Nitroarenes toward 2,1-Benzisoxazole Derivatives. *Heterocycles* **1997**, *45* (2), 235-240.

(194) 4NYW Crystal Structure of the Bromodomain of human CREBBP in complex with a dihydroquinoxalinone ligand. https://doi.org/10.2210/pdb4NYW/pdb (accessed Nov 23, 2023).

(195) Friedel, C.; Craft, J. M. A New General Synthetical Method of Producing Hydrocarbons. *Organic Chemistry* **1877**, *32*, 725.

(196) Barraja, P.; Spanò, V.; Patrizia, D.; Carbone, A.; Cirrincione, G.; Vedaldi, D.; Salvador, A.; Viola, G.; Dall'Acqua, F. Pyrano[2,3-e]isoindol-2-ones, new angelicin heteroanalogues. *Bioorganic & Medicinal Chemistry Letters* **2009**, *19* (6), 1711-1714.

(197) Rancan, E.; Aricò , F.; Quartarone, G.; Ronchin , L.; Tundo, P.; Vavasori, A. Self-catalyzed direct amidation of ketones: A sustainable procedure for acetaminophen synthesis. *Catalysis Communications* **2014**, *54*, 11-16.

(198) Rosano, G. L.; Ceccarelli, E. A. Recombinant protein expression in *Escherichia coli*: advances and challenges. *Frontiers in Microbiology* **2014**, *5* (172), 1-17.

(199) Gutiérrez-González, M.; Farías, C.; Tello, S.; Pérez-Etcheverry, D.; Romero, A.; Zúñiga, R.; Ribeiro, C. H.; Lorenzo-Ferreiro, C.; Molina, M. C. Optimization of culture conditions for the expression of three different insoluble proteins in *Escherichia coli*. *Scientific Reports* **2019**, *9* (1).

(200) Geoghegan, K. F.; Dixon, H. B. F.; Rosner, P. J.; Hoth, L. R.; Lanzetti, A. J.; Borzilleri, K. A.; Marr, E. S.; Pezzullo, L. H.; Martin, L. B.; LeMotte, P. K.*; et al.* Spontaneous α-*N*-6-Phosphogluconoylation of a "His Tag" in *Escherichia coli*: The Cause of Extra Mass of 258 or 178 Da in Fusion Proteins. *Analytical Biochemistry* **1999**, *267* (1), 169-184.

(201) Erlanson, D. A.; Fesik, S. W.; Hubbard, R. E.; Jahnke, W.; Jhoti, H. Twenty years on: the impact of fragments on drug discovery. *Nature Reviews Drug Discovery* **2016**, *15* (9), 605-619.

(202) Linke, P.; Amaning, K.; Maschberger, M.; Vallee, F.; Steier, V.; Baaske, P.; Duhr, S.; Breitsprecher, D.; Rak, A. An Automated Microscale Thermophoresis Screening Approach for Fragment-Based Lead Discovery. *SLAS Discovery* **2016**, *21* (4), 414-421.

(203) Redhead, M.; Satchell, R.; Mccarthy, C.; Pollack, S.; Unitt, J. Thermal Shift as an Entropy-Driven Effect. *Biochemistry* **2017**, *56* (47), 6187-6199.

(204) Bataille, C.; Rabbitts, T.; Claridge, T. NMR waterLOGSY as An Assay in Drug Development Programmes for Detecting Protein-Ligand Interactions–NMR waterLOGSY. *Bio-Protocol* **2020**, *10* (13).

(205) Hill, A. P.; Young, R. J. Getting physical in drug discovery: a contemporary perspective on solubility and hydrophobicity. *Drug Discovery Today* **2010**, *15* (15-16), 648-655.

(206) Li, Q.; Kang, C. A Practical Perspective on the Roles of Solution NMR Spectroscopy in Drug Discovery. *Molecules* **2020**, *25* (13), 2974.

(207) Hammitzsch, A.; Tallant, C.; Fedorov, O.; O'Mahony, A.; Brennan, P. E.; Hay, D. A.; Martinez, F. O.; Al-Mossawi, M. H.; De Wit, J.; Vecellio, M.*; et al.* CBP30, a selective CBP/p300 bromodomain inhibitor, suppresses human Th17 responses. *Proceedings of the National Academy of Sciences* **2015**, *112* (34), 10768-10773.

(208) Jones, G.; Willett, P.; Glen, R. C.; Leach, A. R.; Taylor, R. Development and Validation of a Genetic Algorithm for Flexible Docking. *Journal of Molecular Biology* **1997**, (267), 727-748.

(209) Kumar, V.; Poojary, B.; Prathibha, A.; Shruthi, N. Synthesis of Some Novel 1,2-Disubstituted Benzimidazole-5-carboxylates via One-Pot Method Using Sodium Dithionite and Its Effect on *N*-Debenzylation. *Synthetic Communications* **2014**, *44* (23), 3414-3425.

(210) Yang, D.; Fokas, D.; Li, J.; Yu, L.; Baldino, C. M. A Versatile Method for the Synthesis of Benzimidazoles from *o*-Nitroanilines and Aldehydes in One Step *via* a Reductive Cyclization. *Synthesis* **2005**, *36* (21), 47-56.

(211) Wen, X.; El Bakali, J.; Deprez-Poulain, R.; Deprez, B. Efficient propylphosphonic anhydride (®T3P) mediated synthesis of benzothiazoles, benzoxazoles and benzimidazoles. *Tetrahedron Letters* **2012**, *53* (19), 2440-2443.

(212) Barasa, L.; Yoganathan, S. An efficient one-pot conversion of carboxylic acids into benzimidazoles *via* an HBTU-promoted methodology. *RSC Advances* **2018**, *8* (62), 35824-35830.

(213) Carpino, L. A. 1-Hydroxy-7-azabenzotriazole. An efficient peptide coupling additive. *Journal of the American Chemical Society* **1993**, *115* (10), 4397-4398.

(214) Bhal, S. K.; Kassam, K.; Peirson, I. G.; Pearl, G. M. The Rule of Five Revisited: Applying Log *D* in Place of Log *P* in Drug-Likeness Filters. *Molecular Pharmaceutics* **2007**, *4* (4), 556-560.

(215) Valkó, K.; Bevan, C.; Reynolds, D. Chromatographic Hydrophobicity Index by Fast-Gradient RP-HPLC: A High-Throughput Alternative to log P/log D. *Analytical Chemistry* **1997**, *69* (11), 2022-2029.

(216) Wilcken, R.; Zimmermann, M. O.; Lange, A.; Joerger, A. C.; Boeckler, F. M. Principles and Applications of Halogen Bonding in Medicinal Chemistry and Chemical Biology. *Journal of Medicinal Chemistry* **2013**, *56* (4), 1363-1388.

(217) Patterson, S.; Wyllie, S. Nitro drugs for the treatment of trypanosomatid diseases: past, present, and future prospects. *Trends in Parasitology* **2014**, *30* (6), 289–298.

(218) Patterson, S.; Fairlamb, A. H. Current and Future Prospects of Nitro-compounds as Drugs for Trypanosomiasis and Leishmaniasis. *Current Medicinal Chemistry* **2019**, *26* (23), 4454-4475.

(219) Reguera, R. M.; Pérez-Pertejo, Y.; Gutiérrez-Corbo, C.; Domínguez-Asenjo, B.; Ordóñez, C.; García-Estrada, C.; Martínez-Valladares, M.; Balaña-Fouce, R. Current and promising novel drug candidates against visceral leishmaniasis. *Pure and Applied Chemistry* **2019**, *91* (8), 1385–1404.

(220) Hidalgo, J.; Ortiz, J. F.; Fabara, S. P.; Eissa-Garcés, A.; Reddy, D.; Collins, K. D.; Tirupathi, R. Efficacy and Toxicity of Fexinidazole and Nifurtimox Plus Eflornithine in the Treatment of African Trypanosomiasis. *Cureus* **2021**.

(221) Boelsterli, U. A.; Ho, H. K.; Zhou, S.; Leow, K. Y. Bioactivation and hepatotoxicity of nitroaromatic drugs. *Current Drug Metabolism* **2006**, *7* (7), 715-727.

(222) G.F. Whitmore, A. J. V. The biological properties of reduced nitroheterocyclics and possible underlying biochemical mechanisms. *Biochemical Pharmacology* **1986**, *35* (1), 97-103.

(223) Pal, C.; Bandyopadhyay, U. Redox-Active Antiparasitic Drugs. *Antioxidants and Redox Signaling* **2012**, *17* (4), 555-582.

(224) Fleming, F. F.; Yao, L.; Ravikumar, P. C.; Funk, L.; Shook, B. C. Nitrile-Containing Pharmaceuticals: Efficacious Roles of the Nitrile Pharmacophore. *Journal of Medicinal Chemistry* **2010**, *53* (22), 7902-7917.

(225) Vazquez, M. L.; Kaila, N.; Strohbach, J. W.; Trzupek, J. D.; Brown, M. F.; Flanagan, M. E.; Mitton-Fry, M. J.; Johnson, T. A.; Tenbrink, R. E.; Arnold, E. P.*; et al.* Identification of *N*-{*cis*-3-[Methyl(7*H*-pyrrolo[2,3-*d*]pyrimidin-4-yl)amino]cyclobutyl}propane-1-sulfonamide (PF-04965842): A Selective JAK1 Clinical Candidate for the Treatment of Autoimmune Diseases. *Journal of Medicinal Chemistry* **2018**, *61* (3), 1130-1152.

(226) Boehringer, M.; Fischer, H.; Hennig, M.; Hunziker, D.; Huwyler, J.; Kuhn, B.; Loeffler, B. M.; Luebbers, T.; Mattei, P.; Narquizian, R.*; et al.* Aryl- and heteroaryl-substituted aminobenzo[*a*]quinolizines as dipeptidyl peptidase IV inhibitors. *bioorganic & Medicinal Chemistry Letters* **2010**, *20* (3), 1106-1108.

(227) Pavana, R. K.; Choudhary, S.; Bastian, A.; Ihnat, M. A.; Bai, R.; Hamel, E.; Gangjee, A. Discovery and preclinical evaluation of 7-benzyl-*N*-(substituted)-pyrrolo[3,2-*d*]pyrimidin-4-amines as single agents with microtubule targeting effects along with triple-acting angiokinase inhibition as antitumor agents. *Bioorganic & Medicinal Chemistry* **2017**, *25* (2), 545-556.

(228) Kuntz, K. W.; Campbell, J. E.; Keilhack, H.; Pollock, R. M.; Knutson, S. K.; Porter-Scott, M.; Richon, V. M.; Sneeringer, C. J.; Wigle, T. J.; Allain, C. J.*; et al.* The Importance of Being Me: Magic Methyls, Methyltransferase Inhibitors, and the Discovery of Tazemetostat. *Journal of Medicinal Chemistry* **2016**, *59* (4), 1556-1564.

(229) Schçnherr, H.; Cernak, T. Profound Methyl Effects in Drug Discovery and a Call for New C-H Methylation Reactions. *Angewandte Chemie International Edition* **2013**, *52*, 12256-12267.

(230) Keil, S.; Urmann, M.; Glien, M.; Wendler, W.; Chandross, K.; Lee, L. Derivatives of 2 -Aminthiazoles and 2-aminooxazoles, processes for their preparation and their use as pharmaceuticals. US WO2007039176A1, 2007.

(231) Heck, R. F.; Nolley, J. P. Palladium-catalyzed vinylic hydrogen substitution reactions with aryl, benzyl, and styryl halides. *The Journal of Organic Chemistry* **1972**, *37* (14), 2320-2322.

(232) Tsunoda, T.; Yamamiya, Y.; Itô, S. 1,1‘-(Azodicarbonyl)dipiperidine-Tributylphosphine, A New Reagent System for Mitsunobu Reaction *tetrahedron Letters* **1993**, *34* (10), 1639-1642.

(233) Kumari, A.; Singh, R. K. Morpholine as ubiquitous pharmacophore in medicinal chemistry: Deep insight into the structure-activity relationship (SAR). *Bioorganic Chemistry* **2020**, *96* (103578).

(234) Kramer, C.; Fuchs, J. E.; Liedl, K. R. Strong Nonadditivity as a Key Structure−Activity Relationship Feature: Distinguishing Structural Changes from Assay Artifacts. *Journal of Chemical Information and Modeling* **2015**, *55*, 483-494.

(235) Gomez, L.; Xu, R.; Sinko, W.; Selfridge, B.; Vernier, W.; Ly, K.; Truong, R.; Metz, M.; Marrone, T.; Sebring, K.*; et al.* Mathematical and Structural Characterization of Strong Nonadditive Structure−Activity Relationship Caused by Protein Conformational Changes. *Journal of Medicinal Chemistry* **2018**, *61*, 7754-7766.

(236) Vu, V.; Szewczyk, M. M.; Nie, D. Y.; Arrowsmith, C. H.; Barsyte-Lovejoy, D. Validating Small Molecule Chemical Probes for Biological Discovery. *Annual Review of Biochemistry* **2022**, *91* (1), 61-87.

(237) Sterling, J.; Baker, J. R.; Mccluskey, A.; Munoz, L. Systematic literature review reveals suboptimal use of chemical probes in cell-based biomedical research. *Nature Communications* **2023**, *14* (1).

(238) Frye, S. V. The art of the chemical probe. *Nature Chemical Biology* **2010**, *6* (3), 159-161.

(239) Workman, P.; Collins, I. Probing the Probes: Fitness Factors For Small Molecule Tools. *Chemistry & Biology* **2010**, *17* (6), 561-577.

(240) Croft, S. L.; Engel, J. Miltefosine — discovery of the antileishmanial activity of phospholipid derivatives. *Transactions of The Royal Society of Tropical Medicine and Hygiene* **2006**, *100*, S4-S8.

(241) Docampo, R. Sensitivity of parasites to free radical damage by antiparasitic drugs. *Chemico-Biological Interactions* **1990**, *73* (1), 1-27.

(242) Bichiou, H.; Rabhi, S.; Ben Hamda, C.; Bouabid, C.; Belghith, M.; Piquemal, D.; Trentin, B.; Rabhi, I.; Guizani-Tabbane, L. *Leishmania* Parasites Differently Regulate Antioxidant Genes in Macrophages Derived From Resistant and Susceptible Mice. *Frontiers in Cellular and Infection Microbiology* **2021**, *11* (748738).

(243) Malan, S. F.; Chetty, D. J.; du Plessis, J. Physicochemical properties of drugs and membrane permeability. *South African Journal of Science* **2002**, *98*, 385-391.

(244) Matsson, P. r.; Kihlberg, J. How Big Is Too Big for Cell Permeability? *Journal of Medicinal Chemistry* **2017**, *60*, 1662-1664.

(245) Sander, T.; Freyss, J.; Von Korff, M.; Rufener, C. DataWarrior: An Open-Source Program For Chemistry Aware Data Visualization And Analysis. *Journal of Chemical Information and Modeling* **2015**, *55* (2), 460-473.

(246) Kaur, G.; Grewal, J.; Jyoti, K.; Jain, U. K.; Chandra, R.; Madan, J. Chapter 15 - Oral controlled and sustained drug delivery systems: Concepts, advances, preclinical, and clinical status. In *Drug Targeting and Stimuli Sensitive Drug Delivery Systems*, Grumezescu, A. M. Ed.; Publisher: Place Published, 2018.

(247) Lobo, S. Is there enough focus on lipophilicity in drug discovery? *Expert Opinion on Drug Discovery* **2020**, *15* (3), 261-263.

(248) Lipinski, C.; lLombardo, F.; Dominy, B. W.; Feeney, P. J. Experimental and computational approaches to estimate solubility and permeability in drug discovery and development settings. *Advanced Drug Delivery Reviews* **1997**, *23* (1-3), 3-25.

(249) Bunally, S.; Young, R. J. The role and impact of high throughput biomimetic measurements in drug discovery. *ADMET and DMPK* **2018**, *6* (2), 74-84.

(250) Caron, G.; Ermondi, G. Molecular descriptors for polarity: the need for going beyond polar surface area. *Future Medicinal Chemistry* **2016**, *8* (17), 2013-2016.

(251) Ertl, P.; Rohde, B.; Selzer, P. Fast Calculation of Molecular Polar Surface Area as a Sum of Fragment-Based Contributions and Its Application to the Prediction of Drug Transport Properties. *Journal of Medicinal Chemistry* **2000**, *43*, 3714-3717.

(252) Prasanna, S.; Doerksen, R. J. Topological Polar Surface Area: A Useful Descriptor in 2D-QSAR. *Current Medicinal Chemistry* **2009**, *16* (1), 21-41.

(253) Coimbra, J. T. S.; Feghali, R.; Ribeiro, R. P.; Ramos, M. J.; Fernandes, P. A. The importance of intramolecular hydrogen bonds on the translocation of the small drug piracetam through a lipid bilayer. *RSC Advances* **2021**, *11* (2), 899-908.

(254) Bardal, S. K.; Waechter, J. E.; Martin, D. S. Pharmacokinetics. In *Applied Pharmacology*, Bardal, S. K., Waechter, J. E., Martin, D. S. Eds.; Publisher: Place Published, 2011; pp 17-34.

(255) Galdeano, C.; Ciulli, A. Selectivity on-target of bromodomain chemical probes by structure-guided medicinal chemistry and chemical biology. *Future Medicinal Chemistry* **2016**, *8* (13), 1655-1680.

(256) Padmanabhan, B.; Mathur, S.; Manjula, R.; Tripathi, S. Bromodomain and extra-terminal (BET) family proteins: New therapeutic targets in major diseases. *Journal of Biosciences* **2016**, *41* (2), 295-311.

(257) Belkina, A. C.; Denis, G. V. BET domain co-regulators in obesity, inflammation and cancer. *Nature Reviews Cancer* **2012**, *12* (7), 465-477.

(258) Crystal structure of the first bromodomain of human BRD4 in complex with an isoxazolyl-benzimidazole ligand. https://doi.org/10.2210/pdb4NR8/pdb (accessed 15 Dec, 2023).

(259) Korzekwa, K.; Trager, W.; Gouterman, M.; Spangler, D.; Loew, G. Cytochrome P450 mediated aromatic oxidation: a theoretical study. *Journal of the American Chemical Society* **1985**, *107* (14), 4273-4279.

(260) Ballard, P.; Brassil, P.; Bui, K. H.; Dolgos, H.; Petersson, C.; Tunek, A.; Webborn, P. J. H. Chapter 10 - Metabolism and pharmacokinetic optimization strategies in drug discovery. In *Drug Discovery and Development (Second Edition)*, 2 ed.; Hill, R. G., Rang, H. P. Eds.; Publisher: Place Published, 2013; pp 135-155.

(261) La Du, B. Plasma esterase activity and the metabolism of drugs with ester groups. *Annals of the New York Academy of Sciences* **1971**, *179* (1), 684-694.

(262) Young, R. J.; Green, D. V. S.; Luscombe, C. N.; Hill, A. P. Getting physical in drug discovery II: the impact of chromatographic hydrophobicity measurements and aromaticity. *Drug Discovery Today* **2011**, *16* (17-18), 822-830.

(263) Murray, C. W.; Erlanson, D. A.; Hopkins, A. L.; Keserü, G. M.; Leeson, P. D.; Rees, D. C.; Reynolds, C. H.; Richmond, N. J. Validity of Ligand Efficiency Metrics. *ACS Medicinal Chemistry Letters* **2014**, *5* (6), 616-618.

(264) Gilan, O.; Rioja, I.; Knezevic, K.; Bell, M. J.; Yeung, M. M.; Harker, N. R.; Lam, E. Y. N.; Chung, C. W.; Bamborough, P.; Petretich, M.*; et al.* Selective targeting of BD1 and BD2 of the BET proteins in cancer and immunoinflammation. *Science* **2020**, *368* (6489), 387-394.

(265) Faust, T. B.; Donovan, K. A.; Yue, H.; Chamberlain, P. P.; Fischer, E. S. Small-Molecule Approaches to Targeted Protein Degradation. *Annual Review of Cancer Biology* **2021**, *5* (1), 181-201.

(266) Robers, M. B.; Dart, M. L.; Woodroofe, C. C.; Zimprich, C. A.; Kirkland, T. A.; Machleidt, T.; Kupcho, K. R.; Levin, S.; Hartnett, J. R.; Zimmerman, K.*; et al.* Target engagement and drug residence time can be observed in living cells with BRET. *Nature Communications* **2015**, *6* (1), 10091.

(267) Machleidt, T.; Woodroofe, C. C.; Schwinn, M. K.; Méndez, J.; Robers, M. B.; Zimmerman, K.; Otto, P.; Daniels, D. L.; Kirkland, T. A.; Wood, K. V. NanoBRET—A Novel BRET Platform for the Analysis of Protein–Protein Interactions. *ACS Chemical Biology* **2015**, *10* (8), 1797-1804.

(268) Kurzawa, N.; Leo, I. R.; Stahl, M.; Kunold, E.; Becher, I.; Audrey, A.; Mermelekas, G.; Huber, W.; Mateus, A.; Savitski, M. M.*; et al.* Deep thermal profiling for detection of functional proteoform groups. *Nature Chemical Biology* **2023**, *19* (8), 962-971.

(269) Doudna, J. A.; Charpentier, E. The new frontier of genome engineering with CRISPR-Cas9. *Science* **2014**, *346* (6213), 1258096–1258096.

(270) Di Cristina, M.; Carruthers, V. B. New and emerging uses of CRISPR/Cas9 to genetically manipulate apicomplexan parasites. *Parasitology* **2018**, *145* (9), 1119-1126.

(271) Neggers, J. E.; Kwanten, B.; Dierckx, T.; Noguchi, H.; Voet, A.; Bral, L.; Minner, K.; Massant, B.; Kint, N.; Delforge, M.*; et al.* Target identification of small molecules using large-scale CRISPR-Cas mutagenesis scanning of essential genes. *Nature Communications* **2018**, *9* (1).

(272) BROMOscan Technology. https://www.eurofinsdiscovery.com/solution/bromoscan-technology (accessed Nov 23, 2023).

(273) Fulmer, G. R.; Miller, A. J. M.; Sherden, N. H.; Gottlieb, H. E.; Nudelman, A.; Stoltz, B. M.; Bercaw, J. E.; Goldberg, K. I. NMR Chemical Shifts of Trace Impurities: Common Laboratory Solvents, Organics, and Gases in Deuterated Solvents Relevant to the Organometallic Chemist. *Organometallics* **2010**, *29* (9), 2176-2179.

(274) Kolosov, M.; Shvets, E.; Manuenkov, D.; Vlasenko, S.; Omelchenko, I.; Shishkina, S.; Orlov, V. A synthesis of 6-functionalized 4,7-dihydro[1,2,4]triazolo[1,5-*a*]pyrimidines. *Tetrahedron Letters* **2017**, *58* (12), 1207-1210.

(275) SDBSWeb. https://sdbs.db.aist.go.jp (accessed Jan 12, 2023).

(276) Paudler, W. W.; Helmick, L. S. Ten π -electron nitrogen heterocyclic compounds: X The syntheses and structure determinations of some 1,2,4-Triazolopyrimidines. *Journal of Heterocyclic Chemistry* **1966**, *3* (3), 269-271.

(277) Liscio, P.; Carotti, A.; Asciutti, S.; Karlberg, T.; Bellocchi, D.; Llacuna, L.; Macchiarulo, A.; Aaronson, S. A.; Schüler, H.; Pellicciari, R.*; et al.* Design, synthesis, crystallographic studies, and preliminary biological appraisal of new substituted triazolo[4,3-*b*]pyridazin-8-amine derivatives as tankyrase inhibitors. *Journal of Medicinal Chemistry* **2014**, *57* (6), 2807-2812.

(278) D'Ascenzio, M.; Pugh, K. M.; Konietzny, R.; Berridge, G.; Tallant, C.; Hashem, S.; Monteiro, O.; Thomas, J. R.; Schirle, M.; Knapp, S.*; et al.* An Activity-Based Probe

Targeting Non-Catalytic, Highly Conserved Amino Acid Residues within Bromodomains. *Angewandte Chemie International Edition* **2019**, *58* (4), 1007-1012.

(279) Wilson, B. Developing small molecule inhibitors of bromodomain-histone interactions. PhD Thesis, University of Oxford, 2015.

(280) Alazawe, S.; Elvidge, J. A. Heterocyclic imines and amines. Part XVII. Confirmation of the structures of two aminopyridazinones. *Journal of the Chemical Society, Perkin Transactions 1* **1974**, 696.

(281) Li, X.; Wu, Y.; Tian, G.; Jiang, Y.; Liu, Z.; Meng, X.; Bao, X.; Feng, L.; Sun, H.; Deng, H.*; et al.* Chemical Proteomic Profiling of Bromodomains Enables the Wide-Spectrum Evaluation of Bromodomain Inhibitors in Living Cells. *Journal of the American Chemical Society* **2019**, *141* (29), 11497-11505.

(282) Pollak, A.; Tišler, M. Synthesis of pyridazine derivatives—V : Formation of *s*-triazolo-(4,3-*b*)-pyridazines and bis-*s*-triazolo-(4,3-*b*,3′,4′-*f*)-pyridazines. *Tetrahedron* **1966**, *22* (7), 2073-2079.

(283) Mamta.; Aggarwal, R.; Sadana, R.; Ilag, J.; Sumran, G. Synthesis and bioevaluation of 6-chloropyridazin-3-yl hydrazones and 6-chloro-3-substituted-[1,2,4]triazolo[4,3-*b*]pyridazines as cytotoxic agents. *Bioorganic Chemistry* **2019**, *86*, 288-295.

(284) AG, S. Anti-inflammatory and hypotensive pyridazine derivatives - prepared by reaction of 3-hydrazino-6-chloro-pyridazine with aldehydes or ketones. 1971.

(285) Li, E.; Hu, Z.; Song, L.; Yu, W.; Chang, J. Synthesis of 1,2,4-Triazolo[4,3-*a*]pyridines and Related Heterocycles by Sequential Condensation and Iodine-Mediated Oxidative Cyclization. *Chemistry - A European Journal* **2016**, *22* (31), 11022-11027.

(286) Thiel, O. R.; Achmatowicz, M. M.; Reichelt, A.; Larsen, R. D. Palladium-Catalyzed Coupling of Aldehyde-Derived Hydrazones: Practical Synthesis of Triazolopyridines and Related Heterocycles. *Angewandte Chemie International Edition* **2010**, *49* (45), 8395-8398.

(287) Ye, Z.; Ding, M.; Wu, Y.; Li, Y.; Hua, W.; Zhang, F. Electrochemical synthesis of 1,2,4-triazole-fused heterocycles. *Green Chemistry* **2018**, *20* (8), 1732-1737.

(288) Bhatt, A.; Singh, R. K.; Kant, R. Facile one-pot synthesis of *N*-fused 1,2,4-triazoles via oxidative cyclization using manganese dioxide. *Chemistry of Heterocyclic Compounds* **2018**, *54* (12), 1111-1116.

(289) Kaji, K.; Nagashima, H.; Oda, H. Conversion of Dipyridazino[4,5-*b*:4',5'-*e*][1,4]Thiazines into Dipyridazino[4,5-*b*:4',5'-*d*]Pyrroles through a Base-Induced Extrusion of Sulfur. *Chemical and Pharmaceutical Bulletin* **1984**, *32* (4), 1423-1432.

(290) Laurin, C. M. C. c. Chemical tools to probe the role of bromodomains in the parasite *Trypanosoma cruzi*. PhD Thesis, University of Oxford, 2019.

(291) Mátyus, P.; Czakó, K.; Behr, Á.; Varga, I.; Podányi, B.; von Arnim, M.; Várkonyi, P. Kinetic and Theoretic Aspects of Regiochemistry in the Reaction of 4,5-Dihalo-3(2*H*)-

pyridazinones with Benzylamines. *The Japan Institute of Heterocyclic Chemistry* **1993**, *36* (4), 785-798.

(292) Labadie, S. S. 3-Aryl-2,4-pentanediones from 3,5-Dimethyl-4-iodoisoxazoles: An Application of a Palladium-Catalyzed Cross-Coupling Reaction. *Synthetic Communications* **1994**, *24* (5), 709-719.

(293) Hino, K.; Nagai, Y.; Uno, H. Synthesis and pharmacological activities of 3-phenyl-2-(1-piperazinyl)quinolines and related compounds. *Chemical and Pharmaceutical Bulletin* **1987**, *35* (7), 2819-2824.

(294) Huang, H.-Y.; Lin, X.-Y.; Yen, S.-Y.; Liang, C.-F. Facile access to *N*-formyl imide as an *N*-formylating agent for the direct synthesis of *N*-formamides, benzimidazoles and quinazolinones. *Organic & Biomolecular Chemistry* **2020**, *18* (29), 5726-5733.

(295) Schmidt, C.; Karge, B.; Misgeld, R.; Prokop, A.; Franke, R.; Brönstrup, M.; Ott, I. Gold(I) NHC Complexes: Antiproliferative Activity, Cellular Uptake, Inhibition of Mammalian and Bacterial Thioredoxin Reductases, and Gram-Positive Directed Antibacterial Effects. *Chemistry - A European Journal* **2017**, *23* (8), 1869-1880.

(296) Chen, T.; Zhuo, L.-S.; Liu, P.-F.; Fang, W.-R.; Li, Y.-M.; Huang, W. Discovery of 1,6-naphthyridinone-based MET kinase inhibitor bearing quinoline moiety as promising antitumor drug candidate. *European Journal of Medicinal Chemistry* **2020**, *192*, 112174.

(297) Teuber, H. J.; Benz, S. Reaktionen mit Nitrosodisulfonat, XXXIV. Chinolin-chinone-(7.8). *Chemische Berichte* **1967**, *100* (6), 2077-2092.

(298) Madabhushi, S.; Narsaiah, C.; Sairam, V. V.; Reddy, G. K.; Raveendra, J.; Reddy, M. K. K.; Ramanaiah, B. C. Microwave-assisted efficient one-step synthesis of amides from ketones and benzoxazoles from (2-hydroxyaryl) ketones with acetohydroxamic acid using sulfuric acid as the catalyst. *Tetrahedron Letters* **2011**, *52*, 6103-6107.

(299) Dawson, D. M.; Ke, Z.; Mack, F. M.; Doyle, R. A.; Bignami, G. P. M.; Smellie, I. A.; Bühl, M.; Ashbrook, S. E. Calculation and experimental measurement of paramagnetic NMR parameters of phenolic oximate Cu(II) complexes. *Chemical Communications* **2017**, *53* (76), 10512-10515.

(300) Aakeröy, C. B.; Sinha, A. S. Synthesis of ketoximes via a solvent-assisted and robust mechanochemical pathway. *RSC Advances* **2013**, *3* (22), 8168.

(301) Jennings, L. Development of ligands to target bromodomain-histone interactions. PhD Thesis, University of Oxford, 2015.

(302) Altaf-ur-Rahman.; Boulton, A. Electrophillic substitution in anthranils. *Tetrahedron* **1965**, *22* (7).

(303) Li, D.; Ollevier, T. Iron- or Zinc-Mediated Synthetic Approach to Enantiopure Dihydroquinoxalinones. *European Journal of Organic Chemistry* **2019**, *2019* (6), 1273-1280.

(304) Wang, Y.; Wach, J.-Y.; Sheehan, P.; Zhong, C.; Zhan, C.; Harris, R.; Almo, S. C.; Bishop, J.; Haggarty, S. J.; Ramek, A.*; et al.* Diversity-Oriented Synthesis as a Strategy

for Fragment Evolution against GSK3β. *ACS Medicinal Chemistry Letters* **2016**, *7* (9), 852-856.

(305) Pan, Y.; Chen, C.; Xu, X.; Zhao, H.; Han, J.; Li, H.; Xu, L.; Fan, Q.; Xiao, J. Metal-free tandem cyclization/hydrosilylation to construct tetrahydroquinoxalines. *Green Chemistry* **2018**, *20* (2), 403-411.

(306) Su, Y.; Li, R.; Ning, X.; lin, Z.; Zhao, X.; Zhou, J.; Lui, J.; Jin, Y.; Yin, Y. Discovery of 2,4-diarylaminopyrimidine derivatives bearing dithiocarbamate moiety as novel FAK inhibitors with antitumor and anti-angiogenesis activities | Elsevier Enhanced Reader. *European Journal of Medicinal Chemistry* **2019**, *177*, 32-46.

(307) Cao, X.; Ma, C.; Li, Y.; Zhan, C.; Yang, B. A One-Pot Transition-Metal-Free Tandem Process to 1,4-Benzodiazepine Scaffolds. *Synthesis* **2012**, *45* (01), 111-117.

(308) Wang, Z.; Tang, Y. Mechanistic insights into a catalyst-free method to construct quinazolinones through multiple oxidative cyclization | Elsevier Enhanced Reader. *Tetrahedron* **2016**, *72*, 1330-1336.

(309) Andrews, I. P.; Atkins, R. J.; Breen, G. F.; Carey, J. S.; Forth, M. A.; Morgan, D. O.; Shamji, A.; Share, A. C.; Smith, S. A. C.; Walsgrove, T. C.*; et al.* The Development of a Manufacturing Route for the GPIIb/IIIa Receptor Antagonist SB-214857-A. Part 1: Synthesis of the Key Intermediate 2,3,4,5-Tetrahydro-4-methyl-3-oxo-1*H*-1,4-benzodiazepine-2-acetic Acid Methyl Ester, SB-235349. *Organic Process Research & Development* **2003**, *7* (5), 655-662.

(310) Jarboe, S. G.; Terrazas, M. S.; Beak, P. The Endocyclic Restriction Test: The Geometries of Nucleophilic Substitutions at Sulfur(VI) and Sulfur(II). *The Journal of Organic Chemistry* **2008**, *73* (24), 9627-9632.

(311) Camacho, M. E.; Chayah, M.; García, M. E.; Fernández-Sáez, N.; Arias, F.; Gallo, M. A.; Carrión, M. D. Quinazolinones, Quinazolinthiones, and Quinazolinimines as Nitric Oxide Synthase Inhibitors: Synthetic Study and Biological Evaluation. *Archiv der Pharmazie* **2016**, *349* (8), 638-650.

(312) Boots, M. R.; Boots, S. G.; Moreland, D. E. Conformational aspects of ureas in the inhibition of the Hill reaction. *Journal of Medicinal Chemistry* **1970**, *13* (1), 144-144.

(313) Kornet, M. J. Synthesis and anticonvulsant activity of 3-alkyl-3,4-dihydro-2(1*H*)-quinazolinones. *Journal of Heterocyclic Chemistry* **1992**, *29* (1), 103-105.

(314) Fish, P. V.; Cook, A. S.; Phillips, C.; Bent, A. F.; Mills, J. E. J.; Sciammetta, N. Novel heterocyclic compounds as bromodomain inhibitors. US WO2013027168A1, 2013.

(315) Ferro, S.; De Luca, L.; Germanò, M. P.; Buemi, M. R.; lelo, L.; Certo, G.; Kanteev, M.; Fishman, A.; Rapisarda, A.; Gitto, R. Chemical exploration of 4-(4-fluorobenzyl)piperidine fragment for the development of new tyrosinase inhibitors. *European Journal of Medicinal Chemistry* **2017**, *125*, 992-1001.

(316) De Sousa, N. F.; Da Silva Souza, H. D.; De Menezes, R. P. B.; Da Silva Alves, F.; Acevedo, C. A. H.; De Lima Nunes, T. A.; Sessions, Z. L.; Scotti, L.; Muratov, E. N.;

Mendonça-Junior, F. J. B.*; et al.* Selene-Ethylenelacticamides and *N*-Aryl-Propanamides as Broad-Spectrum Leishmanicidal Agents. *Pathogens* **2023**, *12* (1), 136.

(317) Shen, S.; Picci, C.; Ustinova, K.; Benoy, V.; Kutil, Z.; Zhang, G.; Tavares, M. T.; Pavlíček, J.; Zimprich, C. A.; Robers, M. B.*; et al.* Tetrahydroquinoline-Capped Histone Deacetylase 6 Inhibitor SW-101 Ameliorates Pathological Phenotypes in a Charcot–Marie–Tooth Type 2A Mouse Model. *Journal of Medicinal Chemistry* **2021**, *64* (8), 4810-4840.

(318) Xie, D.; Zhang, S. Selective Reduction of Quinolinones Promoted by a SmI_2/H_2O/MeOH System. *The Journal of Organic Chemistry* **2022**, *87* (13), 8757-8763.

(319) Shi, P.; Tu, Y.; Kong, D.; Wu, P.; Ma, D.; Bolm, C. Iron-Catalyzed Intramolecular Arene C(sp^2)−H Amidations under Mechanochemical Conditions. *Angewandte Chemie International Edition* **2022**, *61* (30).

(320) Tian, X.; Li, X.; Duan, S.; Du, Y.; Liu, T.; Fang, Y.; Chen, W.; Zhang, H.; Li, M.; Yang, X. Room Temperature Benzofused Lactam Synthesis Enabled by Cobalt(III)-Catalyzed C(sp^2)−H Amidation. *Advanced Synthesis & Catalysis* **2021**, *363* (4), 1050-1058.

(321) Guan, M.; Pang, Y.; Zhang, J.; Zhao, Y. Pd-Catalyzed sequential β-C(sp^3)–H arylation and intramolecular amination of δ-C(sp^2)–H bonds for synthesis of quinolinones *via* an *N,O*-bidentate directing group. *Chemical Communications* **2016**, *52* (43), 7043-7046.

(322) Chen, M.; Dong, G. Direct Catalytic Desaturation of Lactams Enabled by Soft Enolization. *Journal of the American Chemical Society* **2017**, *139* (23), 7757-7760.

(323) Mofford, D. M.; Reddy, G. R.; Miller, S. C. Aminoluciferins Extend Firefly Luciferase Bioluminescence into the Near-Infrared and Can Be Preferred Substrates over d-Luciferin. *Journal of the American Chemical Society* **2014**, *136* (38), 13277-13282.

(324) Liu, B.; Fan, Y.; Gao, Y.; Sun, C.; Xu, C.; Zhu, J. Rhodium(III)-Catalyzed *N*-Nitroso-Directed C–H Olefination of Arenes. High-Yield, Versatile Coupling under Mild Conditions. *Journal of the American Chemical Society* **2013**, *135* (1), 468-473.

(325) Mori, M.; Gilardoni, E.; Regazzoni, L.; Pedretti, A.; Colombo, D.; Parkinson, G.; Asai, A.; Meneghetti, F.; Villa, S.; Gelain, A. Towards the Inhibition of Protein–Protein Interactions (PPIs) in STAT3: Insights into a New Class of Benzothiadiazole Derivatives. *Molecules* **2020**, *25* (15), 3509.

(326) Rekunge, D. S.; Khatri, C. K.; Chaturbhuj, G. U. Sulfated polyborate-catalyzed efficient and expeditious synthesis of (un)symmetrical ureas and benzimidazolones. *Tetrahedron Letters* **2017**, *58* (45), 4304-4307.

(327) Yoon, H.; Yoon, Y.-J.; Ryu, K.; Kim, B.; Sung, G. Facile Synthesis of Benzo[*d*]azol-2(3*H*)-ones Using 2-Phenoxycarbonyl-4,5-dichloropyridazin-3(2*H*)-one as Green CO Source. *Synlett* **2015**, *26* (14), 1985-1990.

(328) Rohand, T.; Sopbué Fondjo, E. Synthesis of Novel Structurally Diverse *N*-Mono- and *N*,*N*′-Disubstituted Benzimidazol-2-one Derivatives by the Alkylations of 1,3-

Dihydro-2*H*-benzimidazol-2-one with Some Alkyl Halides under Transfer Catalysis Conditions. *Journal of Heterocyclic Chemistry* **2018**, *55* (10), 2309-2314.

(329) Chernyshev, V. M.; Khazipov, O. V.; Shevchenko, M. A.; Chernenko, A. Y.; Astakhov, A. V.; Eremin, D. B.; Pasyukov, D. V.; Kashin, A. S.; Ananikov, V. P. Revealing the unusual role of bases in activation/deactivation of catalytic systems: O–NHC coupling in M/NHC catalysis. *Chemical Science* **2018**, *9* (25), 5564-5577.

(330) Takamizawa, A.; Hamashima, Y.; Sato, H.; Matsumoto, Y. Studies on Pyrimidine Derivatives and Related Compounds. LXVIII. Reactions of Dialkyl Acylphosphonates with 1, 3-Disubstituted Benzimidazolium Halides. *Chemical and Pharmaceutical Bulletin* **1970**, *18* (8), 1576-1588.

(331) Jin, Y.; Ou, L.; Yang, H.; Fu, H. Visible-Light-Mediated Aerobic Oxidation of *N*-Alkylpyridinium Salts under Organic Photocatalysis. *Journal of the American Chemical Society* **2017**, *139* (40), 14237-14243.

(332) Patil, V. V.; Shankarling, G. S. Steric-Hindrance-Induced Regio- and Chemoselective Oxidation of Aromatic Amines. *The Journal of Organic Chemistry* **2015**, *80* (16), 7876-7883.

(333) Fife, T. H.; Hutchins, J. E. C.; Wang, M. S. Highly efficient intramolecular nucleophilic reactions. Cyclization of *p*-nitrophenyl *N*-(2-mercaptophenyl)-*N*-methylcarbamate and phenyl *N*-(2-aminophenyl)-*N*-methylcarbamate. *Journal of the American Chemical Society* **1975**, *97* (20), 5878-5882.

(334) Ando, K.; Kobayashi, T.; Uchida, N. Practical Methylenation Reaction for Aldehydes and Ketones Using New Julia-Type Reagents. *Organic Letters* **2015**, *17* (10), 2554-2557.

(335) Clark, R. L.; Pessolano, A. A. Synthesis of Some Substituted Benzoxazolones. *Journal of the American Chemical Society* **1958**, *80* (7), 1662-1664.

(336) Shiokawa, Y.; Ohki, S. Studies on Benzimidazoles and Related Compounds. IV. Reactivity of 2-Azido-1-methylbenzimidazole. *Chemical and Pharmaceutical Bulletin* **1971**, *19* (2), 401-408.

(337) Clezy, P.; Fookes, C.; Mirza, A. The chemistry of pyrrolic compounds. XXXVII. Monobenzoporphyrins: The rhodoporphyrin of petroleum deposits. *Australian Journal of Chemistry* **1977**, *30* (6), 1337-1347.

(338) Vodnala, N.; Gujjarappa, R.; Hazra, C. K.; Kaldhi, D.; Kabi, A. K.; Beifuss, U.; Malakar, C. C. Copper-Catalyzed Site-Selective Oxidative C−C Bond Cleavage of Simple Ketones for the Synthesis of Anilides and Paracetamol. *Advanced Synthesis & Catalysis* **2019**, *361* (1), 135-145.

(339) Dziwornu, G. A.; Coertzen, D.; Leshabane, M.; Korkor, C. M.; Cloete, C. K.; Njoroge, M.; Gibhard, L.; Lawrence, N.; Reader, J.; Van Der Watt, M.*; et al.* Antimalarial Benzimidazole Derivatives Incorporating Phenolic Mannich Base Side Chains Inhibit Microtubule and Hemozoin Formation: Structure–Activity Relationship and *In Vivo* Oral Efficacy Studies. *Journal of Medicinal Chemistry* **2021**, *64* (8), 5198-5215.

(340) Noto, N.; Yada, A.; Yanai, T.; Saito, S. Machine-Learning Classification for the Prediction of Catalytic Activity of Organic Photosensitizers in the Nickel(II)-Salt-Induced Synthesis of Phenols. *Angewandte Chemie International Edition* **2023**, *62* (11).

(341) Mali, S. M.; Bhaisare, R. D.; Gopi, H. N. Thioacids Mediated Selective and Mild *N*-Acylation of Amines. *The Journal of Organic Chemistry* **2013**, *78* (11), 5550-5555.

(342) Edmonds, A. K.; Oakes, C. S.; Hassell-Hart, S.; Bruyère, D.; Tizzard, G. J.; Coles, S. J.; Felix, R.; Maple, H. J.; Marsh, G. P.; Spencer, J. Scale-up and optimization of the synthesis of dual CBP/BRD4 inhibitor ISOX-DUAL. *Organic & Biomolecular Chemistry* **2022**, *20* (19), 4021-4029.

(343) Nishiwaki, H.; Nagaoka, H.; Kuriyama, M.; Yamauchi, S.; Shuto, Y. Affinity to the Nicotinic Acetylcholine Receptor and Insecticidal Activity of Chiral Imidacloprid Derivatives with a Methylated Imidazolidine Ring. *Bioscience, Biotechnology and Biochemistry* **2011**, *75* (4), 780-782.

(344) Huang, Z.; Jeff, J.; Timothy, M.; Antonios-McCrea, W. R.; McKenna, M.; Poon, D.; Renhowe, P. A.; Sendzik, M.; Shafer, C.; Smith, A.*; et al.* Novel Heterocyclic Compounds and Uses Thereof. US 2013.

(345) Cheng, Z.; Li, J.; Yang, H.; He, Y.; Shi, Q.; Chang, Q.; Liu, R.; Huang, X.; Li, Y. Discovery of novel benzimidazole derivatives as potent p300 bromodomain inhibitors with anti-proliferative activity in multiple cancer cells. *Bioorganic & Medicinal Chemistry* **2022**, *66*, 116784.

(346) Lindström, S.; Eriksson, M.; Grivas, S. Synthetic routes to nitroamino percursors of the food carcinogen 2-amino-1-methyl-6-phenyl-1*H*-imidazo[4,5-*b*]pyridine and its 3-methyl isomer *via* Pd(0)-catalyzed arylation. *Acta Chemica Scandinavica* **1993**, *47* (8), 805-812.

(347) Wu, C.; Huang, J.; Yu, T.; Dong, J.; Wang, T.-L.; Li, J.; Li, J.; Chen, S. Quinazolinone Compound and Application Thereof. US 2020.

(348) O'Boyle, N. M.; Banck, M.; James, C. A.; Morley, C.; Vandermeersch, T.; Hutchison, G. R. Open Babel: An open chemical toolbox. *Journal of Cheminformatics* **2011**, *3* (1), 33.

(349) Musetti, C.; Bean, M. F.; Quinque, G. T.; Kwiatkowski, C.; Szewczuk, L. M.; Baldoni, J.; Zajac, M. A. High-Throughput Assessment of Structural Continuity in Biologics. *Analytical Chemistry* **2018**, *90* (4), 2970-2975.

Appendices

A1 WaterLOGSY Spectra

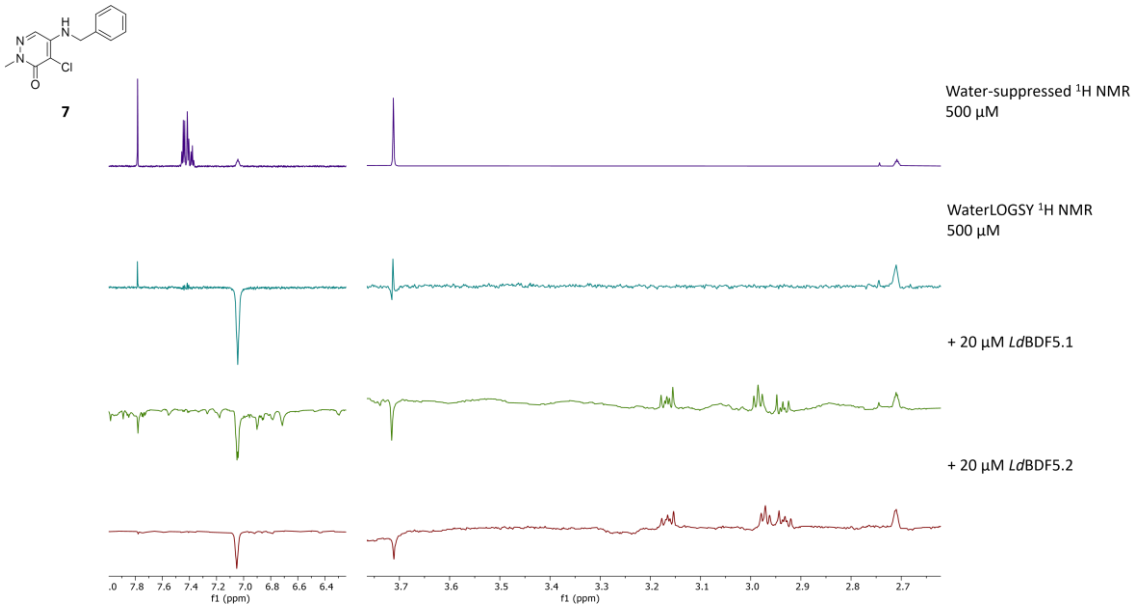

Figure A1.1. Partial waterLOGSY spectra of **7**. The water suppressed ^{1}H spectrum is shown in purple. The waterLOGSY NMR of the compound only (blue) shows no inversion of the compound peaks indicating suitable solubilisation at 500 µM (only the labile N-H proton is inverted). Inversion of the ligand peaks on addition of 20 µM *Ld*BDF5.1 (green), shows potentially weak binding to *Ld*BDF5.1. The waterLOGSY spectrum in the presence of 20 µM *Ld*BDF5.2 (red) also shows partial inversion of the ligand peaks, indicating potential binding.

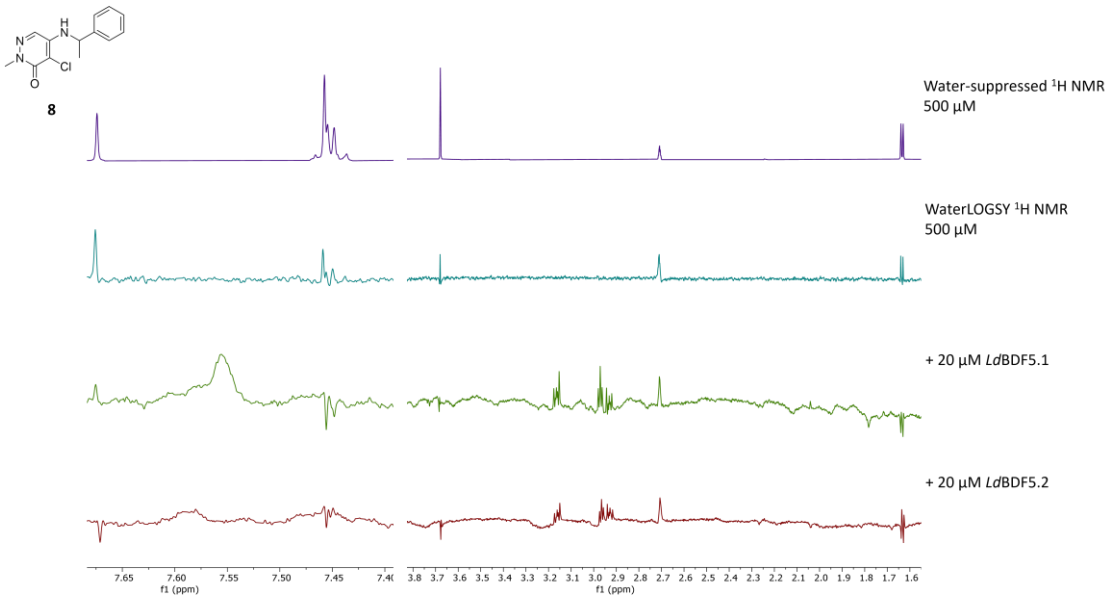

Figure A1.2. Partial waterLOGSY spectra of **8**. The water suppressed ^{1}H spectrum is shown in purple. The waterLOGSY NMR of the compound only (blue) shows no inversion of the compound peaks indicating suitable solubilisation at 500 µM. Inversion of the ligand peaks on addition of 20 µM *Ld*BDF5.1 (green), shows potentially weak binding to *Ld*BDF5.1 (only the labile N-H proton peak is not inverted). The waterLOGSY spectrum in the presence of 20 µM *Ld*BDF5.2 (red) also shows inversion of the ligand peaks, indicating potential binding.

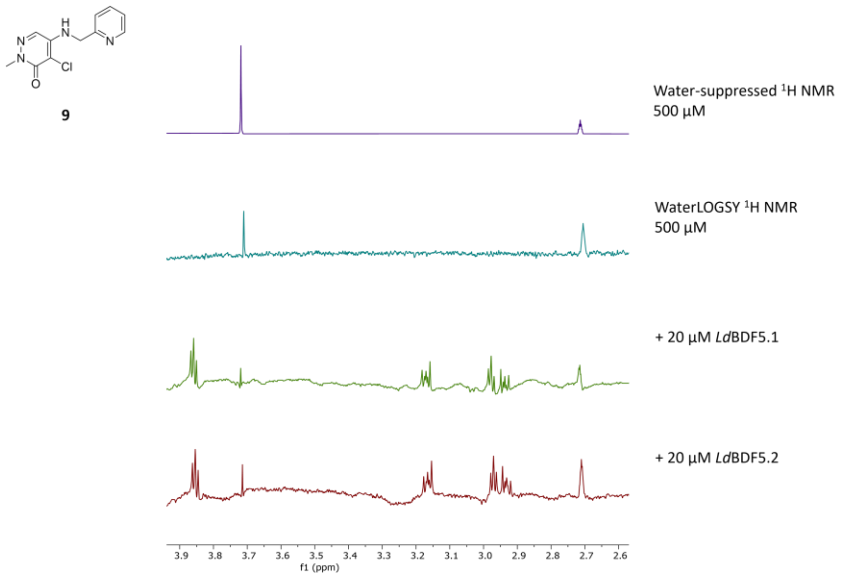

Figure A1.3. Partial waterLOGSY spectra of **9**. The water suppressed ^{1}H spectrum is shown in purple. The waterLOGSY NMR of the compound only (blue) shows no inversion of the compound peaks indicating suitable solubilisation at 500 µM. No inversion of the ligand peaks on addition of 20 µM *Ld*BDF5.1 (green), suggests no binding to *Ld*BDF5.1. The waterLOGSY spectrum in the presence of 20 µM *Ld*BDF5.2 (red) also shows no inversion of the ligand peaks and no binding.

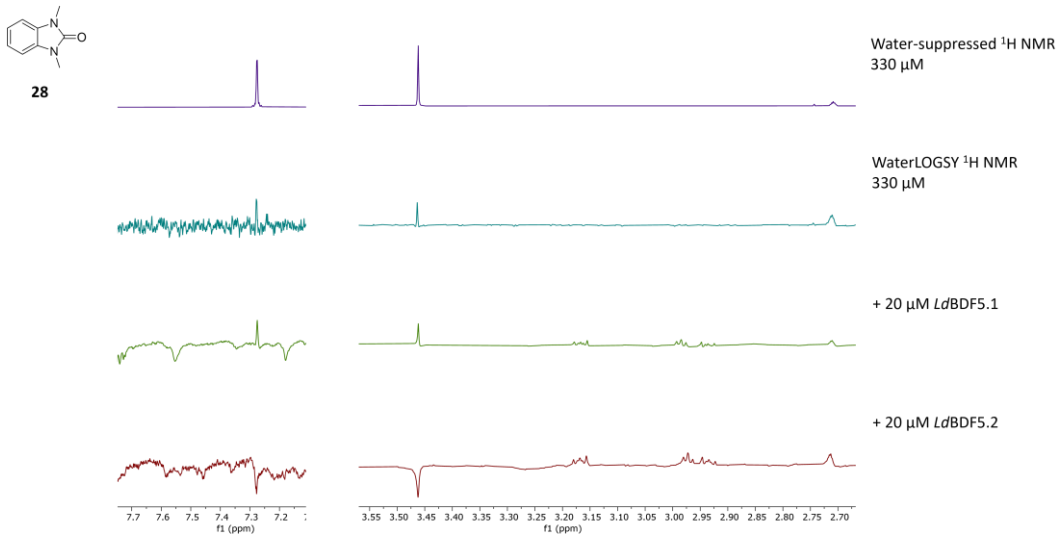

Figure A1.4. Partial waterLOGSY spectra of **28**. The water suppressed ^{1}H spectrum is shown in purple. The waterLOGSY NMR of the compound only (blue) shows no inversion of the compound peaks indicating suitable solubilisation at 330 µM. No inversion of the ligand peaks on addition of 20 µM *Ld*BDF5.1 (green), suggests no binding to *Ld*BDF5.1. The waterLOGSY spectrum in the presence of 20 µM *Ld*BDF5.2 (red) shows inversion of the ligand peaks which indicates potential weak binding.

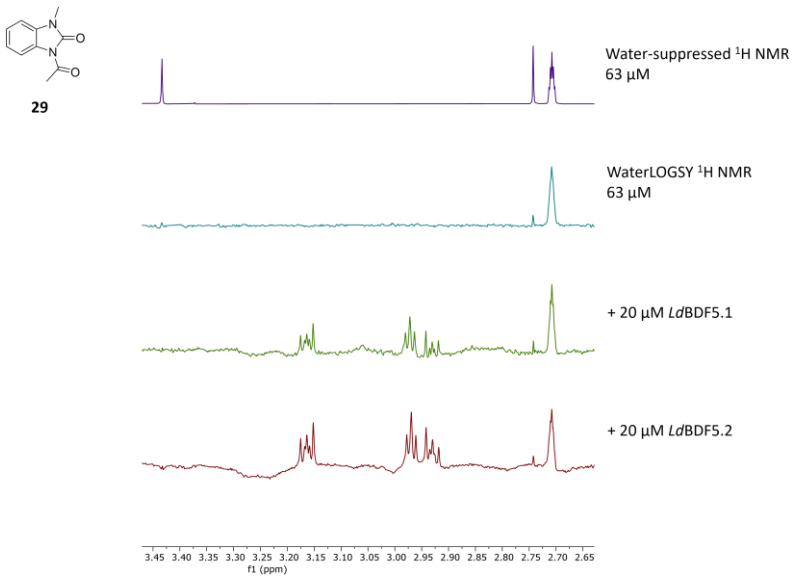

Figure A1.5. Partial waterLOGSY spectra of **29**. The water suppressed ^{1}H spectrum is shown in purple. The waterLOGSY NMR of the compound only (blue) shows no inversion of the compound peaks indicating suitable solubilisation at 63 µM. However, the resolution of the waterLOGSY spectra with protein (shown in green and red) is too low to tell whether any binding occurs.

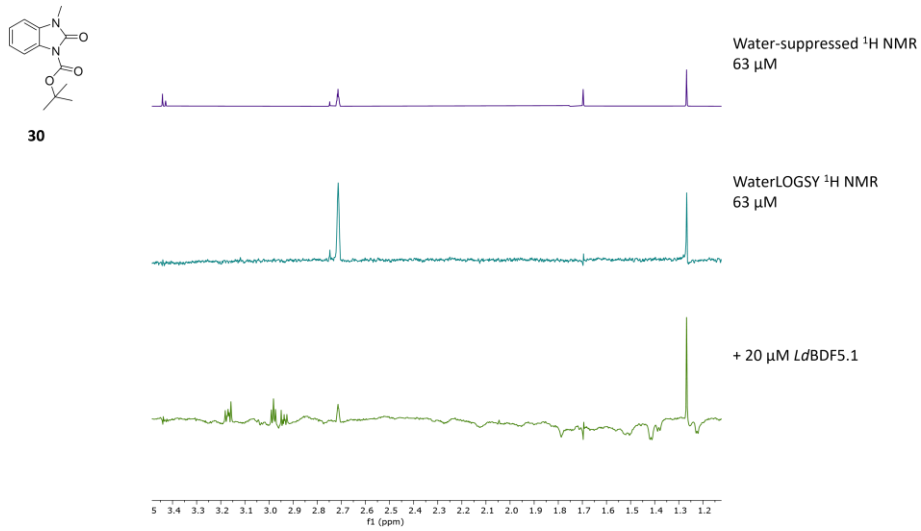

Figure A1.6. Partial waterLOGSY spectra of **30**. The water suppressed ^{1}H spectrum is shown in purple. The waterLOGSY NMR of the compound only (blue) shows no inversion of the compound peaks indicating suitable solubilisation at 63 µM. Inversion of the ligand peaks on addition of 20 µM *Ld*BDF5.1 (green), may indicate binding to *Ld*BDF5.1 however the resolution is very low and it is difficult to confirm.

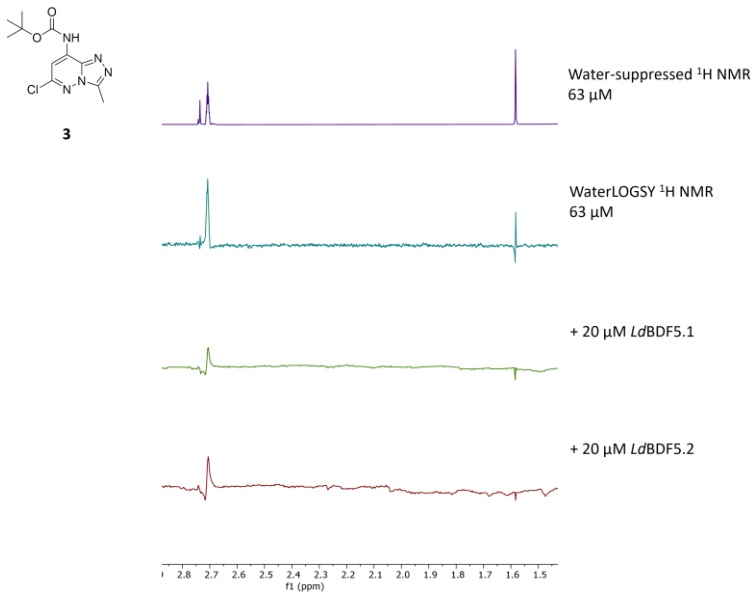

Figure A1.7. Partial waterLOGSY spectra of **3**. The water suppressed ^{1}H spectrum is shown in purple. The waterLOGSY NMR of the compound only (blue) shows no inversion of the compound peaks indicating suitable solubilisation at 63 µM, however the resolution is low. Inversion of the ligand peaks on addition of 20 µM *Ld*BDF5.1 (green), suggests potential binding to *Ld*BDF5.1. The waterLOGSY spectrum in the presence of 20 µM *Ld*BDF5.2 (red) also shows inversion of the ligand peaks which indicates potential weak binding.

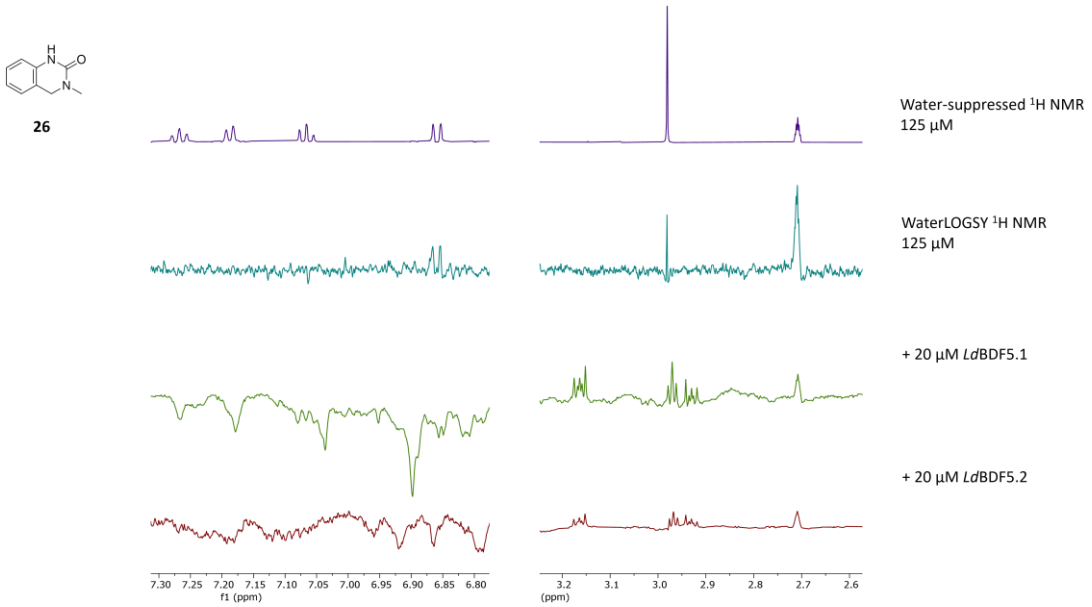

Figure A1.8. Partial waterLOGSY spectra of **26**. The water suppressed ^{1}H spectrum is shown in purple. The waterLOGSY NMR of the compound only (blue) shows no inversion of the compound peaks indicating suitable solubilisation at 125 µM. Resolution of the spectrum is poor but inversion of the ligand peaks on addition of 20 µM *Ld*BDF5.1 (green), suggests binding to *Ld*BDF5.1. The waterLOGSY spectrum in the presence of 20 µM *Ld*BDF5.2 (red) is also poorly resolved but shows inversion of the ligand peaks which indicates potential weak binding.

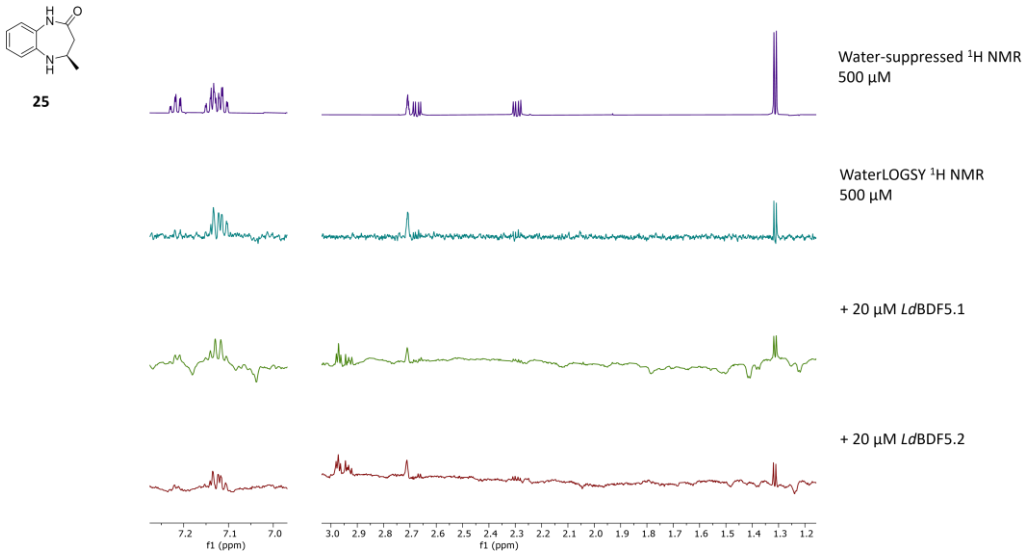

Figure A1.9. Partial waterLOGSY spectra of **25**. The water suppressed ^{1}H spectrum is shown in purple. The waterLOGSY NMR of the compound only (blue) shows no inversion of the compound peaks indicating suitable solubilisation at 500 µM. No inversion of the ligand peaks on addition of 20 µM *Ld*BDF5.1 (green), suggests no binding to *Ld*BDF5.1. The waterLOGSY spectrum in the presence of 20 µM *Ld*BDF5.2 (red) also shows no inversion of the ligand peaks and no binding.

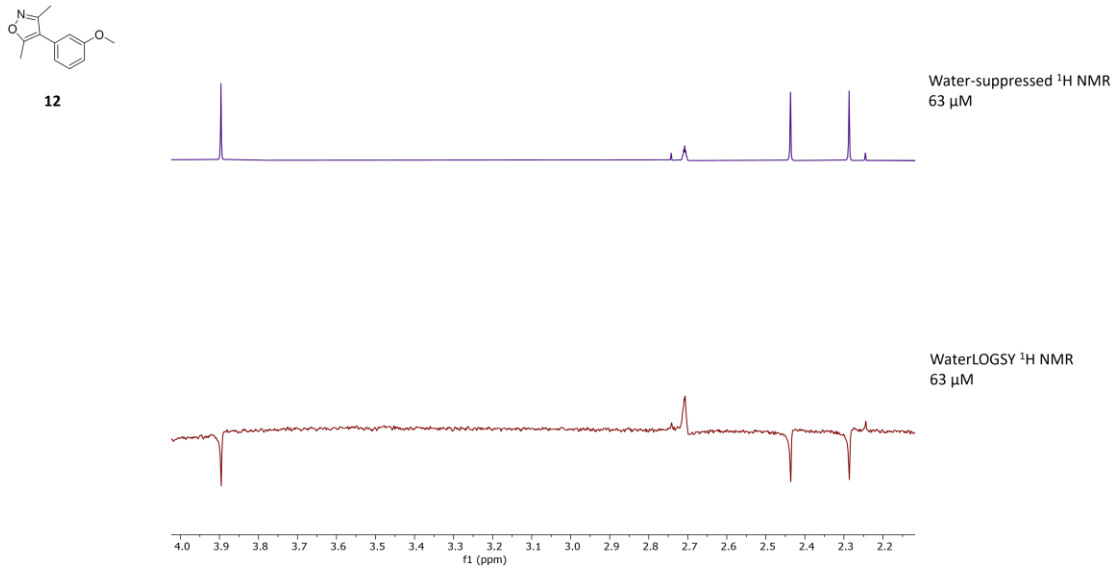

Figure A1.10. Partial waterLOGSY spectra of **12**. The water suppressed ^{1}H spectrum is shown in purple. The waterLOGSY NMR of the compound only (red) shows inversion of the compound peaks indicating the compound is not soluble at 63 µM.

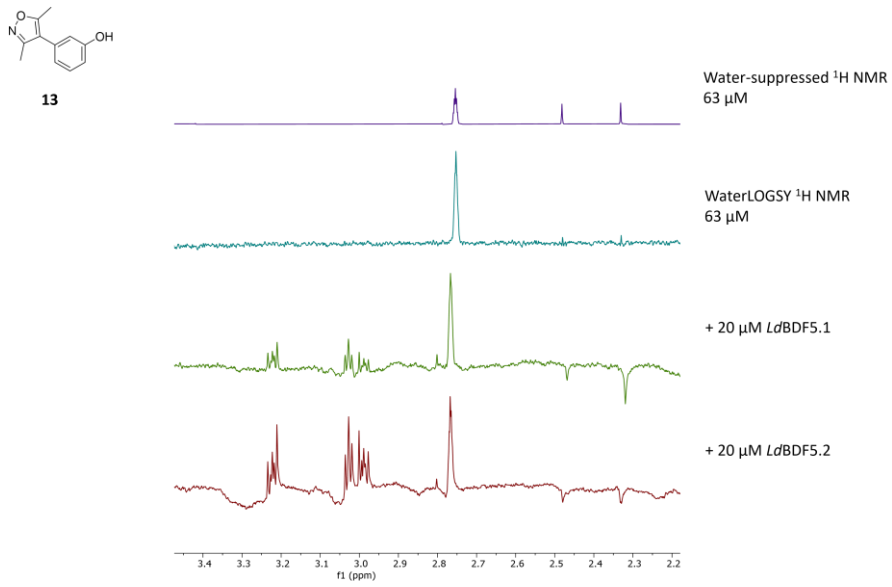

Figure A1.11. Partial waterLOGSY spectra of **13**. The water suppressed ^{1}H spectrum is shown in purple. The waterLOGSY NMR of the compound only (blue) shows no inversion of the compound peaks indicating suitable solubilisation at 63 µM. Inversion of the ligand peaks on addition of 20 µM *Ld*BDF5.1 (green), suggests potential weak binding to *Ld*BDF5.1. The waterLOGSY spectrum in the presence of 20 µM *Ld*BDF5.2 (red) shows inversion of the ligand peaks which also indicates potential weak binding.

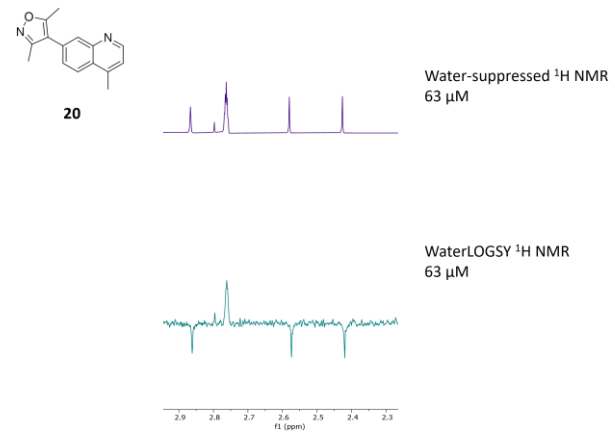

Figure A1.12. Partial waterLOGSY spectra of **20**. The water suppressed ^{1}H spectrum is shown in purple. The waterLOGSY NMR of the compound only (blue) shows inversion of the compound peaks indicating the compound is not soluble at 63 µM.

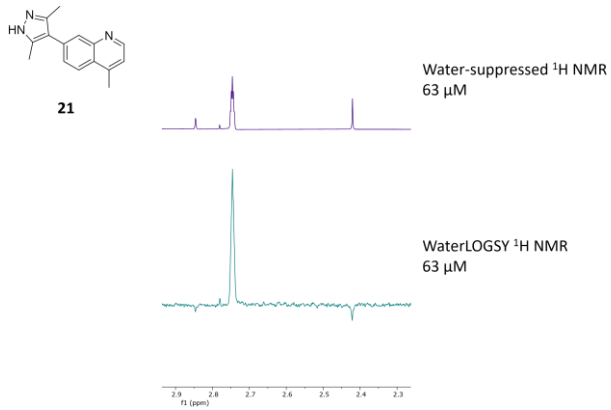

Figure A1.13. Partial waterLOGSY spectra of **21.** The water suppressed ^{1}H spectrum is shown in purple. The waterLOGSY NMR of the compound only (blue) shows inversion of the compound peaks indicating the compound is not soluble at 63 µM.

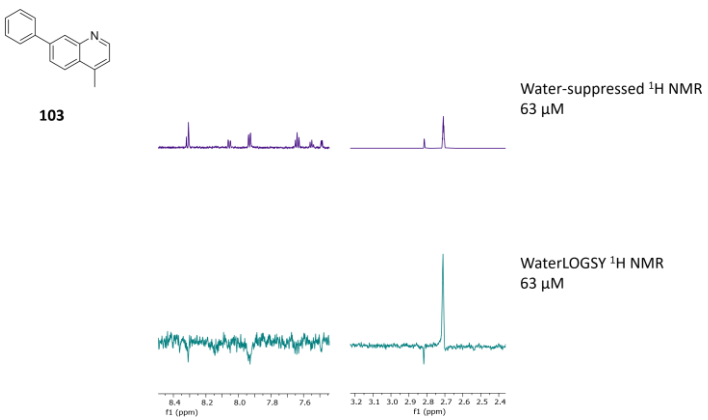

Figure A1.14. Partial waterLOGSY spectra of **103**. The water suppressed ^{1}H spectrum is shown in purple. The waterLOGSY NMR of the compound only (blue) shows inversion of the compound peaks indicating the compound is not soluble at 63 µM.

A2 Thermal Shift Data

T_M (*Ld*BDF5.1) = 51.7 °C

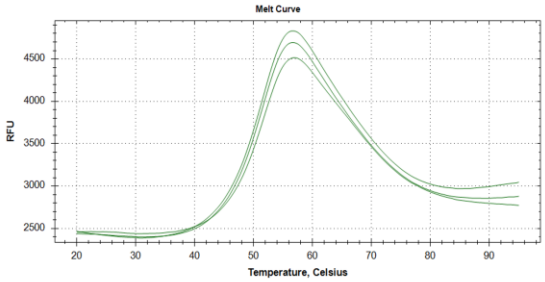

2 ΔT_M = 0.23 ± 0.13 °C

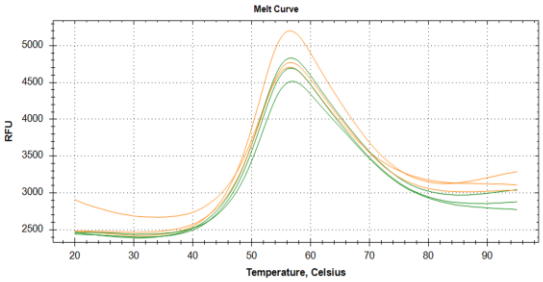

3 ΔT_M = -0.20 ± 0.47 °C

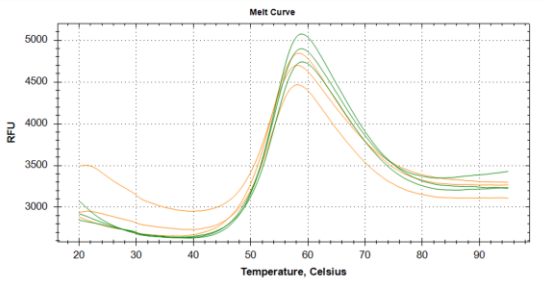

4 ΔT_M = 0.37 ± 0.19 °C

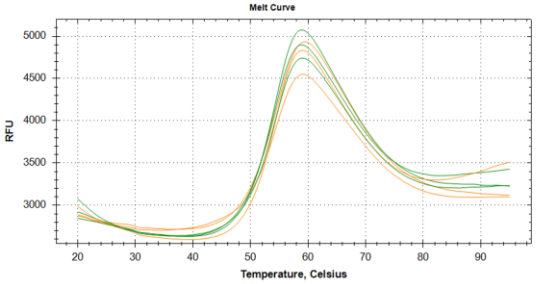

5 ΔT_M = 0.12 ± 0.10 °C

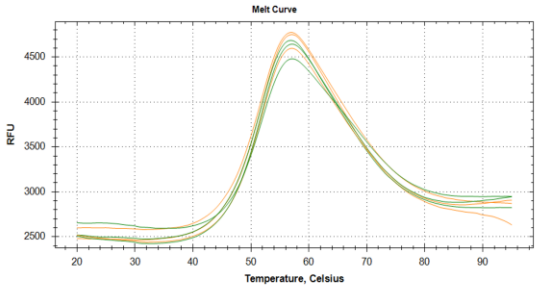

6 ΔT_M = 0.52 ± 0.17 °C

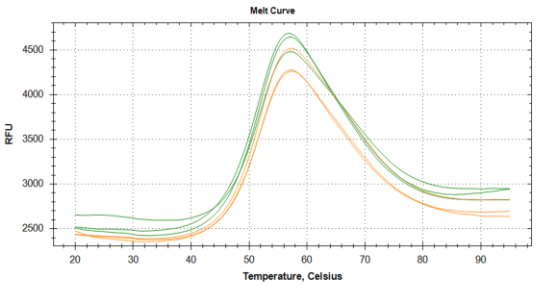

7 ΔT_M = 0.12 ± 0.07 °C

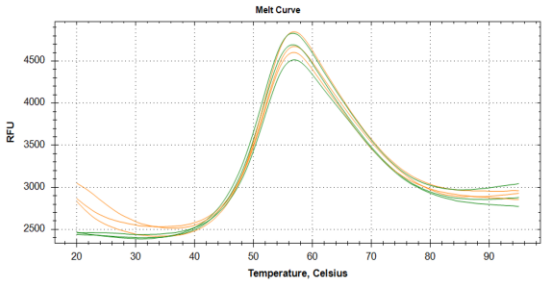

8 ΔT_M = 0.23 ± 0.13 °C

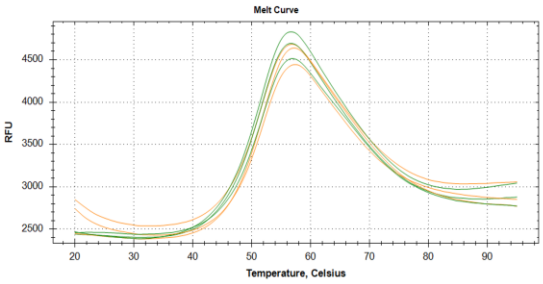

Figure A2.1. Thermal shift assay melting curves for *Ld*BDF5.1 + compounds **2-8** at 250 µM. Curves show three replicate samples of protein with compounds (orange) alongside DMSO control samples (green).

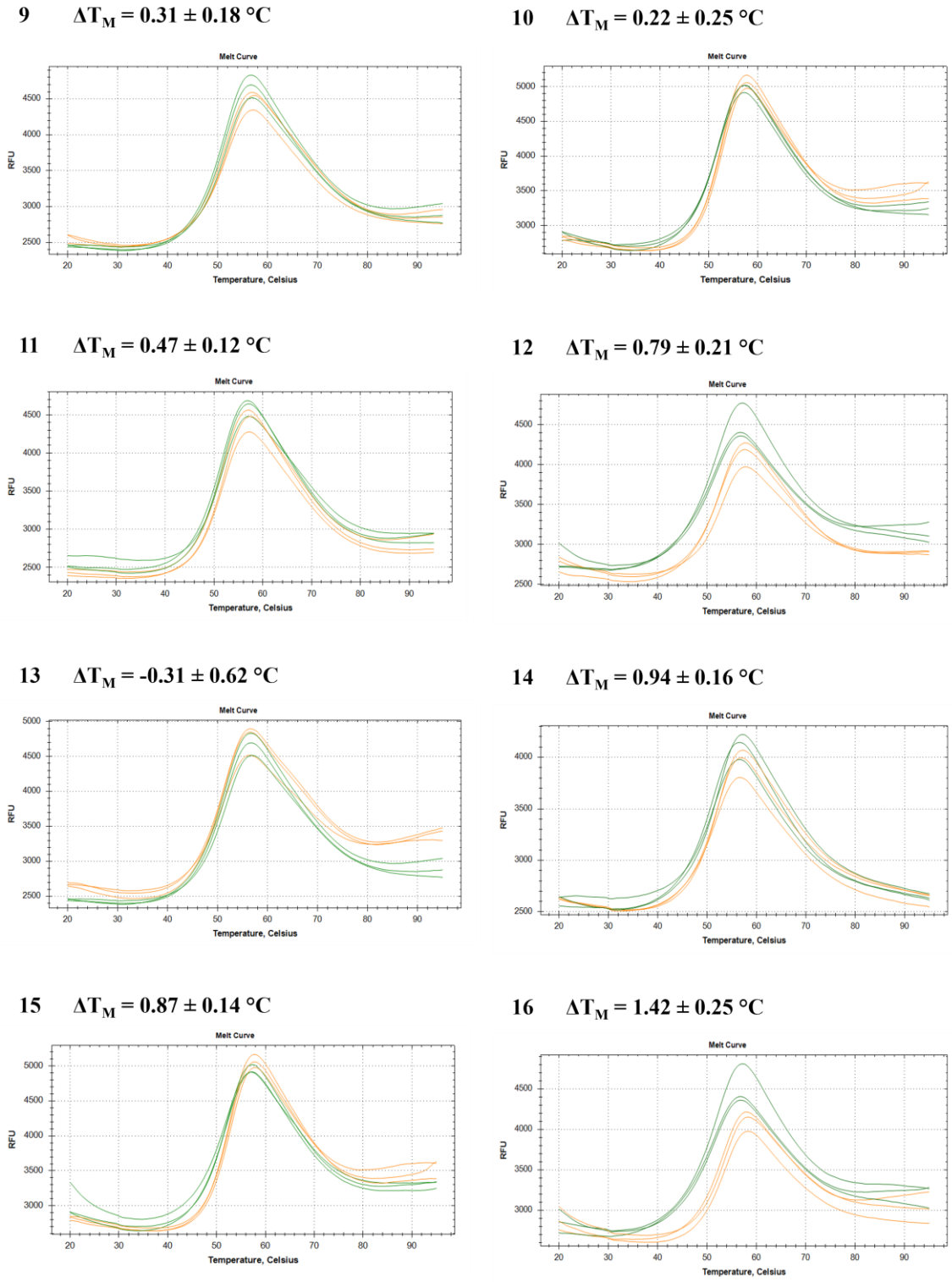

Figure A2.2. Thermal shift assay melting curves for *Ld*BDF5.1 + compounds **9-16** at 250 μM. Curves show three replicate samples of protein with compounds (orange) alongside DMSO control samples (green).

17 $\Delta T_M = 2.12 \pm 0.12$ °C

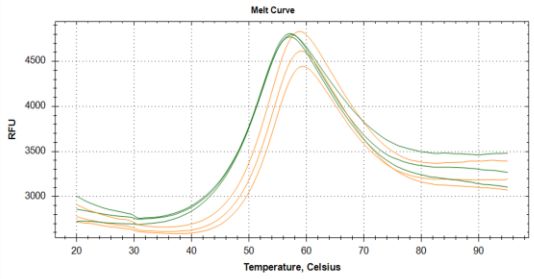

18 $\Delta T_M = 4.67 \pm 0.37$ °C

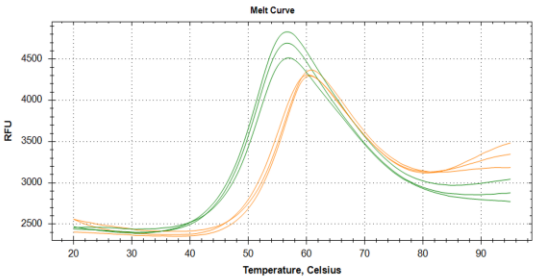

19 $\Delta T_M = 2.42 \pm 0.43$ °C

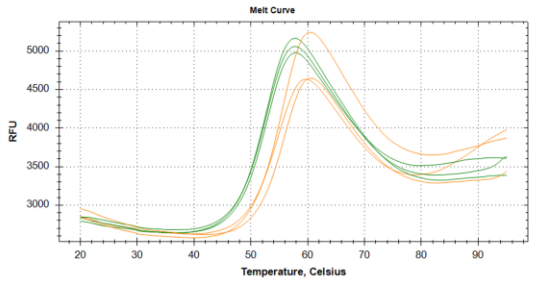

20 $\Delta T_M = 1.31 \pm 0.49$ °C

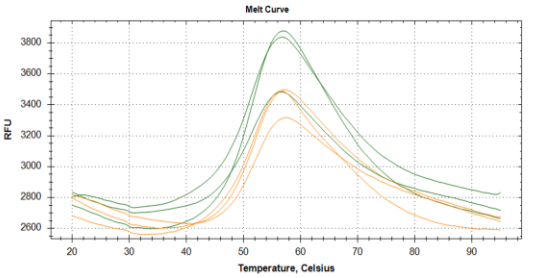

21 $\Delta T_M = 0.31 \pm 0.20$ °C

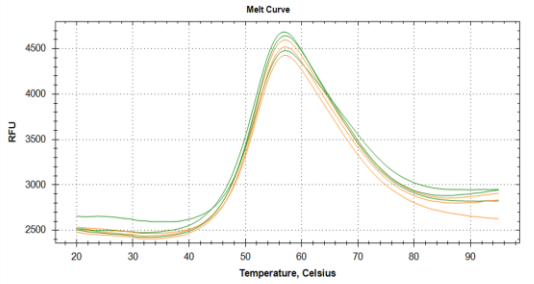

22 $\Delta T_M = 0.23 \pm 0.13$ °C

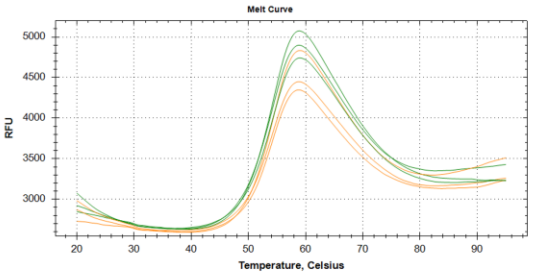

23 $\Delta T_M = 0.04 \pm 0.09$ °C

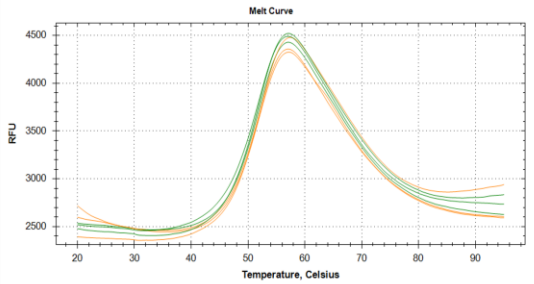

24 $\Delta T_M = 0.12 \pm 0.07$ °C

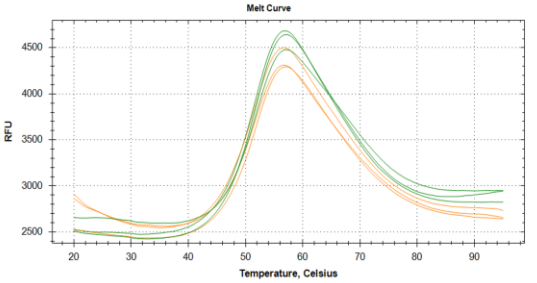

Figure A2.3. Thermal shift assay melting curves for *Ld*BDF5.1 + compounds **17-24** at 250 μM. Curves show three replicate samples of protein with compounds (orange) alongside DMSO control samples (green).

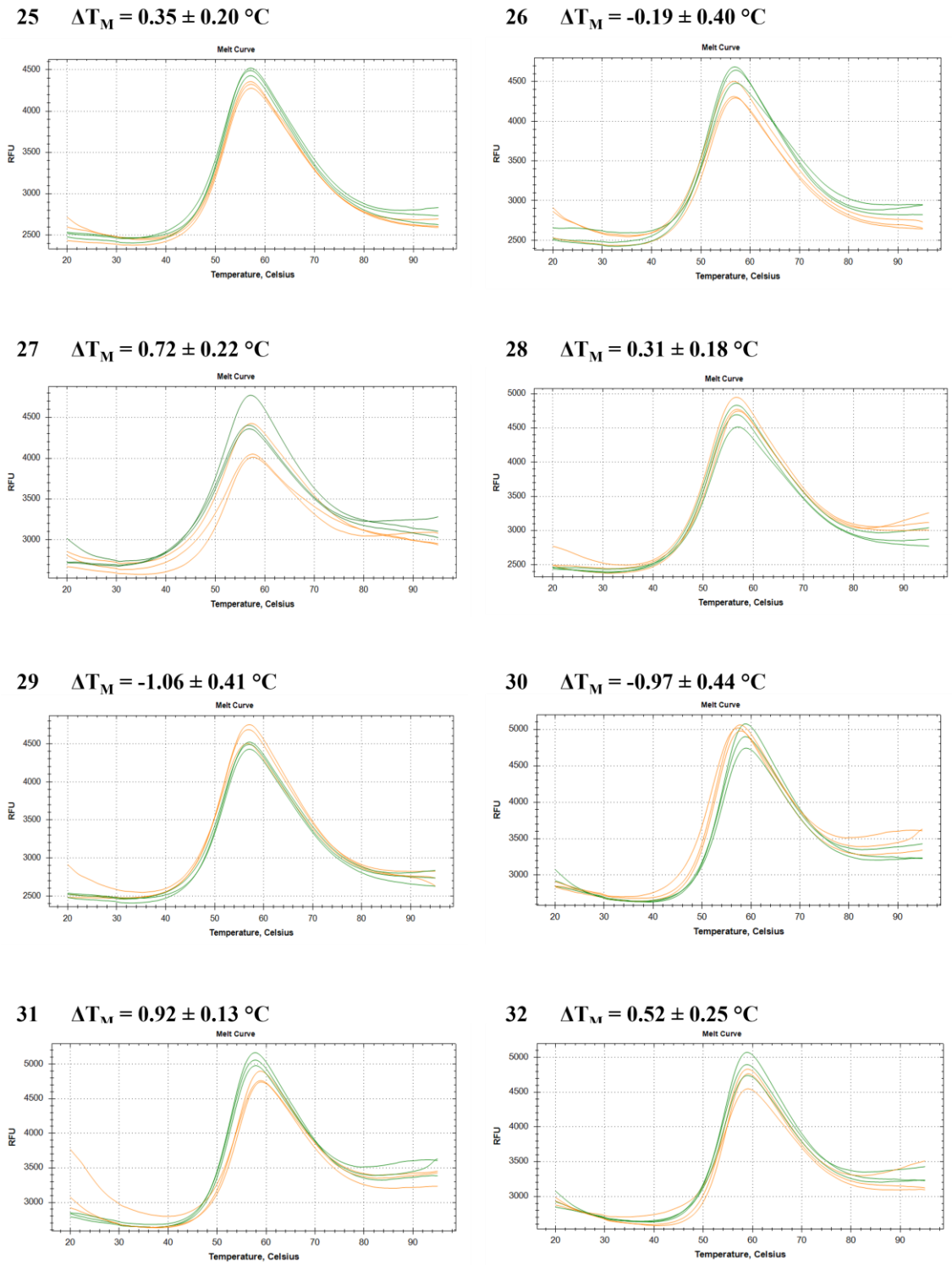

Figure A2.4. Thermal shift assay melting curves for *Ld*BDF5.1 + compounds **25-32** at 250 µM. Curves show three replicate samples of protein with compounds (orange) alongside DMSO control samples (green).

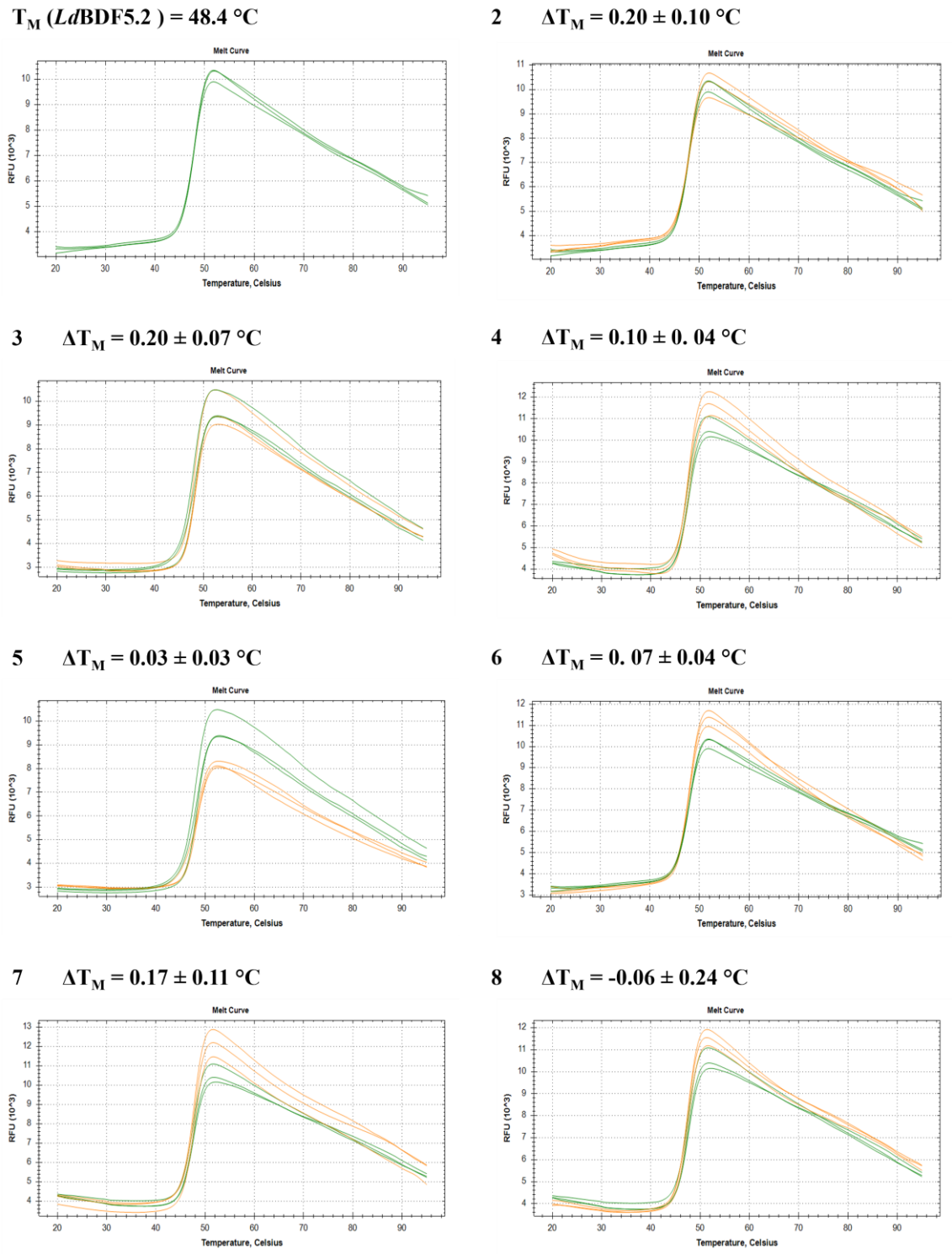

Figure A2.5. Thermal shift assay melting curves for *Ld*BDF5.2 + compounds **2-8** at 250 µM. Curves show three replicate samples of protein with compounds (orange) alongside DMSO control samples (green).

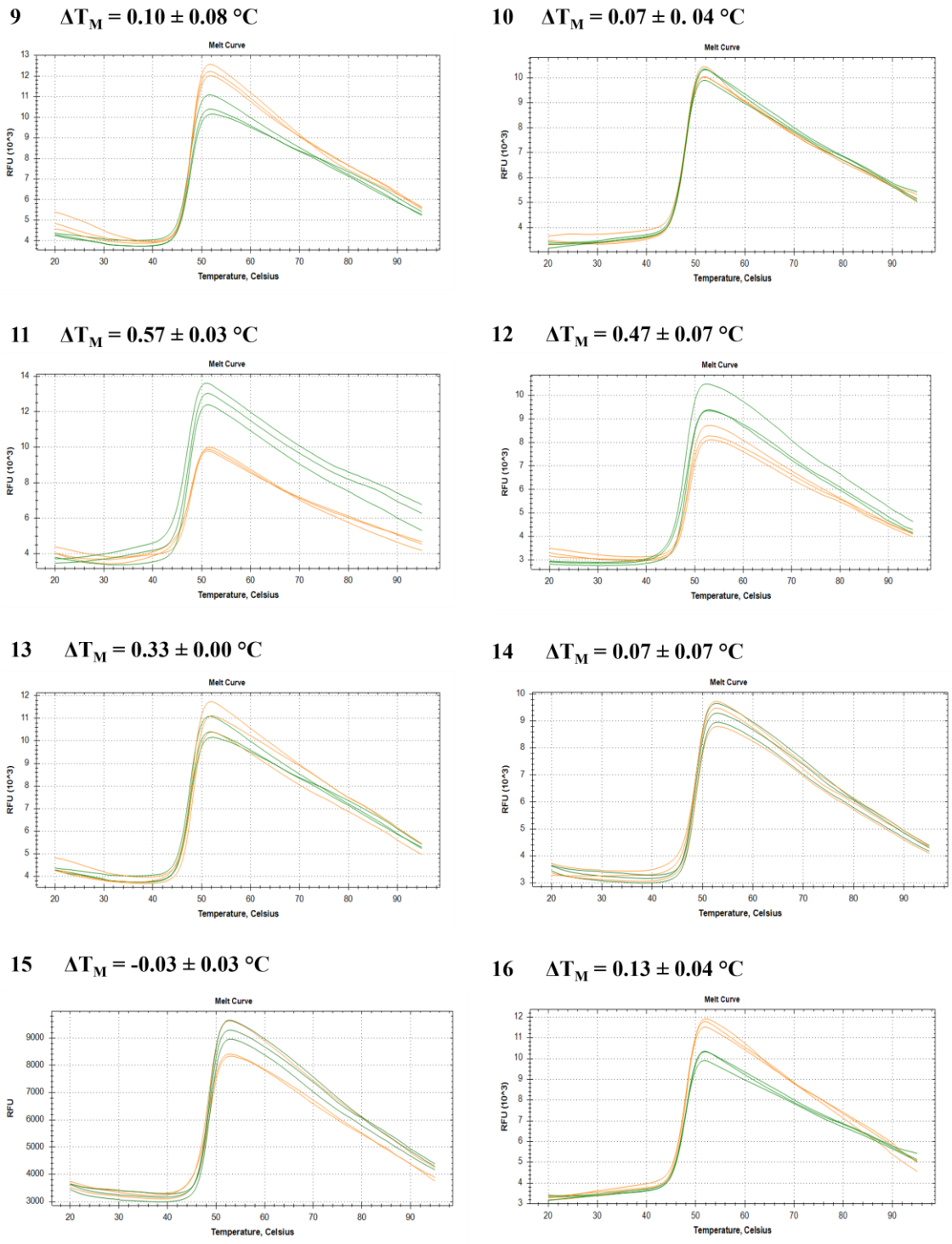

Figure A2.6. Thermal shift assay melting curves for *Ld*BDF5.2 + compounds **9-16** at 250 µM. Curves show three replicate samples of protein with compounds (orange) alongside DMSO control samples (green).

18 $\Delta T_M = 0.20 \pm 0.12$ °C

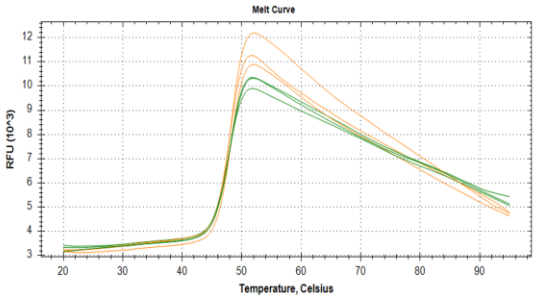

19 $\Delta T_M = 0.00 \pm 0.00$ °C

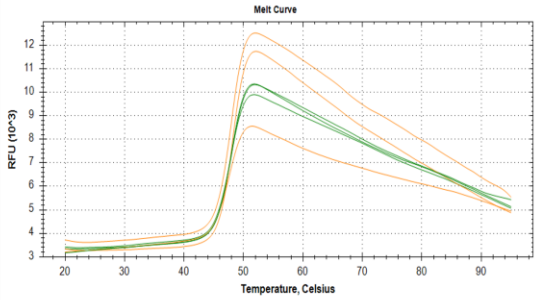

20 $\Delta T_M = 0.33 \pm 0.00$ °C

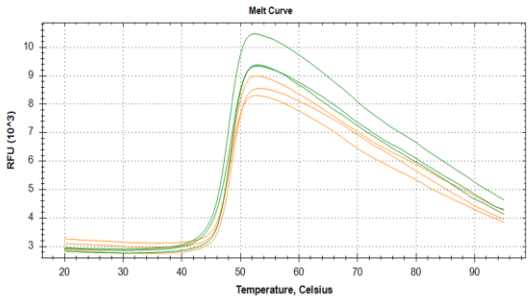

21 $\Delta T_M = 0.17 \pm 0.06$ °C

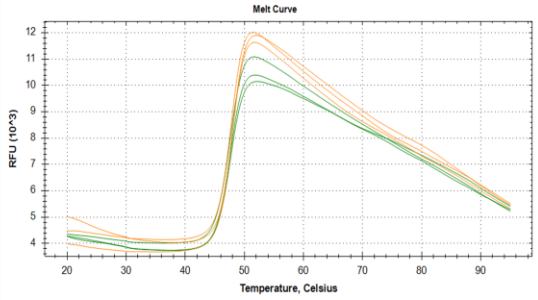

22 $\Delta T_M = 0.33 \pm 0.00$ °C

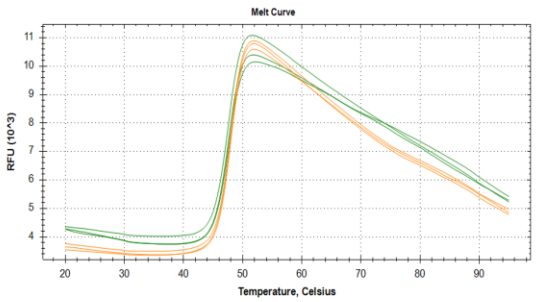

23 $\Delta T_M = 0.03 \pm 0.03$ °C

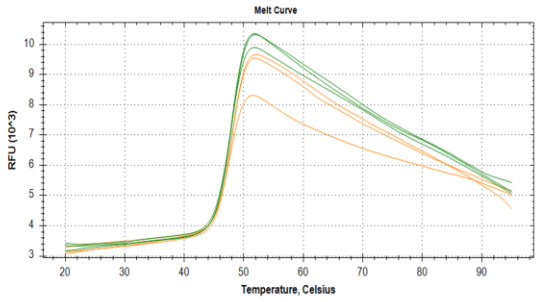

24 $\Delta T_M = 0.17 \pm 0.11$ °C

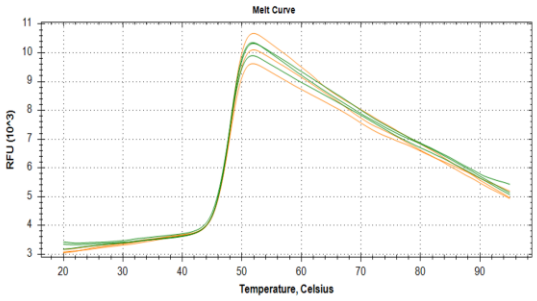

Figure A2.7. Thermal shift assay melting curves for *Ld*BDF5.2 + compounds **18-24** at 250 µM. Curves show three replicate samples of protein with compounds (orange) alongside DMSO control samples (green).

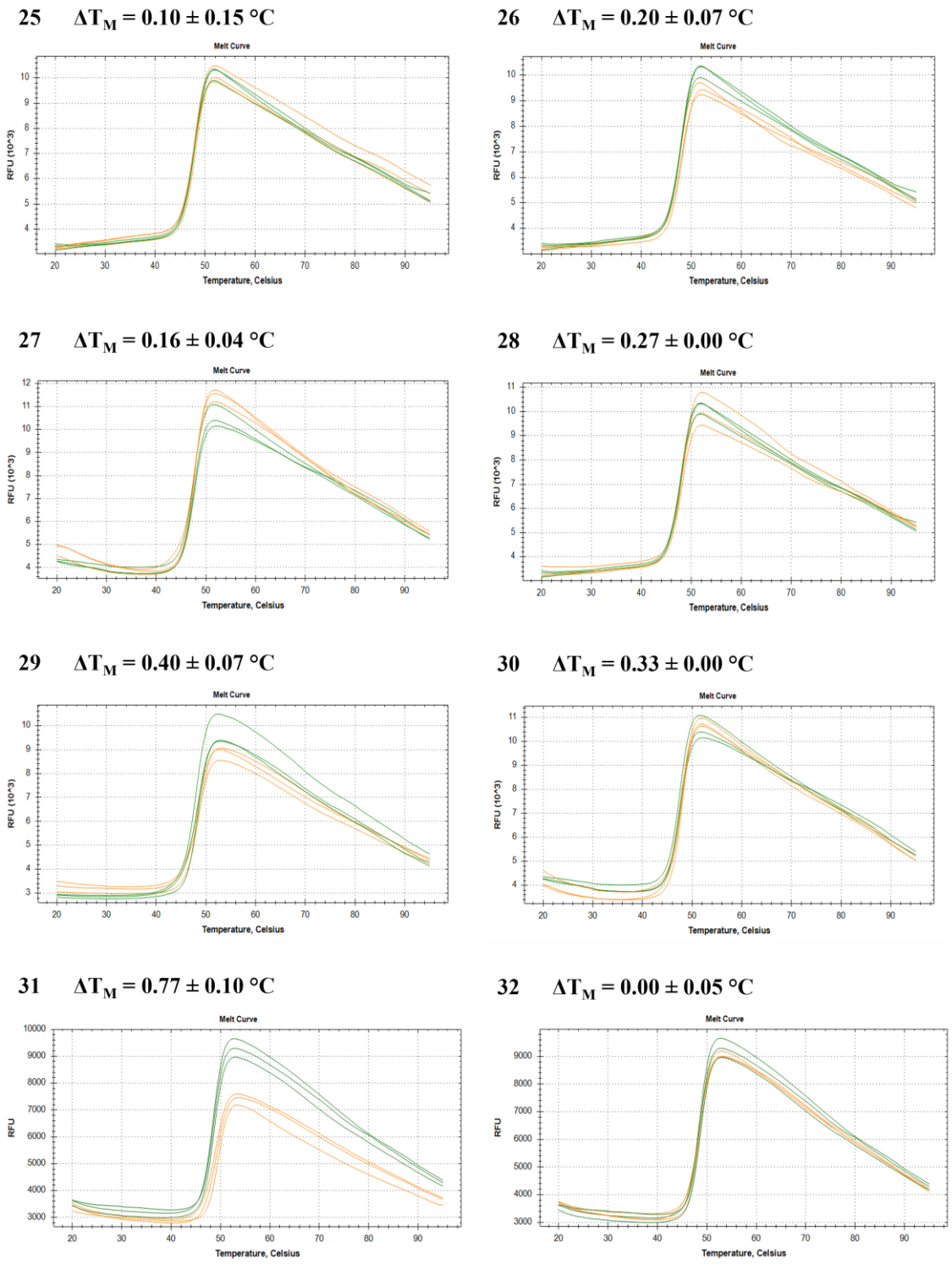

Figure A2.8. Thermal shift assay melting curves for *Ld*BDF5.2 + compounds **25-32** at 250 µM. Curves show three replicate samples of protein with compounds (orange) alongside DMSO control samples (green).

A3 Microscale Thermophoresis (MST) Data

4-(2-Ethyl-1-methyl-1*H*-benzo[*d*]imidazol-5-yl)-3,5-dimethylisoxazole

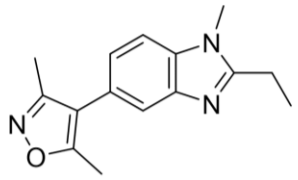

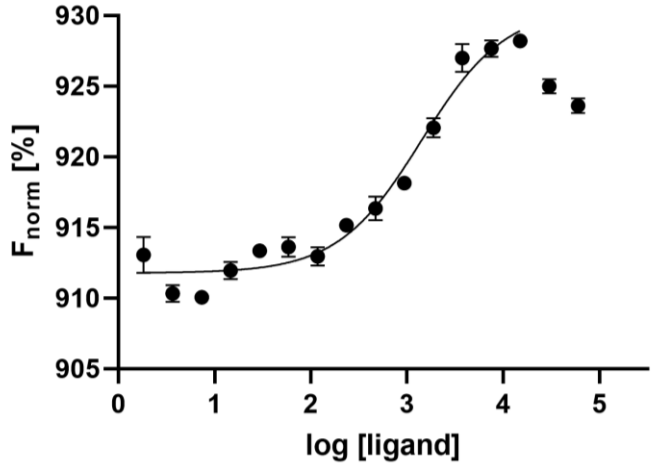

Compound	K_d
18	1410 ± 83 nM

4-(1-(2-Cyclopropylethyl)-2-ethyl-*1H*-benzo[*d*]imidazol-5-yl)-3,5-dimethylisoxazole

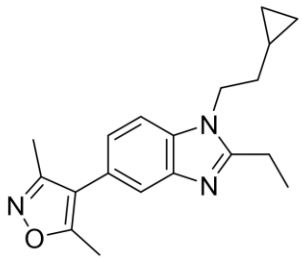

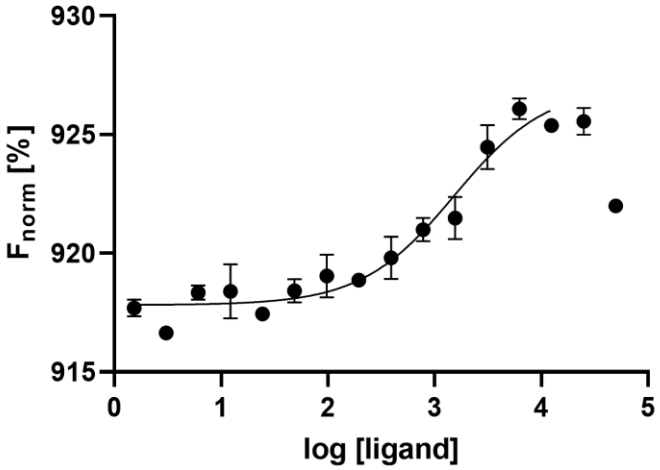

Compound	K_d
110	1641 ± 296 nM

4-(2-Ethyl-1-(2-(pyridin-2-yl)ethyl)-*1H*-benzo[*d*]imidazol-5-yl)-3,5-dimethylisoxazole

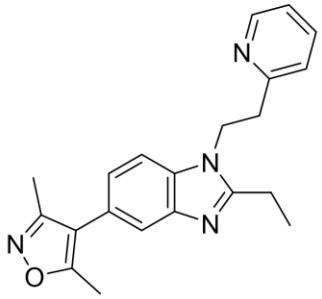

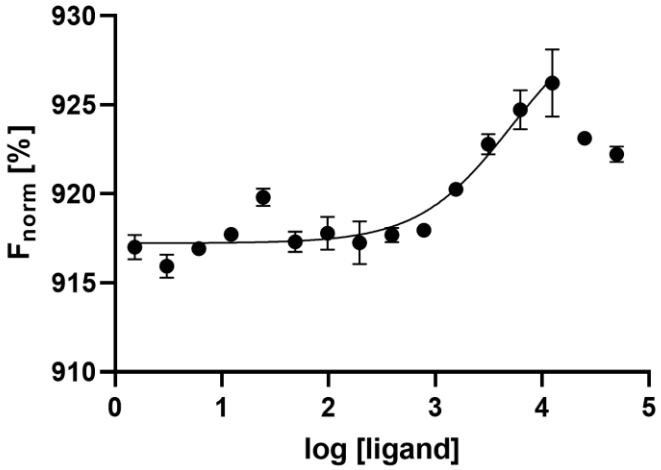

Compound	K_d
108	5125 ± 833 nM

4-(2-Ethyl-1-(2-(pyridin-3-yl)ethyl)-*1H*-benzo[*d*]imidazol-5-yl)-3,5-dimethylisoxazole

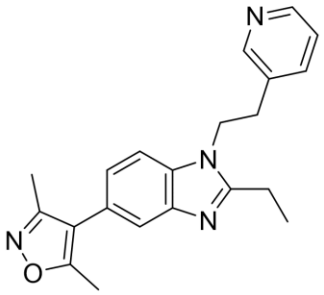

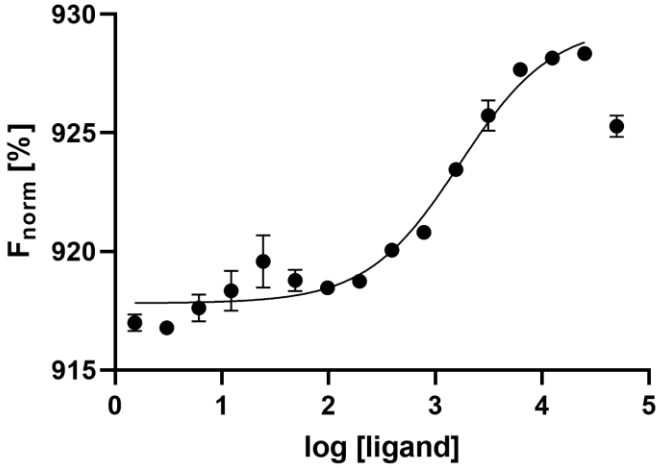

Compound	K_d
109	1720 ± 195 nM

2-(5-(3,5-Dimethylisoxazol-4-yl)-2-ethyl-1*H*-benzo[*d*]imidazol-1-yl)-*N*,*N*-dimethylethan-1-amine

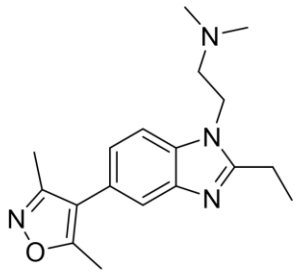

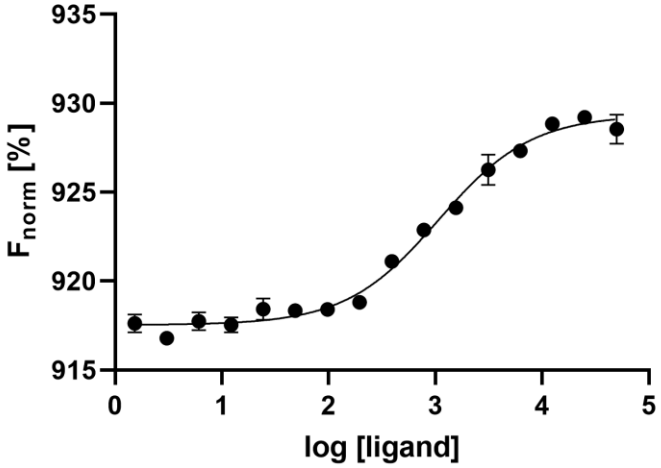

Compound	K_d
104	1119 ± 121 nM

4-(2-Ethyl-1-(2-(4-methylpiperazin-1-yl)ethyl)-1*H*-benzo[*d*]imidazol-5-yl)-3,5-dimethylisoxazole

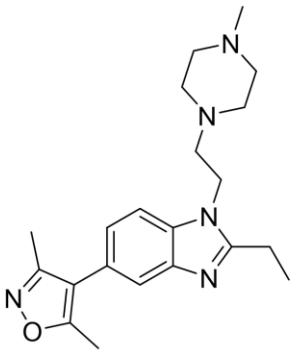

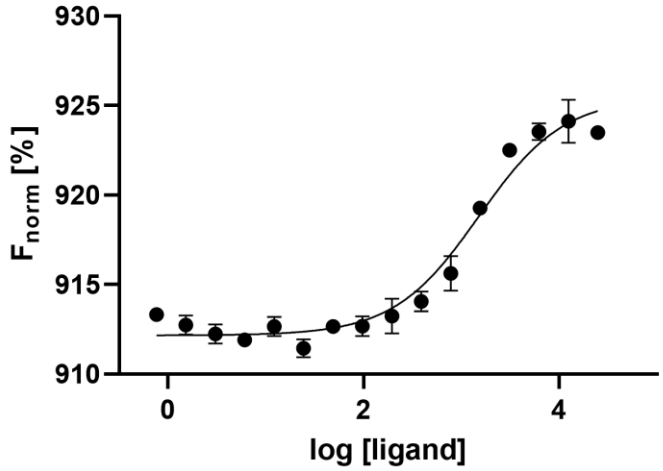

Compound	K_d
105	1537 ± 323 nM

4-(2-(5-(3,5-Dimethylisoxazol-4-yl)-2-ethyl-1*H*-benzo*[d]*imidazol-1-yl)ethyl)morpholine

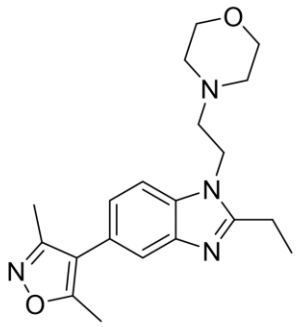

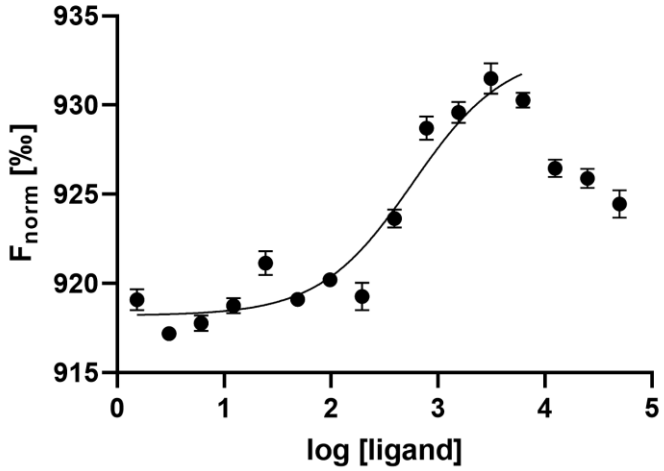

Compound	K_d
106	594 ± 84 nM

(*S*)-4-(1-(5-(3,5-Dimethylisoxazol-4-yl)-2-ethyl-1*H*-benzo[*d*]imidazol-1-yl)propan-2-yl)morpholine

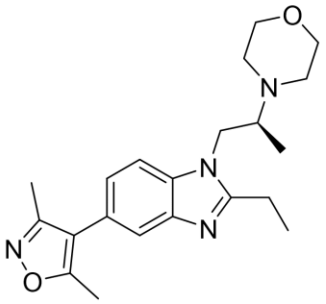

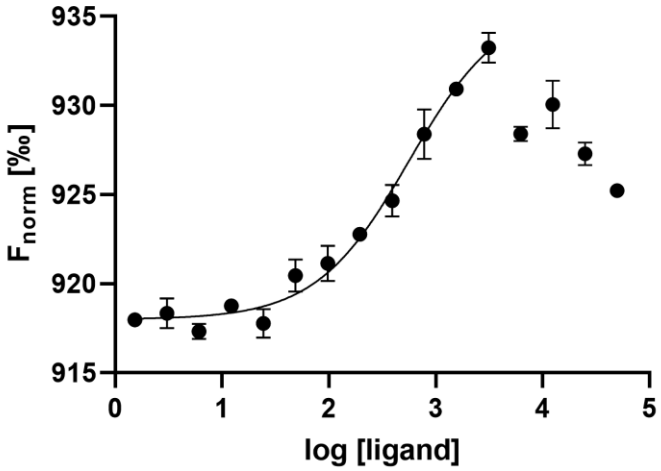

Compound	K_d
107	580 ± 121 nM

3,5-Dimethyl-4-(1-methyl-2-phenethyl-1*H*-benzo[*d*]imidazol-5-yl)isoxazole

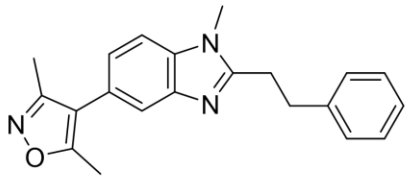

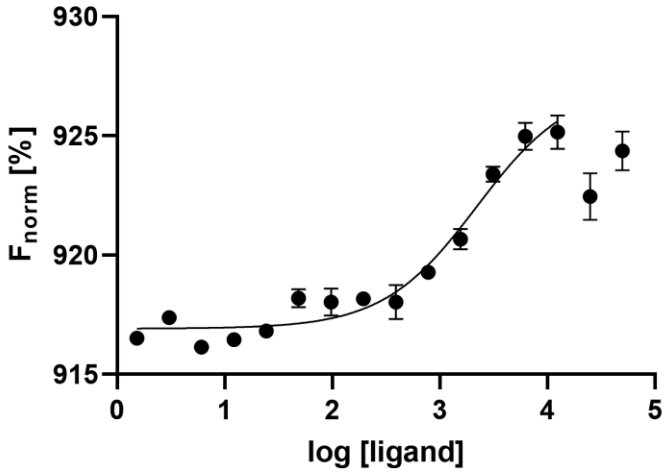

Compound	K_d
137	2474 ± 702 nM

(*S*)-4-(1-(2-(3-Chloro-4-methoxyphenethyl)-5-(3,5-dimethylisoxazol-4-yl)-1*H*-benzo[*d*]imidazol-1-yl)propan-2-yl)morpholine

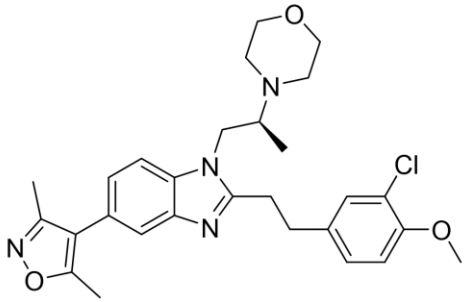

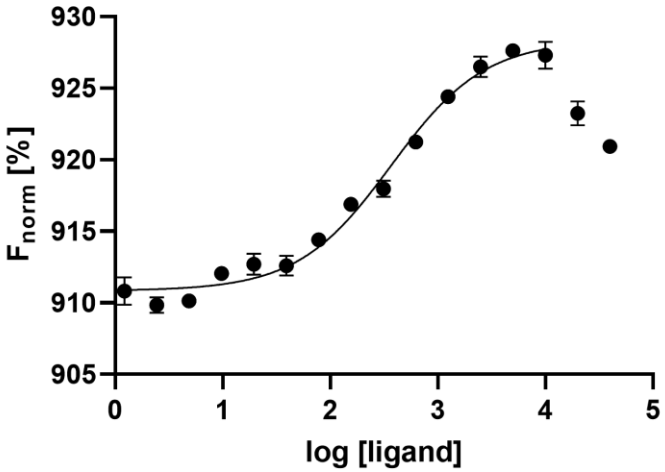

Compound	K_d
SGC-CBP30	369 ± 32 nM

3,5-Dimethyl-4-(1-methyl-2-(3-methylphenethyl)-1*H*-benzo[*d*]imidazol-5-yl)isoxazole

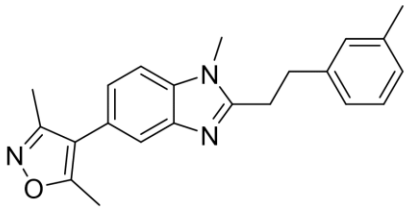

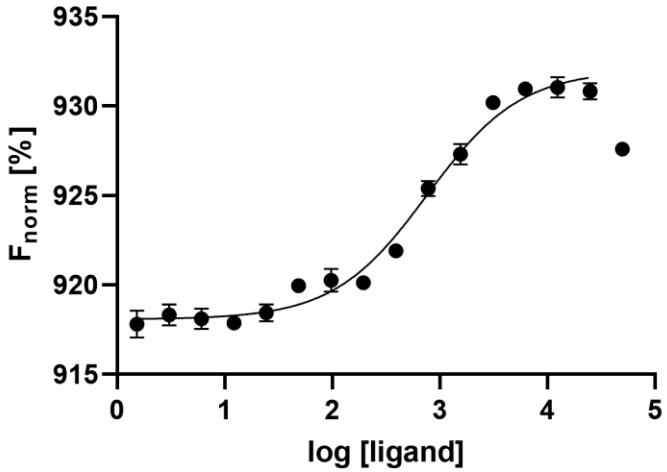

Compound	K_d
121	599 ± 29 nM

3,5-Dimethyl-4-(1-methyl-2-(4-methylphenethyl)-1*H*-benzo[*d*]imidazol-5-yl)isoxazole

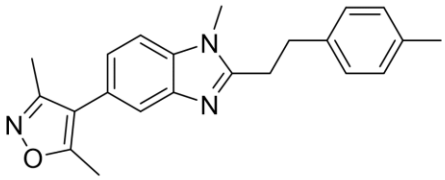

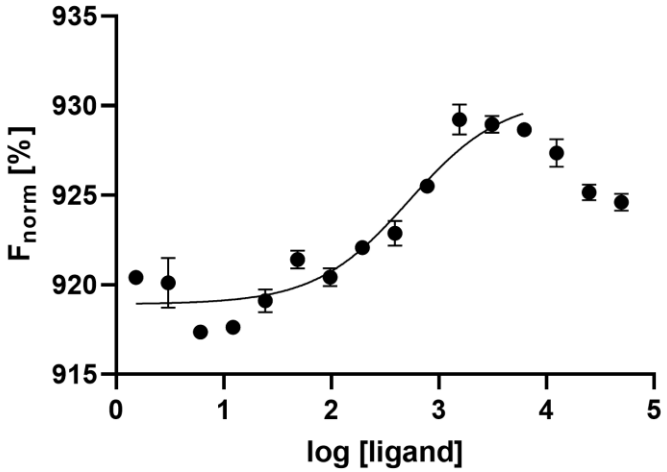

Compound	K_d
138	526 ± 131 nM

4-(2-(3-Fluorophenethyl)-1-methyl-1*H*-benzo[*d*]imidazol-5-yl)-3,5-dimethylisoxazole

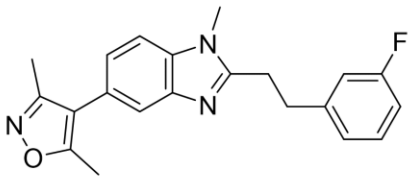

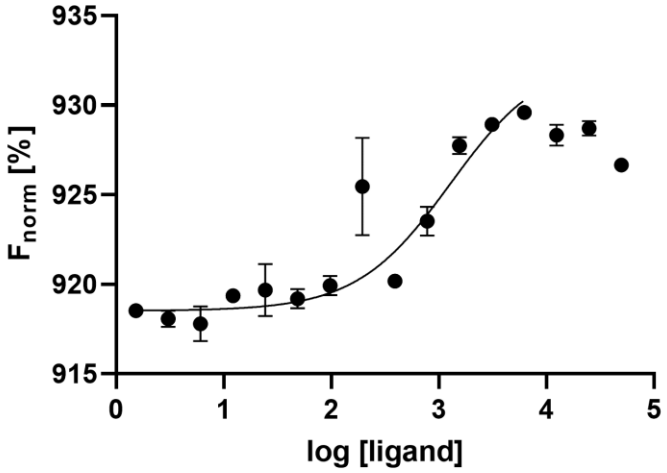

Compound	K_d
122	1294 ± 145 nM

4-(2-(4-Fluorophenethyl)-1-methyl-1*H*-benzo[*d*]imidazol-5-yl)-3,5-dimethylisoxazole

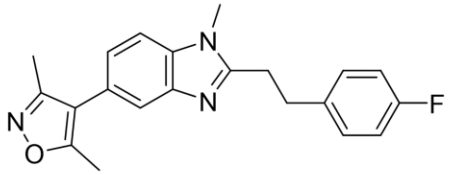

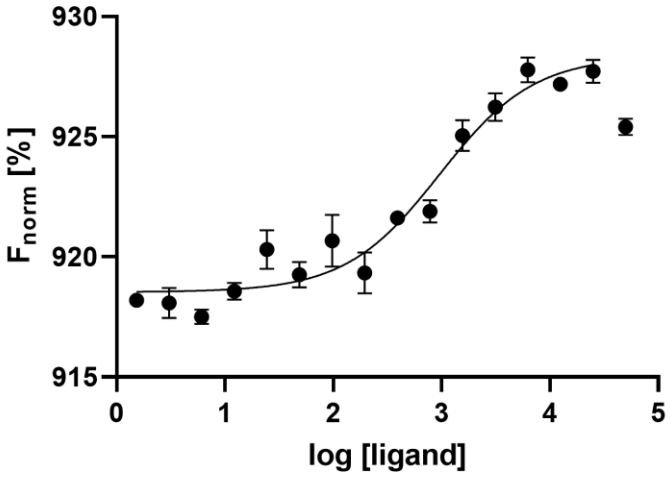

Compound	K_d
123	962 ± 14 nM

4-(2-(3-Chlorophenethyl)-1-methyl-1*H*-benzo[*d*]imidazol-5-yl)-3,5-dimethylisoxazole

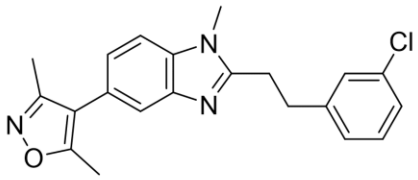

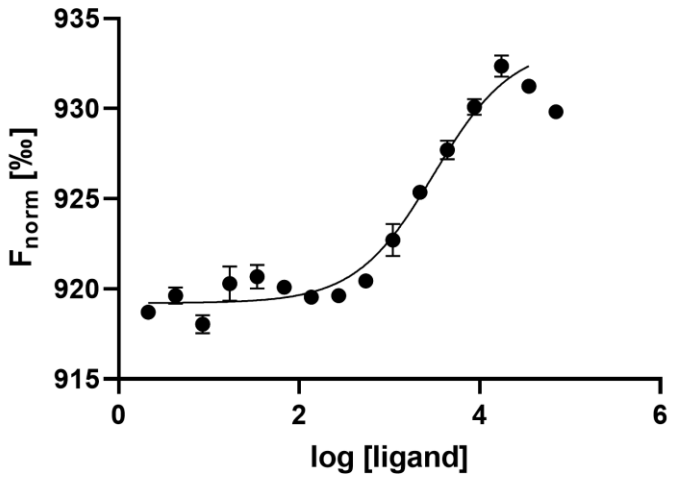

Compound	K_d
149	3139 ± 449 nM

4-(2-(4-Chlorophenethyl)-1-methyl-1*H*-benzo[*d*]imidazol-5-yl)-3,5-dimethylisoxazole

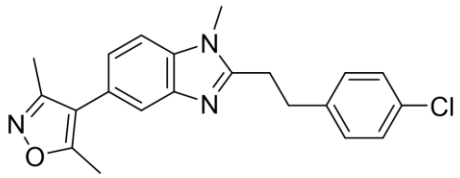

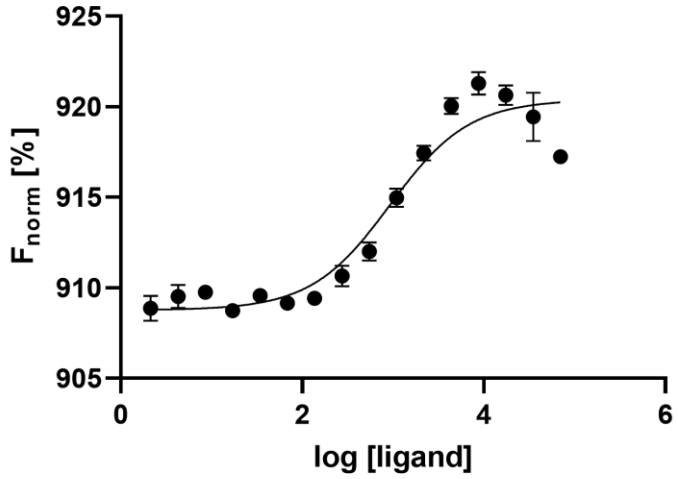

Compound	K_d
176	1451 ± 146 nM

4-(2-(3-Bromophenethyl)-1-methyl-1*H*-benzo[*d*]imidazol-5-yl)-3,5-dimethylisoxazole

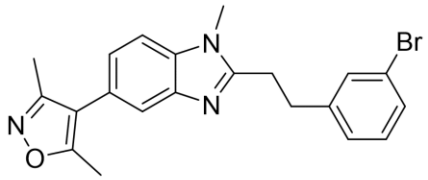

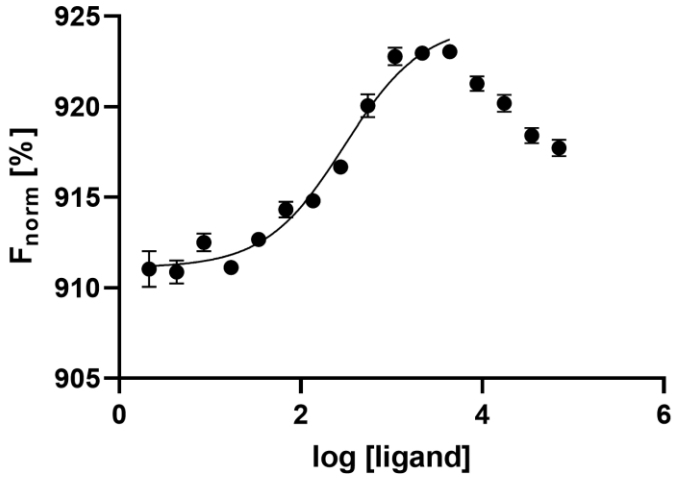

Compound	K_d
150	309 ± 33 nM

4-(2-(4-Bromophenethyl)-1-methyl-1*H*-benzo[*d*]imidazol-5-yl)-3,5-dimethylisoxazole

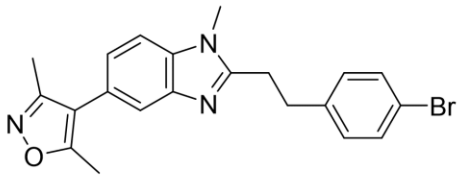

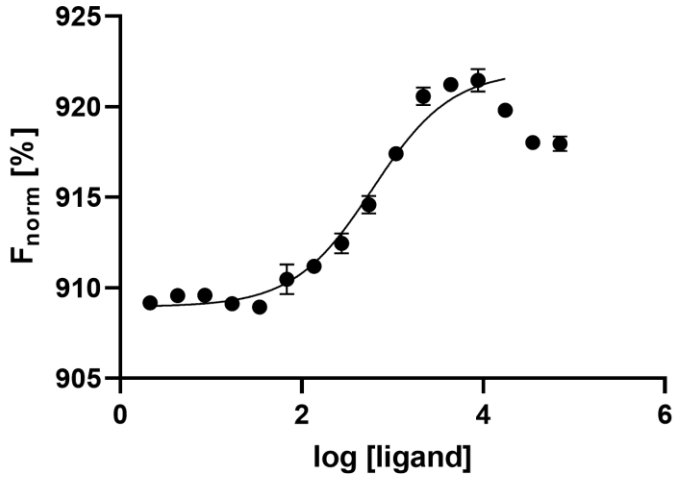

Compound	K_d
125	600 ± 39 nM

3,5-Dimethyl-4-(1-methyl-2-(3-methylphenethyl)-1*H*-benzo[*d*]imidazol-5-yl)isoxazole

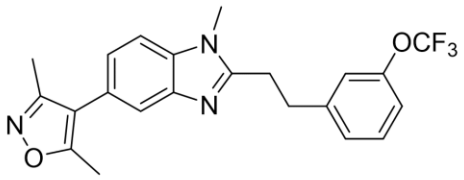

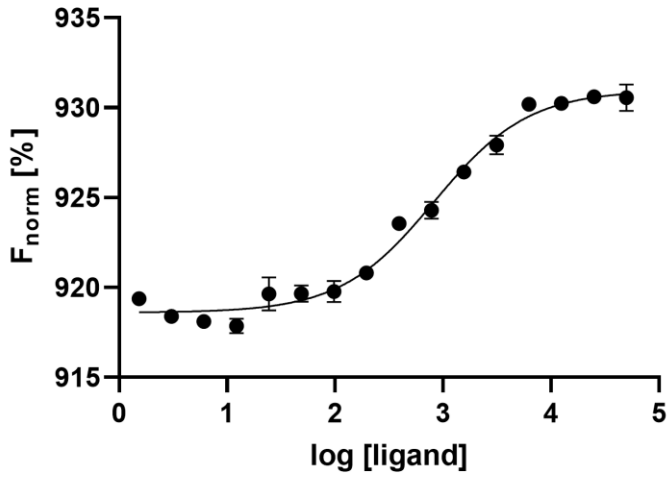

Compound	K_d
120	840 ± 46 nM

3,5-Dimethyl-4-(1-methyl-2-(4-(trifluoromethoxy)phenethyl)-1*H*-benzo[*d*]imidazol-5-yl)isoxazole

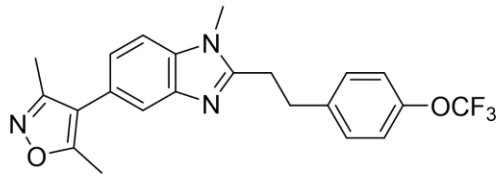

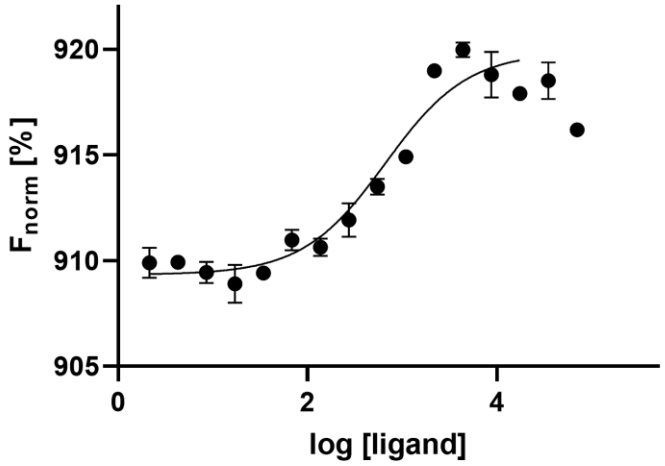

Compound	K_d
144	656 ± 62 nM

4-(2-(3-Methoxyphenethyl)-1-methyl-1*H*-benzo[*d*]imidazol-5-yl)-3,5-dimethylisoxazole

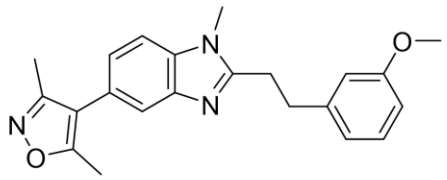

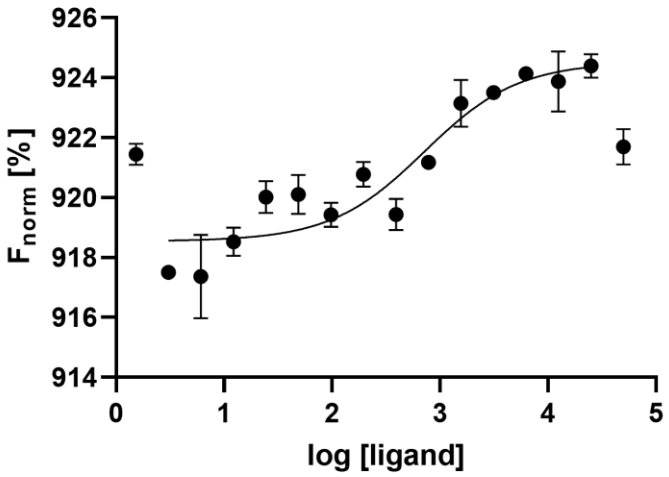

Compound	K_d
139	770 ± 143 nM

4-(2-(4-Methoxyphenethyl)-1-methyl-1*H*-benzo[*d*]imidazol-5-yl)-3,5-dimethylisoxazole

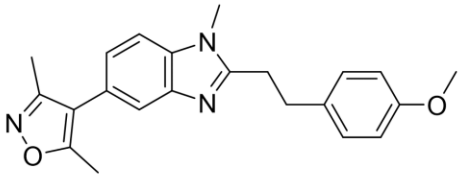

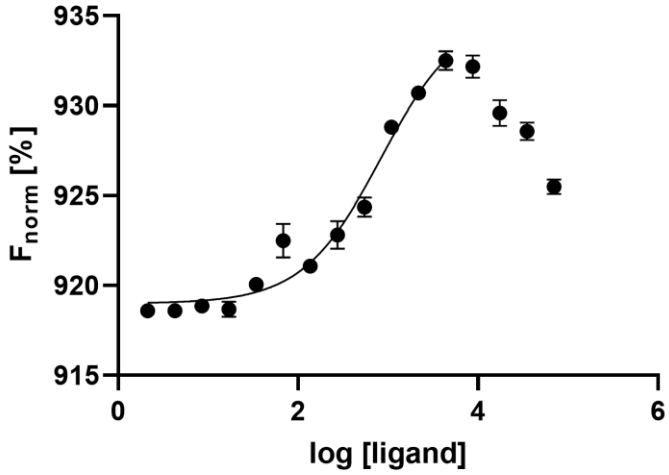

Compound	K_d
142	845 ± 120 nM

3,5-Dimethyl-4-(1-methyl-2-(3-nitrophenethyl)-1*H*-benzo[*d*]imidazol-5-yl)isoxazole

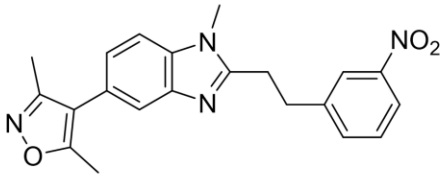

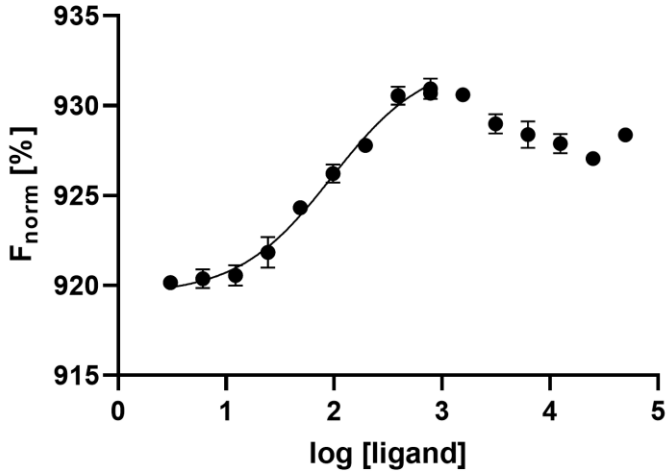

Compound	K_d
151	96 ± 10 nM

3,5-Dimethyl-4-(1-methyl-2-(4-nitrophenethyl)-1*H*-benzo[*d*]imidazol-5-yl)isoxazole

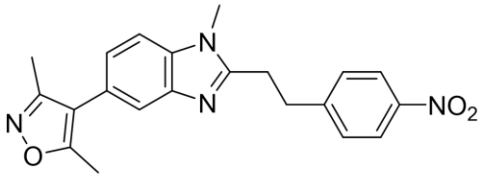

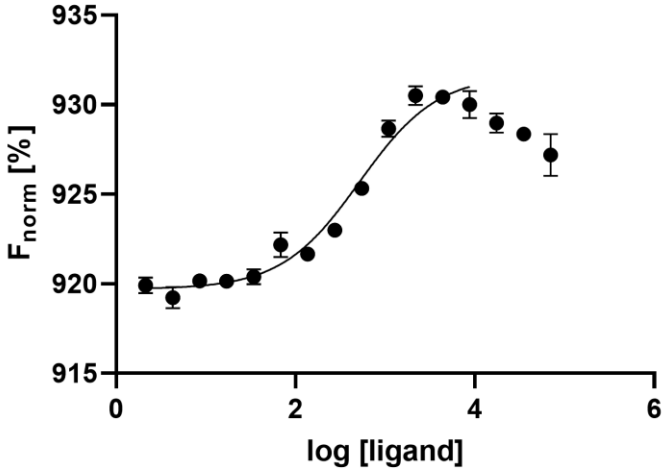

Compound	K_d
152	308 ± 20 nM

3-(2-(5-(3,5-Dimethylisoxazol-4-yl)-1-methyl-1*H*-benzo[*d*]imidazol-2-yl)ethyl)benzonitrile

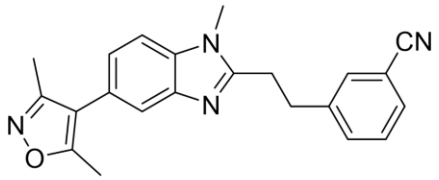

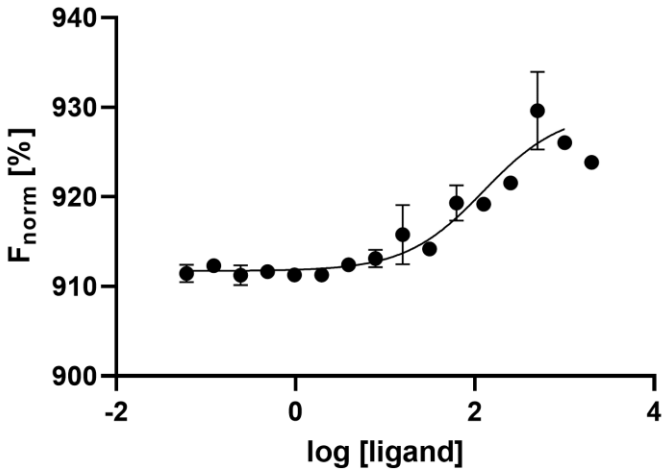

Compound	K_d
154	120 ± 16 nM

4-(2-(5-(3,5-Dimethylisoxazol-4-yl)-1-methyl-1*H*-benzo[*d*]imidazol-2-yl)ethyl)benzonitrile

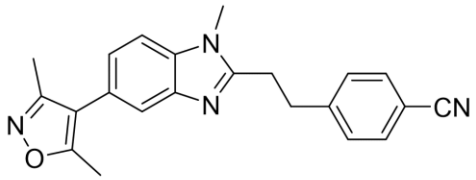

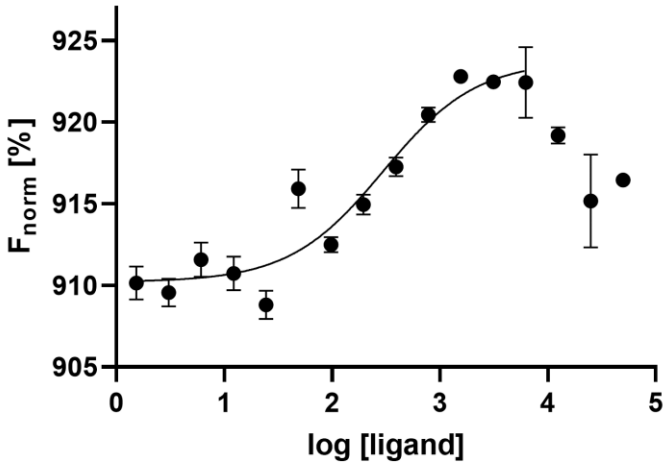

Compound	K_d
155	329 ± 121 nM

3,5-Dimethyl-4-(1-methyl-2-(3-(trifluoromethyl)phenethyl)-1*H*-benzo[*d*]imidazol-5-yl)isoxazole

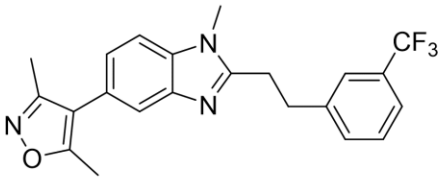

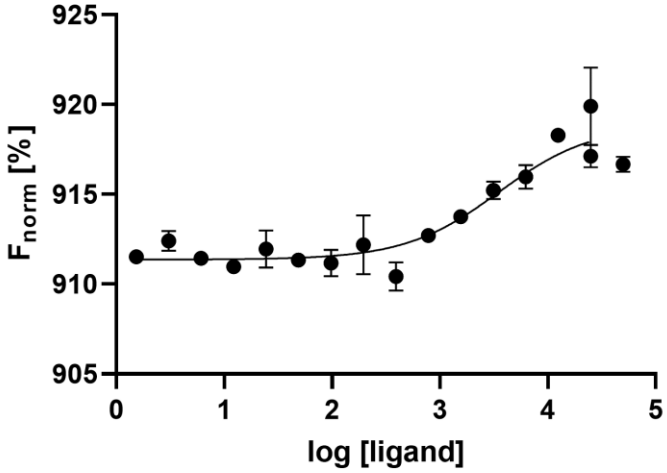

Compound	K_d
153	3605 ± 770 nM

3,5-Dimethyl-4-(1-methyl-2-(4-(trifluoromethyl)phenethyl)-1*H*-benzo[*d*]imidazol-5-yl)isoxazole

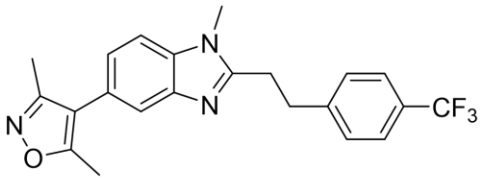

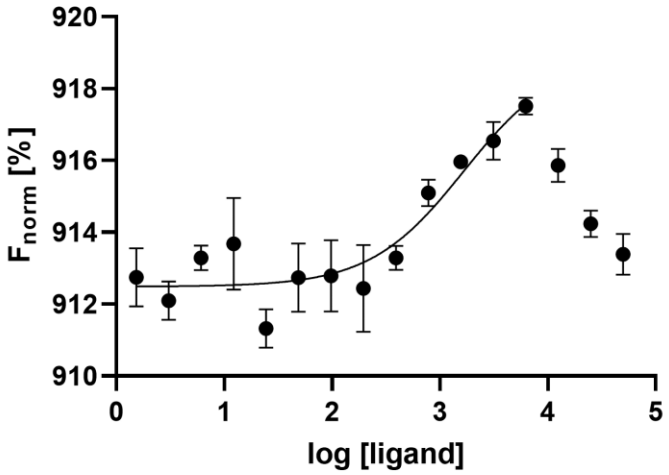

Compound	K_d
177	1829 ± 148 nM

Methyl 3-(2-(5-(3,5-dimethylisoxazol-4-yl)-1-methyl-1*H*-benzo[*d*]imidazol-2-yl)ethyl)benzoate

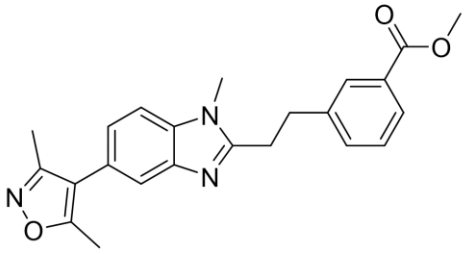

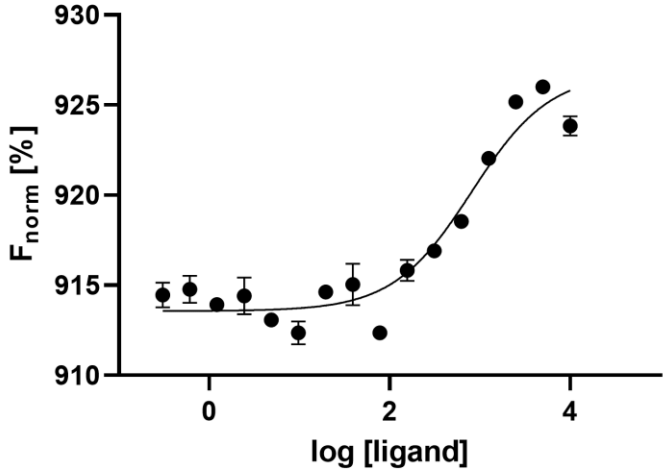

Compound	K_d
145	814 ± 131 nM

Methyl 4-(2-(5-(3,5-dimethylisoxazol-4-yl)-1-methyl-1*H*-benzo[*d*]imidazol-2-yl)ethyl)benzoate

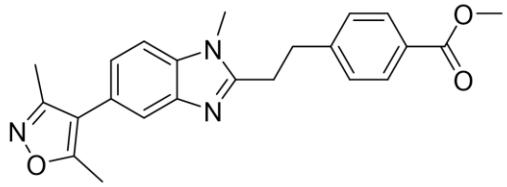

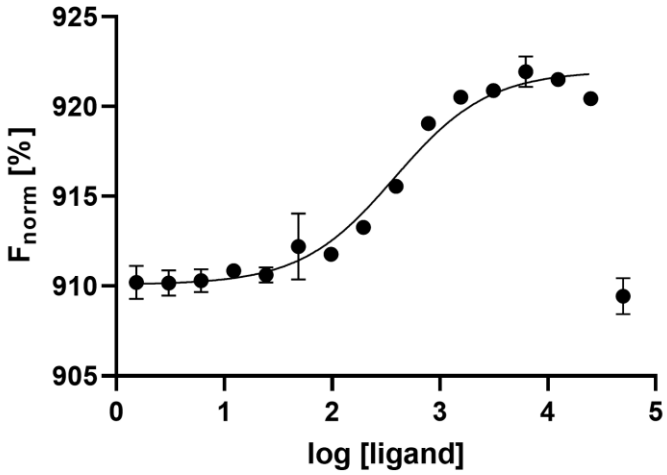

Compound	K_d
146	383 ± 48 nM

3-(2-(5-(3,5-Dimethylisoxazol-4-yl)-1-methyl-1*H*-benzo[*d*]imidazol-2-yl)ethyl)benzoic acid

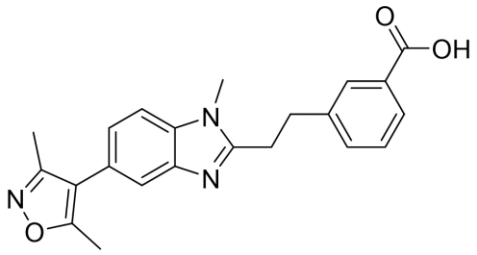

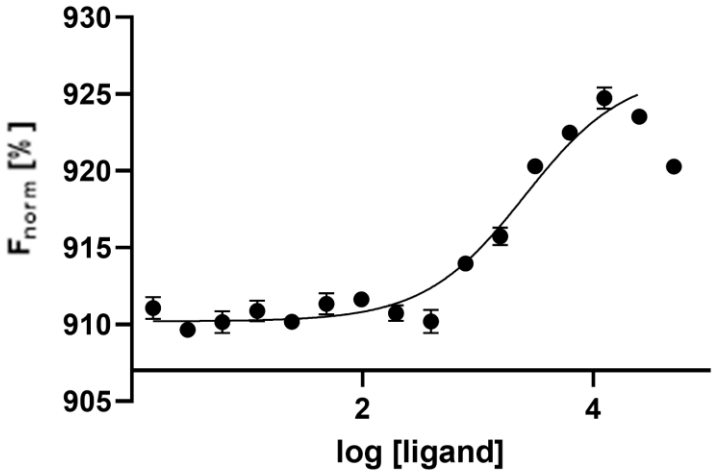

Compound	K_d
147	2548 ± 296 nM

4-(2-(5-(3,5-Dimethylisoxazol-4-yl)-1-methyl-1*H*-benzo[*d*]imidazol-2-yl)ethyl)benzoic acid

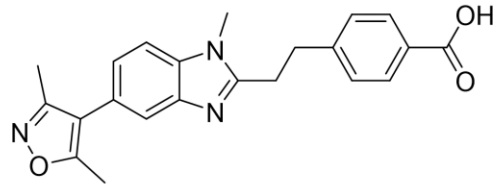

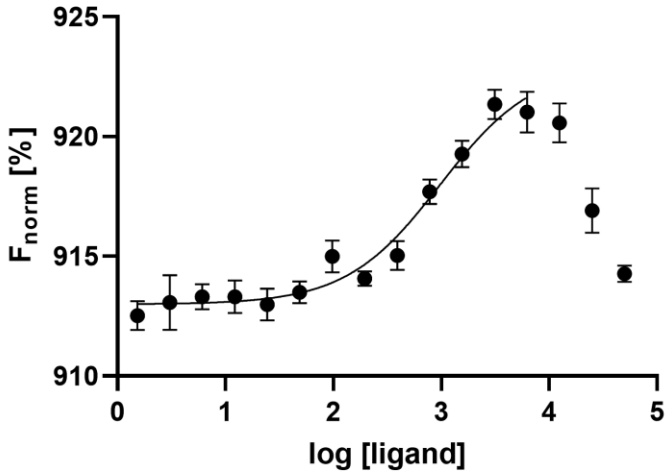

Compound	K_d
148	1147 ± 261 nM

3,5-Dimethyl-4-(1-methyl-2-(3-methylbenzyl)-1*H*-benzo[*d*]imidazol-5-yl)isoxazole

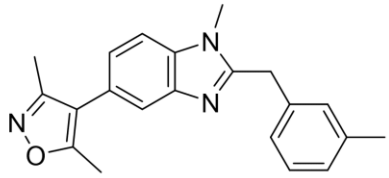

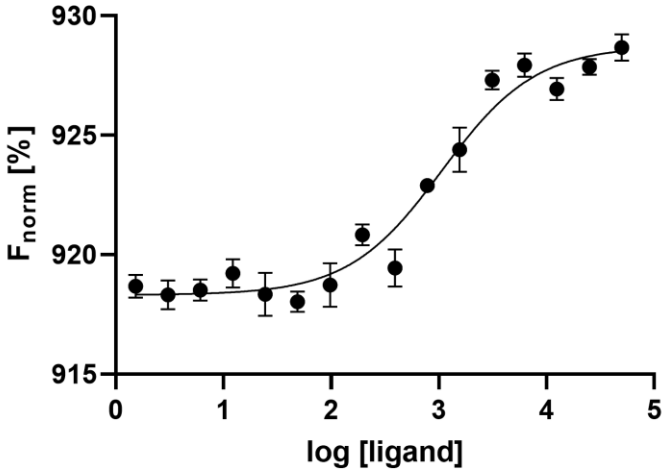

Compound	K_d
112	1084 ± 121 nM

3,5-Dimethyl-4-(1-methyl-2-(4-methylbenzyl)-1*H*-benzo[*d*]imidazol-5-yl)isoxazole

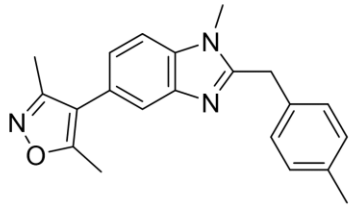

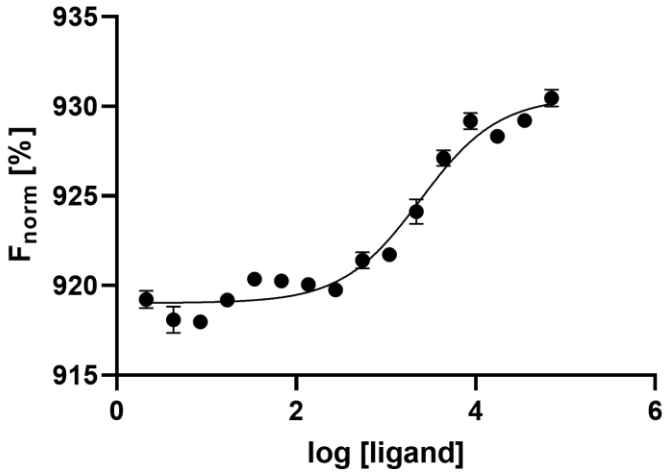

Compound	K_d
111	2420 ± 218 nM

4-(2-(4-Methoxy-3-methylphenethyl)-1-methyl-1*H*-benzo[*d*]imidazol-5-yl)-3,5-dimethylisoxazole

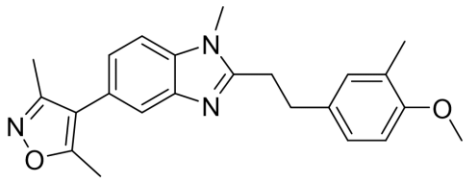

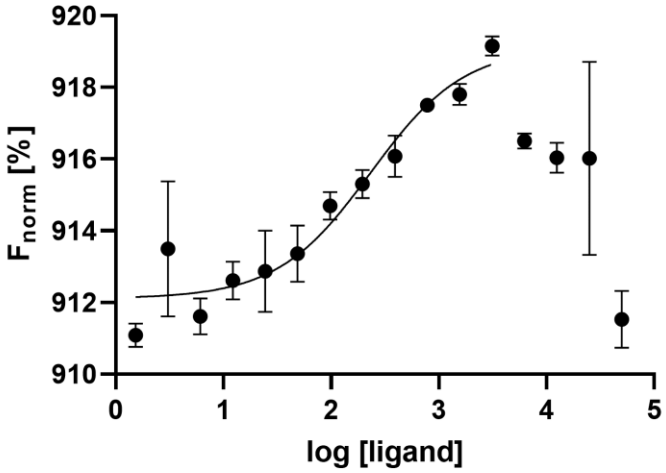

Compound	K_d
141	218 ± 104 nM

4-(2-(3-Chloro-4-methoxyphenethyl)-1-methyl-1*H*-benzo[*d*]imidazol-5-yl)-3,5-dimethylisoxazole

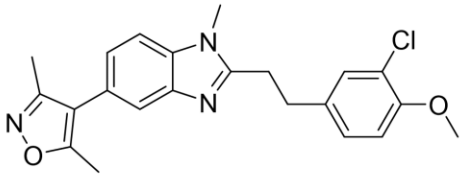

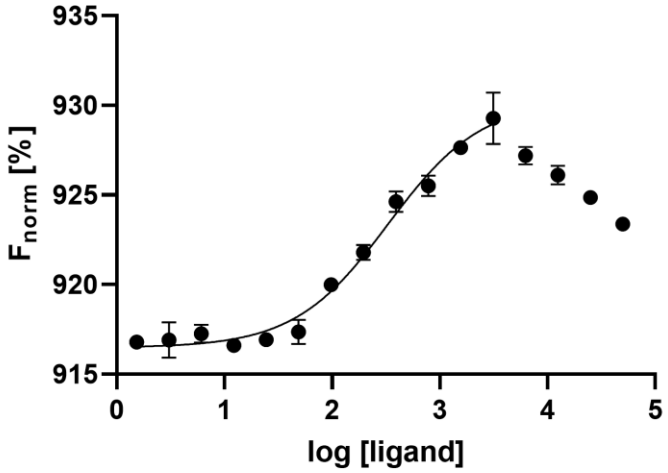

Compound	K_d
143	353 ± 89 nM

5-(2-(5-(3,5-Dimethylisoxazol-4-yl)-1-methyl-1*H*-benzo[*d*]imidazol-2-yl)ethyl)-2-methylbenzonitrile

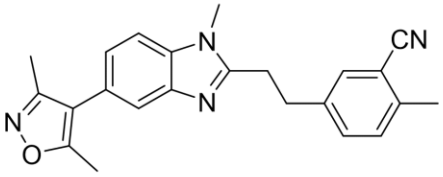

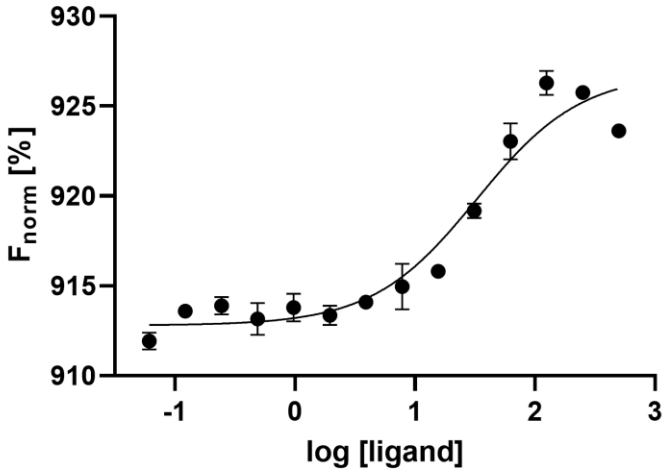

Compound	K_d
156	33 ± 4 nM

4-(2-(5-(3,5-Dimethylisoxazol-4-yl)-1-methyl-1*H*-benzo[*d*]imidazol-2-yl)ethyl)-2-methylbenzonitrile

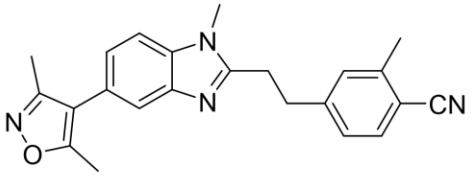

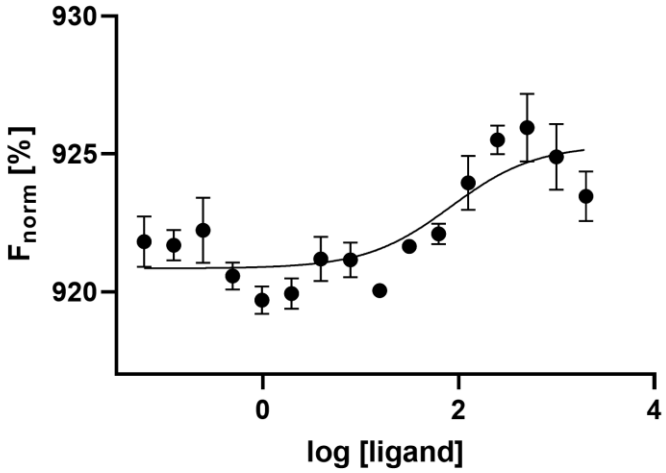

Compound	K_d
157	114 ± 22 nM

4-(2-(5-(3,5-Dimethylisoxazol-4-yl)-2-(3-nitrophenethyl)-1*H*-benzo[*d*]imidazol-1-yl)ethyl)morpholine

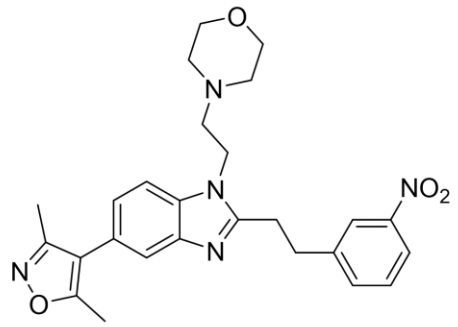

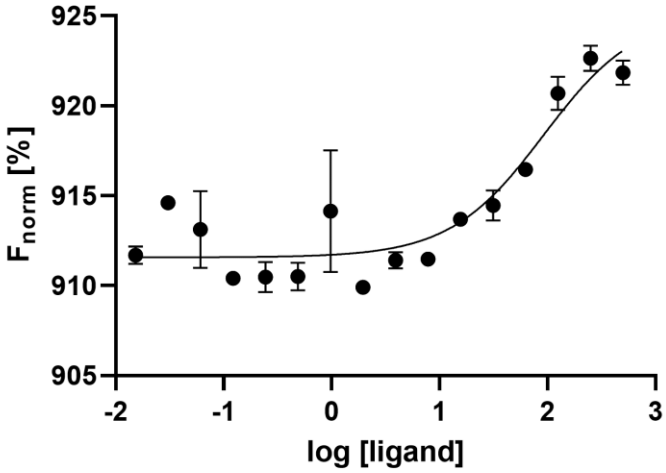

Compound	K_d
172	93 ± 5 nM

4-(2-(5-(3,5-Dimethylisoxazol-4-yl)-2-(4-nitrophenethyl)-1*H*-benzo[*d*]imidazol-1-yl)ethyl)morpholine

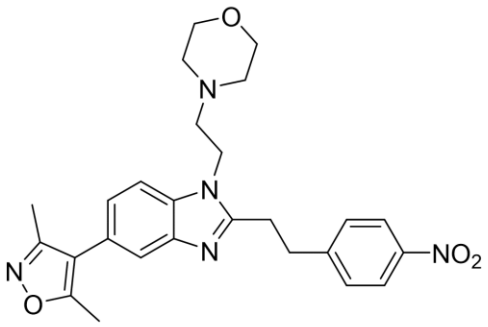

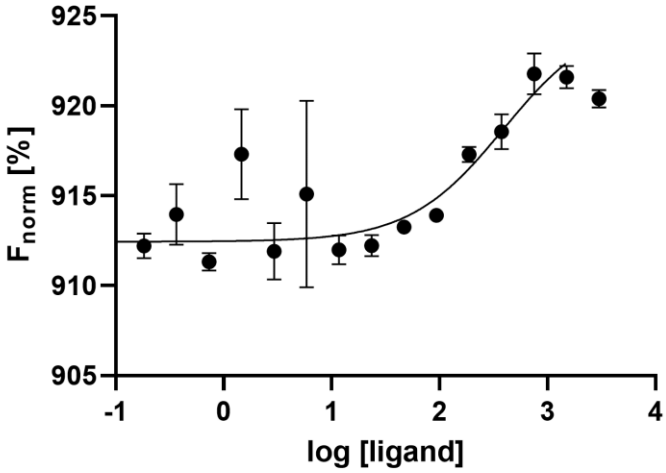

Compound	K_d
173	395 ± 17 nM

3-(2-(5-(3,5-Dimethylisoxazol-4-yl)-1-(2-morpholinoethyl)-1*H*-benzo[*d*]imidazol-2-yl)ethyl)benzonitrile

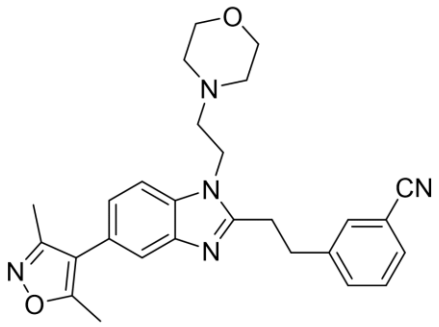

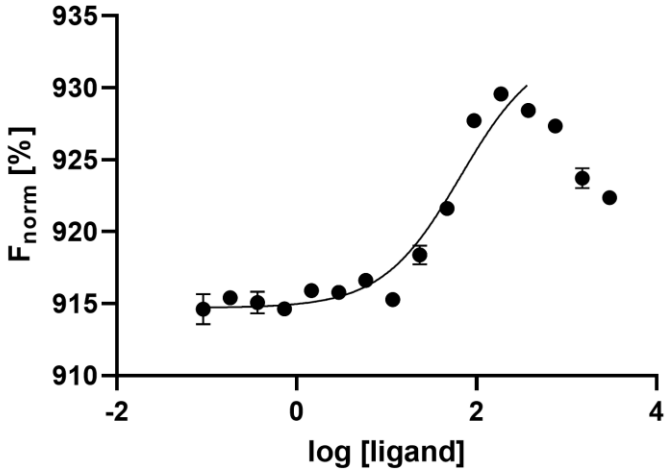

Compound	K_d
170	66 ± 1 nM

4-(2-(5-(3,5-Dimethylisoxazol-4-yl)-1-(2-morpholinoethyl)-1*H*-benzo[*d*]imidazol-2-yl)ethyl)benzonitrile

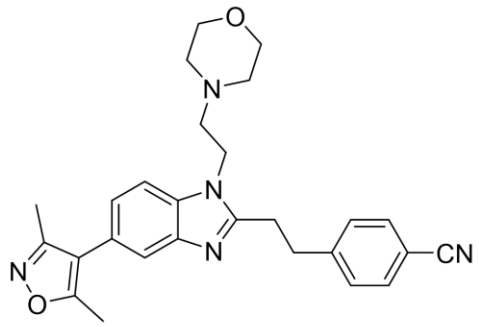

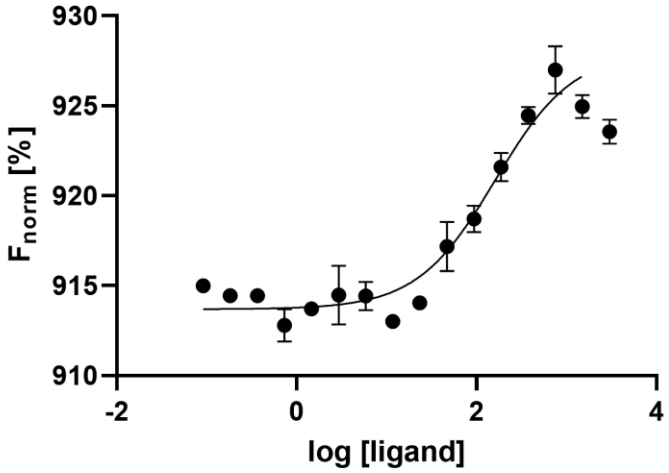

Compound	K_d
178	163 ± 14 nM

4-(2-(5-(3,5-Dimethylisoxazol-4-yl)-2-(3-methylphenethyl)-1*H*-benzo[*d*]imidazol-1-yl)ethyl)morpholine

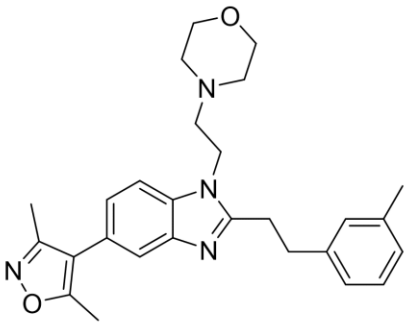

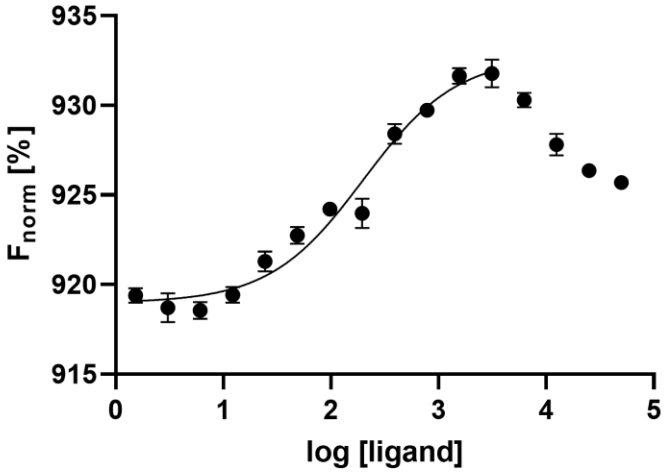

Compound	K_d
171	222 ± 63 nM

4-(2-(5-(3,5-Dimethylisoxazol-4-yl)-2-(4-methylphenethyl)-1*H*-benzo[*d*]imidazol-1-yl)ethyl)morpholine

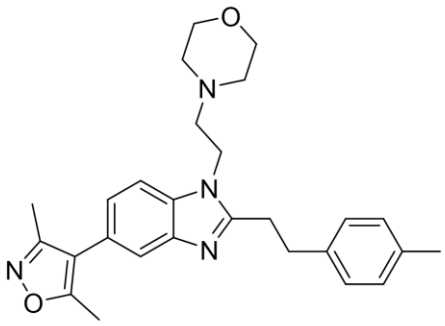

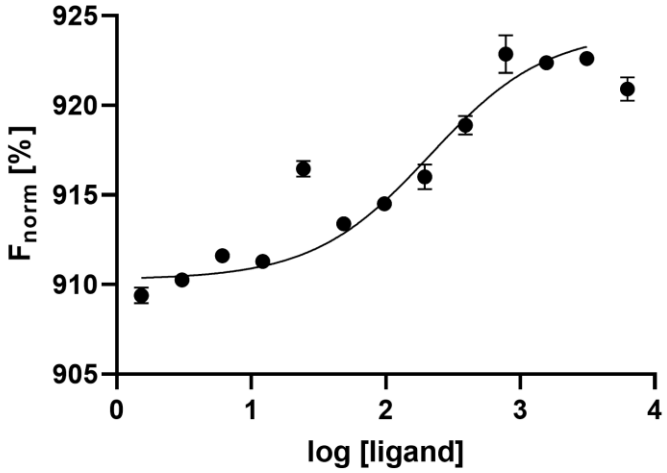

Compound	K_d
179	238 ± 60 nM

5-(2-(5-(3,5-Dimethylisoxazol-4-yl)-1-(2-morpholinoethyl)-1*H*-benzo[*d*]imidazol-2-yl)ethyl)-2-methylbenzonitrile

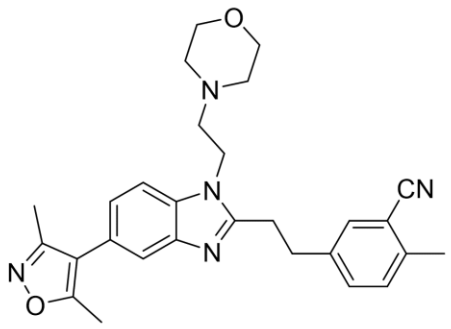

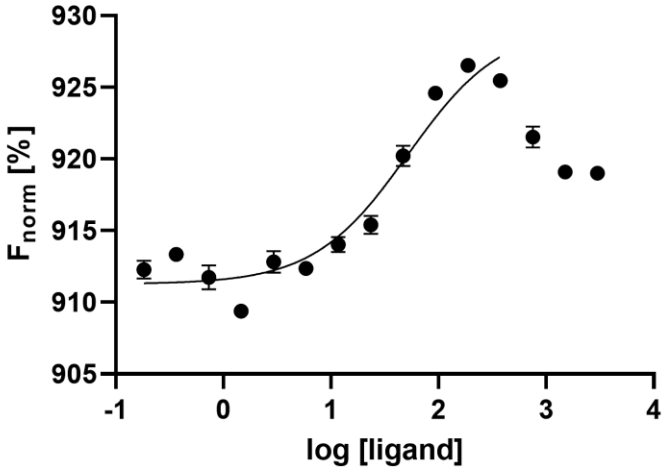

Compound	K_d
174	52 ± 3 nM

4-(2-(5-(3,5-Dimethylisoxazol-4-yl)-1-(2-morpholinoethyl)-1*H*-benzo[*d*]imidazol-2-yl)ethyl)-2-methylbenzonitrile

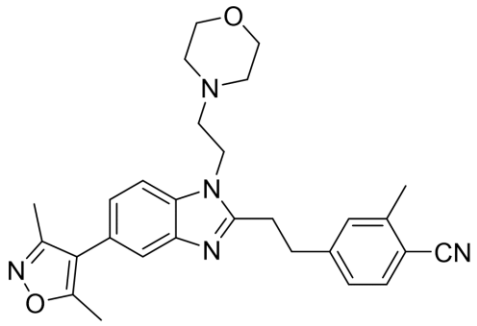

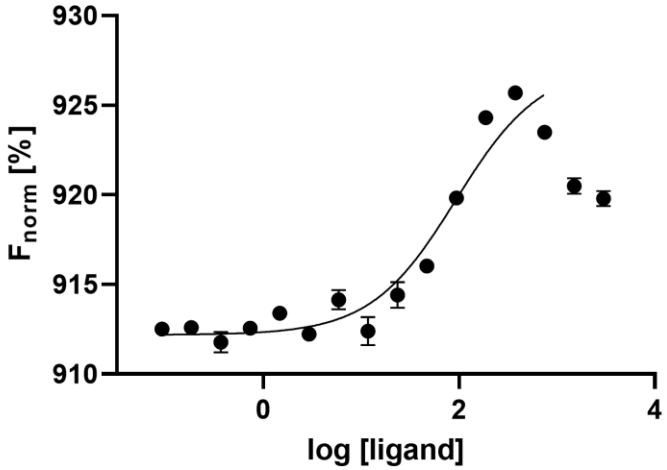

Compound	K_d
175	93 ± 6 nM

4-(2-(5-(3,5-Dimethylisoxazol-4-yl)-1-(2-(piperidin-1-yl)ethyl)-1*H*-benzo[*d*]imidazol-2-yl)ethyl)-2-methylbenzonitrile

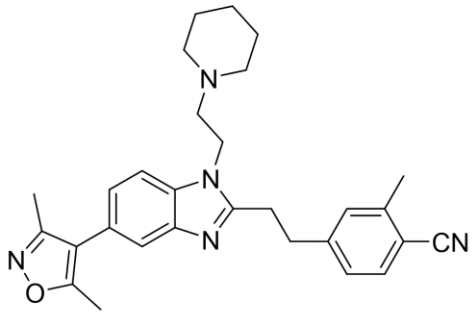

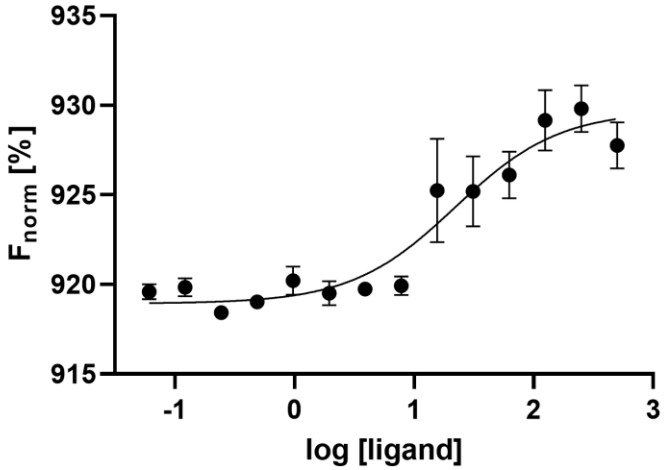

Compound	K_d
180	28 ± 15 nM

4-(2-(5-(3,5-Dimethylisoxazol-4-yl)-1-(2-(tetrahydro-2*H*-pyran-4-yl)ethyl)-1*H*-benzo[*d*]imidazol-2-yl)ethyl)-2-methylbenzonitrile

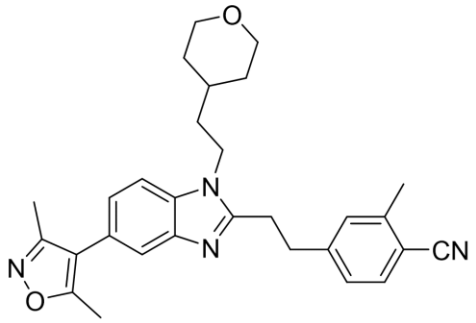

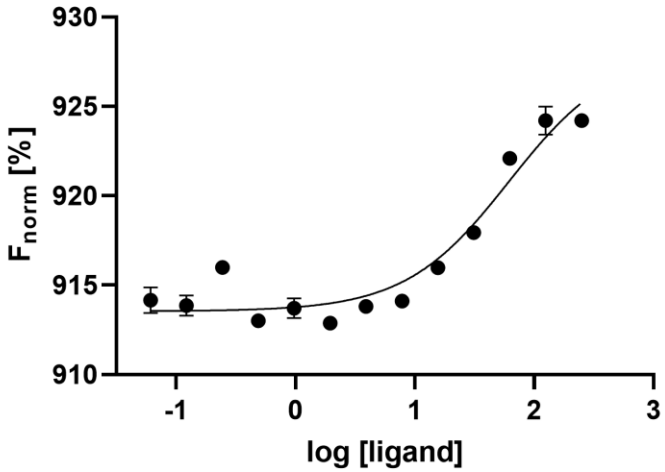

Compound	K_d
186	36 ± 2 nM

5-(2-(5-(3,5-Dimethylisoxazol-4-yl)-1-(2-(4-methylpiperazin-1-yl)ethyl)-1*H*-benzo[*d*]imidazol-2-yl)ethyl)-2-methylbenzonitrile

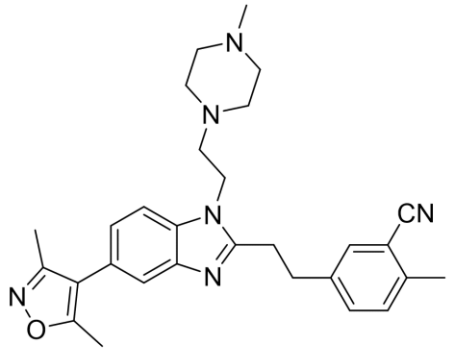

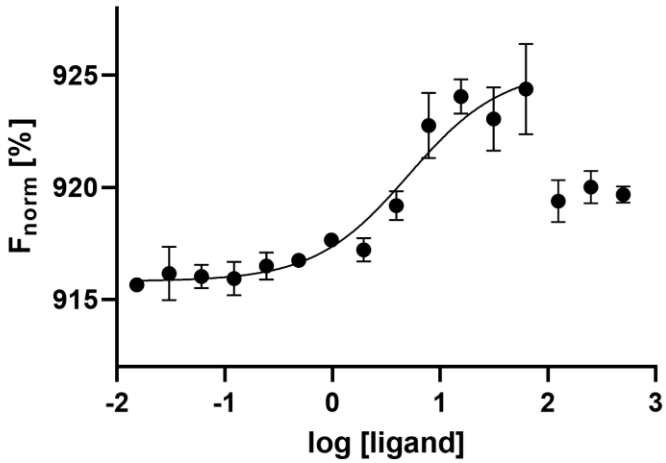

Compound	K_d
183	6 ± 2 nM

4-(2-(5-(3,5-Dimethylisoxazol-4-yl)-1-(2-methoxyethyl)-1*H*-benzo[*d*]imidazol-2-yl)ethyl)-2-methylbenzonitrile

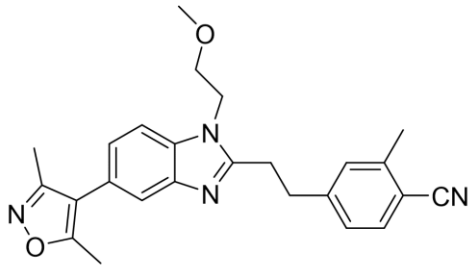

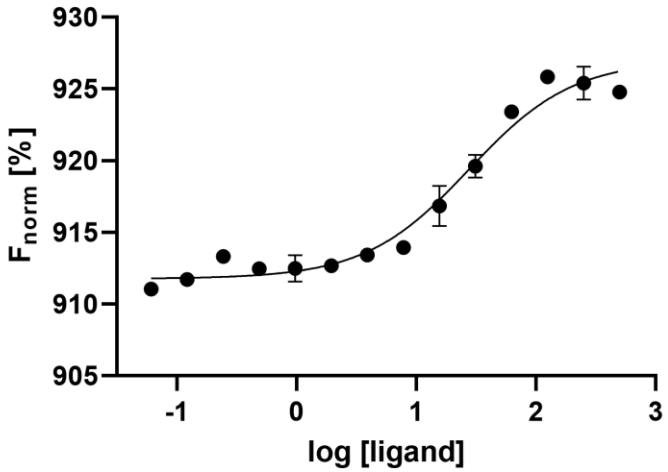

Compound	K_d
185	29 ± 6 nM

4-(2-(1-(2-(4-Acetylpiperazin-1-yl)ethyl)-5-(3,5-dimethylisoxazol-4-yl)-1*H*-benzo[*d*]imidazol-2-yl)ethyl)-2-methylbenzonitrile

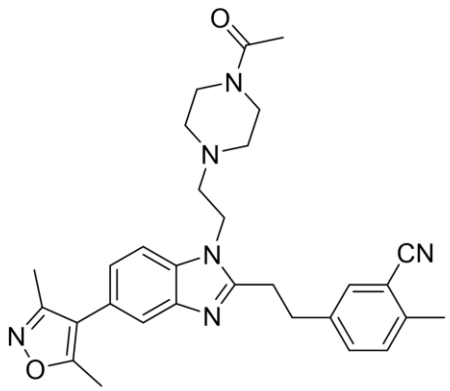

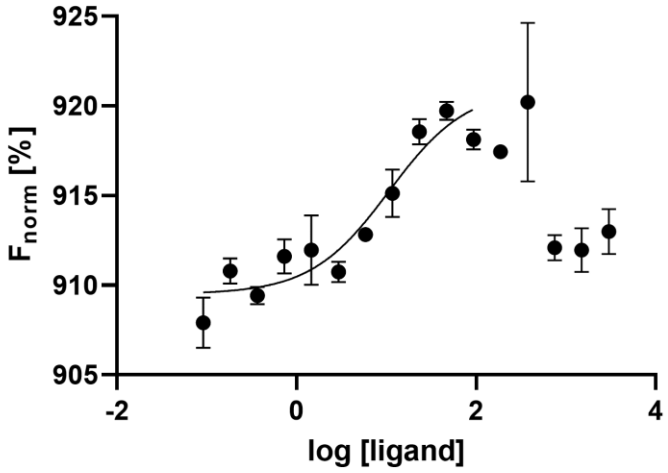

Compound	K_d
181	11 ± 5 nM

5-((5-(3,5-Dimethylisoxazol-4-yl)-1-methyl-1*H*-benzo[*d*]imidazol-2-yl)methoxy)-2-methylbenzonitrile

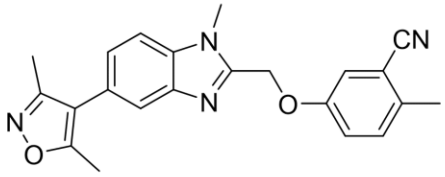

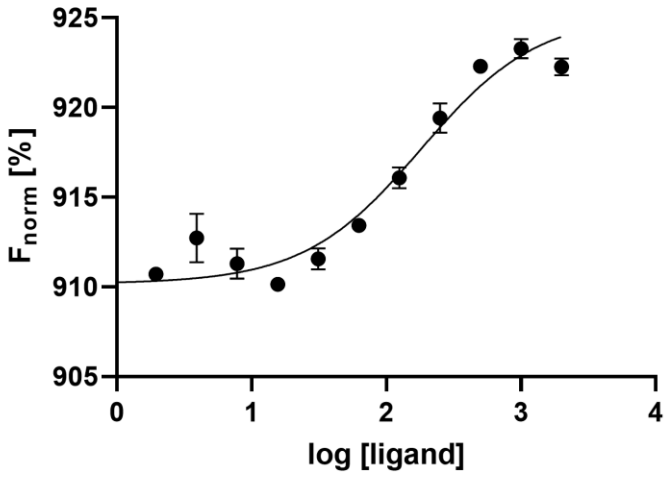

Compound	K_d
168	193 ± 19 nM

A4 MST and ChromlogD$_{7.4}$ Data Tables

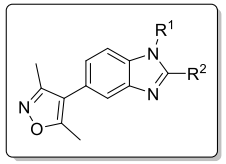

Table A1. Binding affinity (K_d) measured in the MST assay and ChromlogD$_{7.4}$ value for compounds of the general structure shown above. Error quoted is standard error of the mean of 3 technical repeats.

Compound	R^1	R^2	K_d (nM)	ChromlogD$_{7.4}$
18			1410 ± 83	3.59
110			1641 ± 296	5.54
108	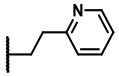		5125 ± 833	3.86
109	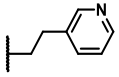		1720 ± 195	3.33
104			1119 ± 121	3.24
105	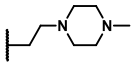		1537 ± 323	2.00
106	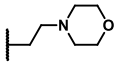		594 ± 84	3.39
107	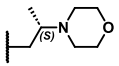		580 ± 121	3.92

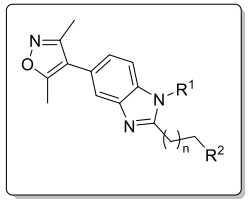

Table A2. Binding affinity (K_d) measured in the MST assay and ChromlogD$_{7.4}$ value for compounds of the general structure shown above. Error quoted is standard error of the mean of 3 technical repeats. Compound **182** was not soluble at the concentrations required for the MST assay and therefore no binding data was obtained.

Compound	n	R^1	R^2	K_d (nM)	ChromlogD$_{7.4}$
137	1	Me		2474 ± 702	5.40
121	1	Me		599 ± 29	5.96
122	1	Me		1294 ± 145	5.48
149	1	Me		3139 ± 449	5.89
150	1	Me		309 ± 33	6.04
120	1	Me	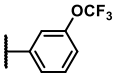	840 ± 46	6.23
139	1	Me	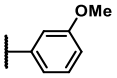	770 ± 143	5.32
151	1	Me	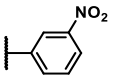	96 ± 10	5.19
154	1	Me		120 ± 16	4.85

Compound	n	R^1	R^2	K_d (nM)	ChromlogD$_{7.4}$
SGC-CBP30		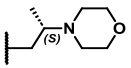	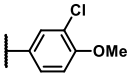	369 ± 32	5.77
138	1	Me	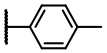	526 ± 131	5.96
123	1	Me	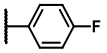	962 ± 14	5.44
176	1	Me	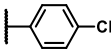	1451 ± 146	5.87
125	1	Me	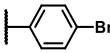	600 ± 39	6.04
144	1	Me	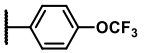	656 ± 62	6.26
142	1	Me	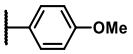	845 ± 120	5.25
152	1	Me	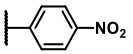	308 ± 20	5.15
155	1	Me	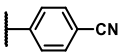	329 ± 121	4.77

153	1	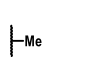	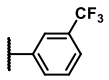	3605 ± 770	6.18	**177**	1		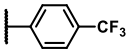	1829 ± 148	6.21
145	1		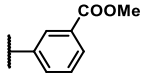	814 ± 131	5.05	**146**	1		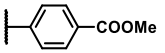	383 ± 48	4.99
147	1	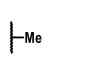	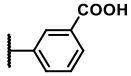	2548 ± 296	2.17	**148**	1		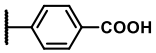	1147 ± 261	2.05
112	0	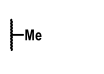		1084 ± 121	5.47	**111**	0		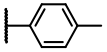	2420 ± 218	5.51
141	1	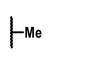	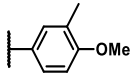	218 ± 104	5.87	**143**	1		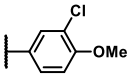	353 ± 89	5.54
156	1	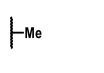	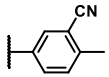	33 ± 4	5.11	**157**	1		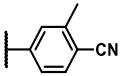	114 ± 22	5.11
224	1	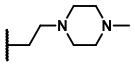	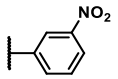	82 ± 15	3.71	**226**	1	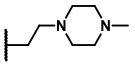	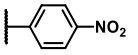	711 ± 174	3.69
172	1	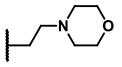	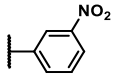	93 ± 5	4.85	**173**	1	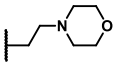	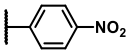	395 ± 17	4.82
170	1	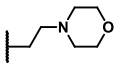	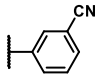	66 ± 1	4.65	**178**	1	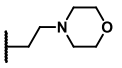	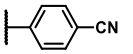	163 ± 14	4.44
171	1	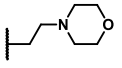		222 ± 63	5.52	**179**	1	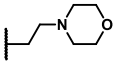	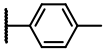	238 ± 60	5.52
174	1			52 ± 3	5.10	**175**	1			93 ± 6	4.82

180	1	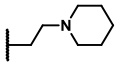	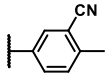	28 ± 15	6.56
183	1	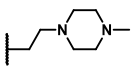	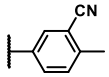	6 ± 2	4.67
181	1	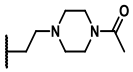	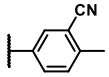	11 ± 5	4.08
182	1	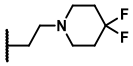	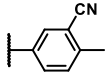	ND	5.98

186	1	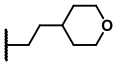	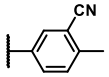	36 ± 2	5.67
185	1		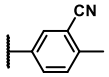	29 ± 6	5.43
168	0		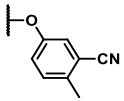	193 ± 19	5.21

A5 NMR Spectra of Novel Compounds

N-Cyclopropyl-3-methyl[1,2,4]triazolo[4,3-*b*]pyridazin-6-amine 4

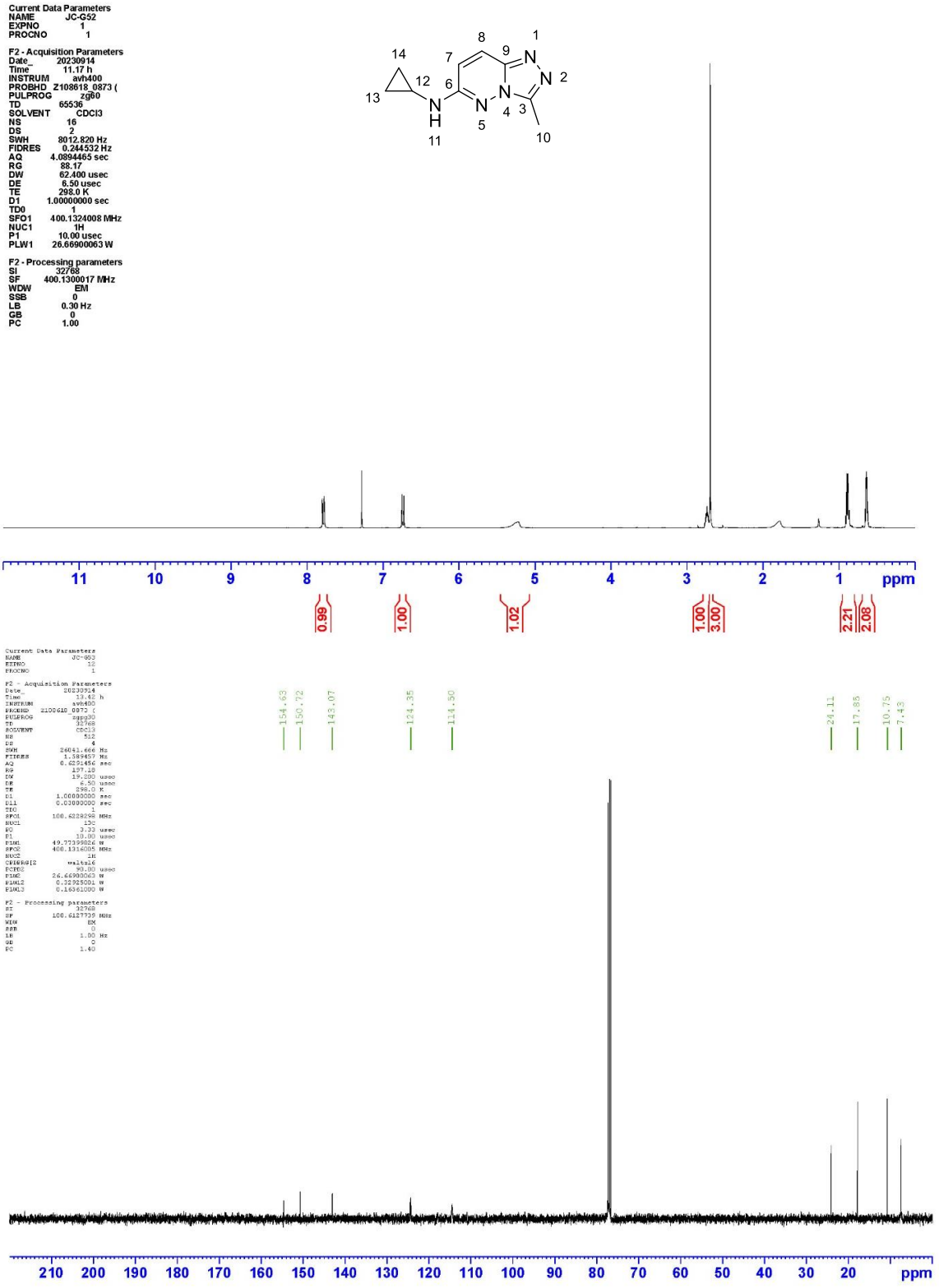

N-Cyclopropyl-3-ethyl[1,2,4]triazolo[4,3-*b*]pyridazin-6-amine 5

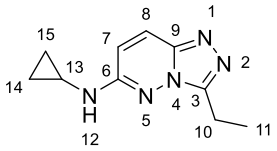

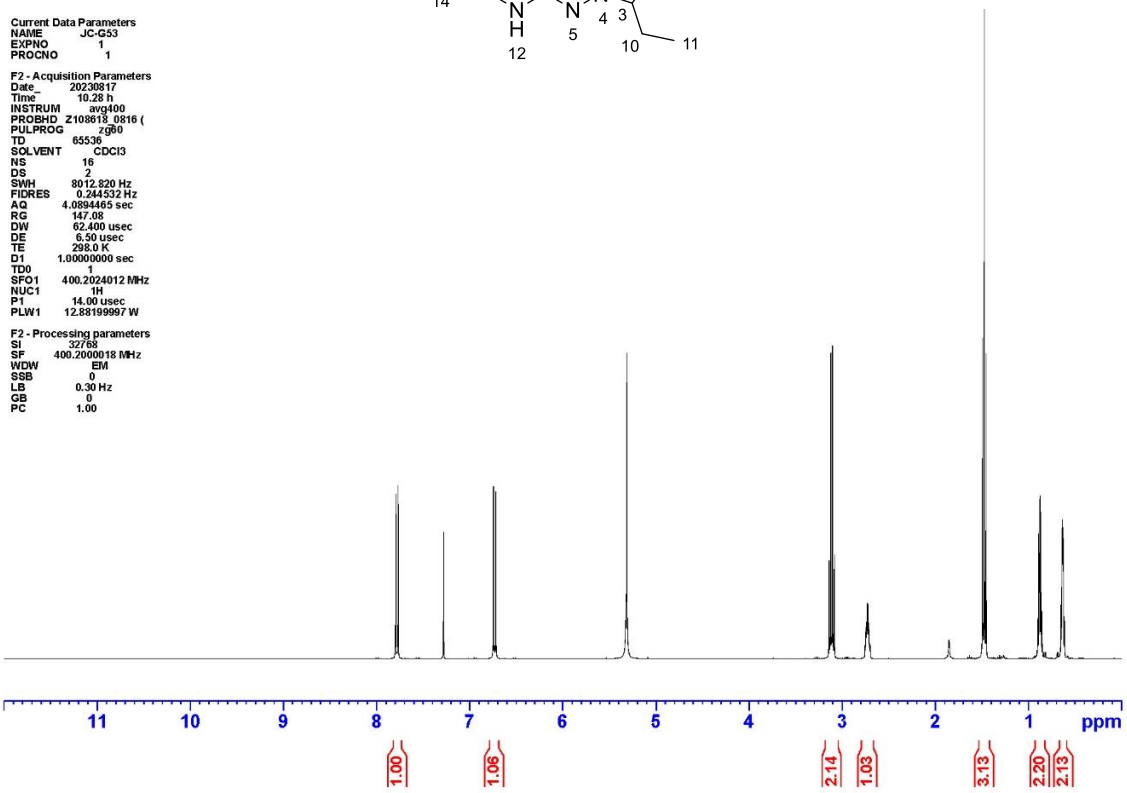

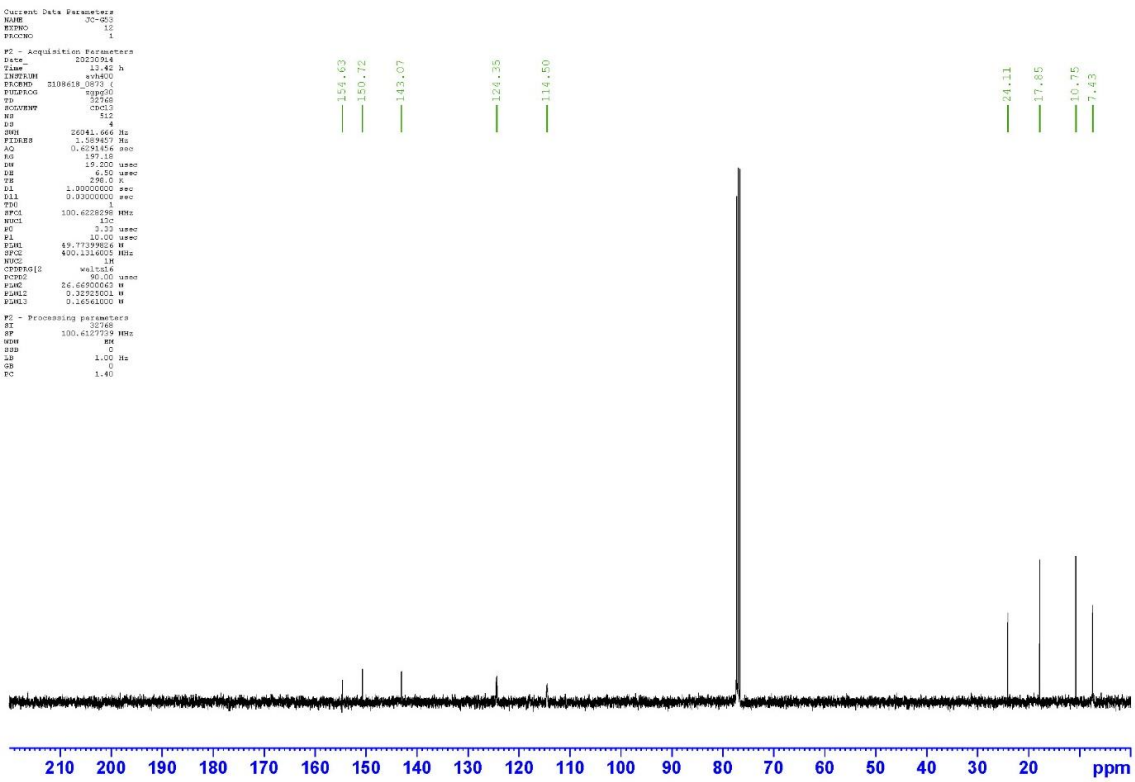

N-Cyclopropyl-3-phenyl[1,2,4]triazolo[4,3-*b*]pyridazin-6-amine 6

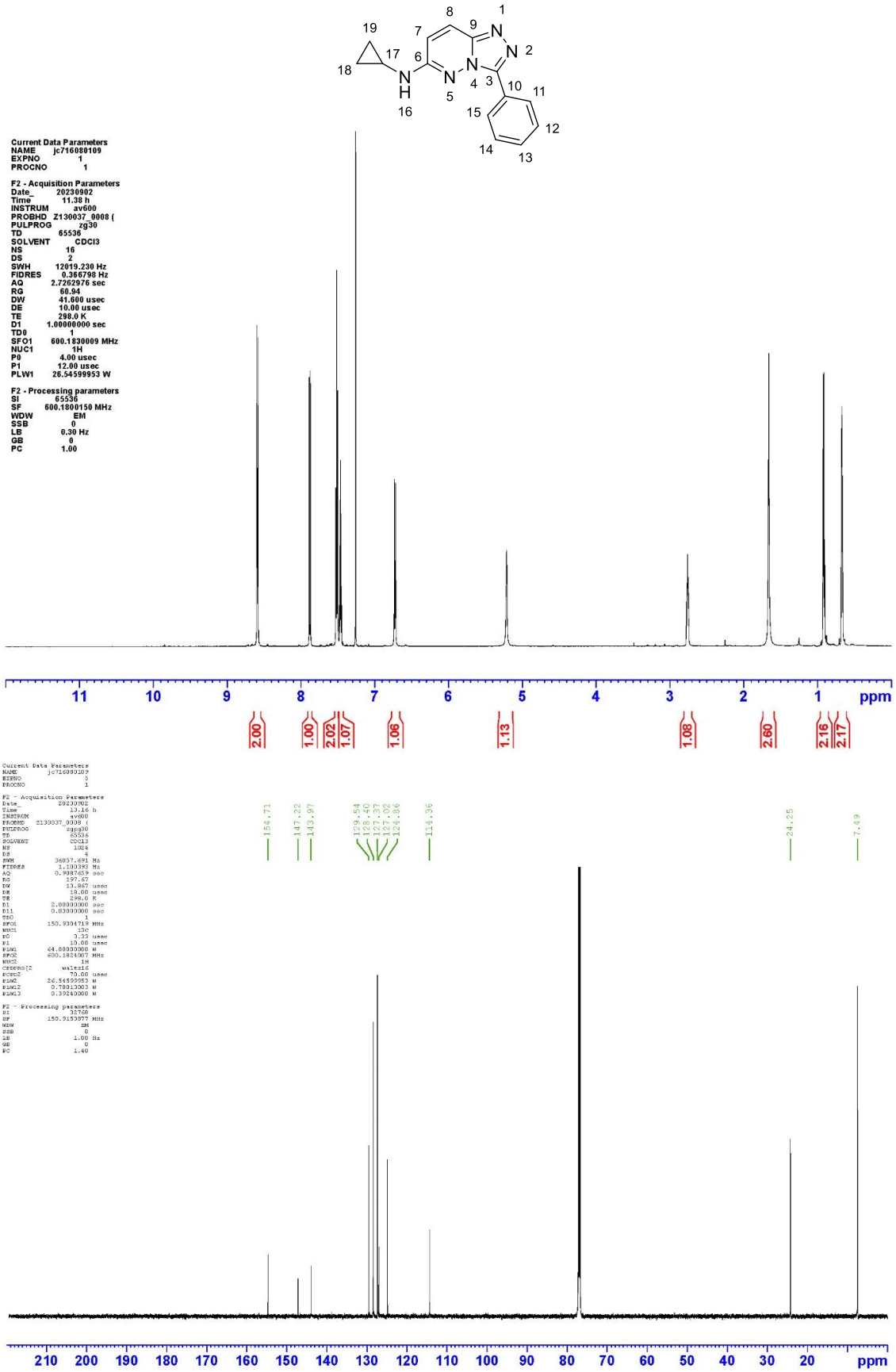

Methyl 2-[(5-bromo-2-nitrophenyl)(hydroxy)methyl]prop-2-enoate 68

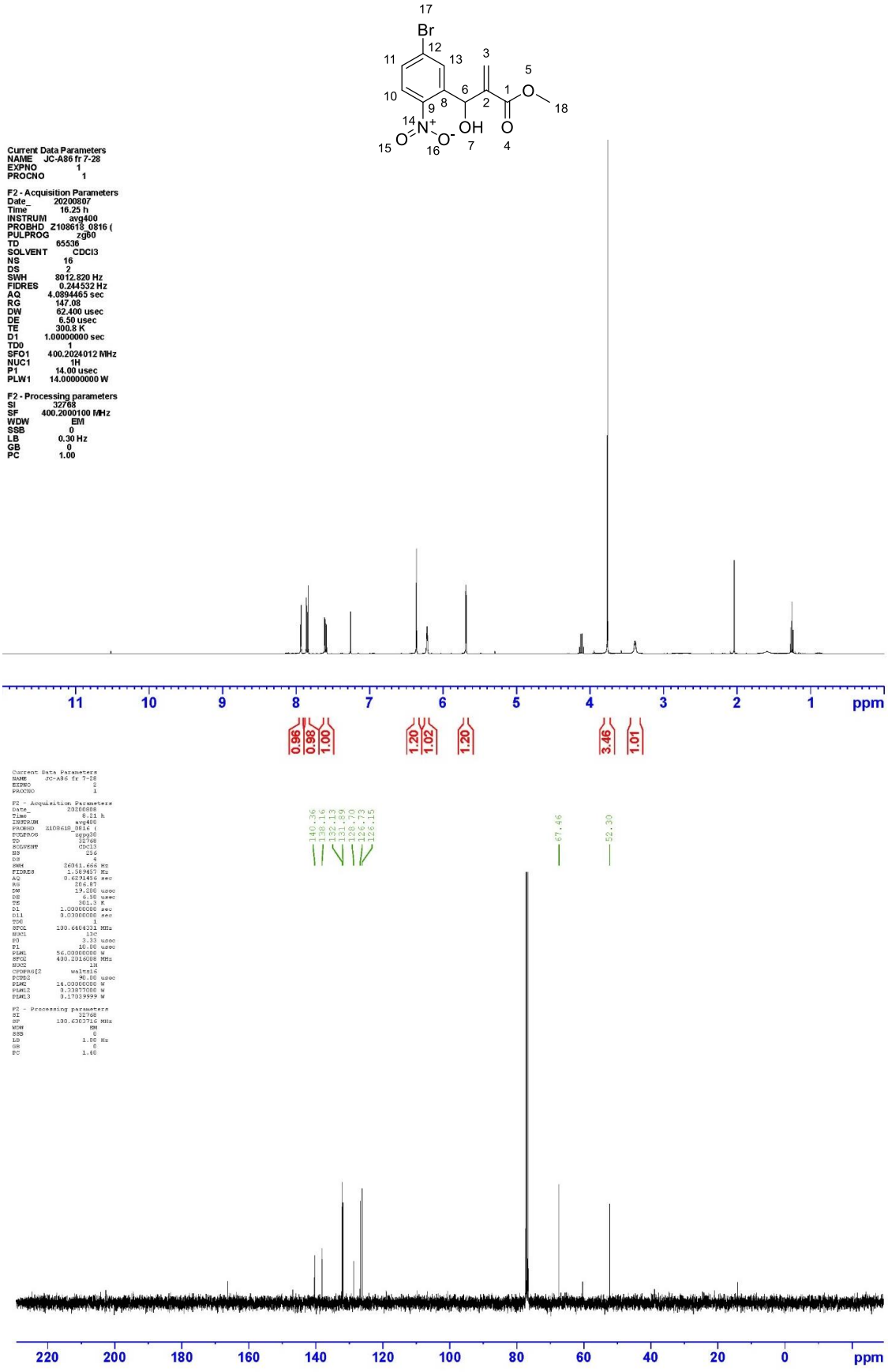

Methyl 3-(5-bromo-2-nitrophenyl)-3-hydroxy-2-methylpropanoate 69

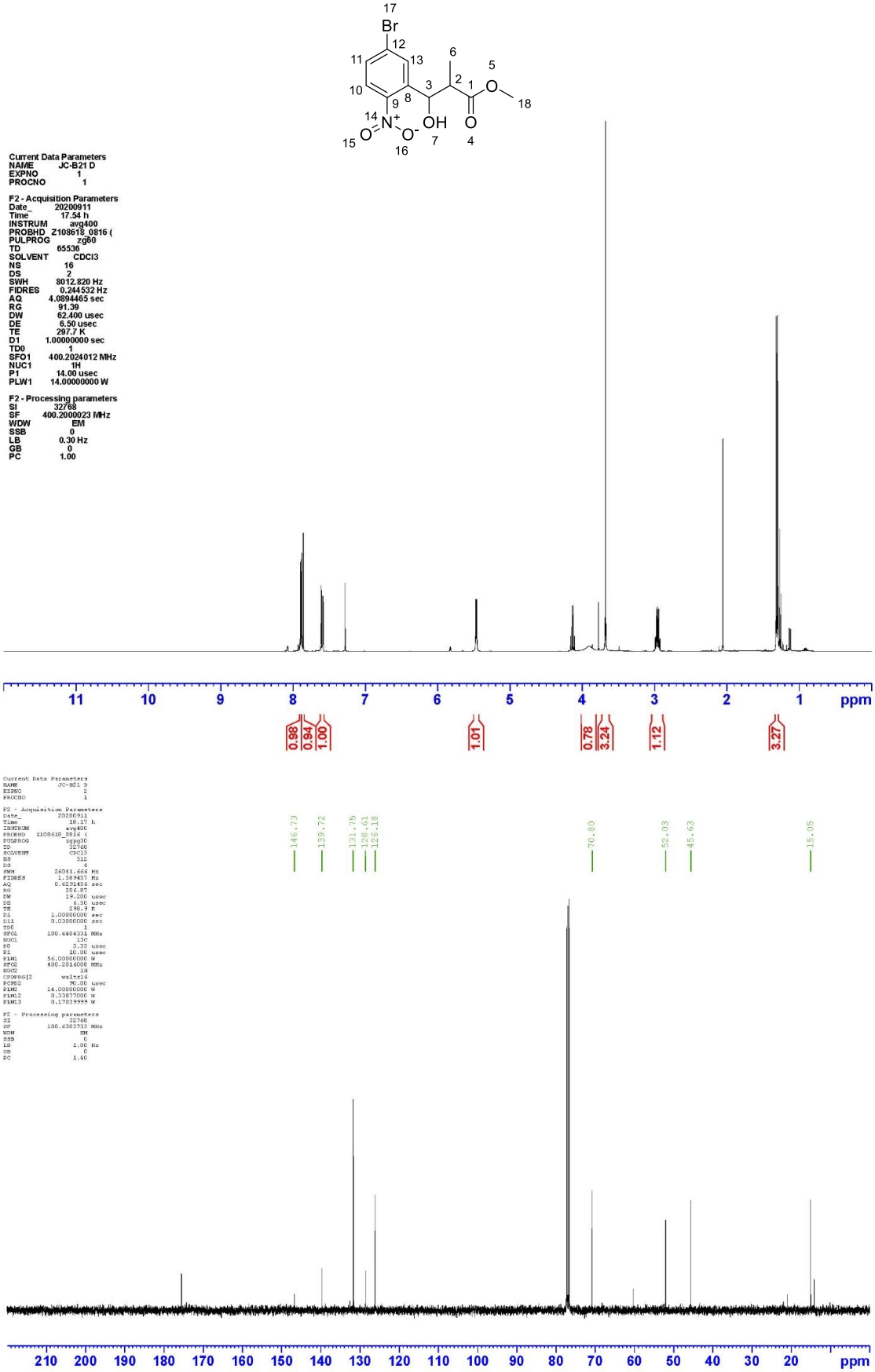

6-(3,5-Dimethyl-1,2-oxazol-4-yl)-3-methylquinolin-2(1*H*)-one 16

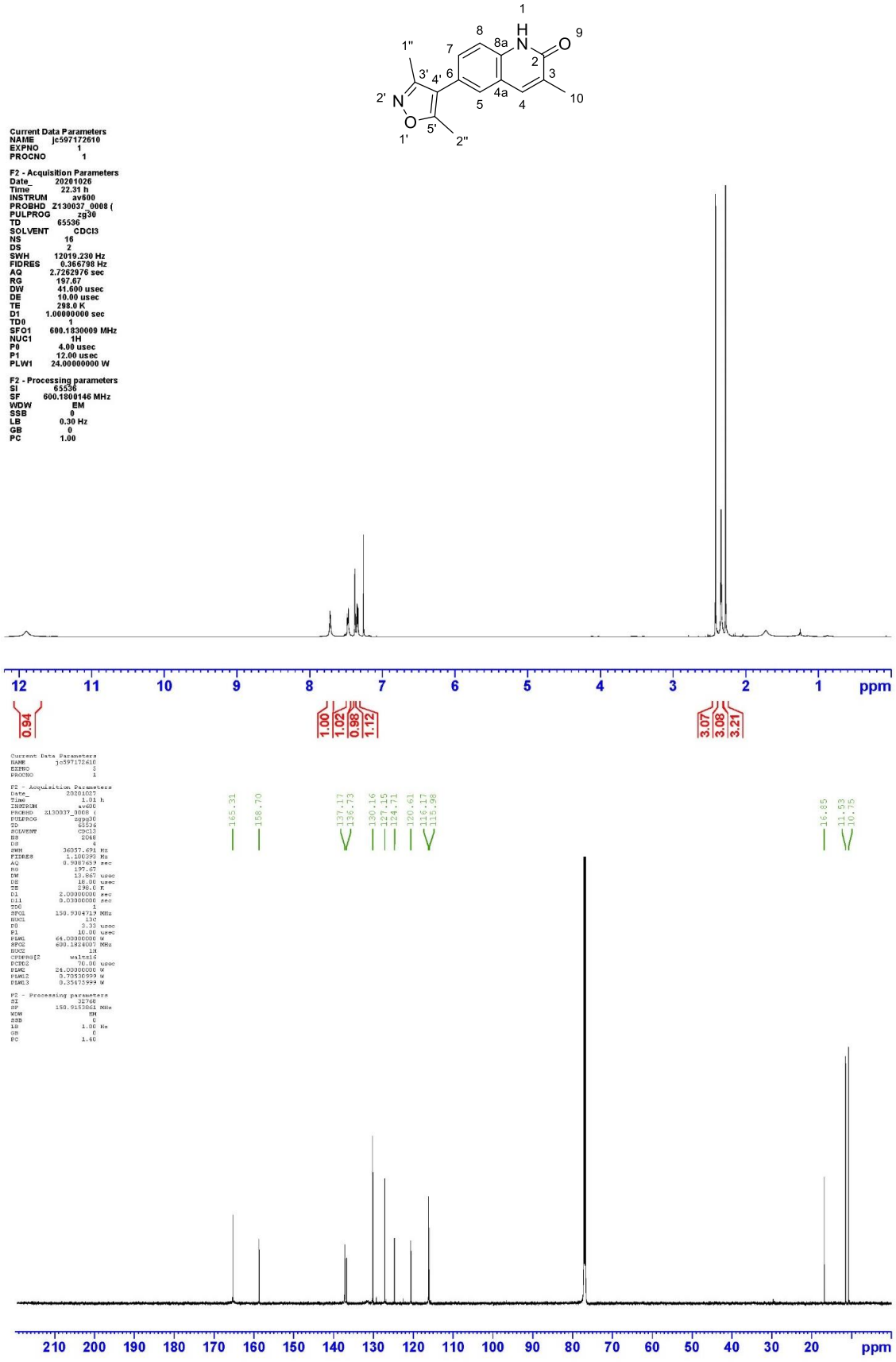

4-(1*H*-Benzo[*d*]imidazol-5-yl)-3,5-dimethylisoxazole 17

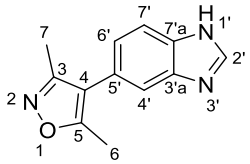

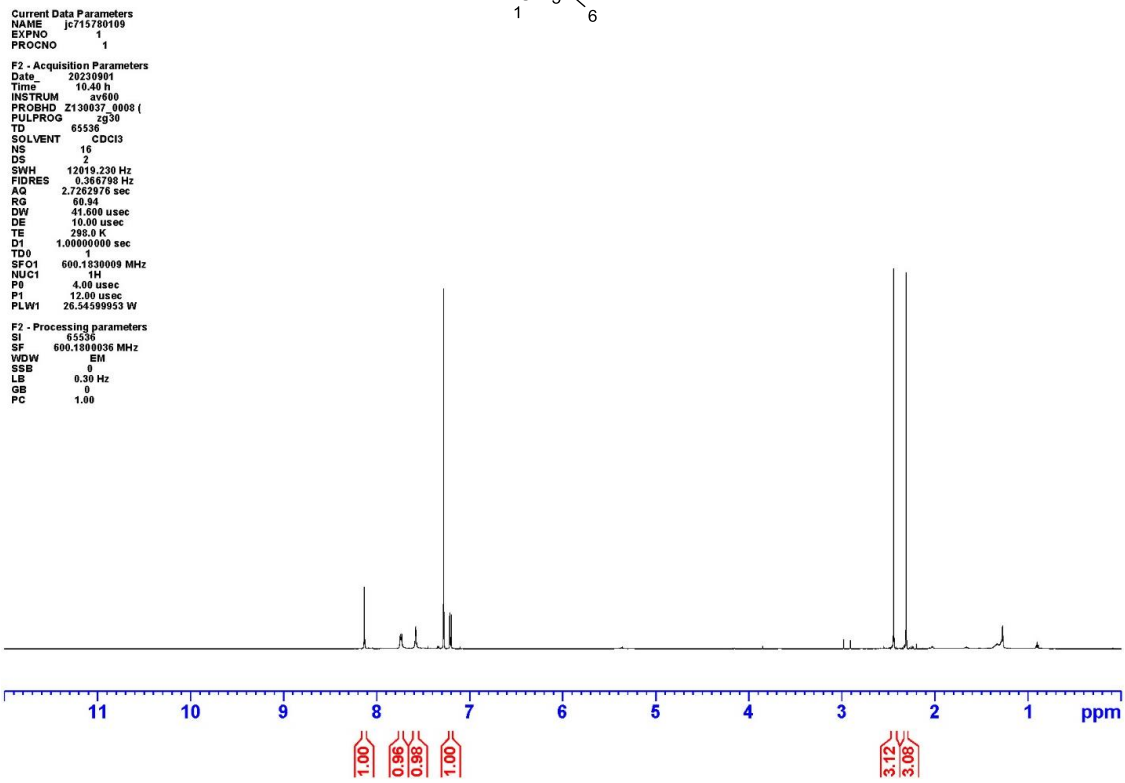

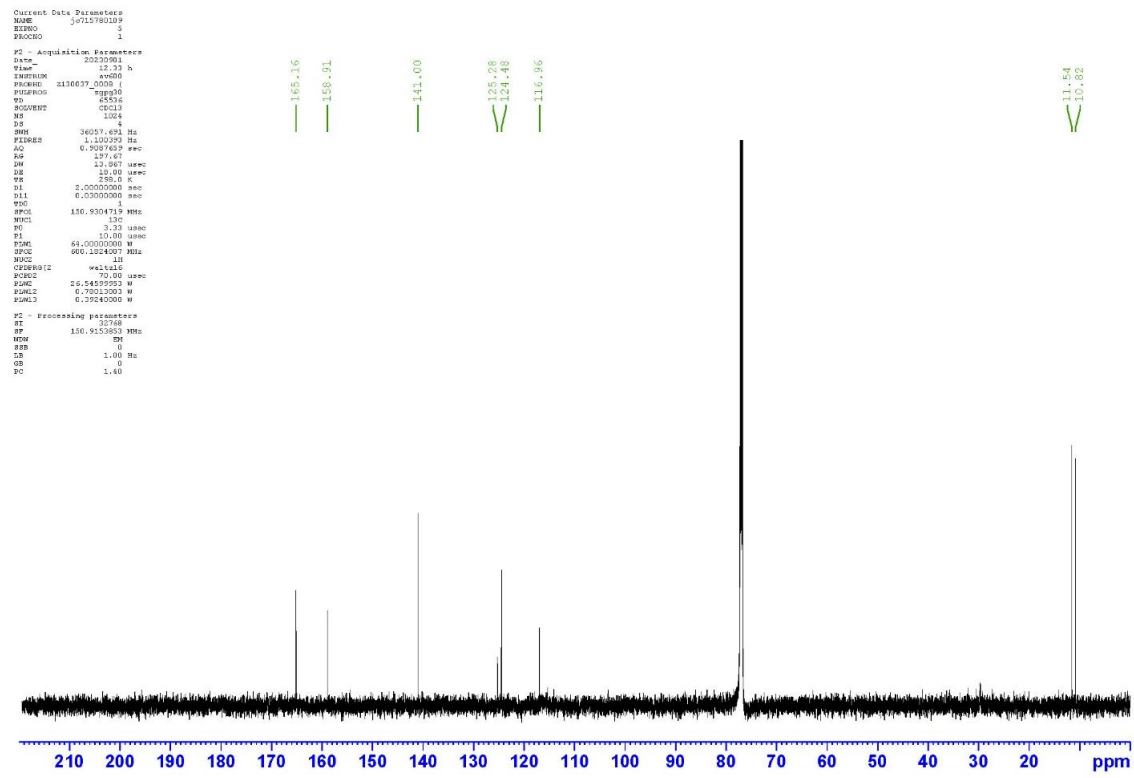

4-(2-Ethyl-1-methyl-1*H*-benzo[*d*]imidazol-5-yl)-3,5-dimethylisoxazole 18

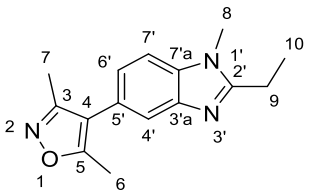

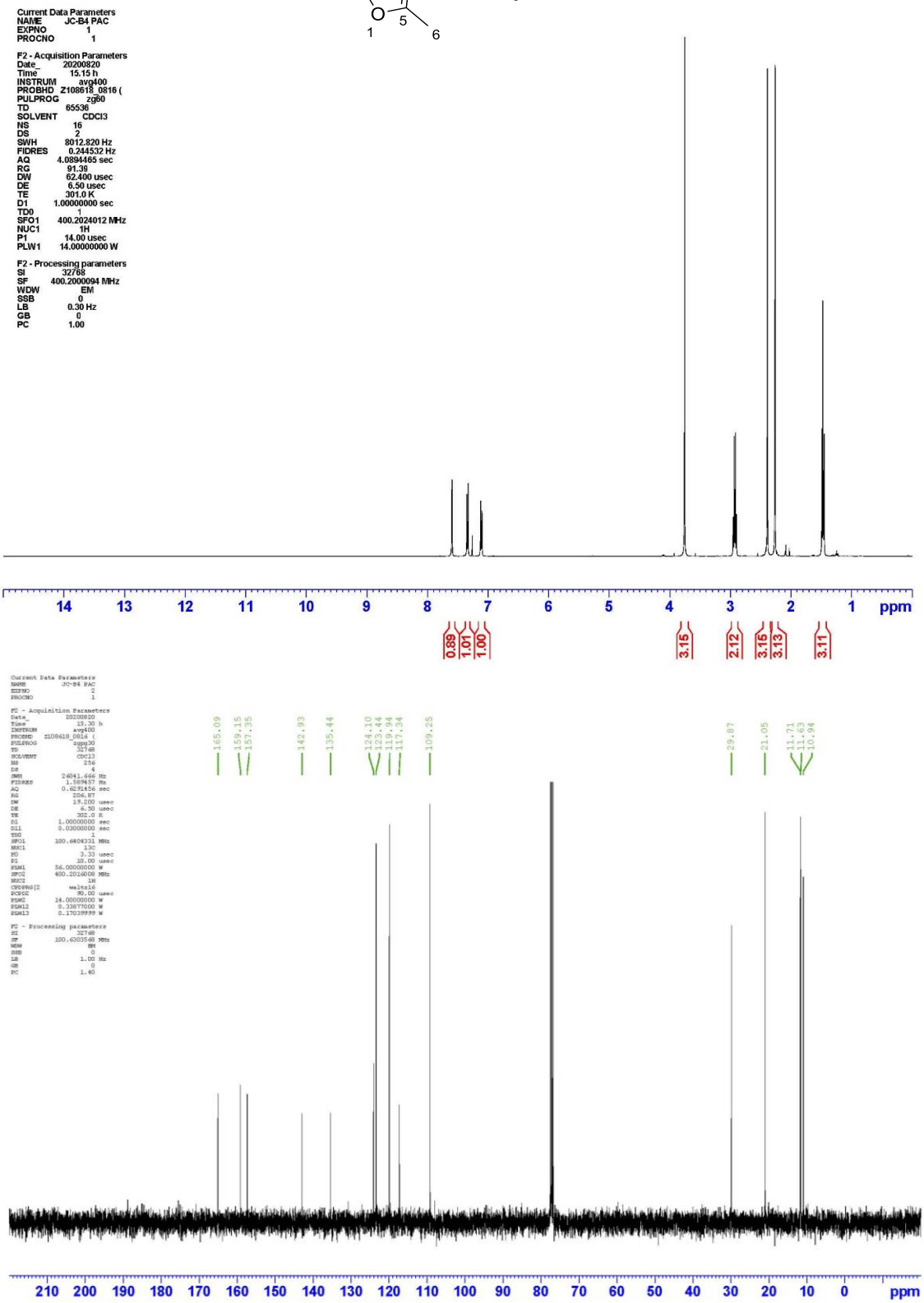

7-(Benzyloxy)-6-methoxy-4-methylquinoline 61

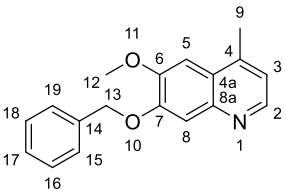

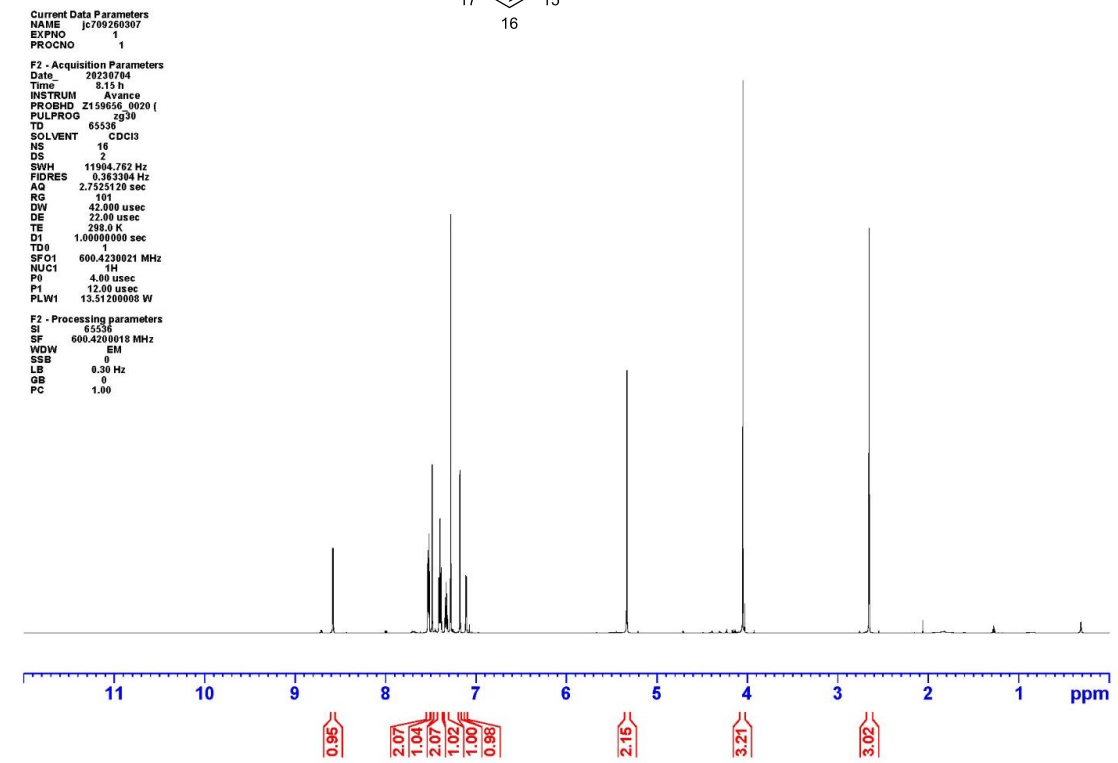

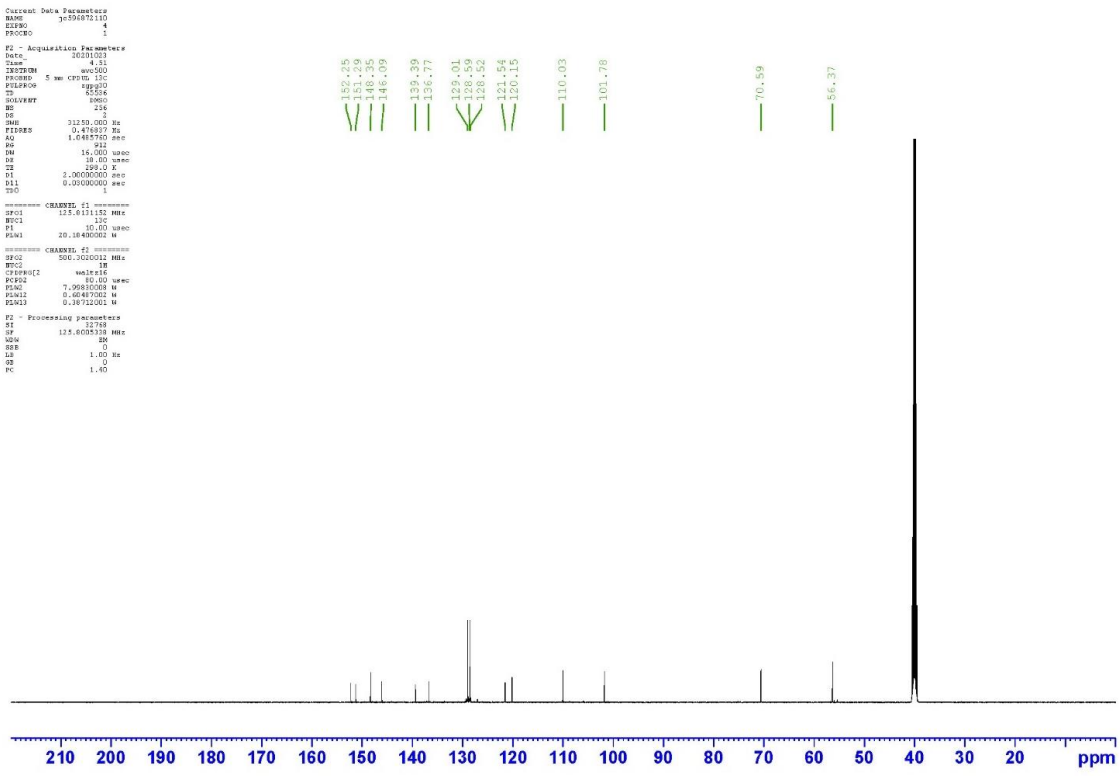

6-Methoxy-4-methylquinolin-7-ol 62

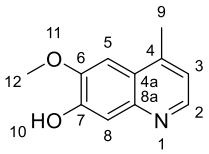

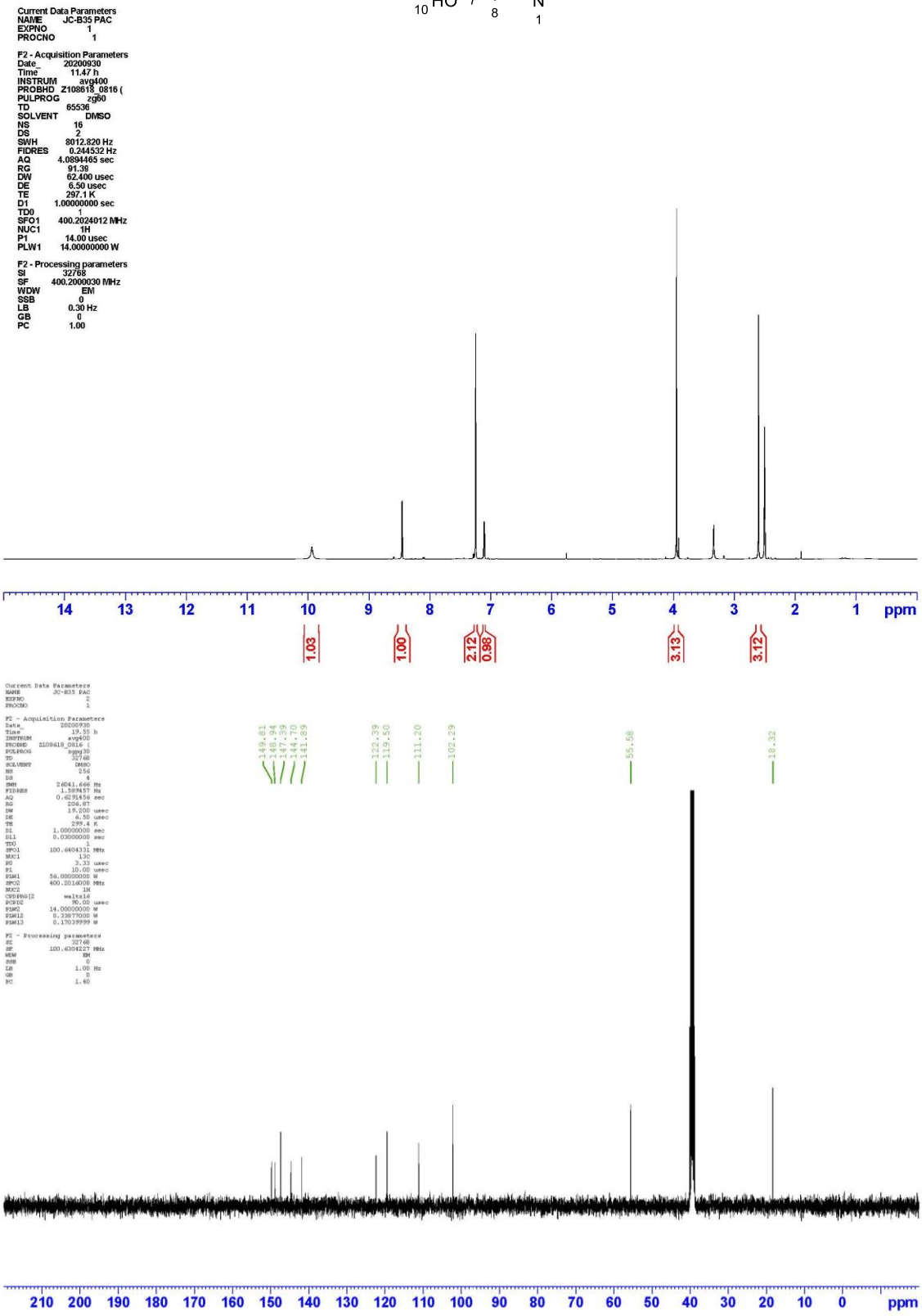

6-Methoxy-4-methylquinolin-7-yl trifluoromethanesulfonate 58

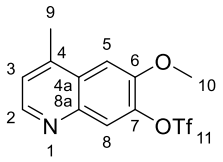

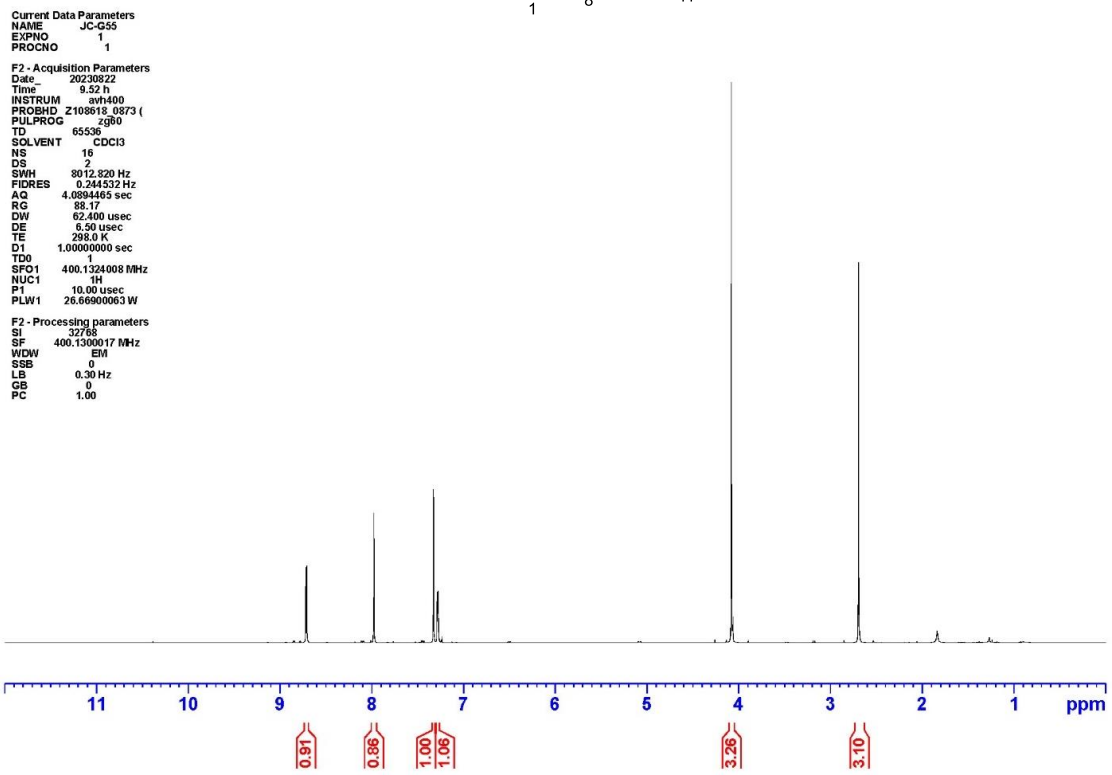

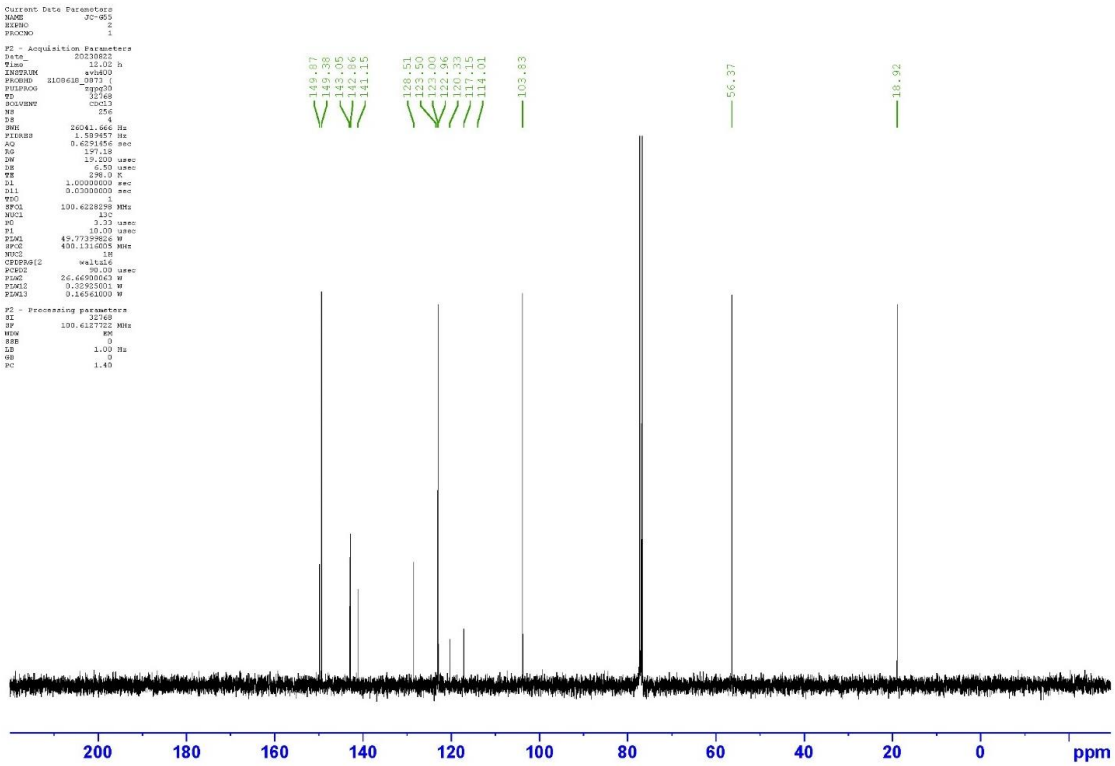

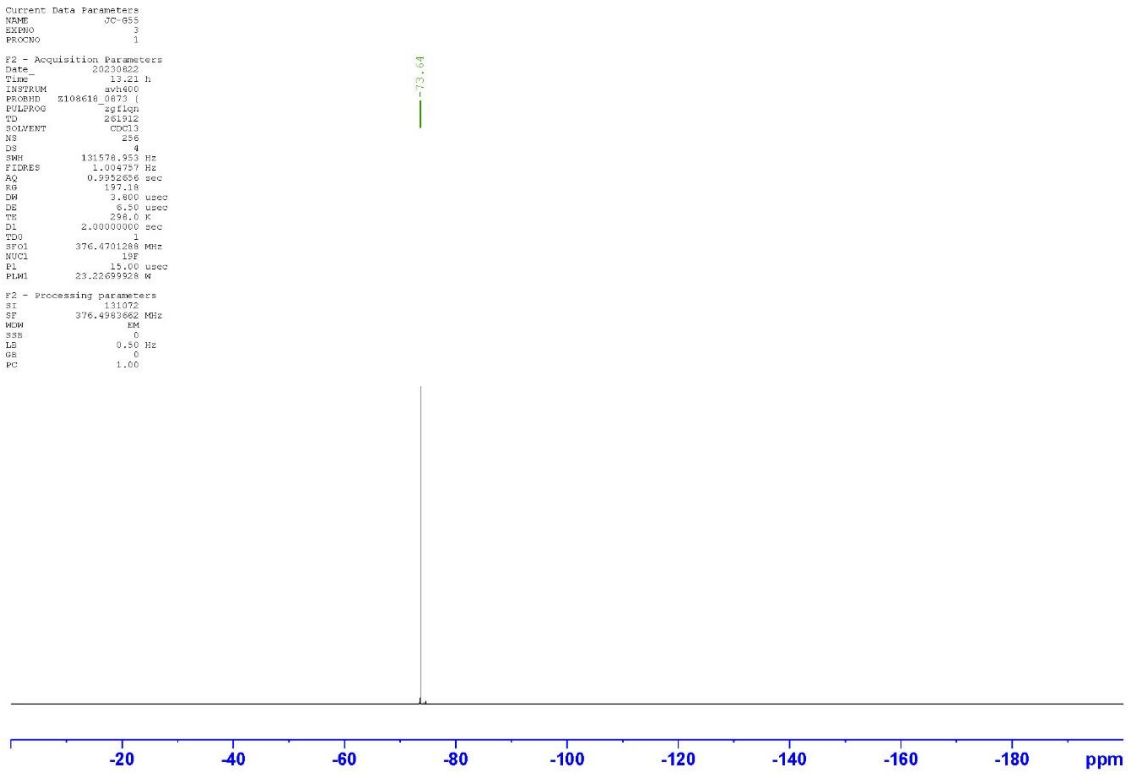
Current Data Parameters
NAME JC-655
EXPNO 3
PROCNO 1
F2 - Acquisition Parameters
Date_ 20230822
Time 13.21 h
INSTRUM avh400
PROBHD Z108618_0873 (
PULPROG zgflqn
TD 261912
SOLVENT CDCl3
NS 256
DS 4
SWH 131578.953 Hz
FIDRES 1.004757 Hz
AQ 0.9952656 sec
RG 197.18
DW 3.800 usec
DE 6.50 usec
TE 298.0 K
D1 2.00000000 sec
TD0 1
SFO1 376.4701288 MHz
NUC1 19F
P1 15.00 usec
PLW1 23.22699928 W
F2 - Processing parameters
SI 131072
SF 376.4983862 MHz
WDW EM
SSB 0
LB 0.50 Hz
GB 0
PC 1.00
-73.64
-20
-40
-60
-80
-100
-120
-140
-160
-180
ppm

7-(3,5-Dimethyl-1,2-oxazol-4-yl)-6-methoxy-4-methylquinoline 19

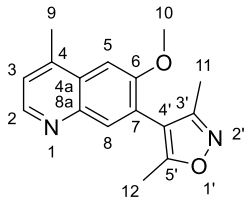

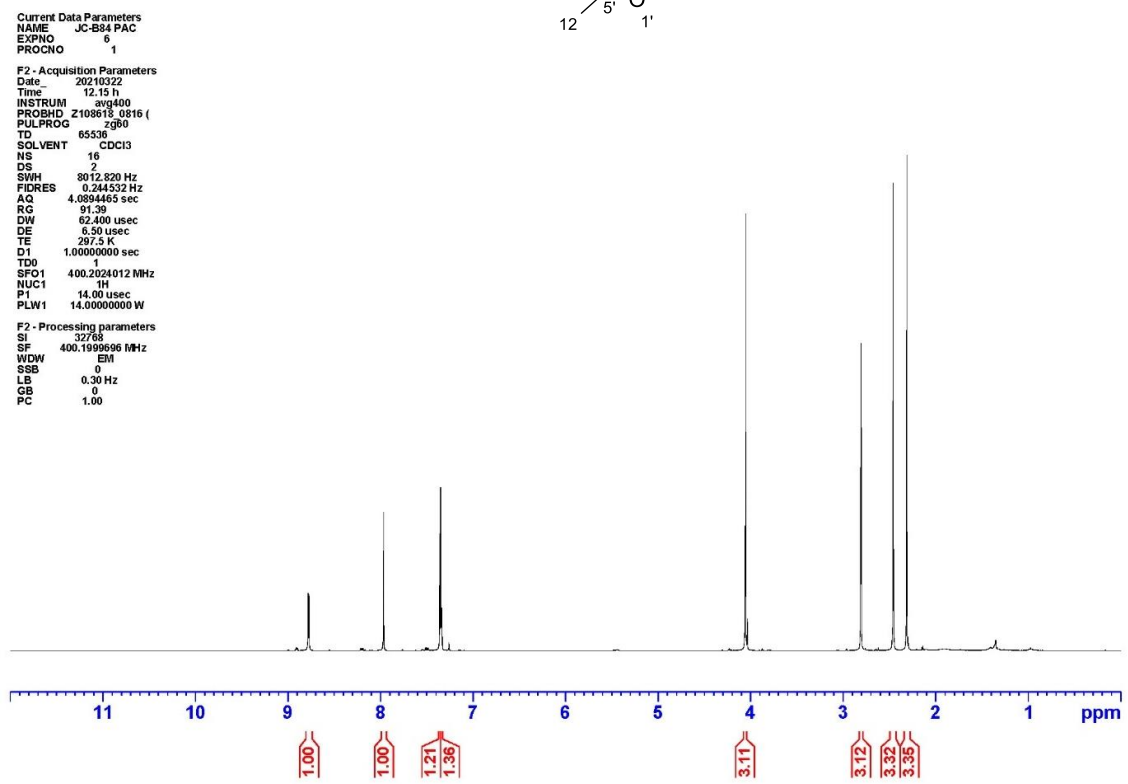

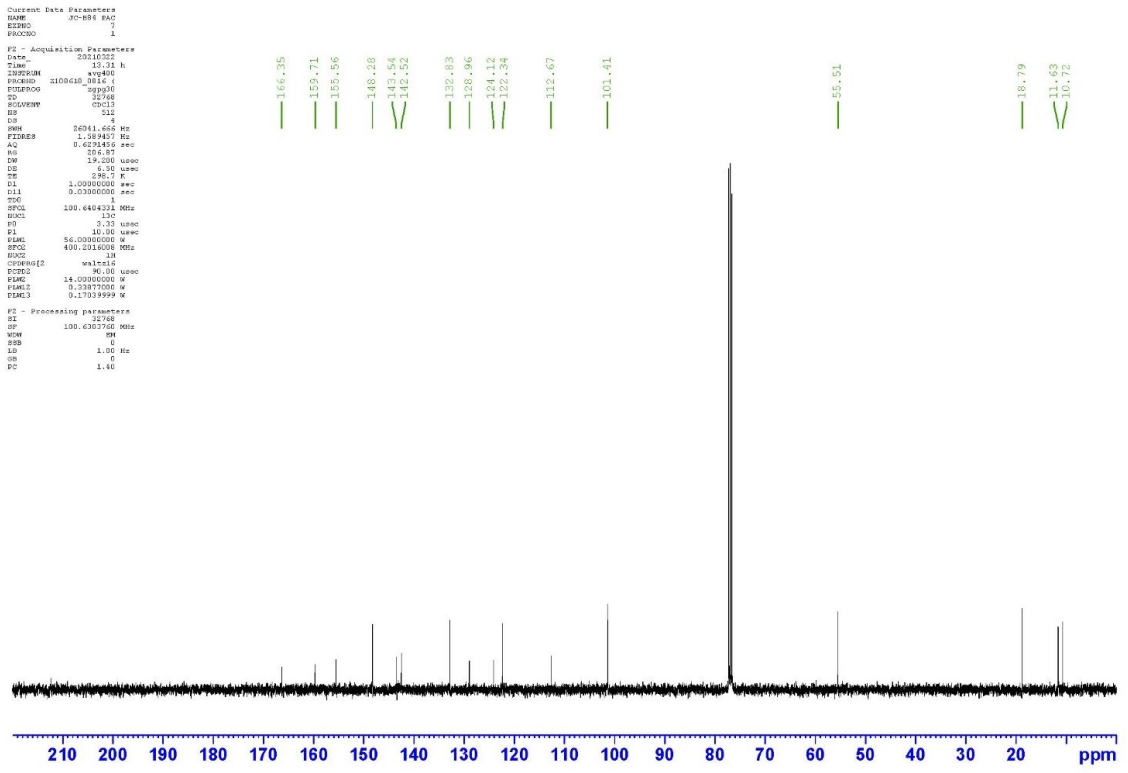

3,5-Dimethyl-4-(4-methylquinolin-7-yl)isoxazole 20

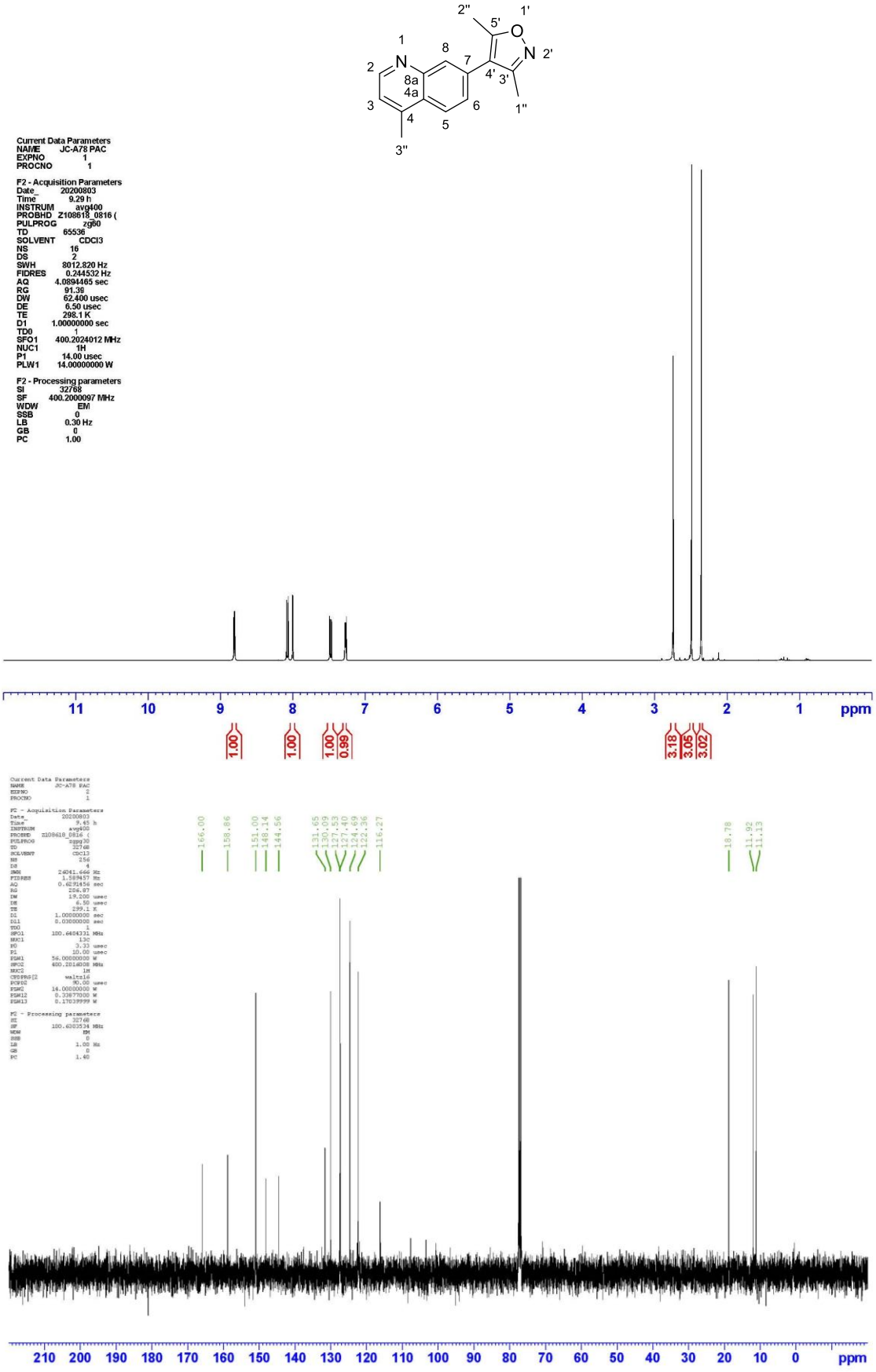

7-(3,5-Dimethyl-1*H*-pyrazol-4-yl)-4-methylquinoline 21

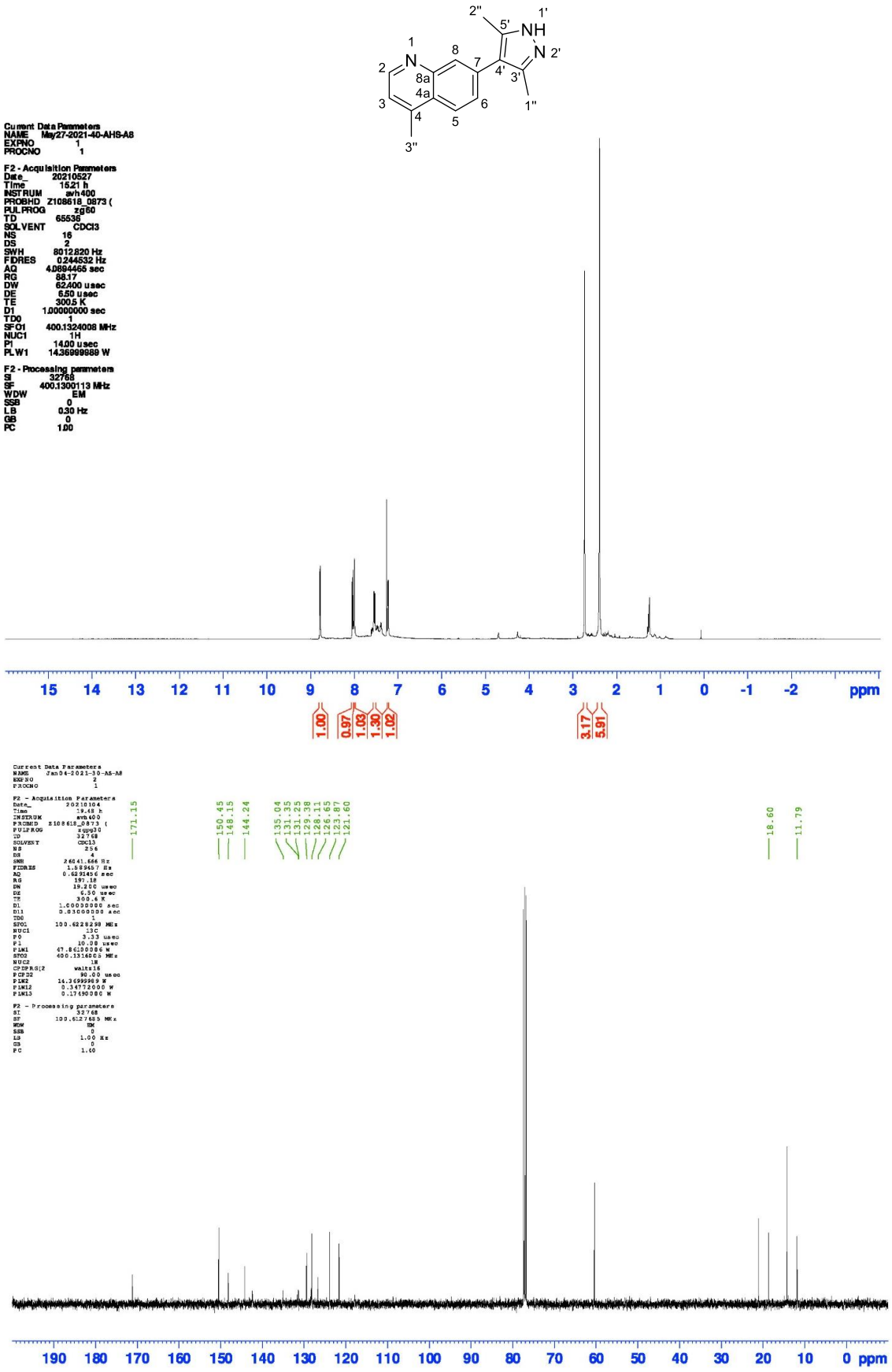

Tert-butyl (R)-3-((2-nitrophenyl)amino)butanoate 93

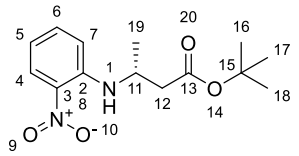

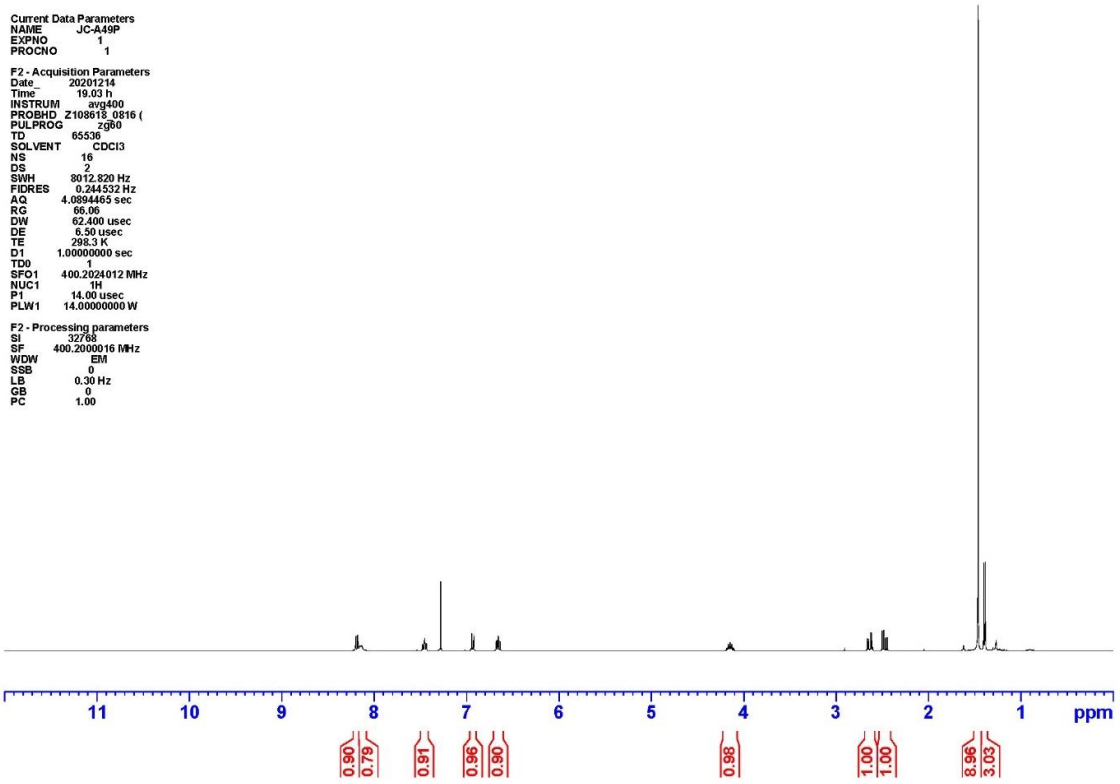

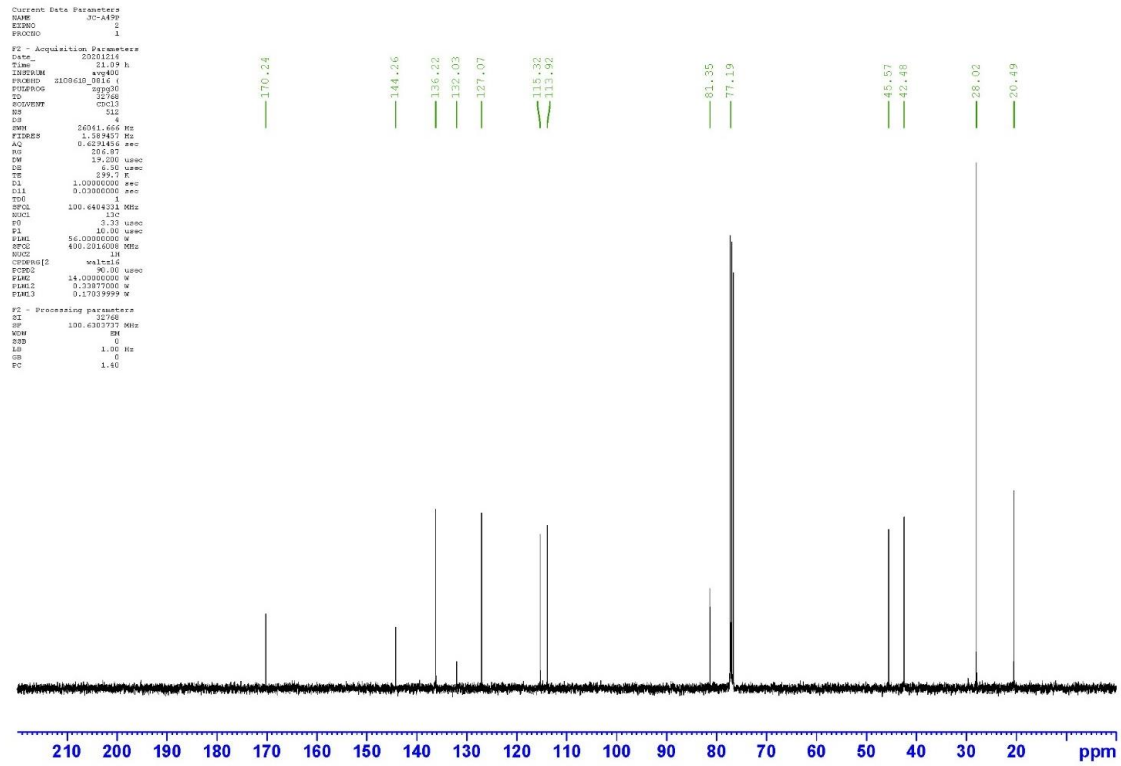

N-(2-Cyclopropylethyl)-4-(3,5-dimethylisoxazol-4-yl)-2-nitroaniline 187

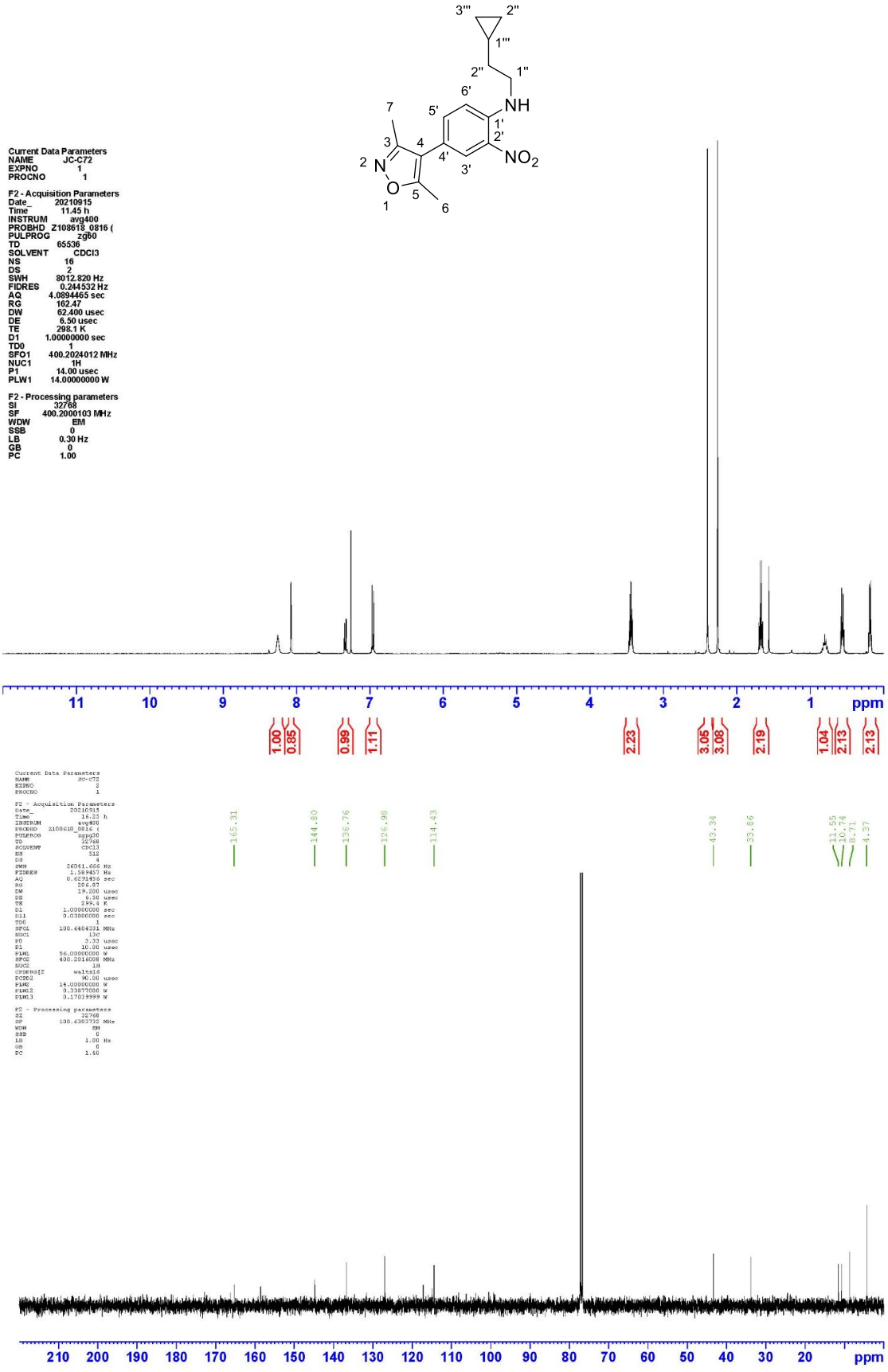

4-(1-(2-Cyclopropylethyl)-2-ethyl-*1H*-benzo[*d*]imidazol-5-yl)-3,5-dimethylisoxazole

110

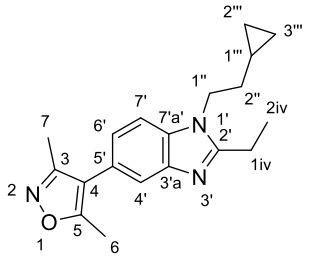

Current Data Parameters
NAME JC-C86 f 13
EXPNO 1
PROCNO 1

F2 - Acquisition Parameters
Date_ 20210920
Time 11.16 h
INSTRUM avg400
PROBHD Z108618_0816 (
PULPROG zg60
TD 65536
SOLVENT CDCl3
NS 16
DS 2
SWH 8012.820 Hz
FIDRES 0.244532 Hz
AQ 4.0894465 sec
RG 91.39
DW 62.400 usec
DE 6.50 usec
TE 297.7 K
D1 1.00000000 sec
TD0 1
SFO1 400.2024012 MHz
NUC1 1H
P1 14.00 usec
PLW1 14.00000000 W

F2 - Processing parameters
SI 32768
SF 400.2000103 MHz
WDW EM
SSB 0
LB 0.30 Hz
GB 0
PC 1.00

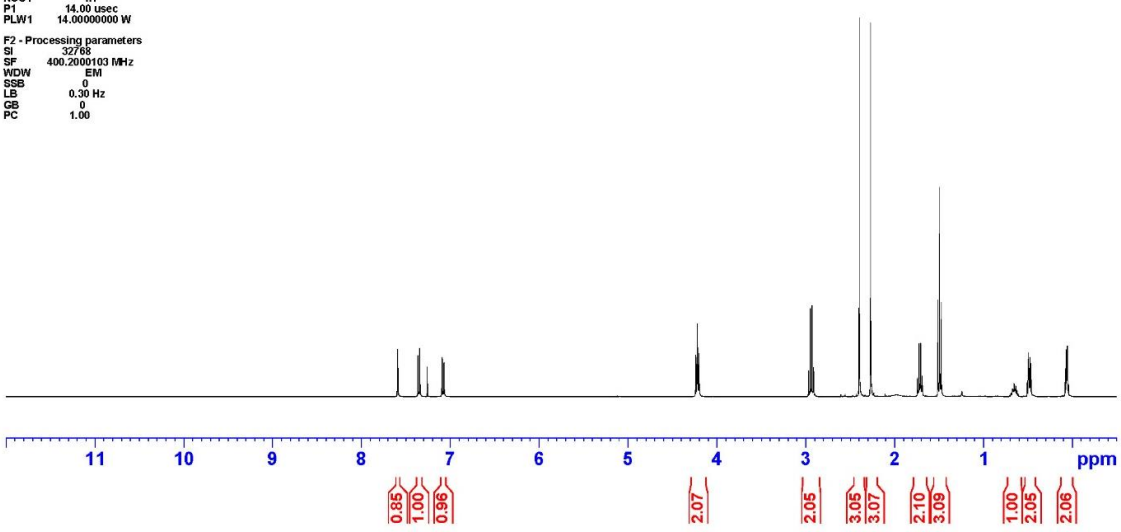

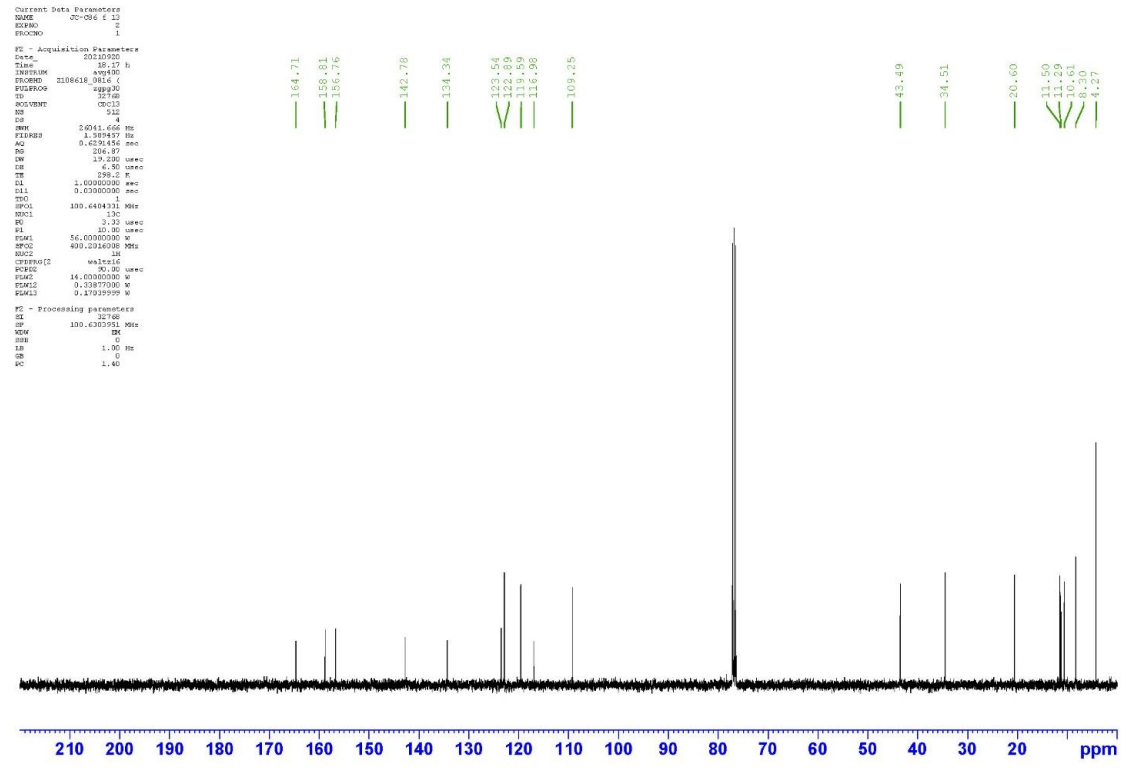

4-(3,5-Dimethylisoxazol-4-yl)-2-nitro-*N*-(2-(pyridin-2-yl)ethyl)aniline 188

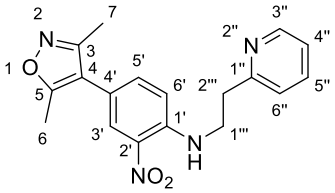

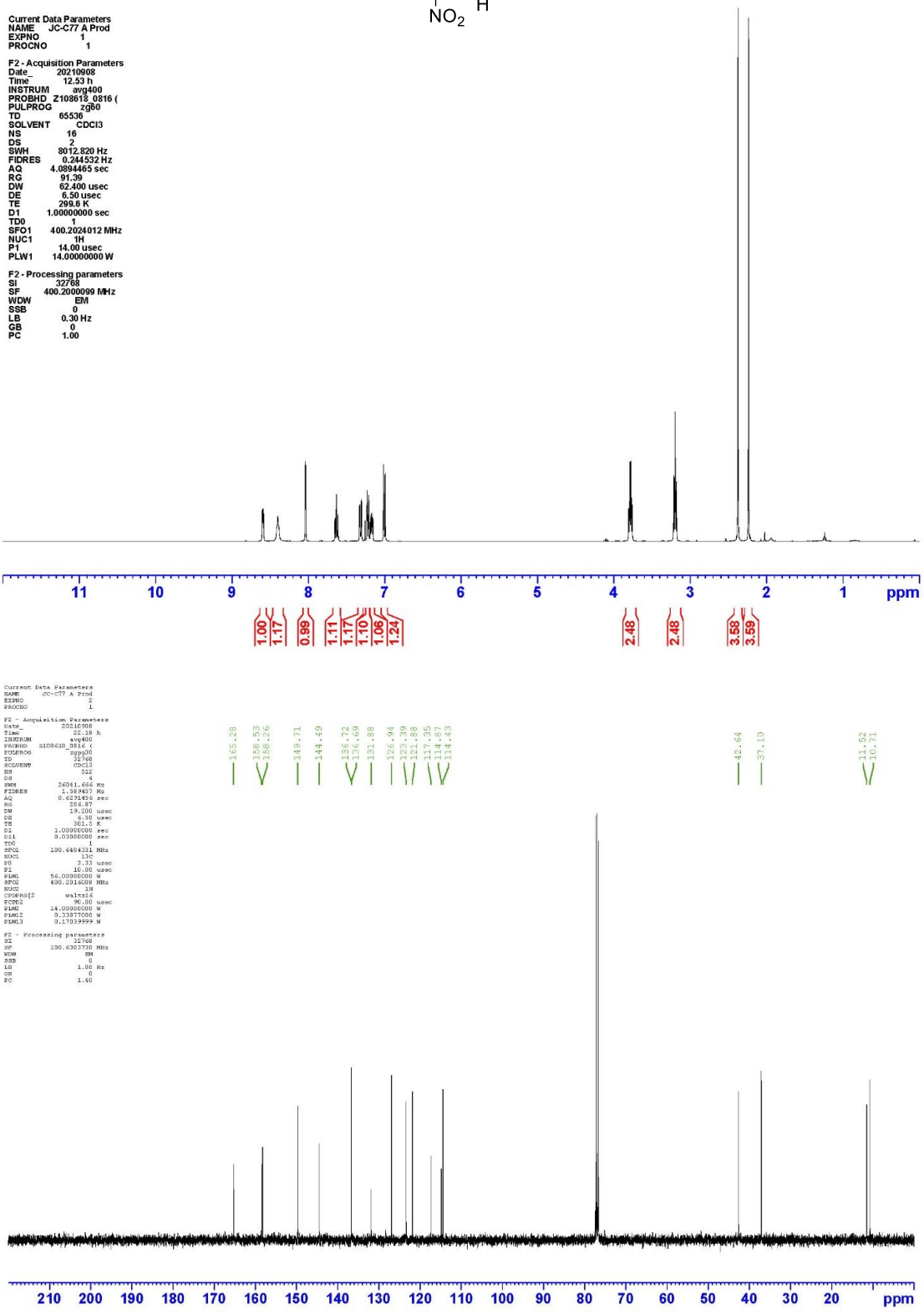

4-(2-Ethyl-1-(2-(pyridin-2-yl)ethyl)-*1H*-benzo[*d*]imidazol-5-yl)-3,5-dimethylisoxazole 108

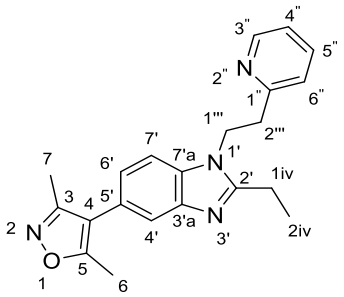

Current Data Parameters
NAME JC-D8
EXPNO 6
PROCNO 1

F2 - Acquisition Parameters
Date_ 20211015
Time 11.46 h
INSTRUM avh400
PROBHD Z108618_0873 (
PULPROG zg60
TD 65536
SOLVENT CDCl3
NS 16
DS 2
SWH 8012.820 Hz
FIDRES 0.244532 Hz
AQ 4.0894465 sec
RG 133.82
DW 62.400 usec
DE 6.50 usec
TE 299.7 K
D1 1.00000000 sec
TD0 1
SFO1 400.1324008 MHz
NUC1 1H
P1 14.00 usec
PLW1 14.36999989 W

F2 - Processing parameters
SI 32768
SF 400.1300109 MHz
WDW EM
SSB 0
LB 0.30 Hz
GB 0
PC 1.00

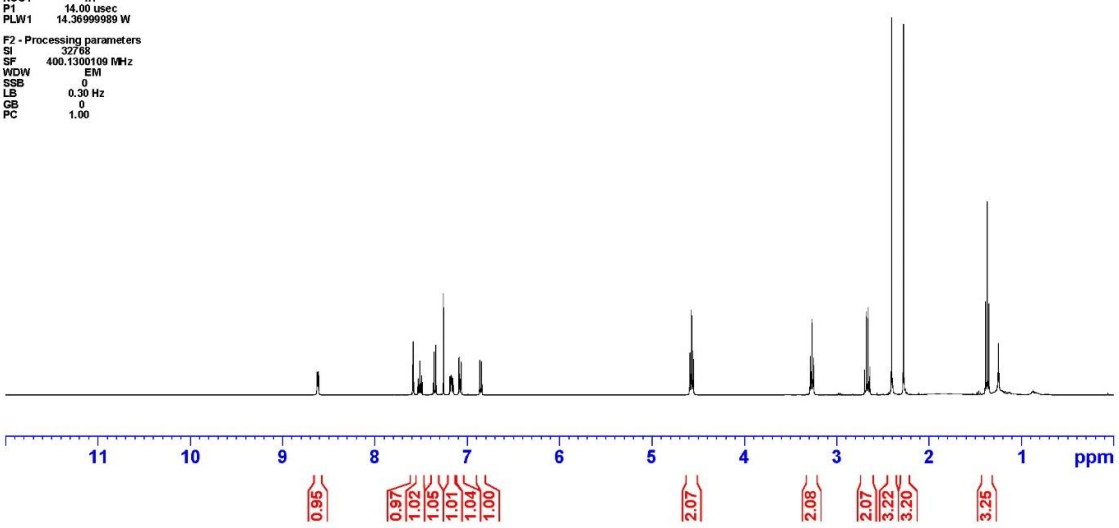

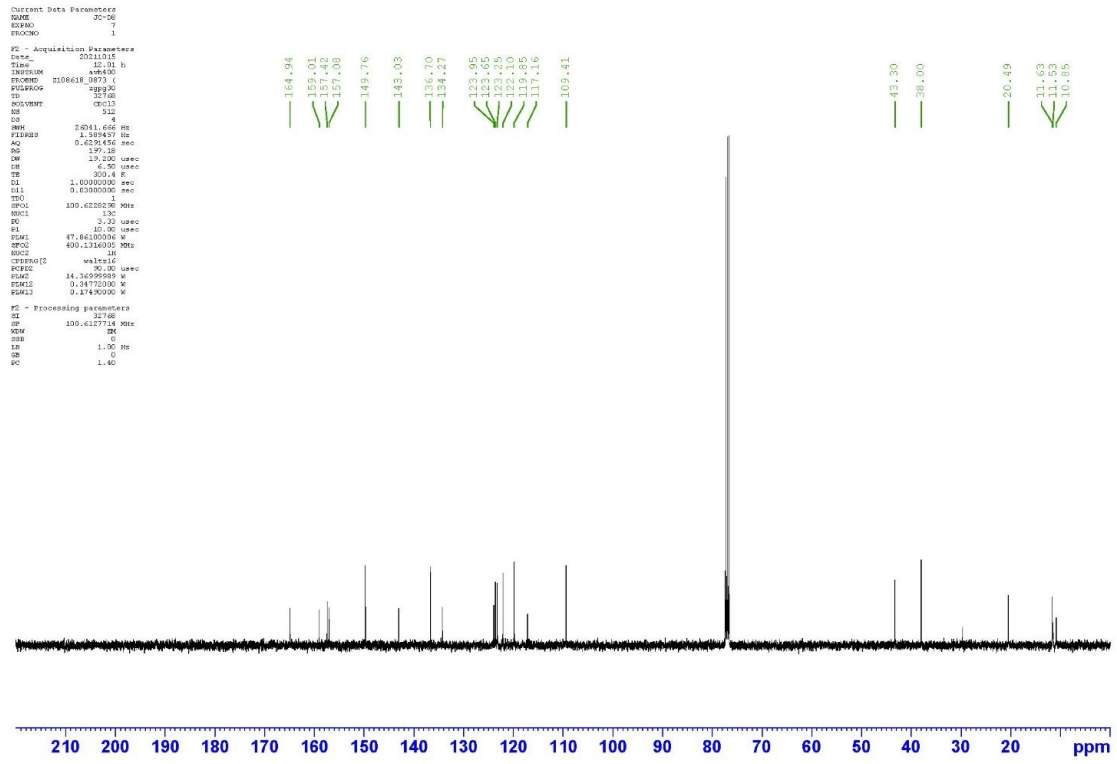

4-(3,5-Dimethylisoxazol-4-yl)-2-nitro-*N*-(2-(pyridin-3-yl)ethyl)aniline 189

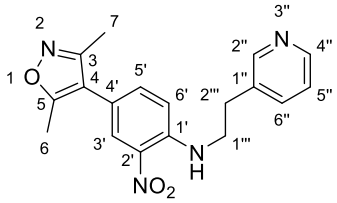

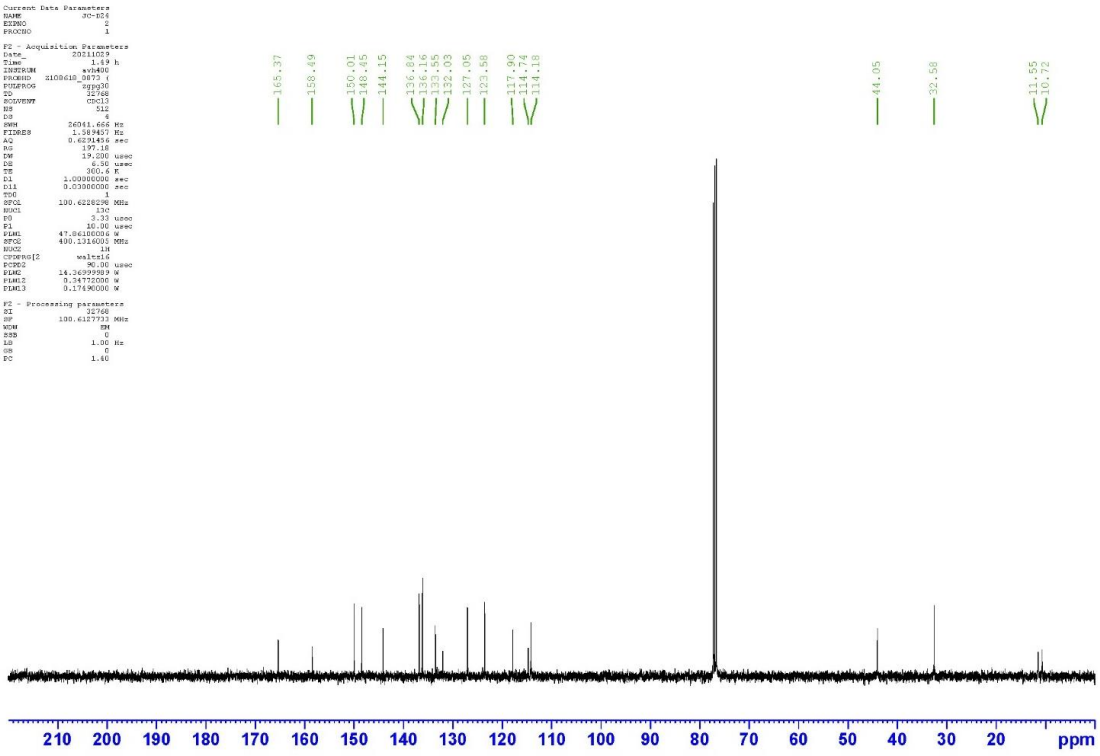

4-(2-Ethyl-1-(2-(pyridin-3-yl)ethyl)-*1H*-benzo[*d*]imidazol-5-yl)-3,5-dimethylisoxazole 109

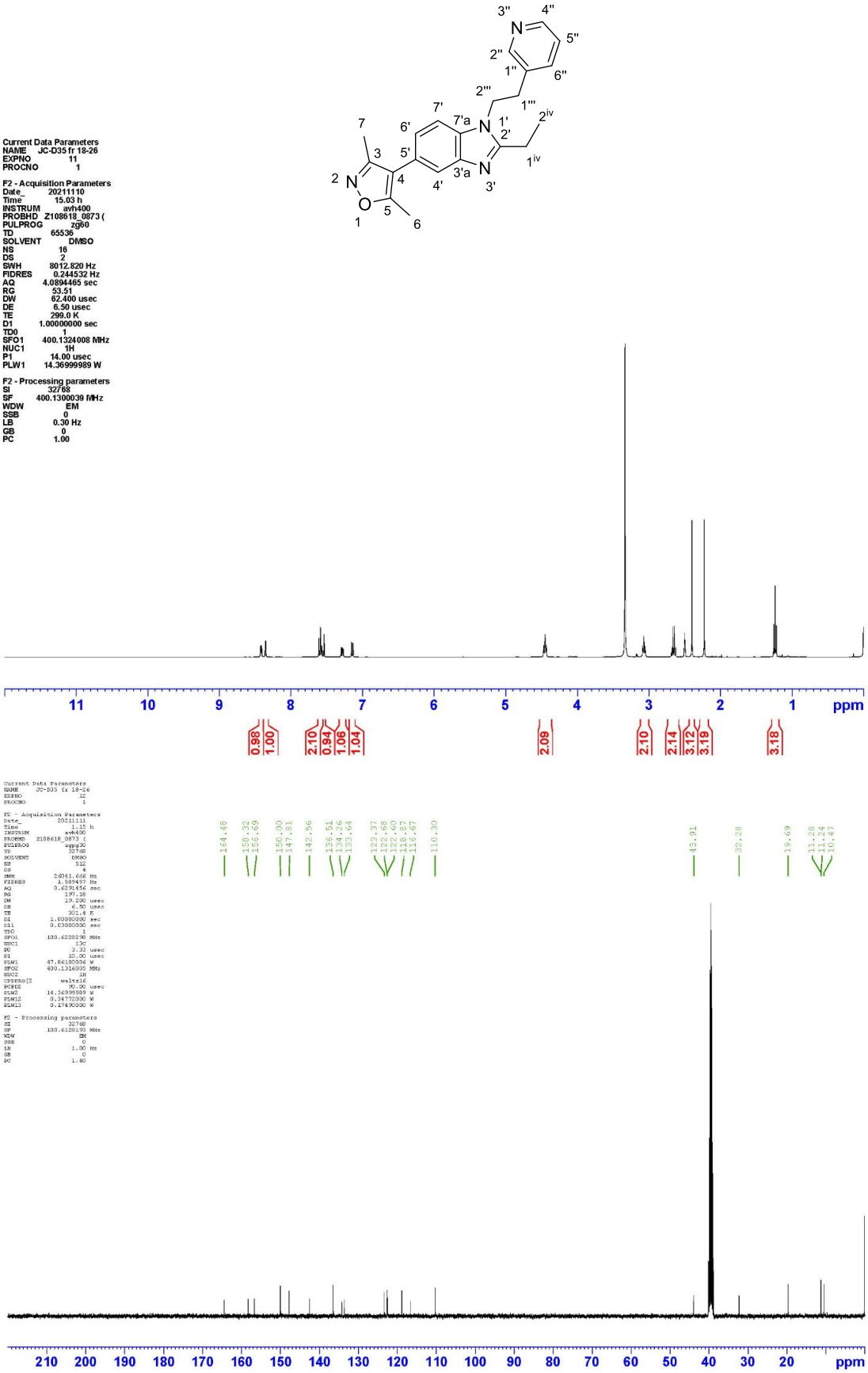

2-(5-(3,5-Dimethylisoxazol-4-yl)-2-ethyl-1*H*-benzo[*d*]imidazol-1-yl)-*N*,*N*-dimethylethan-1-amine 104

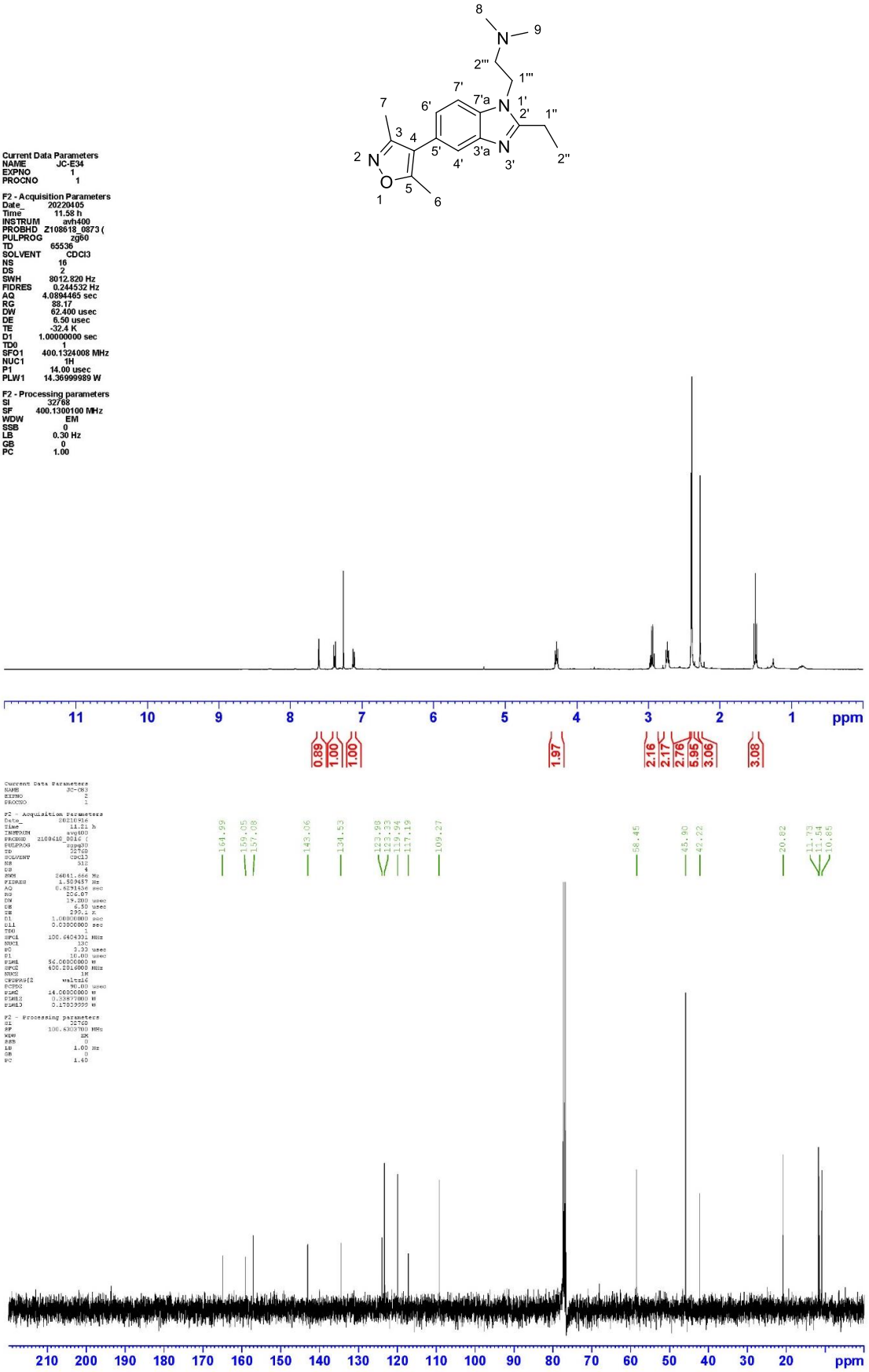

4-(3,5-Dimethylisoxazol-4-yl)-*N*-(2-(4-methylpiperazin-1-yl)ethyl)-2-nitroaniline

193

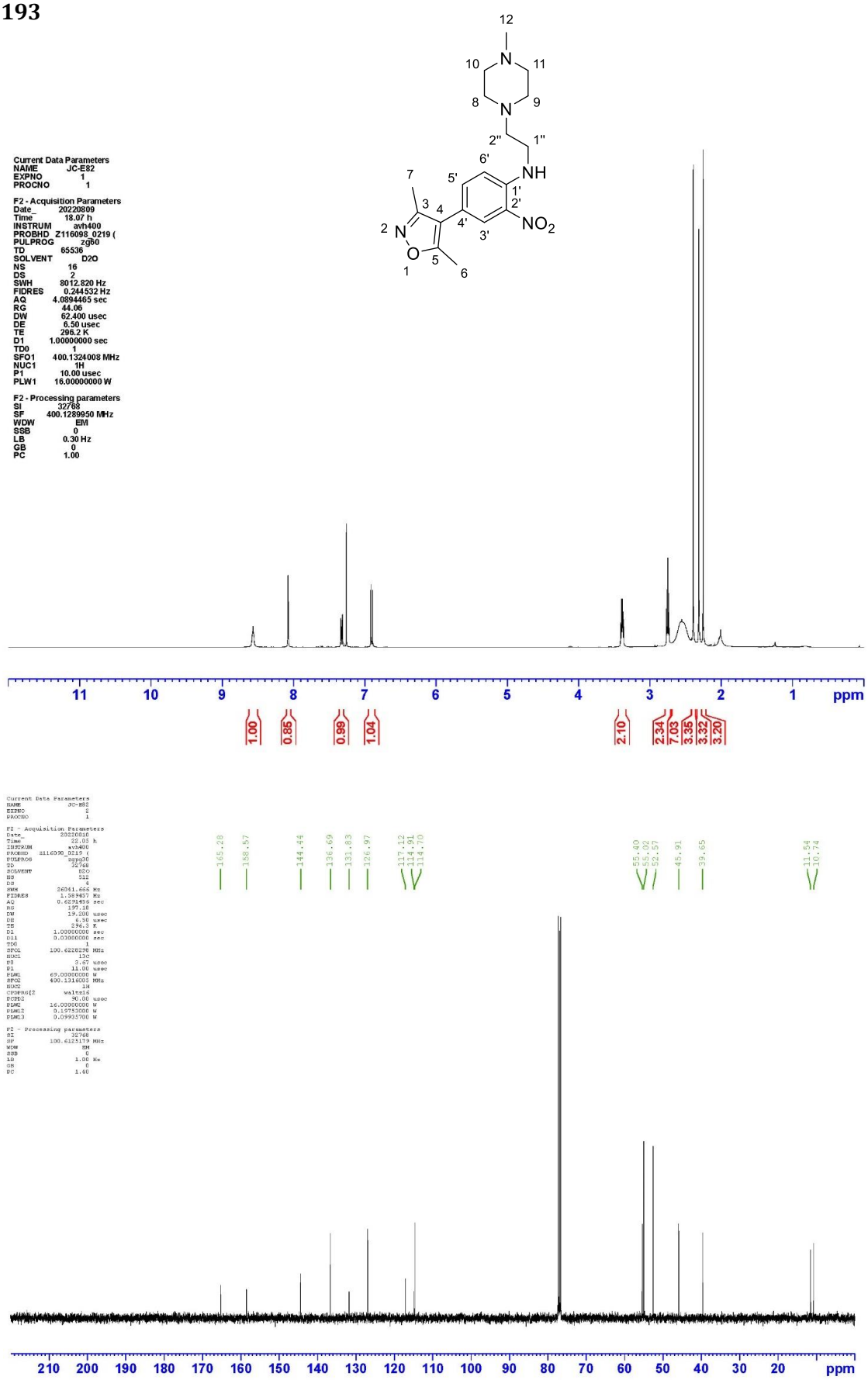

4-(2-Ethyl-1-(2-(4-methylpiperazin-1-yl)ethyl)-1*H*-benzo[*d*]imidazol-5-yl)-3,5-dimethylisoxazole 105

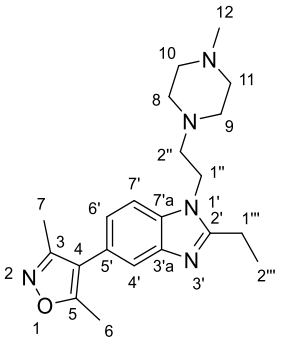

Current Data Parameters
NAME jc673800408
EXPNO 1
PROCNO 1

F2 - Acquisition Parameters
Date_ 20220804
Time 21.54 h
INSTRUM Avance
PROBHD Z159656_0020 (
PULPROG zg30
TD 65536
SOLVENT CDCl3
NS 16
DS 2
SWH 11904.762 Hz
FIDRES 0.363304 Hz
AQ 2.7525120 sec
RG 90.5
DW 42.000 usec
DE 22.00 usec
TE 298.0 K
D1 1.00000000 sec
TD0 1
SFO1 600.4230021 MHz
NUC1 1H
P0 4.00 usec
P1 12.00 usec
PLW1 13.51200008 W

F2 - Processing parameters
SI 65536
SF 600.4200155 MHz
WDW EM
SSB 0
LB 0.30 Hz
GB 0
PC 1.00

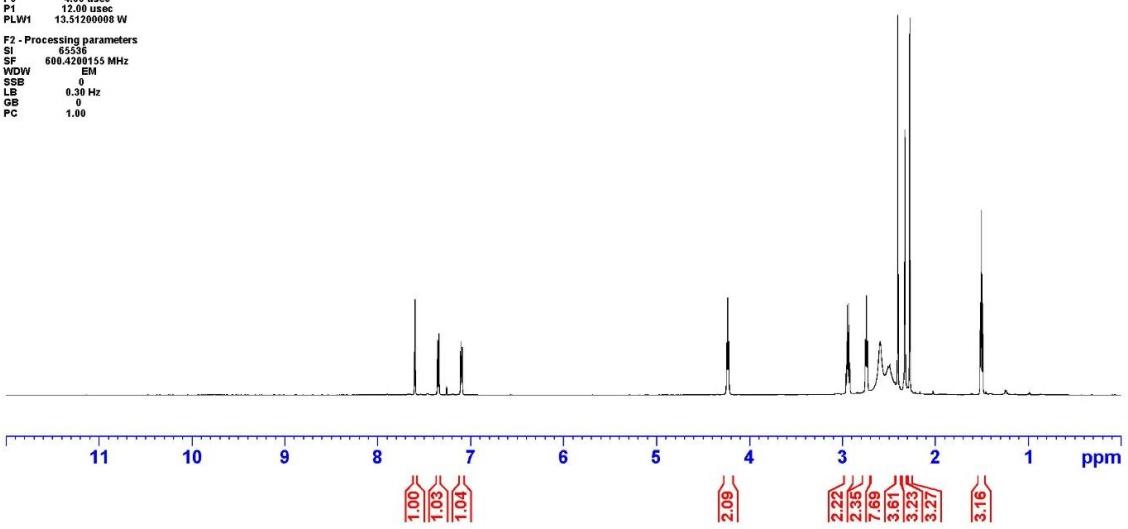

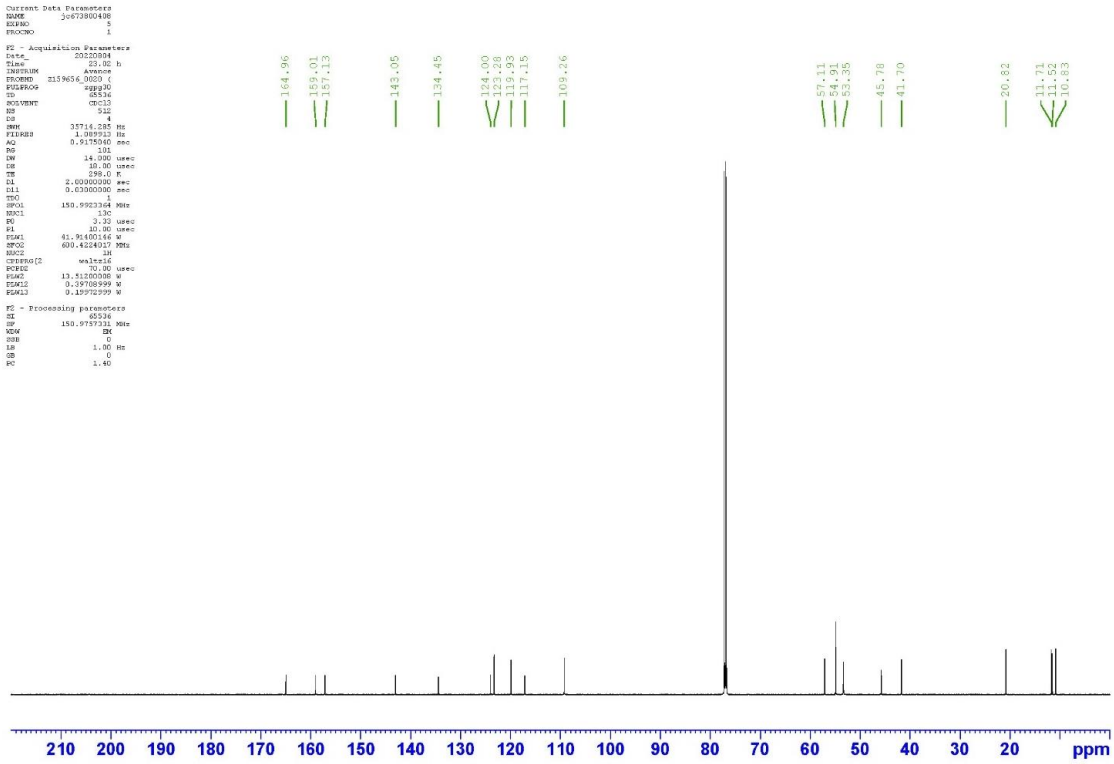

4-(2-(5-(3,5-Dimethylisoxazol-4-yl)-2-ethyl-1*H*-benzo*[d]*imidazol-1-yl)ethyl)morpholine 106

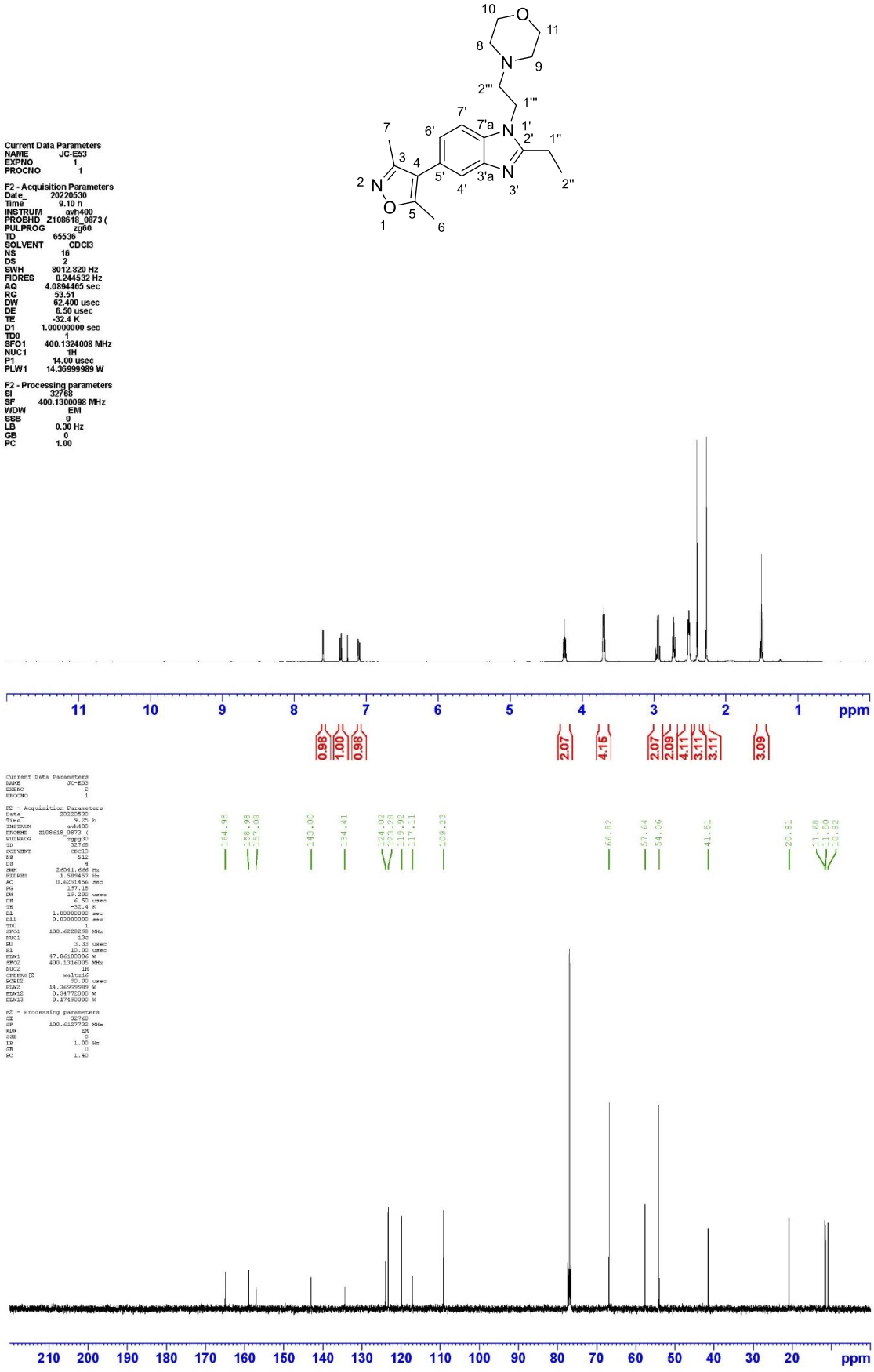

Tert-butyl (*S*)-(1-(1,3-dioxoisoindolin-2-yl)propan-2-yl)carbamate 237

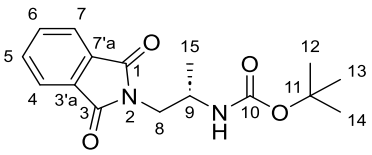

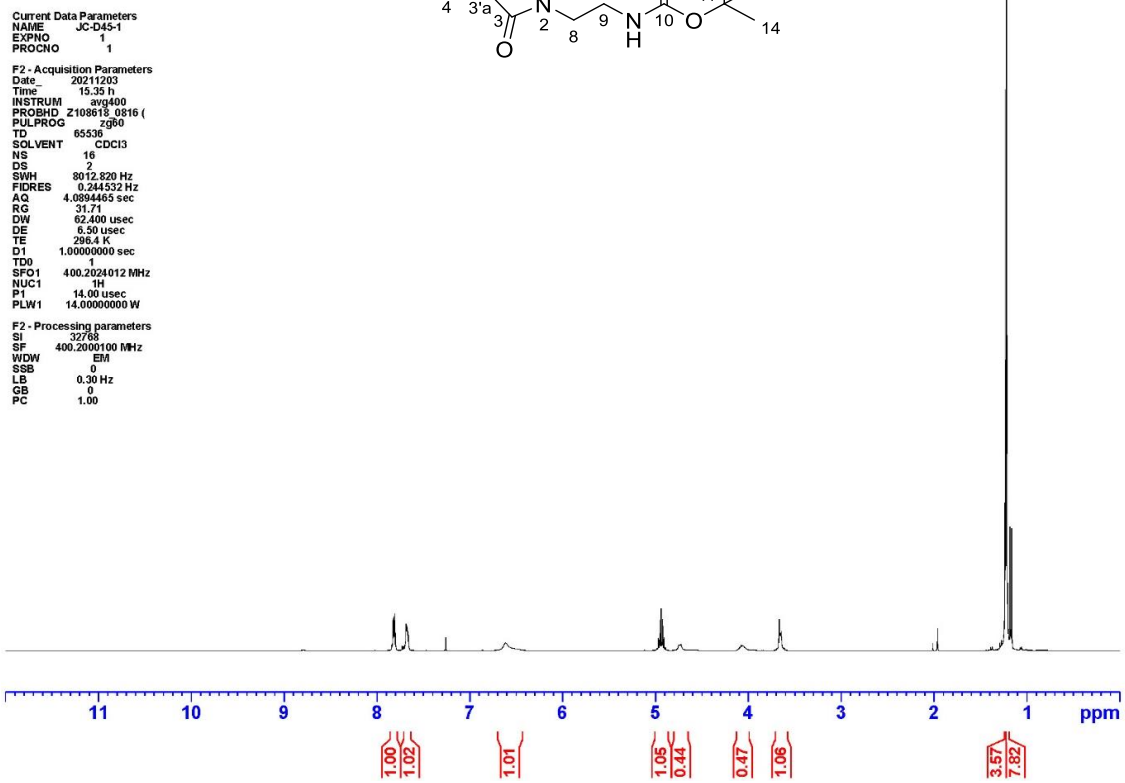

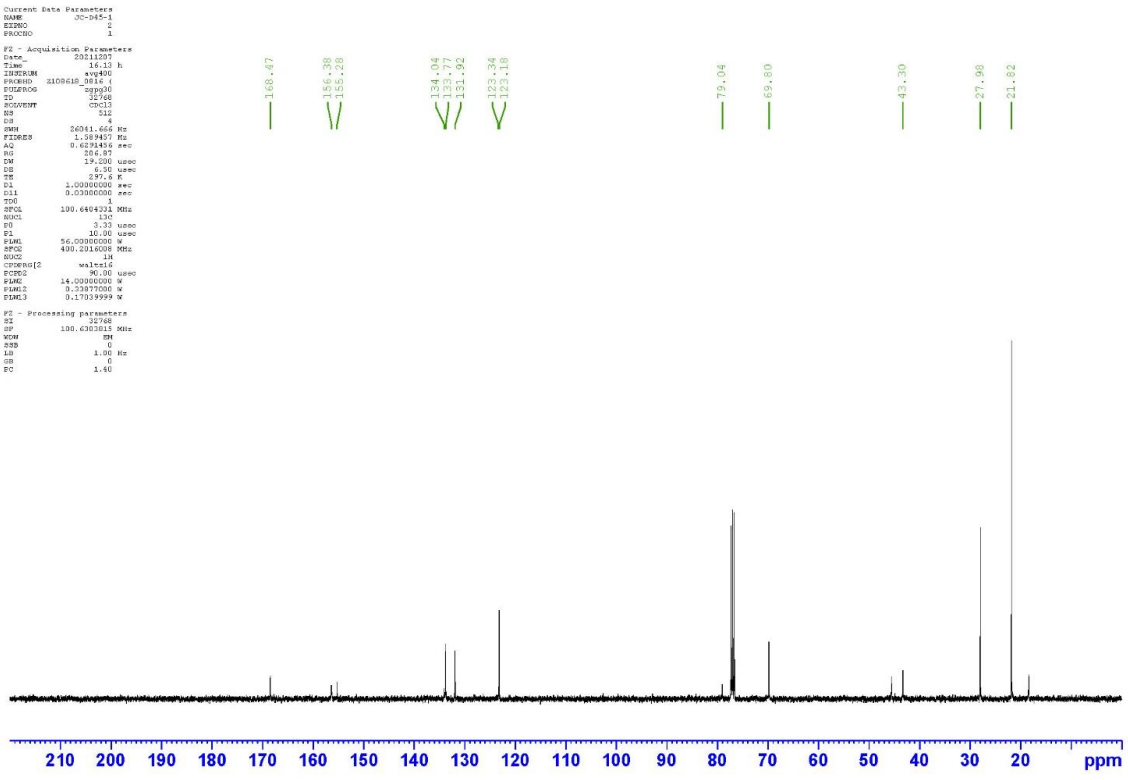

***Tert*-butyl (*S*)-(1-((4-(3,5-dimethylisoxazol-4-yl)-2-nitrophenyl)amino)propan-2-yl)carbamate 133**

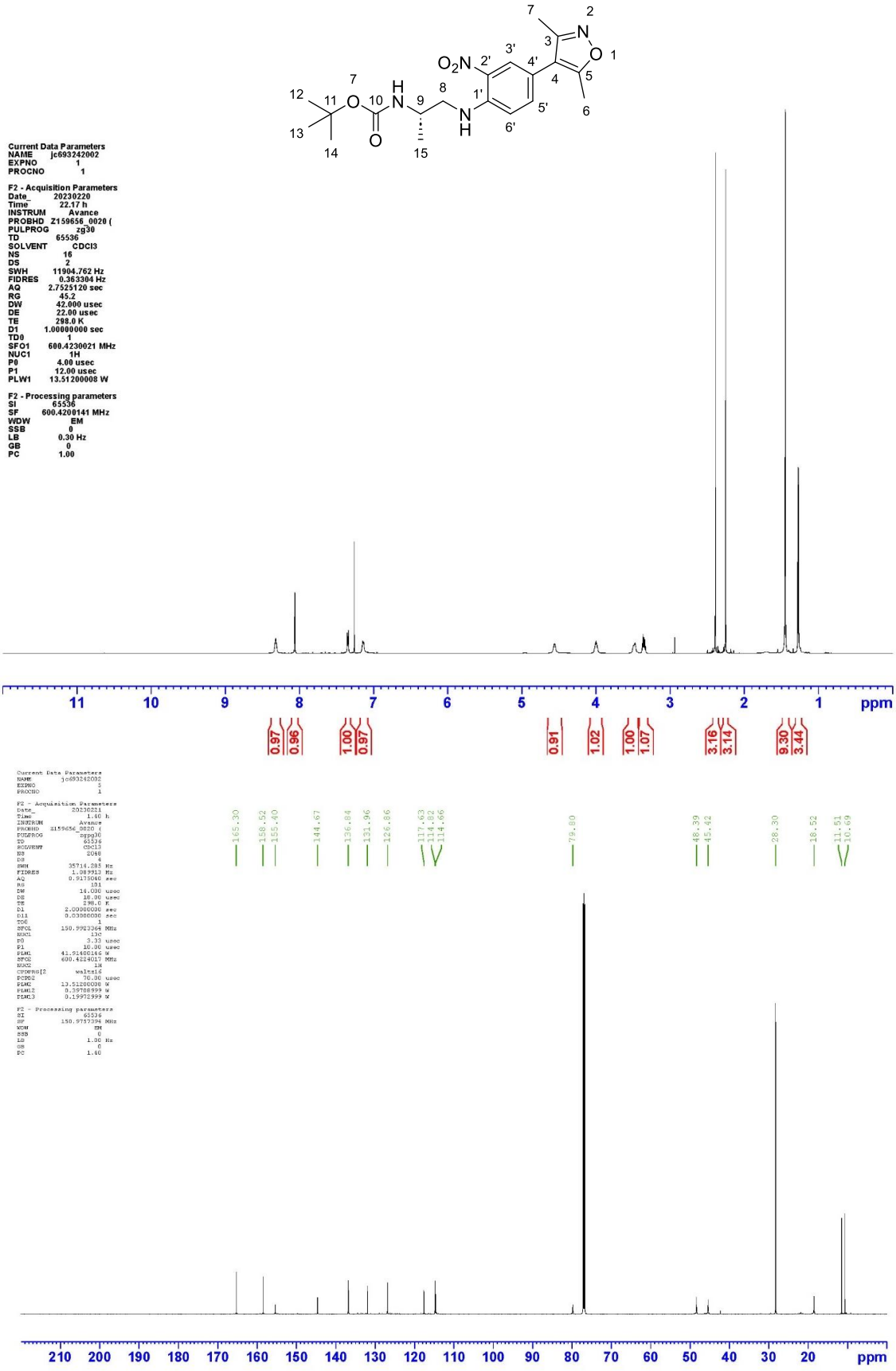

(*S*)-4-(1-(5-(3,5-Dimethylisoxazol-4-yl)-2-ethyl-1*H*-benzo[*d*]imidazol-1-yl)propan-2-yl)morpholine 107

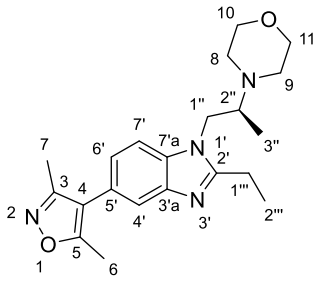

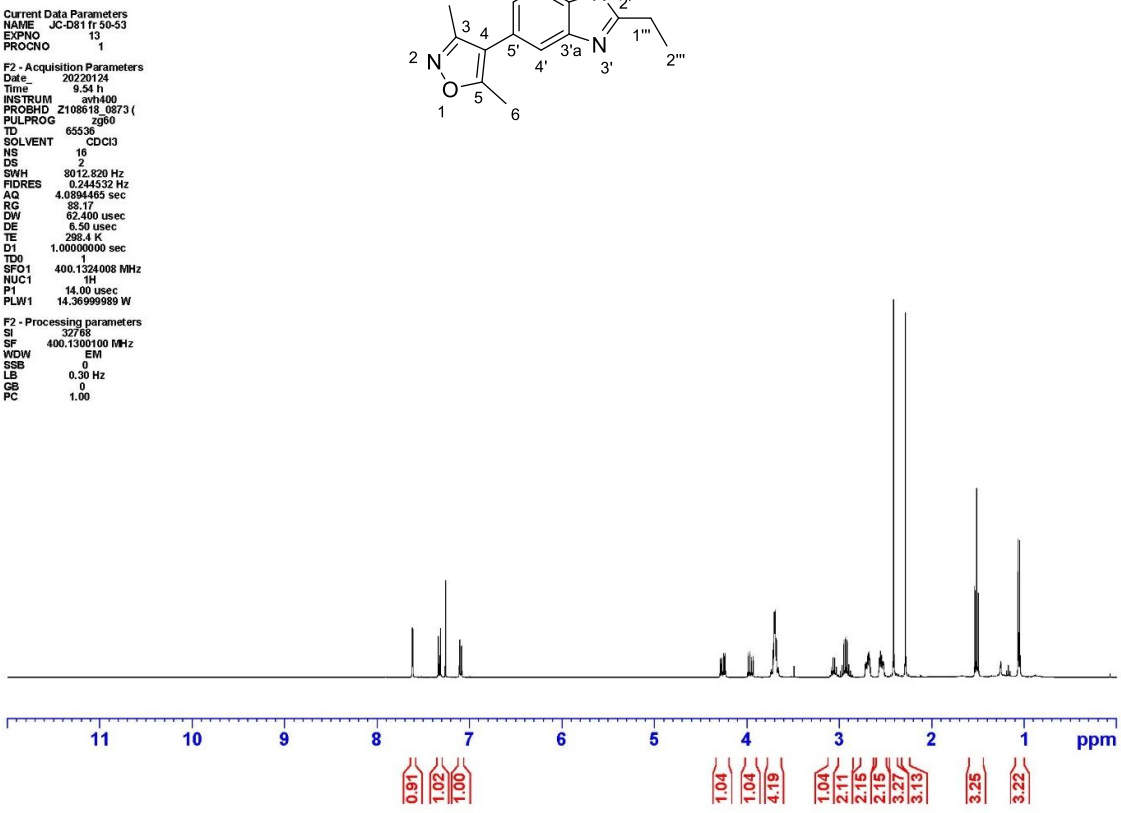

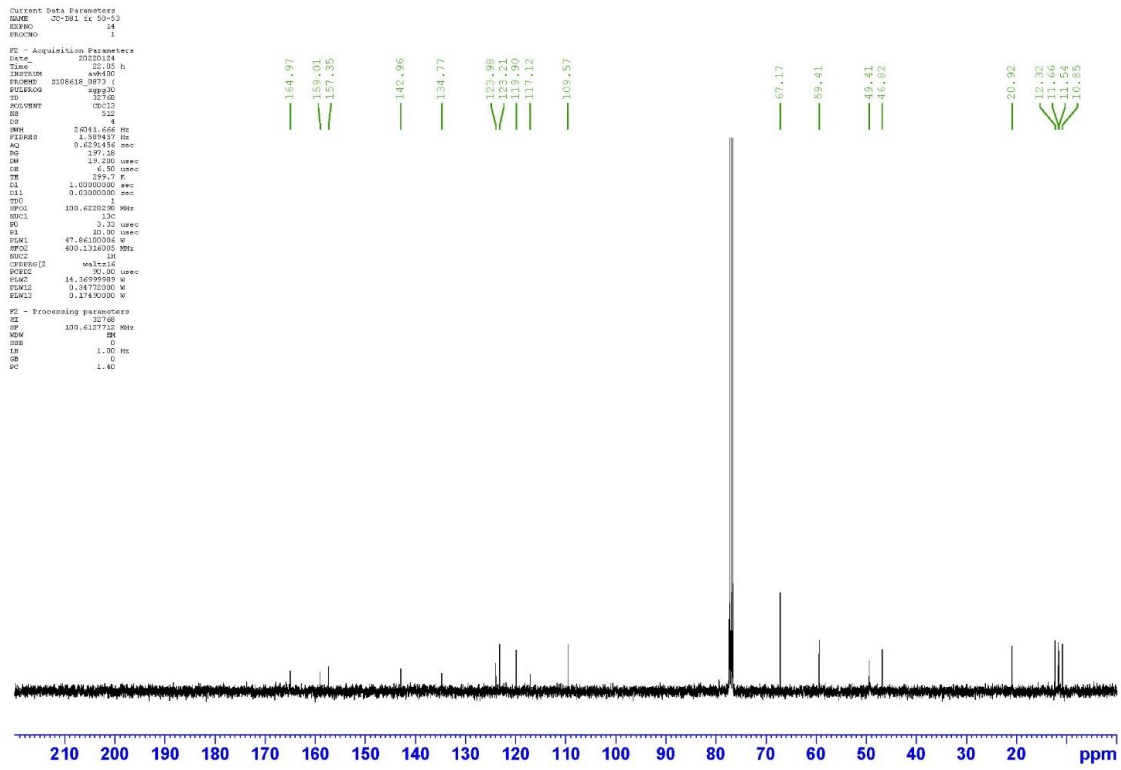

4-(3,5-Dimethyl-1,2-oxazol-4-yl)-*N*-methyl-2-nitroaniline 75

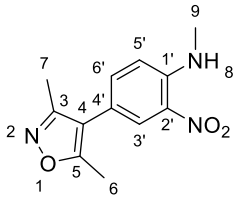

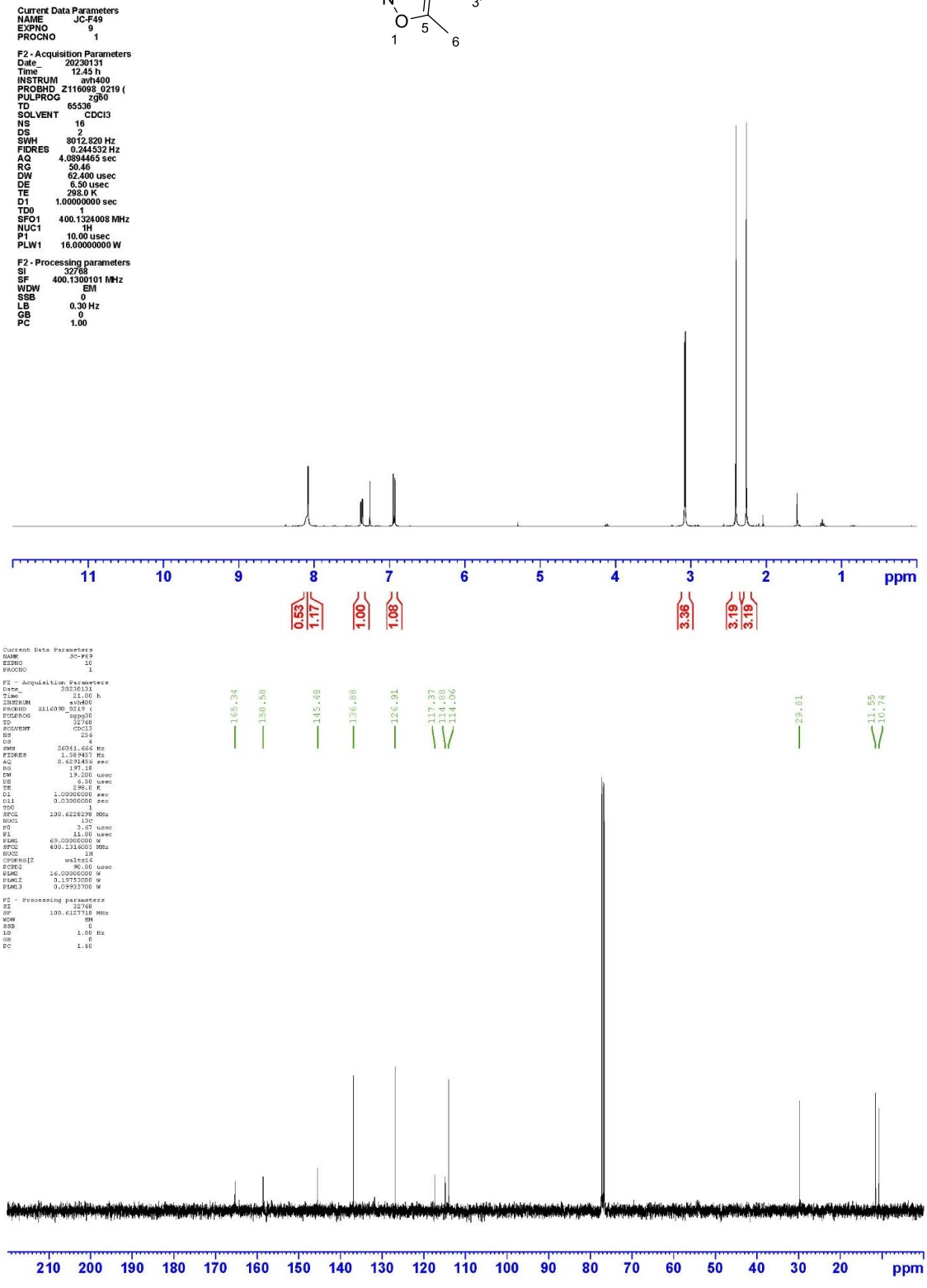

4-(3,5-Dimethylisoxazol-4-yl)-*N*^{1}-methylbenzene-1,2-diamine 76

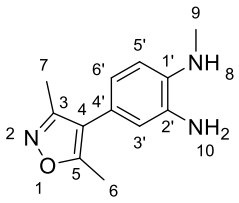

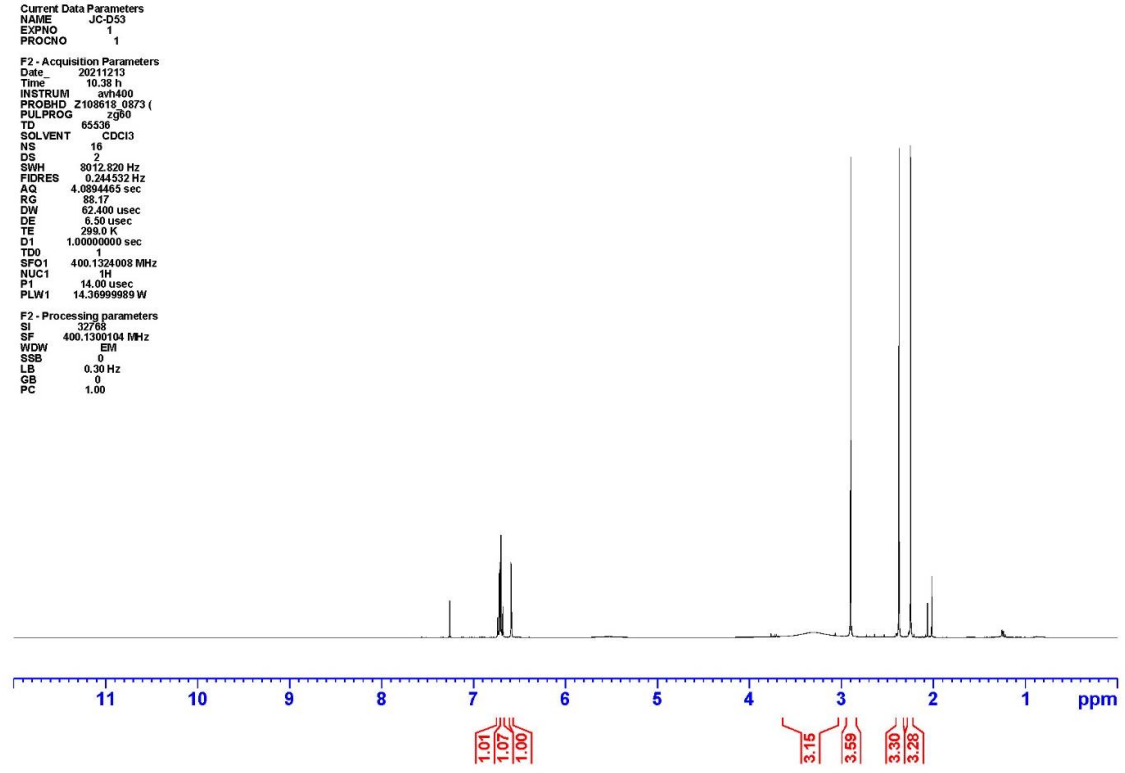

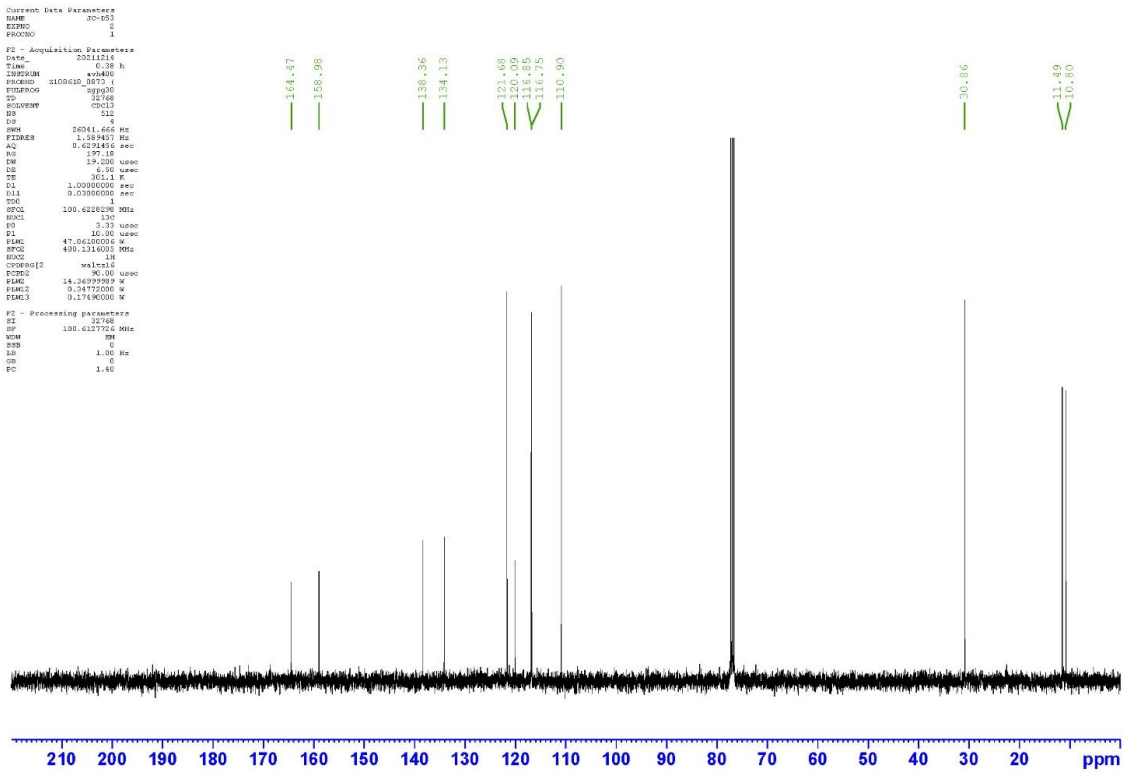

3,5-Dimethyl-4-(1-methyl-2-phenethyl-1*H*-benzo[*d*]imidazol-5-yl)isoxazole 137

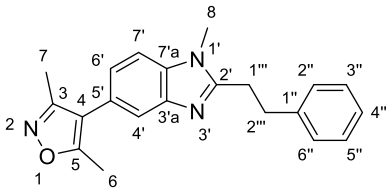

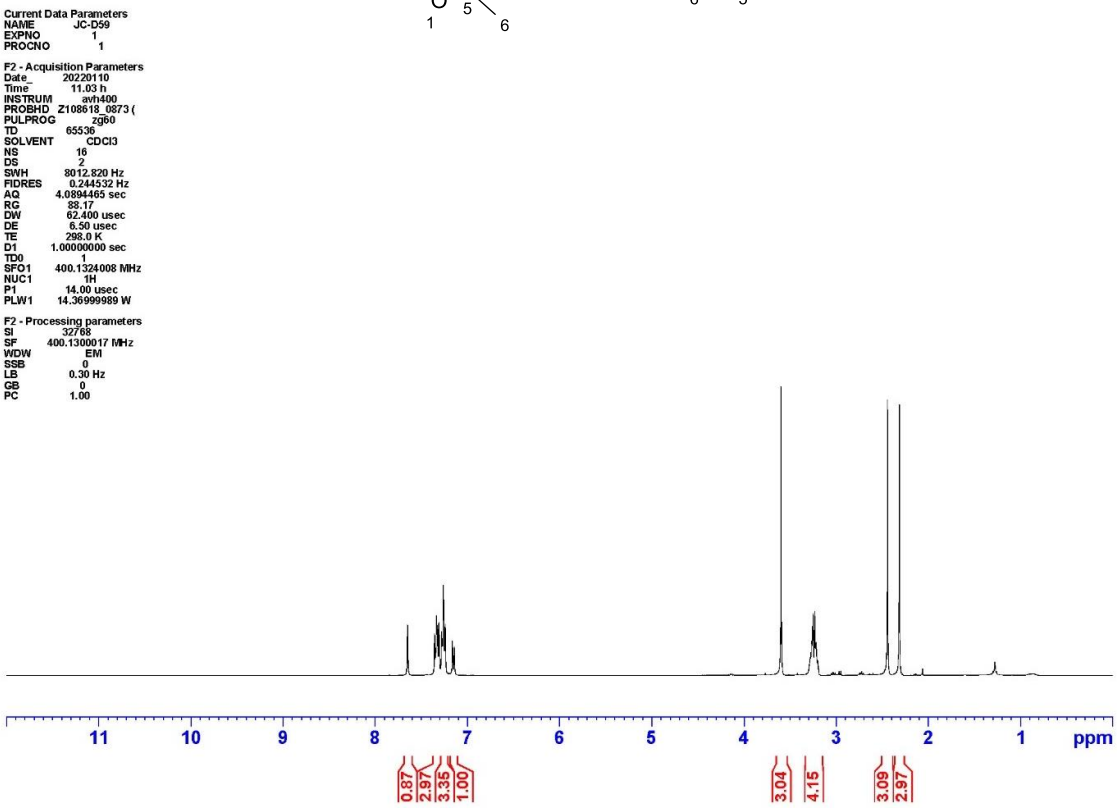

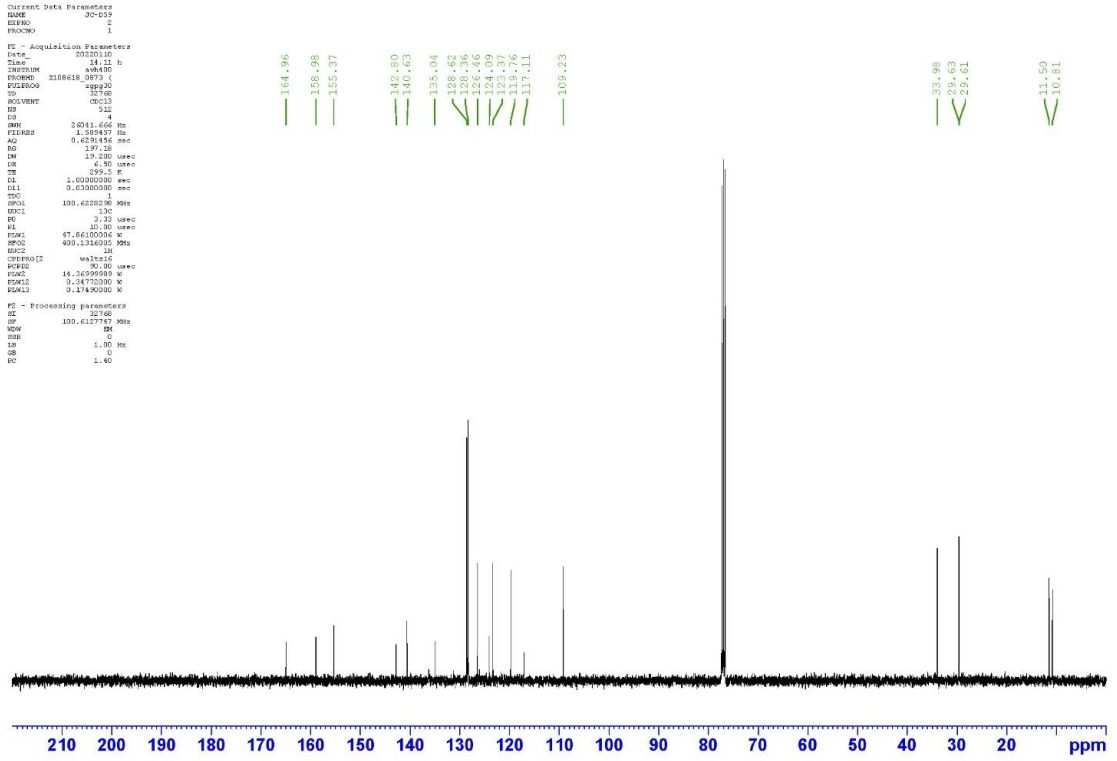

3,5-Dimethyl-4-(1-methyl-2-(3-methylphenethyl)-1*H*-benzo[*d*]imidazol-5-yl)isoxazole 121

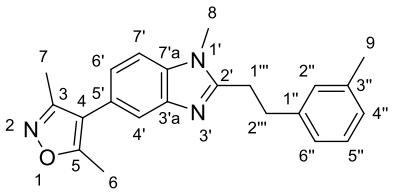

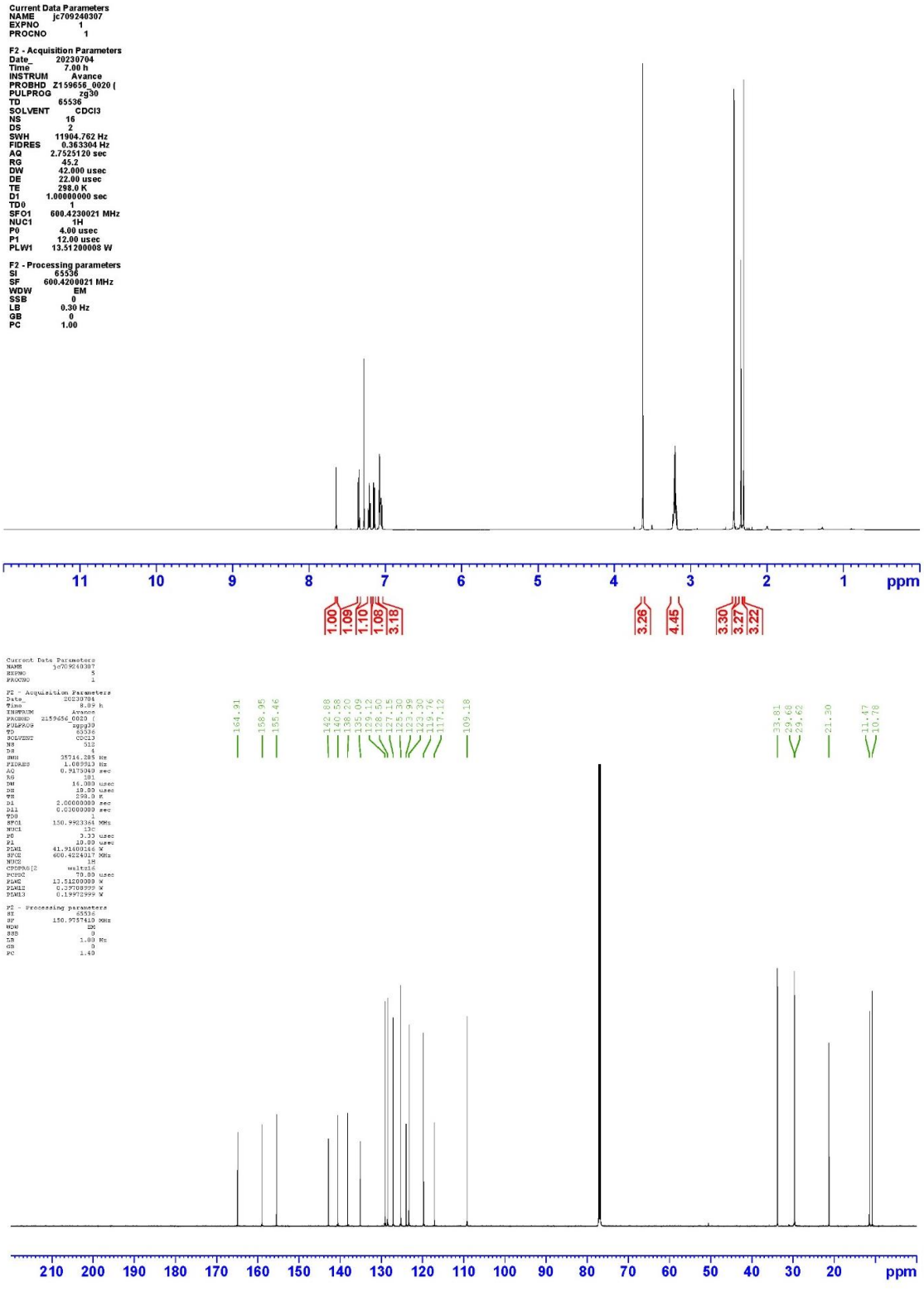

4-(2-(3-Fluorophenethyl)-1-methyl-1*H*-benzo[*d*]imidazol-5-yl)-3,5-dimethylisoxazole 122

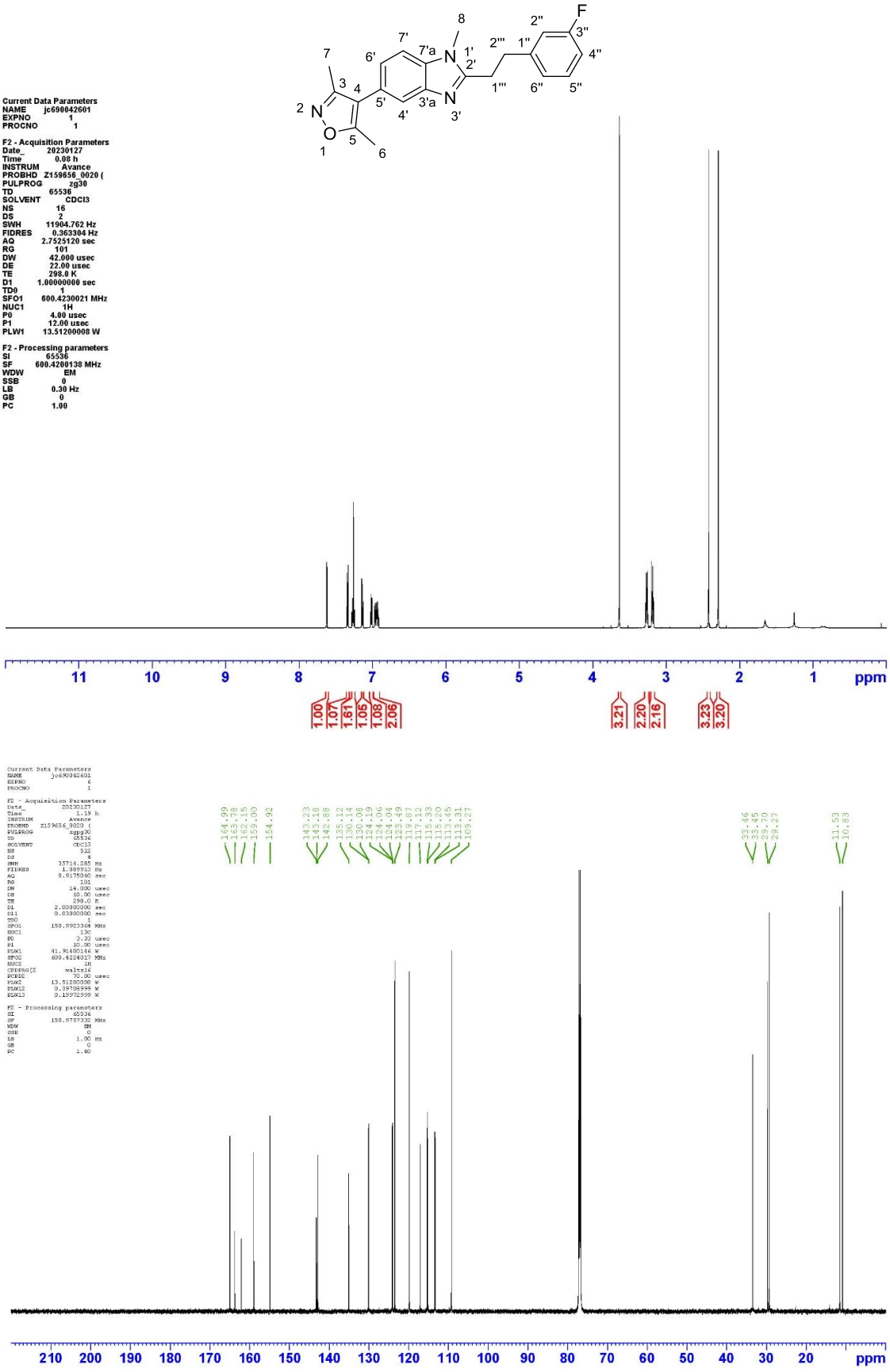

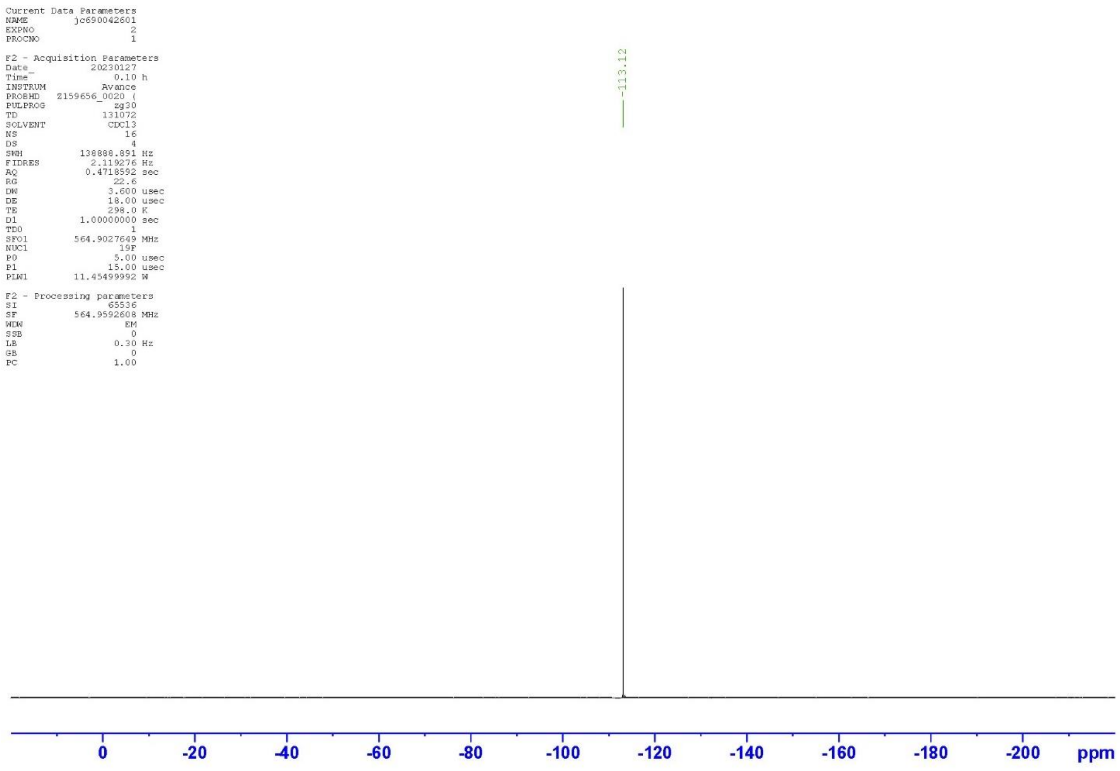
Current Data Parameters
NAME jc690042601
EXPNO 2
PROCNO 1
F2 - Acquisition Parameters
Date_ 20230127
Time 0.10 h
INSTRUM Avance
PROBHD Z159656_0020 (
PULPROG zg30
TD 131072
SOLVENT CDCl3
NS 16
DS 4
SWH 138888.891 Hz
FIDRES 2.119276 Hz
AQ 0.4718592 sec
RG 22.6
DW 3.600 usec
DE 18.00 usec
TE 298.0 K
D1 1.00000000 sec
TD0 1
SFO1 564.9027649 MHz
NUC1 19F
P0 5.00 usec
P1 15.00 usec
PLW1 11.45499992 W
F2 - Processing parameters
SI 65536
SF 564.9592608 MHz
WDW EM
SSB 0
LB 0.30 Hz
GB 0
PC 1.00
-113.12
0
-20
-40
-60
-80
-100
-120
-140
-160
-180
-200
ppm

4-(2-(3-Chlorophenethyl)-1-methyl-1*H*-benzo[*d*]imidazol-5-yl)-3,5-dimethylisoxazole 149

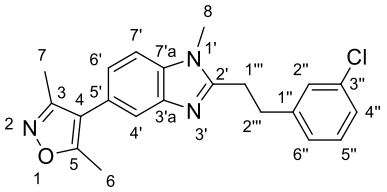

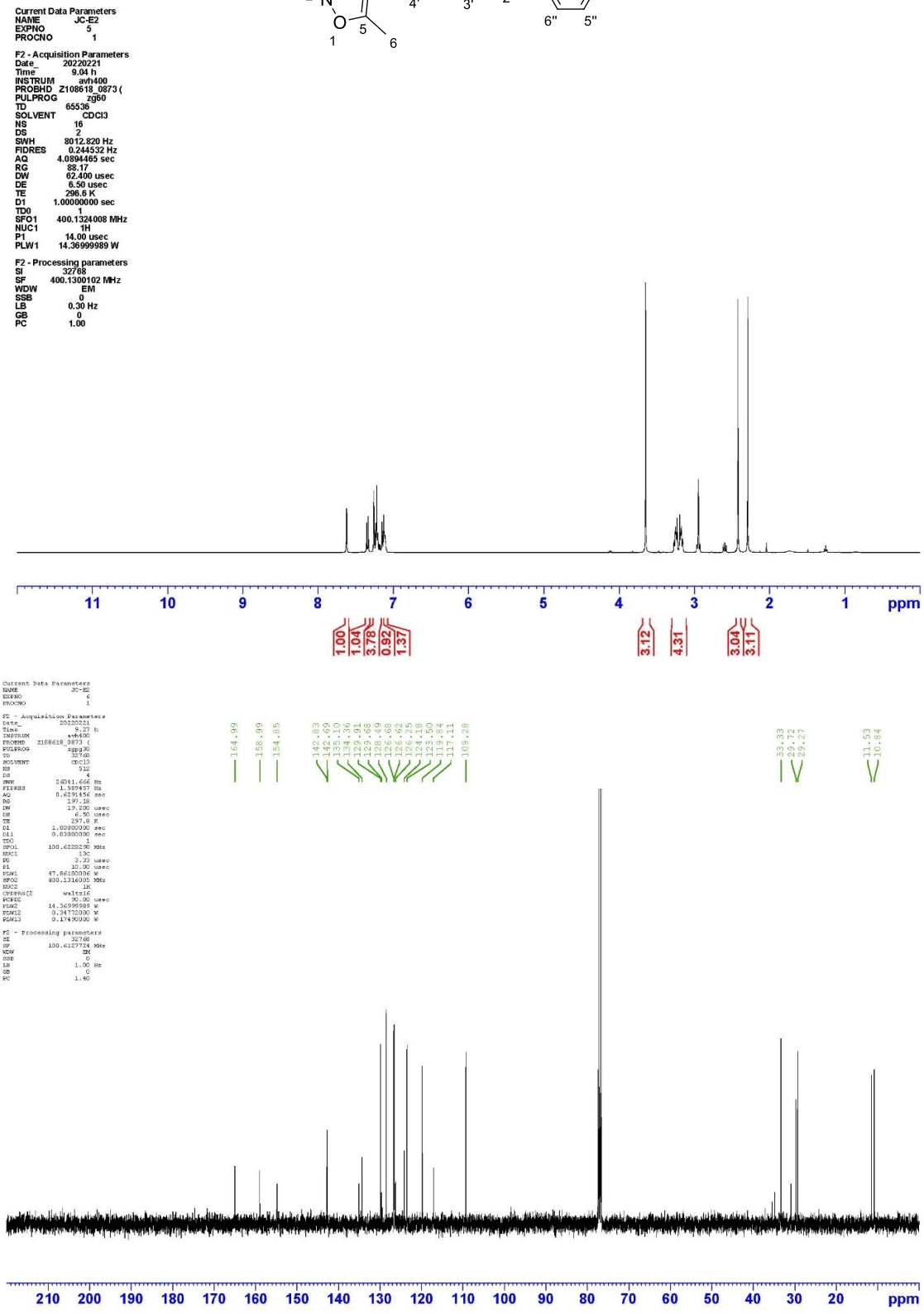

4-(2-(3-Bromophenethyl)-1-methyl-1*H*-benzo[*d*]imidazol-5-yl)-3,5-dimethylisoxazole 150

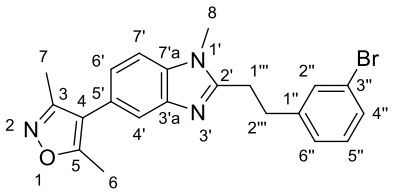

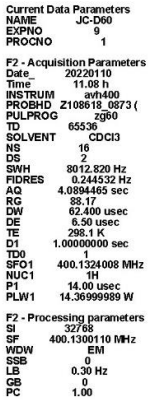

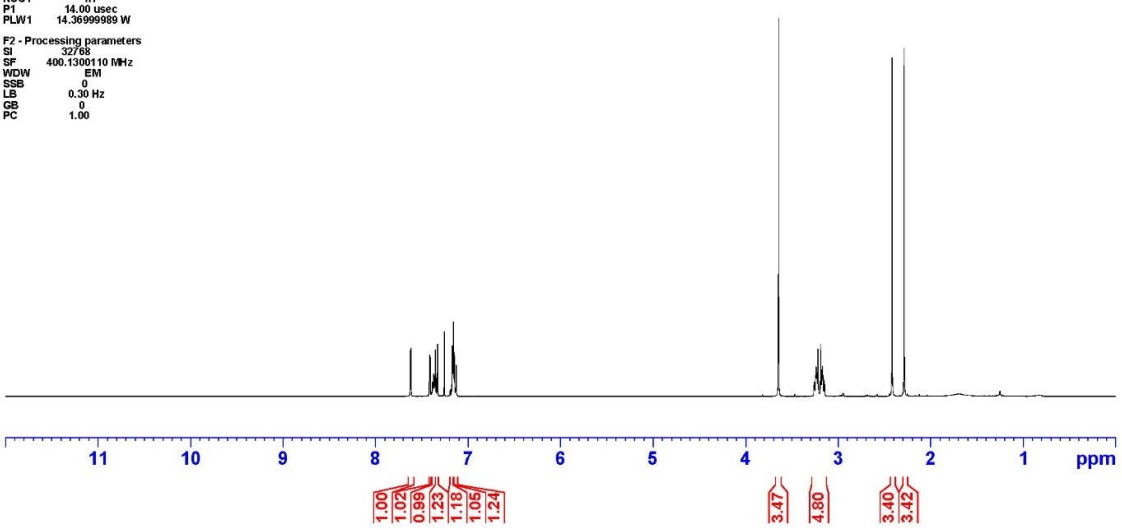

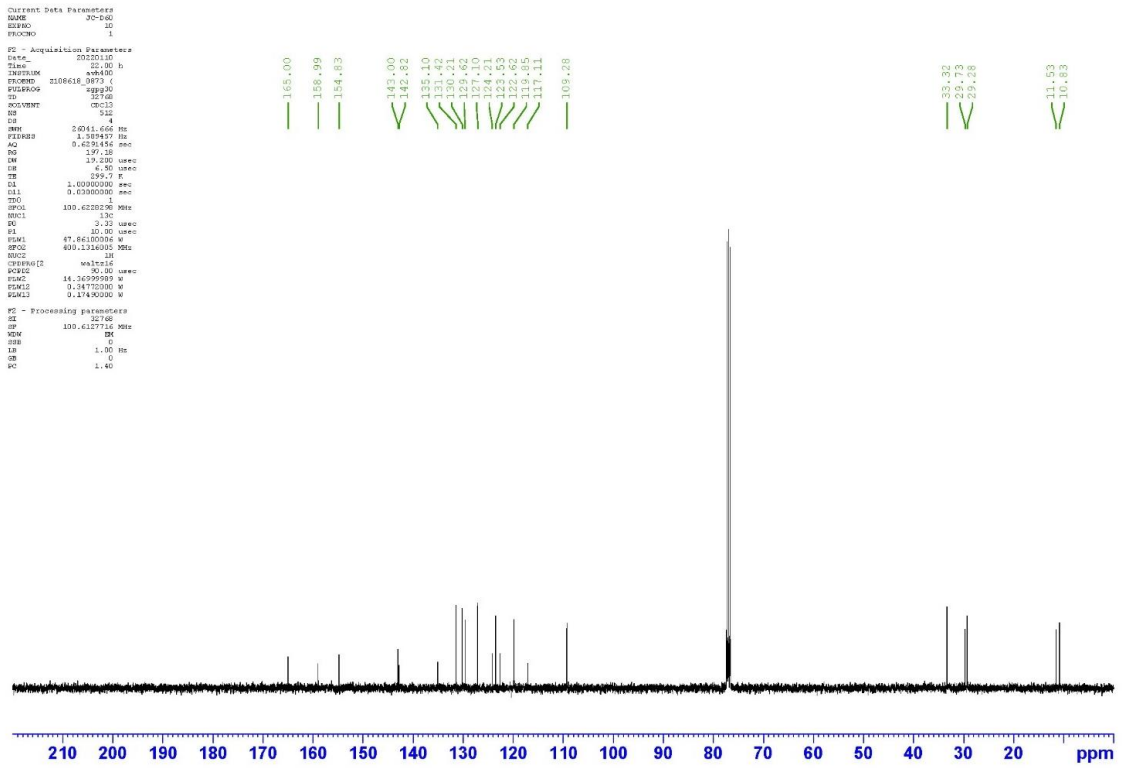

3,5-Dimethyl-4-(1-methyl-2-(3-methylphenethyl)-1*H*-benzo[*d*]imidazol-5-yl)isoxazole 120

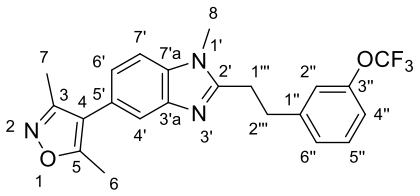

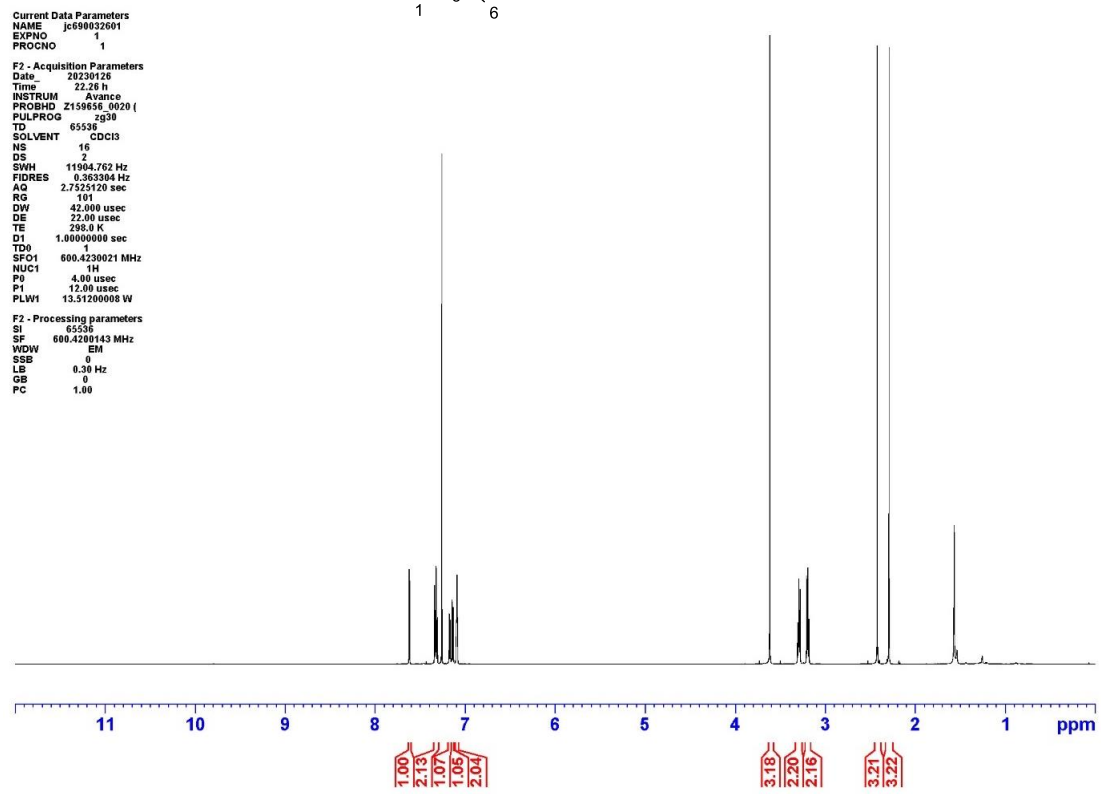

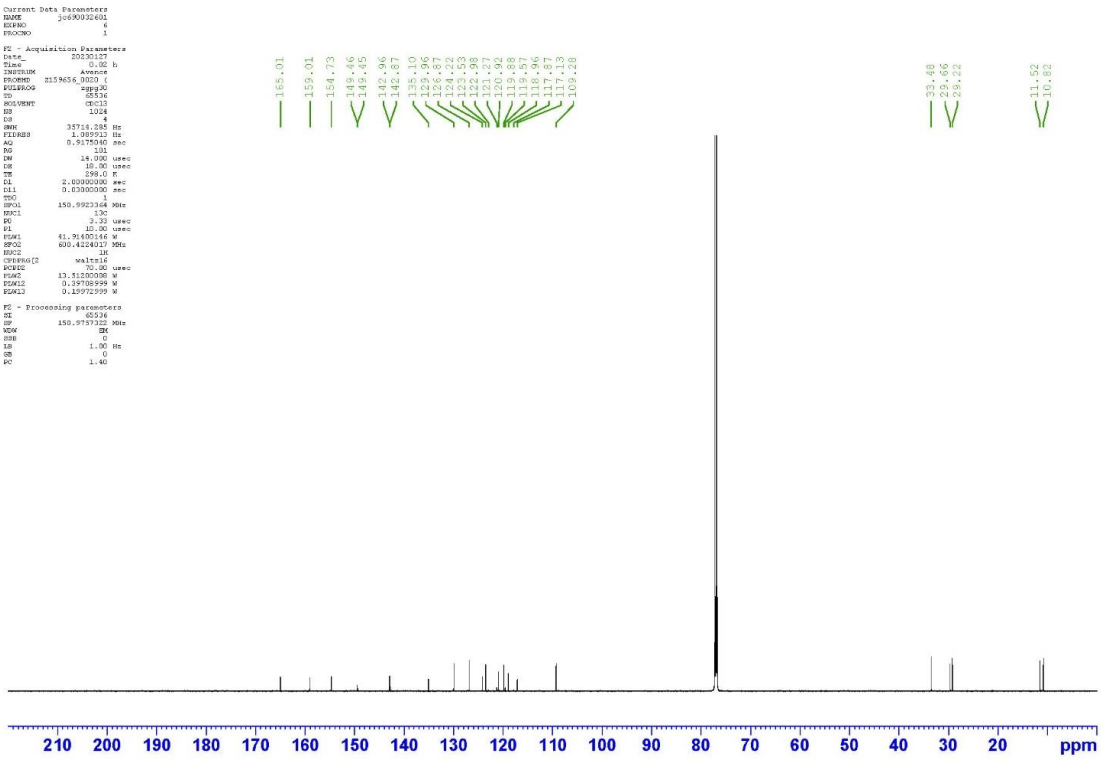

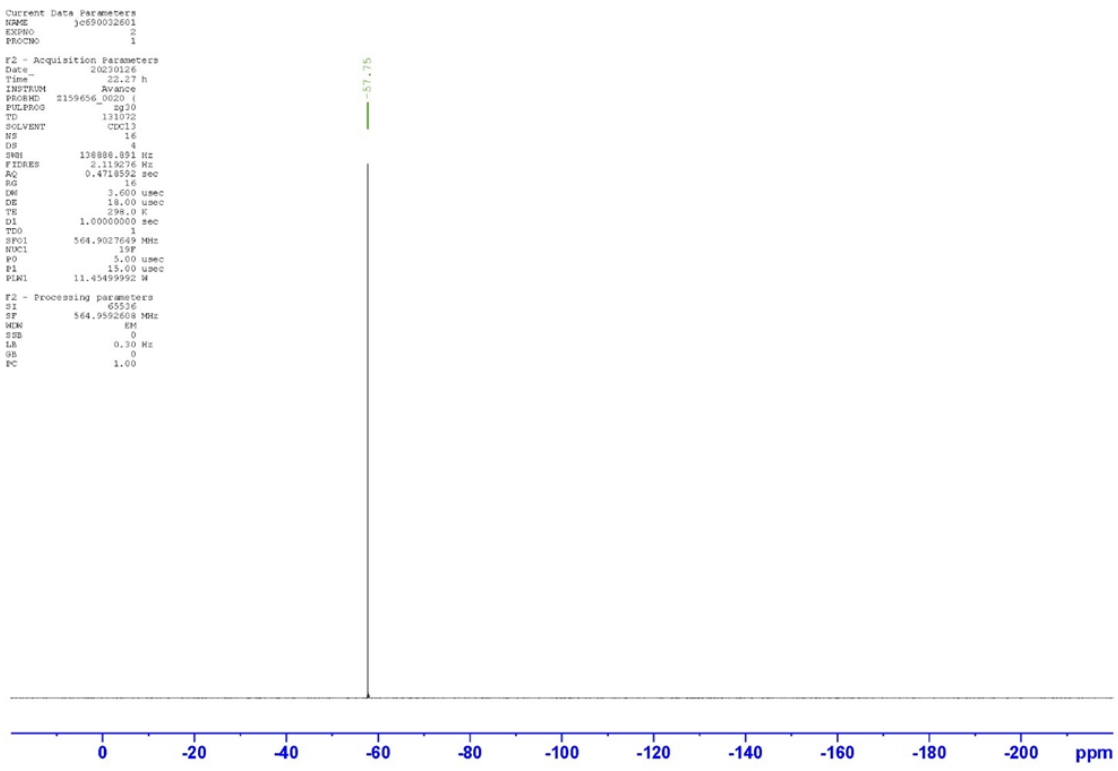
Current Data Parameters
NAME jc690032601
EXPNO 2
PROCNO 1
f2 - Acquisition Parameters
Date_ 20230126
Time_ 22.27 h
INSTRUM Avance
PROBHD 2159656_0020 (
PULPROG zg30
TD 131072
SOLVENT CDCl3
NS 16
DS 4
SWH 138888.891 Hz
FIDRES 2.119276 Hz
AQ 0.4718592 sec
RG 16
DW 3.600 usec
DE 18.00 usec
TE 298.0 K
D1 1.00000000 sec
TD0 1
SFO1 564.9027649 MHz
NUC1 19F
P0 5.00 usec
P1 15.00 usec
PLW1 11.45499992 W
f2 - Processing parameters
SI 65536
SF 564.9592608 MHz
WDW EM
SSB 0
LB 0.30 Hz
GB 0
PC 1.00
-57.75
0
-20
-40
-60
-80
-100
-120
-140
-160
-180
-200
ppm

4-(2-(3-Methoxyphenethyl)-1-methyl-1*H*-benzo[*d*]imidazol-5-yl)-3,5-dimethylisoxazole 139

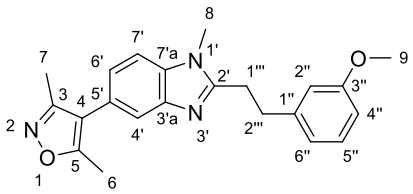

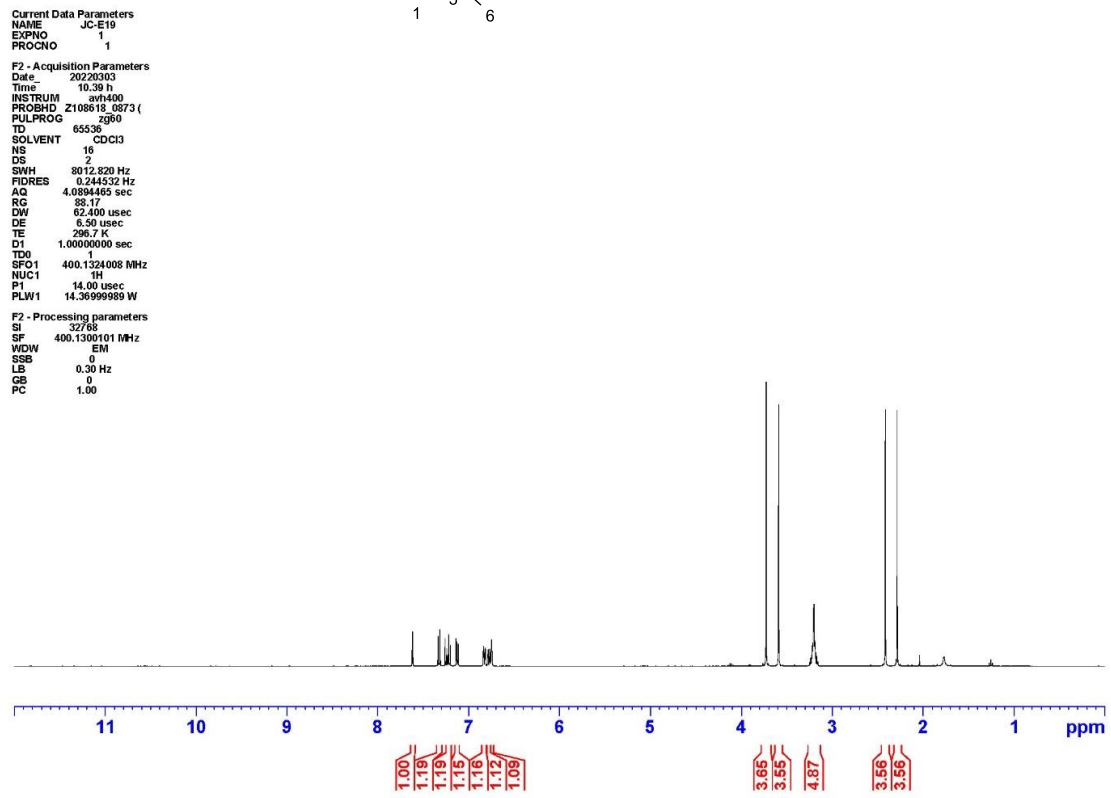

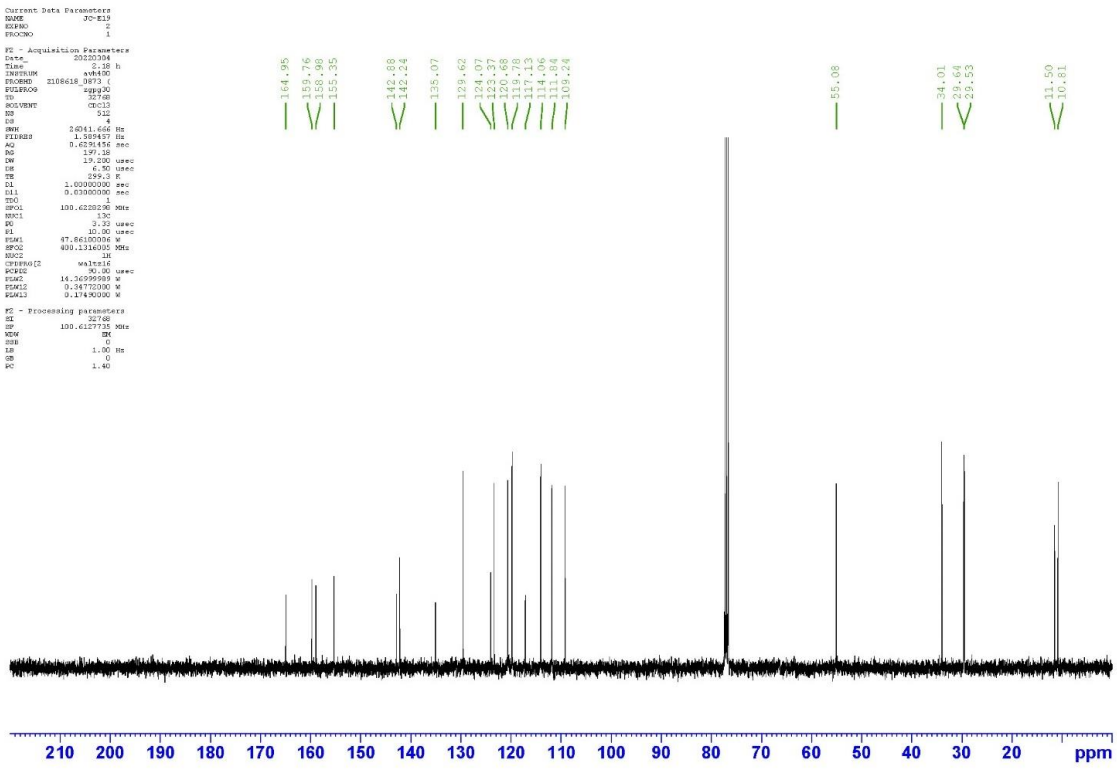

3,5-Dimethyl-4-(1-methyl-2-(3-nitrophenethyl)-1*H*-benzo[*d*]imidazol-5-yl)isoxazole

151

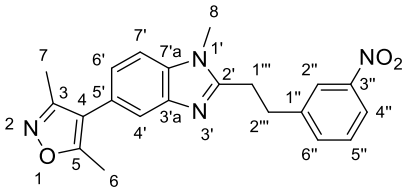

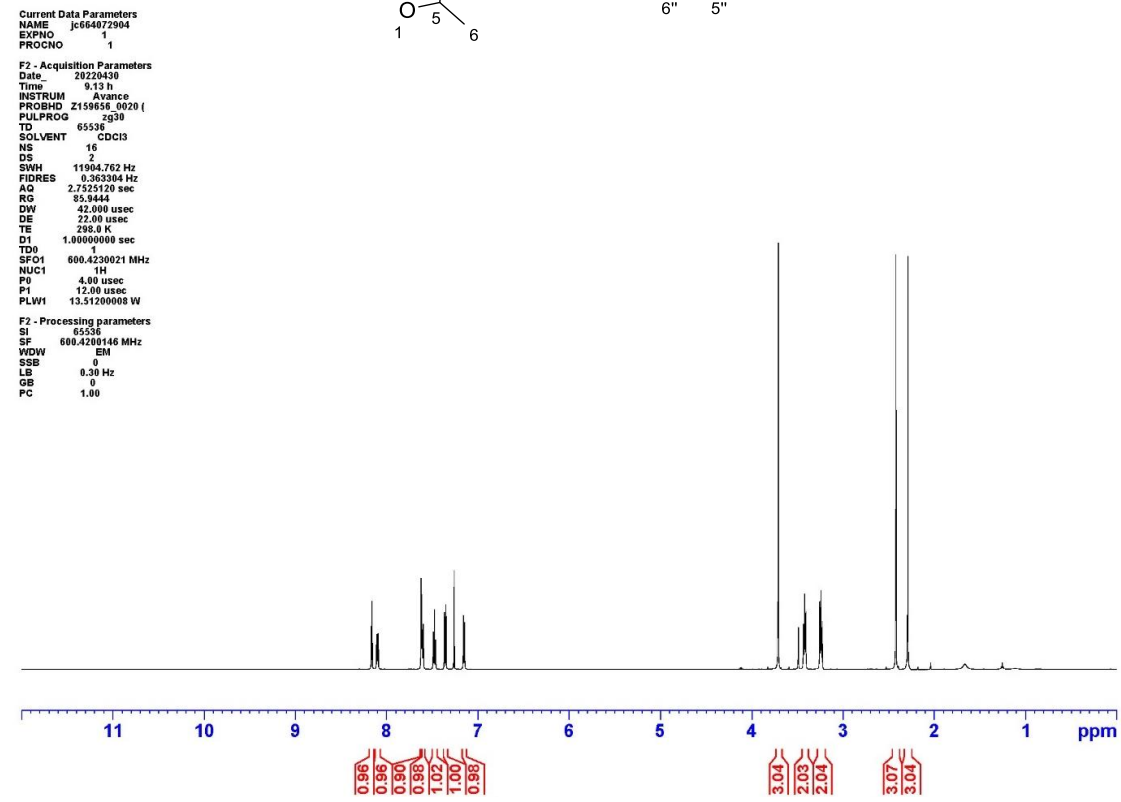

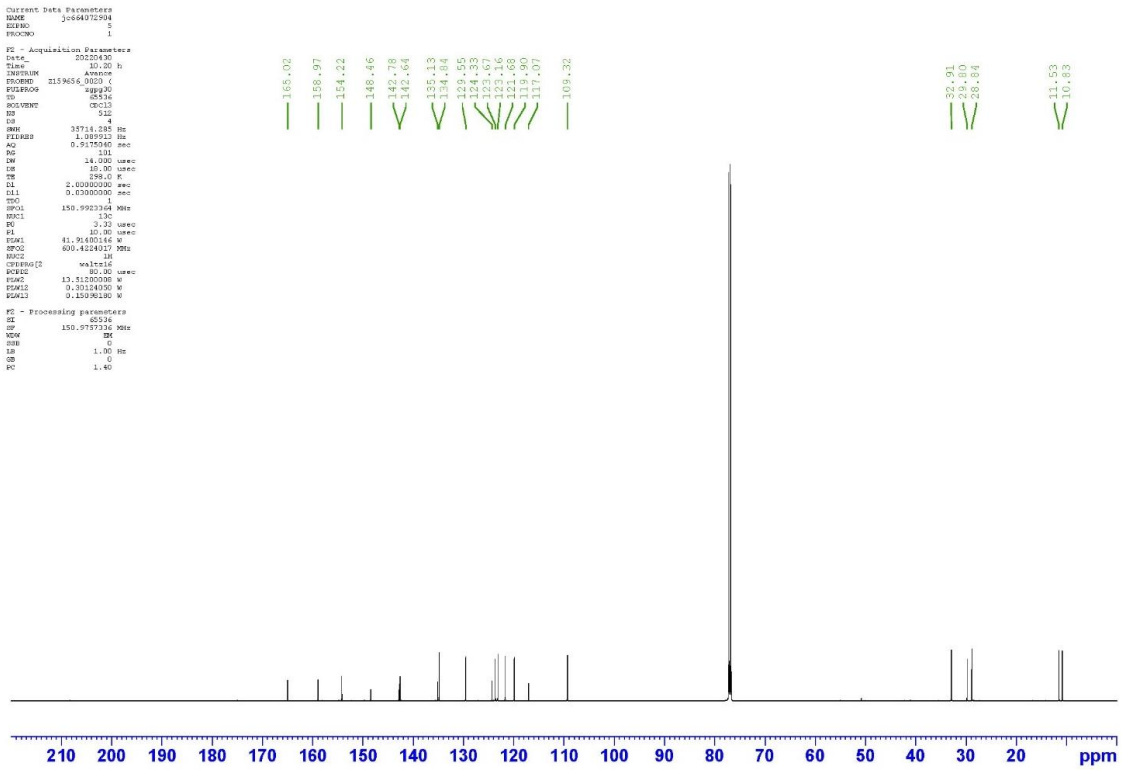

3-(2-(5-(3,5-Dimethylisoxazol-4-yl)-1-methyl-1*H*-benzo[*d*]imidazol-2-yl)ethyl)benzonitrile 154

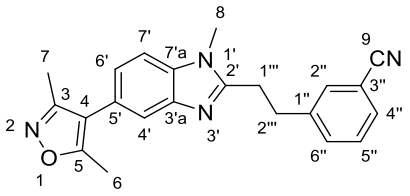

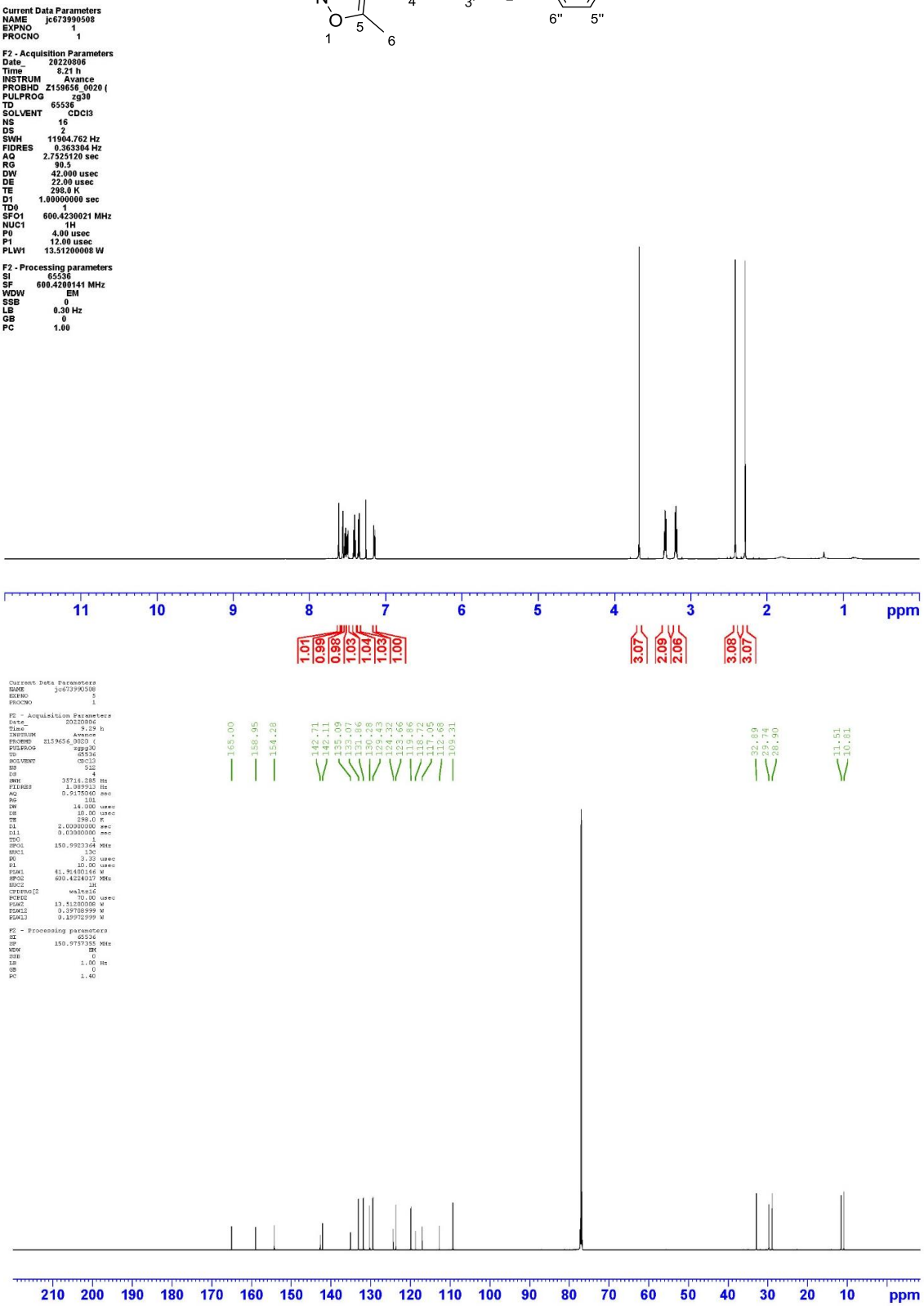

3,5-Dimethyl-4-(1-methyl-2-(3-(trifluoromethyl)phenethyl)-1*H*-benzo[*d*]imidazol-5-yl)isoxazole 153

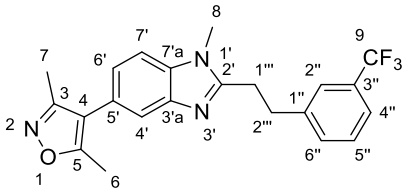

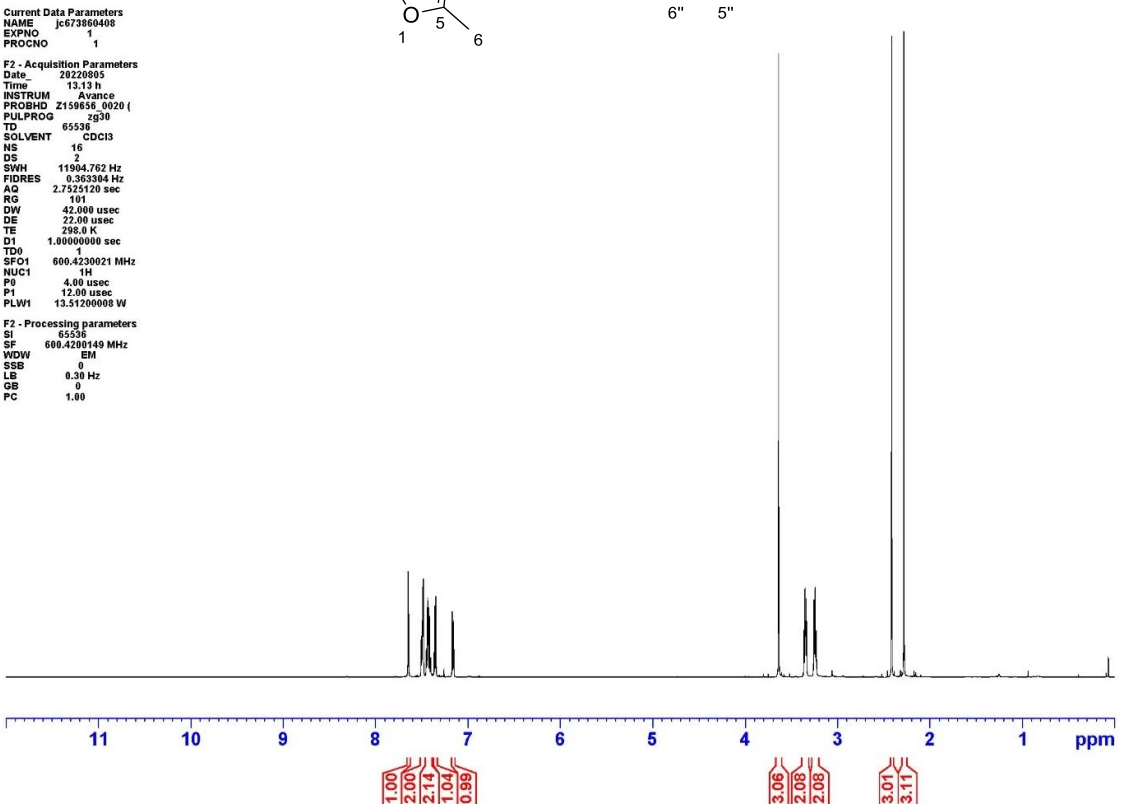

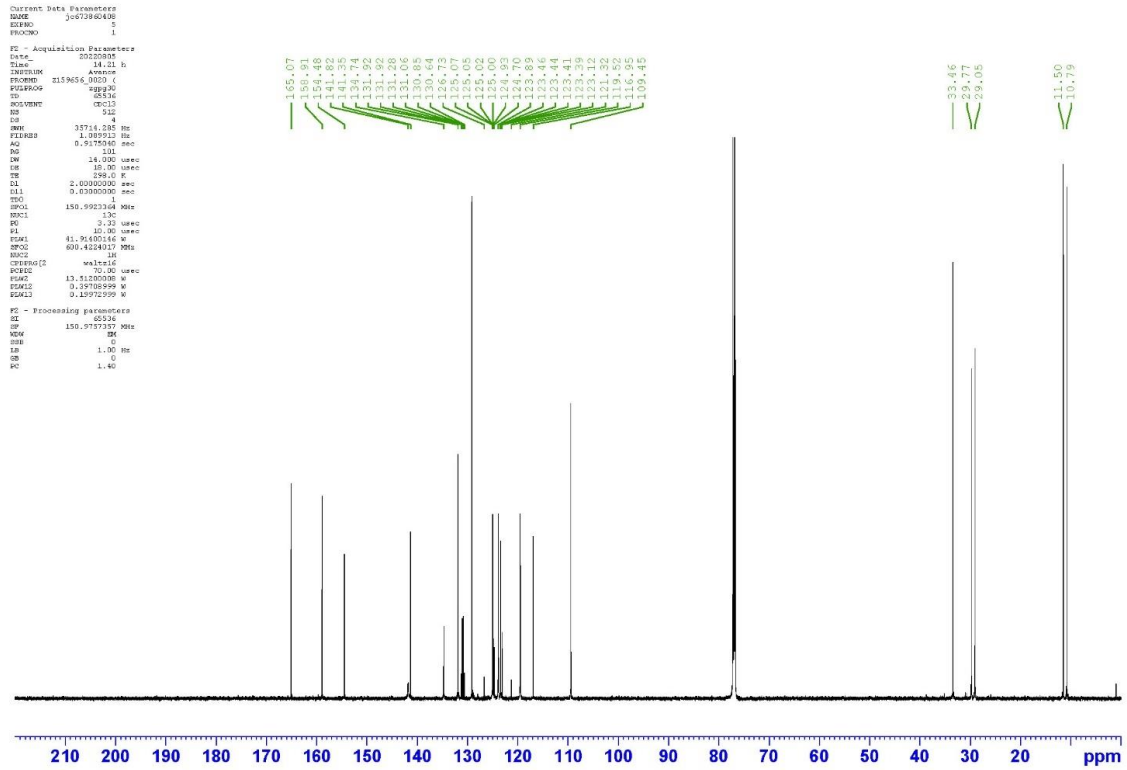

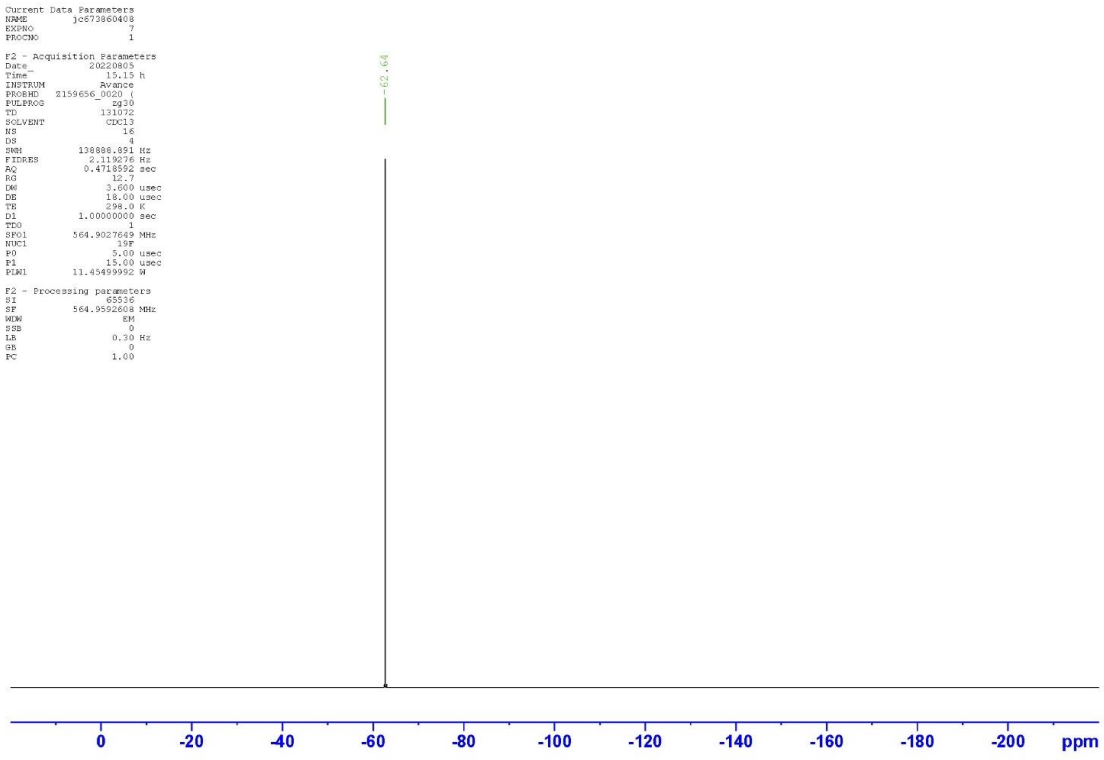
Current Data Parameters
NAME jc673860408
EXPNO 7
PROCNO 1
F2 - Acquisition Parameters
Date_ 20220805
Time_ 15.15 h
INSTRUM Avance
PROBHD 2159656_0020 (
PULPROG zg30
TD 131072
SOLVENT CDCl3
NS 16
DS 4
SWH 138888.891 Hz
FIDRES 2.119276 Hz
AQ 0.4718592 sec
RG 12.7
DW 3.600 usec
DE 18.00 usec
TE 298.0 K
D1 1.00000000 sec
TD0 1
SFO1 564.9027649 MHz
NUC1 19F
P0 5.00 usec
P1 15.00 usec
PLW1 11.45499992 W
F2 - Processing parameters
SI 65536
SF 564.9552608 MHz
WDW EM
SSB 0
LB 0.30 Hz
GB 0
PC 1.00
-62.64
0
-20
-40
-60
-80
-100
-120
-140
-160
-180
-200
ppm

Methyl 3-(2-(5-(3,5-dimethylisoxazol-4-yl)-1-methyl-1*H*-benzo[*d*]imidazol-2-yl)ethyl)benzoate 145

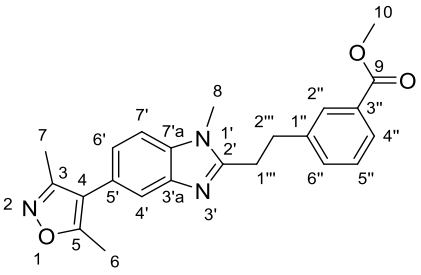

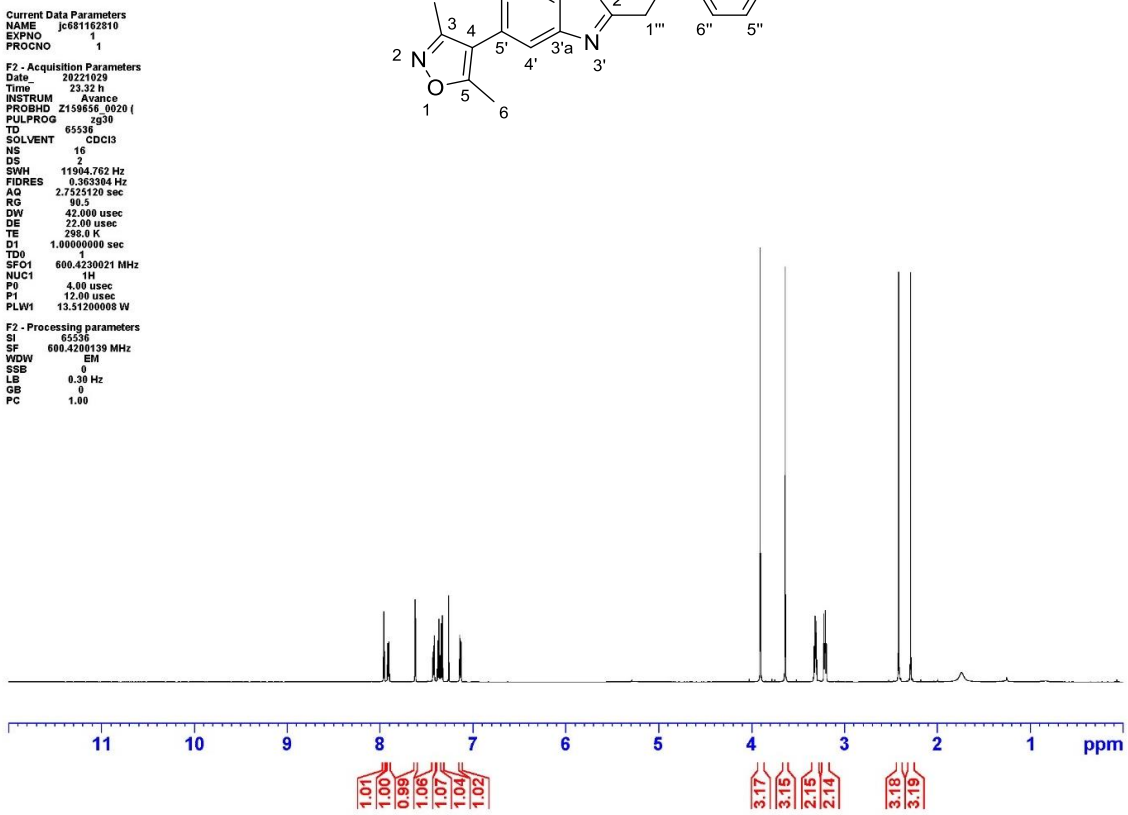

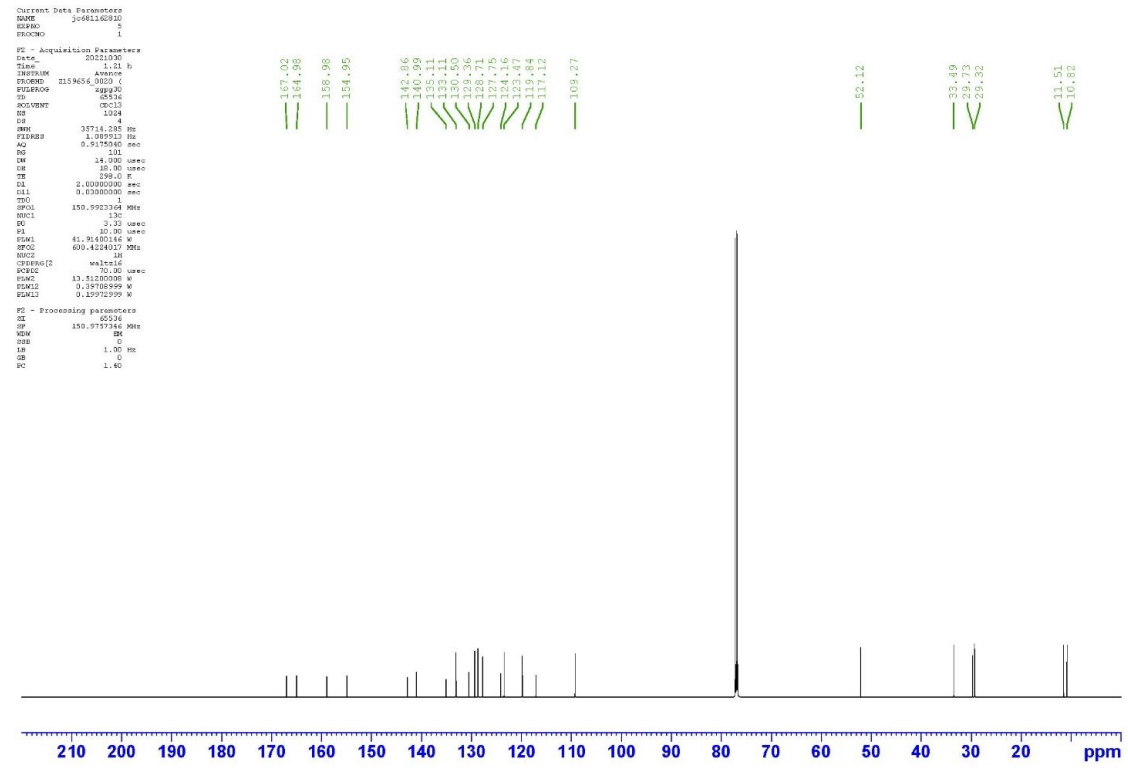

3-(2-(5-(3,5-Dimethylisoxazol-4-yl)-1-methyl-1*H*-benzo[*d*]imidazol-2-yl)ethyl)benzoic acid 147

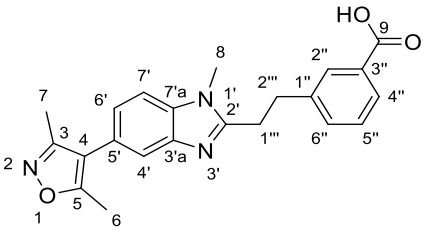

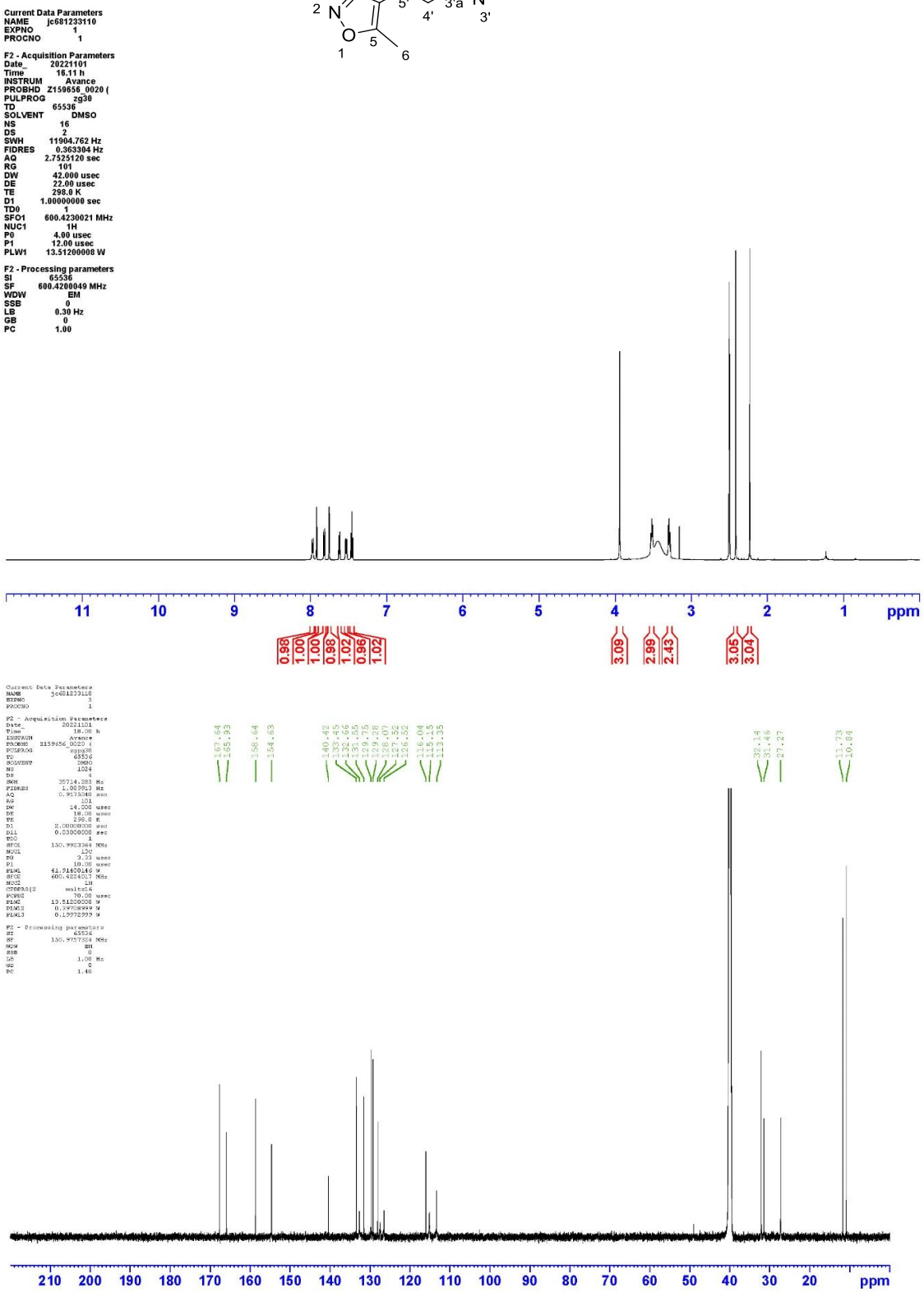

3,5-Dimethyl-4-(1-methyl-2-(4-methylphenethyl)-1*H*-benzo[*d*]imidazol-5-yl)isoxazole 138

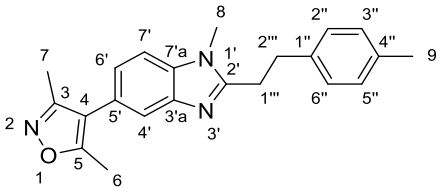

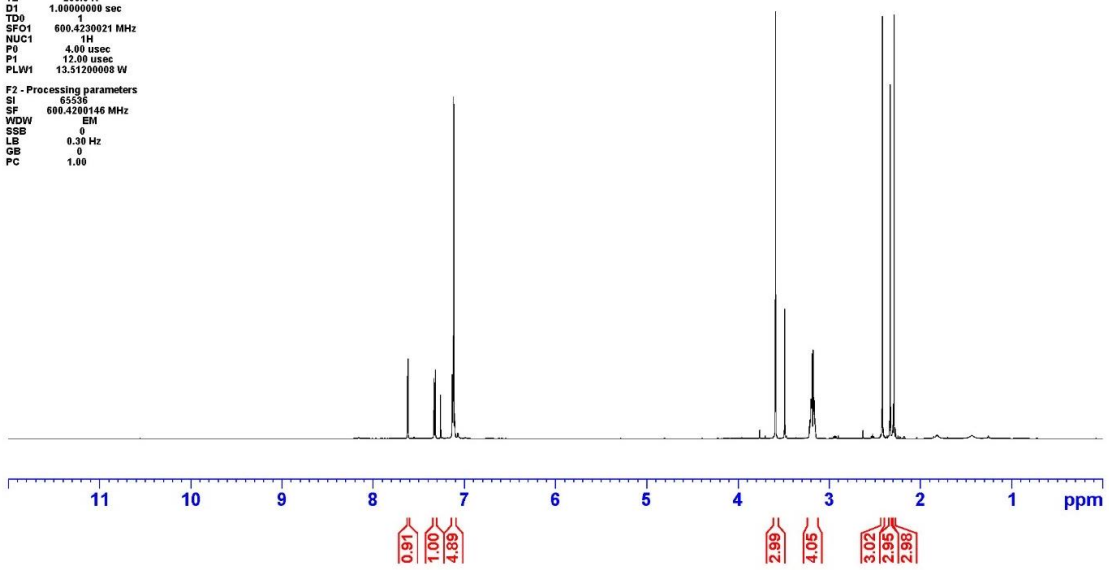

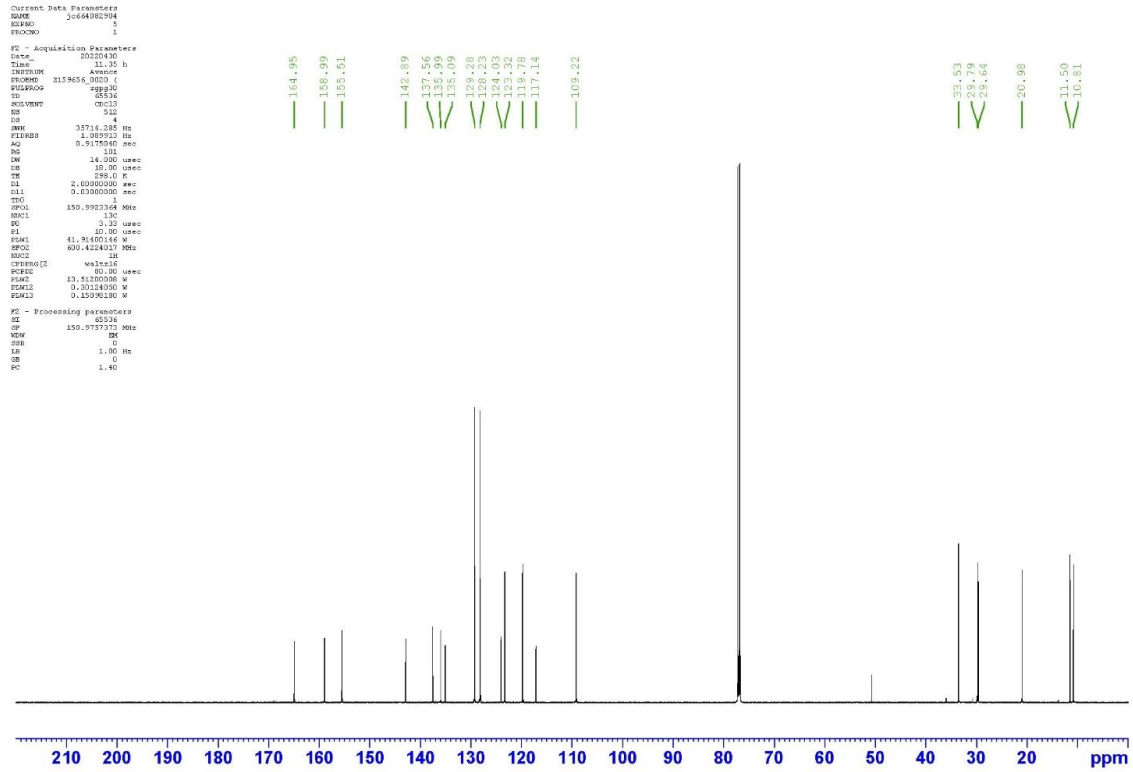

4-(2-(4-Fluorophenethyl)-1-methyl-1*H*-benzo[*d*]imidazol-5-yl)-3,5-dimethylisoxazole 123

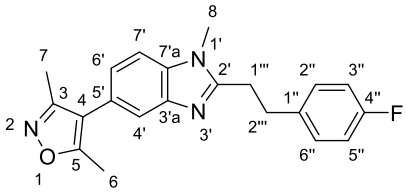

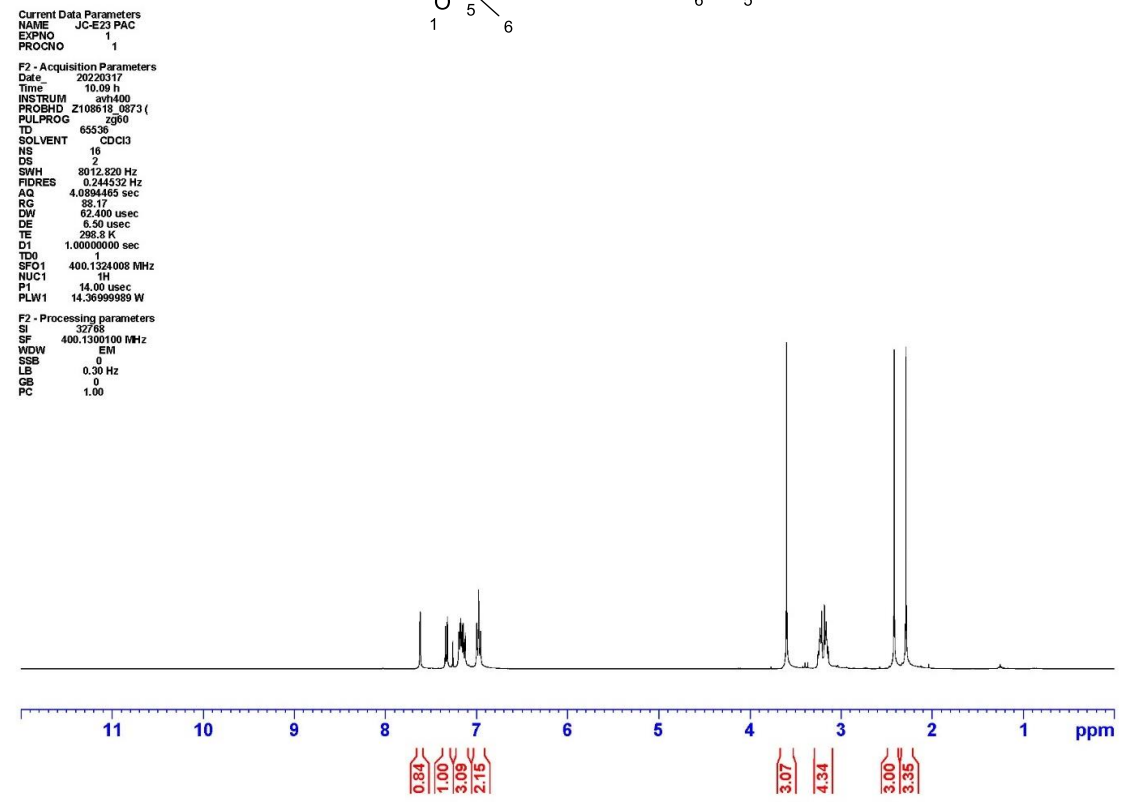

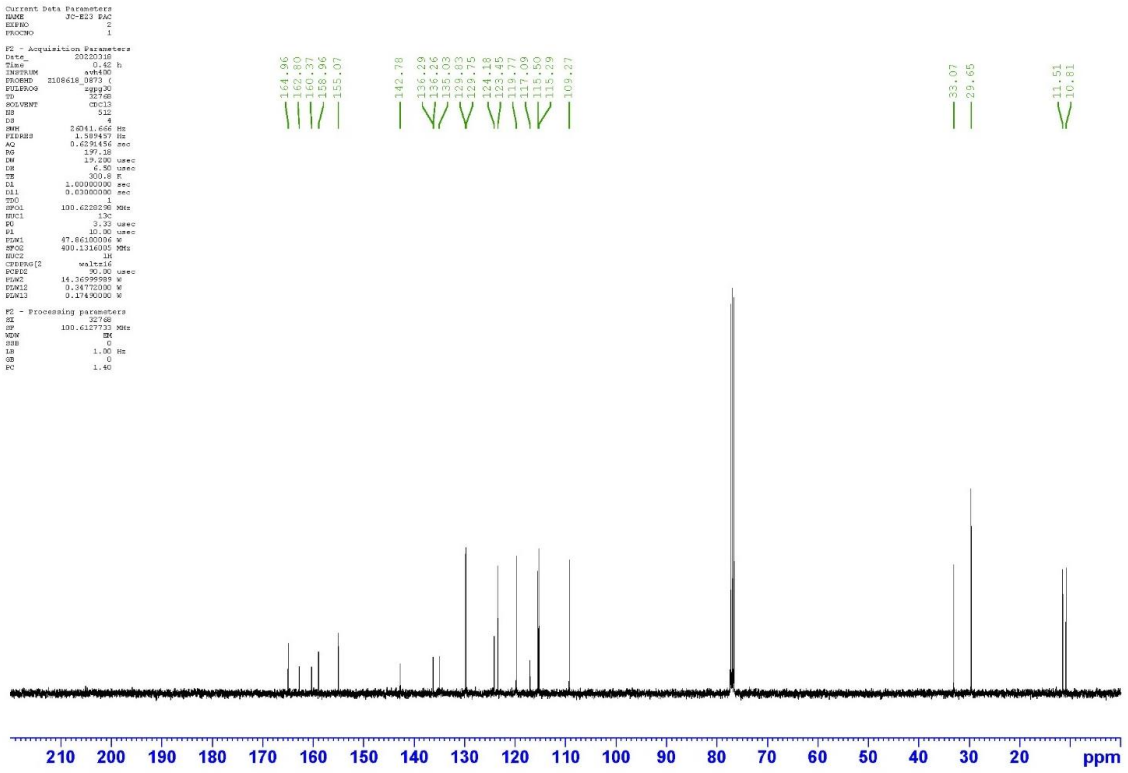

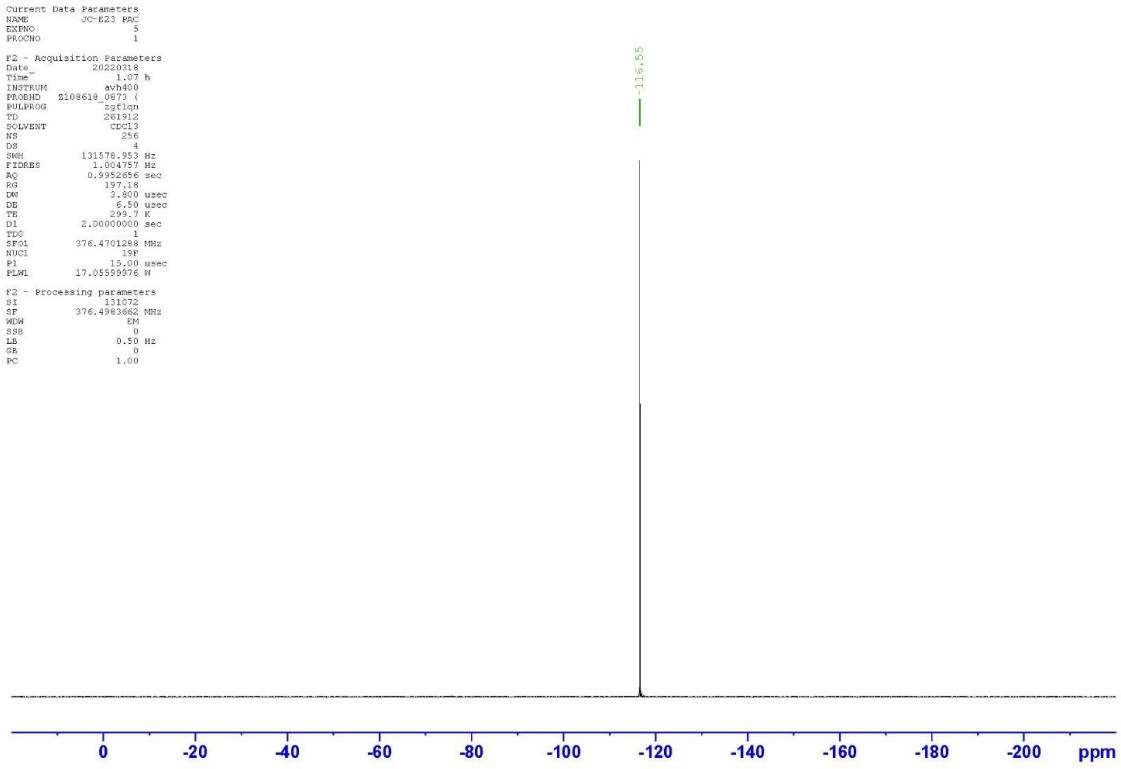
Current Data Parameters
NAME JC-E23 PAC
EXPNO 5
PROCNO 1
F2 - Acquisition Parameters
Date_ 20220318
Time 1.07 h
INSTRUM avh400
PROBHD Z108618_0873 (
PULPROG zgflqn
TD 261912
SOLVENT CDCl3
NS 256
DS 4
SWH 131578.953 Hz
FIDRES 1.004757 Hz
AQ 0.9952656 sec
RG 197.18
DW 3.800 usec
DE 6.50 usec
TE 299.7 K
D1 2.00000000 sec
TD0 1
SFO1 376.4701288 MHz
NUC1 19F
P1 15.00 usec
PLW1 17.05599976 W
F2 - Processing parameters
SI 131072
SF 376.4983662 MHz
WDW EM
SSB 0
LB 0.50 Hz
GB 0
PC 1.00
116.55
0
-20
-40
-60
-80
-100
-120
-140
-160
-180
-200
ppm

4-(2-(4-Chlorophenethyl)-1-methyl-1*H*-benzo[*d*]imidazol-5-yl)-3,5-dimethylisoxazole 176

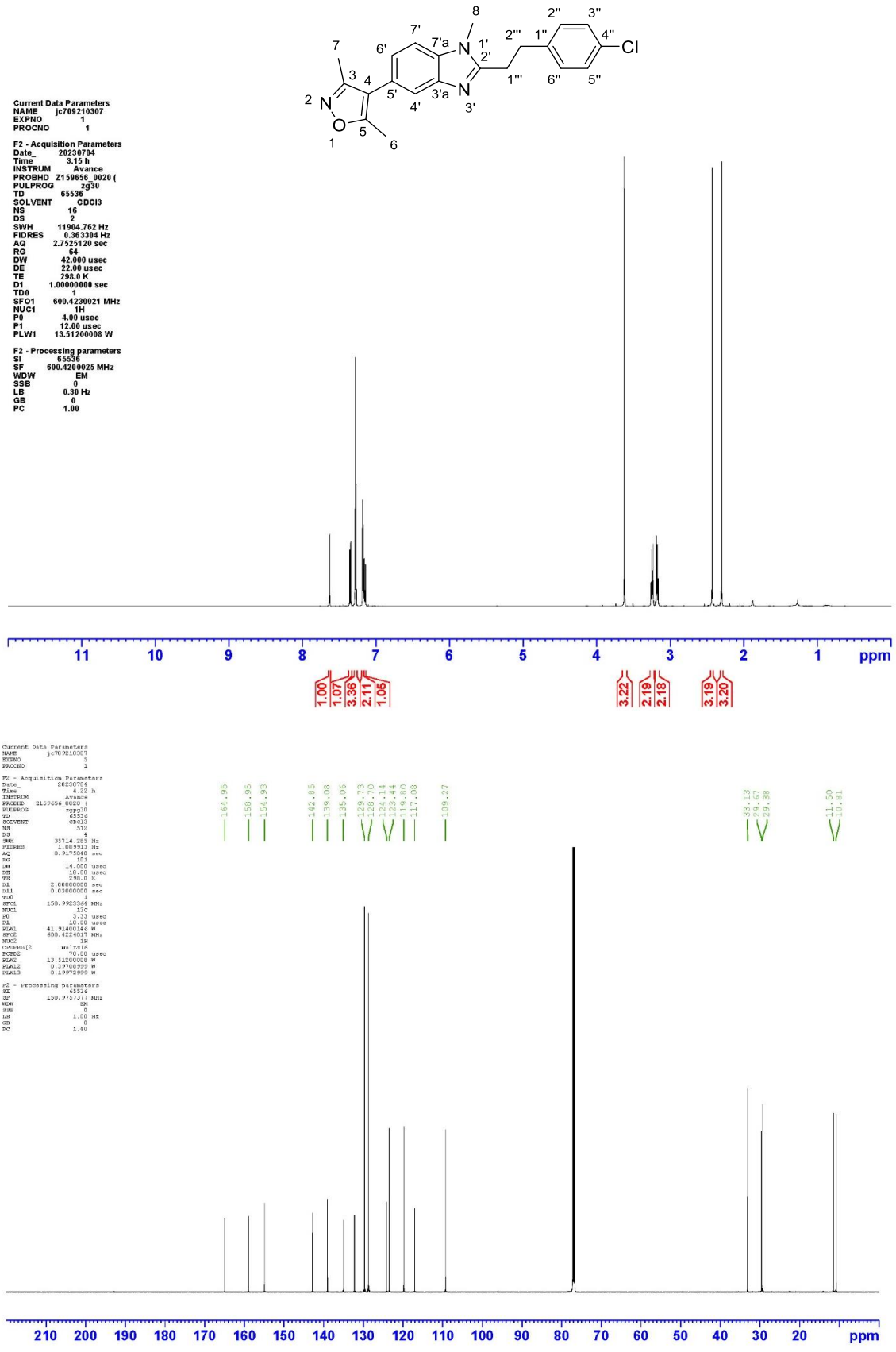

4-(2-(4-Bromophenethyl)-1-methyl-1*H*-benzo[*d*]imidazol-5-yl)-3,5-dimethylisoxazole 125

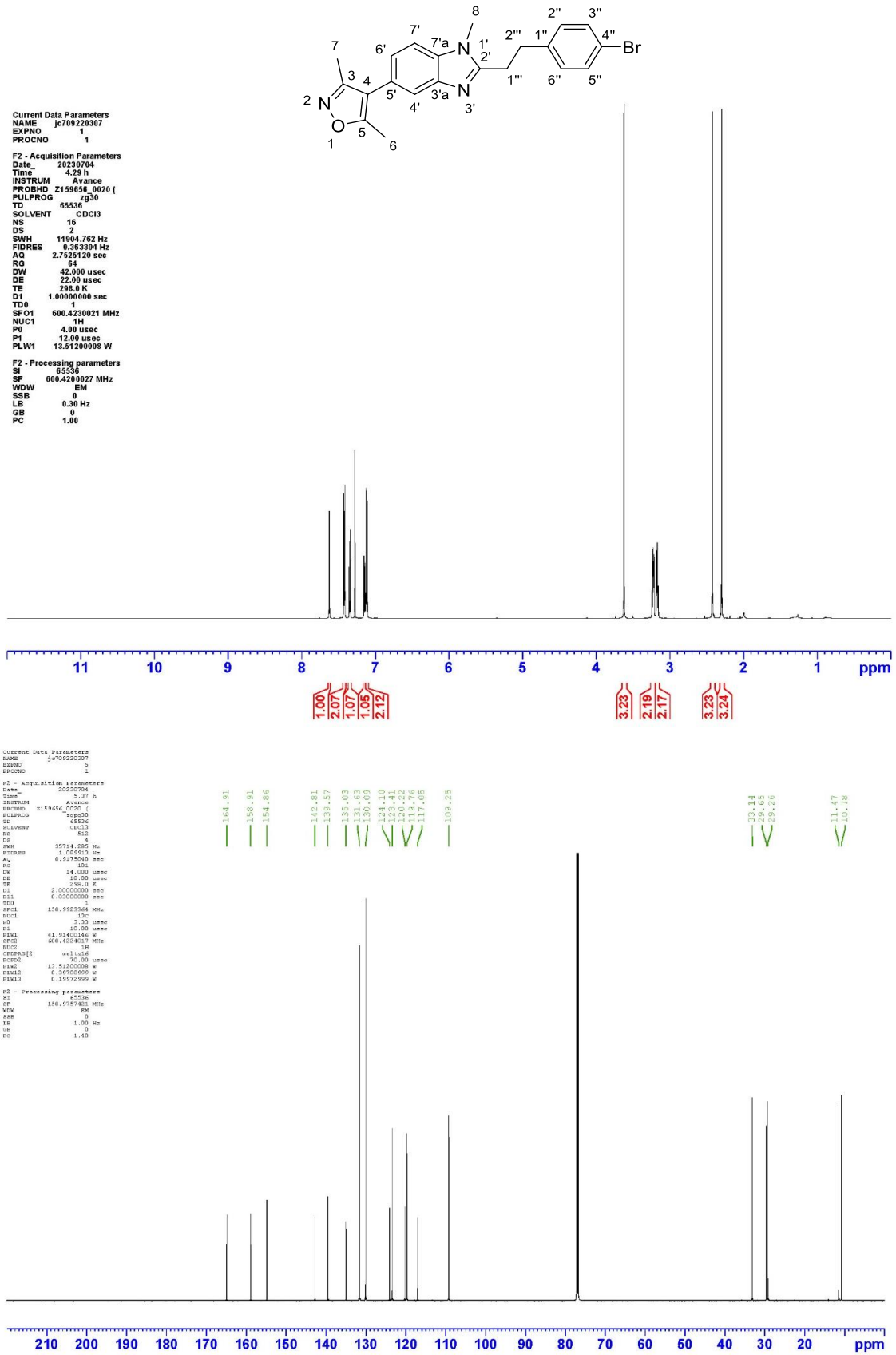

3,5-Dimethyl-4-(1-methyl-2-(4-(trifluoromethoxy)phenethyl)-1*H*-benzo[*d*]imidazol-5-yl)isoxazole 144

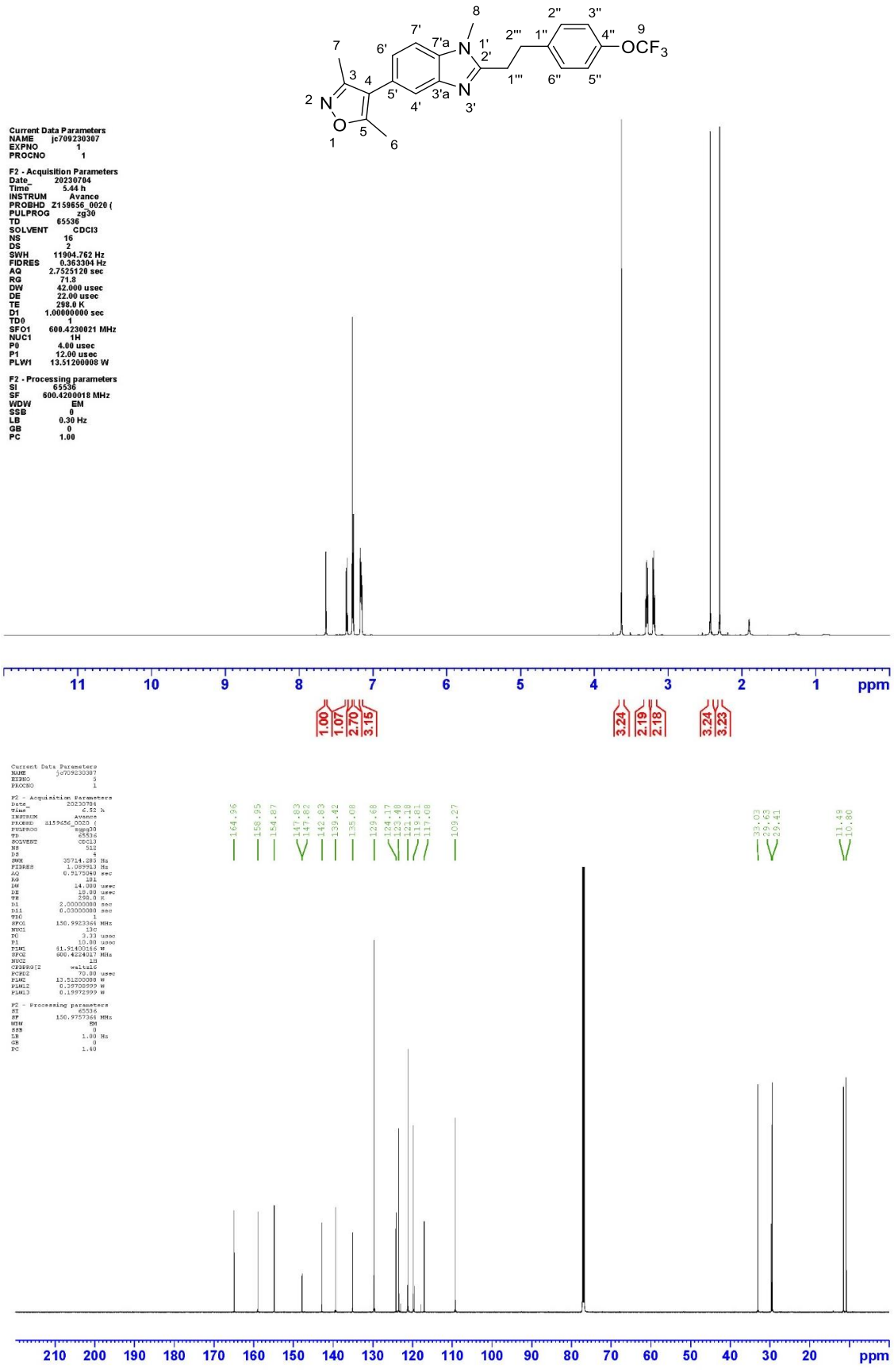

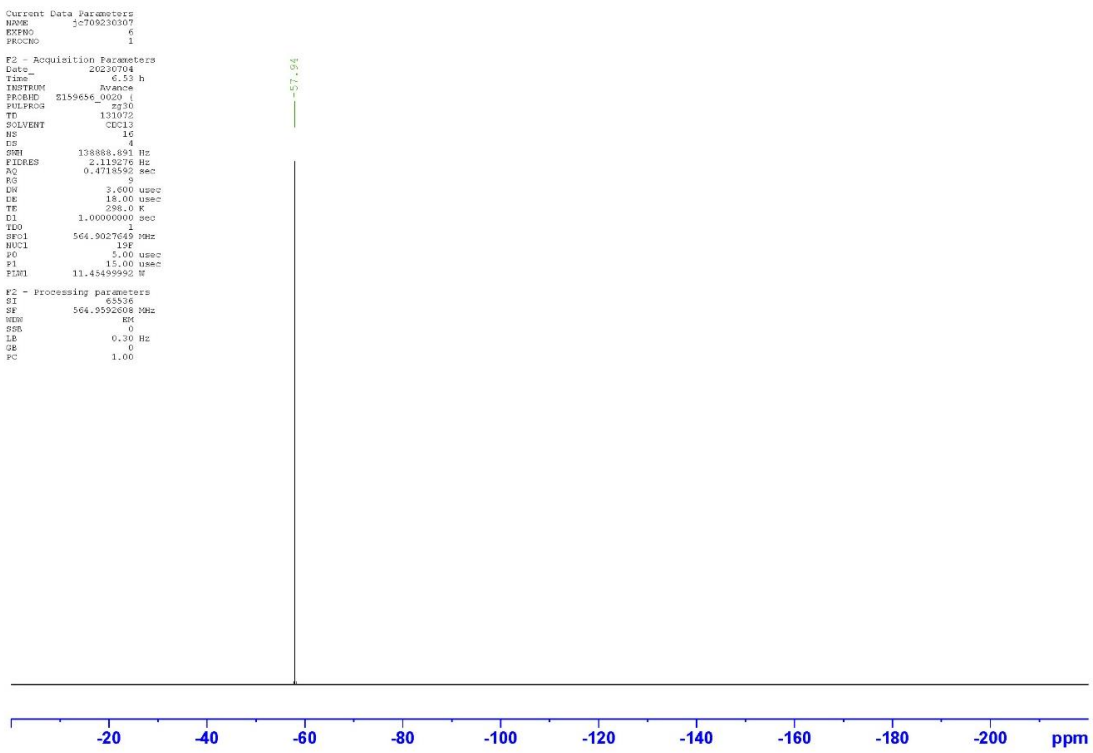
Current Data Parameters
NAME 2c709230307
EXPNO 6
PROCNO 1
F2 - Acquisition Parameters
Date_ 20230704
Time 6.53 h
INSTRUM Avance
PROBHD B159656_0020 (
PULPROG zg30
TD 131072
SOLVENT CDCl3
NS 16
DS 4
SWH 138888.891 Hz
FIDRES 2.119276 Hz
AQ 0.4718592 sec
RG 9
DW 3.600 usec
DE 18.00 usec
TE 298.0 K
D1 1.00000000 sec
TD0 1
SFO1 564.9027649 MHz
NUC1 19F
P0 5.00 usec
P1 15.00 usec
PLW1 11.45499992 W
F2 - Processing parameters
SI 65536
SF 564.9592608 MHz
WDW EM
SSB 0
LB 0.30 Hz
GB 0
PC 1.00
-57.94
-20
-40
-60
-80
-100
-120
-140
-160
-180
-200
ppm

4-(2-(4-Methoxyphenethyl)-1-methyl-1*H*-benzo[*d*]imidazol-5-yl)-3,5-dimethylisoxazole 142

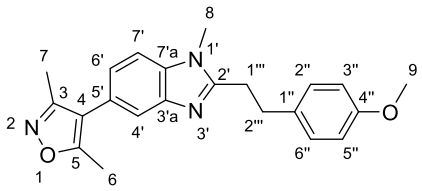

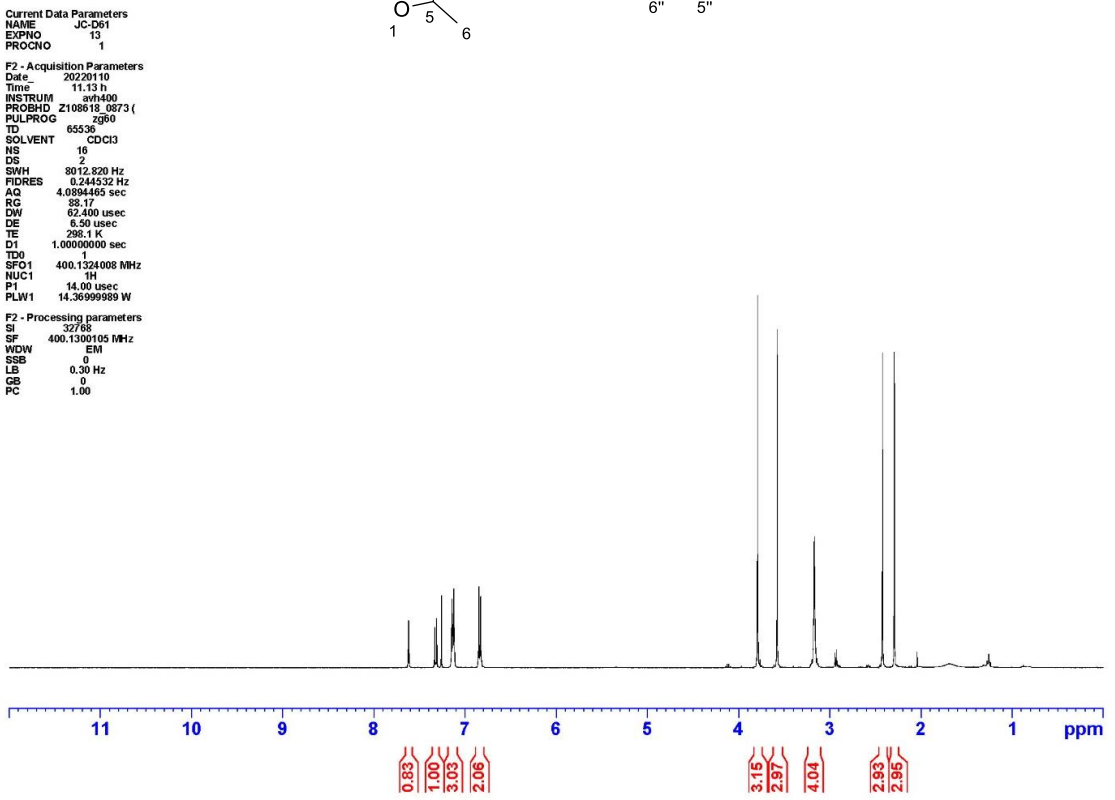

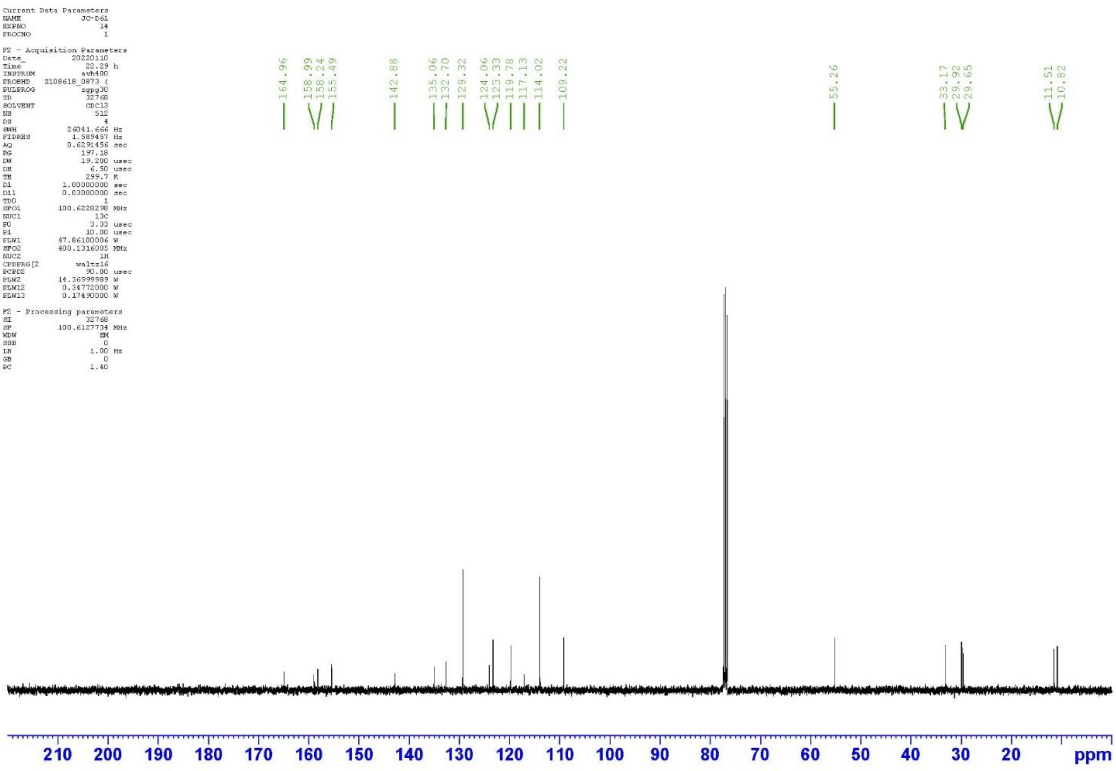

3,5-Dimethyl-4-(1-methyl-2-(4-nitrophenethyl)-1*H*-benzo[*d*]imidazol-5-yl)isoxazole

152

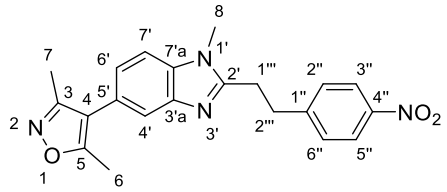

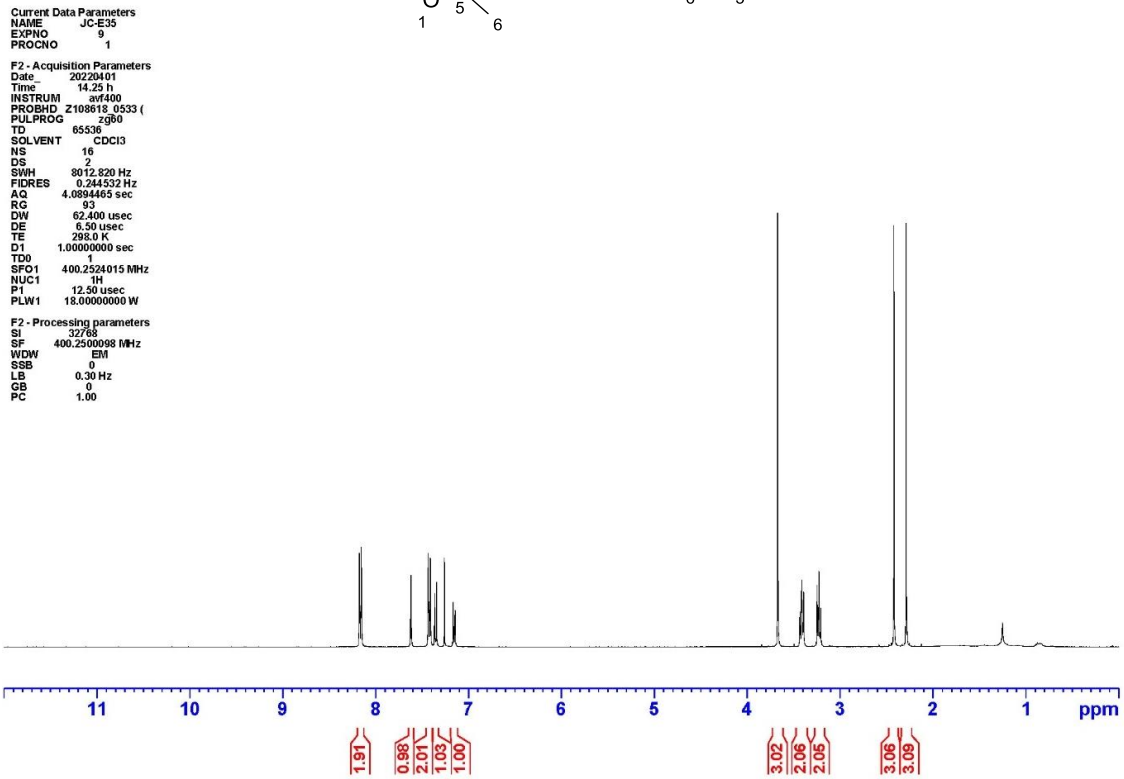

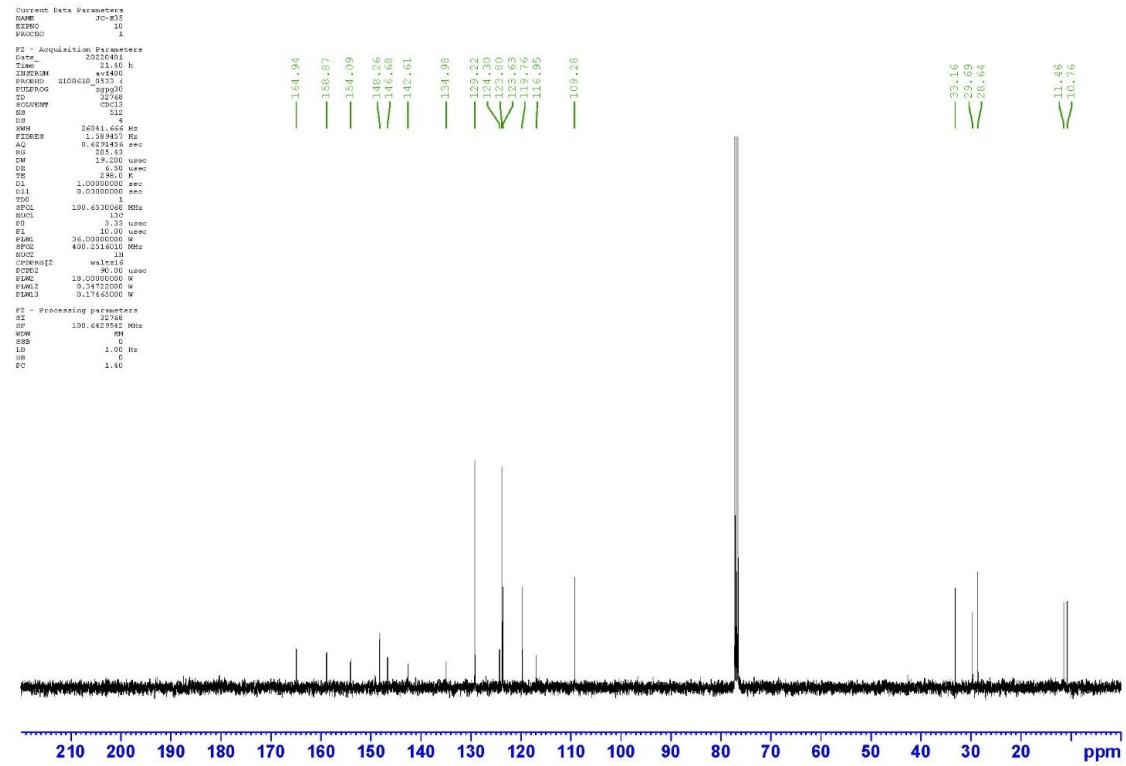

4-(2-(5-(3,5-Dimethylisoxazol-4-yl)-1-methyl-1*H*-benzo[*d*]imidazol-2-yl)ethyl)benzonitrile 155

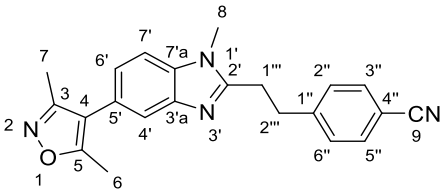

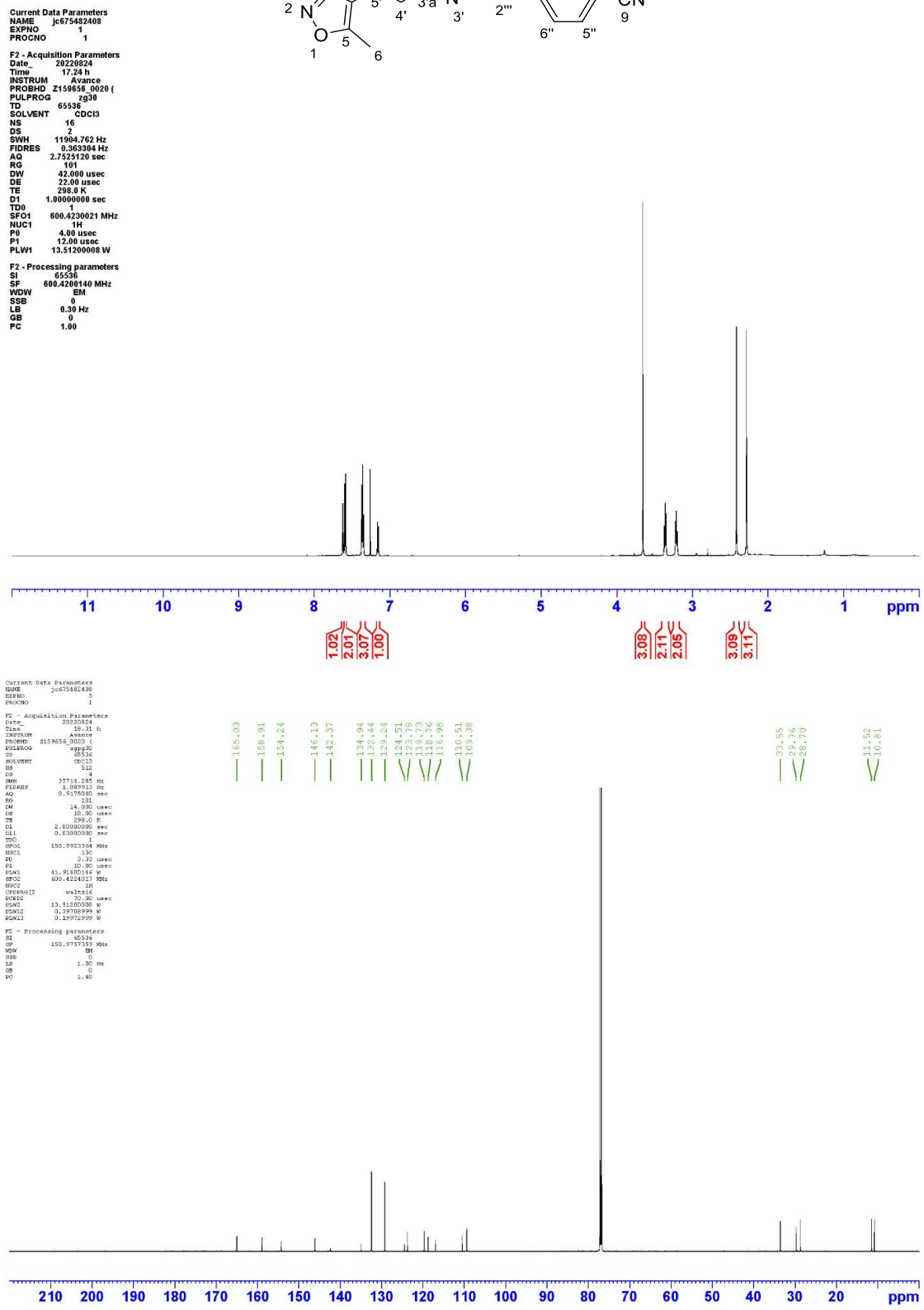

3,5-Dimethyl-4-(1-methyl-2-(4-(trifluoromethyl)phenethyl)-1*H*-benzo[*d*]imidazol-5-yl)isoxazole 177

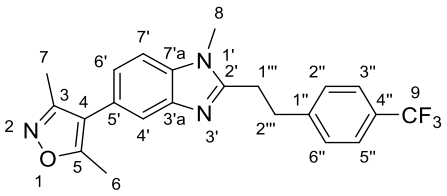

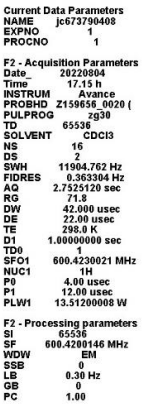

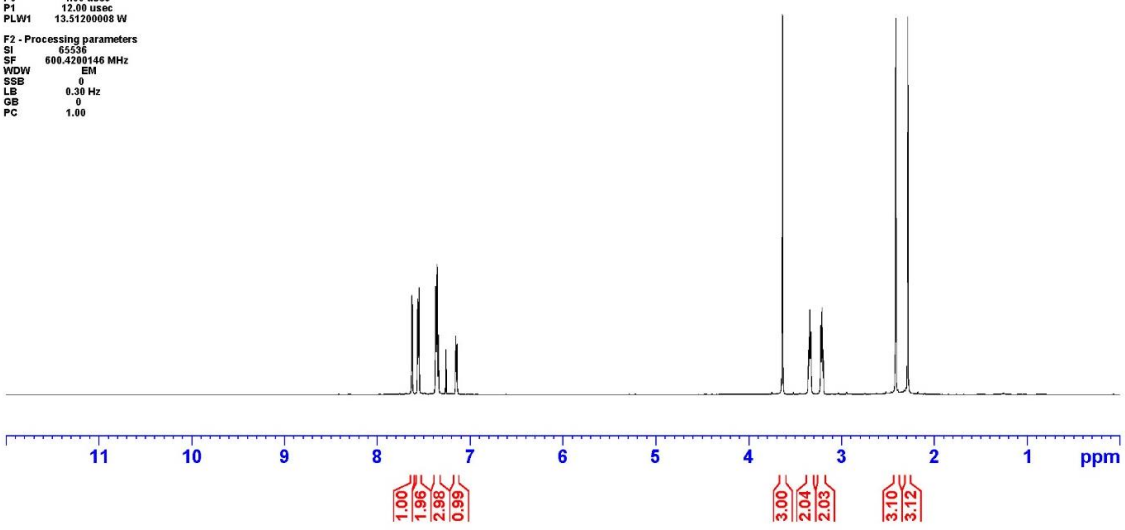

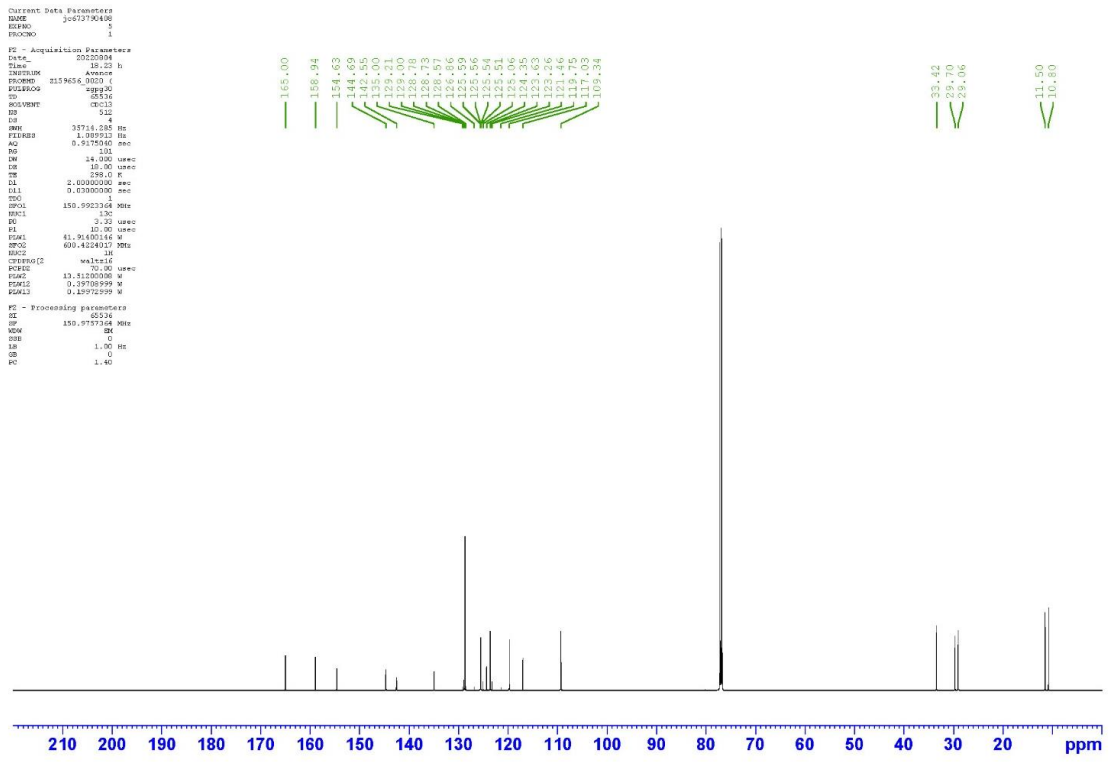

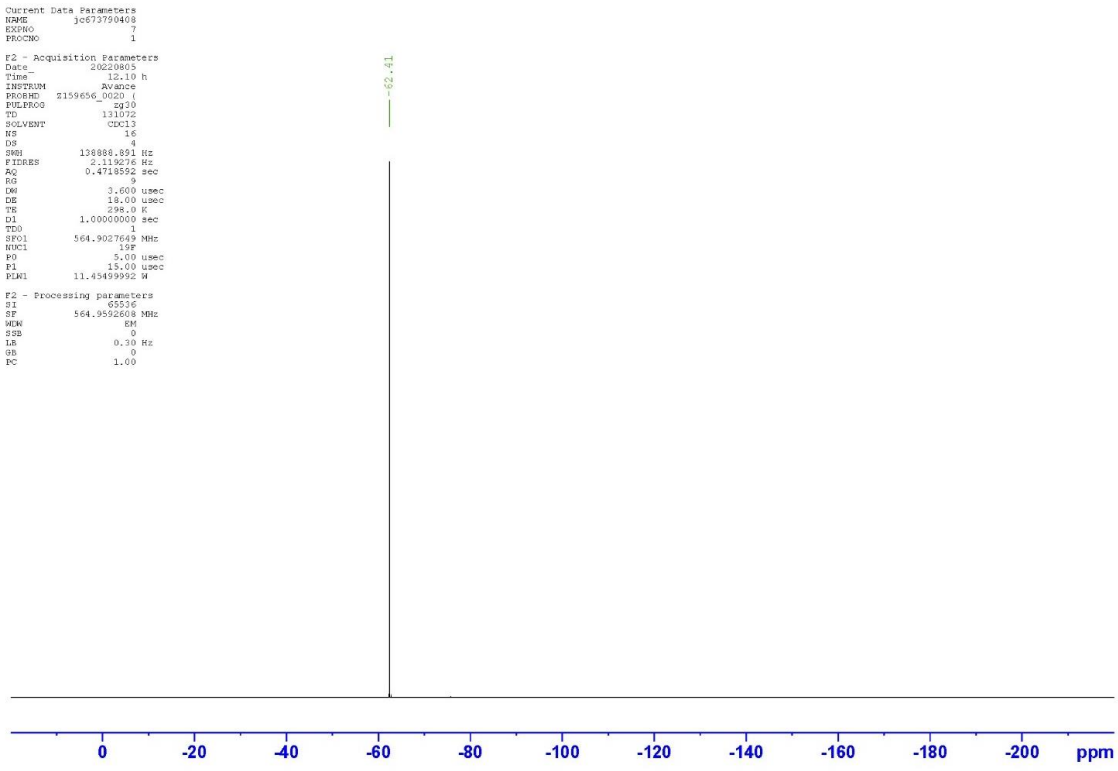
Current Data Parameters
NAME jc673790408
EXPNO 7
PROCNO 1
F2 - Acquisition Parameters
Date_ 20220805
Time 12.10 h
INSTRUM Avance
PROBHD Z159656_0020 (
PULPROG zg30
TD 131072
SOLVENT CDCl3
NS 16
DS 4
SWH 138888.891 Hz
FIDRES 2.119276 Hz
AQ 0.4718592 sec
RG 9
DW 3.600 usec
DE 18.00 usec
TE 298.0 K
D1 1.00000000 sec
TD0 1
SFO1 564.9027649 MHz
NUC1 19F
P0 5.00 usec
P1 15.00 usec
PLW1 11.45499992 W
F2 - Processing parameters
SI 65536
SF 564.9592608 MHz
WDW EM
SSB 0
LB 0.30 Hz
GB 0
PC 1.00
-62.41
0
-20
-40
-60
-80
-100
-120
-140
-160
-180
-200
ppm

Methyl 4-(2-(5-(3,5-dimethylisoxazol-4-yl)-1-methyl-1*H*-benzo[*d*]imidazol-2-yl)ethyl)benzoate 146

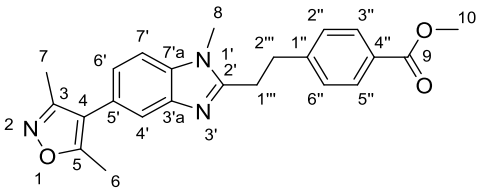

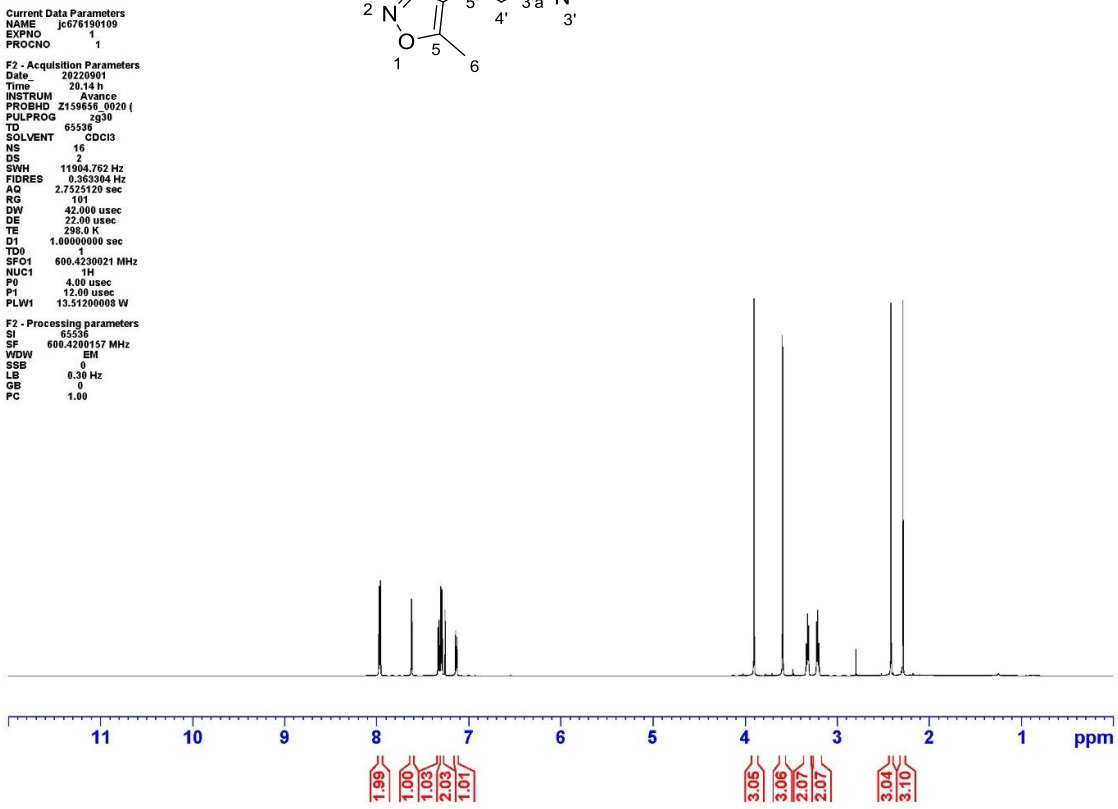

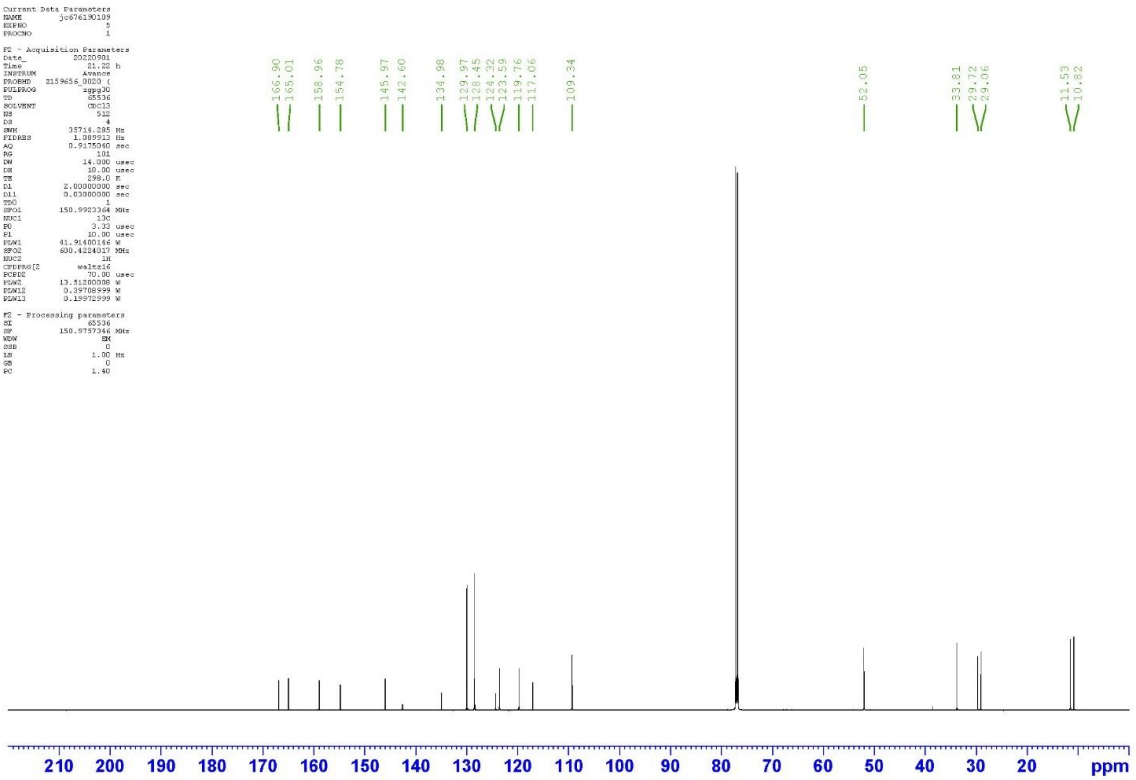

4-(2-(5-(3,5-Dimethylisoxazol-4-yl)-1-methyl-1*H*-benzo[*d*]imidazol-2-yl)ethyl)benzoic acid 148

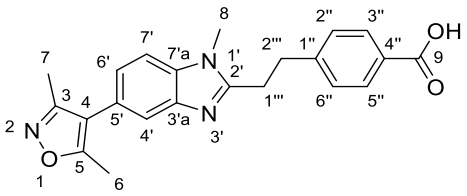

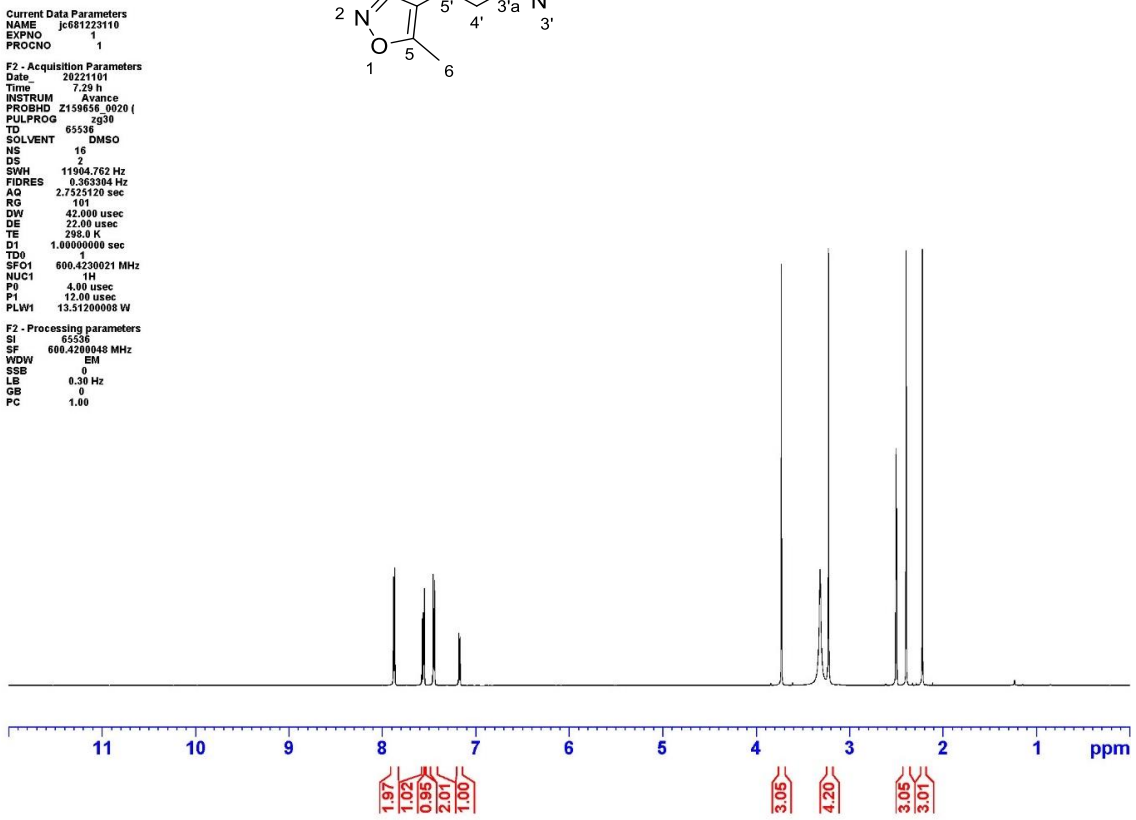

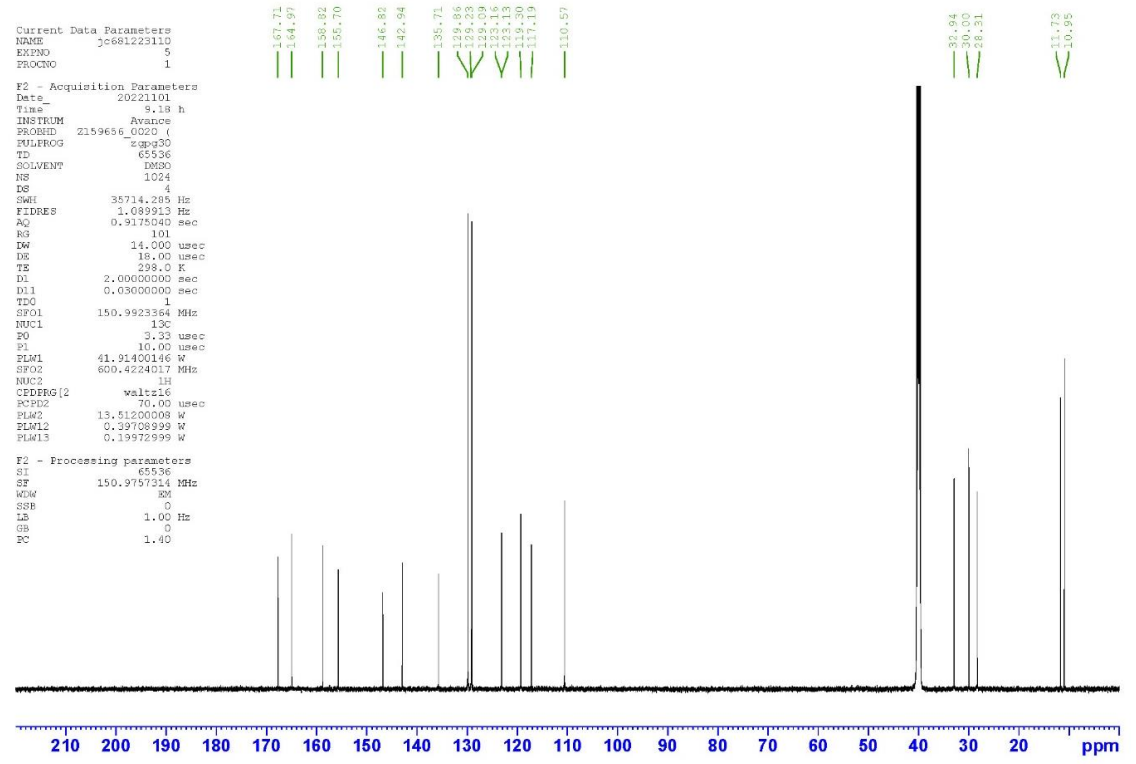

3,5-Dimethyl-4-(1-methyl-2-(3-methylbenzyl)-1*H*-benzo[*d*]imidazol-5-yl)isoxazole

112

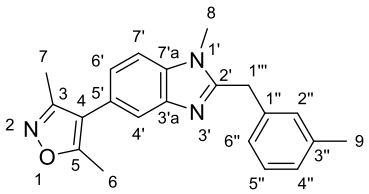

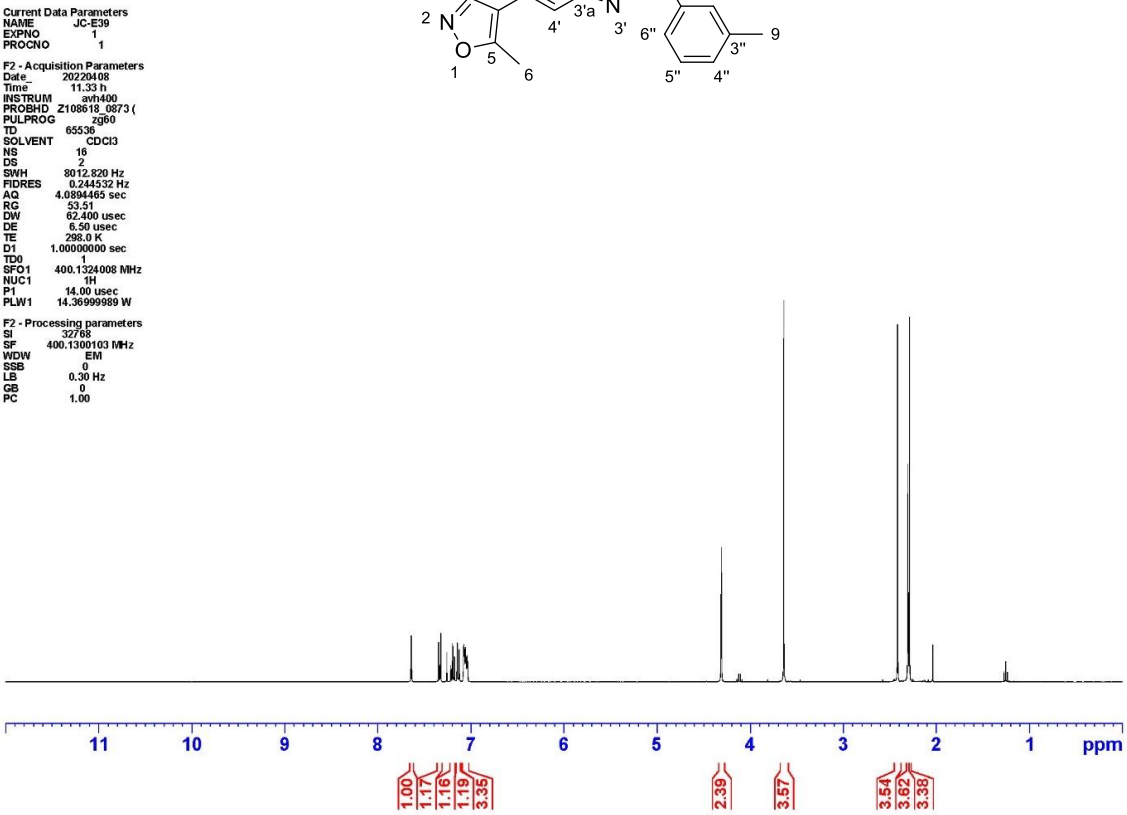

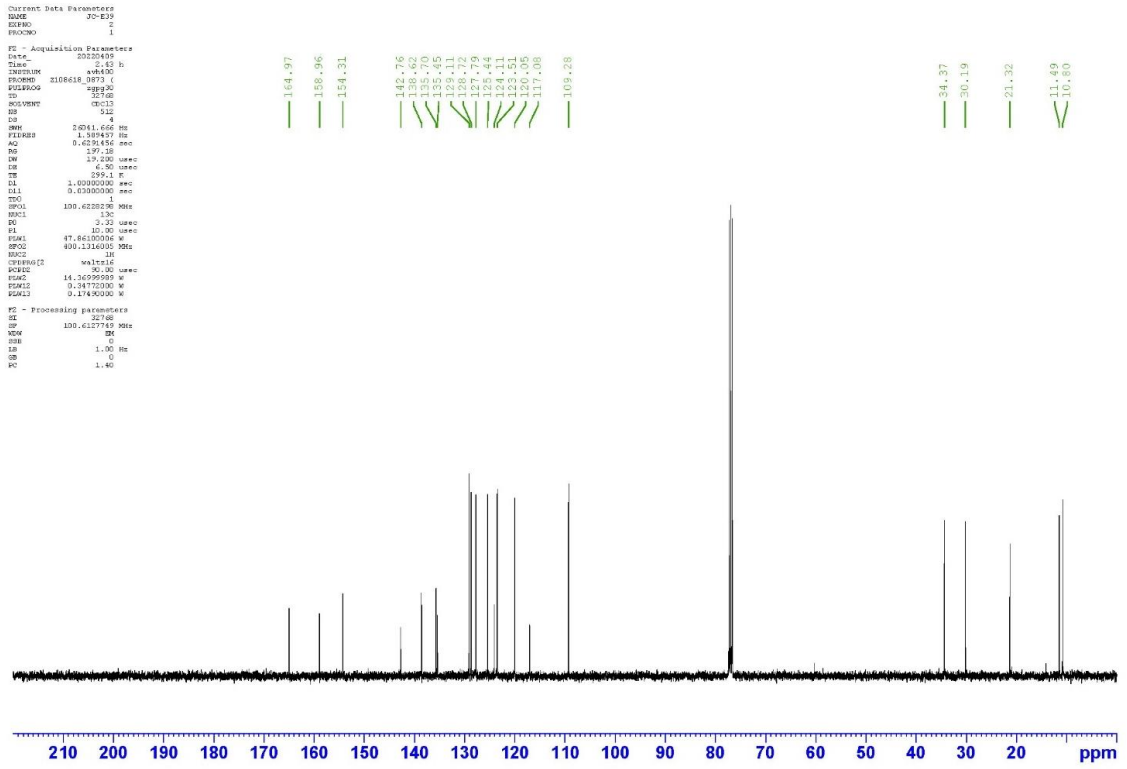

3,5-Dimethyl-4-(1-methyl-2-(4-methylbenzyl)-1*H*-benzo[*d*]imidazol-5-yl)isoxazole

111

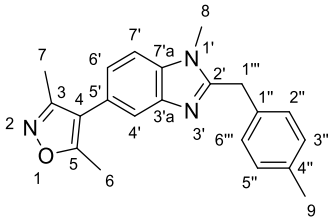

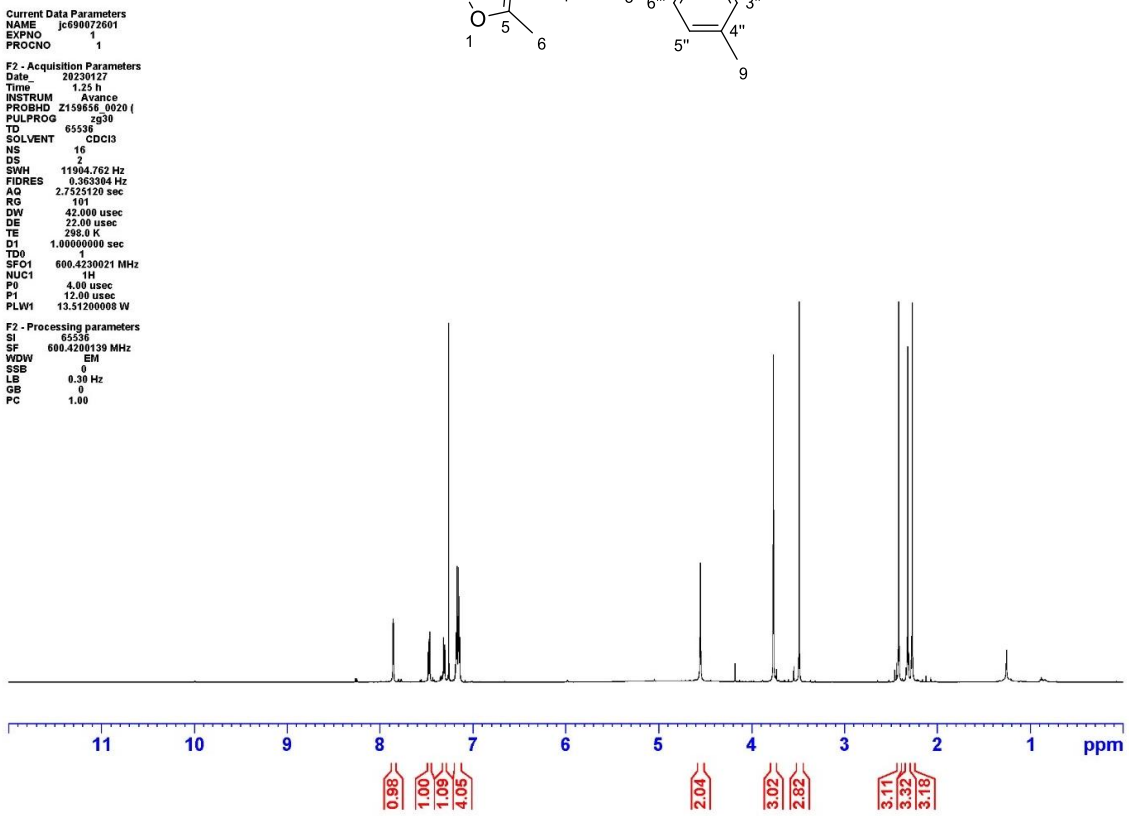

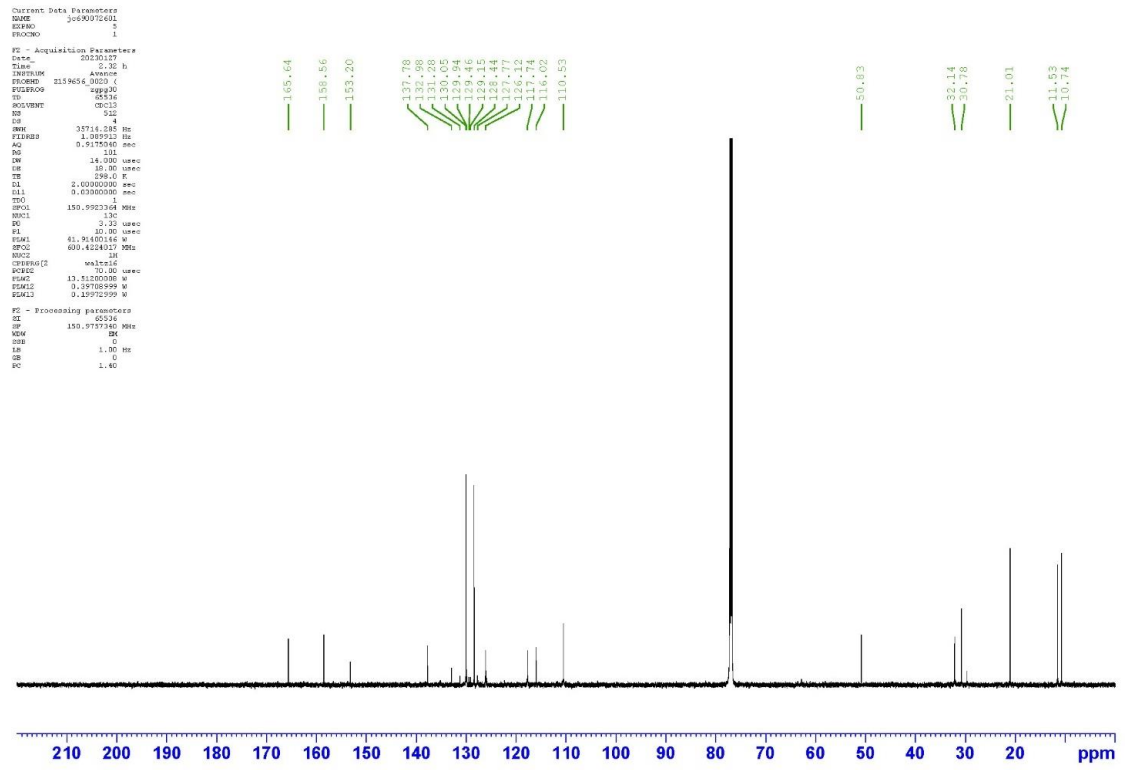

4-(2-Ethyl-3-methyl-3*H*-imidazo[4,5-*b*]pyridin-6-yl)-3,5-dimethylisoxazole 221

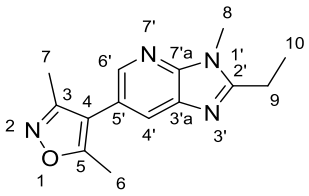

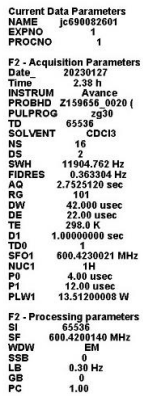

```
Current Data Parameters
NAME      jc690082601
EXPNO             1
PROCNO            1

F2 - Acquisition Parameters
Date_      20230127
Time          2.38 h
INSTRUM       Avance
PROBHD  Z159656_0020 (
PULPROG        zg30
TD            65536
SOLVENT       CDCl3
NS               16
DS                2
SWH       11904.762 Hz
FIDRES        0.363304 Hz
AQ         2.7525120 sec
RG              101
DW           42.000 usec
DE           22.00 usec
TE           298.0 K
D1         1.00000000 sec
TD0               1
SFO1      600.4230021 MHz
NUC1             1H
P0            4.00 usec
P1           12.00 usec
PLW1      13.51200008 W

F2 - Processing parameters
SI            65536
SF       600.4200140 MHz
WDW              EM
SSB               0
LB             0.30 Hz
GB                0
PC             1.00
```

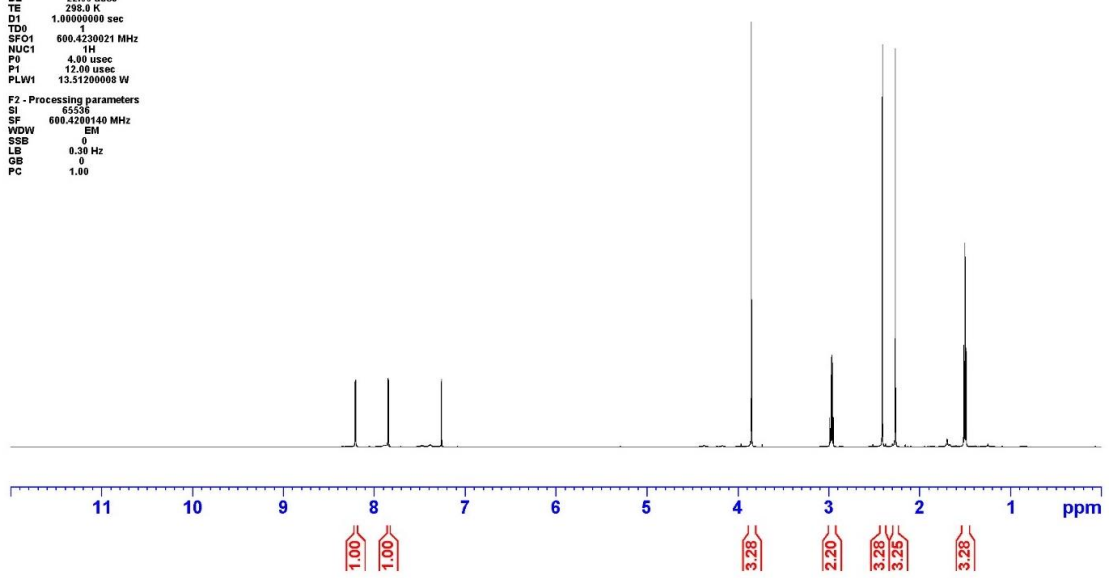

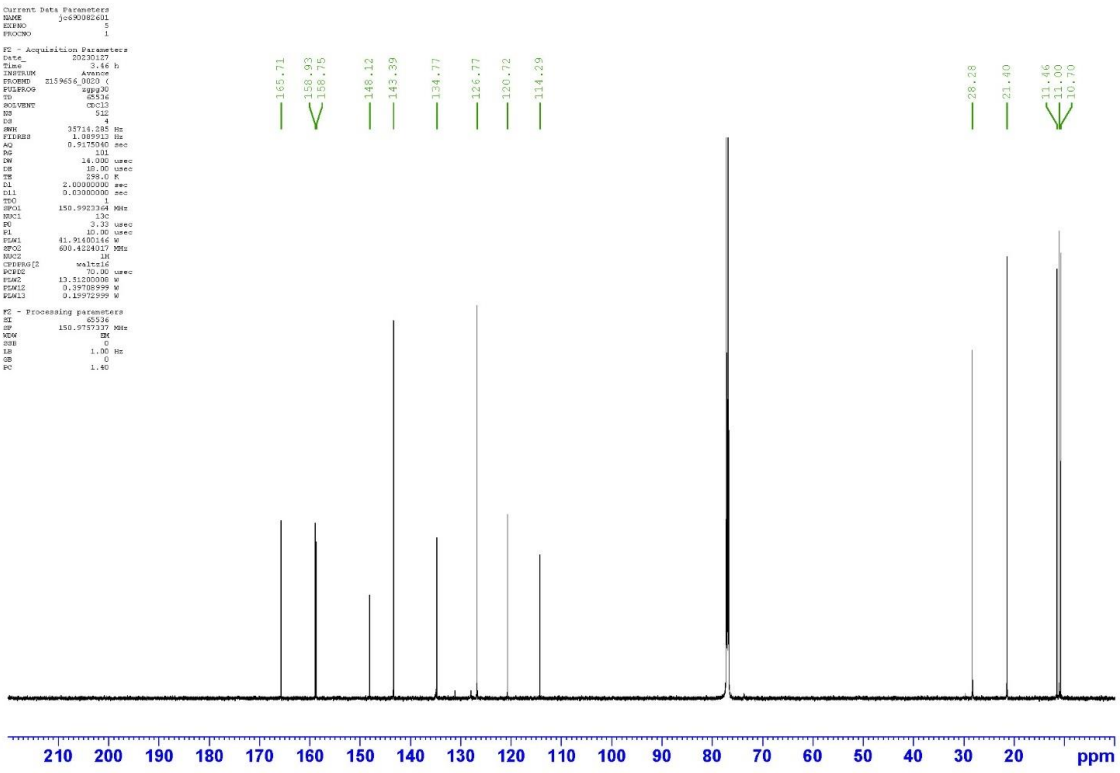

4-(2-(4-Methoxy-3-methylphenethyl)-1-methyl-1*H*-benzo[*d*]imidazol-5-yl)-3,5-dimethylisoxazole 141

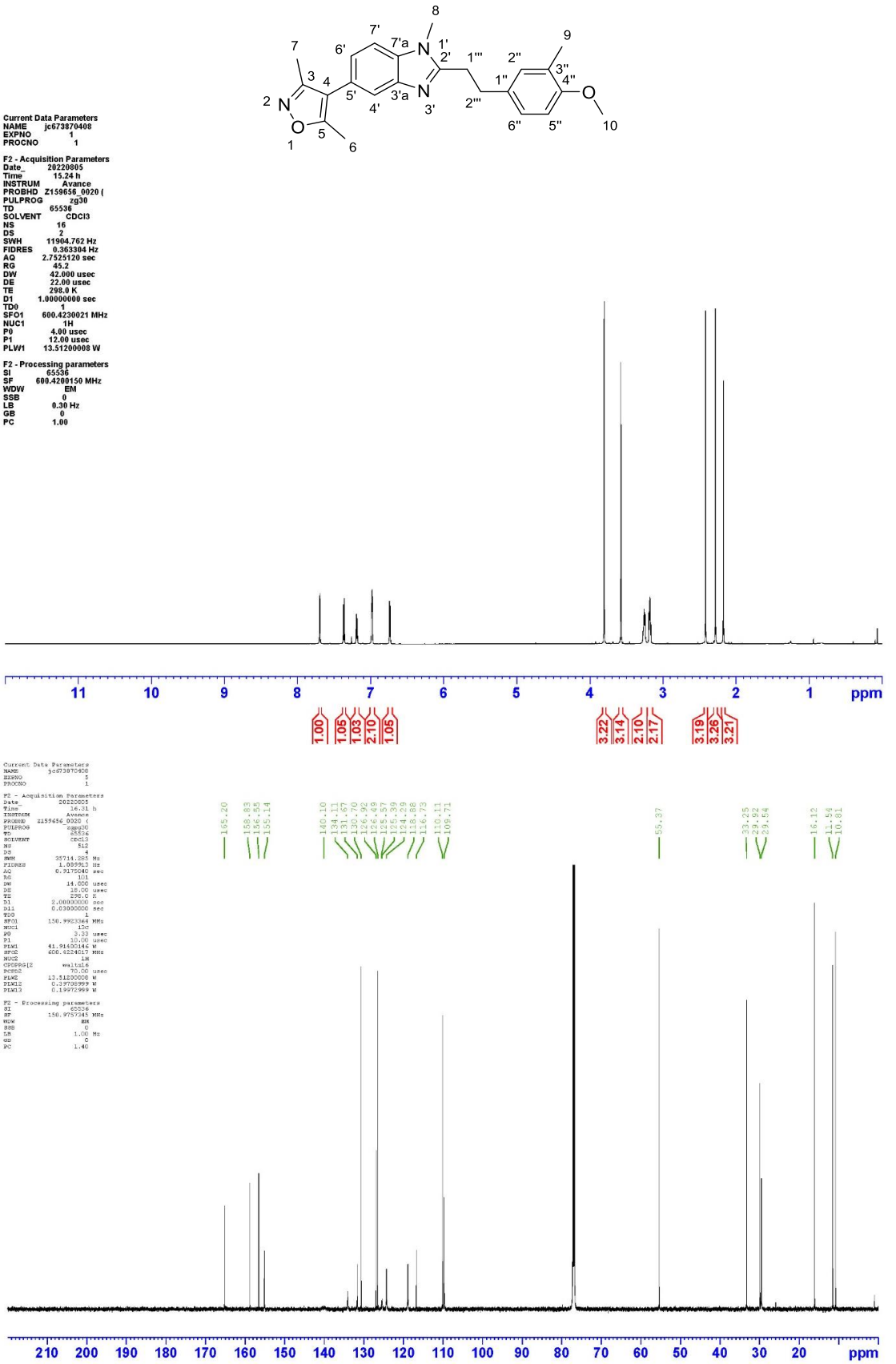

4-(2-(3-Chloro-4-methoxyphenethyl)-1-methyl-1*H*-benzo[*d*]imidazol-5-yl)-3,5-dimethylisoxazole 143

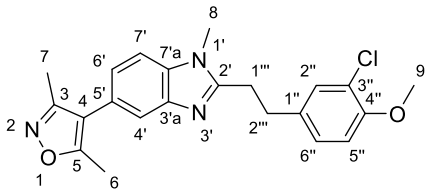

Current Data Parameters
NAME jc668092605
EXPNO 1
PROCNO 1

F2 - Acquisition Parameters
Date_ 20220526
Time 17.43 h
INSTRUM av700
PROBHD Z44908_0059 (C
PULPROG zg60
TD 65536
SOLVENT CDCl3
NS 16
DS 2
SWH 11160.714 Hz
FIDRES 0.340598 Hz
AQ 2.9360127 sec
RG 6.35
DW 44.800 usec
DE 10.00 usec
TE 298.0 K
D1 1.00000000 sec
TD0 1
SFO1 699.8534993 MHz
NUC1 1H
P1 10.65 usec
PLW1 5.01189995 W

F2 - Processing parameters
SI 65536
SF 699.8500179 MHz
WDW EM
SSB 0
LB 0.30 Hz
GB 0
PC 1.00

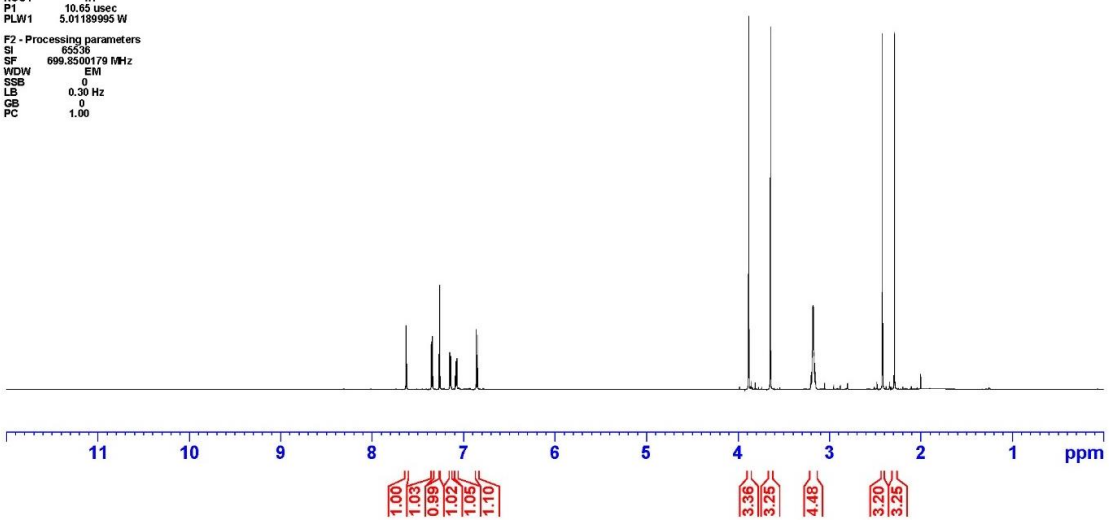

Current Data Parameters
NAME jc668092605
EXPNO 2
PROCNO 1

F2 - Acquisition Parameters
Date_ 20220526
Time 18.32 h
INSTRUM av700
PROBHD Z44908_0059 (C
PULPROG zgpg30
TD 65536
SOLVENT CDCl3
NS 1024
DS 4
SWH 41666.668 Hz
FIDRES 1.271566 Hz
AQ 0.7864320 sec
RG 1030
DW 12.000 usec
DE 10.00 usec
TE 298.0 K
D1 2.00000000 sec
D11 0.03000000 sec
TD0 1
SFO1 175.9950202 MHz
NUC1 13C
P0 5.00 usec
P1 15.00 usec
PLW1 86.00000000 W
SFO2 699.8527994 MHz
NUC2 1H
CPDPRG[2 waltz16
PCPD2 65.00 usec
PLW2 5.01189995 W
PLW12 0.13462000 W
PLW13 0.06776800 W

F2 - Processing parameters
SI 65536
SF 175.9774287 MHz
WDW EM
SSB 0
LB 1.00 Hz
GB 0
PC 1.40

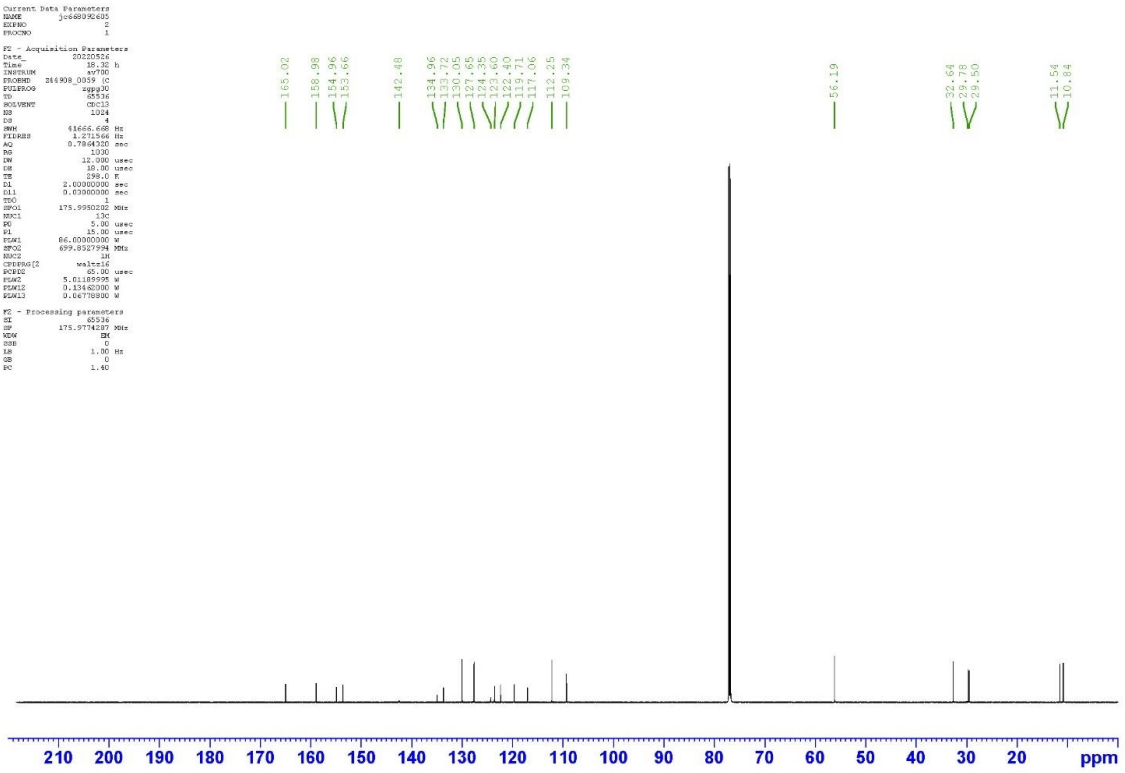

3,5-Dimethyl-4-(1-(2-(4-methylpiperazin-1-yl)ethyl)-2-(3-nitrophenethyl)-1*H*-benzo[*d*]imidazol-5-yl)isoxazole 224

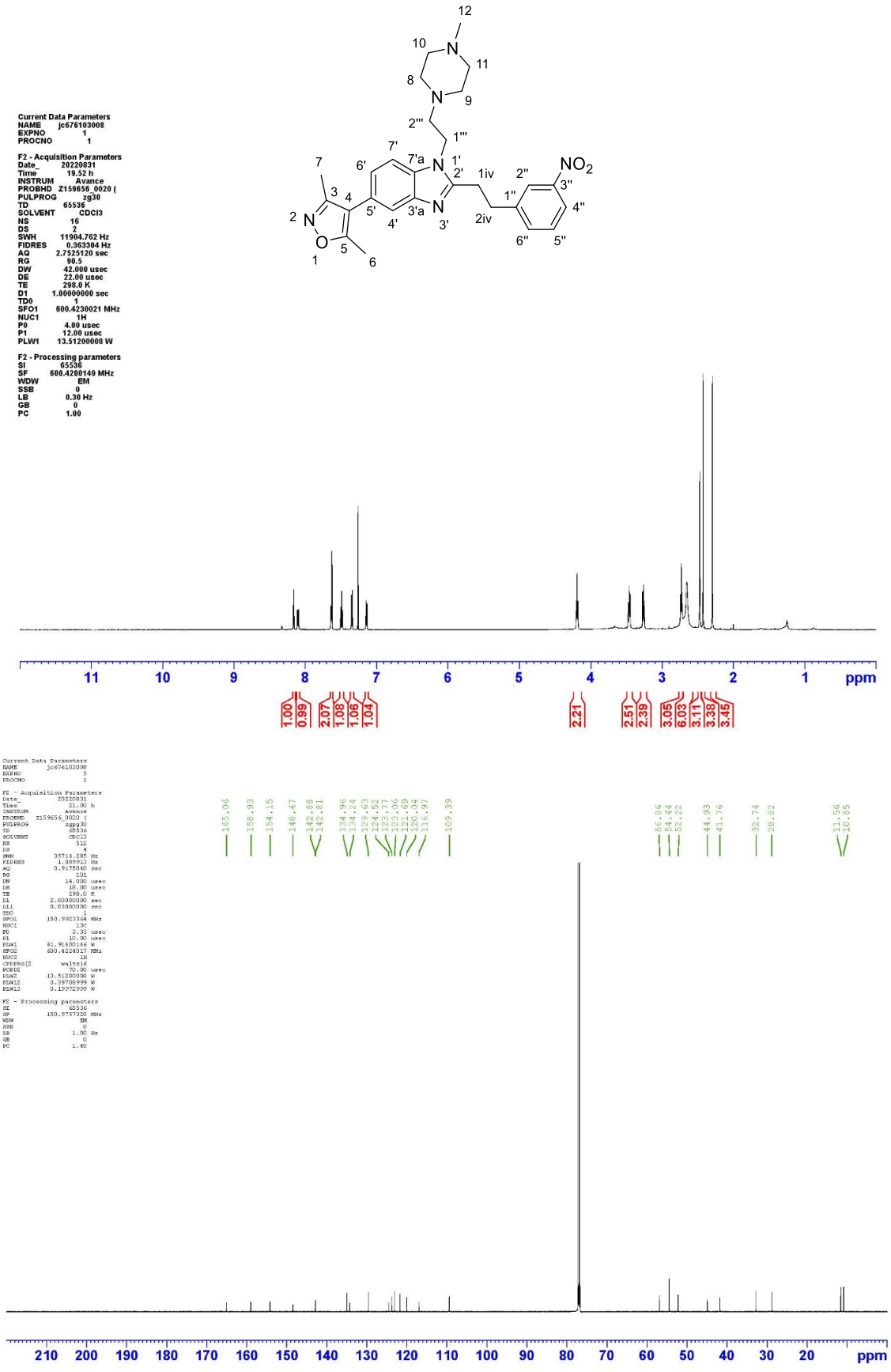

3,5-Dimethyl-4-(1-(2-(4-methylpiperazin-1-yl)ethyl)-2-(4-nitrophenethyl)-1*H*-benzo[*d*]imidazol-5-yl)isoxazole 226

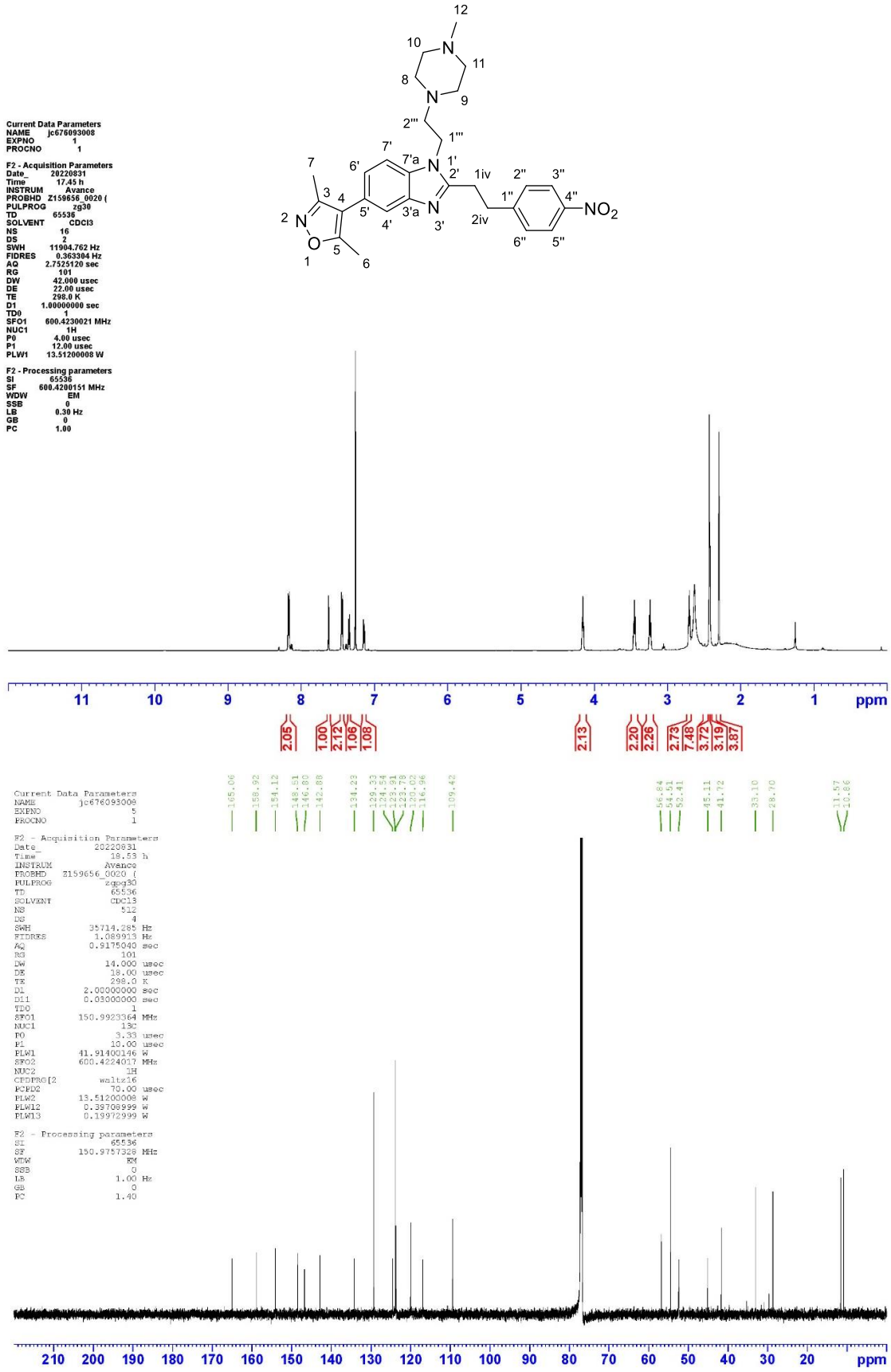

4-(2-(5-(3,5-Dimethylisoxazol-4-yl)-2-(3-nitrophenethyl)-1*H*-benzo[*d*]imidazol-1-yl)ethyl)morpholine 172

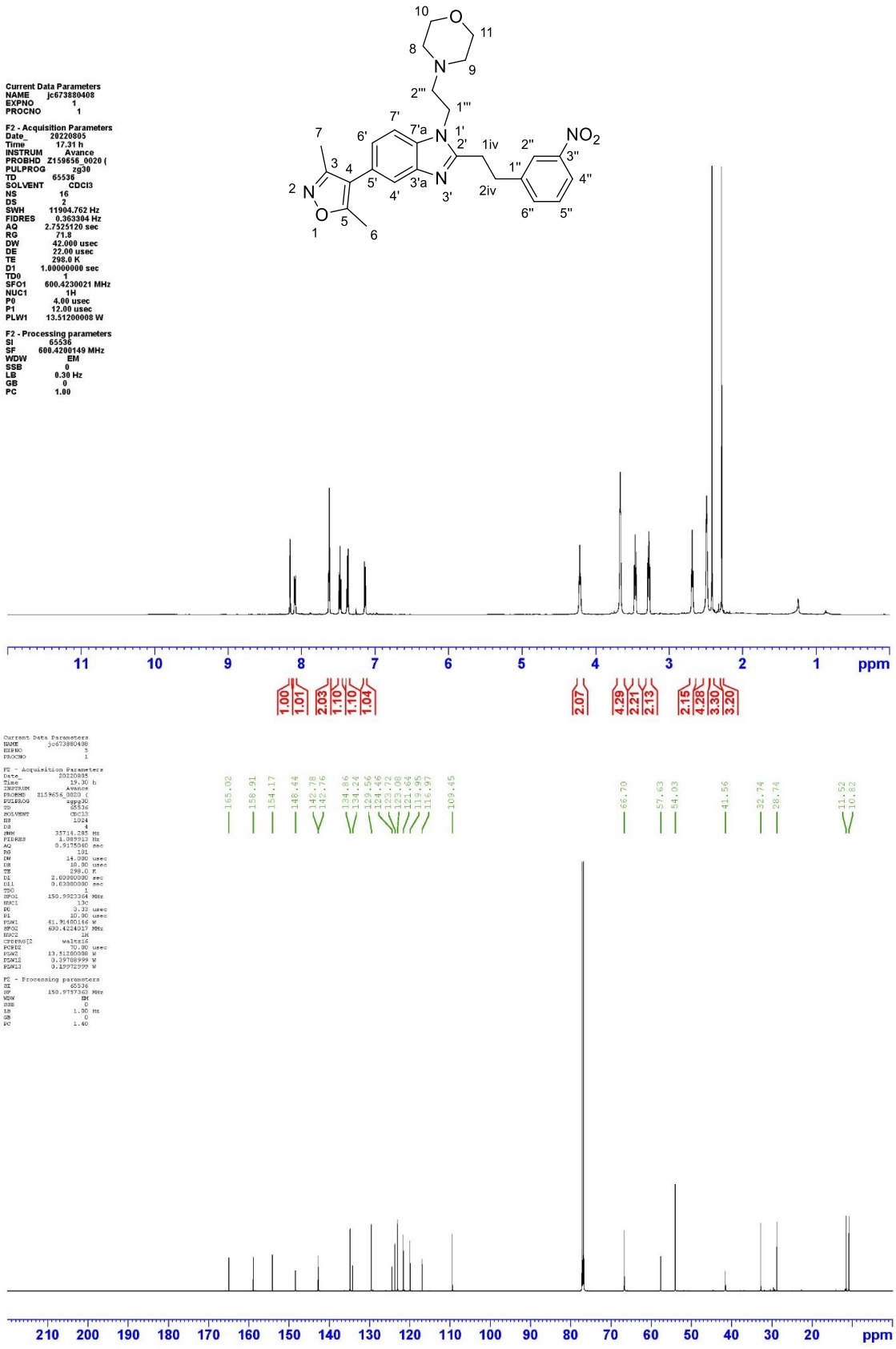

4-(2-(5-(3,5-Dimethylisoxazol-4-yl)-2-(4-nitrophenethyl)-1*H*-benzo[*d*]imidazol-1-yl)ethyl)morpholine 173

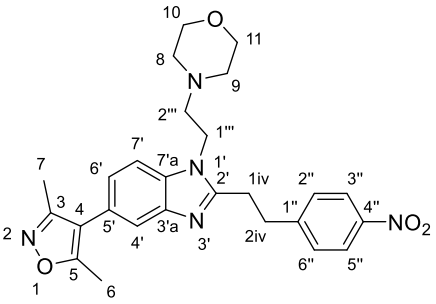

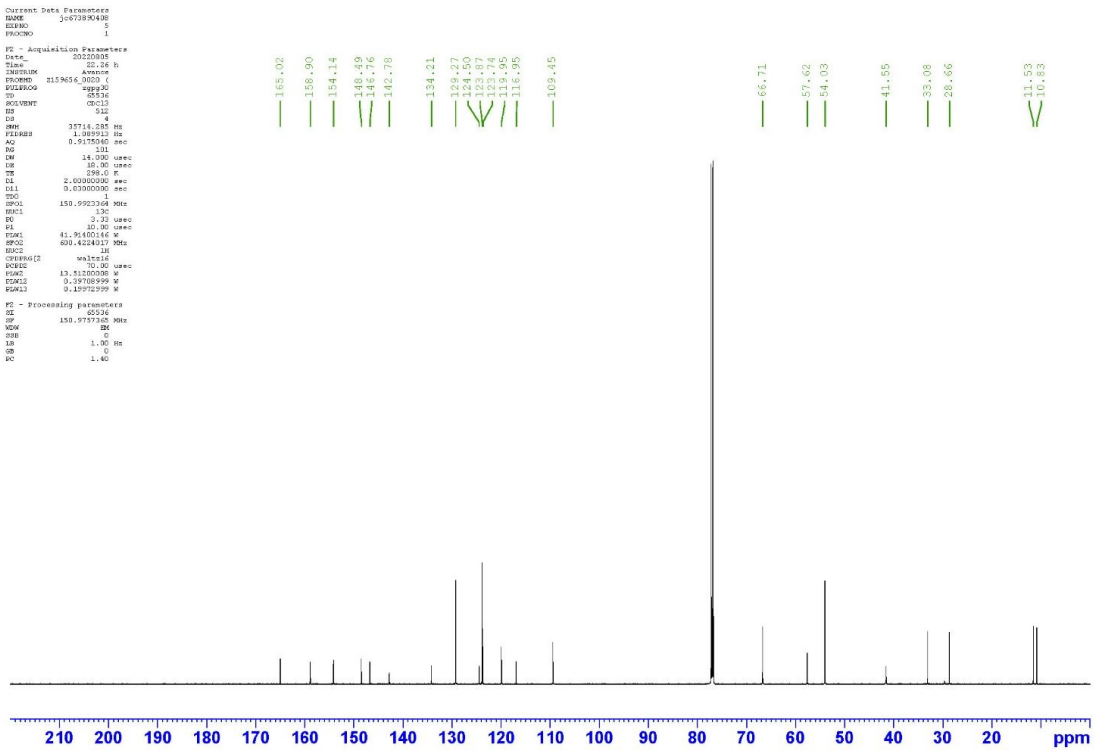

3-(2-(5-(3,5-Dimethylisoxazol-4-yl)-1-(2-morpholinoethyl)-1*H*-benzo[*d*]imidazol-2-yl)ethyl)benzonitrile 170

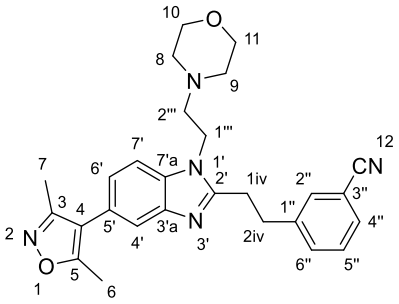

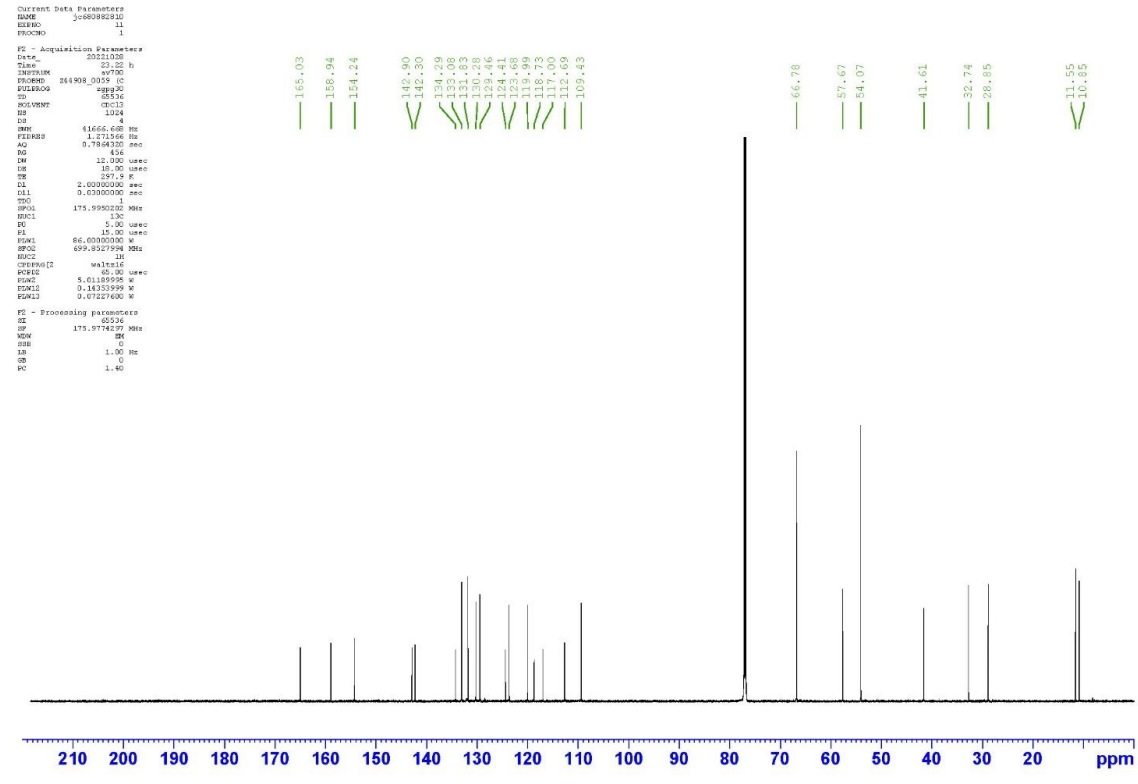

4-(2-(5-(3,5-Dimethylisoxazol-4-yl)-1-(2-morpholinoethyl)-1*H*-benzo[*d*]imidazol-2-yl)ethyl)benzonitrile 178

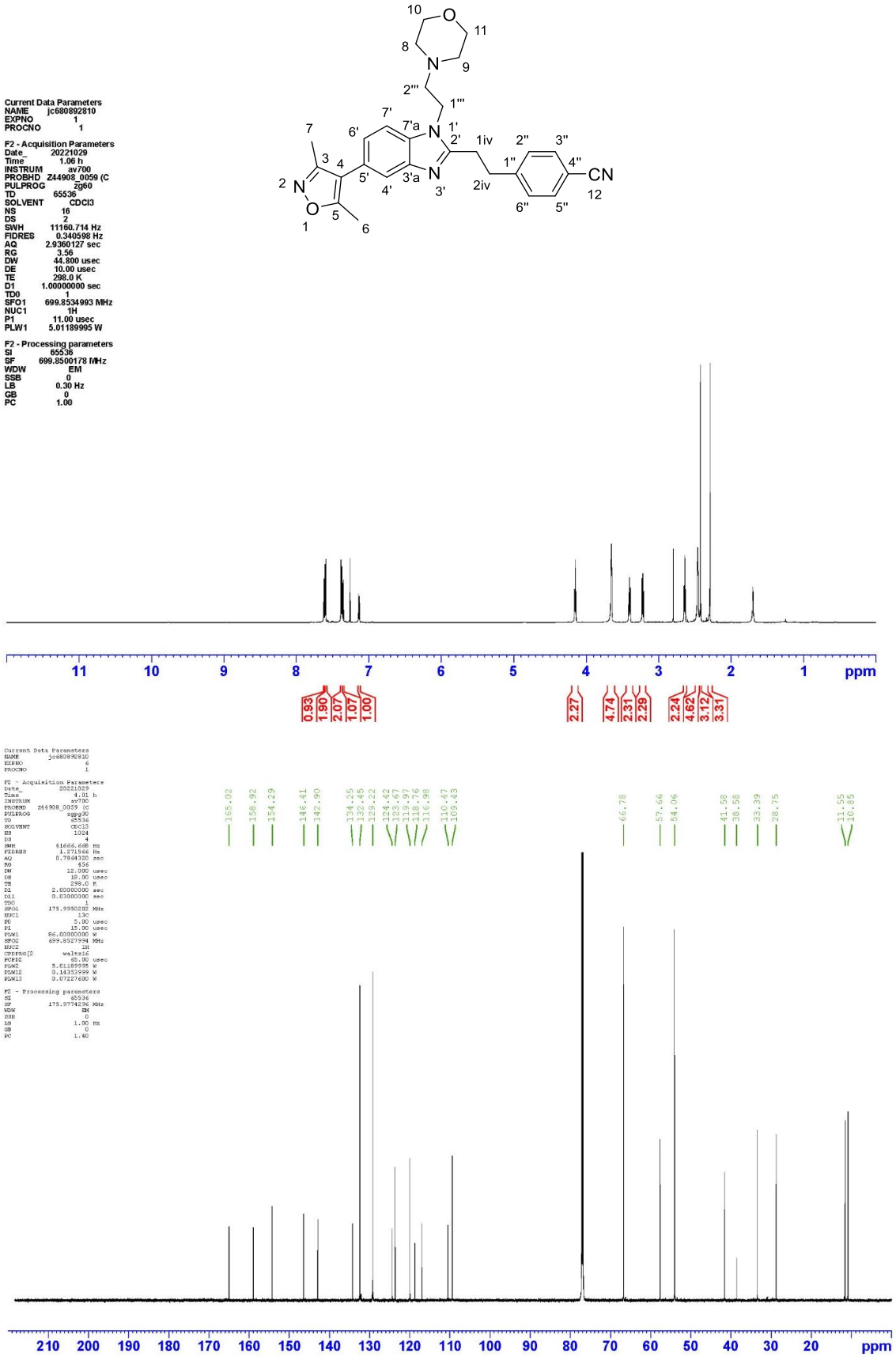

4-(2-(5-(3,5-Dimethylisoxazol-4-yl)-2-(3-methylphenethyl)-1*H*-benzo[*d*]imidazol-1-yl)ethyl)morpholine 171

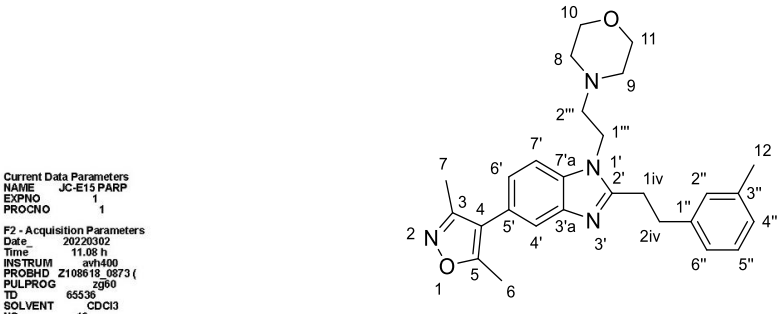

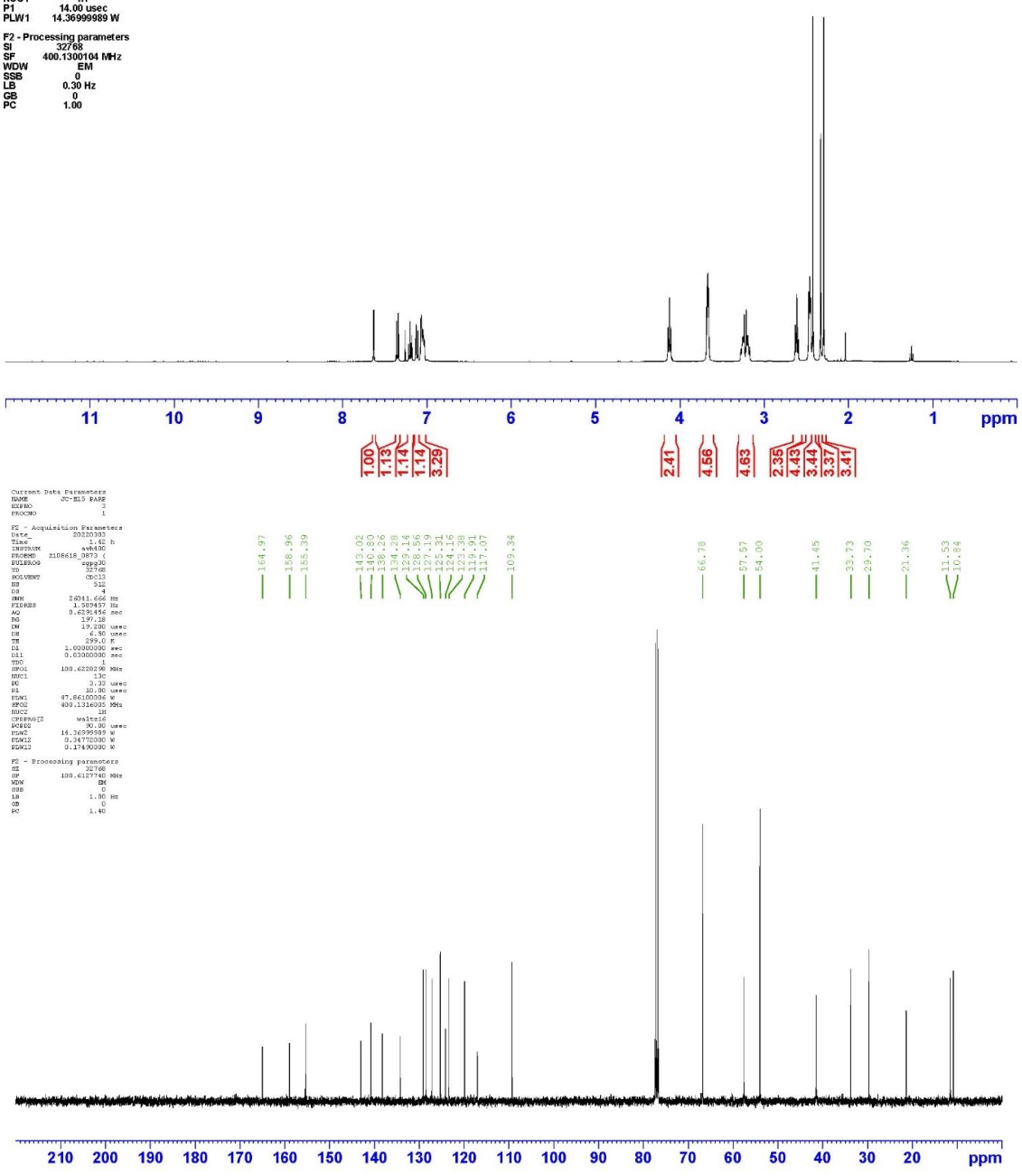

4-(2-(5-(3,5-Dimethylisoxazol-4-yl)-2-(4-methylphenethyl)-1*H*-benzo[*d*]imidazol-1-yl)ethyl)morpholine 179

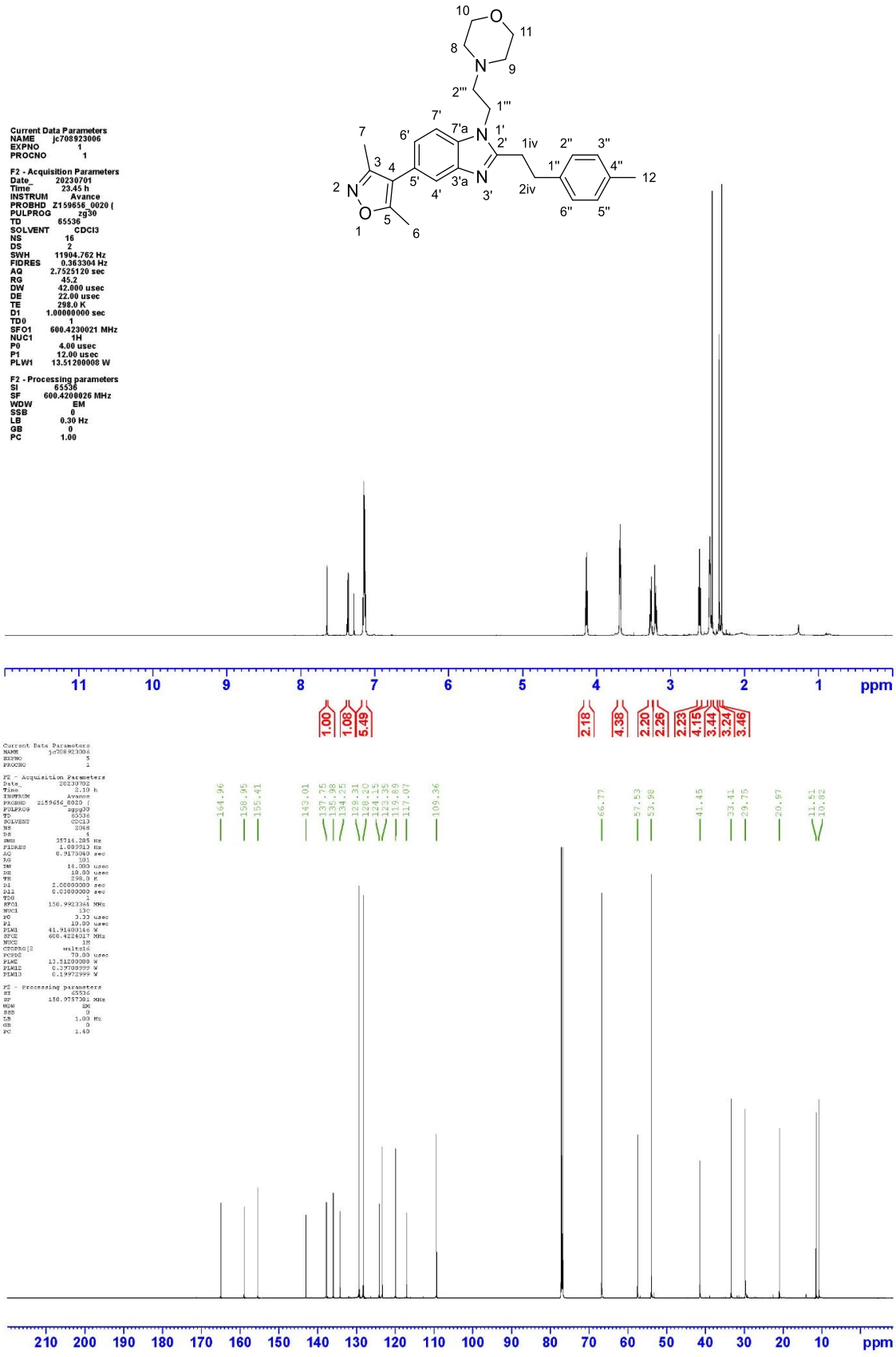

(*E*)-3-(3-Cyano-4-methylphenyl)acrylic acid 162

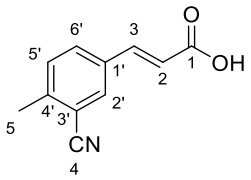

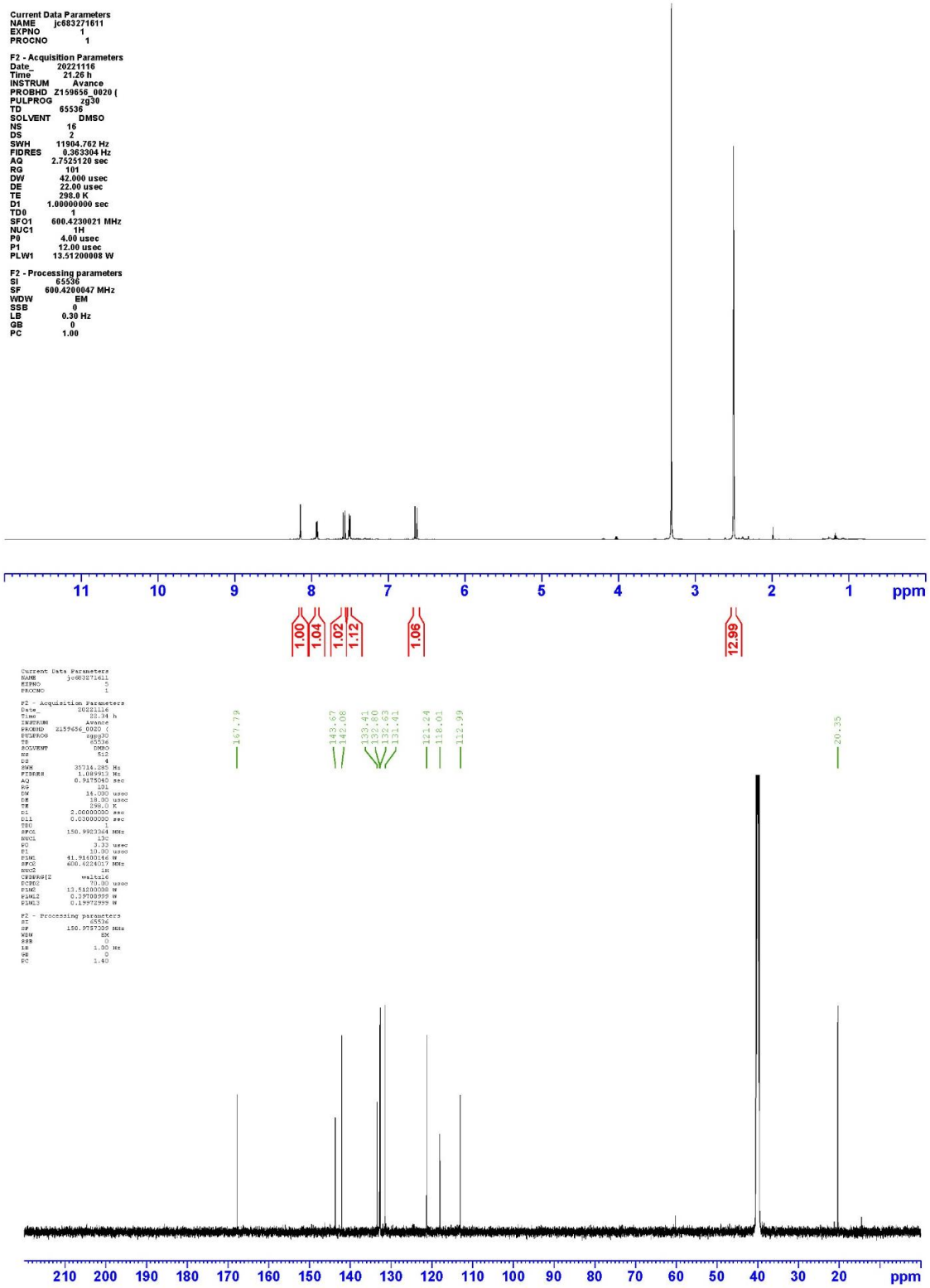

3-(3-Cyano-4-methylphenyl)propanoic acid 158

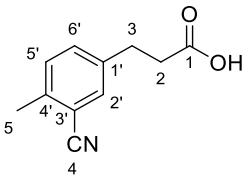

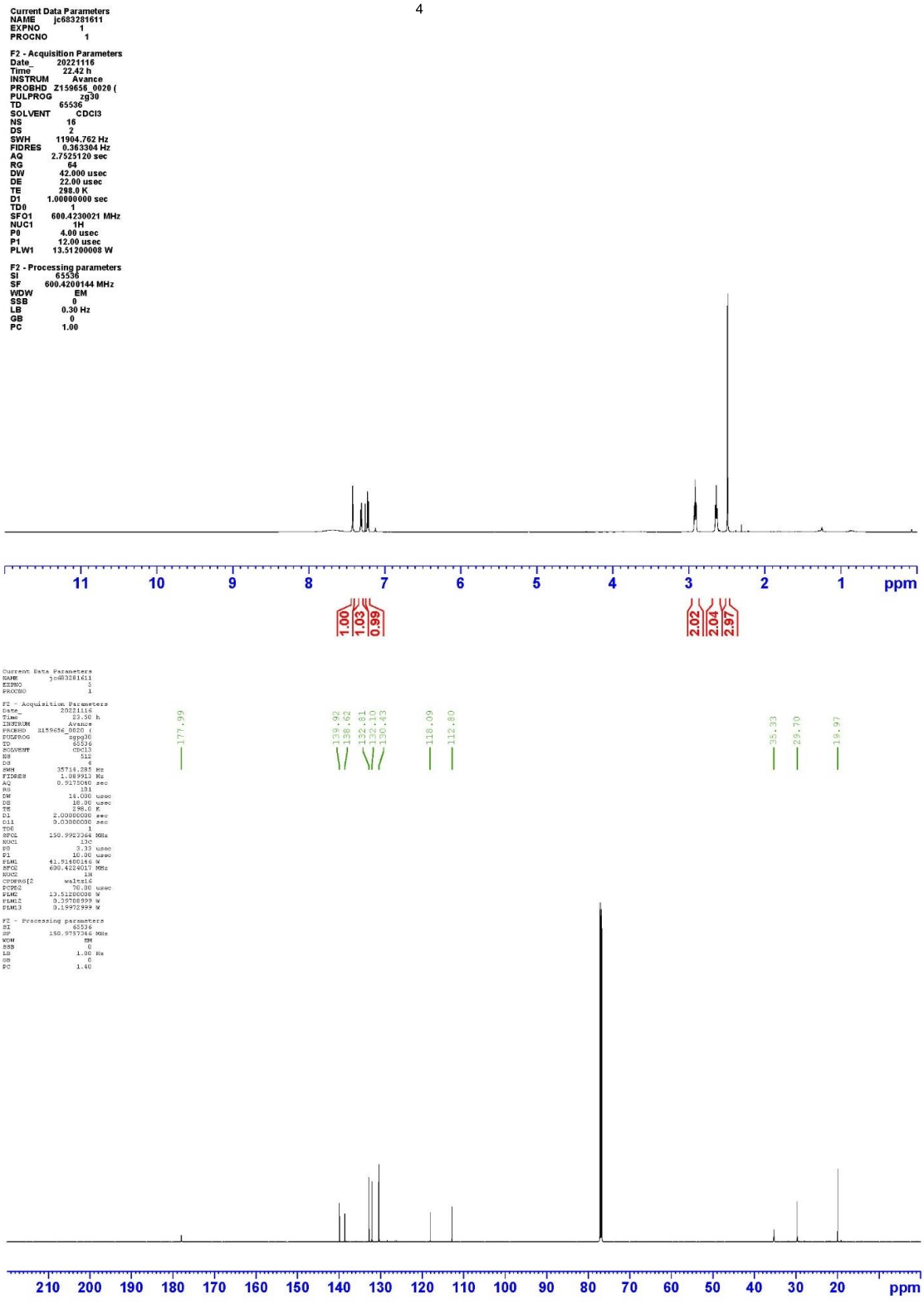

Benzyl (*E*)-3-(3-cyano-4-methylphenyl)acrylate 164

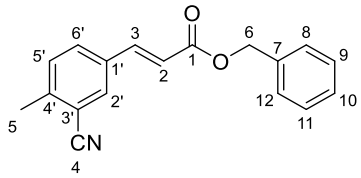

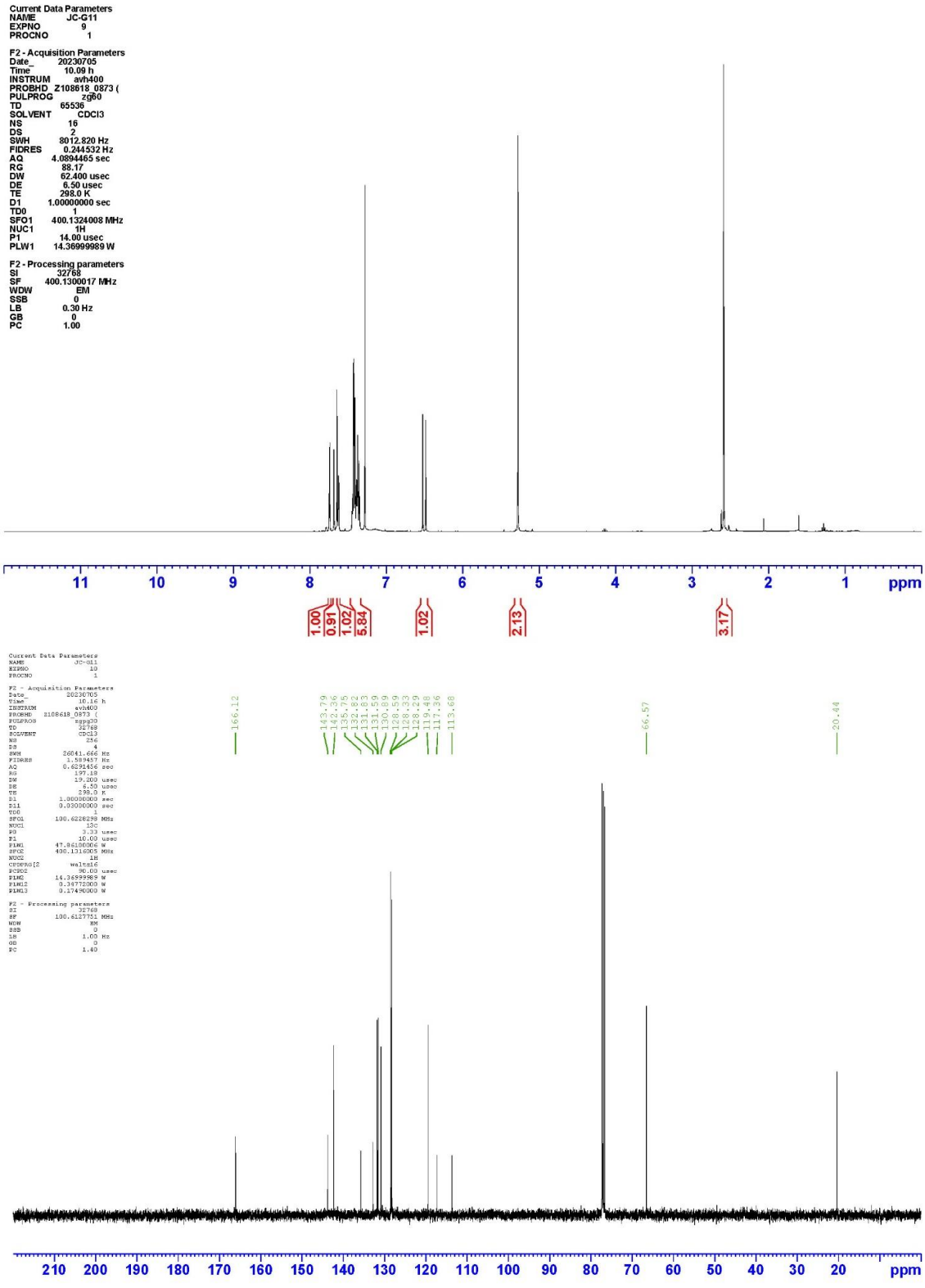

5-(2-(5-(3,5-Dimethylisoxazol-4-yl)-1-methyl-1*H*-benzo[*d*]imidazol-2-yl)ethyl)-2-methylbenzonitrile 156

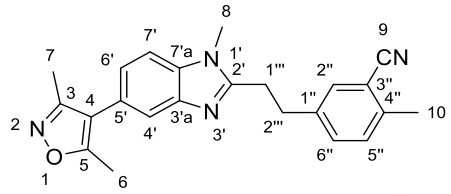

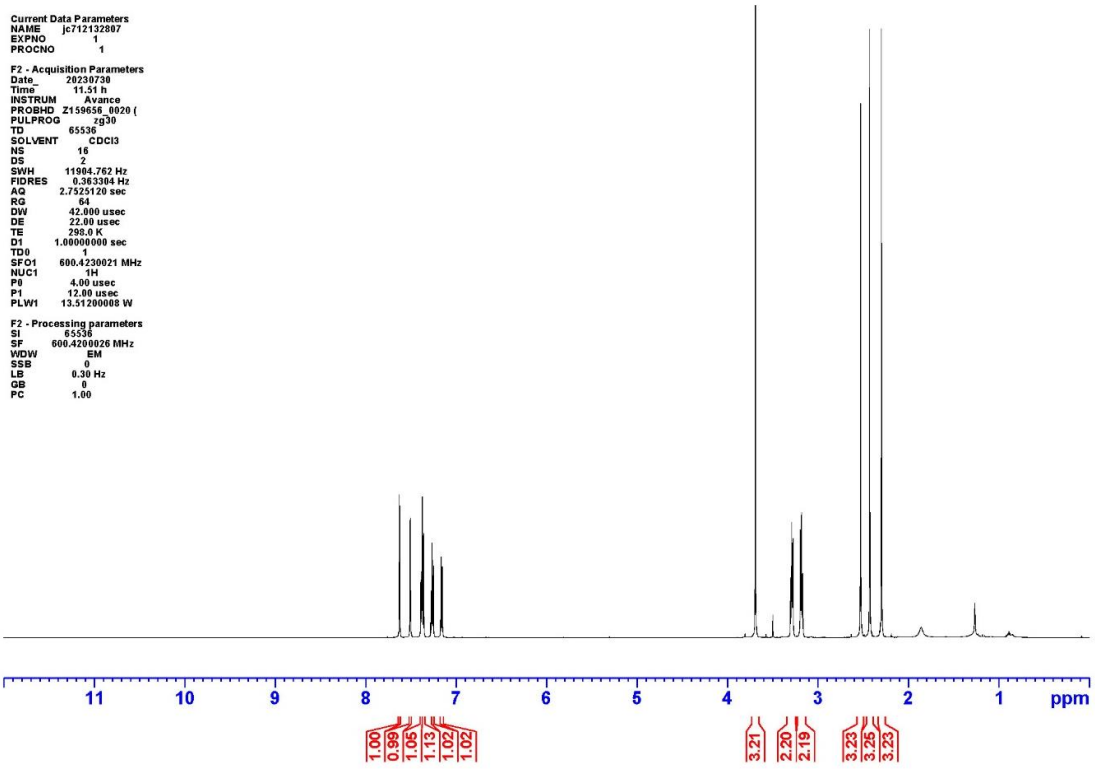

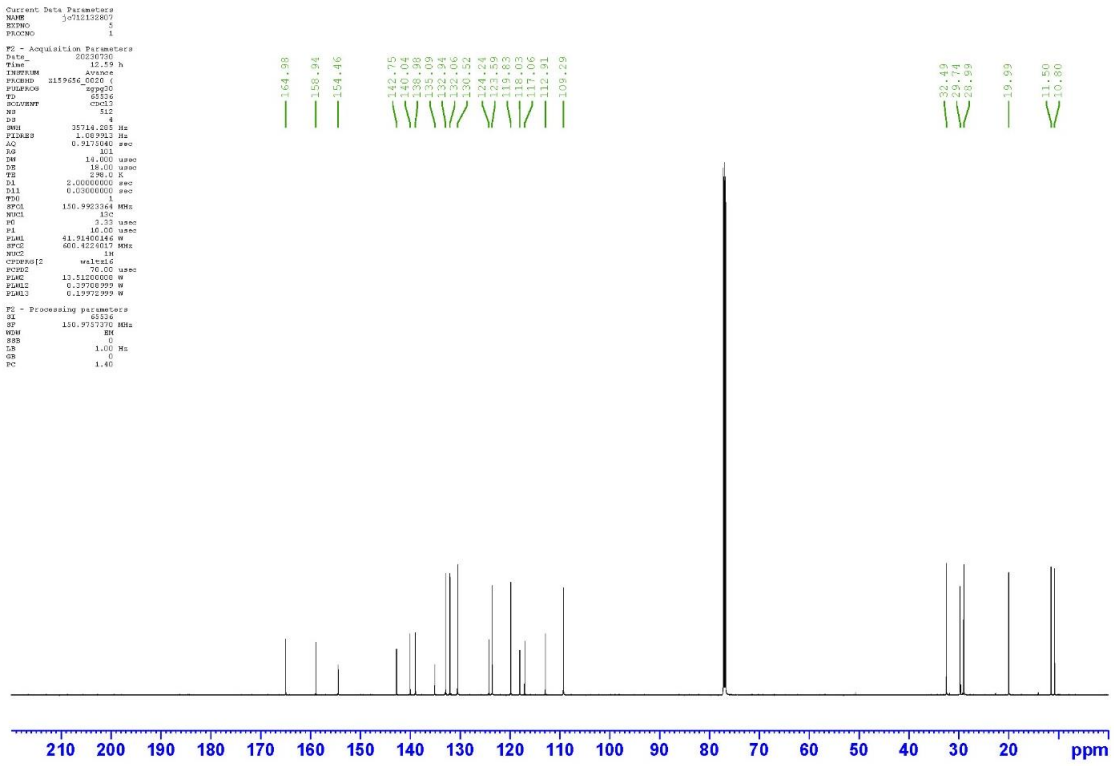

Benzyl (*E*)-3-(4-cyano-3-methylphenyl)acrylate 165

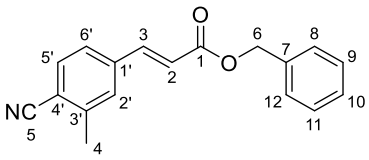

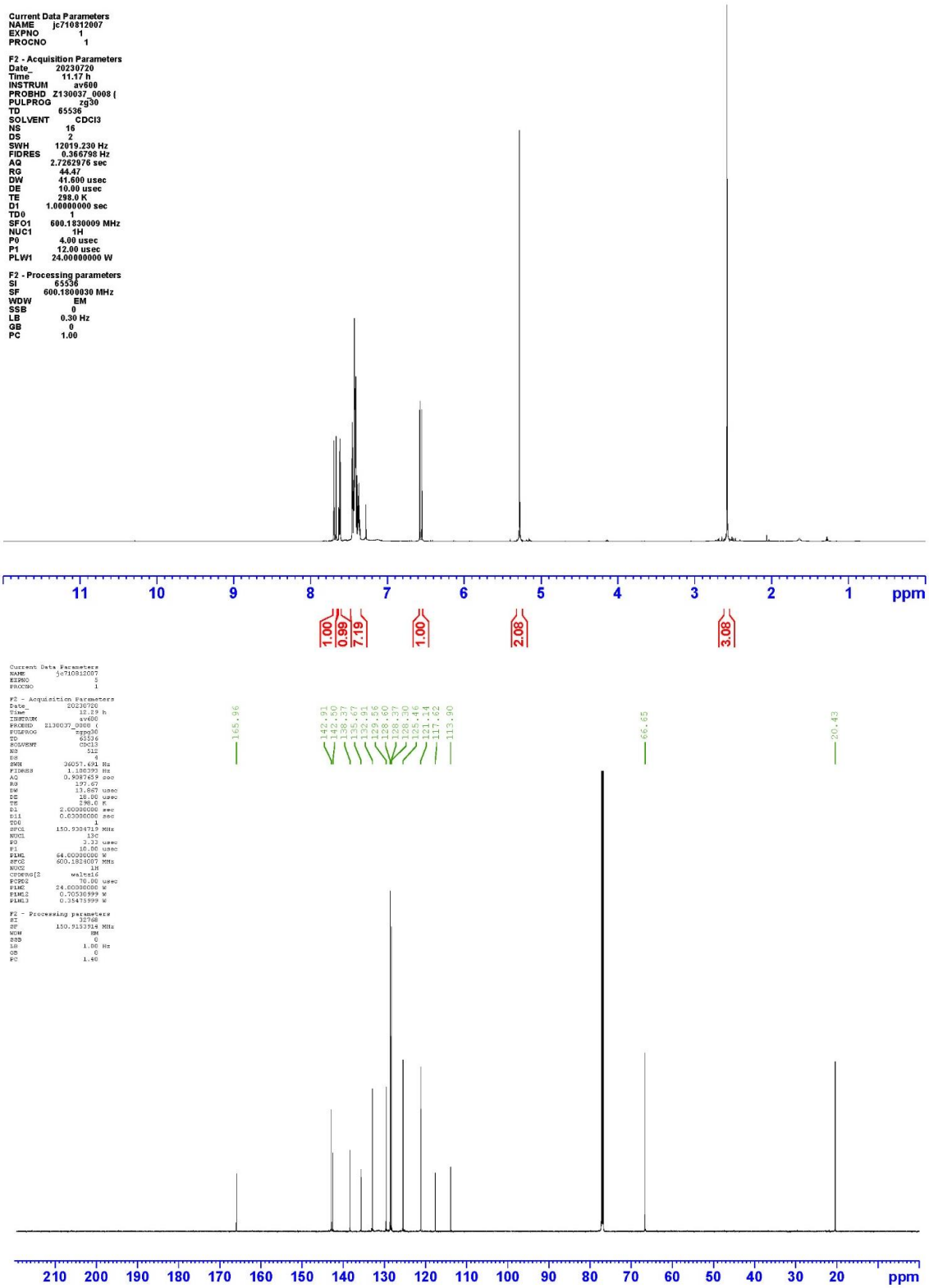

3-(4-Cyano-3-methylphenyl)propanoic acid 159

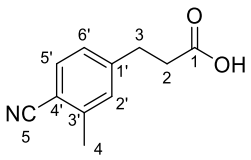

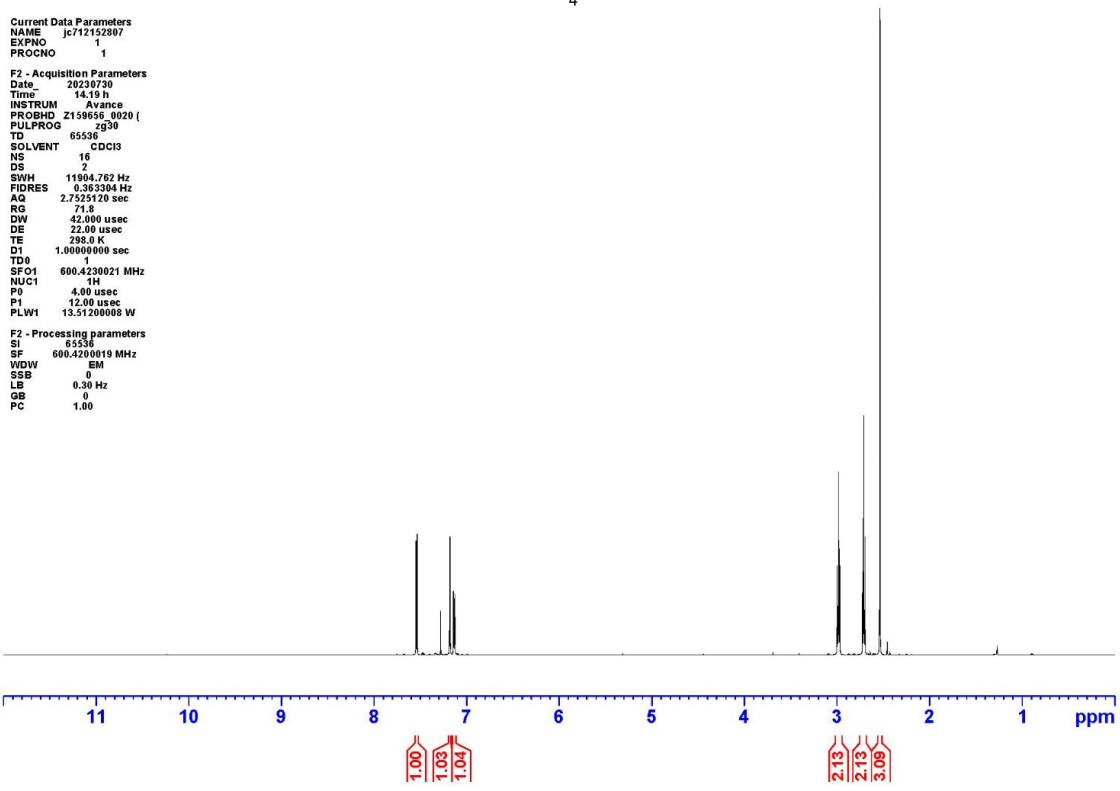

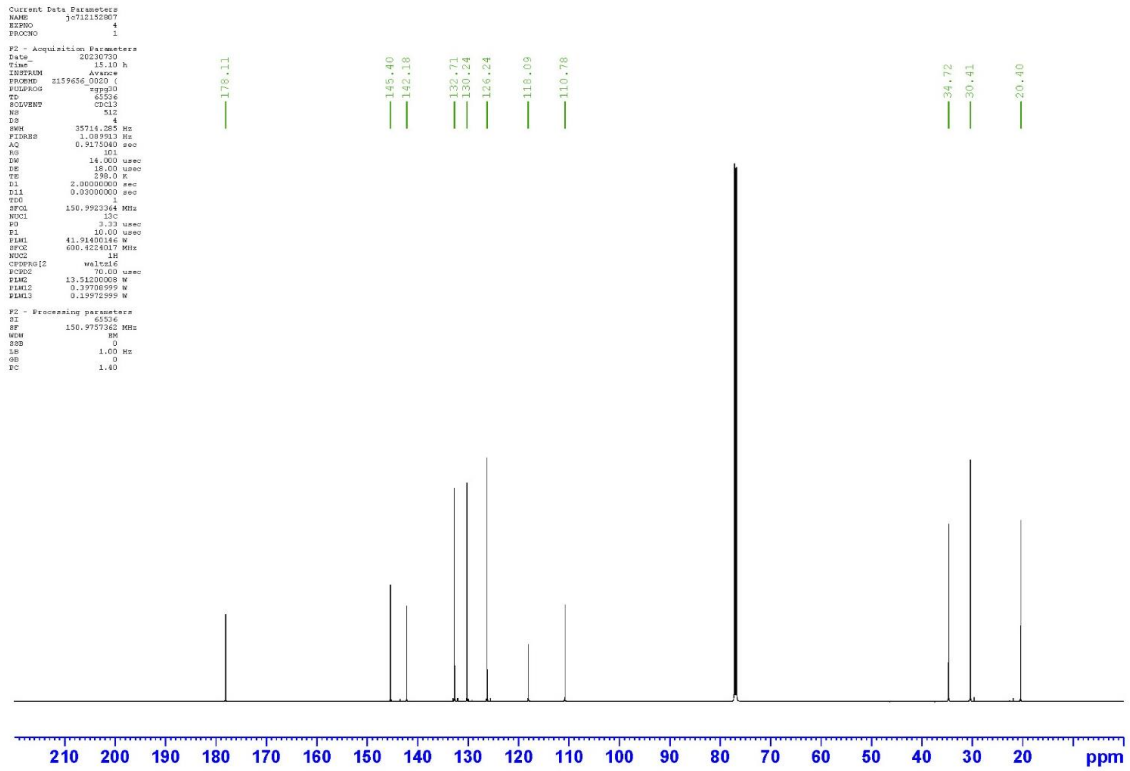

4-(2-(5-(3,5-Dimethylisoxazol-4-yl)-1-methyl-1*H*-benzo[*d*]imidazol-2-yl)ethyl)-2-methylbenzonitrile 157

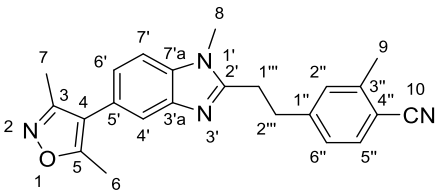

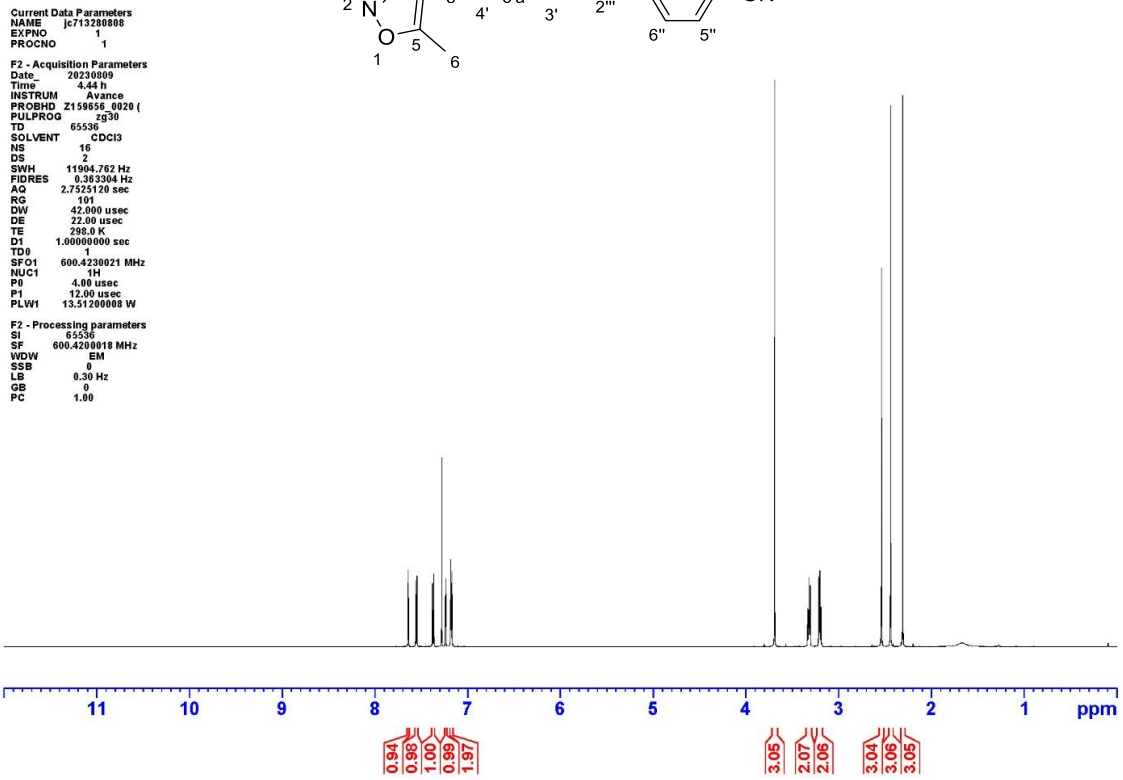

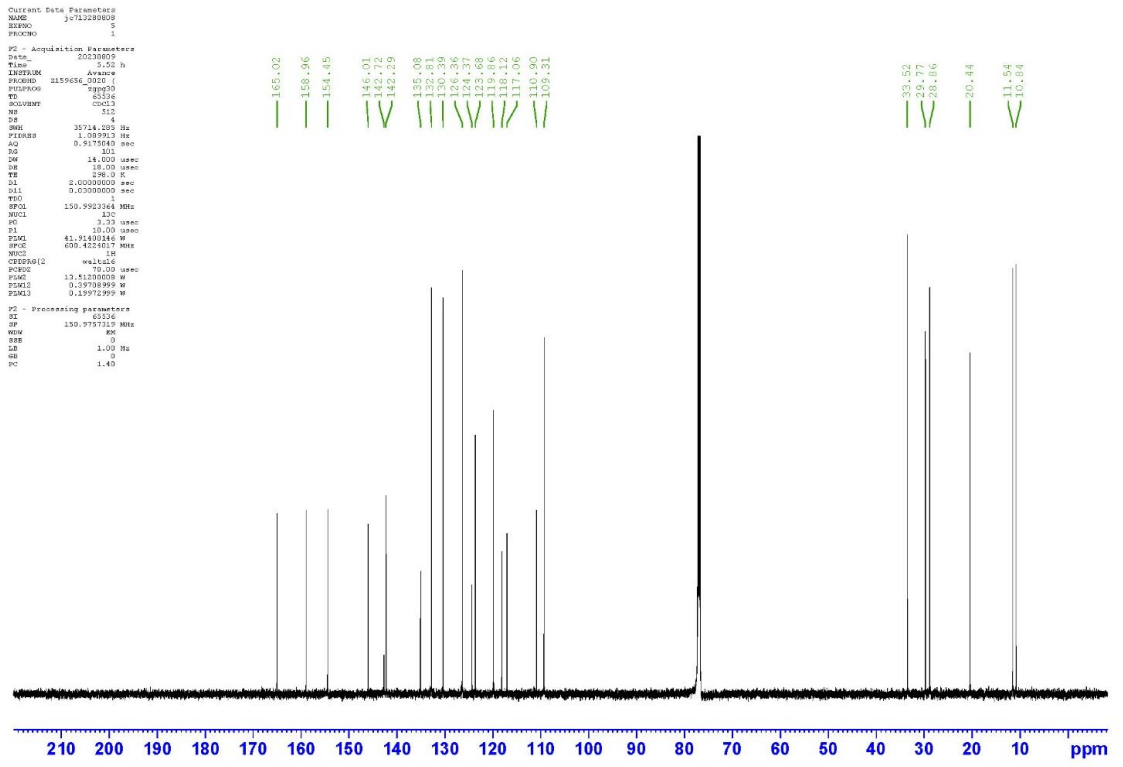

5-(2-(5-(3,5-Dimethylisoxazol-4-yl)-1-(2-morpholinoethyl)-1*H*-benzo[*d*]imidazol-2-yl)ethyl)-2-methylbenzonitrile 174

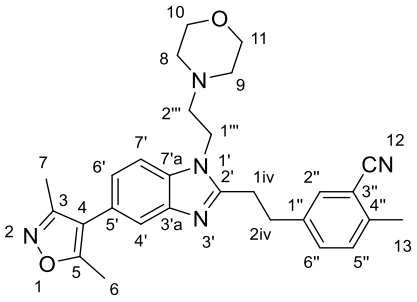

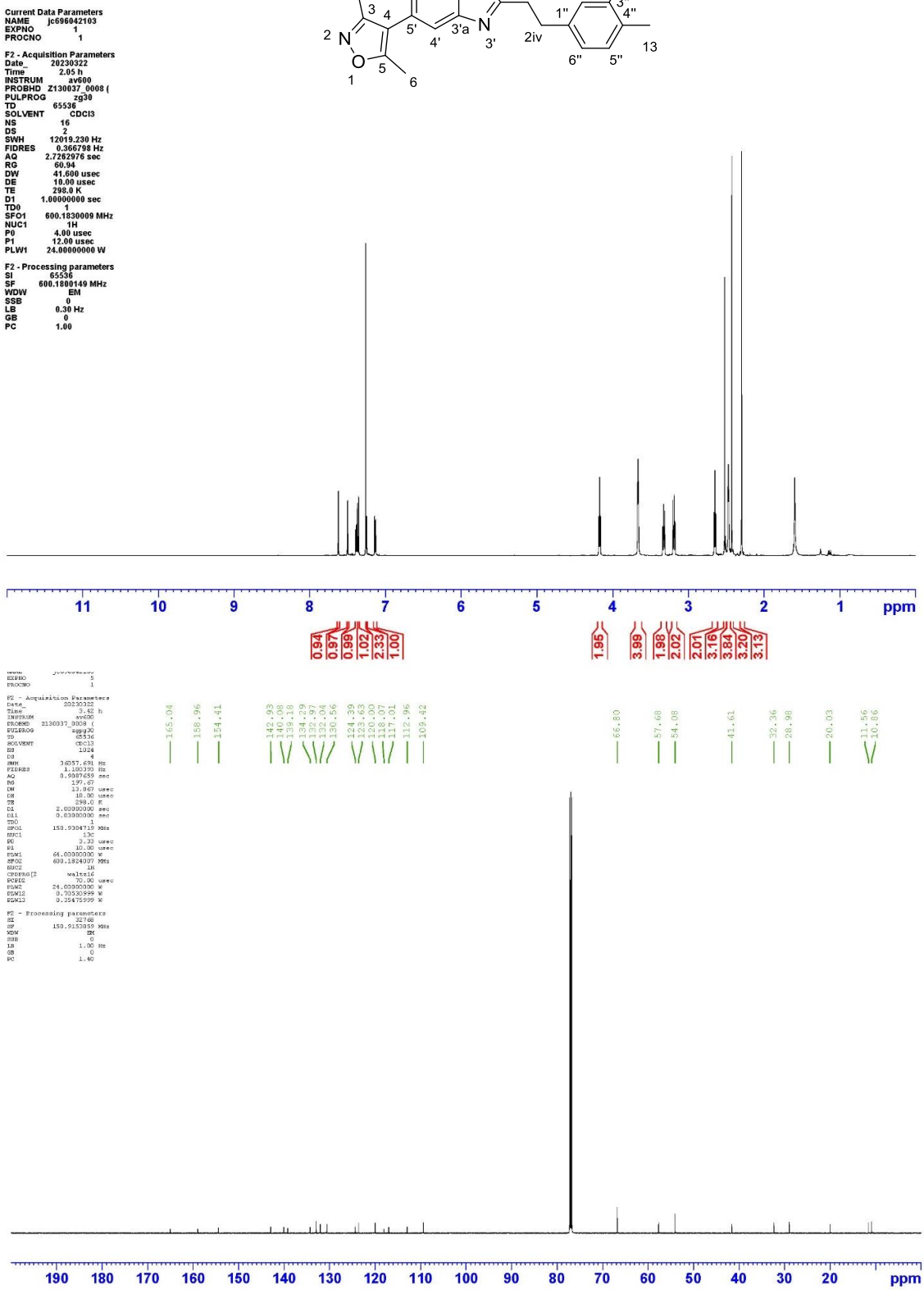

4-(2-(5-(3,5-Dimethylisoxazol-4-yl)-1-(2-morpholinoethyl)-1*H*-benzo[*d*]imidazol-2-yl)ethyl)-2-methylbenzonitrile 175

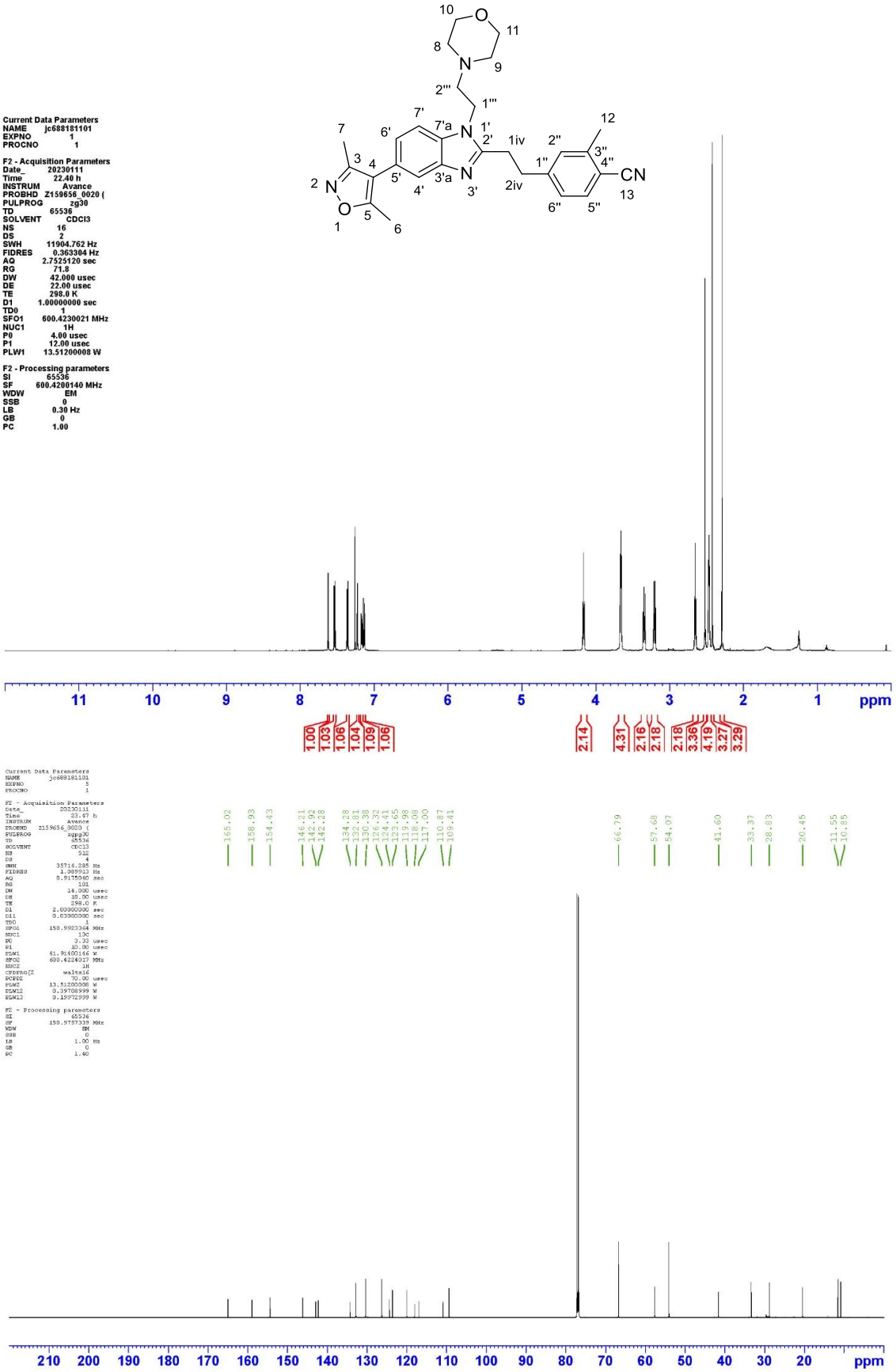

5-(2-(5-(3,5-Dimethylisoxazol-4-yl)-1-(2-(4-methylpiperazin-1-yl)ethyl)-1H-benzo[d]imidazol-2-yl)ethyl)-2-methylbenzonitrile 183

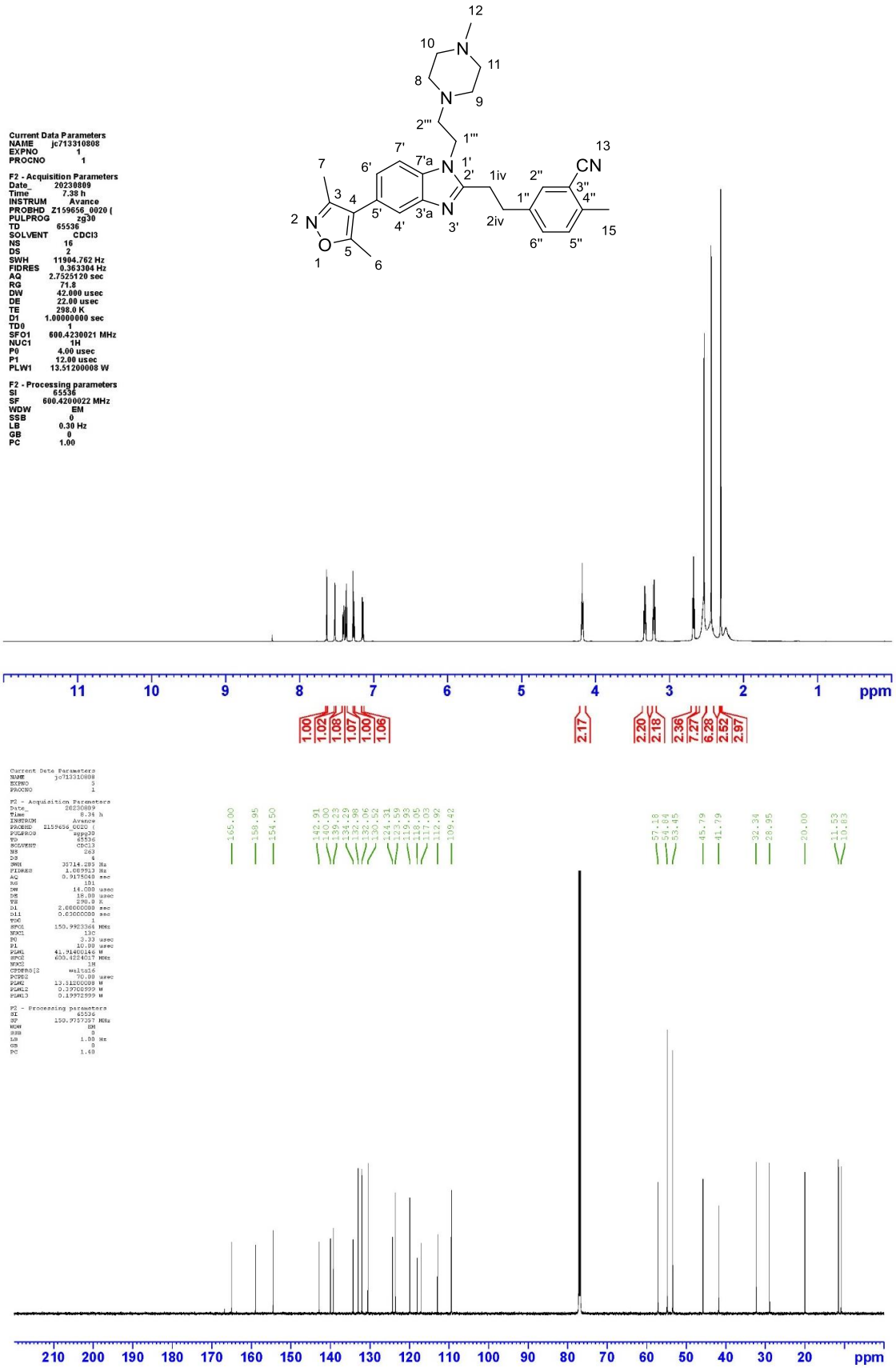

1-(4-(2-((4-(3,5-Dimethylisoxazol-4-yl)-2-nitrophenyl)amino)ethyl)piperazin-1-yl)ethan-1-one 236

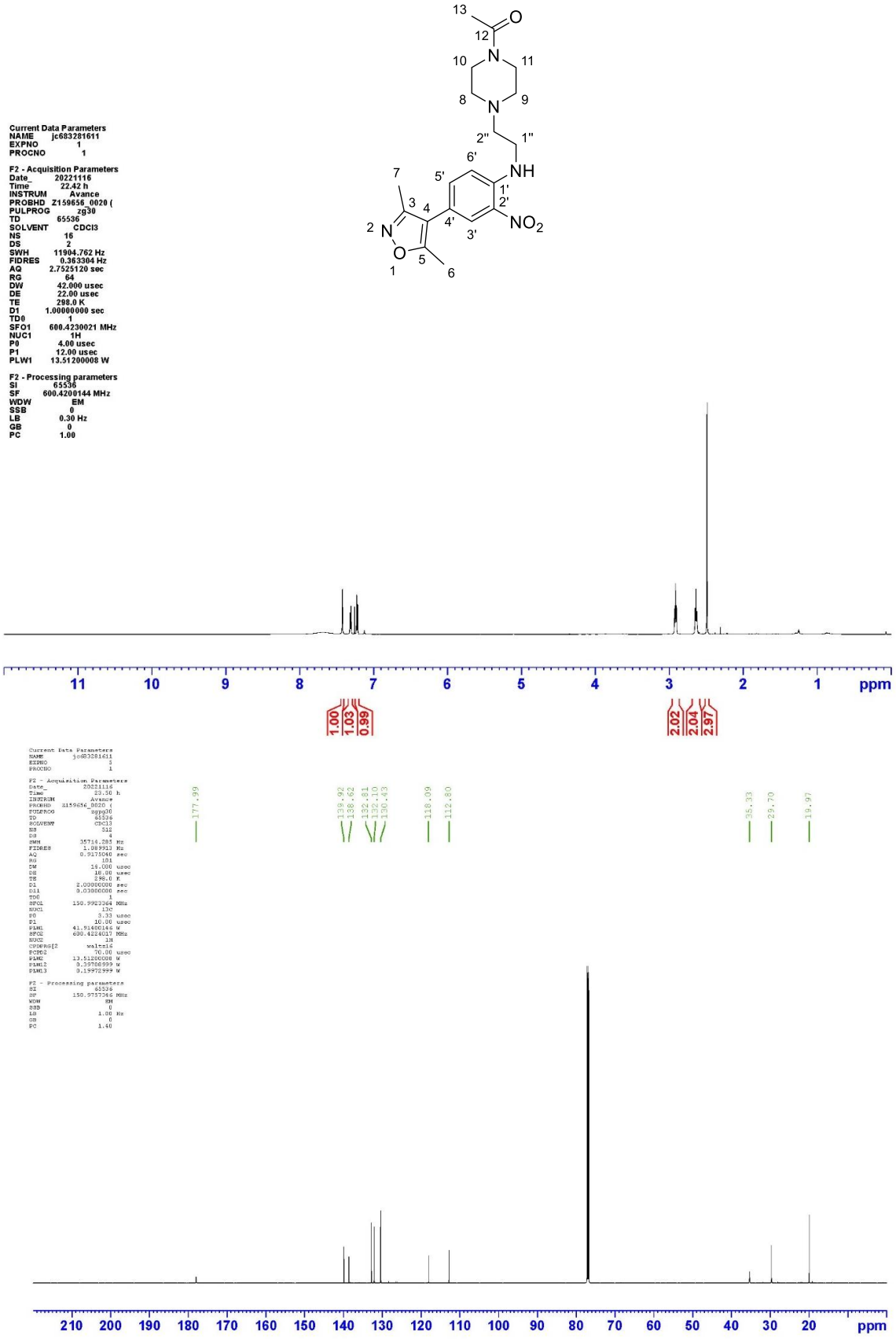

5-(2-(1-(2-(4-Acetylpiperazin-1-yl)ethyl)-5-(3,5-dimethylisoxazol-4-yl)-1*H*-benzo[*d*]imidazol-2-yl)ethyl)-2-methylbenzonitrile 181

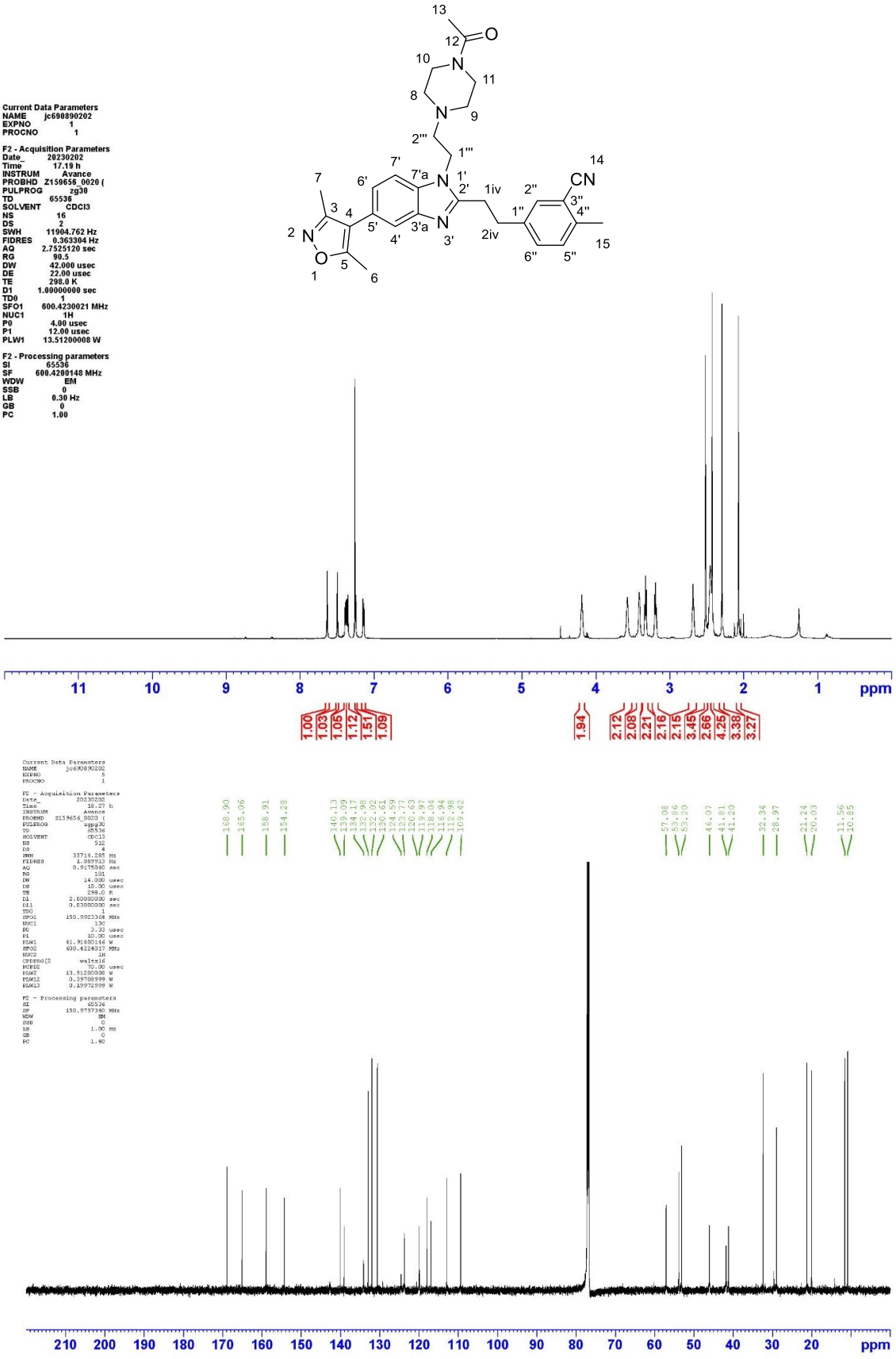

4-(3,5-Dimethylisoxazol-4-yl)-2-nitro-*N*-(2-(piperidin-1-yl)ethyl)aniline 238

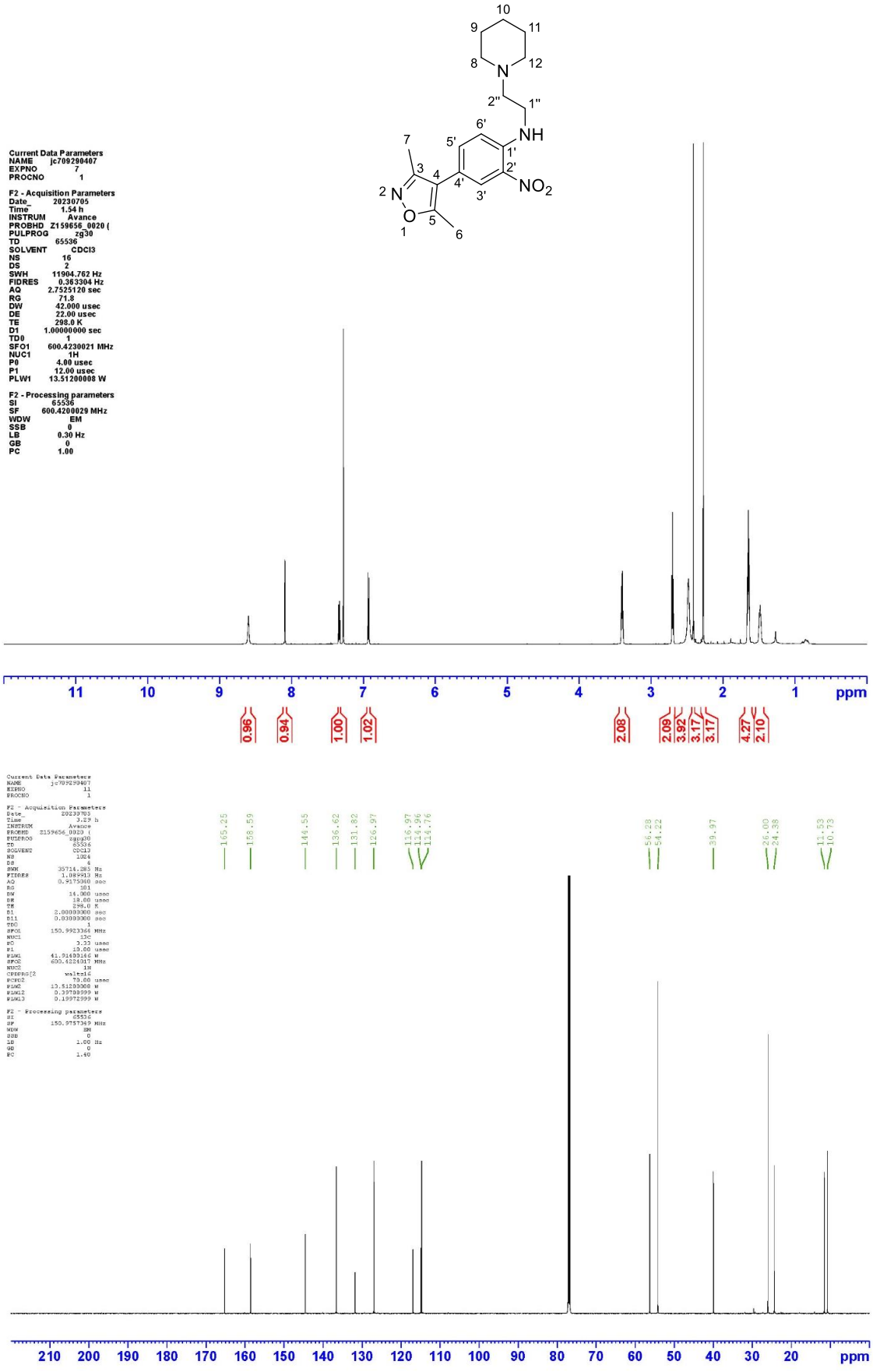

5-(2-(5-(3,5-Dimethylisoxazol-4-yl)-1-(2-(piperidin-1-yl)ethyl)-1*H*-benzo[*d*]imidazol-2-yl)ethyl)-2-methylbenzonitrile 180

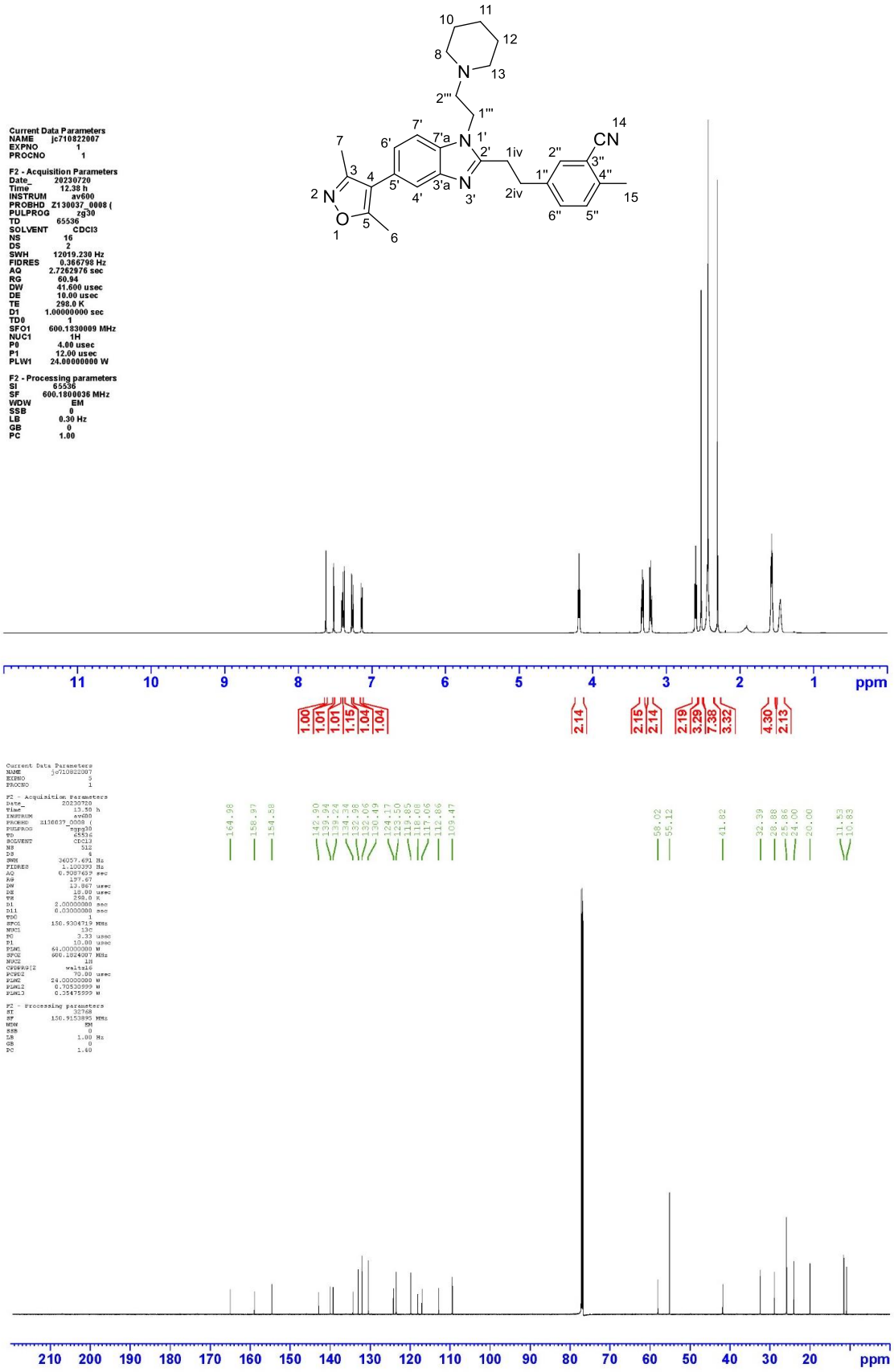

_N_-(2-(4,4-Difluoropiperidin-1-yl)ethyl)-4-(3,5-dimethylisoxazol-4-yl)-2-nitroaniline

240

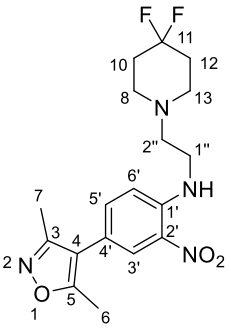

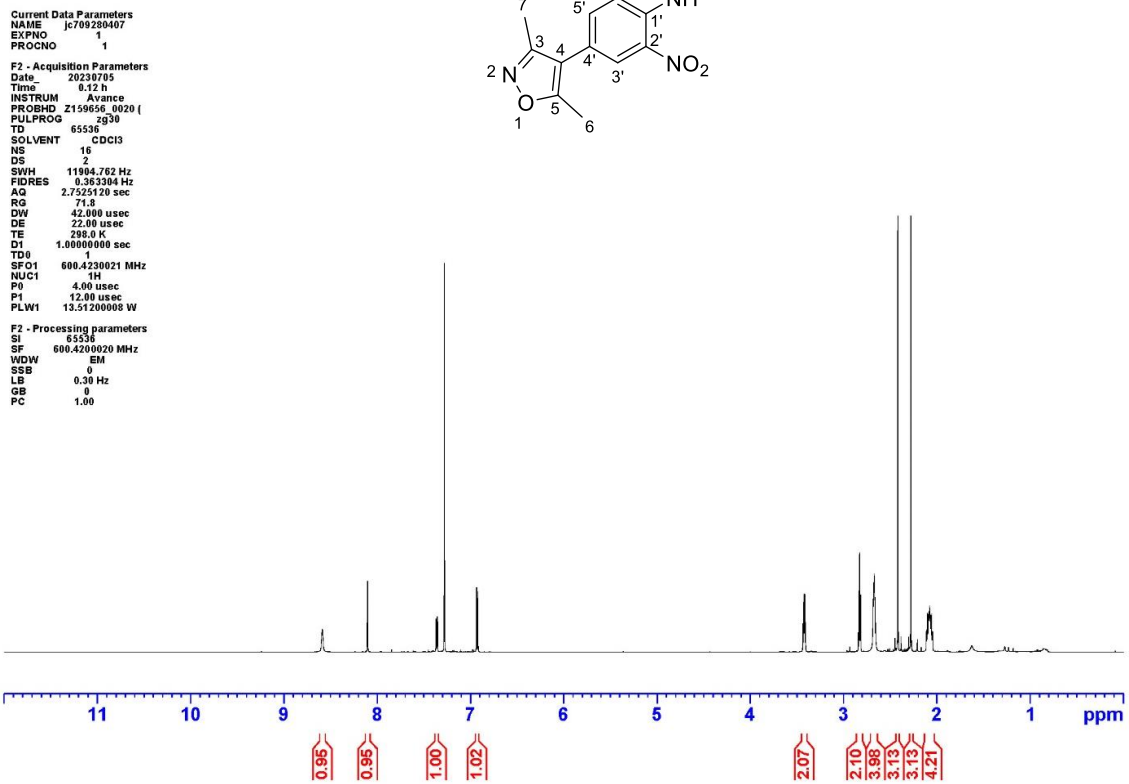

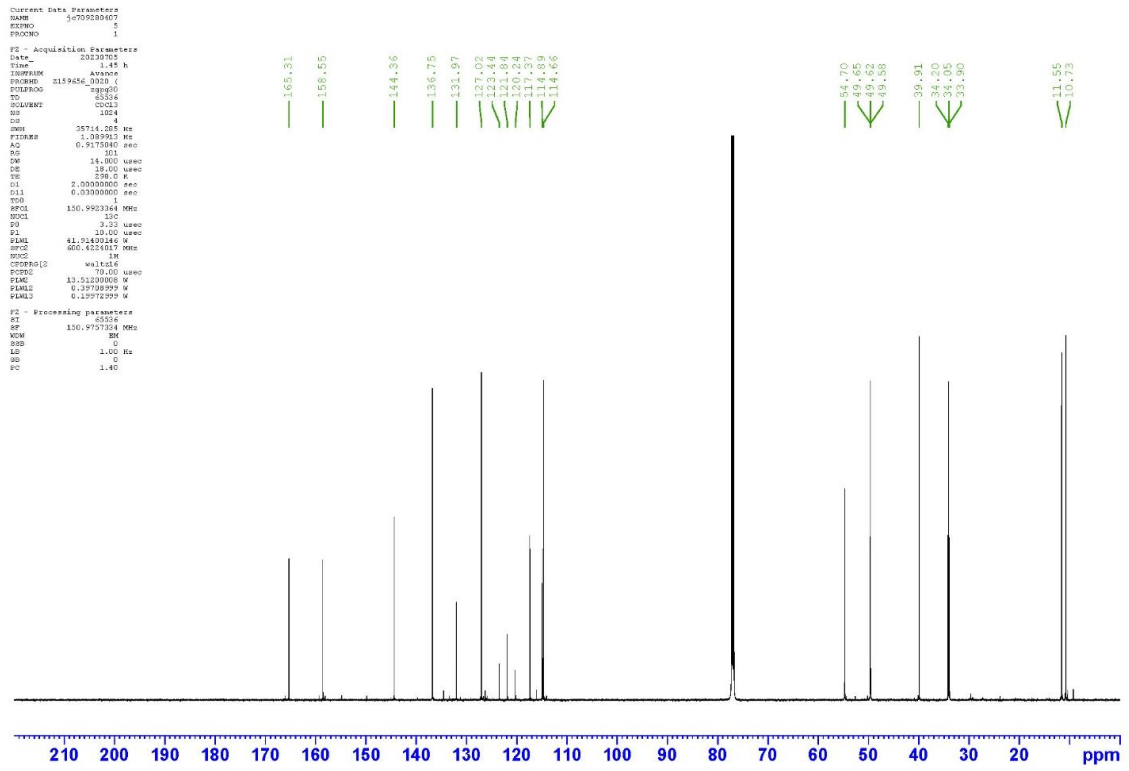

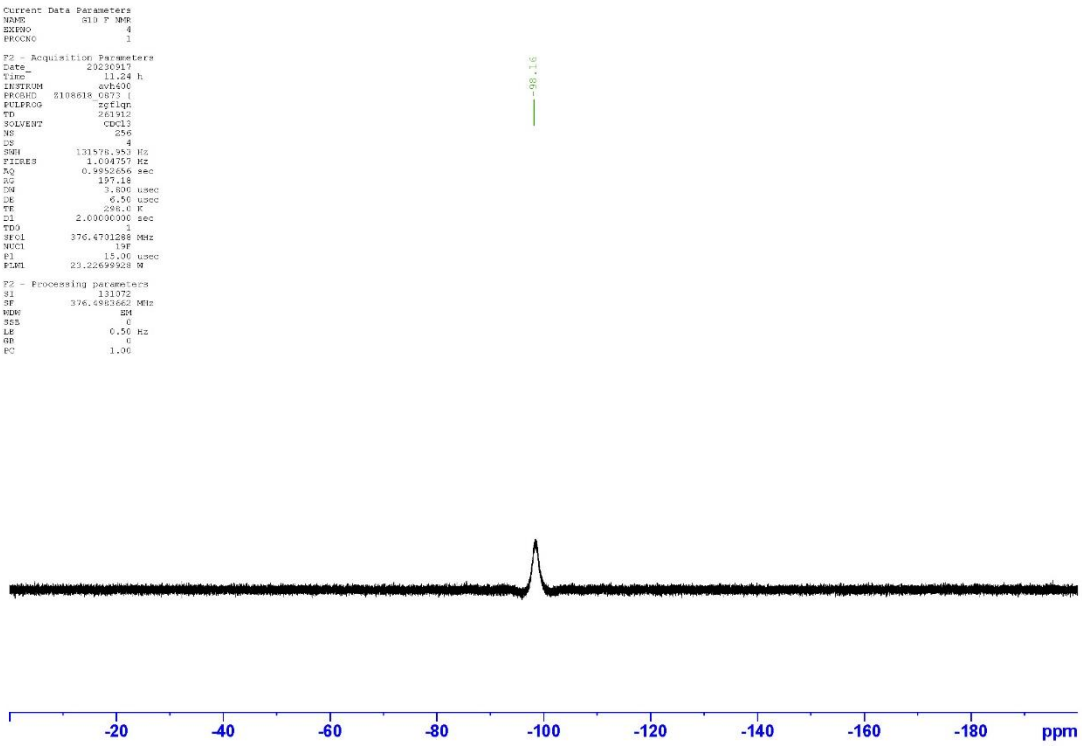
Current Data Parameters
NAME S10 F NMR
EXPNO 4
PROCNO 1
F2 - Acquisition Parameters
Date_ 20230917
Time 11.24 h
INSTRUM avh400
PROBHD 5108618_0673_(
PULPROG zgflqn
TD 261912
SOLVENT CDCl3
NS 256
DS 4
SWH 131578.953 Hz
FIRES 1.004757 Hz
AQ 0.9952656 sec
RG 197.18
DW 3.800 usec
DE 6.50 usec
TE 298.0 K
D1 2.00000000 sec
TD0 1
SFO1 376.4701288 MHz
NUC1 19F
P1 15.00 usec
PLW1 23.22699928 W
F2 - Processing parameters
SI 131072
SF 376.4983662 MHz
WDW EM
SSB 0
LB 0.50 Hz
GB 0
PC 1.00
-98.16
-20
-40
-60
-80
-100
-120
-140
-160
-180
ppm

5-(2-(1-(2-(4,4-Difluoropiperidin-1-yl)ethyl)-5-(3,5-dimethylisoxazol-4-yl)-1*H*-benzo[*d*]imidazol-2-yl)ethyl)-2-methylbenzonitrile 182

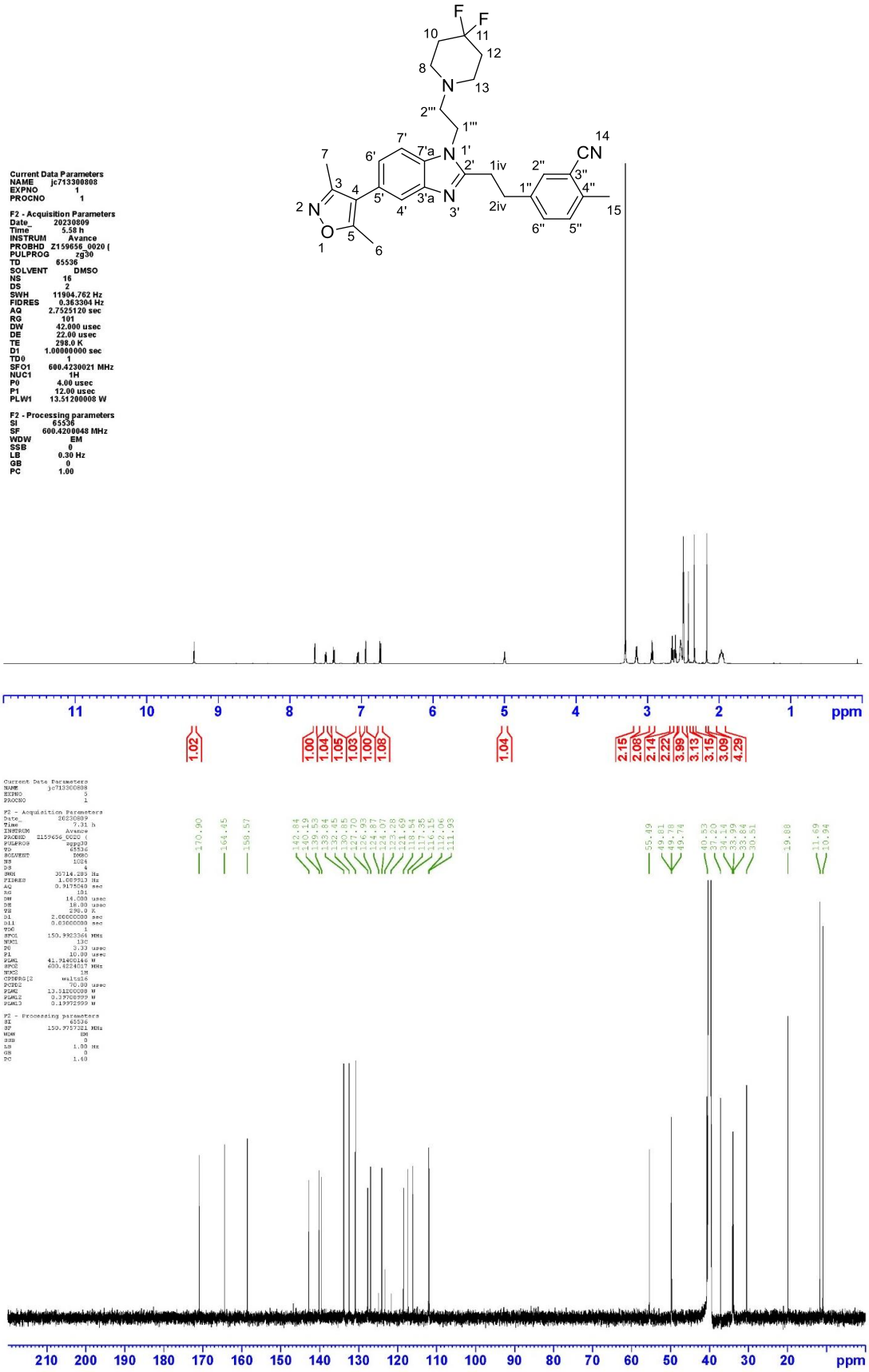

```
Current Data Parameters
NAME        jc-g26 f rmr
EXPNO              12
PROCNO              1

F2 - Acquisition Parameters
Date_         20230917
Time           11.54 h
INSTRUM         avh400
PROBHD   Z108618_0073 (
PULPROG         zgflqn
TD             261912
SOLVENT           CDCl3
NS                256
DS                  4
SWH          131578.953 Hz
FIDRES         1.004757 Hz
AQ           0.9952656 sec
RG              197.18
DW             3.800 usec
DE              6.50 usec
TE             298.0 K
D1          2.00000000 sec
TD0                 1
SFO1       376.4701288 MHz
NUC1              19F
P1              15.00 usec
PLW1       23.22699928 W

F2 - Processing parameters
SI              131072
SF         376.4983662 MHz
WDW               EM
SSB                0
LB              0.50 Hz
GB                 0
PC              1.00
```

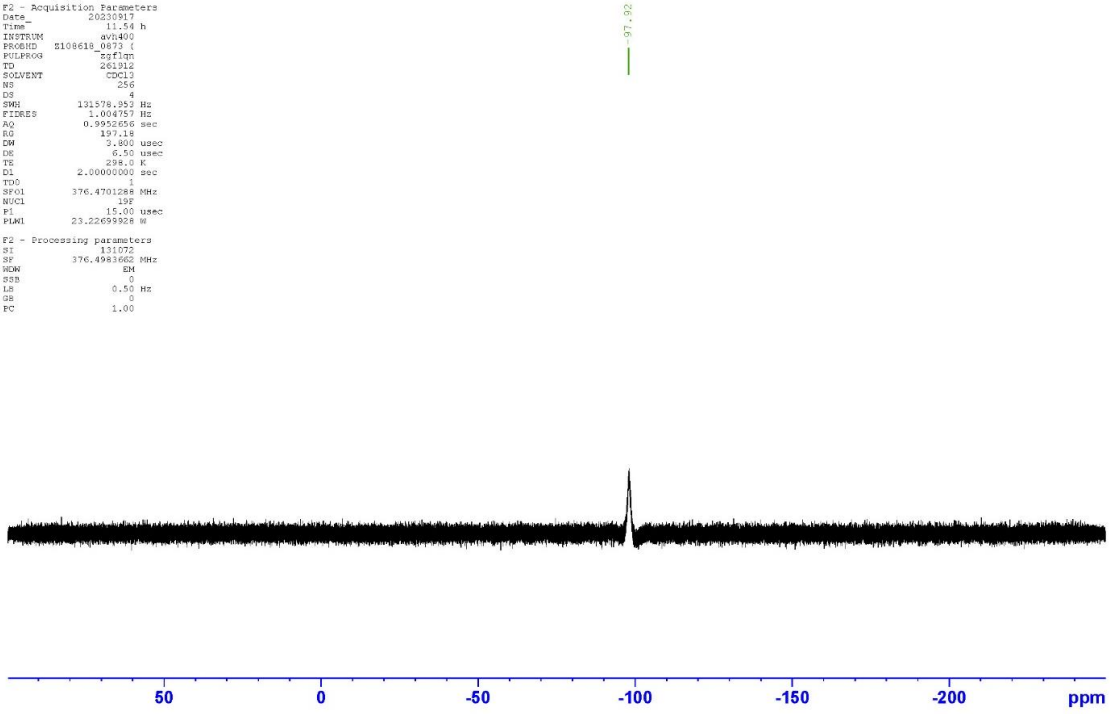

4-(3,5-Dimethylisoxazol-4-yl)-2-nitro-*N*-(2-(tetrahydro-2*H*-pyran-4-yl)ethyl)aniline

242

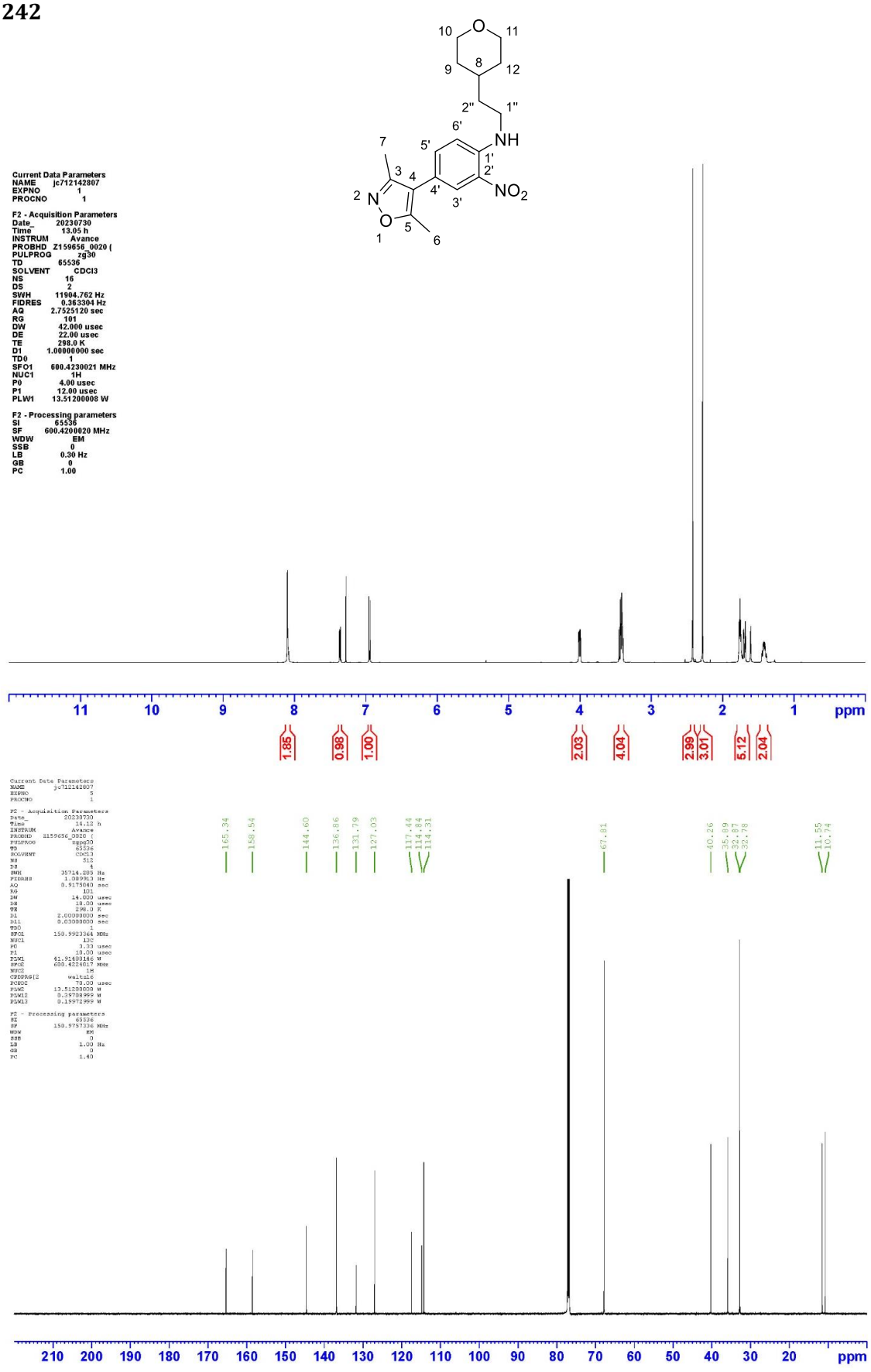

5-(2-(5-(3,5-Dimethylisoxazol-4-yl)-1-(2-(tetrahydro-2*H*-pyran-4-yl)ethyl)-1*H*-benzo[*d*]imidazol-2-yl)ethyl)-2-methylbenzonitrile 186

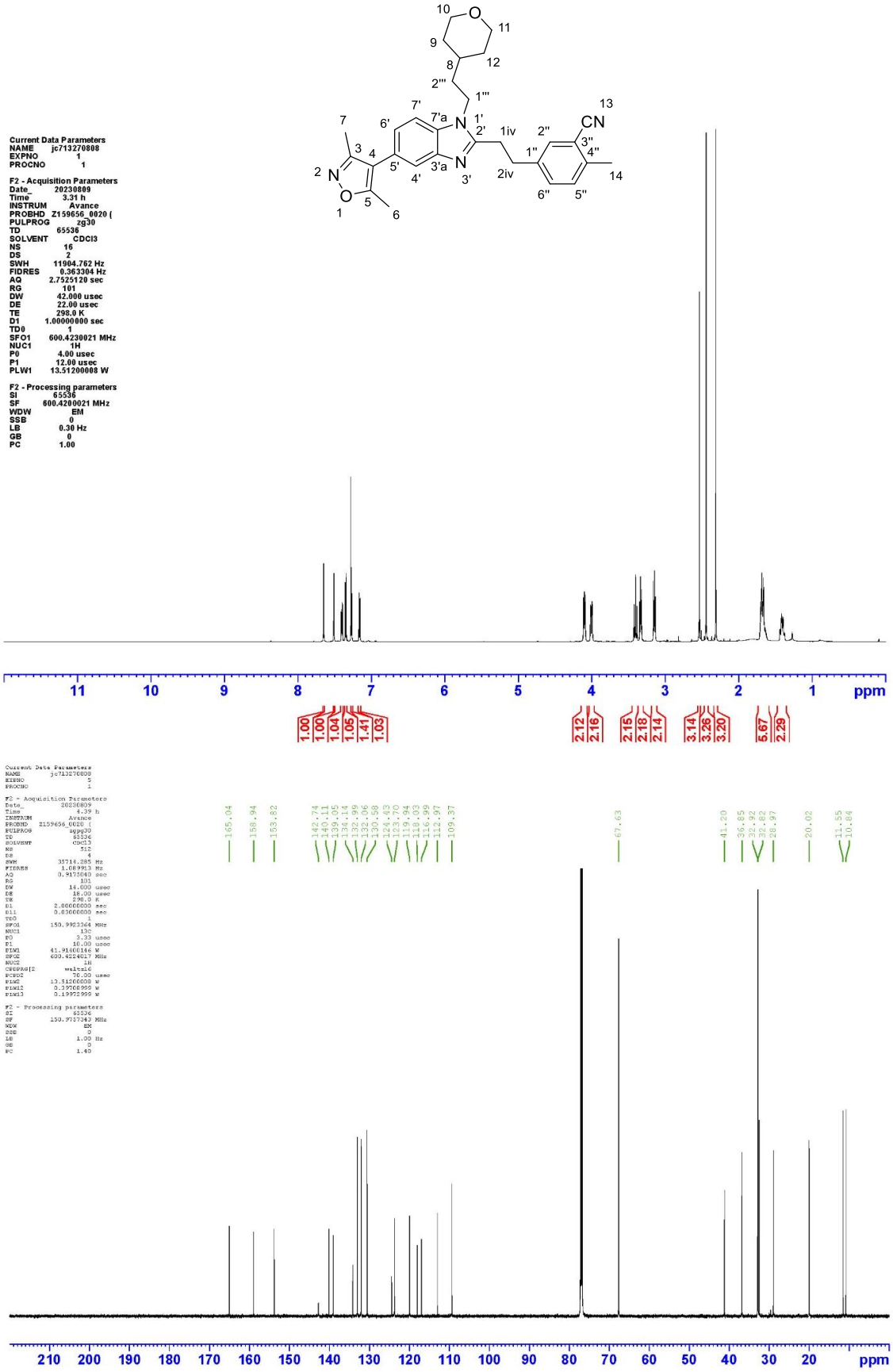

4-(3,5-Dimethylisoxazol-4-yl)-*N*-(2-methoxyethyl)-2-nitroaniline 244

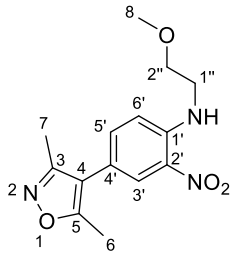

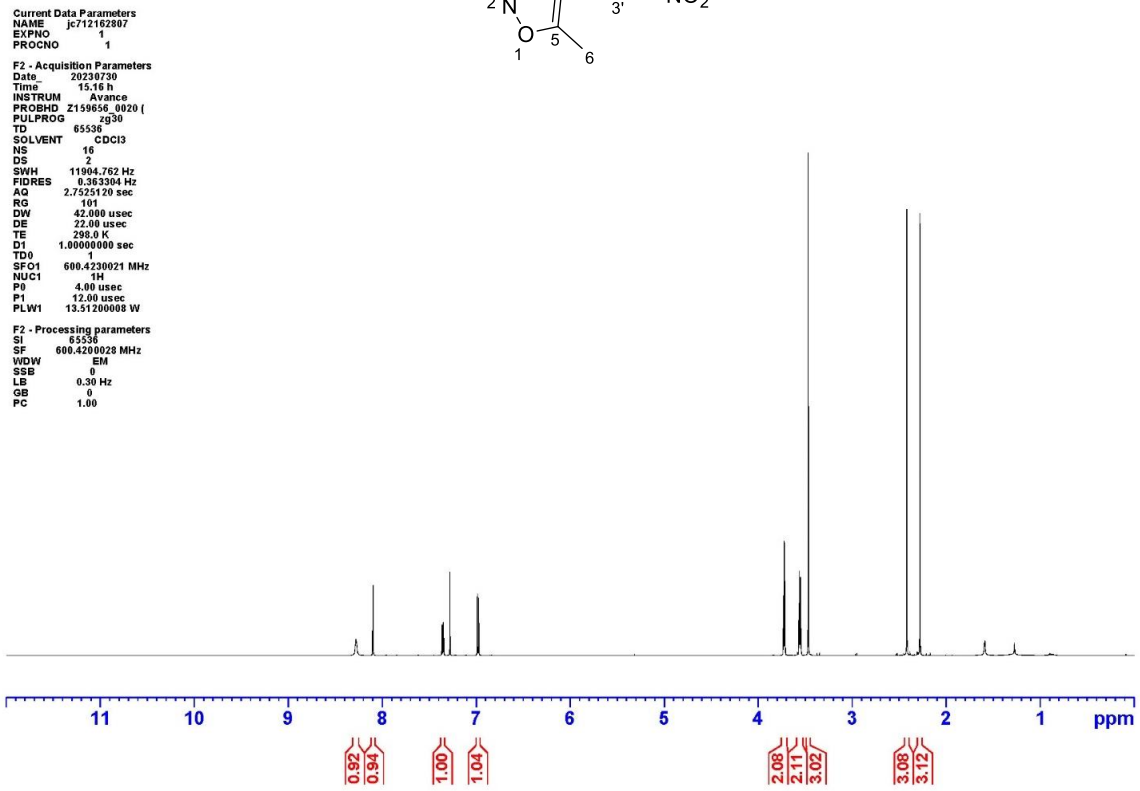

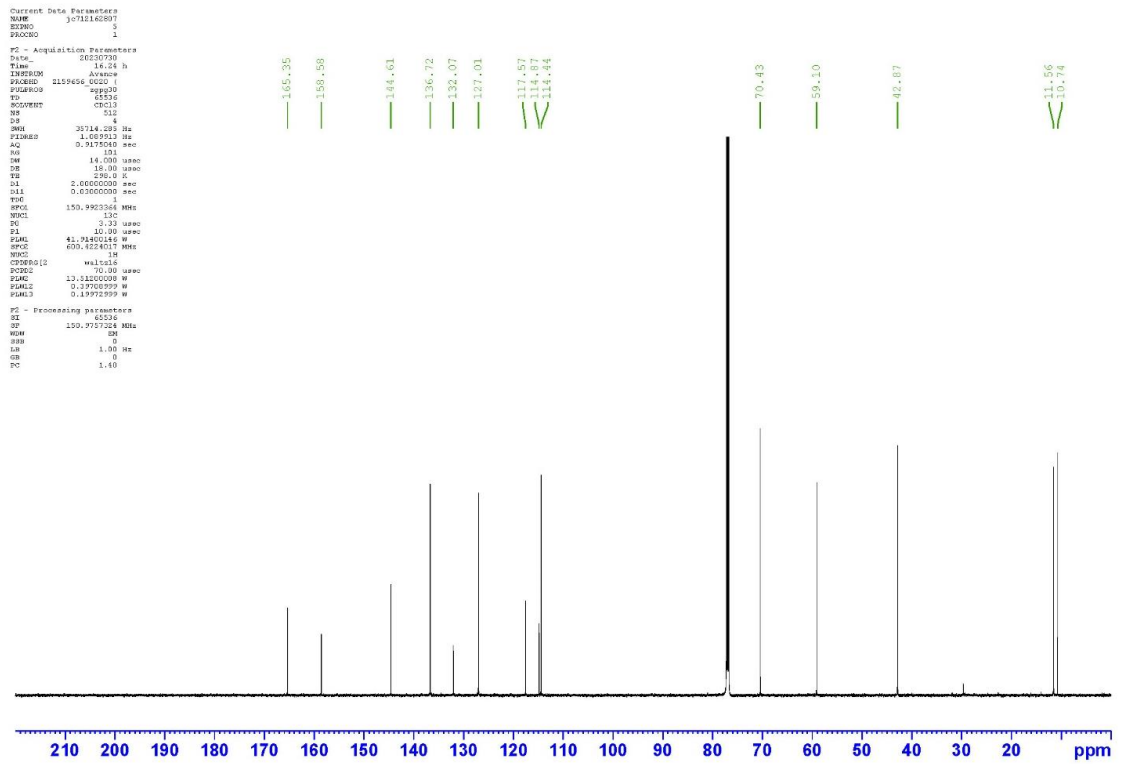

5-(2-(5-(3,5-Dimethylisoxazol-4-yl)-1-(2-methoxyethyl)-1*H*-benzo[*d*]imidazol-2-yl)ethyl)-2-methylbenzonitrile185

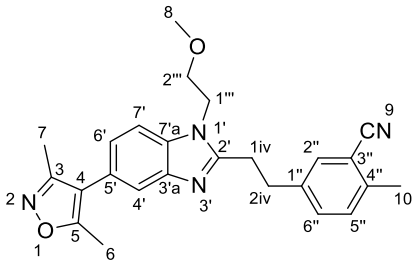

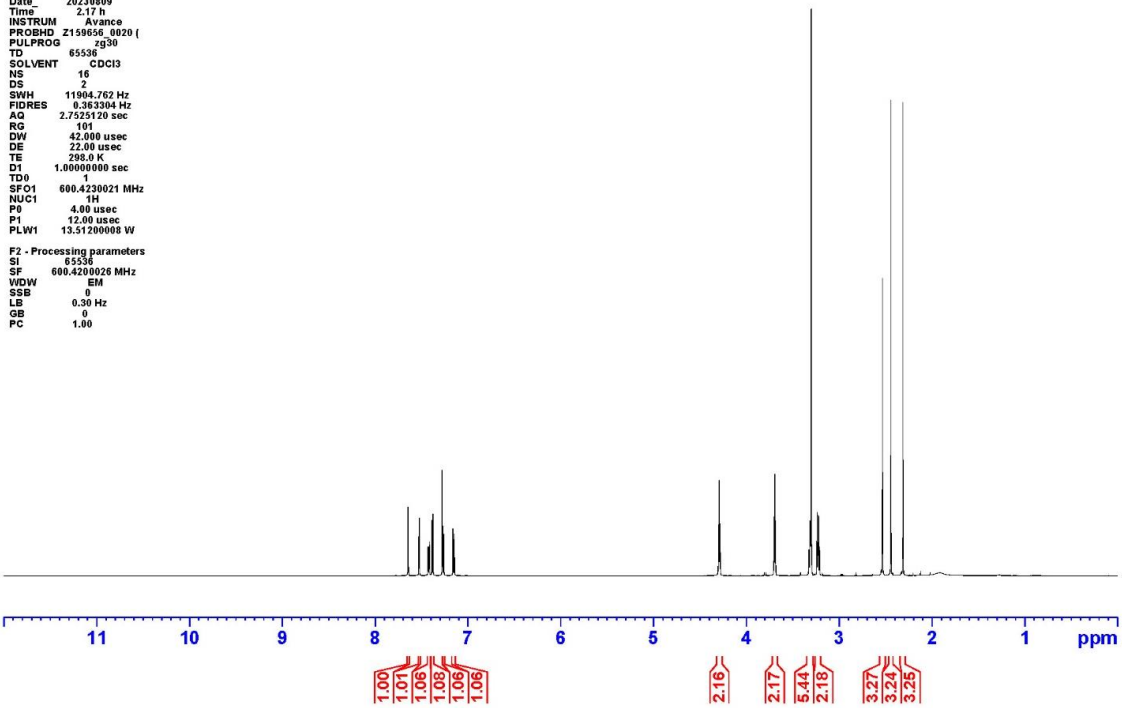

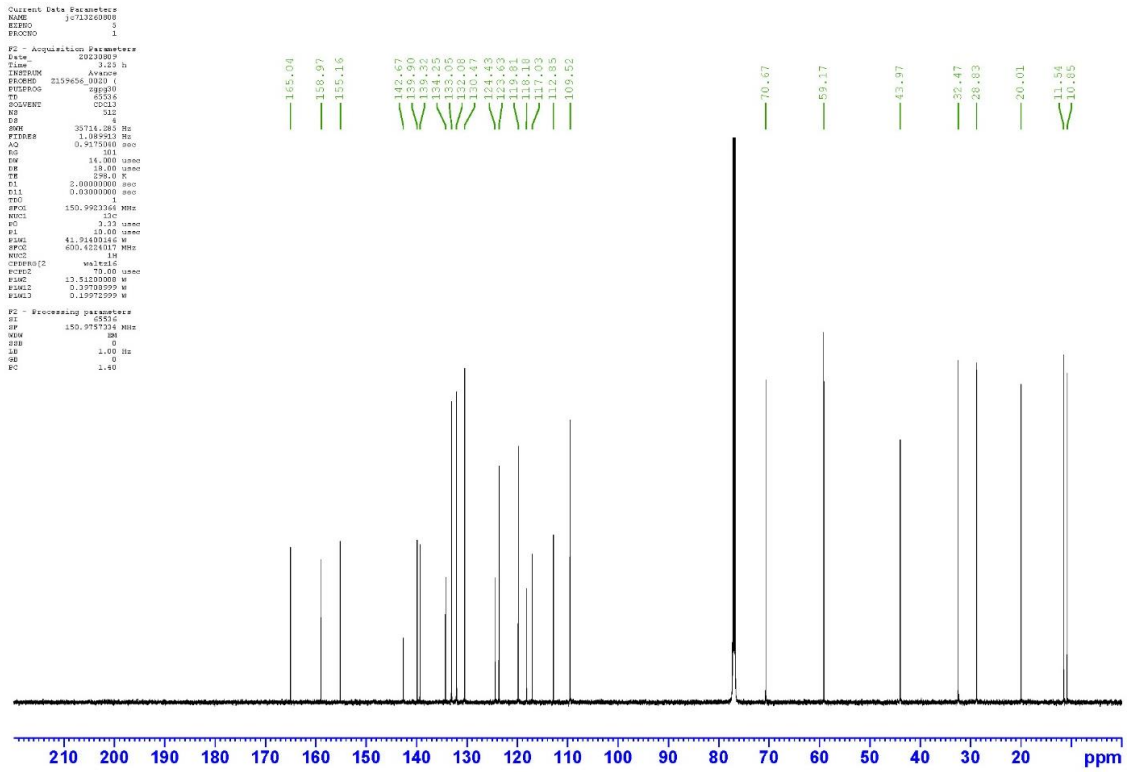

(5-(3,5-Dimethylisoxazol-4-yl)-1-methyl-1*H*-benzo[*d*]imidazol-2-yl)methanol 169

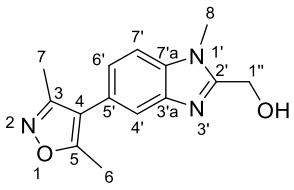

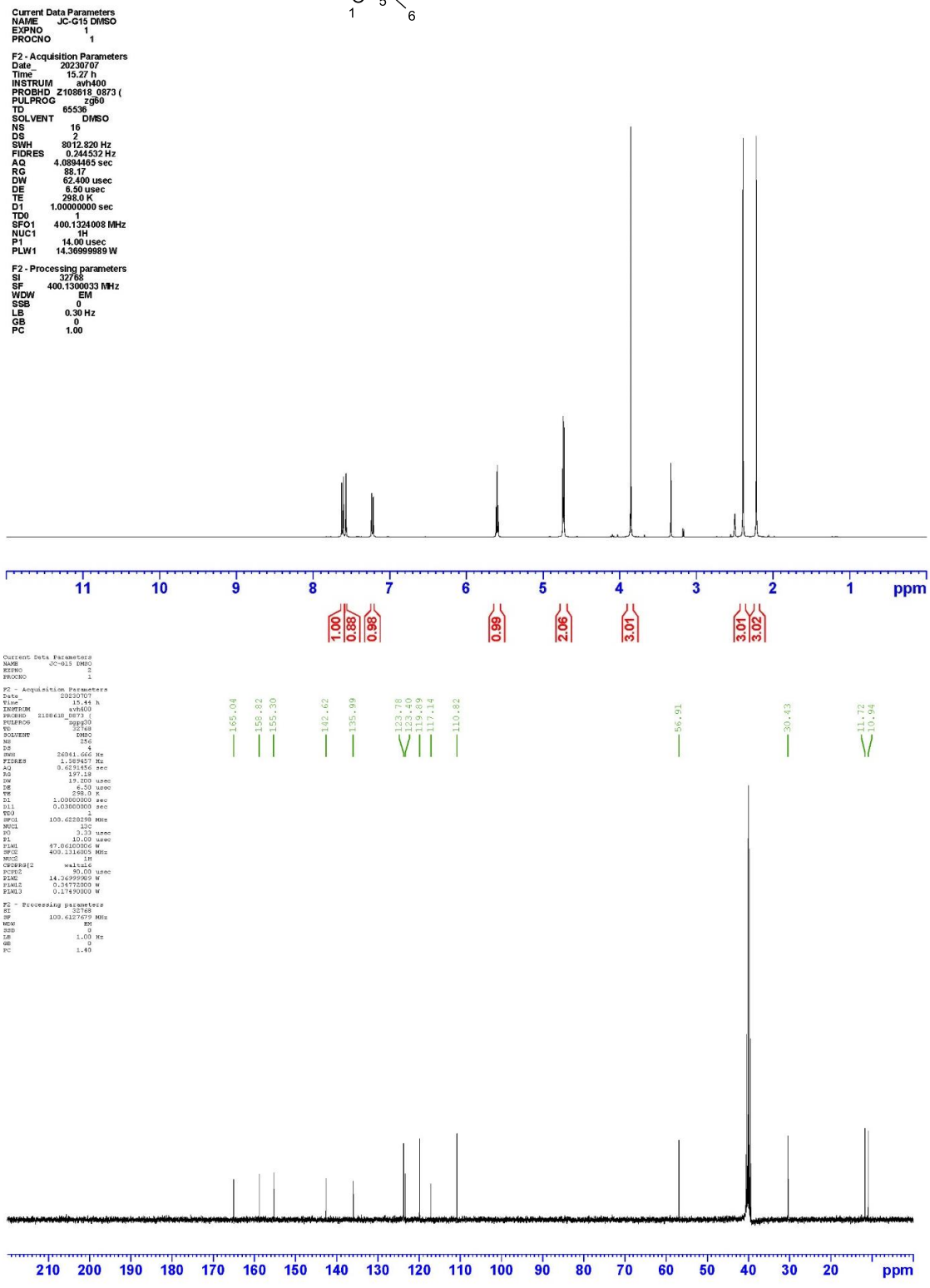

5-((5-(3,5-Dimethylisoxazol-4-yl)-1-methyl-1*H*-benzo[*d*]imidazol-2-yl)methoxy)-2-methylbenzonitrile 168

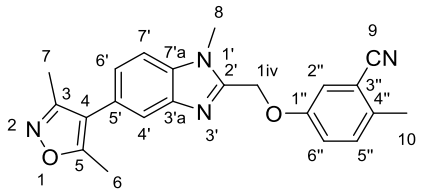

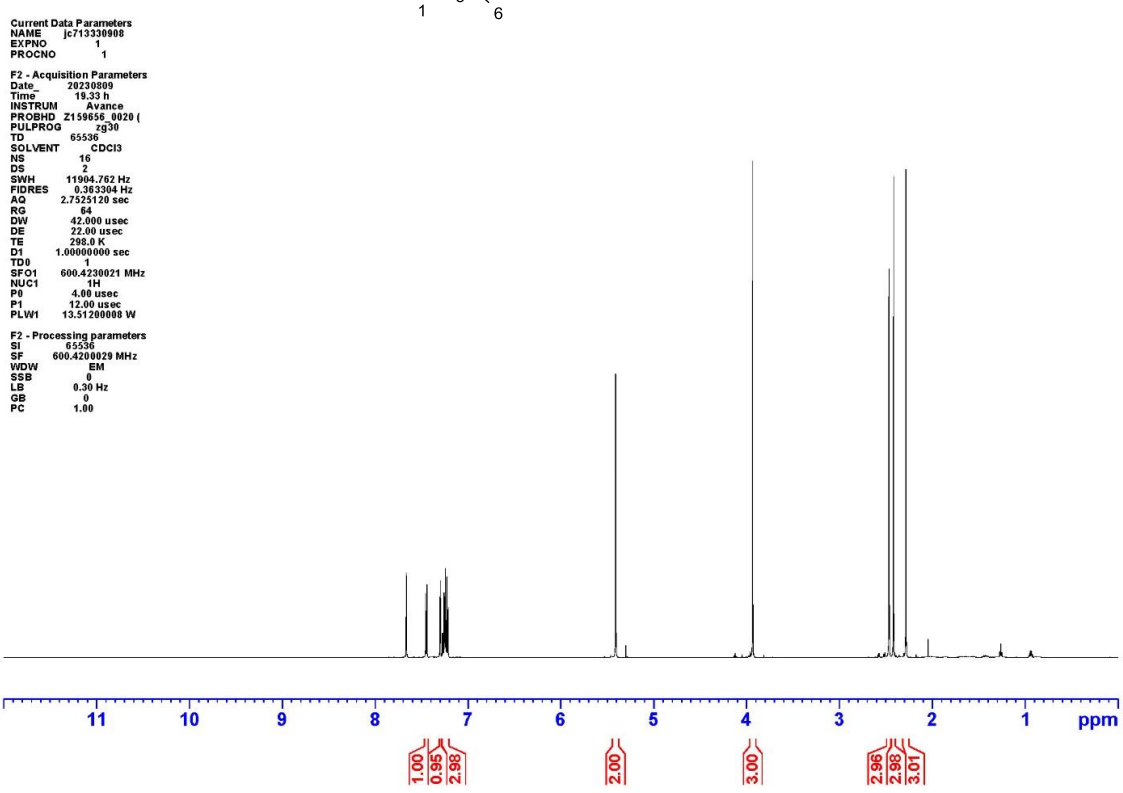

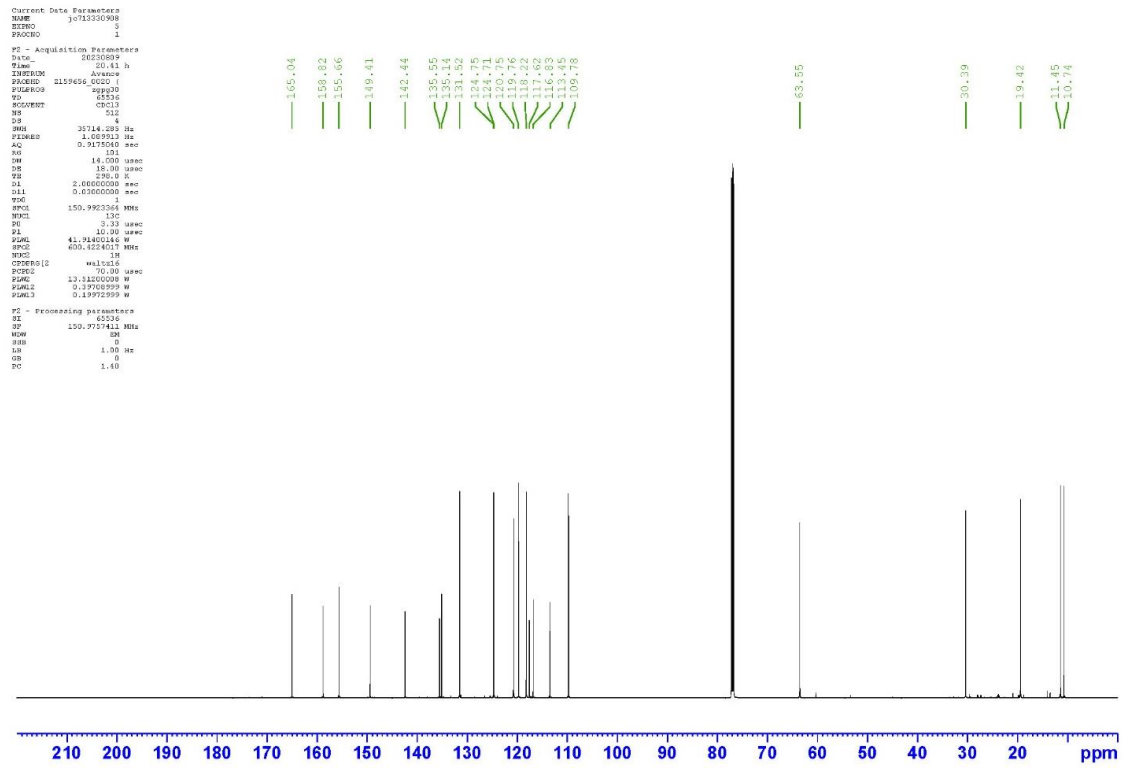

***Tert*-butyl 4-(2-((4-(3,5-dimethylisoxazol-4-yl)-2-nitrophenyl)amino)ethyl)piperazine-1-carboxylate 246**

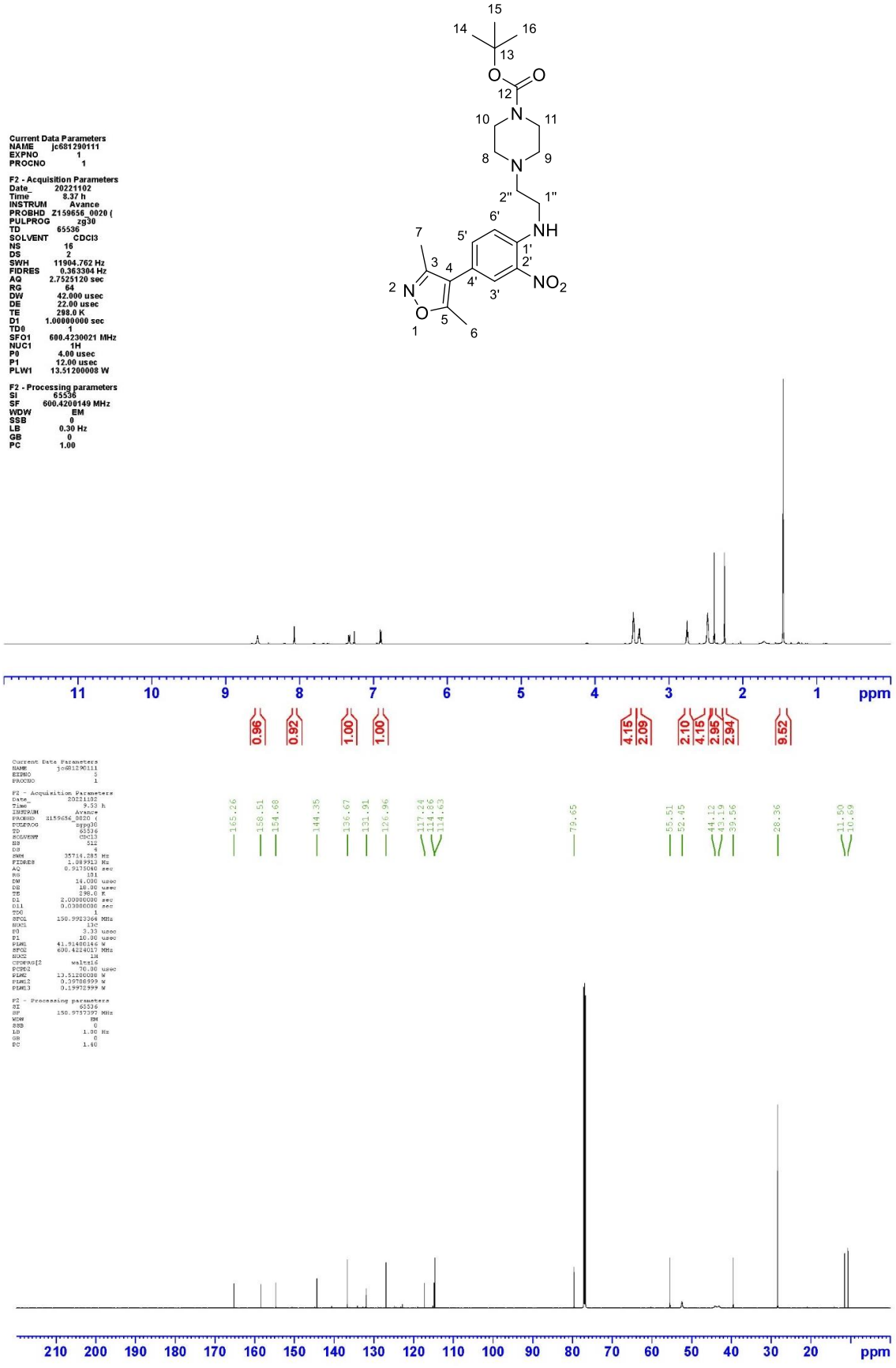

A6 Isothermal Titration Calorimetry (ITC) Data

18 in *Ld*BDF5.1

$K_d = 2.7 \pm 0.35$ μM

n = 3

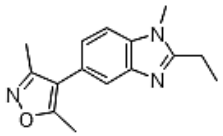

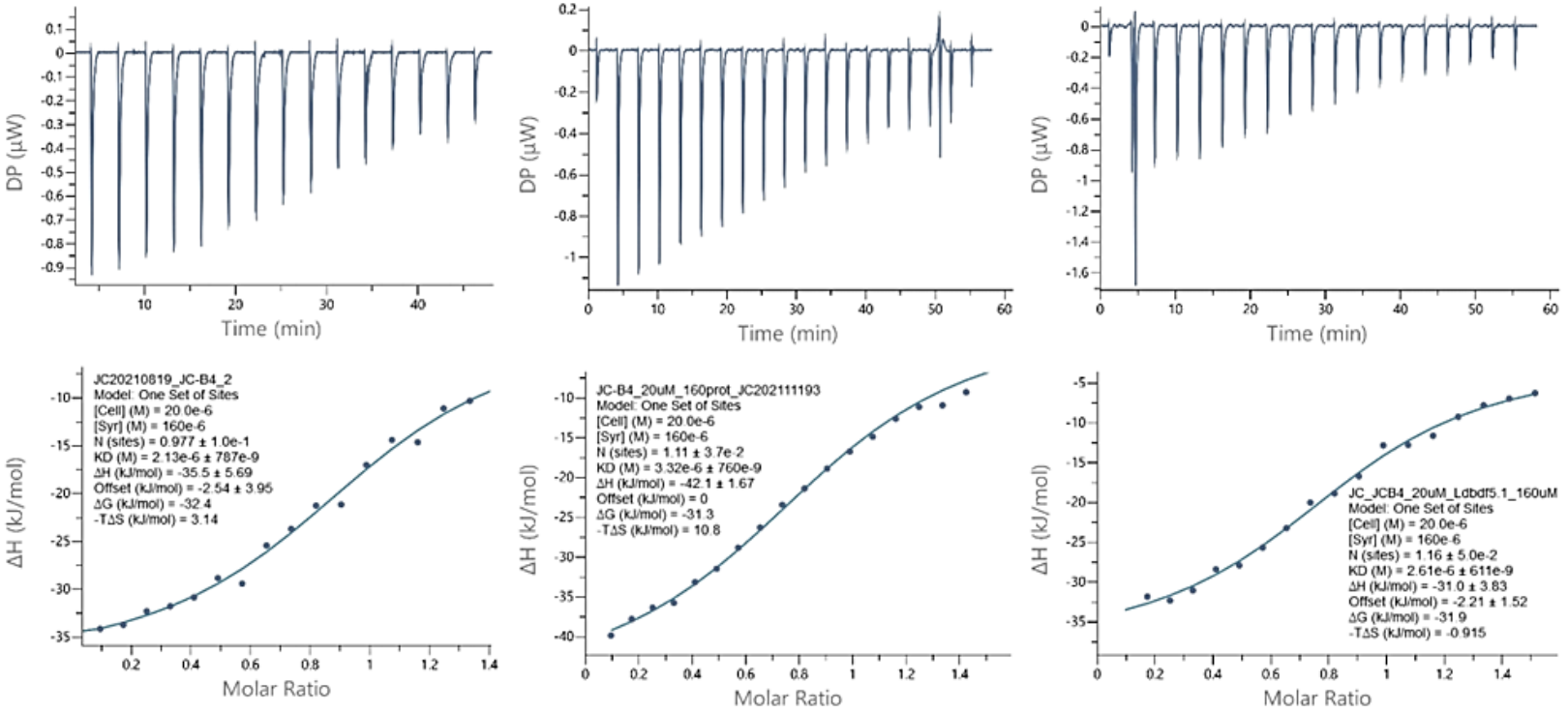

170 in *Ld*BDF5.1

$K_d = 91.8 \pm 0.93$ nM

n = 3

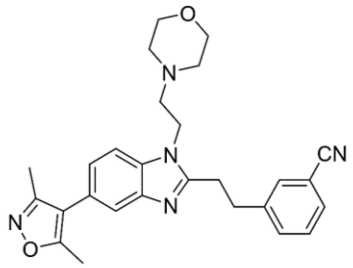

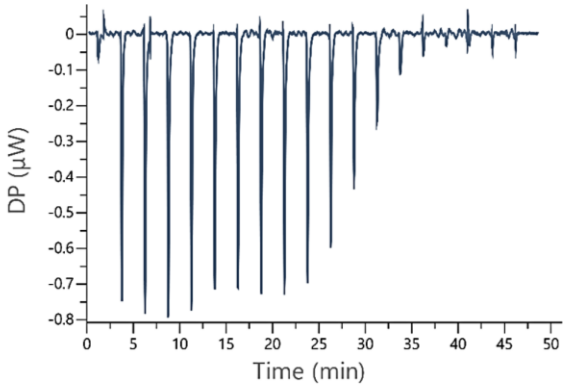

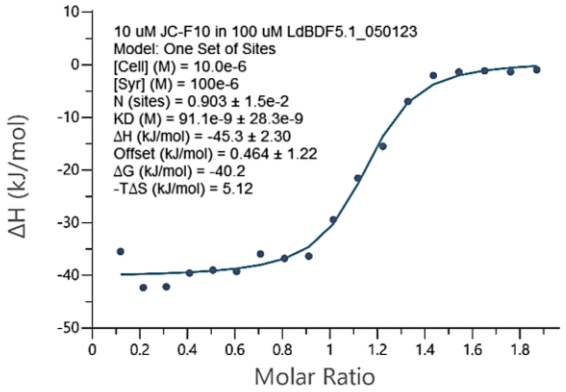

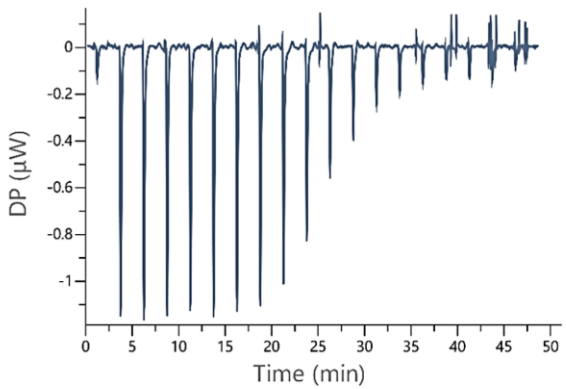

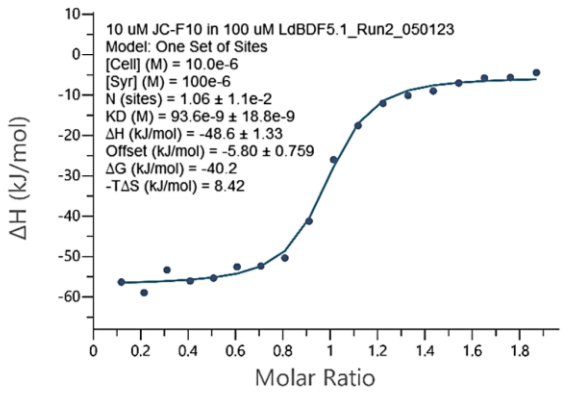

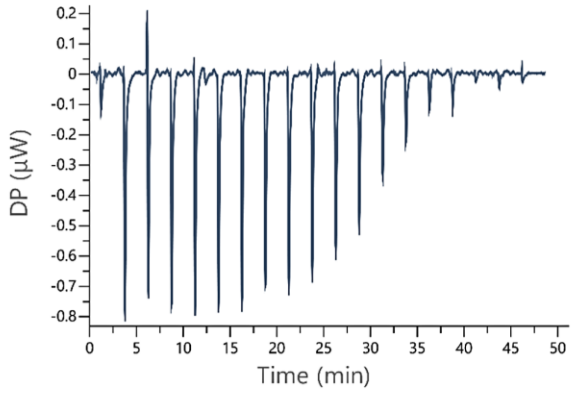

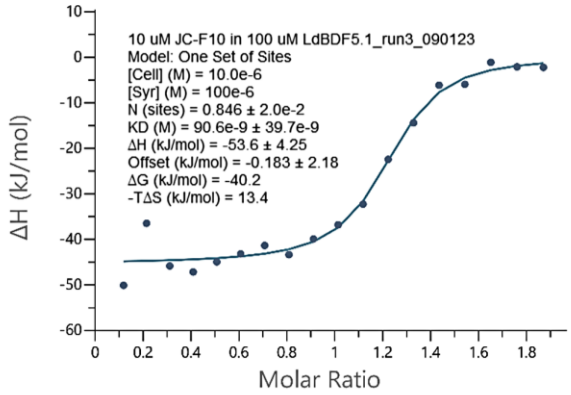

174 in *Ld*BDF5.1

$K_d = 37.0 \pm 12.0$ nM

n = 3

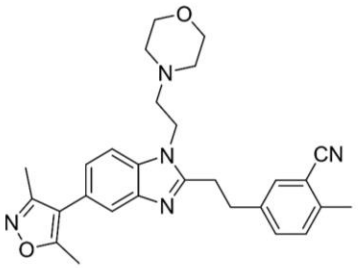

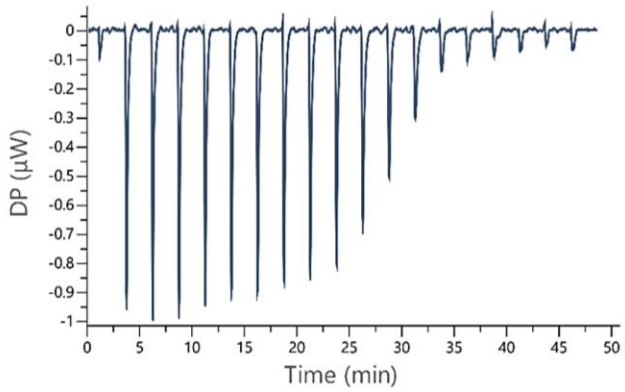

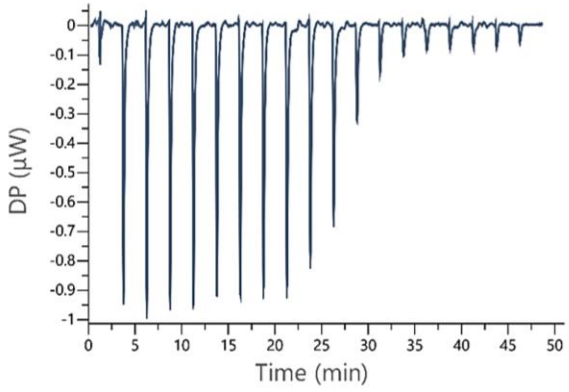

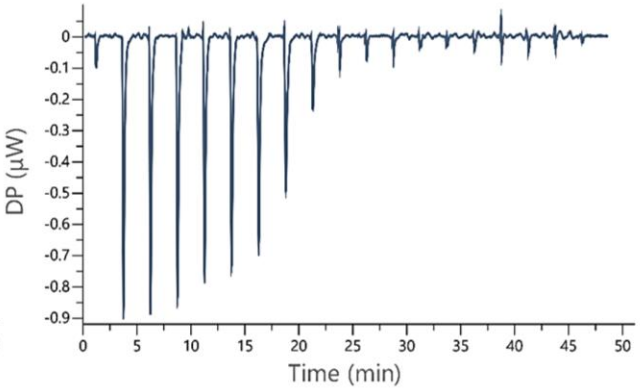

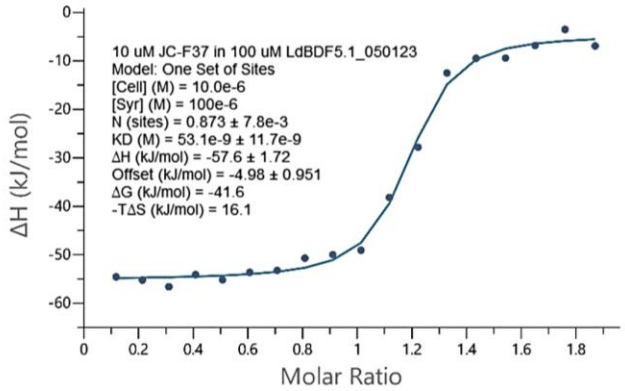

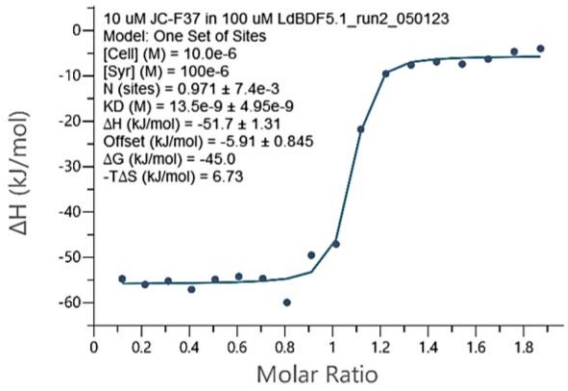

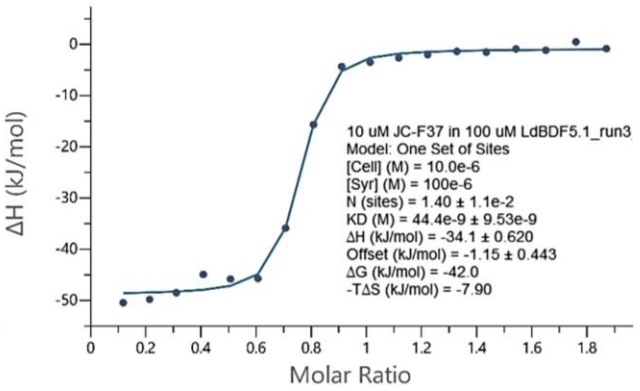

175 in *Ld*BDF5.1

$K_d = 120.2 \pm 13.2$ nM

n = 3

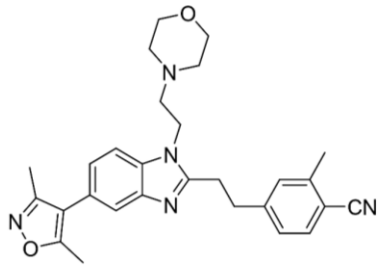

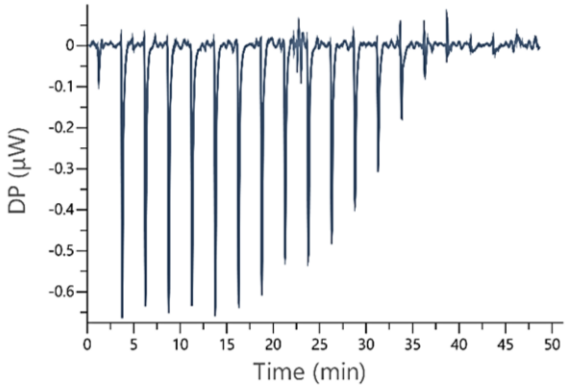

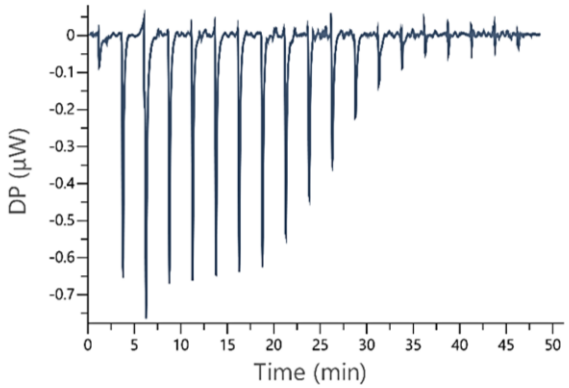

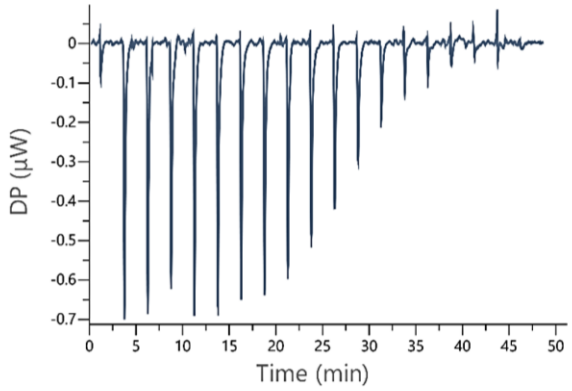

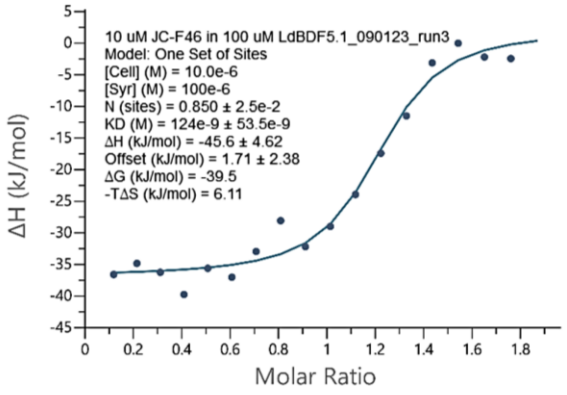

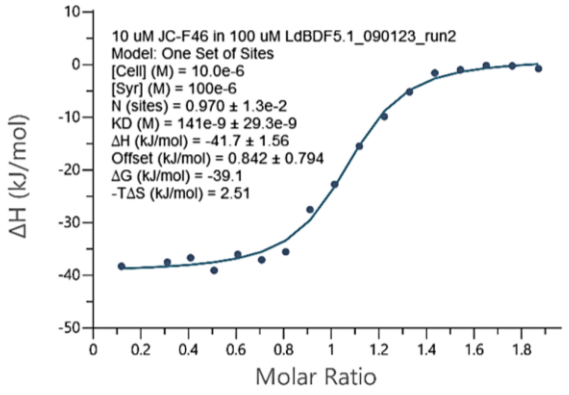

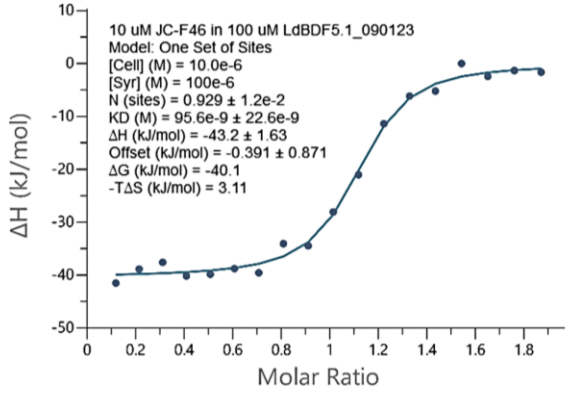

183 in *Ld*BDF5.1

$K_d = 7.2 \pm 2.3$ nM

n = 3

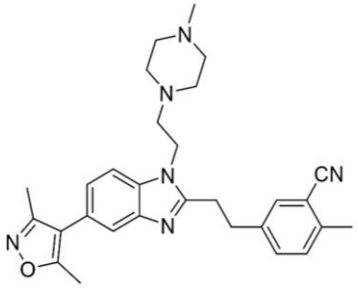

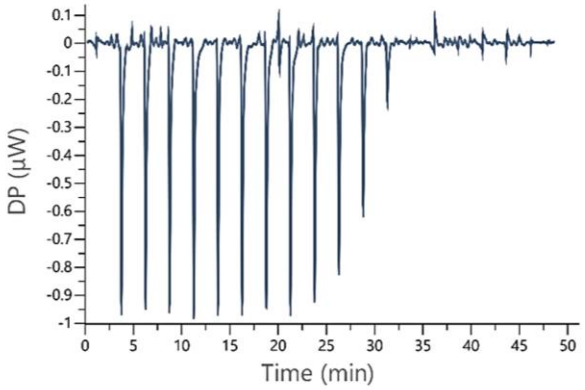

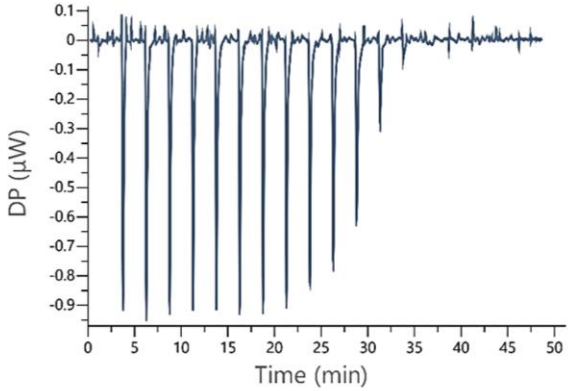

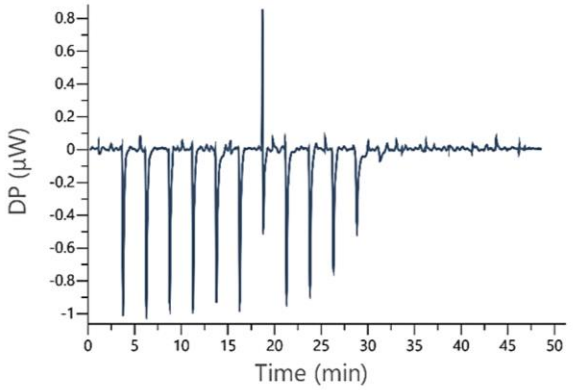

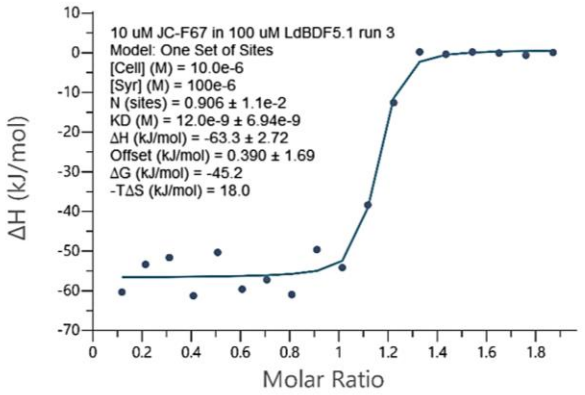

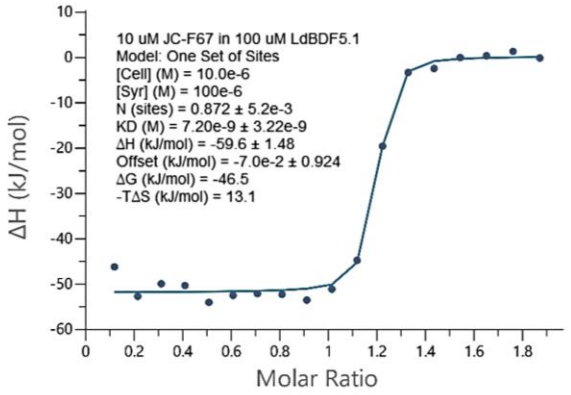

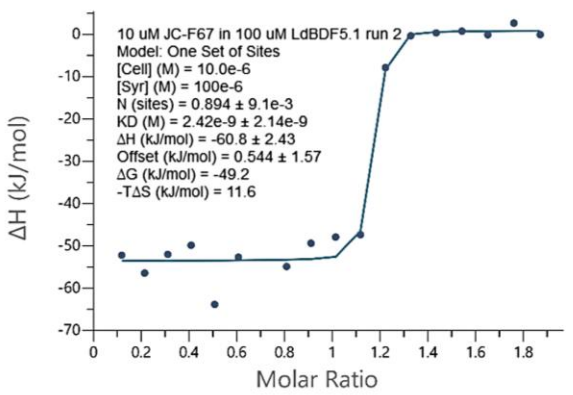

181 in *Ld*BDF5.1

$K_d = 26.4 \pm 4.7$ nM

n = 4

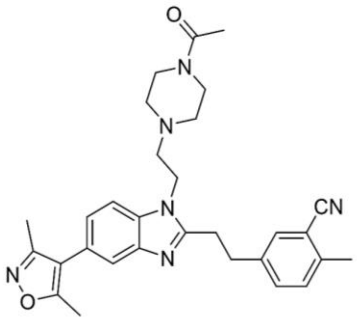

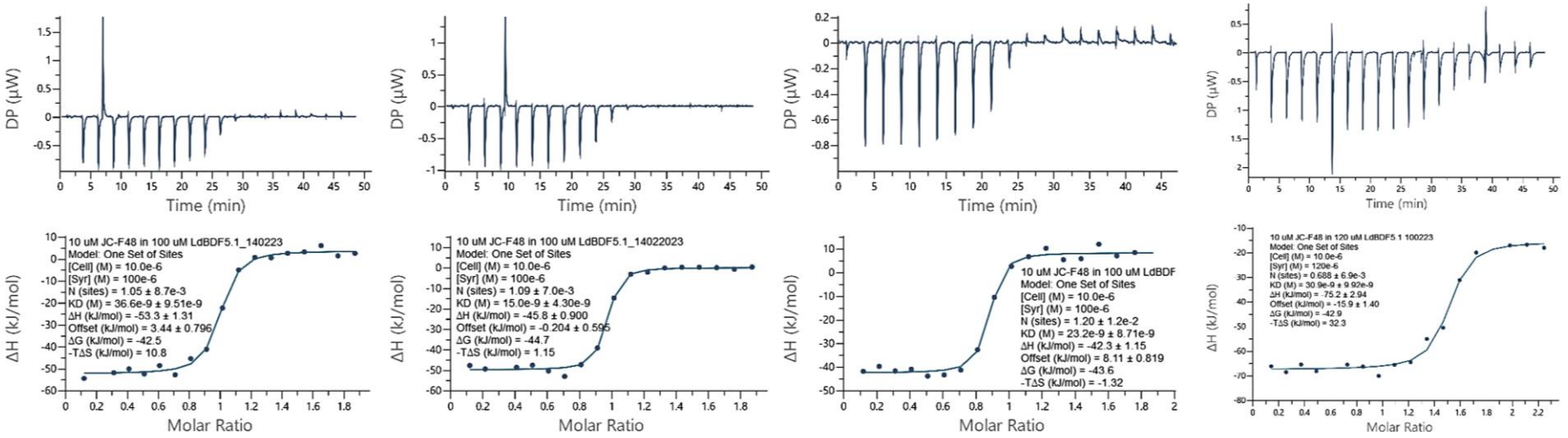

174 in BRD4(1)

$K_d = 9.5 \pm 2.77$ μM

n = 3

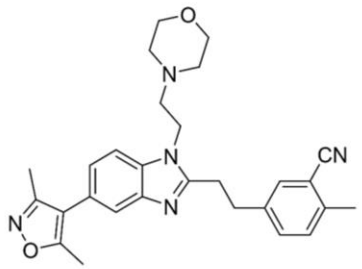

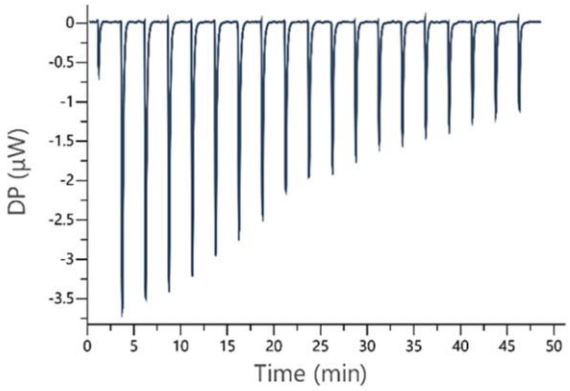

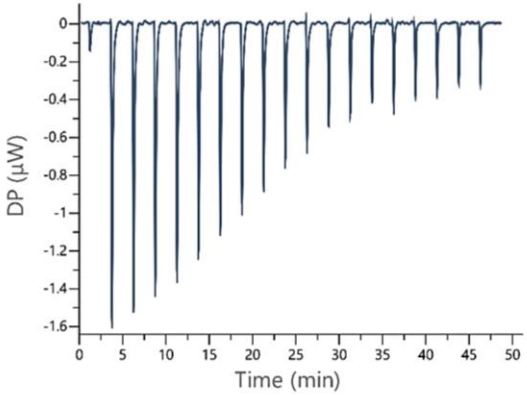

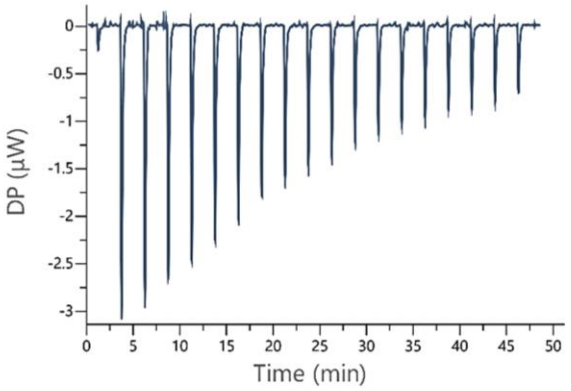

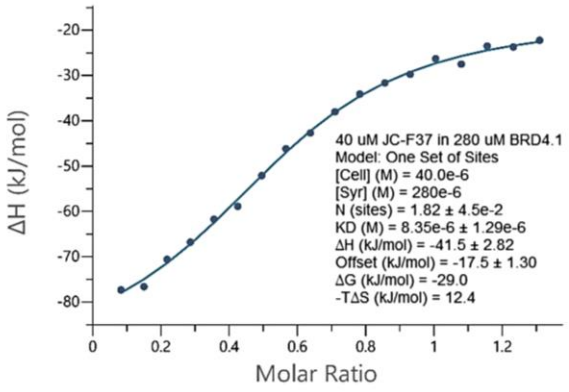

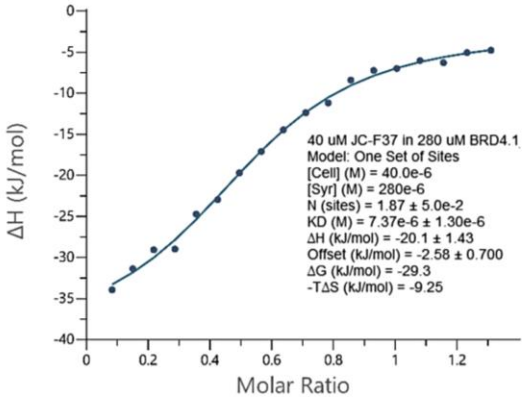

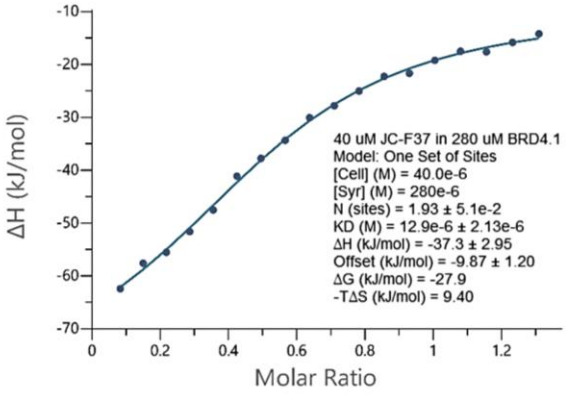

174 in CREBBP

$K_d = 73.3 \pm 40.6$ μM

n = 3

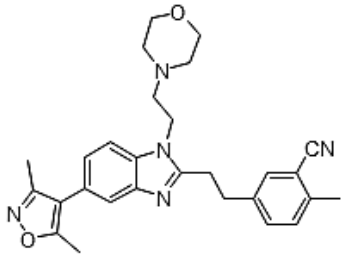

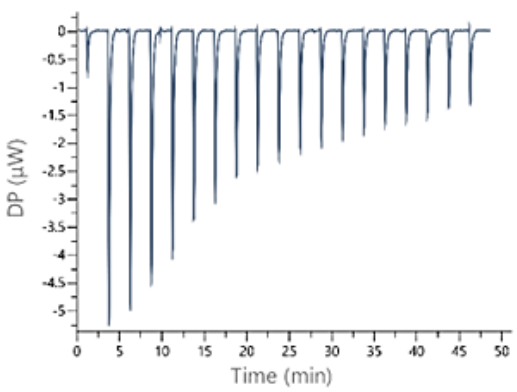

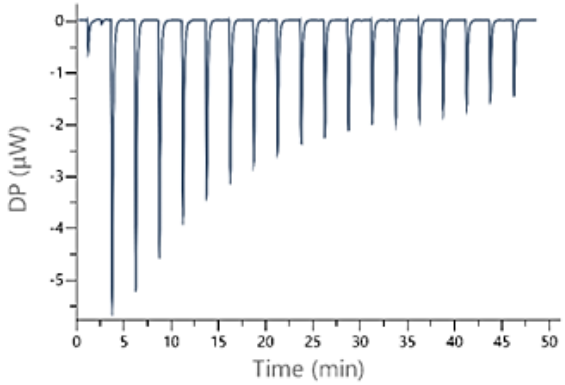

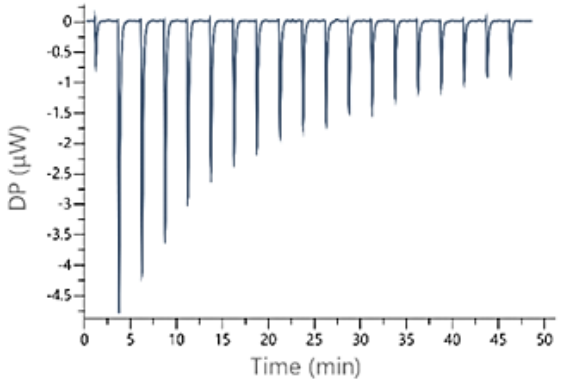

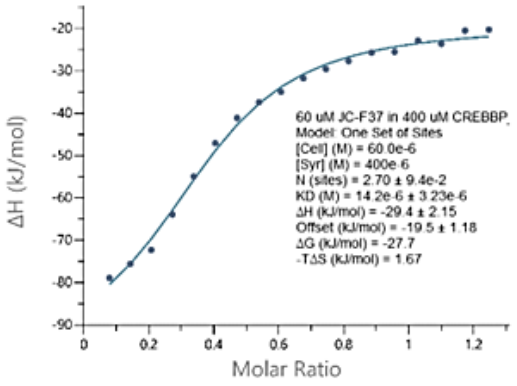

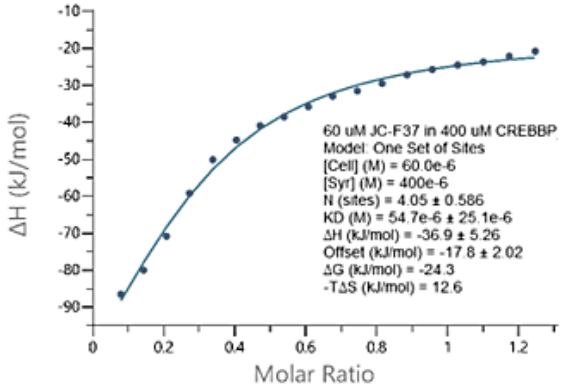

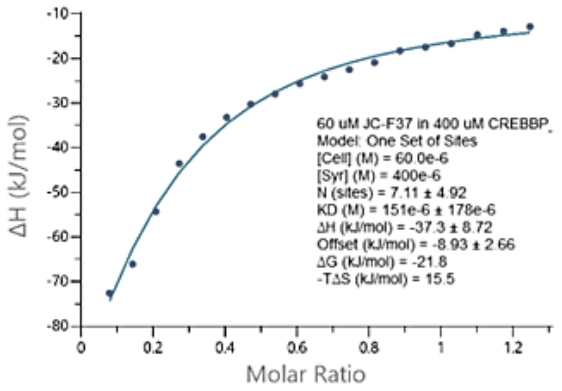

174 in *Lmx*BDF5.2

K_d = 36.1 ± 5.85 µM

n = 2

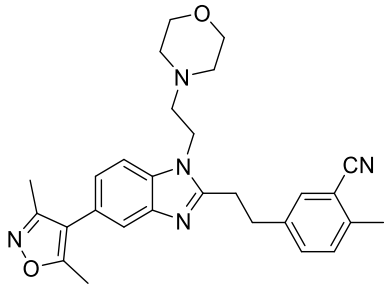

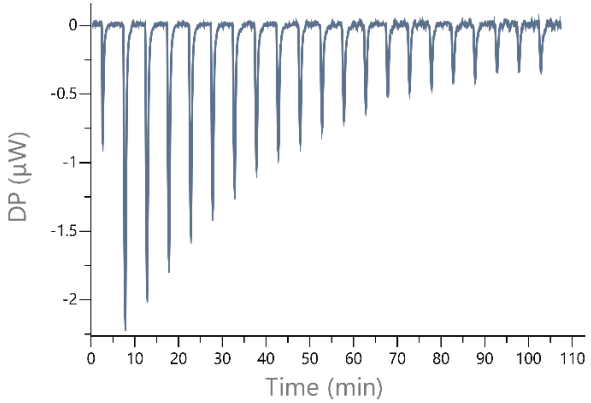

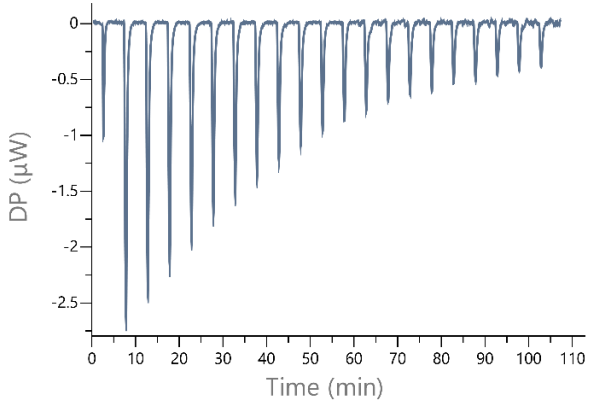

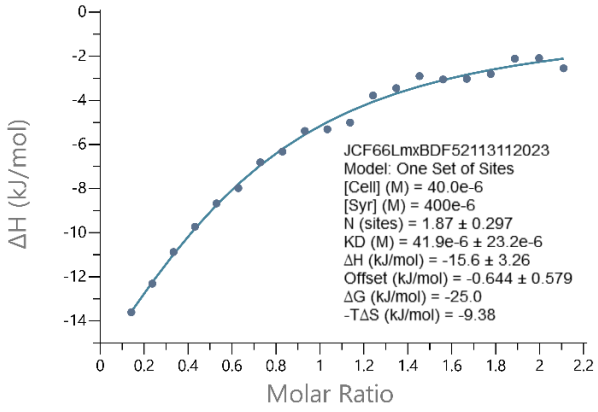

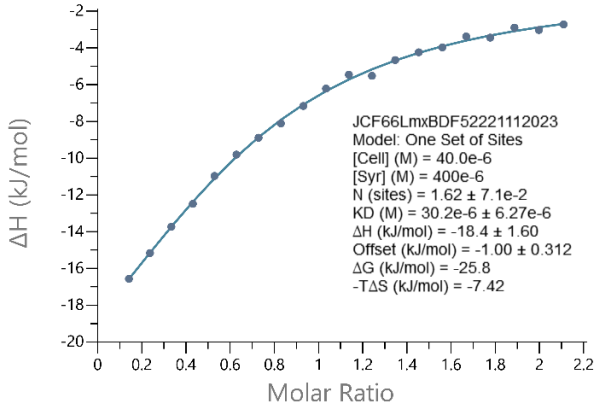

A7 Image Permissions

CCC Marketplace

This is a License Agreement between University of Oxford ("User") and Copyright Clearance Center, Inc. ("CCC") on behalf of the Rightsholder identified in the order details below. The license consists of the order details, the Marketplace Permissions General Terms and Conditions below, and any Rightsholder Terms and Conditions which are included below.

All payments must be made in full to CCC in accordance with the Marketplace Permissions General Terms and Conditions below.

Order Date	18-Dec-2023	Type of Use	Republish in a thesis/dissertation
Order License ID	1428509-1	Publisher	Future Science
ISSN	1756-8919	Portion	Image/photo/illustration

LICENSED CONTENT

Publication Title	Future medicinal chemistry	Country	United Kingdom of Great Britain and Northern Ireland
Date	01/01/2009	Rightsholder	Future Science Ltd.
Language	English	Publication Type	Journal

REQUEST DETAILS

Portion Type	Image/photo/illustration	Distribution	Worldwide
Number of Images / Photos / Illustrations	1	Translation	Original language of publication
Format (select all that apply)	Electronic	Copies for the Disabled?	No
Who Will Republish the Content?	Academic institution	Minor Editing Privileges?	No
Duration of Use	Life of current edition	Incidental Promotional Use?	No
Lifetime Unit Quantity	Up to 499	Currency	GBP
Rights Requested	Main product		

NEW WORK DETAILS

Title	The development of small molecule inhibitors of the essential Leishmania bromodomain LdBDF5	Institution Name	University of Oxford
		Expected Presentation Date	2024-01-12
Instructor Name	Jennifer Carter		

ADDITIONAL DETAILS

Order Reference Number	N/A	The Requesting Person / Organization to Appear on the License	University of Oxford

REQUESTED CONTENT DETAILS

Title, Description or Numeric Reference of the Portion(s)	Figure 2. Post-translational modifications to histone proteins, displayed as amino acid sequences.	Title of the Article / Chapter the Portion Is From	Phenotypic screening and fragment-based approaches to the discovery of small-molecule bromodomain ligands
Editor of Portion(s)	Jennifer Carter	Author of Portion(s)	Laura E Jennings, Angelina R Measures, Brian G Wilson & Stuart J Conway
Volume / Edition	n/a		
Page or Page Range of Portion	181	Issue, if Republishing an Article From a Serial	N/A
		Publication Date of Portion	2014-01-28

Thank you for your order.

This Agreement between University of Oxford -- Jennifer Carter ("You") and Springer Nature ("Springer Nature") consists of your license details and the terms and conditions provided by Springer Nature and Copyright Clearance Center.

Your confirmation email will contain your order number for future reference.

License Number	5676970977150
License date	Nov 27, 2023

Printable Details

Licensed Content

Licensed Content Publisher	Springer Nature
Licensed Content Publication	Journal of Biomolecular NMR
Licensed Content Title	WaterLOGSY as a method for primary NMR screening: Practical aspects and range of applicability
Licensed Content Author	Claudio Dalvit et al
Licensed Content Date	Jan 1, 2001

Order Details

Type of Use	Thesis/Dissertation
Requestor type	academic/university or research institute
Format	electronic
Portion	figures/tables/illustrations
Number of figures/tables/illustrations	1
Will you be translating?	no
Circulation/distribution	1 - 29
Author of this Springer Nature content	no

About Your Work

Title of new work	The development of small molecule inhibitors of the essential Leishmania bromodomain BDF5
Institution name	University of Oxford
Expected presentation date	Jan 2024

Additional Data

Portions	Figure 1, page 350

Requestor Location

Requestor Location	University of Oxford 2 Rymers Lane Oxford, OX4 3LA United Kingdom Attn: University of Oxford

Tax Details



Fragment-Based Approaches in Drug Discovery and Chemical Biology

Author: Duncan E. Scott, Anthony G. Coyne, Sean A. Hudson, et al
Publication: Biochemistry
Publisher: American Chemical Society
Date: Jun 1, 2012

Copyright © 2012, American Chemical Society

PERMISSION/LICENSE IS GRANTED FOR YOUR ORDER AT NO CHARGE

This type of permission/license, instead of the standard Terms and Conditions, is sent to you because no fee is being charged for your order. Please note the following:

- Permission is granted for your request in both print and electronic formats, and translations.
- If figures and/or tables were requested, they may be adapted or used in part.
- Please print this page for your records and send a copy of it to your publisher/graduate school.
- Appropriate credit for the requested material should be given as follows: "Reprinted (adapted) with permission from (COMPLETE REFERENCE CITATION). Copyright (YEAR) American Chemical Society." Insert appropriate information in place of the capitalized words.
- One-time permission is granted only for the use specified in your RightsLink request. No additional uses are granted (such as derivative works or other editions). For any uses, please submit a new request.

If credit is given to another source for the material you requested from RightsLink, permission must be obtained from that source.

BACK

CLOSE WINDOW

© 2023 Copyright - All Rights Reserved | Copyright Clearance Center, Inc. | Privacy statement | Data Security and Privacy | For California Residents | Terms and Conditions
Comments? We would like to hear from you. E-mail us at customercare@copyright.com